Isolated Neutron Stars. Intro.

Stars in the Galaxy

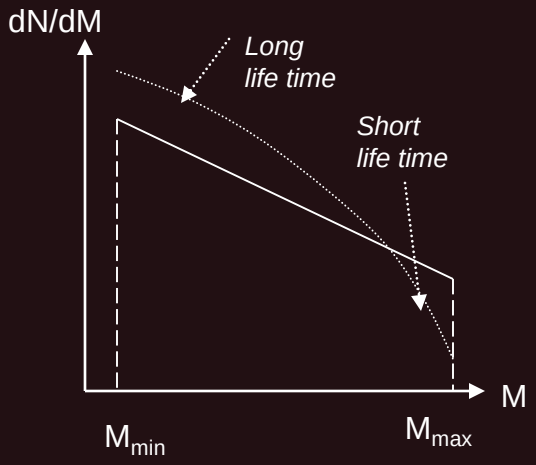

Salpeter (1955) mass function:
$dN/dM \sim M^{-2.35}$

There are many modification (Miller-Scalo, Kroupa etc.).
At high masses the slope is usually steeper.
Note: it is *initial* mass function, not the present day!

It is possible to estimate the number of NS and BH progenitors.
Then using there average lifetime we can estimate the birth rate
and total numbers (with a given age of the Galaxy and assuming constant rate)
taking into account SFR~(3-5) solar mass per year.
[see also Ch.1 in Shapiro, Teukolsky]

Prediction ...

Neutron stars have been predicted in 30s:

L.D. Landau: Star-nuclei (1932) + anecdote

Baade and Zwicky:
neutron stars and supernovae (1934)

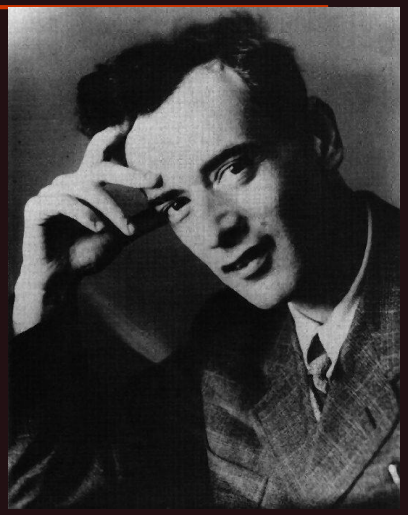

(Landau)

(Baade)

(Zwicky)

(from lectures by D. Yakovlev)

In any case, with the discovery of X-ray sources and quasars, dozens of theoreticians focused their attention on the equilibrium properties of compact stars and on star collapse. But in spite of this mounting theoretical effort, most

[2]Baade and Zwicky (1934): "With all reserve we advance the view that supernovae represent the transitions from ordinary stars into *neutron stars*, which in their final stages consist of extremely closely packed neutrons."

According to Rosenfeld (1974), on the day that word came to Copenhagen from Cambridge telling of Chadwick's discovery of the neutron in 1932, he, Bohr, and Landau spent the evening discussing possible implications of the discovery. It was then that Landau suggested the possibility of cold, dense stars composed principally of neutrons. Landau's only publication on the subject was concerned with neutron cores (Landau, 1938).

[3]Giacconi, Gursky, Paolini, and Rossi (1962).

[4]Chapter 11 is devoted to this subject.

[5]The first QSO identified by Schmidt, 3C273, had a redshift $\delta\lambda/\lambda = 0.158$, which was unprecedented for a normal "star."

[6]Salpeter (1965); in addition to this argument there was strong evidence that quasar redshifts were cosmological in origin.

Shapiro,Teukolsky (1983)

(see detailed description in the book by Haensel, Yakovlev, Potekhin and in the e-print arXiv: 1210.0682)

Landau paper BEFORE neutron discovery

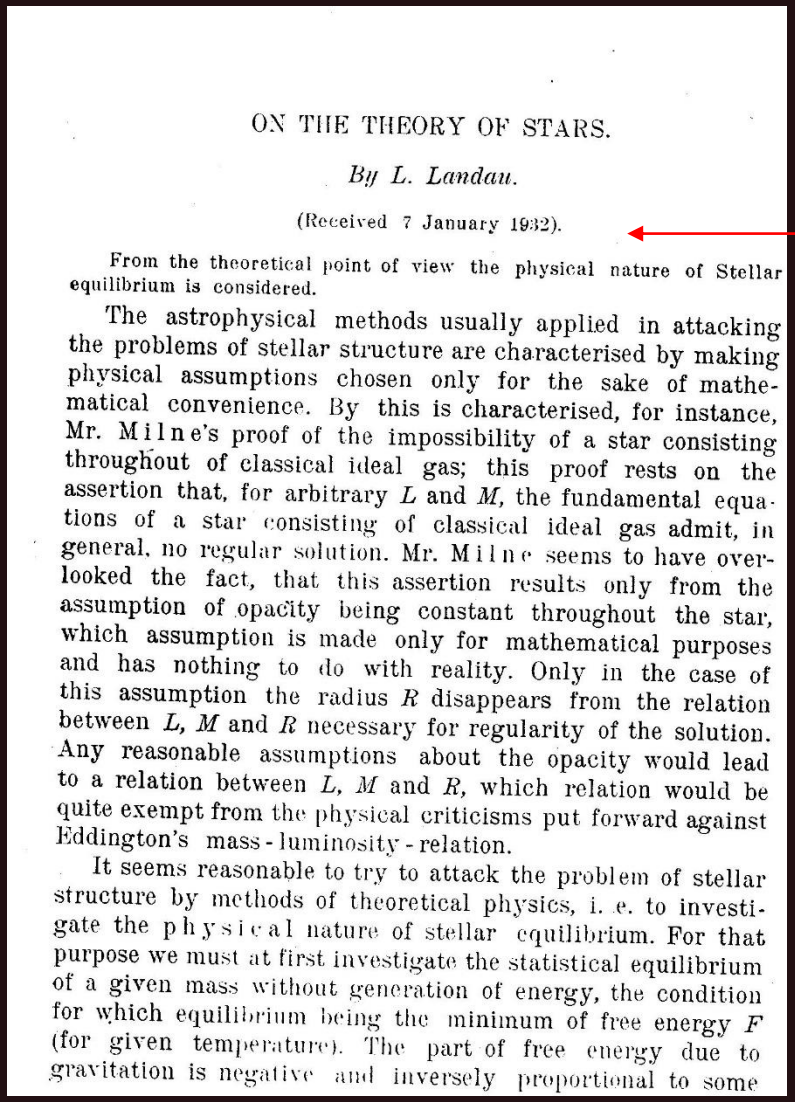

ON THE THEORY OF STARS.

By L. Landau.

(Received 7 January 1932).

From the theoretical point of view the physical nature of Stellar equilibrium is considered.

The astrophysical methods usually applied in attacking the problems of stellar structure are characterised by making physical assumptions chosen only for the sake of mathematical convenience. By this is characterised, for instance, Mr. Milne's proof of the impossibility of a star consisting throughout of classical ideal gas; this proof rests on the assertion that, for arbitrary L and M, the fundamental equations of a star consisting of classical ideal gas admit, in general, no regular solution. Mr. Milne seems to have overlooked the fact, that this assertion results only from the assumption of opacity being constant throughout the star, which assumption is made only for mathematical purposes and has nothing to do with reality. Only in the case of this assumption the radius R disappears from the relation between L, M and R necessary for regularity of the solution. Any reasonable assumptions about the opacity would lead to a relation between L, M and R, which relation would be quite exempt from the physical criticisms put forward against Eddington's mass-luminosity-relation.

It seems reasonable to try to attack the problem of stellar structure by methods of theoretical physics, i. e. to investigate the physical nature of stellar equilibrium. For that purpose we must at first investigate the statistical equilibrium of a given mass without generation of energy, the condition for which equilibrium being the minimum of free energy F (for given temperature). The part of free energy due to gravitation is negative and inversely proportional to some

Physikalische Zeitschrift der Sowjetunion
Vol. 1, No. 2, 285-188, 1932
Written: Feb. 1931, Zurich
Received: Jan. 7, 1932
Published: Feb. 1932

we have no need to suppose that the radiation of stars is due to some mysterious process of mutual annihilation of protons and electrons, which was never observed and has no special reason to occur in stars. Indeed we have always protons and electrons in atomic nuclei very close together, and they do not annihilate themselves; and it would be very strange if the high temperature did help, only because it does something in chemistry (chain reactions!). Following a beautiful idea of Prof. Niels Bohr's we are able to believe that the stellar radiation is due simply to a violation of the law of energy, which law, as Bohr has first pointed out, is no longer valid in the relativistic quantum theory, when the laws of ordinary quantum mechanics break down (as it is experimentally proved by continuous-rays-spectra and also made probable by theoretical considerations).[1] We expect that this must occur when the density of matter becomes so great that atomic nuclei come in close contact, forming one gigantic nucleus.

On these general lines we can try to develop a theory of stellar structure. The central region of the star must consist of a core of highly condensed matter, surrounded by matter in ordinary state. If the transition between these two states were a continuous one, a mass $M < M_0$ would never form a star, because the normal equilibrium state (i. e. without pathological regions) would be quite stable. Because, as far as we know, it is not the fact, we must conclude that the condensed and non-condensed states are separated by some unstable states in the same manner as a liquid and its vapour are, a property which could be easily explained by some kind of nuclear attraction. This would lead to the existence of a nearly discontinuous boundary between the two states.

The theory of stellar structure founded on the above considerations is yet to be constructed, and only such a theory can show how far they are true.

February 1931, Zurich.

[1] L. Landau und R. Peierls, ZS. f. Phys. 69, 56, 1931.

This is correct!

Disappered in reprints, so we have difficulties

Baade and Zwicky – theoretical prediction

W. Baade (Mt. Wilson Observatory)
F. Zwicky (Caltech)

The meeting of American Physical Society
(Stanford, December 15-16, 1933)
Published in Physical Review
(January 15, 1934)

38. Supernovae and Cosmic Rays. W. BAADE, *Mt. Wilson Observatory*, AND F. ZWICKY, *California Institute of Technology*.—Supernovae flare up in every stellar system (nebula) once in several centuries. The lifetime of a super-

nova is about twenty days and its absolute brightness a maximum may be as high as $M_{vis}=-14^{M}$. The visibl radiation L_ν of a supernova is about 10^8 times the radiatio of our sun, that is, $L_\nu=3.78\times10^{41}$ ergs/sec. Calculation indicate that the total radiation, visible and invisible, i of the order $L_\tau=10^7L_\nu=3.78\times10^{48}$ ergs/sec. The super- nova therefore emits during its life a total energy $E_\tau\geqq10^5L_\tau=3.78\times10^{53}$ ergs. If supernovae initially are quite ordinary stars of mass $M<10^{34}$ g, E_τ/c^2 is of the same order as M itself. In the *supernova* process *mass in bulk is annihilated*. In addition the hypothesis suggests itself that *cosmic rays are produced by supernovae*. Assuming that in every nebula one supernova occurs every thousand years, the intensity of the cosmic rays to be observed on the earth should be of the order $\sigma=2\times10^{-3}$ erg/cm² sec. The observational values are about $\sigma=3\times10^{-3}$ erg/cm² sec. (Millikan, Regener). With all reserve we advance the view that supernovae represent the transitions from ordinary stars into *neutron stars*, which in their final stages consist of extremely closely packed neutrons.

$t_1 = 10^6$ years $+410$ seconds for 10^{11} volt electrons.
$t_2 =$ " $+47.6$ days " 10^9 " "
$t_3 =$ " $+44$ years " 10^{11} " protons.

These time lags $t_i - t$ would tend to smear out the change of intensity caused by the flare-up of individual super-novae. Dr. R. M. Langer in one of our seminars was the first to call attention to the straggling of simultaneously ejected particles.

5. *The super-nova process*

We have tentatively suggested that the super-nova process represents the transition of an ordinary star into a neutron star. If neutrons are produced on the surface of an ordinary star they will "rain" down towards the center if we assume that the light pressure on neutrons is practically zero. This view explains the speed of the star's transformation into a neutron star. We are fully aware that our suggestion carries with it grave implications regarding the ordinary views about the constitution of stars and therefore will require further careful studies.

W. BAADE
F. ZWICKY

Mt. Wilson Observatory and
California Institute of Technology, Pasadena.
May 28, 1934.

Phys. Rev. 46, 76, 1934 July 1

Good old classics

For years two main types of NSs have been discussed:
radio pulsars and accreting NSs in close binary systems

The pulsar in the Crab nebula

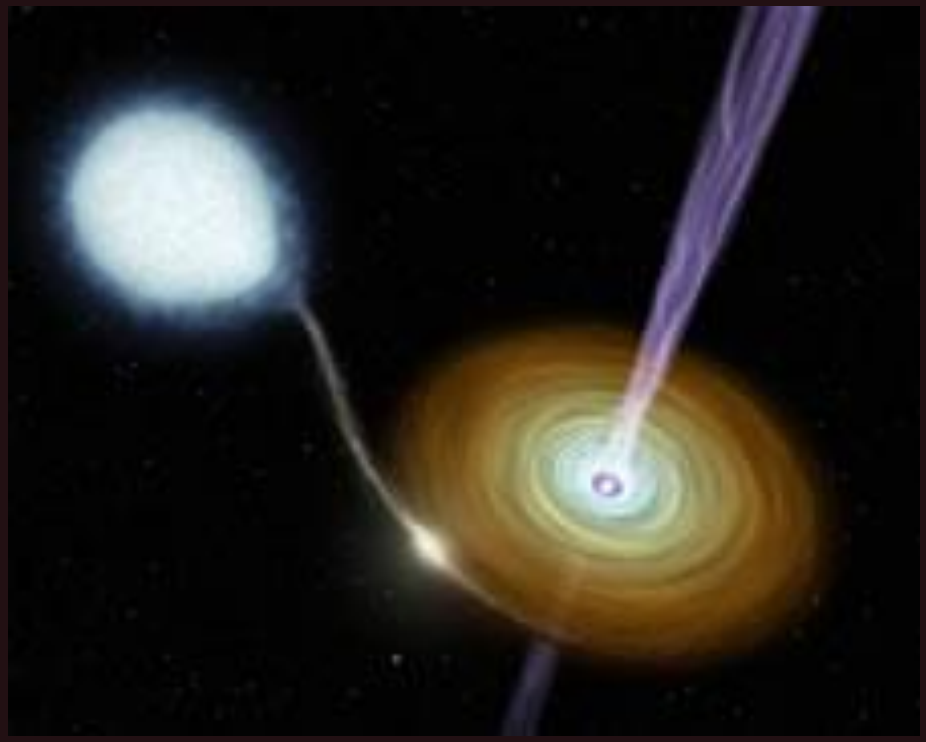

A binary system

What formed in SN 1987A?

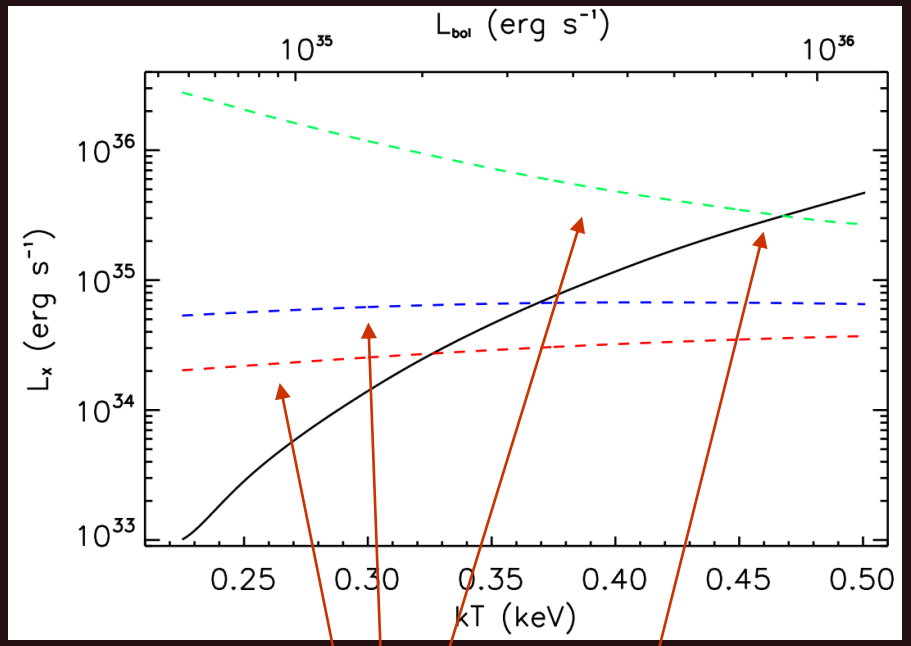

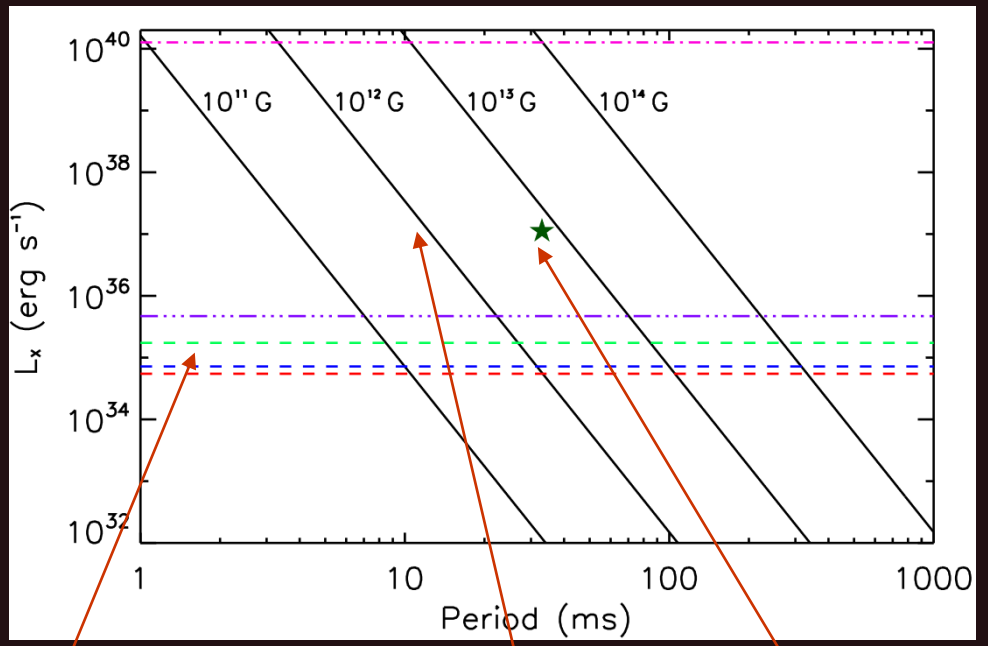

Limits for different N_H.

2-8 keV luminosity
for different temperatures

Dashed and
dot-dashed –
different limits
(as on the left)

Black solid:
2-8 keV luminosity
for different fields.

Crab

1803.04692

See also 1805.04526

More limits on SN1987A

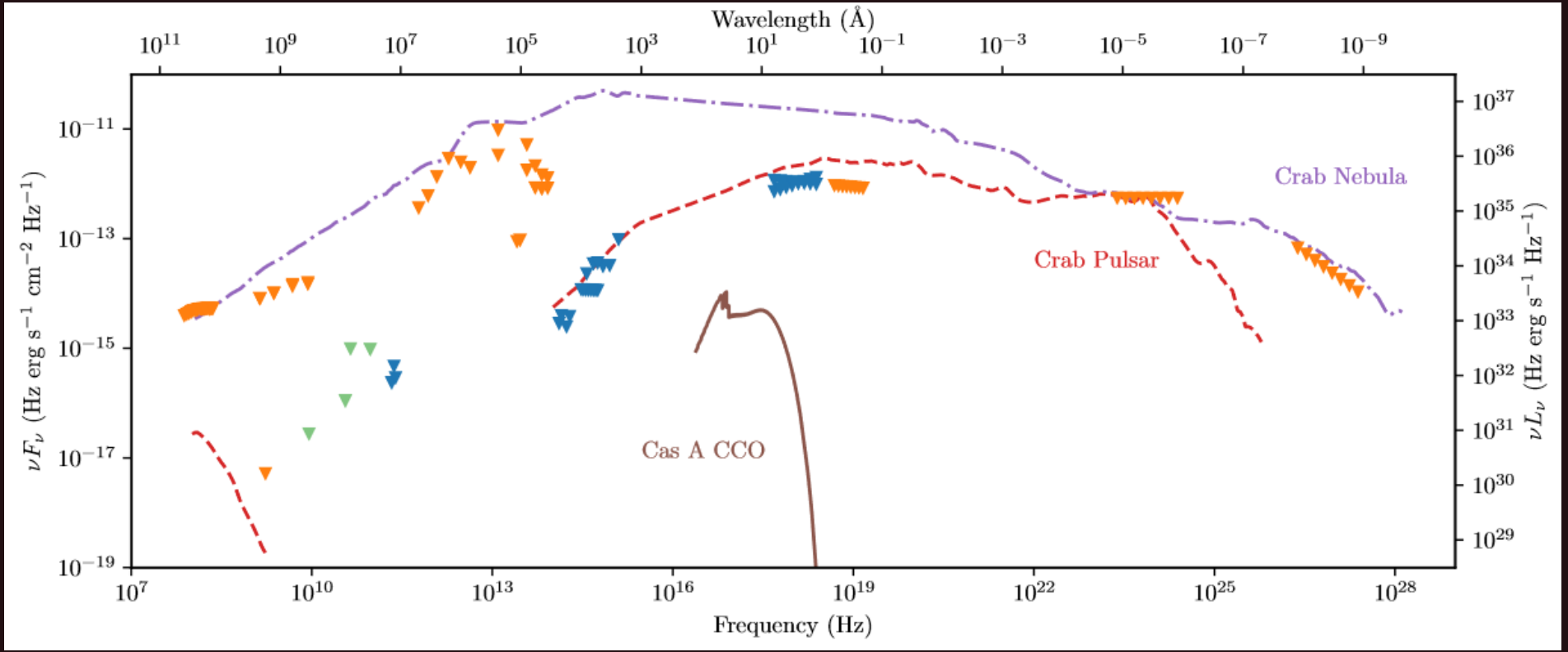

Still, it is possible that a NS is formed in SN 1987A.
But very energetic pulsars or/and magnetars are mostly excluded despite strong uncertainties in absorption.
About absorption see 1805.04528.

1805.04526

The old zoo of neutron stars

In 60s the first X-ray sources have been discovered.

They were neutron stars in close binary systems, BUT ...
.... they were «not recognized»....

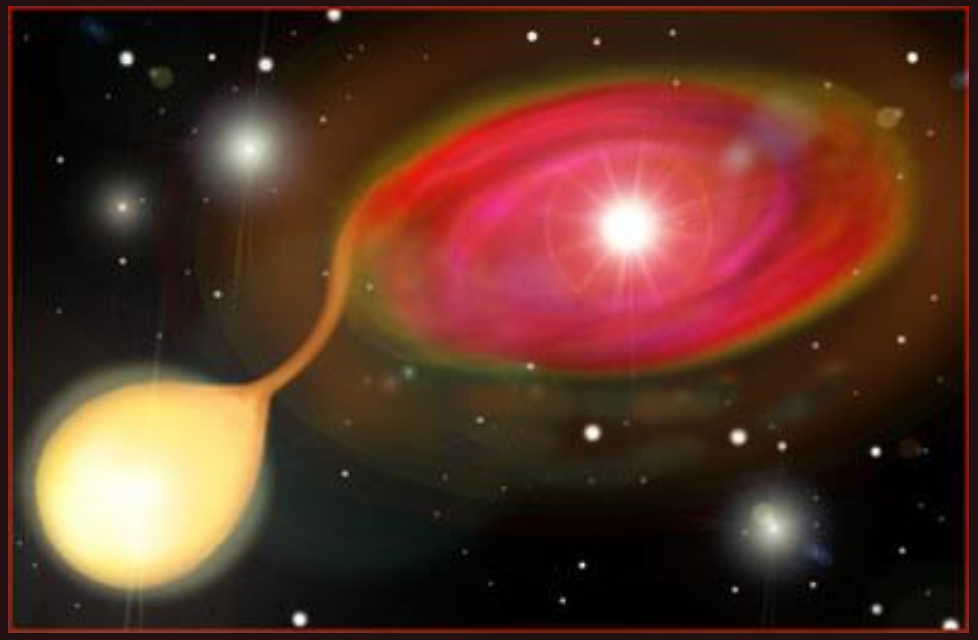

Now we know hundreds of X-ray binaries with neutron stars in the Milky Way and in other galaxies.

Rocket experiments. Sco X-1

Giacconi et al. 1962

In 2002 R. Giacconi was awarded with the Nobel prize.

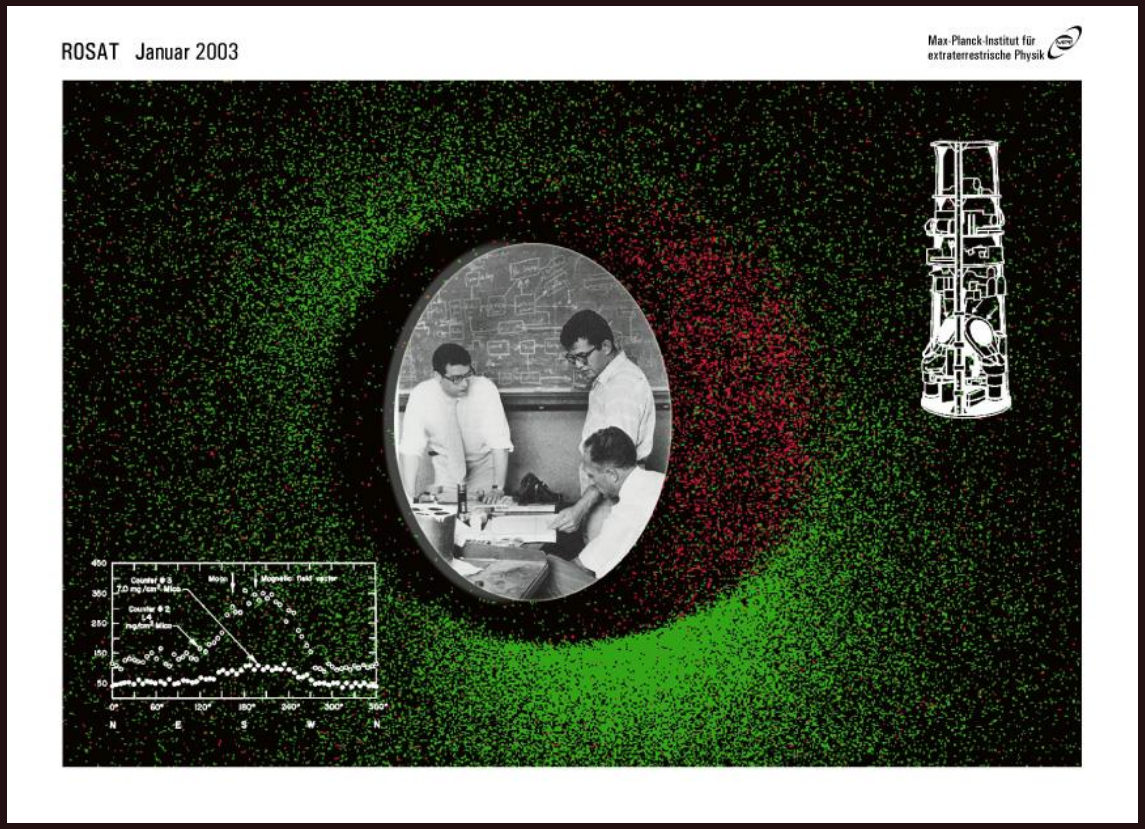

On the photo: Giacconi, Gursky, Hendel

UHURU

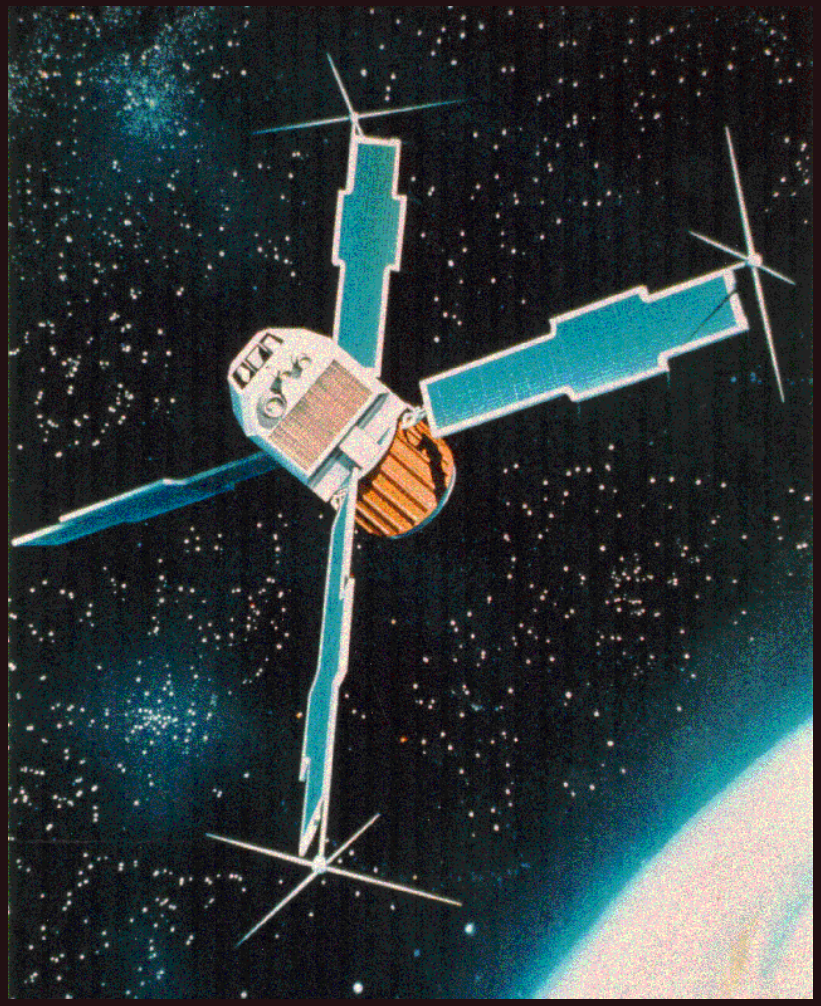

The satellite was launched on December 12, 1970.
The program was ended in March 1973.
The other name SAS-1

2-20 keV

The first full sky survey.
339 sources.

Accretion in close binaries

Accretion is the most powerful source of energy realized in Nature, which can give a huge energy output.

When matter fall down onto the surface of a neutron star up to 10% of mc^2 can be released.

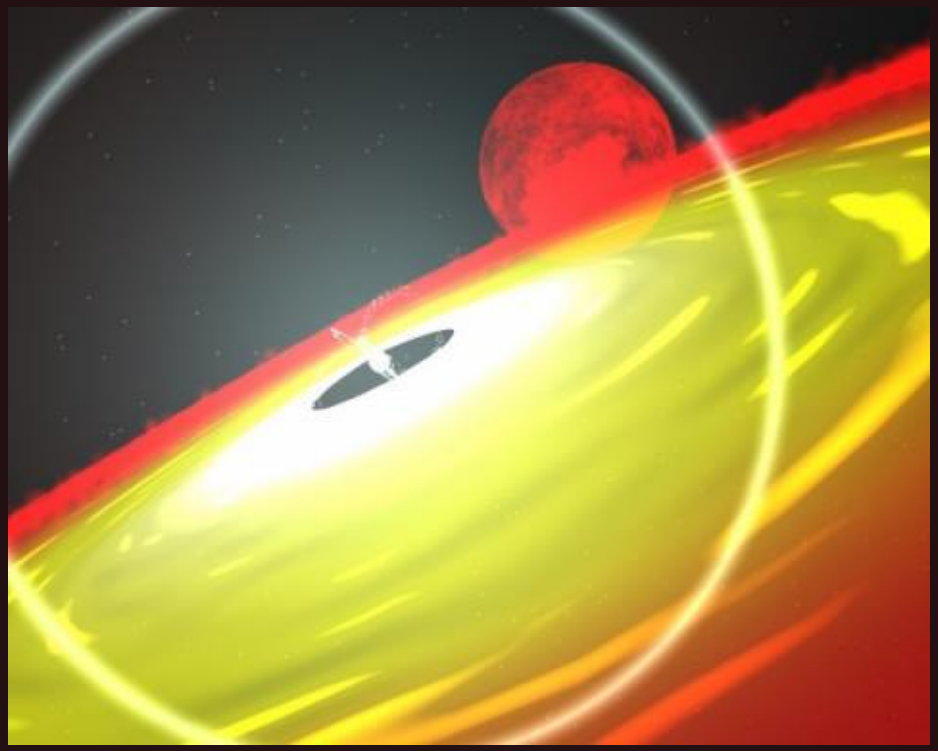

Accretion disc

The theory of accretion discs was developed in 1972-73 by N.I. Shakura and R.A. Sunyaev.

Accretion is important not only in close binaries, but also in active galactic nuclei and many other types of astrophysical sources.

Close binary systems

About ½ of massive stars
Are members of close binary systems.

Now we know many dozens of close binary systems with neutron stars.

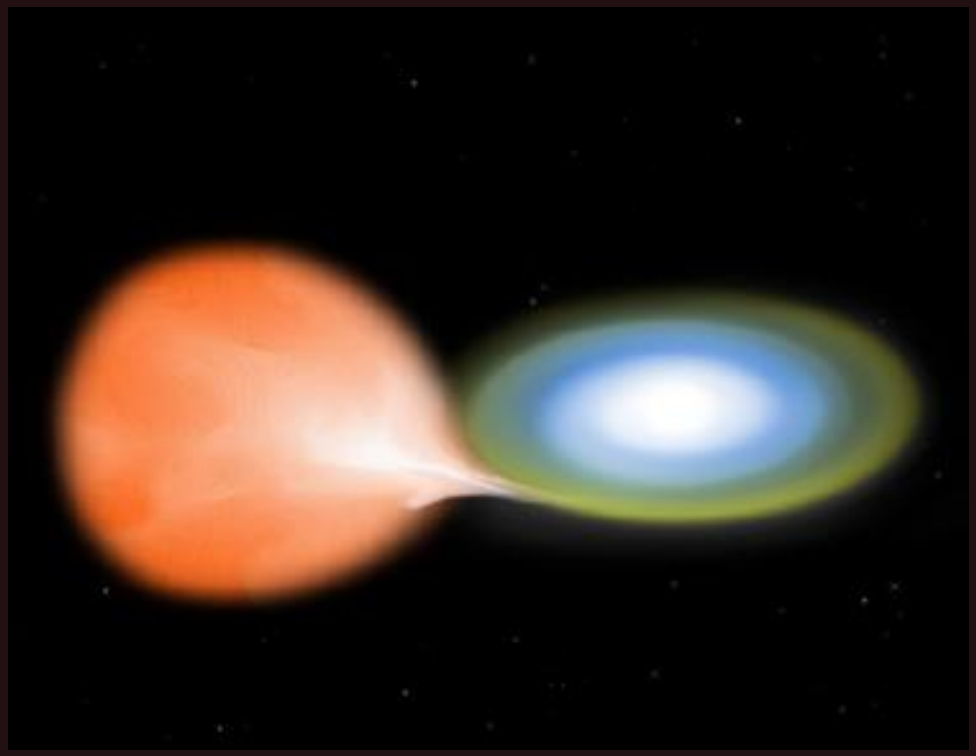

$$L = \dot{M} \eta c^2$$

The accretion rate can be up to 10^{20} g/s;
Accretion efficiency – up to 10%;
Luminosity –thousands of hundreds of the solar.

Discovery !!!!

1967: Jocelyn Bell. Radio pulsars.

Seredipitous discovery.

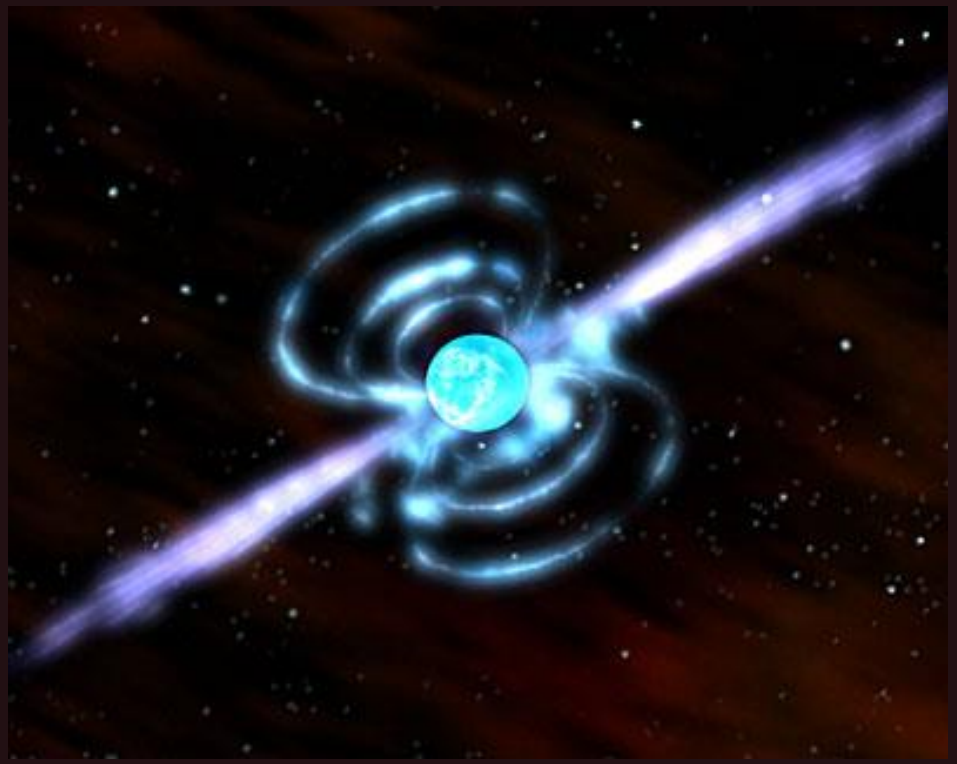

The pulsar in the Crab nebula

Pulsar spin-down: P-Pdot diagram

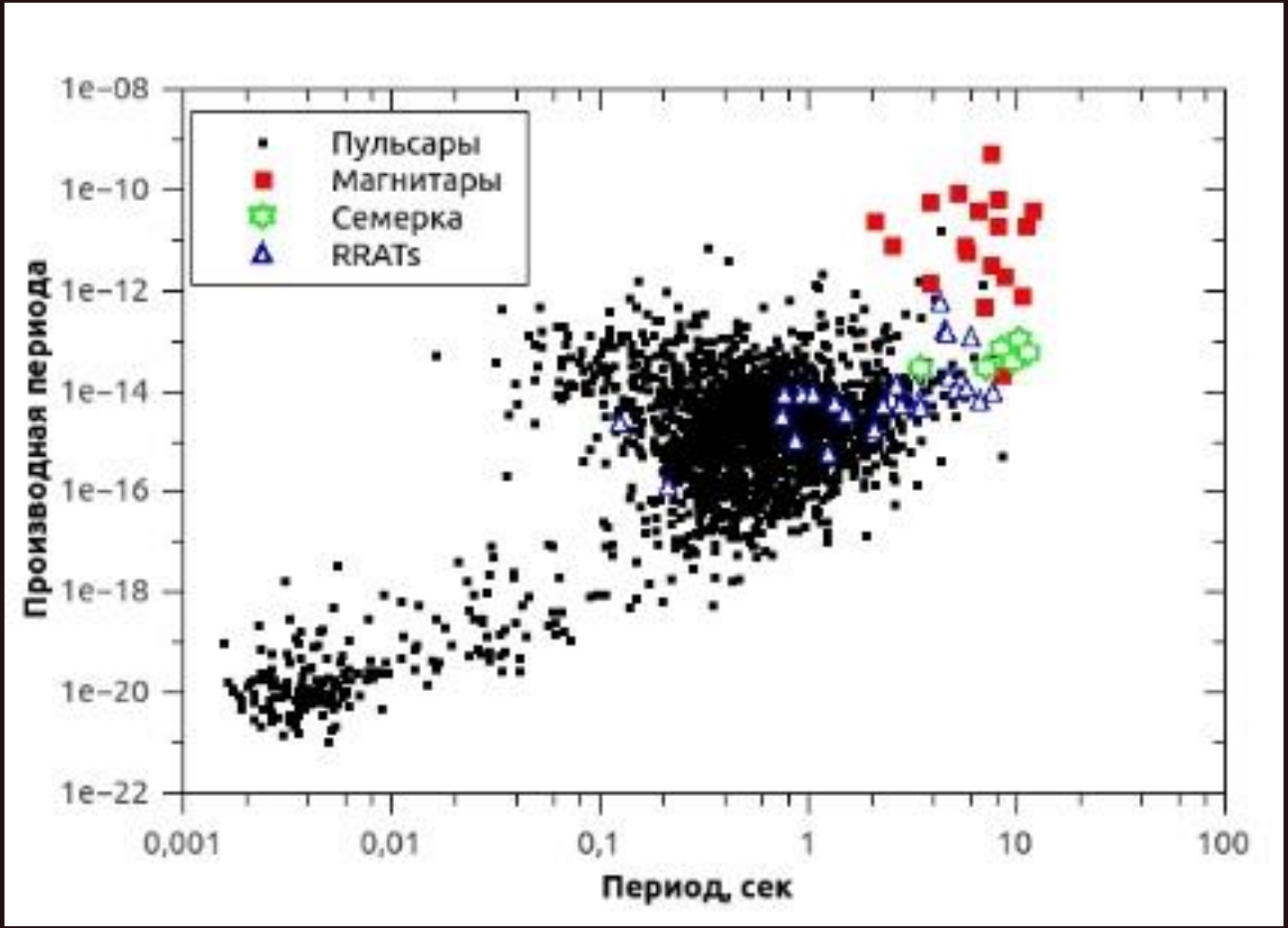

$$L_m = \frac{2}{3}\frac{\mu^2\omega^4}{c^3}\sin^2\beta = \kappa_t\frac{\mu^2}{R_l^3}\omega\,,$$

Slowly rotating NSs – in binaries

AX J1910.7+0917

P>10 hours! (36200+/-100 sec)

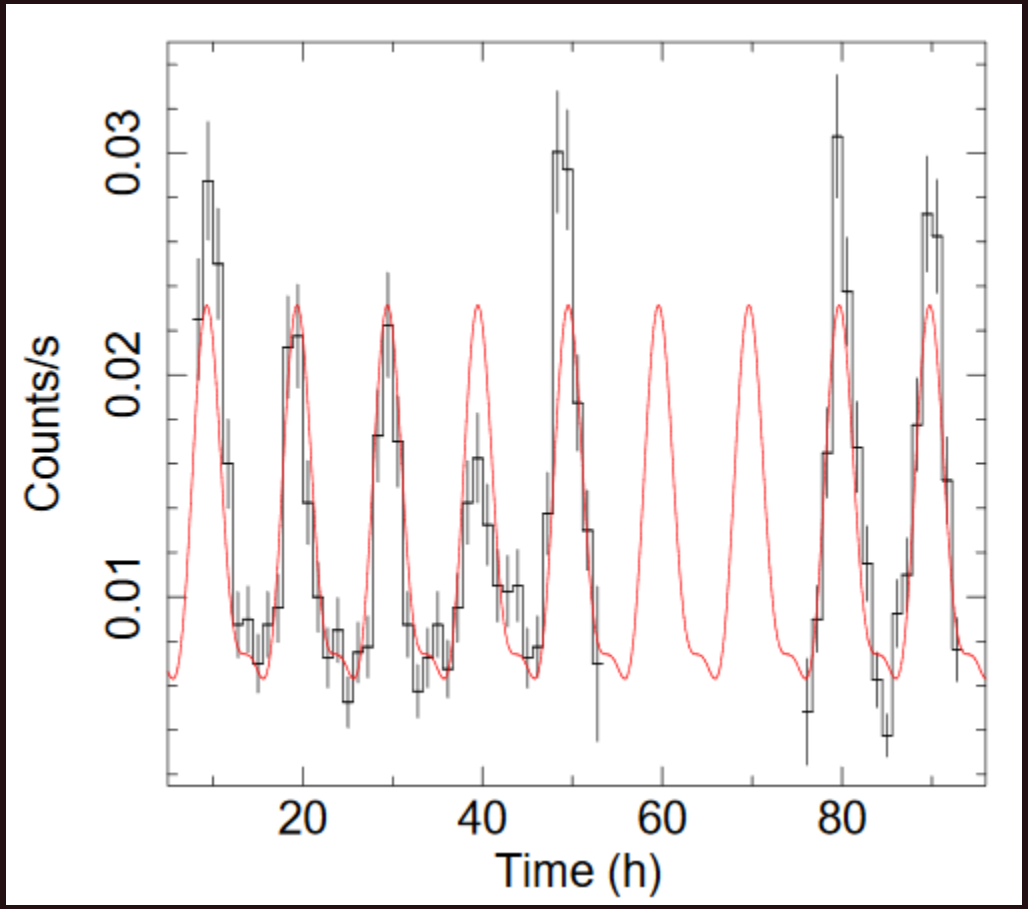

1705.01791

The old Zoo: young pulsars & old accretors

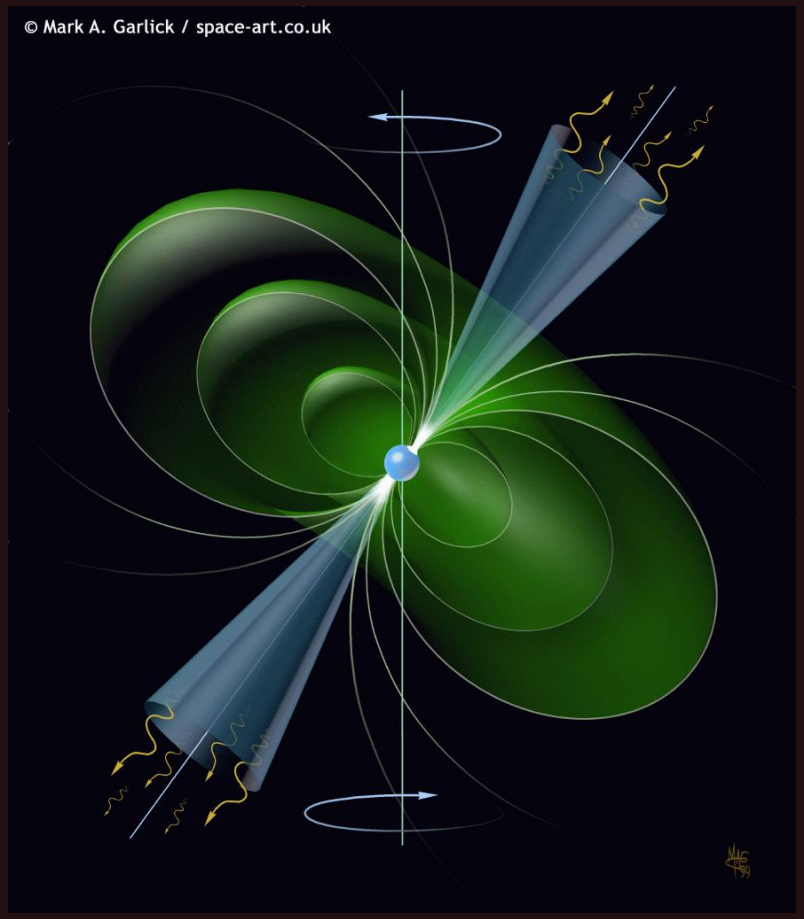

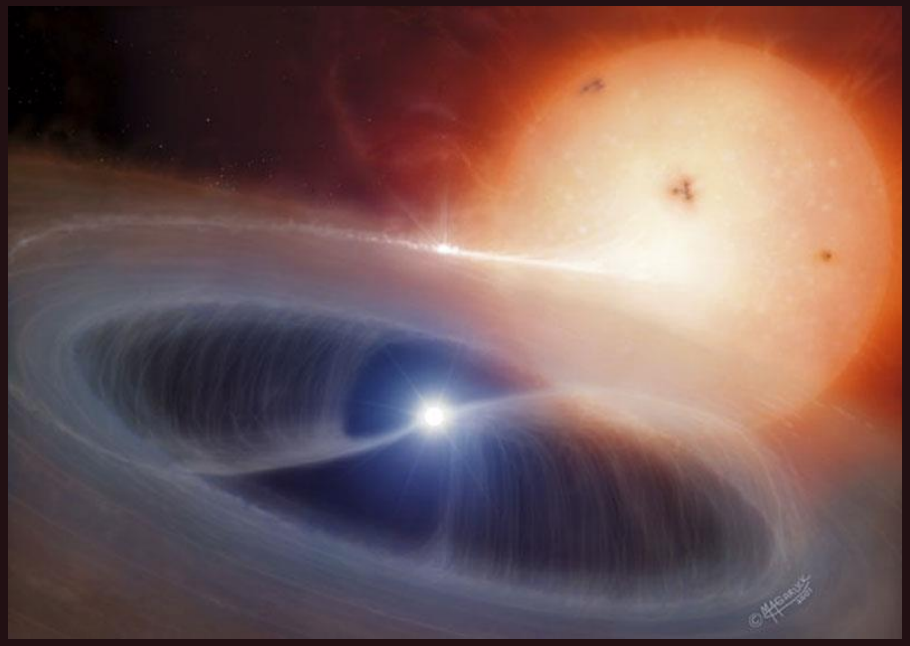

The new zoo of young neutron stars

During last ~25 years
it became clear that neutron stars
can be born very different.
In particular, absolutely
non-similar to the Crab pulsar.

- High-B PSRs
- Compact central X-ray sources in supernova remnants.
- Anomalous X-ray pulsars
- Soft gamma repeaters
- The Magnificent Seven
- Transient radio sources (RRATs)

Old and new zoos: Harding arXiv:1302.0869

See a more recent review in 1712.06040

Compact central X-ray sources in supernova remnants

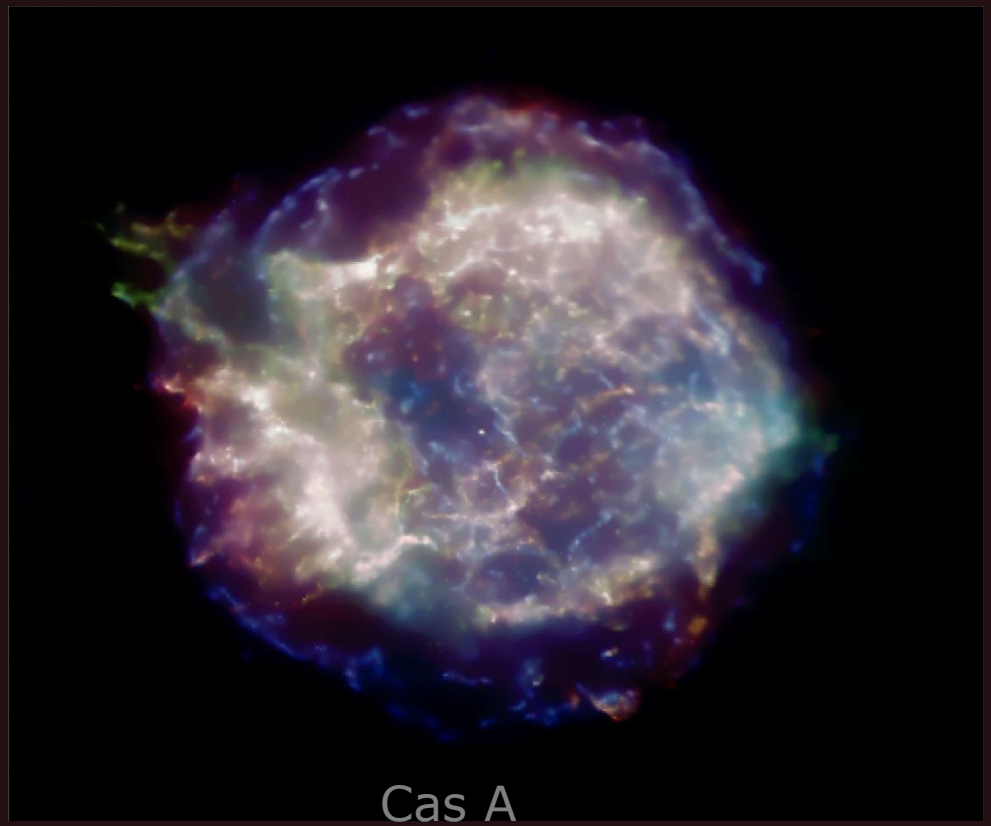

Cas A

Rapid cooling
(Heinke et al. 1007.4719)

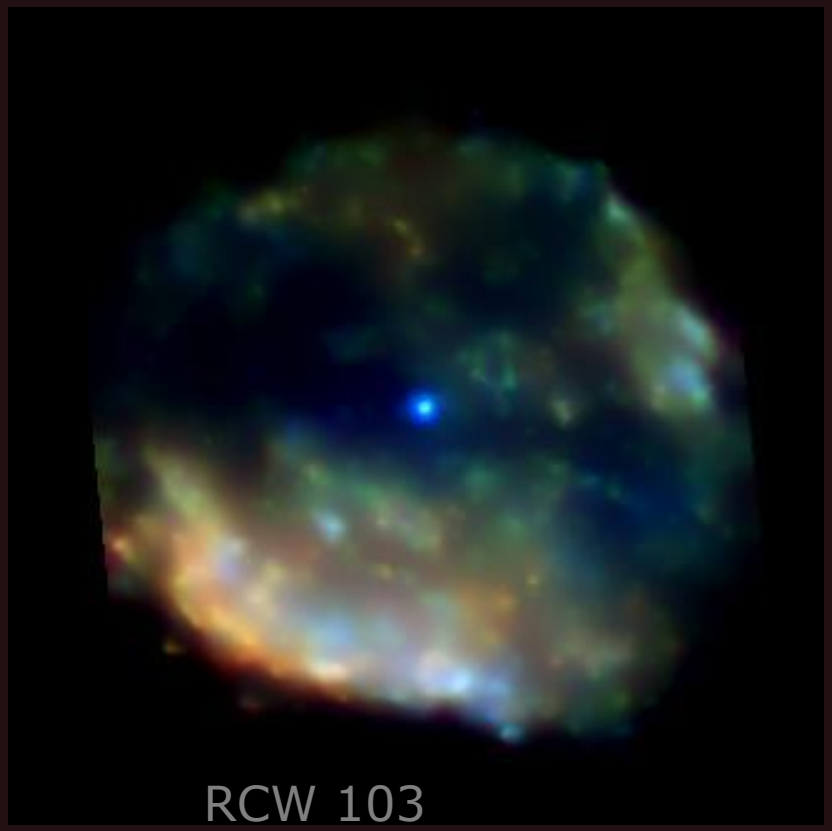

RCW 103

6.7 hour period
(de Luca et al. 2006)

CCOs in SNRs

		Age	Distance
J232327.9+584843	Cas A	0.32	3.3–3.7
J085201.4−461753	G266.1−1.2	1–3	1–2
J082157.5−430017	Pup A	1–3	1.6–3.3
J121000.8−522628	G296.5+10.0	3–20	1.3–3.9
J185238.6+004020	Kes 79	~9	~10
J171328.4−394955	G347.3−0.5	~10	~6

[Pavlov, Sanwal, Teter: astro-ph/0311526,
de Luca: arxiv:0712.2209]

For three sources there are strong indications for large (>~100 msec) initial spin periods and low magnetic fields:

1E 1207.4-5209 in PKS 1209-51/52

PSR J1852+0040 in Kesteven 79

PSR J0821-4300 in Puppis A

[see Halpern et al. arxiv:0705.0978 and 1301.2717]

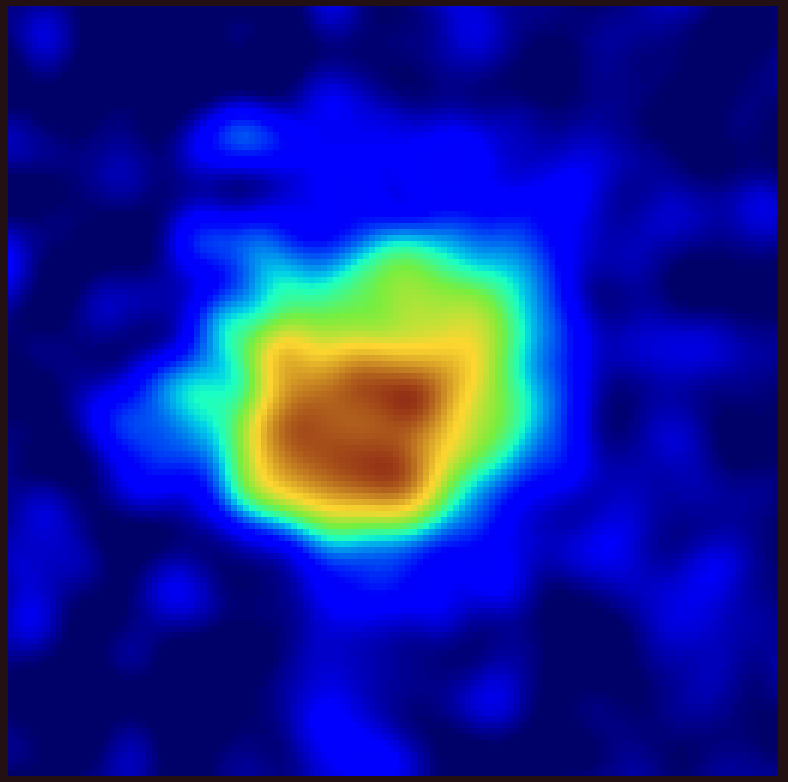

CCOs

High proper motion of CCO in Pup A.
Velocity 672 +/- 115 km/s

1204.3510

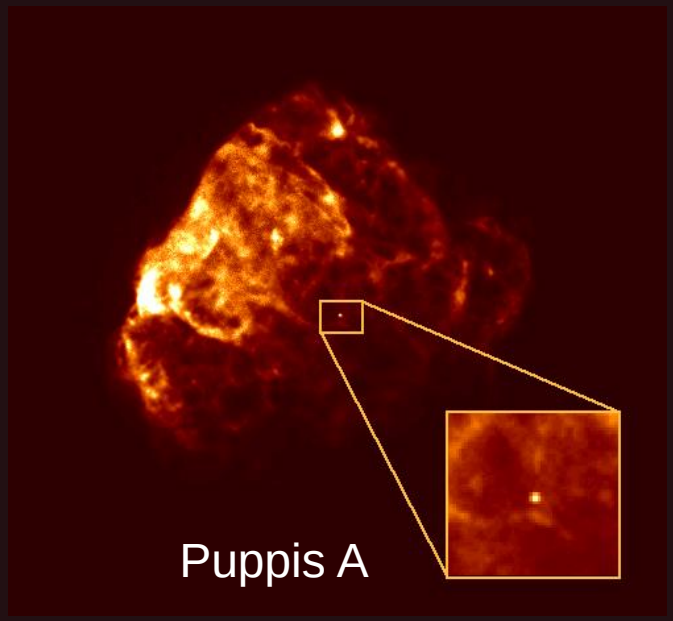

CCO	SNR	Age (kyr)	d (kpc)	P (s)	f_p[a] (%)	B_s (10^{11} G)	$L_{x,\mathrm{bol}}$ (erg s^{-1})	References
RX J0822.0−4300	Puppis A	3.7	2.2	0.112	11	< 9.8	6.5×10^{33}	1,2
CXOU J085201.4−461753	G266.1−1.2	1	1	...	< 7	...	2.5×10^{32}	3,4,5,6,7
1E 1207.4−5209	PKS 1209−51/52	7	2.2	0.424	9	< 3.3	2.5×10^{33}	8,9,10,11,12
CXOU J160103.1−513353	G330.2+1.0	$\gtrsim 3$	5	...	< 40	...	1.5×10^{33}	13,14
1WGA J1713.4−3949	G347.3−0.5	1.6	1.3	...	< 7	...	$\sim 1 \times 10^{33}$	7,15,16
CXOU J185238.6+004020	Kes 79	7	7	0.105	64	0.31	5.3×10^{33}	17,18,19,20
CXOU J232327.9+584842	Cas A	0.33	3.4	...	< 12	...	4.7×10^{33}	20,21,22,23,24
XMMU J172054.5−372652	G350.1−0.3	0.9	4.5	...	...	...	3.4×10^{33}	25
XMMU J173203.3−344518	G353.6−0.7	~ 27	3.2	...	...	...	1.0×10^{34}	26,27,28
CXOU J181852.0−150213	G15.9+0.2	$1 - 3$	(8.5)	...	...	...	$\sim 1 \times 10^{33}$	29

0911.0093

The first CCO in SMC 1E 0102.2-7219

The first CCO identified outside the Galaxy.
L~10^{33} erg/s.

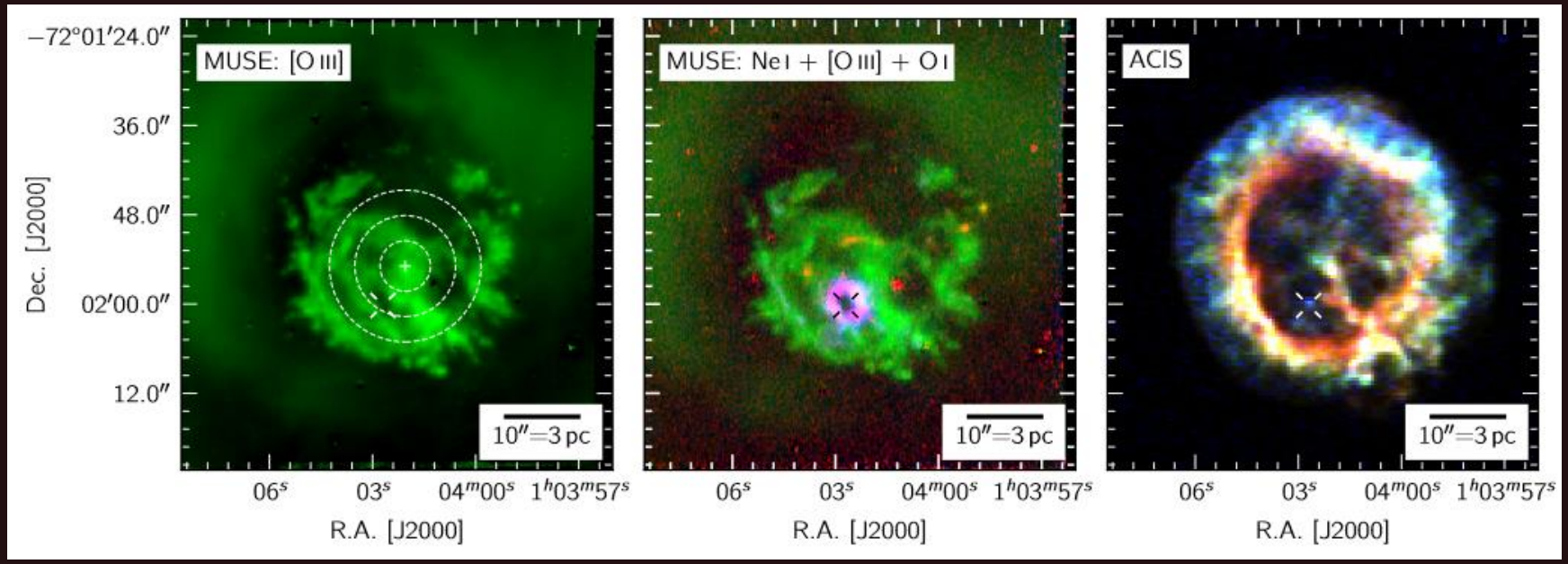

1803.01006

Anti-magnetars

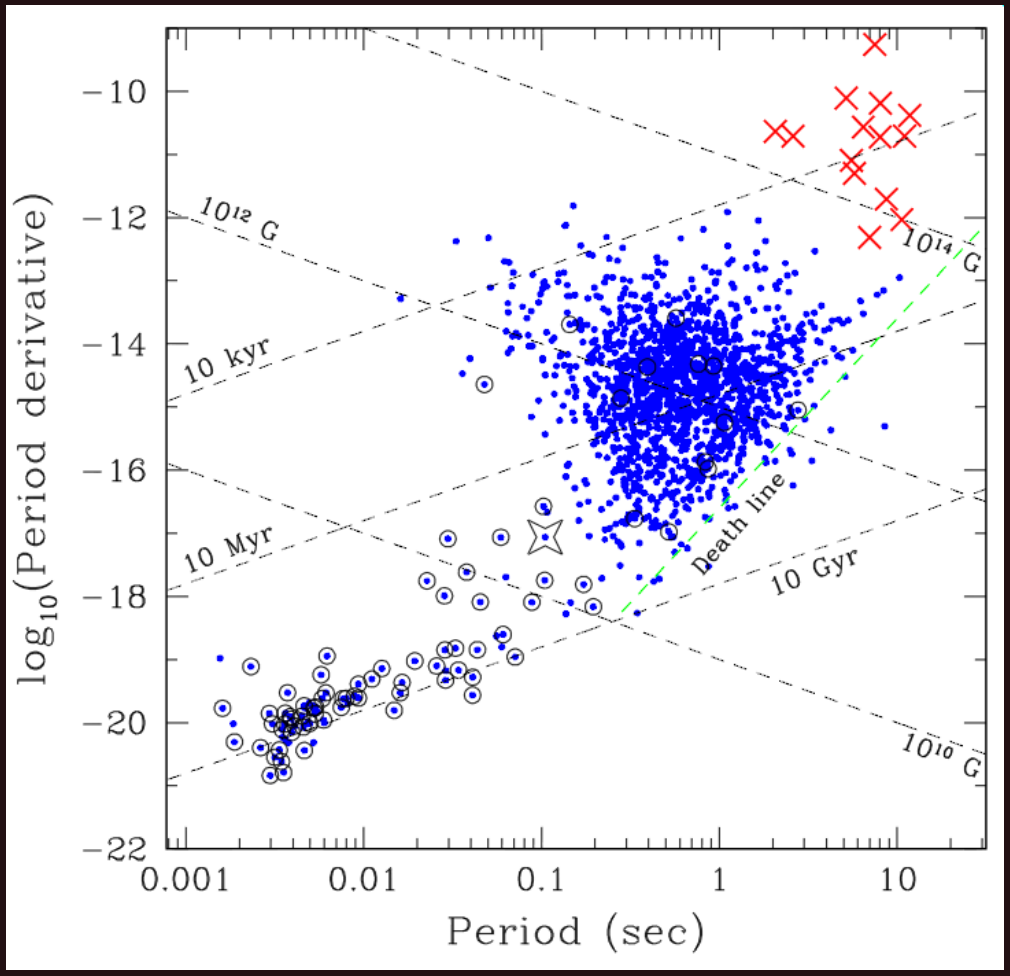

Star marks the CCO from 0911.0093

New results 1301.2717
Spins and derivative are measured for
PSR J0821-4300 and
PSR J1210-5226

0911.0093

“Hidden” magnetars

Kes 79. PSR J1852+0040. P~0.1 s

Shabaltas & Lai (2012) show that large pulse fraction of the NS in Kes 79 can be explained if its magnetic field in the crust is very strong: few $\times 10^{14}$ G.

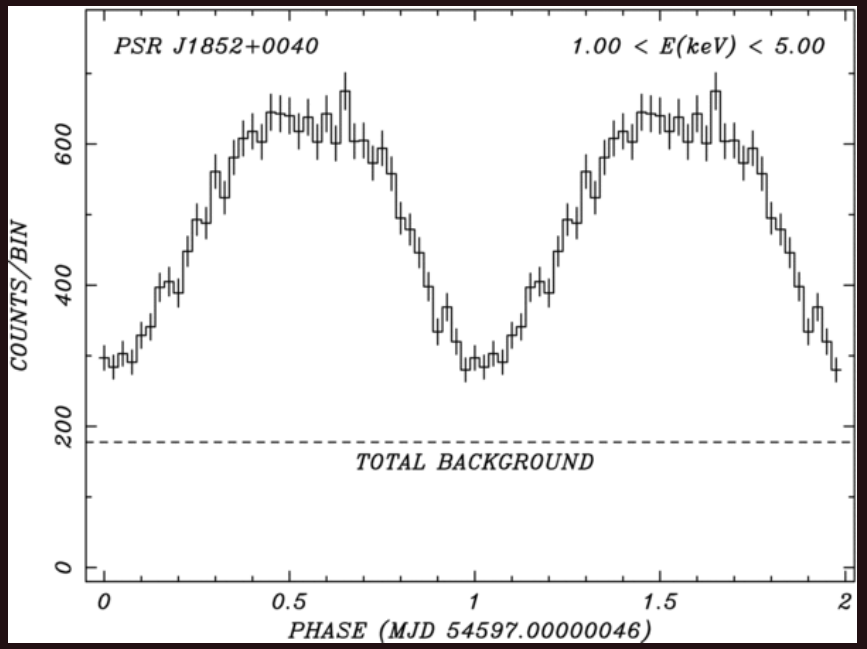

Halpern, Gotthelf 2010

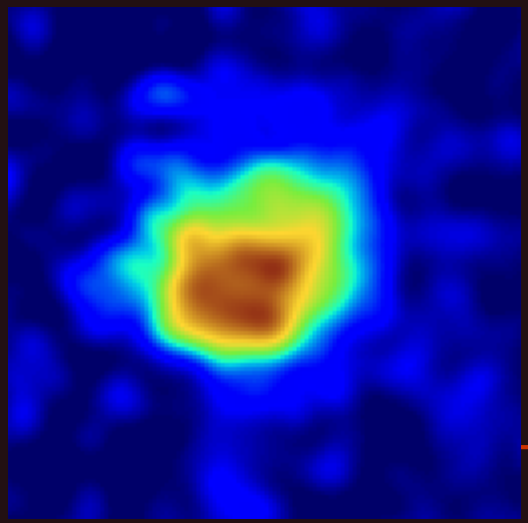

Kes 79

- If submergence of the field happens rapidly, so the present day period represents the initial one
- Then, the field of PSR 1852 was not enhanced via a dynamo mechanism
- Detection of millisecond “hidden” magnetars will be a strong argument in favour of dynamo.

arXiv: 1307.3127

Magnetars

- $dE/dt > dE_{rot}/dt$
- By definition: The energy of the magnetic field is released

Magnetic fields 10^{14}–10^{15} G

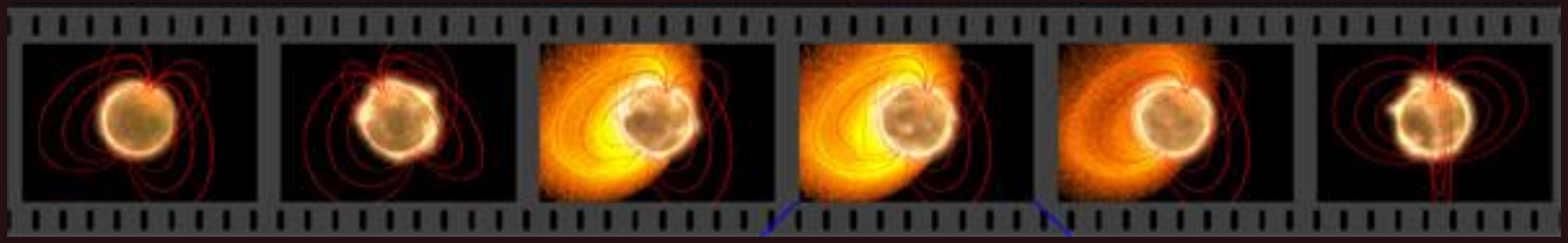

Magnetic field estimates

- Spin down
- Long spin periods

- Energy to support bursts
- Field to confine a fireball (tails)
- Duration of spikes (alfven waves)

- Direct measurements of magnetic field (cyclotron lines)

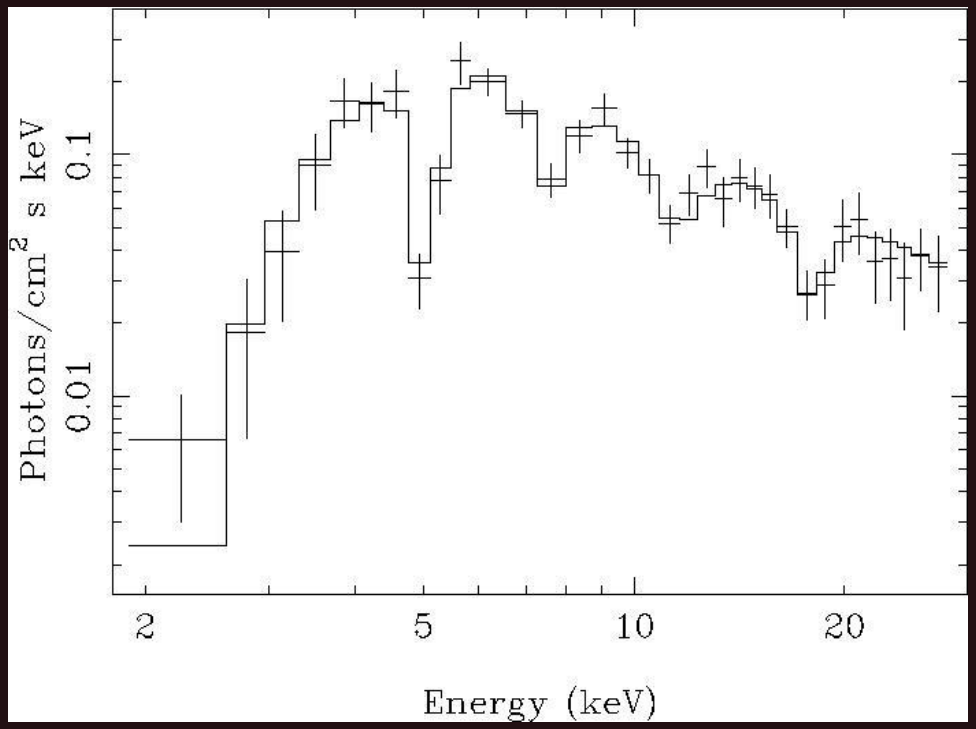

Ibrahim et al. 2002

Some of known magnetars

SGRs

- 0526-66
- 1627-41
- 1806-20
- 1900+14
- 0501+4516
- 0418+5729
- 1833-0832
- 1822-1606
- 1834-0846
- 1801-23 (?)
- 2013+34 (?)

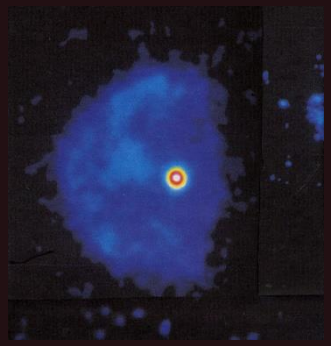

(CTB 109)

AXPs

- CXO 010043.1-72
- 4U 0142+61
- 1E 1048.1-5937
- CXO J1647-45
- 1 RXS J170849-40
- XTE J1810-197
- 1E 1841-045
- AX J1845-0258
- 1E 2259+586
- 1E 1547.0-5408
- PSR J1622-4950
- CXO J171405-381031

Catalogue: http://www.physics.mcgill.ca/~pulsar/magnetar/main.html, 1309.4167

Extragalactic SGRs

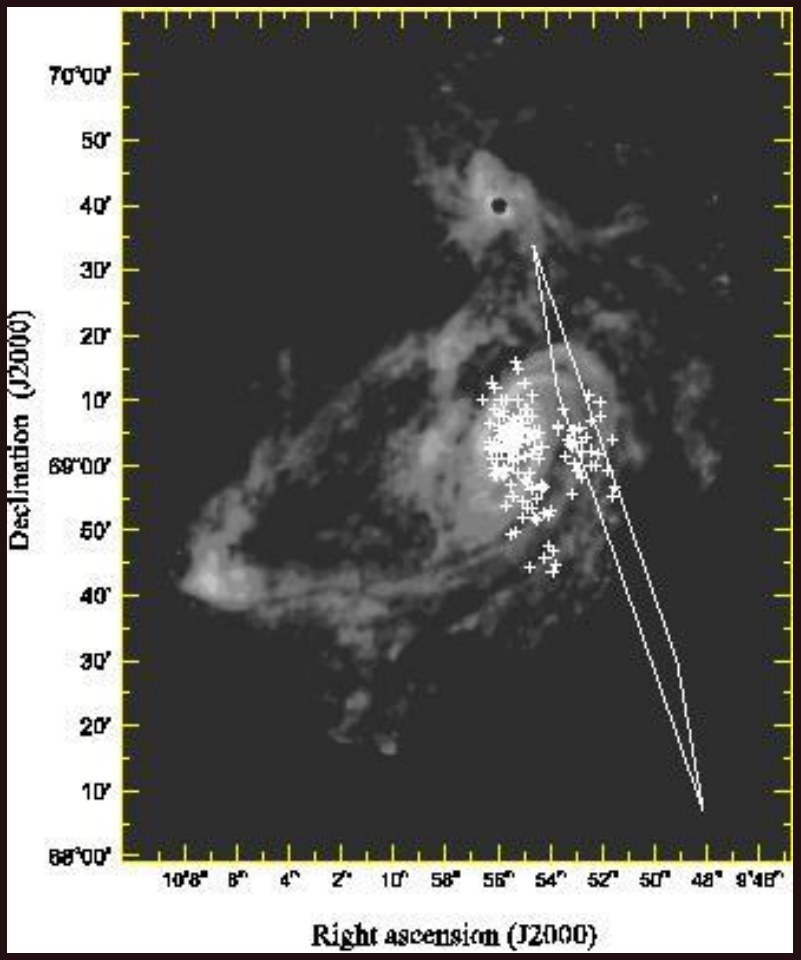

It was suggested long ago (Mazets et al. 1982) that present-day detectors could already detect giant flares from extragalactic magnetars.

However, all searches in, for example, BATSE database did not provide god candidates (Lazzati et al. 2006, Popov & Stern 2006, etc.).

Finally, recently several good candidates have been proposed by different groups (Mazets et al., Frederiks et al., Golenetskii et al., Ofek et al, Crider ...., see arxiv:0712.1502 and references therein, for example).

Burst from M31

[D. Frederiks et al. astro-ph/0609544]

Transient radio emission from AXP

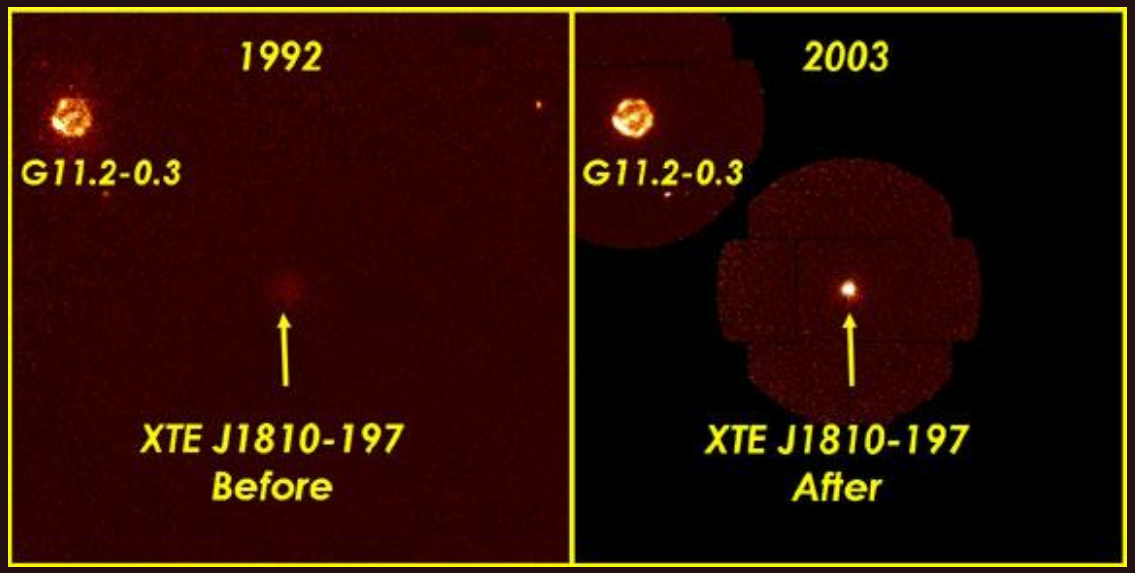

ROSAT and XMM images an X-ray outburst happened in 2003.

AXP has spin period 5.54 s

Radio emission was detected from XTE J1810-197 during its active state.
Clear pulsations have been detected.
Large radio luminosity.
Strong polarization.
Precise Pdot measurement.
Important to constrain models, for better distance and coordinates determinations, etc.

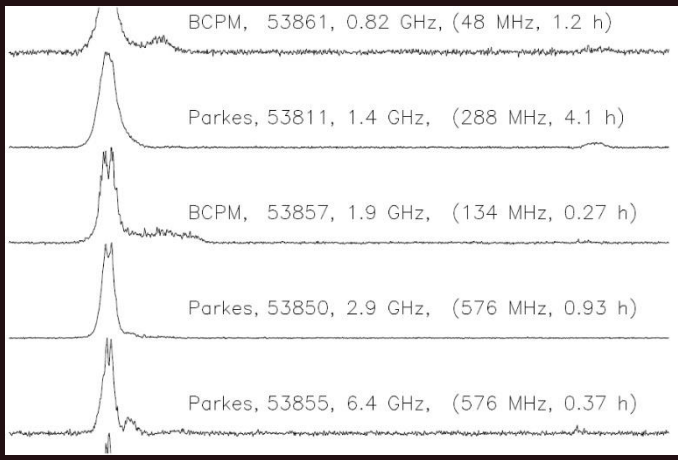

(Camilo et al. astro-ph/0605429)

Another AXP detected in radio

1E 1547.0-5408
P= 2 sec
SNR G327.24-0.13

Pdot changed significantly on the scale of just ~few months
Rotation and magnetic axis seem to be aligned

Also this AXP demonstrated weak SGR-like bursts (Rea et al. 2008, GCN 8313)

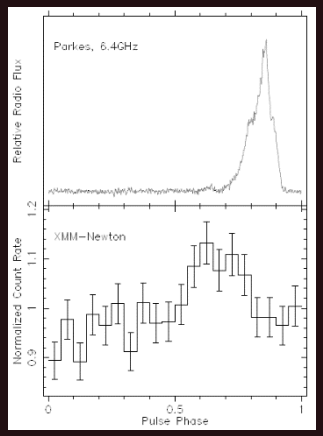

Radio

[simultaneous]

X-rays

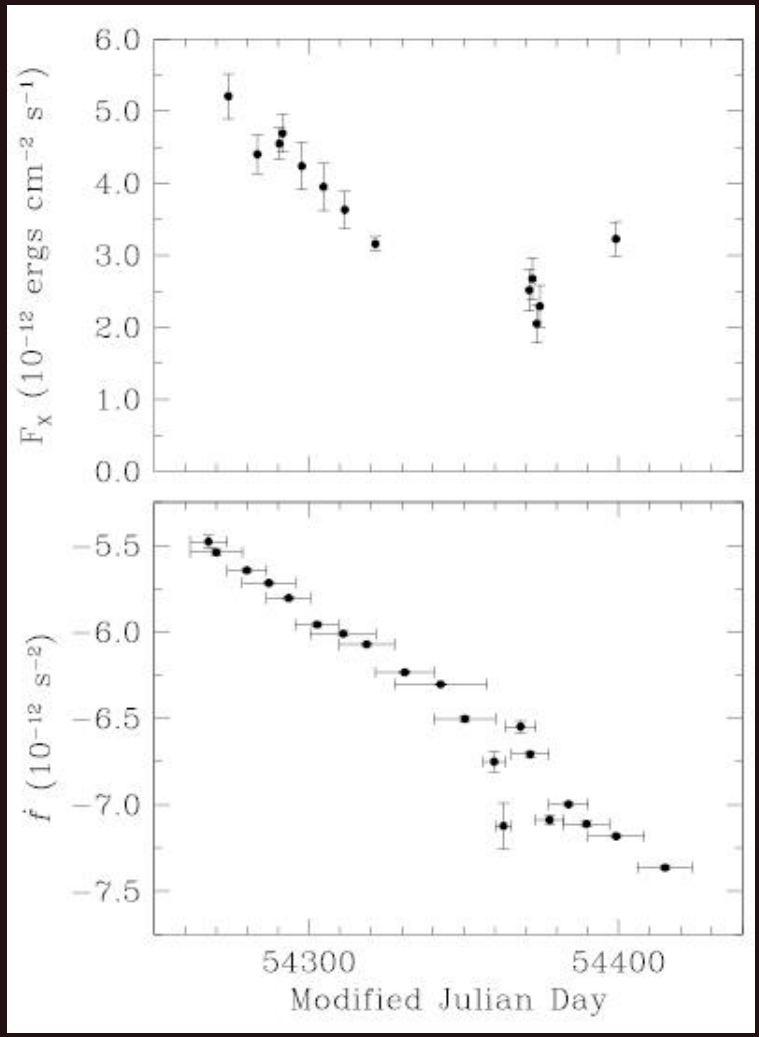

0802.0494 (see also arxiv:0711.3780)

Transient radiopulsar

PSR J1846-0258
P=0.326 sec
B=5 10^{13} G

However, no radio emission detected. Due to beaming?

Among all rotation powered PSRs it has the largest Edot.
Smallest spindown age (884 yrs).

The pulsar increased
its luminosity in X-rays.
Increase of pulsed X-ray flux.
Magnetar-like X-ray bursts (RXTE).
Timing noise.

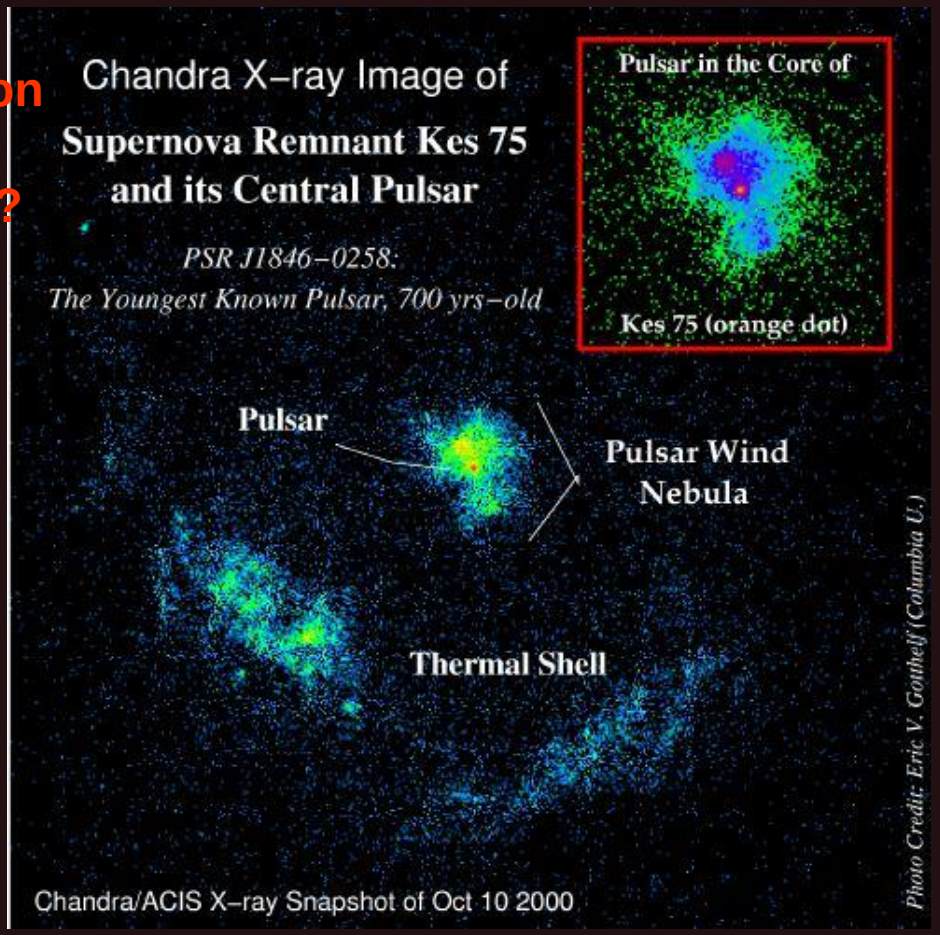

See additional info about this pulsar at the web-site
http://hera.ph1.uni-koeln.de/~heintzma/SNR/SNR1_IV.htm

0802.1242, 0802.1704

Bursts from the transient PSR

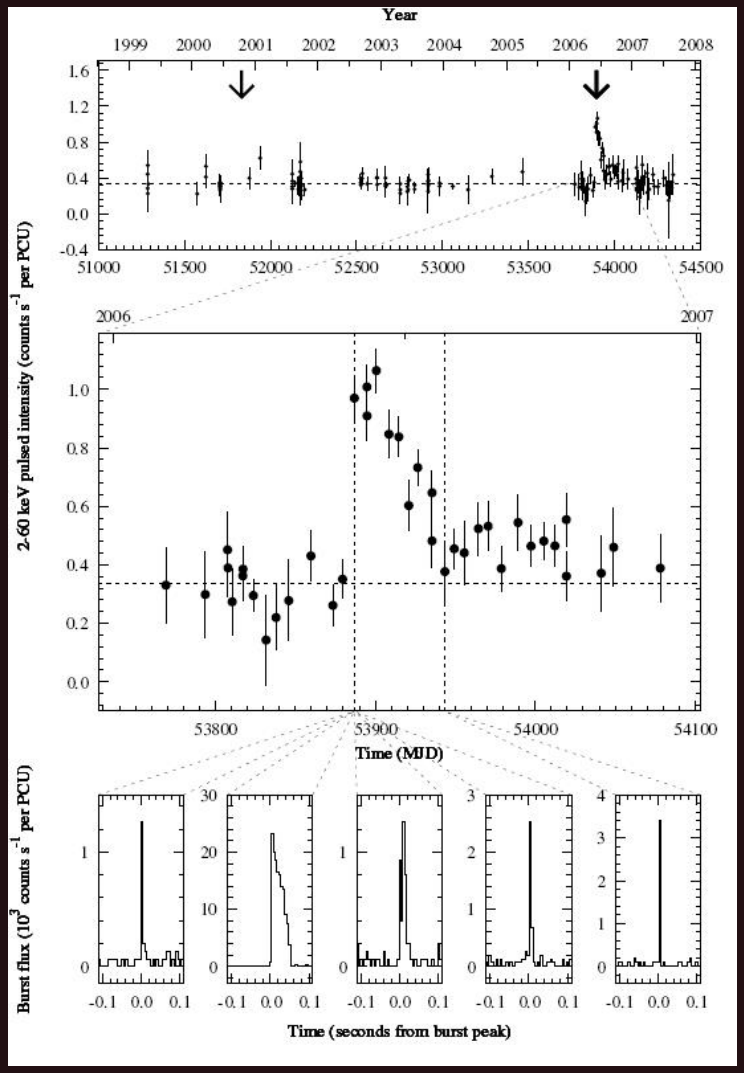

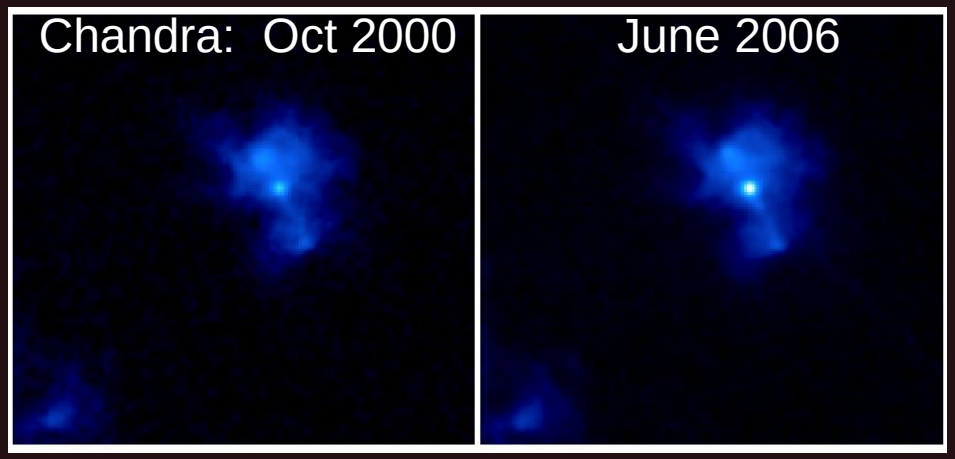

Table 1	PSR J1846−0258 Burst Temporal and Spectral Properties				
	Burst 1	Burst 2	Burst 3	Burst 4	Burst 5
Temporal properties					
Burst day (MJD)	53886	53886	53886	53886	53943
Burst start time (fraction of day)	0.92113966(5)	0.93247134(1)	0.93908845(2)	0.94248467(5)	0.45543551(1)
Rise time, t_r (ms)	$4.2^{+3.5}_{-2.0}$	$1.1^{+0.9}_{-0.5}$	$1.90^{+1.7}_{-0.9}$	$4.1^{+3.1}_{-1.9}$	$0.9^{+2.2}_{-0.7}$
T_{90} (ms)	$71.8^{+38.0}_{-5.5}$	$42.9^{+0.3}_{-0.2}$	$137.0^{+11.4}_{-36.2}$	$33.4^{+29.1}_{-23.1}$	$65.3^{+0.7}_{-0.5}$
Phase (cycles)	-0.49(1)	-0.04(1)	-0.20(1)	-0.05(1)	-0.08(1)
Fluences and fluxes					
T_{90} Fluence (counts/PCU)	8.9±0.7	712.8±2.5	18.3±0.7	18.4±0.7	18.4±1.1
T_{90} Fluence (10^{-10} erg/cm^2)	4.1±2.4	289.9±13.1	6.6±2.5	5.8±1.7	5.3±2.0
Flux for 64 ms (10^{-10} erg/s/cm^2)	57±36	4533±227	99±41	97±31	79±32
Flux for t_r (10^{-10} erg/s/cm^2)	678±427	5783±885	810±385	828±284	2698±1193
Spectral properties					
Power-law index	0.89±0.58	1.05±.04	1.14±0.34	1.36±0.25	1.41±0.31
χ^2/DoF (DoF)	0.42 (1)	1.16 (55)	0.97 (3)	0.35 (2)	1.18 (2)

Gavriil et al. 0802.1704

Weak dipole field magnetar

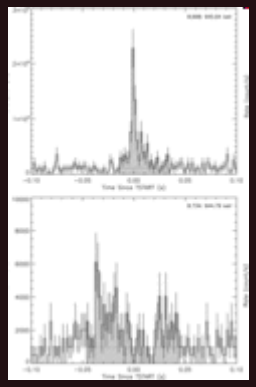

Spin period of a neutron star grows.
The rate of deceleration is related to the dipole magnetic field.
Measuring the spin-down rate we measure the field.

The source is a soft gamma-ray repeater: SGR 0418+5729
P=9.1 s

The straight line in the plot corresponds to a constant spin periods: i.e. no spin-down

B<7.5 10^{12} G (arXiv:1010.2781)

Old magnetar ? (1107.5488)

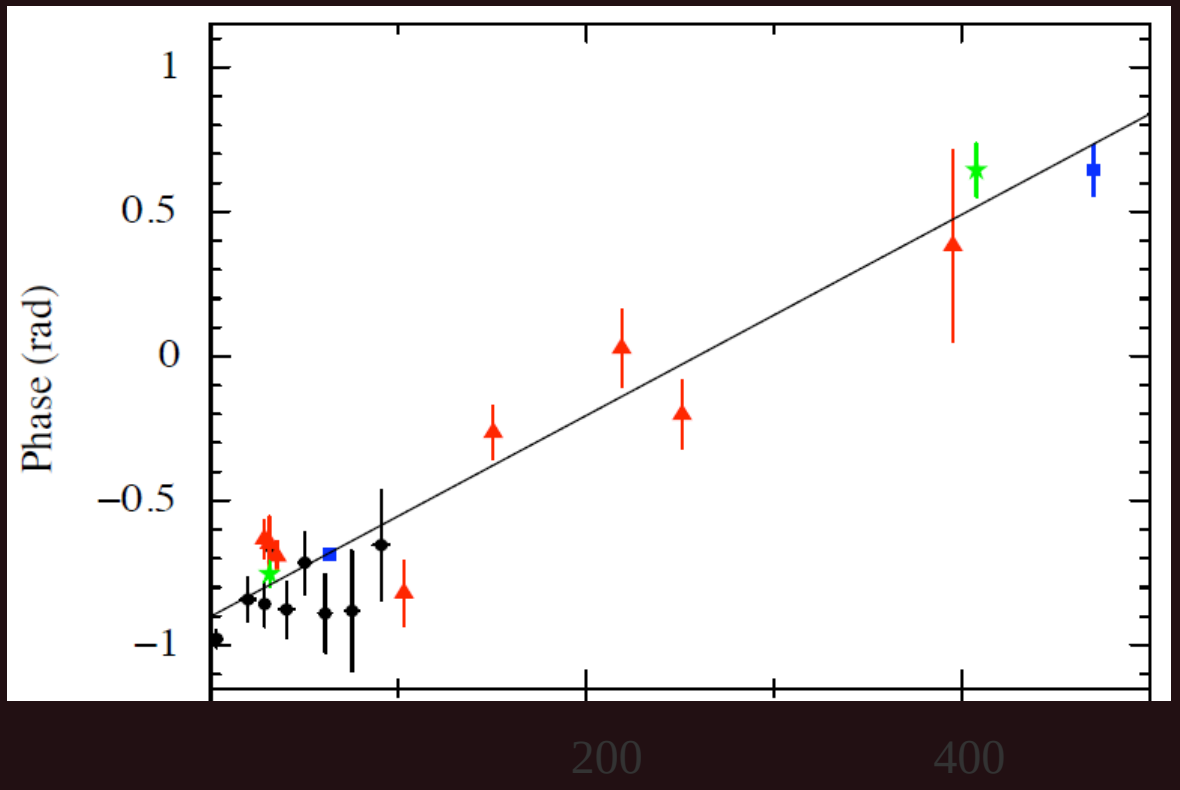

Spectral data suggests high field on the surface: 1103.3024

Another low field magnetar

Swift J1822.3-1606 (SGR 1822-1606)

P=8.44 s

B=3-5 10^{13} G

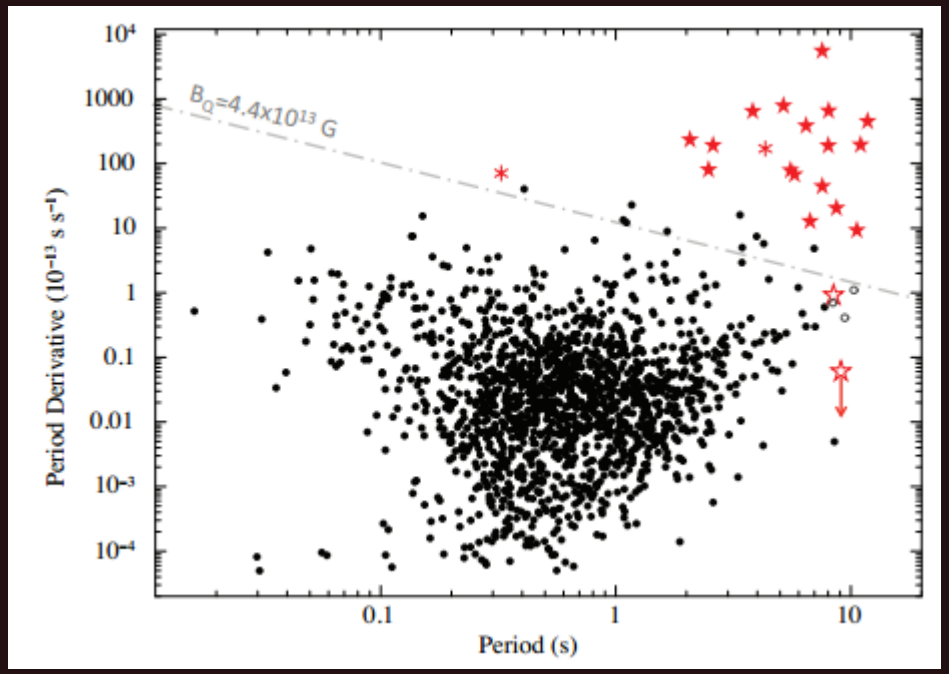

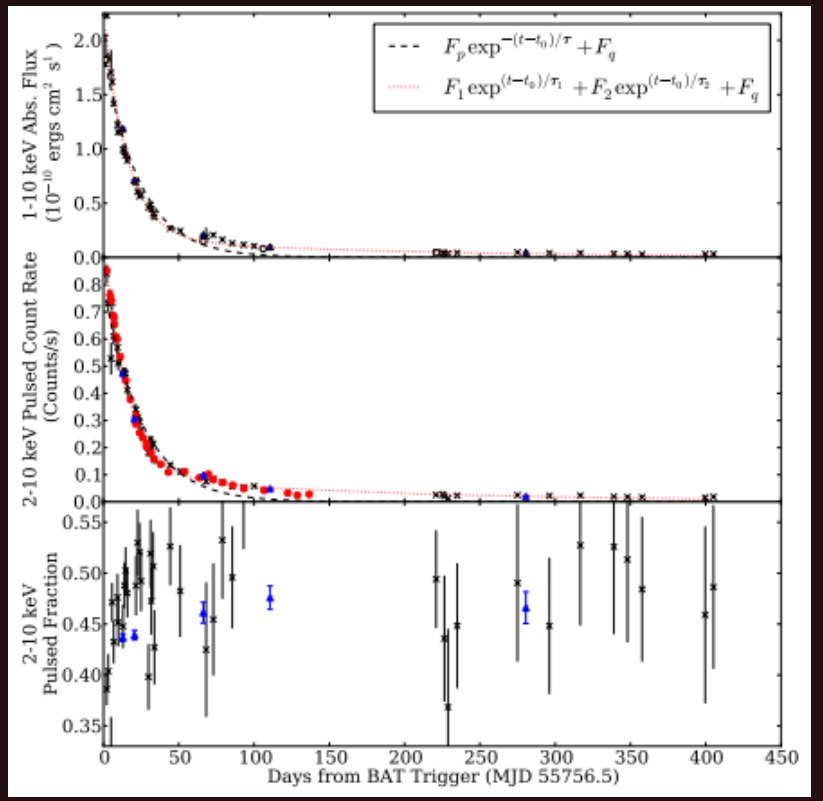

1204.1034

1203.6449

New data: 1211.7347

One more low-field magnetar

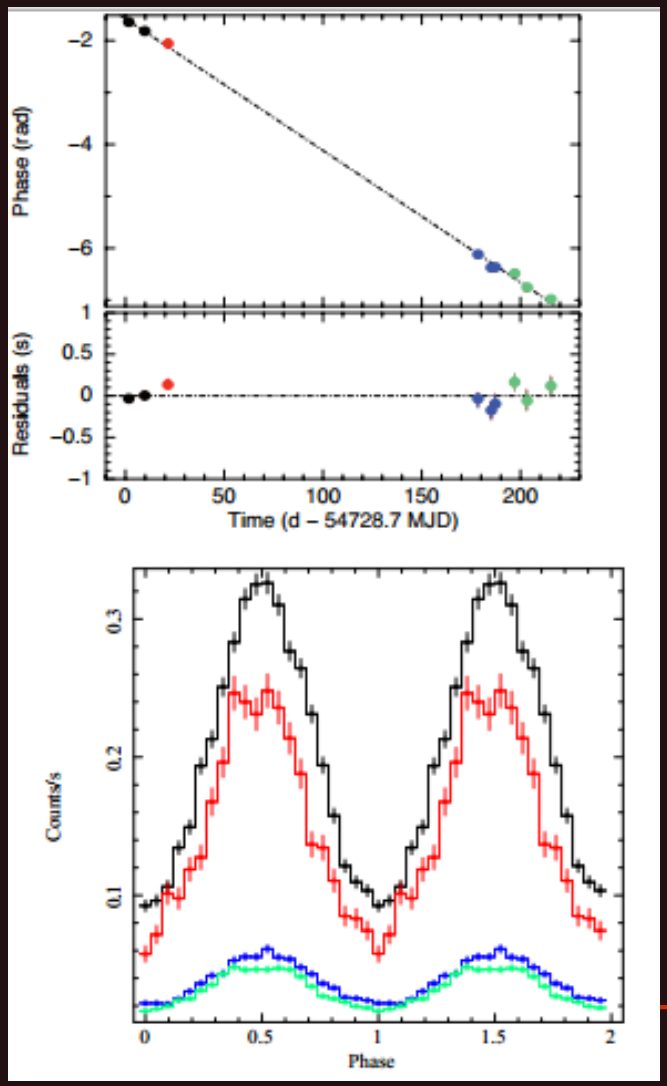

3XMM J185246.6+003317
P=11.5 s No spin-down detected after 7 months
B<4 10^{13} G
Transient magnetar

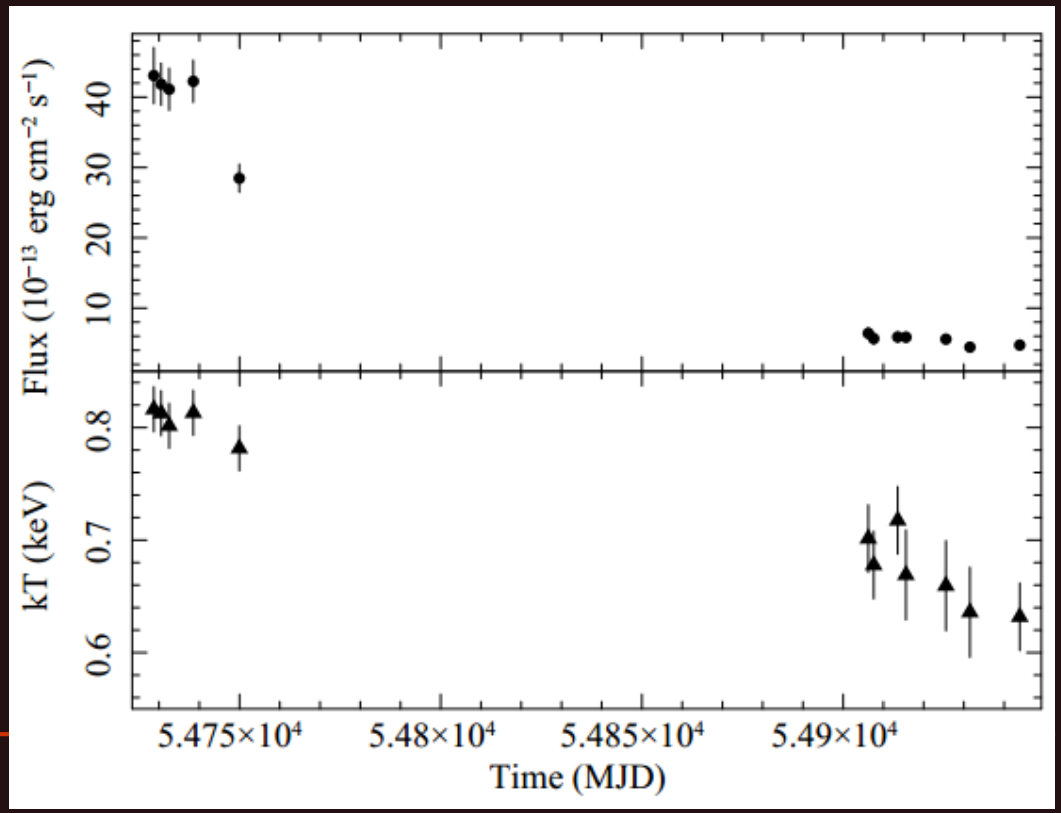

1311.3091

Quiescent magnetar J1622–4950

Normally, magnetars are detected via their strong activity: gamma-ray bursts or enhanced X-ray luminosity.

This one was detected in radio observations
The field is estimated to be B~3 10^{14} G

It seems to be the first magnetar to be Detected in a quiescent state.

PSR J1622–4950 was detected in a radio survey
As a pulsar with P=4.3 s.

Noisy behavior in radio

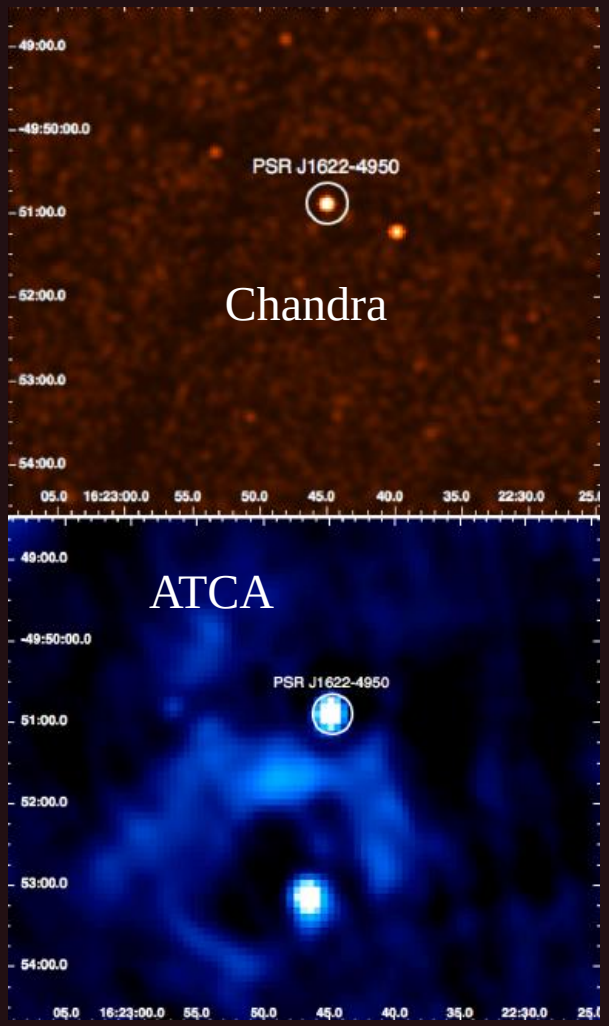

See reviews on high-B PSRs in 1010.4592, 1805.01680

arXiv: 1007.1052

Is J1622–4950 a transient magnetar?

PSR J1622–4950

X-ray flux is decaying for several years. Probably, the source was active years before.

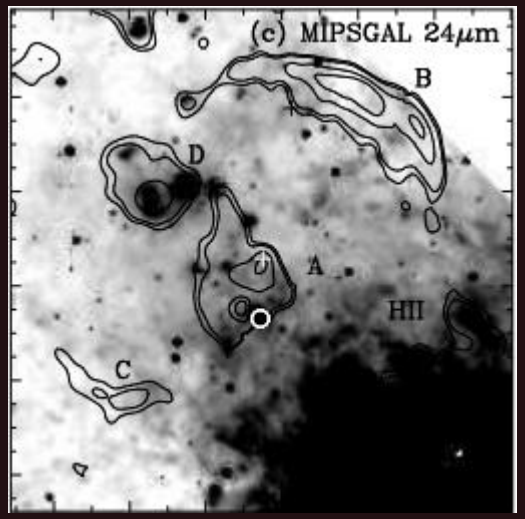

G333.9+0.0 SNR ?

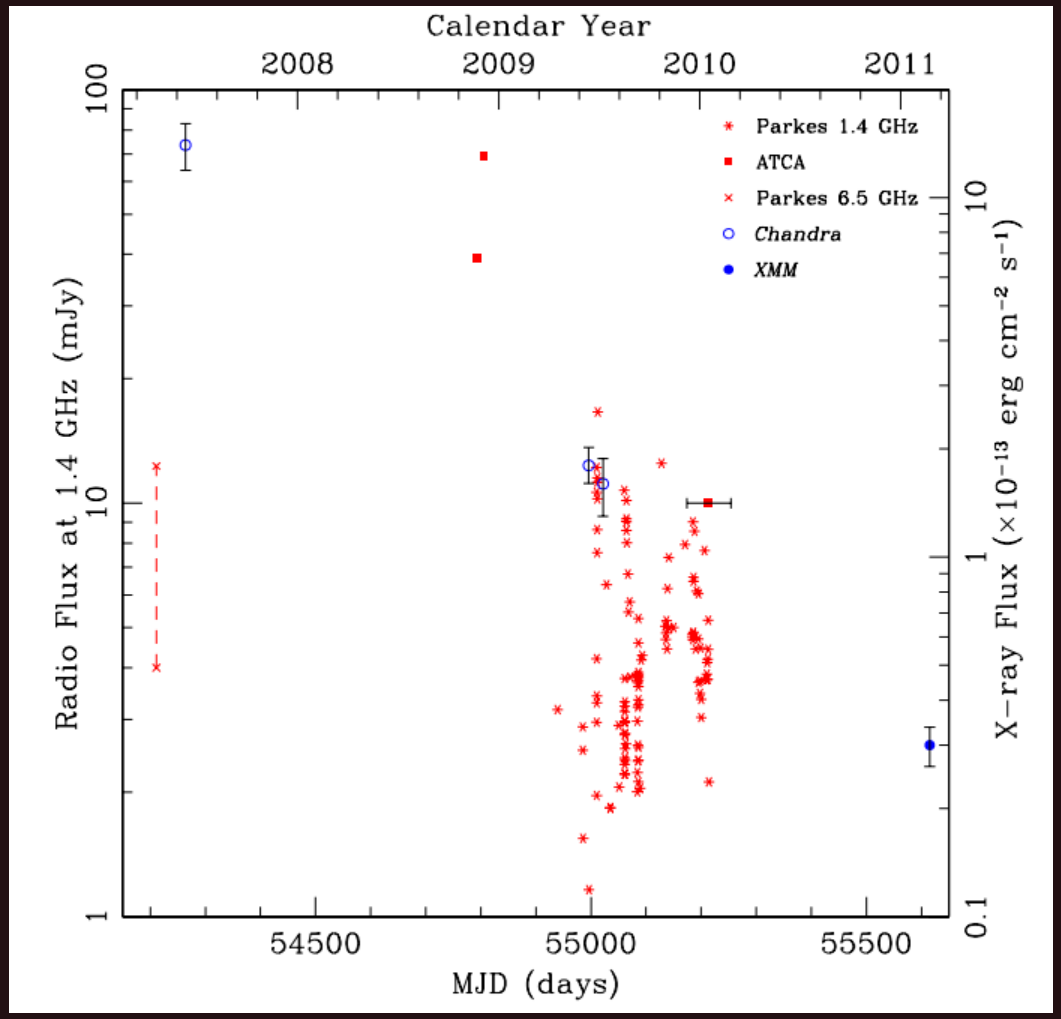

1203.2719

See also 1204.2045

Yes! Revival of J1622–4950

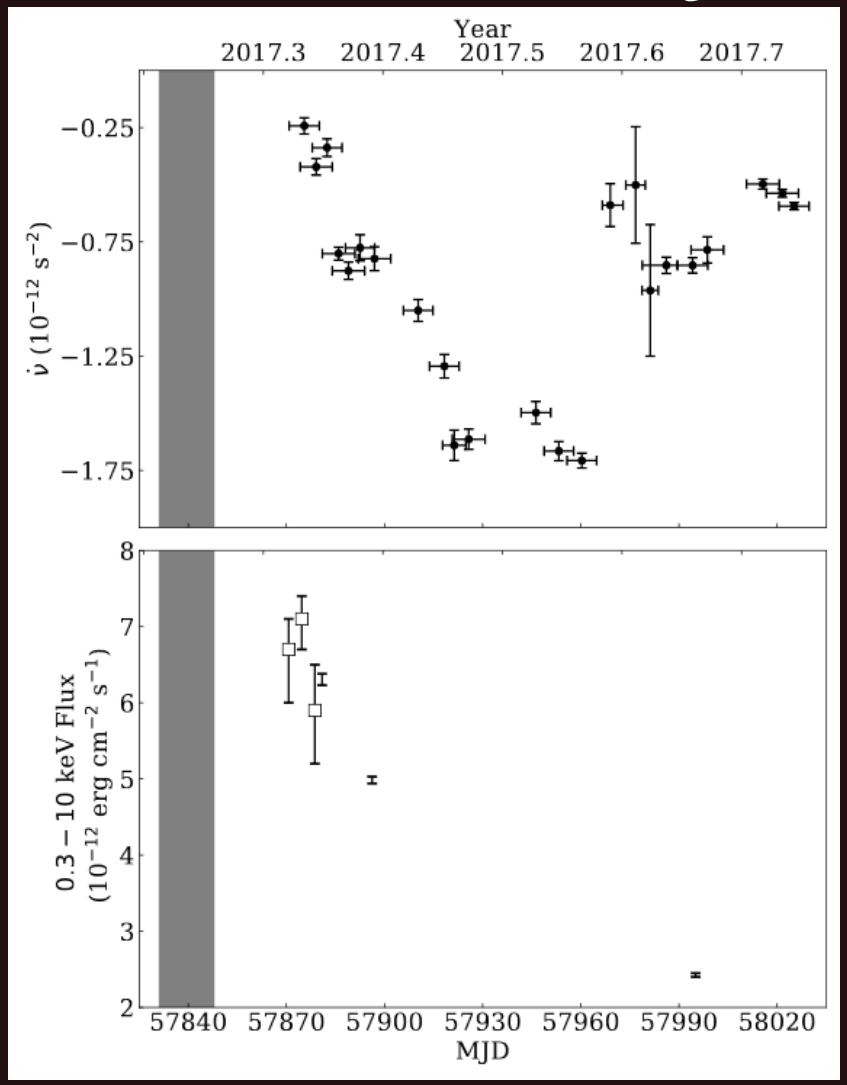

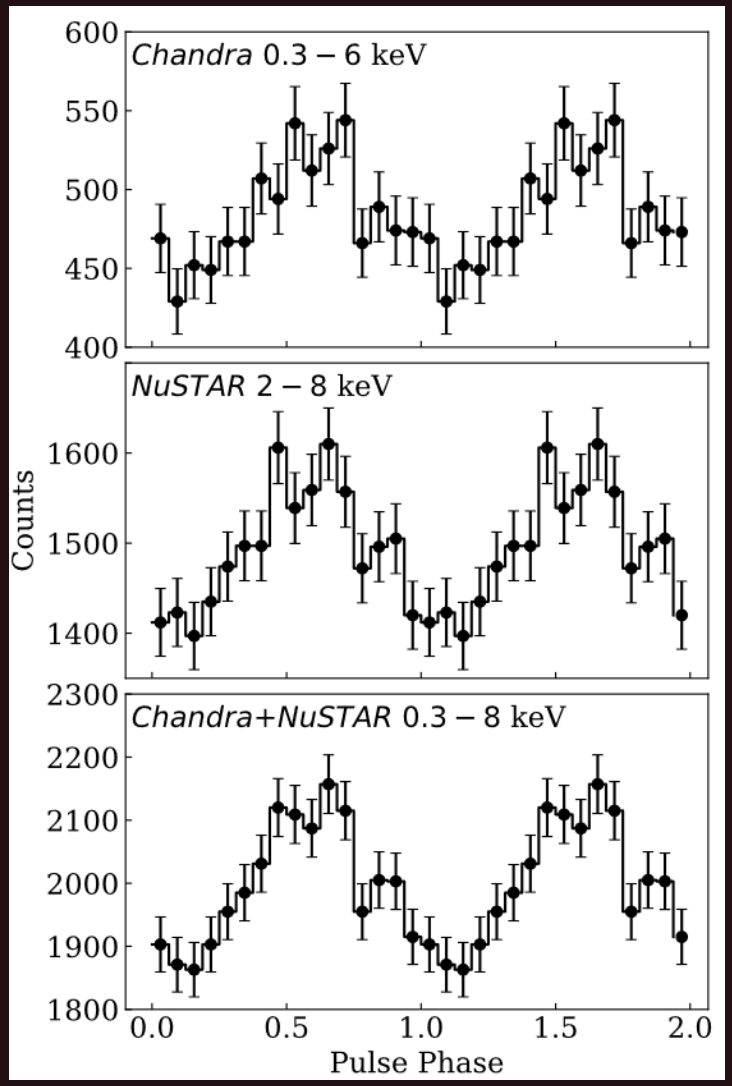

1804.01933 Among few (~5) magnetars with detected radio emission.

A pulsar with growing field?

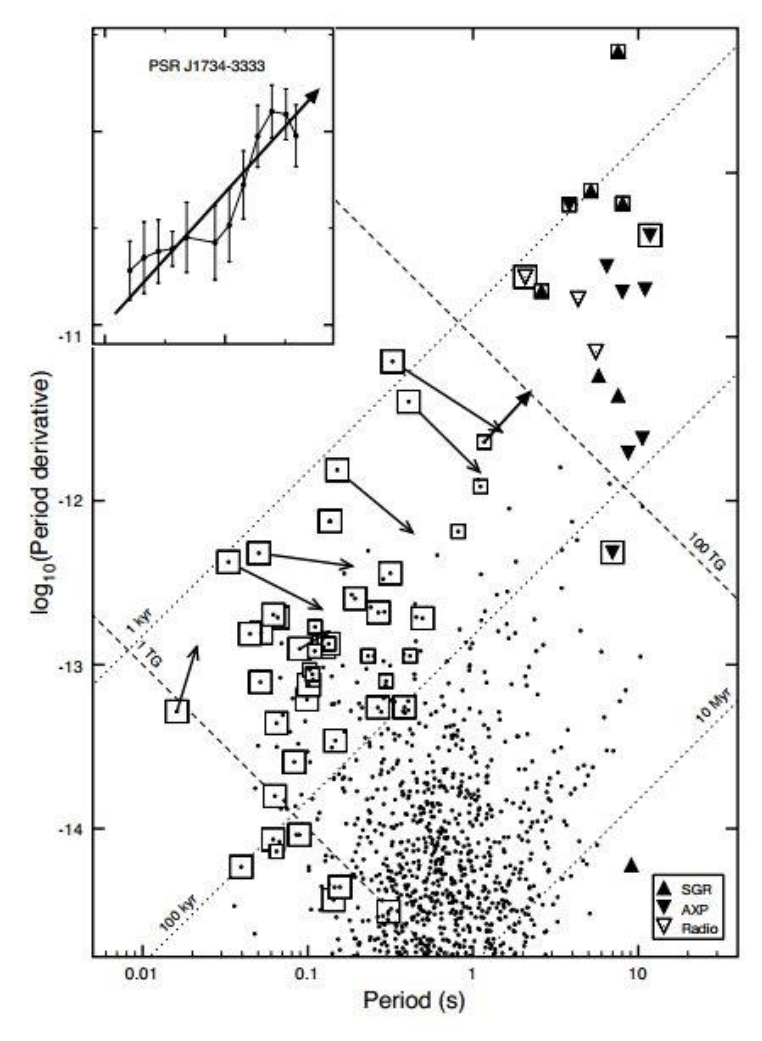

PSR J1734−3333
n=0.9+/-0.2

Will it become a magnetar?

Espinoza et al. arXiv: 1109.2740

ROSAT

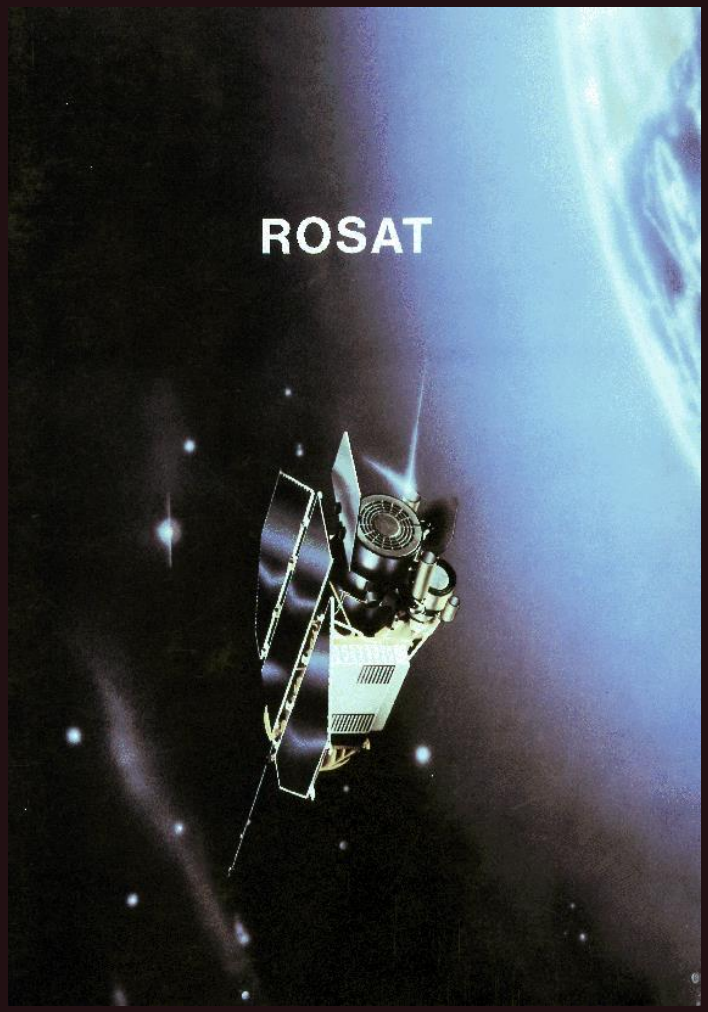

ROentgen SATellite

German satellite
(with participation of US and UK).

Launched 01 June 1990.
The program was successfully ended on 12 Feb 1999.

Close-by radioquiet NSs

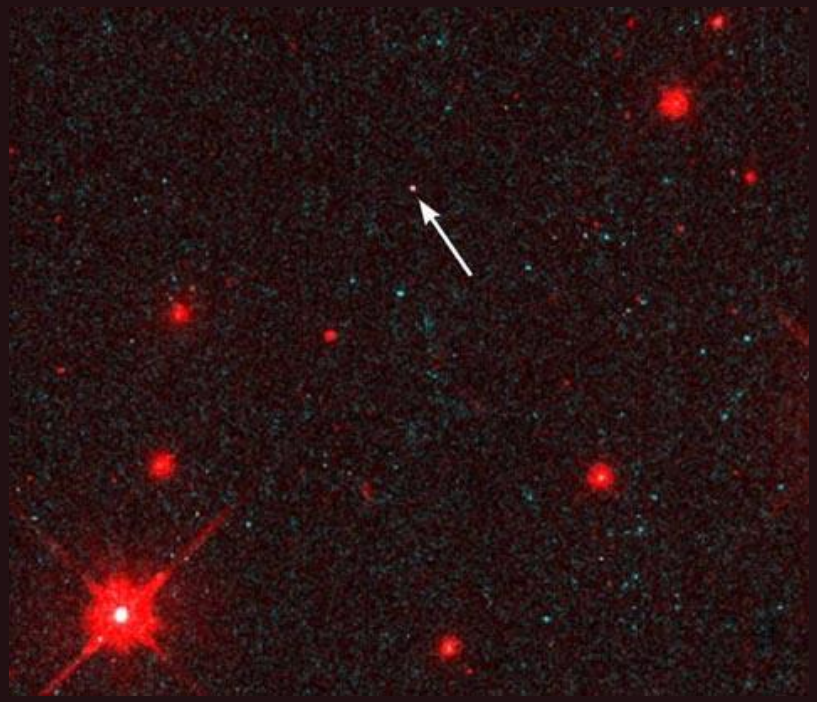

RX J1856.5-3754

- Discovery: Walter et al. (1996)
- Proper motion and distance: Kaplan et al.
- No pulsations
- Thermal spectrum
- Later on: six brothers

Magnificent Seven

Name	Period, s
RX 1856	7.05
RX 0720	8.39
RBS 1223	10.31
RBS 1556	3.39?
RX 0806	11.37
RX 0420	3.45
RBS 1774	9.44

Radioquiet
Close-by
Thermal emission
Absorption features
Long periods

For RBS 1556 (RX J1605) the priod is uncertain: 1901.08533

Spin properties and other parameters

RX J	Spin*			Spectrum†					Astrometry**		References
	P (s)	$\dot{P}$ (10^{-14})	PF (%)	$N_{H,20}$ (cm^{-2})	kT (eV)	PN (s^{-1})	E_{abs} (keV)	m_B (mag)	μ (mas yr^{-1})	d (pc)	
1856.5−3754	7.06	...	1	0.8	62	8.3	...	25.2	333	160	14, 15, 18–20
0720.4−3125‡	8.39	7	11	1.0	87	7.6	0.3	26.6	97	360	21–26
1605.3+3249	...	...	< 3	0.8	93	5.6	0.5(0.6,0.8)	27.2	155	390	27–31
1308.6+2127	10.31	11	18	1.8	102	2.5	0.2(0.4)	28.4§	200¶	...	32–36
2143.0+0654	9.44	...	4	3.6	102	2.0	0.7	> 26‖	...	430	37–39
0806.4−4123	11.37	...	6	1.1	92	1.8	0.3(0.6)	> 24	...	250	29, 40
0420.0−5022	3.45	...	17	2.1	45	0.2	0.3	26.6	...	345	29, 40

Kaplan arXiv: 0801.1143

Updates:

- 1856. vdot=-6 10^{-16} (| vdot|<1.3 10^{-14}) van Kerkwijk & Kaplan arXiv: 0712.3212
- 2143. vdot=-4.6 10^{-16} Kaplan & van Kerkwijk arXiv: 0901.4133
- 0806. |vdot|<4.3 10^{-16} Kaplan and van Kerkwijk arXiv: 0909.5218

Object	kT_∞ (eV)	P (s)	p_f (%)	$\log(\dot{P})$ ($\mathrm{s\,s^{-1}}$)	$\log(\dot{E})$ ($\mathrm{erg\,s^{-1}}$)	$\log(\tau_{ch})$ (yr)	$\log(t_{kin})$ (yr)	$\log(B_{dip})$ (10^{13} G)	$\log(B_{cyc})$ (10^{13} G)	Reference
RX J1856.5-3754	61	7.06	1	−13.527	30.580	6.58	5.62	13.17	–	[1]
RX J0720.4-3125	84 – 93	8.39	11	−13.156	30.726	6.28	5.93	13.39	13.75	[2]
RX J1605.3+3249	100	3.39	4	−11.796	33.267	4.53	5.65	13.87	13.92	[3]
RX J1308.6+2127	100	10.31	18	−12.951	30.663	6.16	5.95	13.54	13.60	[4]
RX J2143.0+0654	104	9.43	4	−13.398	30.332	6.57	–	13.29	14.15	[5]
RX J0806.4-4123	95	11.37	6	−13.260	30.227	6.51	–	13.40	13.96	[6]
RX J0420.0-5022	48	3.45	17	−13.553	31.487	6.29	–	13.00	–	[7]

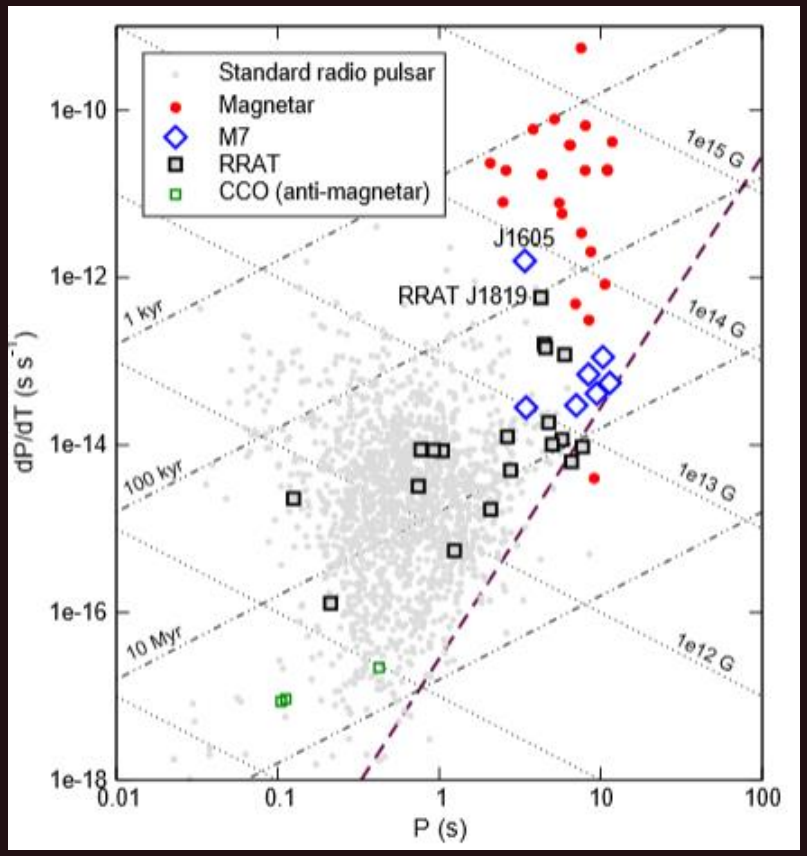

1401.7147

Spectral properties

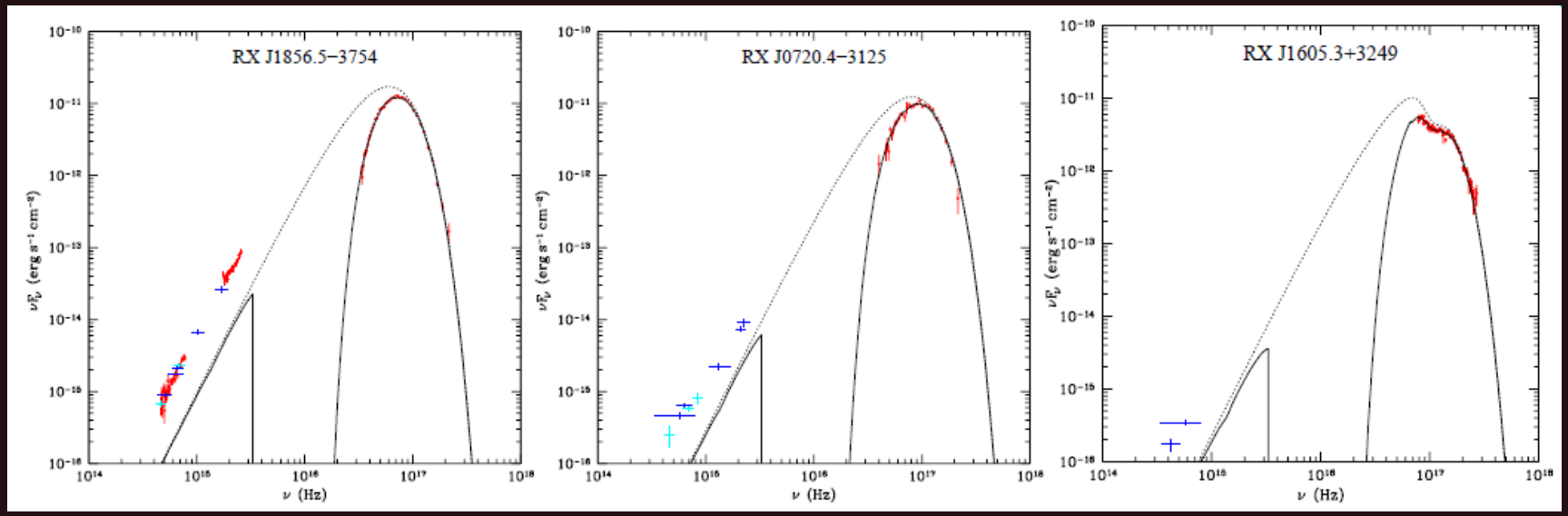

Kaplan arXiv: 0801.1143

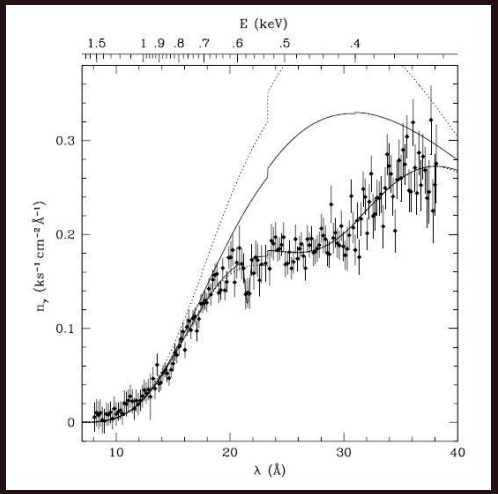

Van Kerkwijk et al. (2004)

Spectra are blackbody plus one or several wide absorption features.
The origin of features is not understood, yet.

New data: Kaplan et al. 1105.4178

The isolated neutron star candidate 2XMM J104608.7-594306

A new INS candidate.

B >26, *V* >25.5, *R* >25
(at 2.5σ confidence level)

$\log(F_X/F_V)$ >3.1
kT = 118 +/-15 eV

unabsorbed X-ray flux:
F_x ~1.3 10^{-12} erg s^{-1} cm^{-2}
in the 0.1–12 keV band.

At 2.3 kpc (Eta Carina)
the luminosity is
L_X ~ 8.2 10^{32} erg s^{-1}
R_∞ ~ 5.7 km

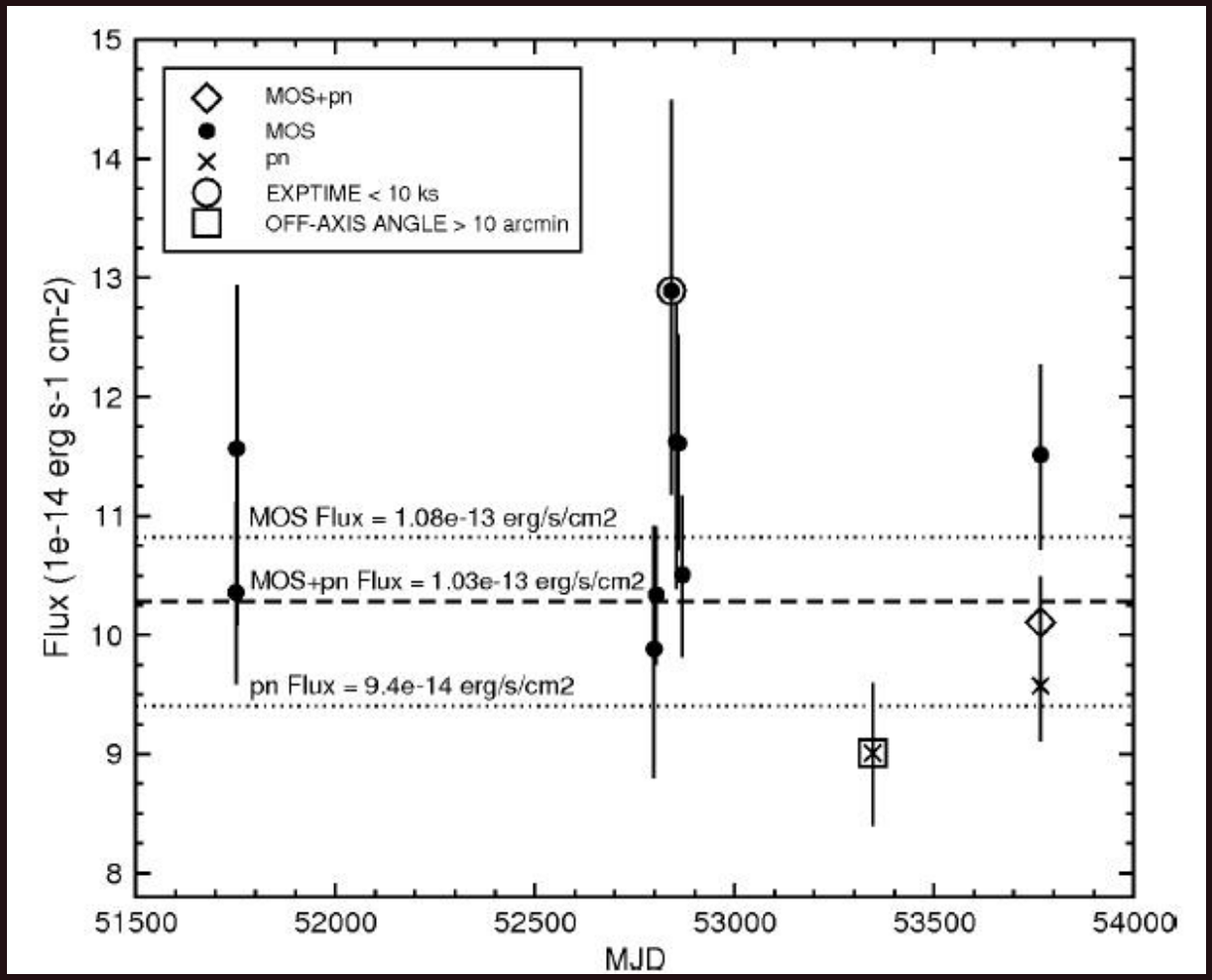

M7-like? Yes!
But P=19 msec

Pires & Motch arXiv: 0710.5192 and Pires et al. arXiv: 0812.4151

Spin period of 2XMM J1046-5943

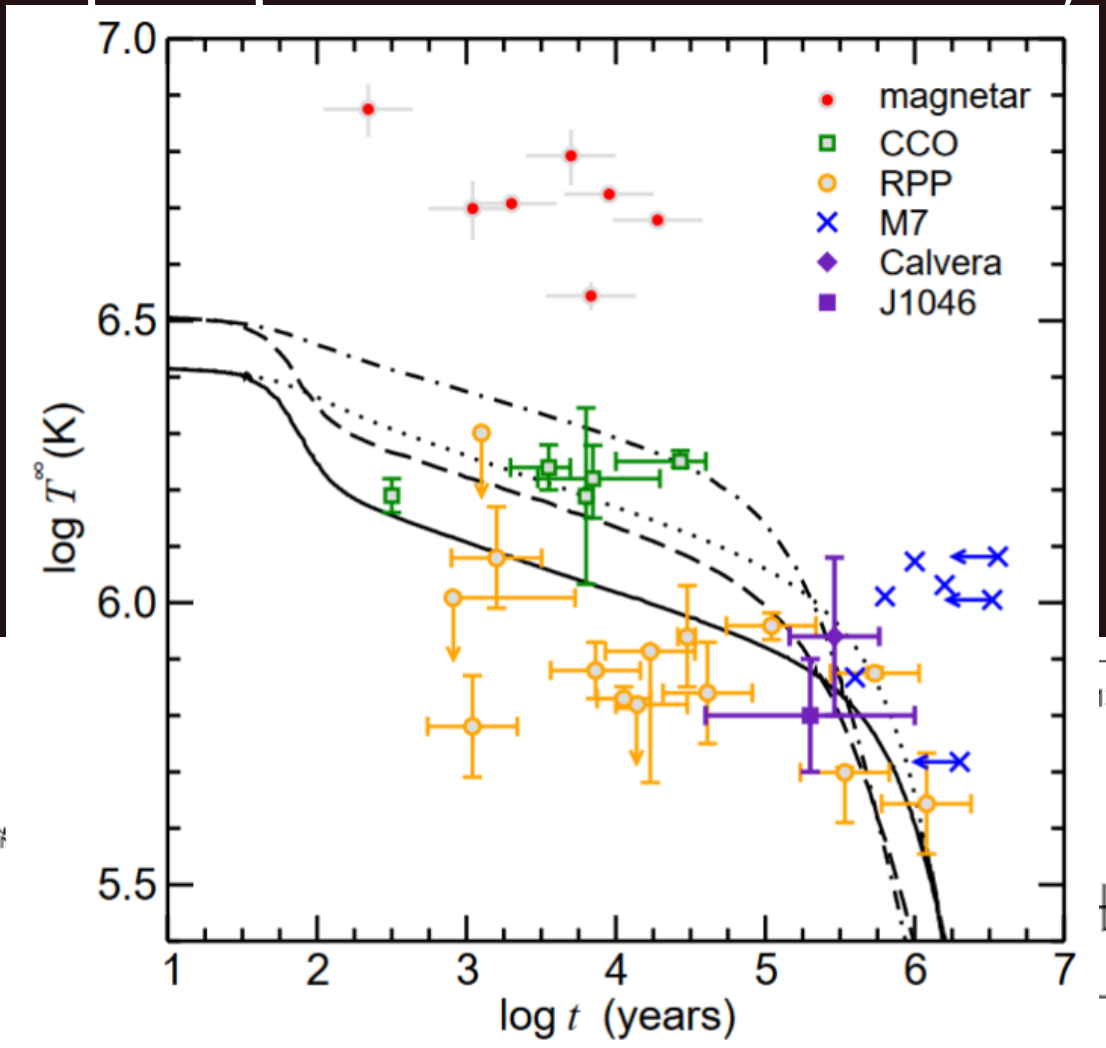

Calvera-like?

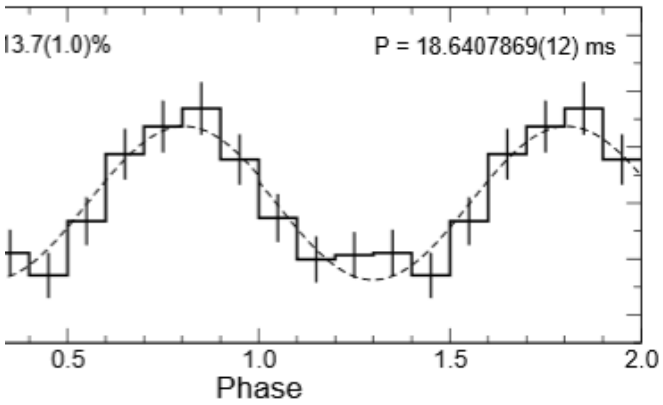

$T_{\rm eff} = (6-10)\times10^5$ K, and $L_{\rm X} = (1.1-7.4)\times10^{32}$ erg s^{-1}.

1508.05246

Radio observations

Up to now the M7 are not detected for sure at radio wavelengths, however, there was a paper by Malofeev et al., in which the authors claim that they had detect two of the M7 at very low wavelength (<~100 MHz).

At the moment the most strict limits are given by Kondratiev et al. Non-detection is still consistent with narrow beams.

XDINS	Pulsed emission			Bursty emission		
	$S_{\rm lim}$ (μJy)	$L_{1400}^{\rm p,max}$ (mJy kpc^2)	$L_{820}^{\rm p,max}$ (mJy kpc^2)	rate upper limit (hr^{-1})	$S_{\rm lim}^{\rm sp}$ (mJy)	$L_{1400}^{\rm b,max}$ (mJy kpc^2)
RX J0720.4−3125	8	4×10^{-4}	10^{-3}	0.25	21	1
RX J0806.4−4123	10	4×10^{-3}	10^{-2}	0.32	18	6.9
RX J1308.6+2127	10	4×10^{-3}	10^{-2}	0.24	17	6.5
RX J1605.3+3249	8	3×10^{-3}	8×10^{-3}	0.25	22	8.4
RX J1856.5−3754	14	1.4×10^{-4}	3.6×10^{-4}	0.32	24	0.2
RX J2143.0+0654	13	5×10^{-3}	1.3×10^{-2}	0.36	20	7.6

Kondratiev et al. arXiv: 0907.0054

M7 among other NSs

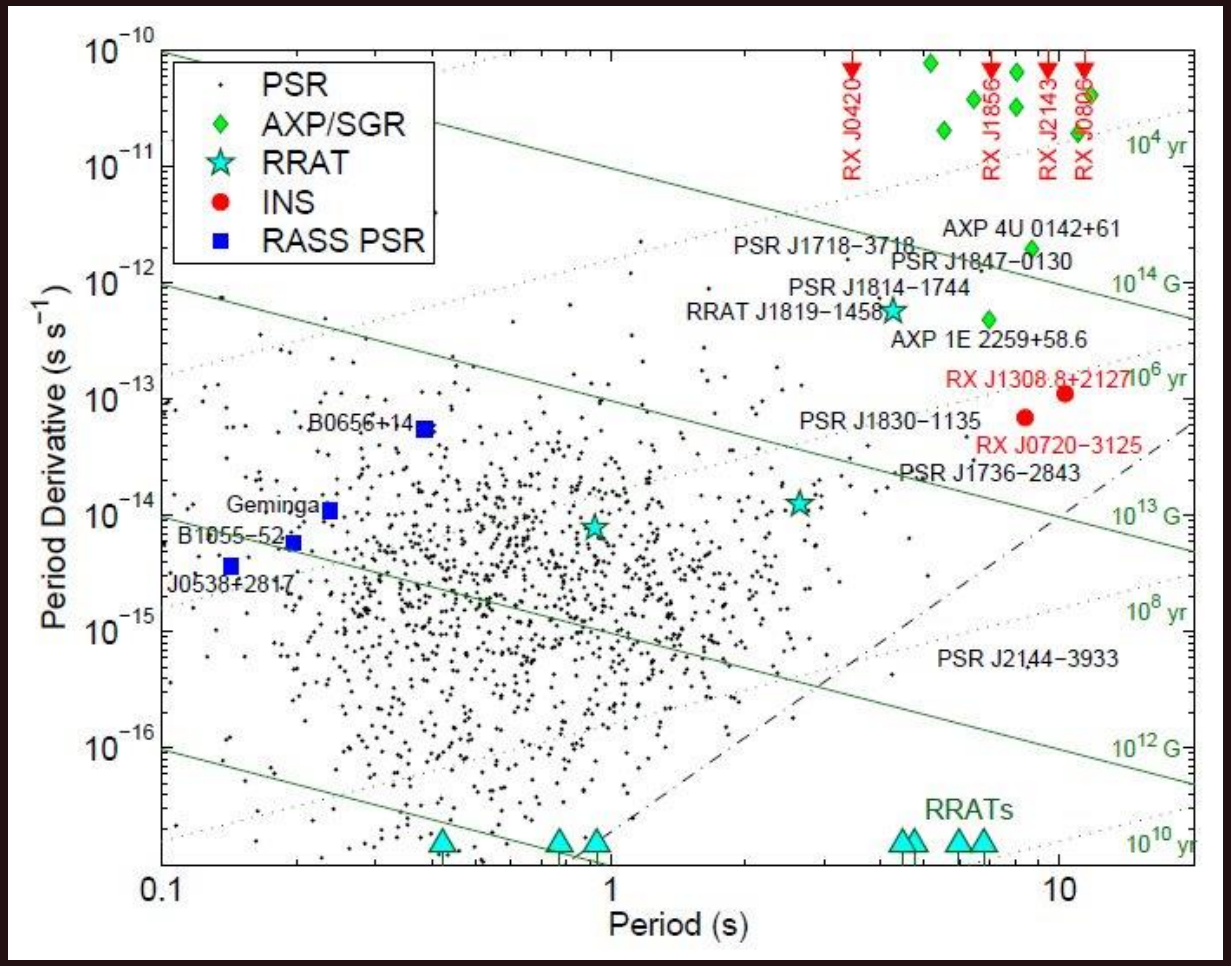

Evolutionary links of M7 with other NSs are not clear, yet.

M7-like NSs can be numerous.

They can be descendants of magnetars.

Can be related to RRATs.

Or, can be a different population.

Kaplan arXiv: 0801.1143

How to find new candidates?

1. Digging the data
   Many attempts failed. One of the latest used SDSS optical data together with ROSAT X-ray. Candidates have been observed by Chandra. Nothing was found (Agueros et al. arXiv: 1103.2132).

2. eROSITA is coming!
   In 2019 spectrum-RG with eROSITA will be launched.
   It is expected that with this telescope tens of
   new M7-like NSs can be found (Boldin et al., Pires et al.)

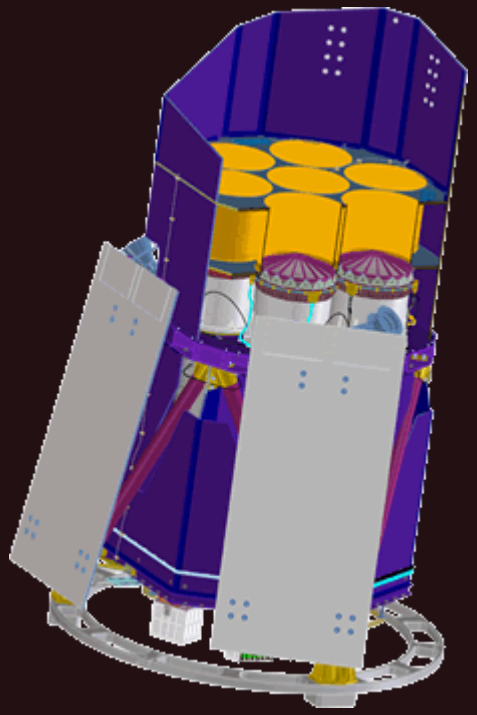

Pulsars invisible in radio?

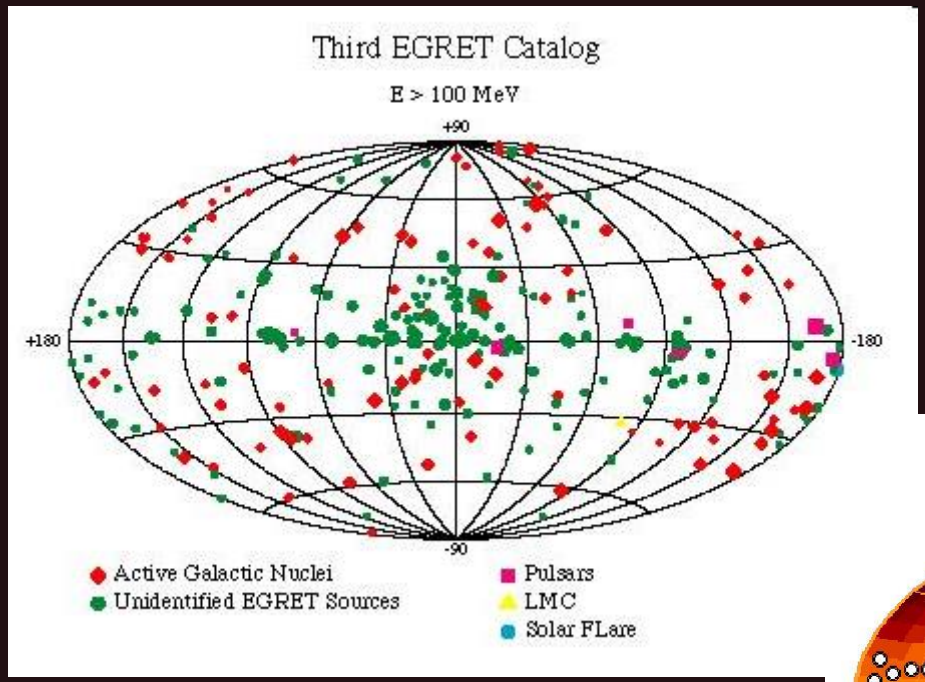

(Nolan et al. astro-ph/9607079)

EGRET data
Many unidentified sources

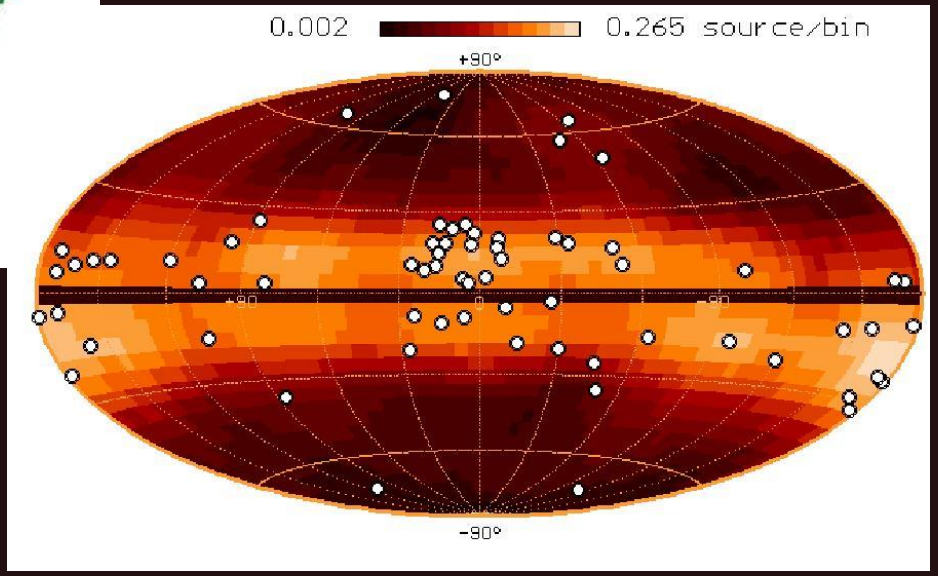

(Grenier astro-ph/0011298)

Fermi pulsars

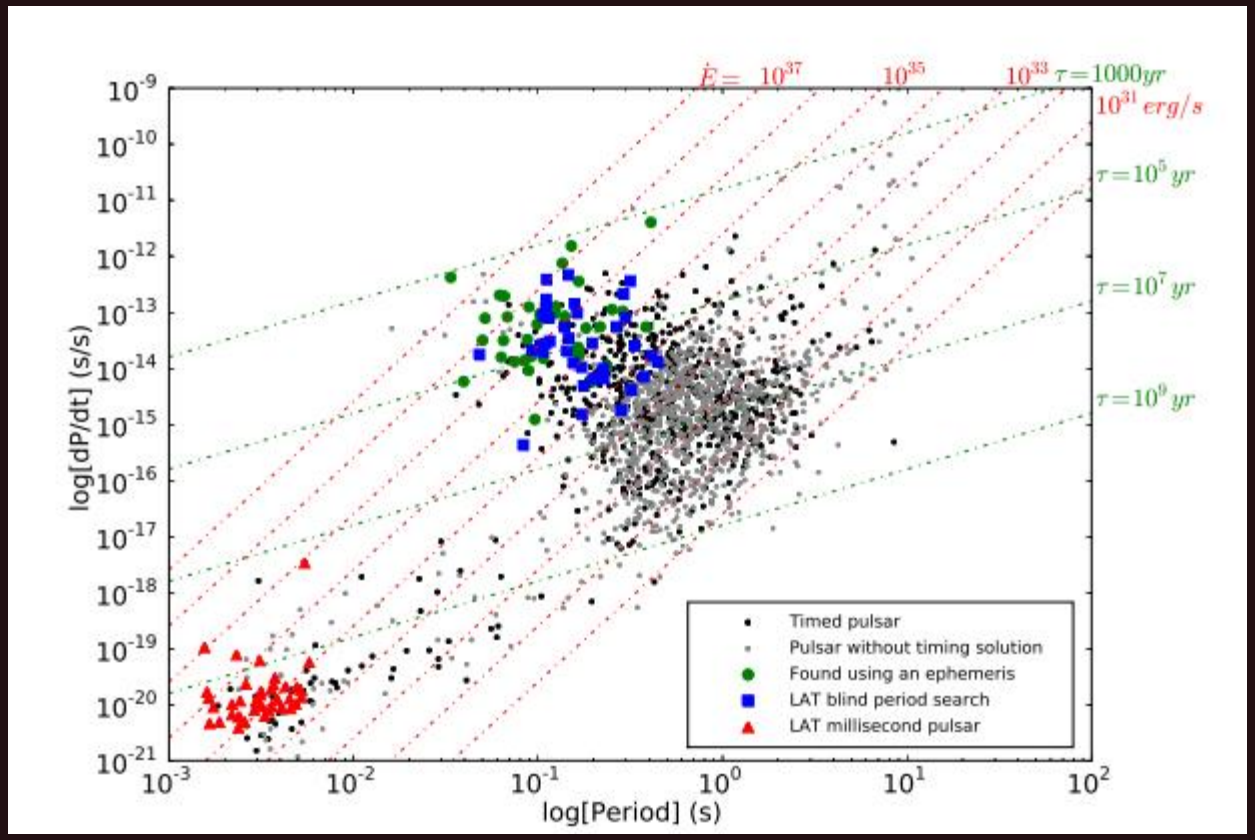

In the 2nd catalogue there are 117 pulsars.

1/3 mPSR

The rest are young:
1/3 radio-loud
1/3 radio-quiet

1211.3726

Full 2nd catalogue is presented in 1305.4385

In the 3rd catalogue there are 167 pulsars
https://fermi.gsfc.nasa.gov/ssc/data/access/lat/4yr_catalog/3FGL-table/

Discovery of radio transients

McLaughlin et al. (2006) discovered a new type of sources– RRATs (Rotating Radio Transients).
For most of the sources periods about few seconds were discovered.
The result was obtained during the Parkes survey of the Galactic plane.

Burst duration 2-30 ms, interval 4 min-3 hr
Periods in the range 0.4-7 s

>100 sources known.

Thermal X-rays were observed from one of the RRATs (Reynolds et al. 2006). This one seems to me the youngest.

Review: 1109.6896

Catalogue: http://www.as.wvu.edu/~pulsar/rratalog/

RRATs. X-ray + radio data

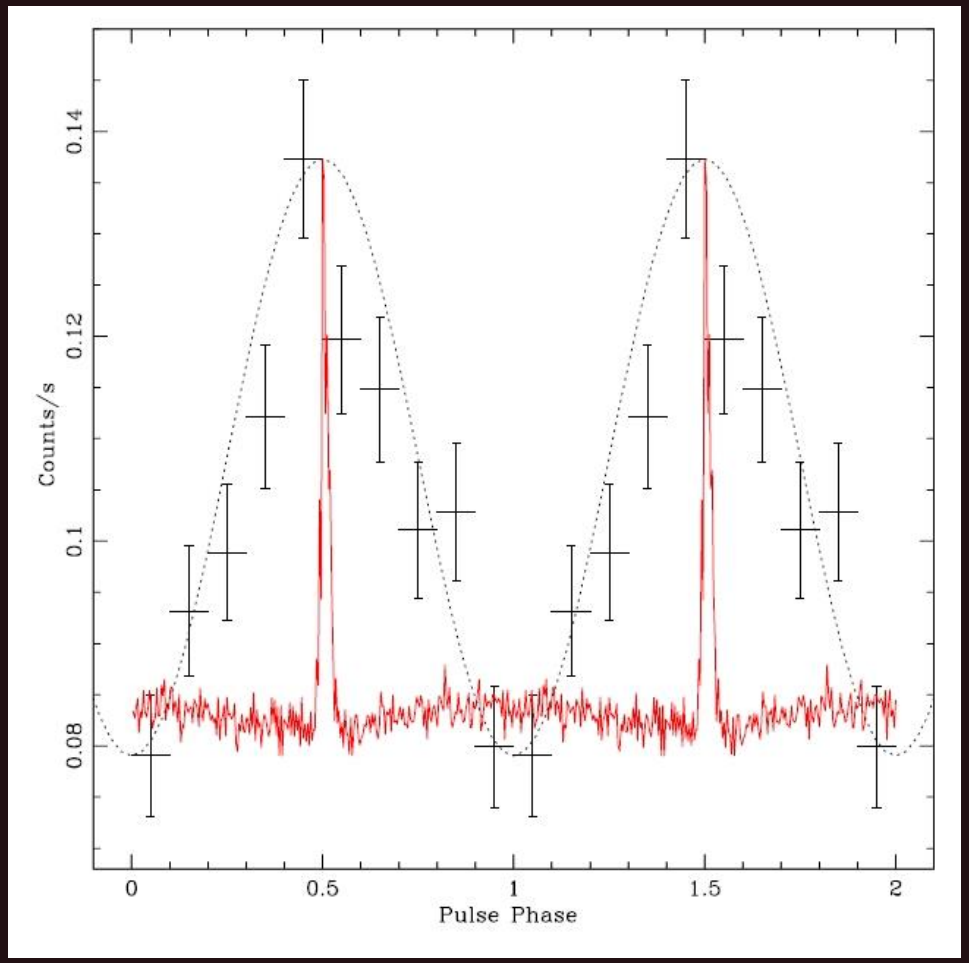

X-ray pulses overlaped on radio data of RRAT J1819-1458.

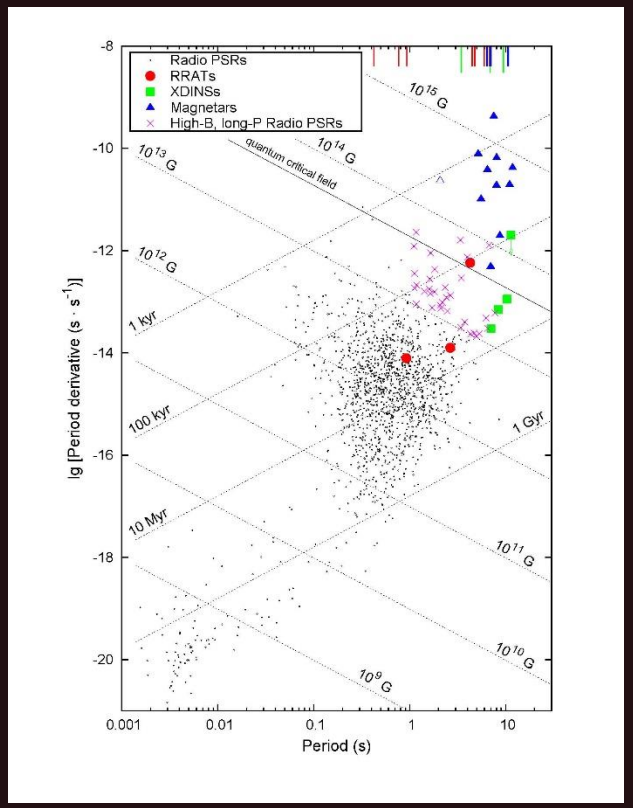

arXiv: 0710.2056

RRAT – are pulsars?

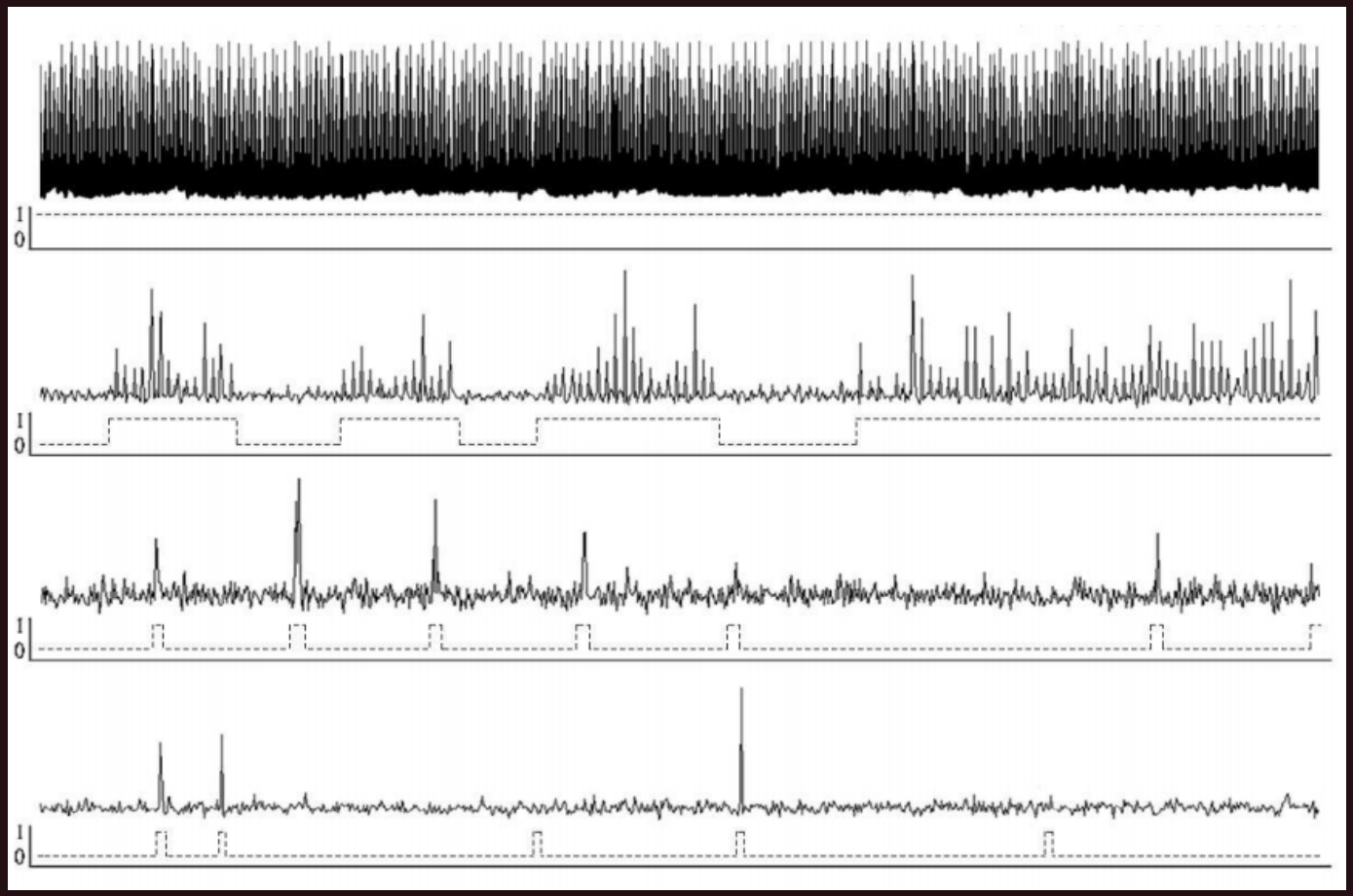

It looks like RRATs bursts are just some kind of magnetospheric activity.
Some PSRs have similar bursts.
It is not easy to plot a boarder line between RRATs and PSRs.

1212.1716

RRATs properties

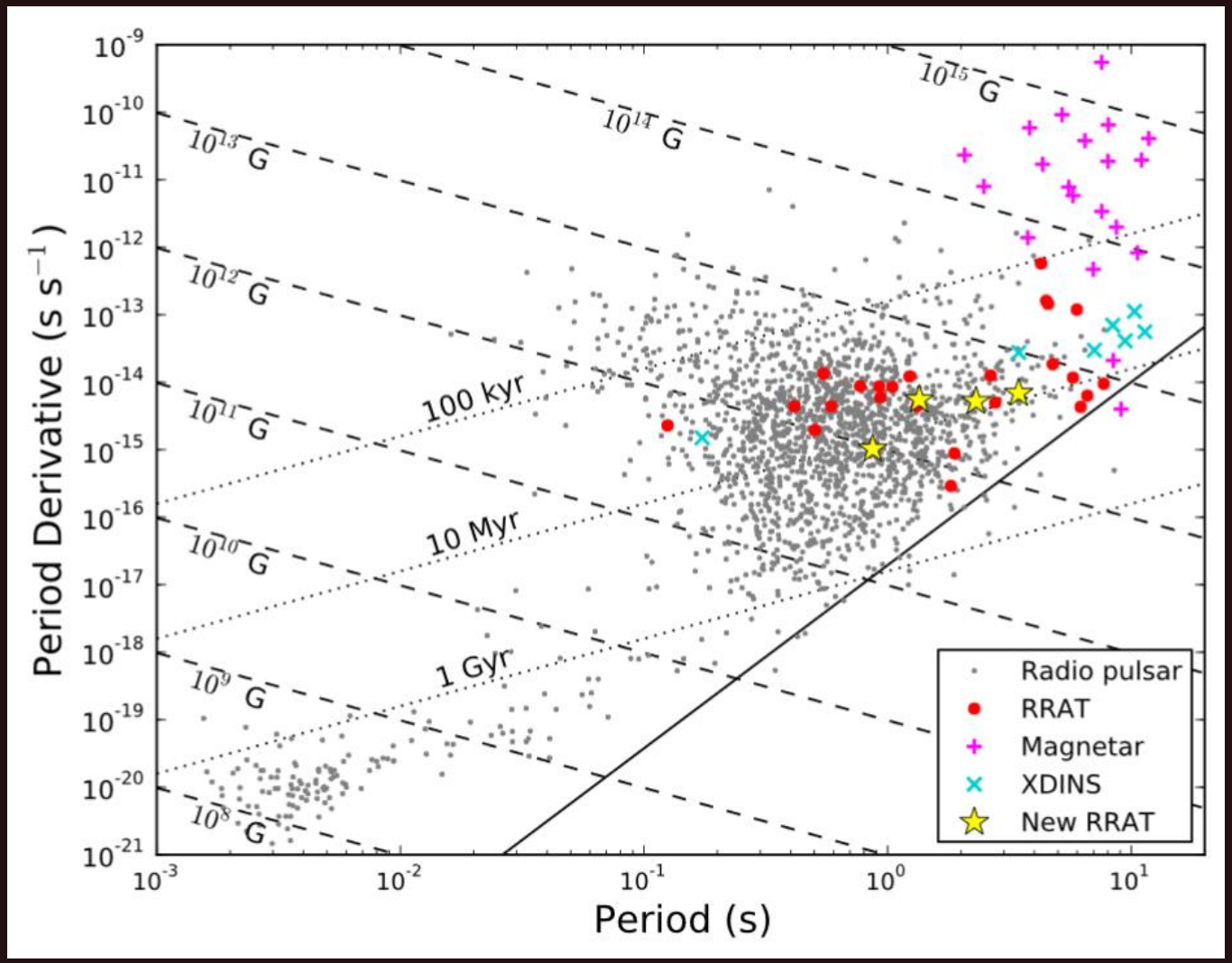

RRATs with P-Pdot seem to be similar to PSRs

About low-frequency detection see 1807.07565.

1503.05170

Catalogue: http://astro.phys.wvu.edu/rratalog
>100 now, see 1706.08412

Calvera et al.

In 2008 Rutledge et al. reported the discovery of an enigmatic NS candidated dubbed *Calvera*. It is high above the galactic plane.

Characteristic	Value
Right Ascension (J2000)	$14^{h}\,12^{m}\,55\overset{s}{.}759$
Declination (J2000)	$+79^{\circ}\,22'\,03\overset{''}{.}41$
Uncertainty Ellipse	$0.31''$ (R.A.) $\times$ $0.25''$ (Dec.)
Absorbed Blackbody[a]	
$N_{\rm H}$	0 (limit)
$kT_{\rm eff}$	229 eV
$(R_{\rm km}/D_{10\,\rm kpc})^2$	26.6
Observed X-ray Flux (0.3–9.5 keV)	7.1×10^{-13} erg cm^{-2} s^{-1}
χ^2_ν (ν)	2.04 (67 dof)
NS Hydrogen Atmosphere (NSA)[b]	
$N_{\rm H}$	$3.1^{+0.9}_{-0.9}\times10^{20}$ cm^{-2}
$kT_{\rm eff}$	109^{+1}_{-1} eV
$D^{-2}_{\rm kpc}$	$7.71^{+0.41}_{-0.38}\times10^{-2}$
Observed X-ray Flux (0.3–9.5 keV)	7.62×10^{-13} erg cm^{-2} s^{-1}
χ^2_ν (ν)	1.31 (67 dof)

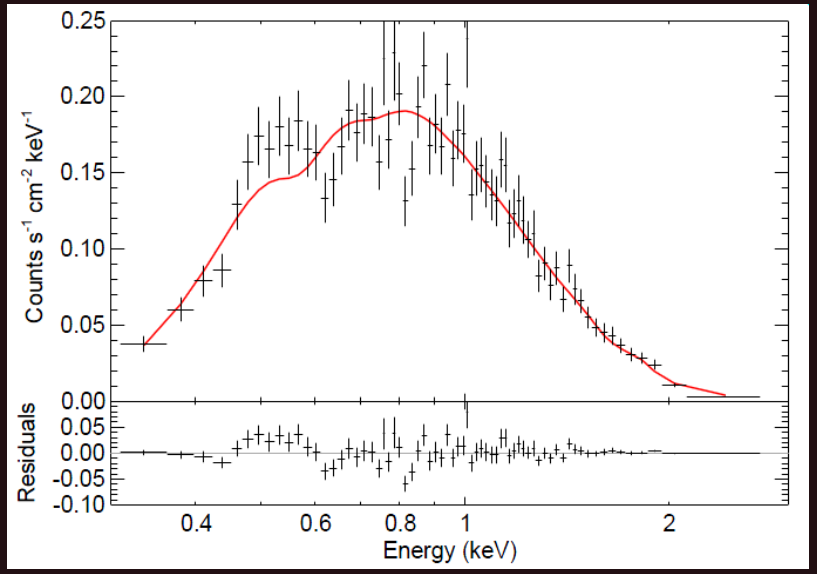

Shevchuk et al. arXiv: 0907.4352

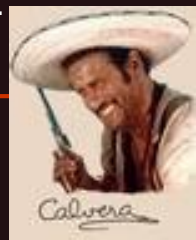

1310.6789

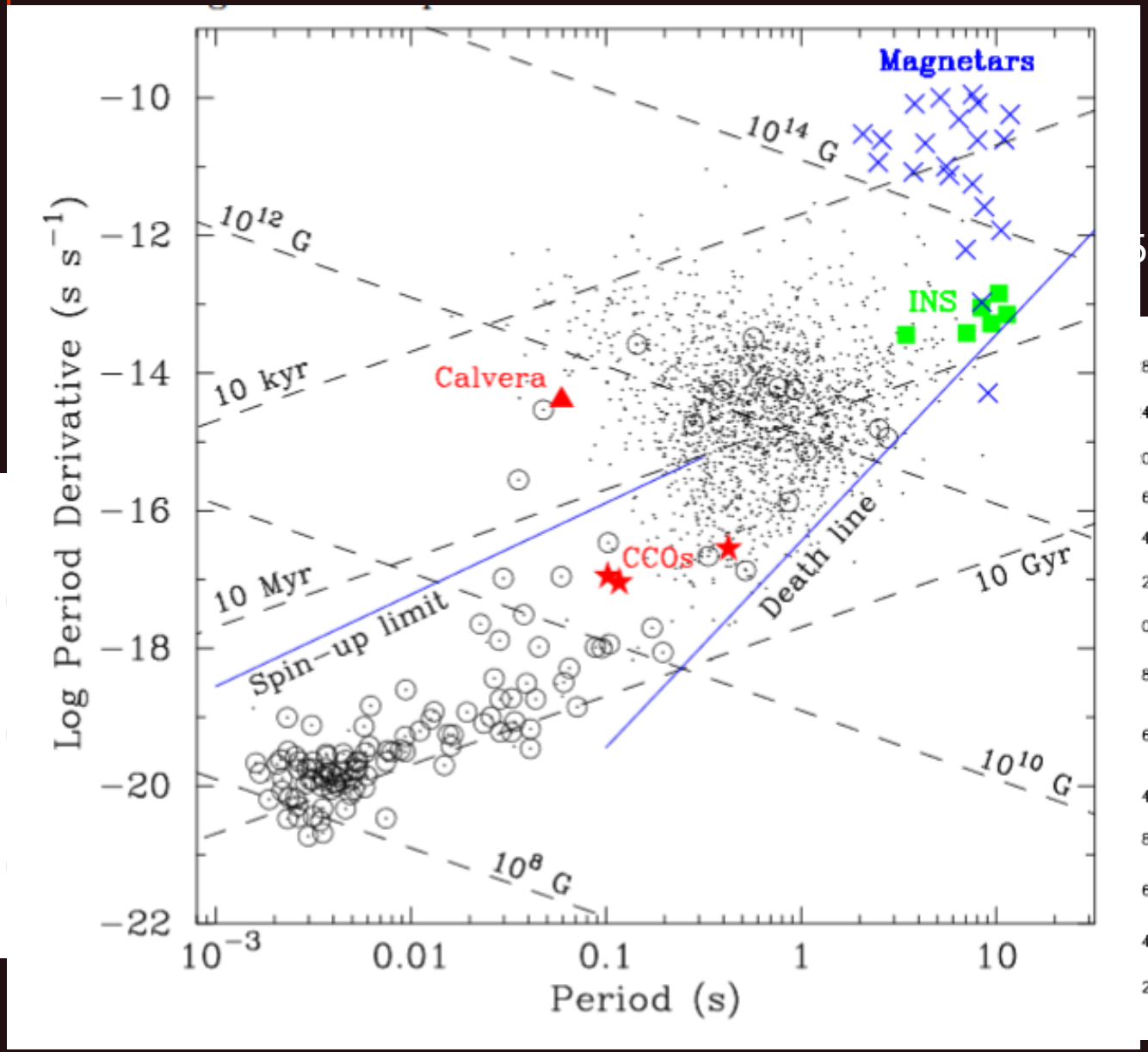

50 eV and ~80/250 eV)

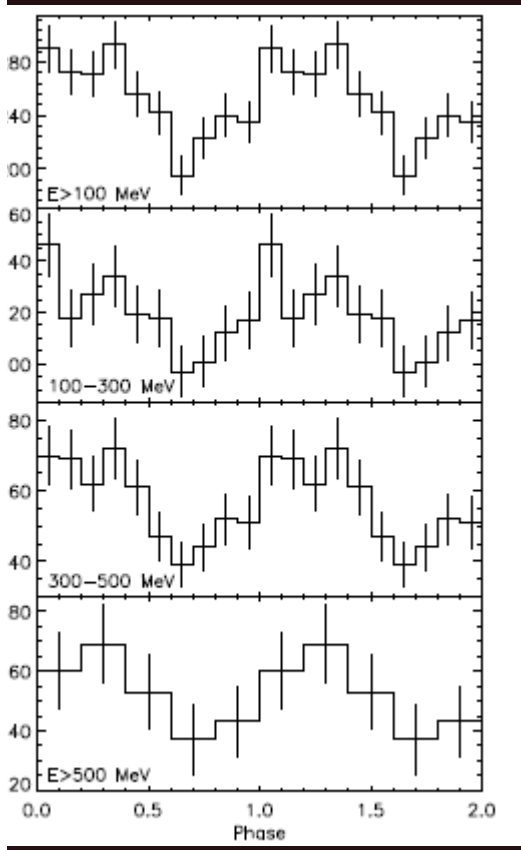

Norm. Intensity

New data 1310.6789, 1510.00683

Some LIGO results

arxiv:1701.07709

First search for gravitational waves from known pulsars with Advanced LIGO

~200 pulsars searched.

Upper limits on GW emission from some known pulsars are becoming constraining.

For Crab <0.002 and for Vela <0.01 of the spin-down can be due to GW.

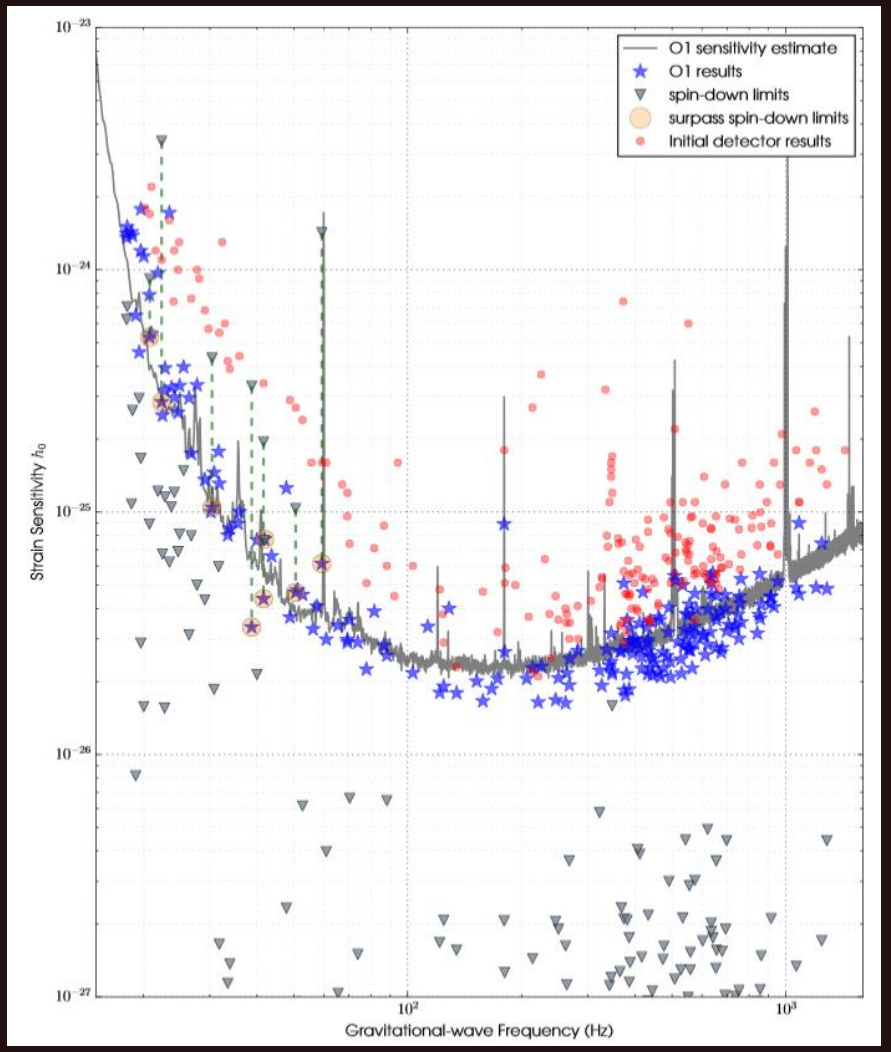

See a review on GW from NSs in 0912.0384, GEO600 results in 1309.4027

arxiv:1701.07709

Limits on ellipticity

$$Q_{22} = h_0 \left(\frac{c^4 d}{16\pi^2 G f_{\mathrm{rot}}^2} \right) \sqrt{\frac{15}{8\pi}}$$

$$\varepsilon = \frac{Q_{22}}{I_{zz}} \sqrt{\frac{8\pi}{15}}$$

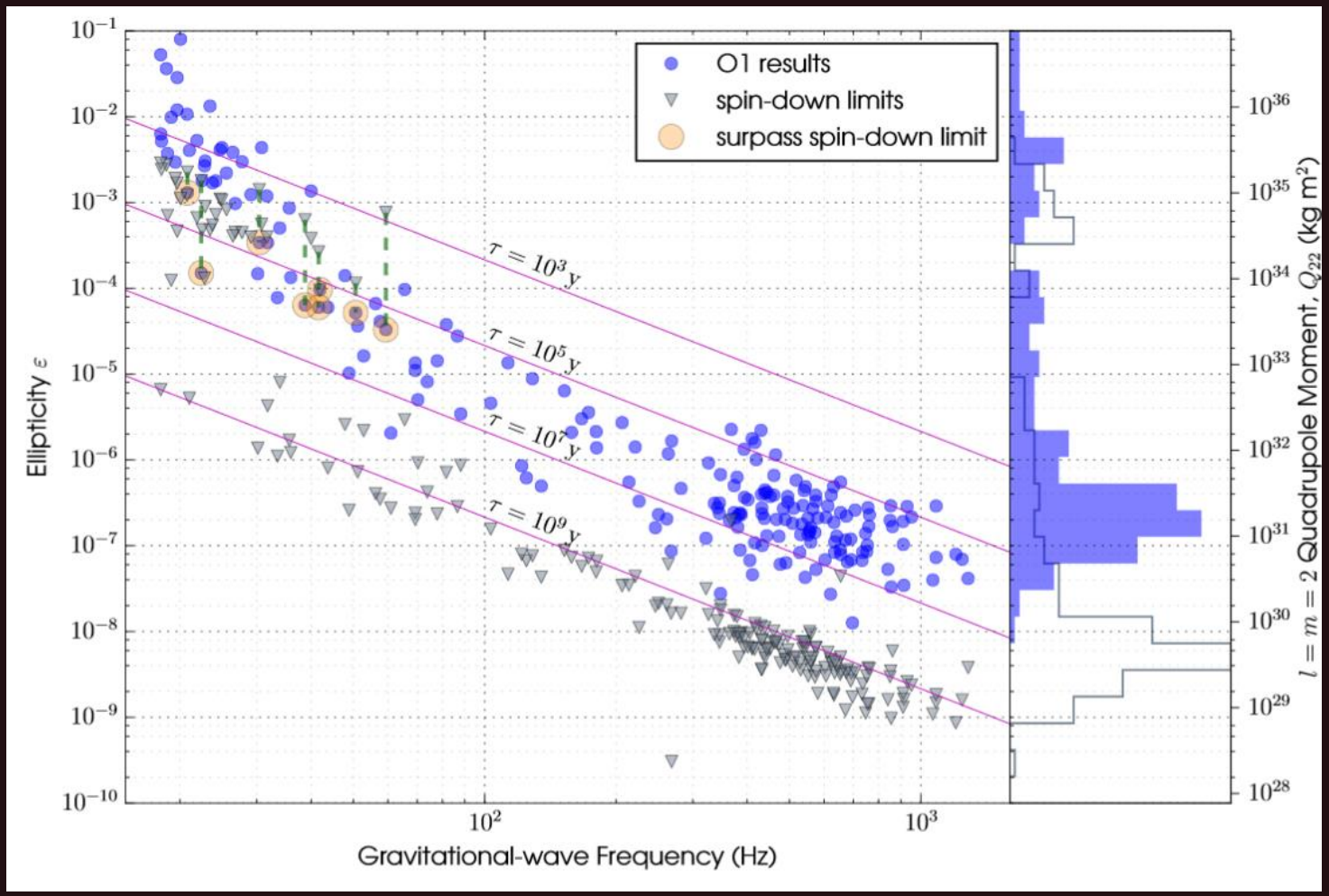

1701.07709

New search

Eleven pulsars in Advanced LIGO first observing run

1710.02327

Name	distance[kpc]	$h_{sd} \cdot 10^{-25}$	$\epsilon_{sd} \cdot 10^{-4}$	h_{ul} 10^{-25}	ϵ_{ul} $\cdot 10^{-4}$	h_{ul}/h_{sd}	$\dot{E}_{rot}/\dot{E}_{GW}$
J0205+6449 [a]	2.0 ± 0.3 [b]	6.9 ± 1.1	14	3.76	7.7	0.54 ± 0.09	0.29
J0534+2200 (Crab)	2.0 ± 0.5 [c]	14 ± 3.5	7.6	1.08	0.58	0.07 ± 0.02	0.005
J0835-4510 (Vela)	0.28 ± 0.02 [c]	34 ± 2.4	18	9.28	5.3	0.27 ± 0.02	0.07
J1400-6326	10 ± 3 [d]	0.90 ± 0.27	2.1	1.17	2.7	1.3 ± 0.4	-
J1813-1246	> 2.5 [e]	< 1.8	< 2.4	1.80	2.5	> 1.0	-
J1813-1749	4.8 ± 0.3 [f]	3.0 ± 0.2	7.0	1.9	4.8	0.64 ± 0.04	0.41
J1833-1034	4.8 ± 0.4 [g]	3.1 ± 0.3	13	3.08	13	0.99 ± 0.09	-
J1952+3252	3.0 ± 0.5 [h]	1.0 ± 0.2	1.1	1.31	1.4	1.31 ± 0.22	-
J2022+3842	10 ± 2 [i]	1.0 ± 0.3	6.0	1.90	11	1.77 ± 0.35	-
J2043+2740	1.5 ± 0.6 [j]	6.9 ± 2.8	23	14.4	47	2.07 ± 0.83	-
J2229+6114	3.0 ± 2 [c]	3.4 ± 2.2	6.2	1.78	3.4	0.54 ± 0.35	0.30

More results on 16 NSs: 1812.11656

Search for periodic signals by LIGO

20-475 Hz
No signals

Could detect ellipticity 8×10^{-7} from 1 kpc at the upper limit.
And 10^{-5} from 1 kpc at 200 Hz.

See a review on GW emission from isolated NSs in 1709.07049

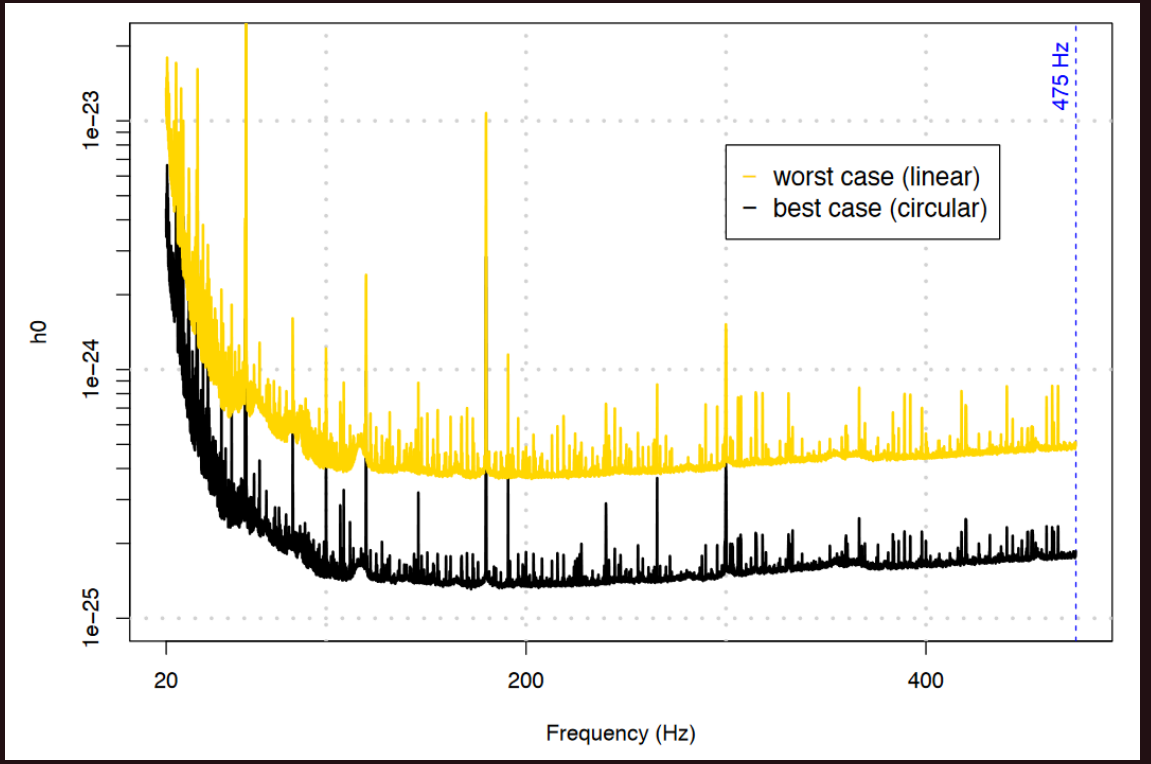

1707.02667

Pulsars, positrons, PAMELA

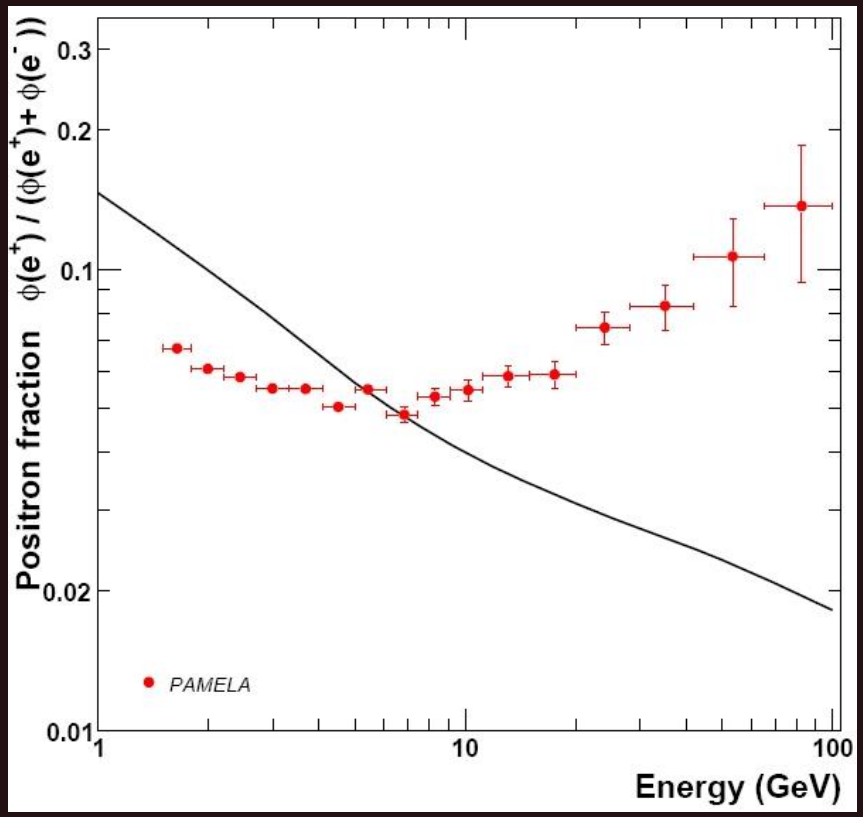

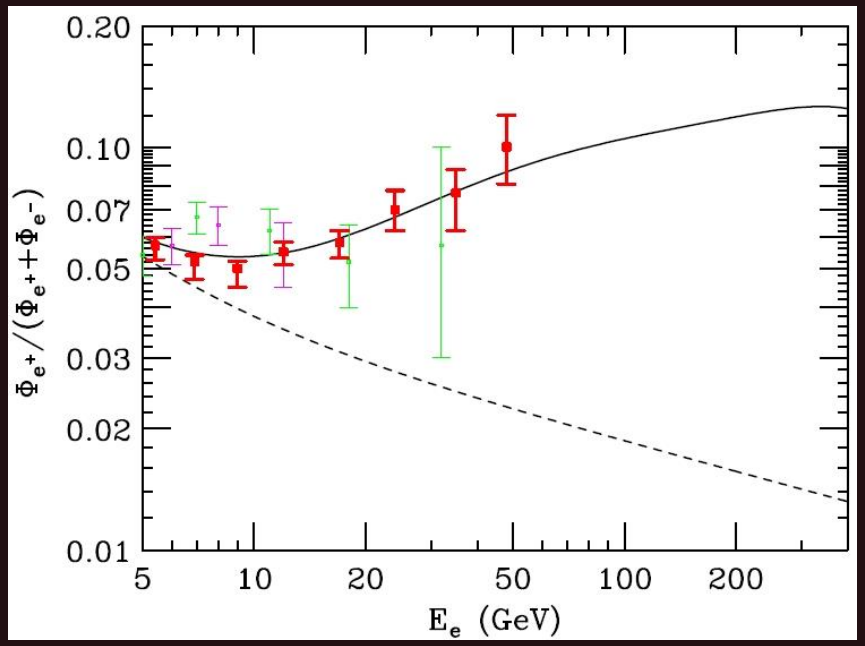

Geminga, PSR B0656+14, and all PSRs

[O. Adriani et al.] arXiv:0810.4995

[Dan Hooper et al. 2008 arXiv: 0810.1527]

NS birth rate

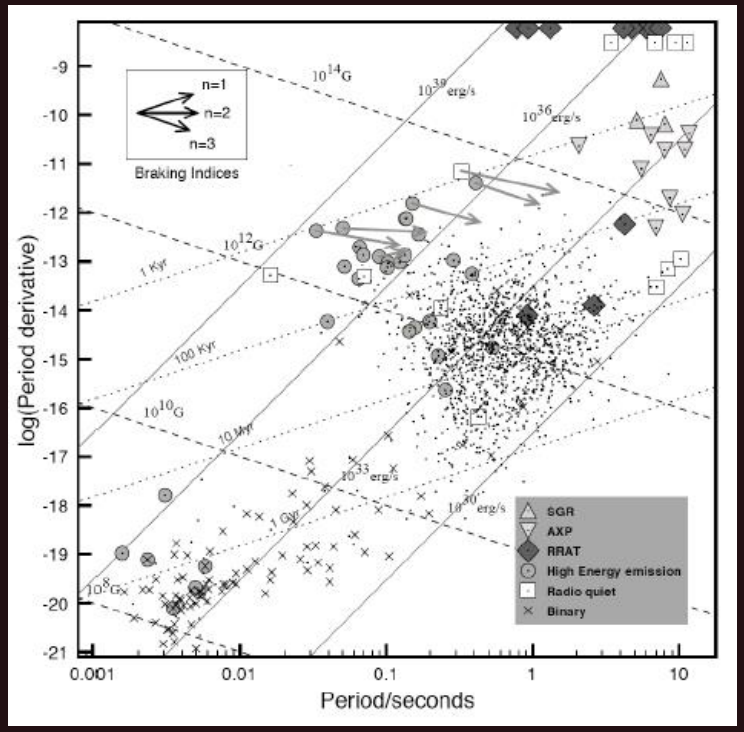

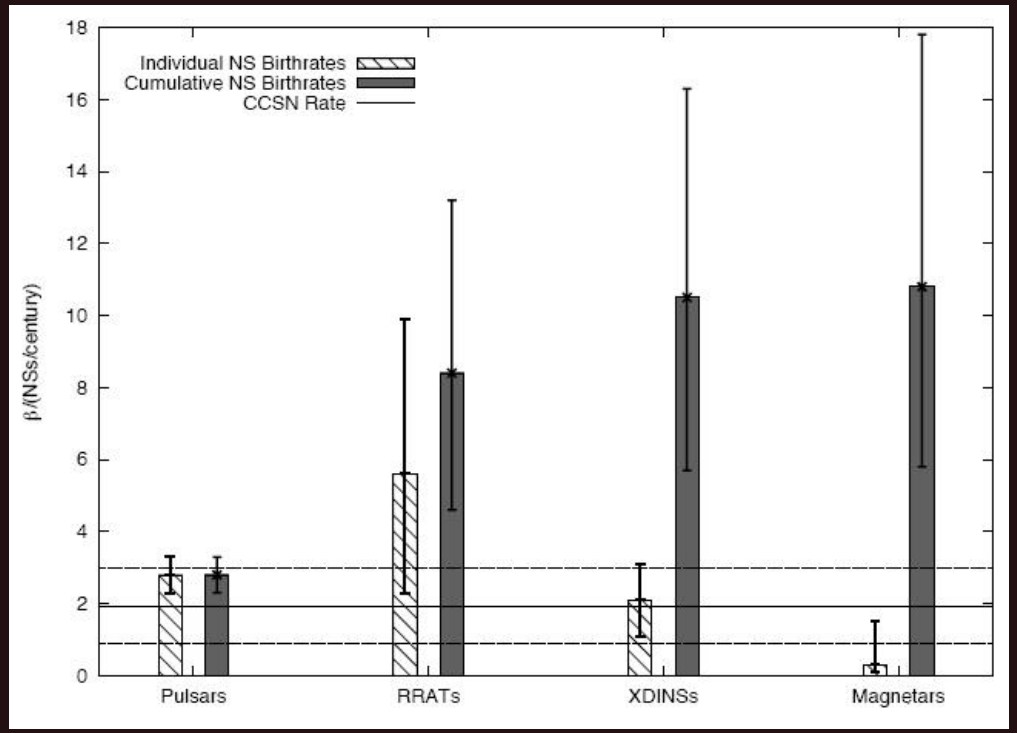

Keane, Kramer 2008, arXiv: 0810.1512

Too many NSs???

$\beta_{\rm PSR}$, $n_{\rm e}$	PSRs	RRATs	XDINSs	Magnetars	Total	CCSN rate
FK06, NE2001	2.8 ± 0.5	$5.6^{+4.3}_{-3.3}$	2.1 ± 1.0	$0.3^{+1.2}_{-0.2}$	$10.8^{+7.0}_{-5.0}$	1.9 ± 1.1
L+06, NE2001	1.4 ± 0.2	$2.8^{+1.6}_{-1.6}$	2.1 ± 1.0	$0.3^{+1.2}_{-0.2}$	$6.6^{+4.0}_{-3.0}$	1.9 ± 1.1
L+06, TC93	1.1 ± 0.2	$2.2^{+1.7}_{-1.3}$	2.1 ± 1.0	$0.3^{+1.2}_{-0.2}$	$5.7^{+4.1}_{-2.7}$	1.9 ± 1.1
V+04, NE2001	1.6 ± 0.3	$3.2^{+2.5}_{-1.9}$	2.1 ± 1.0	$0.3^{+1.2}_{-0.2}$	$7.2^{+5.0}_{-3.4}$	1.9 ± 1.1
V+04, TC93	1.1 ± 0.2	$2.2^{+1.7}_{-1.3}$	2.1 ± 1.0	$0.3^{+1.2}_{-0.2}$	$5.7^{+4.1}_{-2.7}$	1.9 ± 1.1

It seems, that the total birth rate is larger than the rate of CCSN.
e^- - capture SN cannot save the situation, as they are <~20%.

Note, that the authors do not include CCOs.

So, some estimates are wrong, or some sources evolve into others.

See also astro-ph/0603258.

GRAND UNIFICATION: 1005.0876

Keane, Kramer 2008, arXiv: 0810.1512

Conclusion

- There are several types of sources: CCOs, M7,

  SGRs, AXPs, RRATs ...
- Magnetars
- Significant fraction of all newborn NSs are not similar to the Crab pulsar
- Unsolved problems:

  1. Are there links?

  2. Reasons for diversity

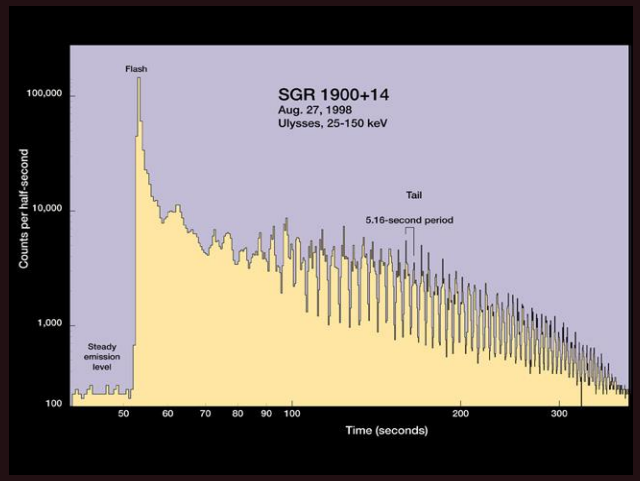

Some reviews on isolated neutron stars

- NS basics: physics/0503245, astro-ph/0405262
- Thermal emission 1507.06186
- Magnetars: 1507.02924
- Magnetar bursts: arXiv: 1101.4472
- CCOs: astro-ph/0311526, arxiv:0712.2209
- Quark stars: arxiv:0809.4228
- The Magnificent Seven: astro-ph/0609066, arxiv:0801.1143
- RRATs: arXiv:1008.3693
- Cooling of NSs: astro-ph/0402143
- NS structure arXiv:0705.2708
- EoS arXiv: 1001.3294, 1512.07820
- NS atmospheres 1403.0074
- NS magnetic fields arxiv:0711.3650
- Different types arXiv:1005.0876, arXiv:1302.0869, arXiv: 1712.06040
- Radio pulsars 1602.07738

- Internal structure and astrophysics 1603.02698
- SN and compact remnants 1806.07267

Lectures can be found at my homepage:

http://xray.sai.msu.ru/~polar/html/presentations.html

Read the OVERVIEW in the book by Haensel, Yakovlev, Potekhin

Internal structure of Neutron Stars

Artistic view

Astronomy meets QCD

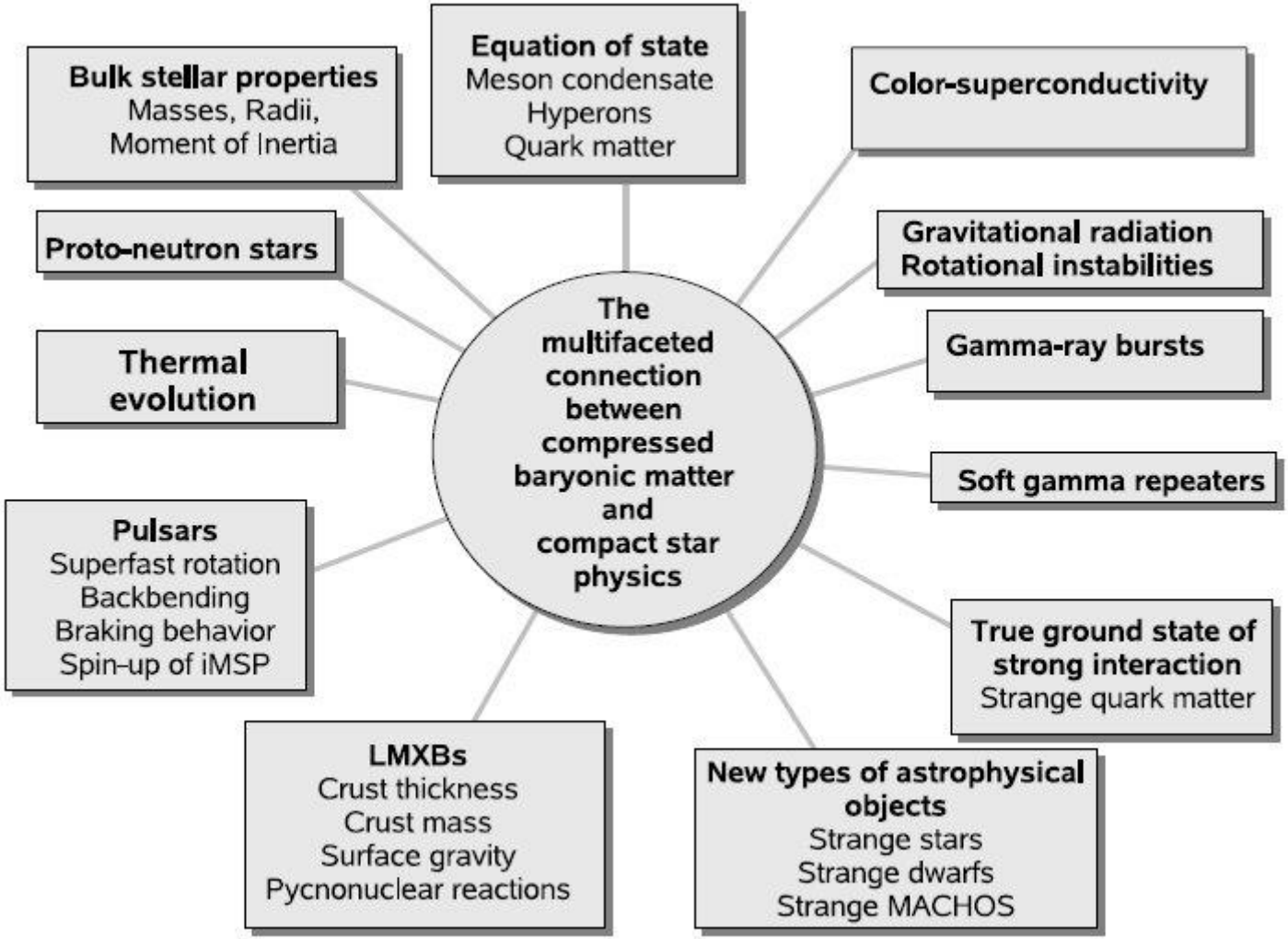

arXiv: 0808.1279

Hydrostatic equilibrium for a star

$$\begin{cases} (1) & \dfrac{dP}{dr} = -\dfrac{Gm\rho}{r^2} \qquad m = m(r) \\ (2) & \dfrac{dm}{dr} = 4\pi\rho\, r^2 \\ (3) & \dfrac{dS}{dt} = Q \\ (4) & P = P(\rho) \end{cases}$$

For NSs we can take T=0
and neglect the third equation

For a NS effects of GR are also important.

$$r_g = \frac{2GM}{c^2} \approx 2.95 \ \frac{M}{M_{SUN}} \ \text{km}$$

$M/R \sim 0.15\ (M/M_\odot)(R/10\ \text{km})^{-1}$
$J/M \sim 0.25\ (1\ \text{ms}/P)\ (M/M_\odot)(R/10\text{km})^2$

Lane-Emden equation. Polytrops.

$$P = K\rho^{\gamma}, \quad K, \gamma = \text{const}, \quad \gamma = 1 + \frac{1}{n}$$

$$\frac{dP}{dr} = -\frac{Gm\rho}{r^2} = g\rho, \qquad g = -\frac{Gm}{r^2} = -\frac{d\varphi}{dr}$$

$$\frac{dP}{dr} = -\rho \frac{d\varphi}{dr}, \qquad \Delta\varphi = 4\pi G\rho$$

$$\rho = \rho_c \Theta^n, \qquad \Theta = 1 \ \text{при} \ r = 0$$

$$P = K\rho_c^{1+1/n} \Theta^{1+n}, \qquad \frac{dP}{dr} = (n+1)K\rho_c^{1+1/n} \Theta^n \frac{d\Theta}{dr}$$

$$\frac{d\varphi}{dr} = -(n+1)K\rho_c^{1/n} \frac{d\Theta}{dr}$$

$$\Delta\Theta = -\frac{4\pi G\rho_c^{1-1/n}}{(n+1)K} \Theta^n$$

$$\xi = r/a, \qquad a^2 = (n+1)K\rho_c^{1/n-1}/(4\pi G)$$

$$\frac{1}{\xi^2}\frac{d}{d\xi}\xi^2\frac{d}{d\xi}\Theta = -\Theta^n$$

$$\Theta = \Theta(\xi)$$

$$0 \le \xi \le \xi_1$$

$$\Theta(0) = 1, \quad \Theta'(0) = 0$$

$$\Theta(\xi_1) = 0$$

Properties of polytropic stars

Analytic solutions:

$$n=0 \qquad \Theta = 1-\frac{\xi^2}{6} \qquad \xi_1 = \sqrt{6}$$

$$n=1 \qquad \Theta = \frac{\sin\xi}{\xi} \qquad \xi_1 = \pi$$

$$n=5 \qquad \Theta = \frac{1}{\sqrt{1+\xi^2/3}} \qquad \xi_1 = \infty$$

$$M = 4\pi \int_0^R dr\, r^2 \rho = 4\pi \rho_c a^3 \xi_1^2 \,|\Theta'(\xi_1)|$$

$$\frac{\rho_c}{\bar{\rho}} = \frac{4\pi R^3 \rho_c}{3M} = \frac{\xi_1}{3|\Theta'(\xi_1)|}$$

↓ γ=5/3 ↓ γ=4/3

n	**0**	**1**	**1.5**	**2**	**3**
ξ_1	**2.449**	**3.142**	**3.654**	**4.353**	**6.897**
$\lvert\Theta'_1\rvert$	**0.7789**	**0.3183**	**0.2033**	**0.1272**	**0.04243**
$\rho_c/\bar{\rho}$	**1**	**3.290**	**5.991**	**11.41**	**54.04**

$$M \sim \rho_c^{(3-n)/(2n)}$$

$$R \sim \rho_c^{(1-n)/(2n)}$$

$$M \sim R^{(3-n)/(1-n)}$$

$$n=0 \qquad M \sim R^3$$

$$n=1 \qquad M \sim \rho_c \qquad R = \text{const}$$

$$n=1.5 \qquad M \sim \sqrt{\rho_c} \sim R^{-3}$$

$$n=3 \qquad M = \text{const} \qquad R \sim \rho_c^{-1/3}$$

Useful equations

White dwarfs

1. Non-relativistic electrons
   $\gamma=5/3$, $K=(3^{2/3}\,\pi^{4/3}/5)\,(\hbar^2/m_e m_u^{5/3}\mu_e^{5/3})$;
   μ_e-mean molecular weight per one electron
   $K=1.0036\,10^{13}\,\mu_e^{-5/3}$ (CGS)

2. Relativistic electrons
   $\gamma=4/3$, $K=(3^{1/3}\,\pi^{2/3}/4)\,(\hbar c/m_u^{4/3}\mu_e^{4/3})$;
   $K=1.2435\,10^{15}\,\mu_e^{-4/3}$ (CGS)

Neutron stars

1. Non-relativistic neutrons
   $\gamma=5/3$, $K=(3^{2/3}\,\pi^{4/3}/5)\,(\hbar^2/m_n^{8/3})$;
   $K=5.3802\,10^{9}$ (CGS)

2. Relativistic neutrons
   $\gamma=4/3$, $K=(3^{1/3}\,\pi^{2/3}/4)\,(\hbar c/m_n^{4/3})$;
   $K=1.2293\,10^{15}$ (CGS)

[Shapiro, Teukolsky]

Neutron stars

Superdense matter and superstrong magnetic fields

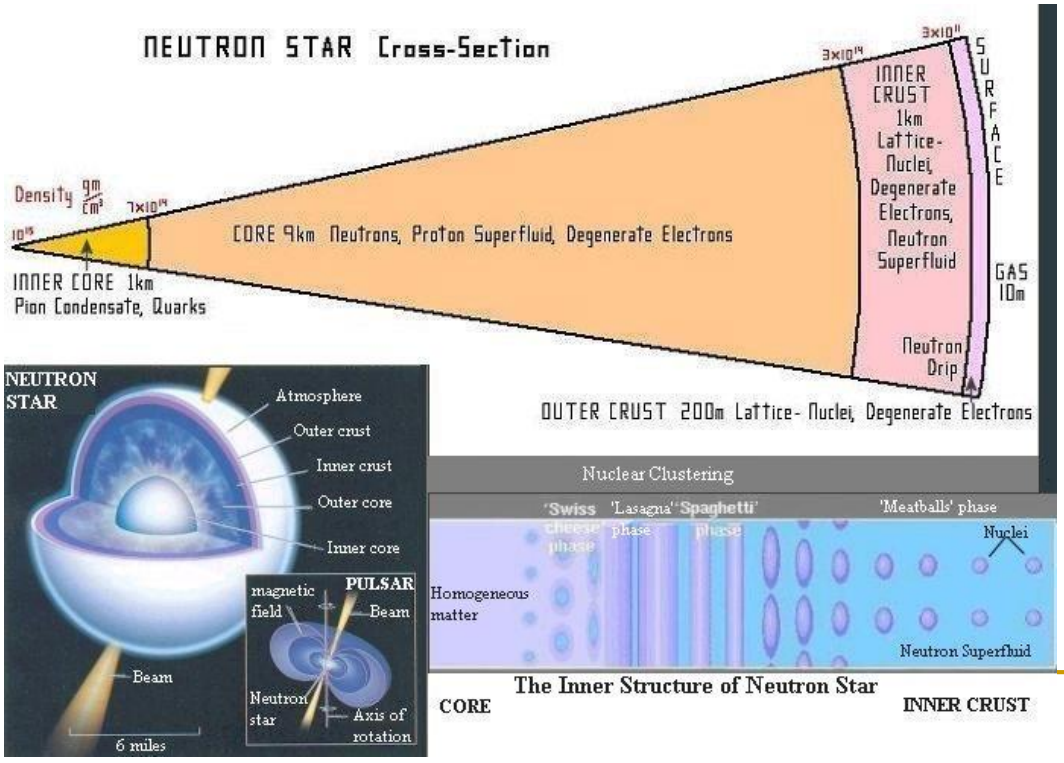

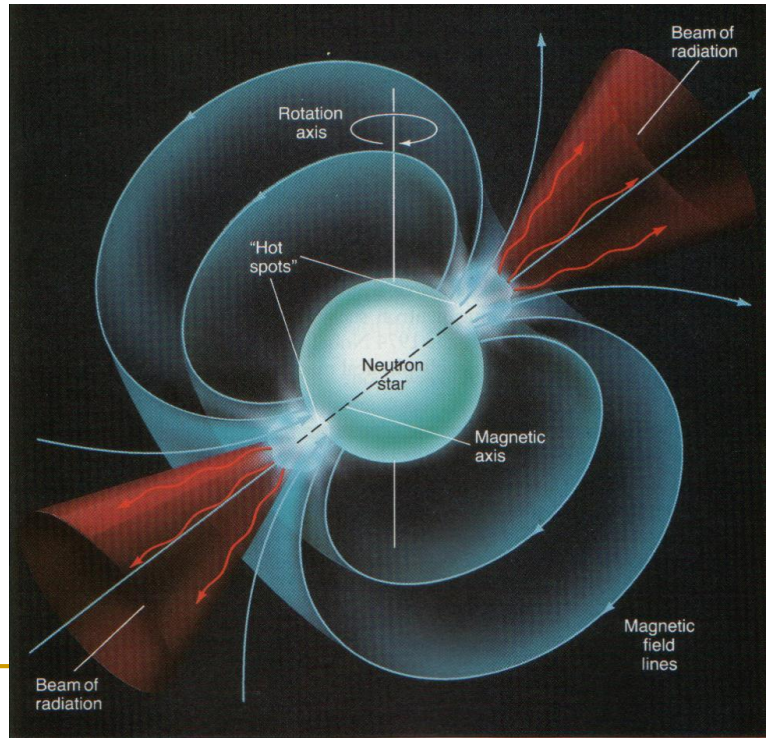

Proto-neutron stars

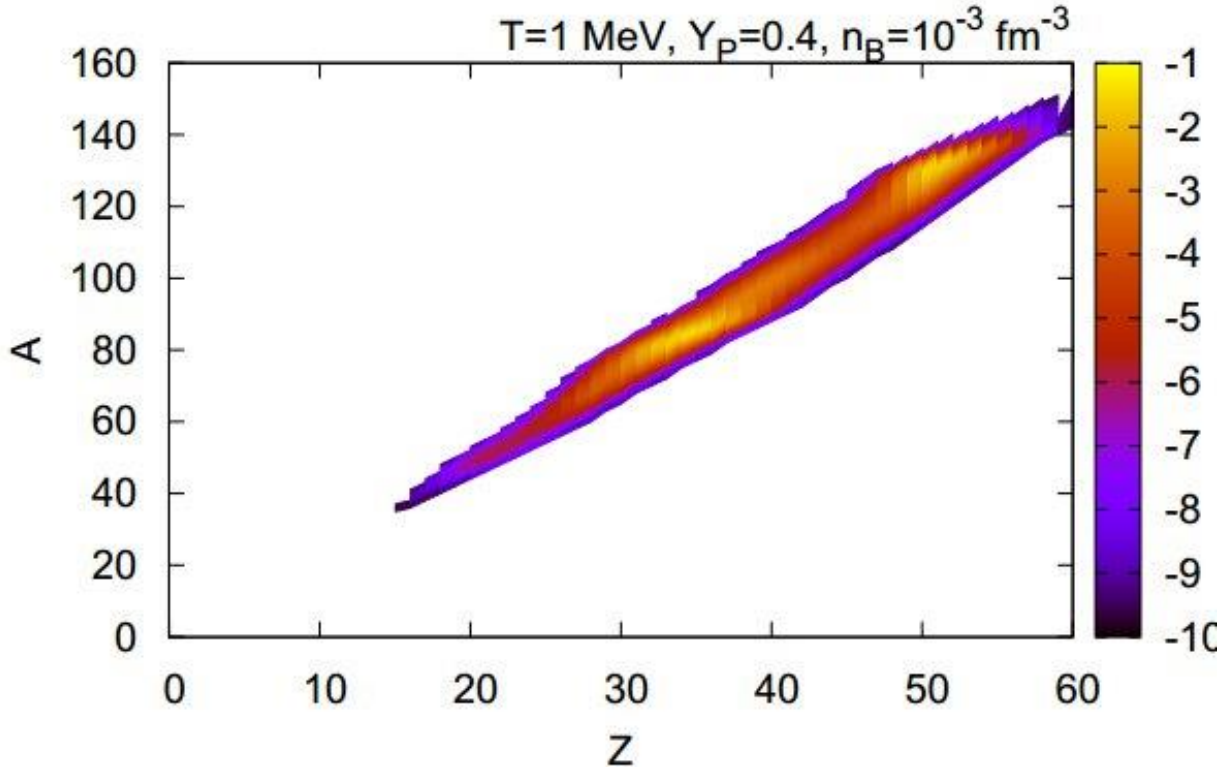

Mass fraction of nuclei in the nuclear chart for matter at T = 1 MeV, $n_B = 10^{-3}$ fm^{-3}, and $Y_P = 0.4$. Different colors indicate mass fraction in Log_{10} scale.

1202.5791

NS EoS are also important for SN explosion calculation, see 1207.2184

EoS for core-collapse, proto-NS and NS-NS mergers

	Core-collapse supernovae	Proto-neutron stars	Mergers of compact binary stars
n/n_s	10^{-8} - 10	10^{-8} - 10	10^{-8} - 10
T(MeV)	0 - 30	0 - 50	0 - 100
Y_e	0.35 - 0.45	0.01 - 0.3	0.01 - 0.6
$S(k_B)$	0.5 - 10	0 - 10	0 - 100

Wide ranges of parameters

1512.07820

Astrophysical point of view

Astrophysical appearence of NSs is mainly determined by:

- **Spin**
- **Magnetic field**
- **Temperature**
- **Velocity**
- **Environment**

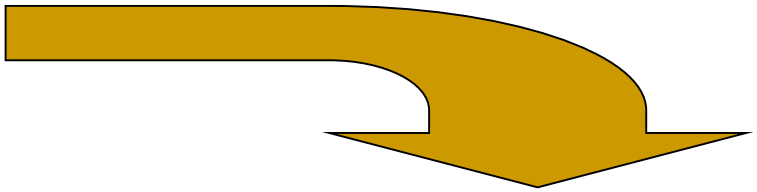

The first four are related to the NS structure!

Equator and radius

$$ds^2=c^2dt^2e^{2\Phi}-e^{2\lambda}dr^2-r^2[d\theta^2+\sin^2\theta d\varphi^2]$$

In flat space $\Phi(r)$ and $\lambda(r)$ are equal to zero.

- $t=\text{const},\ r=\text{const},\ \theta=\pi/2,\ 0<\Phi<2\pi$ ⇒ $l=2\pi r$
- $t=\text{const},\ \theta=\text{const},\ \varphi=\text{const},\ 0<r<r_0$ ⇒ $dl=e^{\lambda}dr$ ⇒ $l=\int_0^{r_0} e^{\lambda}dr \neq r_0$

Gravitational redshift

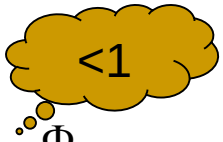

$$d\tau = dt\, e^{\Phi}, \qquad \nu_r = \frac{dN}{d\tau} = e^{-\Phi}\frac{dN}{dt}$$

→ Frequency emitted at r

$$r \to \infty \qquad \Phi \to 0 \qquad \nu_\infty = \frac{dN}{dt}$$

→ Frequency detected by an observer at infinity

$$\nu_\infty = \nu_r\, e^{\Phi} \quad \Rightarrow \quad \Phi(r)$$

→ This function determines gravitational redshift

$$e^{2\lambda} \equiv \frac{1}{1-\dfrac{2Gm}{c^2 r}}$$

It is useful to use m(r) – gravitational mass inside r – instead of λ(r)

Outside of the star

$$r > R \Rightarrow m(r) = M = \text{const}$$

$$e^{2\Phi} = 1 - \frac{2GM}{c^2 r} = 1 - \frac{r_g}{r}, \qquad r_g = \frac{2GM}{c^2}$$

$$ds^2 = \left(1 - \frac{r_g}{r}\right) c^2\, dt^2 - \left(1 - \frac{r_g}{r}\right)^{-1} dr^2 - r^2\, d\Omega^2$$

$$\nu_\infty = \nu_r \sqrt{1 - \frac{r_g}{r}} \longrightarrow \text{redshift}$$

Bounding energy $\longrightarrow$ $\Delta M = M_b - M \sim 0.2\ M_{\text{sun}}$

Apparent radius $\longrightarrow$ $R_\infty = R / \sqrt{1 - r_g / R}$

Bounding energy

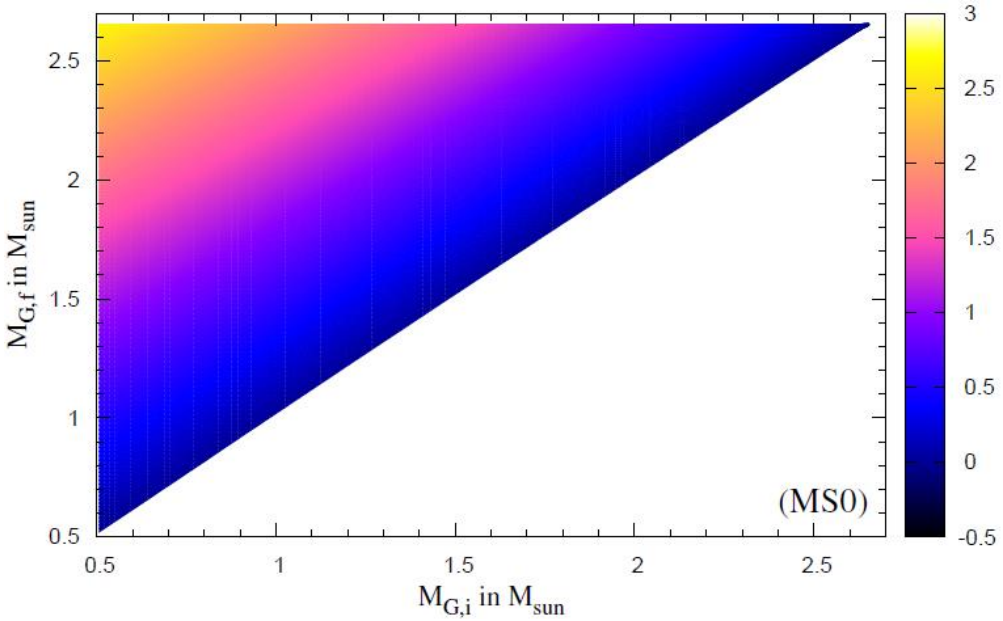

If you drop a kilo on a NS, then you increase its mass for < kilo

M_{acc} is shown with color

$M_{G,i}$ $(M_\odot)$	ΔM_G $(M_\odot)$	$M_{B,i}$ $(M_\odot)$		M_{acc} (ΔM_B) $(M_\odot)$	
		APR	MS0	APR	MS0
1.4	0.57	1.554	1.525	0.768	0.712
1.5	0.47	1.681	1.647	0.641	0.591
1.6	0.37	1.811	1.767	0.511	0.470
1.7	0.27	1.943	1.892	0.379	0.345
1.8	0.17	2.080	2.018	0.242	0.219
1.9	0.07	2.221	2.146	0.101	0.091

$M_{acc}=\Delta M_G+\Delta BE/c^2=\Delta M_B$
BE- binding energy
$BE=(M_B-M_G)c^2$

1102.2912

TOV equation

$$R_{ik} - \frac{1}{2} g_{ik} R = \frac{8\pi G}{c^4} T_{ik}$$

$$\begin{cases} (1) & \dfrac{dP}{dr} = -\dfrac{G\rho m}{r^2}\left(1+\dfrac{P}{\rho c^2}\right)\left(1+\dfrac{4\pi r^3 P}{mc^2}\right)\left(1-\dfrac{2Gm}{rc^2}\right)^{-1} \\ (2) & \dfrac{dm}{dr} = 4\pi r^2 \rho \\ (3) & \dfrac{d\Phi}{dr} = -\dfrac{1}{\rho c^2}\dfrac{dP}{dr}\left(1+\dfrac{P}{\rho c^2}\right)^{-1} \\ (4) & P = P(\rho) \end{cases}$$

Tolman (1939)
Oppenheimer-Volkoff (1939)

Structure and layers

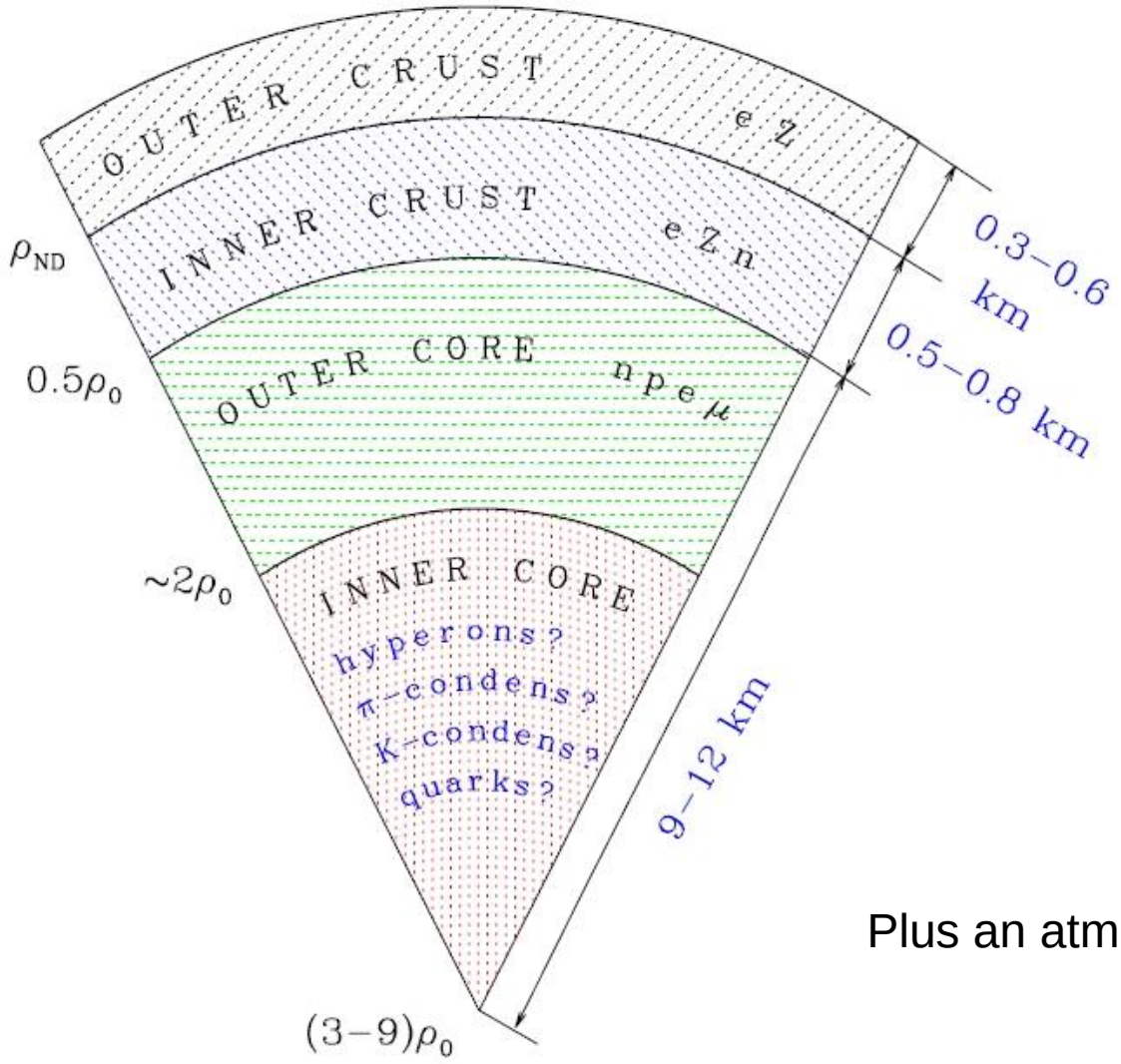

Plus an atmosphere...

Neutron star interiors

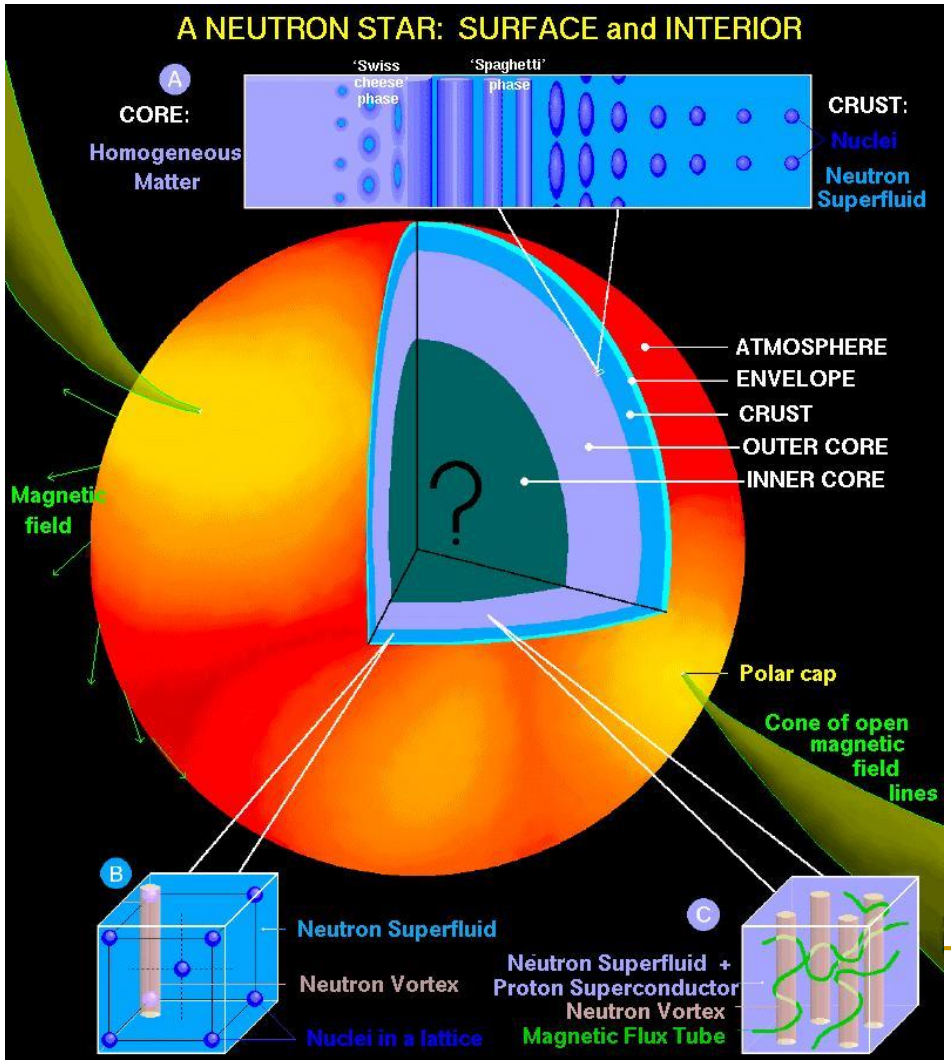

Radius: 10 km
Mass: 1-2 solar
Density: above the nuclear
Strong magnetic fields

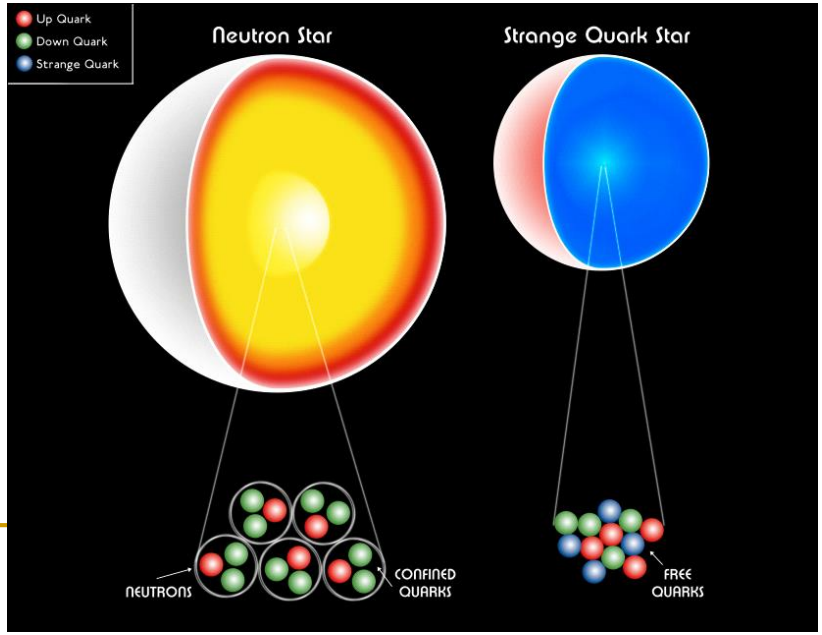

Neutron star crust

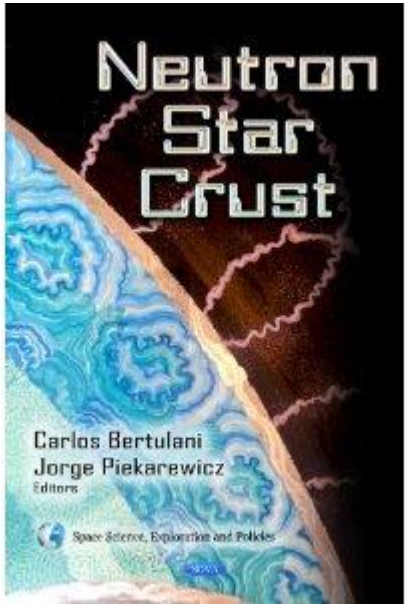

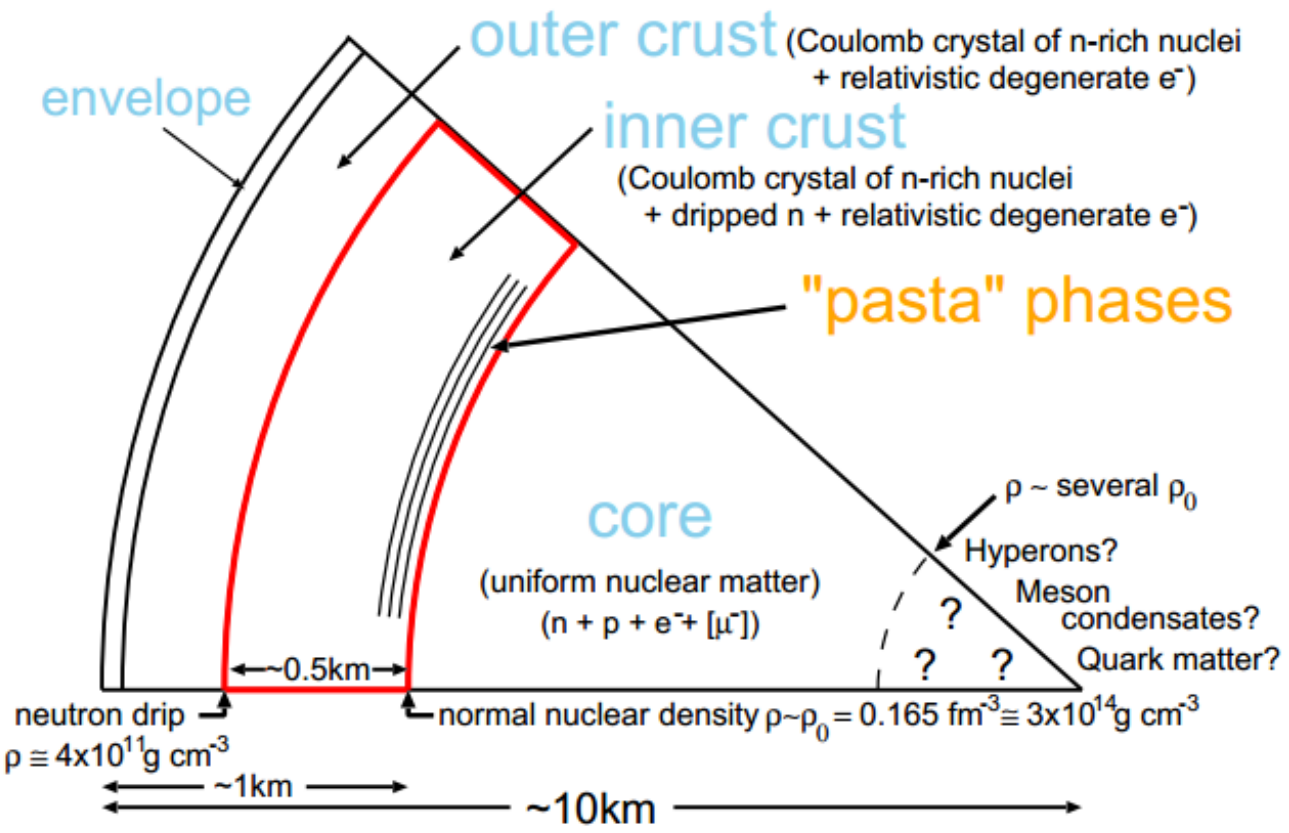

Many contributions to the book are available in the arXiv.

Mechanical properties of crusts are continuosly discussed, see 1208.3258

Inner crust properties

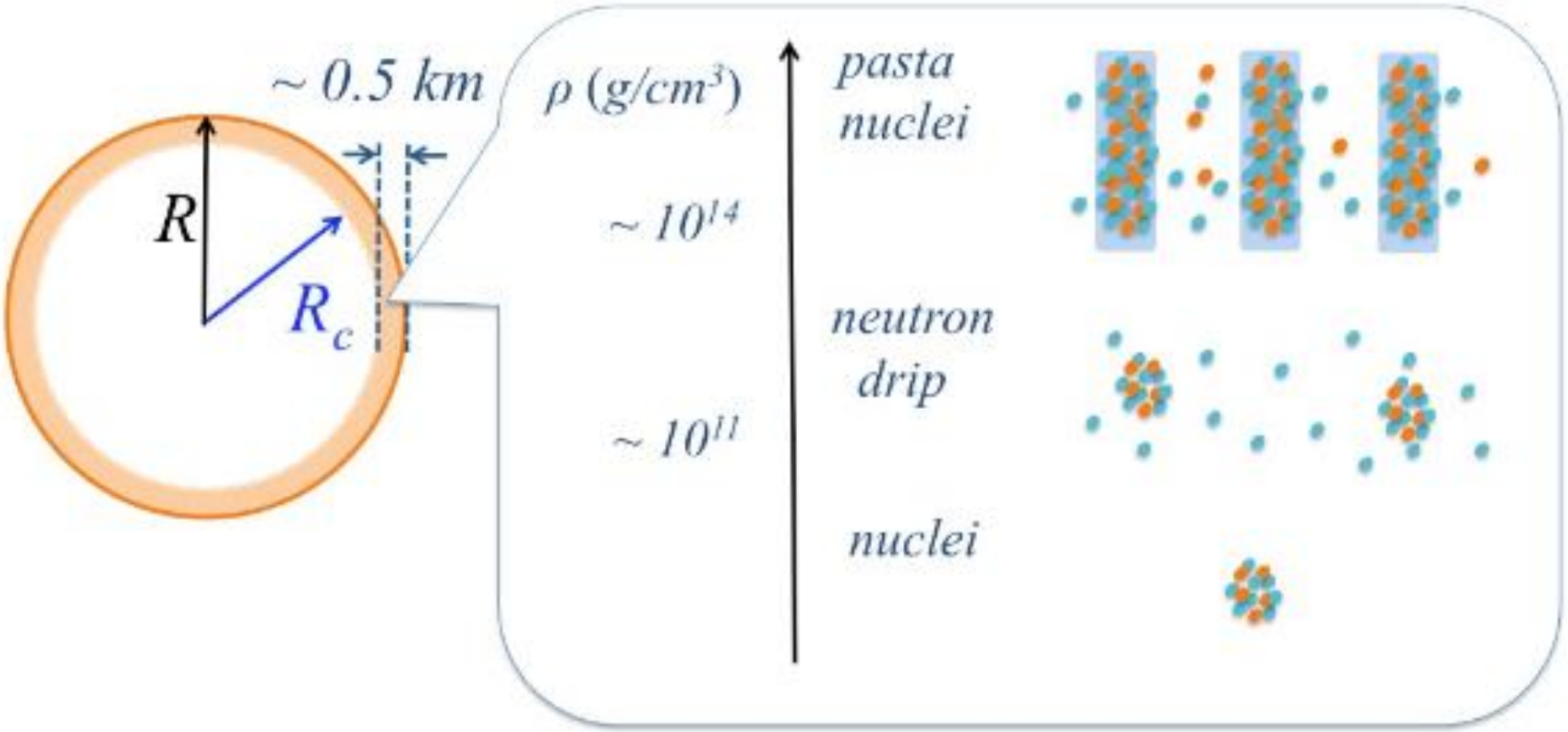

1707.04966

Accreted crust

It is interesting that the crust formed by accreted matter differs from the crust formed from catalyzed matter. The former is thicker.

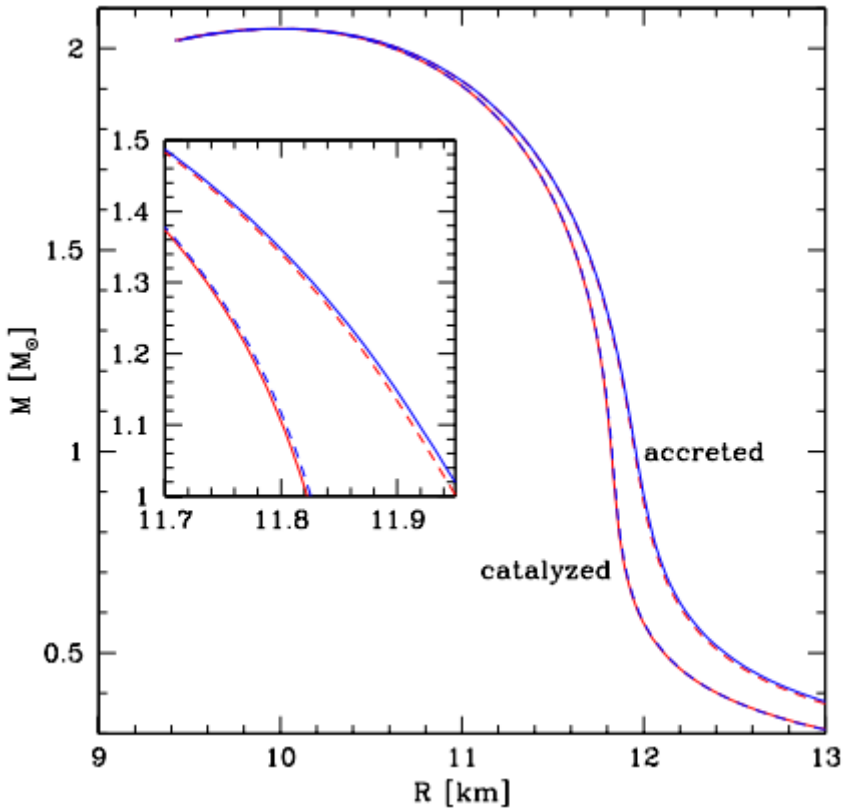

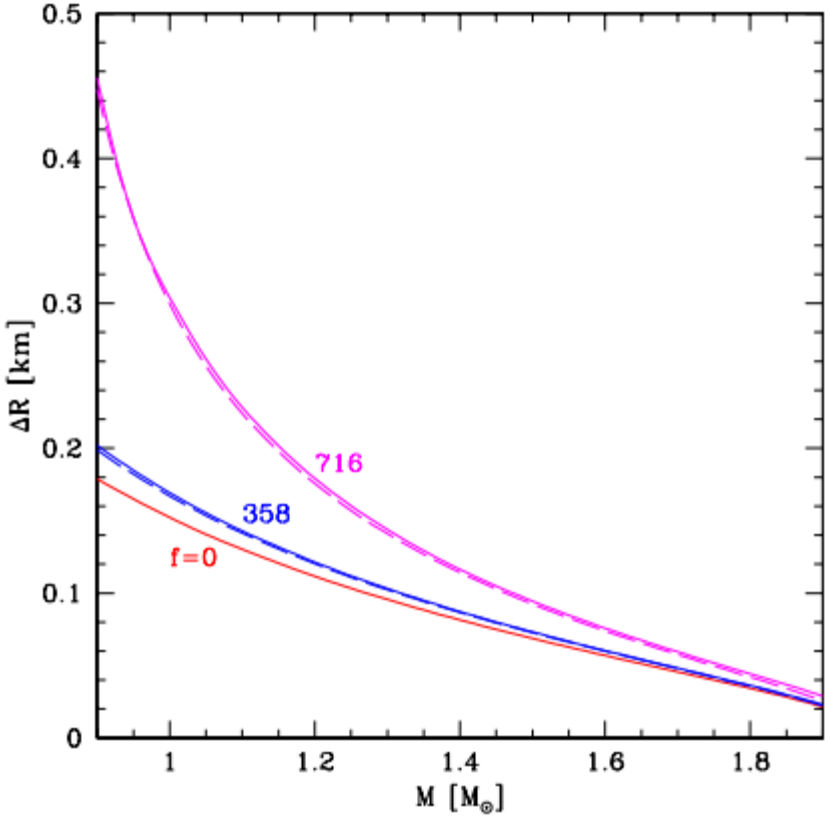

1104.0385

Crust and limiting rotation

Model	σ	$f_{\rm in}^{1.4}$ (Hz)	$f_{\rm fin}^{1.4}$ (Hz)	$f_{\rm in}^{1.8}$ (Hz)	$f_{\rm fin}^{1.8}$ (Hz)
HLPSStiff	0.05	0	326	35	368
	0.10	136	479	236	569
IU-FSU	0.05	349	515	909	1022
	0.10	781	947	1875	1988
IU-FSUmax	0.05	35	358	374	586
	0.10	232	555	854	1066

Failure of the crust can be the reason of the limiting frequency.
Spinning-up of a NS due to accretion can result in crust failure.
Then the shape of the star is deformed, it gains ellipticity.
So, GWs are emitted which slow down the compact object.

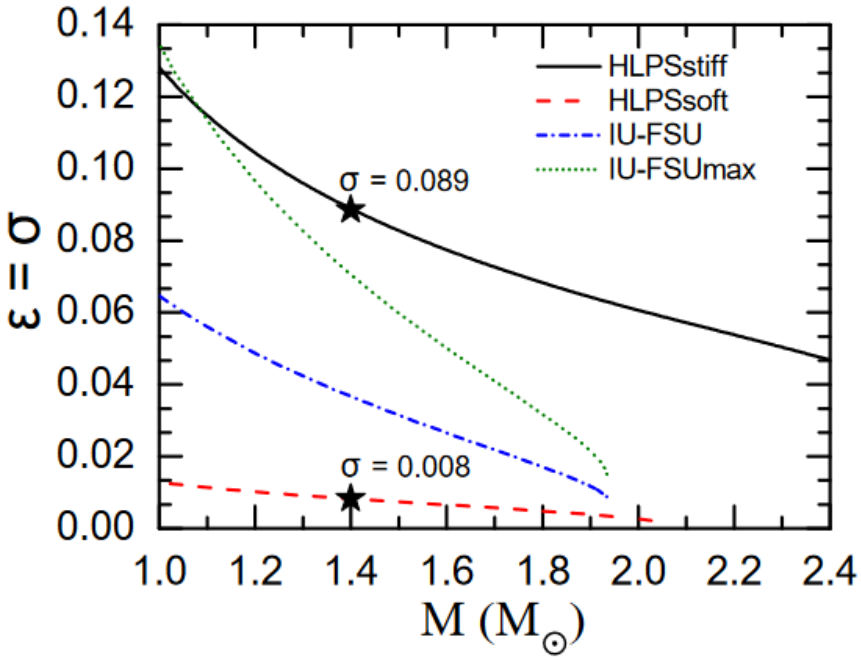

1804.04952

(about limits based on EoS see 1805.11277)

Configurations

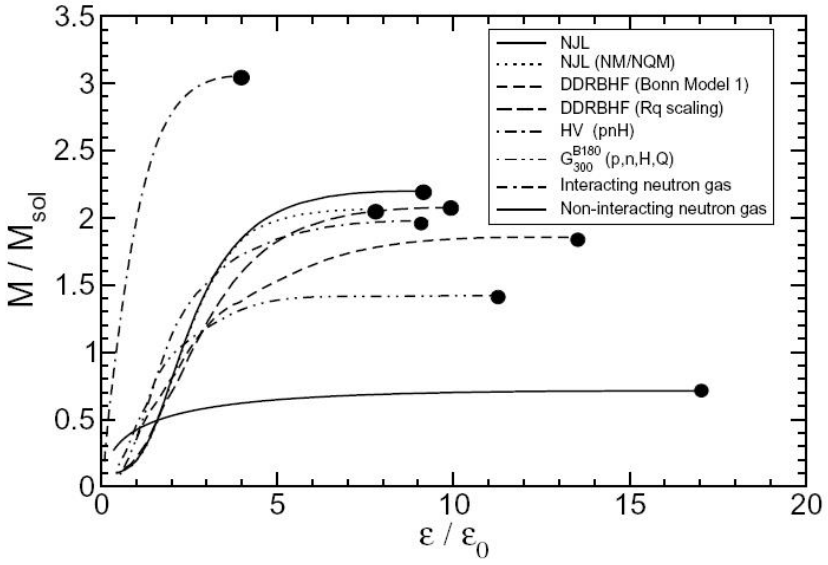

NS mass vs. central density (Weber et al. arXiv: 0705.2708)

Stable configurations for neutron stars and hybrid stars (astro-ph/0611595).

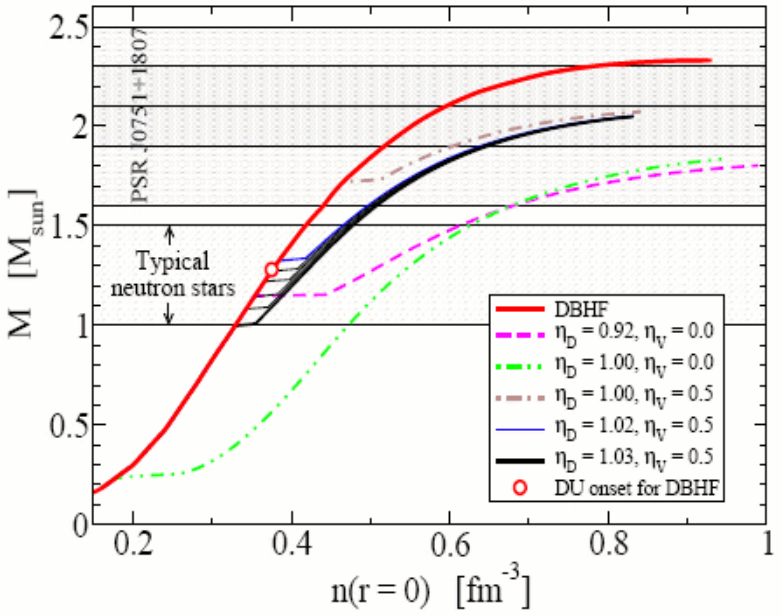

A RNS code is developed and made available to the public by Sterligioulas and Friedman ApJ 444, 306 (1995) http://www.gravity.phys.uwm.edu/rns/

EoS

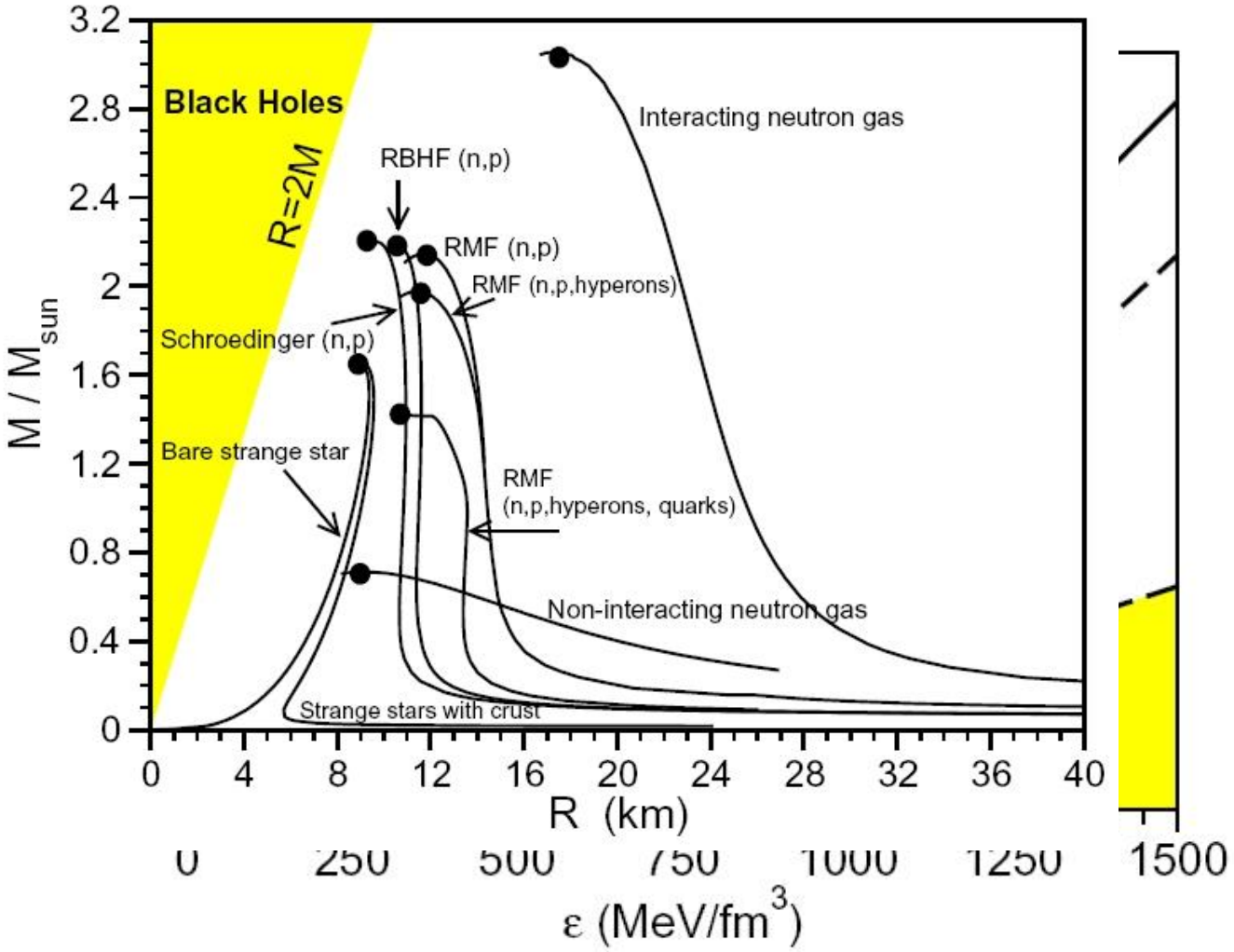

(Weber et al. ArXiv: 0705.2708)

Mass-radius

Mass and radius
are marcoscopical
potentially measured
parameters.
Thus, it is important
to formulate EoS
in terms of these
two parameters.

Mass-radius relations for CSs
with possible phase transition
to deconfined quark matter.

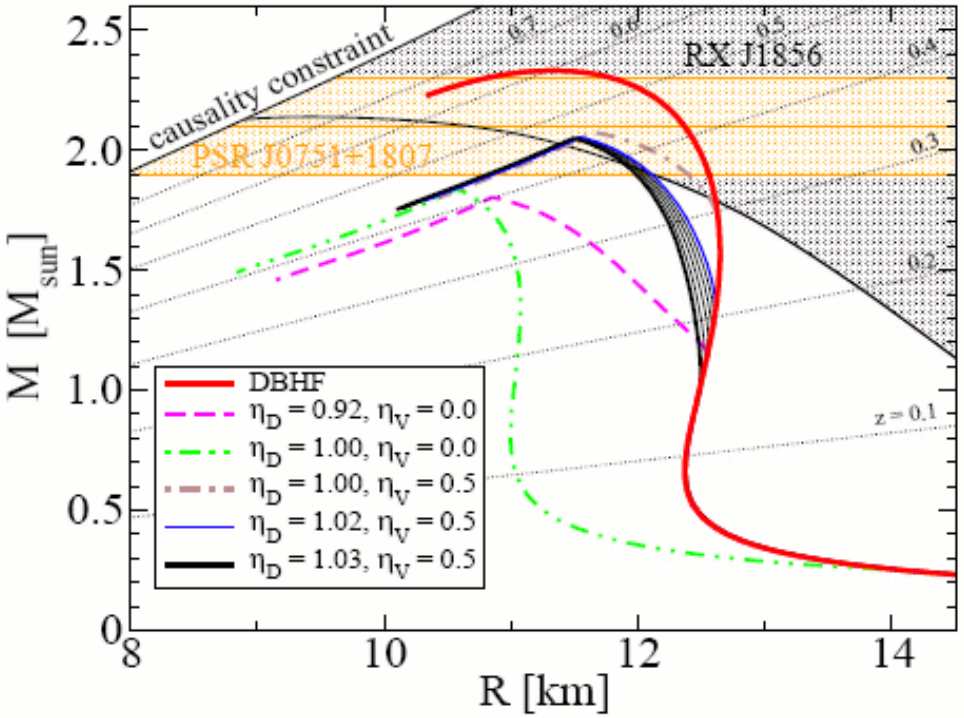

About hyperon stars see a
review in 1002.1658.
About strange stars and some other
exotic options – 1002.1793

astro-ph/0611595

Mass-radius relation

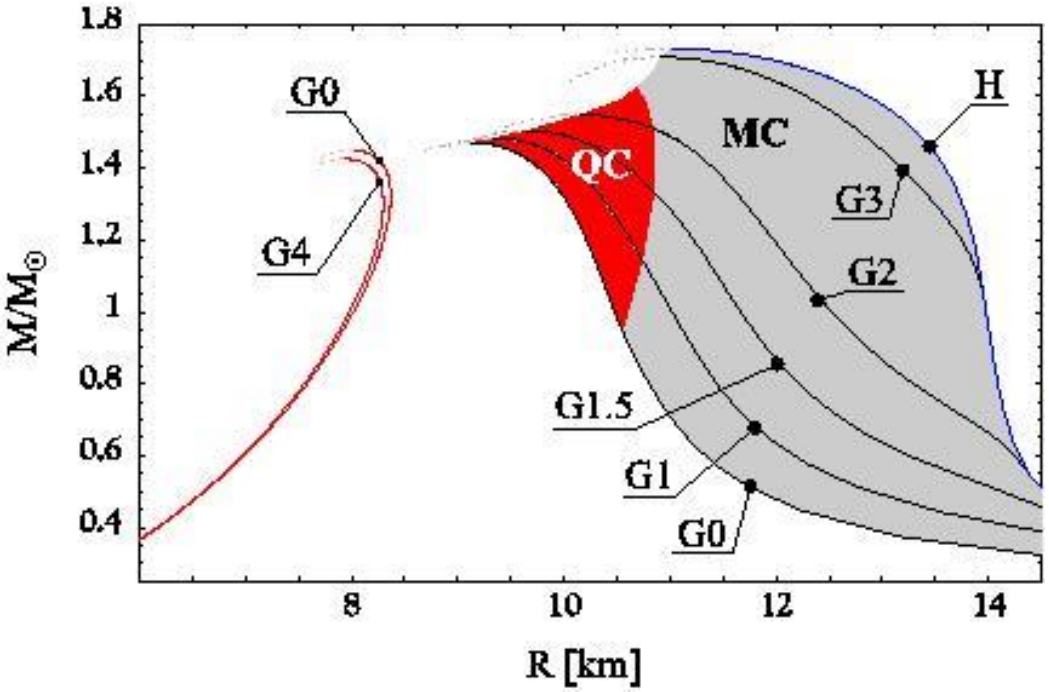

Main features

- Max. mass
- Diff. branches (quark and normal)
- Stiff and soft EoS
- Small differences for realistic parameters
- Softening of an EoS with growing mass

Rotation is neglected here.
Obviously, rotation results in:
- larger max. mass
- larger equatorial radius

Spin-down can result in phase transition, as well as spin-up (due to accreted mass), see 1109.1179

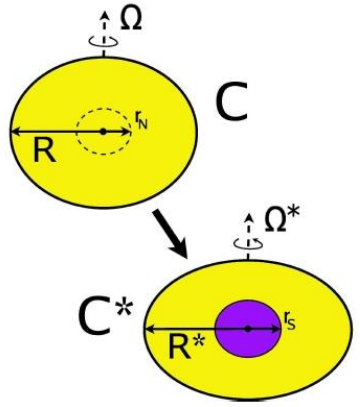

Haensel, Zdunik
astro-ph/0610549

Fitting formulae for moment of inertia

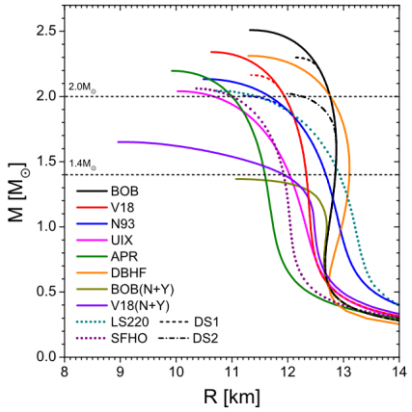

$$\frac{I}{M^3} \equiv 0.8134\,\beta^{-1} + 0.2101\,\beta^{-2} + 0.003175\,\beta^{-3} - 0.0002717\,\beta^{-4} \qquad (18)$$

$$\frac{I}{M^3} \equiv 1.0334\,M^{-1} + 30.7271\,M^{-2} - 12.8839\,M^{-3} + 2.8841\,M^{-4} \qquad (19)$$

$$\beta = Gm/(Rc^2)$$

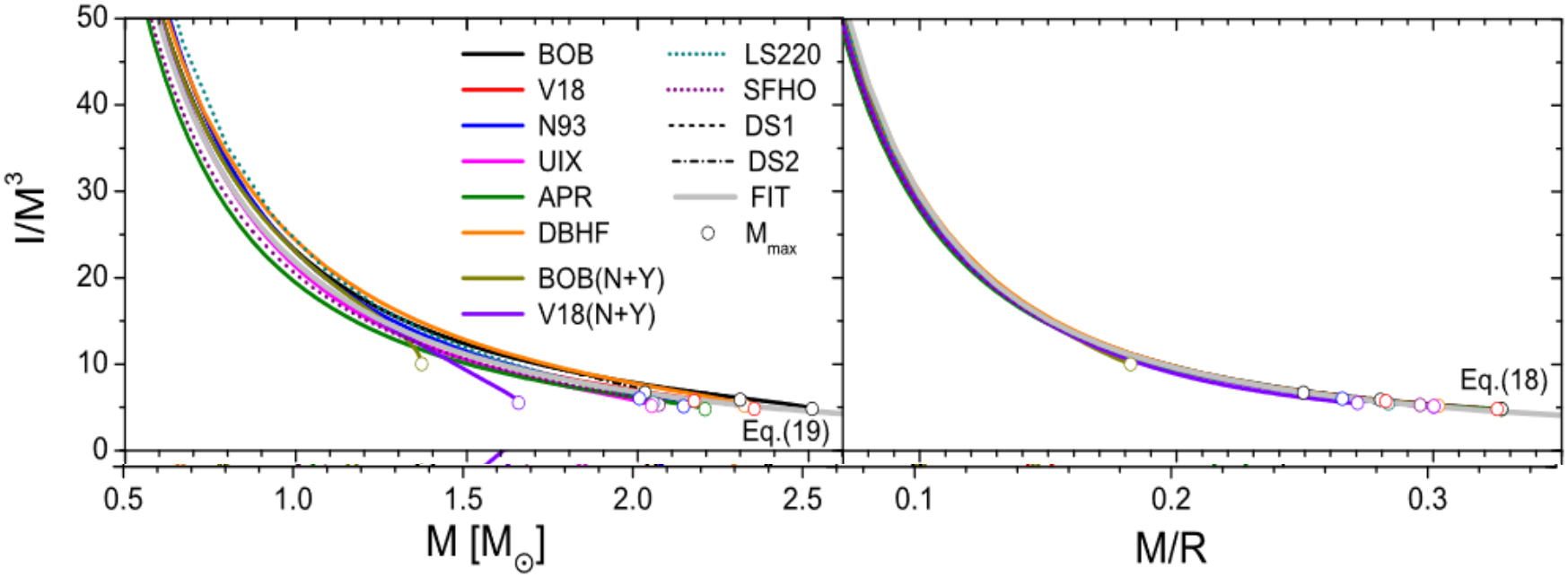

1809.04315

Fits for I/MR^2

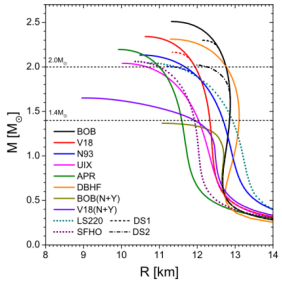

$$\frac{I}{MR^2} \approx (0.237 \pm 0.008)(1 + 2.844\beta + 18.91\beta^4)$$

$$\frac{I}{MR^2} \approx 0.189 + 0.118\frac{M}{M_\odot} \pm 0.016\,.$$

$$\frac{I}{MR^2} \equiv 0.207 + 0.857\beta \pm 0.011$$

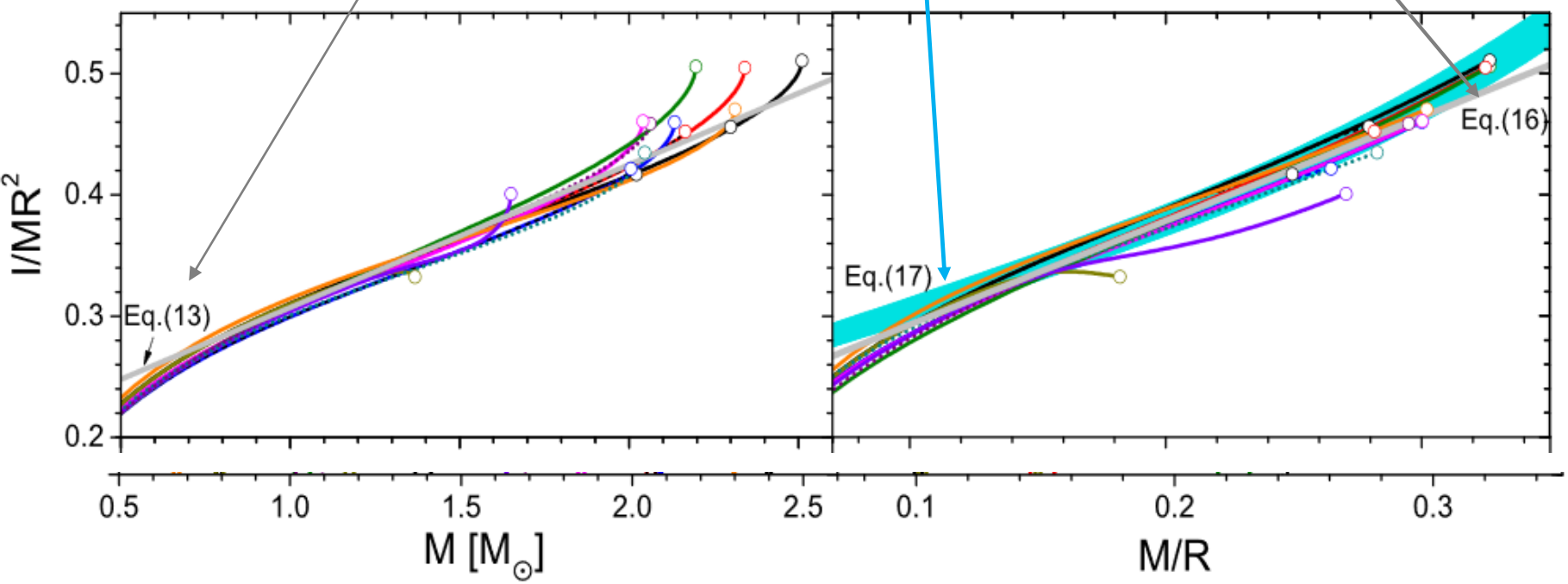

1809.04315

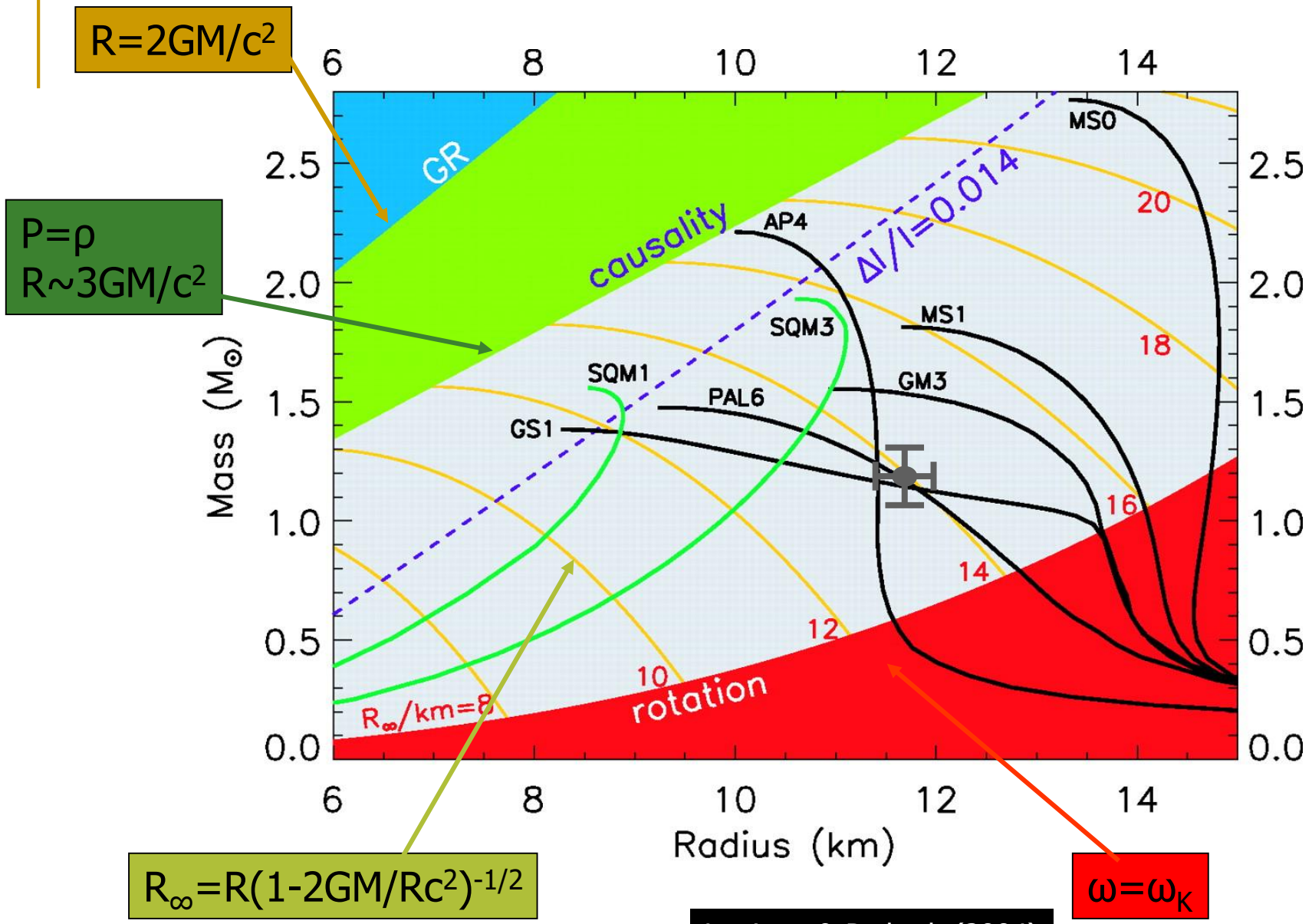

Lattimer & Prakash (2004)

Theory vs. observations

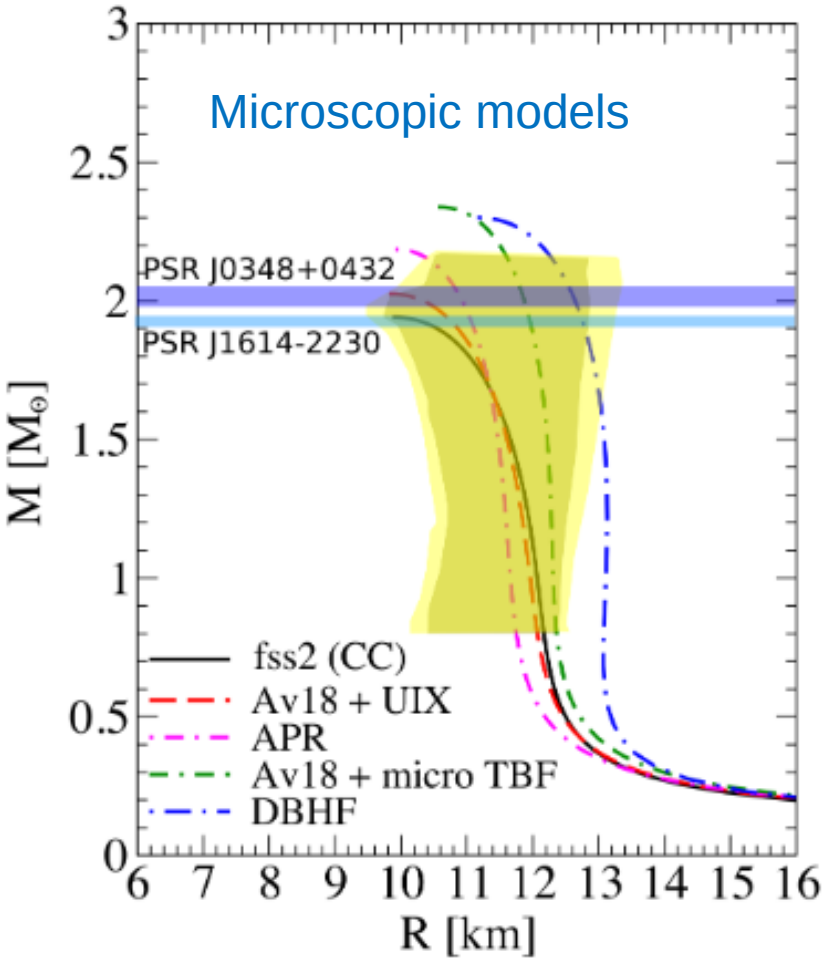

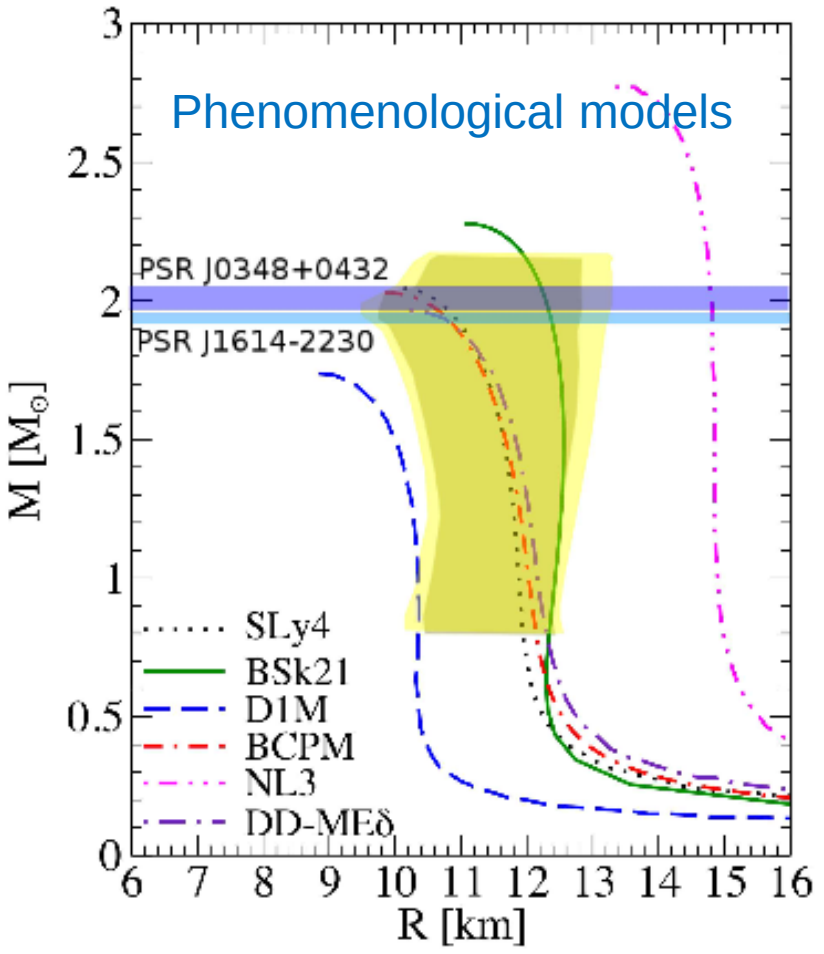

1804.03020

Au-Au collisions

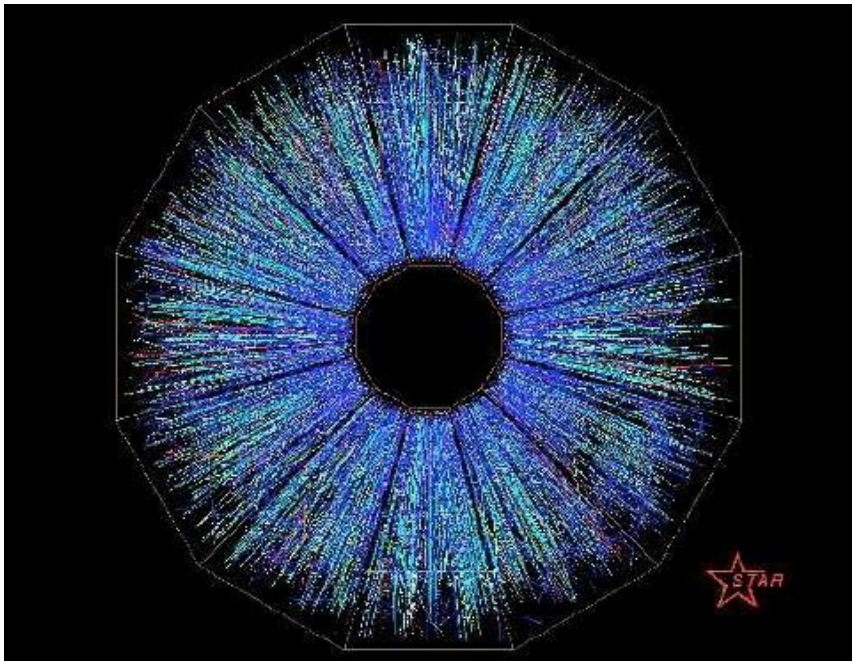

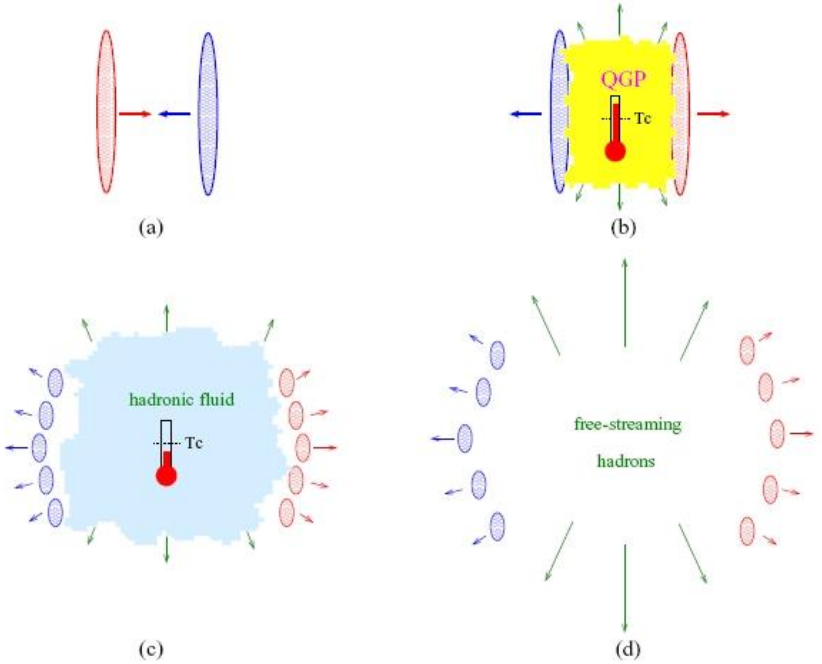

Experimental results and comparison

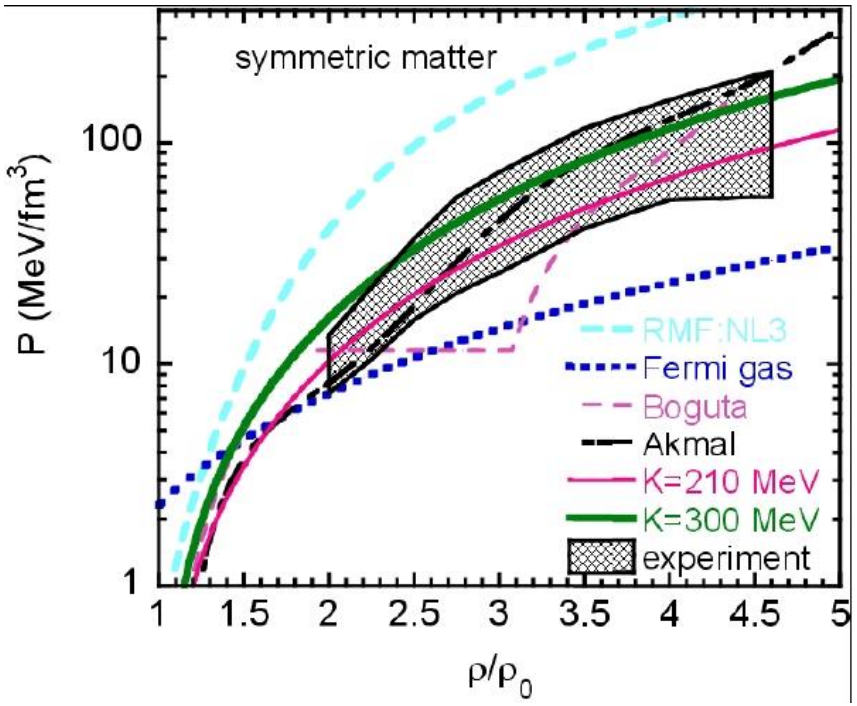

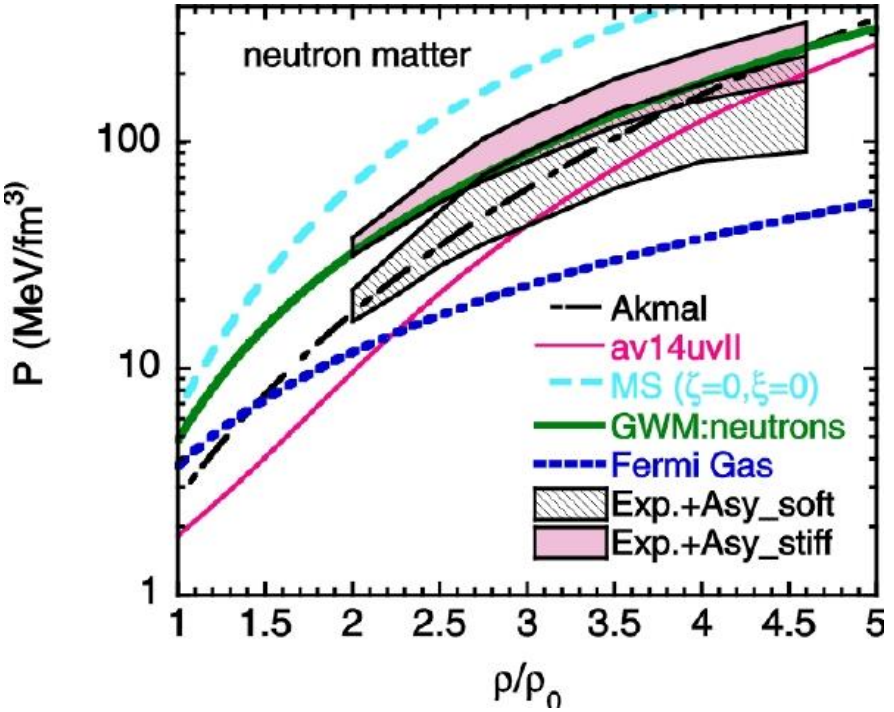

1 Mev/fm^3 = 1.6 10^{32} Pa

GSI-SIS and AGS data

Danielewicz et al. nucl-th/0208016

New heavy-ion data and discussion: 1211.0427

Also laboratory measurements of lead nuclei radius can be important, see 1202.5701

Phase diagram

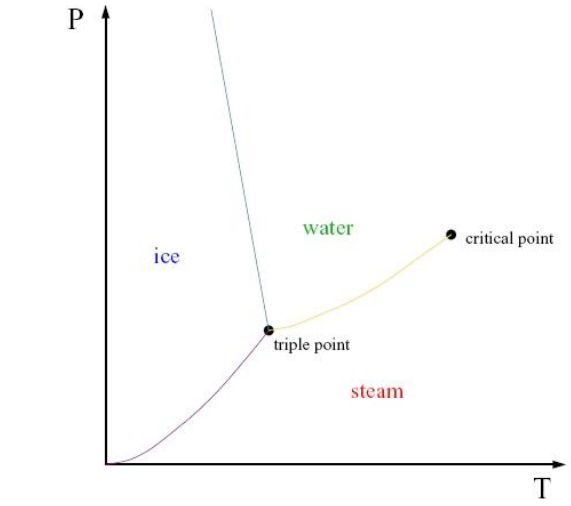

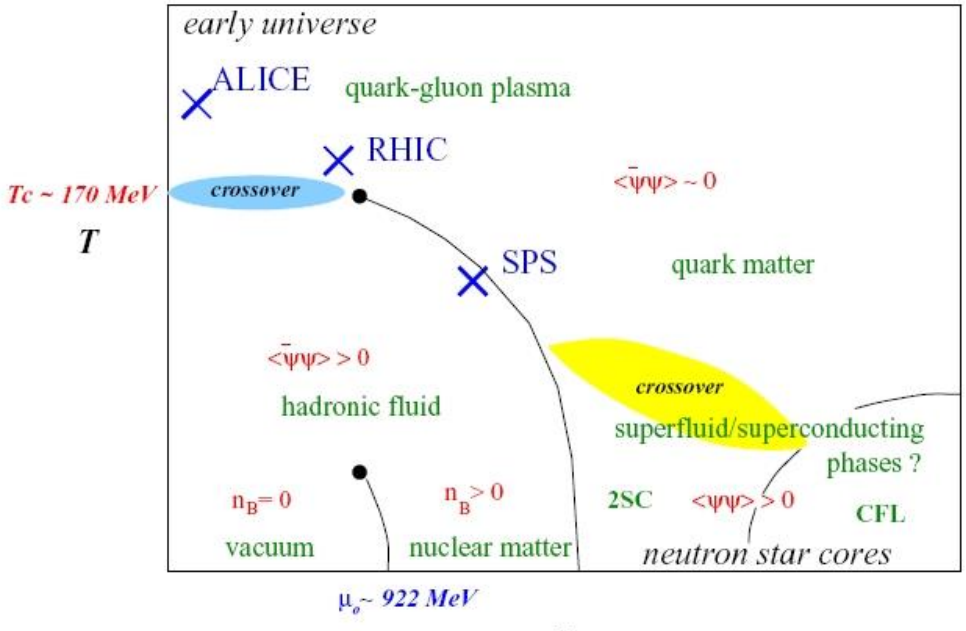

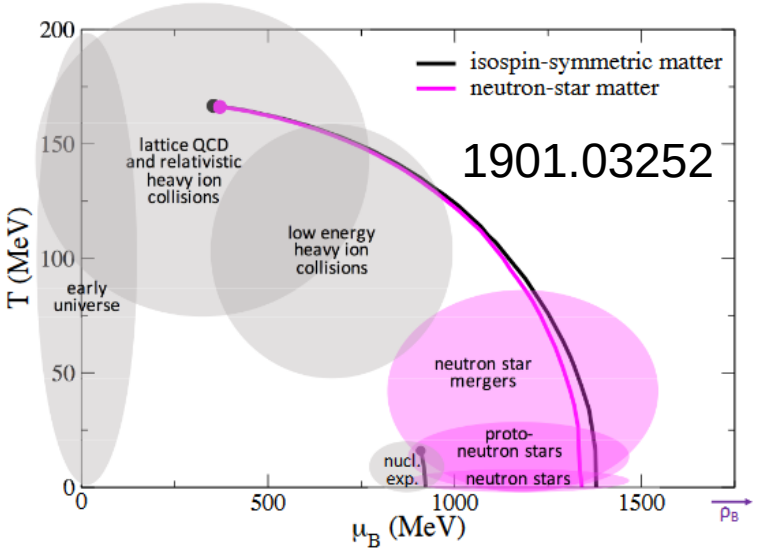

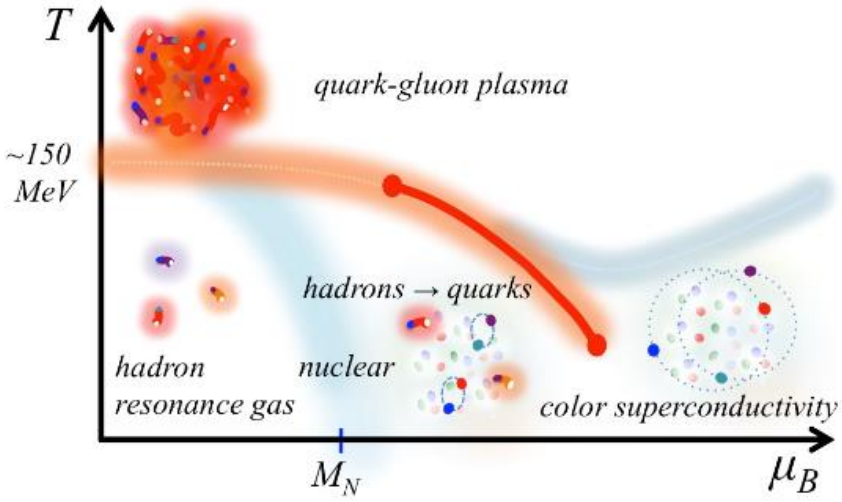

See 1803.01836

Phase diagram

Phase diagram for isospin symmetry using the most favorable hybrid EoS studied in astro-ph/0611595.

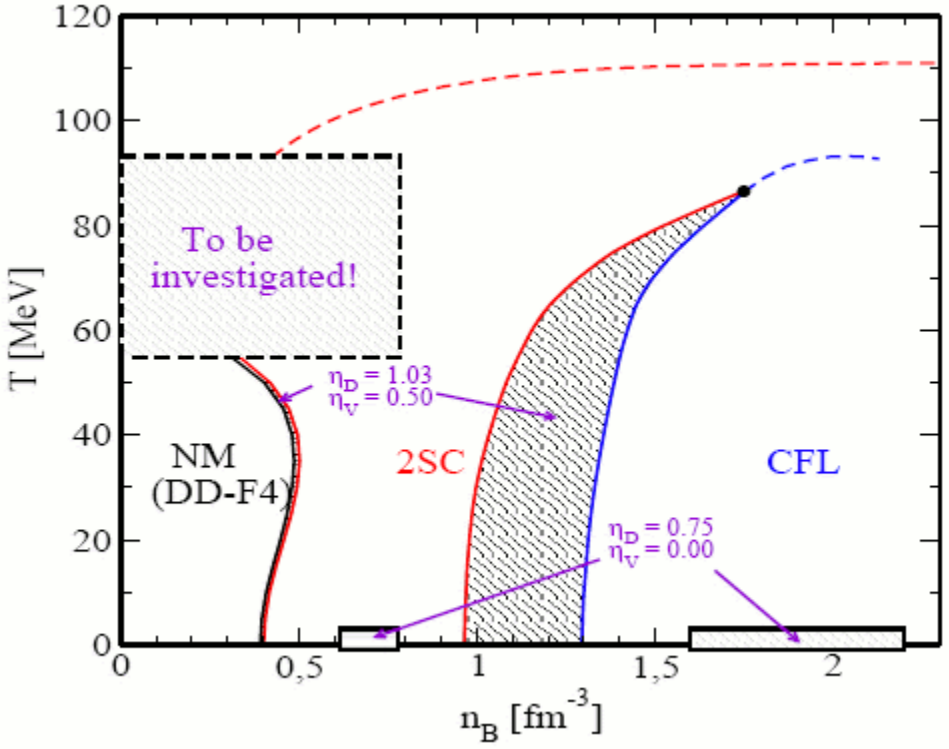

(astro-ph/0611595)

Particle fractions

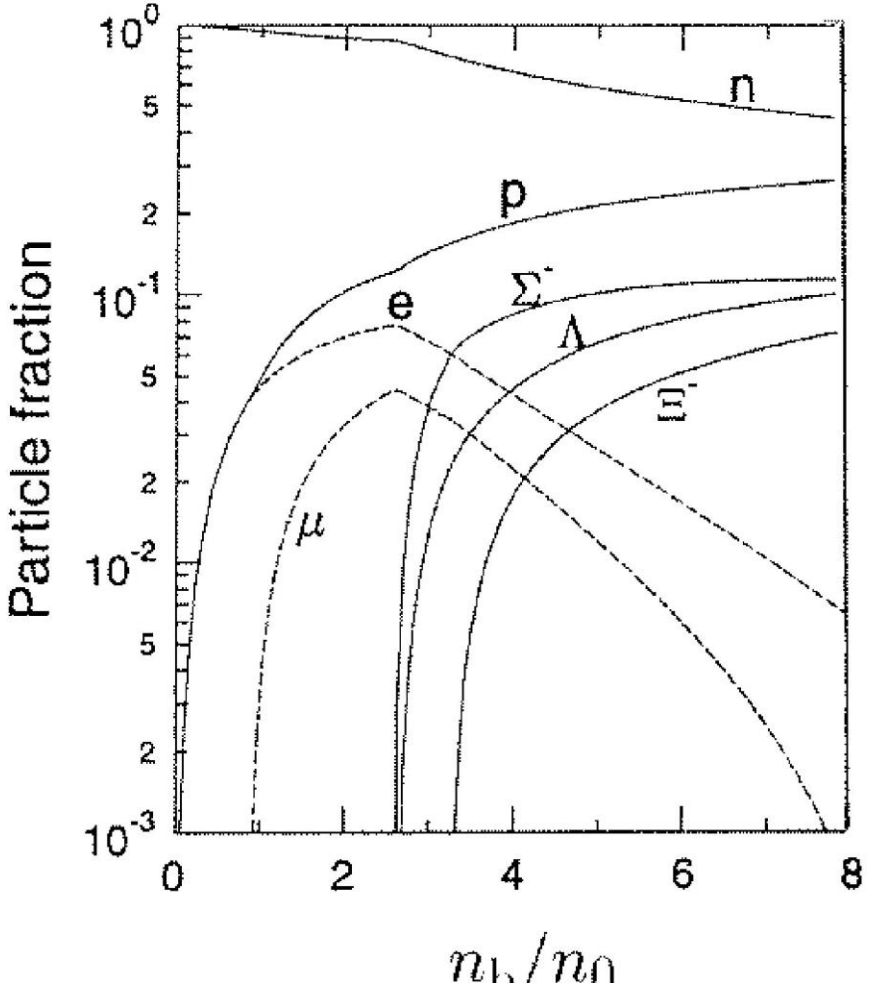

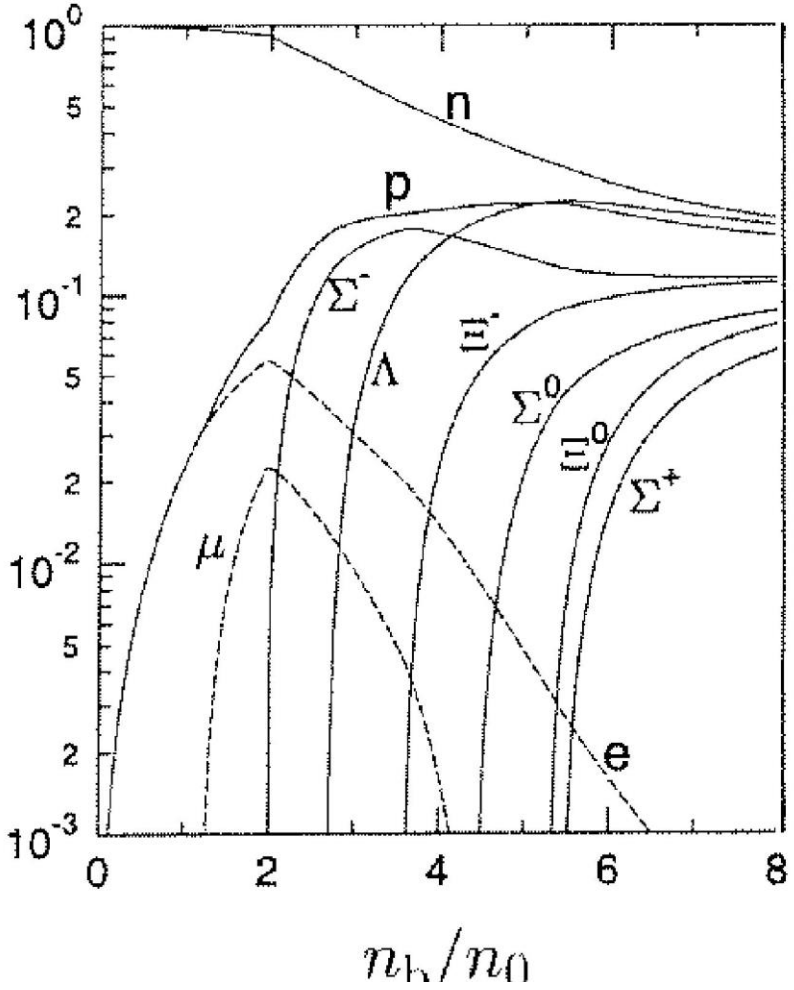

Effective chiral model of Hanauske et al. (2000)

Relativistic mean-field model TM1 of Sugahara & Toki (1971)

Superfluidity in NSs

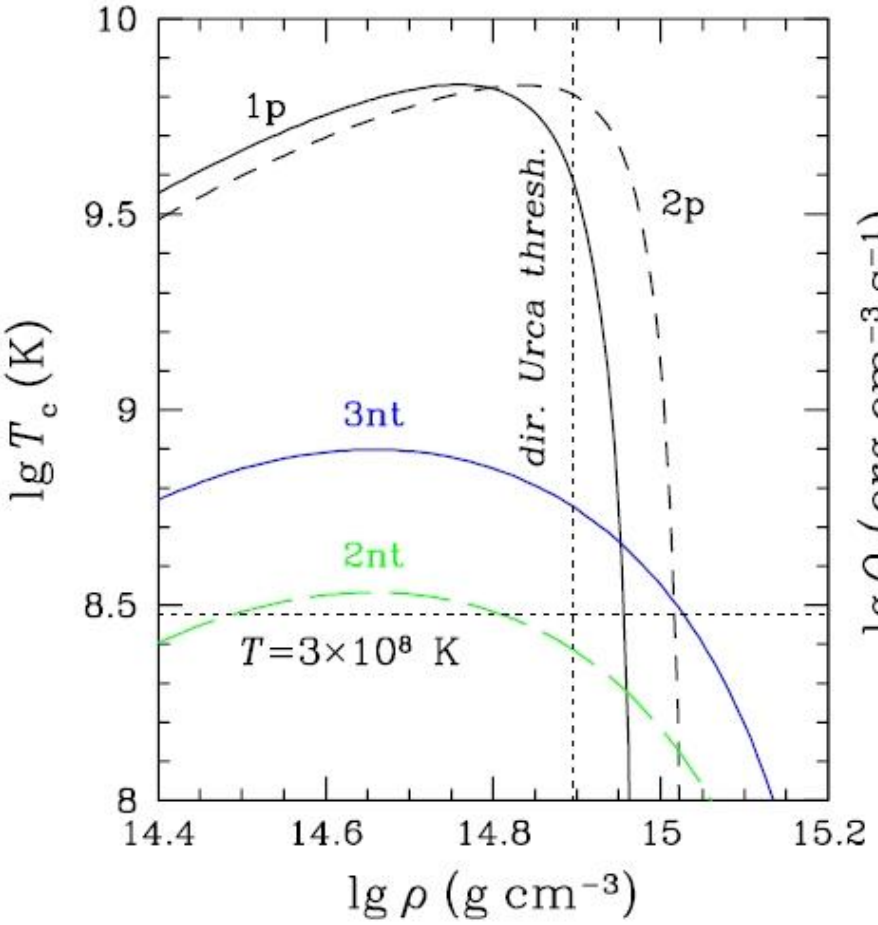

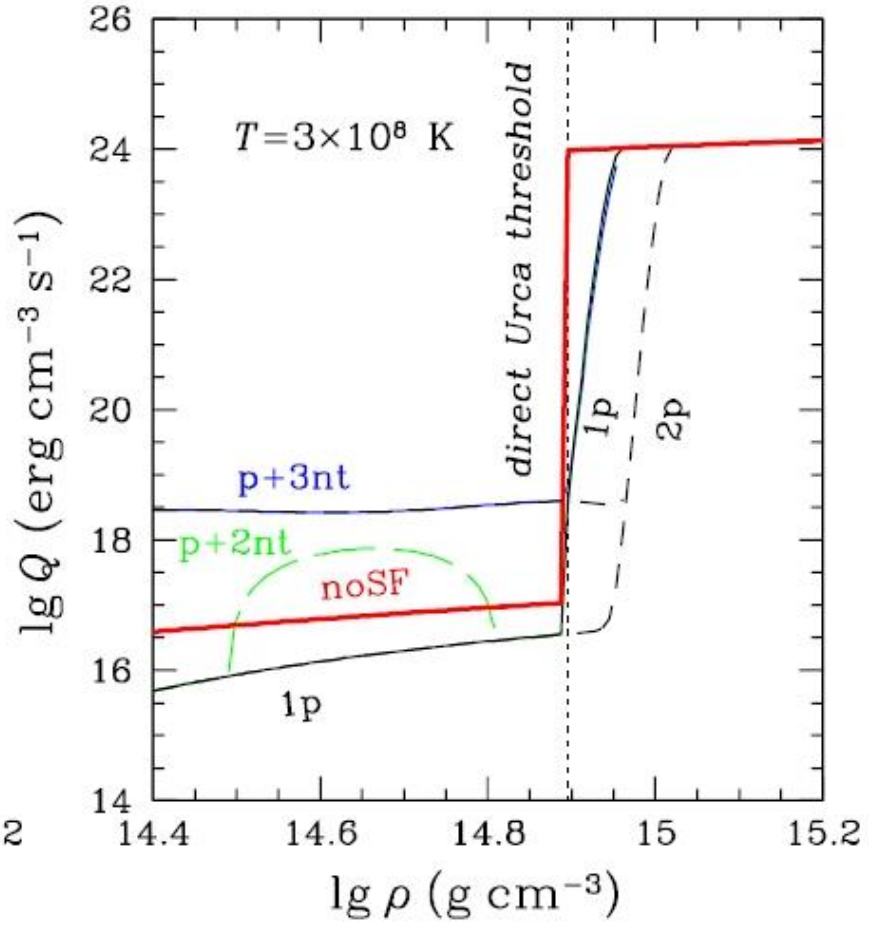

(Yakovlev)

Яковлев и др. УФН 1999

Quark stars

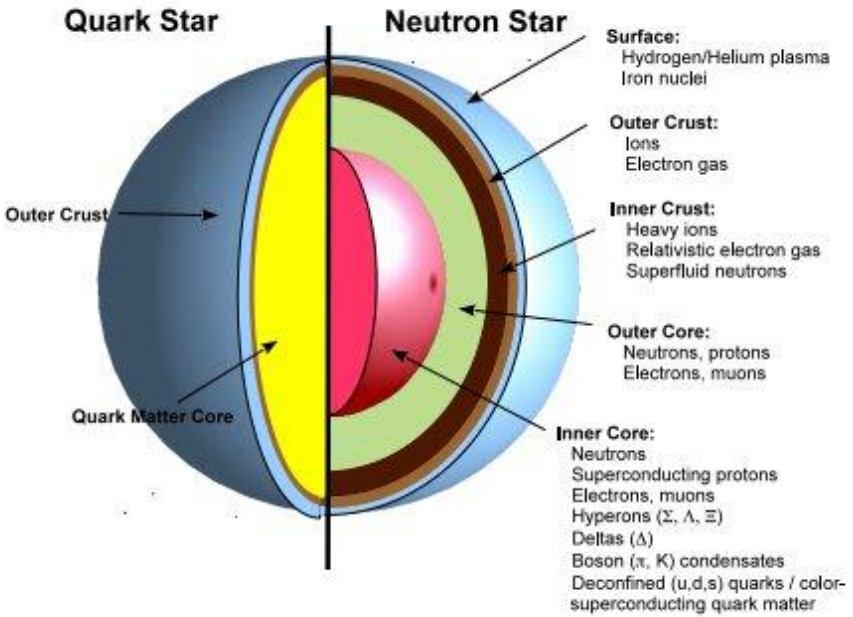

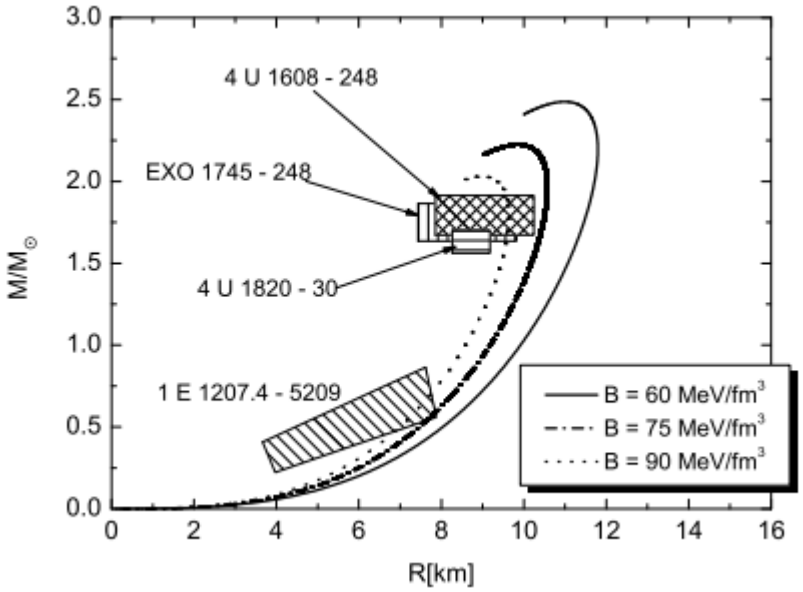

1210.1910

See also 1112.6430

Formation of quark stars

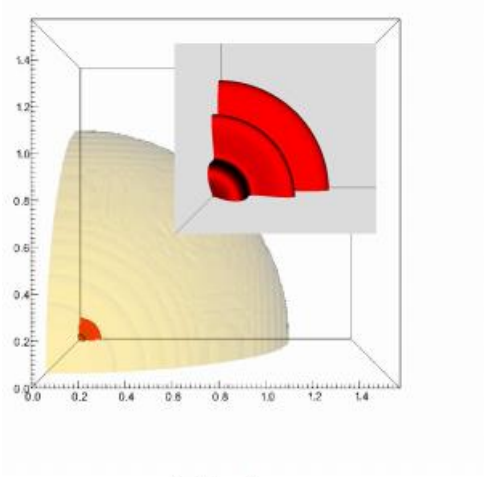

(a) $t = 0$

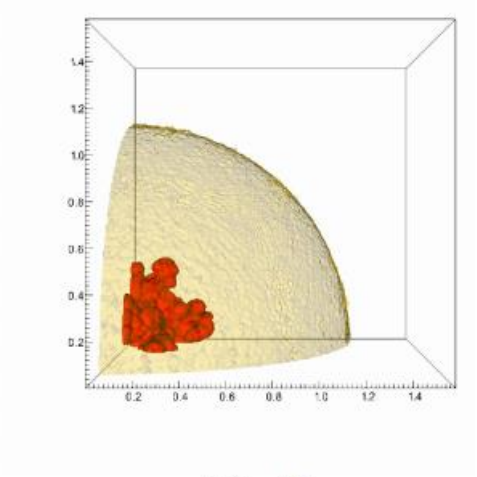

(b) $t = 0.7\,\mathrm{ms}$

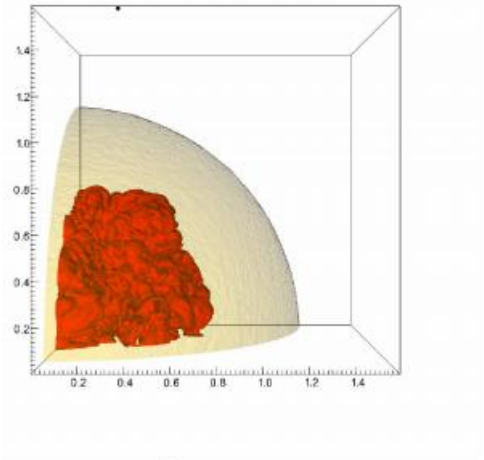

(c) $t = 1.2\,\mathrm{ms}$

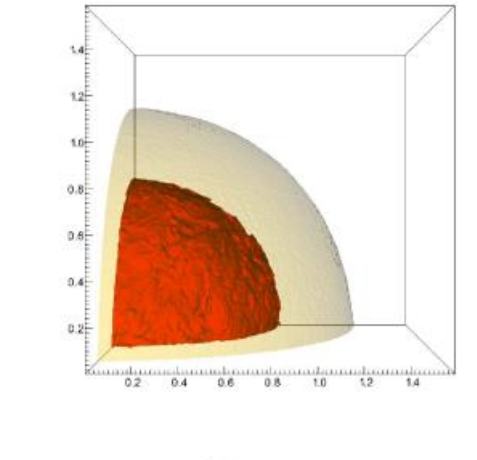

(d) $t = 4.0\,\mathrm{ms}$

Turbulent deflagration,
as in SNIa.

Neutrino signal due to
conversion of a NS into
a quark star was calculated
in 1304.6884

1109.0539

Hybrid stars

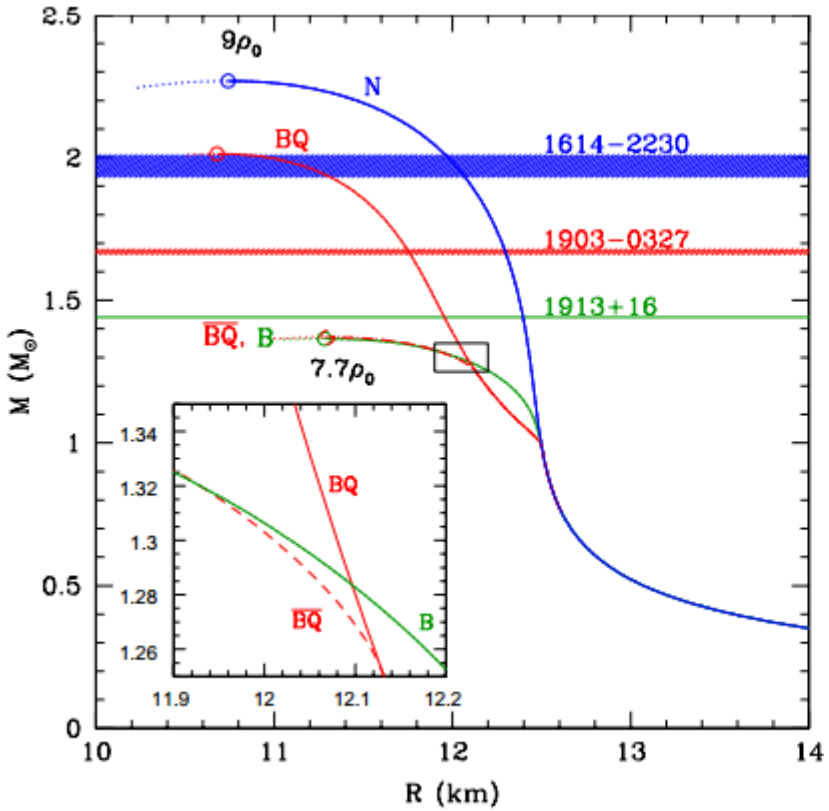

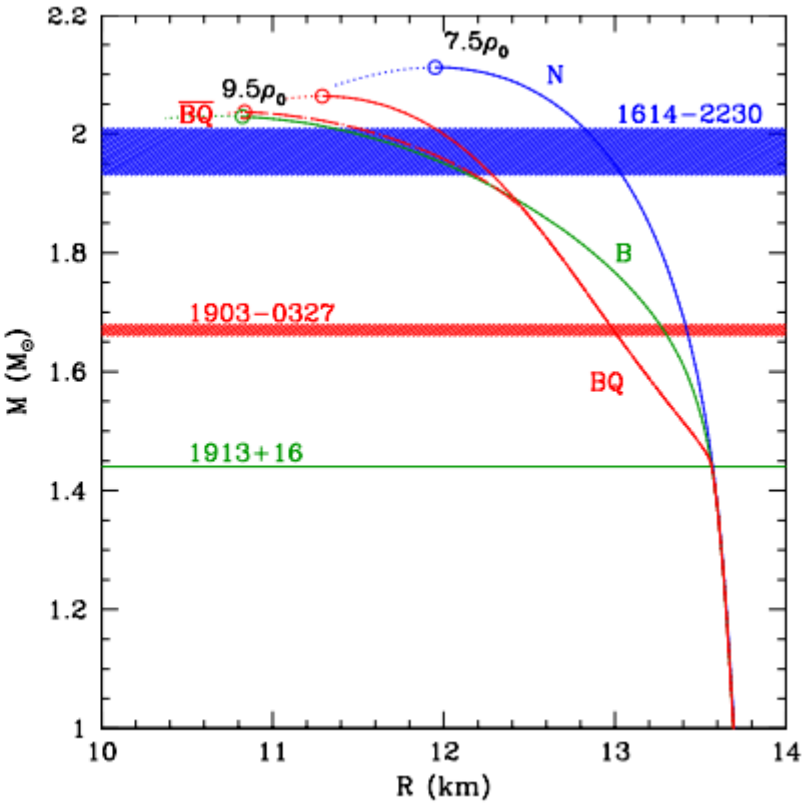

1211.1231

See also **1302.4732**

Massive hybrid stars

Stars with quark cores can be massive, and so this hypothesis is compatible with existence of pulsars with M>2 Msolar

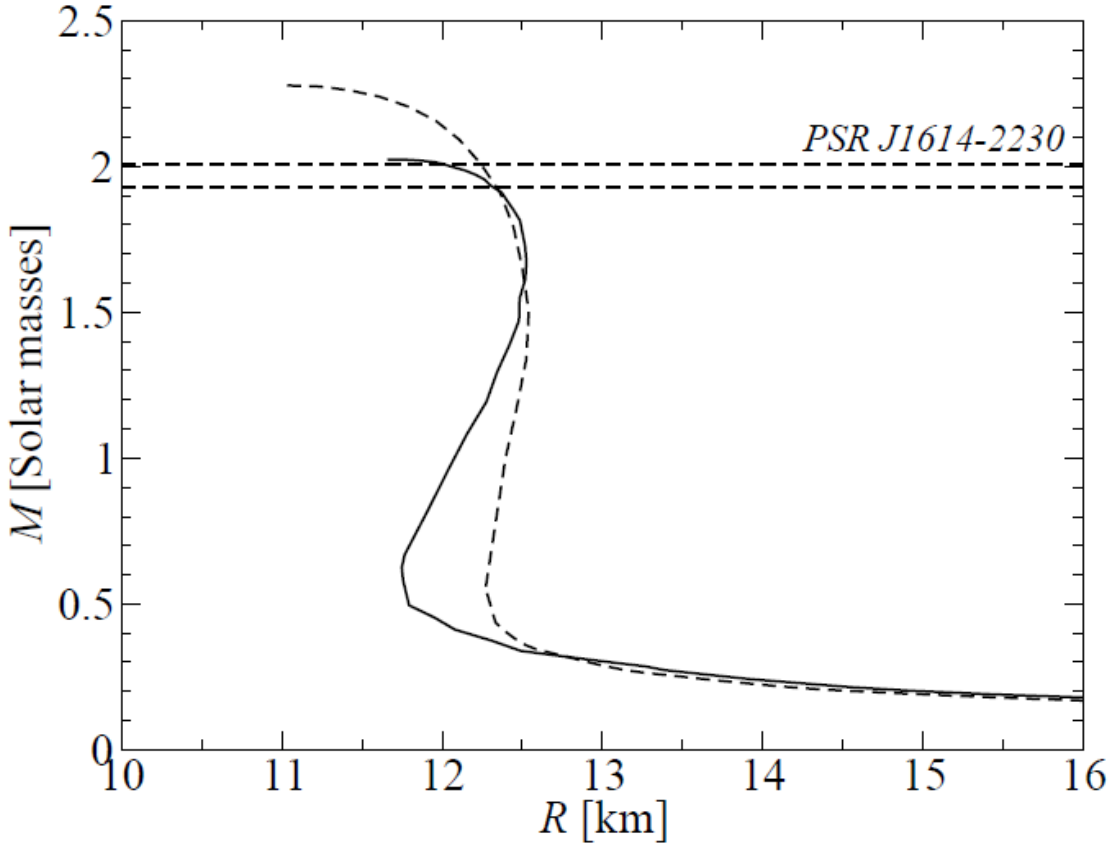

1304.6907

Pion stars

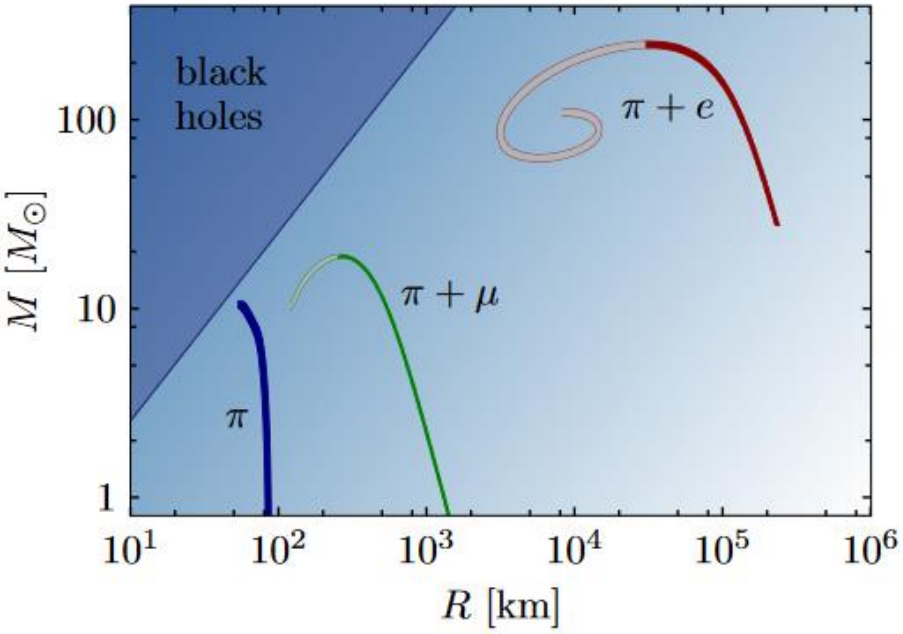

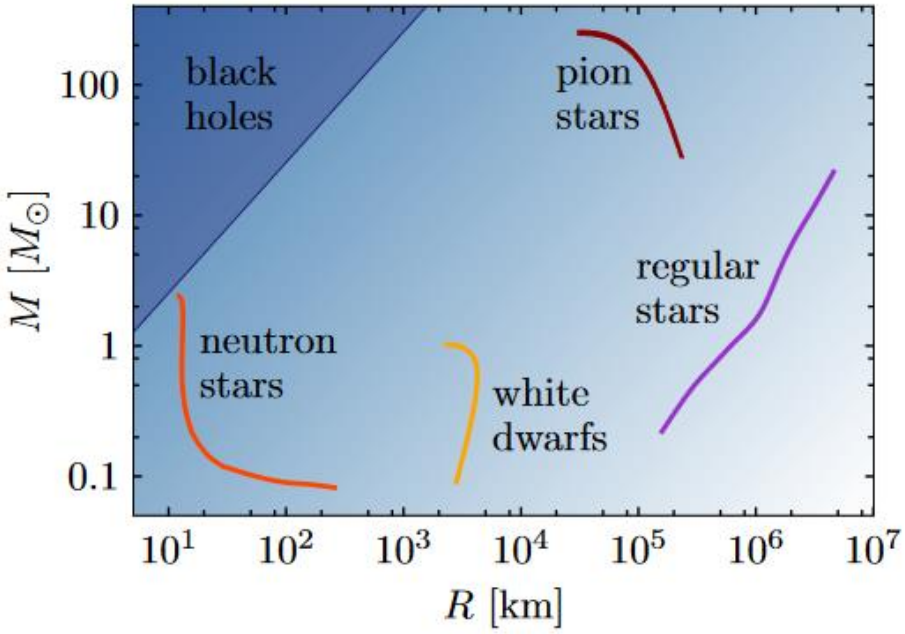

New exotic solution.

It is not clear if it can be applied to any known type of sources.

1802.06685

NS interiors: resume

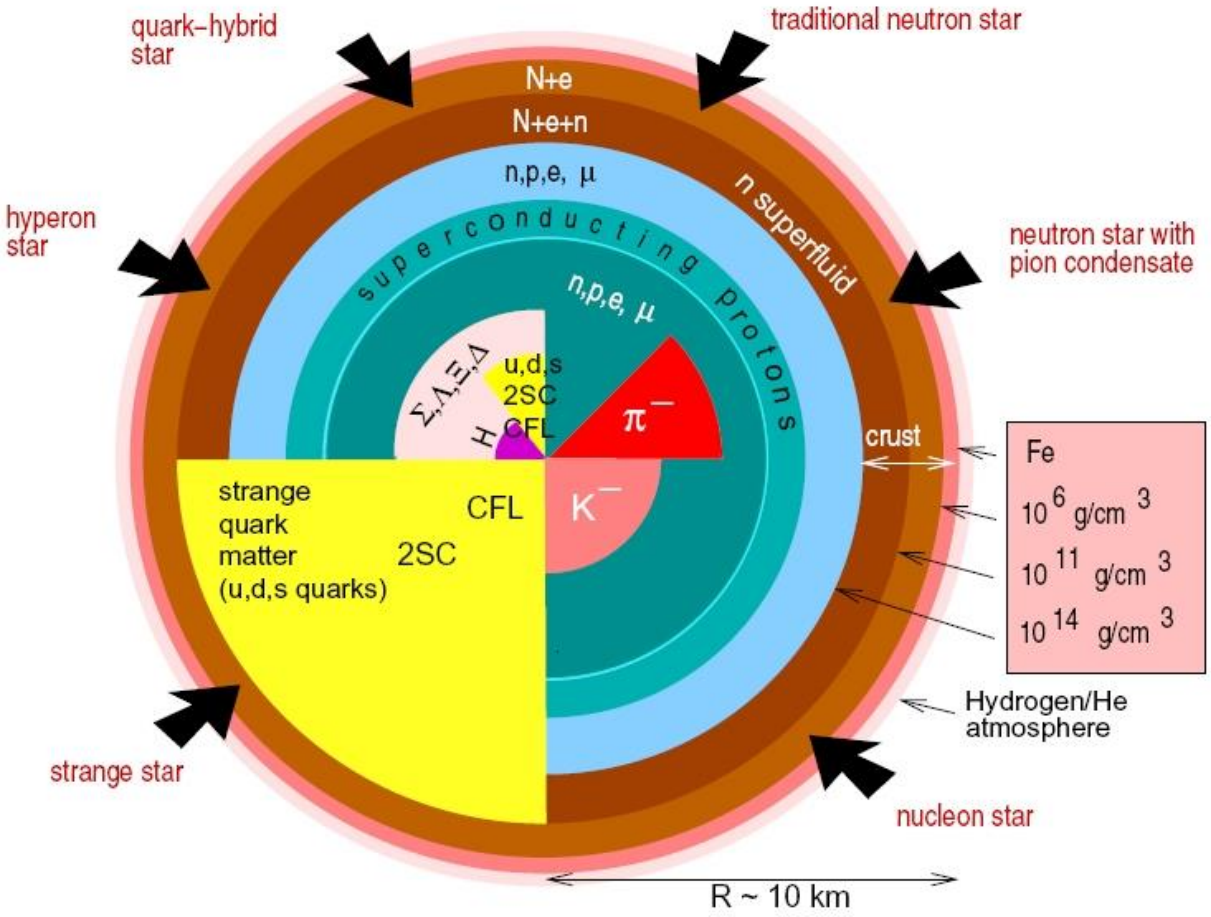

(Weber et al. ArXiv: 0705.2708)

Maximum mass

Maximum mass of NSs depends on the EoS, however, it is possible to make calculations on the base of some fundamental assumptions.

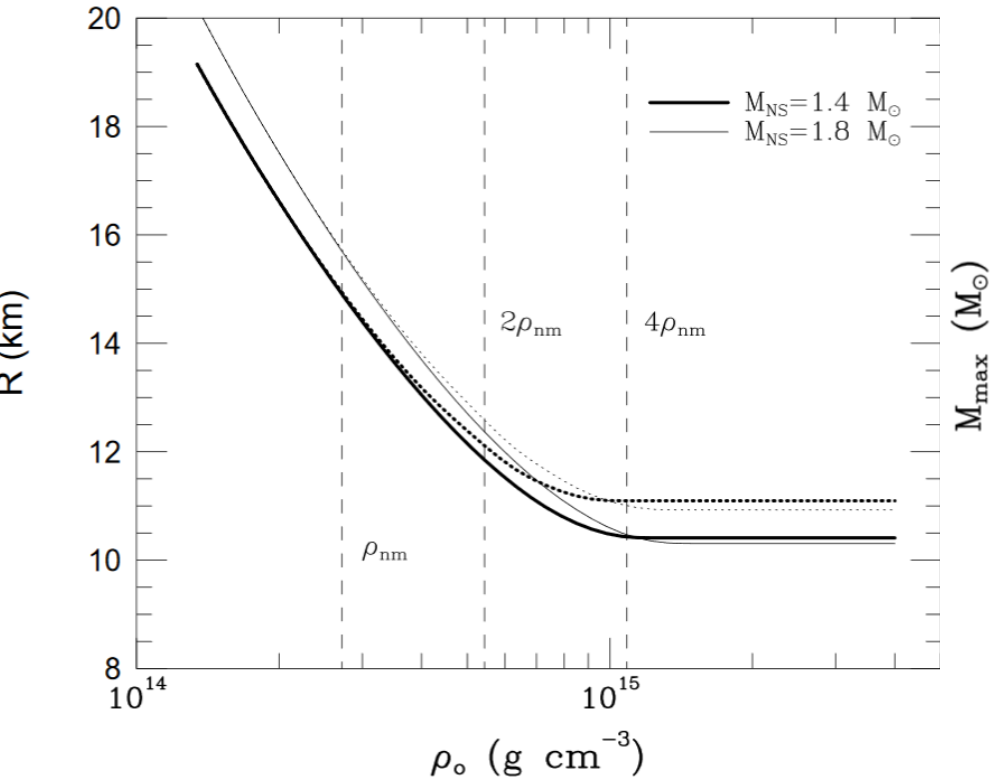

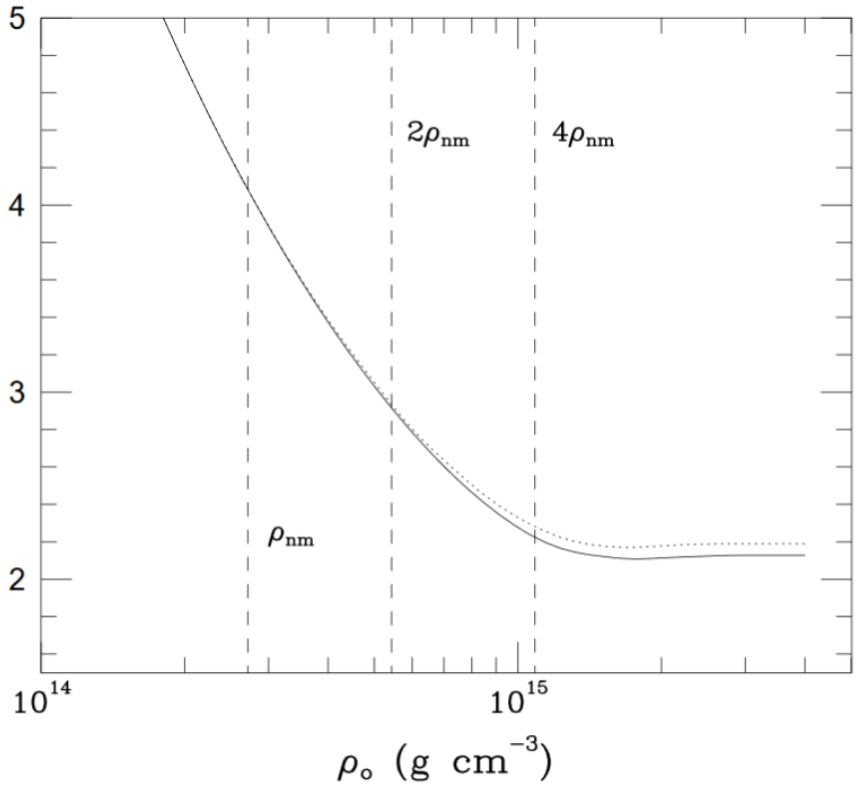

astro-ph/9608059

Seminal paper: Rhoades, Ruffini 1974
http://prl.aps.org/abstract/PRL/v32/i6/p324_1

$$c_s^2 = \frac{dP}{d\rho} = c^2.$$

Calculations based on recent data on NS-NS coalescence

What uniform rotation can give: $M_{\rm max} = \left(1.20^{+0.02}_{-0.02}\right) M_{\rm TOV}$ independently of the EOS

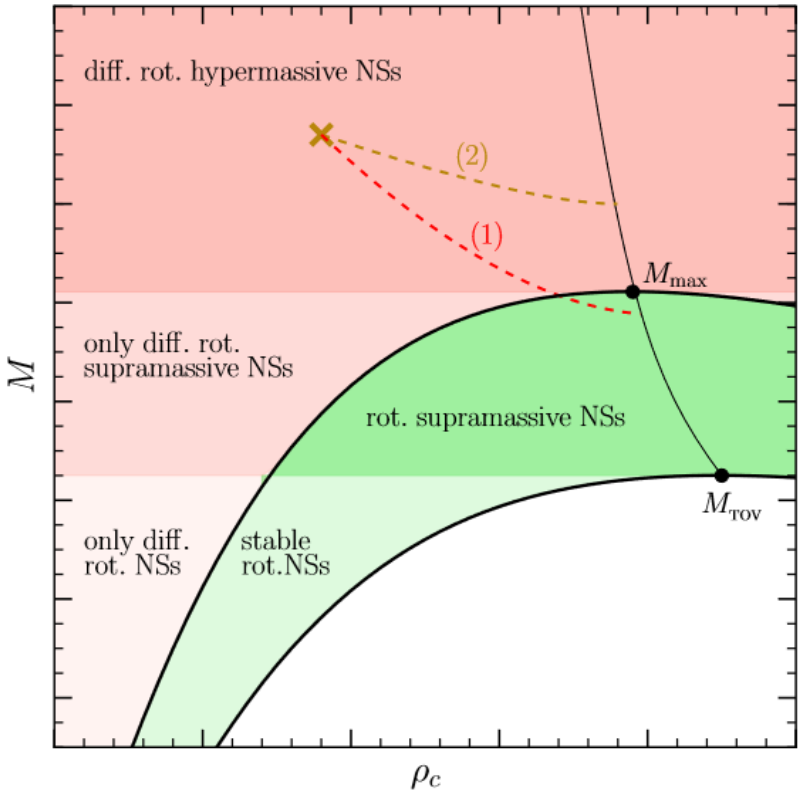

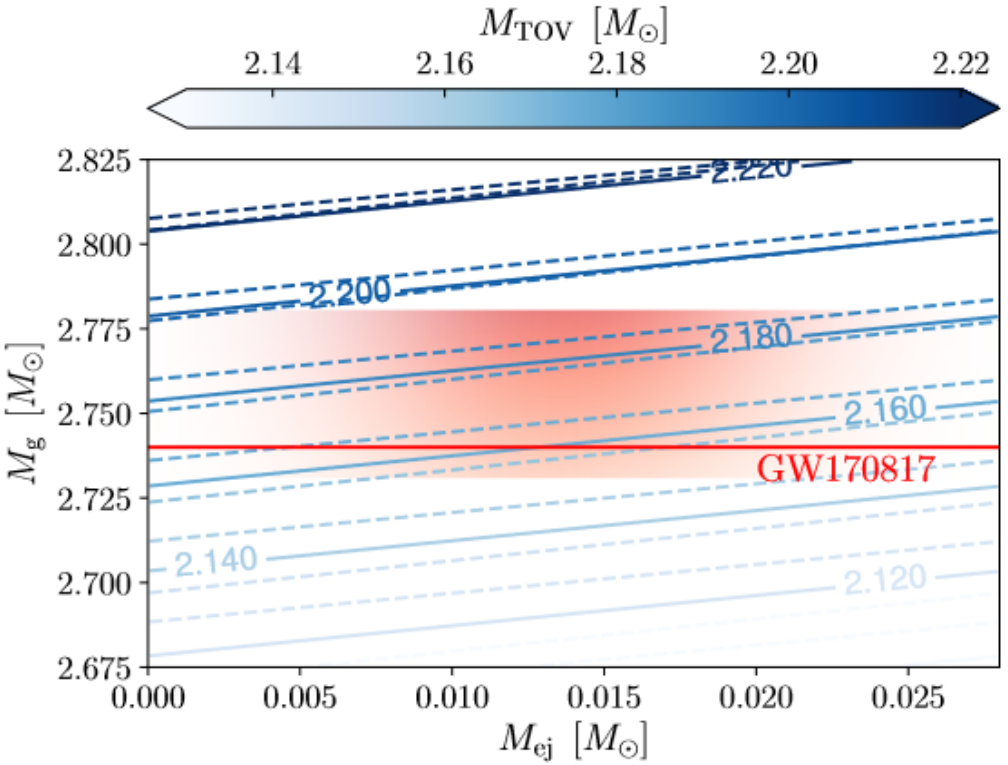

1711.00314

M_{TOV}=2-2.3 solar masses

Another constraint from GW170817

$$M_{\rm NSNS} \approx 2.74 \lesssim M_{\rm thresh} \approx \alpha M^{\rm sph}_{\rm max}.$$

As there was no prompt collapse

Here $\alpha \approx 1.3 - 1.7$ is the ratio of the HMNS threshold mass limit to the NS spherical maximum mass as gleaned from multiple numerical experiments of merging NSNSs

$$M_{\rm NSNS} \approx 2.74 \gtrsim M^{\rm sup}_{\rm max} \approx \beta M^{\rm sph}_{\rm max},$$

where $\beta \approx 1.2$ is the ratio of the uniformly rotating supramassive NS limit to the nonrotating spherical maximum

$$M^{\rm sph}_{\rm max} = 4.8 \left(\frac{2 \times 10^{14}\ {\rm gr/cm^3}}{\rho_m/c^2} \right)^{1/2} M_\odot\,,$$

$$M^{\rm sup}_{\rm max} = 6.1 \left(\frac{2 \times 10^{14}\ {\rm gr/cm^3}}{\rho_m/c^2} \right)^{1/2} M_\odot\,,$$

$$\beta \approx 1.27.$$

$$2.74/\alpha \lesssim M^{\rm sph}_{\rm max} \lesssim 2.74/\beta$$

$$M^{\rm sph}_{\rm max} \lesssim 2.16. \quad \beta \approx 1.27.$$

$$M^{\rm sph}_{\rm max} \lesssim 2.28. \quad \beta = 1.2$$

1711.00473

Papers to read

1. astro-ph/0405262 Lattimer, Prakash "Physics of neutron stars"
2. 0705.2708 Weber et al. "Neutron stars interiors and equation of state …"
3. physics/0503245 Baym, Lamb "Neutron stars"
4. 0901.4475 Piekarewicz "Nuclear physics of neutron stars" (first part)
5. 0904.0435 Paerels et al. "The Behavior of Matter Under Extreme Conditions"
6. 1512.07820 Lattimer, Prakash "The EoS of hot dense matter …."
7. 1001.3294 Schmitt "Dense matter in compact stars - A pedagogical introduction "
8. 1303.4662 Hebeler et al. "Equation of state and neutron star properties constrained by nuclear physics and observation "
9. 1210.1910 Weber et al. Structure of quark star
10. 1302.1928 Stone "High density matter "
11. 1707.04966 Baym et al. "From hadrons to quarks in neutron stars: a review"
12. 1804.03020. Burgio, Fantina. "Nuclear Equation of state for Compact Starsand Supernovae"
13. 1803.01836 Blaschke, Chamel. "Phases of dense matter in compact stars"

+ the book by Haensel, Yakovlev, Potekhin

Lectures on the Web

Lectures can be found at my homepage:

http://xray.sai.msu.ru/~polar/html/presentations.html

Neutron Star masses and radii

NS Masses

- Stellar masses are directly measured only in binary systems
- Accurate NS mass determination for PSRs in relativistic systems by measuring PK corrections
- Gravitational redshift may provide M/R in NSs by detecting a *known* spectral line,

  $E_\infty = E(1-2GM/Rc^2)^{1/2}$

Neutron stars and white dwarfs

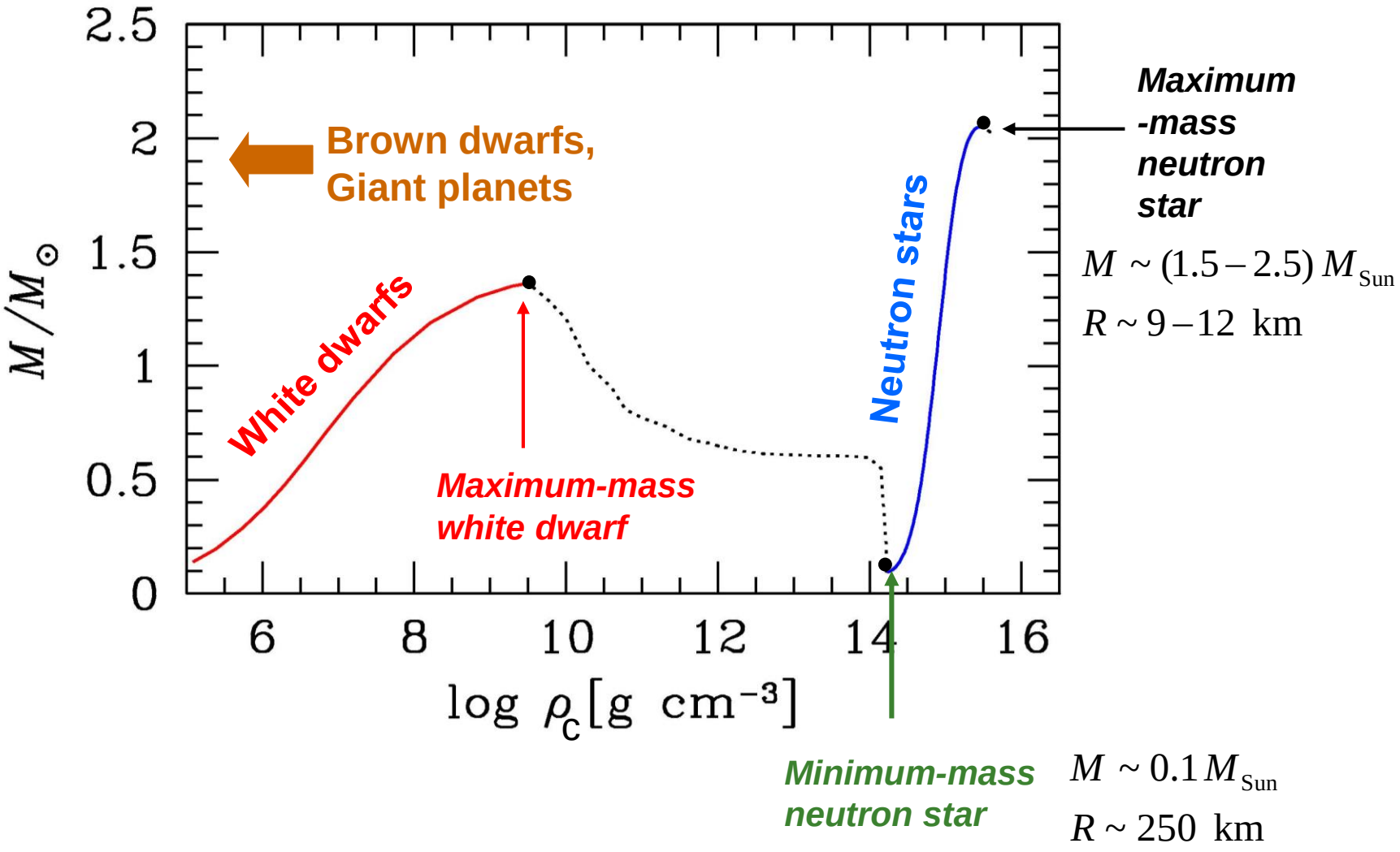

Remember about the difference between baryonic and gravitational masses in the case of neutron stars!

Minimal mass

In reality, minimal mass is determined by properties of protoNSs.
Being hot, lepton rich they have much higher limit: about 0.7 solar mass.

Stellar evolution does not produce
NSs with baryonic mass
less than about 1.1-1.2 solar.

Fragmentation of a core
due to rapid rotation
potentially can lead
to smaller masses,
but not as small as
the limit for cold NSs.

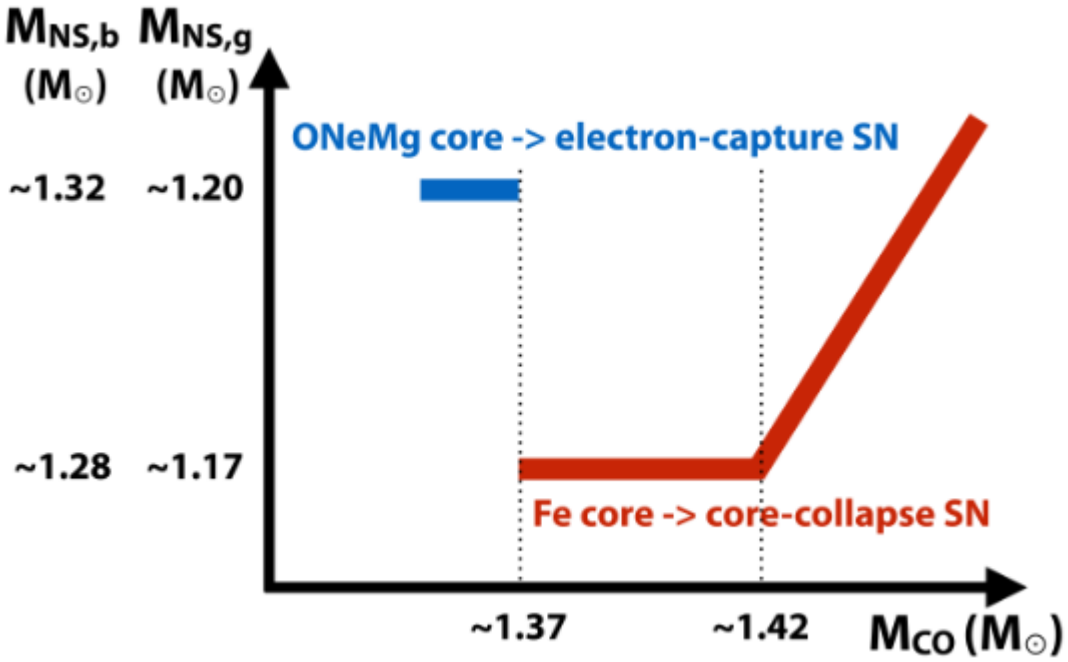

1808.02328

Maximum mass

Detailed discussion about the maximum mass is given in 1307.3995

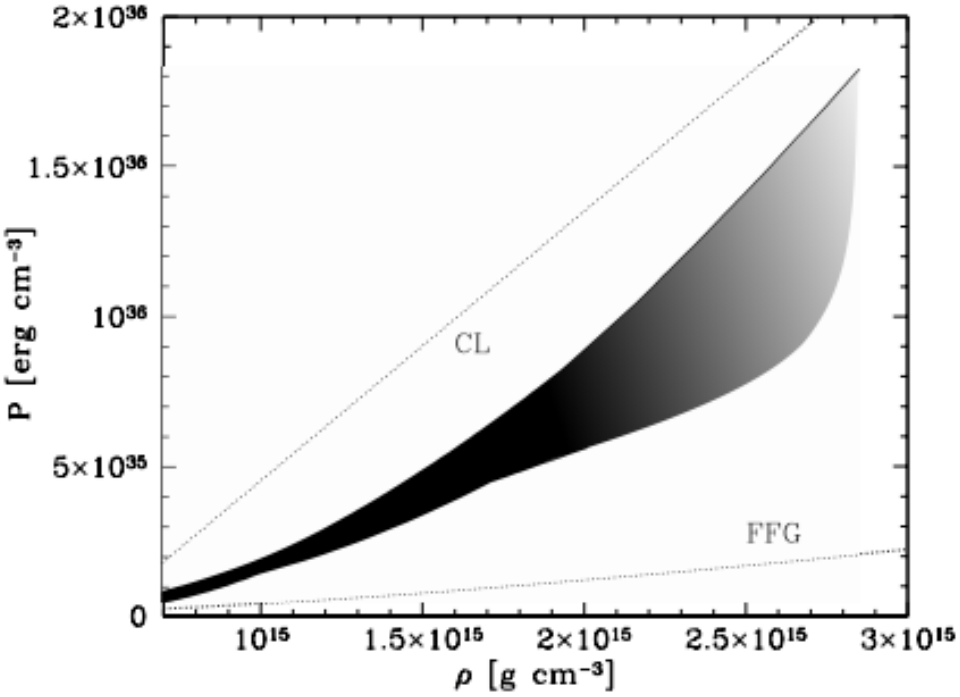

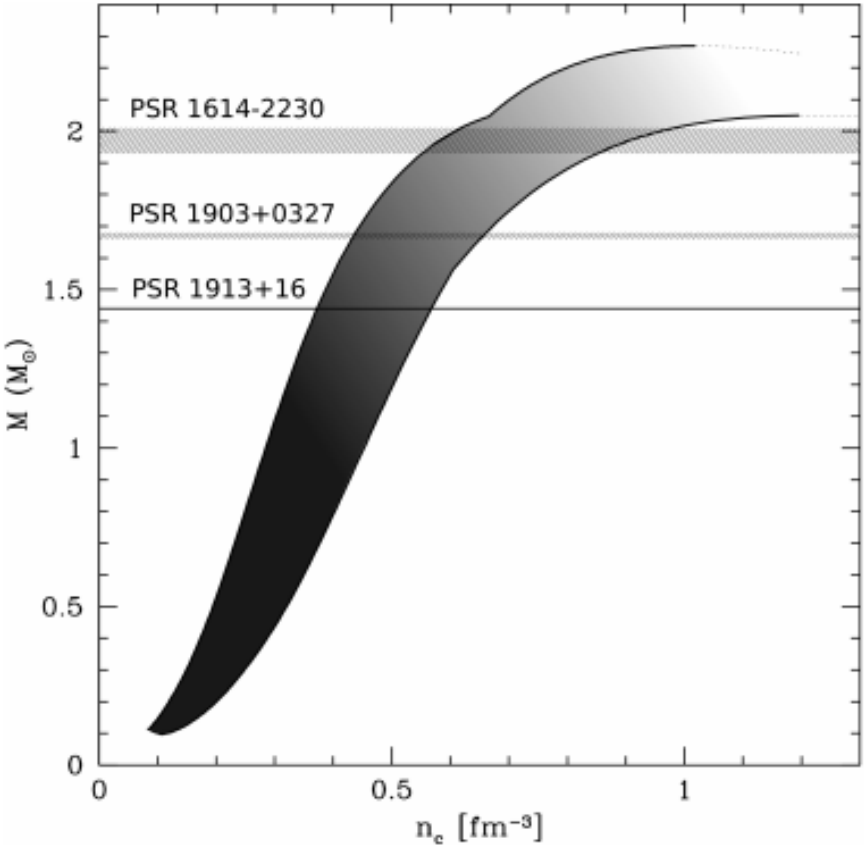

Maximum mass and cut-off

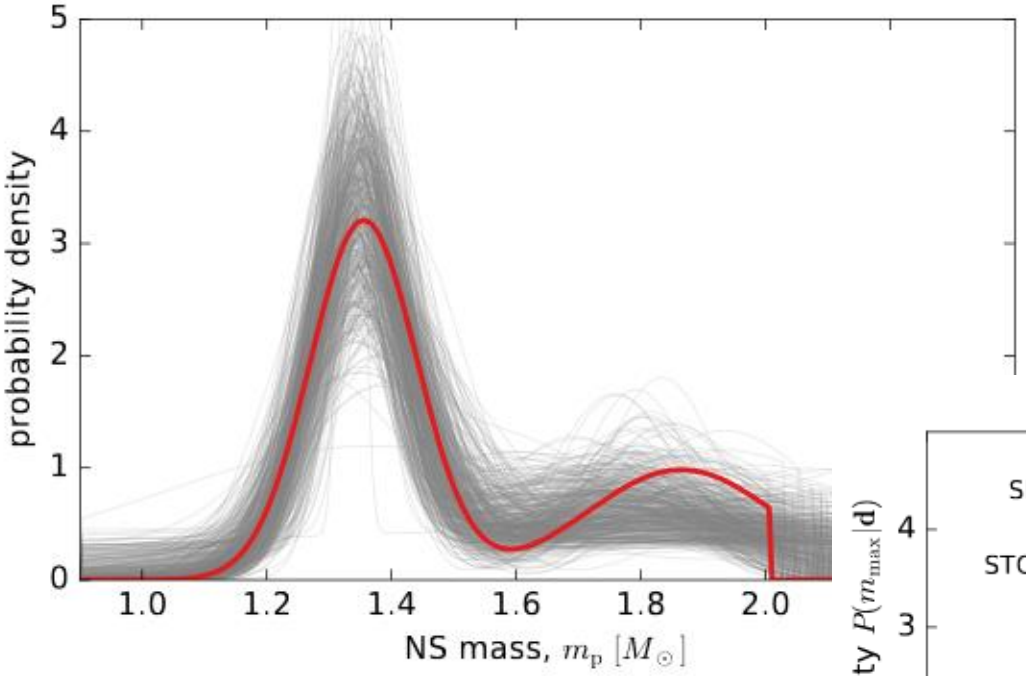

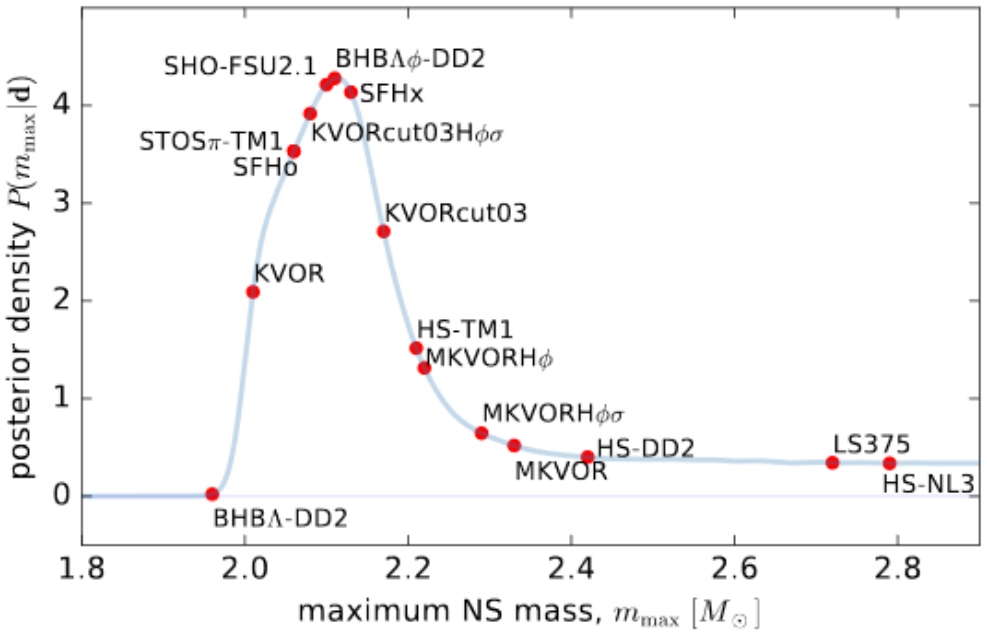

1709.07889

Neutron star masses

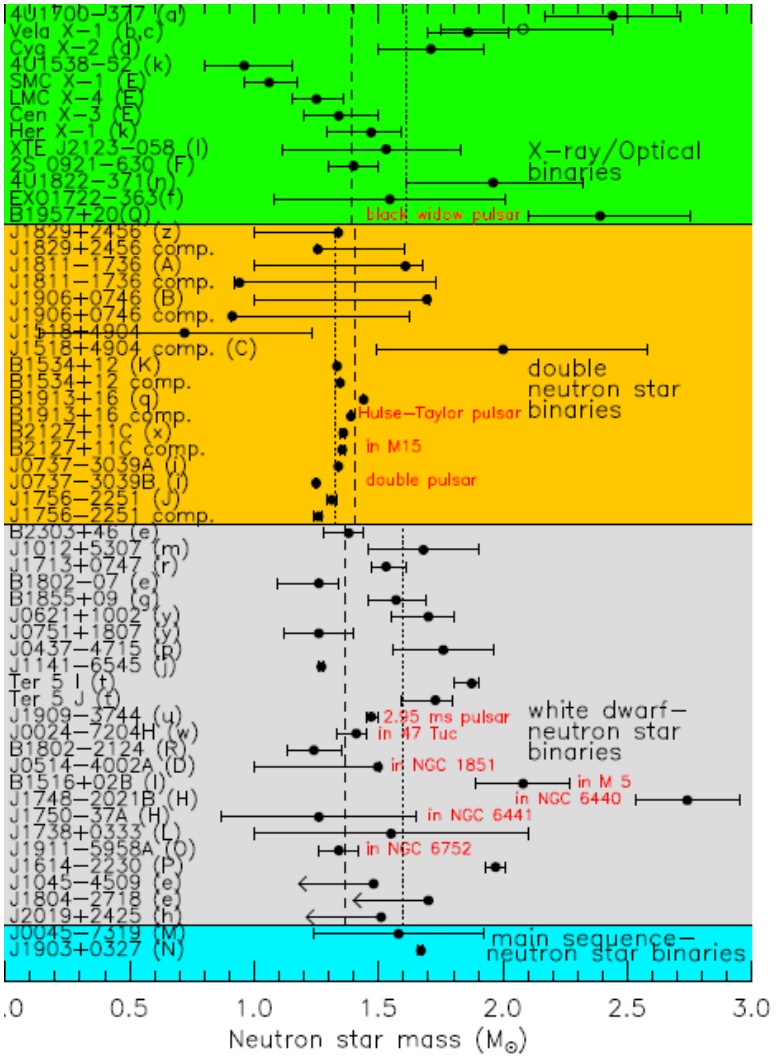

Object	Mass ($M_\odot$)	Reference	Object	Mass ($M_\odot$)	Reference
X-Ray/Optical Binaries (mean = 1.609 $M_\odot$, weighted mean = 1.393 $M_\odot$)					
4U1700-377	$2.44^{+0.27}_{-0.27}$	a (10)	Vela X-1	$1.86^{+0.16}_{-0.16}$	b, c (11, 12)
Cyg X-2	$1.71^{+0.21}_{-0.21}$	d (13)	4U1538-52	$0.96^{+0.19}_{-0.16}$	k (14)
SMC X-1	$1.06^{+0.11}_{-0.10}$	E (15)	LMC X-4	$1.25^{+0.11}_{-0.10}$	E (15)
Cen X-3	$1.34^{+0.16}_{-0.14}$	E (15)	Her X-1	$1.47^{+0.12}_{-0.18}$	k (14)
XTE J2123-058	$1.53^{+0.30}_{-0.42}$	I (16, 17)	2S 0921-630	$1.4^{+0.1}_{-0.1}$	F (18)
4U 1822-371	$1.96^{+0.36}_{-0.35}$	n (19)	EXO 1722-363	$1.545^{+0.465}_{-0.465}$	f (47)
B1957+20	$2.39^{+0.36}_{-0.29}$	Q (49)			
Neutron Star – Neutron Star Binaries (mean = 1.325 $M_\odot$, weighted mean = 1.403 $M_\odot$)					
J1829+2456	$1.338^{+0.002}_{-0.338}$	z (20)	J1829+2456 (c)	$1.256^{+0.346}_{-0.003}$	z (20)
J1811-1736	$1.608^{+0.066}_{-0.608}$	A (21)	J1811-1736 (c)	$0.941^{+0.787}_{-0.021}$	A (21)
J1906+07	$1.694^{+0.012}_{-0.694}$	B (22)	J1906+07 (c)	$0.912^{+0.710}_{-0.004}$	B (22)
J1518+4904	$0.72^{+0.51}_{-0.58}$	C (23)	J1518+4904 (c)	$2.00^{+0.58}_{-0.51}$	C (23)
1534+12	$1.3332^{+0.0010}_{-0.0010}$	K (24)	1534+12 (c)	$1.3452^{+0.0010}_{-0.0010}$	K (24)
1913+16	$1.4398^{+0.0002}_{-0.0002}$	q (25)	1913+16 (c)	$1.3886^{+0.0002}_{-0.0002}$	q (25)
2127+11C	$1.358^{+0.010}_{-0.010}$	x (26)	2127+11C (c)	$1.354^{+0.010}_{-0.010}$	x (26)
J0737-3039A	$1.3381^{+0.0007}_{-0.0007}$	i (27)	J0737-3039B	$1.2489^{+0.0007}_{-0.0007}$	i (27)
J1756-2251	$1.312^{+0.017}_{-0.017}$	J (28)	J1756-2251 (c)	$1.258^{+0.017}_{-0.017}$	J (28)
Neutron Star – White Dwarf Binaries (mean = 1.599 $M_\odot$, weighted mean = 1.362 $M_\odot$)					
B2303+46	$1.38^{+0.06}_{-0.10}$	e (29)	J1012+5307	$1.68^{+0.22}_{-0.22}$	m (30)
J1713+0747	$1.53^{+0.08}_{-0.04}$	r (31, 51)	B1802-07	$1.26^{+0.08}_{-0.17}$	e (29)
B1855+09	$1.57^{+0.12}_{-0.11}$	g (32, 51)	J0621+1002	$1.70^{+0.10}_{-0.17}$	y (33)
J0751+1807	$1.26^{+0.14}_{-0.14}$	y (33)	J0437-4715	$1.76^{+0.20}_{-0.20}$	p (34)
J1141-6545	$1.27^{+0.01}_{-0.01}$	j (35)	Ter 5 I	$1.874^{+0.32}_{-0.068}$	t (36)
Ter 5 J	$1.728^{+0.066}_{-0.136}$	t (36)	J1909-3744	$1.47^{+0.03}_{-0.02}$	u (37)
J0024-7204H	$1.41^{+0.04}_{-0.08}$	w (38)	B1802-2124	$1.24^{+0.11}_{-0.11}$	R (50)
J0514-4002A	$1.497^{+0.008}_{-0.497}$	D (39)	B1516+02B	$2.08^{+0.19}_{-0.19}$	I (40)
J1748-2021B	$2.74^{+0.21}_{-0.21}$	H (41)	J1750-37A	$1.26^{+0.39}_{-0.39}$	H (41)
J1738+0333	$1.55^{+0.55}_{-0.55}$	L (42)	J1911-5958A	$1.34^{+0.08}_{-0.08}$	O (43)
J1614-2230	$1.97^{+0.04}_{-0.04}$	P (48)	J1045-4509	< 1.48	e (29)
J1804-2718	< 1.70	e (29)	J2019+2425	< 1.51	h (44)
Neutron Star – Main Sequence Binaries					
J0045-7319	$1.58^{+0.34}_{-0.34}$	M (45)	J1903+0327	$1.67^{+0.01}_{-0.01}$	N (46)

Follow updates at https://stellarcollapse.org/nsmasses

arXiv: 1012.3208

Update - 2012

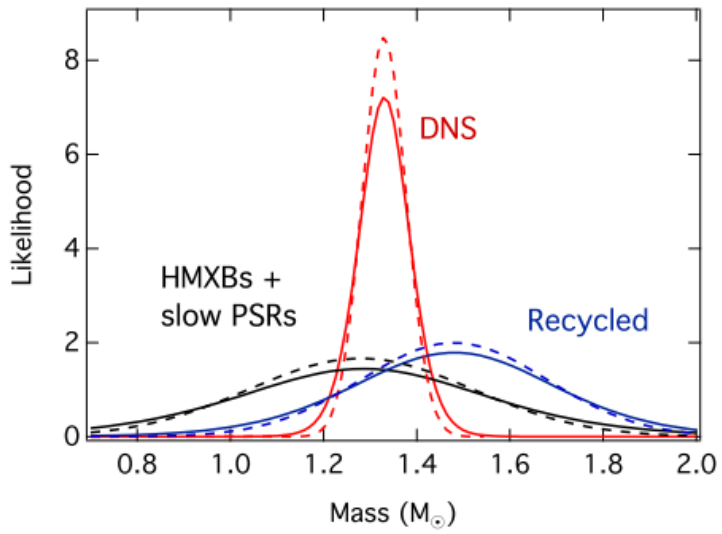

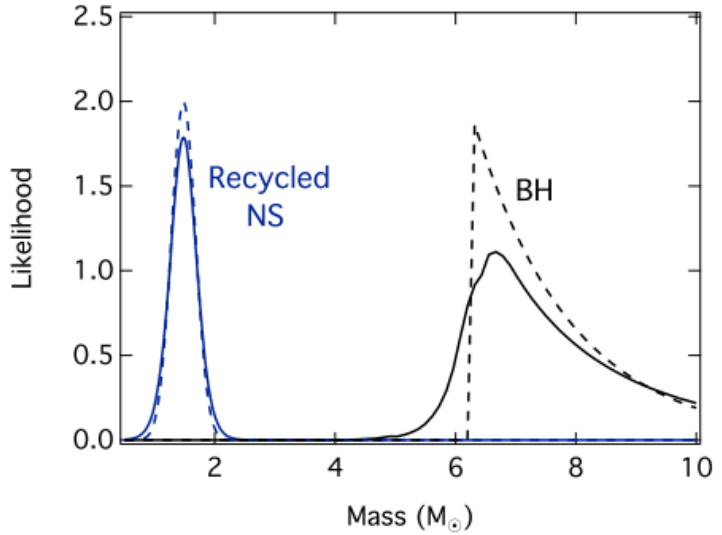

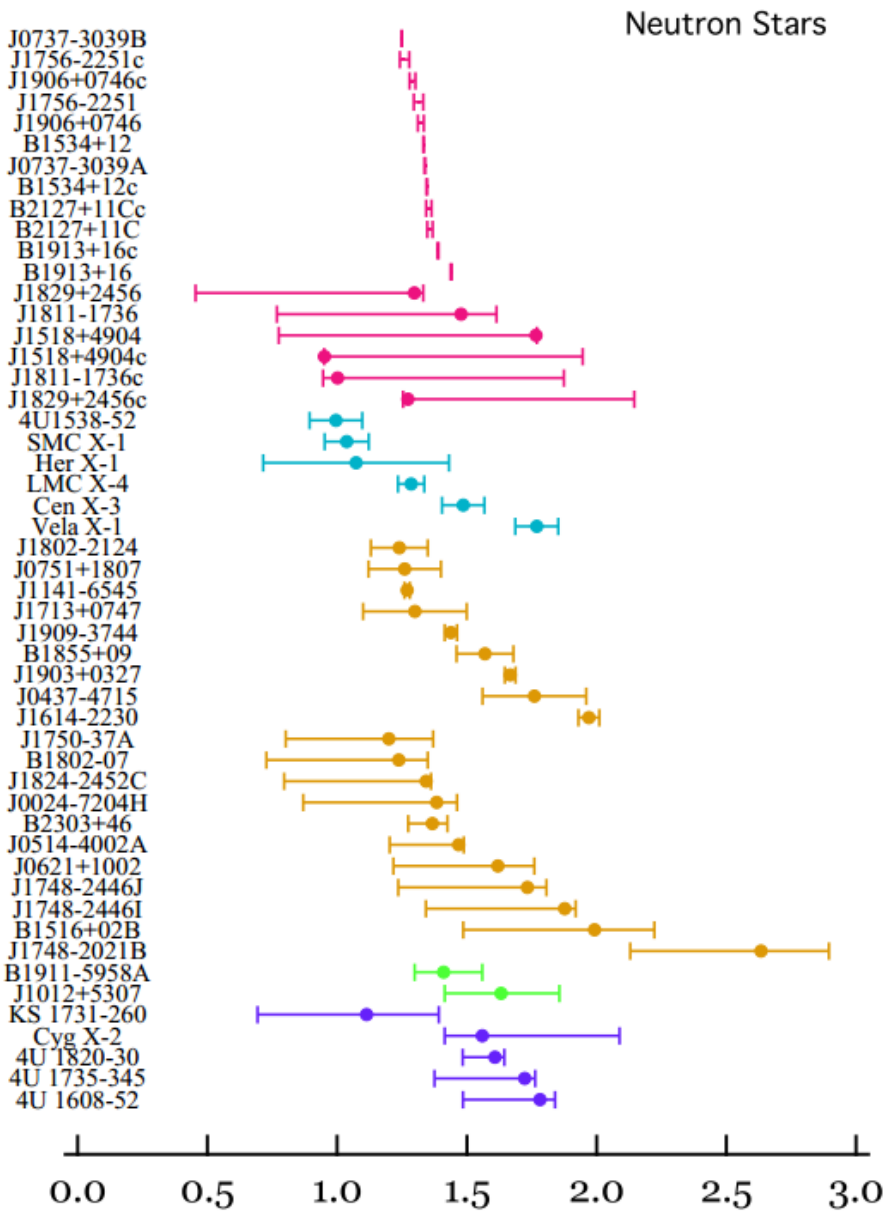

1201.1006

Update - 2013

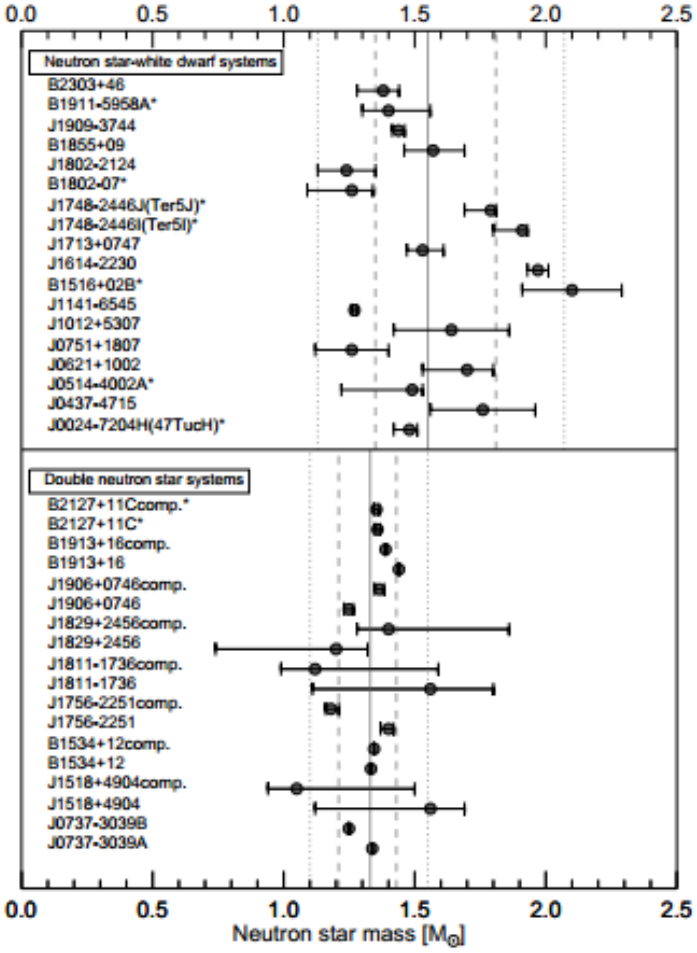

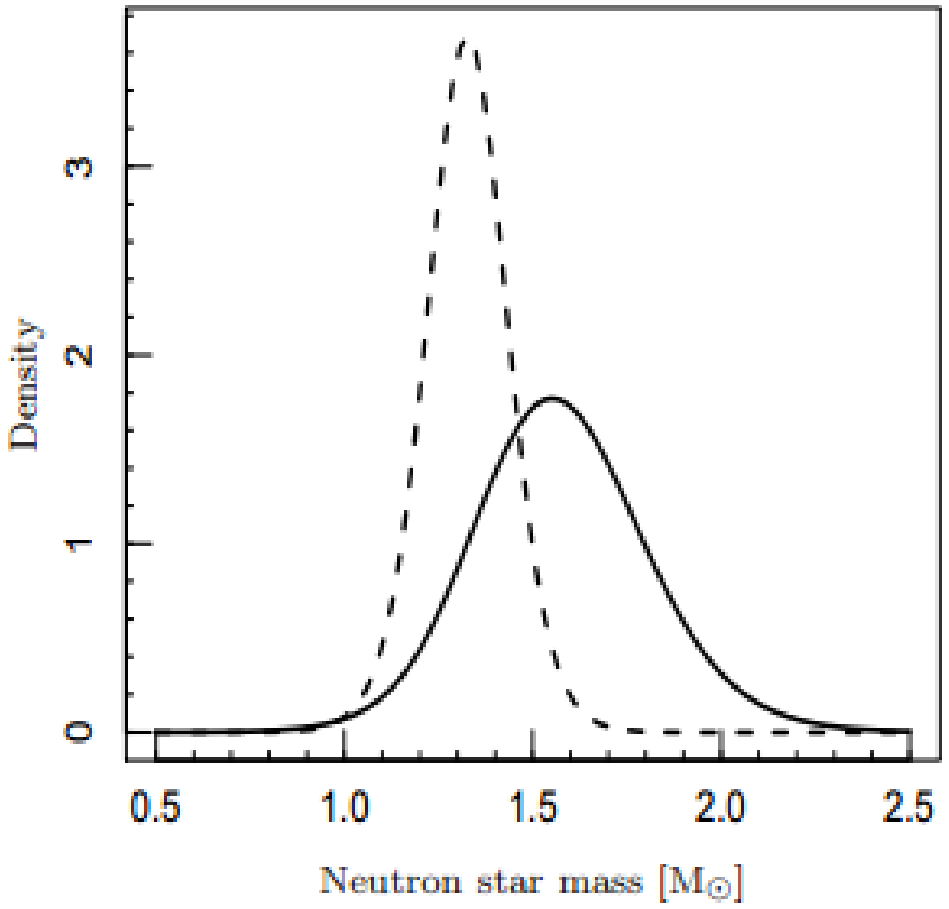

1309.6635

Compact objects and progenitors. Solar metallicity.

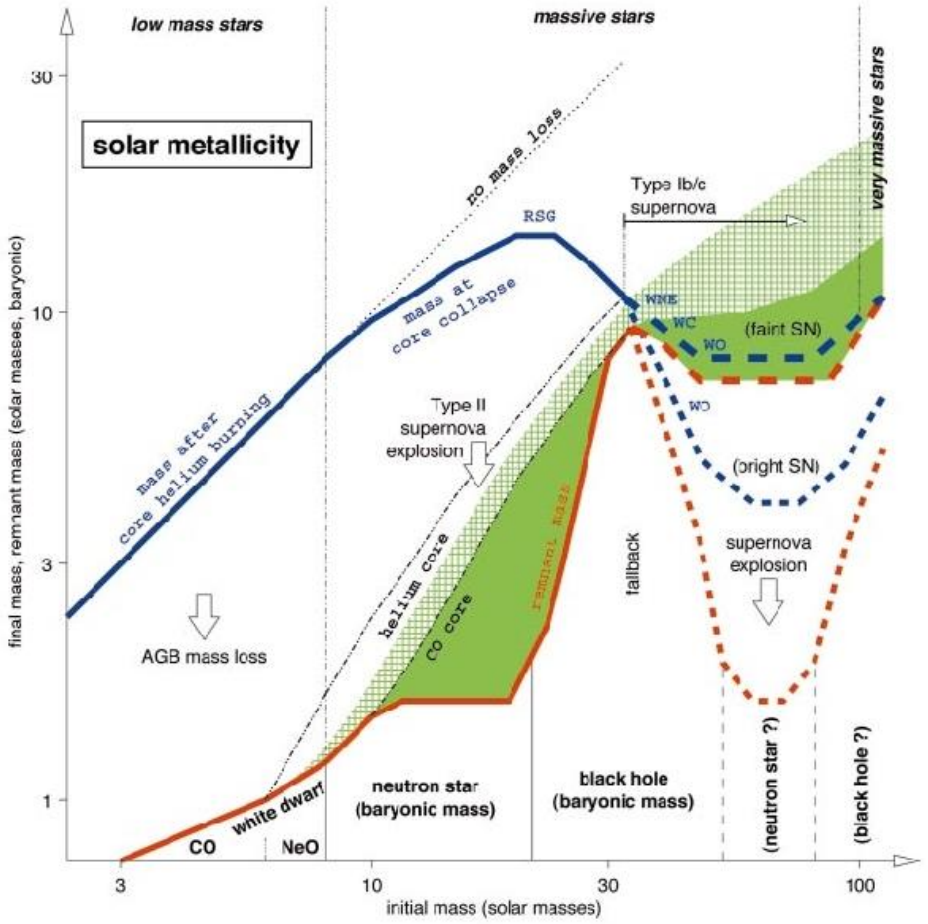

There can be a range of progenitor masses in which NSs are formed, however, for smaller and larger progenitors masses BHs appear.

Woosley et al. 2002

Mass spectrum of compact objects

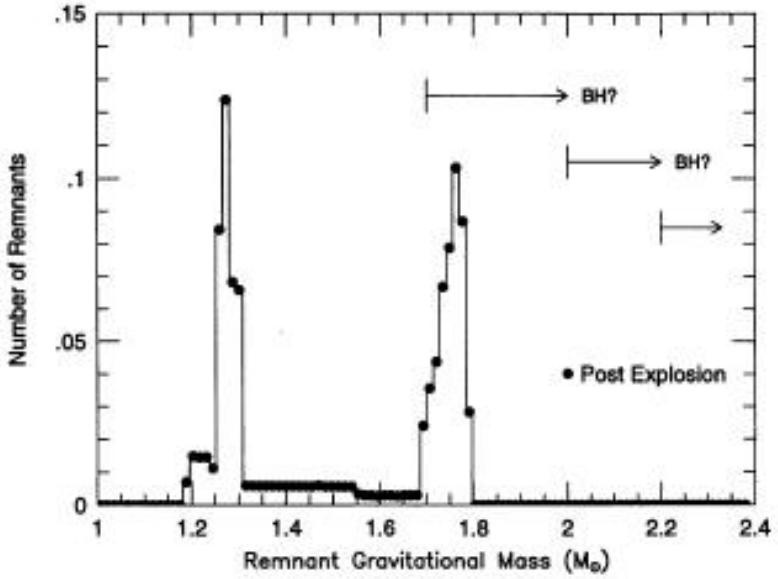

Results of calculations
(depend on the assumed model
of explosion)

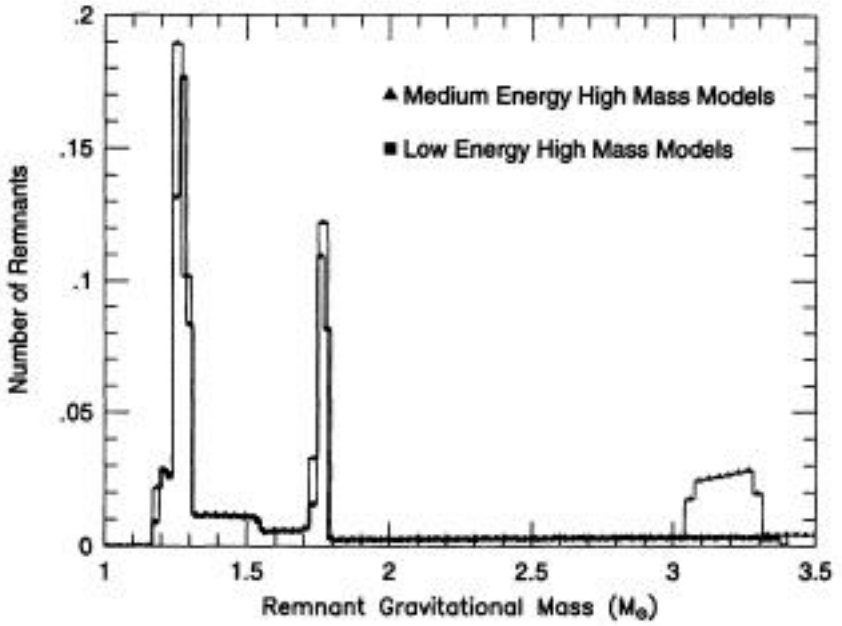

Timmes et al. 1996, astro-ph/9510136

Mass spectrum of compact objects

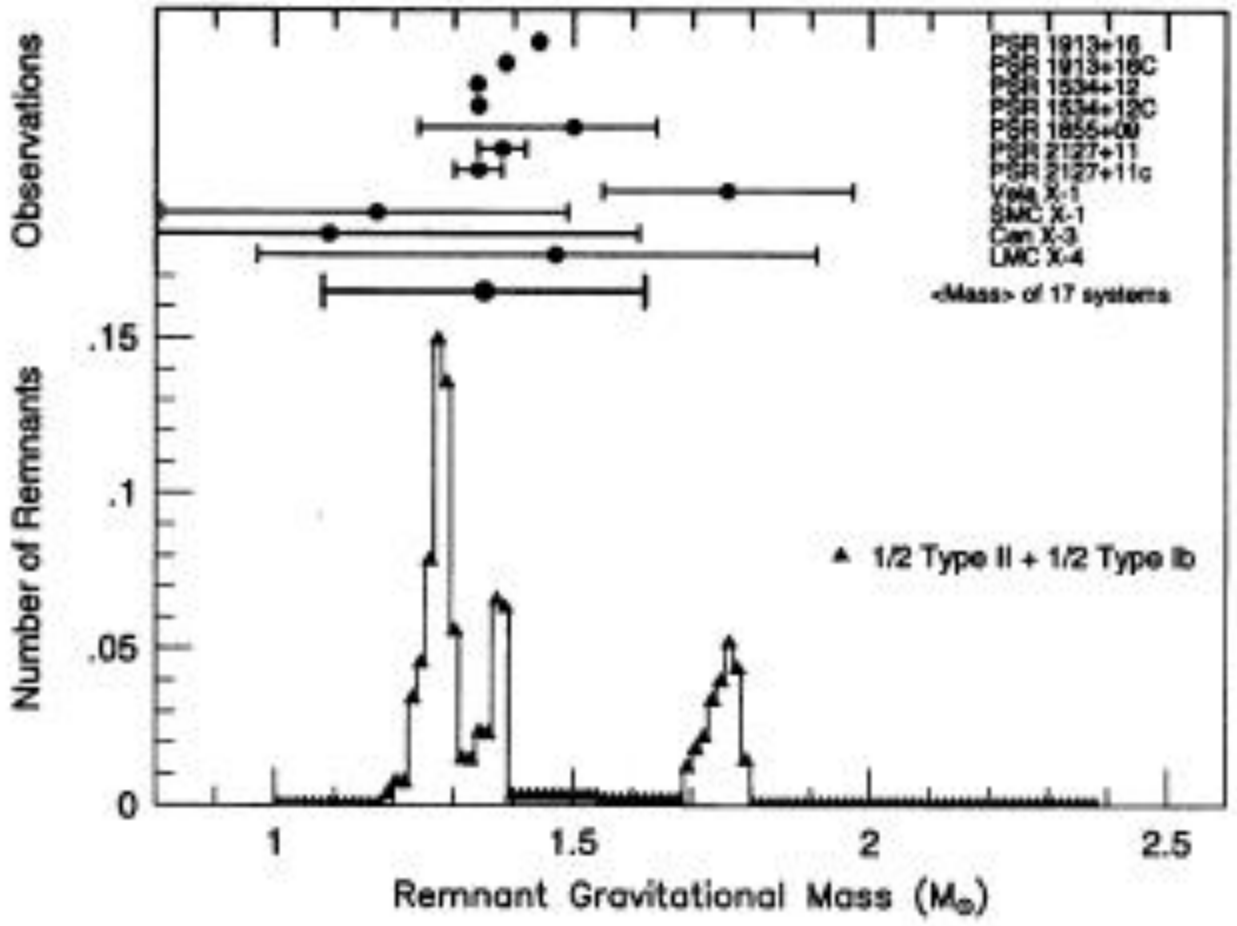

Comparison of one of the model with observations.

However, selection effects can be important as observed NSs a all in binaries.

Timmes et al. 1996, astro-ph/9510136

Newer calculations of the mass spectrum

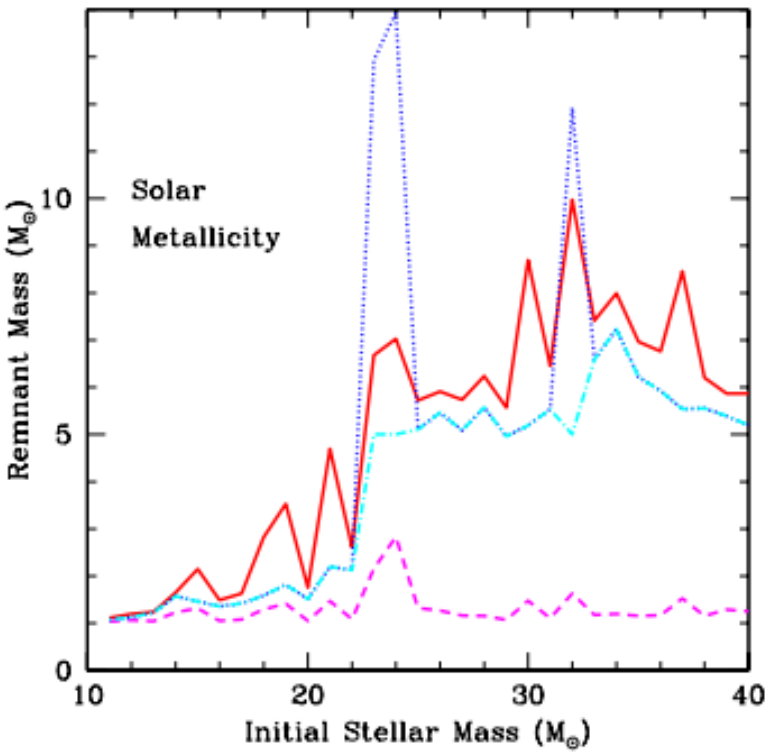

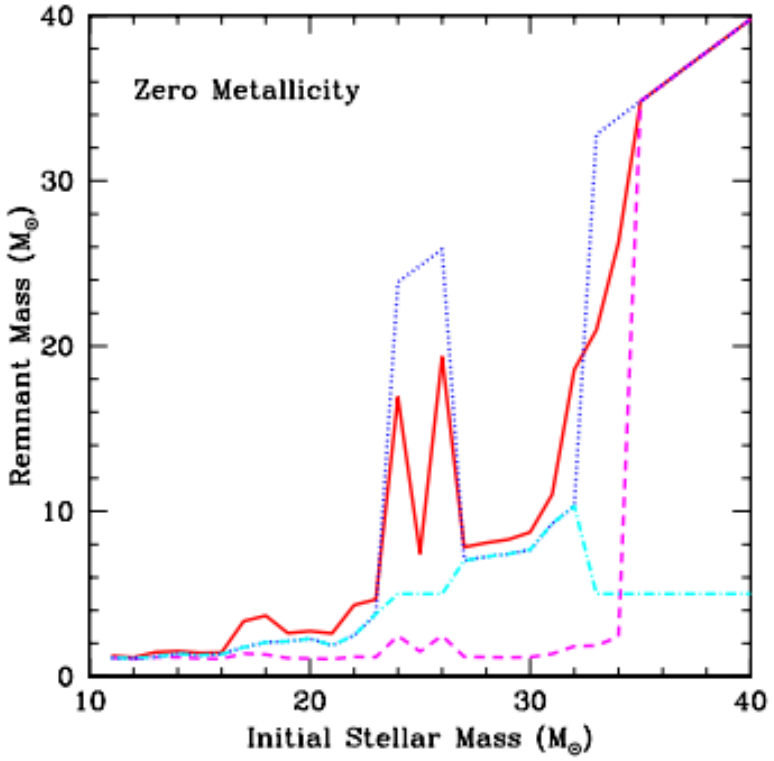

Different curves are plotted for different models of explosion:
dashed – with a magnetar

1110.1726

Bi-modal mass spectrum?

Pulsar Name	Mass of Recycled Neutron Star ($M_\odot$)	Mass of Young Neutron Star ($M_\odot$)	P_{orb} (hours)	Eccentricity	Pulse Period (ms)	Reference
J0737-3039A/B	1.3381 ± 0.0007	1.2489 ± 0.0007	2.4	0.088	23	Kramer et al. (2006)
B1534+12	1.3332 ± 0.0010	1.3452 ± 0.0010	10.1	0.273	38	Stairs et al. (2002)
J1756-2251	1.32 ± 0.02	1.24 ± 0.02	7.67	0.18	28	Stairs (2008)
J1906+0746	1.365 ± 0.018	1.248 ± 0.018	3.98	0.085	144†	Kasian (2008)
B1913+16	1.4414 ± 0.0002	1.3867 ± 0.0002	7.92	0.617	59	Weisberg & Taylor (2005)
B2127+11C	1.358 ± 0.010	1.354 ± 0.010	8.05	0.681	30	Jacoby et al. (2006)
J1909-3744	1.438 ± 0.024	white dwarf	36.7	$\lesssim 10^{-6}$	2.9	Jacoby et al. (2005)
J1141-6545	white dwarf	1.27 ± 0.01	4.74	0.172	393†	Bhat et al. (2008)

The low-mass peak the authors relate to e$^-$-capture SN.

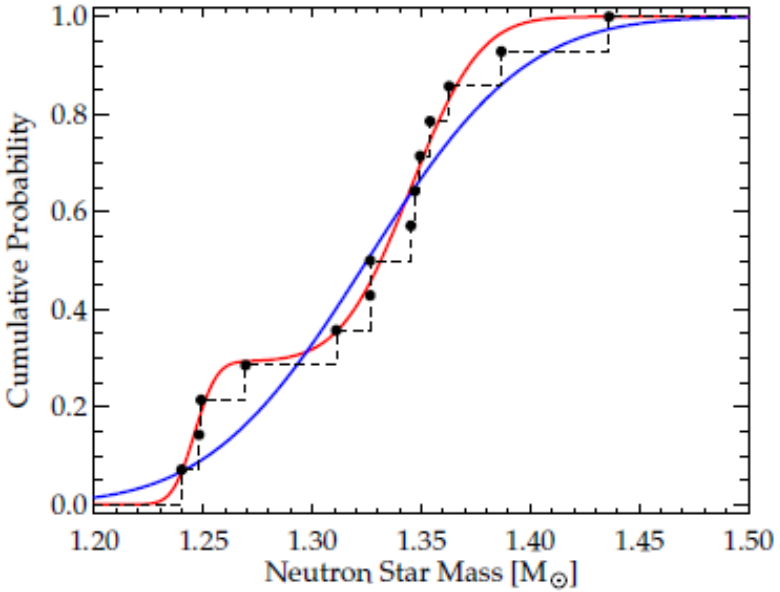

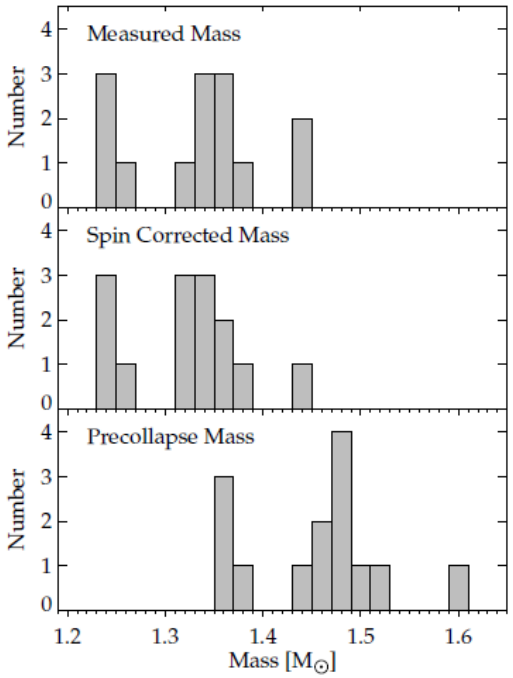

Based on 14 observed systems

1006.4584

Comparison of observations with theory

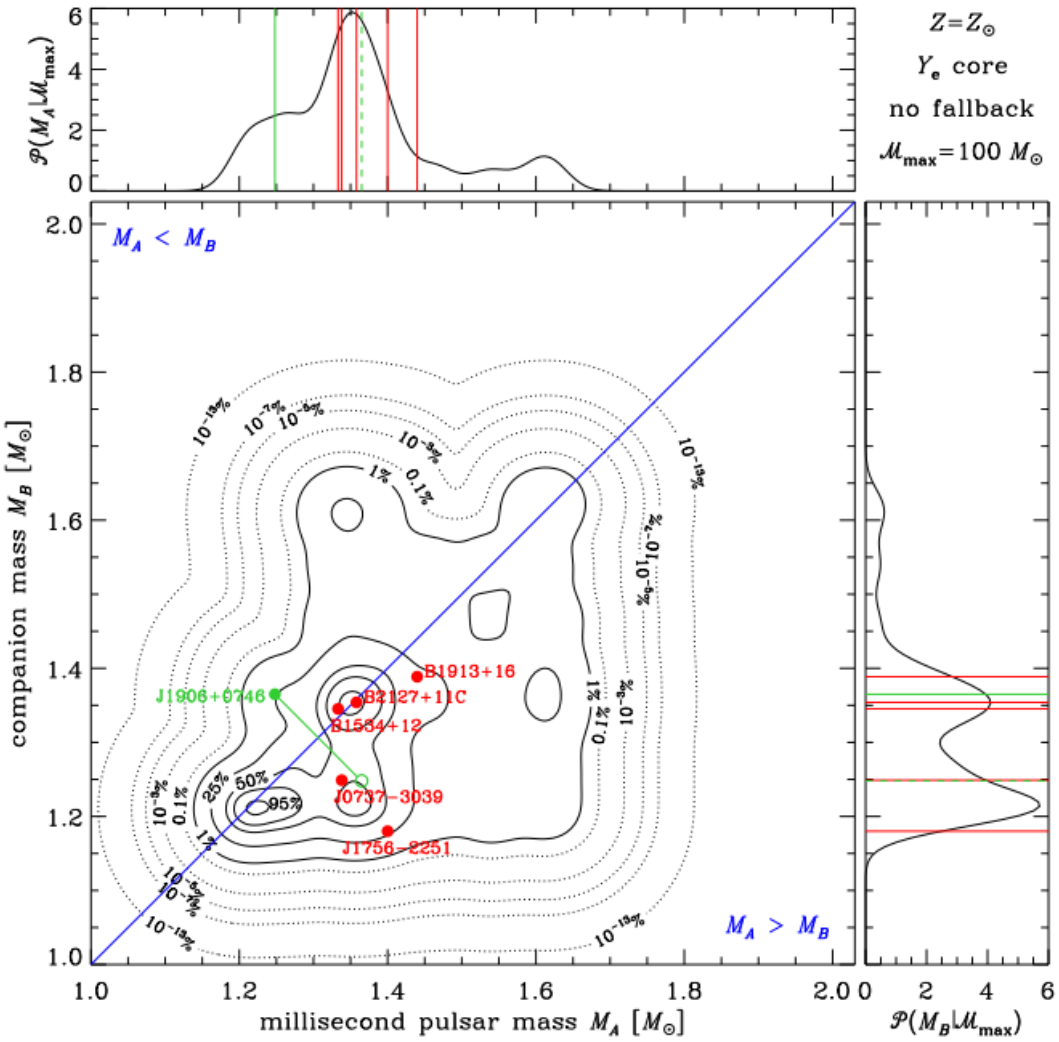

1204.5478

Bimodality in mPSR mass distribution

#	PSR Name	Mass [$M_\odot$]
1	J0337+1715	1.4378(13)
2	J0348+0432	2.01(4)
3	J0437−4715	1.44(7)
4	J0751+1807	1.64(15)
5	J1012+0507	1.83(11)
6	J1023+0038	1.71(16)
7	J1614−2230	1.928(17)
8	J1713+0747	1.31(11)
9	J1738+0333	1.47(7)
10	J1802−2124	1.24(11)
11	J1807−2500B	1.3655(21)
12	B1855+09	1.30(11)
13	J1903+0327	1.667(7)
14	J1909−3744	1.540(27)
15	J1910−5959A	1.34(8)
16	J1918−0642	1.18(11)
17	J1946+3417	1.832(13)
18	J2234+0611	1.396(11)

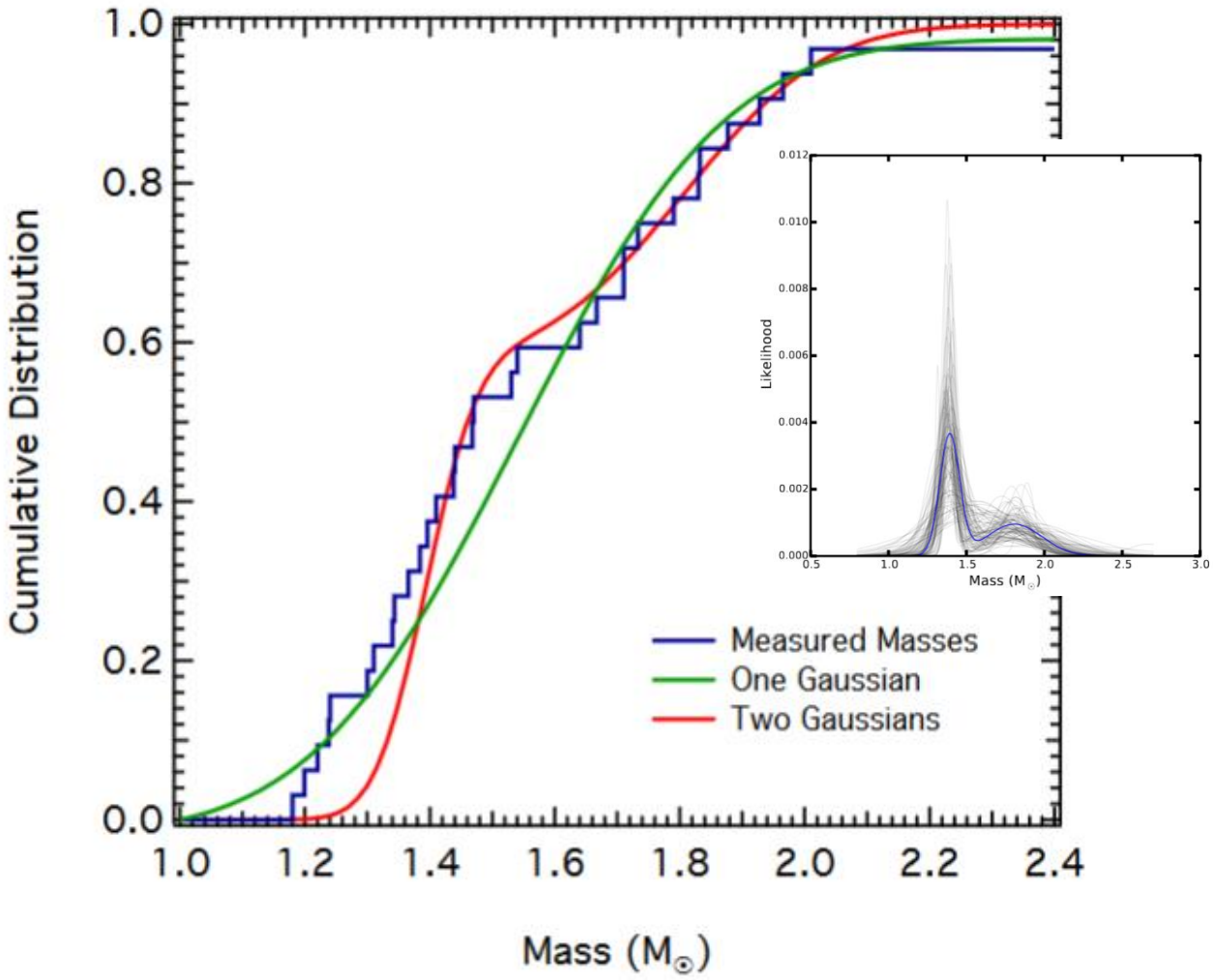

+ 14 PSR with less precisely determined masses

The bimodality reflects birth properties?

1605.01665

Massive born NS

PSR J2222−0137
WD companion
P=32.8 msec
M_{NS}~1.7-1.8

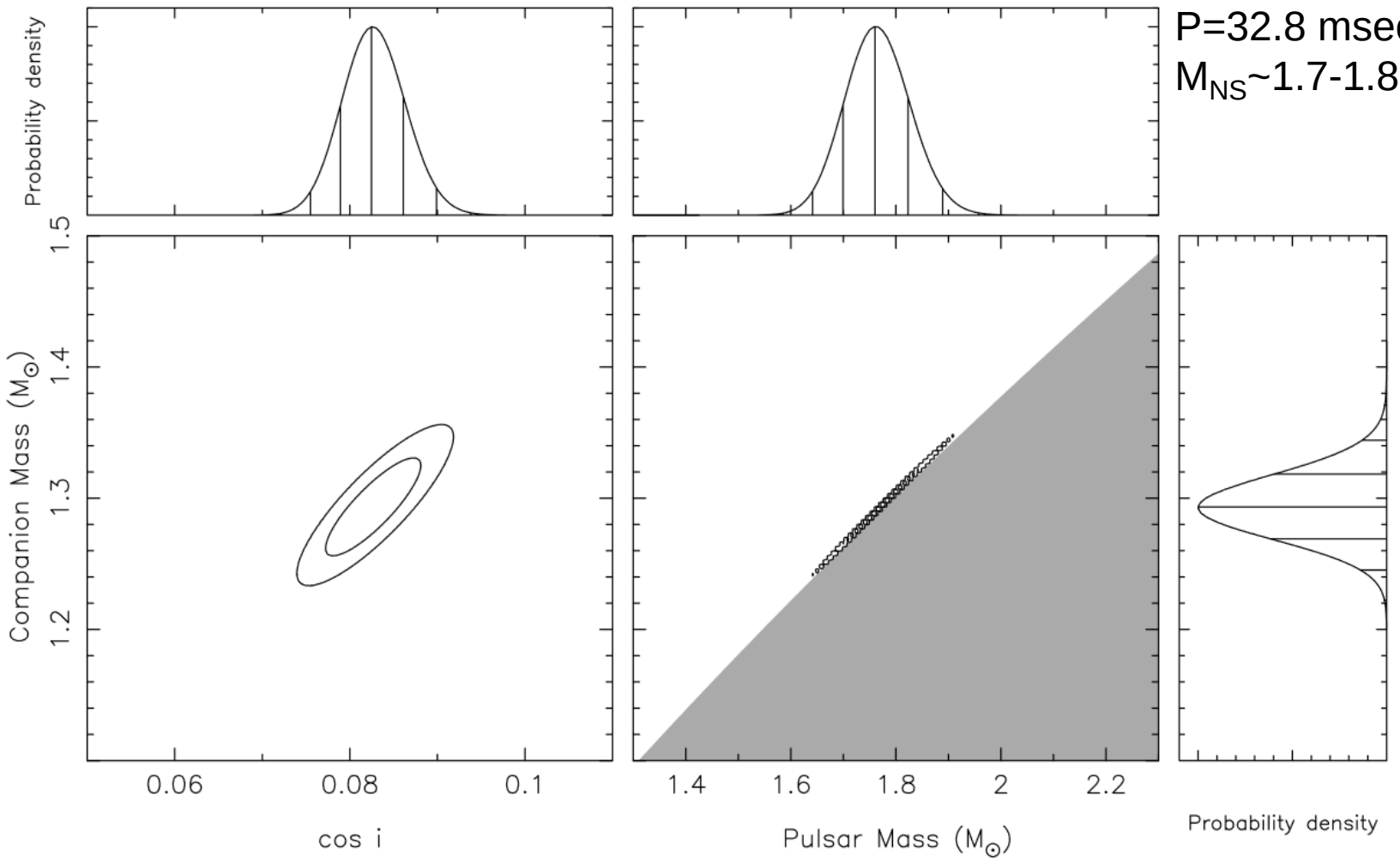

1706.08060

A NS from a massive progenitor

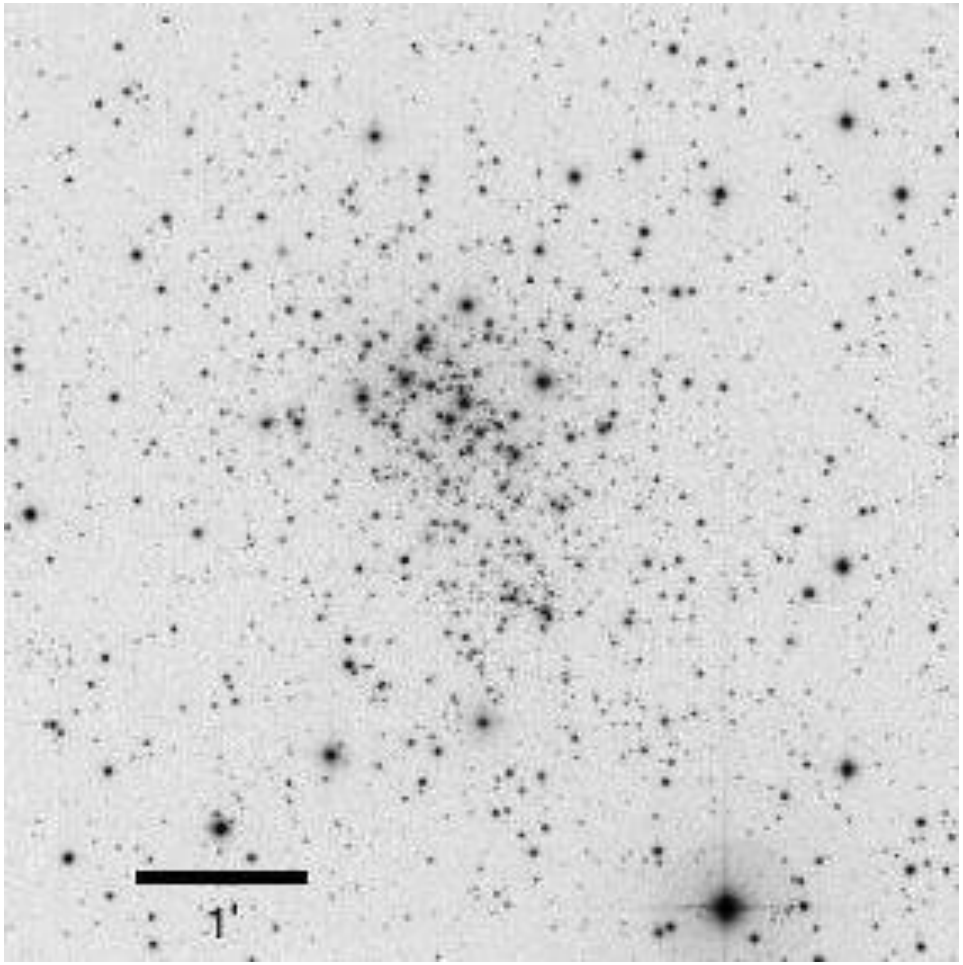

Anomalous X-ray pulsar
in the association
Westerlund1 most probably has
a very massive progenitor, >40 M_O.

astro-ph/0611589

The case of zero metallicity

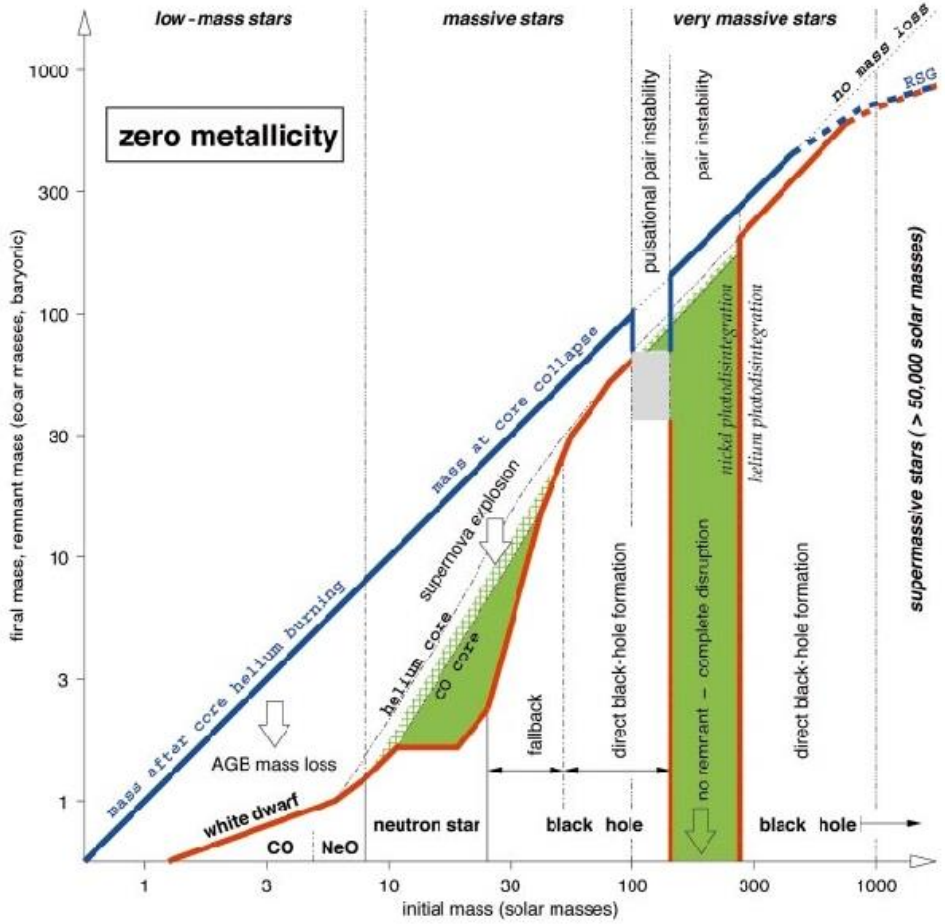

No intermediate mass range for NS formation.

Woosley et al. 2002

DNS

Radio Pulsar	Type	P (ms)
J0453+1559[a]	recycled	45.8
J0737−3039A[b]	recycled	22.7
J0737−3039B[b]	young	2773.5
J1518+4904[c]	recycled	40.9
B1534+12[d]	recycled	37.9
J1753−2240[e]	recycled	95.1
J1755−2550[f]*	young	315.2
J1756−2251[g]	recycled	28.5
J1811−1736[h]	recycled	104.2
J1829+2456[i]	recycled	41.0
J1906+0746[j]*	young	144.1
J1913+1102[k]	recycled	27.3
B1913+16[l]	recycled	59.0
J1930−1852[m]	recycled	185.5
J1807−2500B[n]*	GC	4.2
B2127+11C[p]	GC	30.5

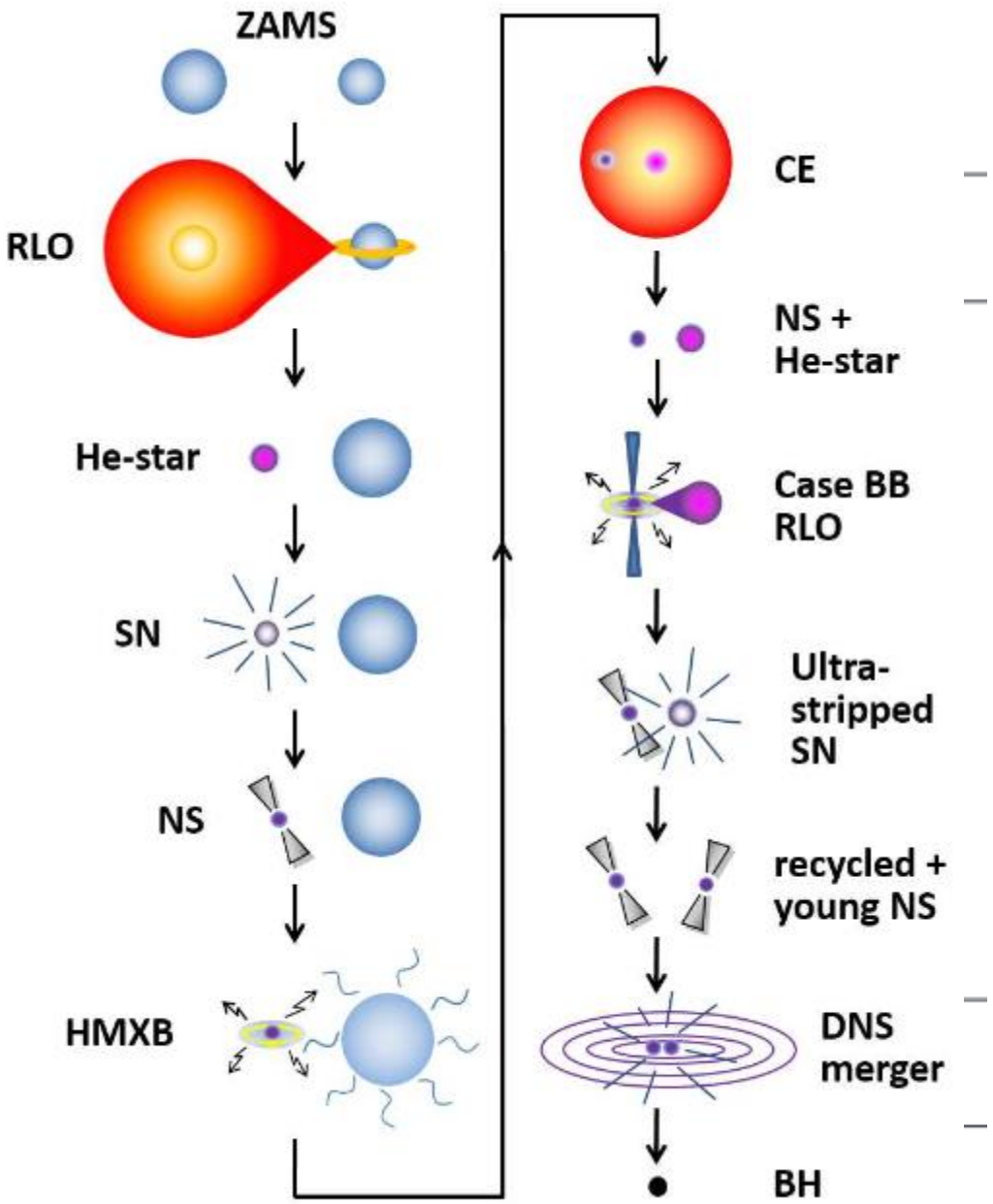

1706.09438

Mass distribution

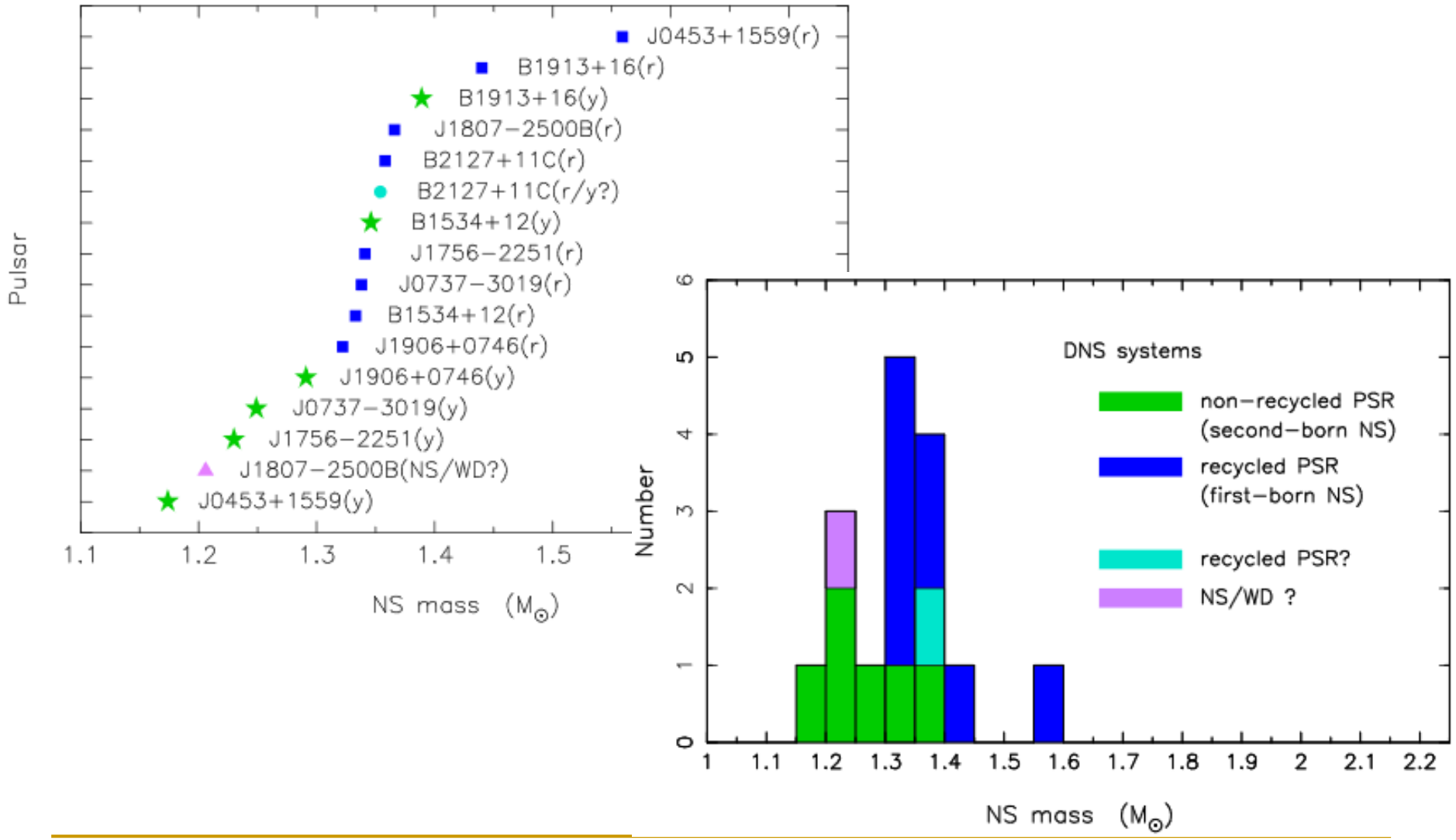

1706.09438

PSR J1518+4904

[Janssen et al. arXiv: 0808.2292]

Surprising results !!!

Mass of the recycled pulsar is <1.17 solar masses

Mass of its component is >1.55 solar masses

<u>Central values are even more shocking:</u>

$0.72^{+0.51}_{-0.58}$ and $2.00^{+0.58}_{-0.51}$

V~25 km/s, e~0.25

The second SN was e^--capture?

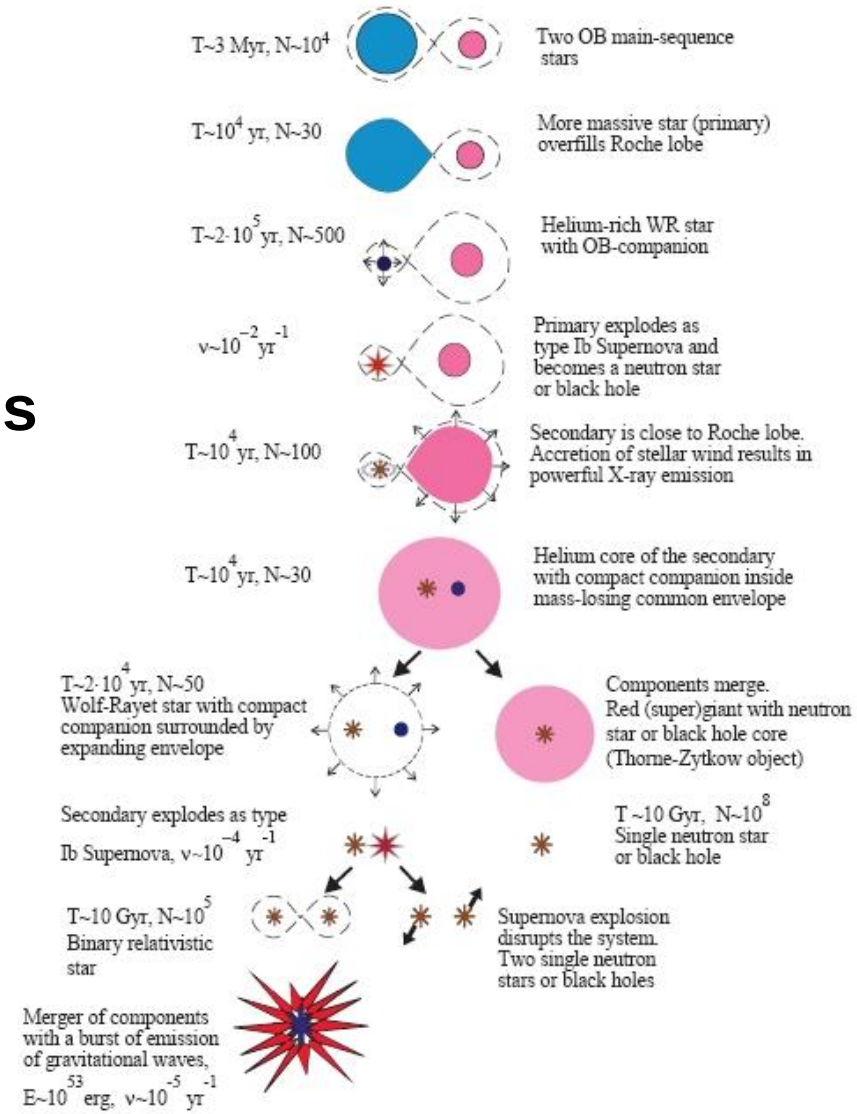

New measurements show less extreme values, see table 1 in 1603.02698: <1.768 and >0.95 solar masses. Total mass is the same 2.7183 solar masses.

Recent discoveries with records

PSR J1757−1854
4.4 hours

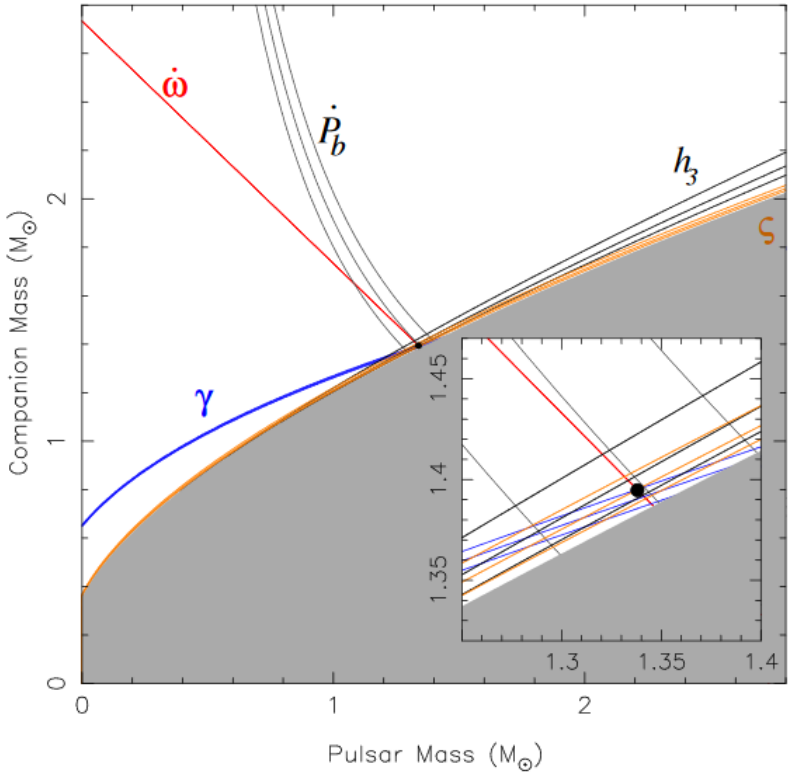

$$\dot{\omega} \simeq 10.37^\circ\,\mathrm{yr}^{-1},$$

1711.07697

PSR J1946+2052
1.88 hours

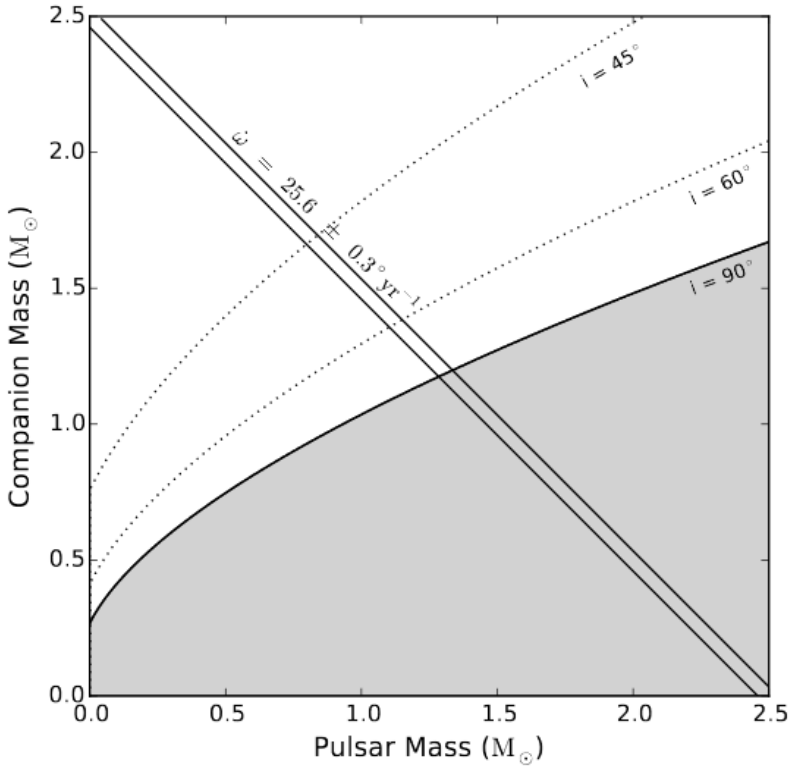

$$\dot{\omega} = 25.6 \pm 0.3\,\mathrm{deg\,yr}^{-1},$$

1802.01707

Binary pulsars

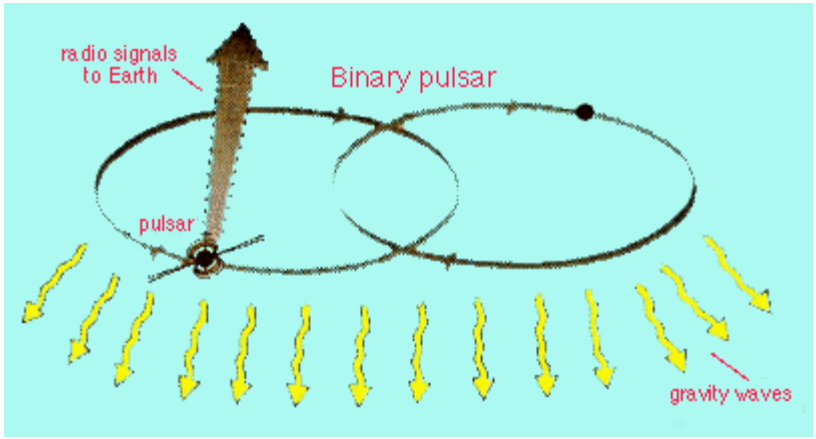

$$\frac{d\Delta_{E\odot}}{dt} = \sum_i \frac{Gm_i}{c^2 r_i} + \frac{v_\oplus^2}{2c^2} - \text{constant} .$$

$$\Delta_{S\odot} = -\frac{2GM_\odot}{c^3} \log (1 + \cos\theta) ,$$

$$T = t_{\text{obs}} - t_0 + \Delta_C - D/f^2 + \Delta_{R\odot}(\alpha, \delta, \mu_\alpha, \mu_\delta, \pi)$$
$$+ \Delta_{E\odot} - \Delta_{S\odot}(\alpha, \delta)$$
$$- \Delta_R(x, e, P_b, T_0, \omega, \dot{\omega}, \dot{P}_b) - \Delta_E(\gamma) - \Delta_S(r, s)$$

See 1502.05474 for a recent detailed review

Relativistic corrections and measurable parameters

$$\dot{\omega} = 3\left(\frac{P_b}{2\pi}\right)^{-5/3}(T_\odot M)^{2/3}(1-e^2)^{-1}\,,$$

$$\gamma = e\left(\frac{P_b}{2\pi}\right)^{1/3} T_\odot^{2/3} M^{-4/3} m_2(m_1+2m_2)\,,$$

$$\dot{P}_b = -\frac{192\pi}{5}\left(\frac{P_b}{2\pi}\right)^{-5/3}\left(1+\frac{73}{24}e^2+\frac{37}{96}e^4\right) \times (1-e^2)^{-7/2} T_\odot^{5/3} m_1 m_2 M^{-1/3}\,,$$

$$r = T_\odot m_2\,,$$

$$s = x\left(\frac{P_b}{2\pi}\right)^{-2/3} T_\odot^{-1/3} M^{2/3} m_2^{-1}\,.$$

For details see
Taylor, Weisberg 1989
ApJ 345, 434

Shapiro delay

$$\Delta_S = -2r \log(1 - s \cos[2\pi(\phi - \phi_0)])$$

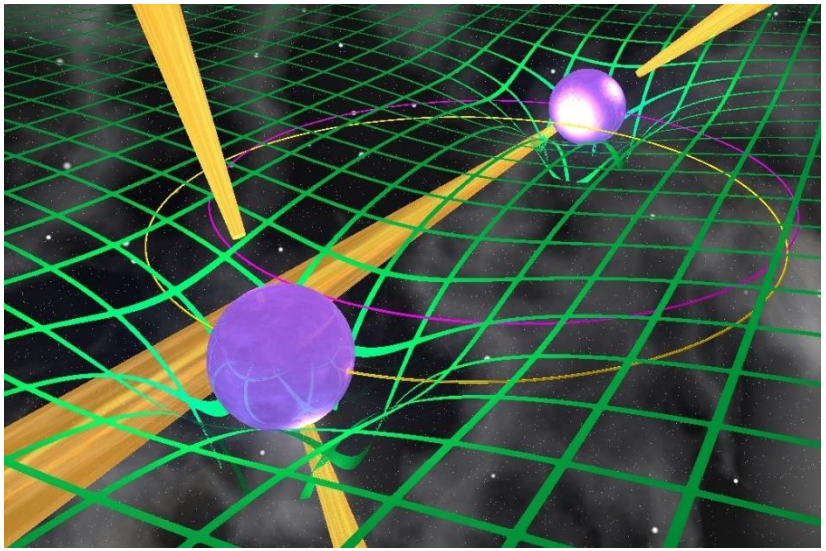

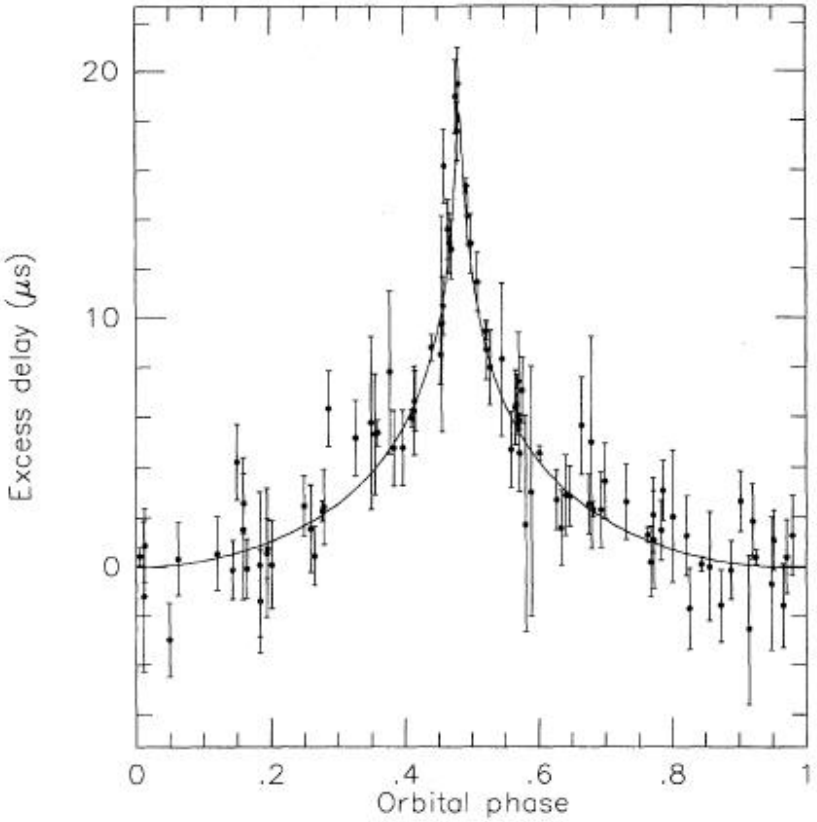

PSR 1855+09 (Taylor, Nobel lecture)

Mass measurements

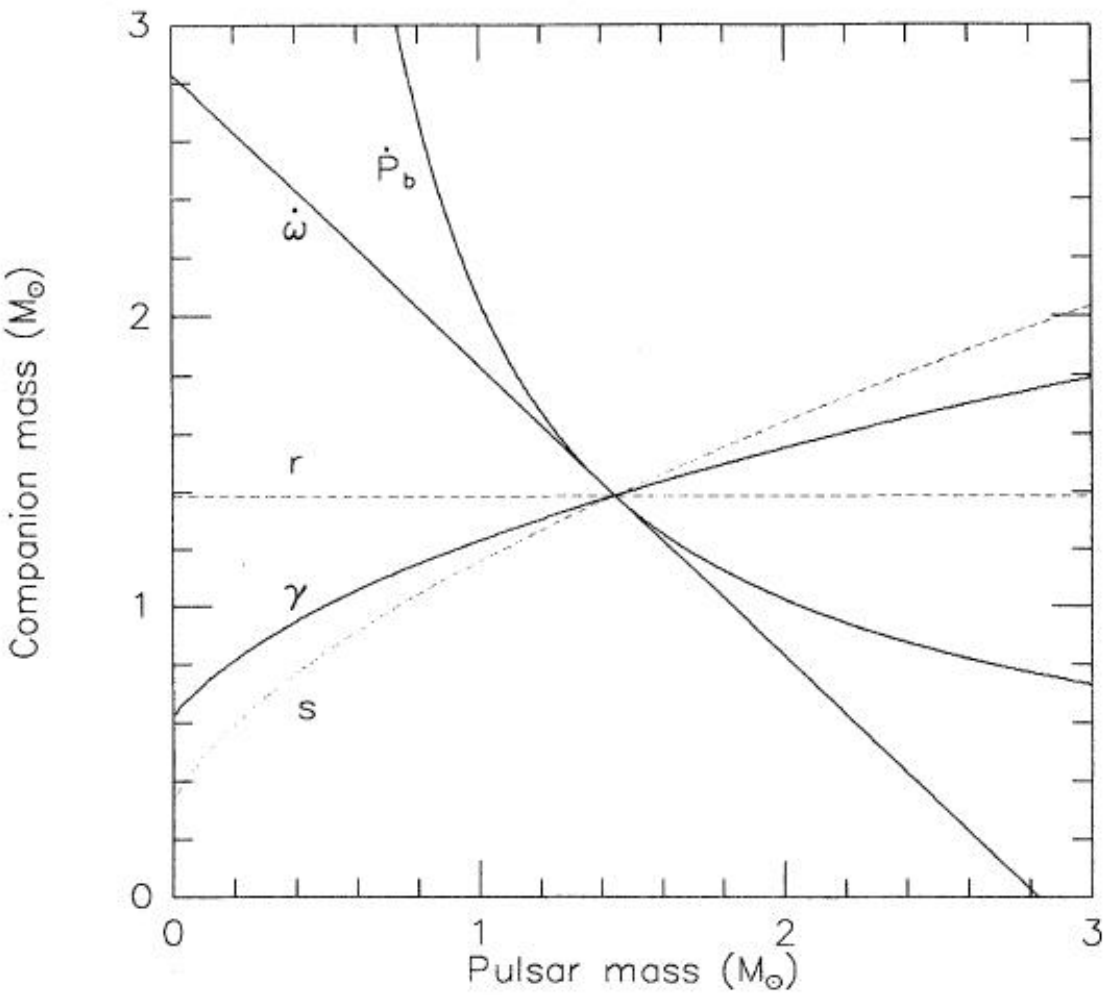

PSR 1913+16

Taylor

Uncertainties and inverse problems

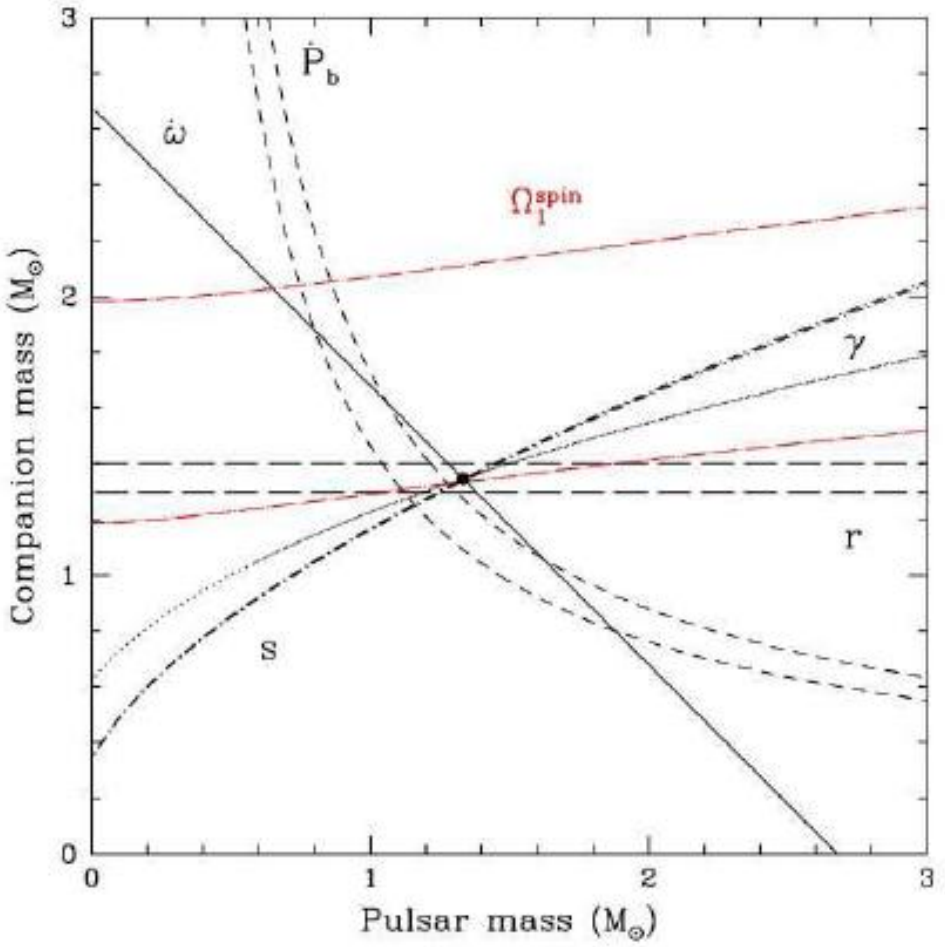

$P_b$dot depends on the Shklovskii effect. So, if distance is not certain, it is difficult to have a good measurement of this parameter.

It is possible to invert the problem. Assuming that GR is correct, one can improve the distance estimate for the given source.

PSR B1534+12.

1502.05474

Double pulsar J0737-3039

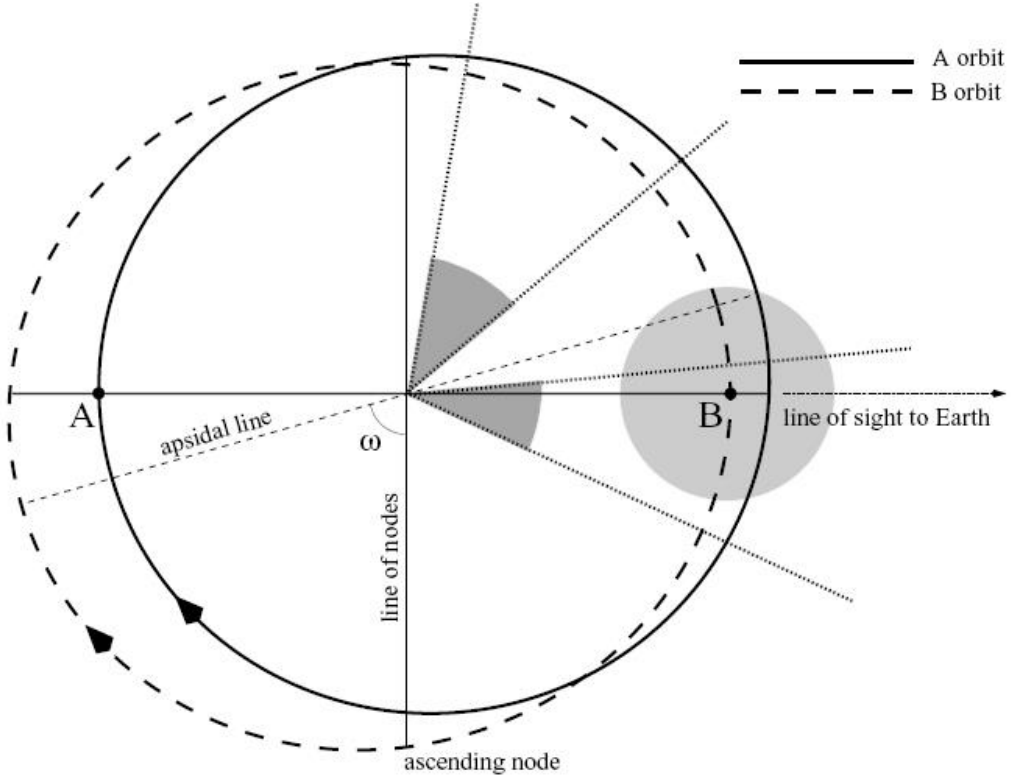

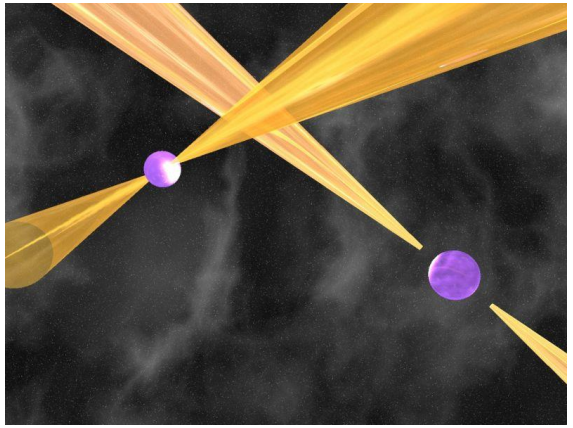

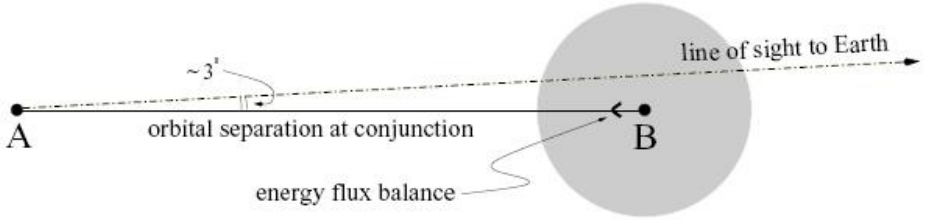

Lyne et al. astro-ph/0401086

Masses for PSR J0737-3039

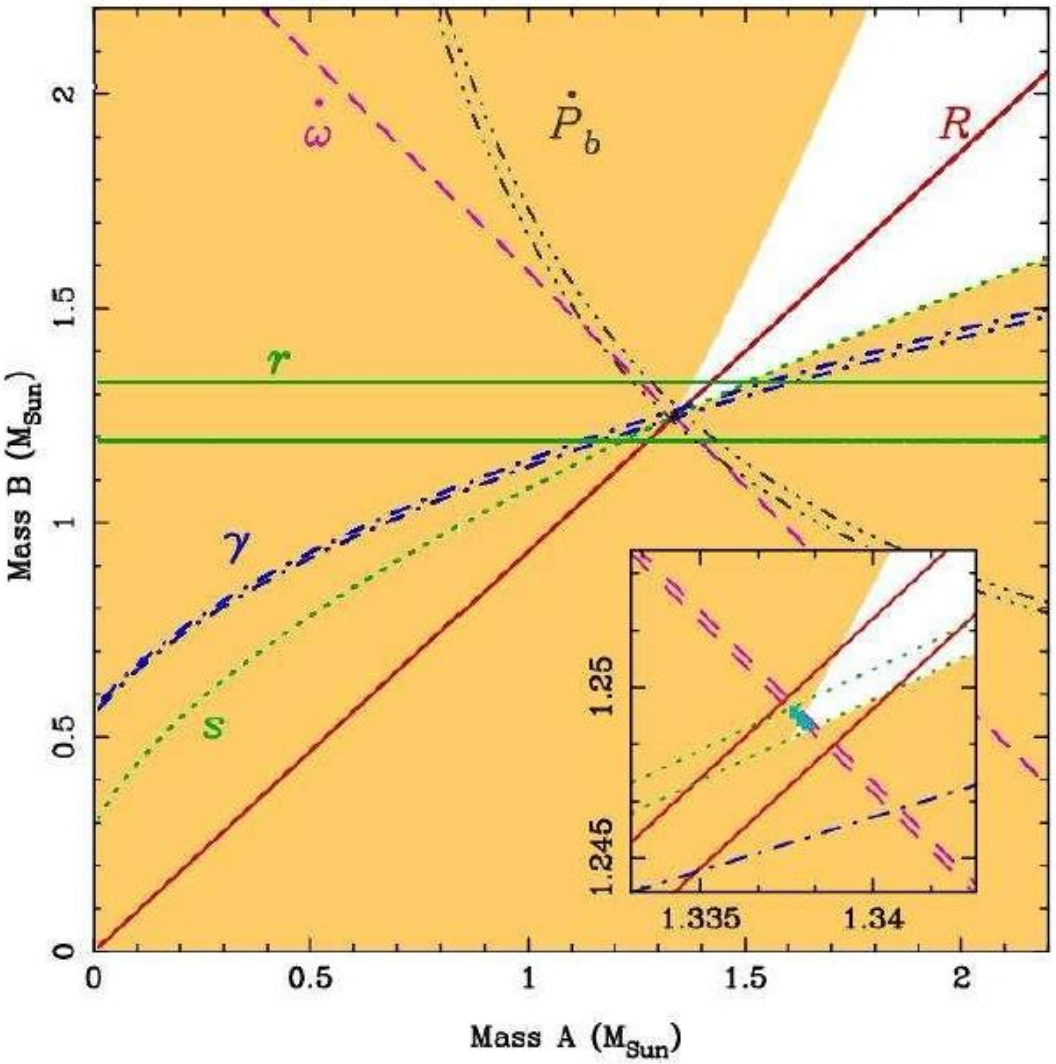

The most precise values.

New mass estimates have uncertainties <0.001

Kramer et al. astro-ph/0609417

Tests of theories of gravity

J1713+0747

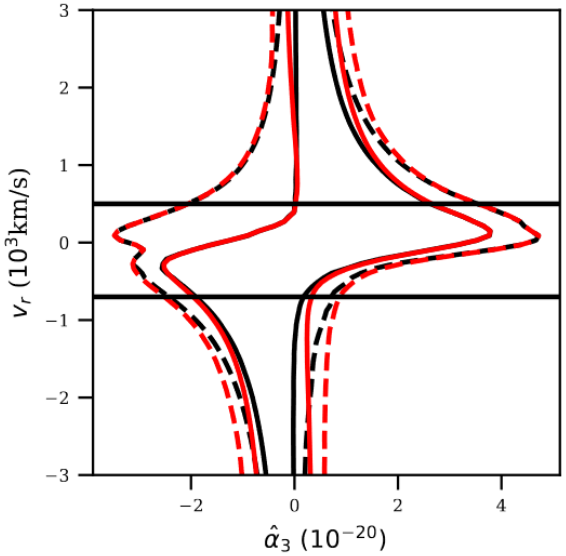

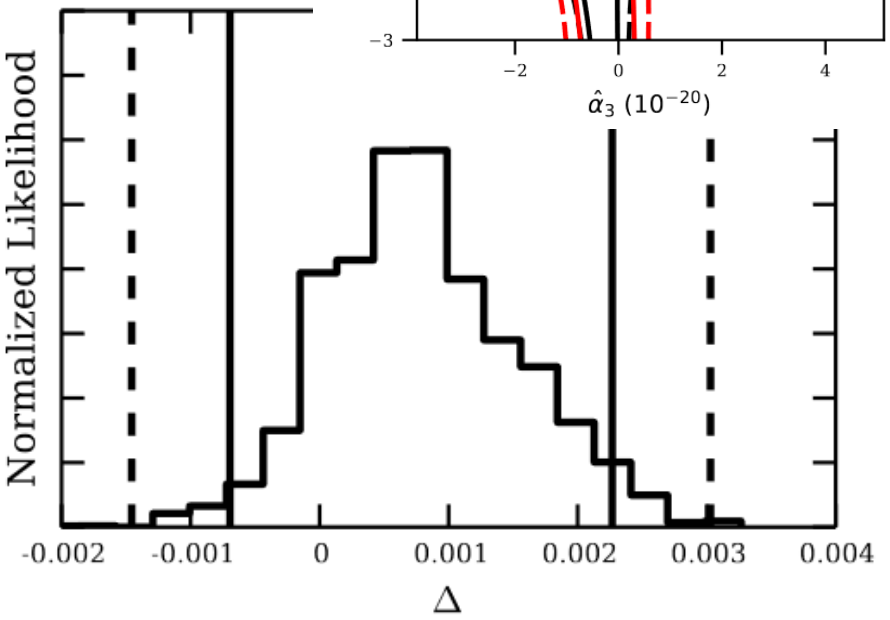

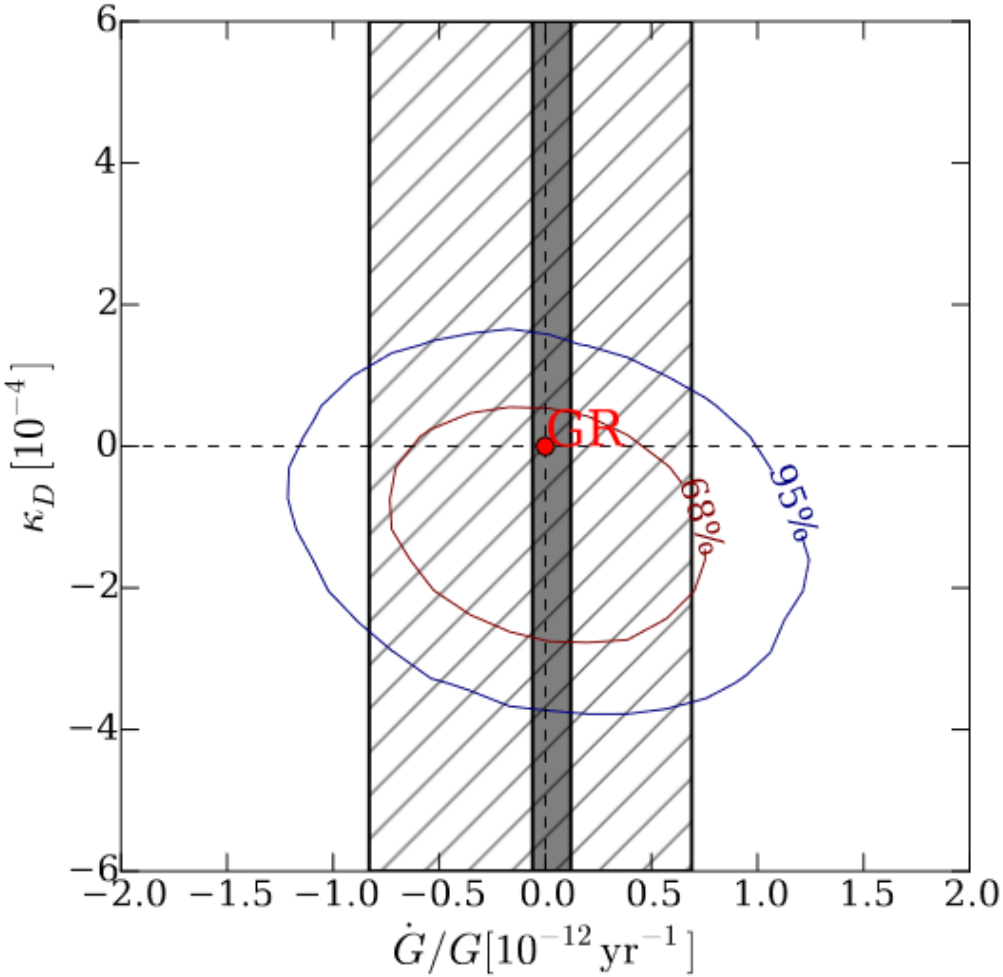

1802.09206

Testing strong equivalence principle with triple pulsar PSR J0337+1715

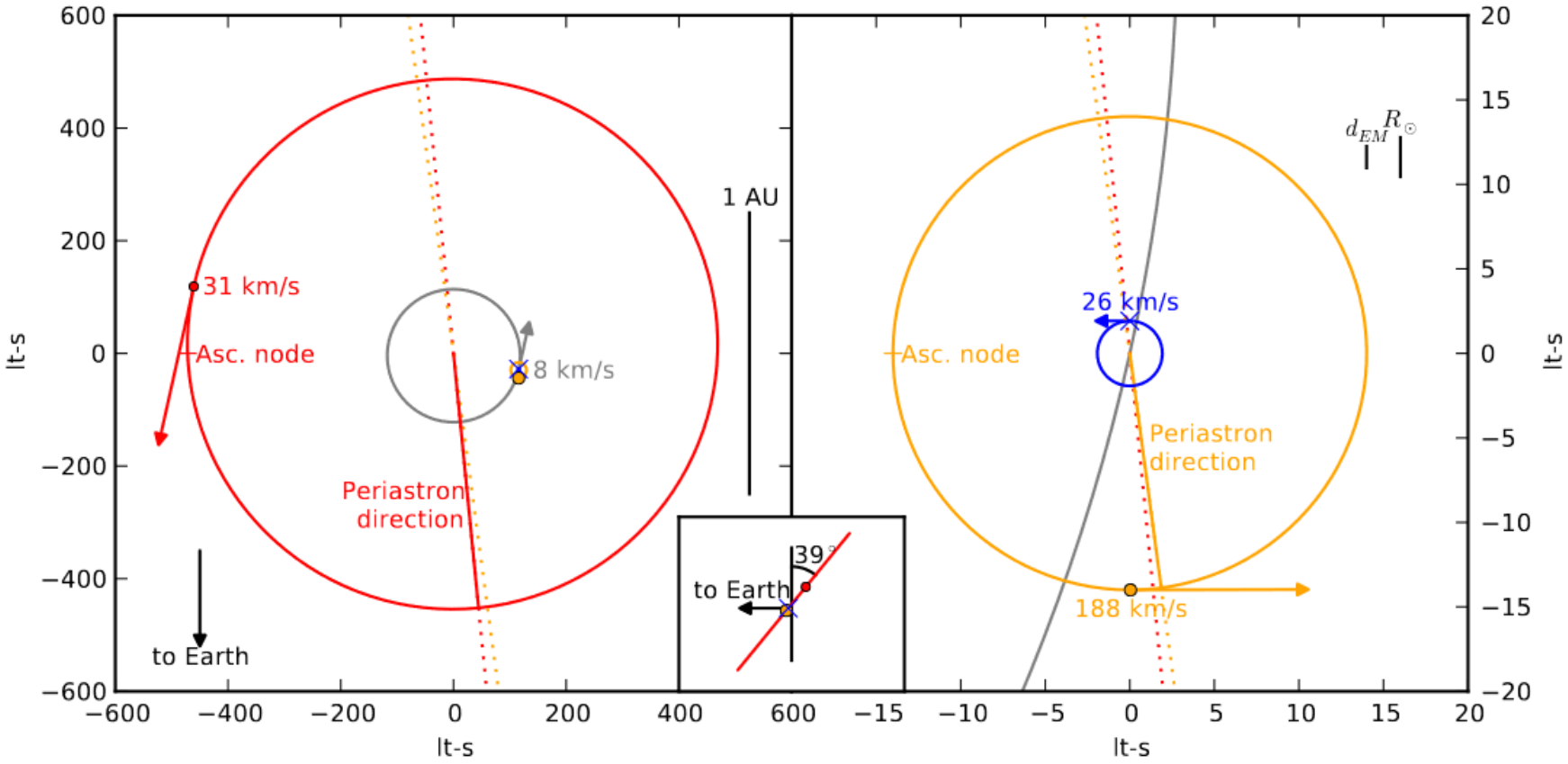

NS+WD+WD

1401.0535

NS+WD binaries

Some examples

PSR J0437-4715. WD companion [0801.2589, 0808.1594].
The closest millisecond PSR. M_{NS}=1.76+/-0.2 solar.

The case of PSR J0751+1807.
Initially, it was announced that it has a mass ~2.1 solar [astro-ph/0508050].
However, then in 2007 at a conference the authors announced that the result was incorrect. Actually, the initial value was 2.1+/-0.2 (1 sigma error).
New result: 1.26 +/- 0.14 solar
[Nice et al. 2008, Proc. of the conf. "40 Years of pulsars"]

It is expected that most massive NSs get their additional "kilos" due to accretion from WD companions [astro-ph/0412327].

Very massive neutron star

Binary system: pulsar + white dwarf
PSR 1614-2230

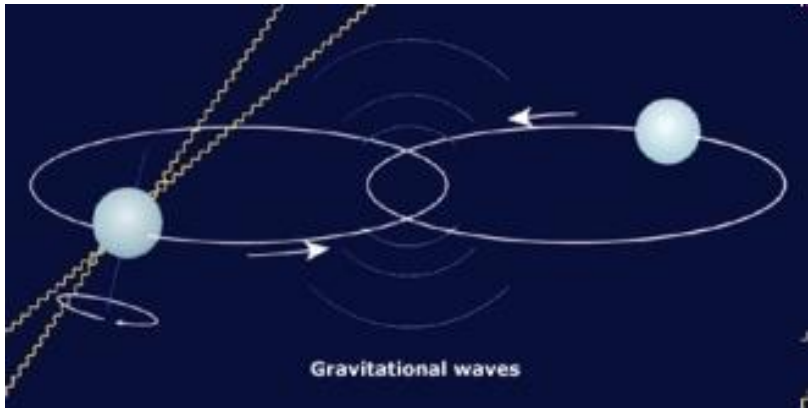

Mass ~ 2 solar

About the WD see 1106.5497.
The object was identified in optics.

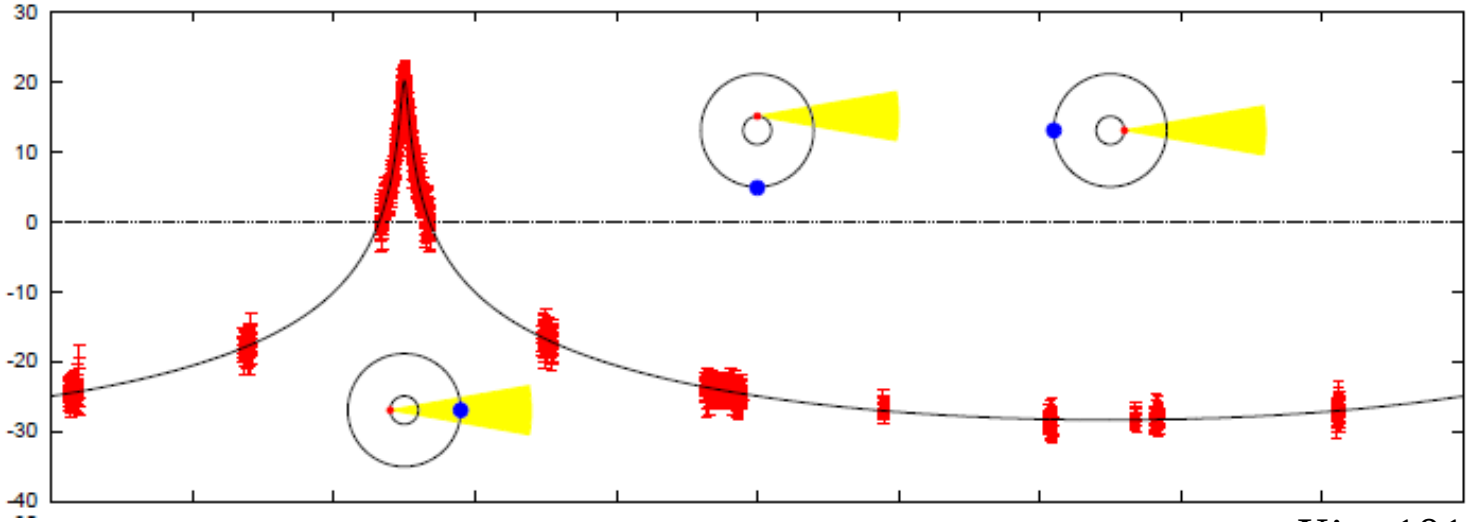

arXiv: 1010.5788

About formation of this objects see 1103.4996

Why is it so important?

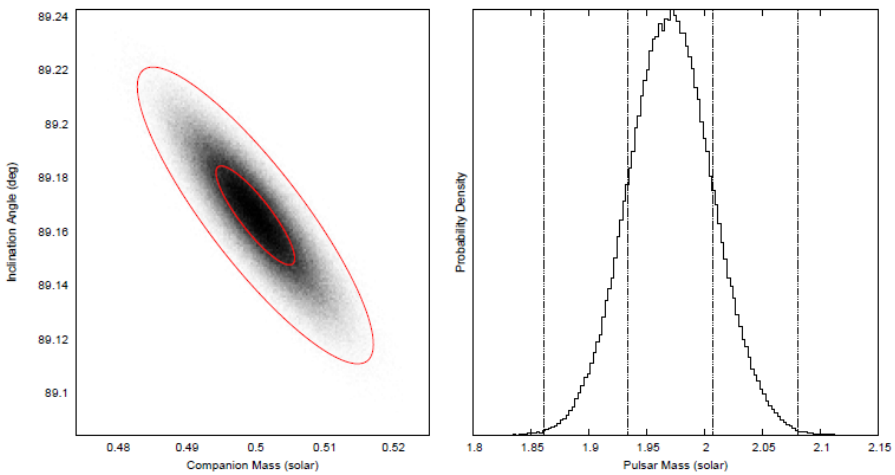

The maximum mass is a crucial property of a given EoS

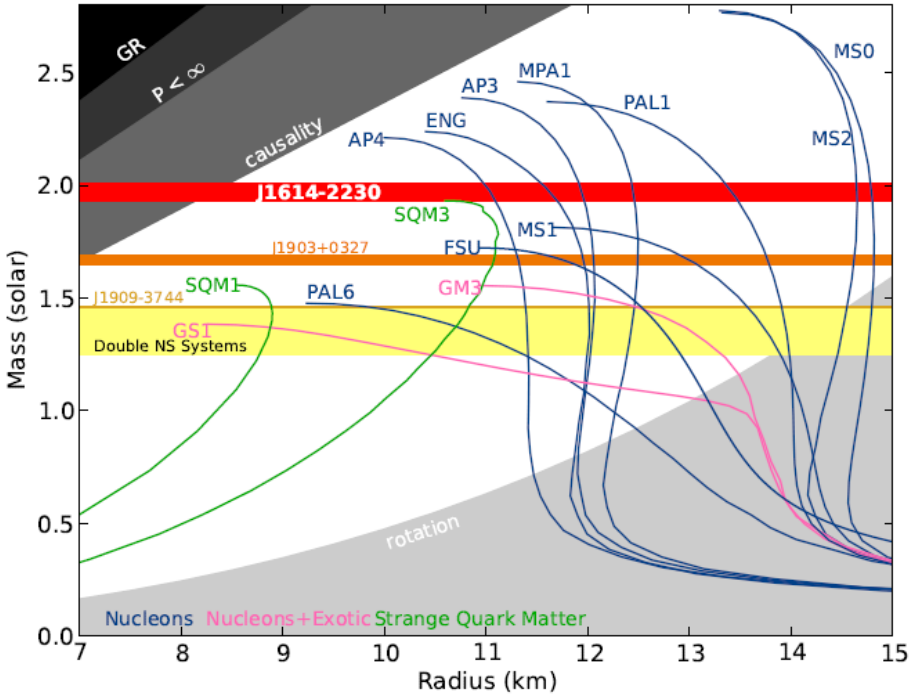

Collapse happens earlier for softer EoSs, see however, 1111.6929 about quark and hybrid stars to explain these data.

Interestingly, it was suggested that just <0.1 solar masses was accreted (1210.8331)

arXiv: 1010.5788

In the future specific X-ray sources (eclipsing msec PSR like SWIFT J1749.4−2807) can show Shapiro delay and help to obtain masses for a different kind of systems, see 1005.3527 , 1005.3479 .

2.01 solar masses NS

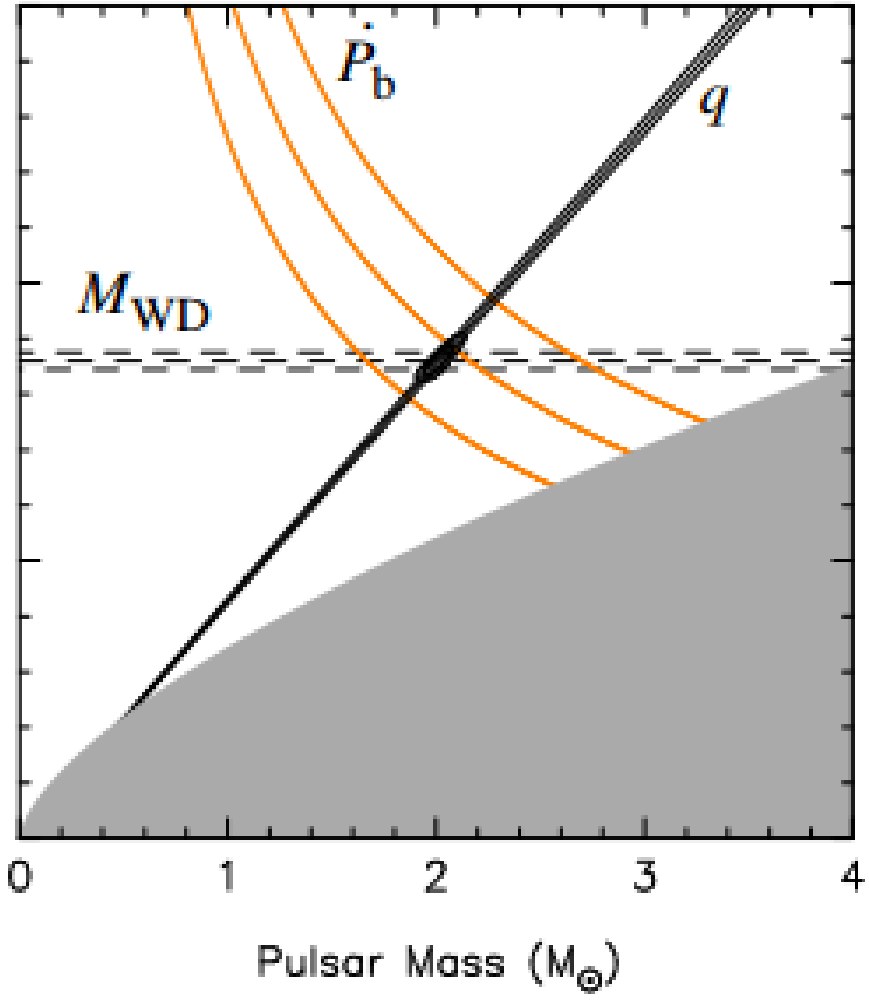

PSR J0348+0432
39 ms, 2.46 h orbit
WD companion

The NS mass is estimated to be:
1.97 – 2.05 solar mass at 68.27%
1.90 – 2.18 solar mass at 99.73% confidence level.

System is perfect for probing theories of gravity as it is very compact.

1304.6875

The most extreme (but unclear) example

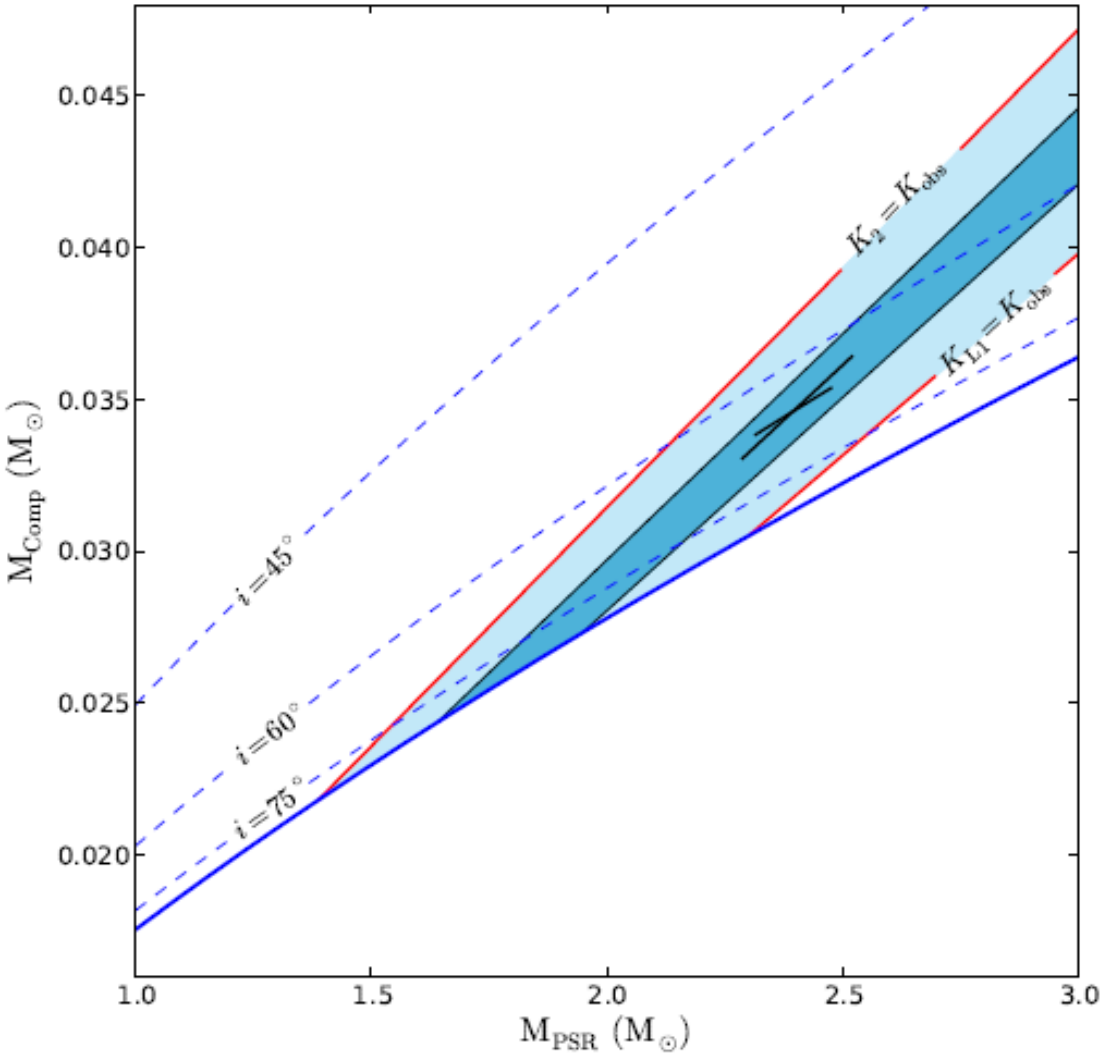

BLACK WIDOW PULSAR
PSR B1957+20

2.4+/-0.12 solar masses

1009.5427

More measurements

PSR J1738+0333 NS+WD arXiv: 1204.3948

M_{WD} = 0.181+0.007-0.005 M_O
M_{PSR} = 1.47+0.07-0.06 M_O

PSR J1311−3430
arXiv: 1210.6884
MPSR>2.1 at least!

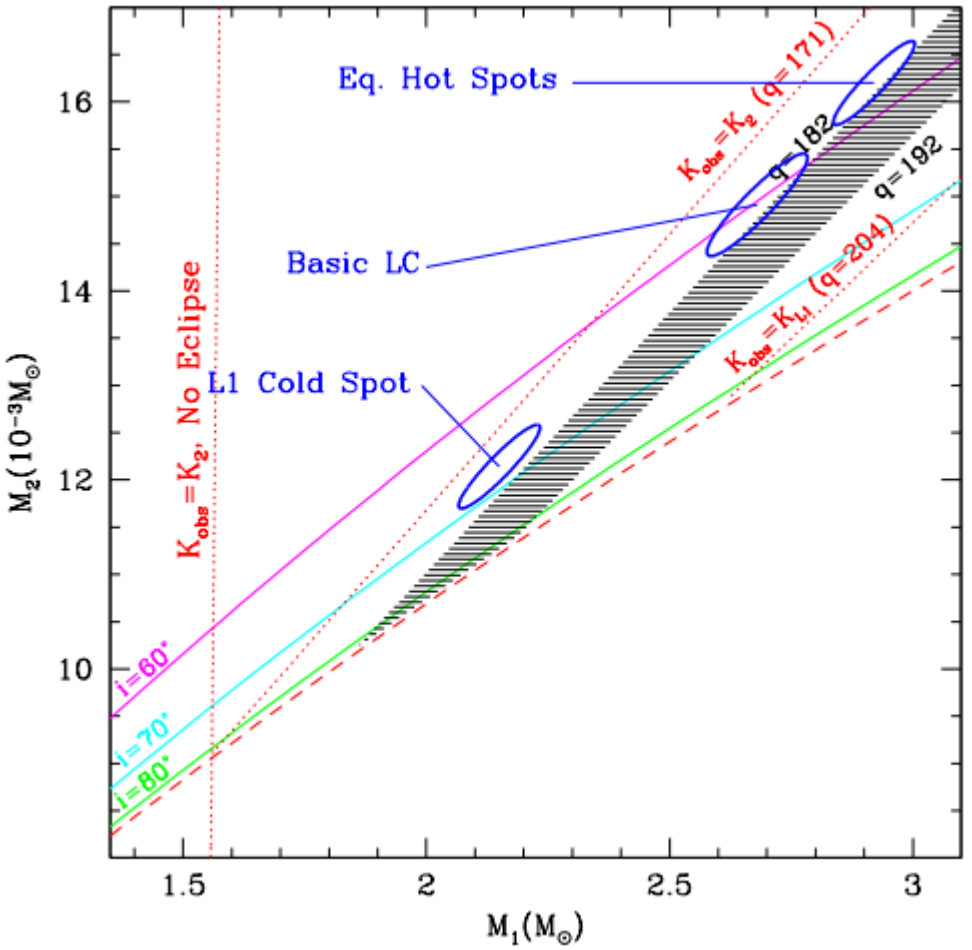

A massive NS in PSR J2215+5135

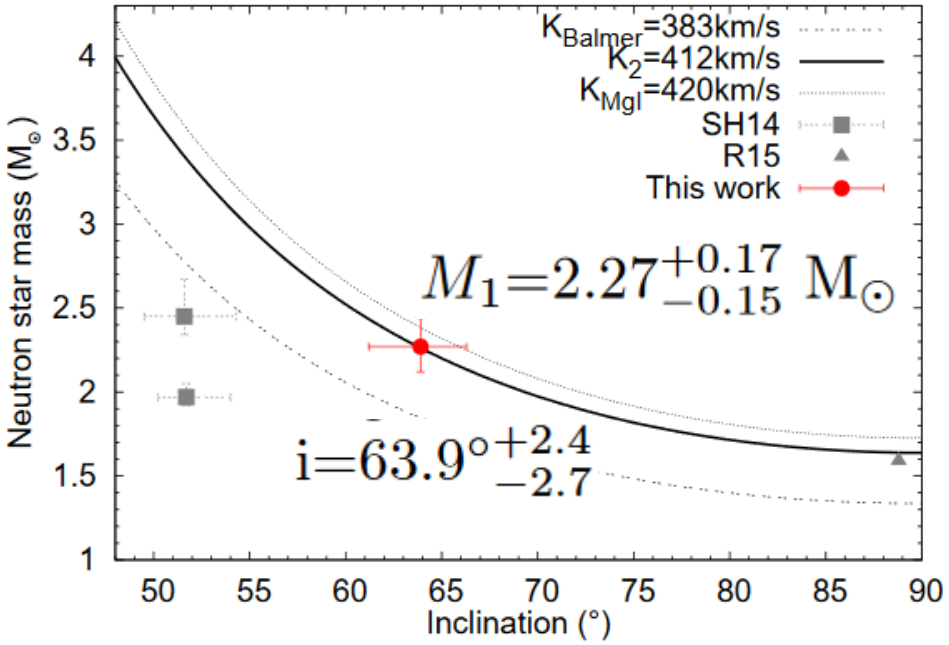

Different lines provide different velocity as they are emitted from different sides of the companion.

Different sides of the companion move with different velocity.

Thus, a correct model provides new mass determination.

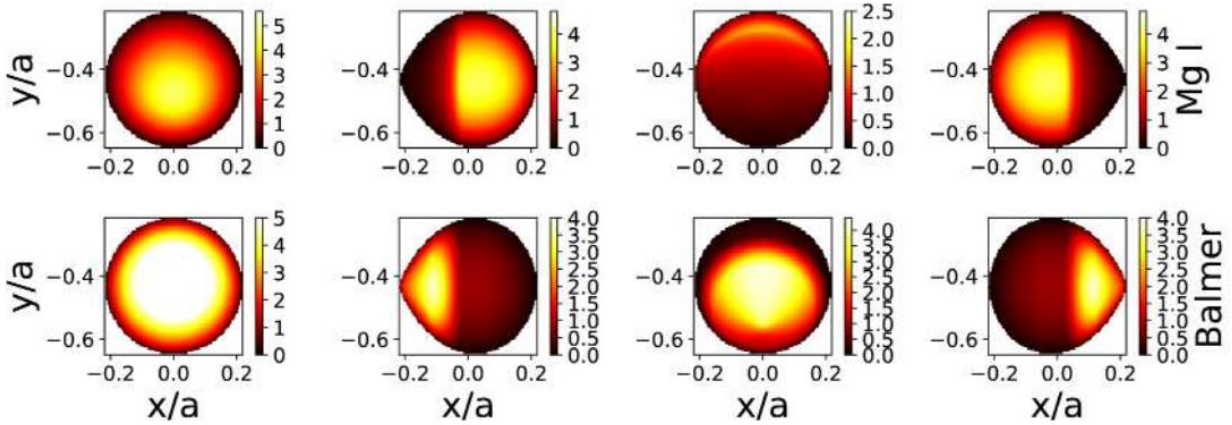

1805.08799

How much do PSRs accrete?

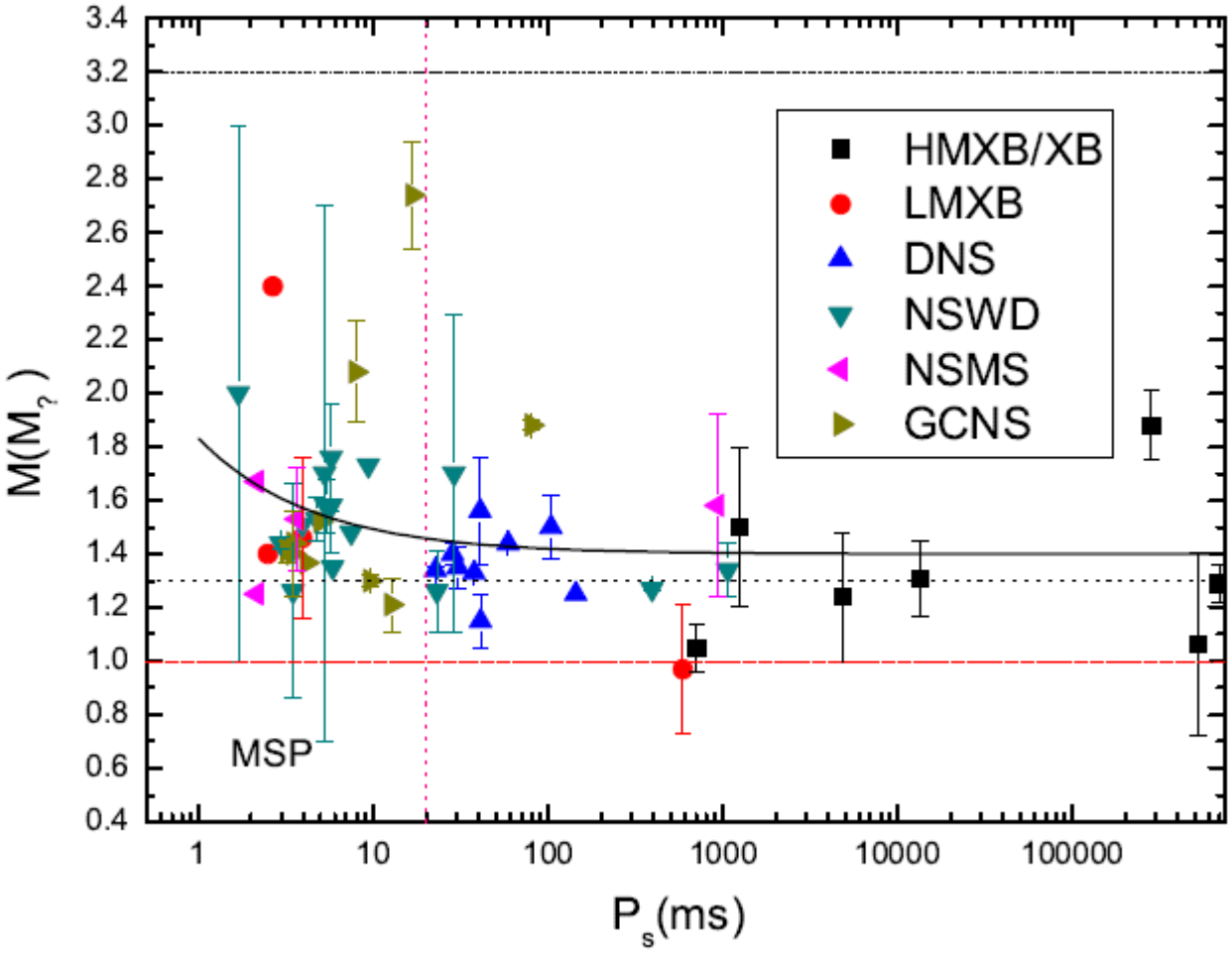

$M=1.4+0.43(P/ms)^{-2/3}$

Millisecond pulsars are ~0.2 solar masses more massive than the rest ones.

1010.5429

DNS and NS+WD binaries

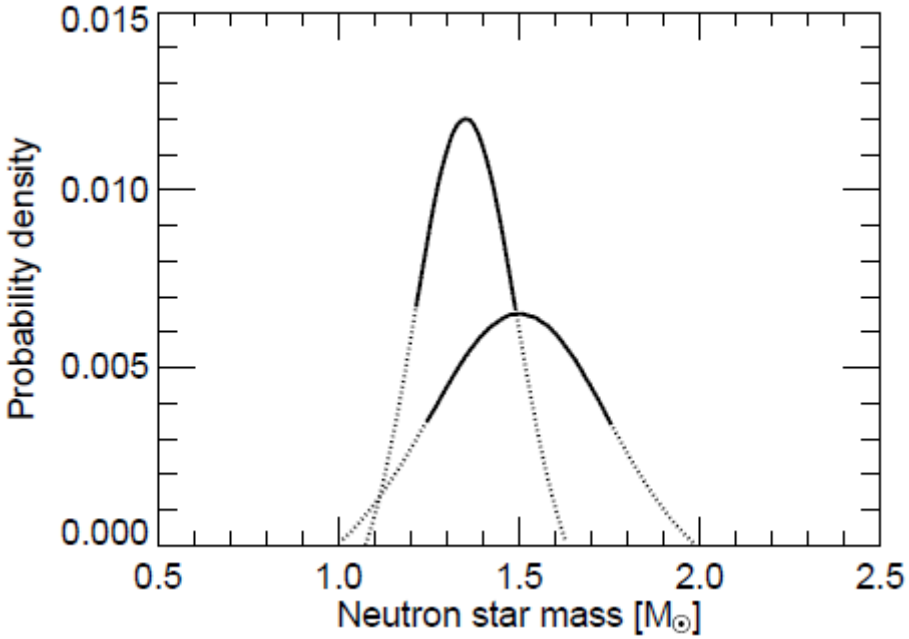

1.35+/-0.13 and 1.5+/-0.25

Cut-off at ~2.1 solar masses can be mainly due to evolution in a binary, not due to nuclear physics (see 1309.6635)

1011.4291

Neutron stars in binaries

Study of close binary systems gives an opportunity to obtain mass estimate for progenitors of NSs (see for example, Ergma, van den Heuvel 1998 A&A 331, L29).
For example, an interesting estimate was obtained for GX 301-2.
The progenitor mass is >50 solar masses.
On the other hand, for several other systems with both NSs and BHs progenitor masses a smaller: from 20 up to 50.
Finally, for the BH binary LMC X-3 the progenitor mass is estimated as >60 solar.
So, the situation is tricky.
Most probably, in some range of masses, at least in binary systems, stars can produce both types of compact objects: NSs and BHs.

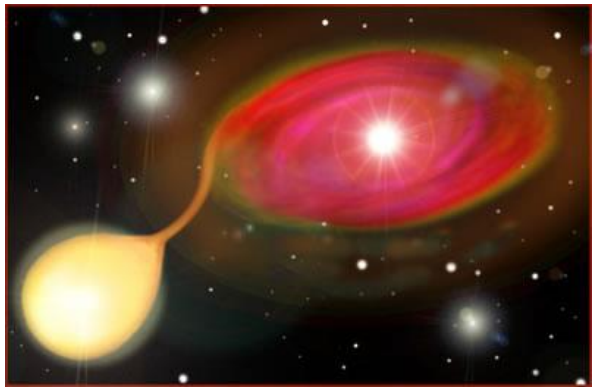

Mass determination in binaries: mass function

$$f_v(m)\frac{m_x^3 \sin i^3}{(m_x+m_v)^2} = 1,038 \cdot 10^{-7} K_v^3 P (1-e^2)^{3/2}\,,$$

m_x, m_v - masses of a compact object and of a normal star (in solar units),
K_v – observed semi-amplitude of line of sight velocity of the normal star (in km/s),
P – orbital period (in days), e – orbital eccentricity, i – orbital inclination
(the angle between the orbital plane and line of sight).

One can see that the mass function is the lower limit for the mass of a compact star.

The mass of a compact object can be calculated as:

$$m_x = f_v(m)\left(1+\frac{m_v}{m_x}\right)^2 \frac{1}{\sin i^3}\,.$$

So, to derive the mass it is necessary to know (besides the line of sight velocity) independently two more parameters: mass ration $q=m_x/m_v$, and orbital inclination i.

Some mass estimates

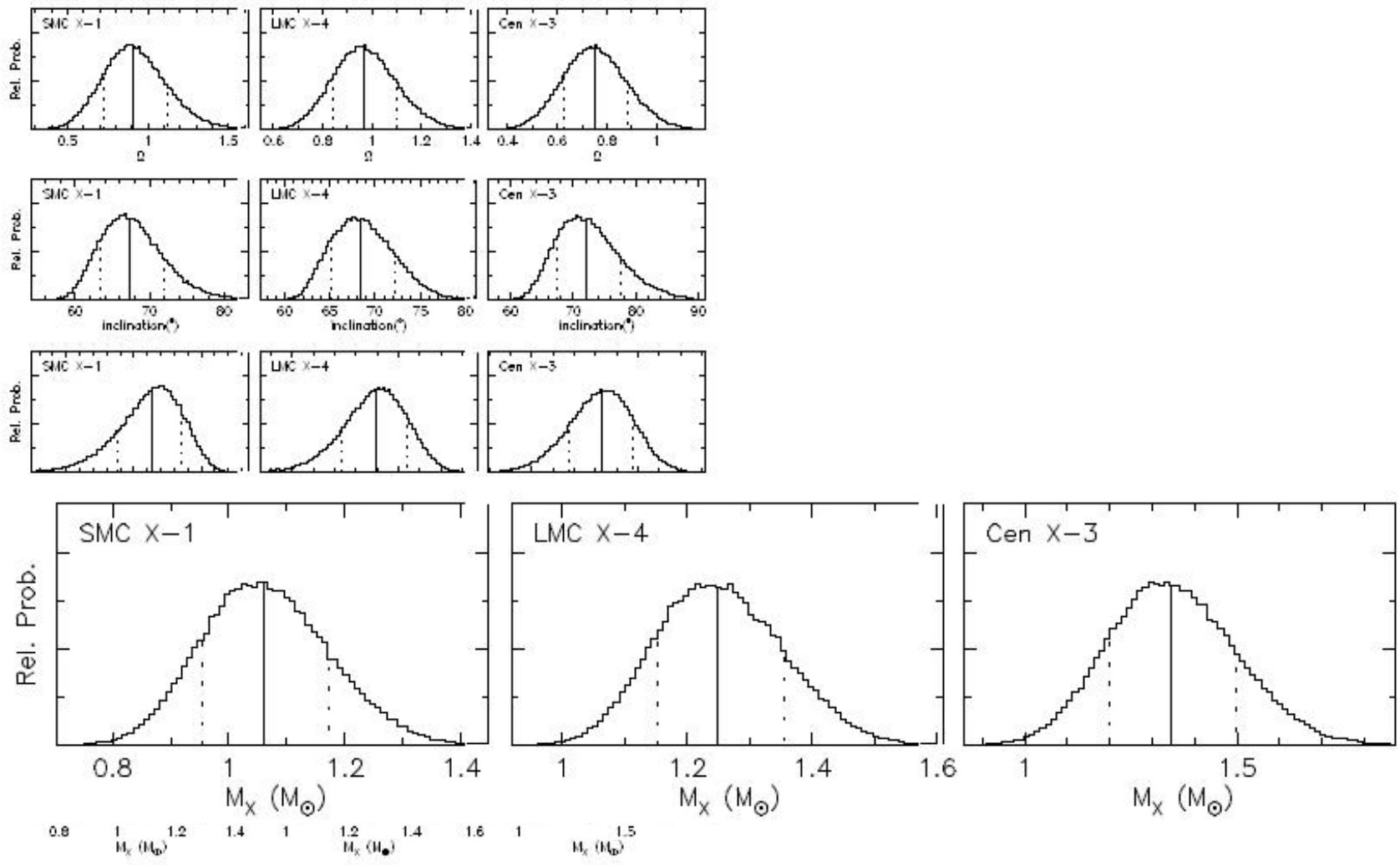

ArXiv: 0707.2802

More measurements

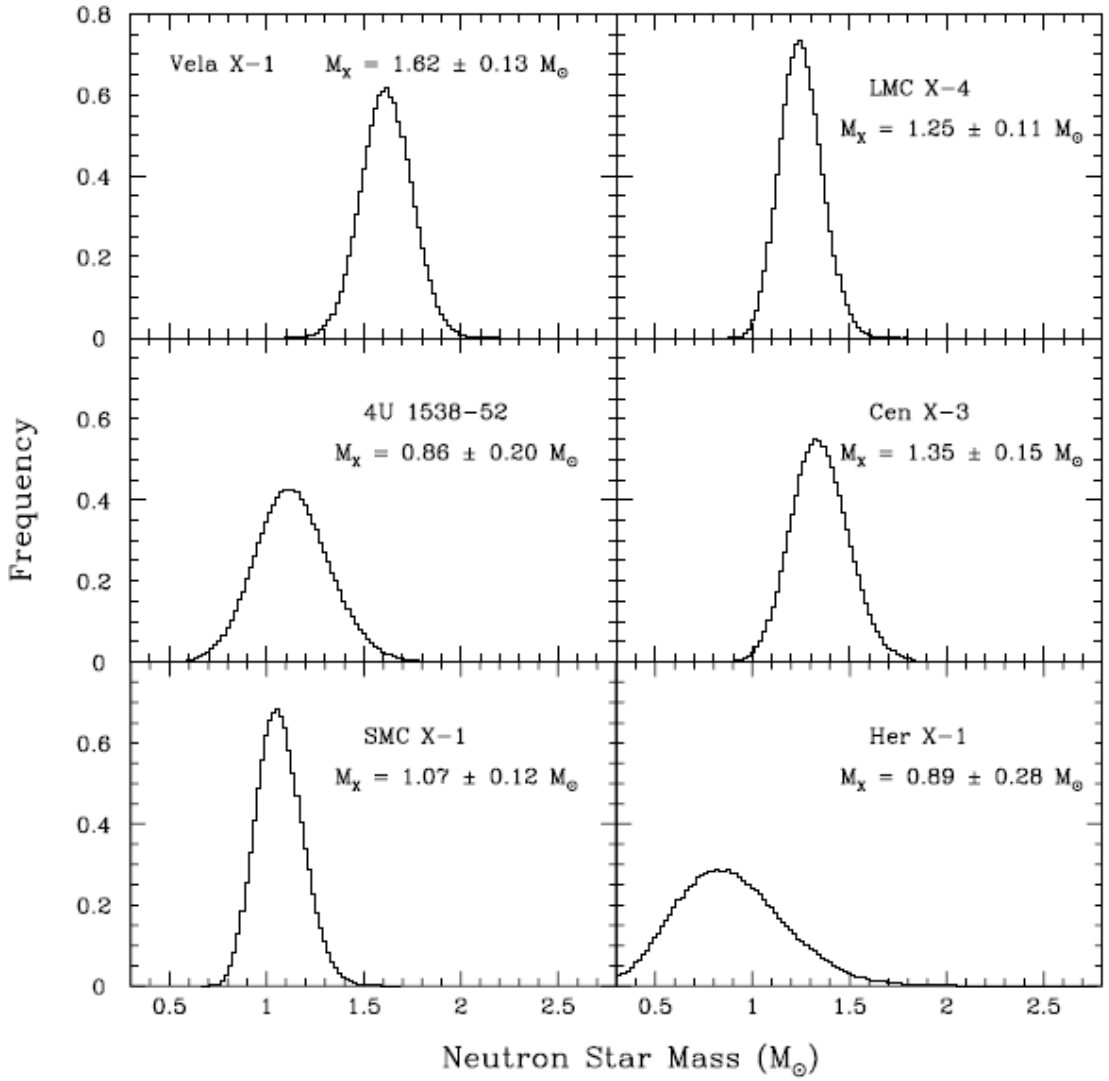

Six X-ray binary systems.
All are eclipsing pulsars.

1101.2465

Altogether

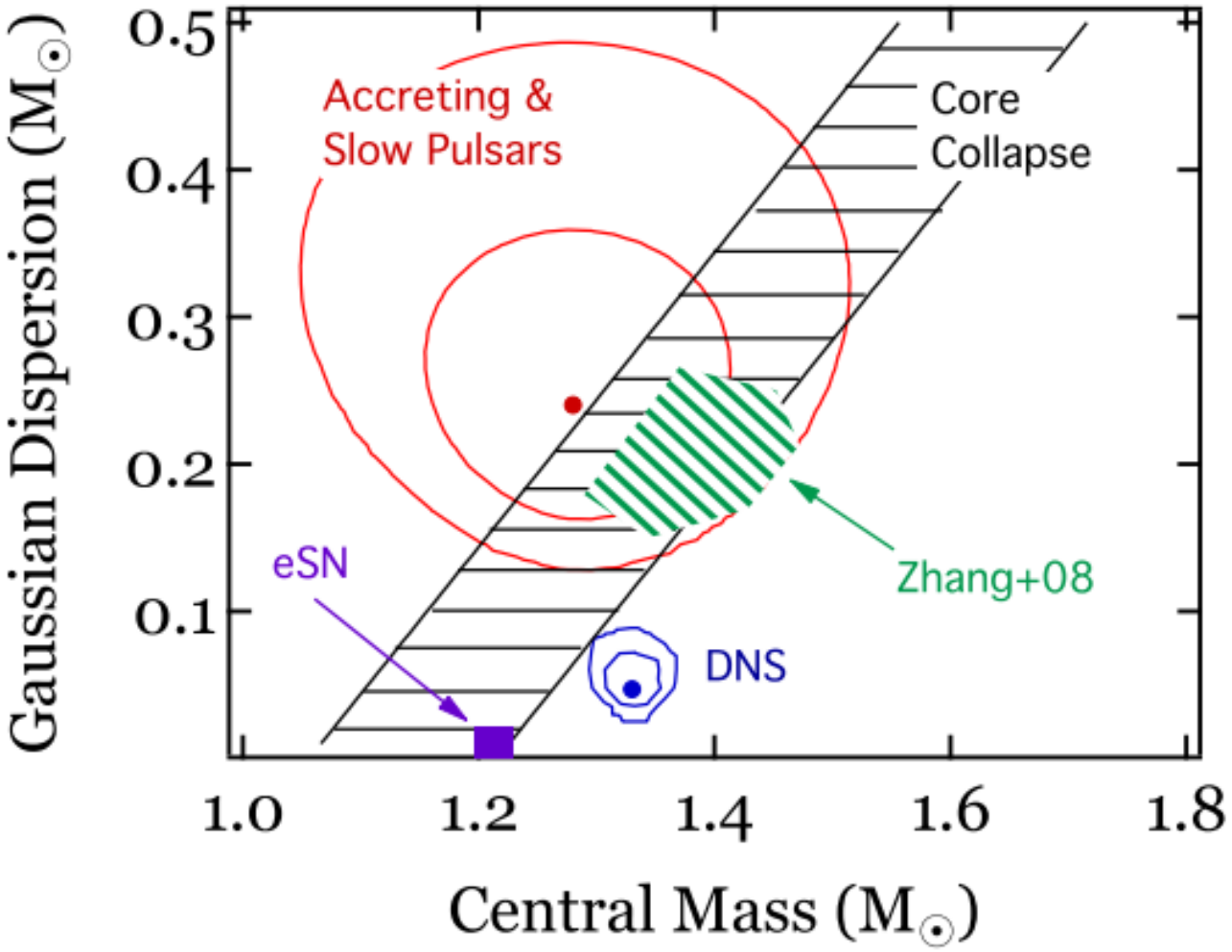

1201.1006

Mass-radius diagram and constraints

Unfortunately, there are no good data on independent measurements of masses and radii of NSs.

Still, it is possible to put important constraints.
Most of recent observations favour stiff EoS.

Useful analytical estimates for EoS can be found in 1310.0049).

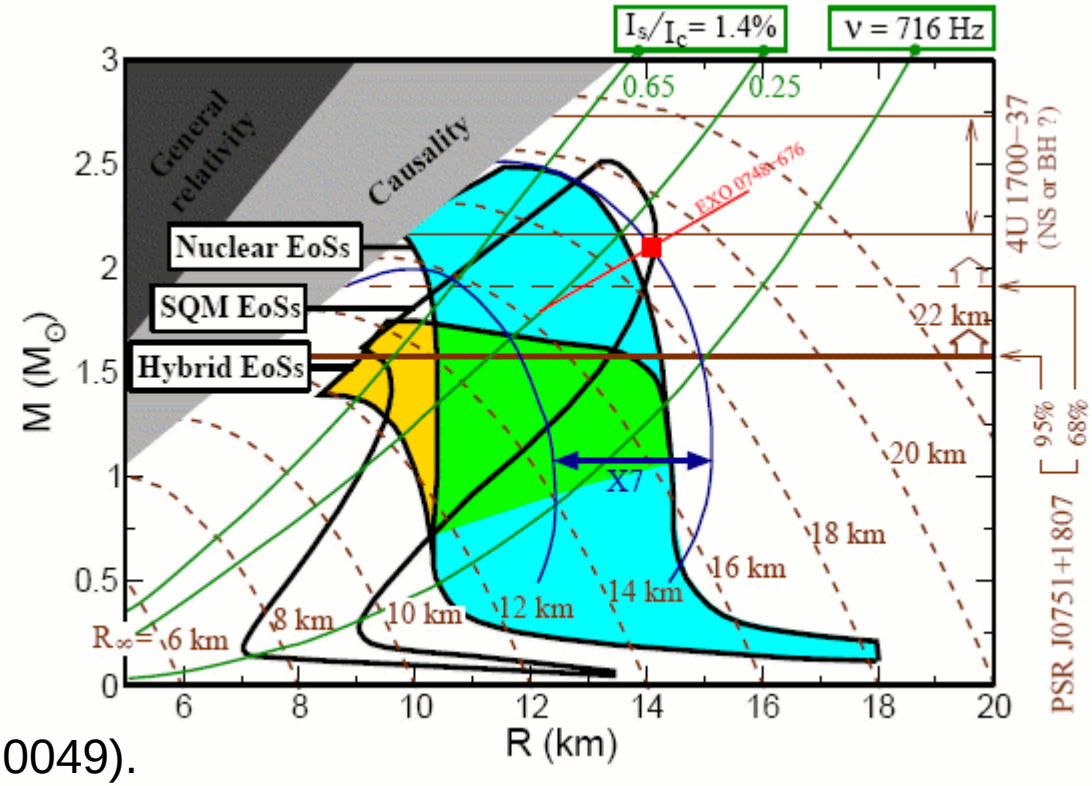

astro-ph/0608345, 0608360

Observations vs. data

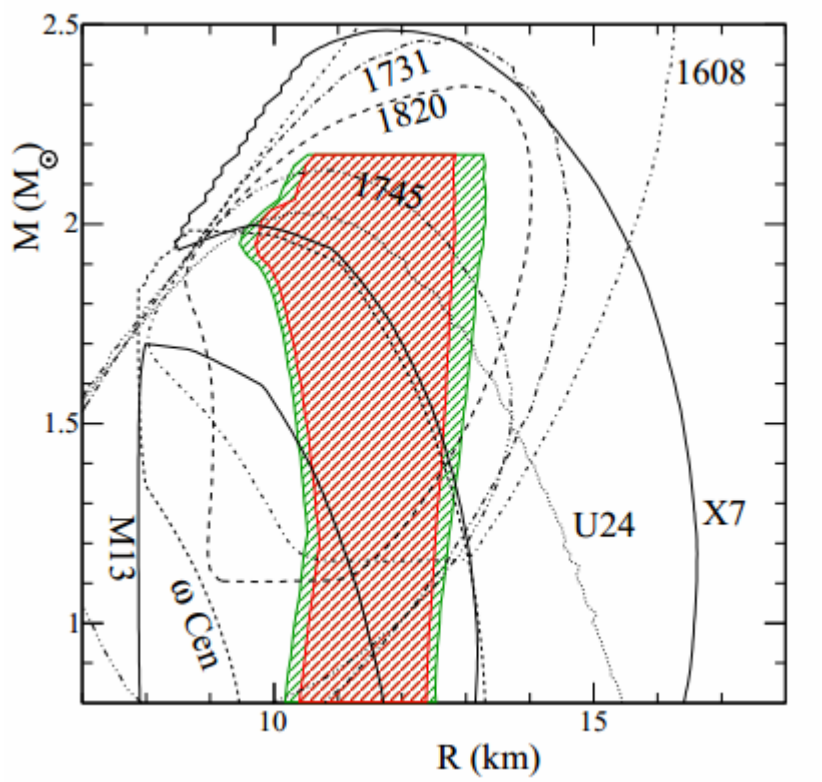

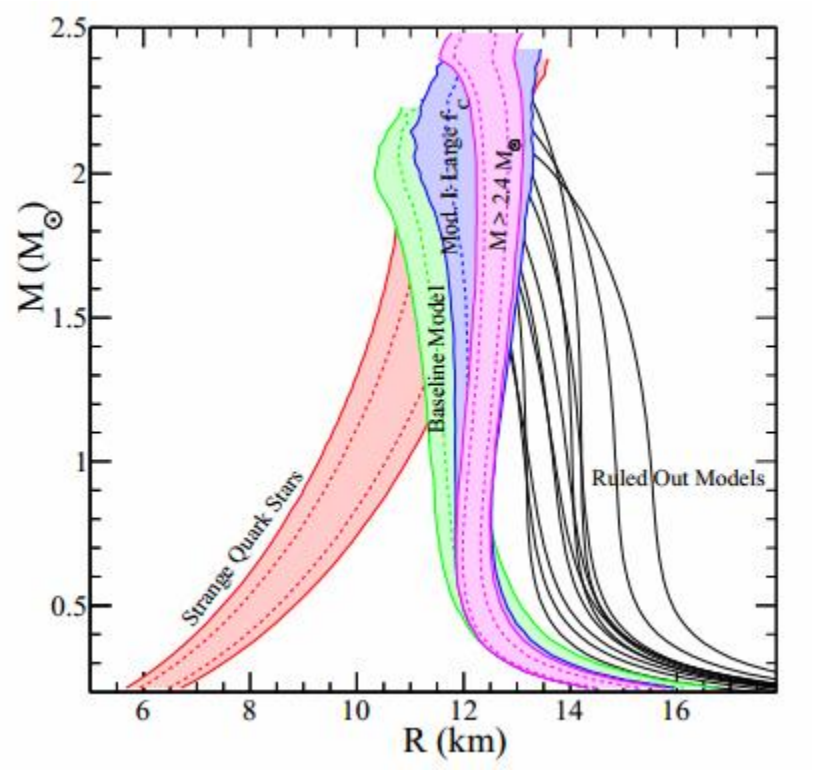

1205.6871

Some newer results by the same group are presented in 1305.3242

Mass and radius for a pulsar!

PSR J0437–4715 NS+WD

The nearest known mPSR
155-158 pc

XMM-Newton observations showed thermal emission.

H-atmosphere model fits.

Hot caps are non-antipodal.

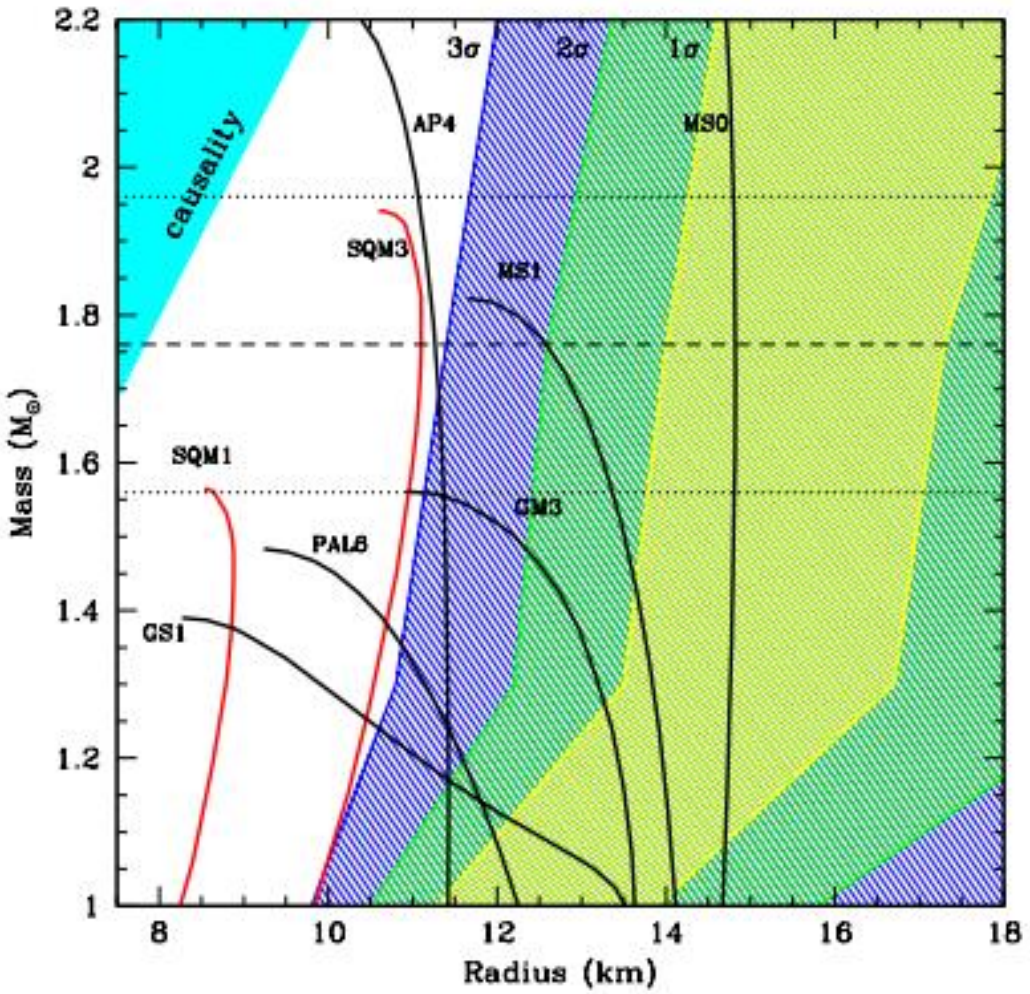

1211.6113

Combination of different methods

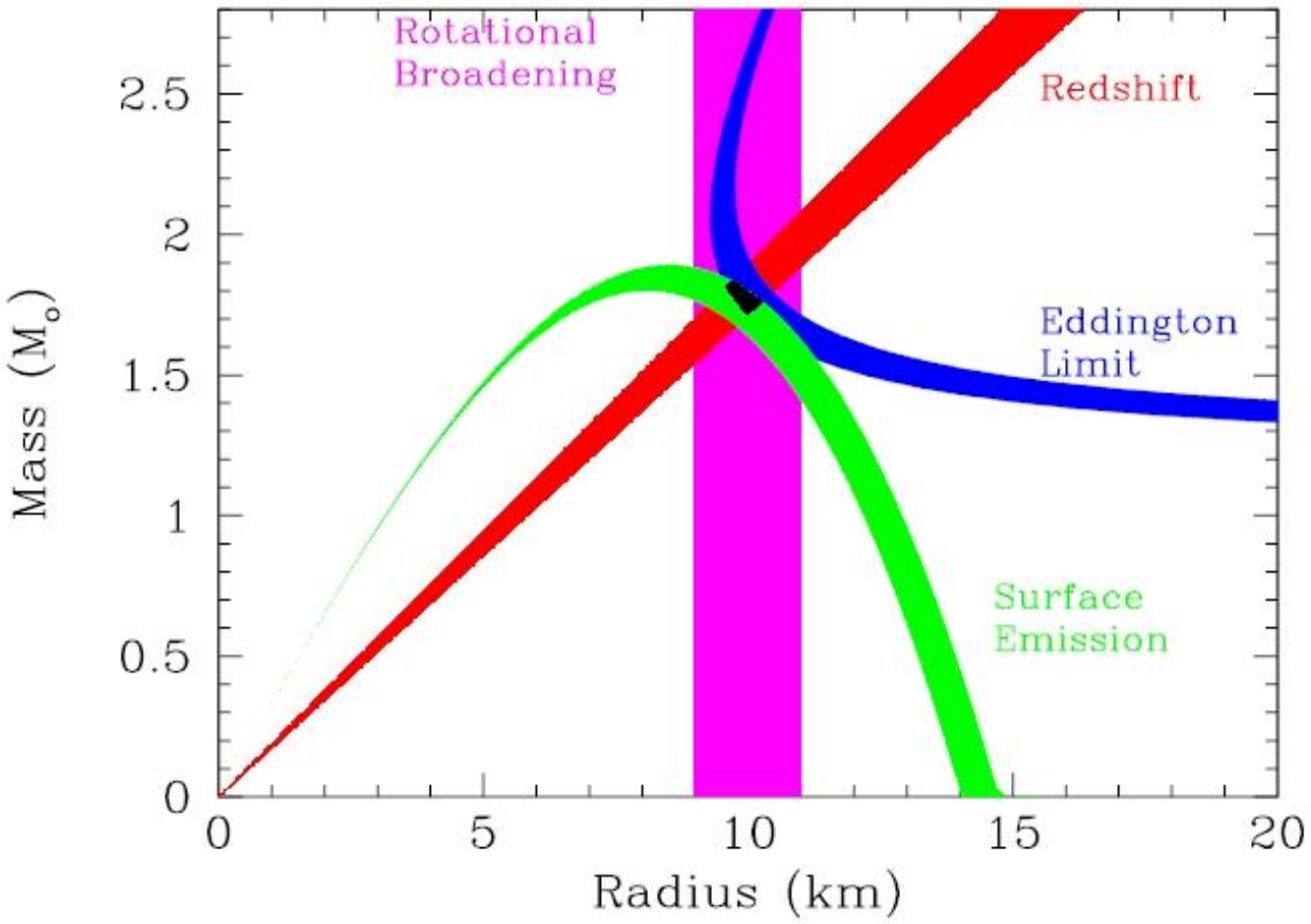

EXO 0748-676

Ozel astro-ph/0605106

Radius determination in bursters

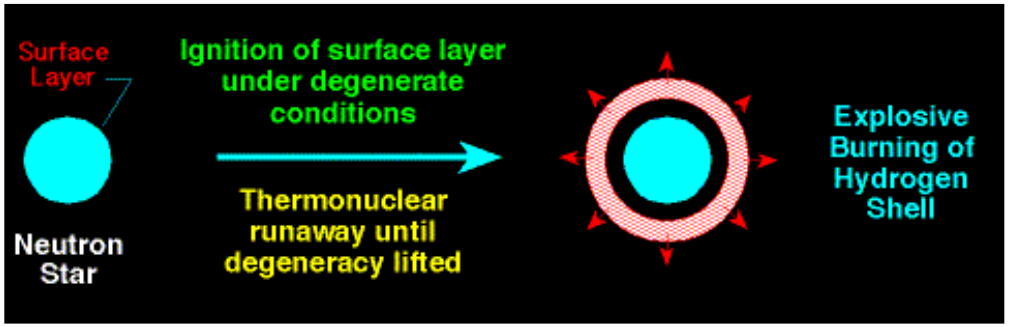

Explosion with a ~ Eddington liminosity.

Modeling of the burst spectrum and its evolution.

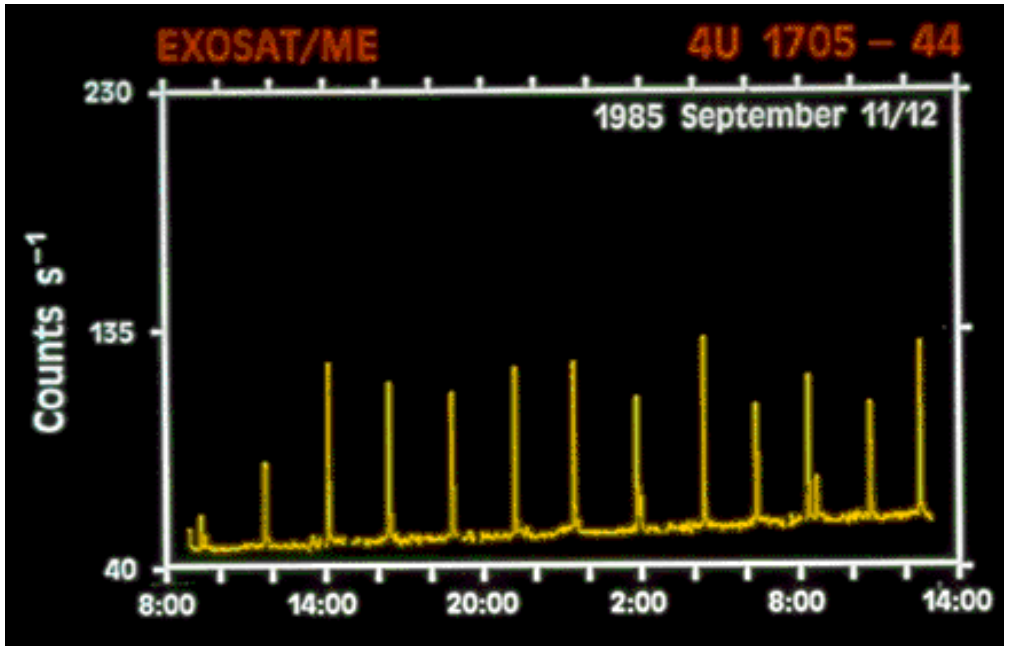

See, for example,
Joss, Rappaport 1984,
Haberl, Titarchuk 1995

http://www.astro.washington.edu/ben/a510/NSTARS.new.html

More measurements

Continuously new measurements, critics and discussion appears

- 1104.2602 Systematic Uncertainties in the Spectroscopic Measurements of Neutron-Star Masses and Radii from Thermonuclear X-ray Bursts. II. Eddington Limit
- 1104.5027 The Mass and Radius of the Neutron Star in the Bulge Low-Mass X-ray Binary KS 1731-260
- 1103.5767 Systematic Uncertainties in the Spectroscopic Measurements of Neutron-Star Masses and Radii from Thermonuclear X-ray Bursts. I. Apparent Radii
- 1105.1525 Mass and radius estimation for the neutron star in X-ray burster 4U 1820-30
- 1105.2030 New Method for Determining the Mass and Radius of Neutron Stars
- 1106.3131 Constraints on the Mass and Radius of the Neutron Star XTE J1807-294
- 1111.0347 Constraints on neutron star mass and radius in GS 1826-24 from sub-Eddington X-ray bursts
- 1201.1680 On the consistency of neutron-star radius measurements from thermonuclear bursts
- 1204.3627 Constraints on the mass and radius of the accreting neutron star in the Rapid Burster
- 1301.0831 The mass and the radius of the neutron star in the transient low mass X-ray binary SAX J1748.9-2021

Limits on the EoS from EXO 0748-676

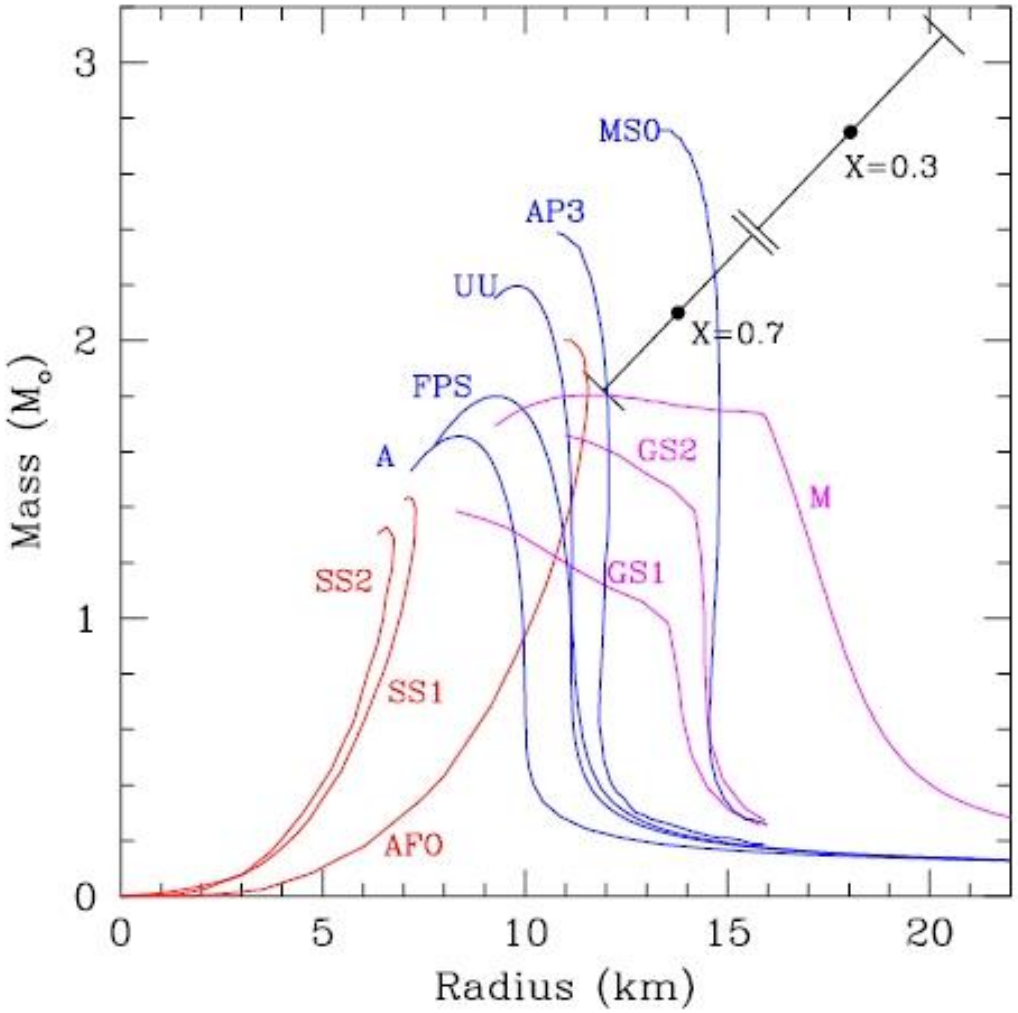

Stiff EoS are better.
Many EoS for strange matter are rejected.
But no all! (see discussion in Nature).

X- hydrogen fraction in the accreted material

Ozel astro-ph/0605106

Some optimistic estimates

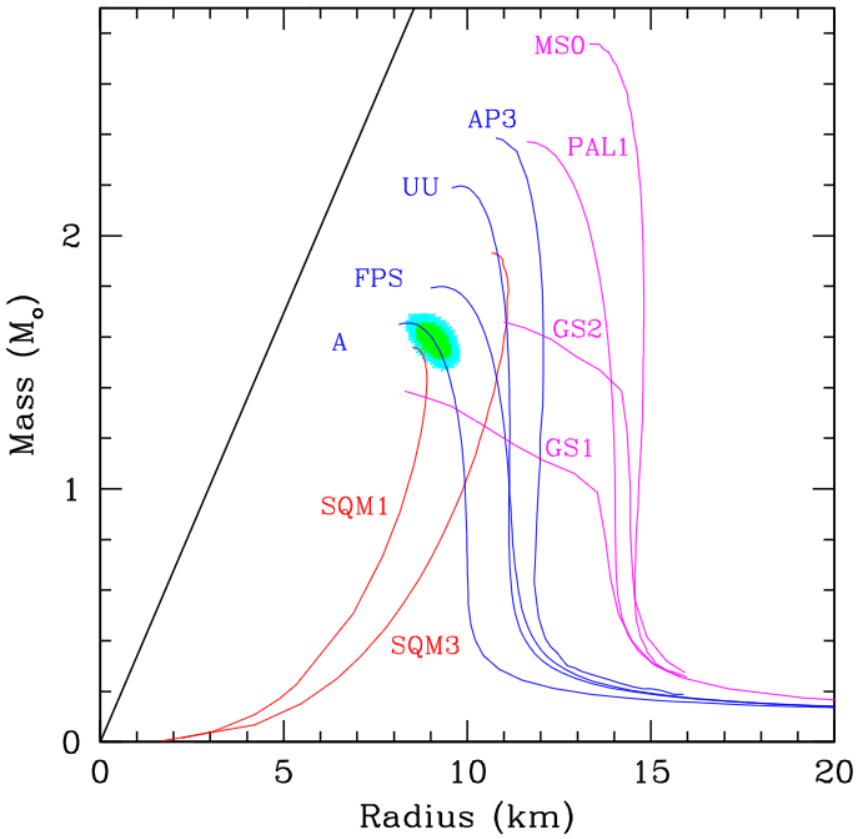

4U 1820-30 1002.3825

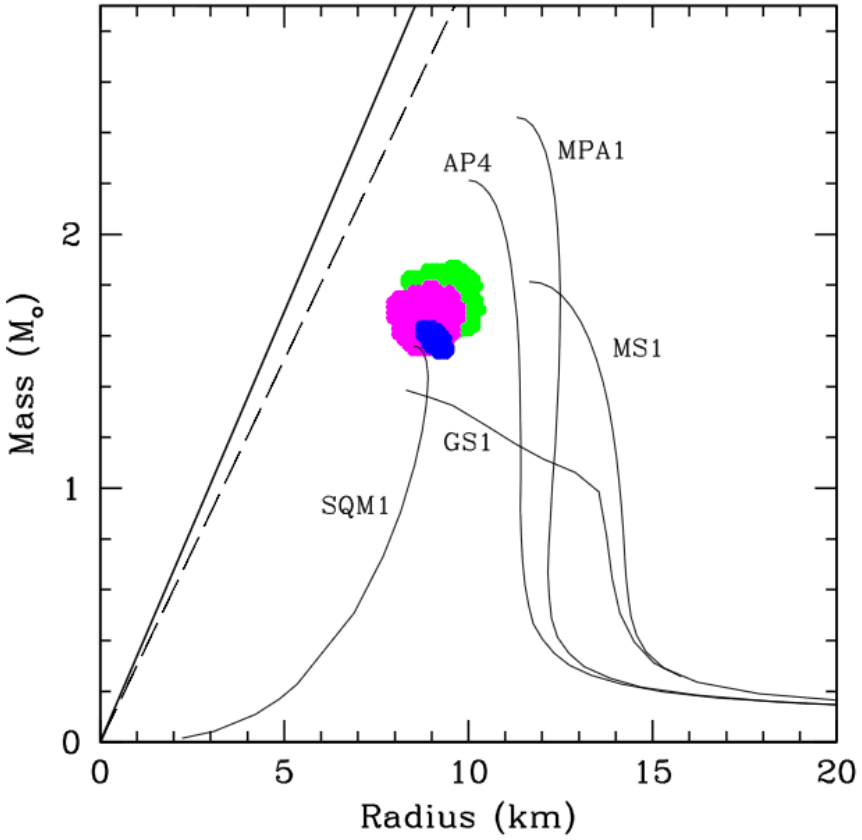

1002.3153

Pessimistic estimates

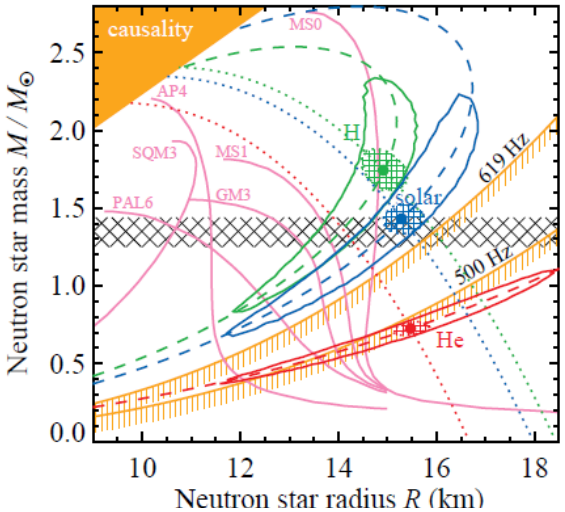

1004.4871

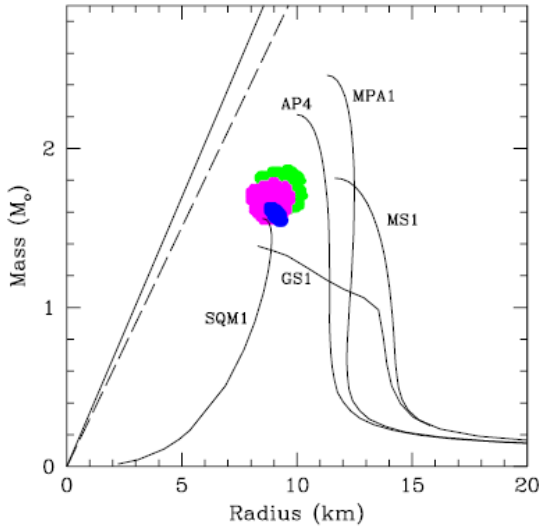

1005.0811

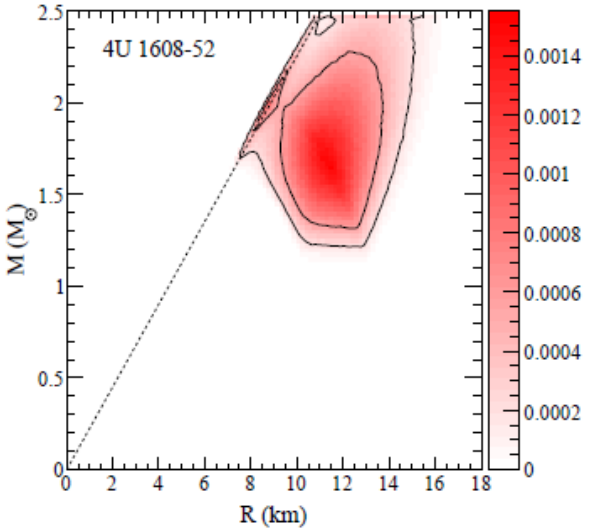

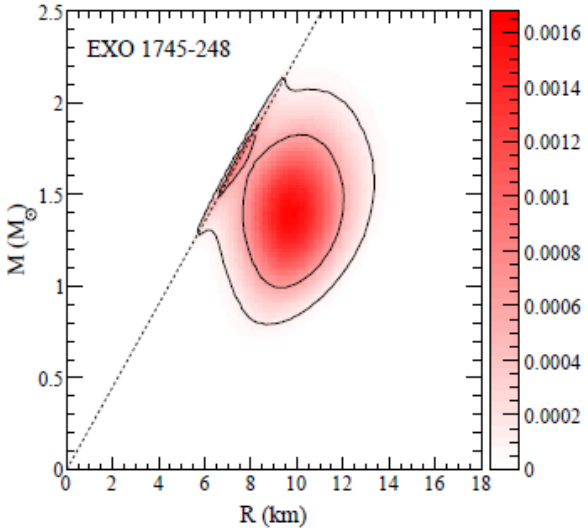

It seems that Ozel et al. underestimate different uncertainties and make additional assumptions.

1002.3153

Radius measurement

Fitting X-ray spectrum of a low-mass X-ray binary in quiescent state.

Mostly sources in globular clusters.

For 4 objects ~10% precision. But this is for fixed mass.

For U24 in NGC 6397 $R_{NS}=8.9^{+0.9}_{-0.6}$ km for 1.4 solar masses.
For the radius observed from infinity: $11.9^{+2.2}_{-2.5}$ km

1007.2415

Radii measurements for qLMXBs in GCs

5 sources

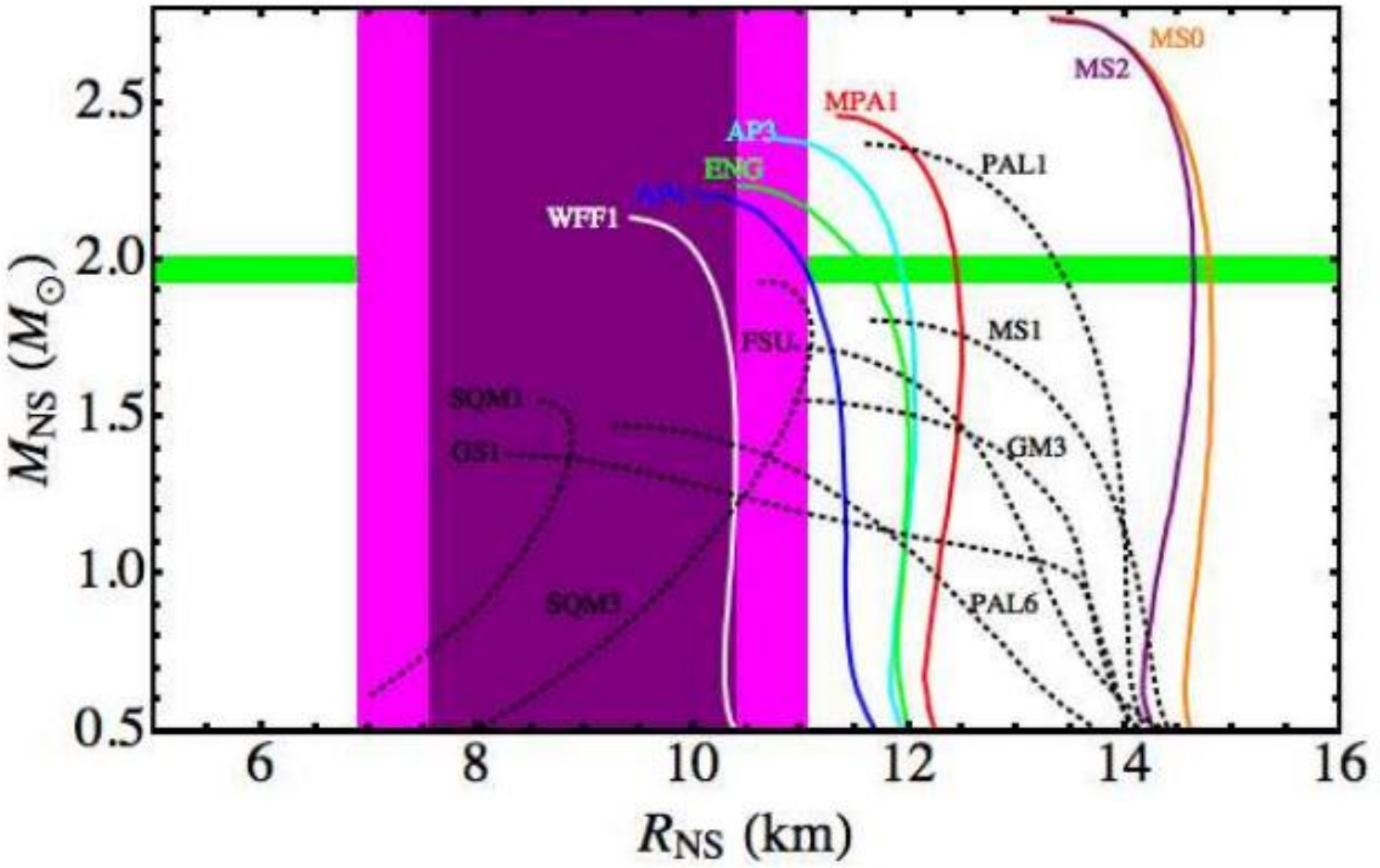

1302.0023

Distance uncertainty

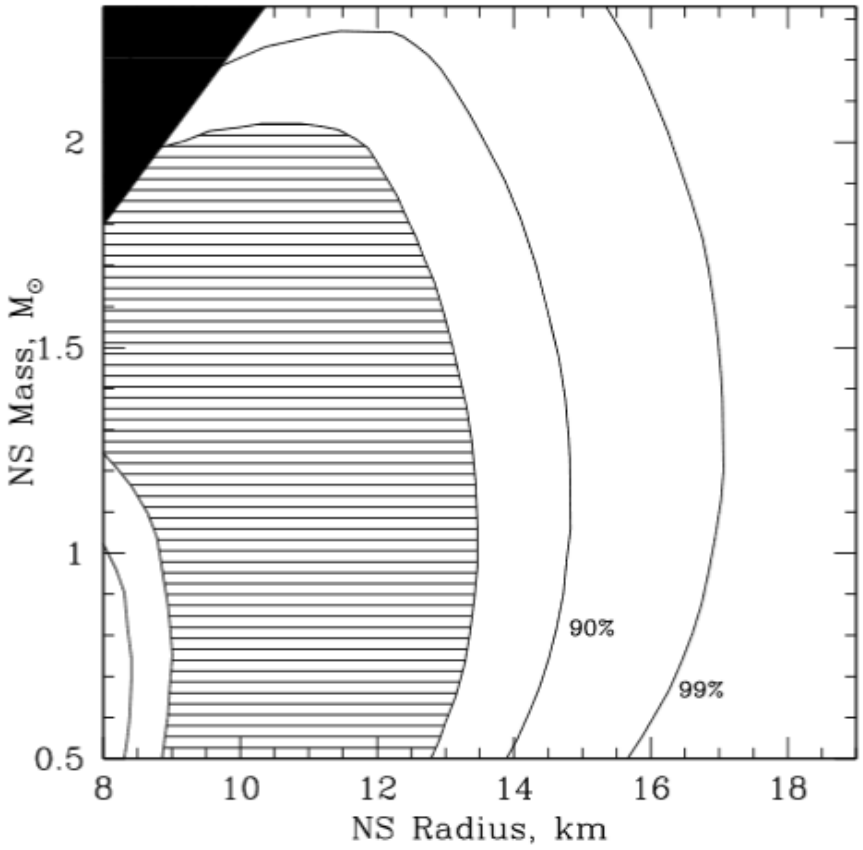

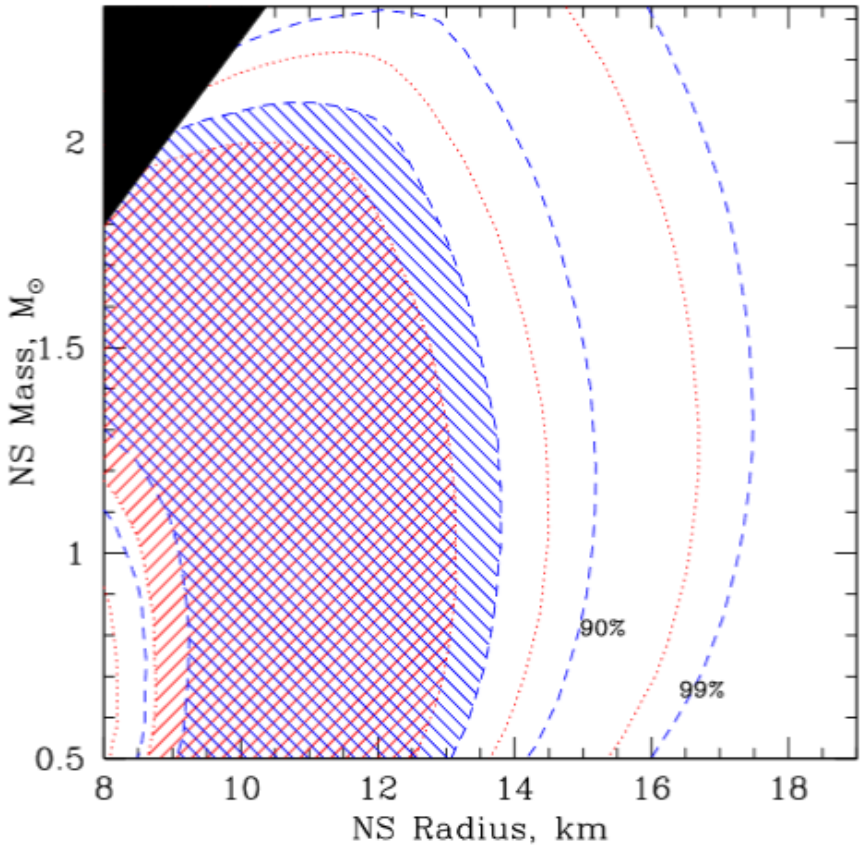

1406.1497

Atmospheric uncertainties

qLMXB in M13

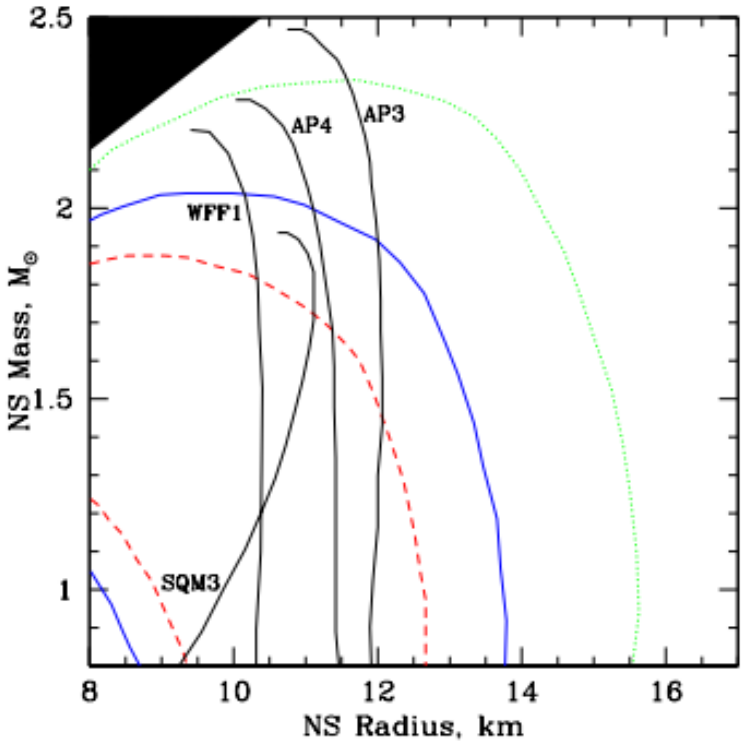

Hydrogene

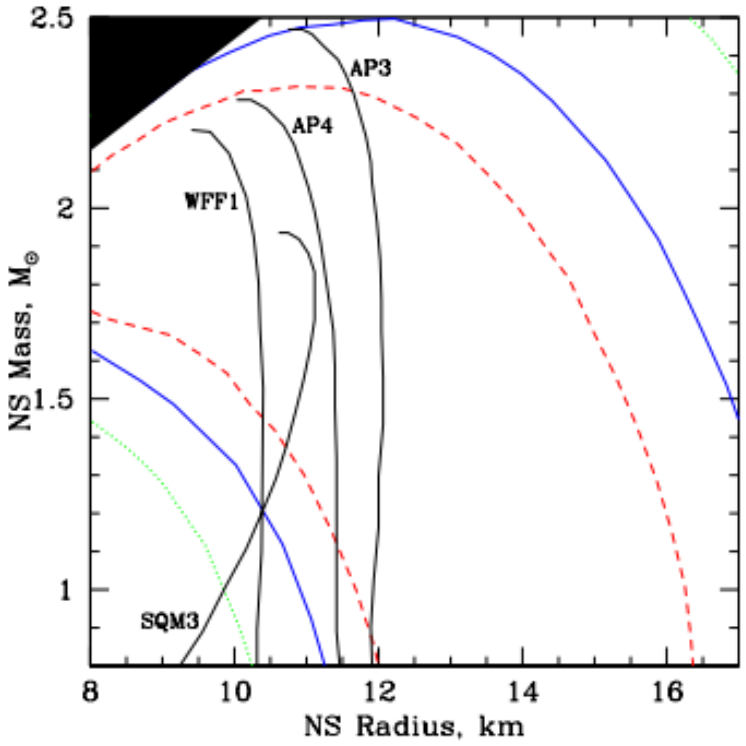

Helium

1301.3768

Limits from RX J1856

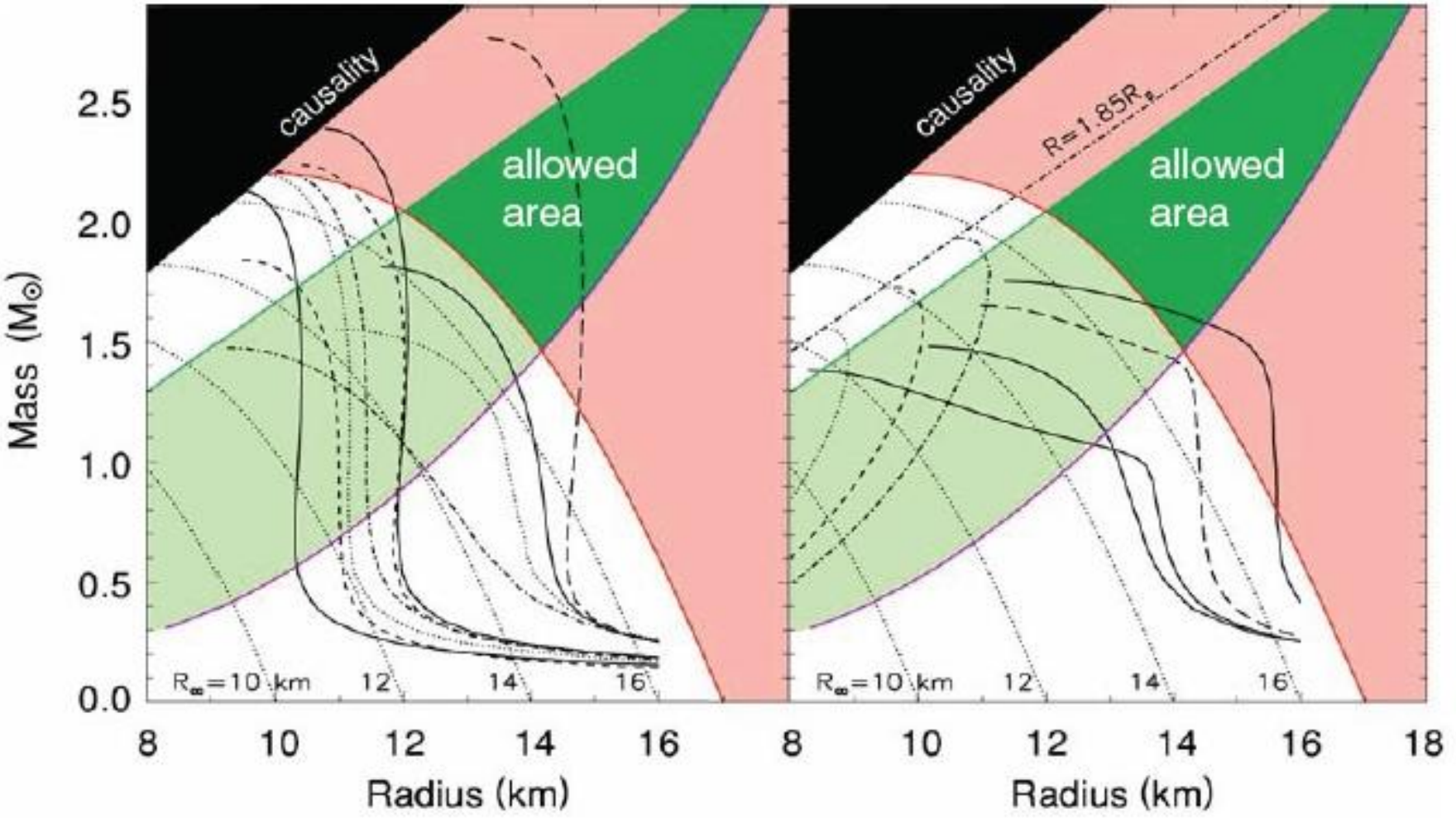

Trumper

About M7 for constraints on the EoS see 1111.0447

PSR 0751+1807

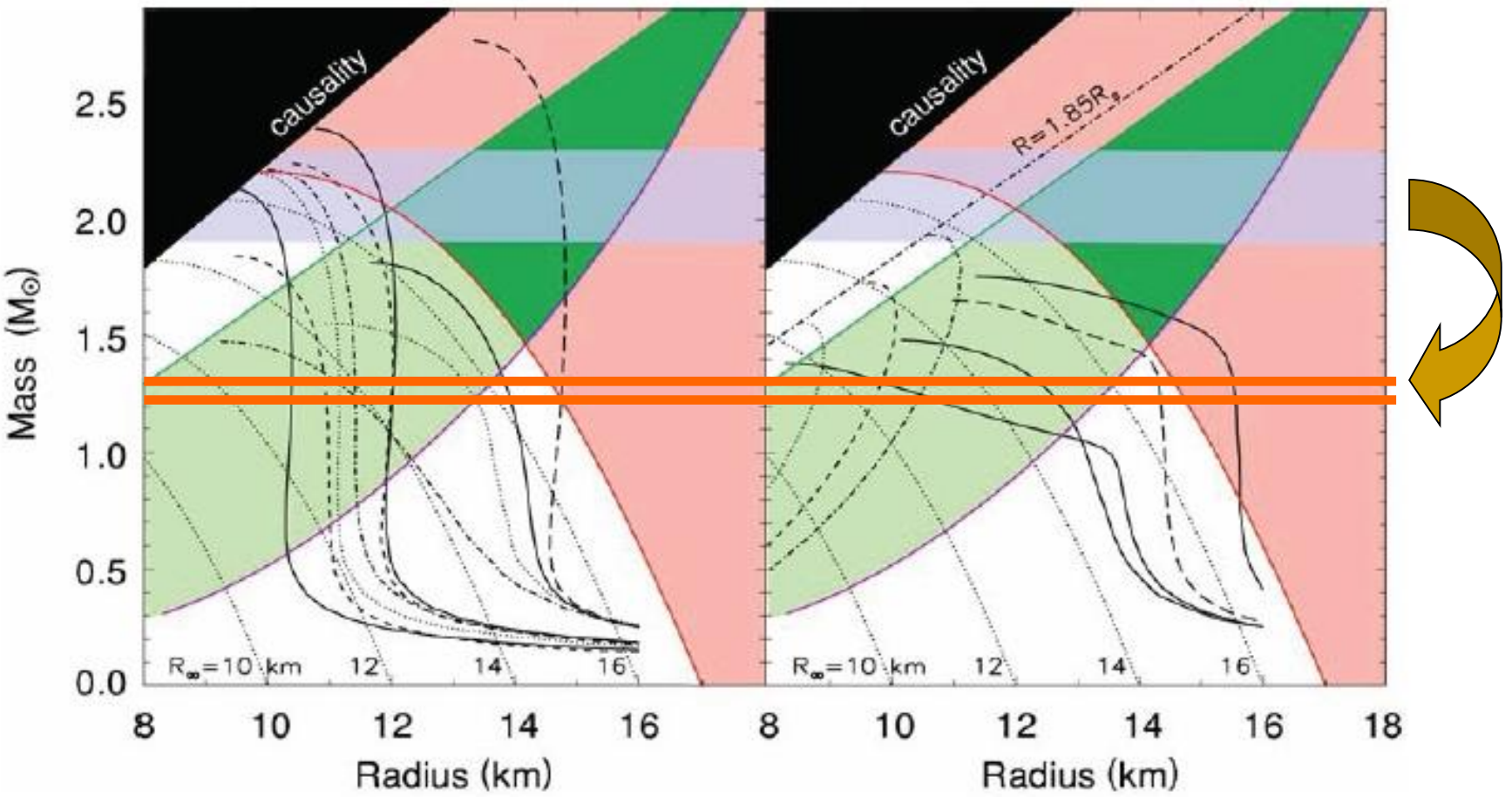

Massive NS: 2.1+/-0.3 solar masses – Now shown to be wrong (!)
[see Nice et al. 2008]

Trumper

Burst oscillations

Fitting light curves of X-ray bursts.
Oscillations due to rotation of a NS.
$Rc^2/GM > 4.2$ for the neutron star in XTE J1814-338.

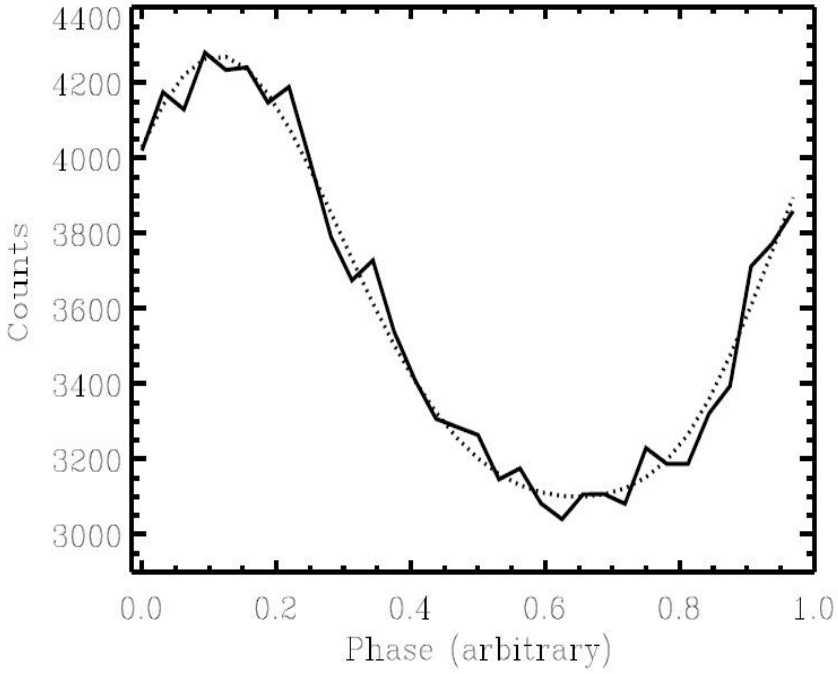

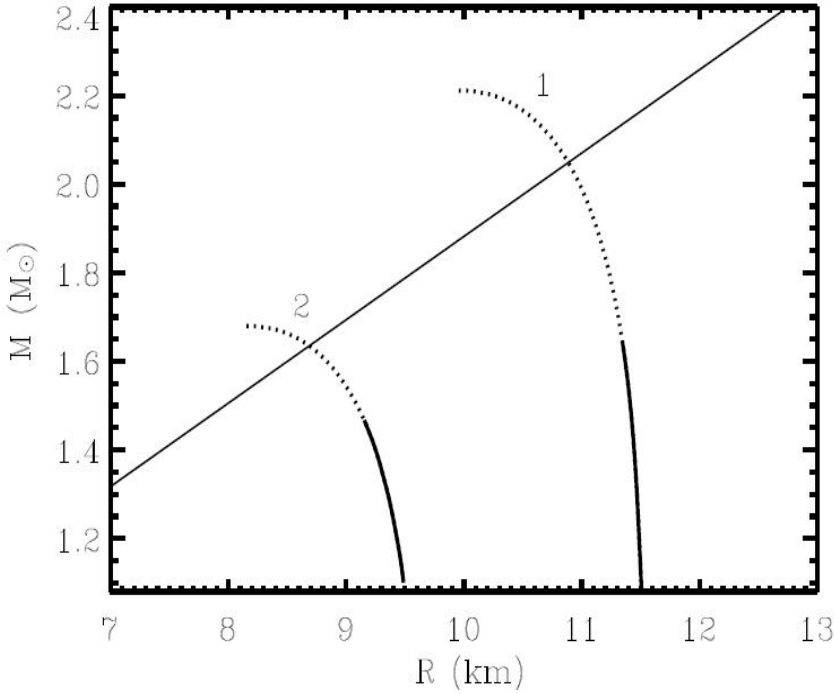

Bhattacharyya et al. astro-ph/0402534

Pulse profile constraints

The idea is that: sharp pulses are possible only in the case of a large star

Green – excluded region

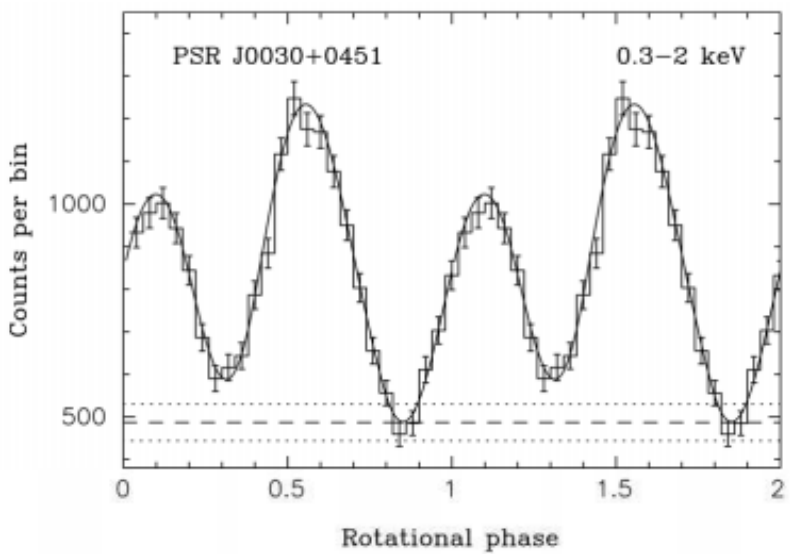

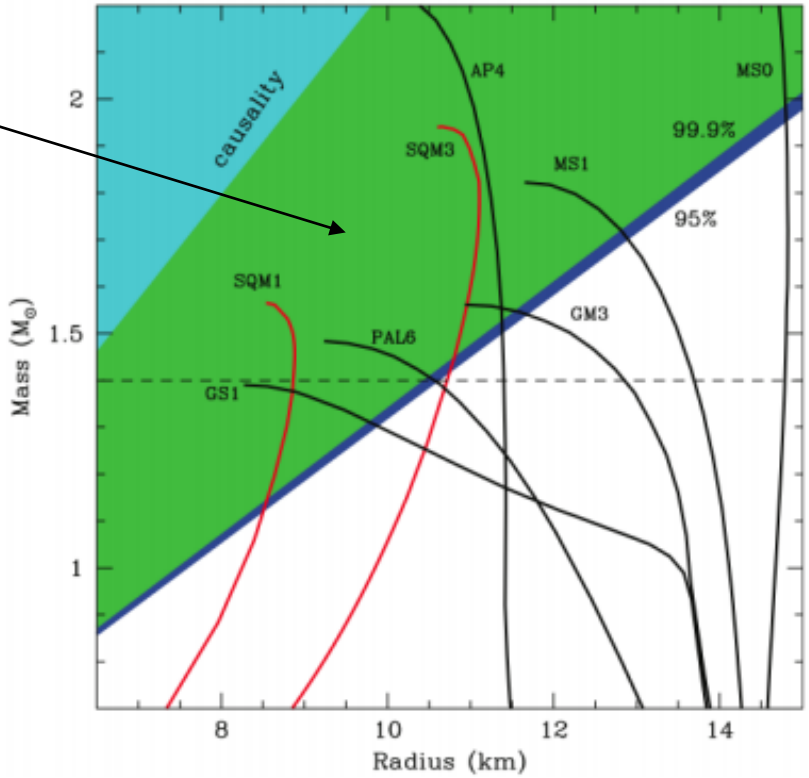

Based on Bogdanov, Grindlay 2009

1303.0317

Hot spots and pulse profiles

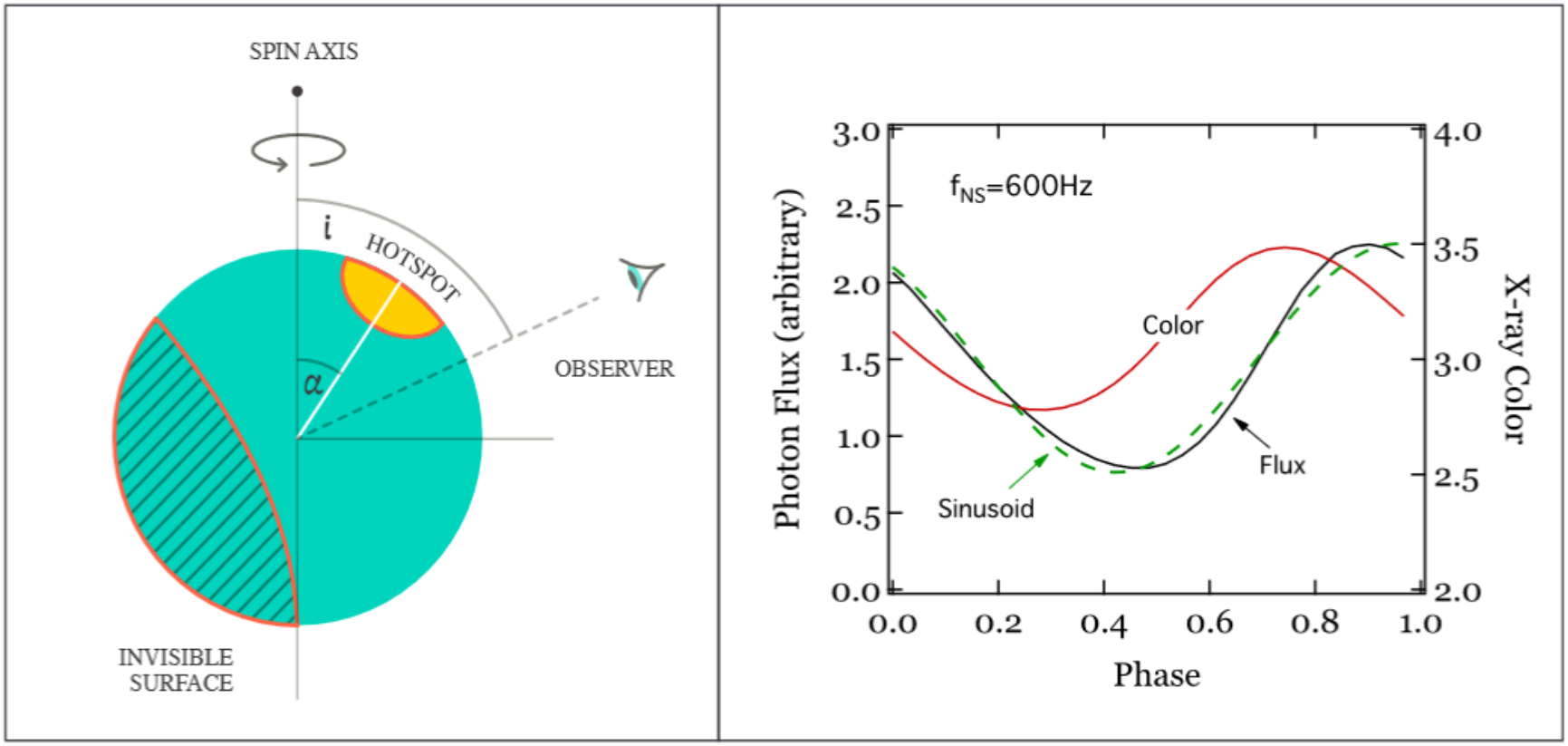

As the neutron star rotates, emission from a surface hotspot generates a pulsation.
The figure shows observer inclination i, and hotspot inclination α.
The invisible surface is smaller than a hemisphere due to relativistic light-bending.

1602.01081

Astroseismology

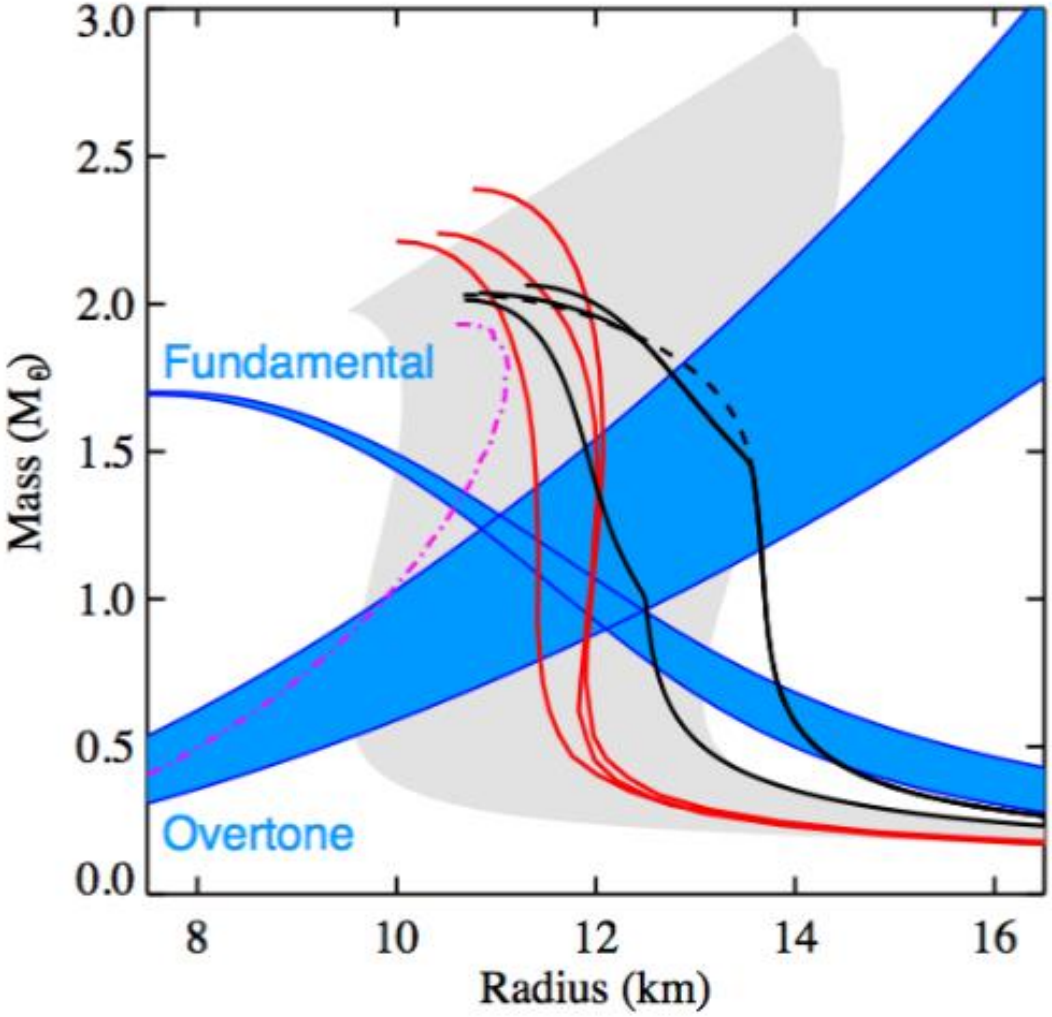

M – R diagram showing the seismological constraints for the soft gamma-ray repeater SGR 1806–20 using the relativistic torsional crust oscillation model of Samuelsson and Andersson (2007), in which the 29 Hz QPO is identified as the fundamental and the 625 Hz QPO as the first radial overtone. The neutron star lies in the box where the constraints from the two frequency bands overlap.

This is a simplified model. More detailed are in progress.

1602.01081

Fe K lines from accretion discs

Measurements of the inner disc radius provide upper limits on the NS radius.

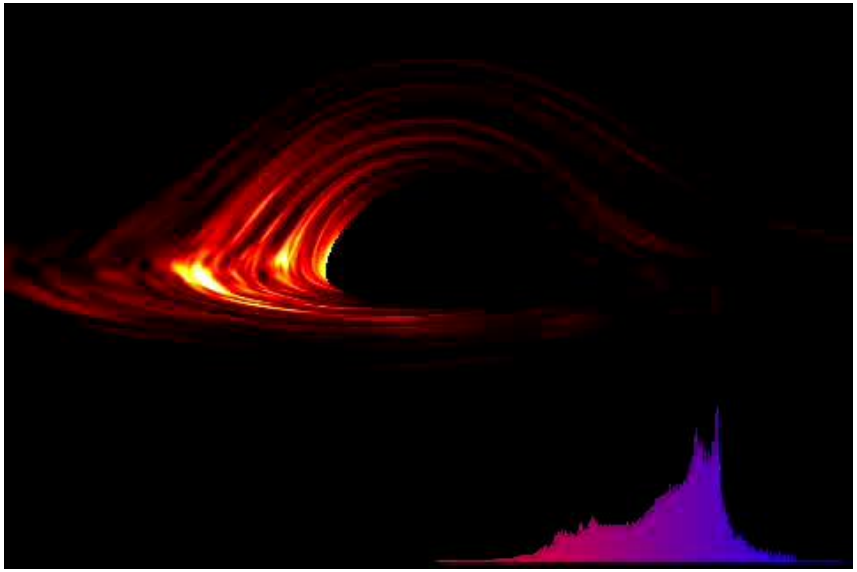

Ser X-1 <15.9+/-1
4U 1820-30 <13.8+2.9-1.4
GX 349+2 <16.5+/-0.8
(all estimates for 1.4 solar mass NS)

[Cackett et al. arXiv: 0708.3615]

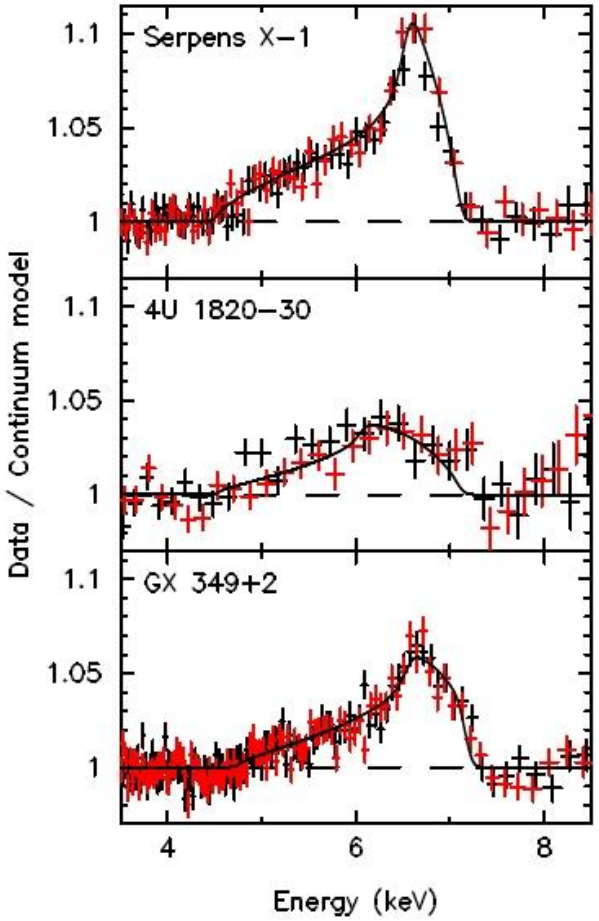

Suzaku observations

See also Papito et al. arXiv: 0812.1149,
a review in Cackett et al. 0908.1098, and theory in 1109.2068.

Limits on the moment of inertia

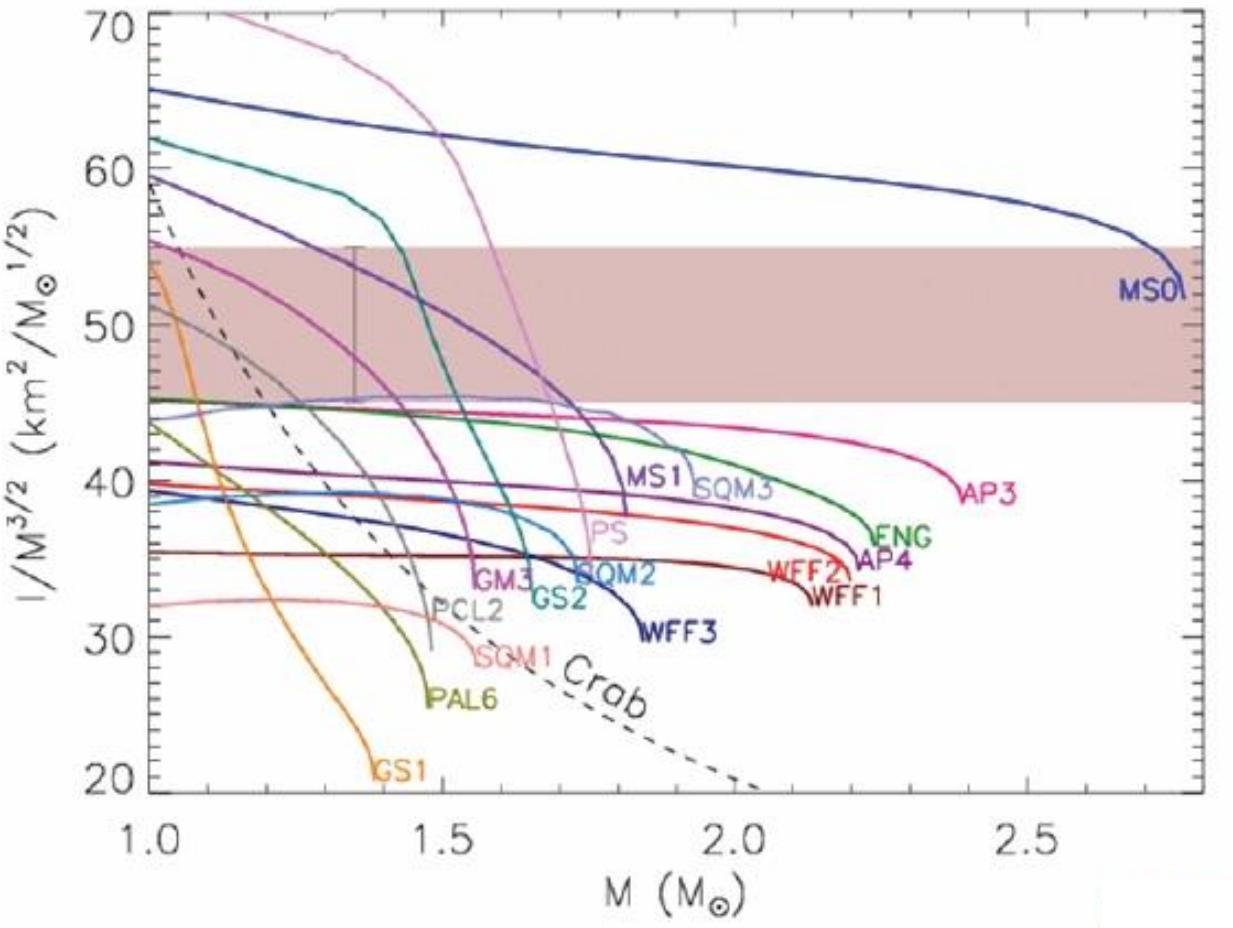

Spin-orbital interaction

PSR J0737-3039 (see Lattimer, Schutz astro-ph/0411470)

The band refers to a *hypothetical* 10% error. This limit, hopefully, can be reached in several years of observ.

See a more detailed discussion in 1006.3758

Most rapidly rotating PSR

716-Hz eclipsing binary radio pulsar in the globular cluster Terzan 5

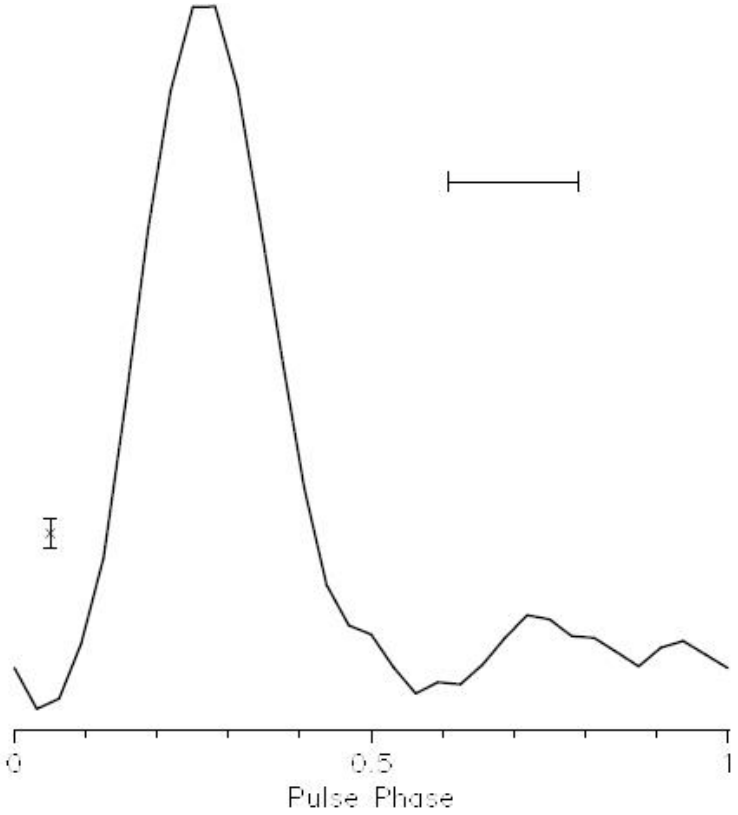

Previous record
(642-Hz pulsar B1937+21)
survived for more than 20 years.

Interesting calculations for rotating NS have been performed recently by Krastev et al. arXiv: 0709.3621

Rotation starts to be important from periods ~3 msec.

Jason W.T. Hessels et al. astro-ph/0601337

QPO and rapid rotation

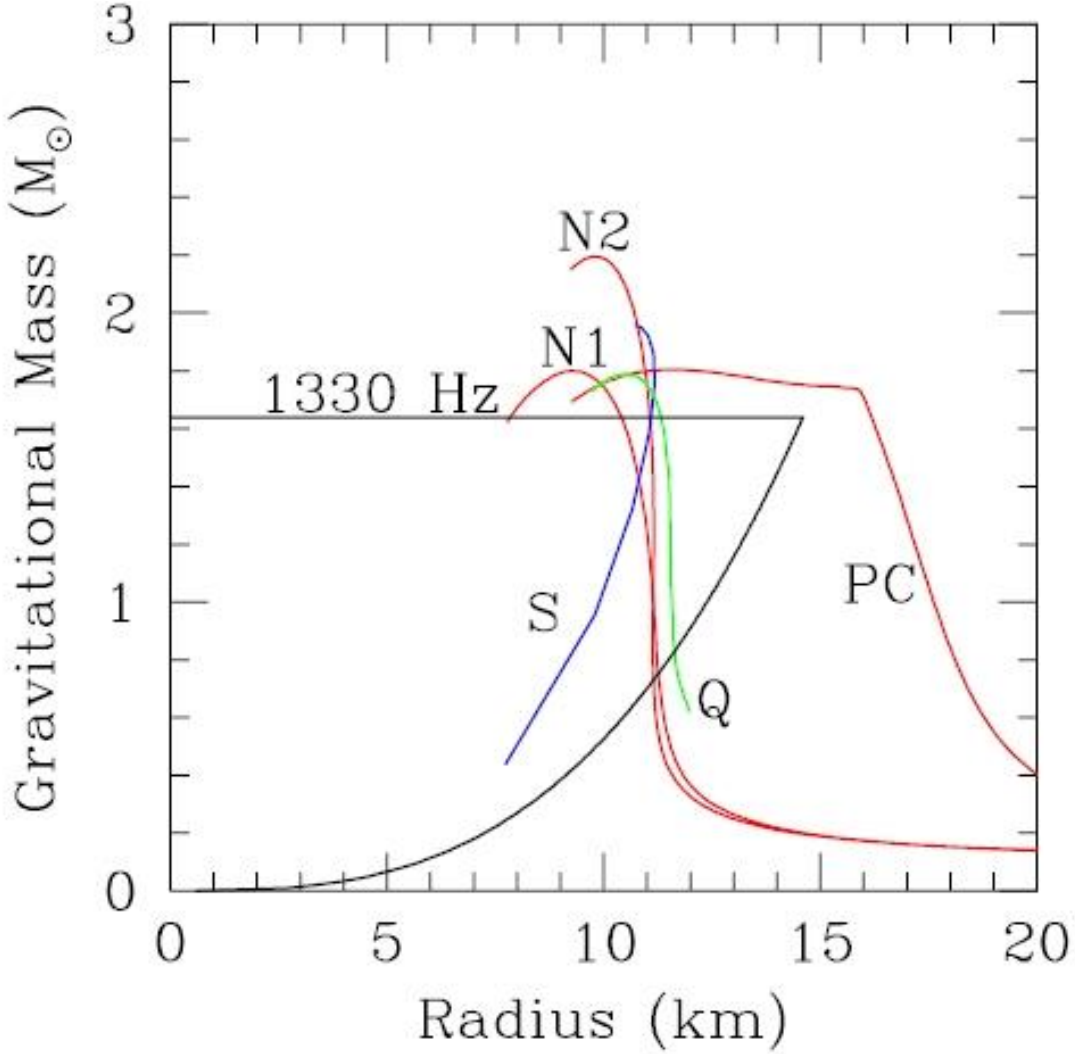

XTE J1739-285
1122 Hz
P. Kaaret et al.
astro-ph/0611716

1330 Hz – one of the highest QPO frequency

The line corresponds to the interpretation, that the frequency is that of the last stable orbit, $6GM/c^2$

Miller astro-ph/0312449

New measurements for 4U 0614+09

$$M \leq 2.2(\nu_{orb}/1000\ \mathrm{Hz})^{-1}(1+0.75j)M_{\odot}$$

$$R \leq 19.5(\nu_{orb}/1000\ \mathrm{Hz})^{-1}(1+0.2j)\mathrm{km}$$

$$j \equiv cJ/GM^2$$

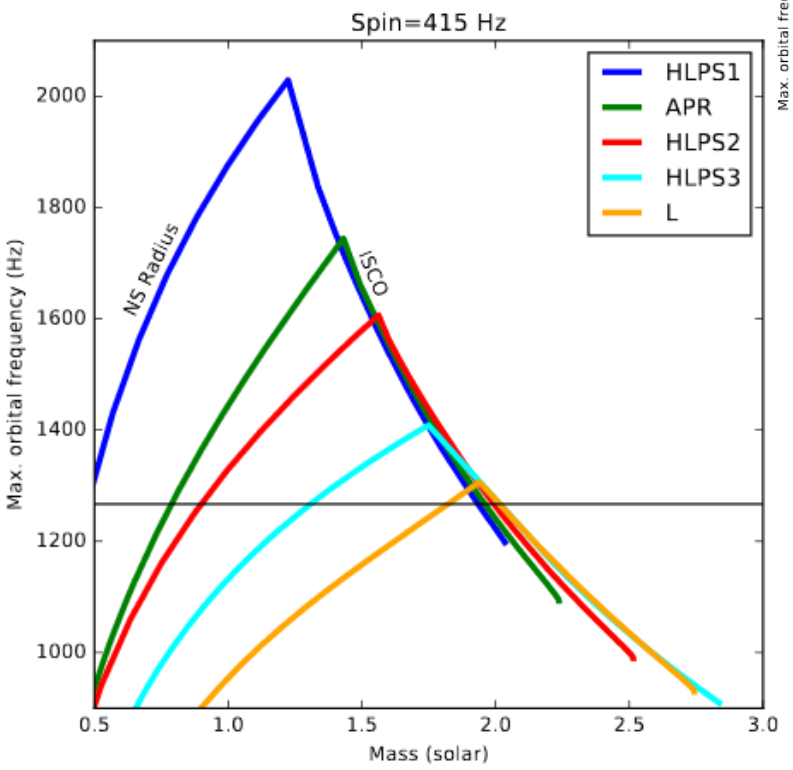

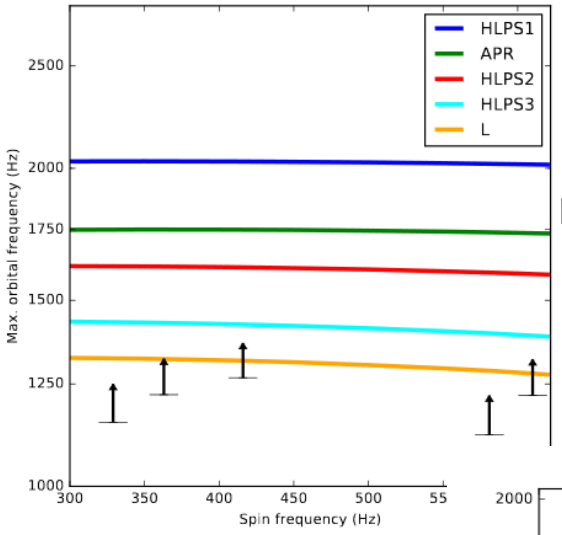

r_{min}= 6GM/c2, $r_{ISCO} > R_{NS}$

R_{NS}, $r_{ISCO} < R_{NS}$

1267 Hz

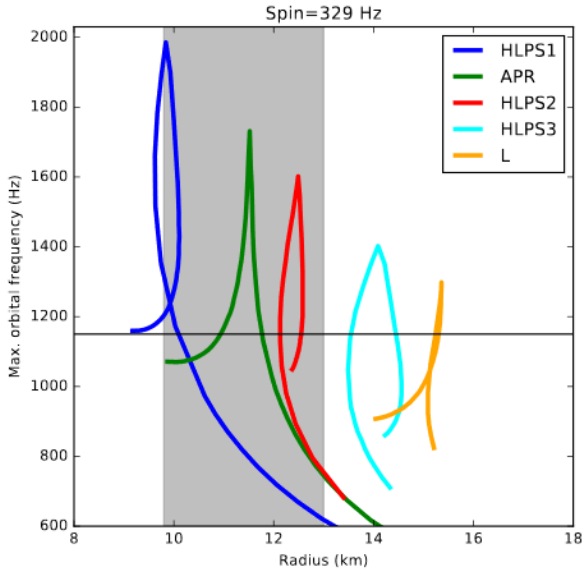

1805.11361

Rotation and composition

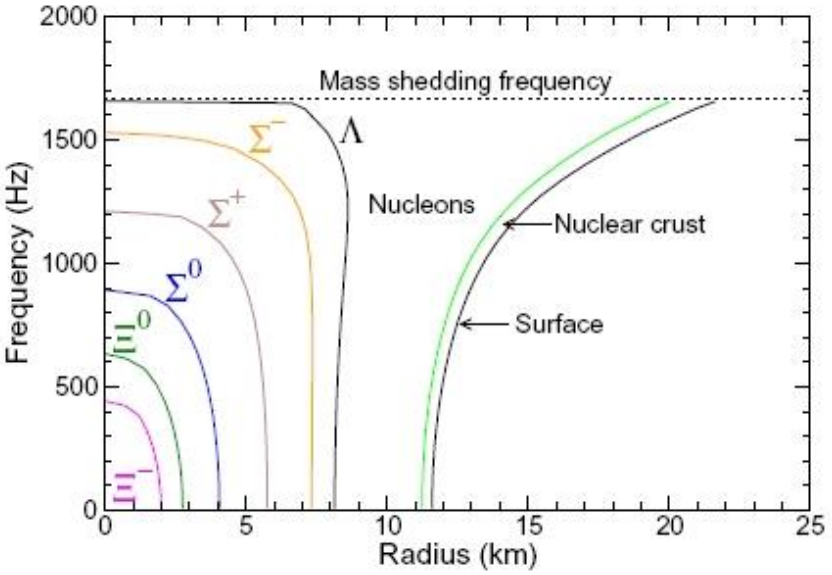

(equatorial)

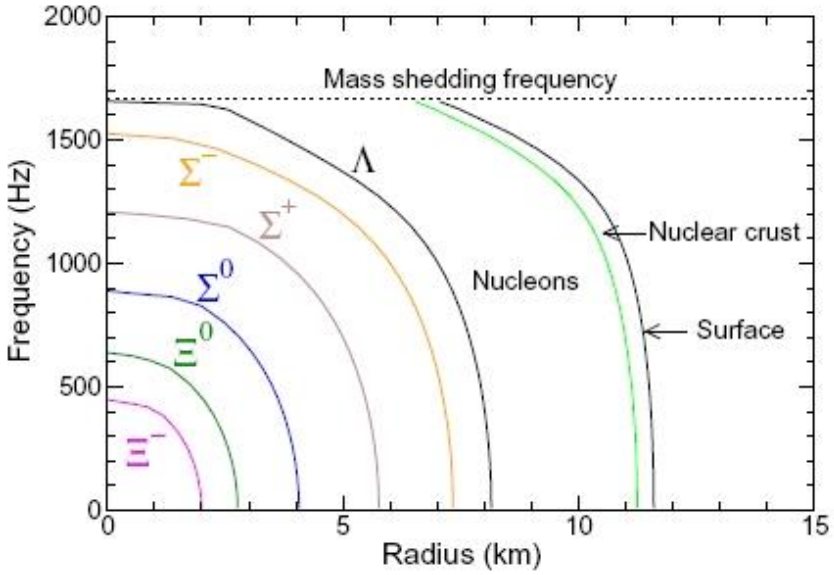

(polar)

Computed for a particular model:
density dependent relativistic Brueckner-Hartree-Fock (DD-RBHF)

(Weber et al. arXiv: 0705.2708)

Detailed study of the influence of rotation onto structure and composition is given in 1307.1103

Rotation and composition

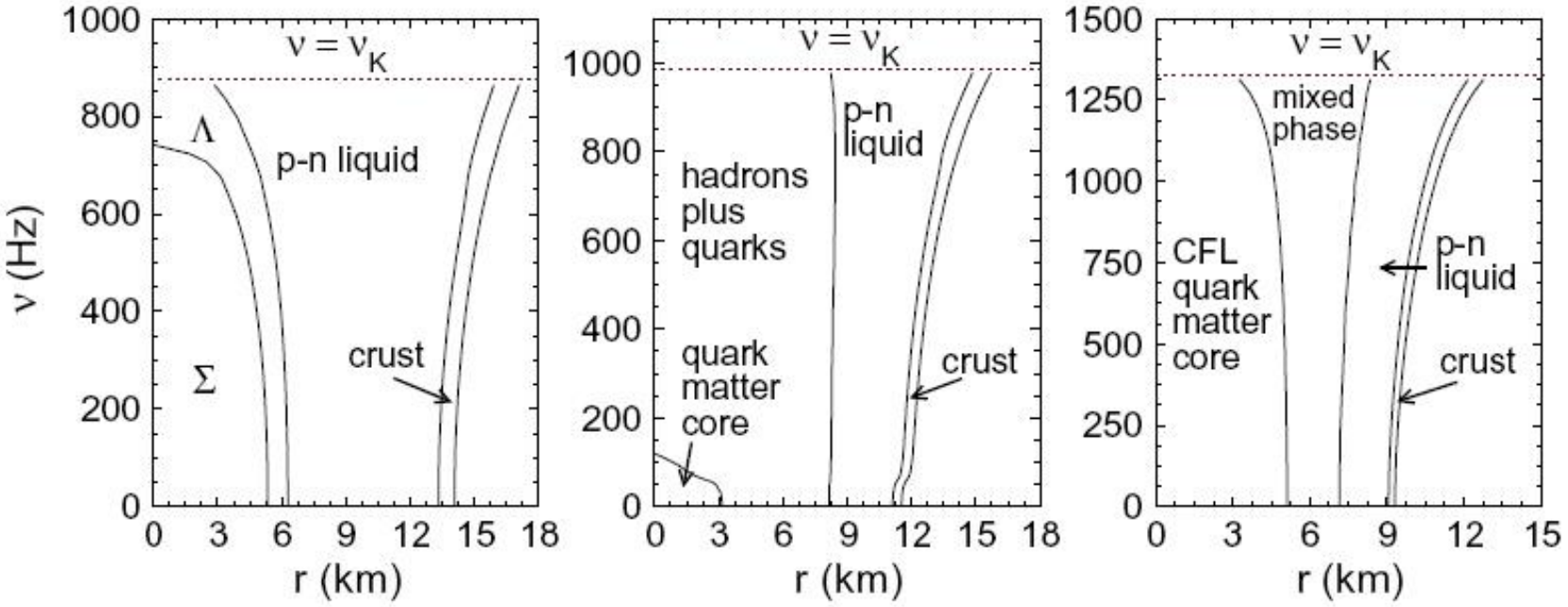

hyperon **quark-hybrid** **quark-hybrid (quarks in CFL)**

(Weber et al. arXiv: 0705.2708) 1.4 solar mass NS (when non-rotating)

Limiting rotation

$$f_{\max}^{\mathrm{EOS}} = C_{\max} \left(\frac{M_{\max}^{\mathrm{stat}}}{M_\odot} \right)^{1/2} \left(\frac{R_{M_{\max}}^{\mathrm{stat}}}{10\ \mathrm{km}} \right)^{-3/2}$$

$$C_{\max} = 1.22\ \mathrm{kHz}$$

Without additional assumptions for realistic EoS it is expected that NS can rotate faster than f=716 Hz for masses close to the limiting value.

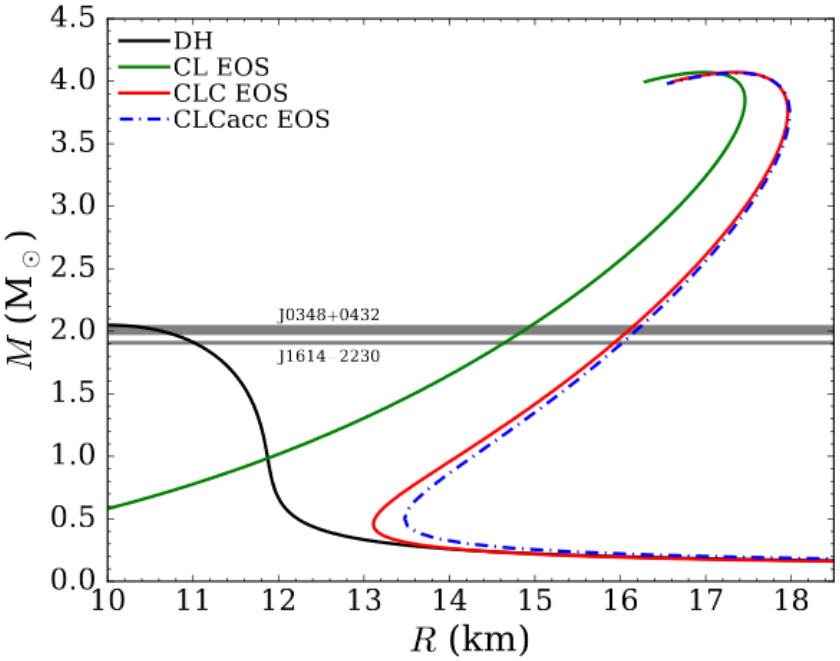

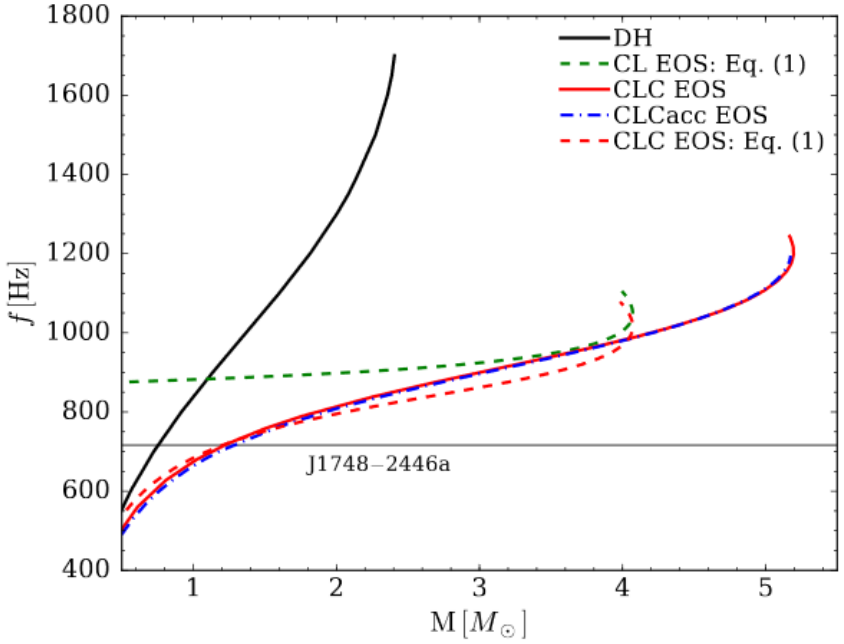

1805.11277

Limits on the EoS from GW observations

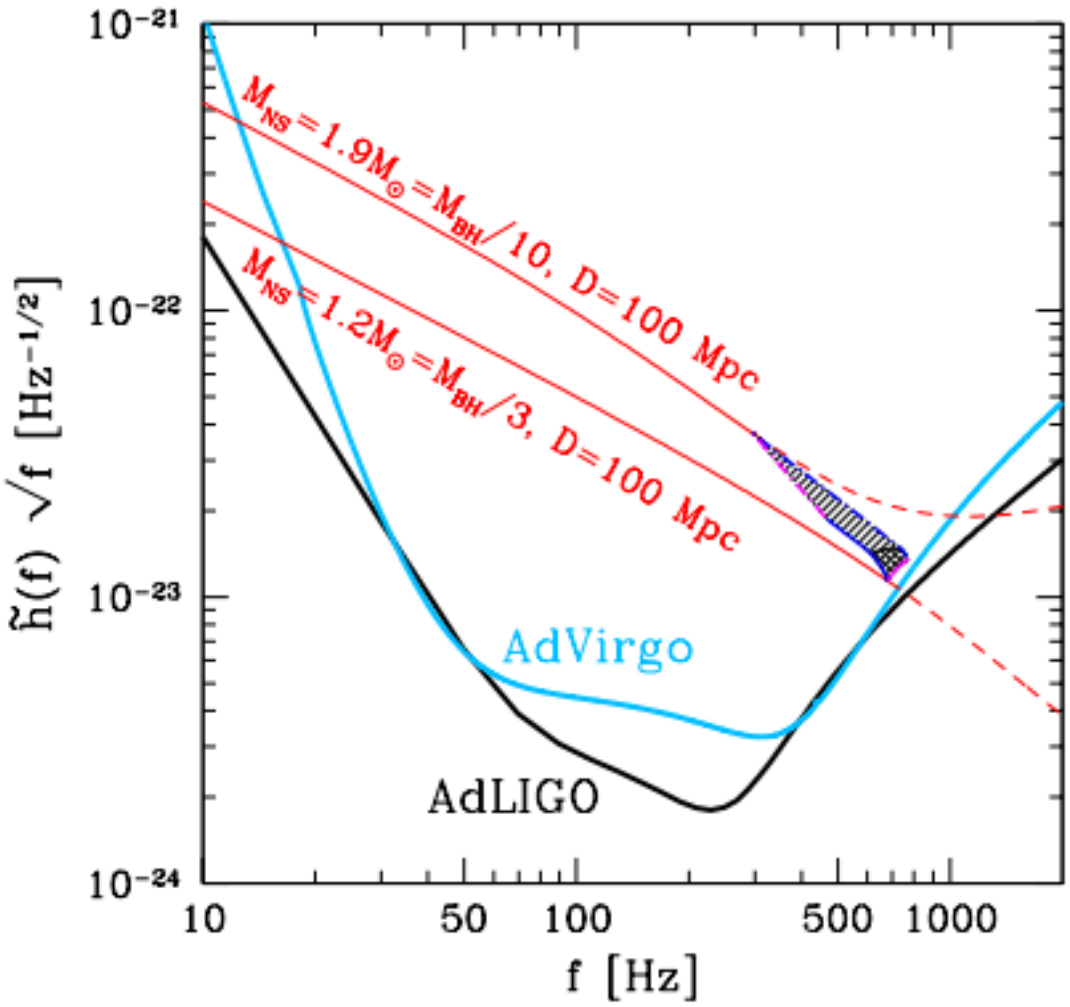

For stiff EoS
AdLIGO and AdVIRGO
can detect signatures
in the GW signal
during BH-NS mergers.

1103.3526

Another constraint

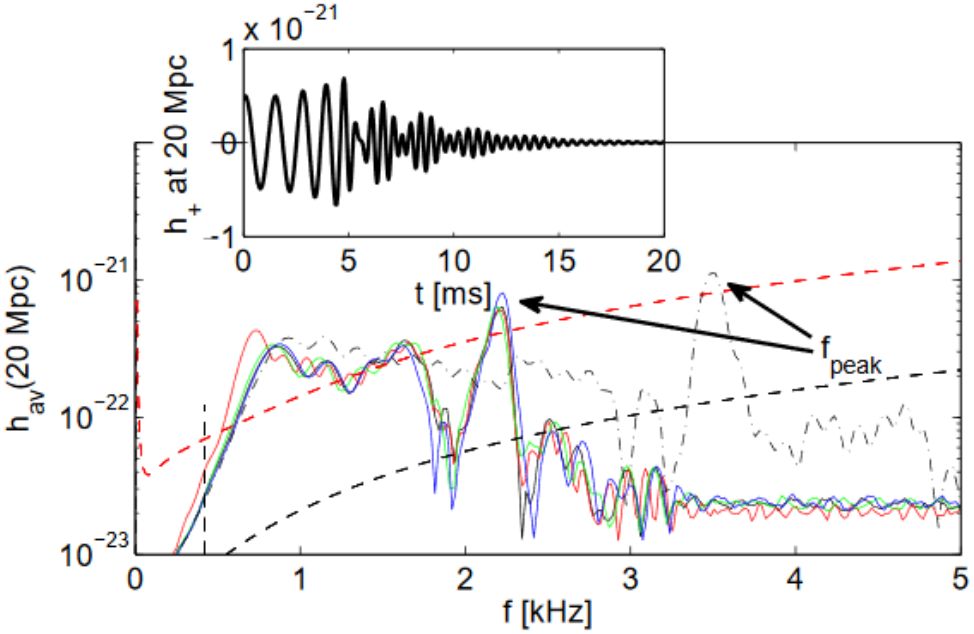

Measuring NS-NS mergers
one can better constraint the EoS.

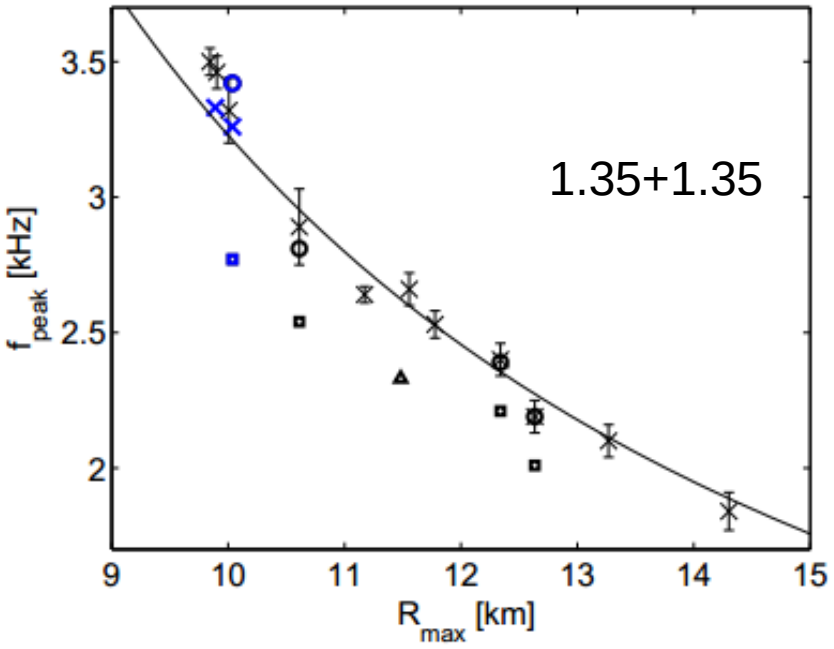

1106.1616

GW170817: deformability Λ

Many papers are published based on detection of GW signal from GW170817: 1803.00549, 1804.08583, 1805.09371, 1805.11579, 1805.11581, 1901.04138.

$$\tilde{\Lambda} = \frac{16}{13}\frac{(12q+1)\Lambda_1 + (12+q)q^4\Lambda_2}{(1+q)^5},$$

$$q = m_2/m_1 \leq 1$$

$$\Lambda_{1,2} = \frac{2}{3}k_2\left(\frac{R_{1,2}c^2}{Gm_{1,2}}\right)^5$$

$$\beta = Gm/(Rc^2)$$

$k_2 \sim \beta^{-1}$
$\Lambda \sim \beta^{-6}$

Low spin proiors

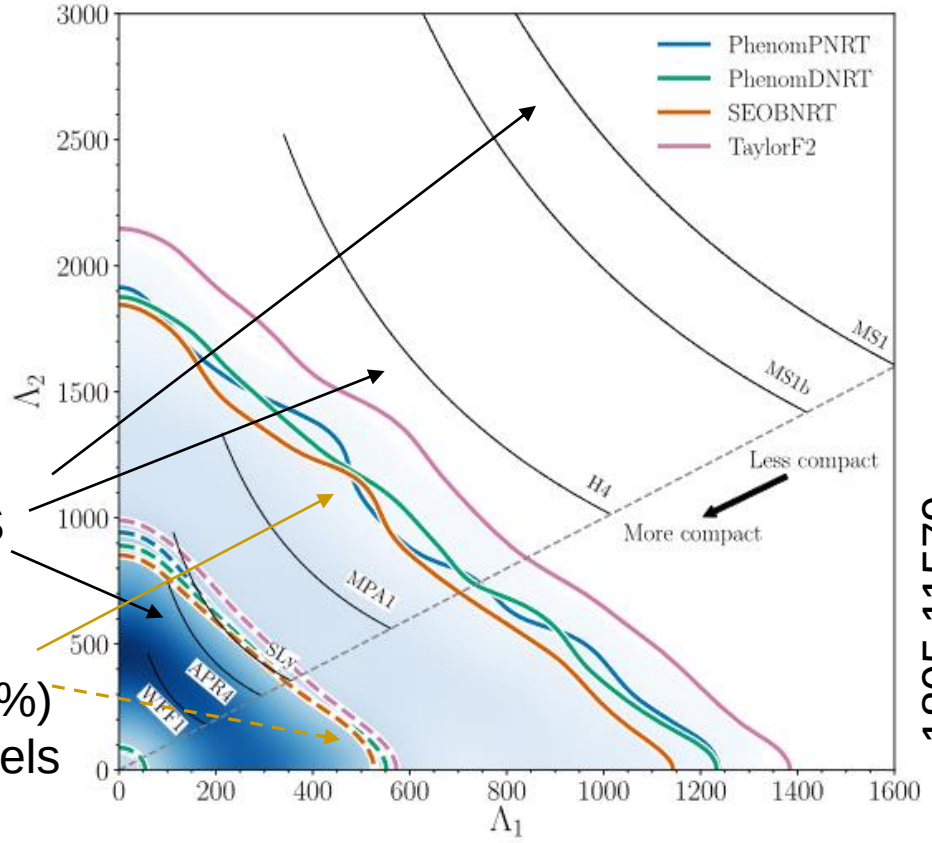

Solid – theoretical EoS

Colored – limits
(dashed 50%, solid 90%)
for four waveform models

1805.11579

Collapse to a BH after ~1 sec? (1901.04138)

GW170817: M-R

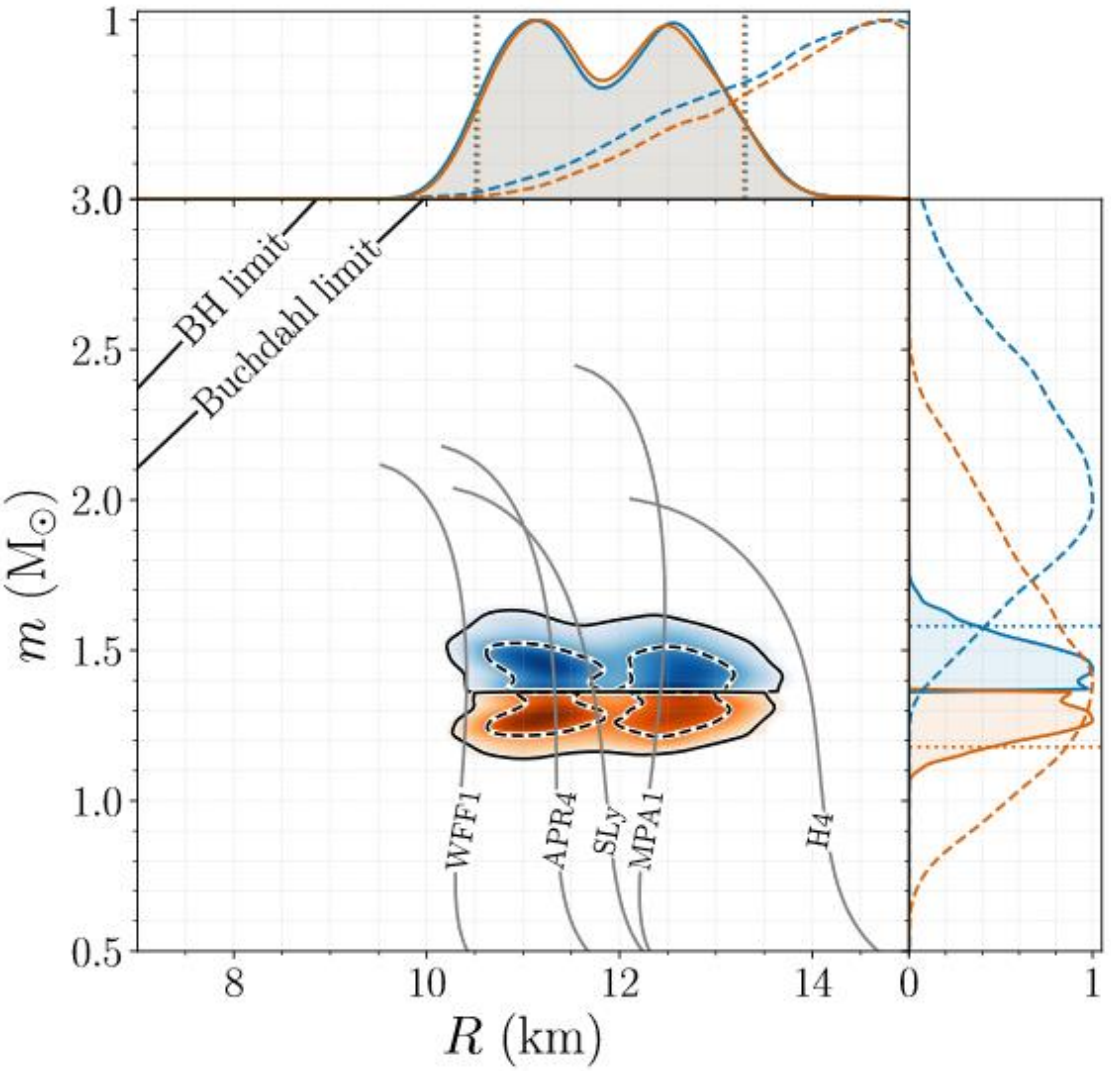

$$R_1 = 11.9^{+1.4}_{-1.4}\,\mathrm{km}$$

$$R_2 = 11.9^{+1.4}_{-1.4}\,\mathrm{km}$$

1805.11581

Microlensing and weak lensing

In the future (maybe already with Gaia)
it can possible to determine NS mass with lensing.
Different techniques can be discussed:
photometric (normal) microlensing (1009.0005),
astrometric microlensing, weak lensing (1209.2249).

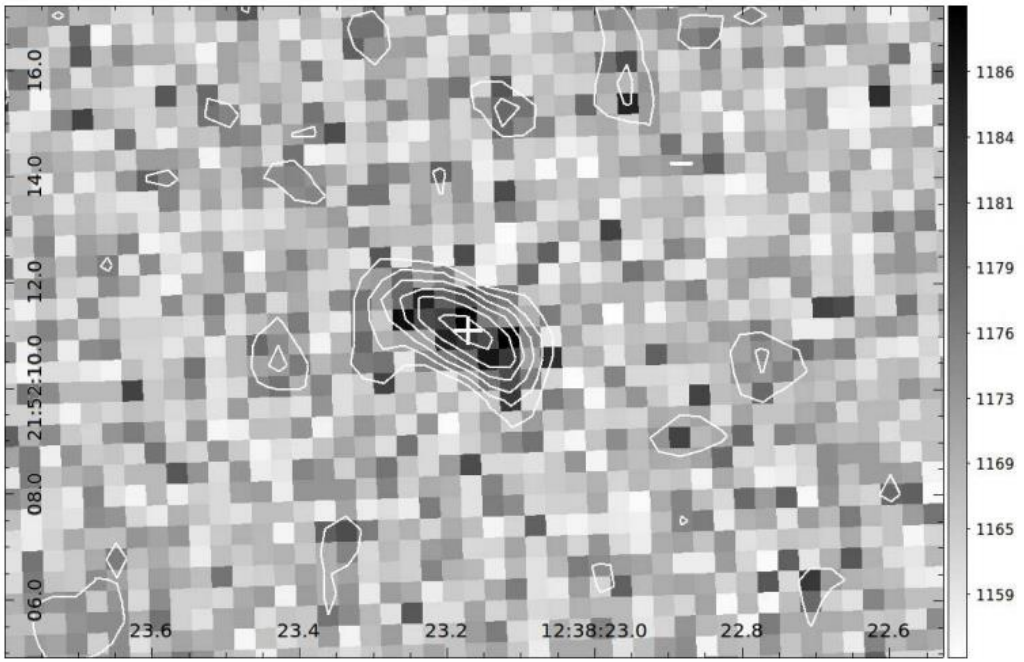

1209.2249

Future X-ray measurements

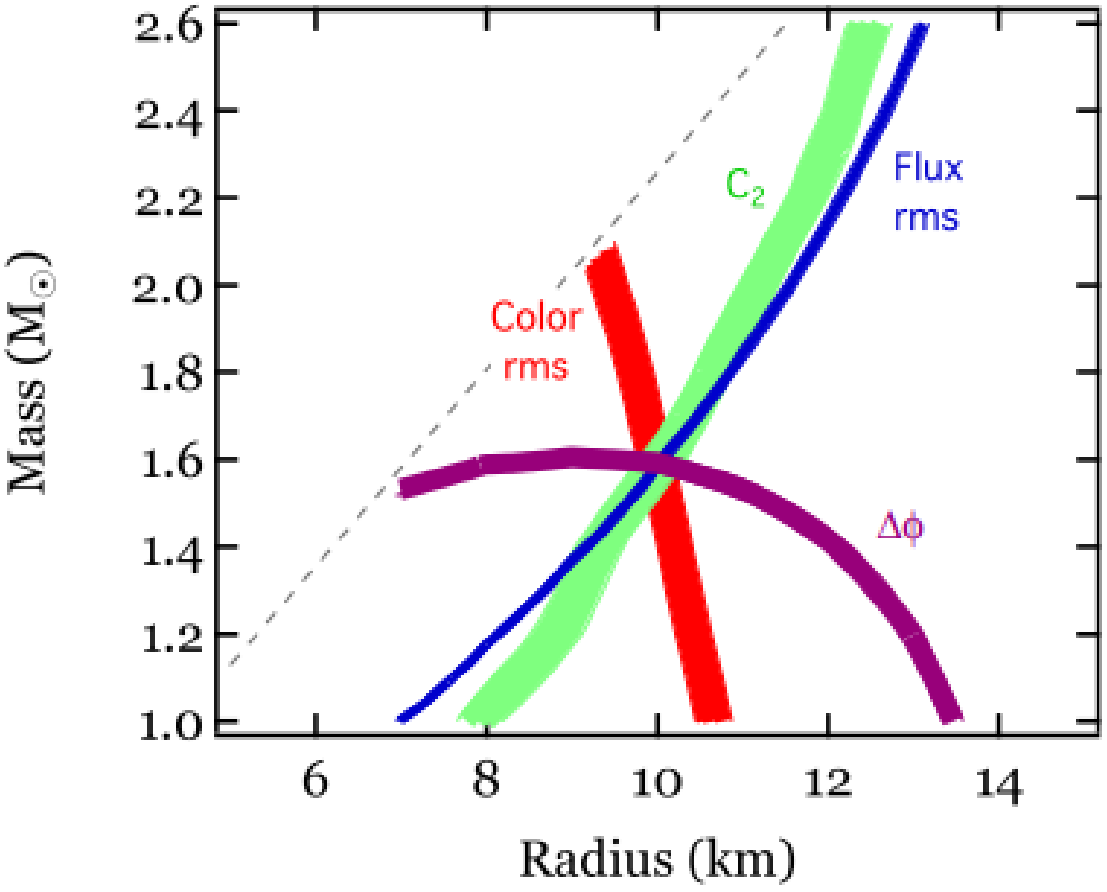

Valid for future observations aboard NICER and LOFT space projects.

Data based on pulse profile.

The idea is to observe X-ray pulsars with spin periods ~few msec and to collect about 10^6 counts.

It allows to derive from the pulse profile a lot of info about a NS.

1311.1571

References

- Observational Constraints on Neutron Star Masses and Radii 1604.03894
  The review is about X-ray systems
- Mass, radii and equation of state of neutron stars 1603.02698
  The review about different kinds of measurements, including radio pulsars. Recent lists of mass measurements for different NSs.
- Measuring the neutron star equation of state using X-ray timing 1602.01081
  The review about EoS and X-ray measurements
- The masses and spins of neutron stars and stellar-mass black holes 1408.4145
  The review covers several topics. Good brief description of radio pulsar mass measurements.
- Properties of DNS systems. 1706.09438
  The review covers all aspects of observations, formation and evolution.
- Testing the equation of state of neutron stars with electromagnetic observations. 1806.02833 The review describes observational tests of the EoS.

NS+NS binaries

Secondary companion in double NS binaries can give a good estimate of the initial mass if we can neglect effects of evolution in a binary system.

	Pulsar	Pulsar mass	Companion mass	
	B1913+16	1.44	1.39	
GC →	B2127+11C	1.36	1.35	
	B1534+12	1.33	1.35	
	J0737-3039	1.34	1.25	
	J1756-2251	1.40	1.18	
	J1518+4904	<1.17	>1.55	→ 0808.2292
Non- →	J1906+0746	1.25	1.37	
recycled	J1811-1736	1.56	1.12	
	J1829+2456	1.2	1.4	

Also there are candidates, for example PSR J1753-2240 arXiv:0811.2027

In NS-NS systems we can neglect all tidal effects etc.

See a review on formation and evolution of DNS binaries in 1706.09438

Pulsar masses

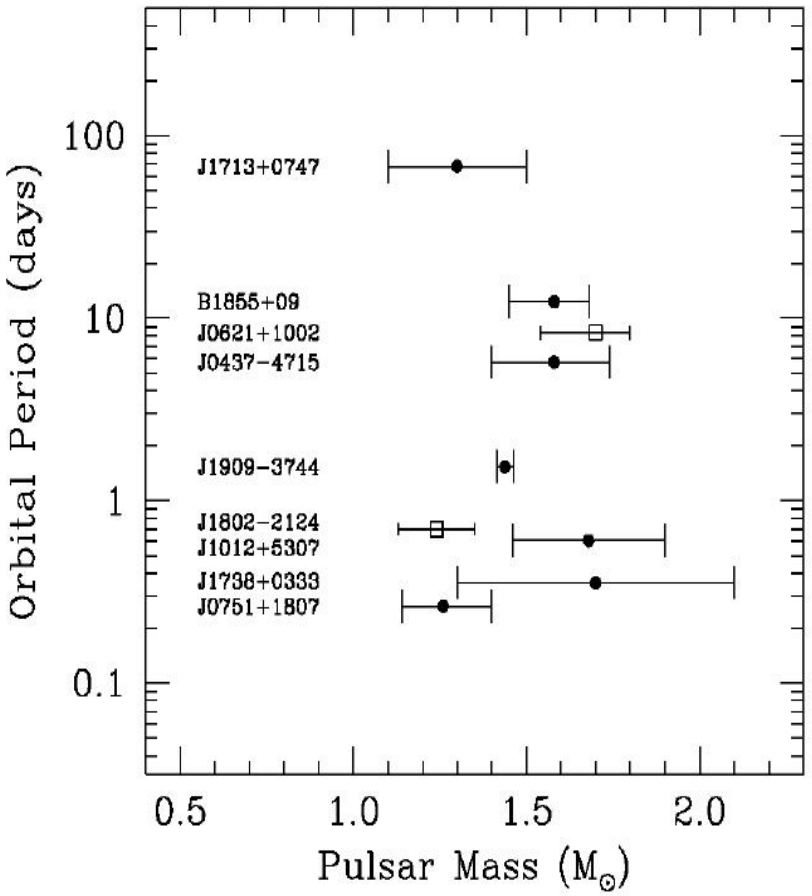

With WD companions

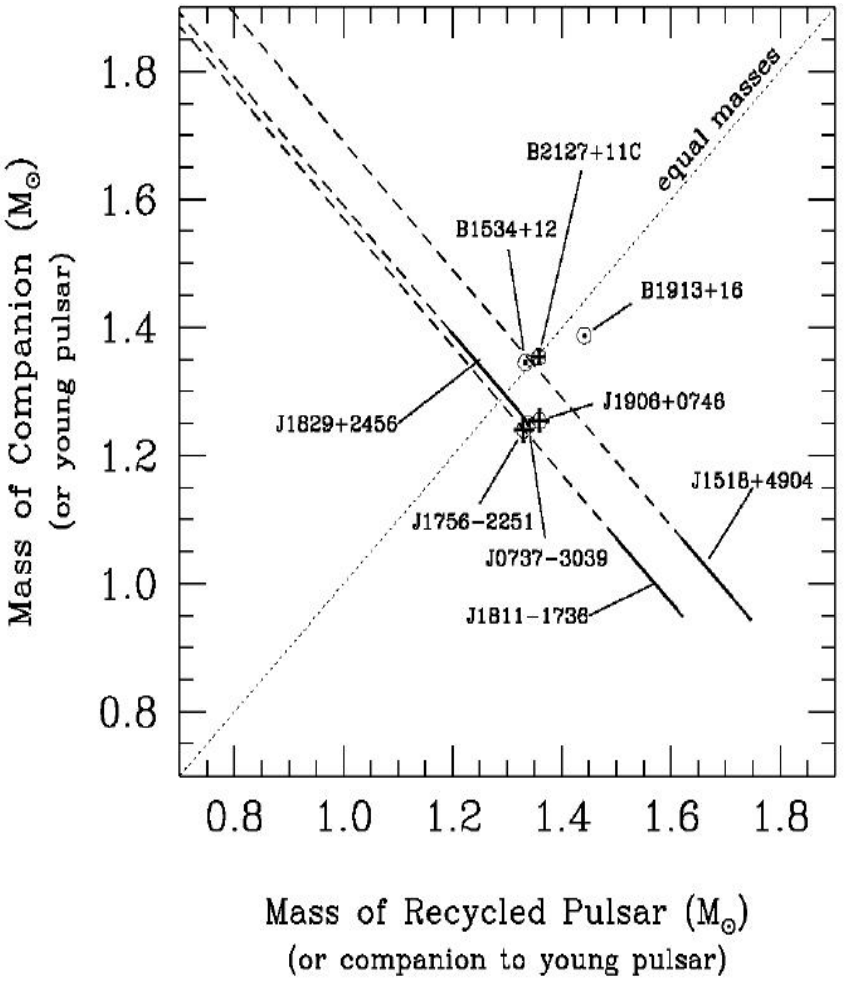

With NS companions

[Nice et al. 2008]

Glitches and precession

What is a glitch?

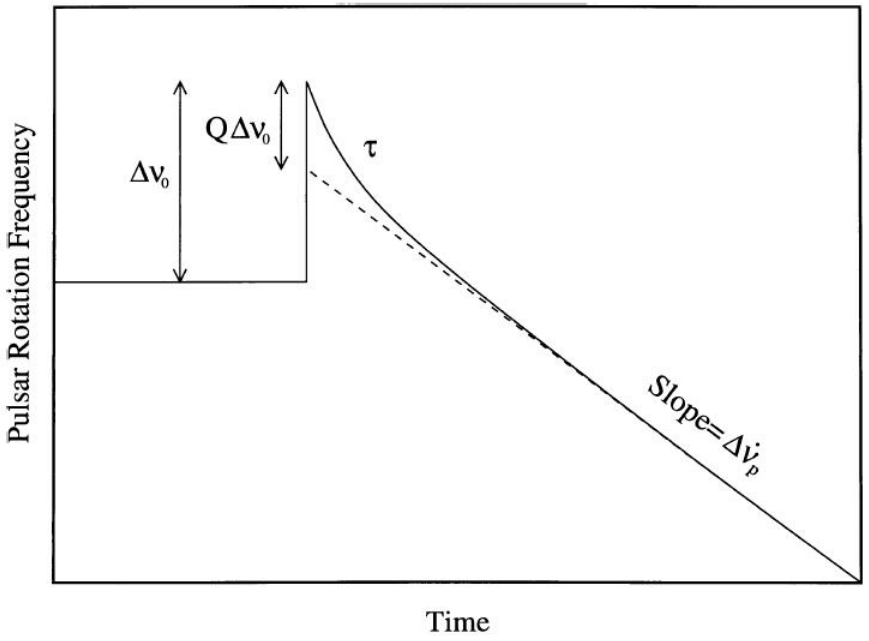

A sudden increase of rotation rate (limits are down to <40 sec in Vela).

ATNF catalogue gives >130 normal PSRs with glitches.

The most known: Crab and Vela

$$\Delta\Omega/\Omega \sim 10^{-9} - 10^{-6}$$

Spin-down rate can change after a glitch. Vela is spinning down faster after a glitch.

Starquakes or/and vortex lines unpinning - new configuration or transfer of angular momentum

Glitches are important because they probe internal structure of a NS.

See a review in 1502.07062

Anti-glitch of a magnetar

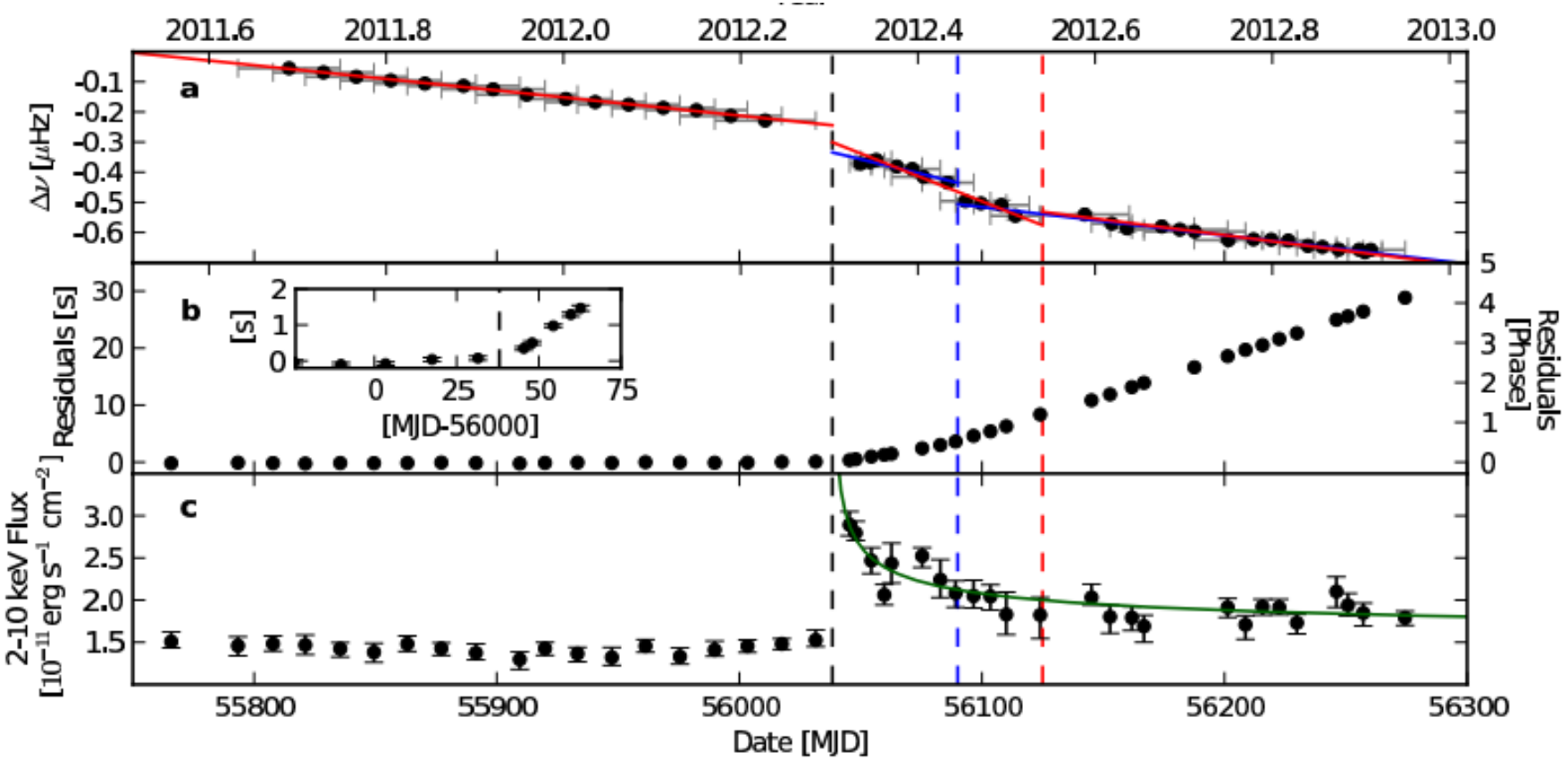

AXP 1E 2259+586

1305.6894

Crab glitch and the general idea

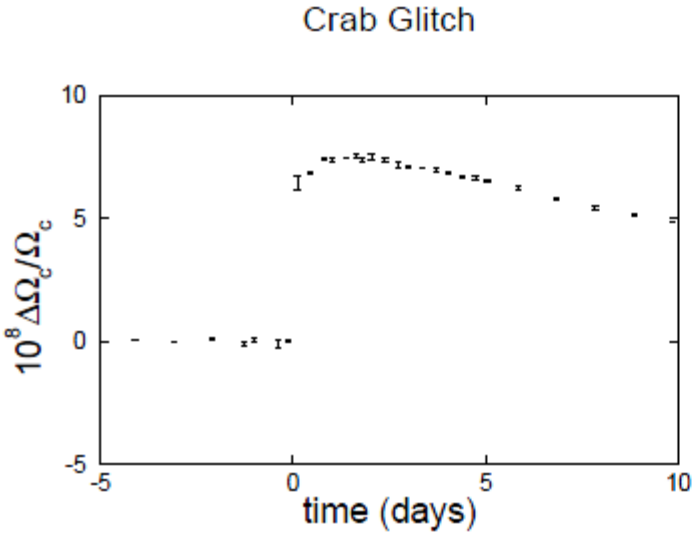

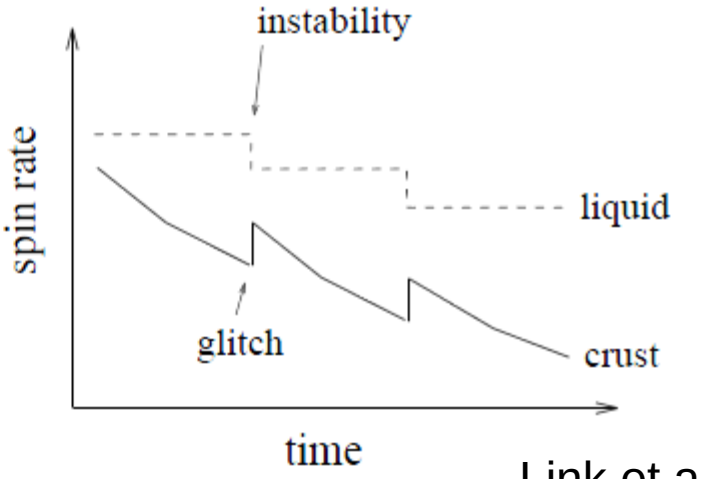

Link et al. (2000)

While the crust we see (and all coupled to it) is slowing down,
some component of a star is not.
Then suddenly (<40 sec) an additional momentum stored in such a “reservoir” is released and given to the crust.
The crust spins-up,
up the internal reservoir – down.

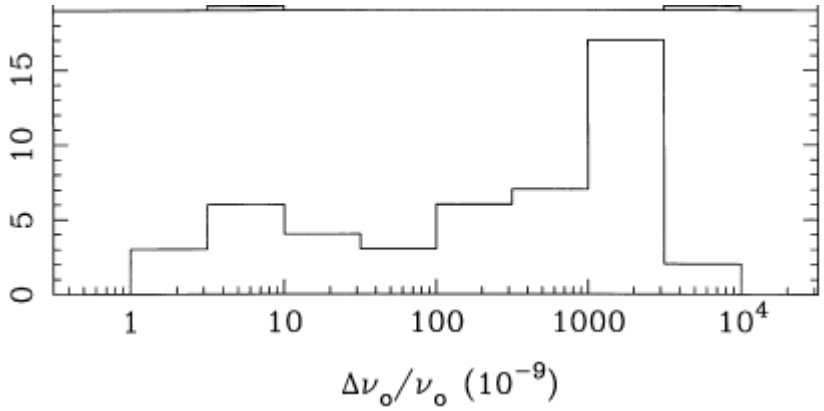

Lyne et al. (2000)

Glitches

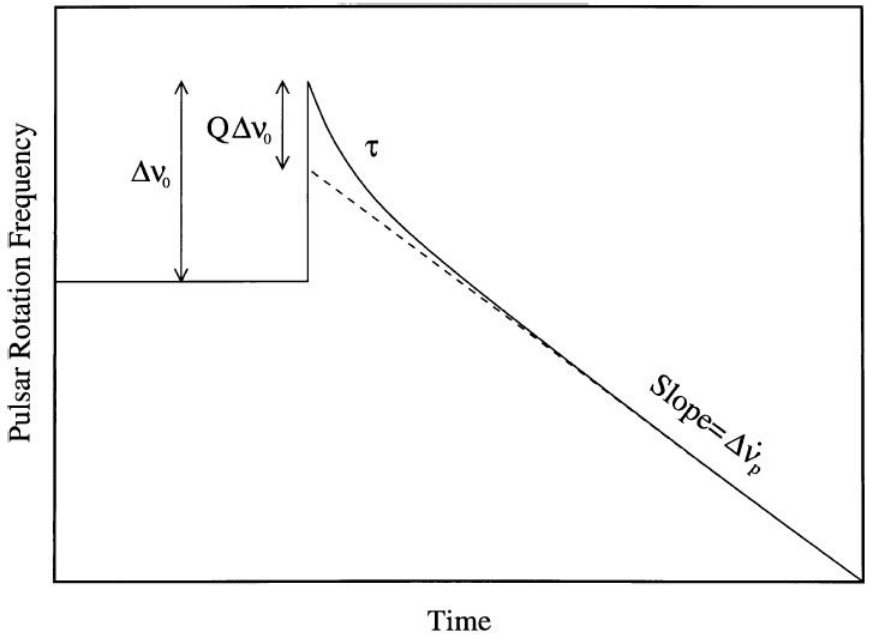

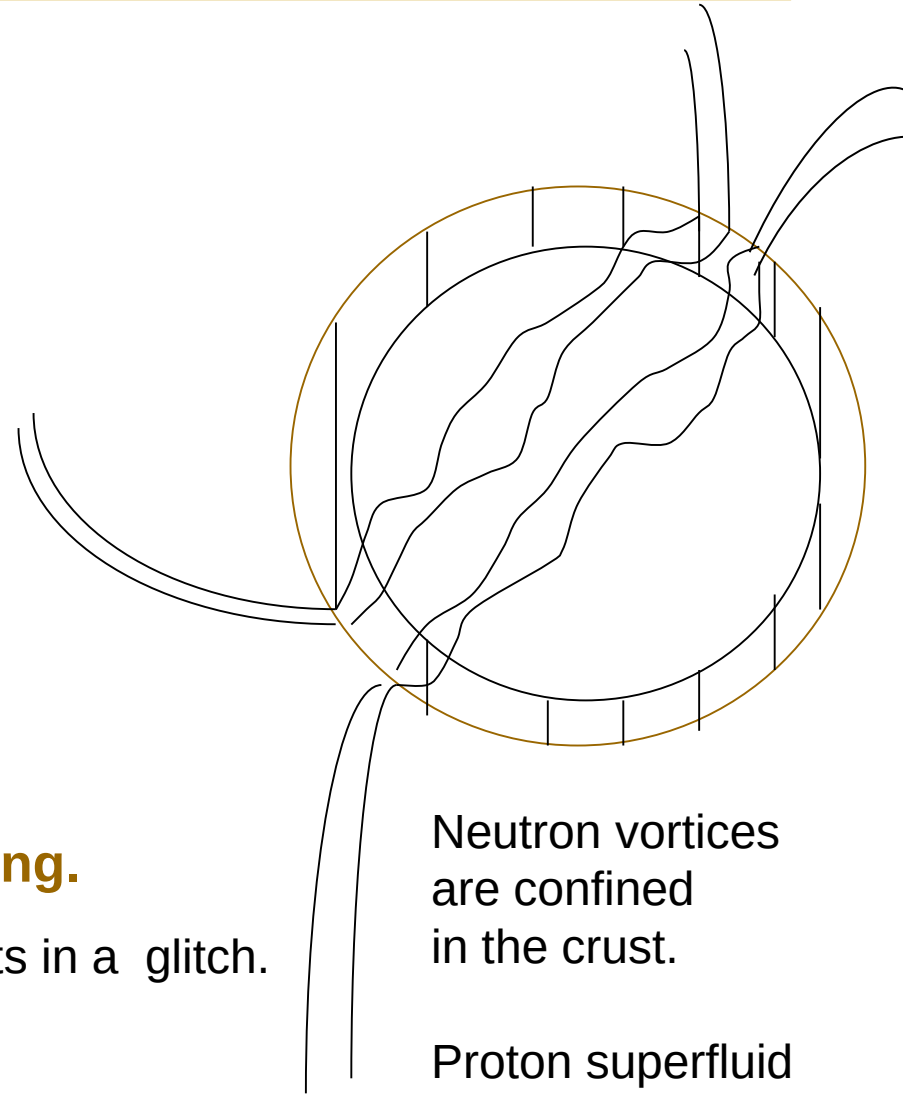

Starquakes or vortex lines unpinning.

Unpinning of superfluid vortex lines results in a glitch.

Vortex density is about 10^4 cm^{-2} P^{-1}

Flux lines density is 5 10^{18} B_{12} cm^{-2}

Neutron vortices are confined in the crust.

Proton superfluid is strongly coupled to the crust.

A recent review about superfluidity in NS and its relation to glitches, etc.: 1709.10340

Glitch discovery and observations

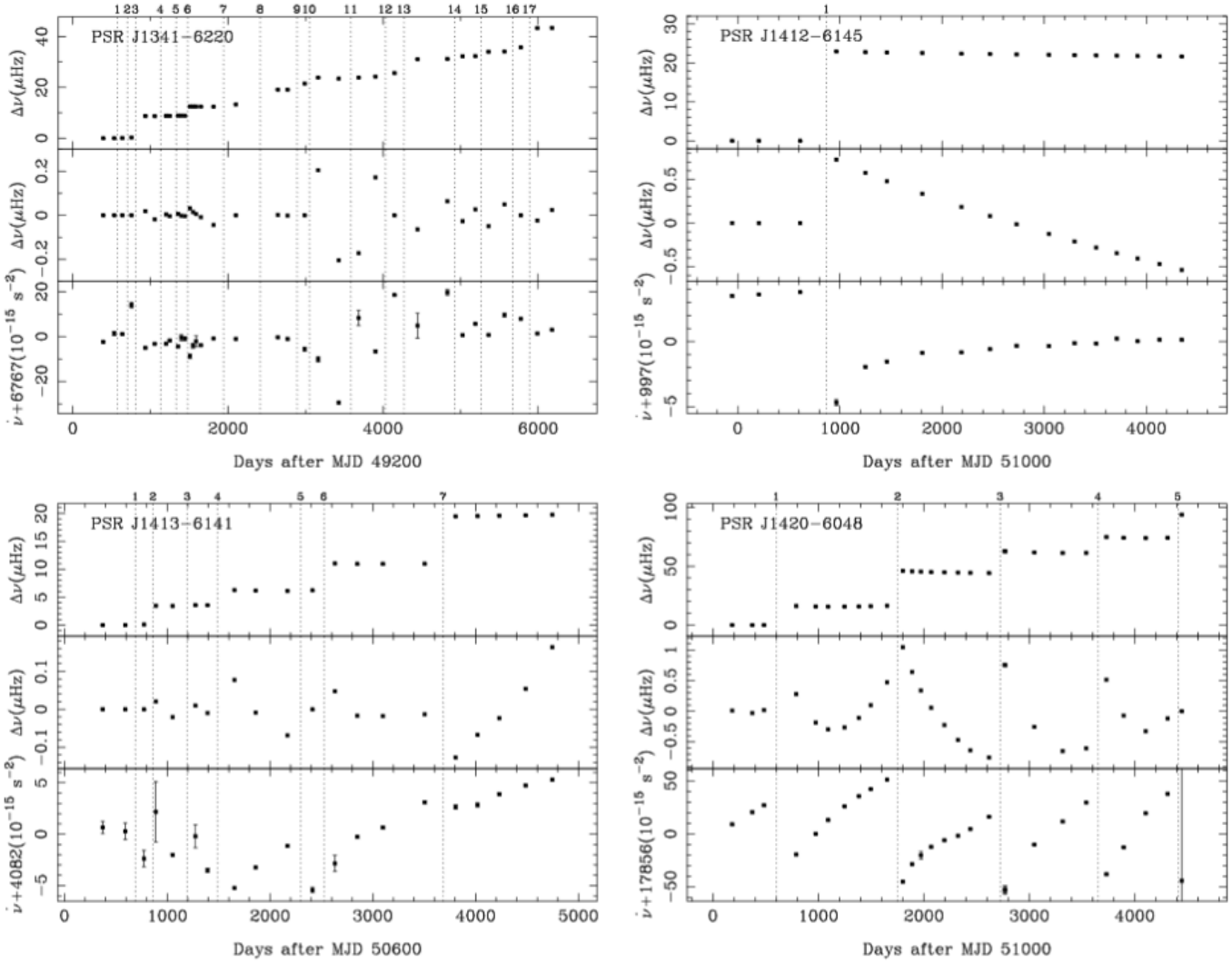

1211.2035

The largest glitch of the Crab pulsar

2017 November 8

$\Delta\nu = 1.530 \times 10^{-5}$ Hz

$\Delta\nu/\nu = 0.516 \times 10^{-6}$

$\Delta\dot{\nu}/\dot{\nu} = 7 \times 10^{-3}$

The glitch occurred after the longest period of glitch inactivity – 6 years, - since beginning of daily monitoring in 1984.

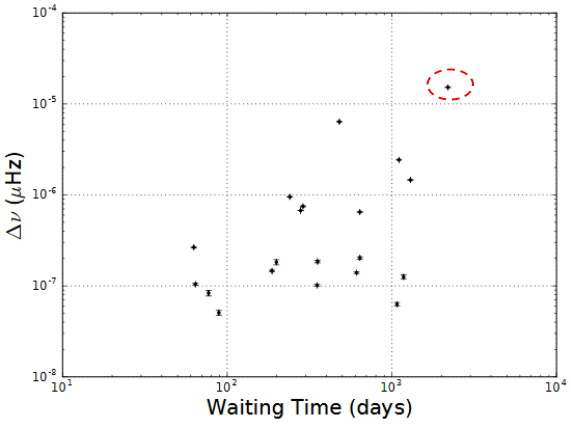

No changes in the shape of the pulse profile, no changes in the X-ray flux.

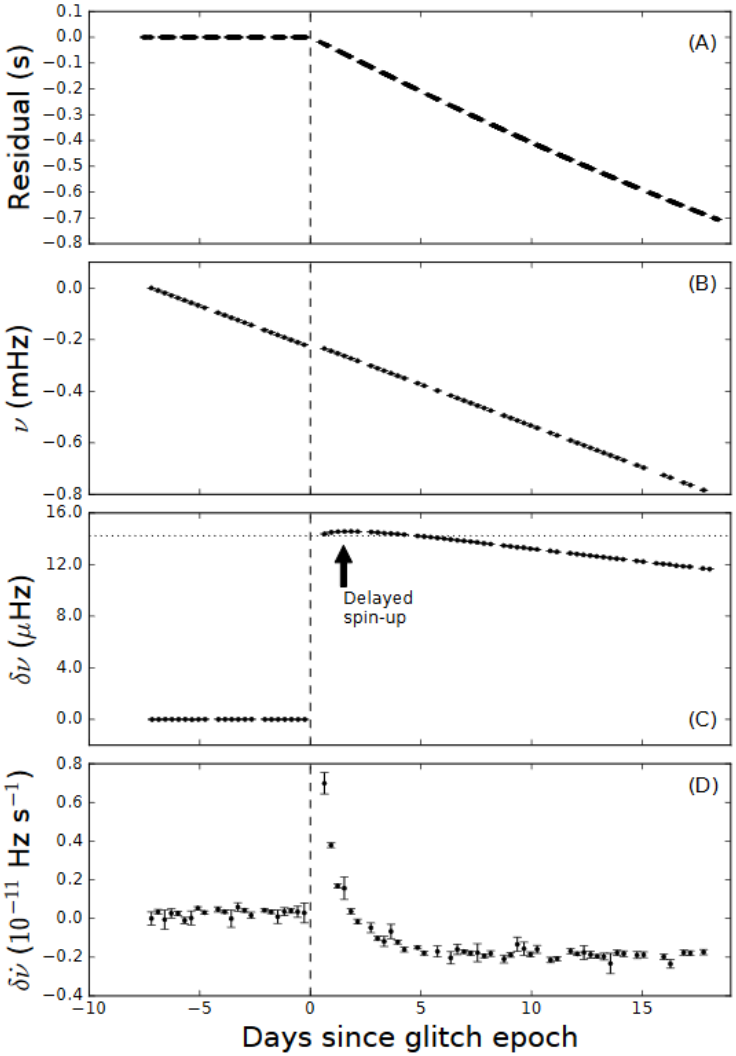

1805.05110

(See theoretical discussion in 1806.10168)

Glitch size – spin down rate correlation

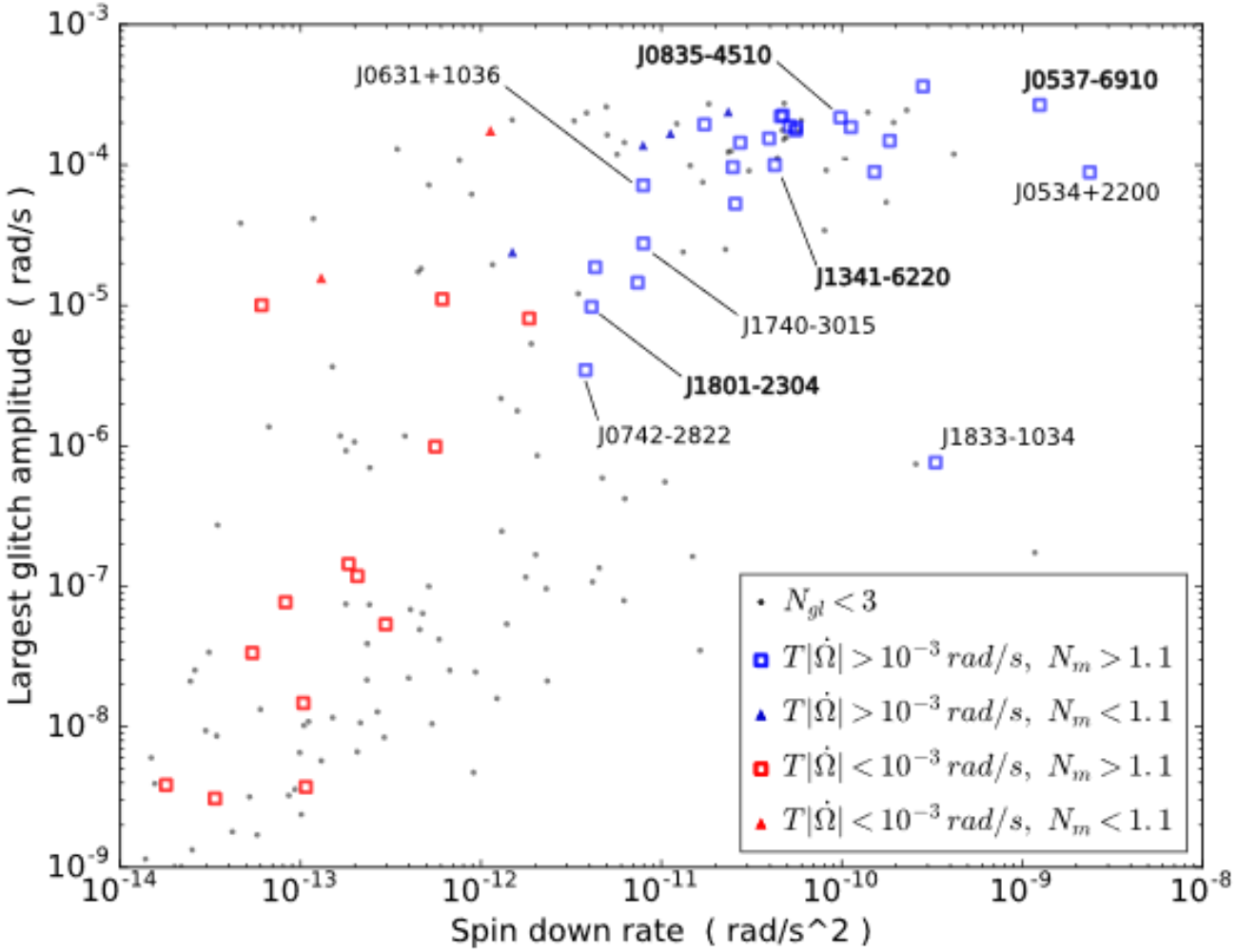

1809.07834

Phenomenology and the Vela pulsar

$$\Delta J_i = I_c \Delta\Omega_i,$$

$$J(t) = I_c \bar{\Omega} \sum_i \frac{\Delta\Omega_i}{\bar{\Omega}},$$

Glitches are driven by the portion of the liquid interior that is differentially rotating with respect to the crust.

I_c – crust + everything coupled with (i.e., nearly all the star, except superfluid neutrons).

The average rate of angular momentum transfer associated with glitches is $I_c \bar{\Omega} A,$

$$A = (6.44 \pm 0.19) \times 10^{-7}\ \mathrm{yr}^{-1}.$$ - Pulsar activity parameter

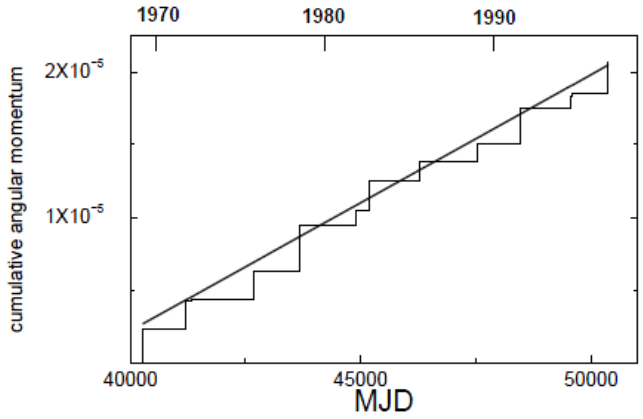

Vela glitches are not random, they appear every ~840 days.

A – the slope of the straight line in the figure.

(Values are for the Vela PSR)

In Vela glitches can be related also to the outer core 1806.10168

General features of the glitch mechanism

Glitches appear because some fraction (unobserved directly) rotates faster than the observed part (crust plus charged parts), which is decelerated (i.e., which is spinning-down).

$$\dot{J}_{\rm res} \leq I_{\rm res}|\dot{\Omega}|,$$

The angular momentum is “collected” by the reservoir, related to differentially rotating part of a star (SF neutrons)

$$\frac{I_{\rm res}}{I_c} \geq \frac{\bar{\Omega}}{|\dot{\Omega}|}A \equiv G,$$

G – the coupling parameter. It can be slightly different in different sources.

$$\frac{I_{\rm res}}{I_c} \geq G_{\rm Vela} = 1.4\%.$$

Glitch statistics for Vela provide an estimate for G.

Superfluid is a good candidate to form a “reservoir” because relaxation time after a glitch is very long (~months) which points to very low viscosity.

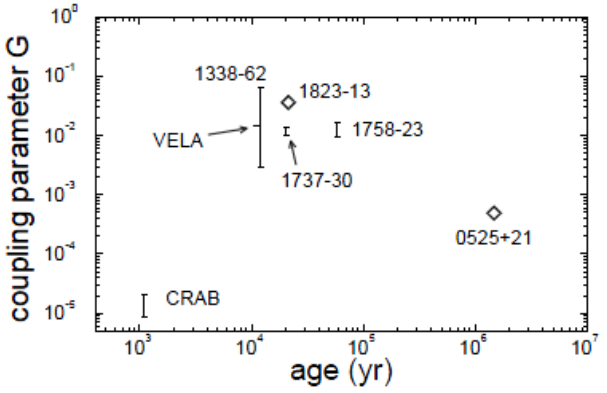

Link et al. 0001245

KERS

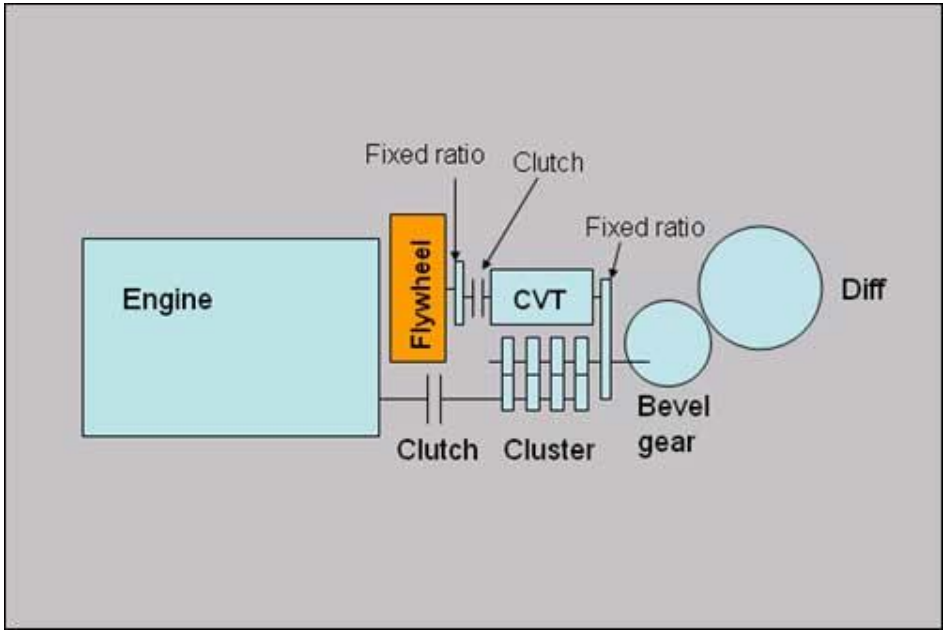

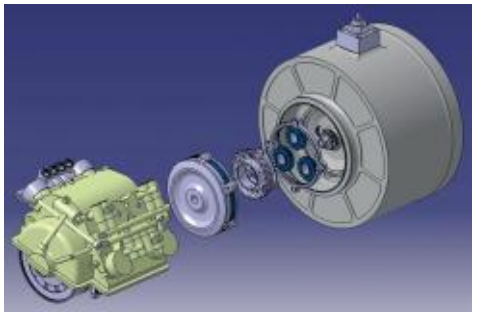

Williams-F1 used mechanical KERS.
Energy is stored in a flywheel.

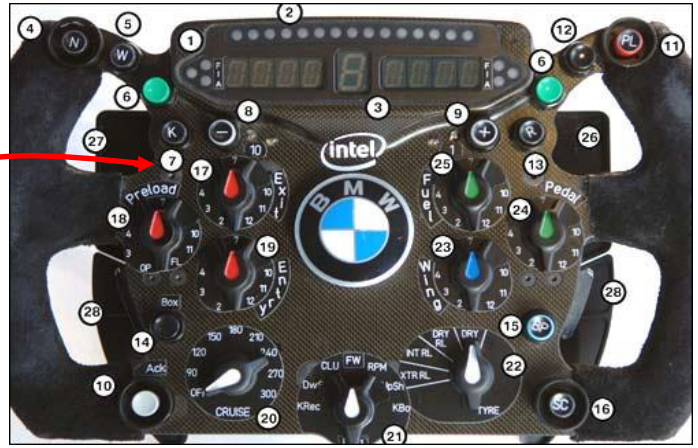

Critical velocity difference

In most popular models glitches appear when the difference in angular velocity between the crust and the superfluid reaches some critical value.

$I_{super}/I_{crust} \sim 10^{-2}$
$\Delta\Omega/\Omega \sim 10^{-6}$
$\Delta\Omega$ – is for the crust (we see it!)
$\Delta\Omega\, I_{crust} = \Delta\Omega_{super}\, I_{super}$

$\Delta\Omega_{super} = \Delta\Omega\, I_{crust}/I_{super} = \Omega\, 10^{-6}\, 10^{2} = 10^{-4}\, \Omega$

Glitch size – waiting time correlation

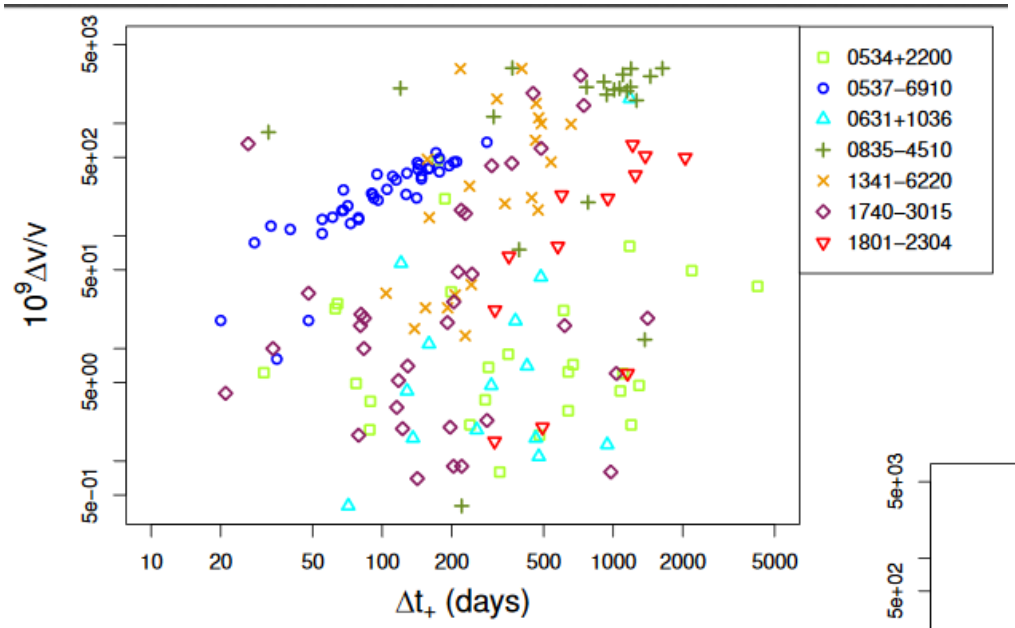

No correlation of a glitch size with time since the previous glitch, or with time before the next one.

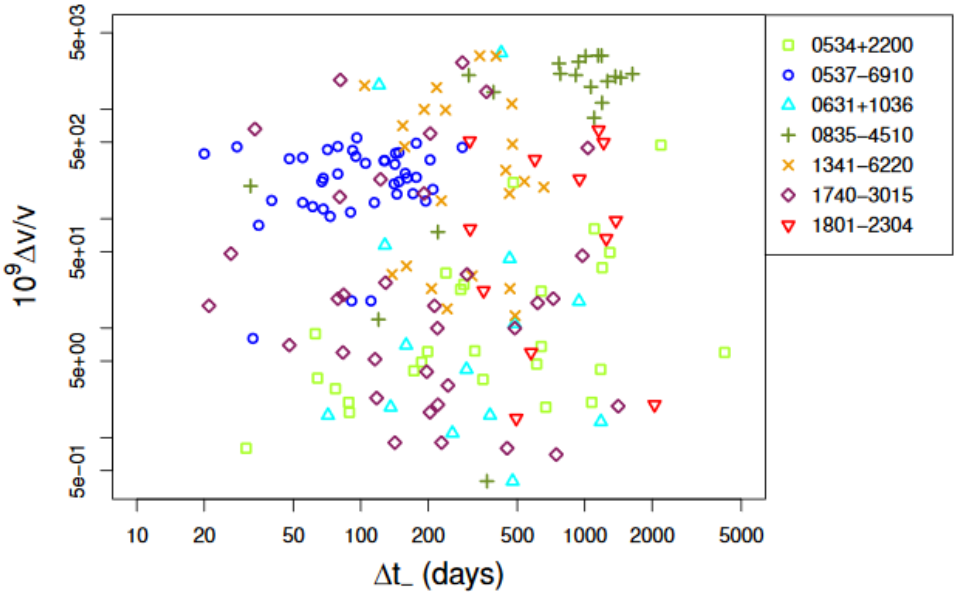

1809.03064

EoS and glitches

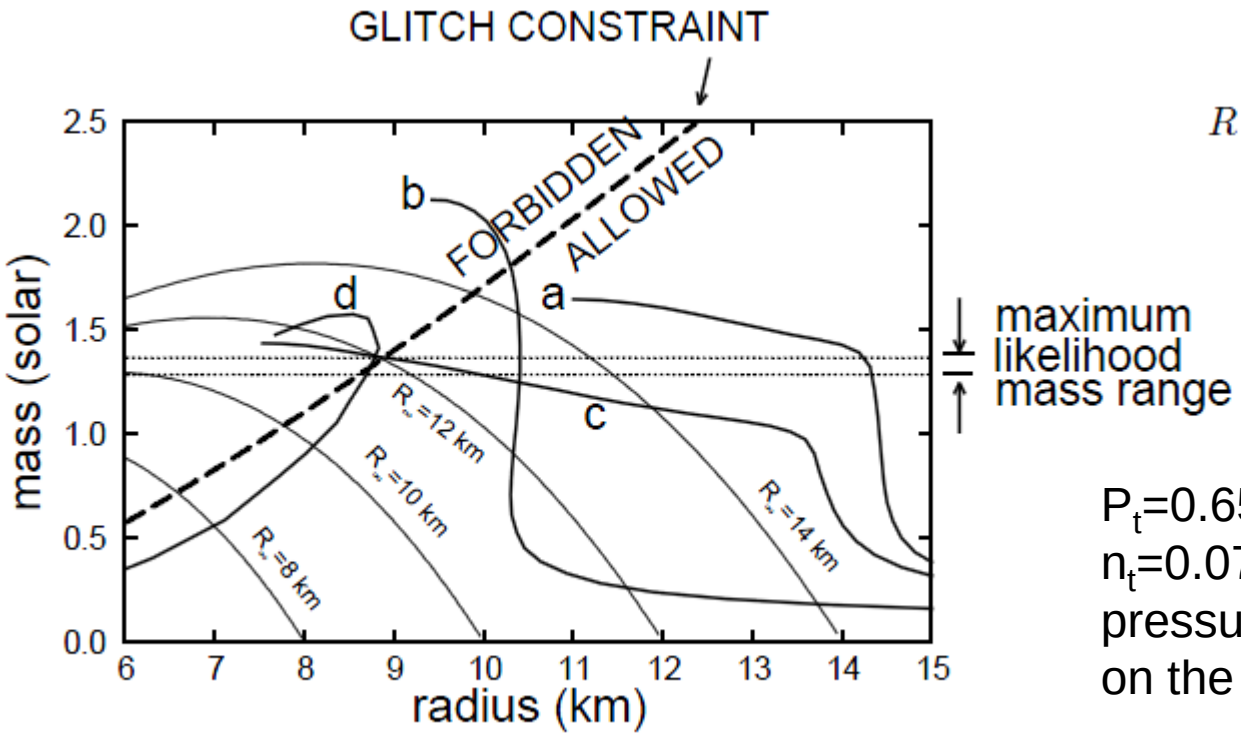

$$R = 3.6 + 3.9M/M_\odot\,.$$

P_t=0.65 MeV fm^{-3}
n_t=0.075 fm^{-3}
pressure and density
on the core-crust boundary.

$$\Lambda \equiv (1 - 2GM/Rc^2)^{-1}$$

$$\frac{\Delta I}{I} \simeq \frac{28\pi}{3}\frac{P_t R^4}{GM^2}\left[1 + \frac{8P_t}{n_t m_n c^2}\frac{4.5 + (\Lambda-1)^{-1}}{\Lambda - 1}\right]^{-1}$$

$$\Delta I/(I - \Delta I) \geq \Delta I/I_c \geq I_{\rm res}/I_c \geq 0.014.$$

Link et al. 0001245

See some critics in 1207.0633 “Crust is not enough” and 1210.8177
Further discussion – in 1404.2660, 1809.07834.

Which PSRs do glitch?

On average young pulsars with larger spin-down glitch more frequently

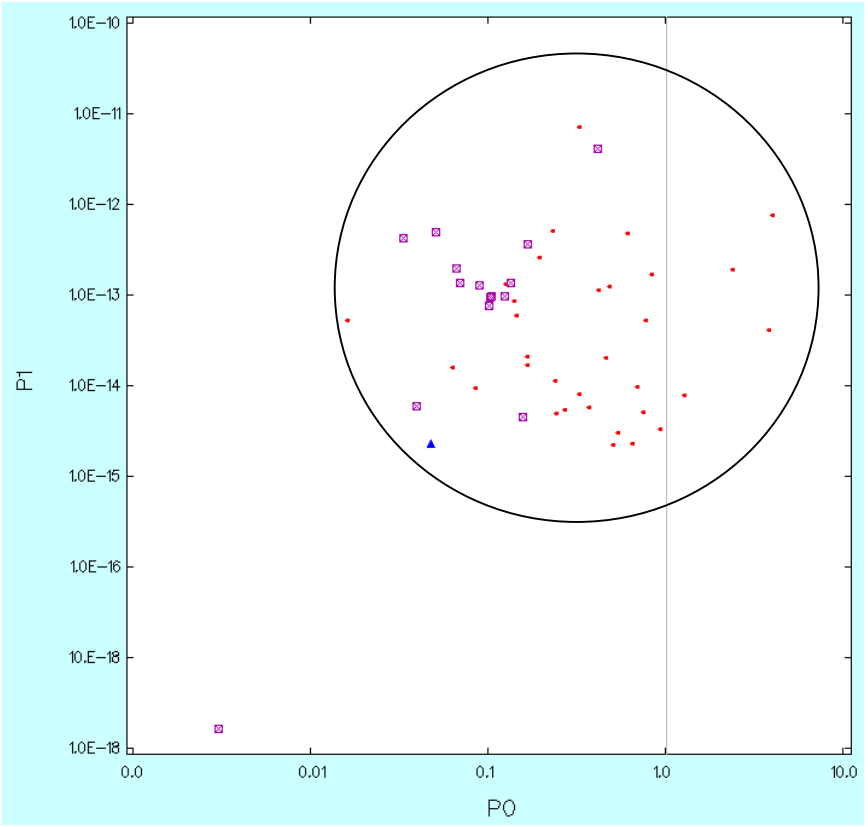

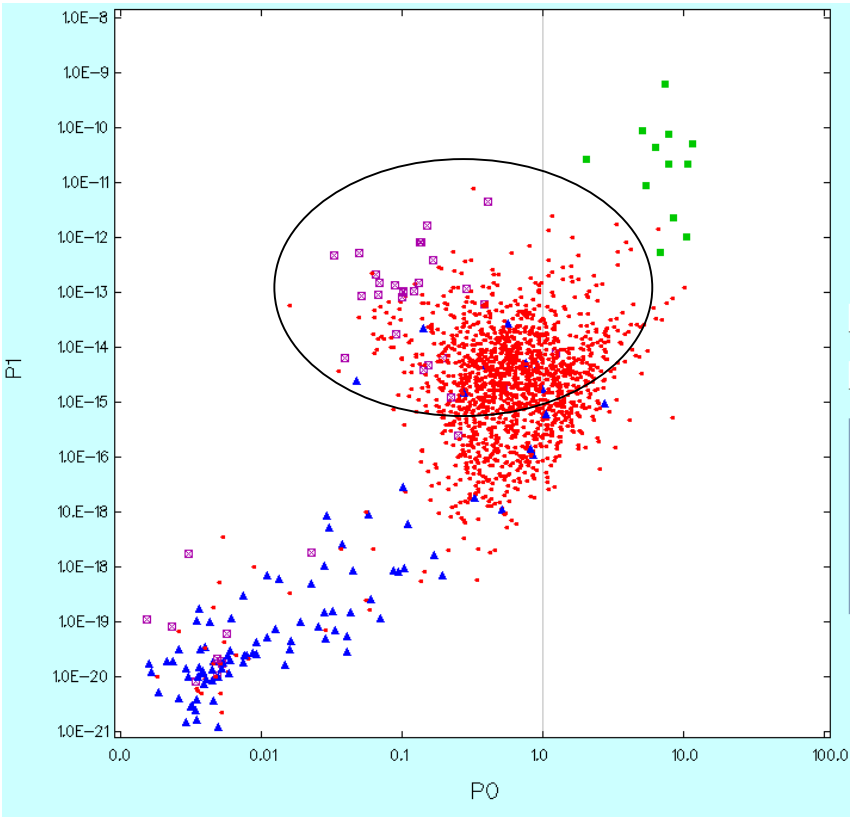

P-Pdot

>520 glitches
in >180 PSRs

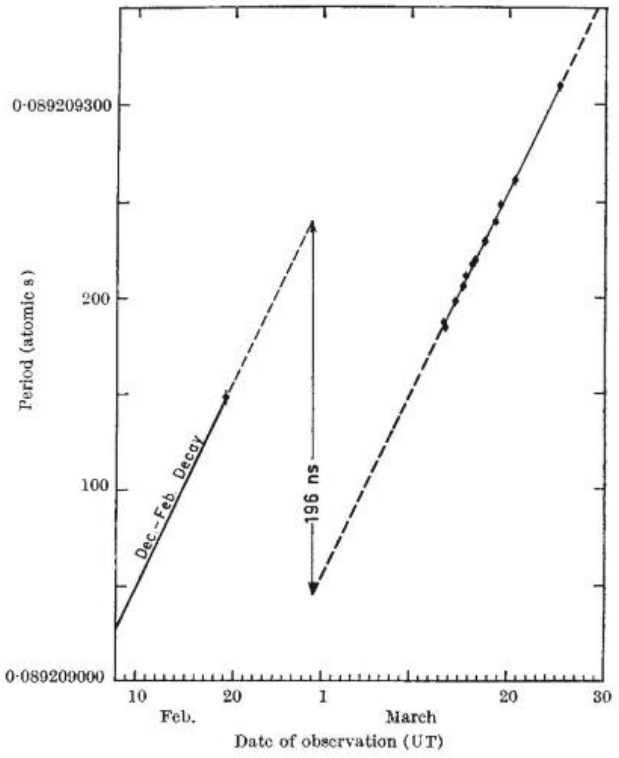

Vela glitch in 1969

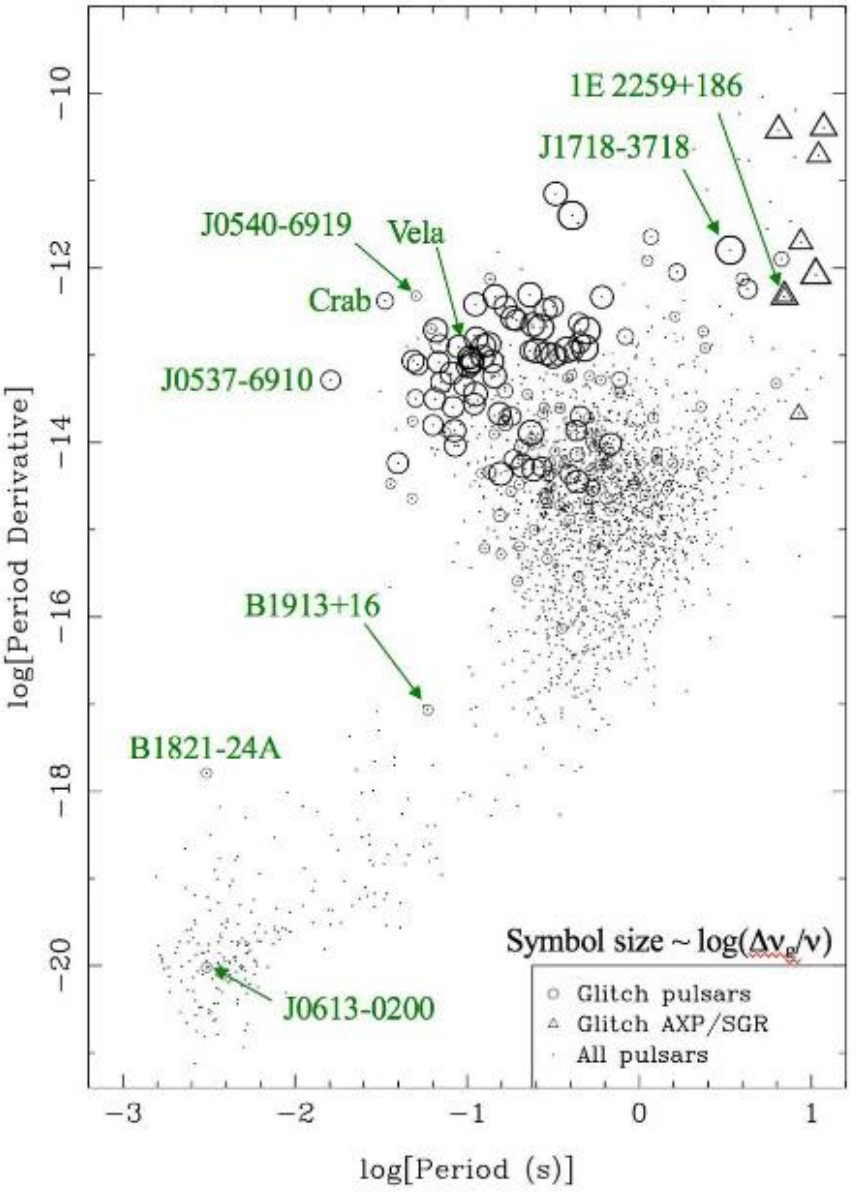

1801.04332

Statistics

384 glitches in 141 NSs

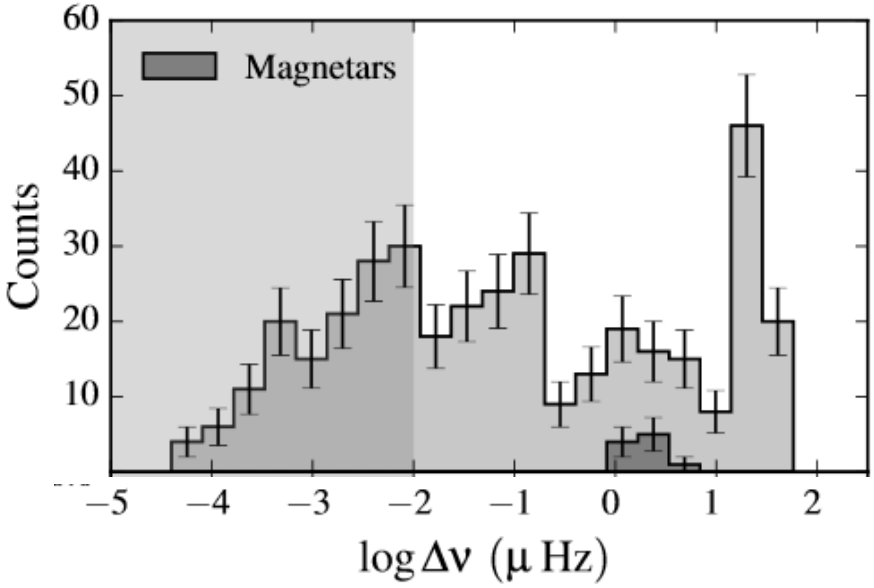

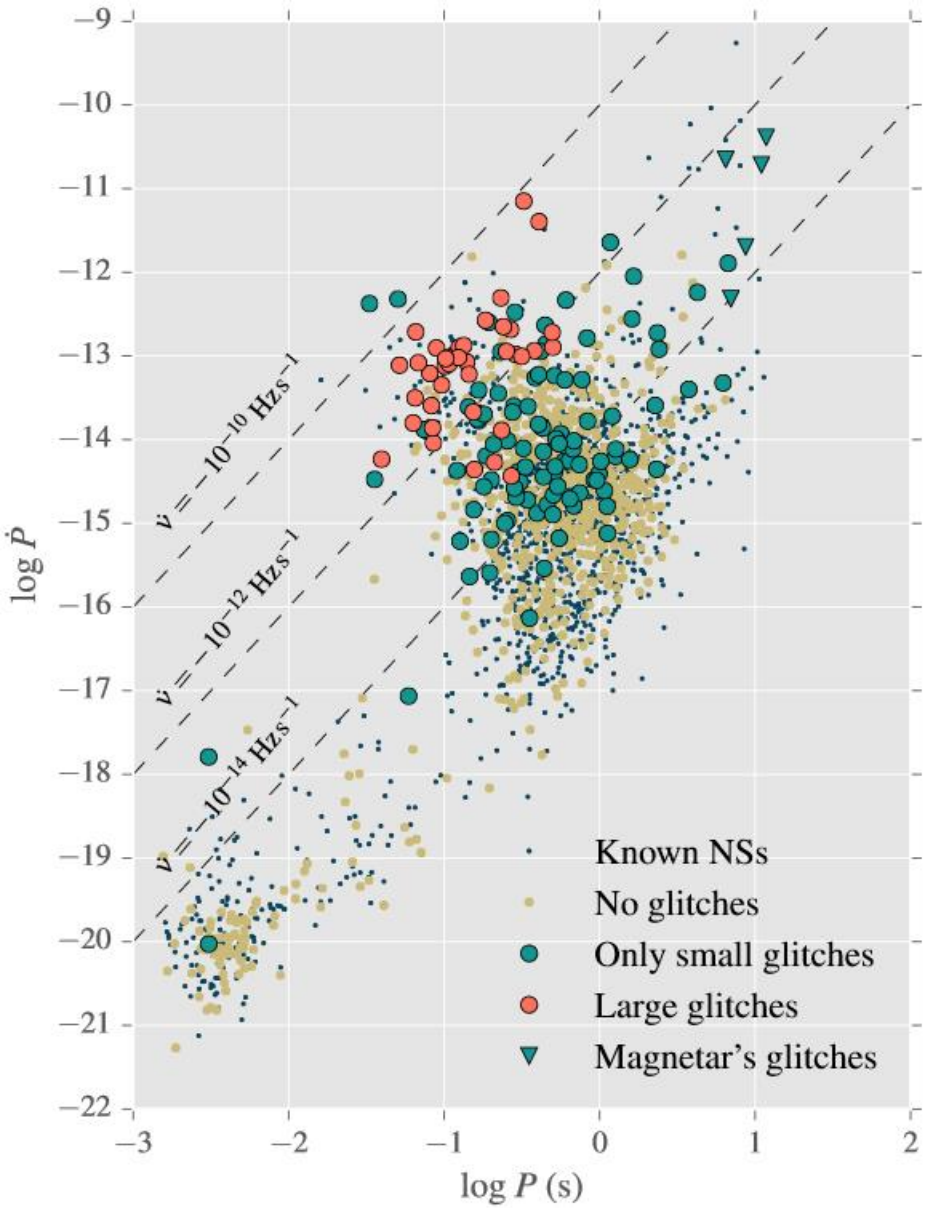

1710.00952

Catalogue http://www.jb.man.ac.uk/pulsar/glitches.html

Glitches properties

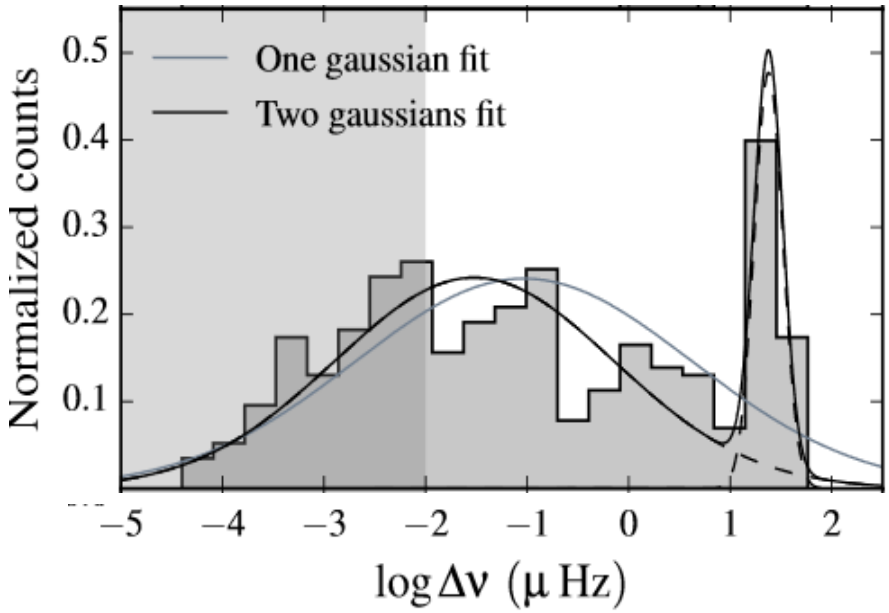

384 glitches in 141 NSs

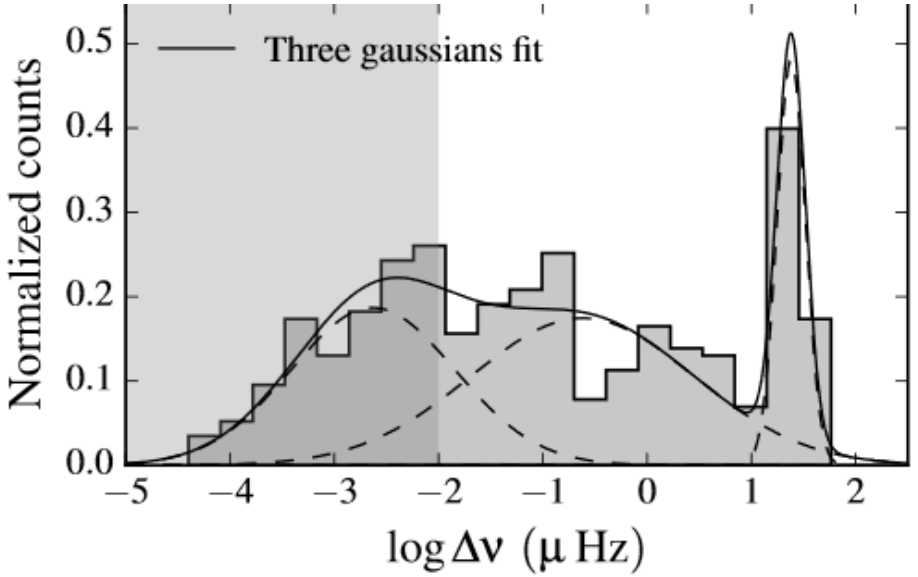

1710.00952

# bin	$\log \lvert\dot{\nu}\rvert$ (Hz s^{-1})	$\sum T_i$ (yr)	N_ℓ	N_t	N_{pg}	N_p
1	−16.75	117	0	0	0	7
2	−16.25	430	0	0	0	25
3	−15.75	1233	0	0	0	70
4	−15.25	2478	0	3	3	139
5	−14.75	2675	0	11	8	142
6	−14.25	1973	0	25	16	105
7	−13.75	2083	0	35	20	113
8	−13.25	1706	1	29	18	105
9	−12.75	1312	3	26	14	81
10	−12.25	745	4	38	15	48
11	−11.75	493	8	74	15	33
12	−11.25	357	37	78	18	20
13	−10.75	66	13	19	5	5
14	−10.25	44	4	8	2	3
15	−9.75	16	0	2	1	1
16	−9.25	46	0	25	1	1

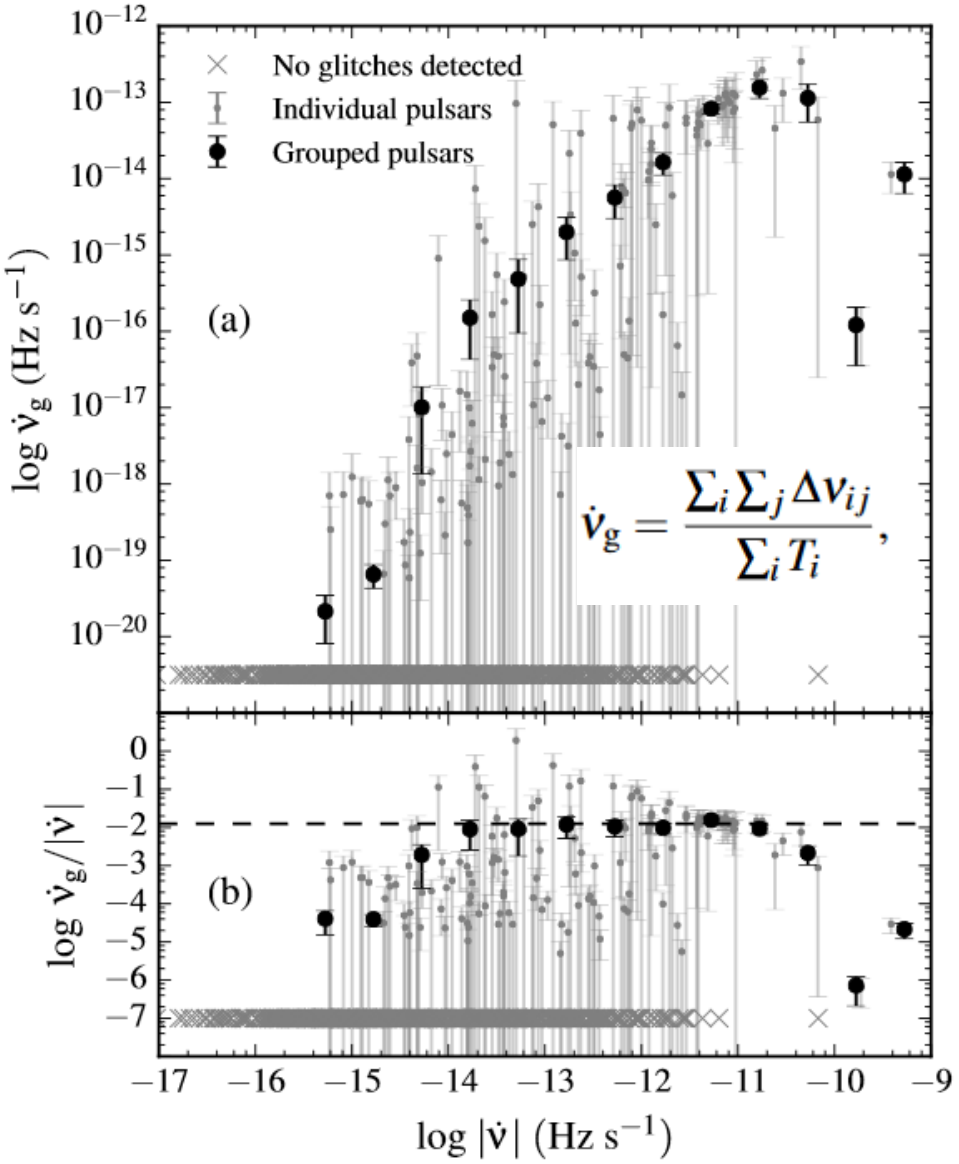

1710.00952

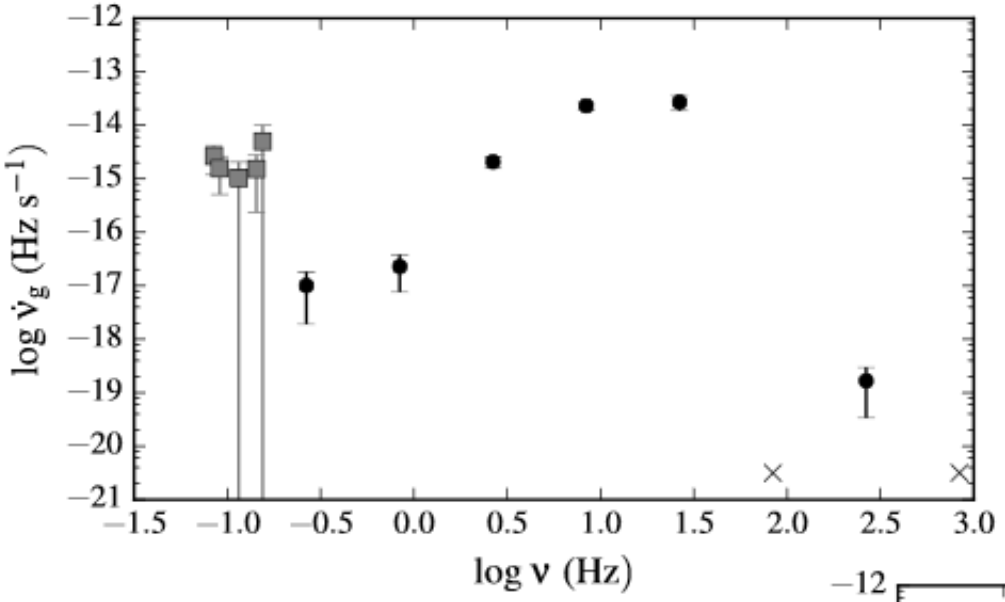

All PSRs in the survey are included, also those with no detected glitches.

$$\dot{\nu}_{\rm gg} = \frac{\sum_i \sum_j \Delta\nu_{ij}}{\sum_i T_i},$$

The double sum runs over every change in frequency $\Delta\nu_{ij}$ due to the glitch j of the pulsar i, and T_i is the time over which pulsar i has been searched for glitches.

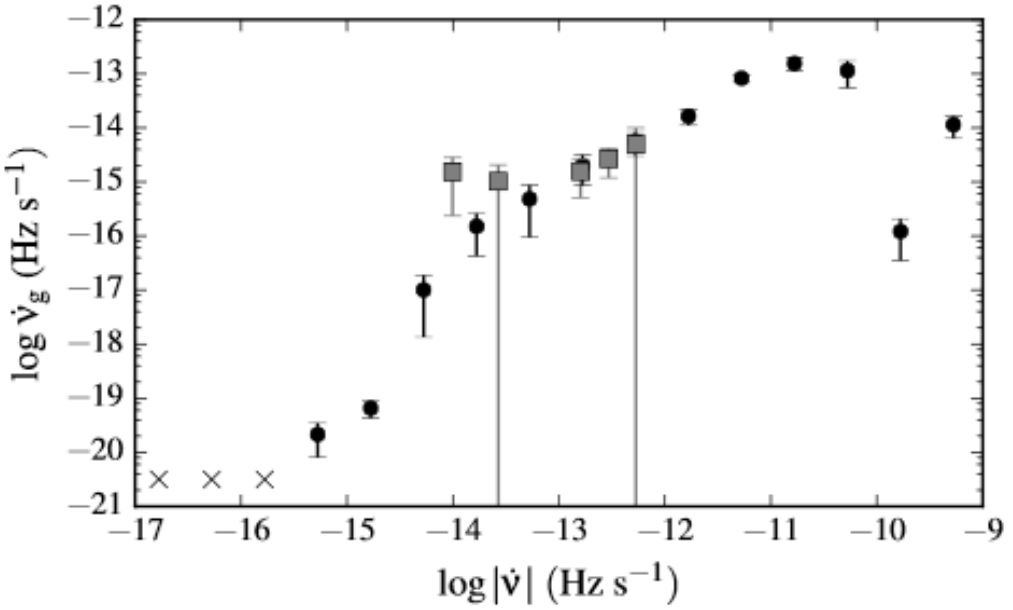

1710.00952

$$\dot{\nu}_{\rm g} = \frac{\sum_i \sum_j \Delta\nu_{ij}}{\sum_i T_i},$$

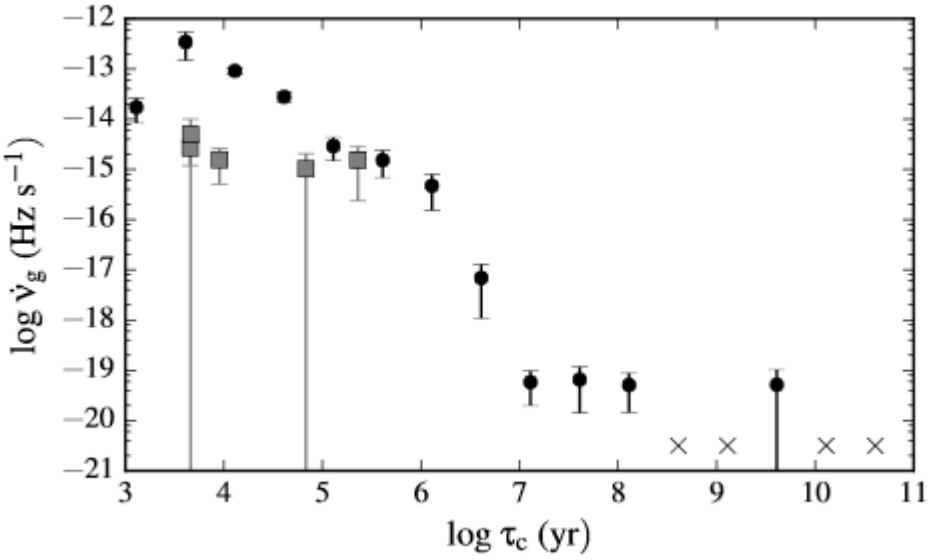

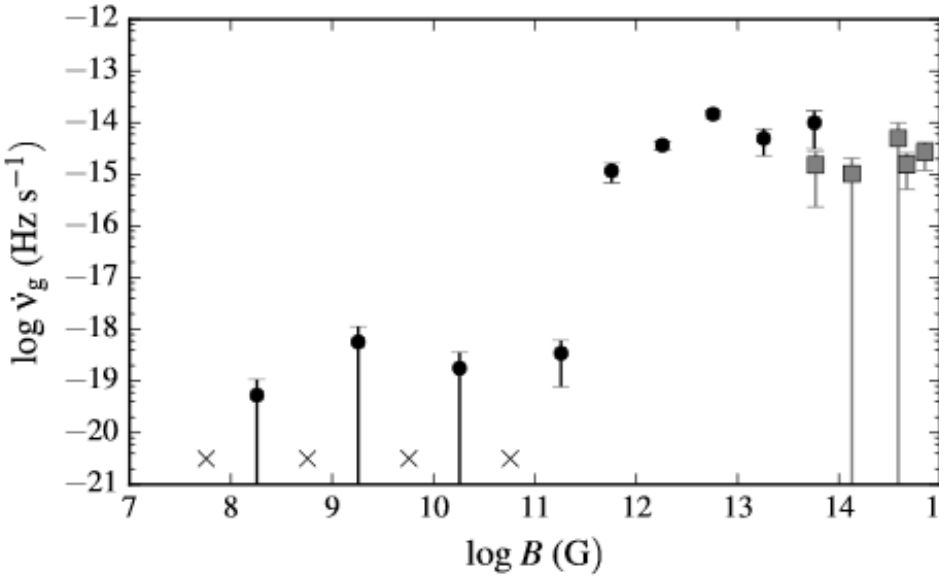

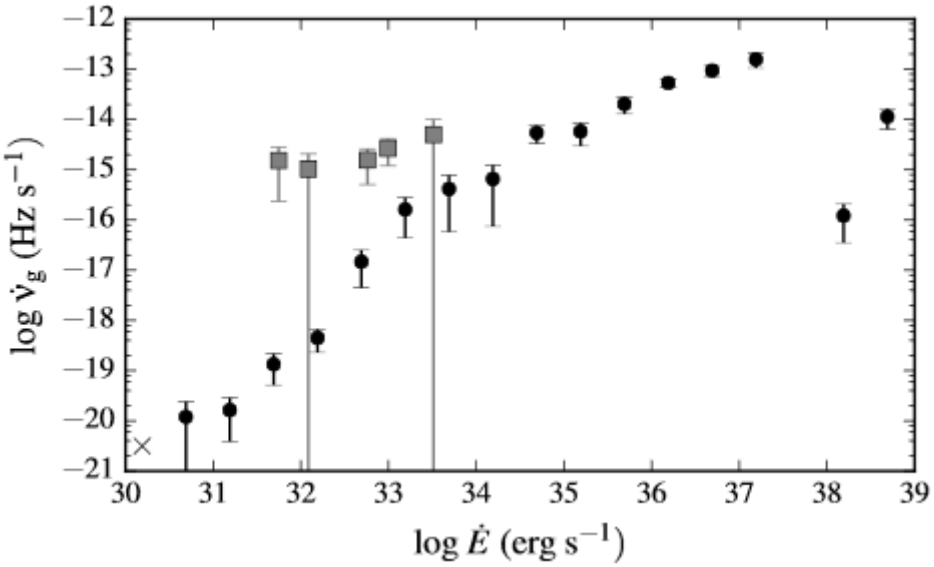

1710.00952

The largest glitch

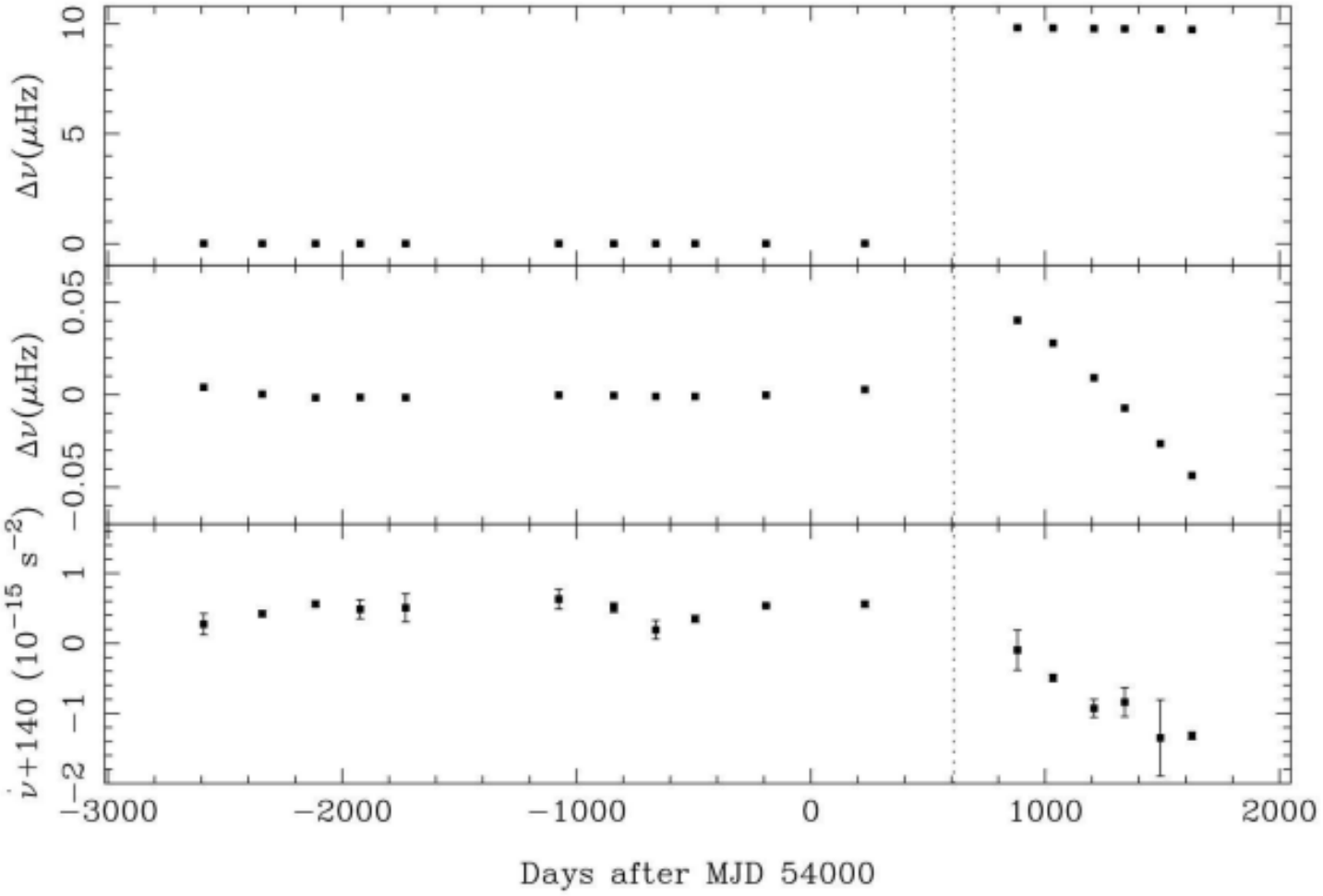

33 10^{-6}

1106.5192

Glitch and radio properties

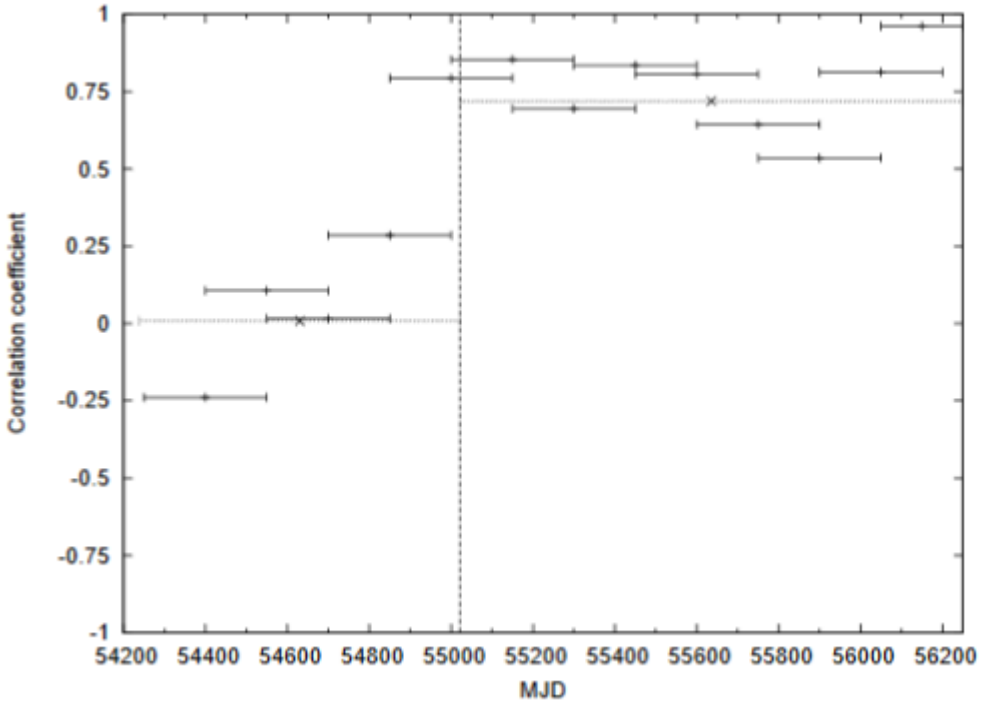

PSR J0742−2822
exhibits two distinct emission states that are identified by discrete changes in the observed pulse profile.

Correlation between frequency derivative and smoothed pulse shape parameter for overlapping 300-day intervals. The vertical dashed line at MJD 55022 indicates the epoch of a glitch.
Also shown with dotted bars is the same correlation when computed for the entire pre and post-glitch epochs.

Thermal effect of a glitch

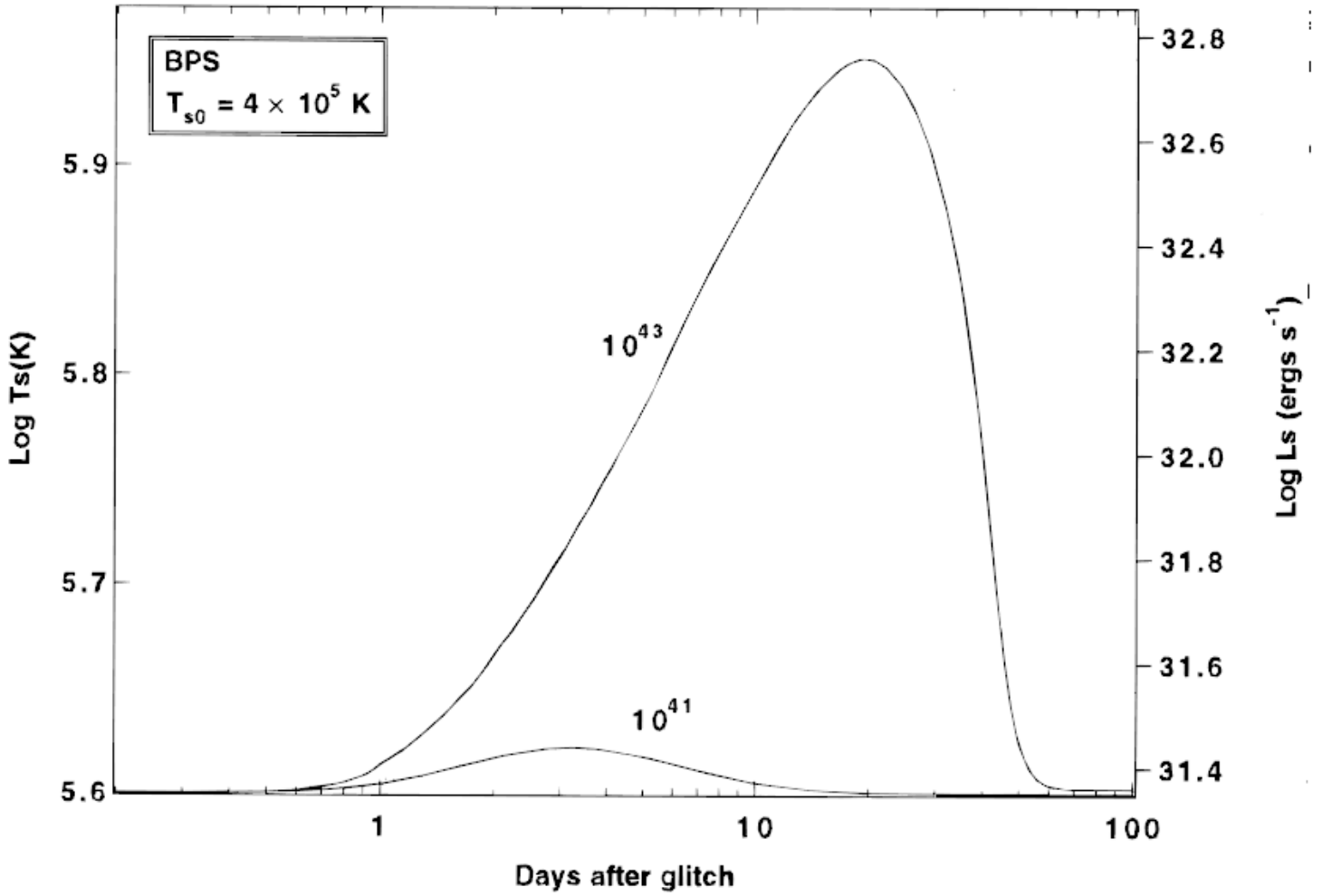

Hirano et al. 1997

Gravitational waves from glitches

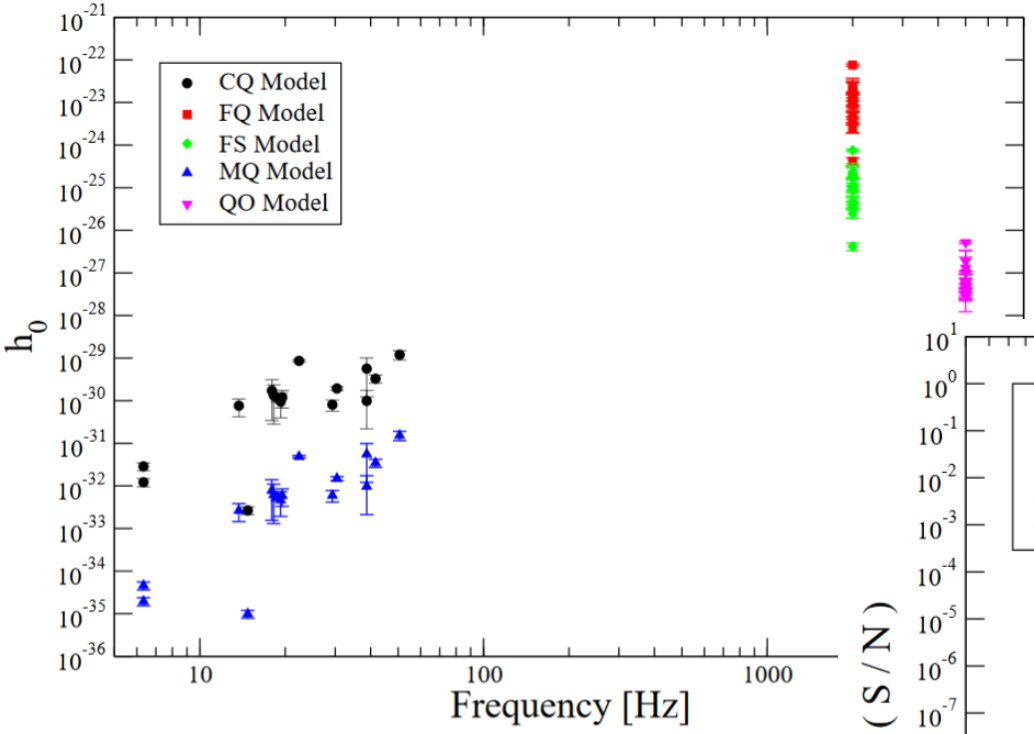

In some very optimistic models GW signals from PSRs glitches can be detected already with existing detectors (aLIGO, adVIRGO).

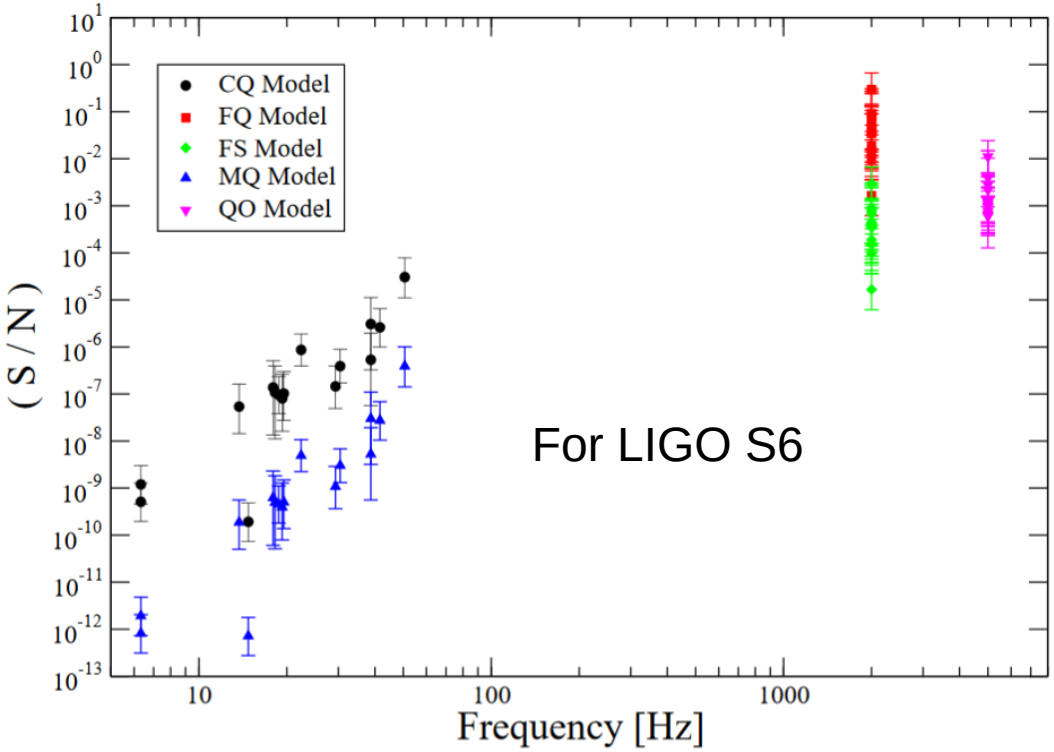

For LIGO S6

1305.2466

Glitches of magnetars

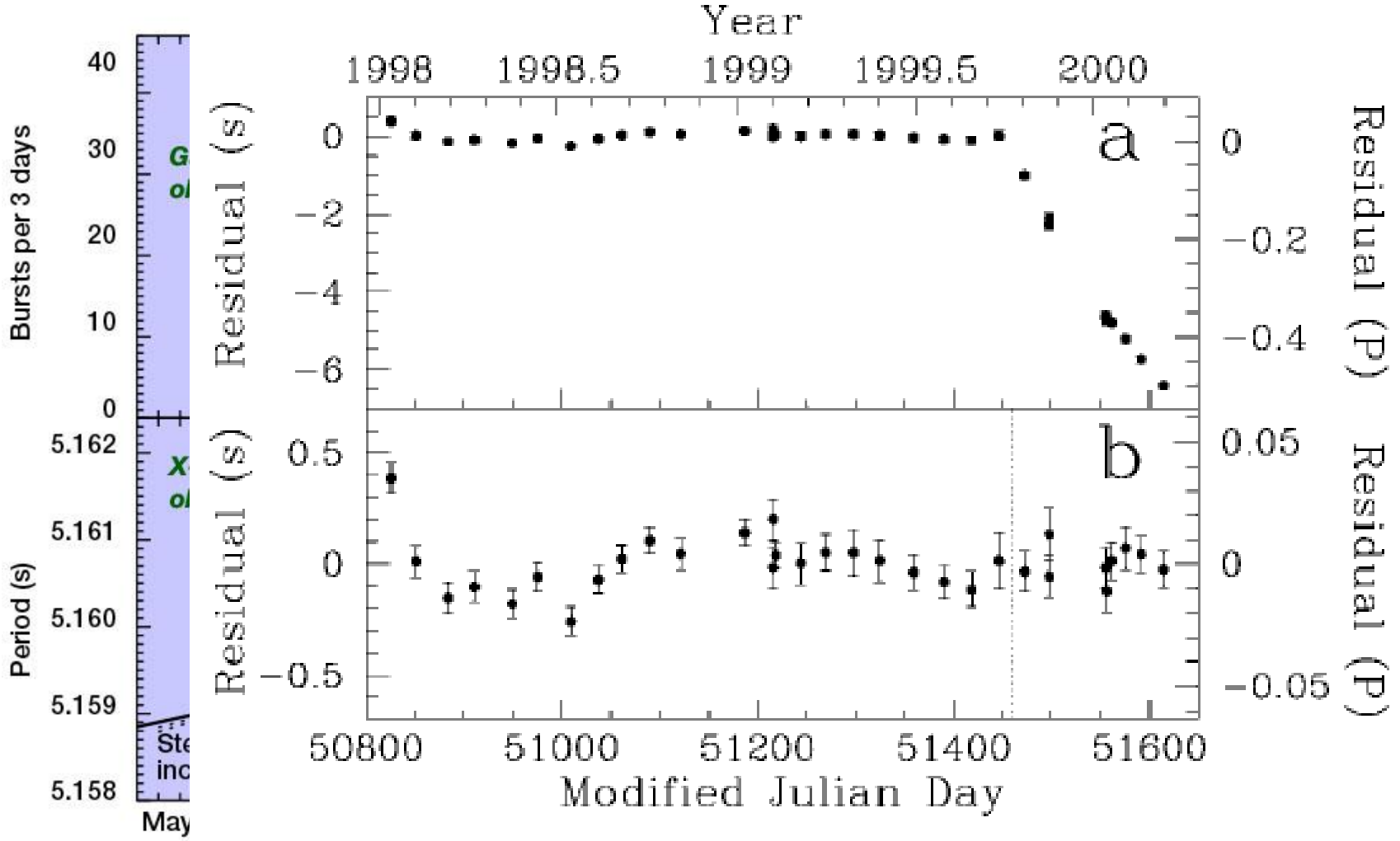

es.

Rs'.

)00:

About modeling of magnetar bursts see 1203.4506:
glitches always are accompanied by energy release.

Glitches and bursts

Sometime magnetar glitches are related to bursts, sometime – not.

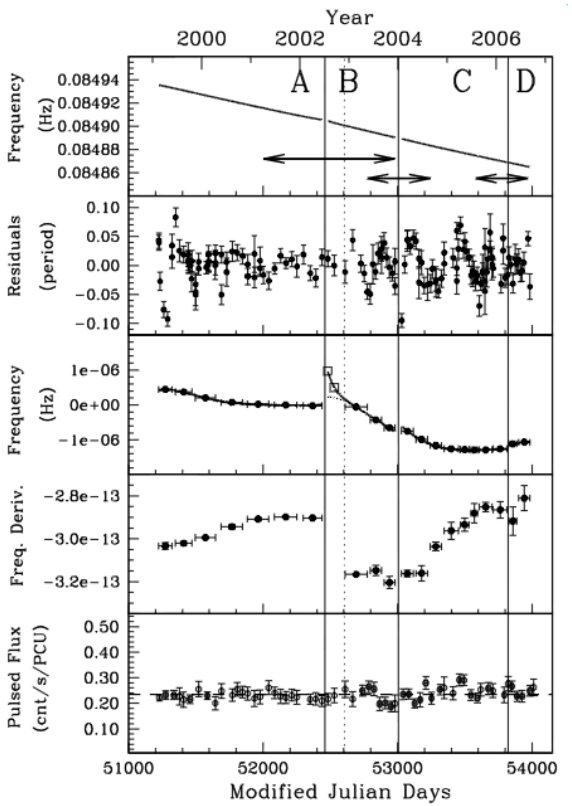

The pulsed flux was nearly constant during glitches.

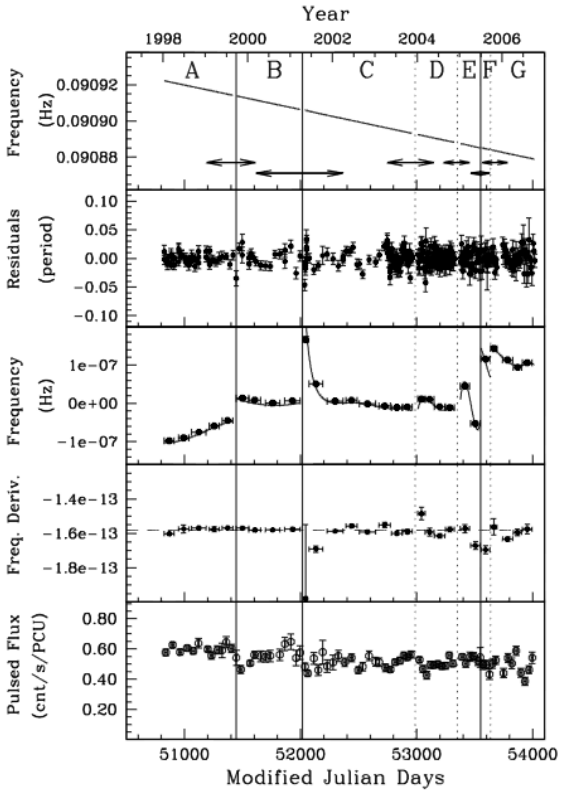

1E 1841-045

From Dib et al. 2008

RXS J170849.0-400910

Glitch and bursts from PSR J1119−6127

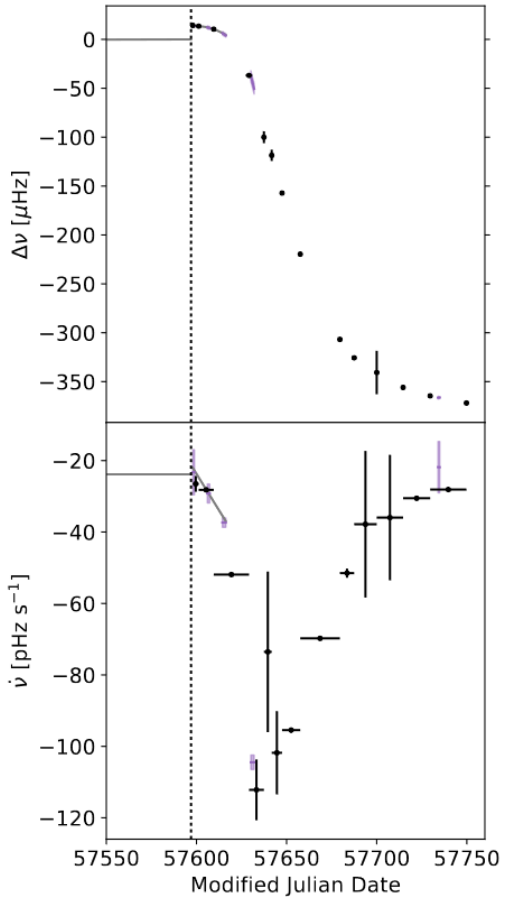

Young
highly magnetizes
radio pulsar.

Outburst with
many flares.

Glitch properties
confirm the model
of magnetospheric
perturbation and
energy release.
Spin behavior
correlates with
pulse profile
and spectral changes.

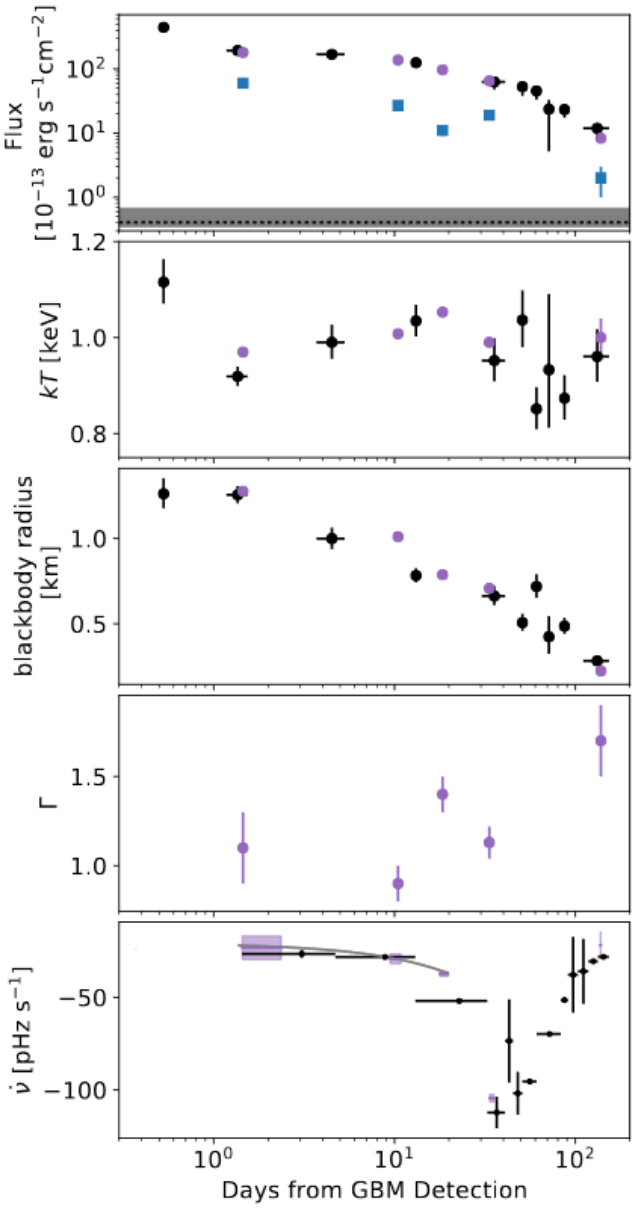

1806.01414 (see also 1806.05064)

PSRs vs. magnetars

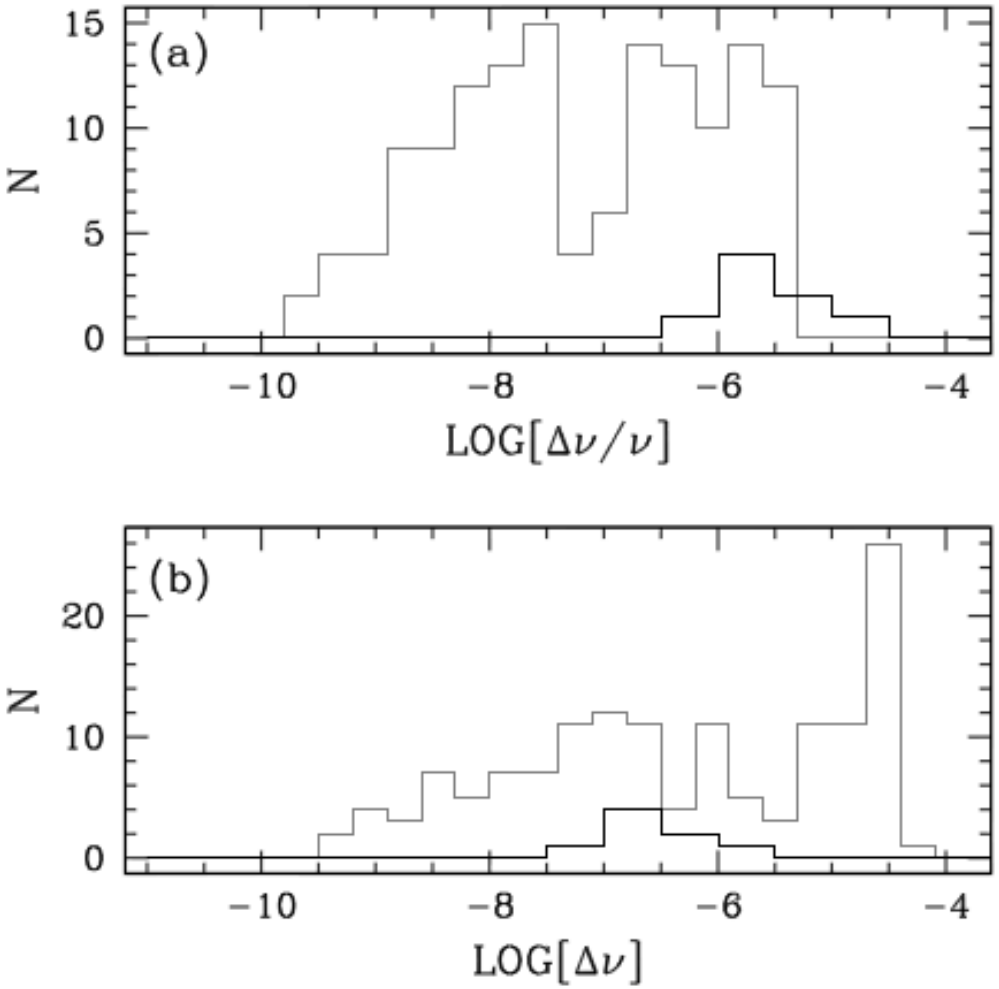

Nearly all known persistent AXPs now seem to glitch.

In terms of fractional frequency change, AXPs are among the most actively glitching neutron stars, with glitch amplitudes in general larger than in radio pulsars.

However, in terms of absolute glitch amplitude, AXP glitches are unremarkable.

Dib et al. 2008

Are PSRs and magnetar glitches similar?

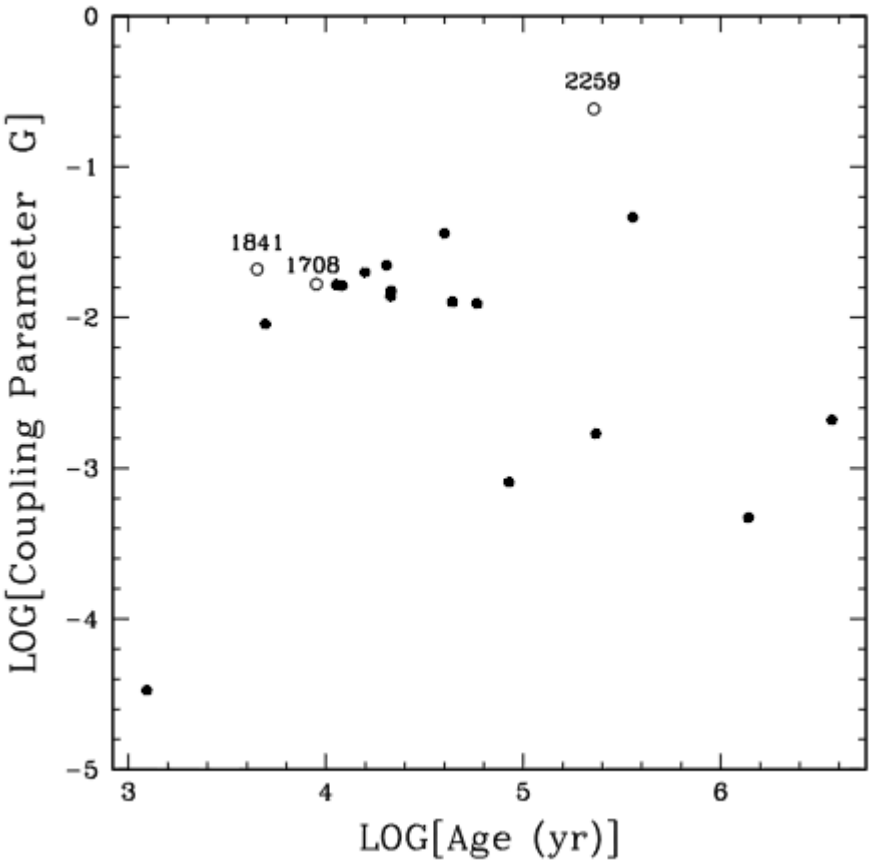

$$\dot{J}_{\rm res} \le I_{\rm res}|\dot{\Omega}|, \quad \frac{I_{\rm res}}{I_c} \ge \frac{\bar{\Omega}}{|\dot{\Omega}|} A \equiv G,$$

$$\frac{I_{\rm res}}{I_c} \ge G_{\rm Vela} = 1.4\%.$$

It seems that for some AXP glitches G is much larger than for PSRs. Dib et al. propose that it can be related to the role of core superfluid.

Many others proposed that glitches of magnetars can be related to magnetic field dissipation in the crust. As the field can be dynamically important there, its decay can result in crust cracking.

Dib et al. (2008), see arXiv: 0706.4156

PSRs vs. Magnetars

Glitch activity of the magnetars with the smallest characteristic ages is lower than that of the rotation-powered pulsars with similar characteristic ages.
However, their activity is larger than that of pulsars of equal spin-down power.

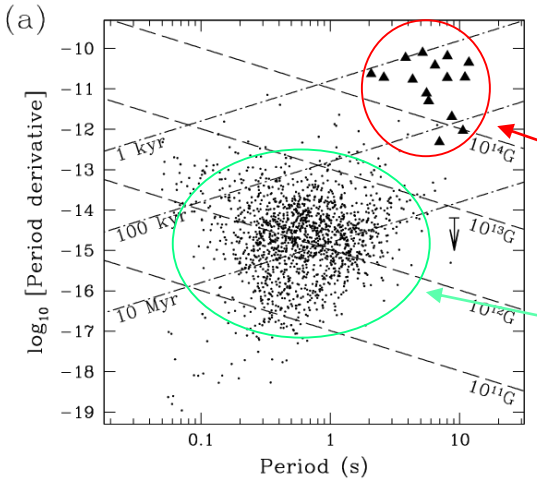

Magnetars

PSRs

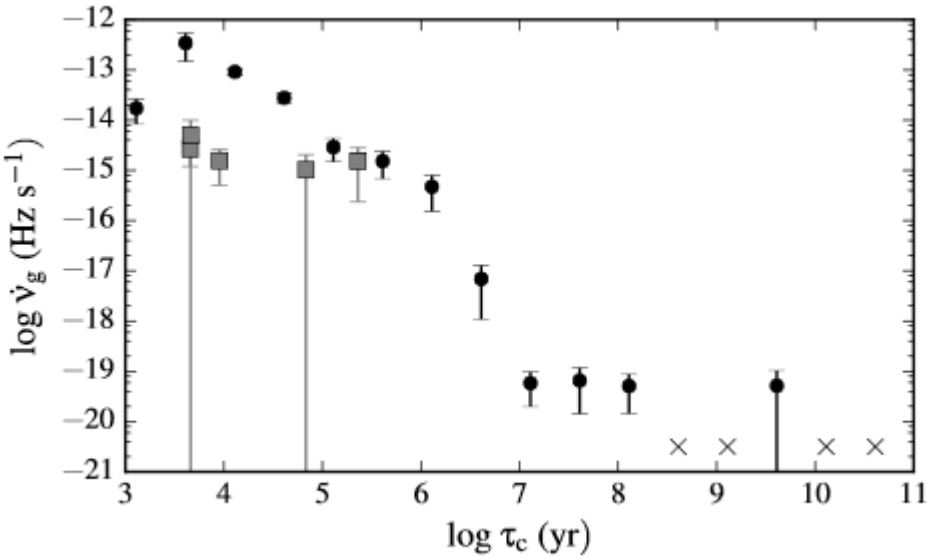

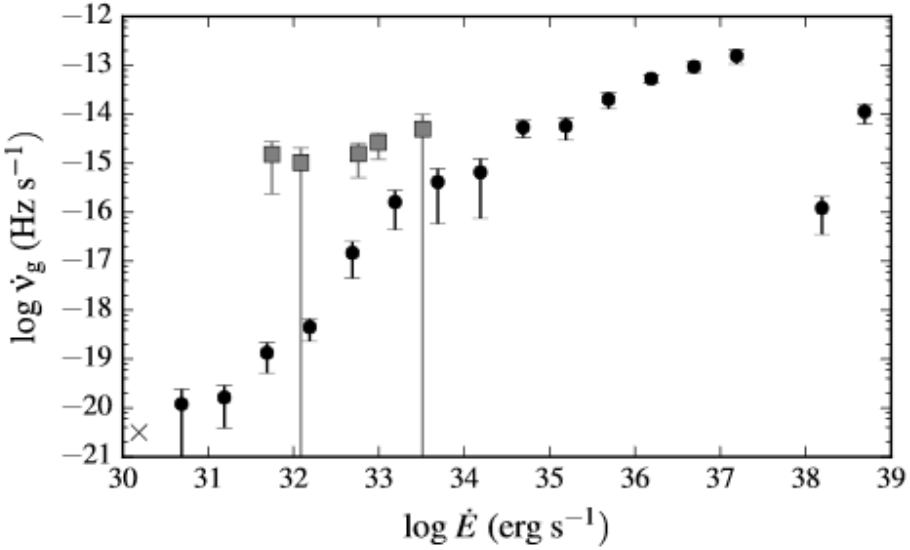

CCOs also glitch!

1E 1207.4−5209

0.424 s

$B_s \approx 9 \times 10^{10}$ G

$\Delta f/f = (2.8 \pm 0.4) \times 10^{-9}$

Parameter	Pre-glitch[a]	Post-glitch[b]
Epoch	2012	2017
$N_{\rm H}$ ($\rm cm^{-2}$) (fixed)	1.66×10^{21}	1.66×10^{21}
kT_1 (keV)	$0.0801^{+0.0046}_{-0.0042}$	$0.0742^{+0.0042}_{-0.0037}$
kT_2 (keV)	$0.2513^{+0.0022}_{-0.0021}$	$0.2509^{+0.0021}_{-0.0021}$
E_0 (keV)	$0.712^{+0.012}_{-0.011}$	$0.710^{+0.017}_{-0.015}$
σ_0 (keV) (fixed)	0.08	0.08
τ_0	0.26	0.22
E_1 (keV)	$1.4292^{+0.0087}_{-0.0088}$	$1.4216^{+0.0089}_{-0.0090}$
σ_1 (keV) (fixed)	0.08	0.08
τ_1	0.098	0.10
F_x(pn)[c]	$2.084^{+0.010}_{-0.011}$	$2.078^{+0.010}_{-0.012}$
χ^2_ν(DoF)	1.39(283)	1.32(276)

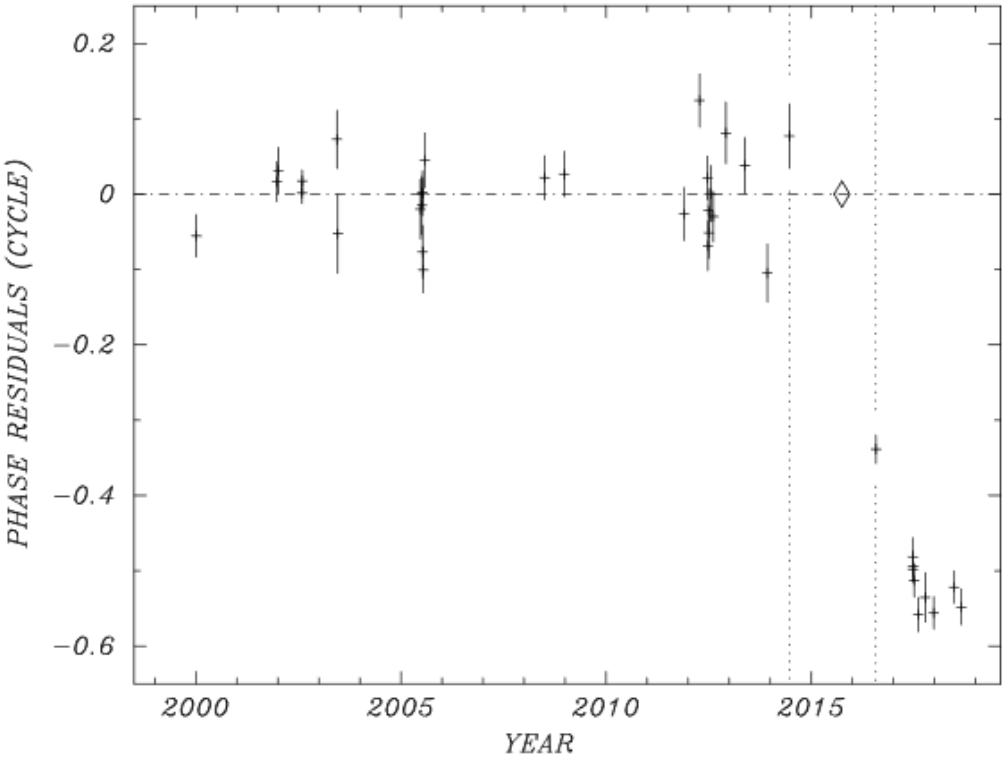

Glitch Parameters

Epoch (MJD)	57295[b]
Δf	$(1.23 \pm 0.19) \times 10^{-8}$ $\rm s^{-1}$
$\Delta f/f_{\rm pred}$	$(5.22 \pm 0.80) \times 10^{-9}$
$\Delta \dot{f}$	$(-1.58 \pm 0.31) \times 10^{-16}$ $\rm s^{-2}$
$\Delta \dot{f}/\dot{f}_{\rm pred}$	1.27 ± 0.25

1809.04678

Slow glitches

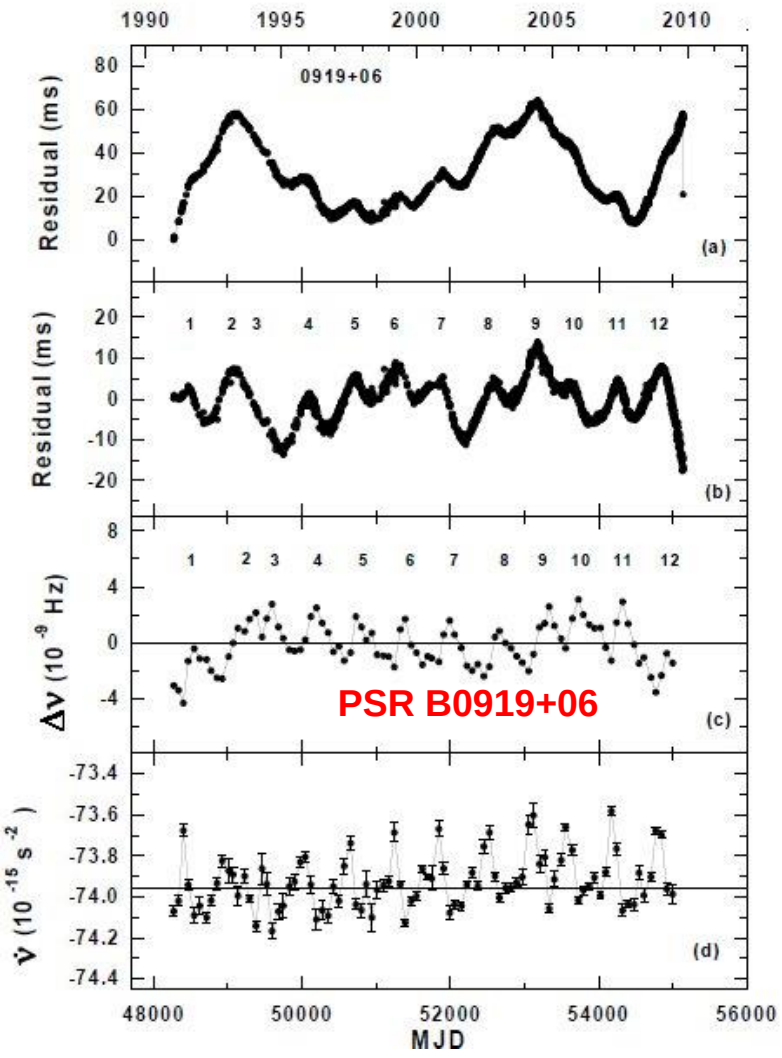

Below: a slow glitch by PSR B1822-09 (Shabanova 1998)

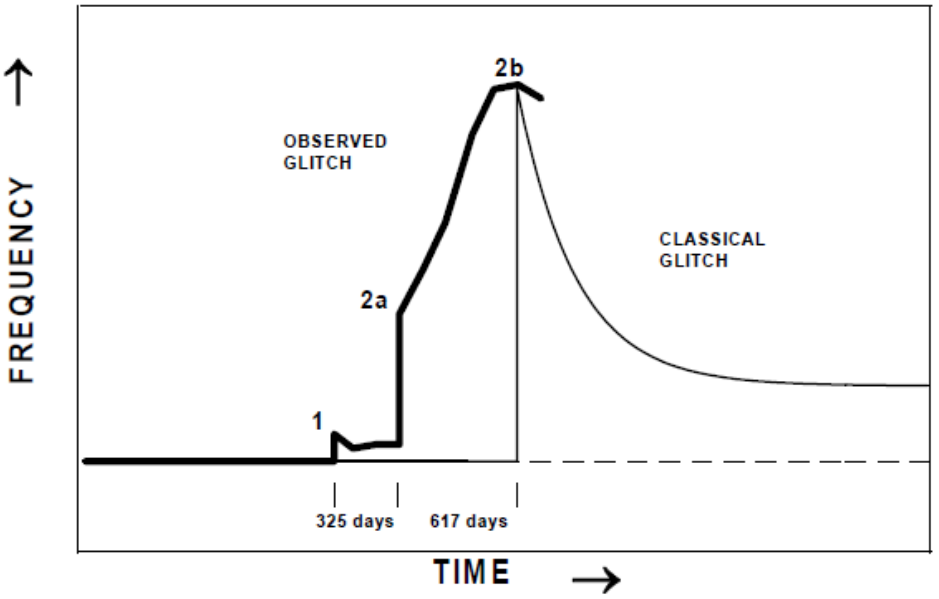

1007.0125

Timing irregularities

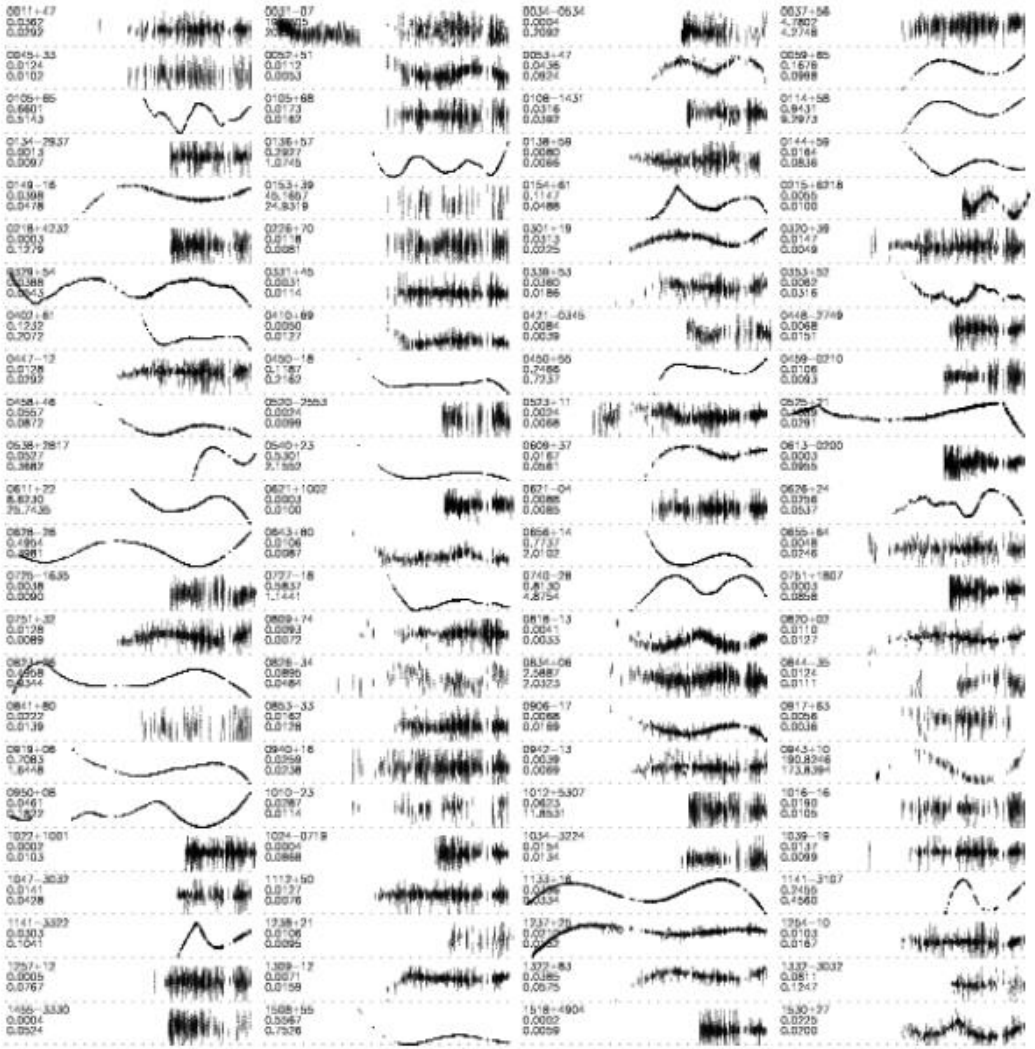

Analysis demonstrates different type of irregularities including quasi-periodic.

0912.4537

Possible explanation?

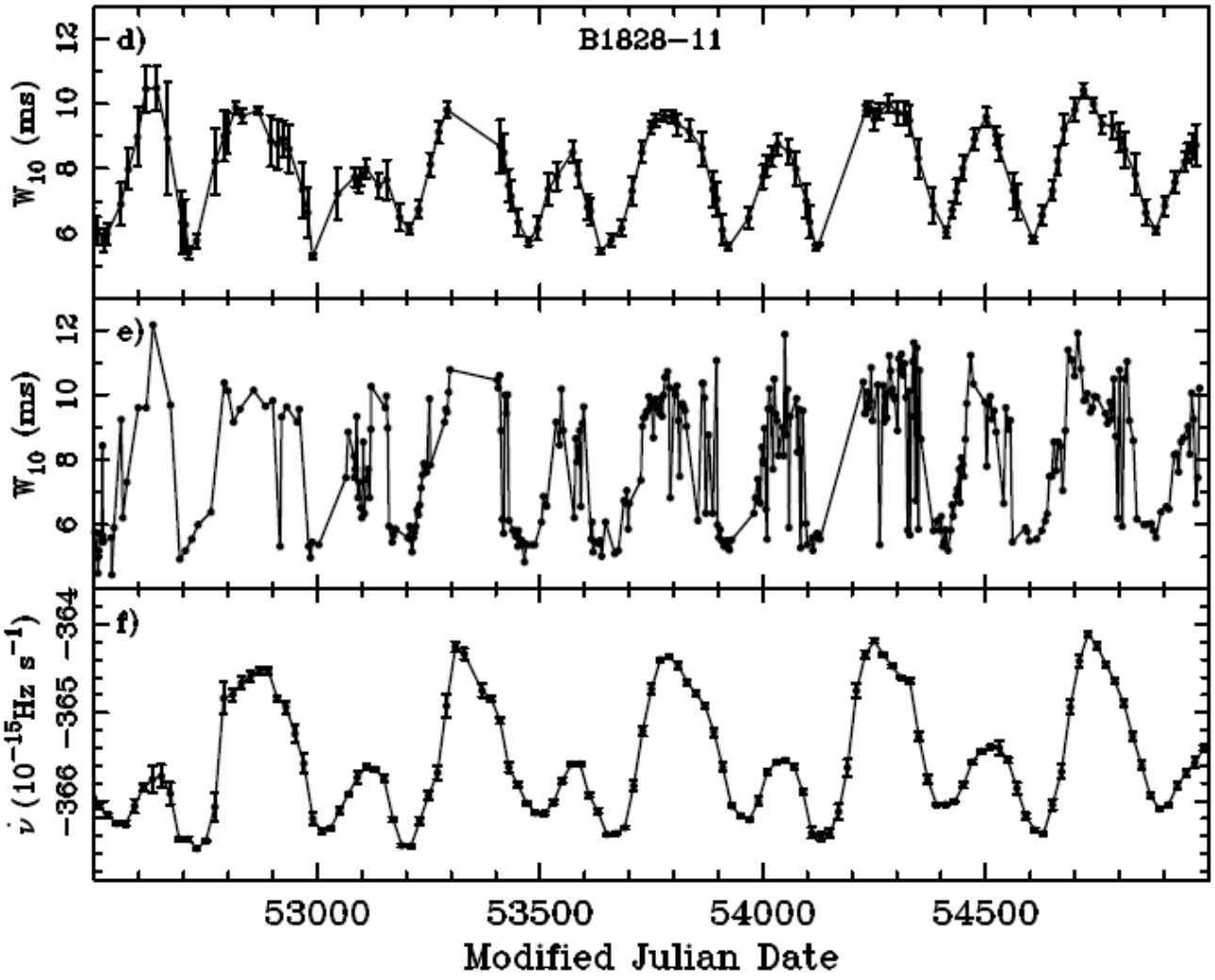

Magnetospheric effect?

Two stages characterized by particular pulse profile and spin-down rate.

Switching between these states happens rapidly.

1006.5184

Polarization angle variations

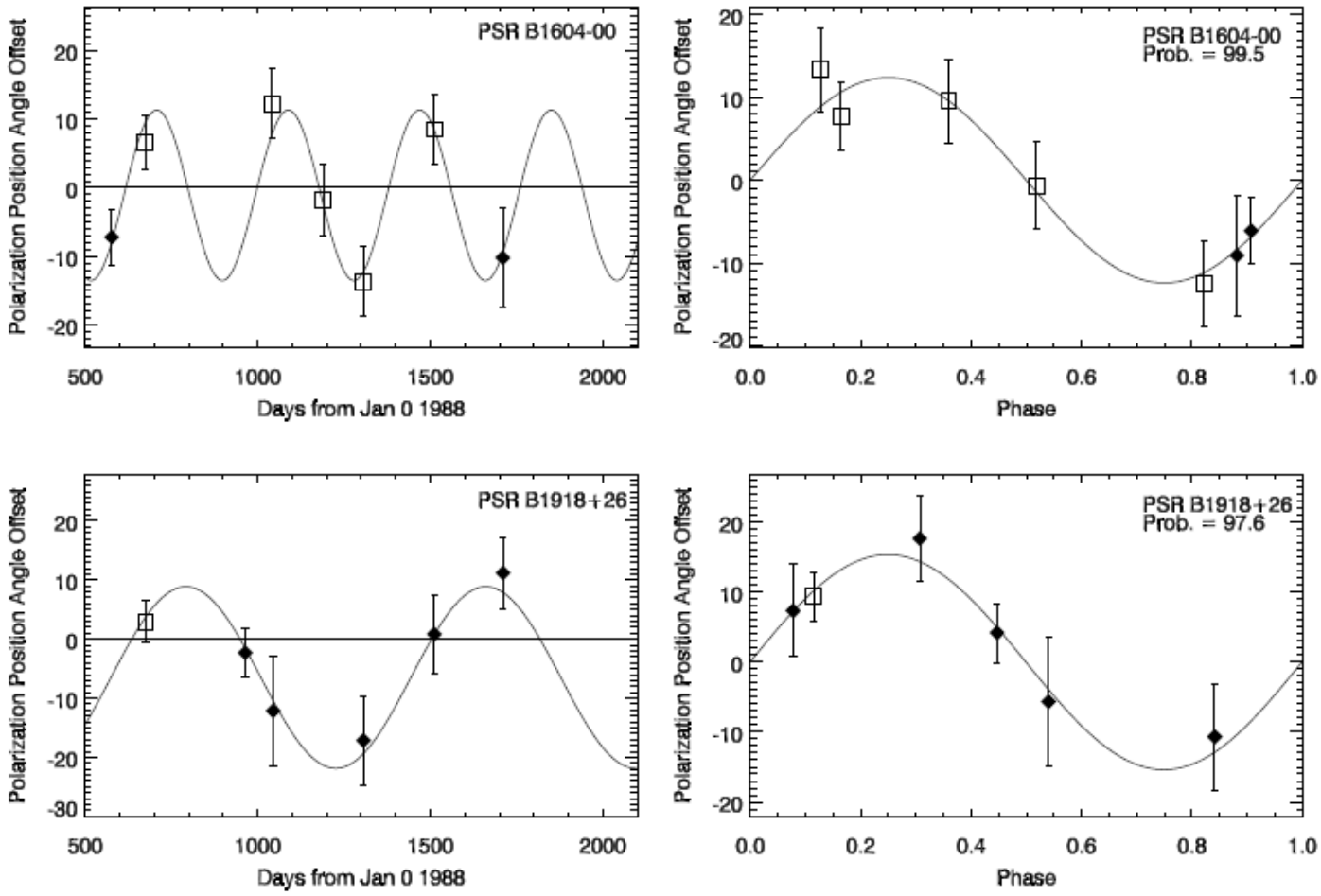

Such variations could be caused by precession

Weisberg et al. 2010 1008.0454

Precession in NSs

$P_{prec}=P/\varepsilon$,
ε-oblateness: $\varepsilon \sim 10^{-8}$ ⇨ P_{prec} ~ year

(More complicated models are developed, too.
See Akgun, Link, Wasserman, 2005)

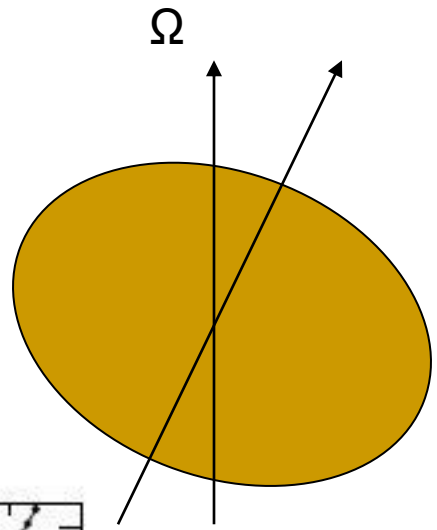

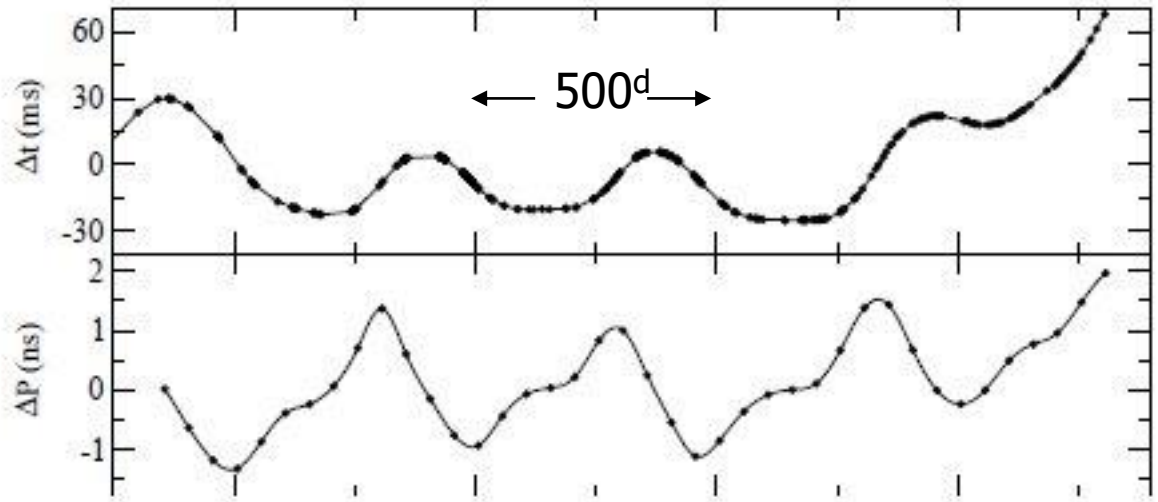

Time of arrival
and period residuals
for PSR B1828-11.
Wobbling angle is ~3-5°

But why among ~1500 there are just 1-2 candidates… ?

New analysis confirms that PSR 1826-11 can have precession (1510.03579).
Still, it is difficult to bring it in correspondence with glitches from this PSR (1610.03509).

Precession (nutation)

Θ_w – is small
Ω and L are very close

If we consider the free precession,
then we have a superposition of two motions:

1. Rapid (~Ω) rotation around total angular momentum axis – L
2. Slow (Ω_p) retrograde rotation around the symmetry axis (s)

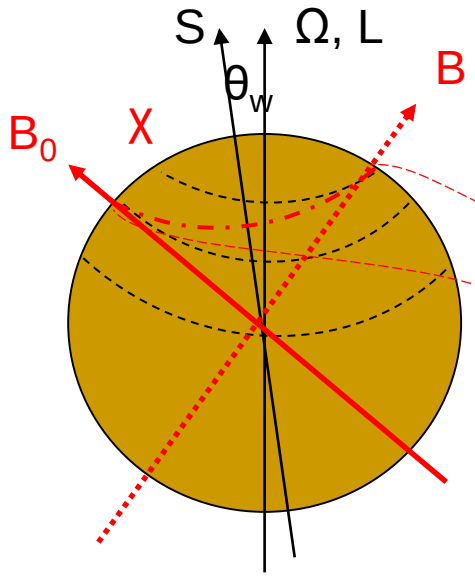

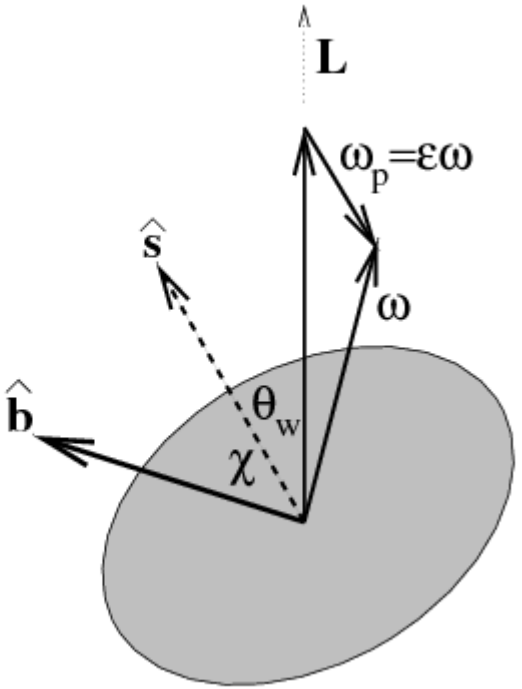

$\Delta\varphi=\varphi_{max}-\varphi_{min}=(\chi+\theta_w)-(\chi-\theta_w)=2\theta_w$

Beam width variation

See B. Link astro-ph/0211182

A toy model

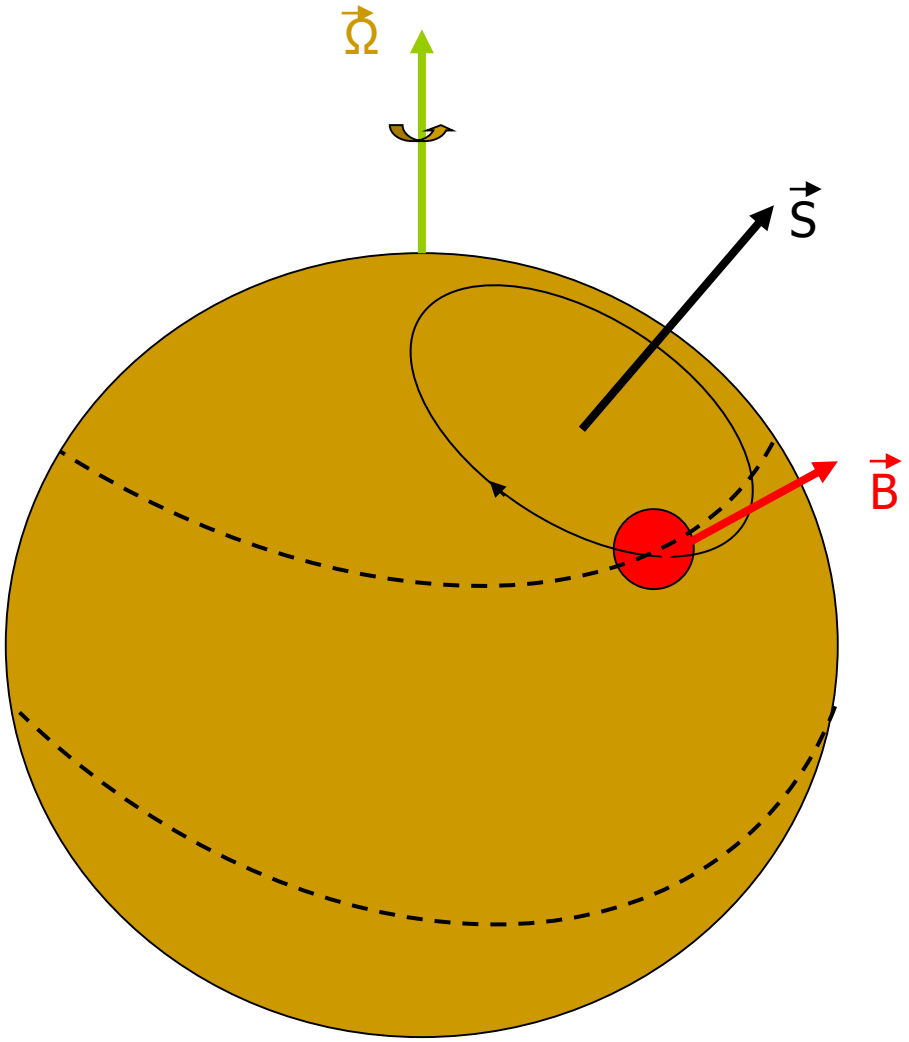

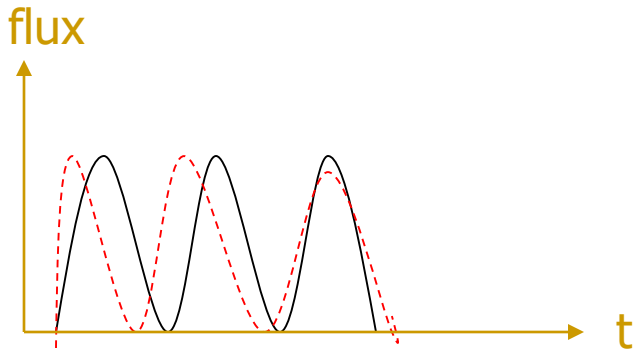

This is a picture seen
by an external observer.

In the coordinate frame of the body

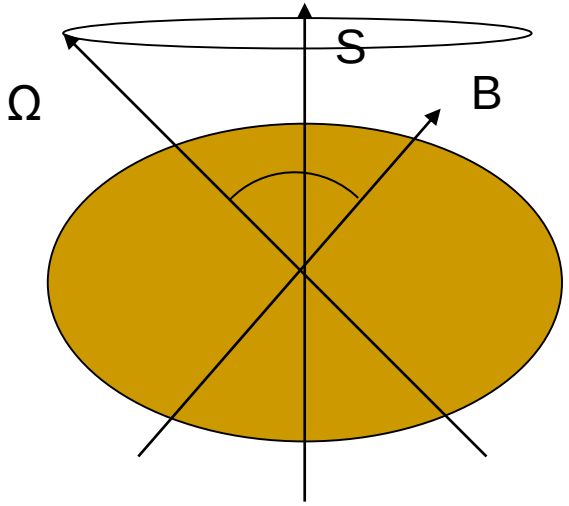

In this system the rotation axis is rotating around the symmetry axis.
So, it is clear that the angle between spin axis and the magnetic axis changes.

This results in an additional effect in timing:
Now the spin-down rate changes with the period of precession.

$$\frac{1}{2} I_1 \frac{d\omega^2}{dt} \simeq \boldsymbol{\omega} \cdot \mathbf{N},$$

$$\mathbf{N} = \frac{2\omega^2}{3c^3}(\boldsymbol{\omega} \times \mathbf{m}) \times \mathbf{m},$$

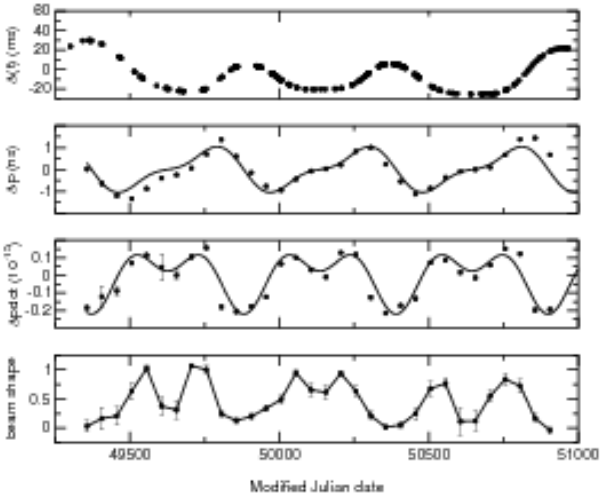

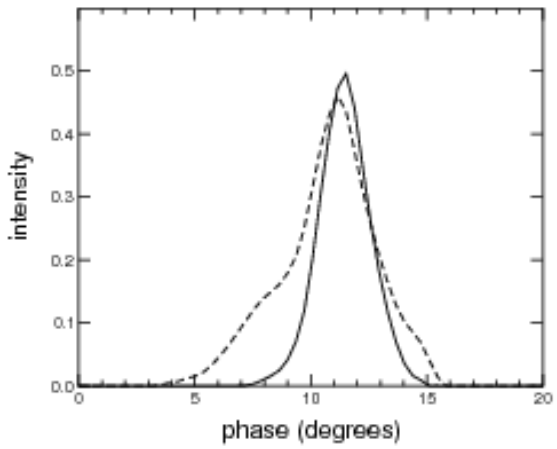

astro-ph/0211182

Complications …

A neutron star is not a solid body …
At least crust contains superfluid neutron vortices.
They are responsible for $I_p \sim 0.01$ of the total moment of inertia.

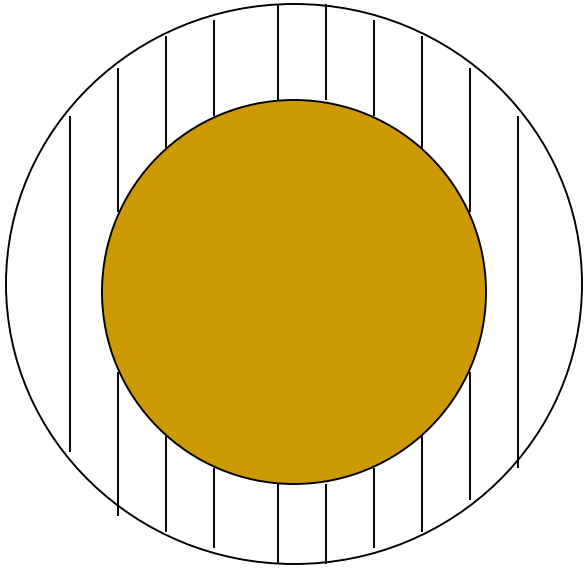

There are several effects related to vortices.

Neutron vortices can interact with the crust.
So-called "pinning" can happen.

The vortex array works as a gyroscope.
If vortices are absolutely pinned to the crust then $\omega_{prec}=(I_p/I)\Omega \sim 10^{-2}\Omega$ (Shaham, 1977).
But due to finite temperature the pinning is not that strong, and precession is possible (Alpar, Ogelman, 1987).

Superfluidity in NSs

50 years ago it was proposed (Migdal, 1959) that neutrons in NS interiors can be *superfluid*.

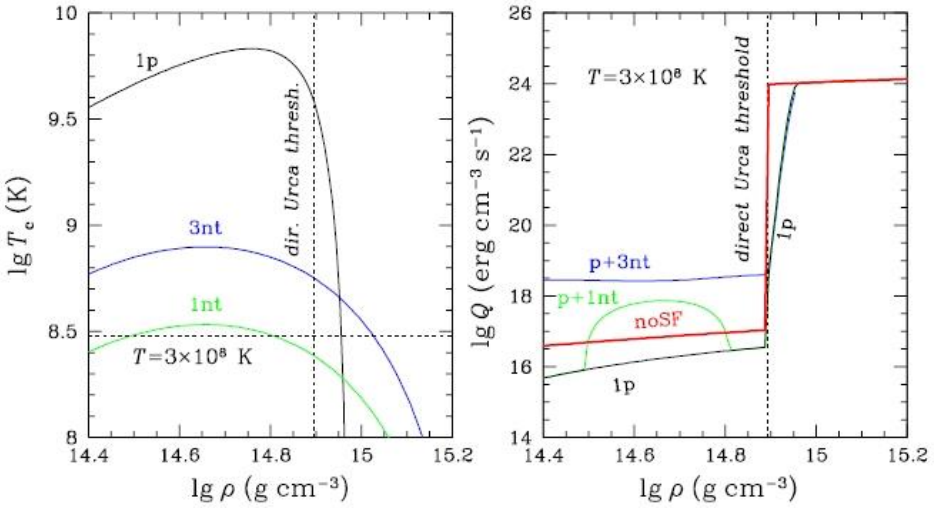

Various baryons in neutron star matter can be in *superfluid* state produced by Cooper pairing of baryons due to an attractive component of baryon-baryon interaction.

Now it is assumed that

- neutrons are supefluid in the crust (singlet)
- protons are superfluid in the core (singlet)
- neutrons can also be superfluid in the core (triplet)

Onsager and Feynman revealed that rotating superfluids were threaded by an array of quantized vortex lines.

Peculiar behavior of RX J0720

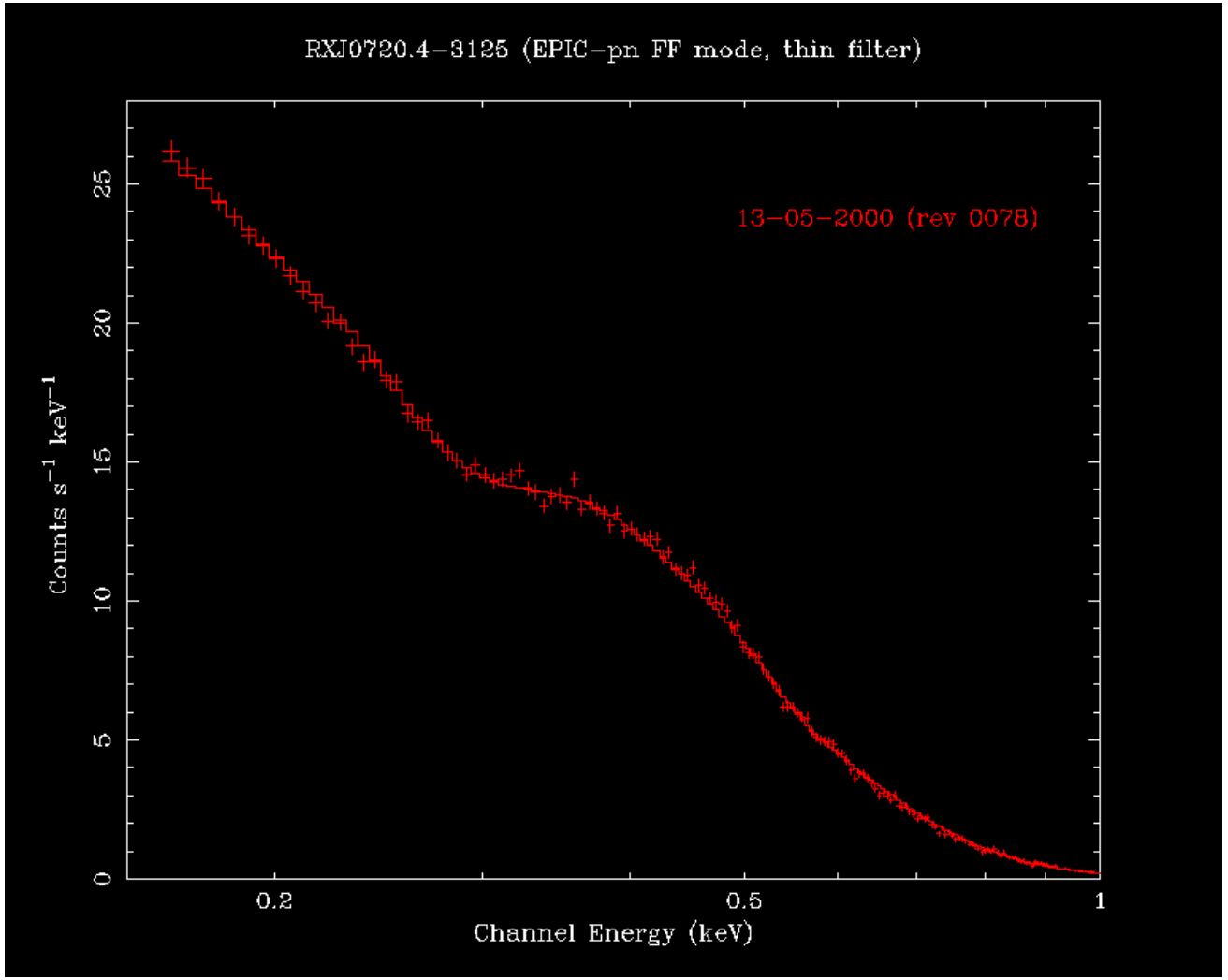

RX J0720.4-3125 as a variable source

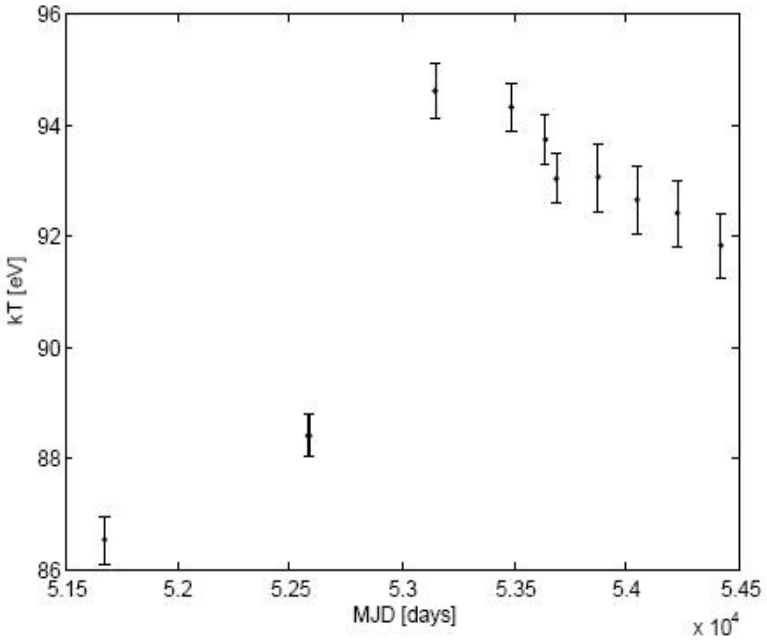

Long term phase averaged spectrum variations

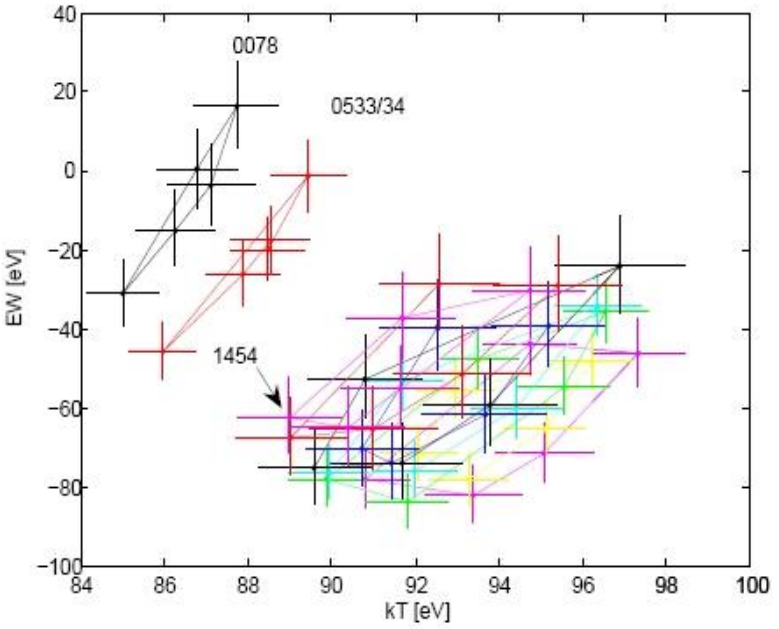

Phase dependent variations during different observations.

[Hohle et al. 2009 arXiv:0810.5319]

~10 years period: precession???

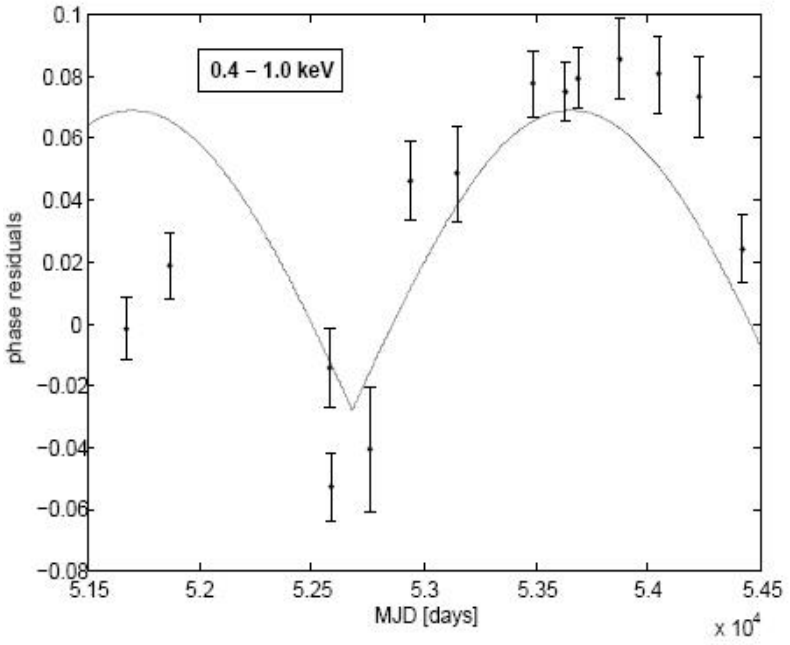

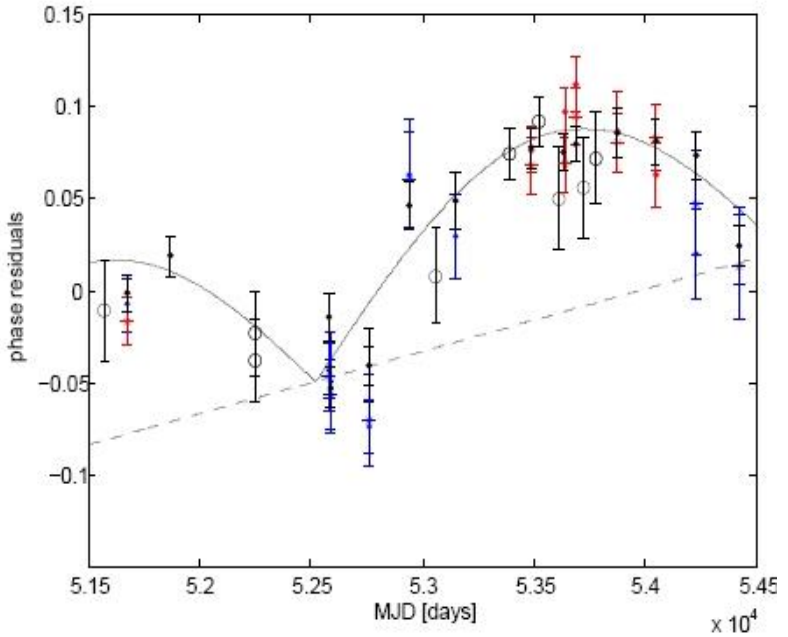

10.711 +/-0.058 yrs

However, the situation is not clear.
New results and a different timing solution.
The estimate of the period of precession slightly changed down to ~7 years.

[Hohle et al. 2009]

RX J0720.4-3125: timing residuals

-for $P(t_0)$ and dP/dt : phase coherent timing -in Kaplan & van Kerkwijk (2005) and van Kerkwijk 2007, without energy restriction

-now: restricting to the hard band (except for ROSAT and Chandra/HRC) +five new XMM-Newton +two new Chandra/HRC observations

$P(t_0)$=8.3911132650(91)s
dP/dt=6.9742(19) 10^{-14} s/s

-long term period: (6.91 +/- 0.17) yrs
Haberl (2007): (7.70 +/- 0.60) yrs
for two hot spots: abs(sine)
with 13-15.5yrs period

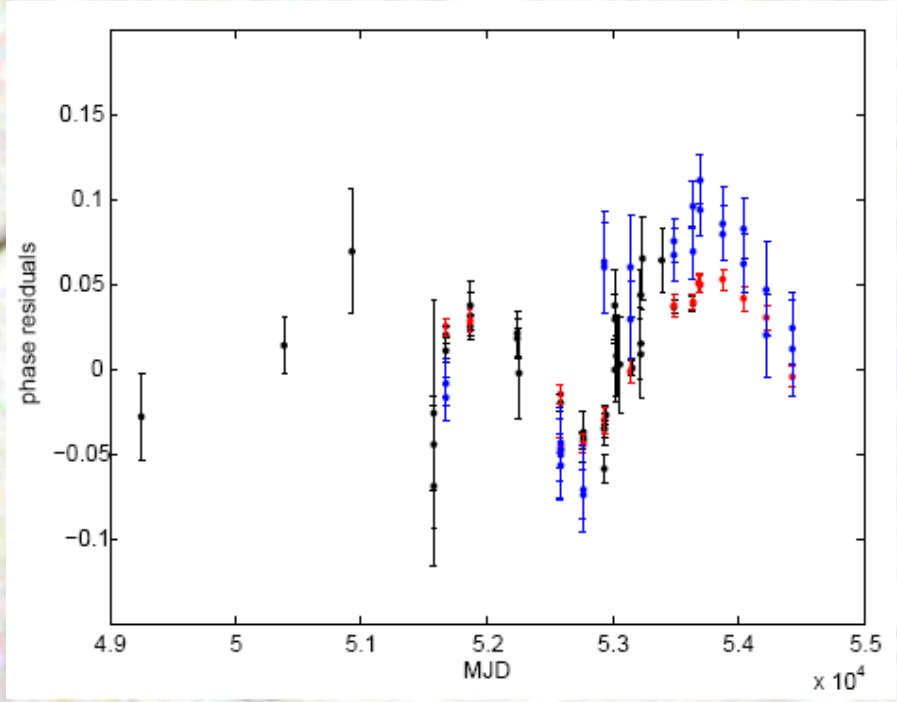

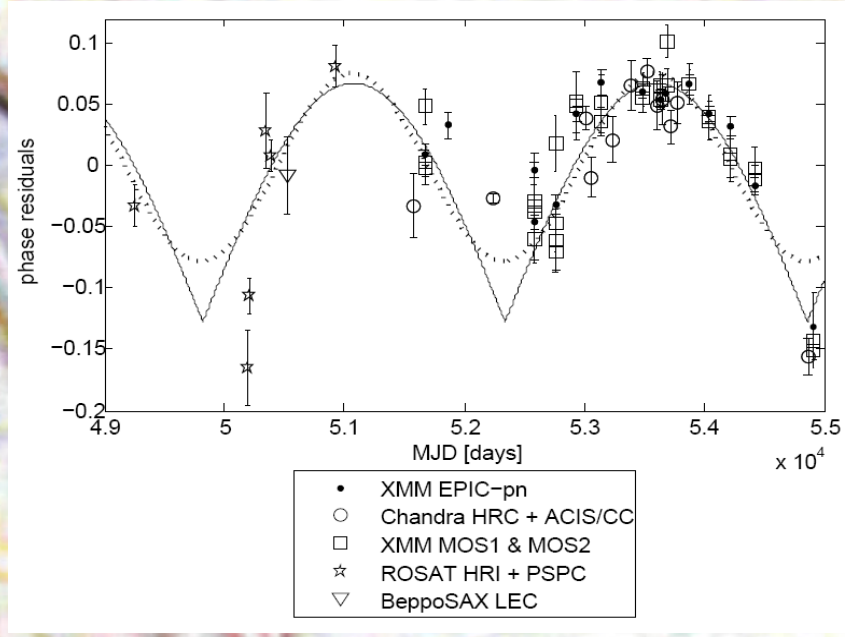

The slide from a talk by
Markus Hohle (Jena observatory).

Another interpretation: glitch + ?

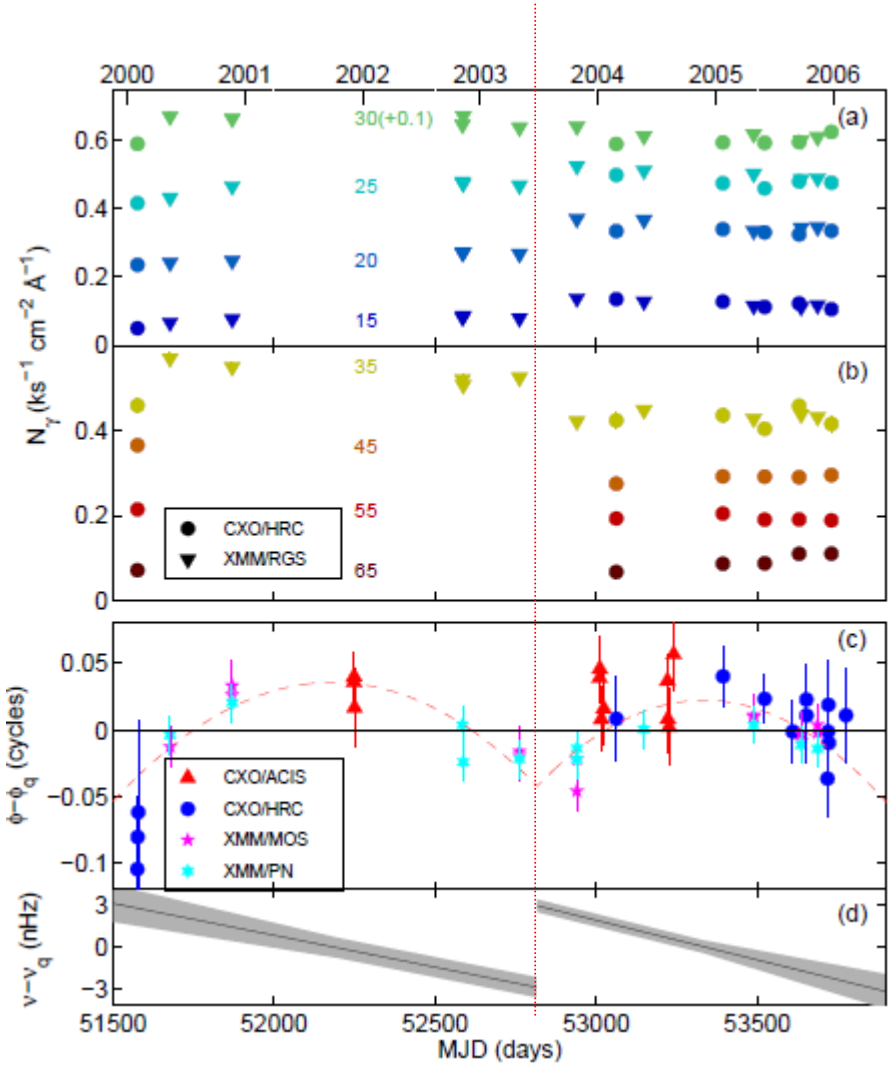

TIMING SOLUTIONS FOR RX J0720.4–3125

Quantity	Excl. *ROSAT*	All Data
Spindown only		
t_0 (MJD)	53010.2635646(7)	53010.2635626(6)
ν (Hz)	0.11917366979(12)	0.11917366954(11)
$\dot{\nu}$ (Hz s^{-1})	$-9.74(4) \times 10^{-16}$	$-9.88(13) \times 10^{-16}$
TOA rms (s)	0.26	0.29
χ^2/dof	77.6/46=1.69	150.8/49=3.08
Spin-down + Glitch		
t_0 (MJD)	53010.2635686(10)	53010.2635667(10)
ν (Hz)	0.1191736716(9)	0.1191736716(9)
$\dot{\nu}$ (10^{-15} Hz s^{-1})	–1.04(3)	–1.04(3)
t_g (MJD)	52817(61)	52866(73)
$\Delta\nu$ (nHz)	5.7(17)	4.1(12)
$\Delta\dot{\nu}$ (10^{-17} Hz s^{-1})	–1(4)	–4(3)
TOA rms (s)	0.15	0.24
χ^2/dof	37.0/43=0.86	45.1/46 = 0.98

NOTE. — The parameters determine the cycle count plus phase via $\phi(t) = \nu(t-t_0) + \frac{1}{2}\dot{\nu}(t-t_0)^2 + \Delta\phi_g(t)$, where $\Delta\phi_g(t) = -\Delta\nu(t-t_g) - \frac{1}{2}\Delta\dot{\nu}(t-t_g)^2$ for $t < t_g$ in the glitch model and zero otherwise. For all fits, a 0.11 s systematic uncertainty has been added in quadrature to the times of arrival (TOAs), and the uncertainties quoted are twice the formal 1σ values.

Van Kerkwijk et al. astro-ph/0703326

RX J0720.4-3125: a glitch

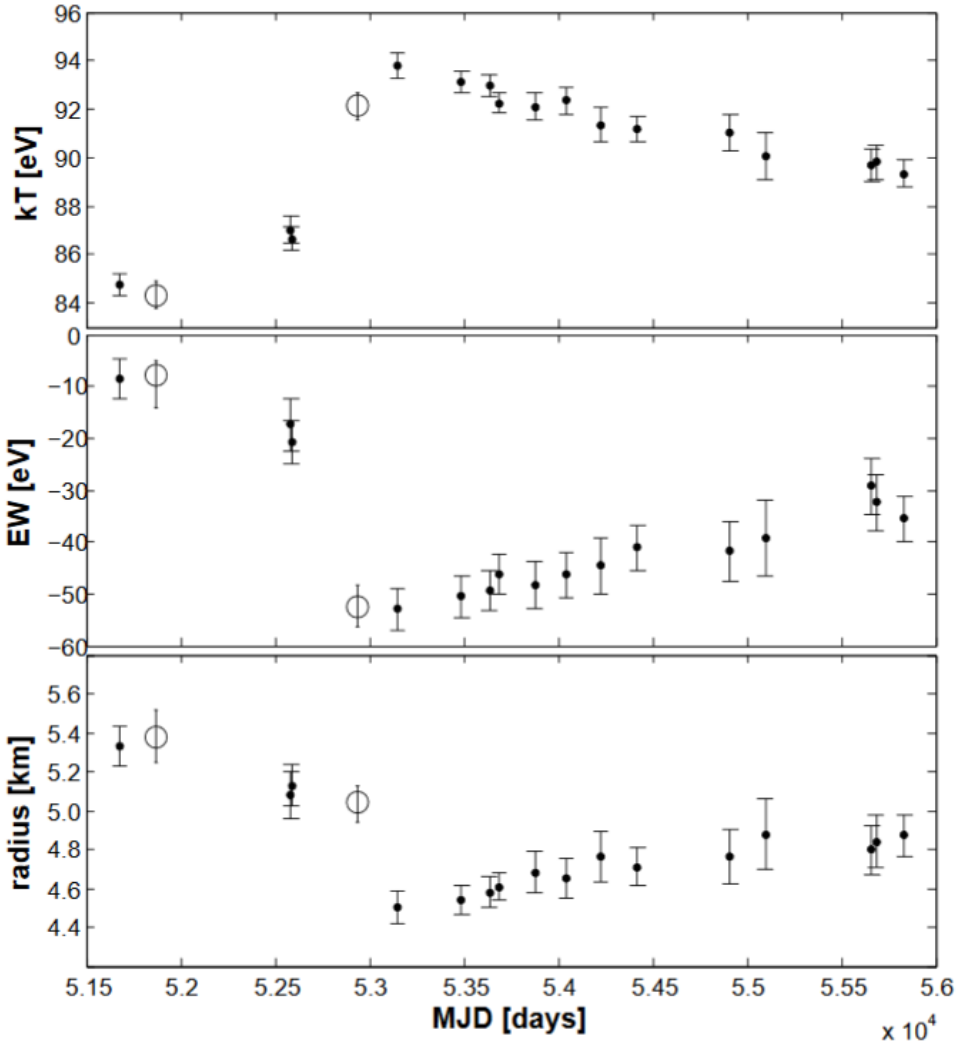

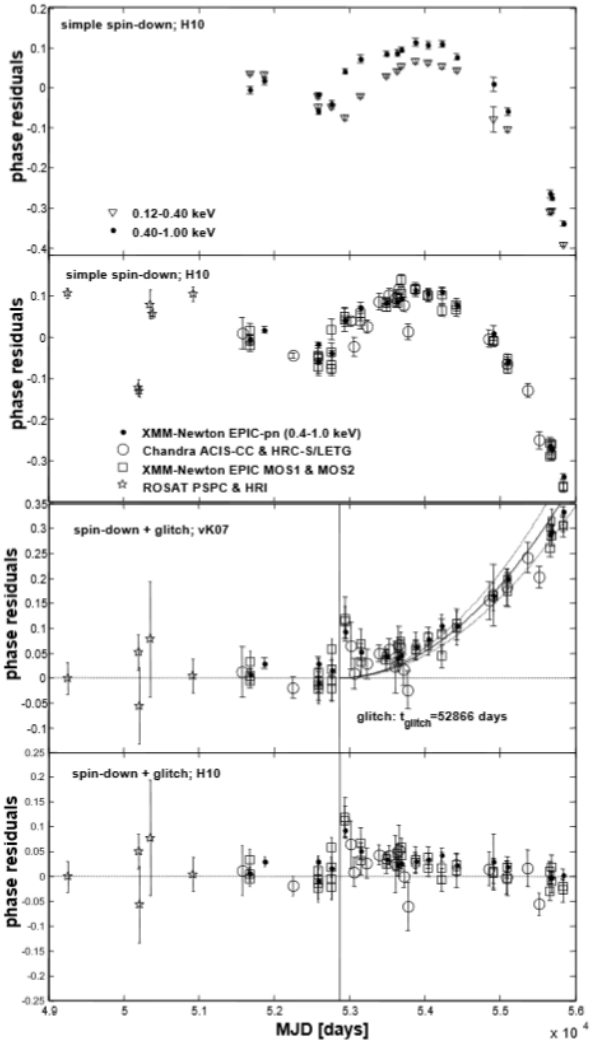

1203.3708

Glitch+? in a PSR

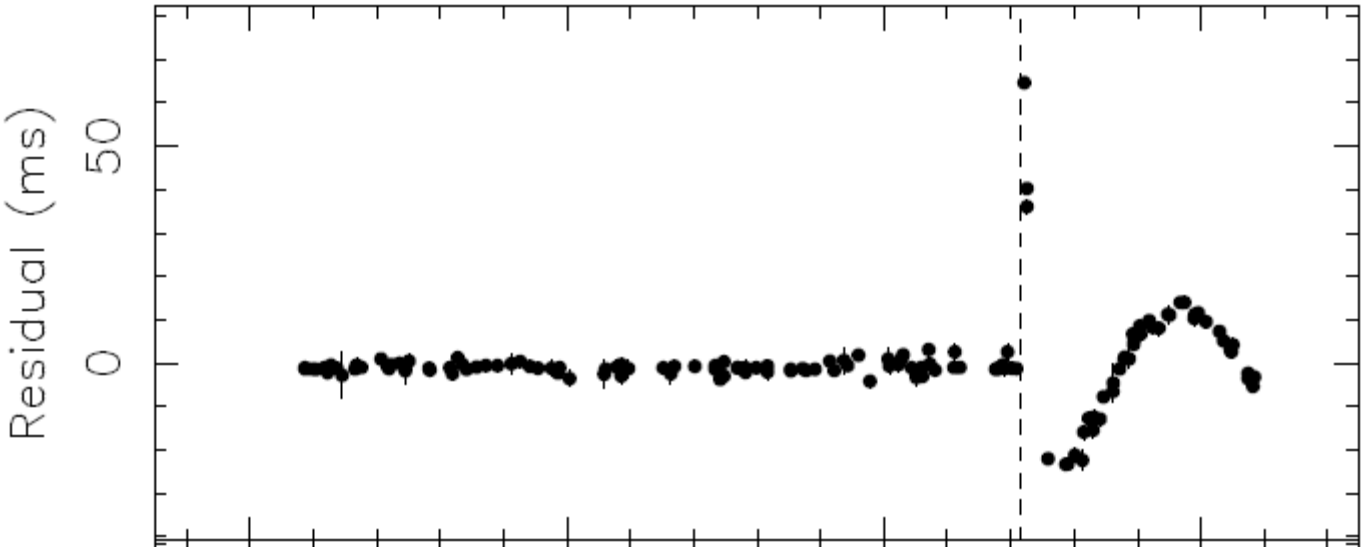

PSR B2334+61

arXiv: 1007.1143

Precession after a glitch was proposed as possible feature due to Tkachenko waves excitation (arXiv: 0808.3040).

Precession as a viable mechanism for long-term modulation was recently discussed in details in 1107.3503.

Free precession of a magnetar?

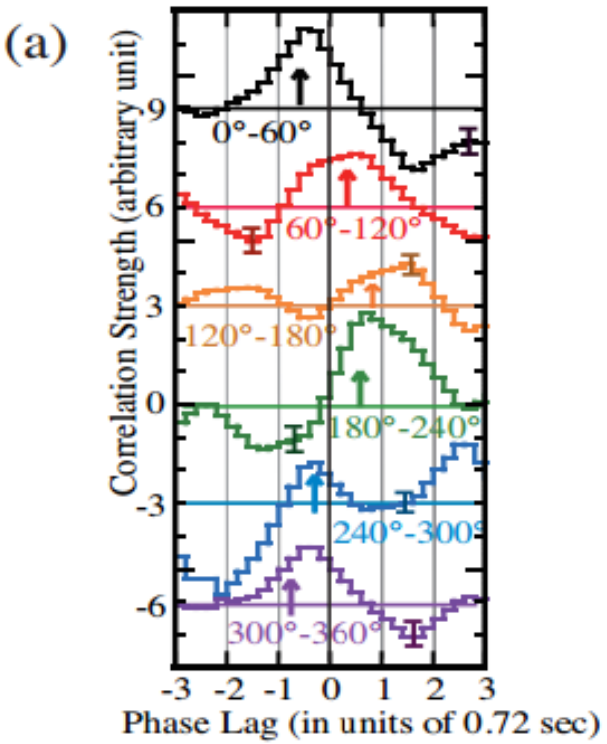

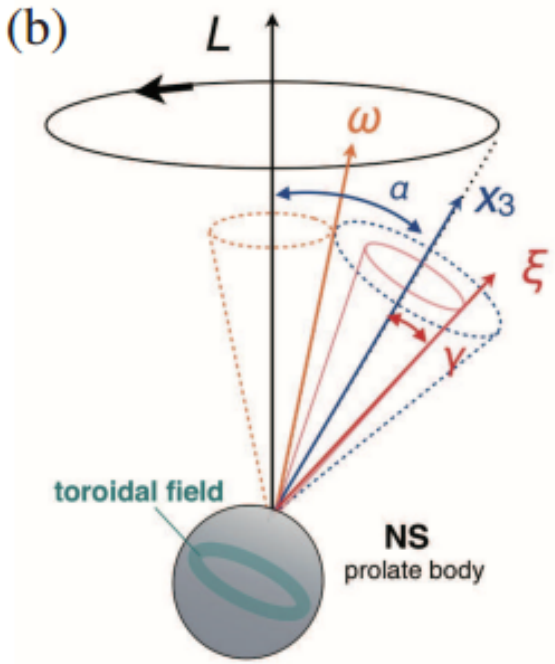

The authors observe modulation of the pulse profile with a period ~15 hours.
If it is interpreted by a free precession, than the NS is significantly deformed which can be due to strong toroidal field. This field might be ~10^{16} G.

1404.3705

New precession candidates among PSRs

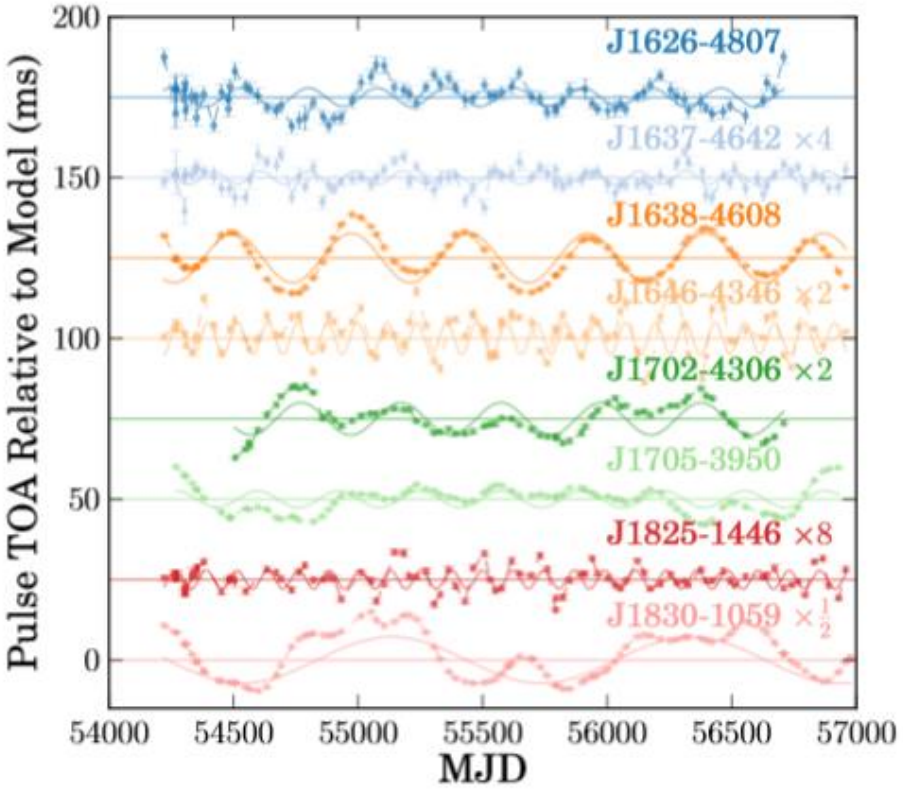

Periodic modulations which can be interpreted as free precession.

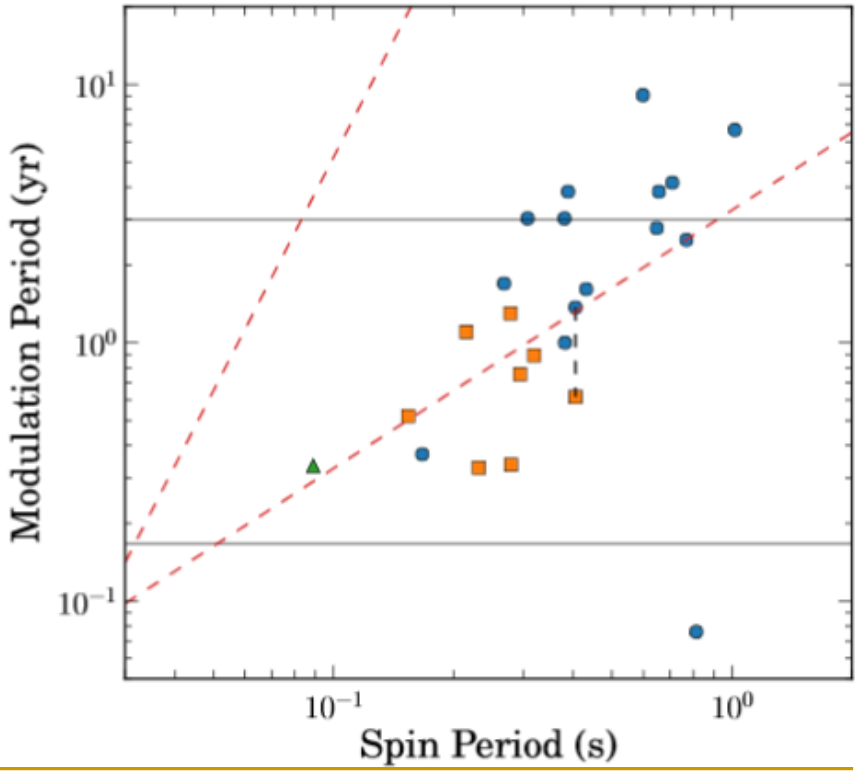

Correlations of the modulation period with spin period, characteristic age and spin-down power.

1510.06078

Conclusion

Many observed phenomena are related to internal dynamics of NSs.

- Glitches
- Precession

Glitches are related to the existence of some reservoir for angular momentum. Most probably, it is a layer of superfluid neutrons in the inner crust.

Some glitches of magnetars can be related to a different process.

Main papers

- Link et al. astro-ph/0001245 Glitches
- Link astro-ph/0211182 Precession
- Jones, Andersson astro-ph/0011063 Precession
- Dib et al. arXiv: 0706.4156 AXP glitches
- Haskell, Melatos arXiv: 1502.07062 Big review
- Haskell, Sedrakian arXiv: 1709.10340 Big review on superfluidity
- Fuentes et al. arXiv: 1710.00952 Glitch statistics
- Manchester arXiv: 1801.04332 Brief review on glitches

Many-many glitches …

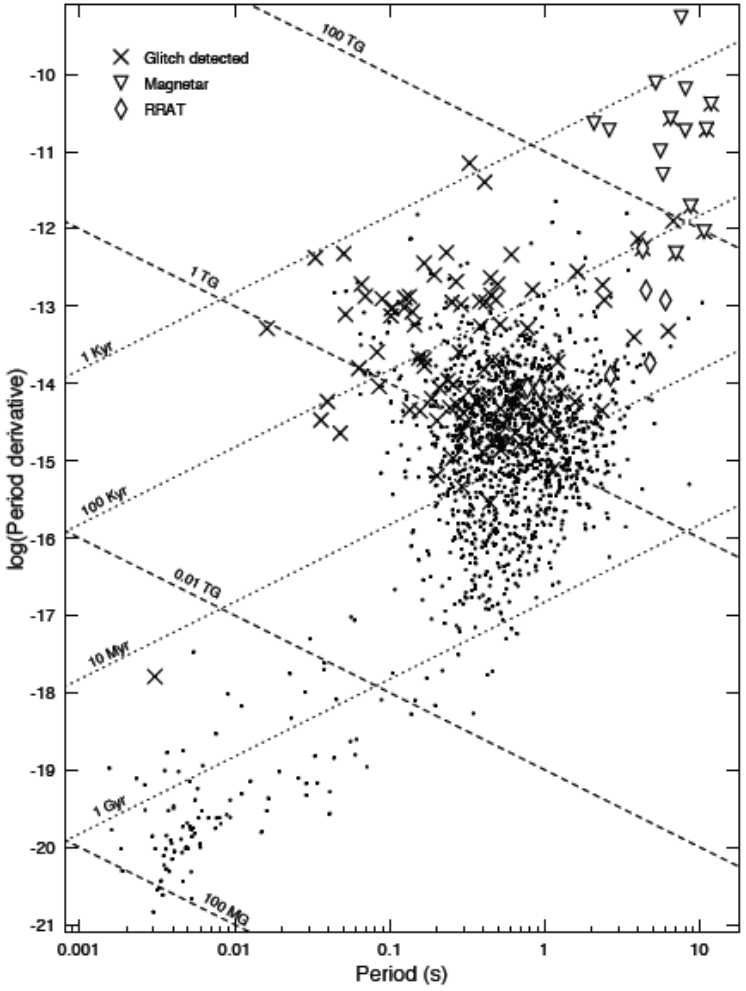

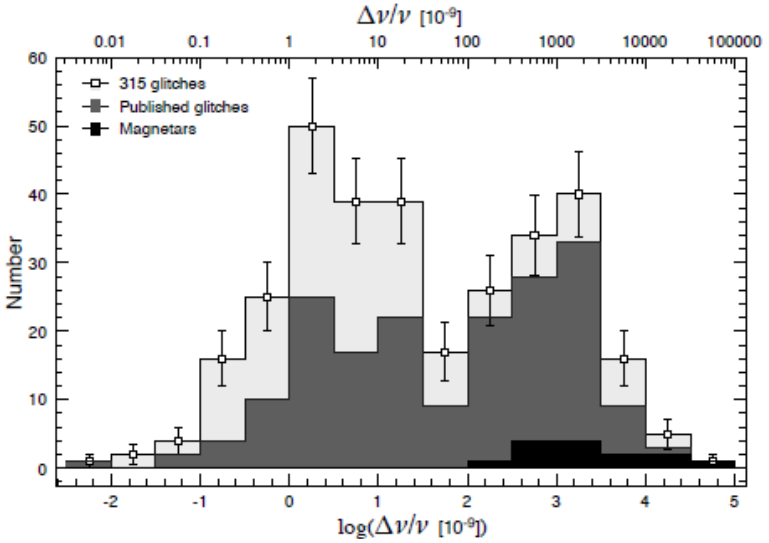

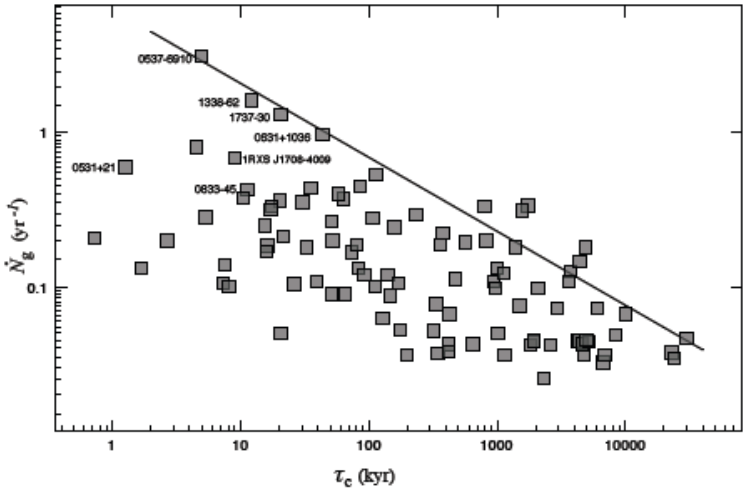

1102.1743

315 glitches in 102 PSRs

107 new glitches in 36 pulsars

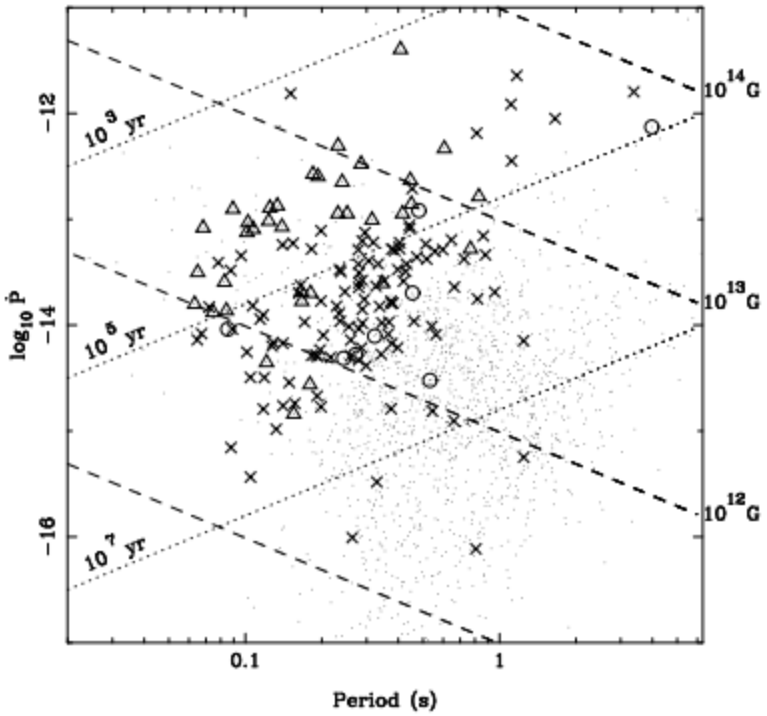

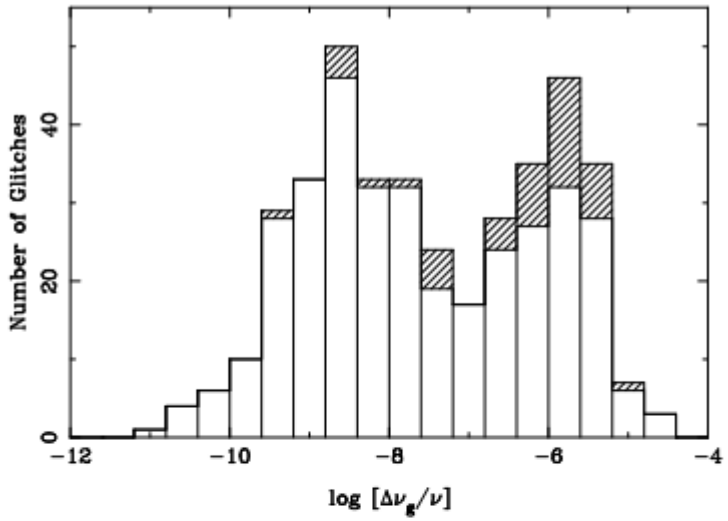

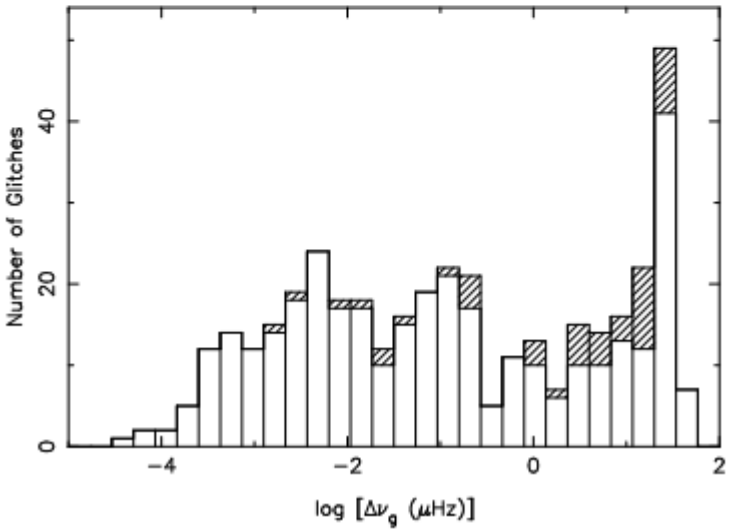

1211.2035

P–Pdot diagrams for glitch-related quantities

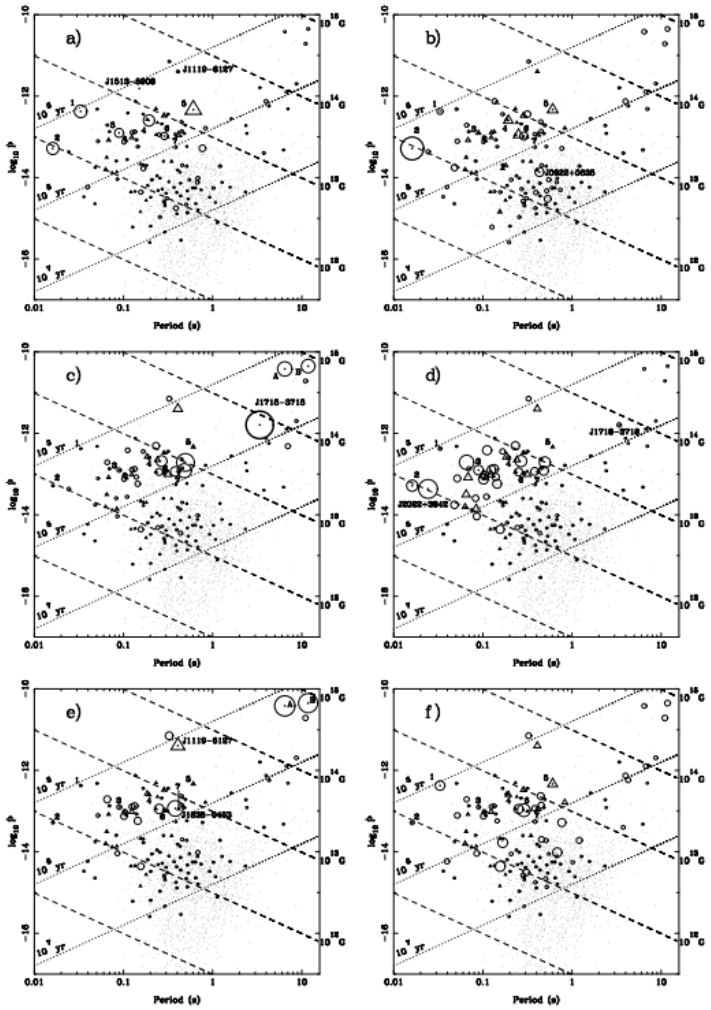

a) number of detected glitches; b) average number of glitches per year;
c) maximum fractional glitch size; d) maximum glitch size; e) rms fractional glitch size; and f) rms fractional size normalised by the mean. A circle indicates the parameter was obtained from the ATNF Pulsar Catalogue glitch table, whereas a triangle symbol indicates a parameter from this work. In the various plots, the seven pulsars exhibiting ten or more glitches are marked: 1 – PSR B0531+21 (Crab pulsar); 2 – PSR J0537−6910; 3 – PSR B0833−45 (Vela pulsar); 4 – PSR J1341−6220; 5 – PSR J1740−3015; 6 – PSR J0631+1036; 7 – PSR J1801−2304; and two magnetars: A – PSR J1048−5937 (1E 1048.1−5937) and B – PSR J1841−0456 (1E 1841−045).

1211.2035

Modeling glitches

Mean field approach to describe vortex dynamics

Kick velocity

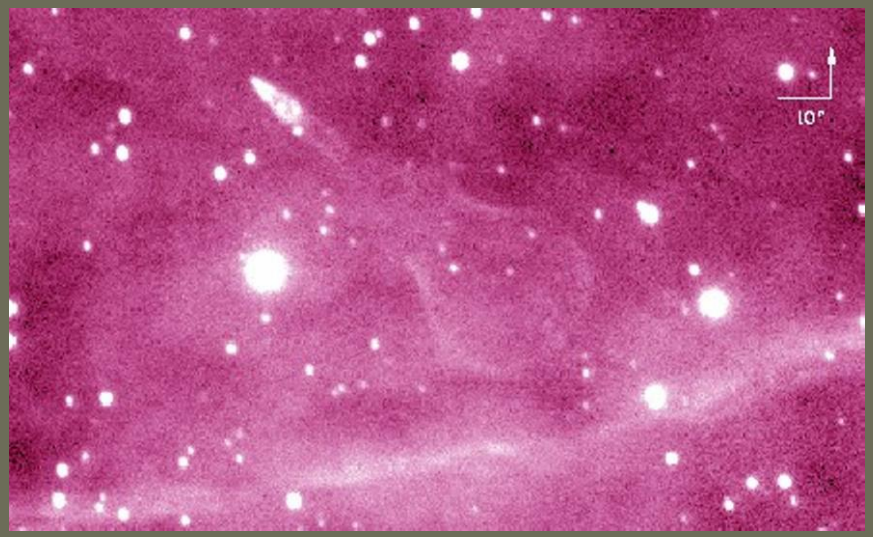

Why do neutron stars move so rapidly?

Stars vs. Neutron Stars

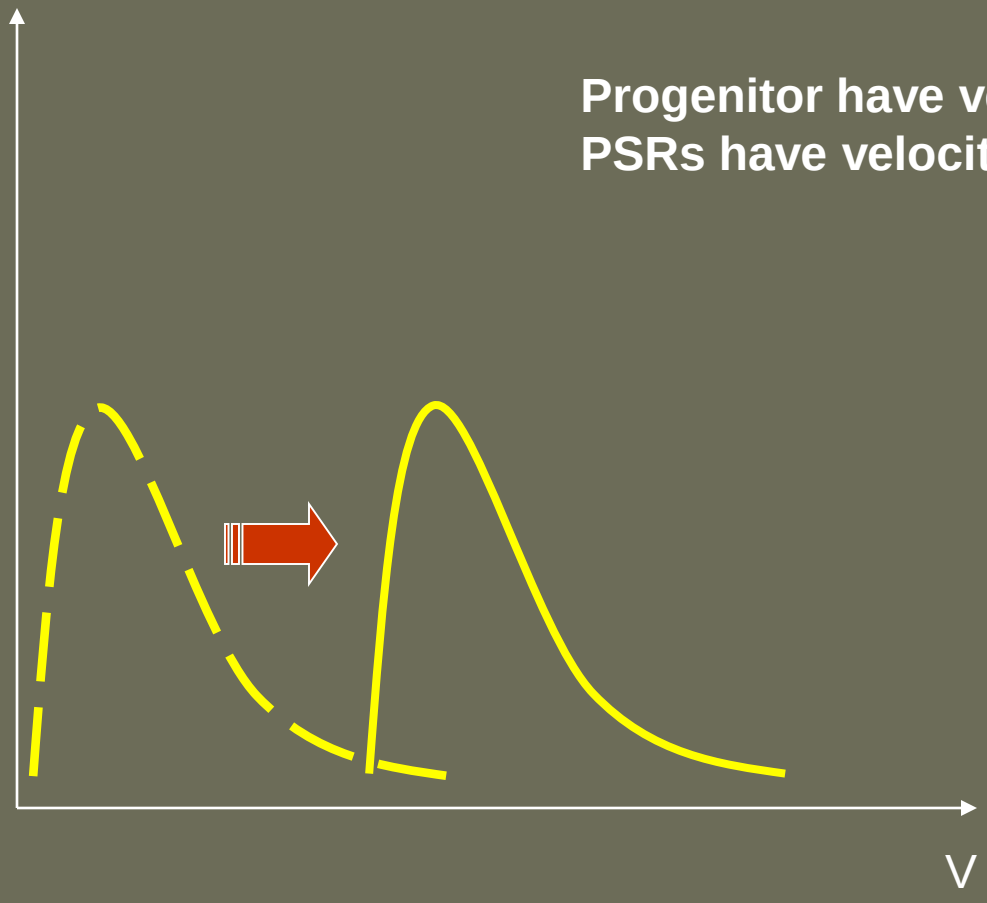

Progenitor have velocities about ~10-30 km/s
PSRs have velocities ~100-500 km/s

Pulsar velocity distribution

Normal stars have velocities ~10-30 km/s.

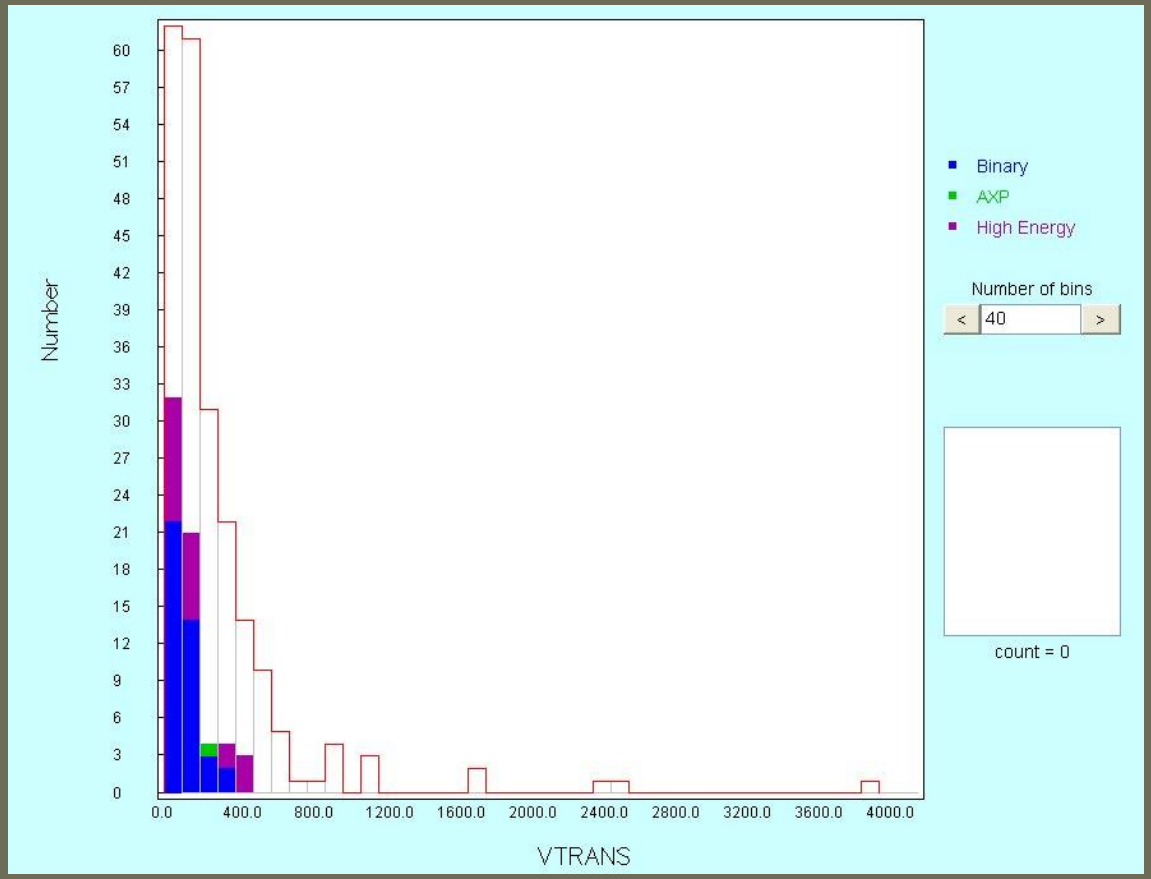

Already in 70s it became clear that PSRs have high spatial velocities (>>10 km/s).

A breakthrough happened in 1994 when Lyne and Lorimer in a seminal paper in Nature showed that velocities are even higher than it was thought before – hundreds km/s.

Note, that the observed distribution is much different from the initial one.
To derive the later it is necessary to calculate a model.

ATNF catalogue

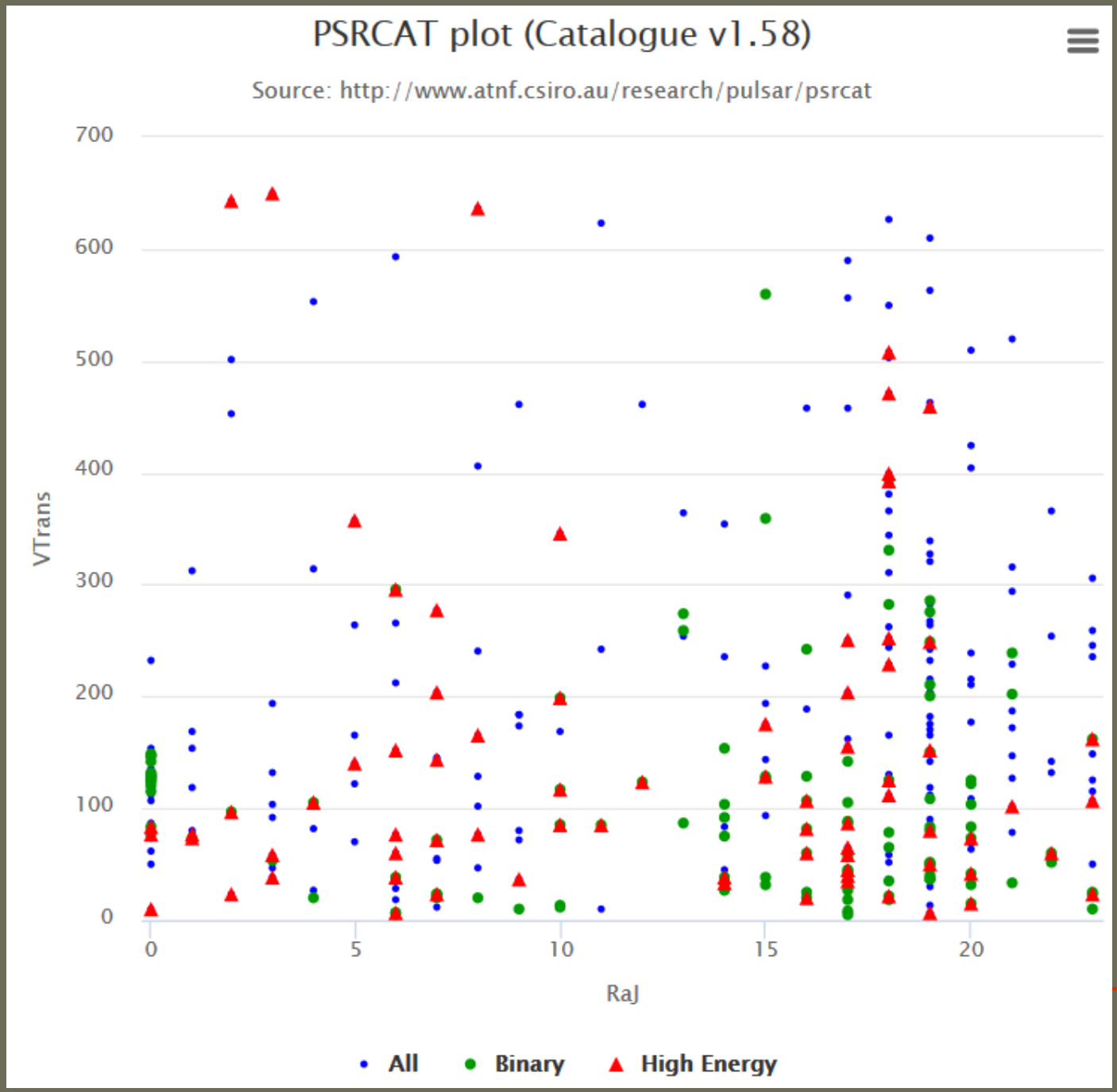
PSRCAT plot (Catalogue v1.58)
Source: http://www.atnf.csiro.au/research/pulsar/psrcat
VTrans
700
600
500
400
300
200
100
0
0
5
10
15
20
RaJ
All
Binary
High Energy

ATNF

SN explosions should not be symmetric!

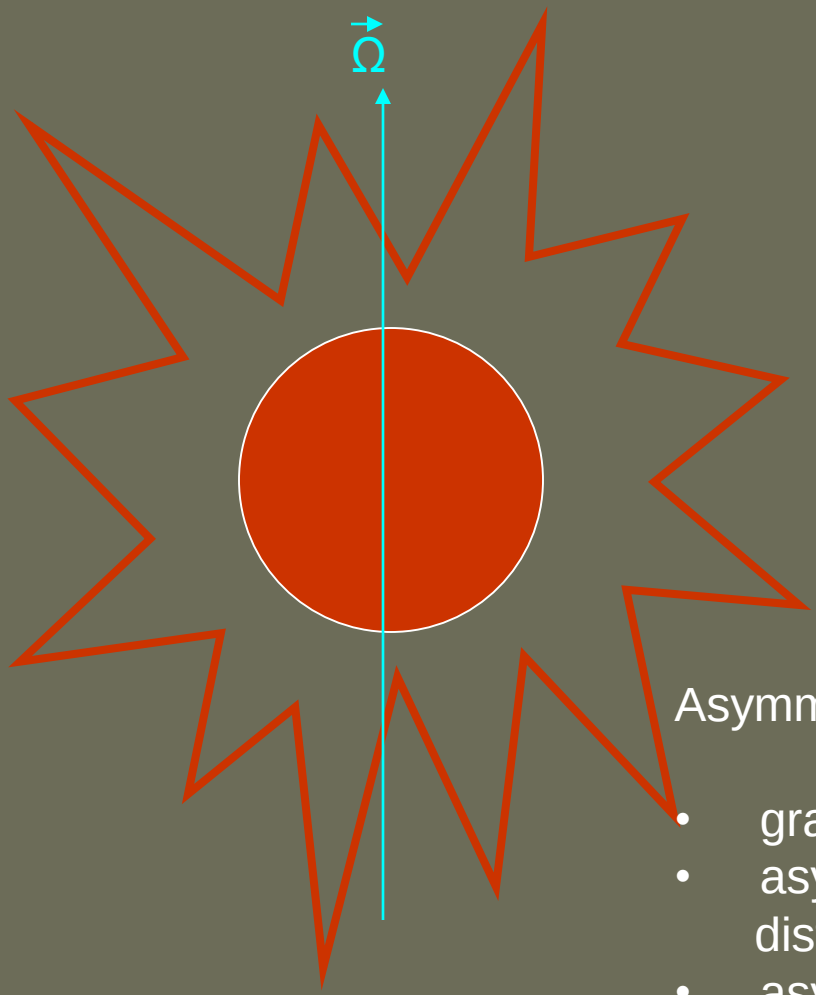

E_{total}~3 10^{53} erg
Most of energy is carried away by neutrinos.

~Few % asymmetry in energy release
can produce a strong kick up to 1000 km/s.

Main kick mechanisms

- Asymmetric mass ejection (Shklovsky 1970)
- Asymmetric neutrino emission (Chugai 1984)

Asymmetric mass ejection includes three mechanisms:

- gravitational pull due to asymmetric matter
- asymmetric neutrino emission due to matter distribution
- asymmetric matter jets (Khokhlov et al.1999)

Leonid Ozernoy in 1965 discussed asymmetry of SN explosions in the context of GW radiation.

SN and kick explosion mechanisms

Mechanism	Time scale	$V_{\max}$, km s^{-1}	Alignment (spin and V)	Main recent refs.
Hydrodynamical	0.1 s	$\sim (100 - 200)$	random	Lai et al. (2001)
ν-driven	$\sim$ few s	$\sim 50\ B_{15}$	parallel	Lai et al. (2001)
Electromagnetic rocket	long	$1400\ R_{10}^2\ P_{\rm ms}^{-2}$	parallel	Lai et al. (2001), Huang et al. (2003)
Binary disruption (without add. kick)	$<< P_{\rm orb}$	~ 1000	perpendicular	Iben & Tutukov (1996)
NS instability	few ms	~ 1000	perpendicular	Colpi & Wasserman (2002), Imshennik & Ryazhskaya (2004)
Magnetorotational	0.2 s – minutes	~ 300 (up to 1000)	quasirandom	Moiseenko et al. (2003), Ardeljan et al. (2004)

For neutrino emission: $V_{kick}=\varepsilon\ E_{tot}/Mc \sim 1000$ km/s $(\varepsilon/0.1)\ (E_{tot}/10^{53}$ erg).
Also it depends on the magnetic field.

Kick modeling

Recently, new results on the origin of NS and BH kicks have been obtained:

- Neutrino-triggered asymmetric magnetorotational mechanism arXiv:1110.1041
- Hydrodynamic Origin of Neutron Star Kicks arXiv: 1112.3342
- Three-dimensional neutrino-driven supernovae arXiv:1210.8148
- BH kicks arXiv:1203.3077

A review on SNae properties and explosion mechanisms: arXiv:1210.4921

To kick or not to kick?

Up to mid-90s it was not clear if kicks are absolutely necessary.

- Tademaru (rocket) mechanism
- Binary disruption (Blaaw mechanism)
- Core fragmentation (Berezinski et al., Imshennik)

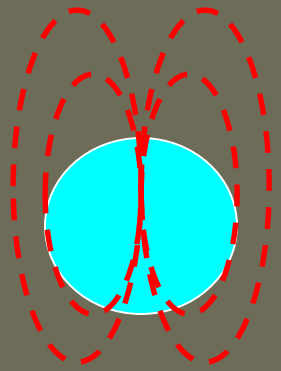

Asymmetric dipole

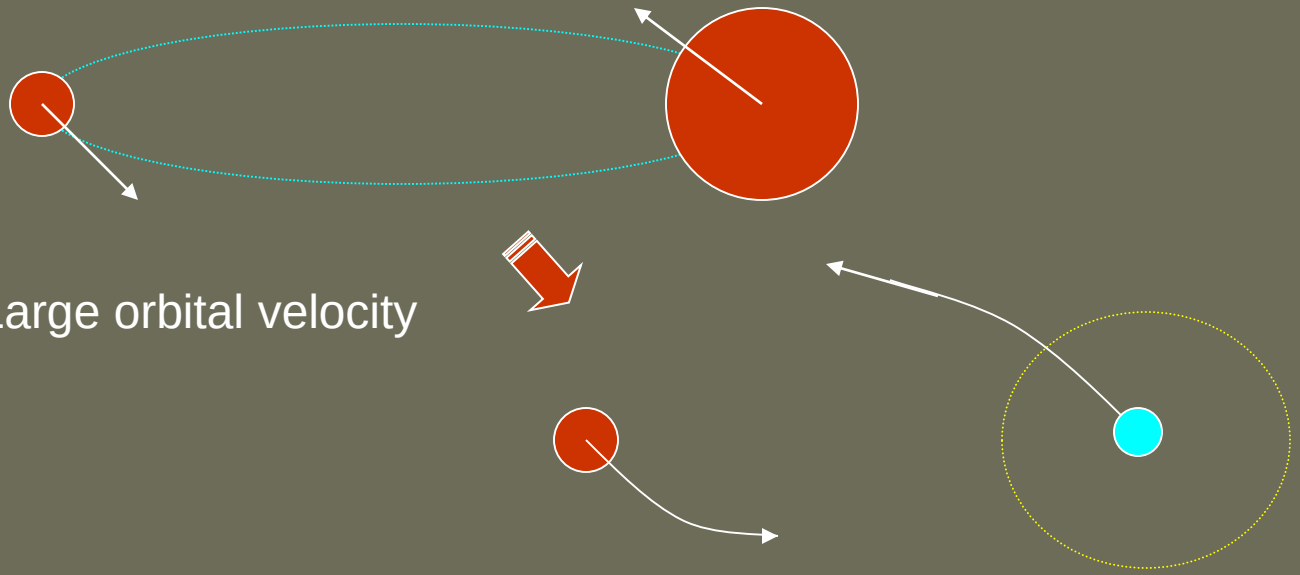

Large orbital velocity

However, some discoveries directly point to necessity of natal kicks.

Direct evidence

1. High-velocity NSs and binaries
2. Spin inclination in binaries and geodetic precession

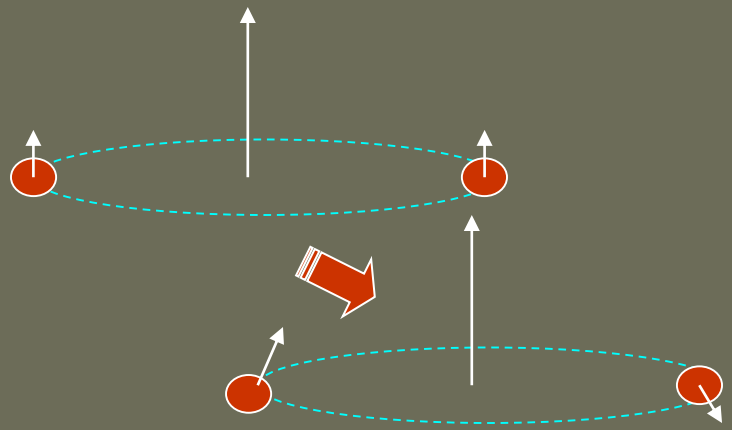

Orbit inclination relative
to a normal star equator
can be measure due to:
- orbital precession due to spin-orbit interaction (Kaspi et al. 1996)
- circumstellar disc inclination (Prokhorov, Postnov 1997)

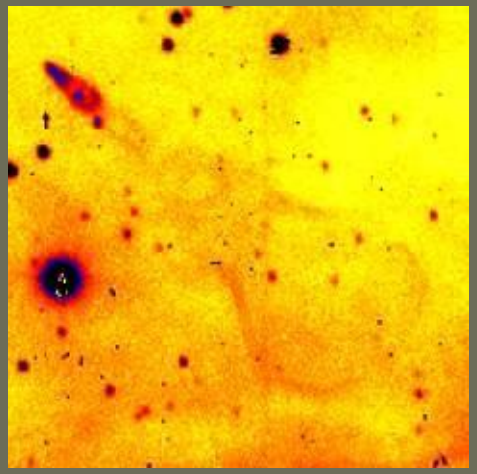

Guitar nebula, B2224+65

The most spectacular 3D velocity measurements for NSs are related to nebulae around these objects.

The transversal velocity can be measured by proper motion observations of radio pulsars and other neutron stars

For binaries large velocities are measured (Cir X-1: Johnston et al. 1999).

Double pulsar PSR J0737-3039

Pulsar A's spin is tilted from the orbital angular momentum by
no more than 14 degrees at 95% confidence;
pulsar B's -- by 130 ± 1 degrees at 99.7% confidence.

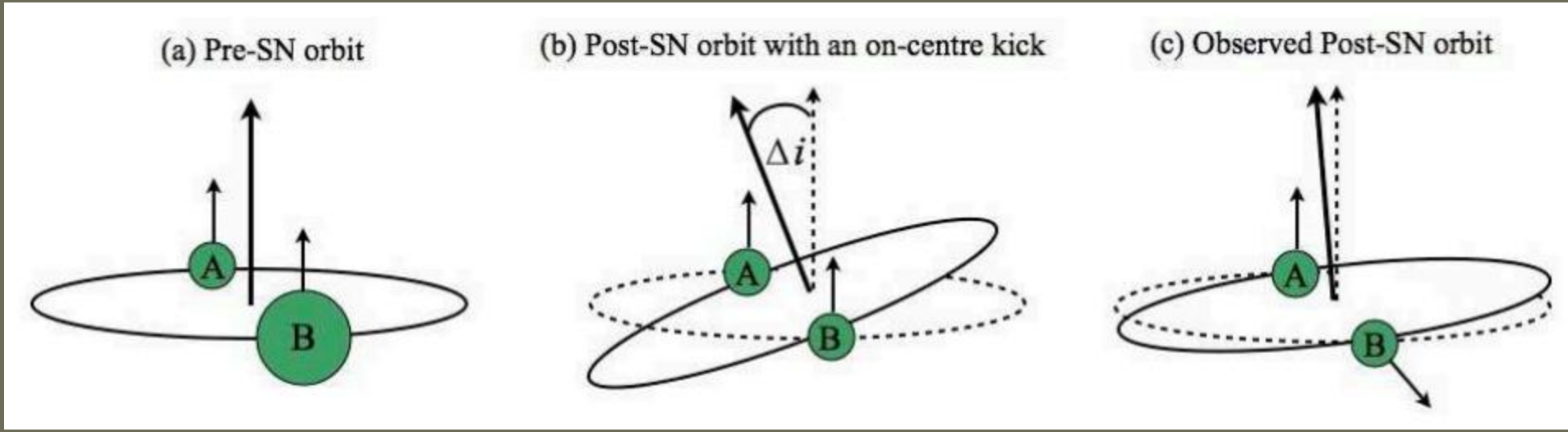

This spin-spin misalignment requires that the origin of most of B's present-day spin is connected to the supernova that formed pulsar B.
The spin could be thought of as originating from the off-center nature of the kick.

1104.5001

See also 1302.2914 about probably near-zero kick for the pulsar A.

Many kick velocity distributions are proposed

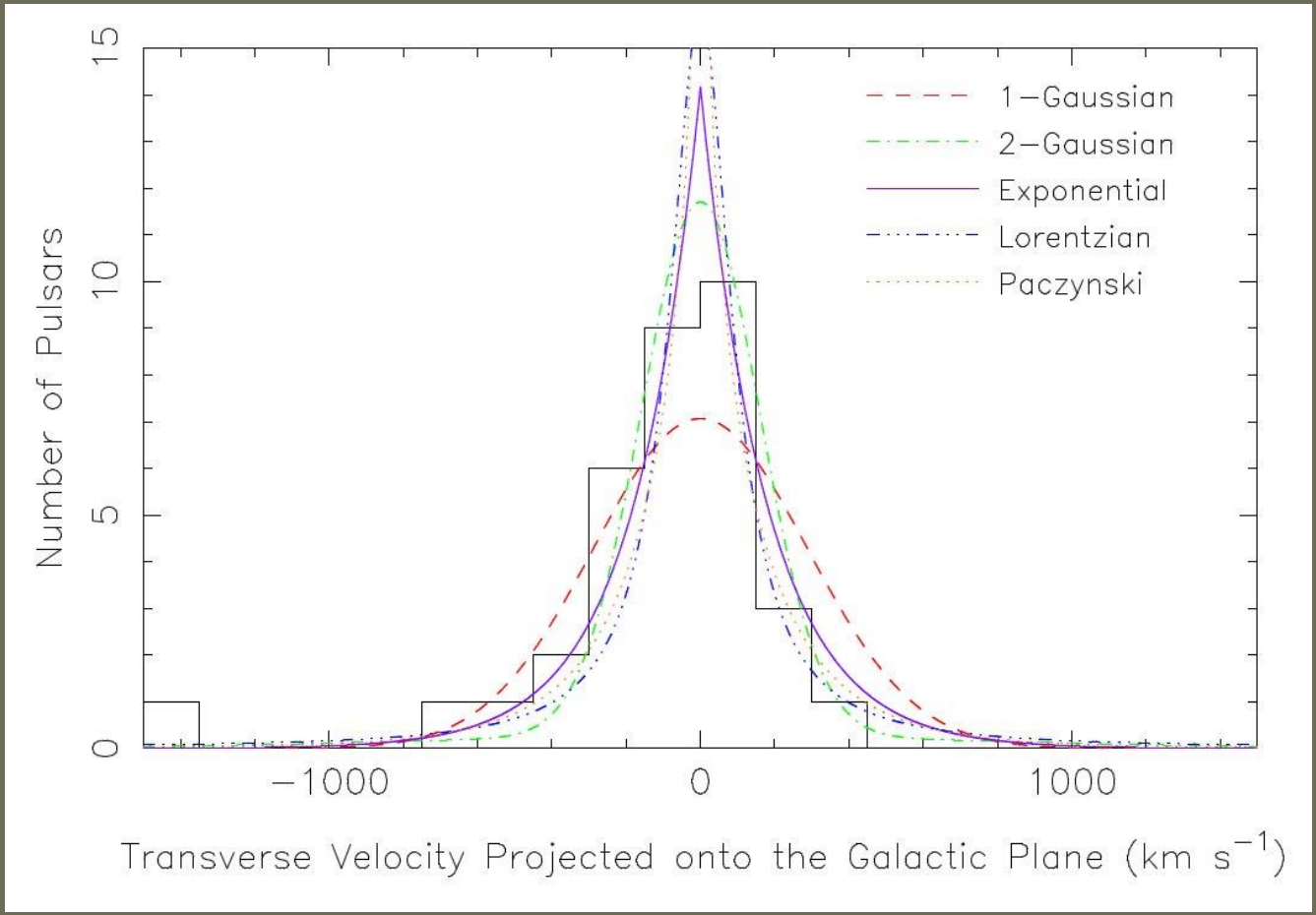

Three popular models:

- Arzoumanian, Chernoff, Cordes (2002)
- Hobbs et al. (2005)
- Faucher-Giguer and Kaspi (2006)

Note the difference:
We observe present day velocities with selection and evolutionary effects, but we are interested in the velocity at birth!

(Faucher-Giguer, Kaspi 2006)

Bimodal distribution

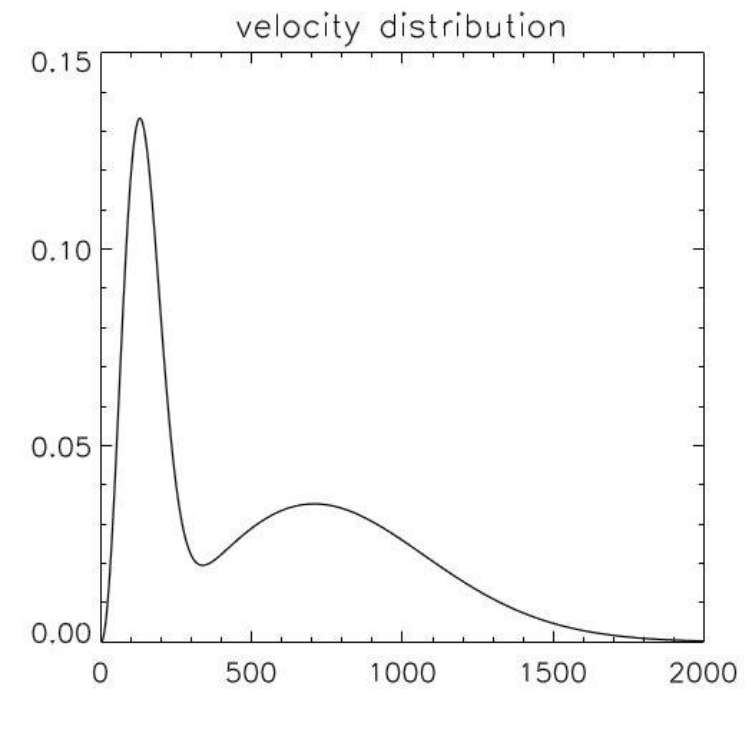

Arzoumanian et al. 2002

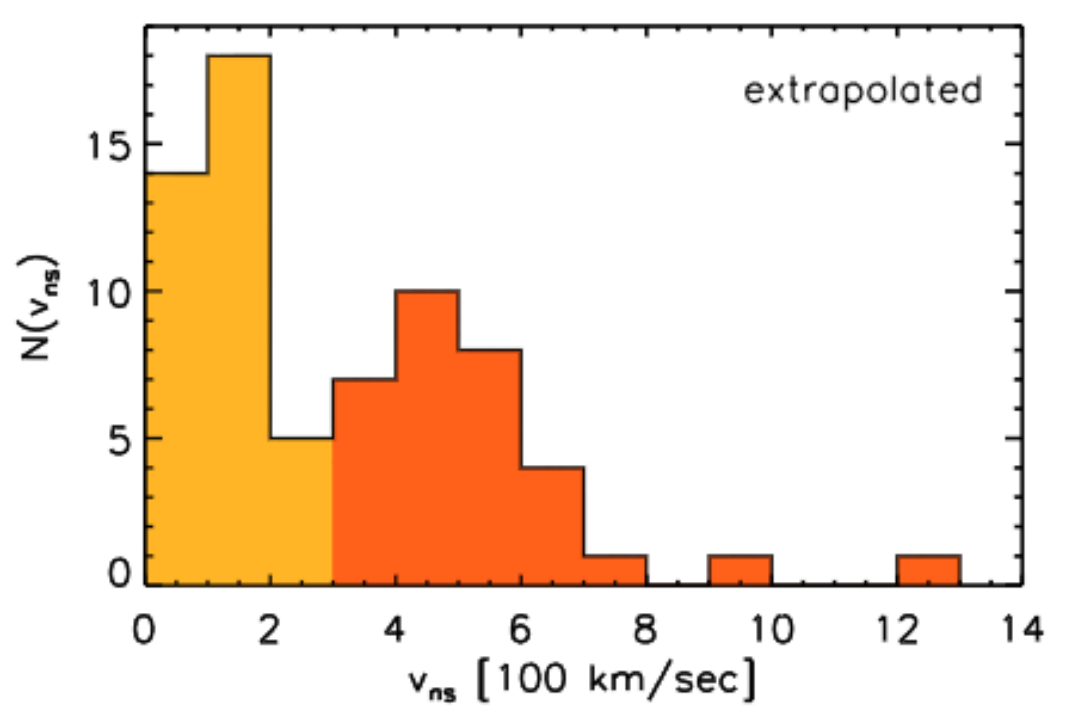

Scheck et al. 2006

Hydrodynamical models

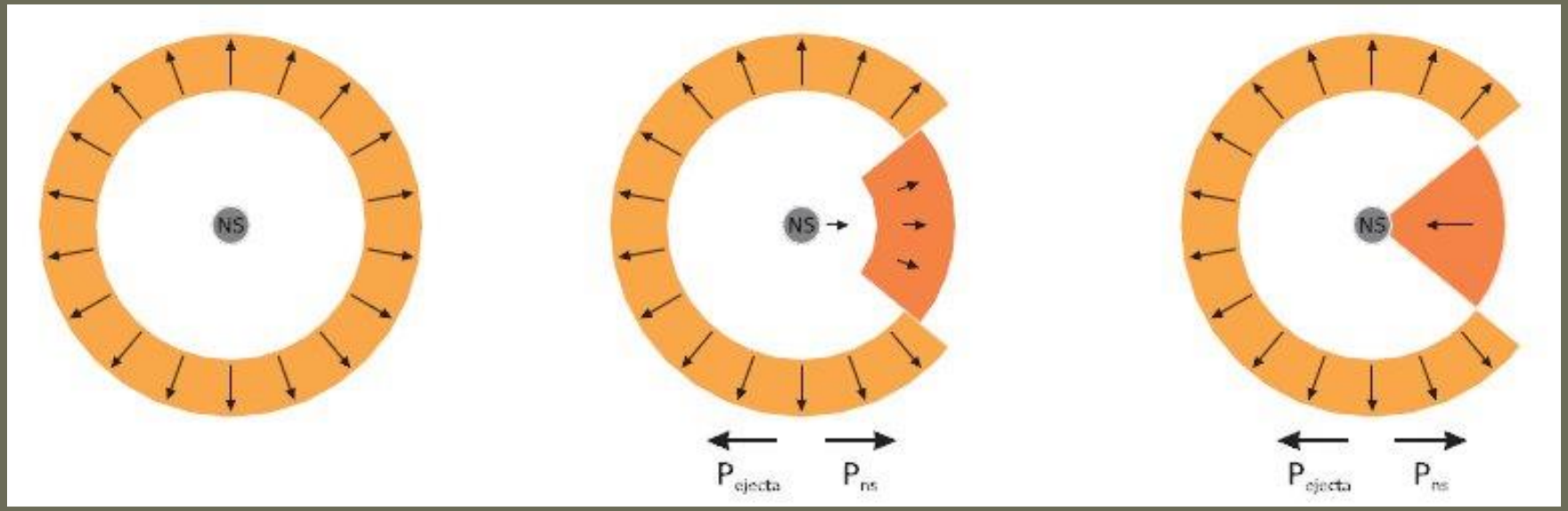

astro-ph/0601302

2D simulations

Acceleration of a NS is mainly due to gravitational pull of the anisotropic ejecta

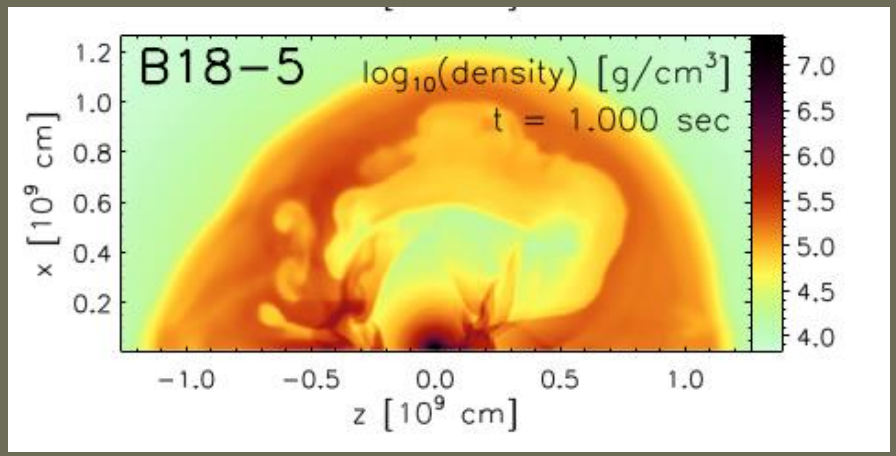

Scheck et al.

See 3D calculations in 1010.0167

3D hydrodynamics kicks

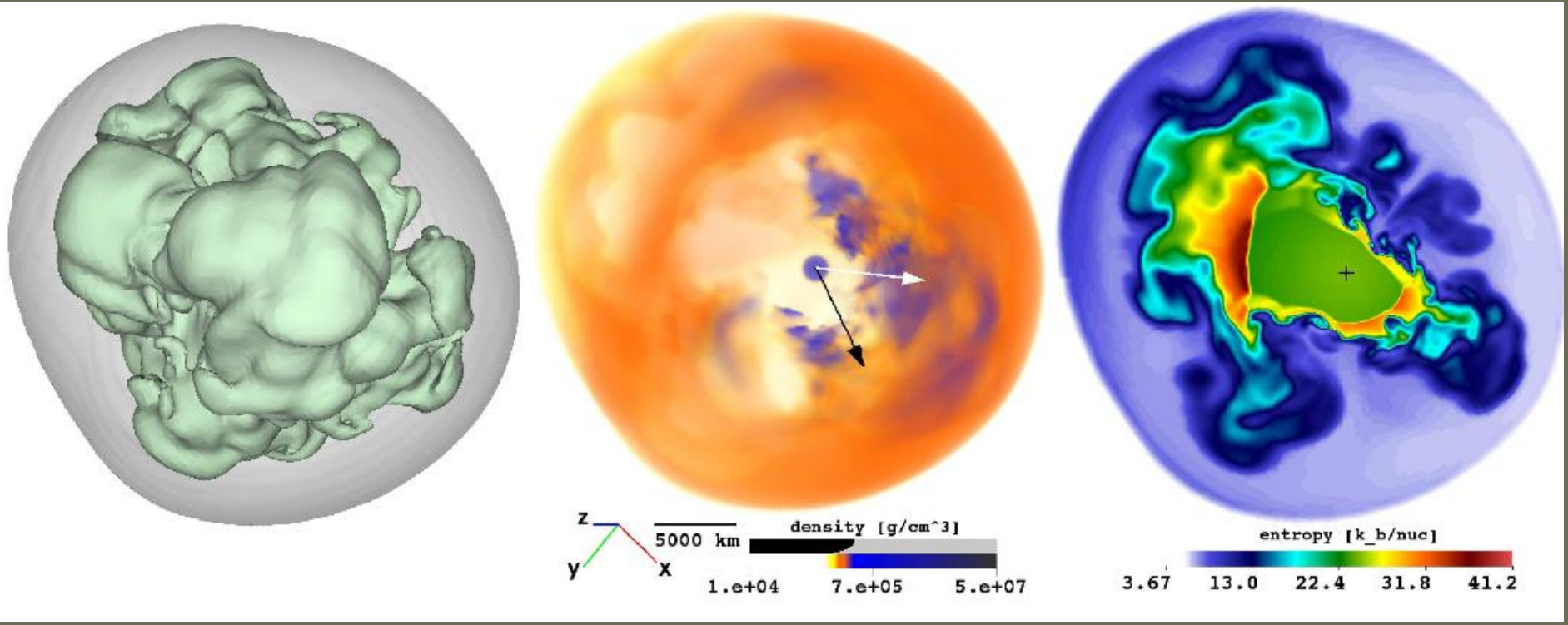

$$\mathbf{v}_{\rm ns}(t) = -\mathbf{P}_{\rm gas}(t)/M_{\rm ns}(t)$$

$$\mathbf{P}_{\rm gas} = \int_{R_{\rm ns}}^{R_{\rm ob}} {\rm d}V\,\rho\mathbf{v}.$$

$$v_{\rm ns} \approx 2G\Delta m/(r_{\rm i}v_{\rm s}) \approx 2700\,{\rm km\,s^{-1}}$$

$$r_{\rm i} = 100\,{\rm km} \qquad \Delta m = \pm 10^{-3}\,M_\odot$$

$$v_{\rm s} = 1000\,{\rm km\,s^{-1}}$$

1010.0167

NS kick models

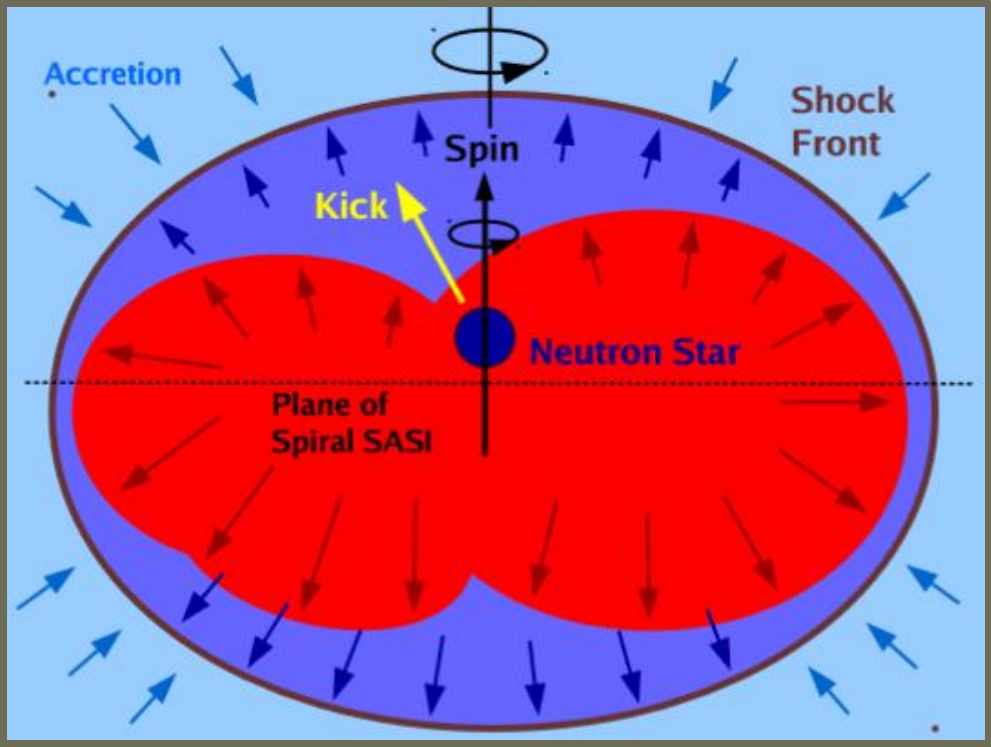

Spin-kick alignment resulting from a neutrino-driven explosion launched from a phase of strong spiral-SASI activity.

While the explosion starts by equatorial expansion, the final NS kick is determined by the slower mass ejection in the polar directions.

The NS is accelerated by the gravitational attraction of the mass in these more slowly expanding, dense regions.
In the cartoon the NS is pulled more strongly towards the northern direction and therefore opposite to the (southern) hemisphere where the explosion is more powerful.

1611.07562

Spin-velocity alignment

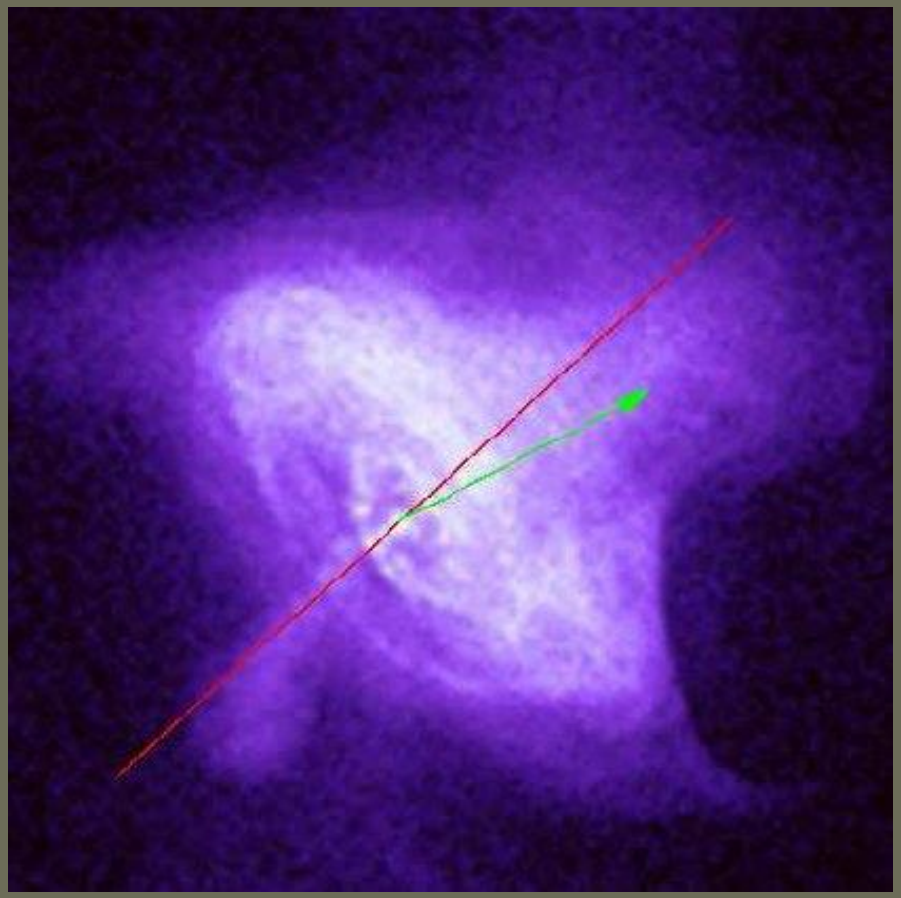

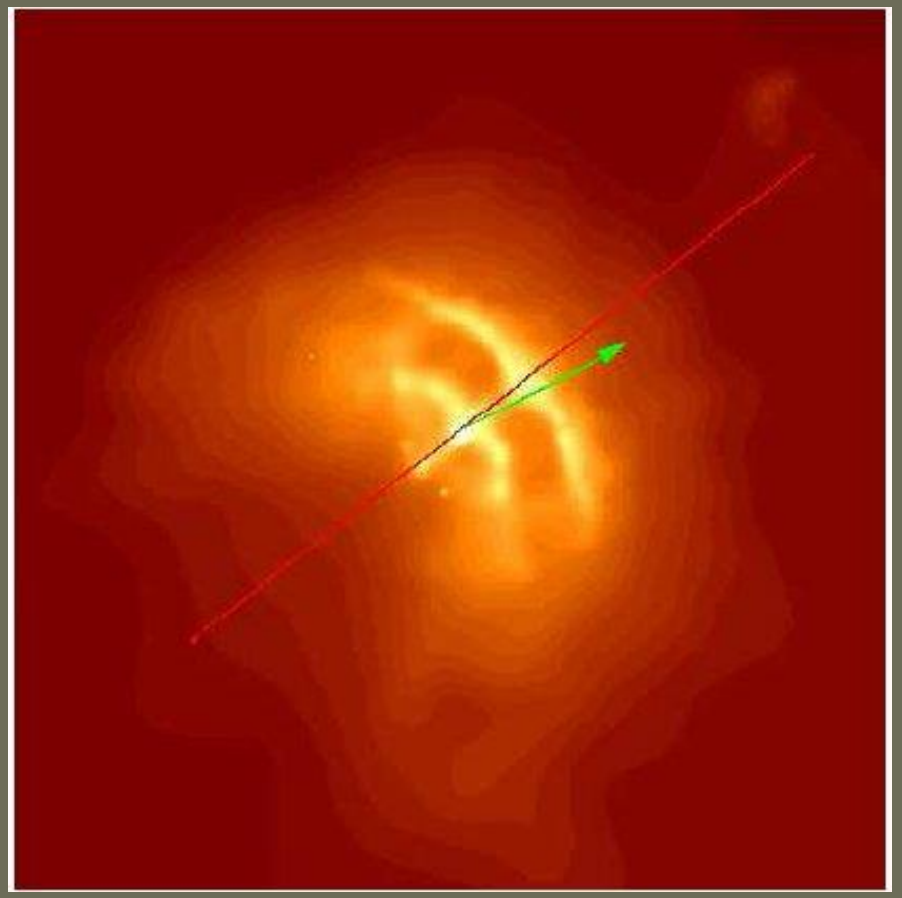

Spatial velocity and spin axis are nearly coincident.
Nearly is important: there is some misalignment.

[Ng & Romani]

The best studied cases: Crab and Vela

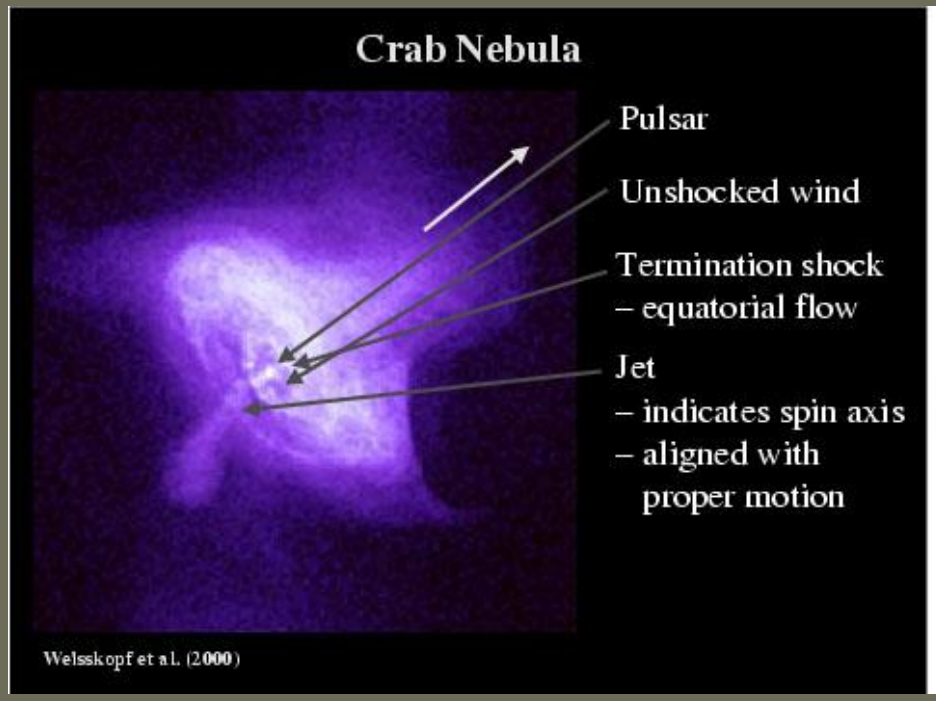

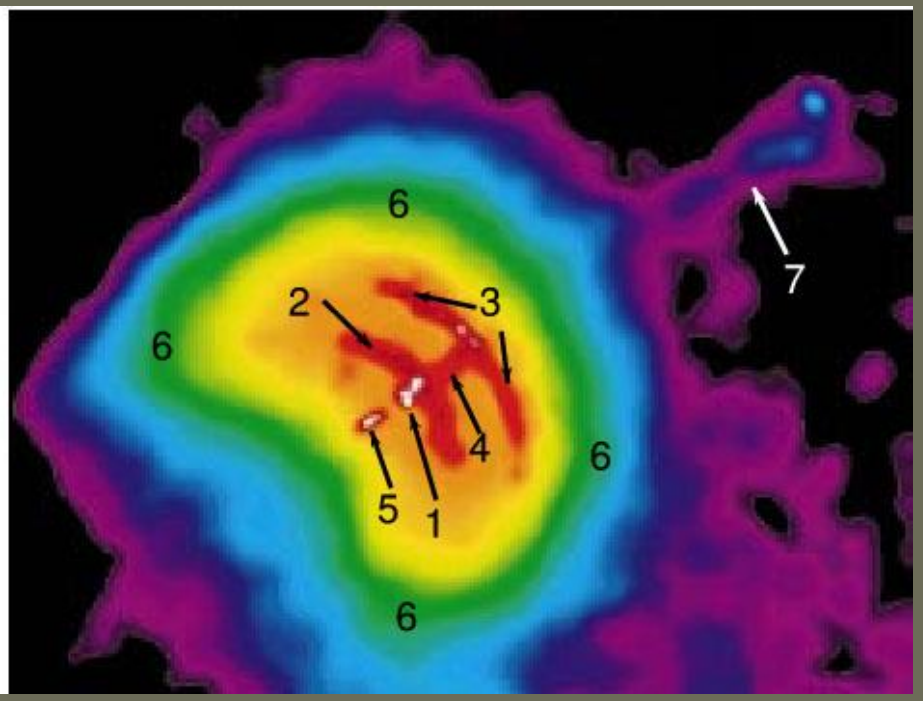

Crab and Vela are not the only cases, but are the best studied ones.
Spin-velocity correlation (in direction) is reported for many radio pulsar.
For some of them pulsar wind nebula observations are used,
for some only direction of proper motion and polarization properties can be used.

Some set of PSRs with known spin-velocity orientation

		2D Pulsars	
B0628−28	318	+61/−64	5 ± 4
B0740−28	259	+190/−149	7 ± 5
B0823+26	189	+55/−34	21 ± 7
B0835−41	170	±30	13 ± 11
B0919+06	506	±80	32 ± 17
B1133+16	639	+38/−35	22 ± 2
B1325−43	597	±254	31 ± 22
B1426−66	150	+40/−24	5 ± 9
B1449−64	219	+55/−18	1 ± 3
B1508+55	1082	+103/−90	23 ± 7
B1642−03	160	+34/−32	26 ± 5
B1800−21	347	+48/−57	7 ± 8
B1842+14	512	+51/−50	5 ± 15
B1929+10	173	+4/−5	16 ± 2
B2045−16	304	+39/−38	3 ± 6
IC 443	250	±50	45 ± 10
		3D Pulsars	
J0205+6449	838	±251	21 ± 10
B0531+21	140	±8	26 ± 3
J0537−6910	634	±50	3 ± 5
J0538+2817	407	+116/−74	12 ± 4
B0540−69	1300	±612	34 ± 33
B0833−45	61	±2	10 ± 2
B1706−44	645	±194	35 ± 10
J1833−1034	125	±30	16 ± 15
B1951+32	273	±11	18 ± 5

[Ng & Romani 2007]

Recent data on radio pulsars

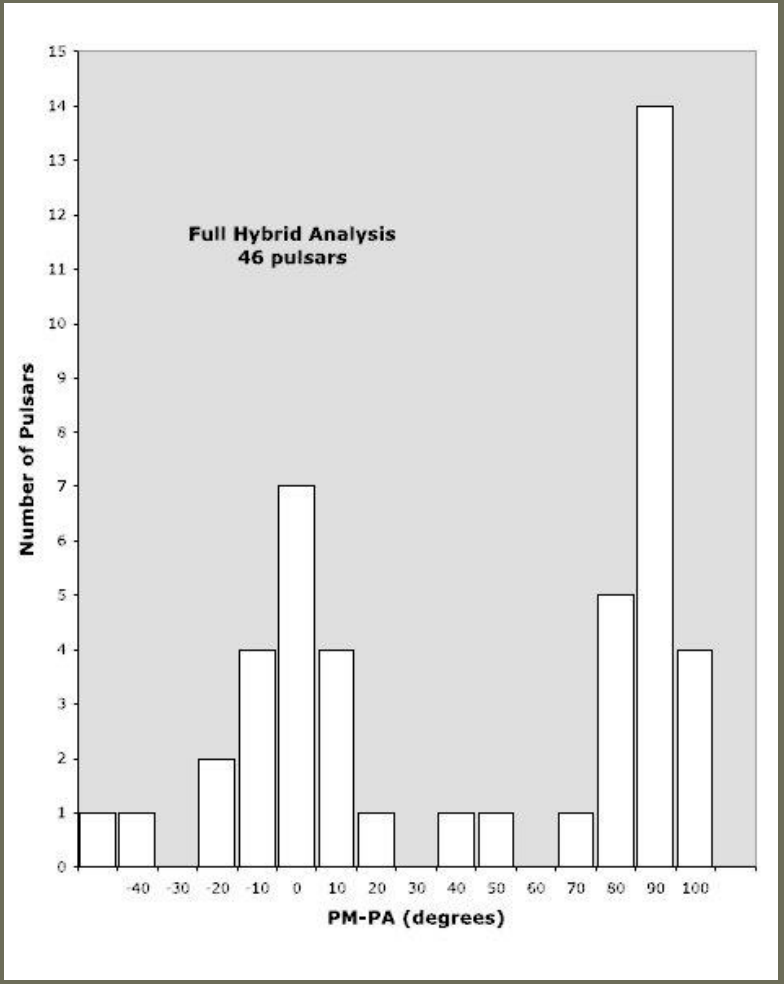

Rankin (2007)

J name	B name	log[age] (yr)	V_T km s^{-1}	PA_v (°)	PA_0 (°)	Ψ (°)
J0452−1759	B0450−18	6.2	185	72(23)	47(3)	25(23)
J0659+1414	B0656+14	5.0	65	93.1(4)	−86(2)	−1(5)
J0738−4042	B0736−40	6.6	180	313(5)	−21(2)	−26(5)
J0837+0610	B0834+06	6.5	170	2(5)	18(5)	−16(7)
J0837−4135	B0835−41	6.5	360	187(6)	−84(5)	−89(8)
J1604−4909	B1600−49	6.7	510	268(6)	−17(3)	−75(7)
J1735−0724	B1732−07	6.7	570	355(3)	55(5)	−60(6)
J1801−2451	B1757−24	4.2	300	270	−55(5)	−35(5)
J1820−0427	B1818−04	6.2	190	338(17)	42(3)	−64(17)
J1850+1335	B1848+13	6.6	300	237(16)	−45(3)	−78(16)
J1915+1009	B1913+10	5.6	280	174(15)	85(3)	89(15)
J1937+2544	B1935+25	6.7	210	220(9)	−9(5)	49(10)
J2048−1616	B2045−16	6.5	330	92(2)	−13(5)	−75(6)
J2330−2005	B2327−20	6.7	180	86(2)	21(10)	65(10)

Johnston et al. (2007)

The tendency is clear,
but it is only a tendency.

New data and discussion in 1502.05270

Alignment

47 pulsars with well-determined parameters.

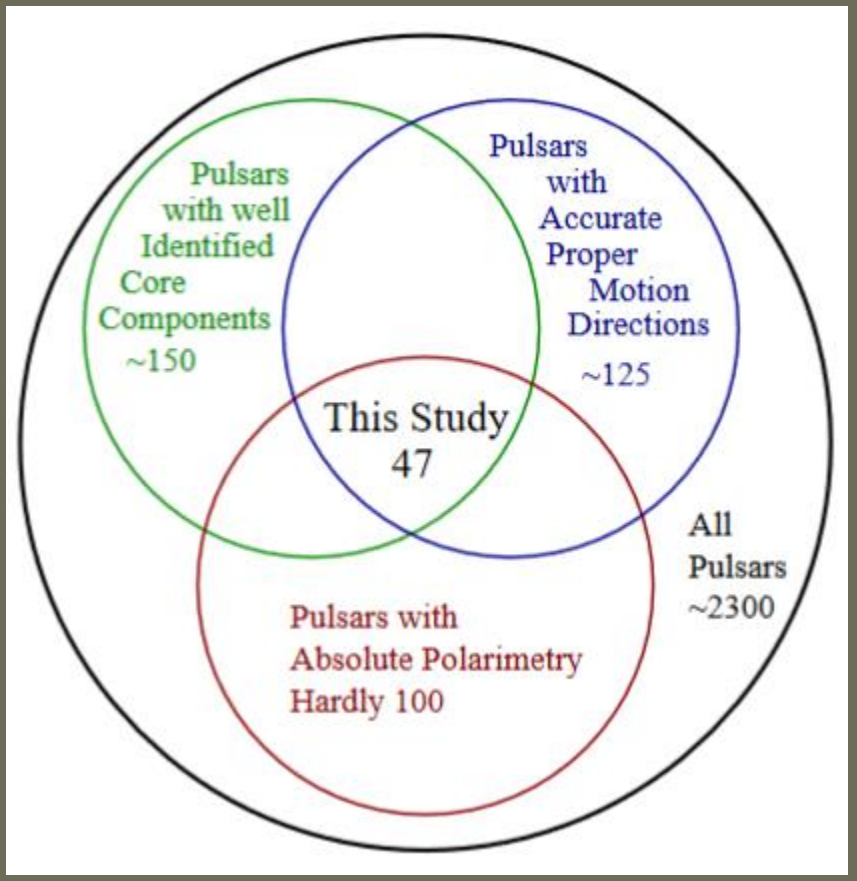

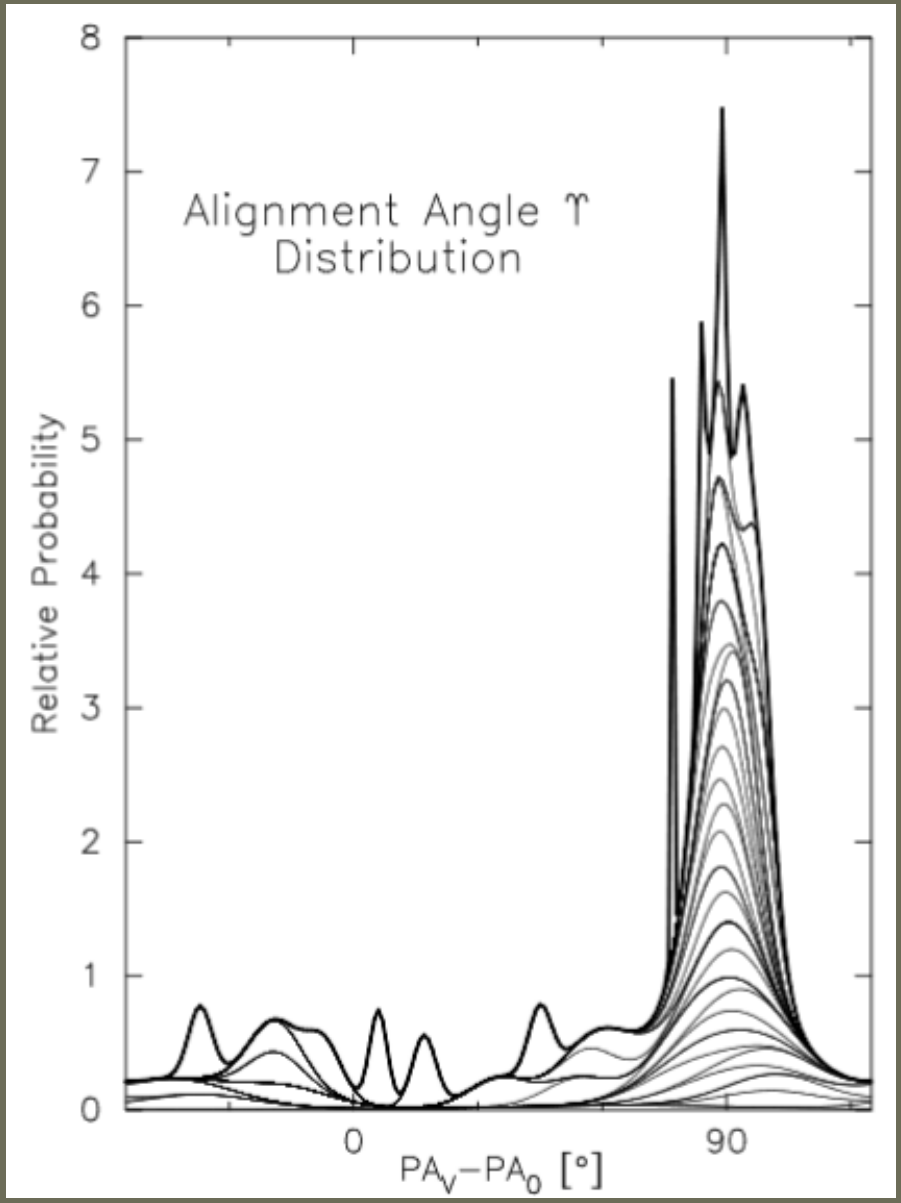

1502.05270

Why?

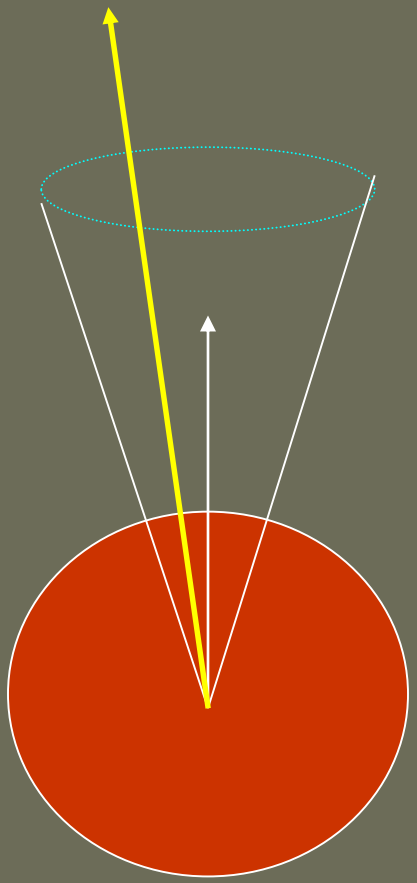

Kick can be confined in some angle around the spin axis. Typical cones must be <~10^{o} (see, for example, Kuranov et al. 2009).

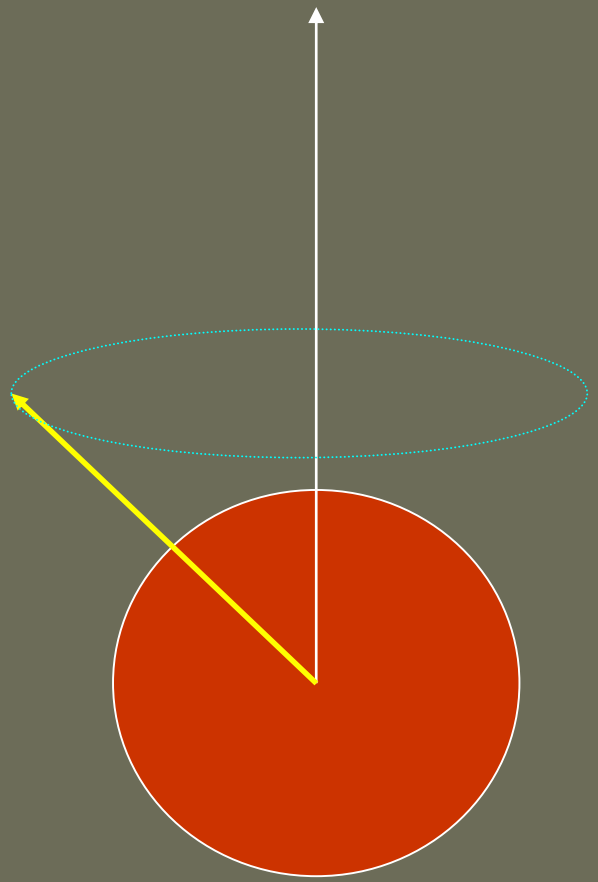

Kick mechanism can be operative for a long time (many spin periods), so that its influence is average. Typical duration must be 1-10 sec.

Kicks in binary evolution

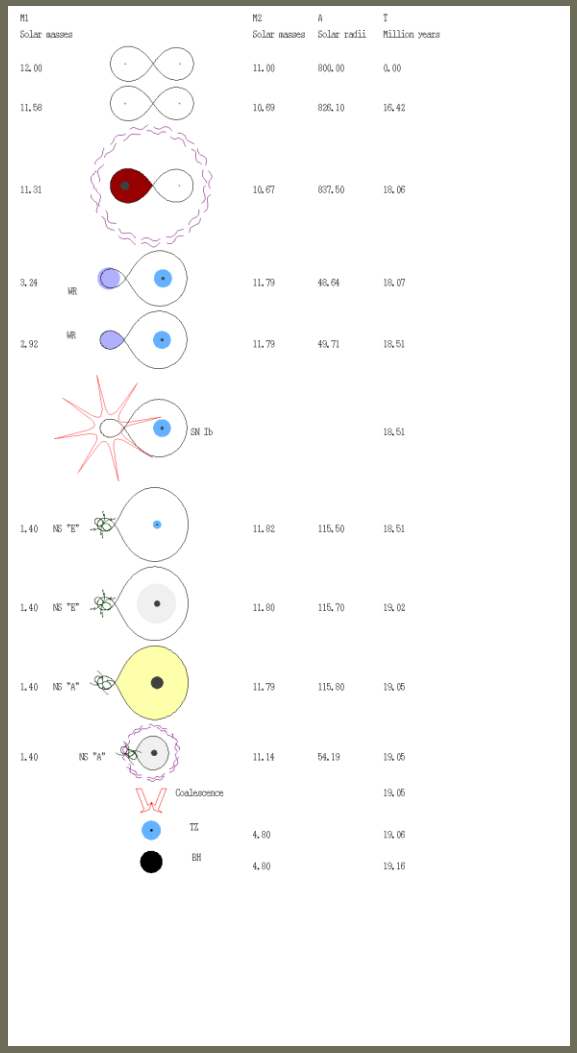

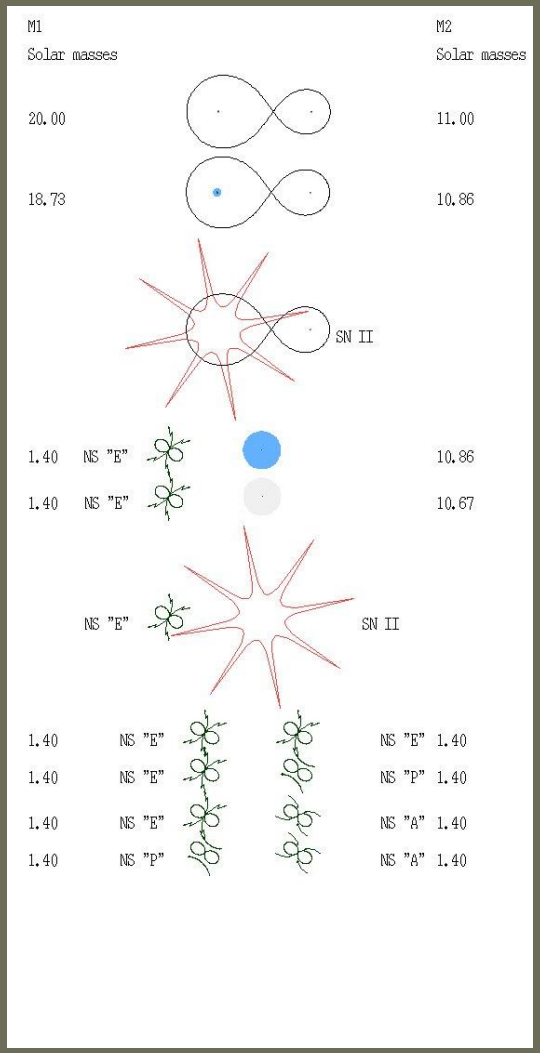

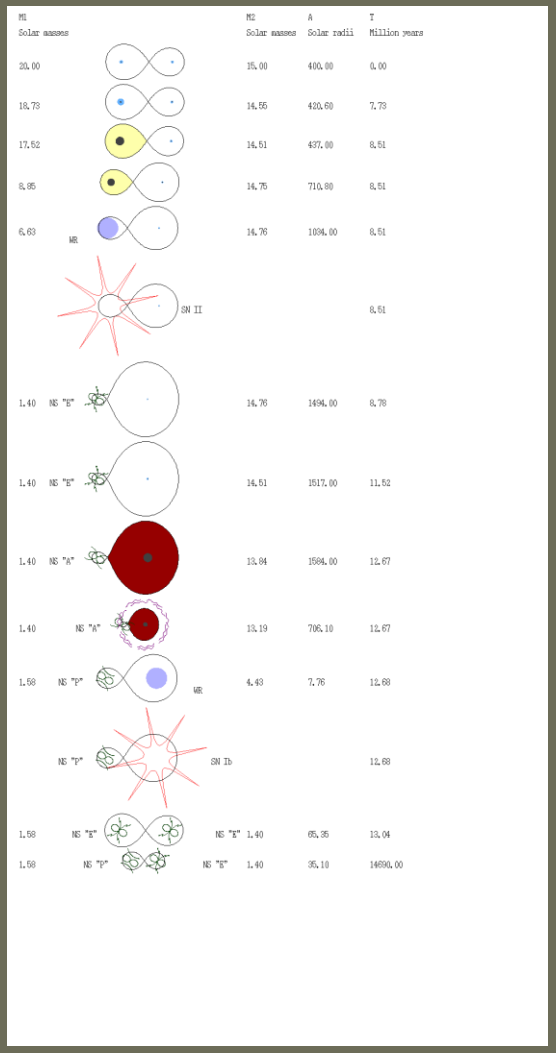

Influence of kicks on binaries

Kicks can both – destroy and **save** – binaries!

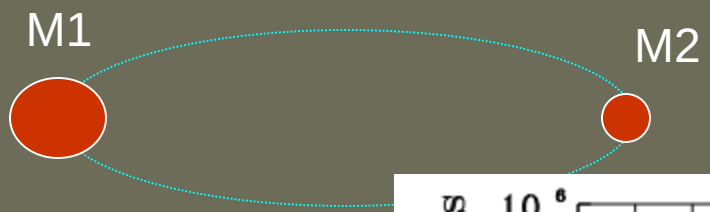

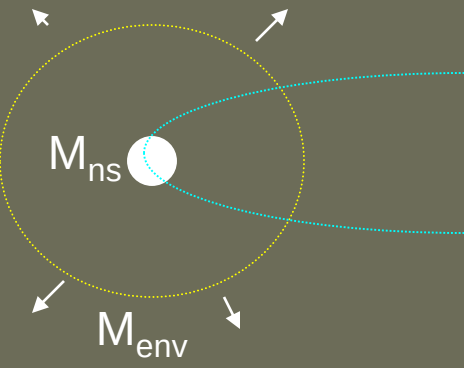

If a more massive star is about to explode, and the lost mass sum of the nd the secondary mass, should be destroyed. k can save it.

+BH, BH+BH binaries. l the more massive star ns to produce GW.

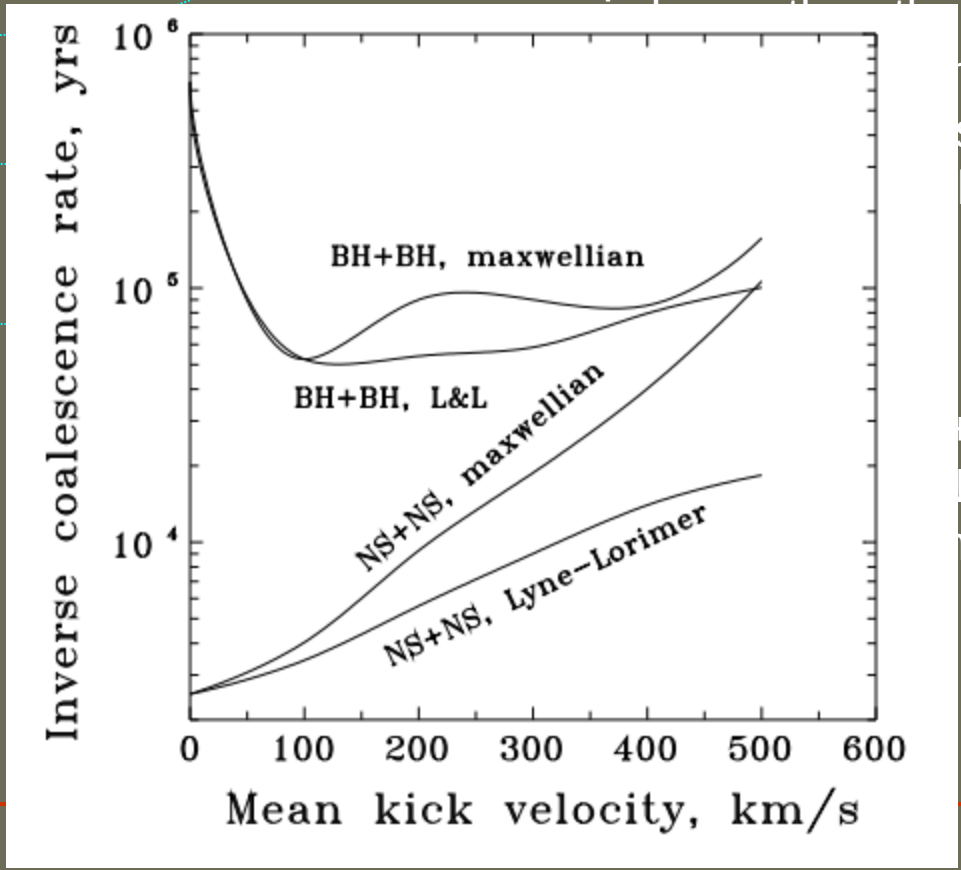

astro-ph/9702060

Parameters of binaries after kicks

Kicks significantly influence binary parameters (for example, eccentricity distribution). This is specially important for systems which survived the second explosion (NS+NS).

There are examples, when a NS rotates “in a wrong direction”, i.e. its orbital motion is in the direction opposite to the spin of the second companion.

For detailed description see Postnov, Yungelson (astro-ph/0701059) pp. 18-22.

$$\frac{a_\mathrm{f}}{a_\mathrm{i}} = \left[2 - \chi\left(\frac{w_x^2 + w_z^2 + (V_\mathrm{i} + w_y)^2}{V_\mathrm{i}^2}\right)\right]^{-1}$$

$$1 - e^2 = \chi \frac{a_\mathrm{i}}{a_\mathrm{f}}\left(\frac{w_z^2 + (V_\mathrm{i} + w_y)^2}{V_\mathrm{i}^2}\right)$$

$$\cos\theta = \frac{\vec{J}_\mathrm{f}\cdot\vec{J}_\mathrm{i}}{|\vec{J}_\mathrm{f}|\,|\vec{J}_\mathrm{i}|},$$

$$\cos\theta = \frac{V_\mathrm{i} + w_y}{\sqrt{w_z^2 + (V_\mathrm{i} + w_y)^2}}.$$

$$\chi \equiv (M_1 + M_2)/(M_\mathrm{c} + M_2) \geq 1.$$

$$\frac{V_\mathrm{f}}{V_\mathrm{i}} \geq \sqrt{\frac{2}{\chi}}.$$

Disruption condition

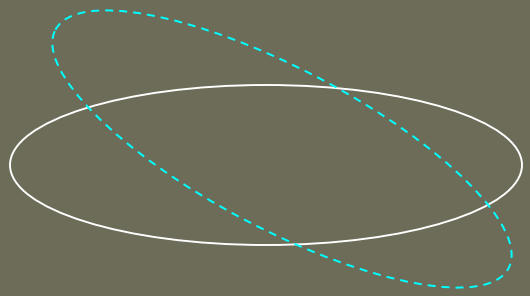

e^--supernovae with low kicks

In 80s it was proposed by Nomoto, Miyaji et al. that in some cases a SN explosion can happen due to electron capture by ^{24}Mg and ^{20}Ne (no iron core is formed).

It was noticed (Pfahl et al. 2002, Podsiadlowski et al. 2004;
van den Heuvel 2004, 2007) that among Be/X-ray binaries there is
a group of systems with small eccentricities.
But they suffered one SN explosion and there was no Roche-lobe overflow.
This means that kicks in these systems were low.
The same is true for some of NS+NS binaries.

The proposed mechanism is related to e^- -capture SN.

Such explosions can appear not only in binary systems,
but in binaries they can be more frequent.
Among isolated stars about 4% (up to ~20%!) of SN can be of this type
(Poelarends et al. 2008). [It is not clear if they appear among normal PSRs.]

Why kick is low? Uncertain. Low core mass, rapid explosion, low mass ejection…

e^- -capture SN in binaries

Poelarends et al. 2008. 0705.4643

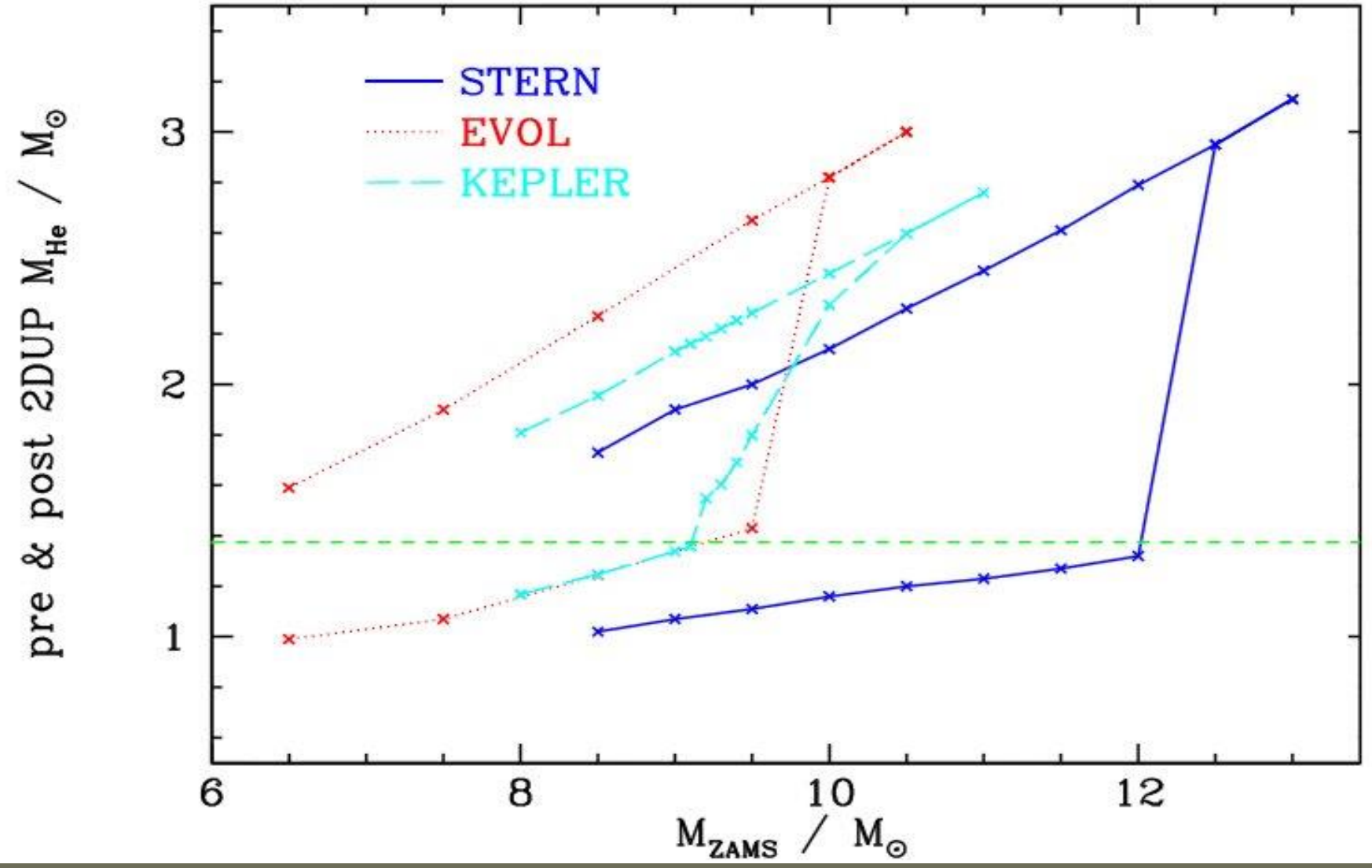

Evolution of e^--capture SN progenitors

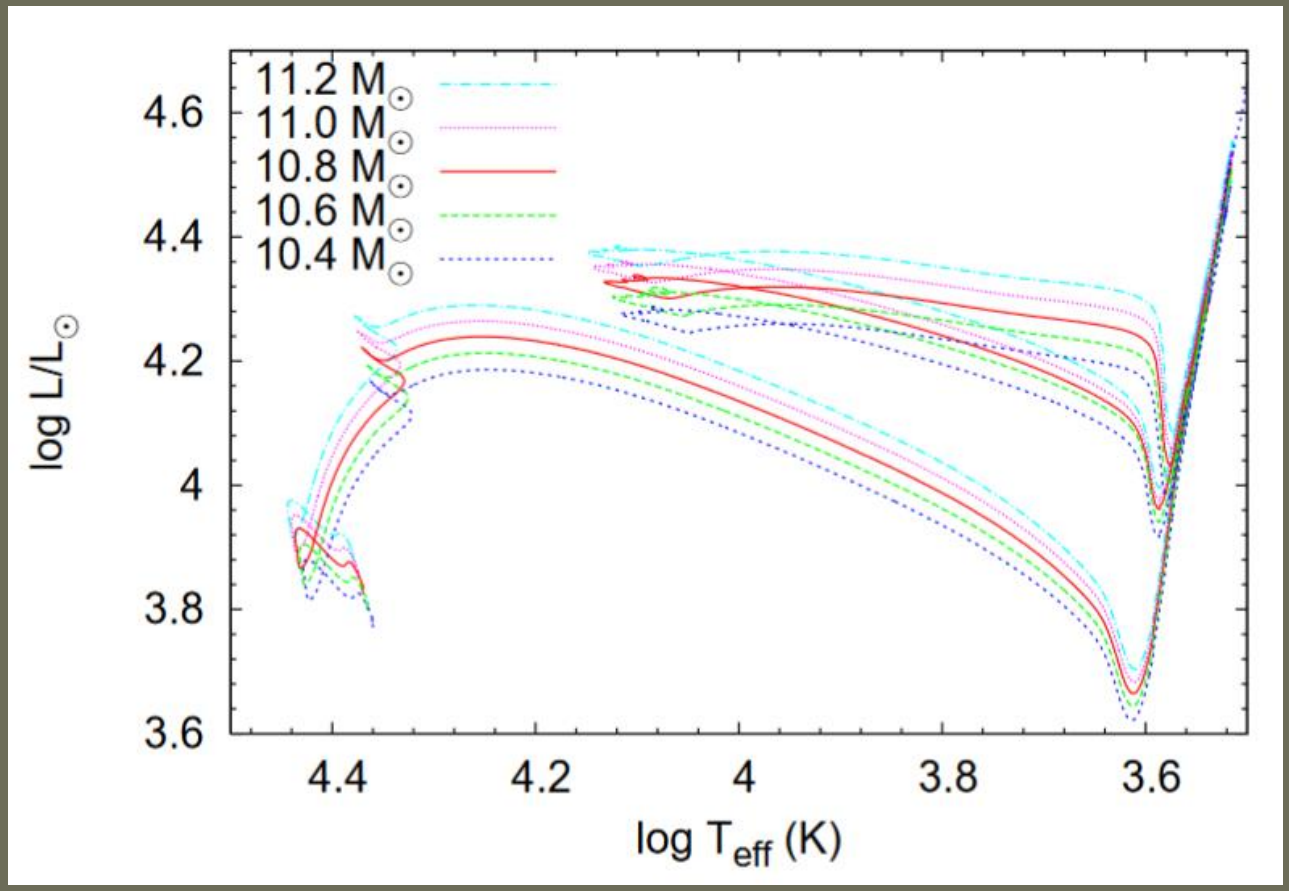

Critical core mass 1.367 solar masses.

For initial stellar masses >11 solar neon is ignited, and later on a Fe-core is formed.

1302.6402

e^--capture SN in close binaries

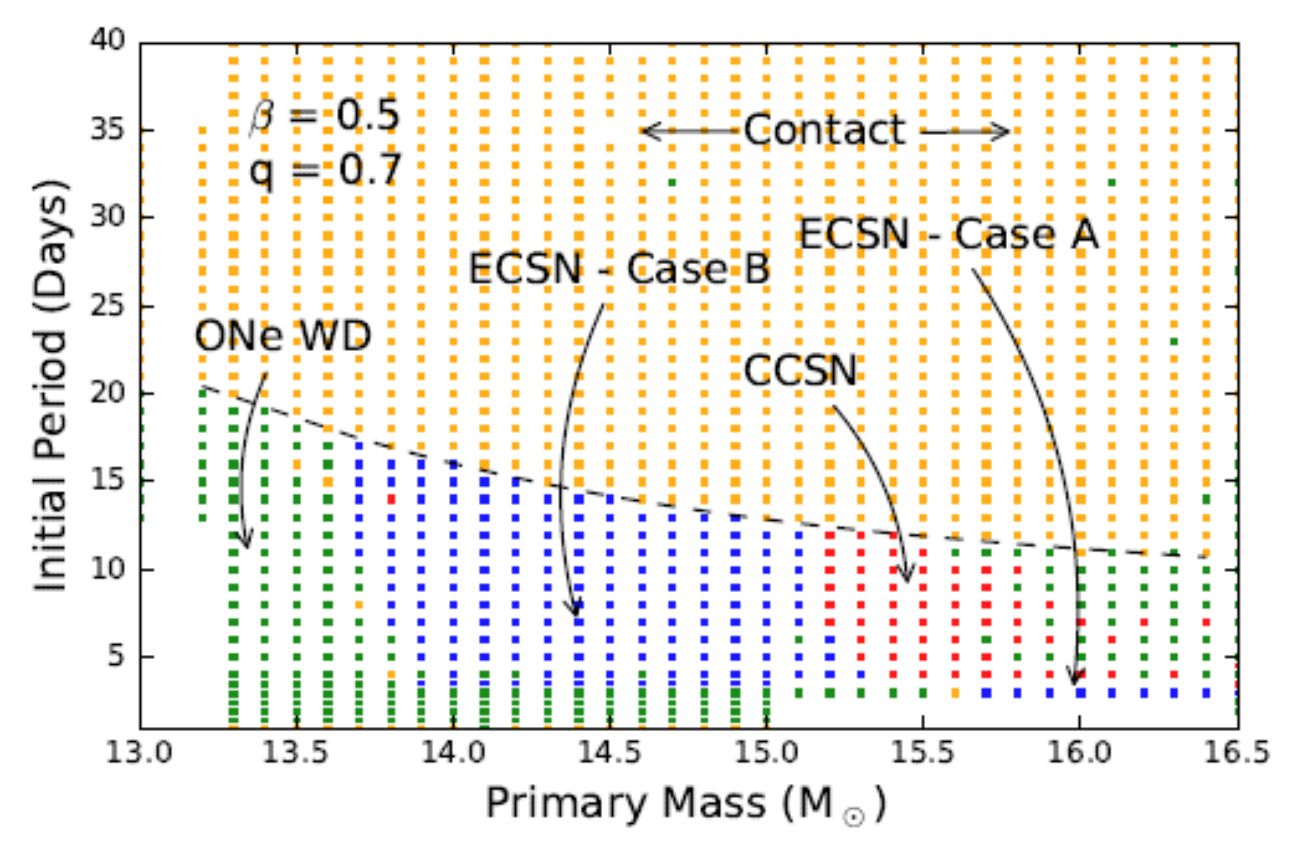

The initial primary mass and the mass transfer evolution are important factors in the final fate of stars in this mass range

1710.11143

e⁻-capture SN and Crab

Calculations confirm that in e- -capture SN kicks are low (tag-boat, i.e. gravitational pull mechanism, is not effective). Thus, Crab pulsar was not born in an e- -capture explosion.

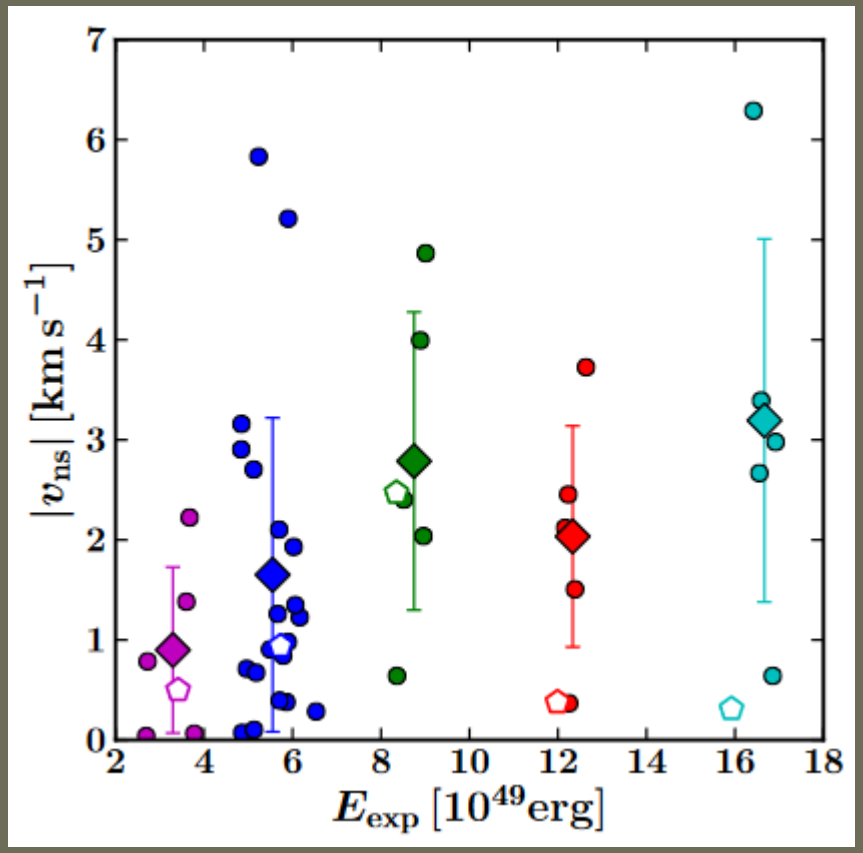

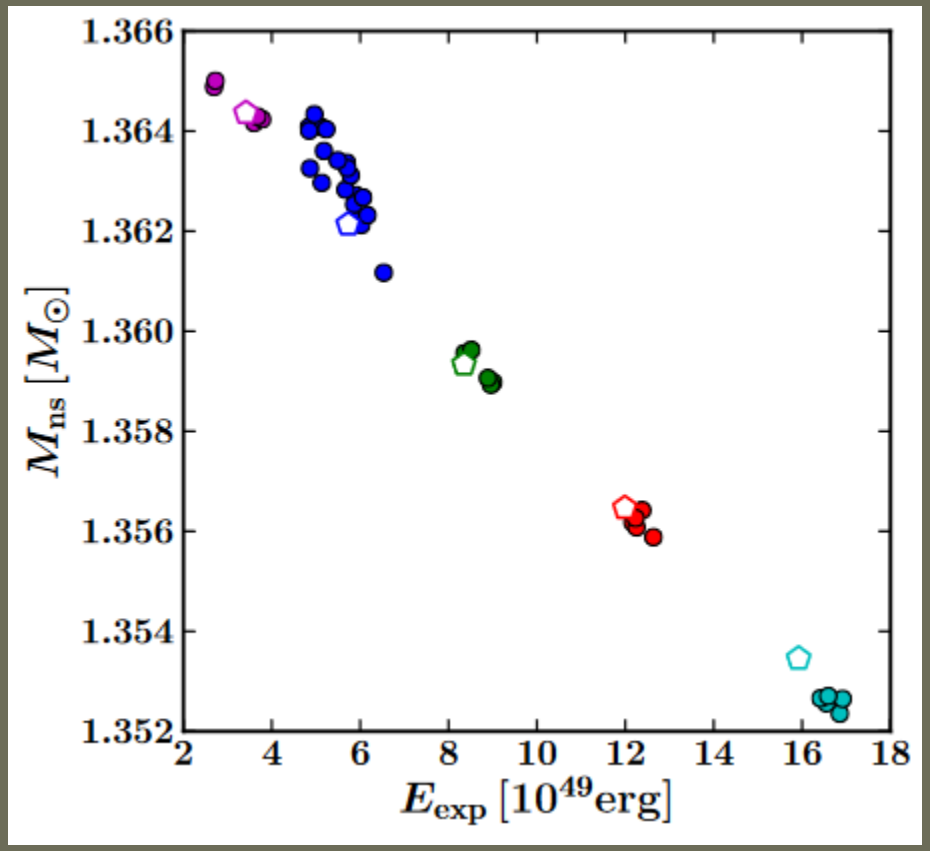

1802.05274

Pulsars with low velocities

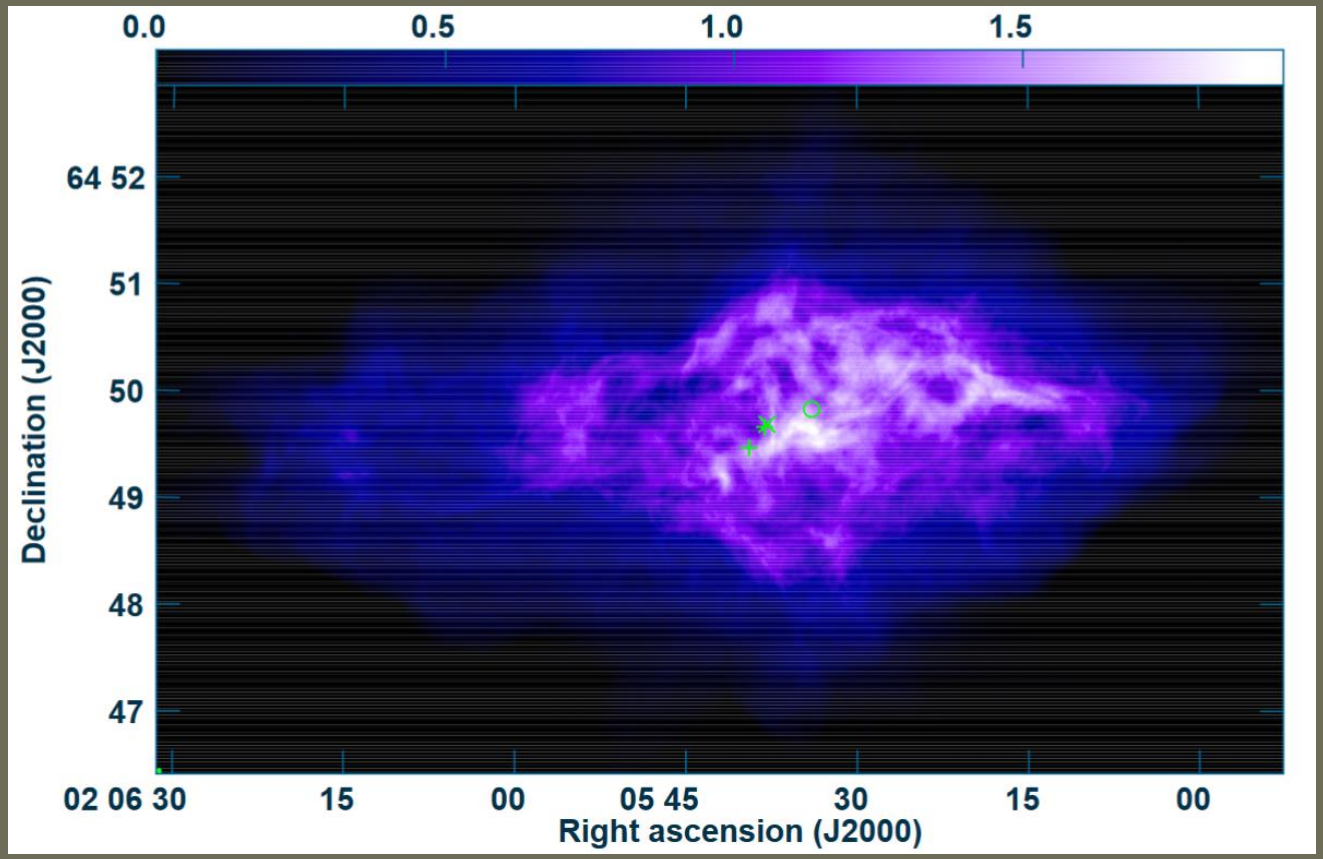

Some NSs demonstrate low spatial velocities. Obviously, this is due to low kicks.

3C58.
Low kick velocity.
Projected velocity 30-40 km/s

1302.5625

Kicks as fingerprints

Think about young highly magnetized NSs of different types:

- SGR
- AXP
- RRATs
- Magnificent Seven

Are they relatives?

It is a difficult question, but velocity measurements can give you a hint.
Even if fields are decayed, rotation is slowed down, thermal energy is emitted …
if they are relatives – velocity distributions must be identical.
Unfortunately, now we do not know the answer.

Magnetar velocity measurements

SGR 1806-20	350 +/- 100 km/s	arXiv:1210.8151
SGR 1900+14	130 +/- 30 km/s	arXiv:1210.8151
PSR J1550-5418	280 +/- 130 km/s	arXiv:1201.4684
XTE J1810-197	200 km/s	Helfand et al. (2007)

Record velocities

1. PSR J1357-6429 1600-2000 km/s arXiv:1206.5149 - shown to be wrong
2. IGR J11014-6103 2400-2900 km/s arXiv: 1204.2836

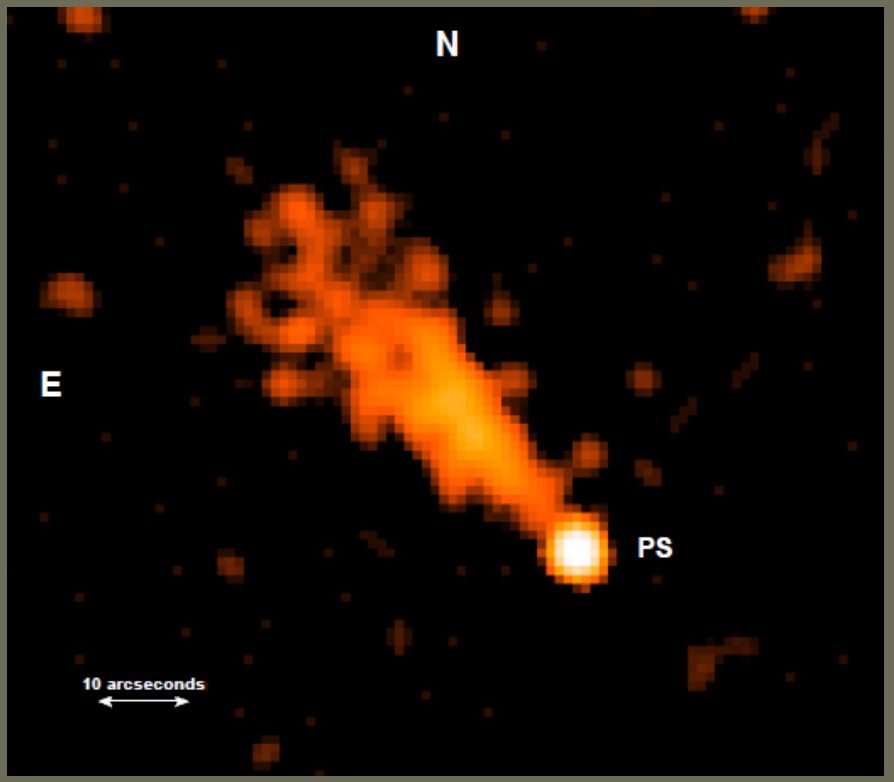

CCO velocities

RX J0822-4300 in the Supernova Remnant Puppis A
672 +/- 115 km/s
arXiv: 1204.3510

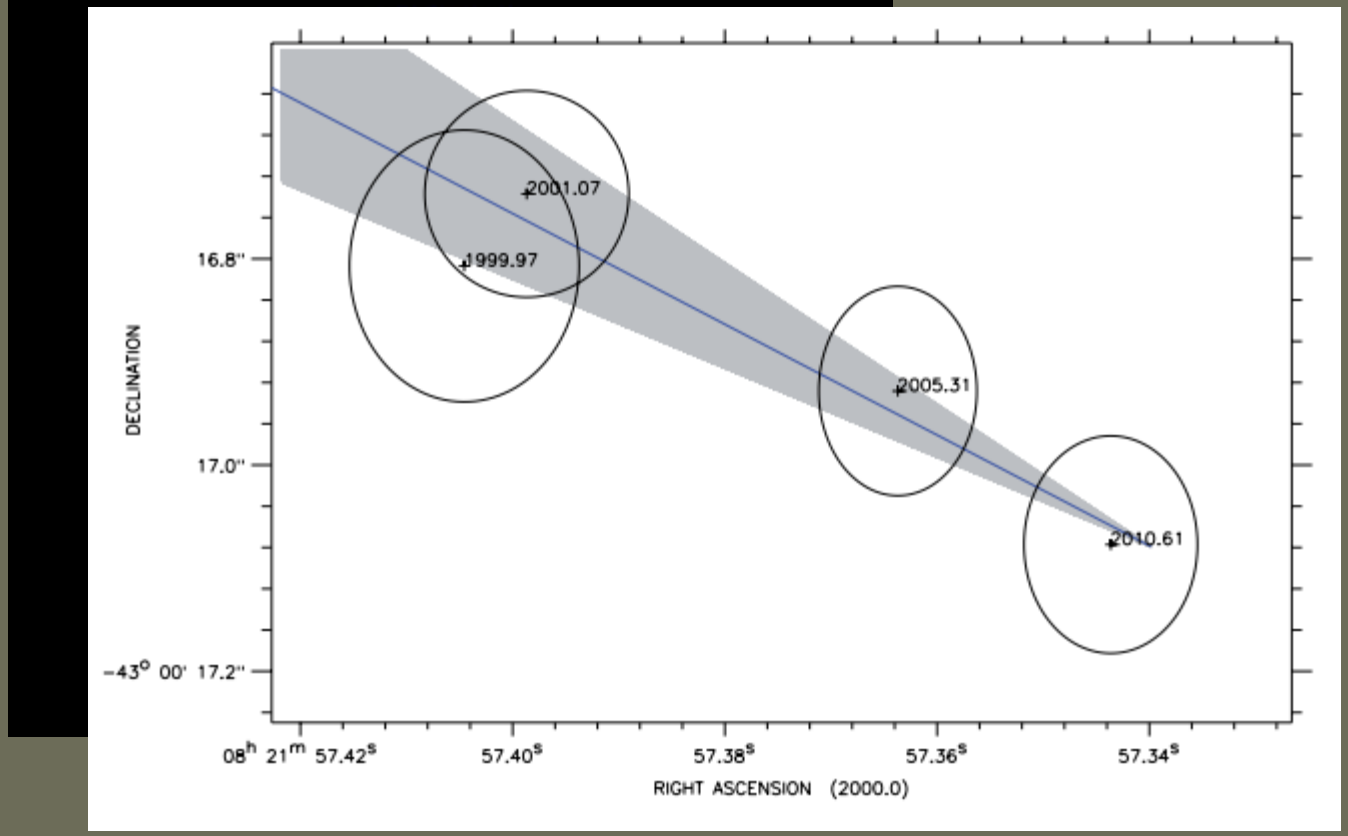

Kick velocity and SNR morphology

18 young (<20 kyr) SNR with NSs (with velocity) fully imaged by Chandra or ROSAT. Thermal X-ray emission distribution is stidued.

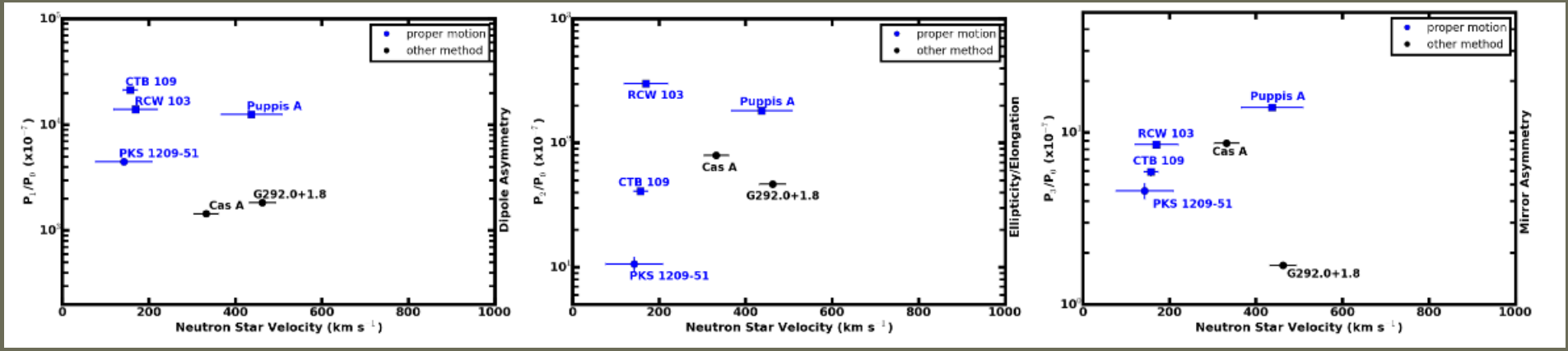

1705.08454

Dipole anisotropy and velocity

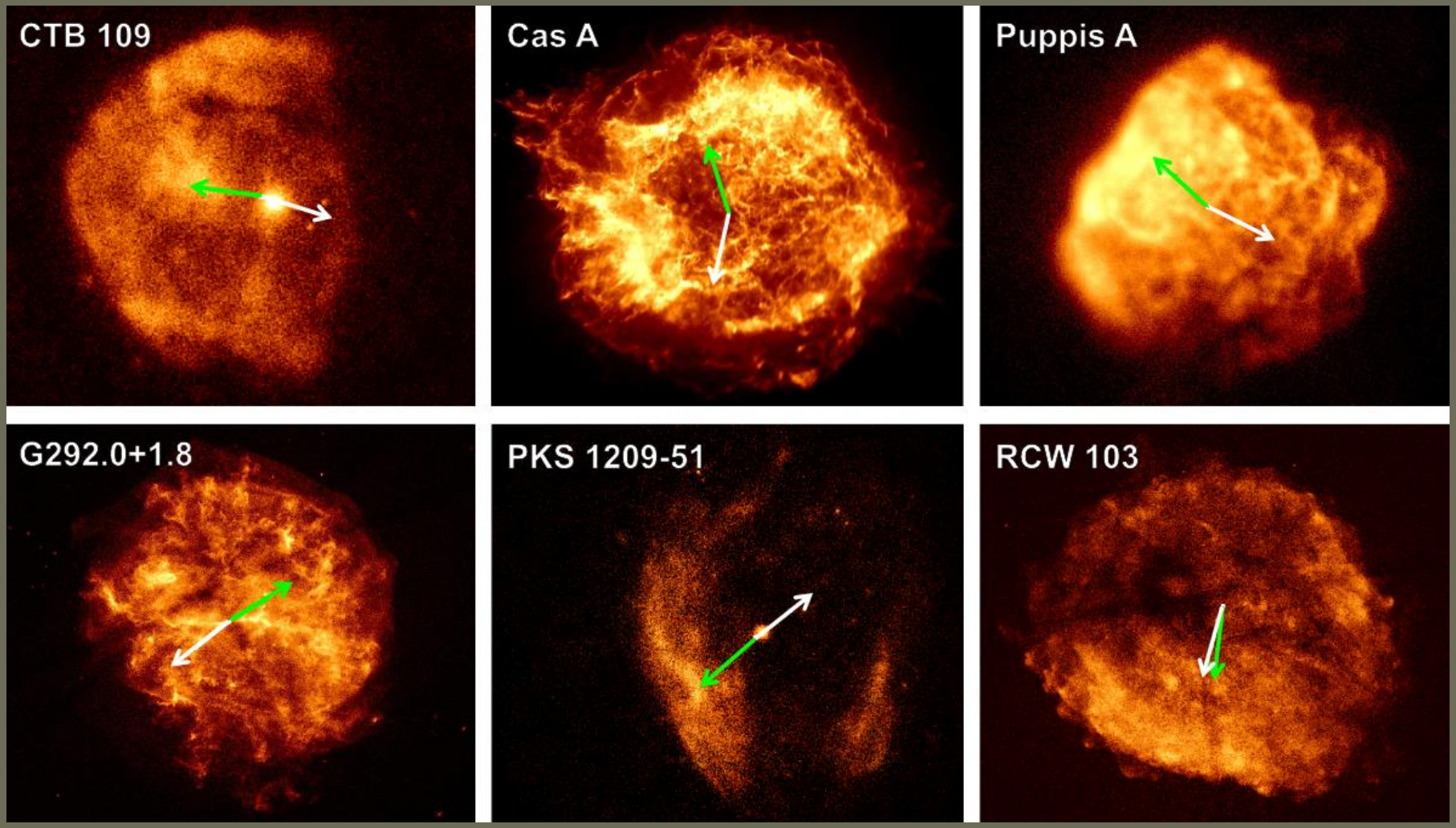

Green – dipole anisotropy of X-ray thermal emission distribution

1705.08454

Spinnig-up kicks

Do you play billiard?

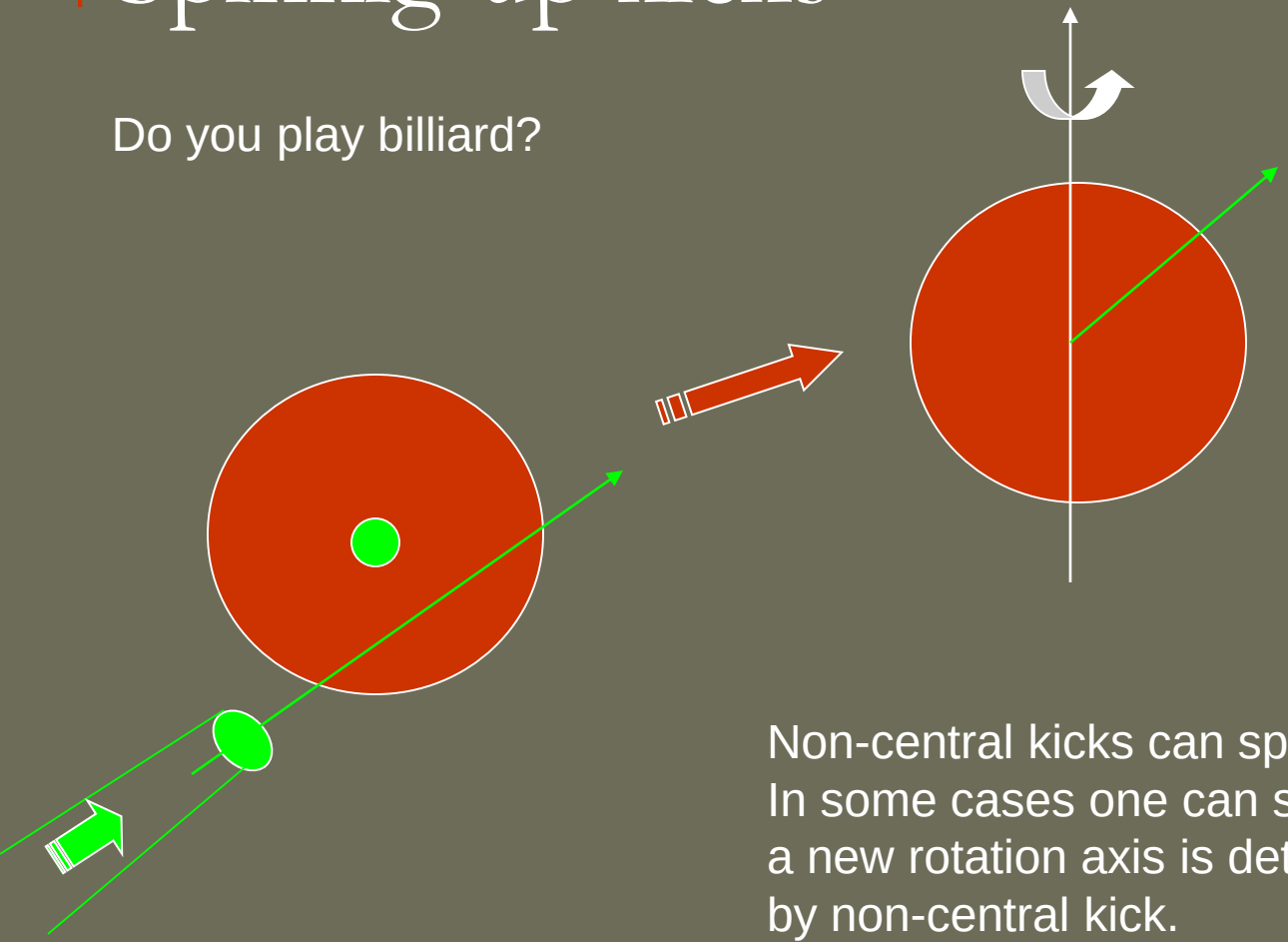

Non-central kicks can spin-up a NS.
In some cases one can speculate that
a new rotation axis is determined mainly
by non-central kick.
But then velocity - spin period correlation is expected.

Evolution of isolated NSs and kicks

Evolution of an isolated NS depends on the intensity of its interaction with the ISM. This intensity depends on the relative velocity of a NS and the ISM.

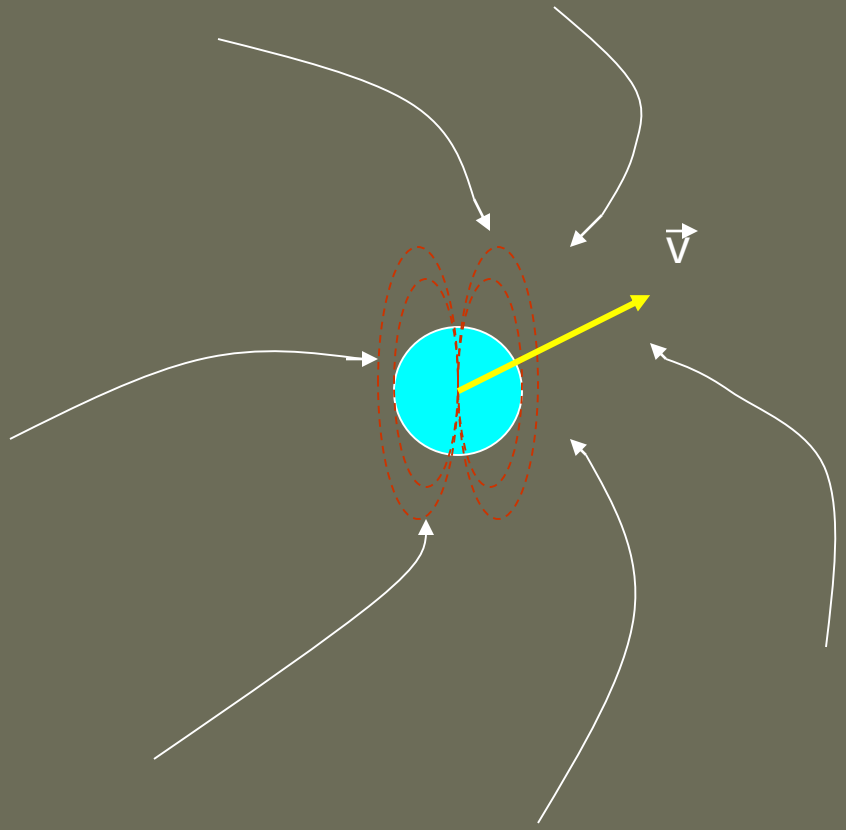

Will a NS start to accrete from the ISM, or will it stay as Ejector, or Propeller, or will in enter another regime strongly depends on the relative velocity of a NS and the ISM.

Galactic potential

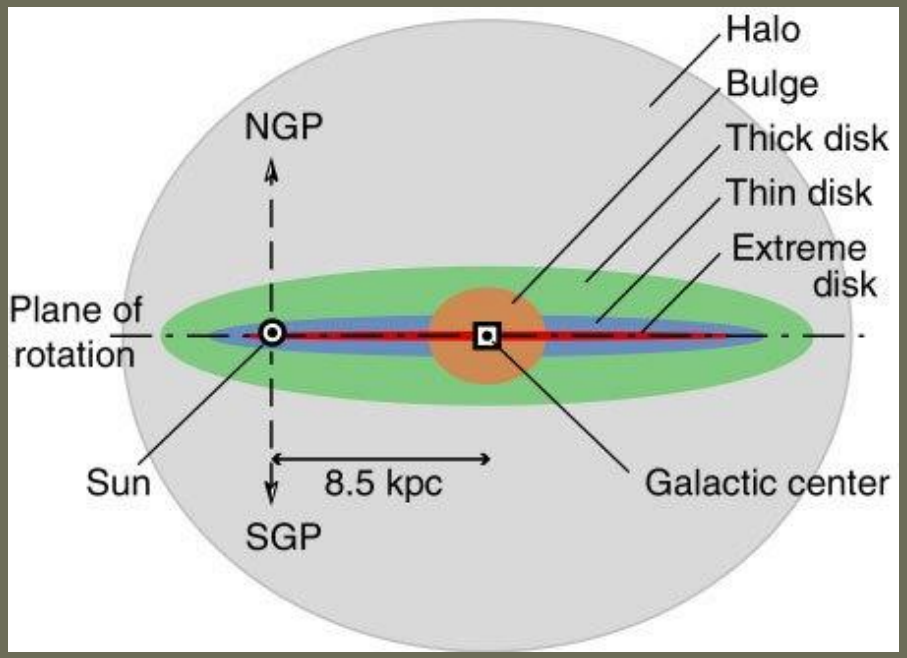

Clearly, some NSs are rapid enough to leave the Galaxy.

Z-distribution of PSRs is much wider than the progenitors' one.

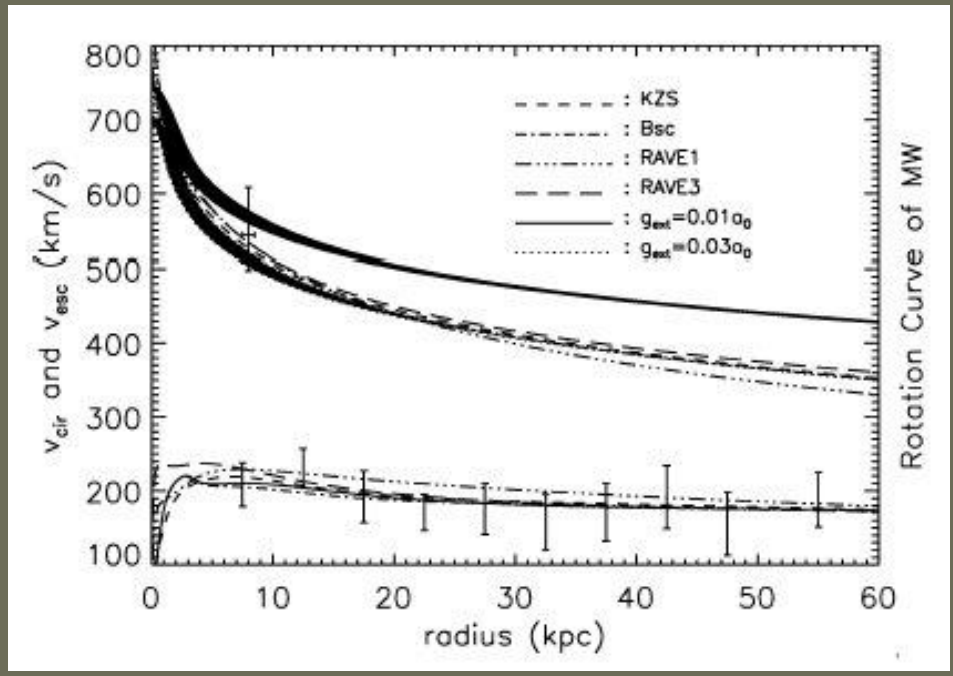

Wu et al. 2008

Mass distribution in the Galaxy

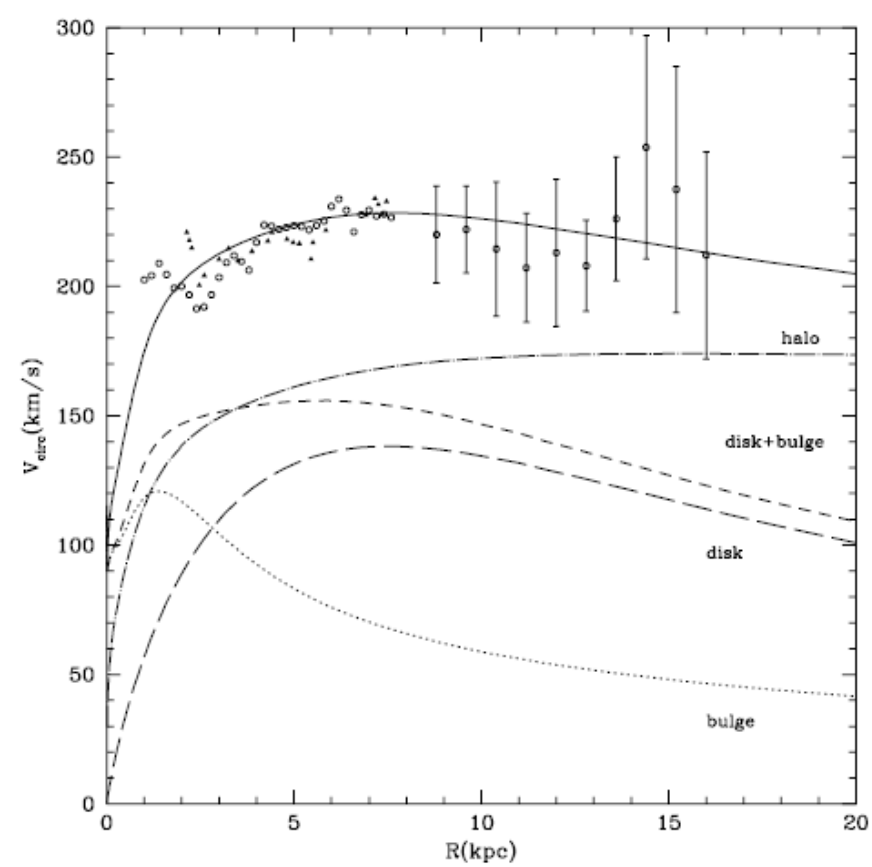

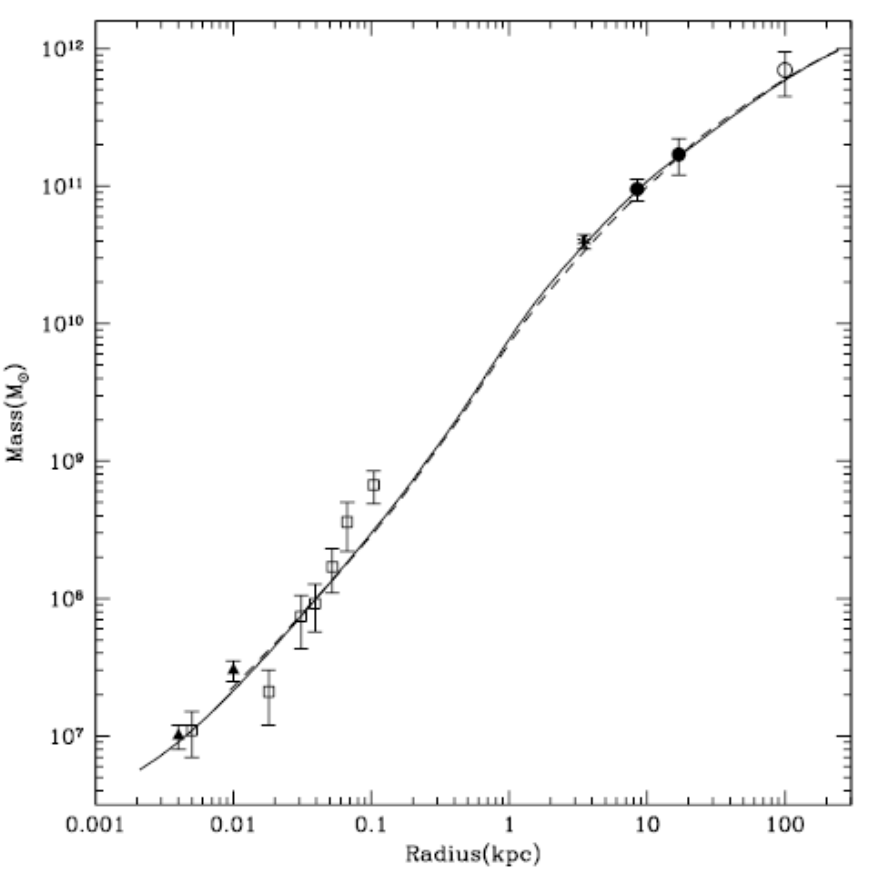

Klypin et al. (2002)

“Paczynski” model

Disc+Buldge+Halo
Actually, it is Miyamoto, Nagai (1975) model.
It is simple and popular in NS motion calculations.

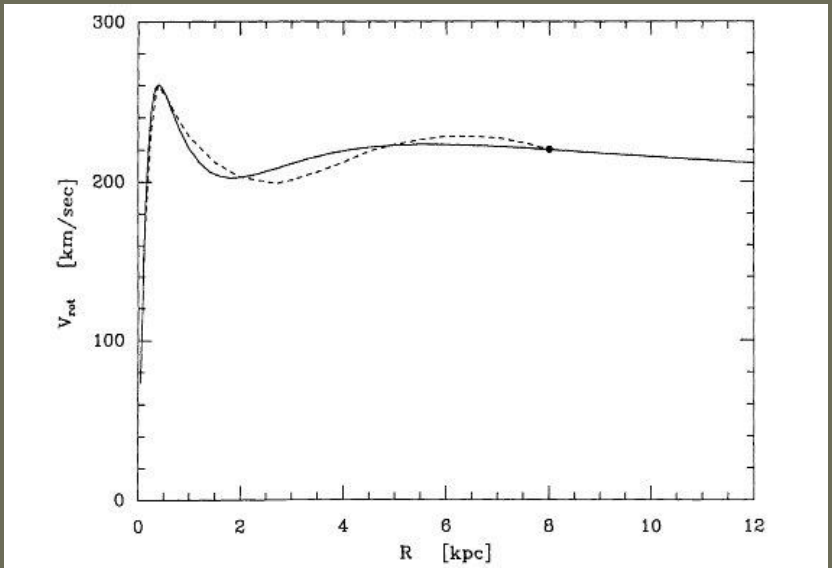

$$\Phi_i(R,z) = \frac{GM_i}{\{R^2 + [a_i + (z^2 + b_i^2)^{1/2}]^2\}^{1/2}}, \quad R^2 = x^2 + y^2$$

$$\Phi_h = -\frac{GM_c}{r_c}\left[\frac{1}{2}\ln\left(1 + \frac{r^2}{r_c^2}\right) + \frac{r_c}{r}\,\mathrm{atan}\left(\frac{r}{r_c}\right)\right],$$

$$M_c \equiv 4\pi\rho_c r_c^3$$

$$a_1 = 0, \quad b_1 = 0.277\ \mathrm{kpc}, \quad M_1 = 1.12 \times 10^{10}\ M_\odot,$$
$$a_2 = 3.7\ \mathrm{kpc}, \quad b_2 = 0.20\ \mathrm{kpc}, \quad M_2 = 8.07 \times 10^{10}\ M_\odot,$$
$$r_c = 6.0\ \mathrm{kpc}, \quad M_c = 5.0 \times 10^{10}\ M_\odot,$$

At the very center one has to add the central BH potential

Examples of old NS distribution

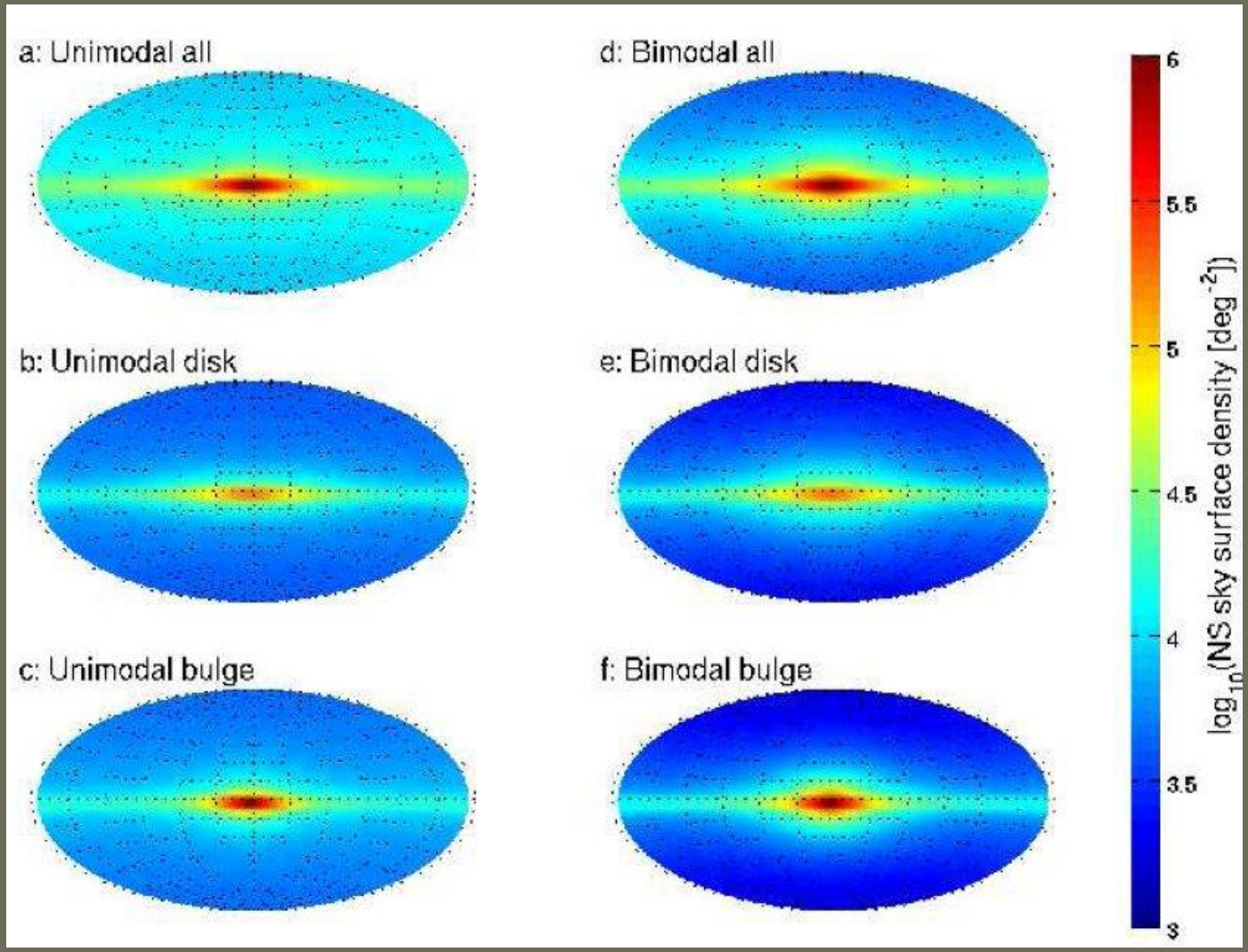

0910.3684

Spatial density of NSs

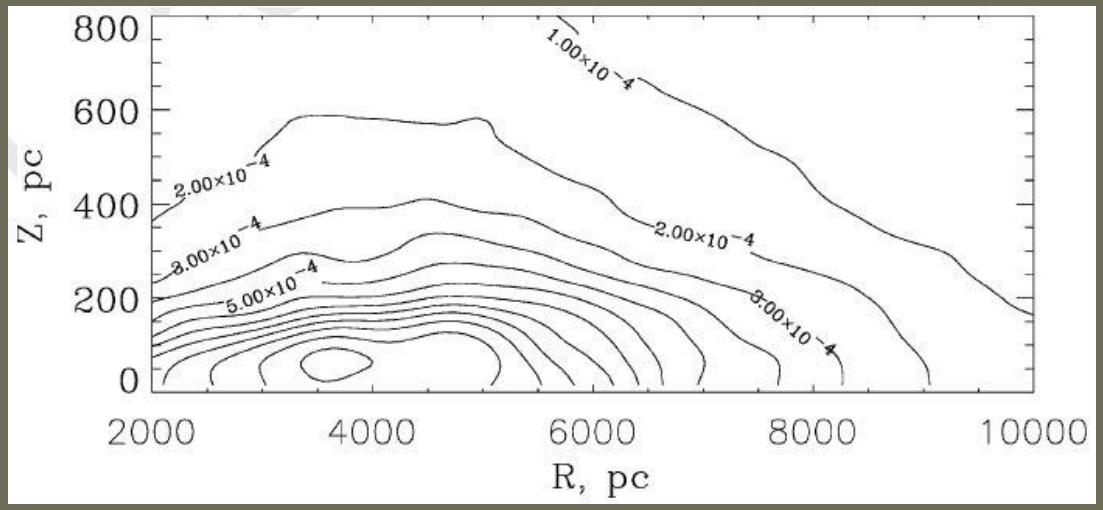

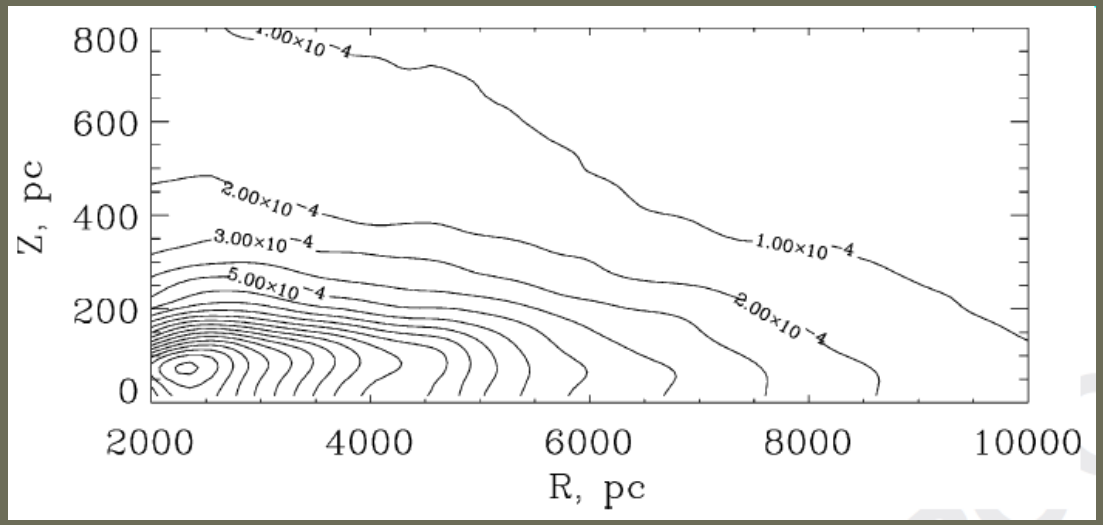

In both models N=5 10^8.
Kick: ACC02.
Potential: Paczynski 1990

NS formation rate is assumed to be proportional to the square of the ISM density at the birthplace.

Formation rate is proportional to [exp(−*z*/75 pc) exp(−*R*/4 kpc)].

astro-ph/0305599

X-ray sources in other galaxies

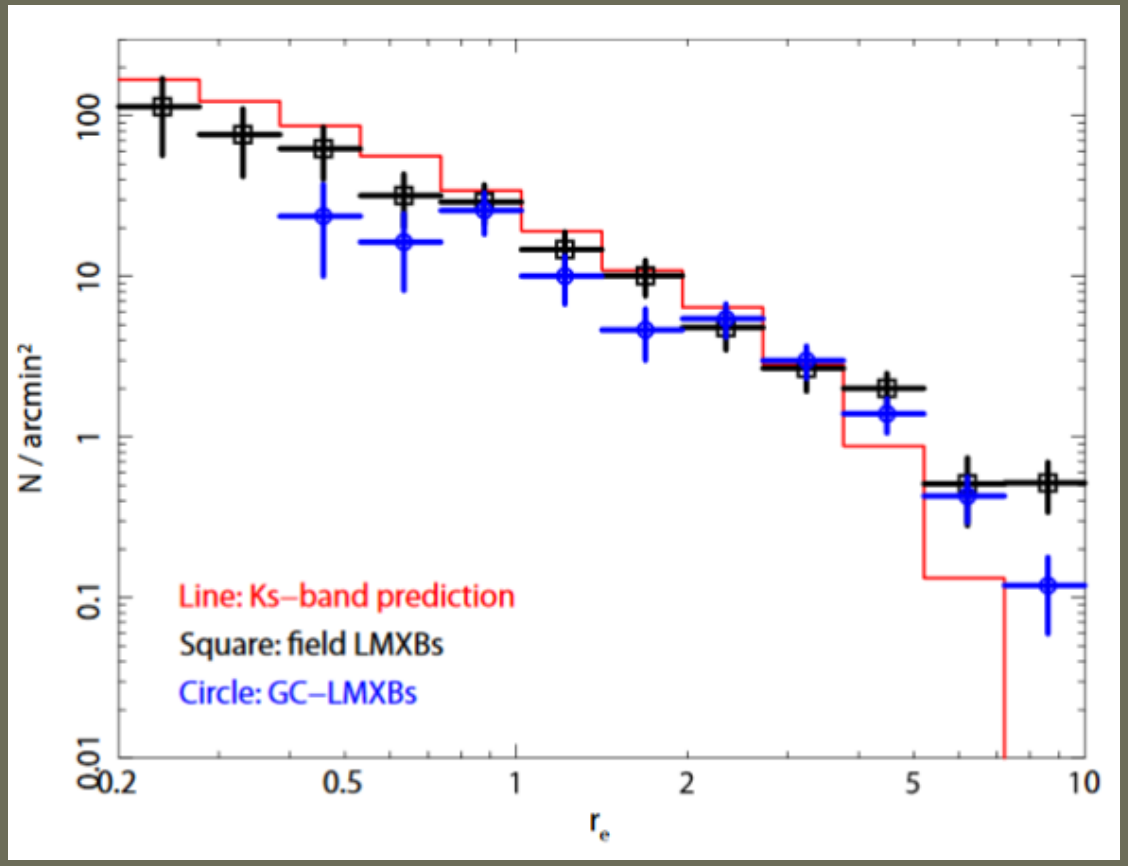

X-ray sources are shifted from the stellar light distribution.
This might be due to kicks, especially in the case of NS binaries.

The effect cannot be explained by sources in globular clusters.

1211.0399

Black hole kicks

Do BHs obtain kicks?

- they are more massive
- horizon is formed
- SN mechanism can be different

If before the horizon formation
a “protoNS-like” object is formed,
then there should be a kick, but
smaller (in km/s) due to larger mass.

We do not know isolated BHs,
but we know binaries.
It is possible to measure velocity.

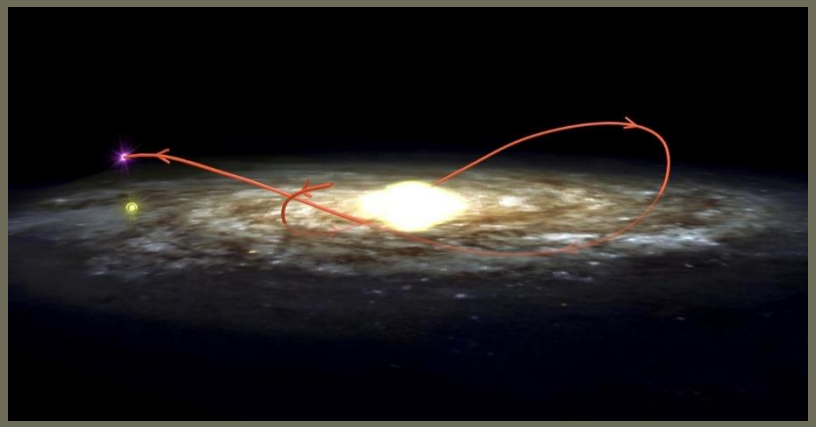

XTE J1118+480

Knowing just a velocity it is difficult
to distinguish kick from dynamical
interaction or initially large velocity
(for example, a system can be
from a globular cluster).

On the mechanism of BH kick see 1306.0007

GROJ1655-40

Kick 45-115 km/s

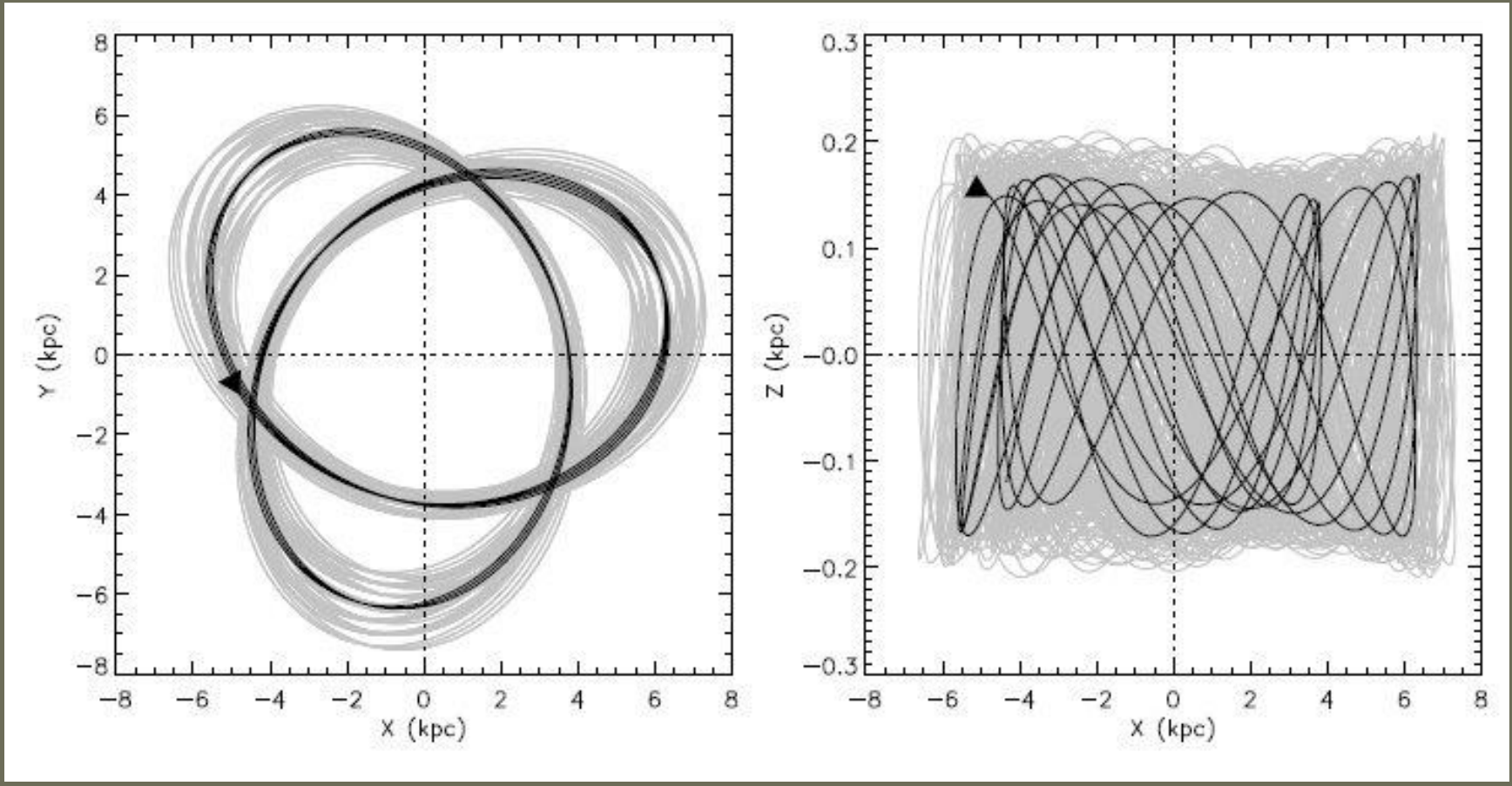

Willems et al. (2005)

Cyg X-1

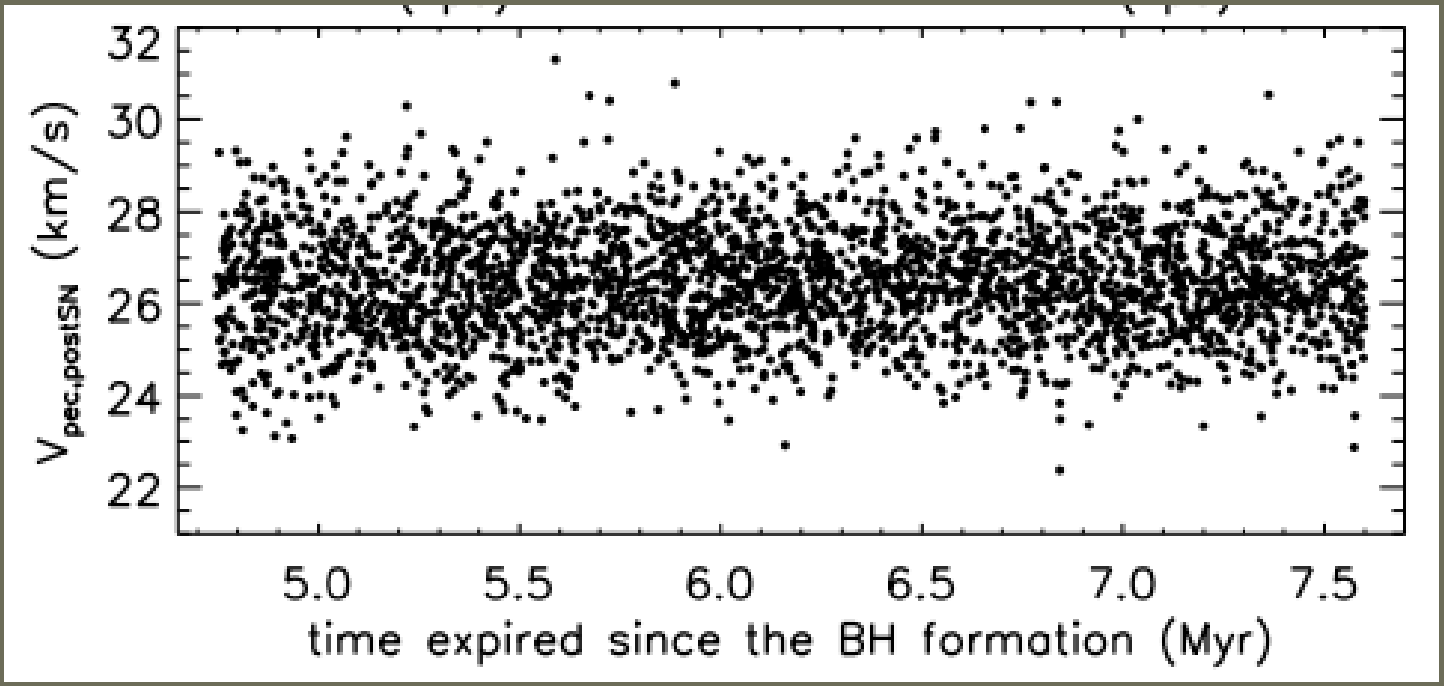

For this system the distance is known very precisely.
This allows to trace the trajectory back
and derive the value of post-SN peculiar velocity.

It is equal to 22-32 km/s.
Probably, the BH obtained a moderate kick <77 km/s.

1107.5585

BH binaries in the Galaxy

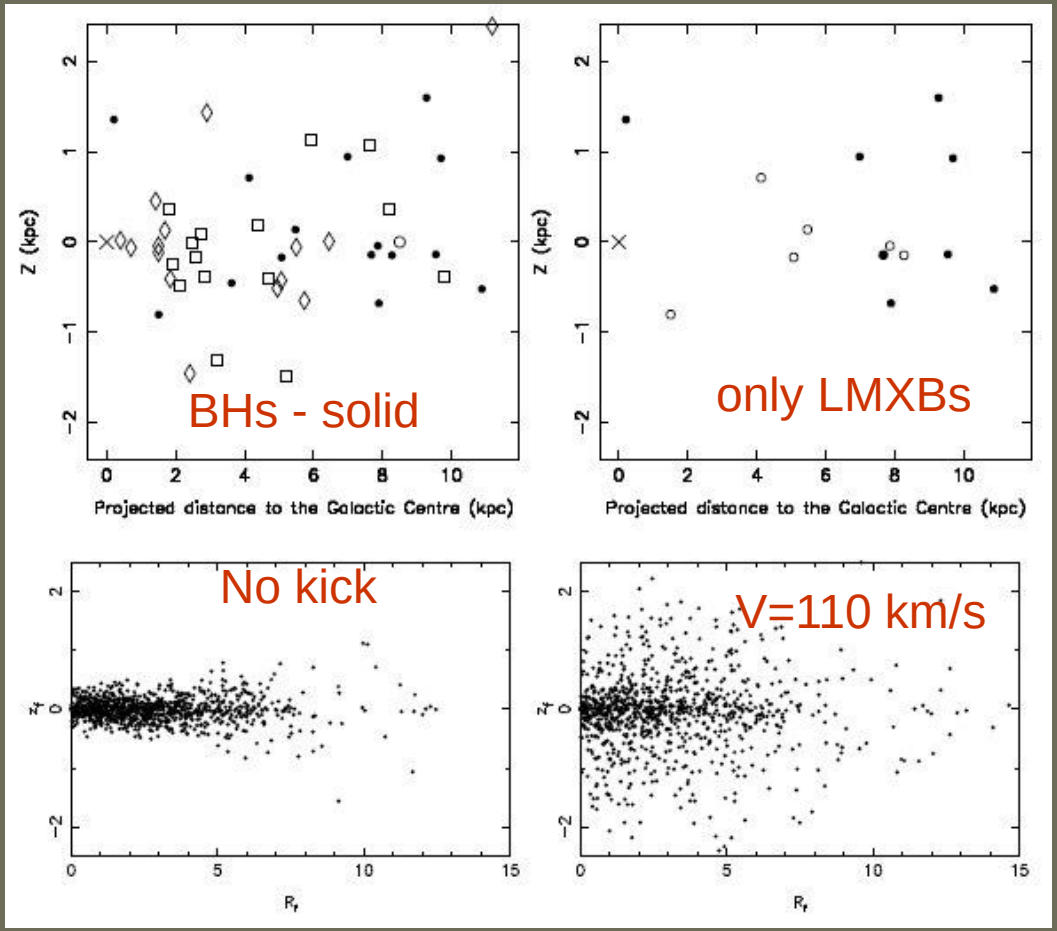

The situation is not clear when we look at the whole population:

- Distribution for BHs is similar to the one for NS (for kick)
- Modeled distribution for zero kick can explain, roughly, the spatial distribution (against large kick)

Also line-of-site velocities are not high

Nelemans (2004)

Black hole kick velocities

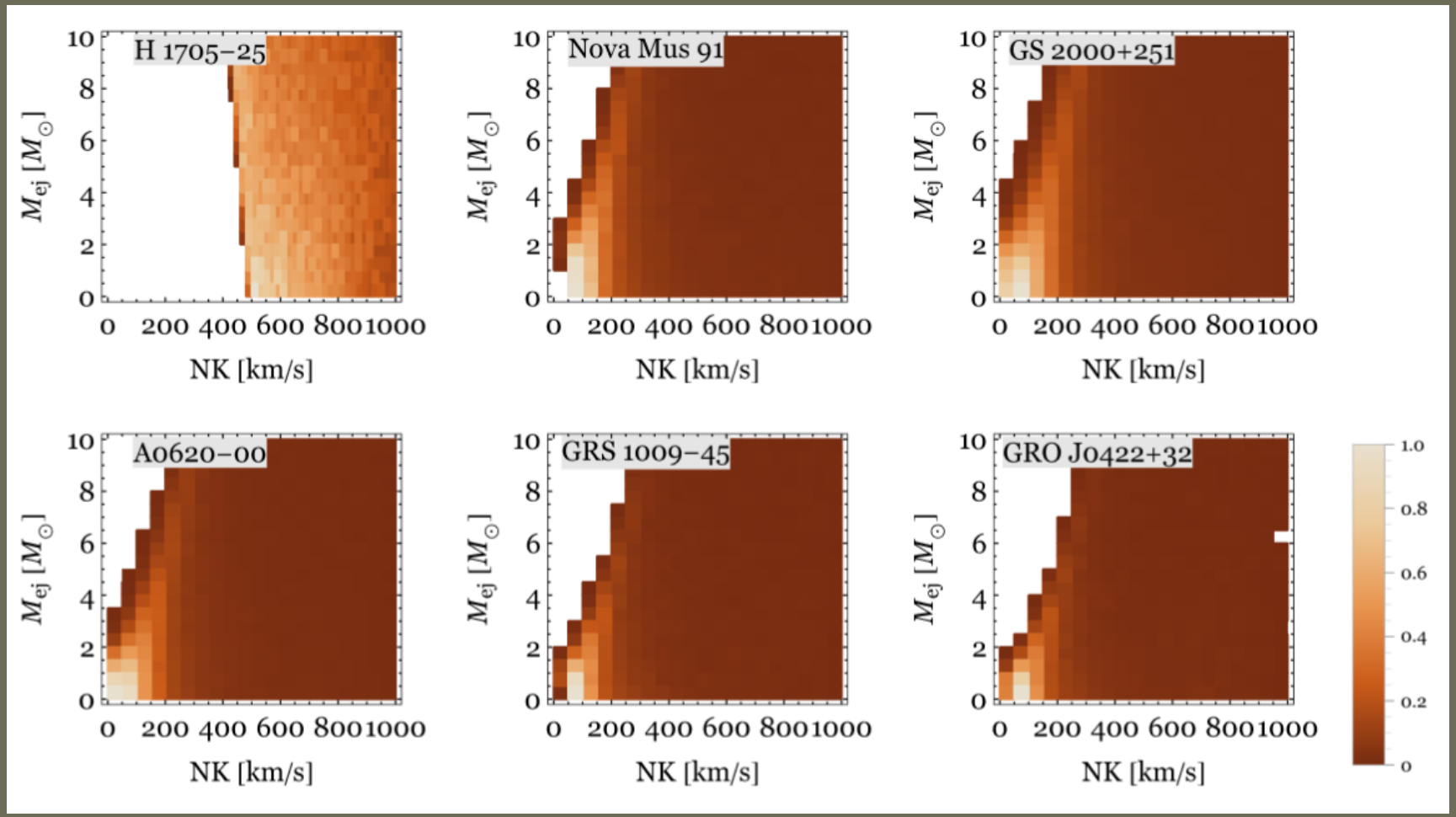

Some BHs receive large kicks at birth. Difficult to explain by scaling from NSs.

1507.08105

H 1705-250

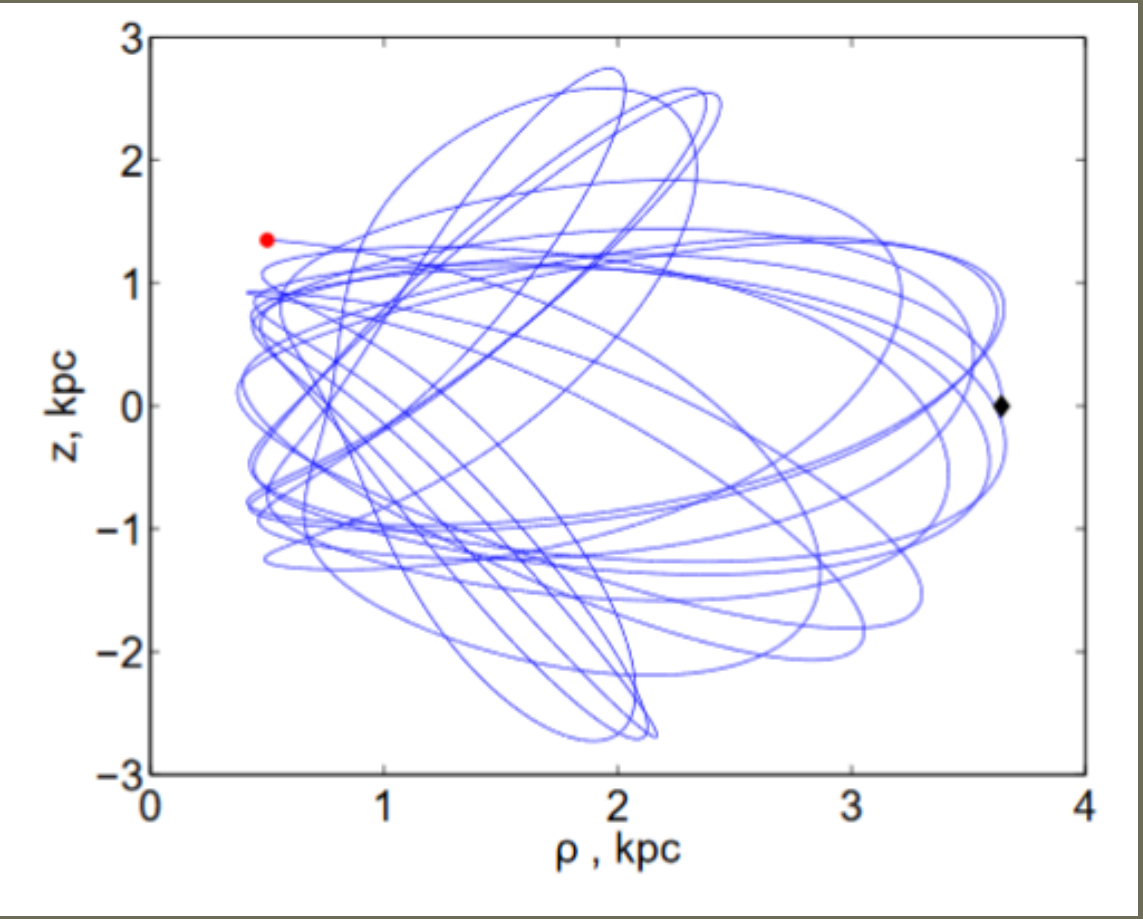

Large kick is not necessary.
~100 km/s is enough.

1510.03871

IC 10 X-1

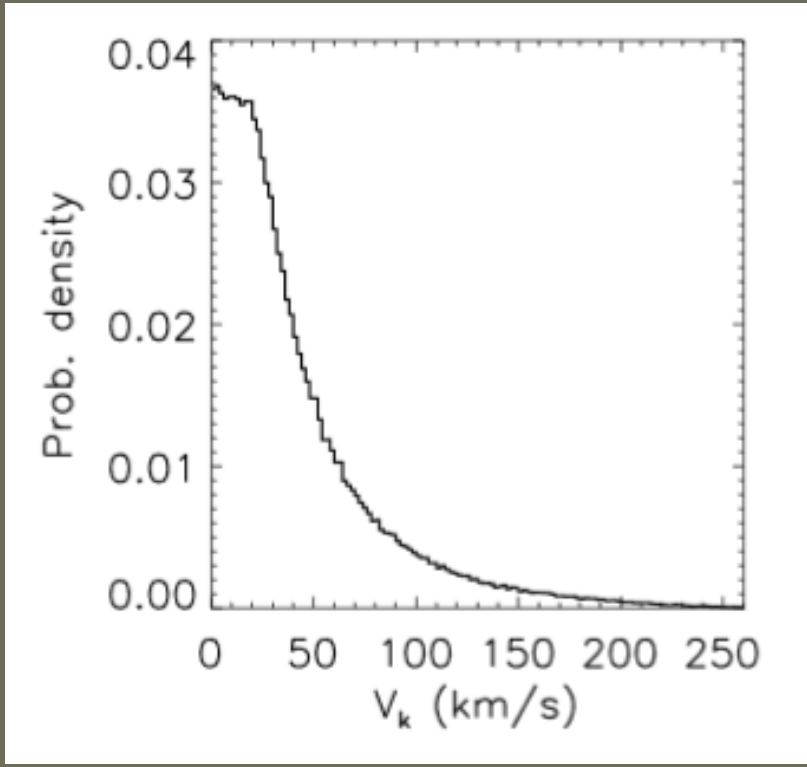

Low kick <130 km/s.

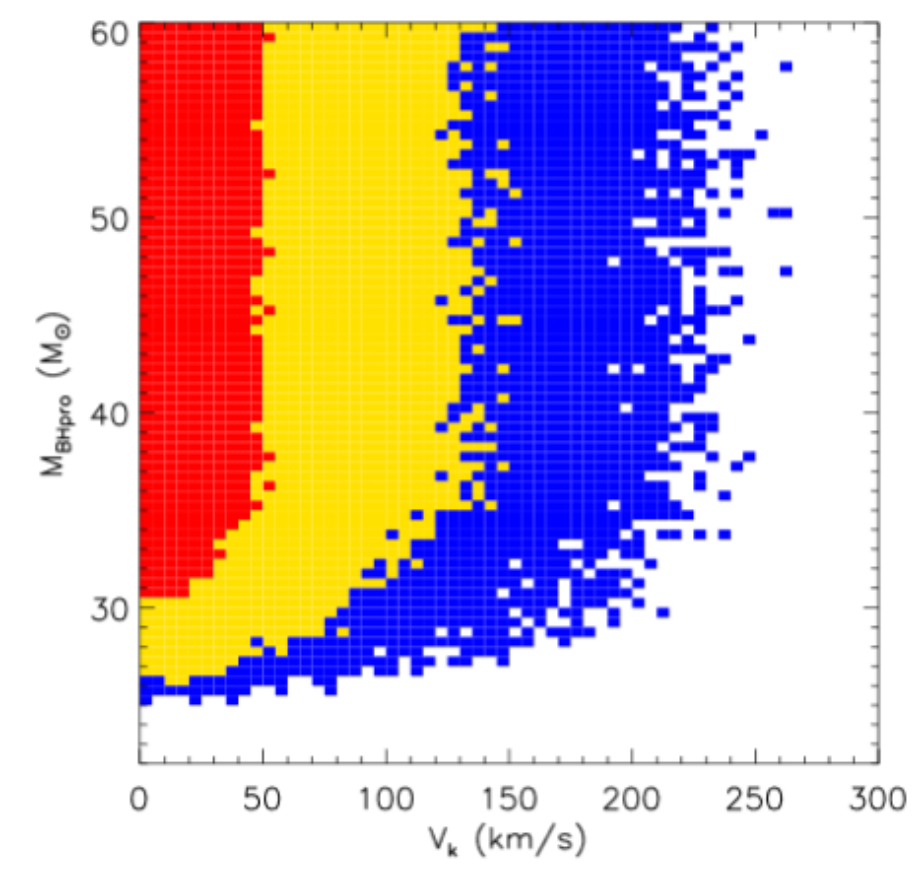

$M_{BH\ Pro}$ – progenitor mass before BH formation

1304.3756

Velocity of BH and NS X-ray binaries

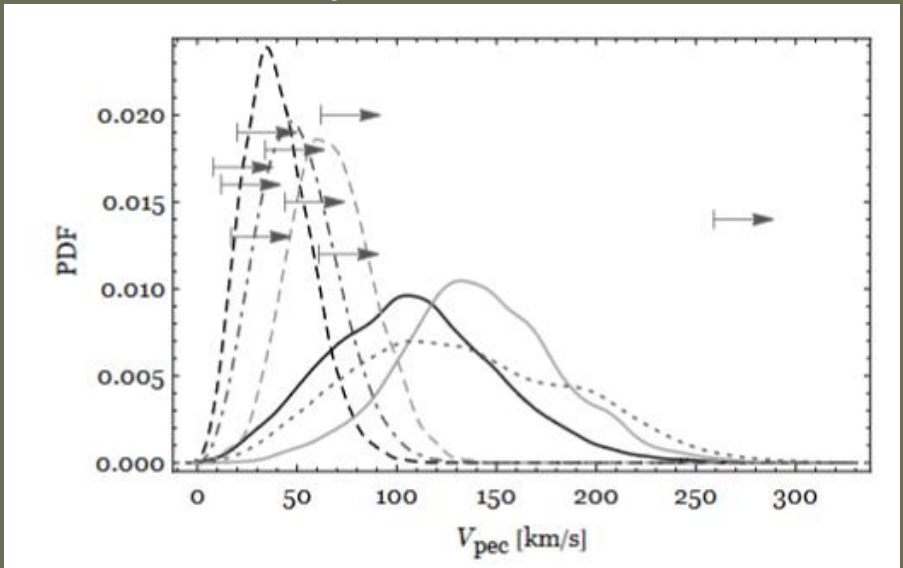

Some BHs might obtain significant kick.

NS binaries kick distribution is compatible with the one derived from PSRs.

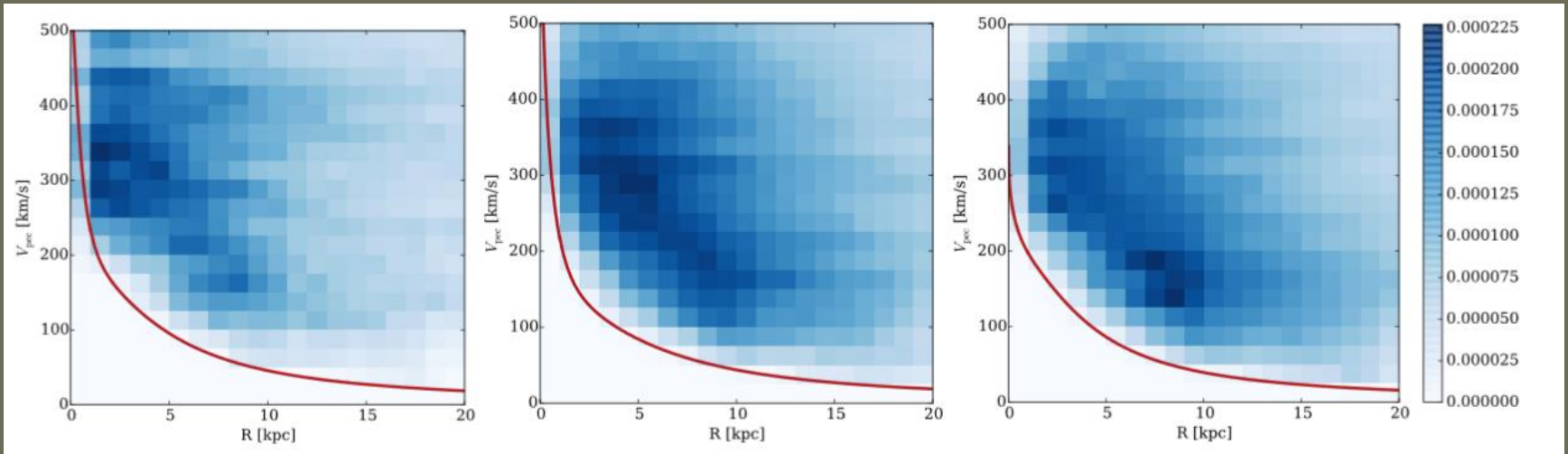

$$V_{\rm pec,min} = \sqrt{2[\Phi(R_0, z) - \Phi(R_0, 0)]},$$

1701.01347

EMRI and compact objects kicks

Kicks received by NSs and BHs in the nuclear cluster around a SMBH can result in extreme mass ratio inspirals (EMRI).
The rate is >~10^{-8} per year per galaxy.
eLISA can detect up to tens of event per year of observations.

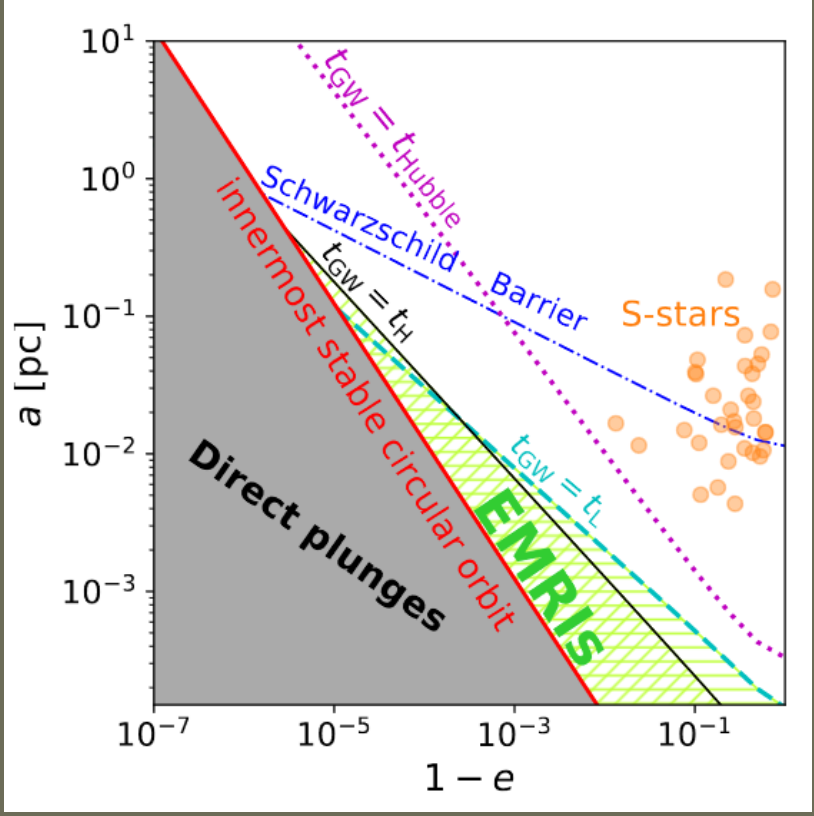

Populations with higher kick produce more SN-EMRI.

SN-EMRI contribute ~10% of all EMRI (in the case of the Milky Way).

1902.04581

Conclusions

- NSs and (most probably) BHs obtain natal kicks
- For NSs kick velocity can be as large as >1000 km/s
- The direction of the kick and rotation are correlated
- Kicks depend on the SN mechanism
- Kicks influence parameters of binaries
- Kicks influence evolution of isolated NSs

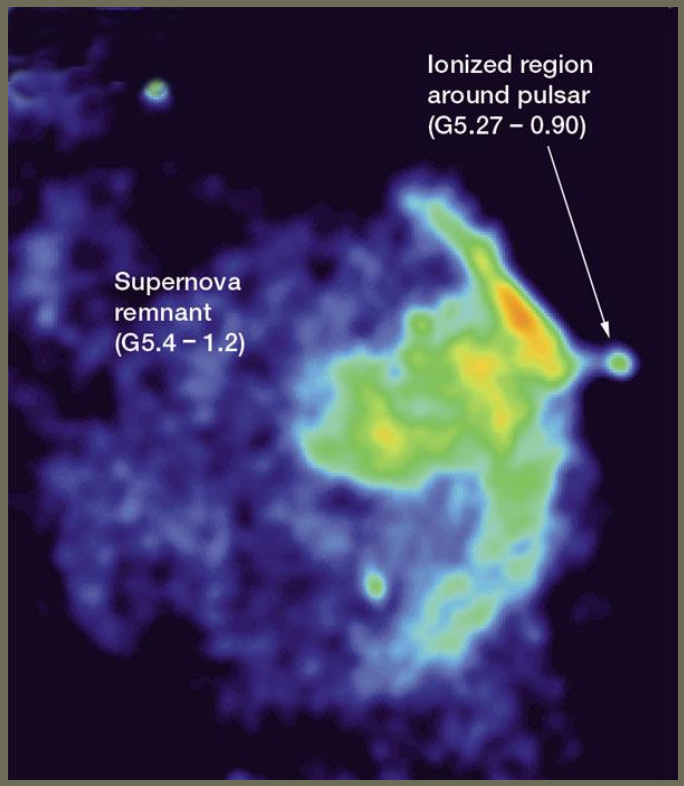

Important papers

- Lai astro-ph/0212140– different kick mechanisms
- ATNF catalogue – database including PSR transversal velocities
- Ng & Romani, ApJ 660, 1357 (2007) – spin-velocity alignment in PSRs with nebulae
- Johnston et al. MNRAS 381, 1625 (2007) and Rankin ApJ 664, 443 (2007) – spin-velocity alignment in dozens of radio pulsars (polarization)
- Postnov, Yungelson astro-ph/0701059 – kicks in binaries (pp.18-23)
- Ofek et al. NS spatial distribution. arXiv: 0910.3684

Spin evolution of NSs

Evolution of neutron stars

Thermal

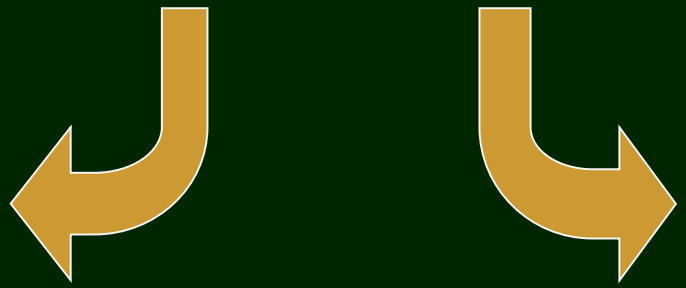

Magneto-rotational

Observational appearence of a NS can depend on:

- Temperature
- Period
- Magnetic field
- Velocity

Evolution of NSs: temperature

Neutrino cooling stage

Photon cooling stage

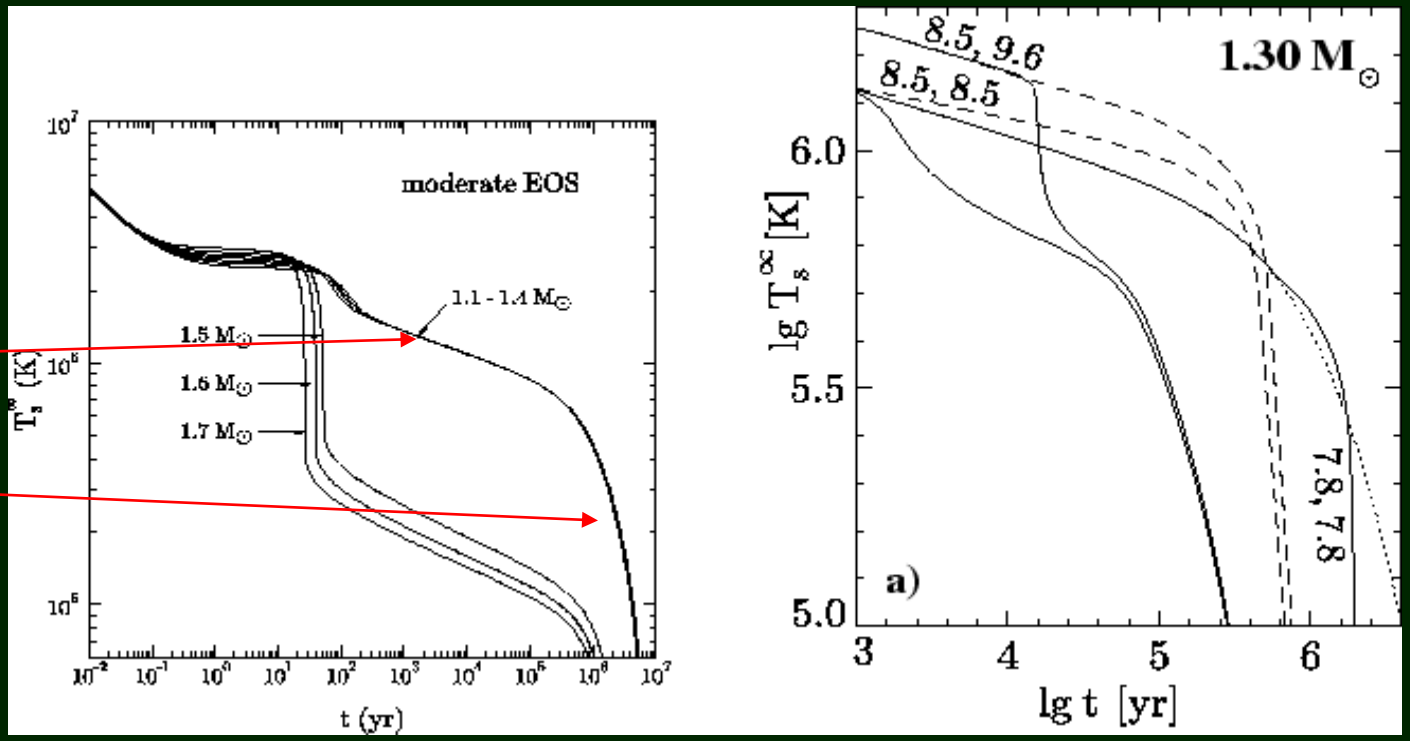

First papers on the thermal evolution appeared already in early 60s, i.e. before the discovery of radio pulsars.

[Yakovlev et al. (1999) Physics Uspekhi]

Evolution of neutron stars: rotation + magnetic field

Ejector → Propeller → Accretor → Georotator

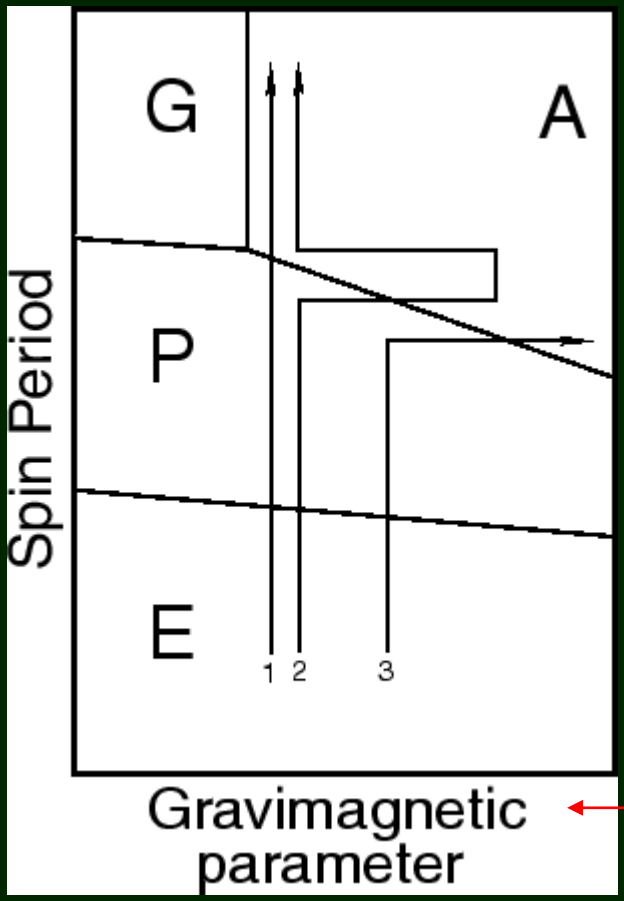

1 – spin down
2 – passage through a molecular cloud
3 – magnetic field decay

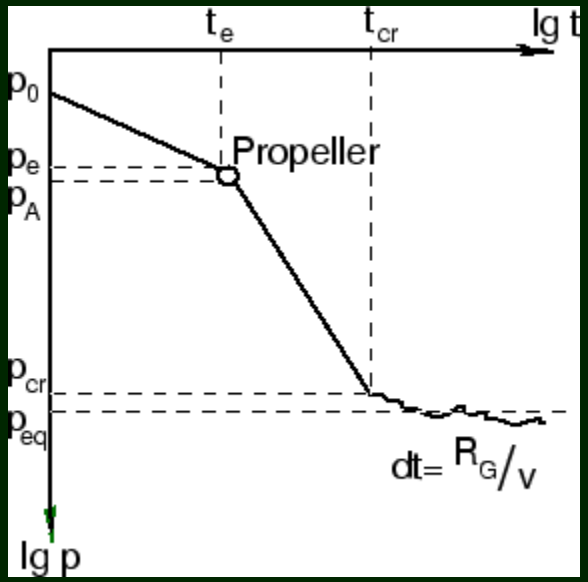

Mdot/μ²

astro-ph/0101031

See the book by Lipunov (1987, 1992)

Magnetic rotator

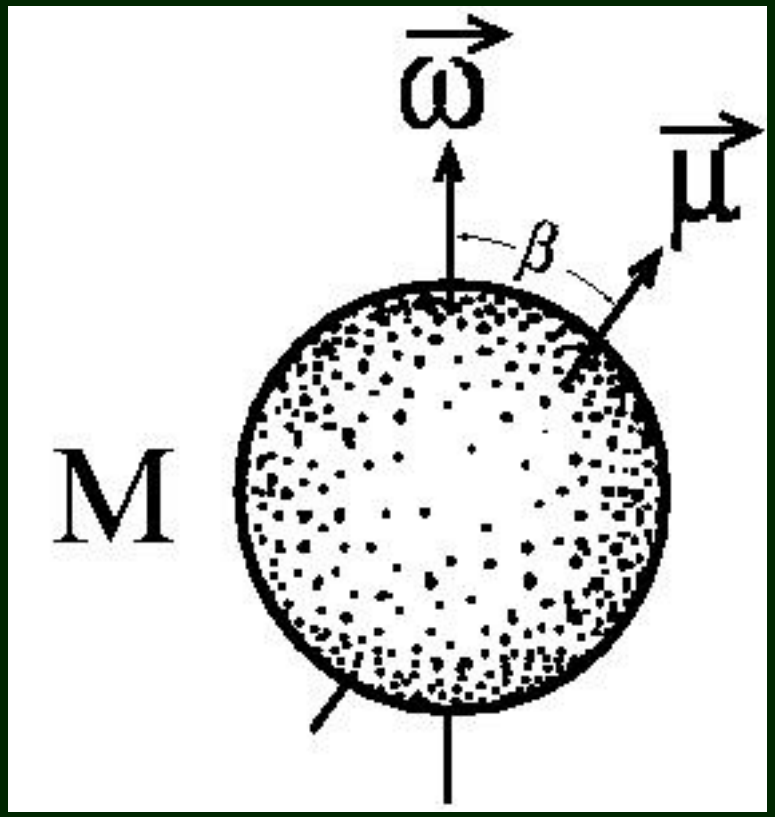

Observational appearances of NSs
(if we are not speaking about cooling)
are mainly determined by P, Pdot, V, B,
(and, probably, by the inclination angle χ),
and properties of the surrounding medium.
B is not evolving significantly in most cases,
so it is important to discuss spin evolution.

Together with changes in B (and χ)
one can speak about

magneto-rotational evolution

We are going to discuss the main stages
of this evolution, namely:
Ejector, Propeller, Accretor, and *Georotator*
following the classification by Lipunov

Magneto-rotational evolution of radio pulsars

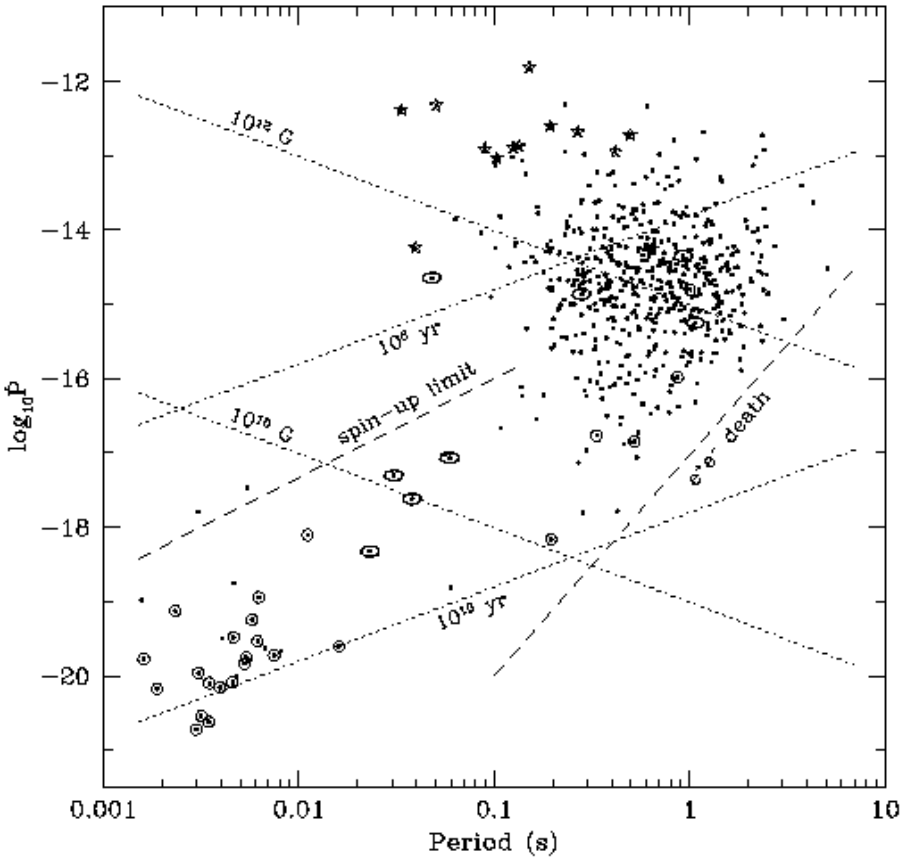

For radio pulsar magneto-rotational evolution is usually illustrated in the P-Pdot diagram.
However, we are interested also in the evolution after this stage.

$$L_m = \frac{2}{3}\frac{\mu^2\omega^4}{c^3}\sin^2\beta = \kappa_t\frac{\mu^2}{R_l^3}\omega\,,$$

$$B \sim 3.2\times10^{19}\,(PdP/dt)^{1/2}\ \mathrm{G}.$$

Spin-down.
Rotational energy is released.
The exact mechanism is still unknown.

Fields in binaries: cyclotron line

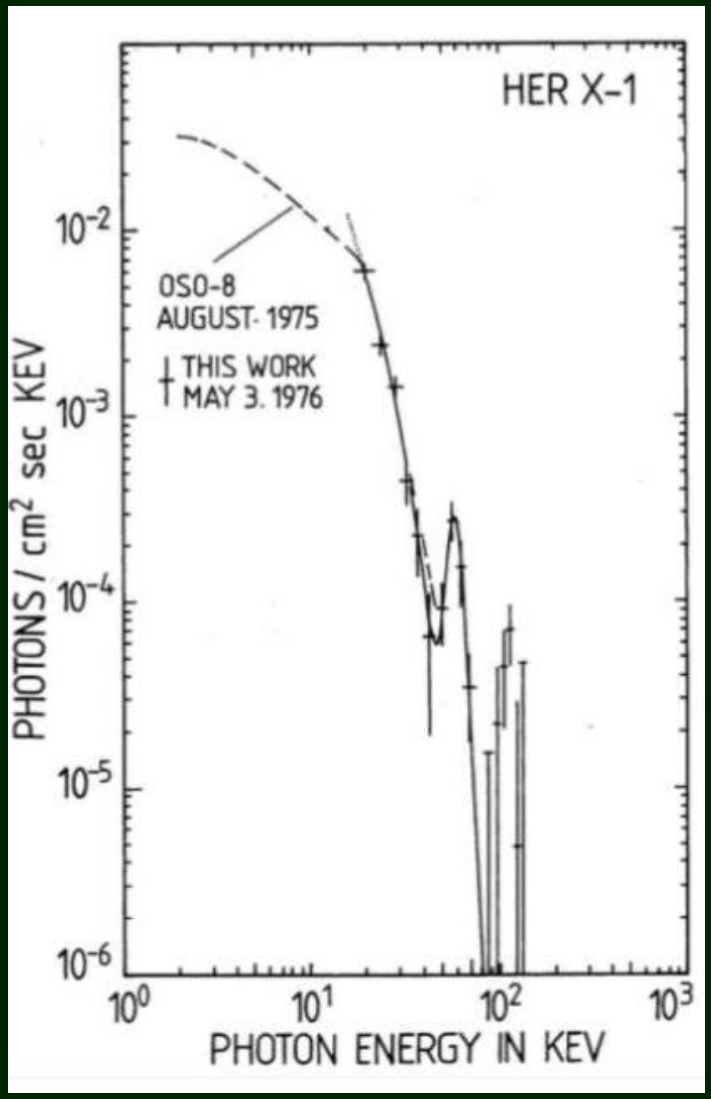

Now 36 X-ray pulsars in binaries.

$$E_{cyc} = \frac{n}{(1+z)}\frac{\hbar e B}{m_e c} \approx \frac{n}{(1+z)} 11.6\,[keV] \times B_{12},$$

$$E_{cyc}(\dot{M}) = E_0 \left(\frac{R_{NS}}{H_l(\dot{M}) + R_{NS}} \right)^3$$

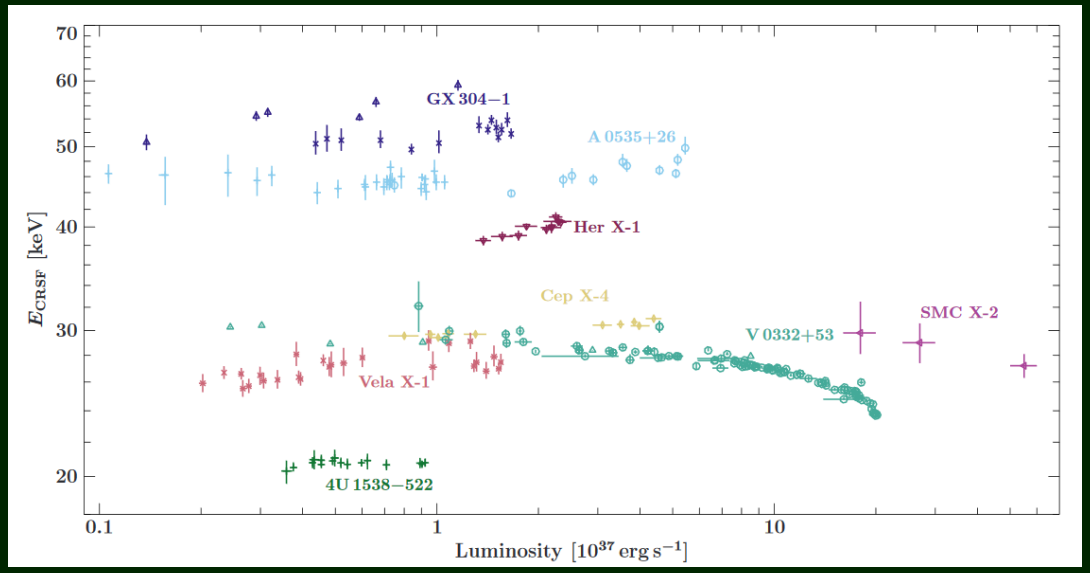

1812.03461

Radio pulsar braking: current losses

The model of pulsar emission is not known, and also the model for spin-down is not known, too. Well-known magneto-dipole formula is just a kind of approximation.

One of models is the ***longitudinal current losses*** model (Beskin et al. see astro-ph/0701261)

$$\dot{P} = 10^{-15} B_{12}^{10/7} P^{1/14} \cos^{3/2}\chi.$$

Longitudinal current losses

$$\dot{P} = 0.24 \times 10^{-15} B_{12}^{2} P^{-1} \sin^{2}\chi.$$

Magneto-dipole

Both models predict evolution of the angle between spin and magnetic axis. Surprisingly, both are wrong!

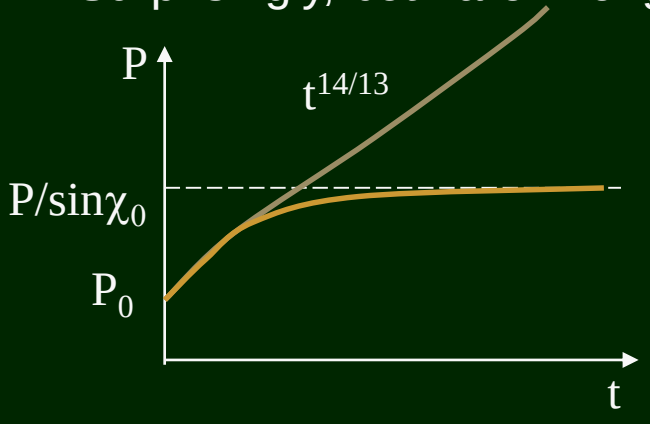

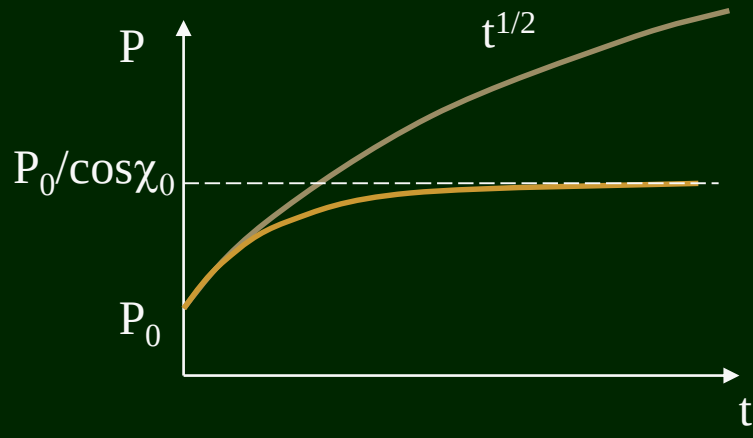

Models of spin-down are not certain up to now, see 1903.01528

Radio pulsar braking: braking index

$$n_{\rm br} = \frac{\Omega\ddot{\Omega}}{\dot{\Omega}^2}.$$

Braking index (definition)

$$n_{\rm br} = 3 + 2\cot^2\chi.$$

Magneto-dipole formula

$$n_{\rm br} = 1.93 + 1.5\tan^2\chi.$$

Longitudinal current losses

For well-measured braking indices n<3.
However, for many pulsars they are very large.
This can be simply an observational effect (microglitches, noise, etc.),
but it can also be something real.
For example, related to the magnetic field evolution.

Crab pulsar and angle evolution

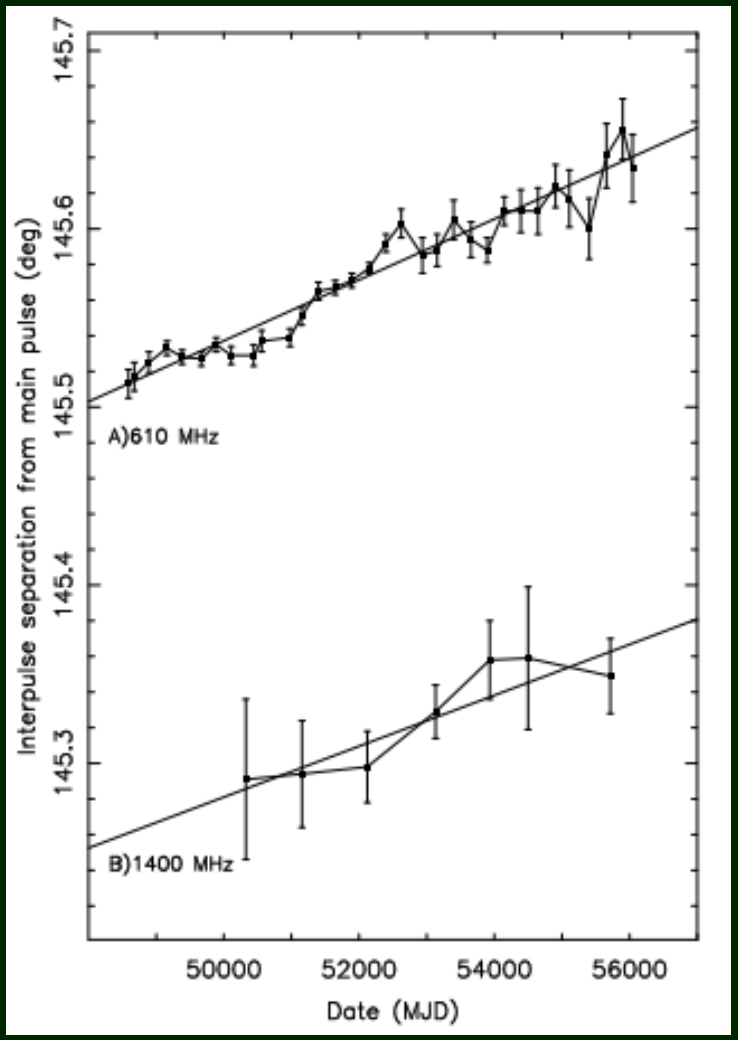

It seems that the angle is changing with the rate 0.6 degrees per century. It is visible as the separation between the main pulse and interpulse is changing.

The axis of the dipolar magnetic field is moving towards the equator.

$$n = 3 + 2\nu/\dot{\nu} \times \dot{\alpha}/\tan(\alpha).$$

1311.0408

Pulsar emission

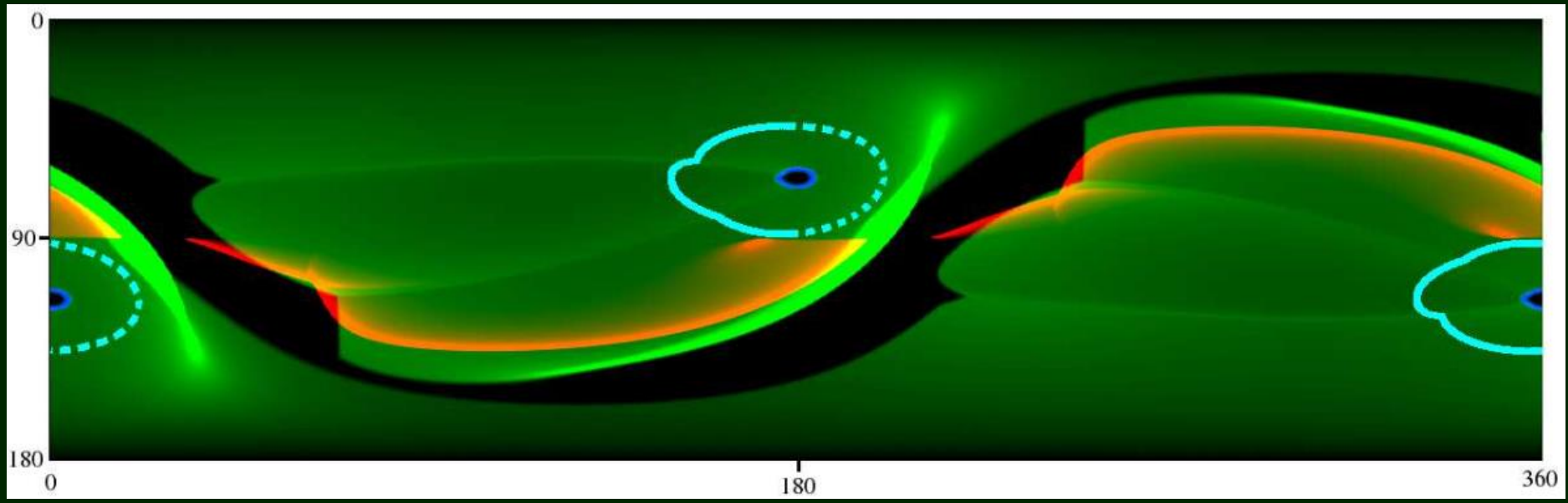

The TPC model for w=0.05 is shown in green, the OG model for w=0.1 is shown in red and the PC emission site is shown in blue.
The cyan lines show the locus of the possible high altitude (r=500 km, here for P=0.2s) radio emission, with the radiating front half shown solid and the back half dashed

0812.3931

Peaks separation for different parameters

Increasing of magnetic inclination results in growth of the separation up to 180º

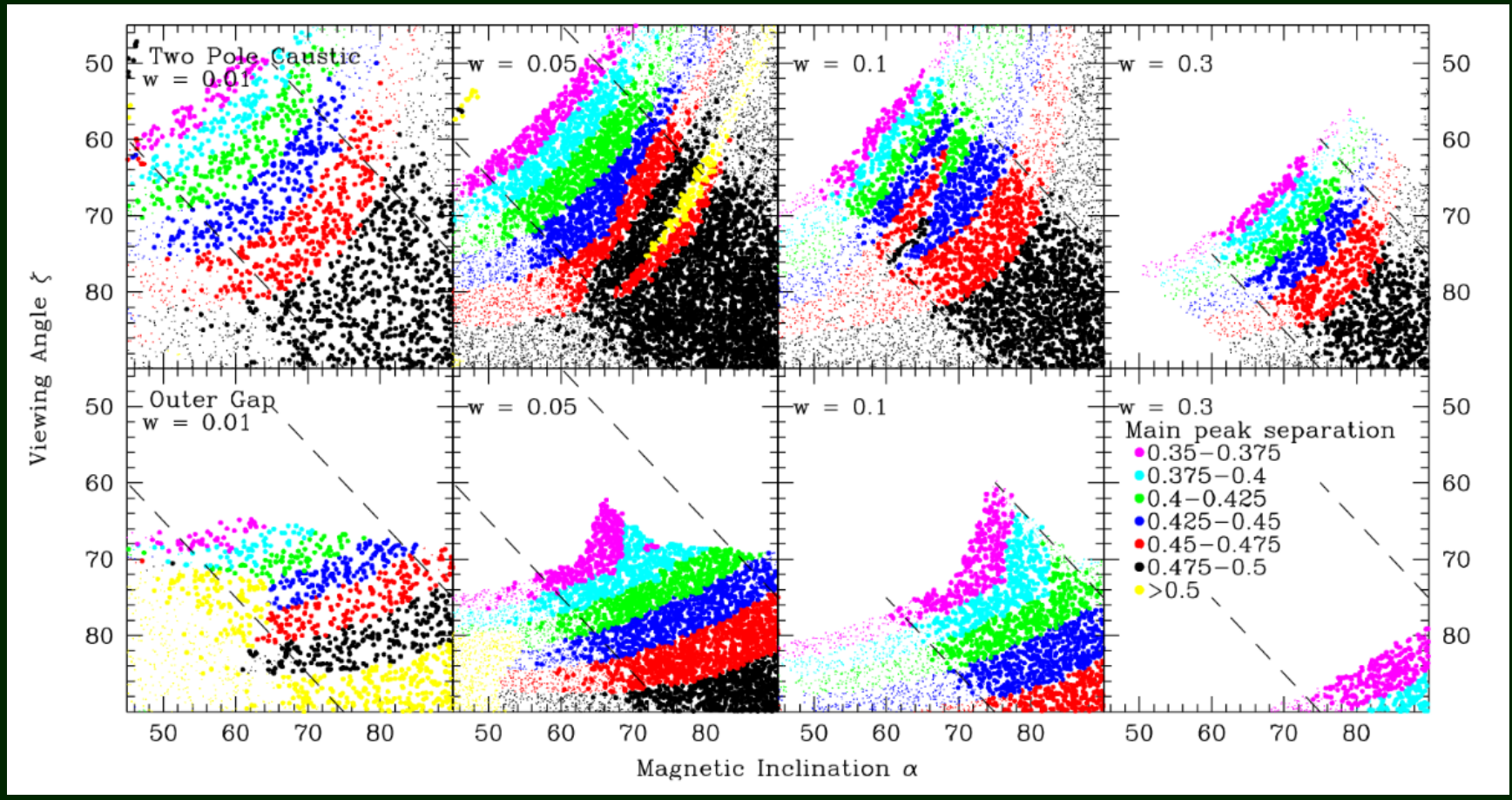

0812.3931

Theoretical studies of the angle evolution

The authors studied the case of plasma filled magnetosphere.
The angle should evolve towards zero.

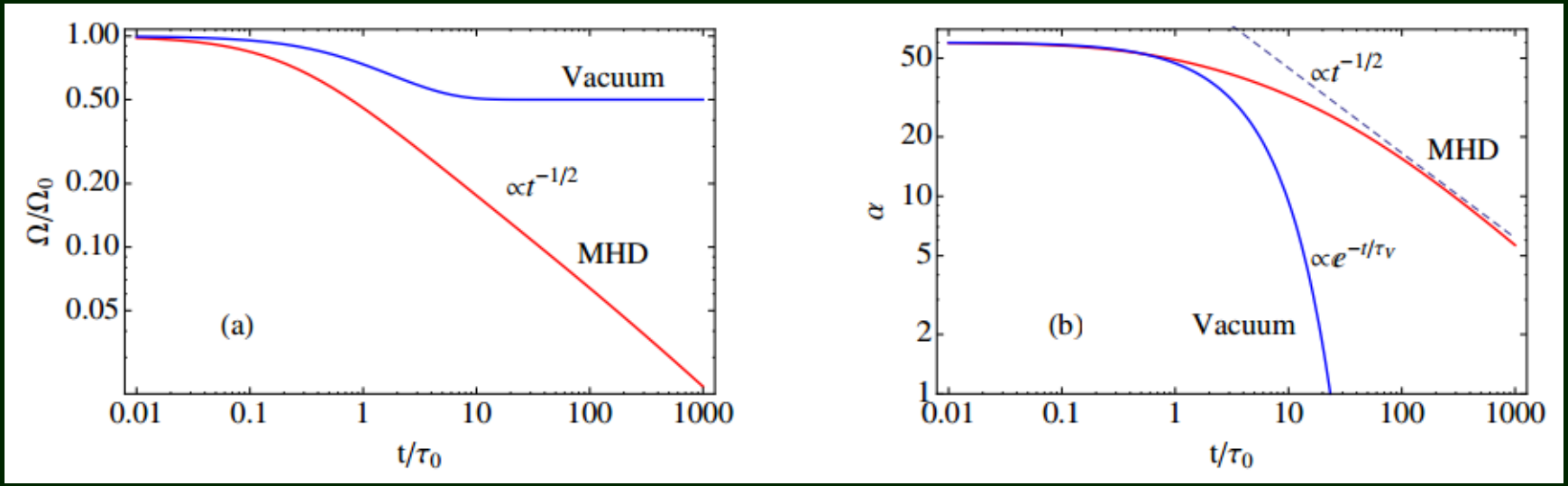

1311.1513

Initial tilt angle distribution

The distribution of pulsar tilt angles is not consistent with a random distribution at birth. Deficit of PSRs with intermediate angles. Bimodality of initial angles?

Viscous damping of precession results in the angle evolution for an oblique rorator.

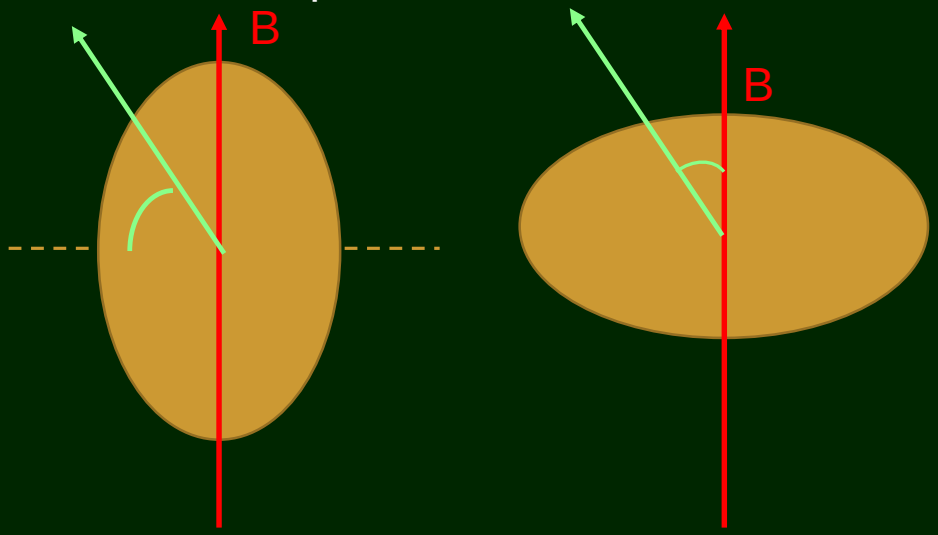

Toroidal field. Prolate. The angle evolves towards 90 degrees.

Poloidal field. Oblate. The angle evolves towards alignment

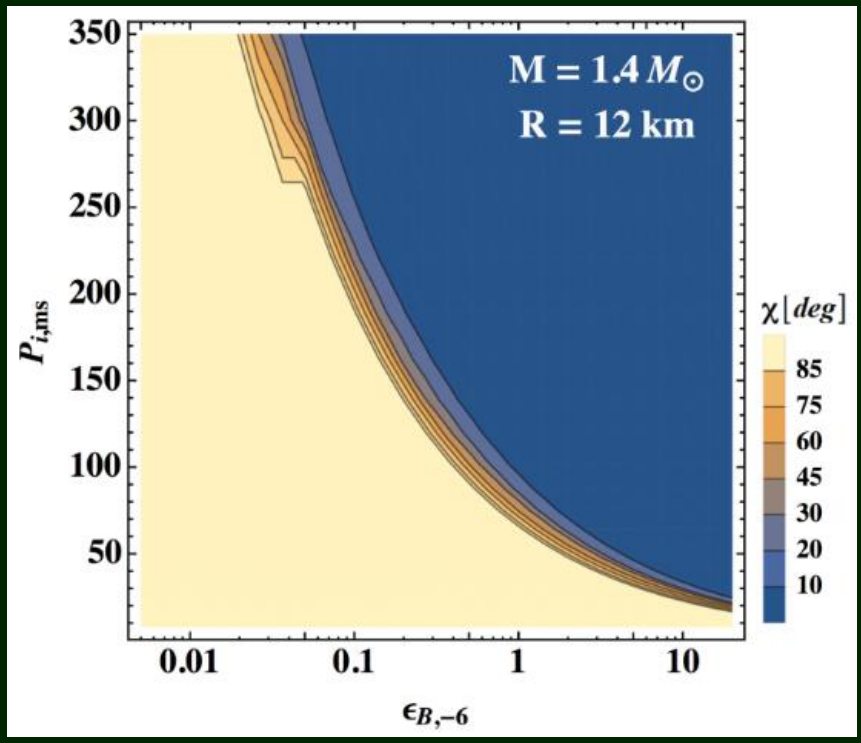

(i) the NS has a non-spherical shape which is mostly determined by magnetic stresses,

(ii) the internal magnetic field is dominated by a toroidal component, thus - prolate deformation,

(iii) at birth, the magnetic axis has a small tilt angle.

1708.08925

Angle evolution

Precession, viscous dissipation, electromagnetic radiation reaction.

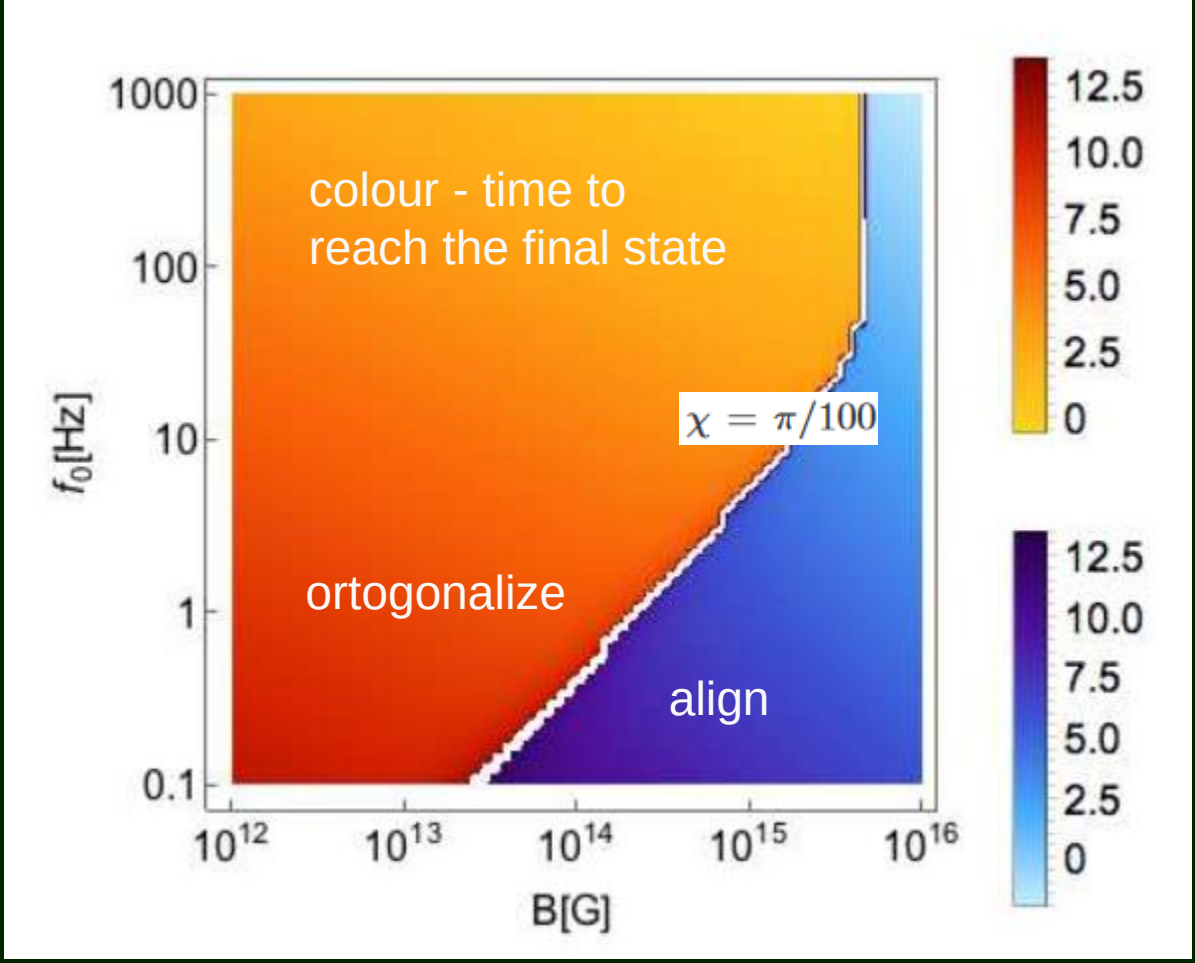

1807.01289

Magneto-rotational evolution of NSs

Ejector → Propeller → Accretor → Georotator

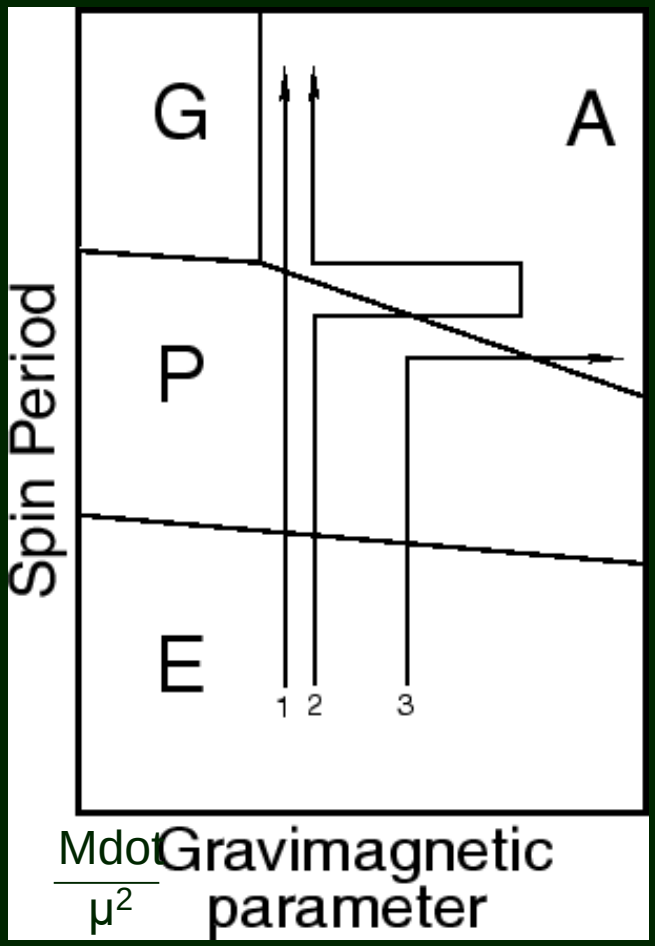

1 – spin down
2 – passage through a molecular cloud
3 – magnetic field decay

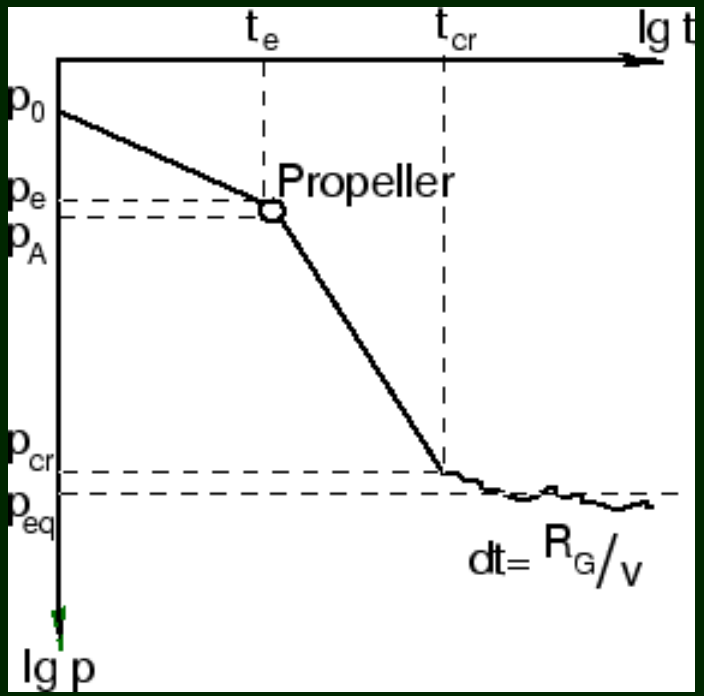

astro-ph/0101031

See the book by Lipunov (1987, 1992)

Critical radii -I

Transitions between different evolutionary stages can be treated in terms of

critical radii

- Ejector stage. Radius of the light cylinder. $R_l=c/\omega$.
  Shvartsman radius. R_{sh}.
- Propeller stage. Corotation radius. R_{co}
- Accretor stage. Magnetospheric (Alfven) radius. R_A
- Georotator stage. Magnetospheric (Alfven) radius. R_A

As observational appearence is related to interaction with the surrounding medium the radius of *gravitational capture* is always important. $R_G=2GM/V^2$.

Critical radii-II

1. Shvartsman radius
   It is determined by
   relativistic particles wind

$$R_{\rm Sh} = \left(\frac{8\kappa_t \mu^2 G^2 M^2 \omega^4}{\dot{M}_c v_\infty^5 c^4} \right)^{1/2}, \qquad R_{\rm Sh} > R_G$$

2. Corotation radius

$$\omega R_{\rm St} < \sqrt{GM_x / R_{\rm St}}$$

$$R_c = (GM_x/\omega^2)^{1/3} \sim 2.8 \times 10^8 m_x^{1/3} (P/1\ {\rm s})^{2/3}\ {\rm cm}$$

3. Alfven radius

$$P_m(R_{\rm st}) = P_a(R_{\rm st})$$

$$R_\Lambda = \begin{cases} \left(\dfrac{2\mu^2 G^2 M^2}{\dot{M}_c v_\infty^5} \right)^{1/6}, & R_\Lambda > R_G \\ \left(\dfrac{\mu^2}{2\dot{M}_c \sqrt{2GM}} \right)^{2/7}, & R_\Lambda \le R_G \end{cases}$$

Pressure

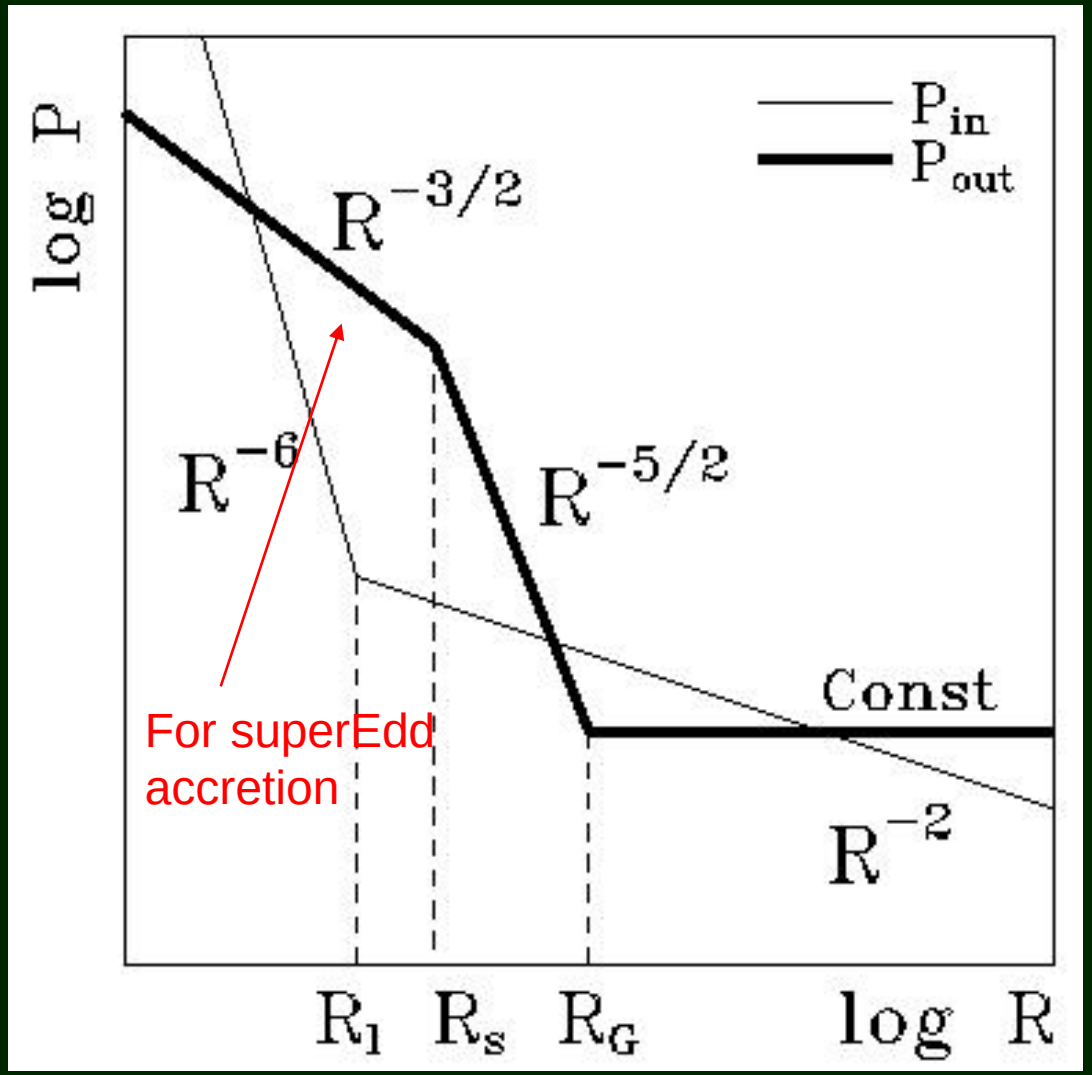

$$P_m = \begin{cases} \dfrac{\mu^2}{8\pi R^6}, & R \le R_l \\ \dfrac{L_m}{4\pi R^2 c}, & R > R_l \end{cases}$$

$$L_m = \kappa_t \frac{\mu^2}{R_l^3}\omega$$

We can define a stopping radius R_{st}, at which external and internal pressures are equal.

The stage is determined by relation of this radius to other critial radii.

Classification

Abbrevi-ation	Type	Characteristic radii relation	Accretion rate	Observational appearances
E	Ejector	$R_{st} > R_G$ $R_{st} > R_l$	$\dot{M}_c \leq \dot{M}_{cr}$	Radiopulsars, Soft γ-ray repeaters, Cyg X-3? LSI+61 303?
P	Propeller	$R_c < R_{st}$ $R_{st} \leq R_G$ $R_{st} \leq R_l$	$\dot{M}_c \leq \dot{M}_{cr}$	X-ray transients? Rapid burster? γ-bursters??? Magnetic Ap-stars
A	Accretor	$R_{st} \leq R_G$ $R_{st} \leq R_l$	$\dot{M}_c \leq \dot{M}_{cr}$	X-ray pulsars, bursters, cataclysmic variables, intermediate polars
G	Georotator	$R_G < R_{st}$ $R_{st} \leq R_c$	$\dot{M}_c \leq \dot{M}_{cr}$	Earth, Jupiter
M	Magnetor	$R_{st} > a$ $R_c > a$???	$\dot{M}_c \leq \dot{M}_{cr}$	AM Her, polars

Alfven radius in different situations

Simple estimate of R_A presented before is just a zero approximation.
Many different variants for different accretion regimes were obtained.
In particular, R_A is modified in the case of disc accretion,
and for low accretion rates.

1806.11516

$$R_M^{GL79} \simeq 0.52 R_A = 0.52 \mu^{4/7} (2GM)^{-1/7} \dot{M}^{-2/7}$$
$$\simeq 1.6 \times 10^6 \mu_{26}^{4/7} M_{1.4}^{-1/7} \dot{M}_{16}^{-2/7} \text{ cm},$$

In the plot the radius
in the case of disc accretion
according to GL79
is compared for different
accretion rate and inclination
with the model originally
developed by Wang (1997).

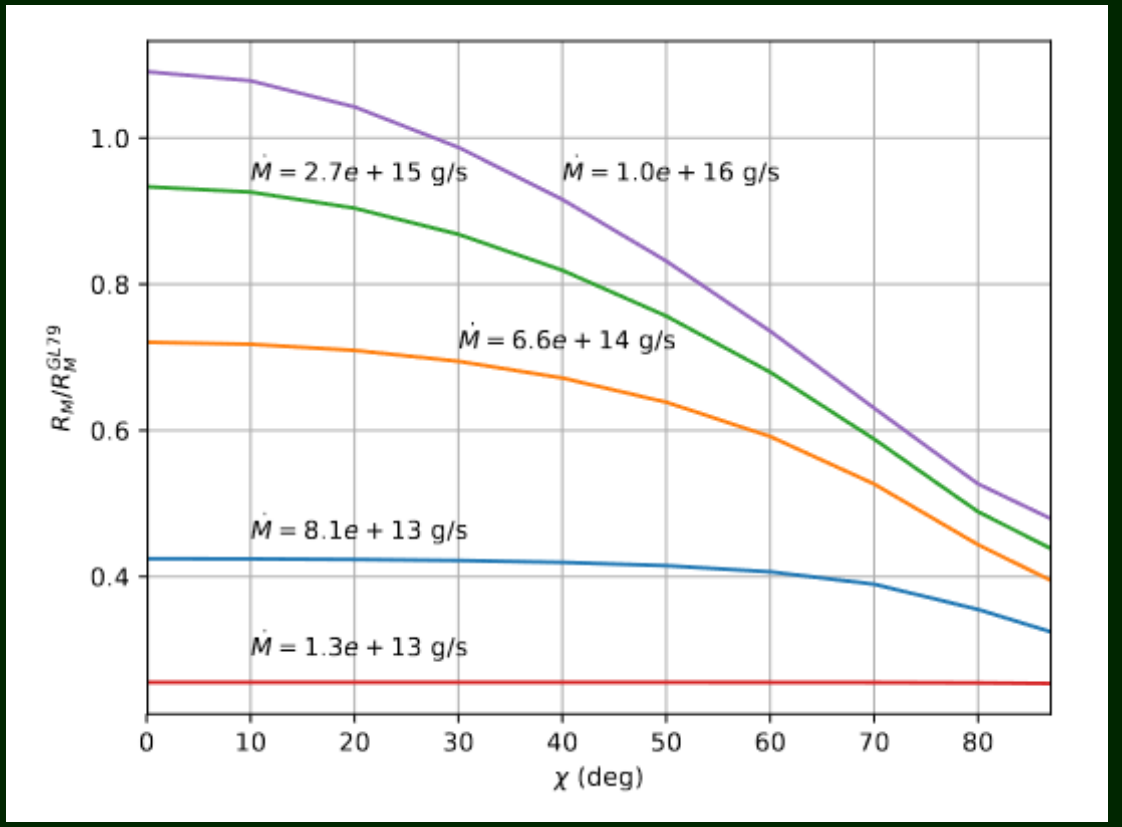

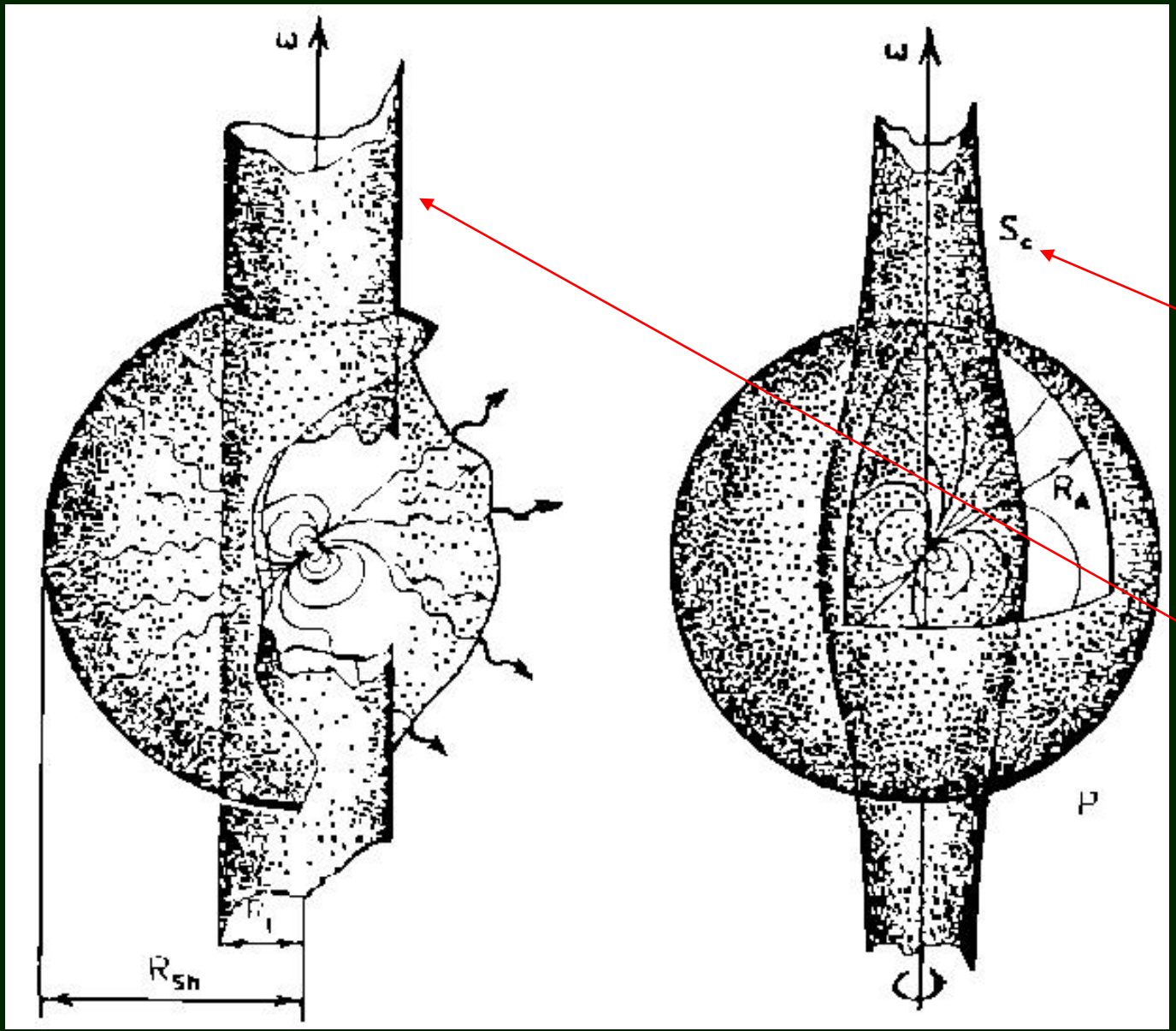

$R=R_{co}\cos^{-2/3}\theta$

$R_{co}=(GM/\omega^2)^{1/3}$

Light cylinder

$R_l=\omega/c$

Ejector **Propeller**

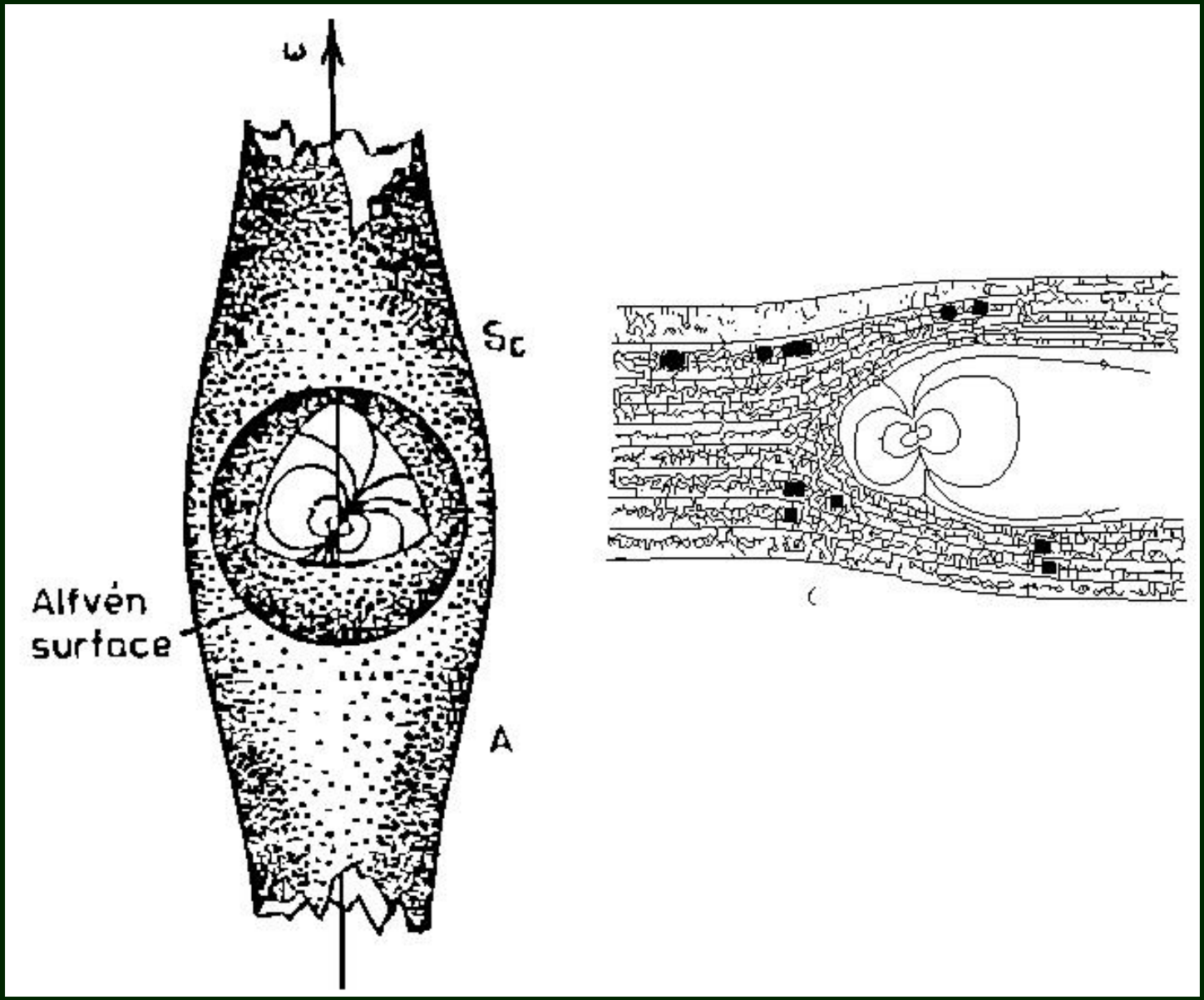

Accretor **Georotator**

Critical periods for isolated NSs

$$P_E(E \to P) \simeq 10\,\mu_{30}^{1/2}\,n^{-1/4}\,v_{10}^{1/2}\ \mathrm{s}$$

Transition from Ejector to Propeller (supersonic)

$$t_E \simeq 10^9\,\mu_{30}^{-1}\,n^{-1/2}\,v_{10}\ \mathrm{yr}$$

Duration of the ejector stage

$$P_A(P \to A) \simeq 420\,\mu_{30}^{6/7}\,n^{-3/7}\,v_{10}^{9/7}\ \mathrm{s}$$

Transition from supersonic Propeller to subsonic Propeller or Accretor

$$P_{eq} = 2.6 \times 10^3\,v_{(t)10}^{-2/3}\,\mu_{30}^{2/3}\,n^{-2/3}\,v_{10}^{13/3}\ \mathrm{s}$$

A kind of equilibrium period for the case of accretion from turbulent medium

$$v < 410\,n^{1/10}\,\mu_{30}^{-1/5}\ \mathrm{km\,s^{-1}}$$

Condition for the Georotator formation (instead of Propeller or Accretor)

(see, for example, astro-ph/9910114)

Spin-up/down at the stage of accretion

$$\frac{dI\omega}{dt} = \dot{M} k_{\rm su} - \kappa_t \frac{\mu^2}{R_t^3}$$

$$k_{\rm su} = \begin{cases} (GM_x R_d)^{1/2}, & \text{Keplerian disk accretion,} \\ \eta_t \Omega R_G^2, & \text{wind accretion in a binary,} \\ \sim 0, & \text{a single magnetic rotator.} \end{cases}$$

For a single rotator (i.e. an isolated NS) spin-up can be possible due to turbulence in the interstellar medium.

In the case of isolated accreting NS one can estimate the accretion rate as:

$$\dot{M}_c = 4\pi R_G^2 \rho_\infty v_\infty$$

Unified approach to spin-down

One can find it comfortable to represent the spin-down moment by such a formula

$$-\kappa_t \frac{\mu^2}{R_t^3}$$

k_t and R_t are different for different stages.
k_t can be also frequency dependent.

Parameter	Regime					
	E, SE	P, SP	A	SA	G	M
$\dot{M}$	0	0	$\dot{M}_c$	$\dot{M}_c(R_A/R_s)$	0	$\dot{M}_c$
κ_t	$\sim 2/3$	$\lesssim 1/3$	$\sim 1/3$	$\sim 1/3$	$\sim 1/3$	$\sim 1/3$
R_t	R_l	R_m	R_c	R_c	R_A	a

Equilibrium period

$$\dot{M} k_{su} = -\kappa_t \frac{\mu^2}{R_t^3}$$

The hypothesis of equilibrium can be used to determine properties of a NS.

The corotation radius is decreasing as a NS is spinning up.
So, before equilibrium is reached the transition to the propeller stage can happen.

Looking at this formula (and remembering that for Accretors $R_t=R_{co}$) it is easy to understand why millisecond PSRs have small magnetic field.
Spin-up can not be very large (Eddington rate).
So, to have small spin periods (and so small corotation radii),
it is necessary to have small magnetic fields.
High magnetic field NS can not be spun-up to millisecond periods.

Accreting isolated neutron stars

Why are they so important?

- Can show us how old NSs look like
  1. Magnetic field decay
  2. Spin evolution
- Physics of accretion at low rates
- NS velocity distribution
- New probe of NS surface and interiors
- ISM probe

Expected properties

1. **Accretion rate**

An upper limit can be given by the Bondi formula:
Mdot = $\pi R_G^2 \rho v$, $R_G \sim v^{-2}$
Mdot = 10^{11} g/s $(v/10 \text{ km/s})^{-3}$ n
$L=0.1 \dot{M} c^2 \sim 10^{31}$ erg/s

However, accretion can be smaller due to the influence of a magnetosphere of a NS

2. **Periods**

Periods of old accreting NSs are uncertain, because we do not know evolution well enough.

a) $p_A = 2^{5/14}\pi(GM)^{-5/7}(\mu^2/\dot{M})^{3/7} \simeq$

$R_A=R_{co}$

$$300\,\mu_{30}^{6/7}(v/10\,\mathrm{km\,s^{-1}})^{9/7}n^{-3/7}\,\mathrm{s}.$$

Subsonic propeller

Even after $R_{co}>R_A$ accretion can be inhibited.
This have been noted already in the pioneer papers by Davies et al.

Due to rapid (however, subsonic) rotation a hot envelope is formed around the magnetosphere. So, a new critical period appear.

$$P_{\rm br} \simeq 450\ \mu_{30}^{16/21}\ \dot{M}_{15}^{-5/7}\ m^{-4/21}\ {\rm s}.$$

(Ikhsanov astro-ph/0310076)

If this stage is realized (inefficient cooling) then
- accretion starts later
- accretors have longer periods

Initial spin periods

Determination of initial spin periods is closely linked with models of magneto-rotational evolution of neutron stars.

Among thousands of known NSs just for a few tens there are estimates of initial spin periods. Just for a few such estimates a robust enough.

Typically, it is necessary to have a independent estimate of a NS age. Then, using *some* model of magneto-rotational evolution the initial spin period is reconstructed.

Independent ages:
- SNR
- Kinematic
- Cooling

Sample of NSs+SNRs

Table 1. Sample of PSRs associated with SNRs

PSR	SNR	$\tau_{SNR}/10^3$ yrs	$\tau_{sd}/10^3$ yrs	Ref.
J0537-6910	N157B	as the PSR	4.9	Wang and Gotthelf (1998)
J1119-6127	G292.2-0.5	as the PSR	1.6	Pivovaroff et al. (2001)
J1747-2809	G0.9+0.1	as the PSR	5.3	Aharonian and et al. (2005)
				Porquet et al. (2003)
J1747-2958	G359.23-0.82	as the PSR	25.5	Camilo et al. (2002b)
J1846-0258	Kes75	as the PSR	0.73	Leahy and Tian (2008)
J1930+1852	G54.1+0.3	as the PSR	2.9	Camilo et al. (2002a)
J0007+7303	CTA 1	10.2-15.8	13.9	Slane et al. (2004)
J0205+6449	3C58	4.3-7	5.4	Slane et al. (2008)
J0538+2817	S147	40-200	618.1	Anderson et al. (1996)
				Ng et al. (2007)
B0540-69	0540-693	0.66-1.1	1.67	Williams et al. (2008)
B0656+14	Monogem Ring	86-170	110.9	Thorsett et al. (2003)
J0821-4300	Puppis A	3.3-4.1	1489.	Gotthelf and Halpern (2009)
B0833-45	Vela	11-27	11.3	Aschenbach et al. (1995)
J1124-5916	G292.0+1.8	2.4-2.85	2.85	Gonzalez and Safi-Harb (2003)
B1509-58	G320.4-1.2	6-20	1.6	Yatsu et al. (2005)
J1809-2332	G7.5-1.7	10-100	67.6	Roberts and Brogan (2008)
J1813-1749	G12.8-0.0	0.285-2.5	4.7	Brogan et al. (2005)
J1833-1034	G21.5-0.9	0.8-40.	4.9	Safi-Harb et al. (2001)

Table 1—Continued

PSR	SNR	$\tau_{SNR}/10^3$ yrs	$\tau_{sd}/10^3$ yrs	Ref.
B1853+01	W44	6.5-20	20.3	Harrus et al. (1997)
J1957+2831	G65.1+0.6	40-140	1568.	Tian and Leahy (2006)
B1951+32	CTB80	> 18	107.	Castelletti et al. (2003)
B1338-62	G308.8-0.1	< 32.5	12.1	Caswell et al. (1992)
J2229+6114	G106.6+2.9	> 3.9	10.5	Kothes et al. (2006)
B0531+21	Crab	0.957	1.24	Stephenson and Green (2002)
J1210-5226	G296.5+10.0	10-20	101817.	Vasisht et al. (1997)
J1437-5959	G315.9-0.0	22	114.	Camilo et al. (2009)
J1811-1925	G11.2-0.3	1.6	23.2	Torii et al. (1999)
J1852+0040	Kes79	6	191502.	Sun et al. (2004)
J2021+4026	G78.2+2.1	6.6	76.9	Uchiyama et al. (2002)
B2334+61	G114.3+0.3	7.7	40.6	Yar-Uyaniker et al. (2004)

30 pairs: PSR+SNR
Popov, Turolla arXiv: 1204.0632

Table 2. Spin parameters of PSRs in the sample

PSR	P s	$\dot{P}$	$B/10^{12}$ G	P_0 s	P_0/P
J0537-6910	0.016	5.18E-14	0.92	$\ll P$	~ 0
J1119-6127	0.408	4.02E-12	41.	$\ll P$	~ 0
J1747-2809	0.052	1.56E-13	2.9	$\ll P$	~ 0
J1747-2958	0.099	6.13E-14	2.5	$\ll P$	~ 0
J1846-0258	0.326	7.08E-12	48.6	$\ll P$	~ 0
J1930+1852	0.137	7.51E-13	10.3	$\ll P$	~ 0
J0007+7303	0.316	3.6E-13	10.8	< 0.163	< 0.52
J0205+6449	0.066	1.94E-13	3.6	< 0.029	< 0.45
J0538+2817	0.143	3.67E-15	0.73	< 0.134	< 0.93
	0.143	3.67E-15	0.73	> 0.118	> 0.82
B0540-69	0.05	4.79E-13	5.0	< 0.039	< 0.78
	0.05	4.79E-13	5.0	> 0.03	> 0.59
B0656+14	0.385	5.5E-14	4.7	< 0.183	< 0.48
J0821-4300	0.113	1.2E-15	0.37	< 0.113	~ 1
	0.113	1.2E-15	0.37	> 0.113	~ 1
B0833-45	0.089	1.25E-13	3.4	< 0.016	< 0.2
J1124-5916	0.135	7.53E-13	10.2	< 0.054	< 0.40
	0.135	7.53E-13	10.2	> 0.004	> 0.03
J1210-5226	0.424	6.6E-17	0.17	0.424	~ 1
B1509-58	0.151	1.54E-12	15.4	—	—

Table 2—Continued

PSR	P s	$\dot{P}$	$B/10^{12}$ G	P_0 s	P_0/P
J1809-2332	0.147	3.44E-14	2.3	< 0.136	< 0.92
J1813-1749	0.045	1.5E-13	2.6	< 0.043	< 0.97
	0.045	1.5E-13	2.6	> 0.031	> 0.69
J1833-1034	0.062	2.02E-13	3.6	< 0.057	< 0.91
B1853+01	0.267	2.08E-13	7.5	< 0.221	< 0.83
	0.267	2.08E-13	7.5	> 0.036	> 0.14
J1957+2831	0.308	3.11E-15	0.99	< 0.3	< 0.99
	0.308	3.11E-15	0.99	> 0.29	> 0.95
B1951+32	0.04	5.84E-15	0.49	< 0.036	< 0.91
B1338-62	0.193	2.53E-13	7.1	—	—
J2229+6114	0.052	7.83E-14	2.0	< 0.041	< 0.79
B0531+21	0.033	4.23E-13	3.8	0.016	0.48
J1437-5959	0.062	8.59E-15	0.74	0.055	0.9
J1811-1925	0.065	4.40E-14	1.7	0.062	0.97
J1852+0040	0.105	8.68E-18	0.03	0.105	~ 1
J2021+4026	0.265	5.47E-14	3.9	0.254	0.96
B2334+61	0.495	1.93E-13	9.9	0.45	0.91

B vs. P_0

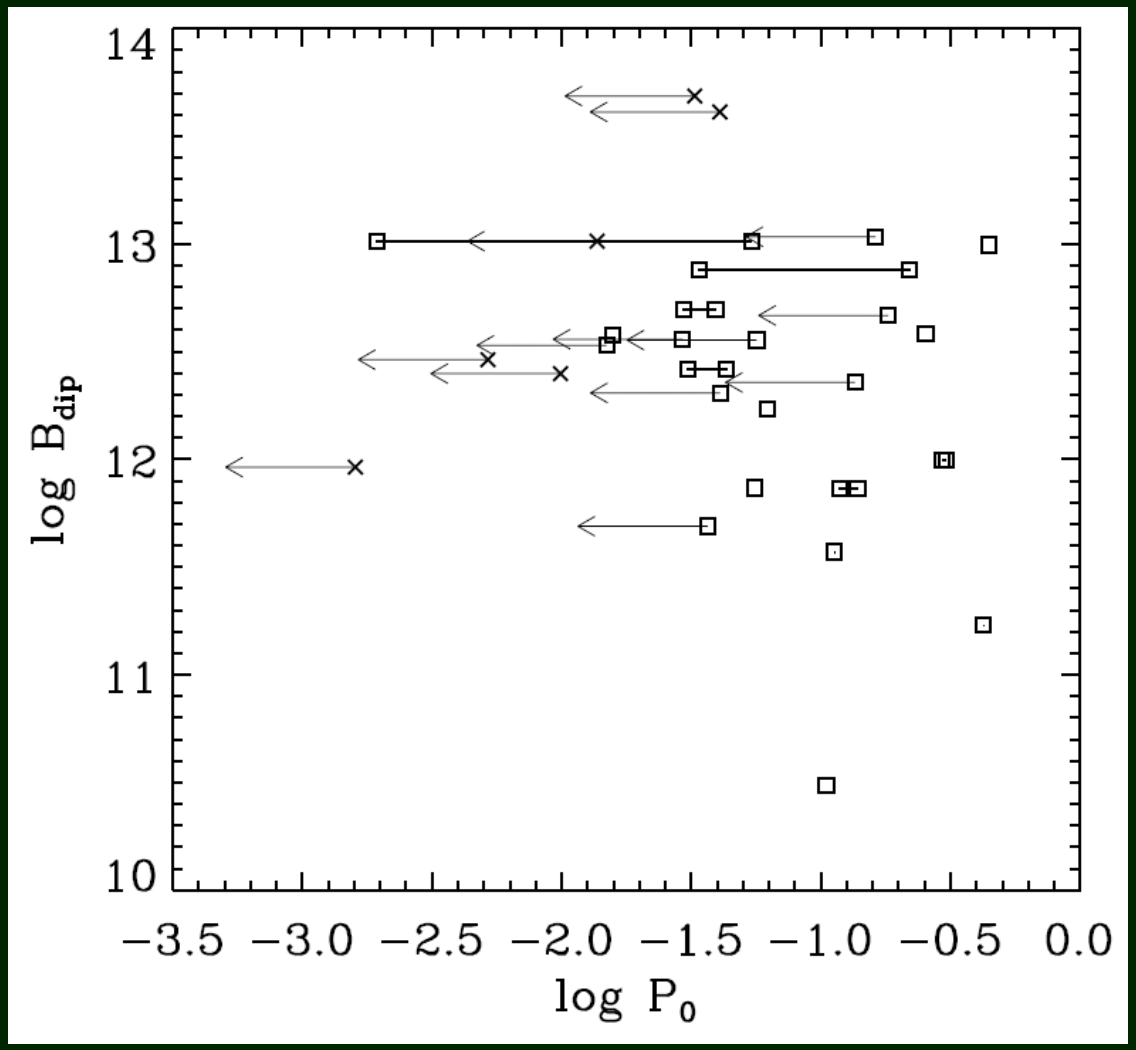

All presented estimates are made for standard assumptions:
n=const=3.
So, field is assumed to be constant, as well as the angle between spin and magnetic axis.

Crosses – PSRs in SNRs (or PWN) with ages just consistent with spin-down ages.
We assume that P_0<0.1P

1204.0632

Checking gaussian

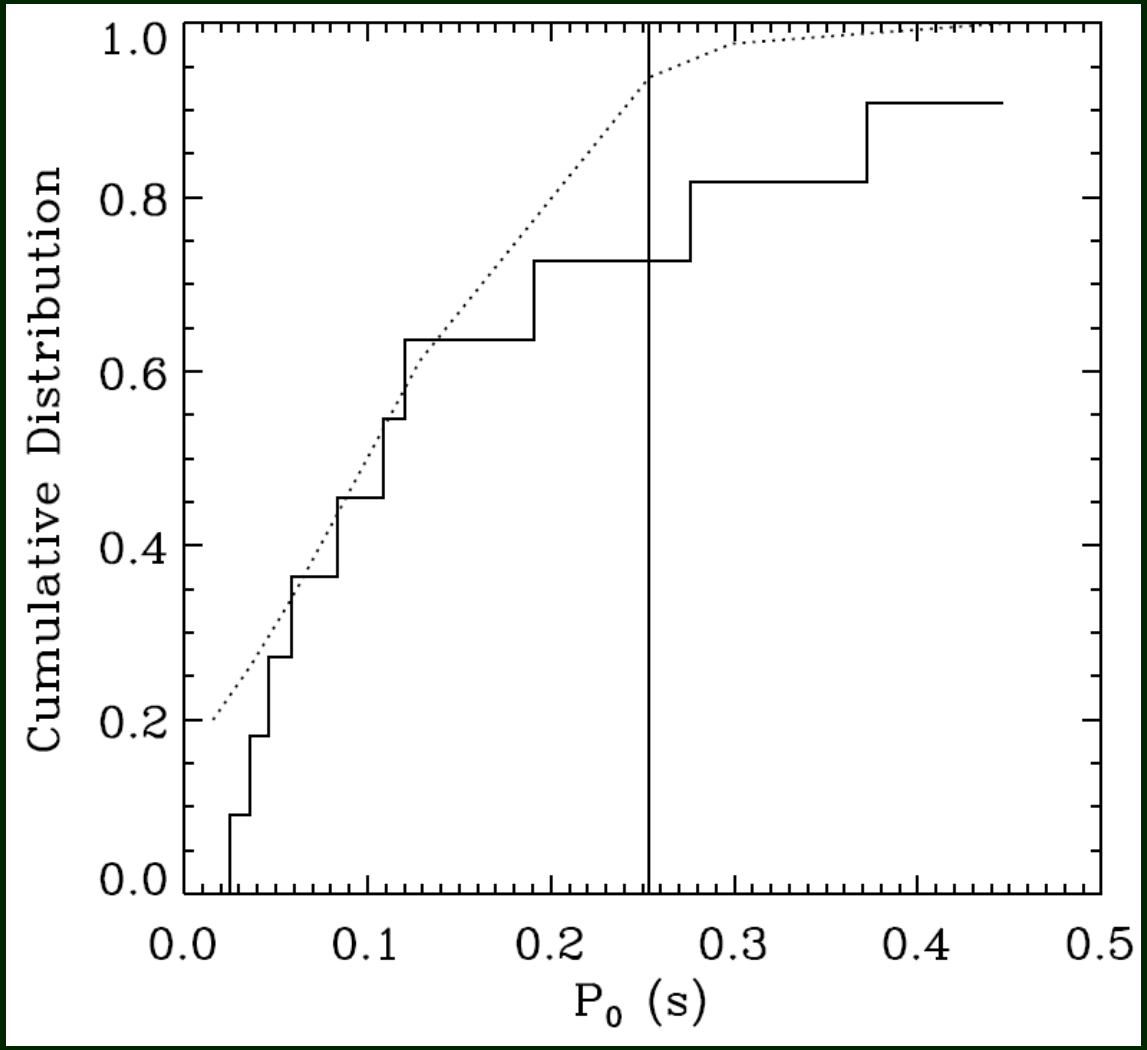

The data we have is not enough to derive the shape of the P_0 distribution.
However, we can exclude very wide and very narrow distributions, and also we can check if some specific distributions are compatible with our results.

Here we present a test for a gaussian distribution, which fits the data.

Still, we believe that the fine tuning is premature with such data.

P_0=0.1 s; σ=0.1 s

Checking flat distrbution

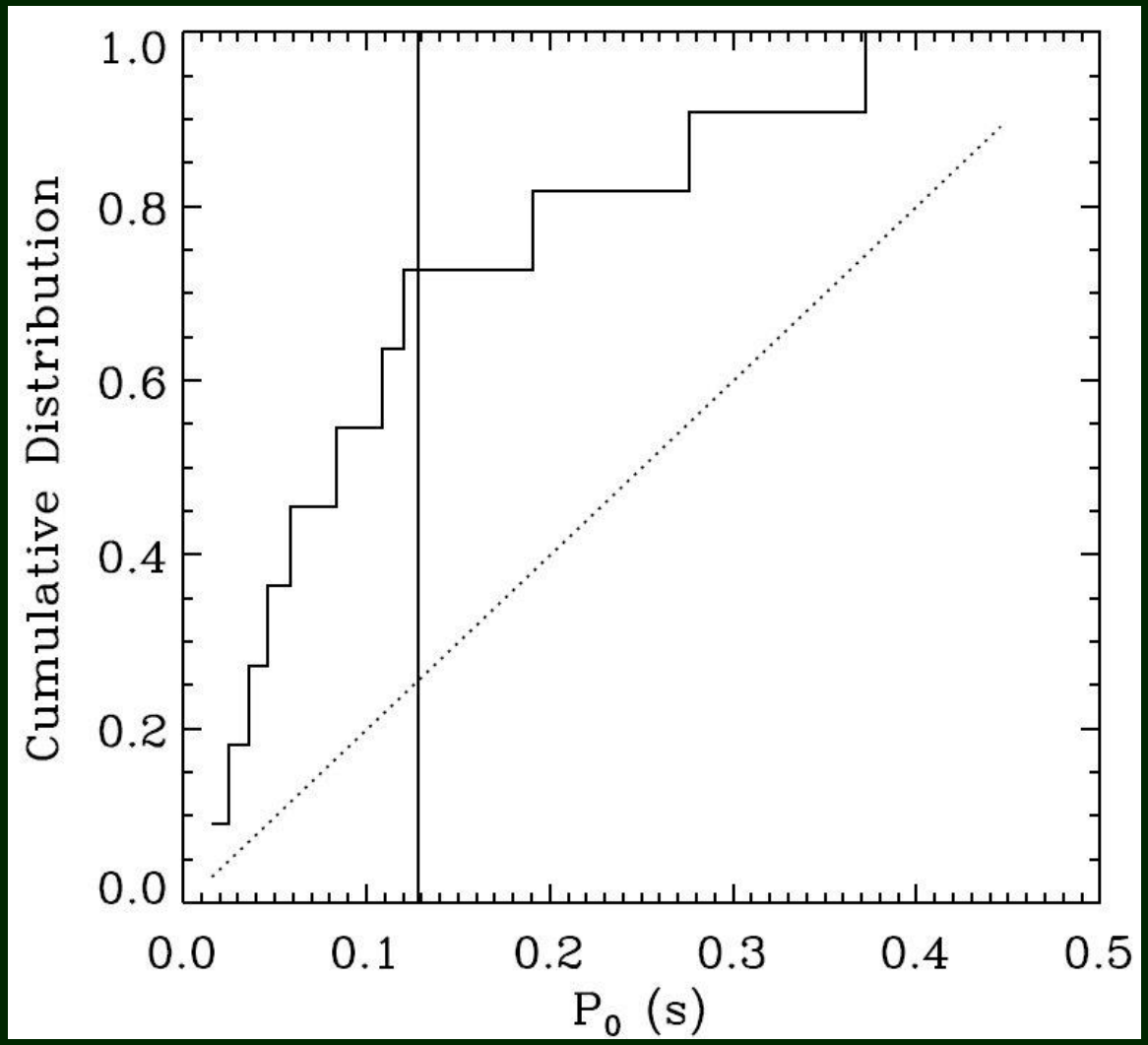

Flat between 0.001 and 0.5 s.

Very wide distributions in general do not fit the data we have.

Wide initial spin period distribution

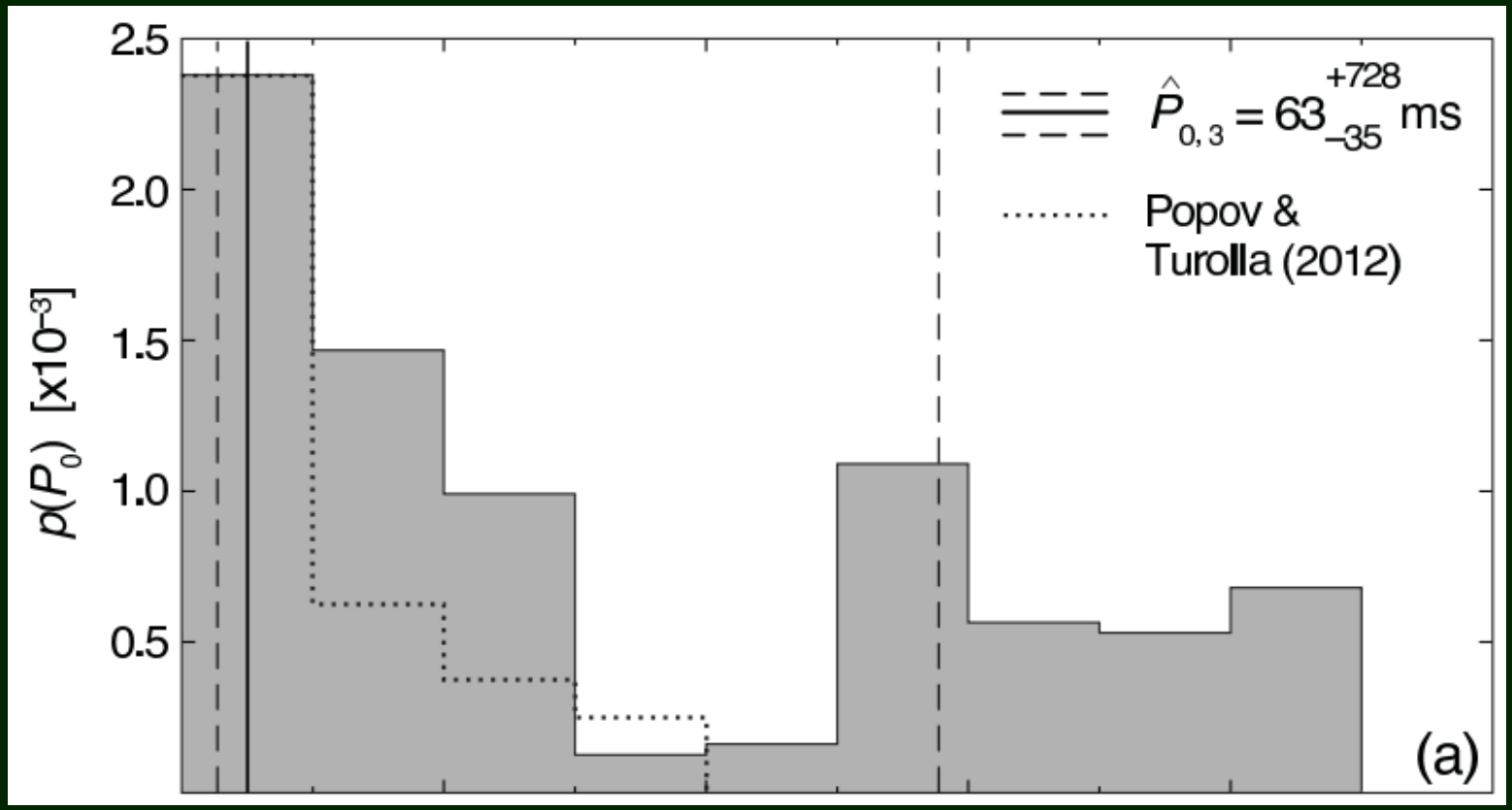

Based on kinematic ages. Mean age – few million years.
Note, that in Popov & Turolla (2012) only NSs in SNRs were used, i.e. the sample is much younger!
Can it explain the difference?

1301.1265

Magnetic field decay and P_0

One can suspect that magnetic field decay can influence the reconstruction of the initial spin period distribution.

Exponential field decay with τ=5 Myrs.
$\langle P_0 \rangle$=0.3 s, σ_P=0.15 s; $\langle \log B_0/[G] \rangle$=12.65, σ_B=0.55

$$P_0 = P\sqrt{1 - \frac{t}{\tau}}.$$

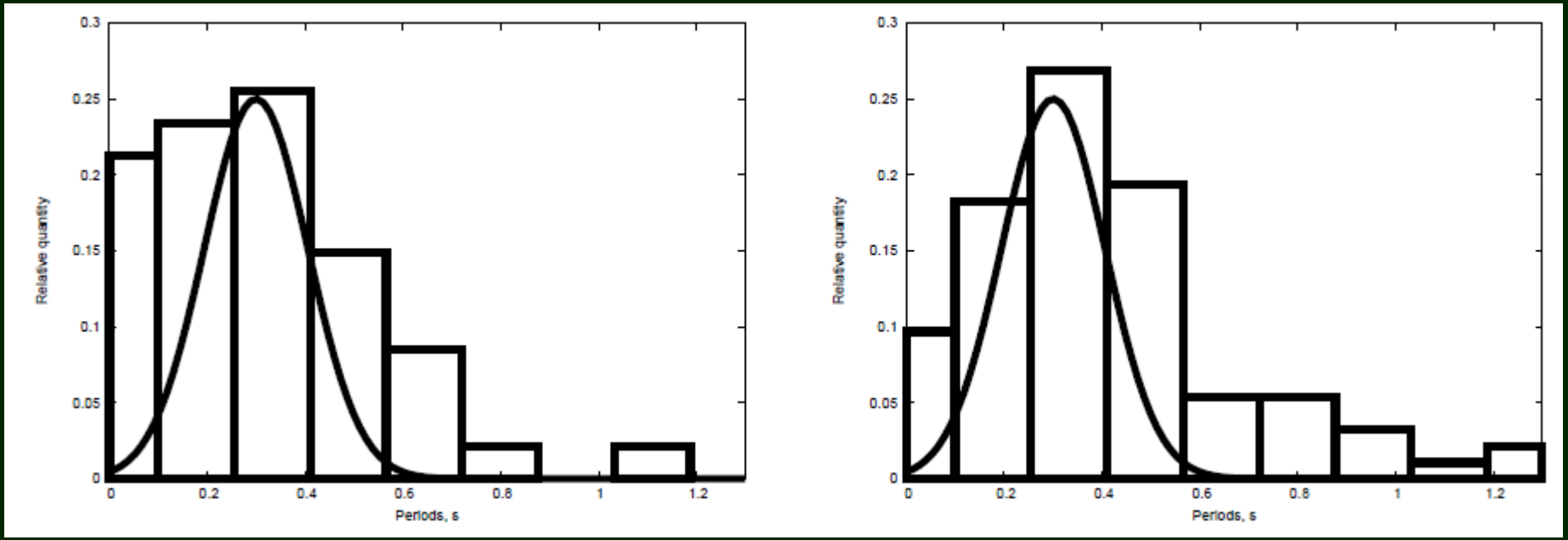

$\tau<10^7$ yrs, $10^5<t$

$10^5<t<10^7$ yrs

Igoshev, Popov 2013

Real vs. reconstructed P_0

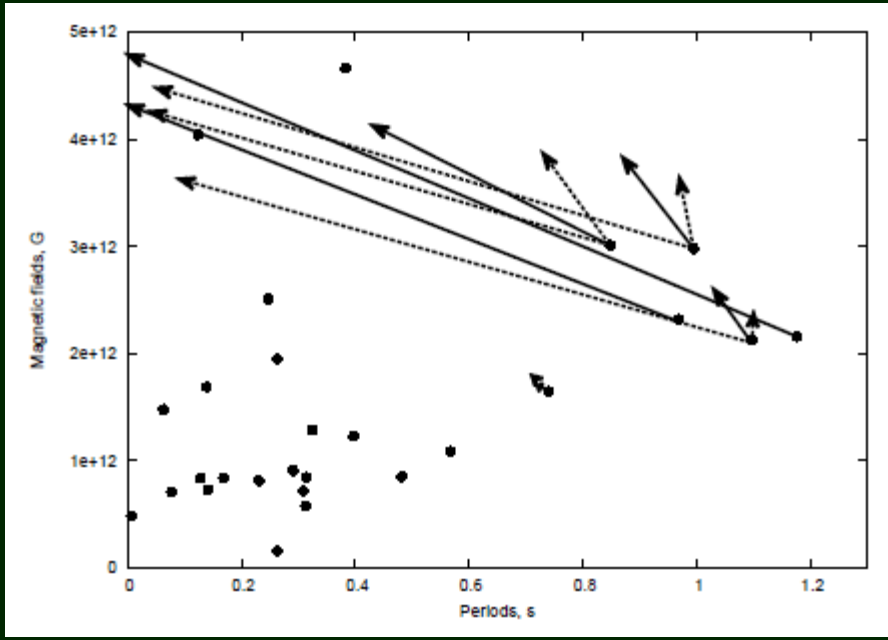

How much the reconstructed initial periods are changed due to not taking into account the exponential field decay?

Igoshev, Popov 2013

Complications for magneto-rotational evolution

1. Internal structure can be important.
   For example, neutron vorticies can pin magnetic flux tubes (1106.5997).
   Estimates indicate that this can be important for magnetars.
2. In young NSs a core can rotates faster than the crust (1210.5872).
3. Non-trivial topology of the magnetosphere can be important.
   In magnetars a twisted magnetosphere can result in a different spin-down rate (1201.3635, and see the lecture on magnetars)
4. Magnetic field can have a very non-trial evolution (see the next lecture)
5. Initial spin-periods can depend on additional phenomenae.
   Gravitational wave emission (1302.2649).
   Neutrino emission (1301.7495).
   Different instabilities (1110.3937).

Conclusions

- We have some framework for spin evolution of NSs.
  They are expected to pass several well-defined stages:
  Ejector (including radio pulsar),
  Propeller (probably, with subsonic substage),Accretor.
  NSs with large velocities (or fields) after the Ejector stage
  can appear as Georotators.

- In binaries we observe Ejectors, Propellers and Accretor.
  For isolated NSs – only Ejectors (even, mostly radiopulsars).

- There are still many uncertainties related to the spin evolution:

  1. Spin-down rate and angle evolution for radio pulsars
  2. Subsonic propeller stage for isolated NSs
  3. Inhibition of accretion at low rates
  4. The role of the field decay

Conclusions-2

- Observations of isolated accreting NSs can help a lot to understand *all* unknown questions of NS spin evolution and low-rate accretion.
- Magnetic field decay can be important also for young NSs, especially for highly magnetized ones, as a source of energy.

So, we have some coherent picture ..... But .....

A lot of funny thing a still waitng for us!

Papers and books to read

- Lipunov V.M. “**Astrophysics of neutron stars**” (1992)
- Lipunov, Postnov, Prokhorov “**The Scenario Machine: Binary Star Population Synthesis” Astrophysics and Space Science Reviews (1996)**
  http://xray.sai.msu.ru/~mystery/articles/review/
- Boldin, Popov ``Evolution of isolated neutron stars till accretion'' 1004.4805

Evolution with decaying and re-emerging magnetic field

Diversity of young neutron stars

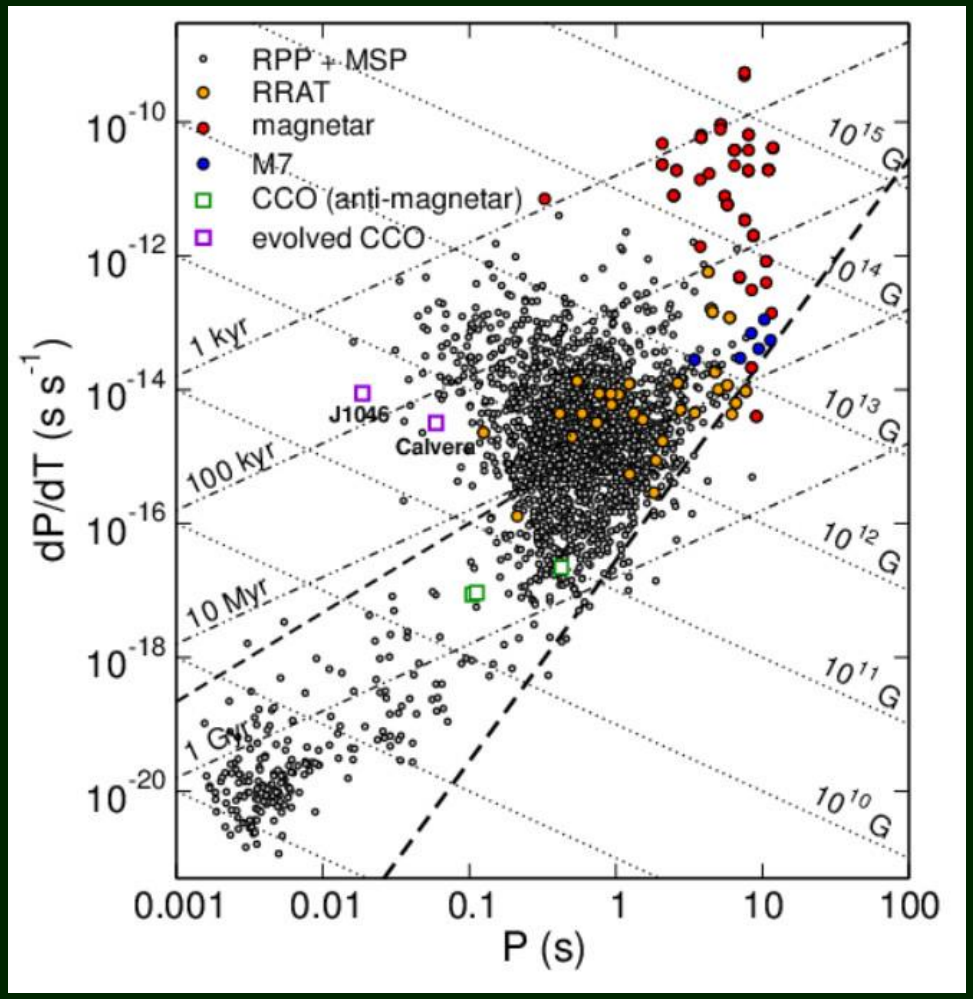

Young isolated neutron stars can appear in many flavors:

- o Radio pulsars
- o Compact central X-ray sources in supernova remnants.
- o Anomalous X-ray pulsars
- o Soft gamma repeaters
- o The Magnificent Seven & Co.
- o Transient radio sources (RRATs)

The term "GRAND UNIFICATION FOR NEUTRON STARS" was coined by Kaspi (2010)

PSRs, magnetars and M7 unified in the model by Popov et al. (2010).

Pires et al. 2015

Three main ingredients of a unified model

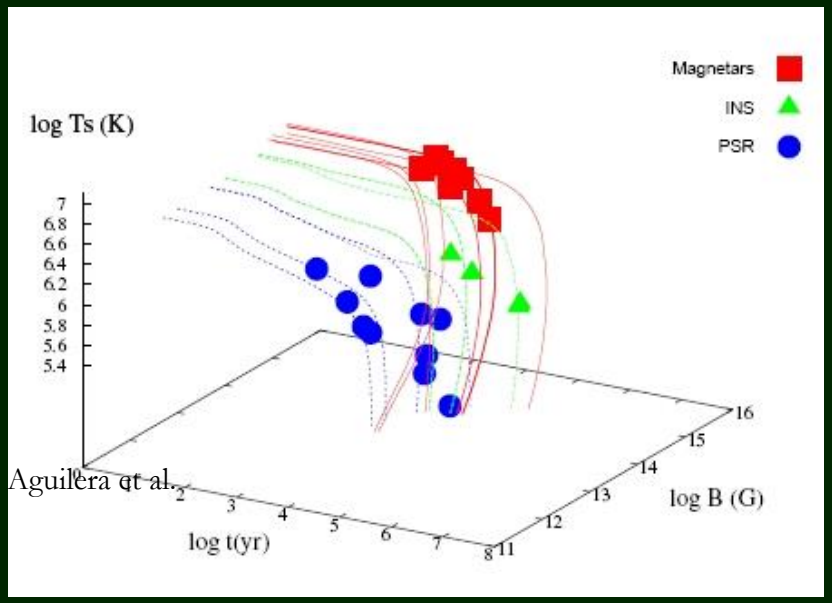

Aguilera et al.

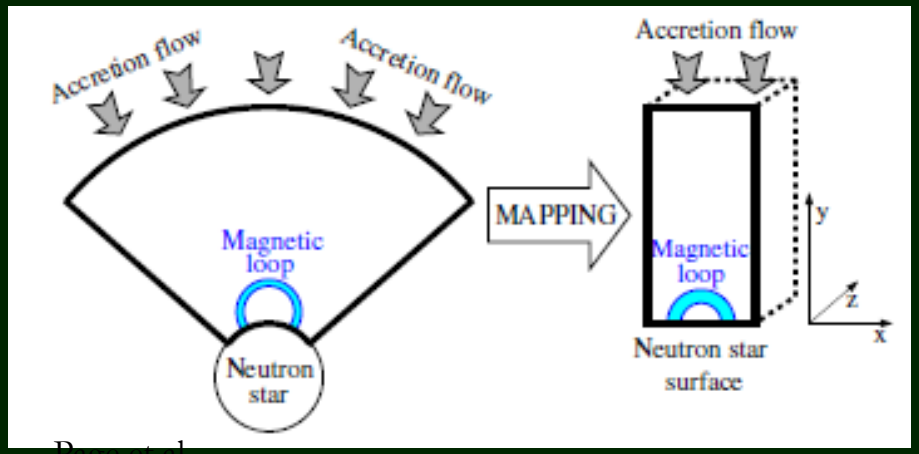

Page et al.

- Field decay
- Emerging magnetic field
- Toroidal magnetic field

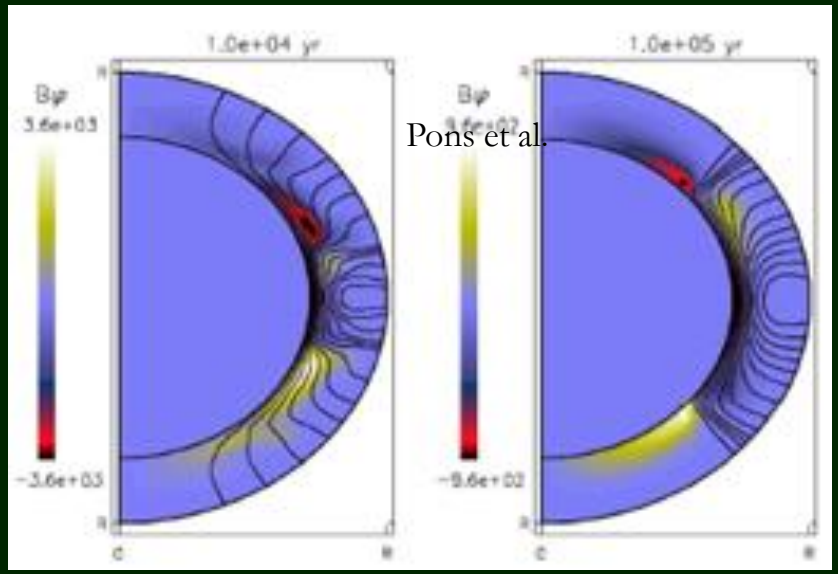

Pons et al.

Magnetic field decay

Magnetic fields of NSs are expected to decay due to decay of currents which support them.

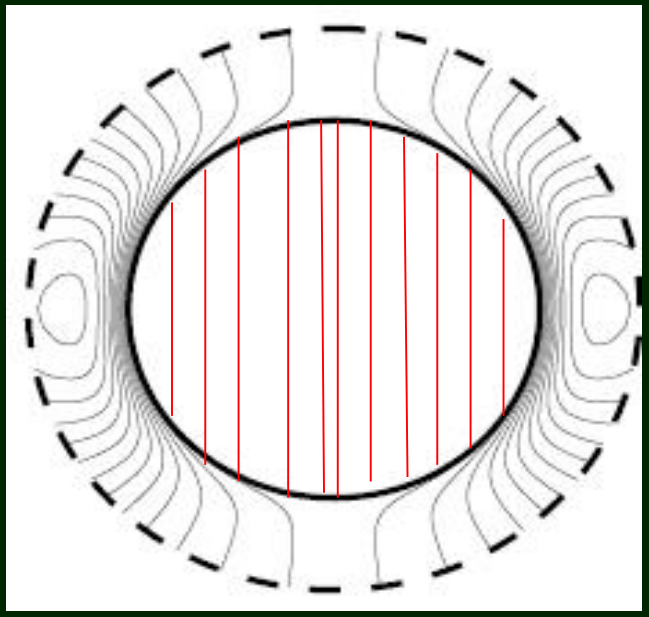

Crustal field of core field?

It is easy to decay in the crust.

In the core the filed is in the form of superconducting vortices.
They can decay only when they are moved into the crust (during spin-down).

Still, in most of models strong fields decay.

Period evolution with field decay

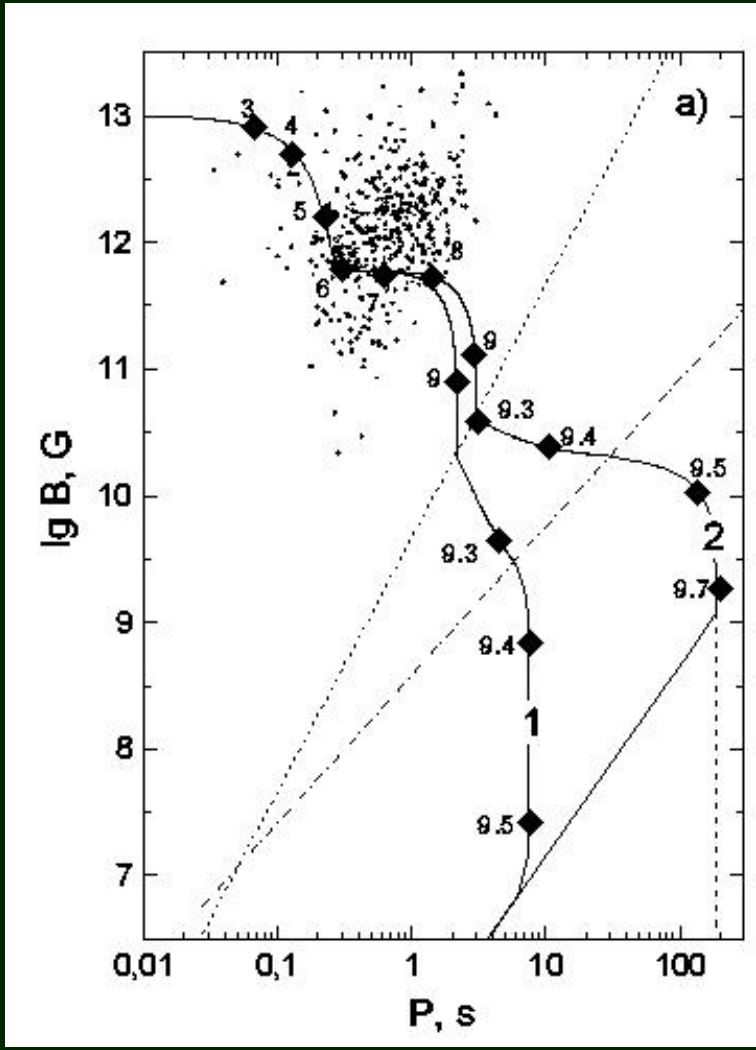

An evolutionary track of a NS is very different in the case of decaying magnetic field.

The most important feature is slow-down of spin-down. Finally, a NS can nearly freeze at some value of spin period.

Several episodes of relatively rapid field decay can happen.

Number of isolated accretors can be both decreased or increased in different models of field decay. But in any case their average periods become shorter and temperatures lower.

astro-ph/9707318

Magnetars, field decay, heating

A model based on field-dependent decay of the magnetic moment of NSs can provide an evolutionary link between different populations (Pons et al.).

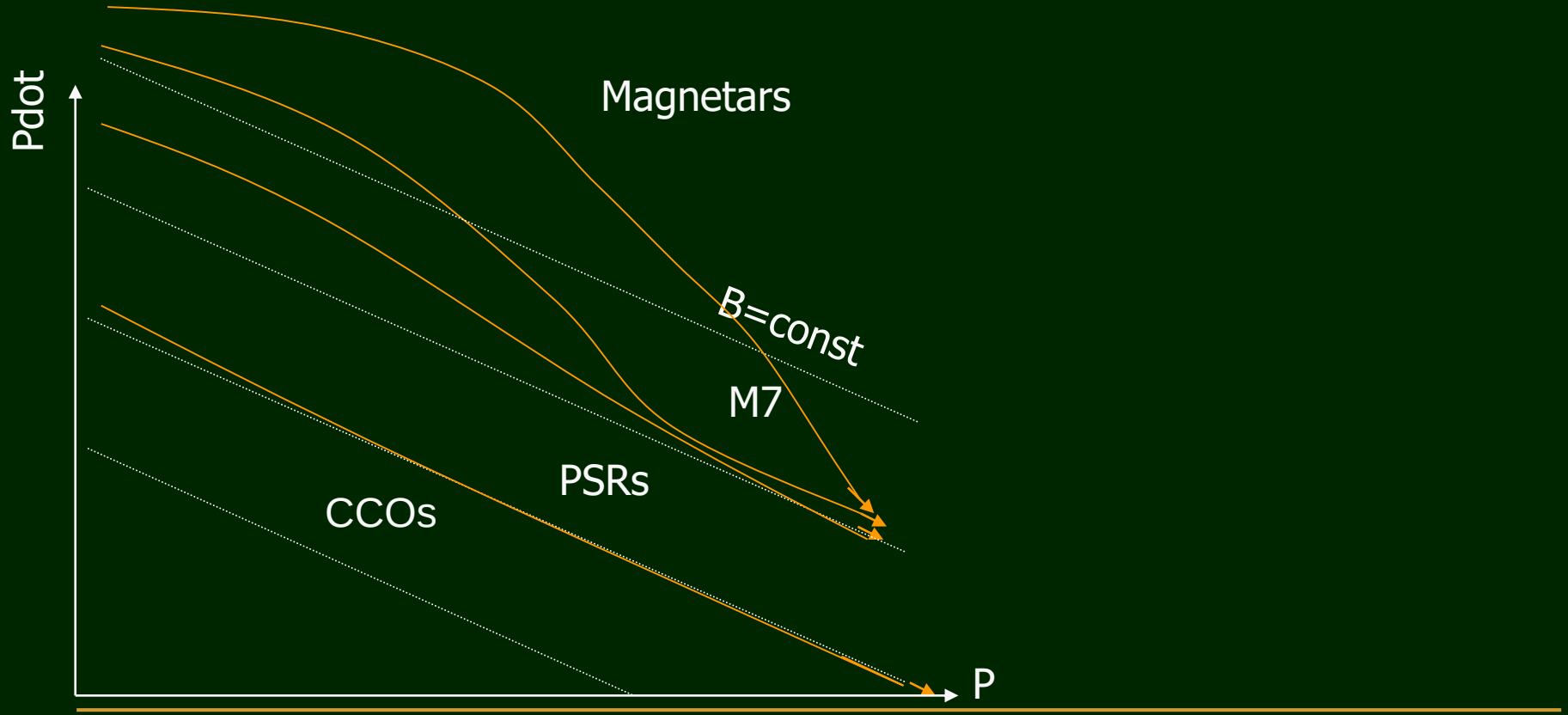

Magnetic field decay vs. thermal evolution

Magnetic field decay can be an important source of NS heating.

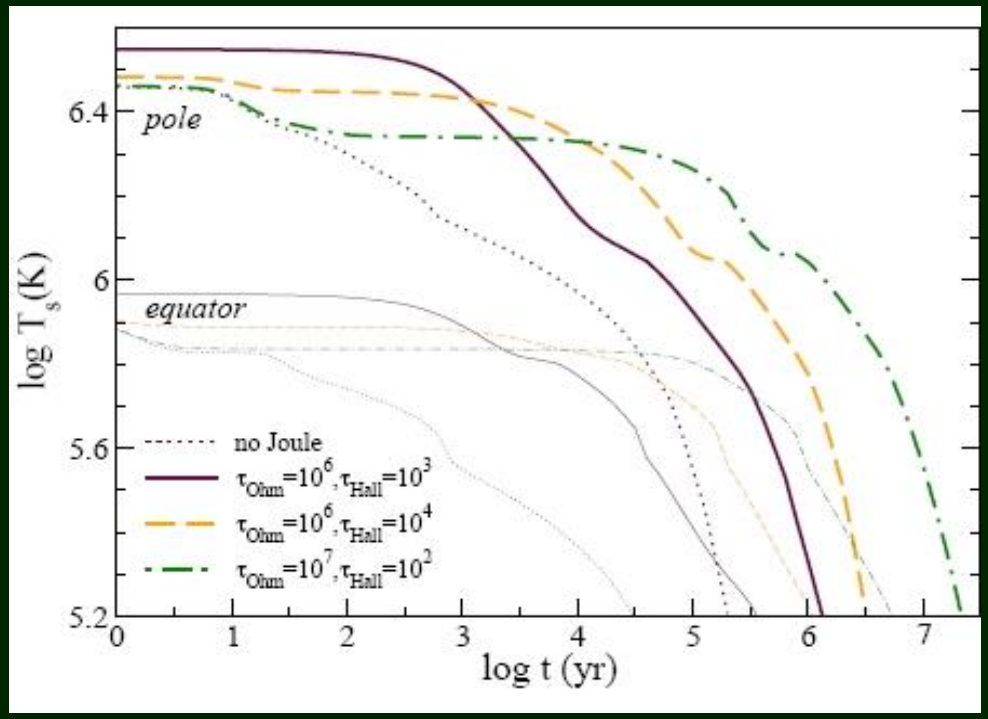

Heat is carried by electrons.
It is easier to transport heat along field lines. So, poles are hotter.
(for light elements envelope the situation can be different).

Ohm and Hall decay

arxiv:0710.0854 (Aguilera et al.)

$$B = B_0 \frac{\exp\left(-t/\tau_{\rm Ohm}\right)}{1+\frac{\tau_{\rm Ohm}}{\tau_{\rm Hall}}\left(1-\exp\left(-t/\tau_{\rm Ohm}\right)\right)}$$

Joule heating for everybody?

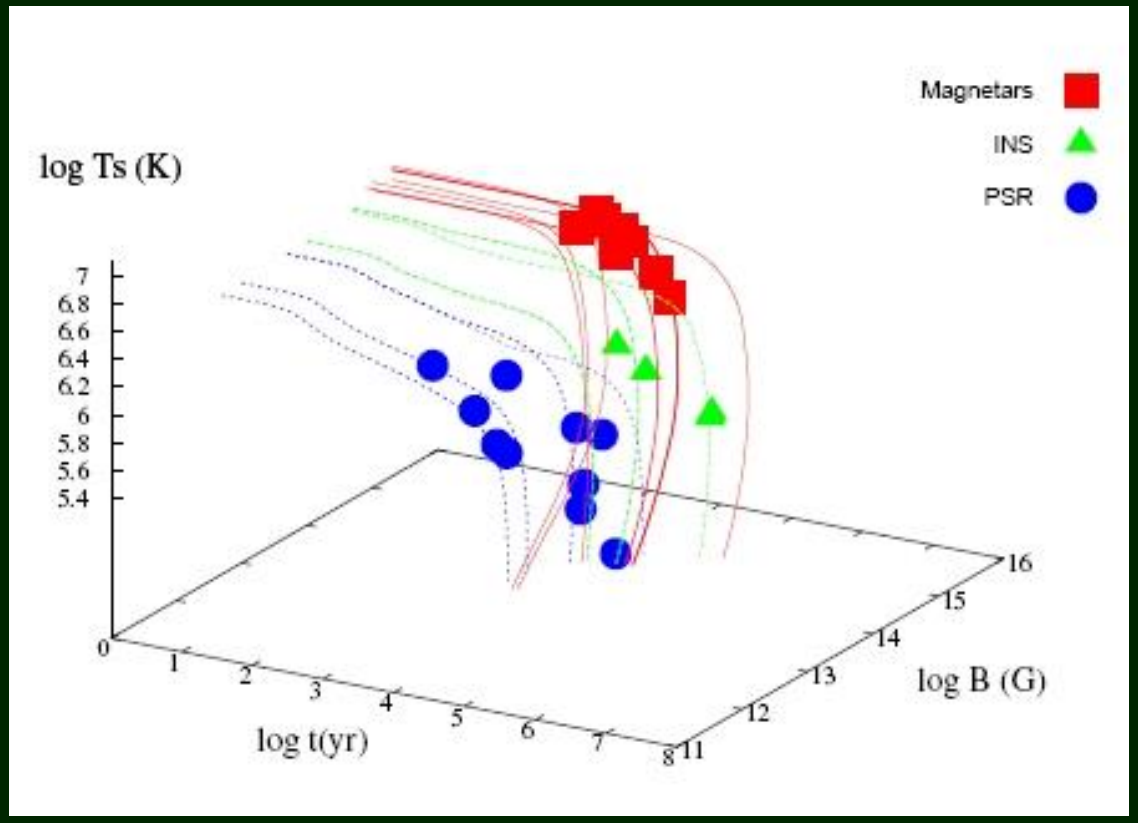

It is important to understand the role of heating by the field decay for different types of INS.

In the model by Pons et al. the effect is more important for NSs with larger initial B.

Note, that the characteristic age estimates (P/2 Pdot) are different in the case of decaying field!

arXiv: 0710.4914 (Aguilera et al.)

Magnetic field vs. temperature

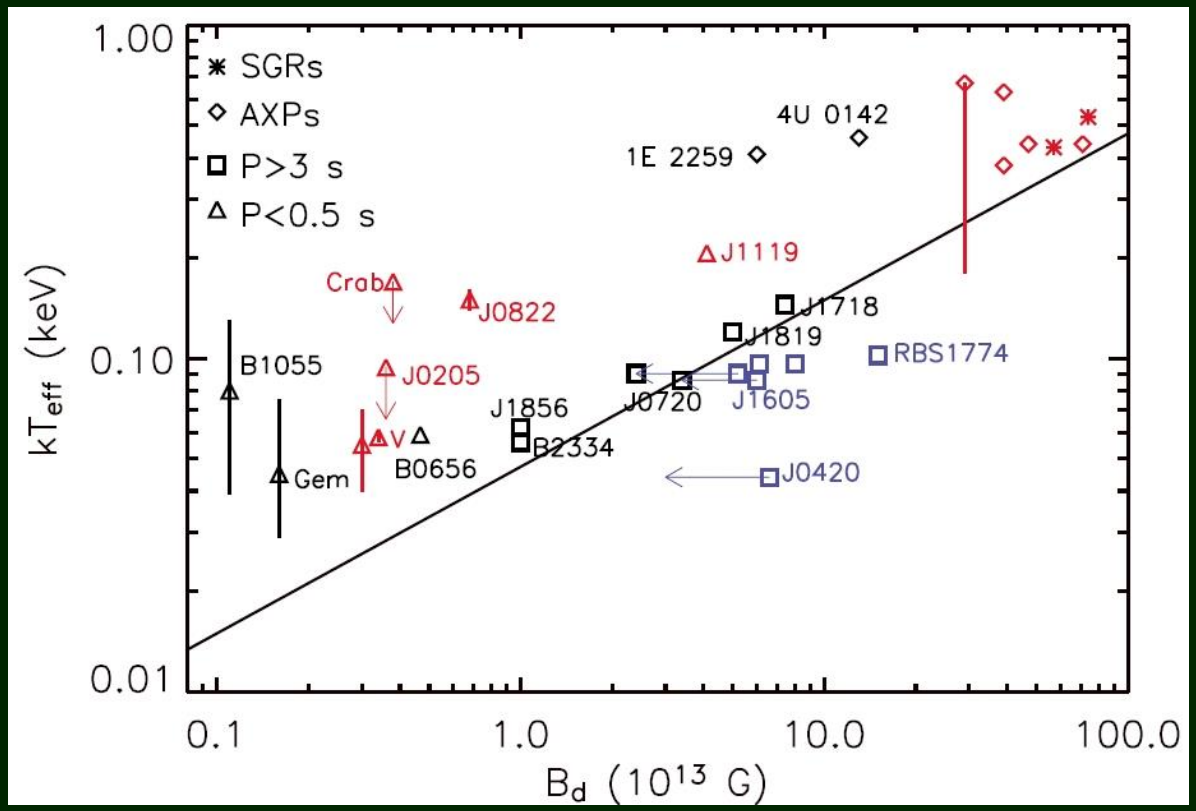

(astro-ph/0607583)

The line marks balance between heating due to the field decay and cooling
It is expected that a NS evolves downwards till it reaches the line, then the evolution proceeds along the line: $T_{eff} \sim B_d^{1/2}$

Selection effects are not well studied here.
A kind of population synthesis modeling is welcomed.

What kind of decay do we see?

Ohmic decay due to phonons

Hall cascade

Both time scales fit, and in both cases we can switch of decay at ~1
either due to cooling, or due to the Hall attractor.

$$B = B_0 \frac{\exp\left(-t/\tau_{\rm Ohm}\right)}{1 + \frac{\tau_{\rm Ohm}}{\tau_{\rm Hall}}\left(1 - \exp\left(-t/\tau_{\rm Ohm}\right)\right)}$$

Hall cascade and field evolution

$$\frac{\partial B}{\partial t} = -c\nabla \times E,$$

advection

Ohm

Hall

$$E = -\frac{1}{c} v \times B + \frac{J}{\sigma} + \frac{J \times B}{n_e e c},$$

$$\tau_{\rm Ohm} = \frac{4\pi\sigma L^2}{c^2}.$$

$$J = (c/4\pi)(\nabla \times B)$$

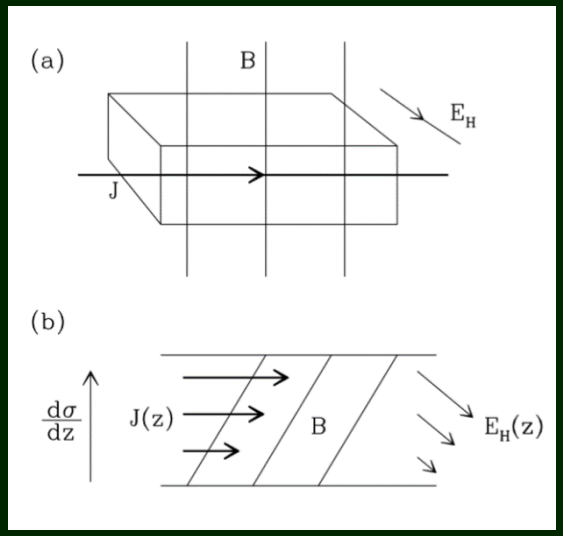

With only Hall term we have:

$$\frac{\partial B}{\partial t} = -\nabla \times \left(\frac{J \times B}{n_e e} \right),$$

$$t_{\rm Hall} = \frac{n_e e L}{J} = \frac{4\pi n_e e L^2}{cB},$$

astro-ph/0402392

Characteristic timescales

$$\tau_{\rm Hall} = \frac{4\pi e n_e L^2}{cB(t)},$$

$$\tau_{\rm Hall} = \tau_{\rm Hall,0}\frac{B_0}{B(t)}.$$

Hall time scale strongly depends on the current value of the field.

$$\tau_{\rm Ohm} = \frac{4\pi\sigma L^2}{c^2},$$

$$\sigma = \frac{\sigma_{\rm Q}\sigma_{\rm ph}}{\sigma_{\rm Q}+\sigma_{\rm ph}}.$$

Ohmic decay depends on the conductivity

$$\tau_{\rm Ohm}^{-1} = \tau_{\rm Ohm,ph}^{-1} + \tau_{\rm Ohm,Q}^{-1}.$$

Resistivity can be due to

- Phonons
- Impurities

$$\sigma_Q = 4.4\times10^{25}{\rm s}^{-1}\left(\frac{\rho_{14}^{1/3}}{Q}\right)\left(\frac{Y_e}{0.05}\right)^{1/3}\left(\frac{Z}{30}\right),$$

$$Q = n_{\rm ion}^{-1}\Sigma_i n_i \times (Z^2 - \langle Z\rangle^2).$$

$$\sigma_{\rm ph} = 1.8\times10^{25}{\rm s}^{-1}\left(\frac{\rho_{14}^{7/6}}{T_8^2}\right)\left(\frac{Y_e}{0.05}\right)^{5/3},$$

P-Pdot diagram and field decay

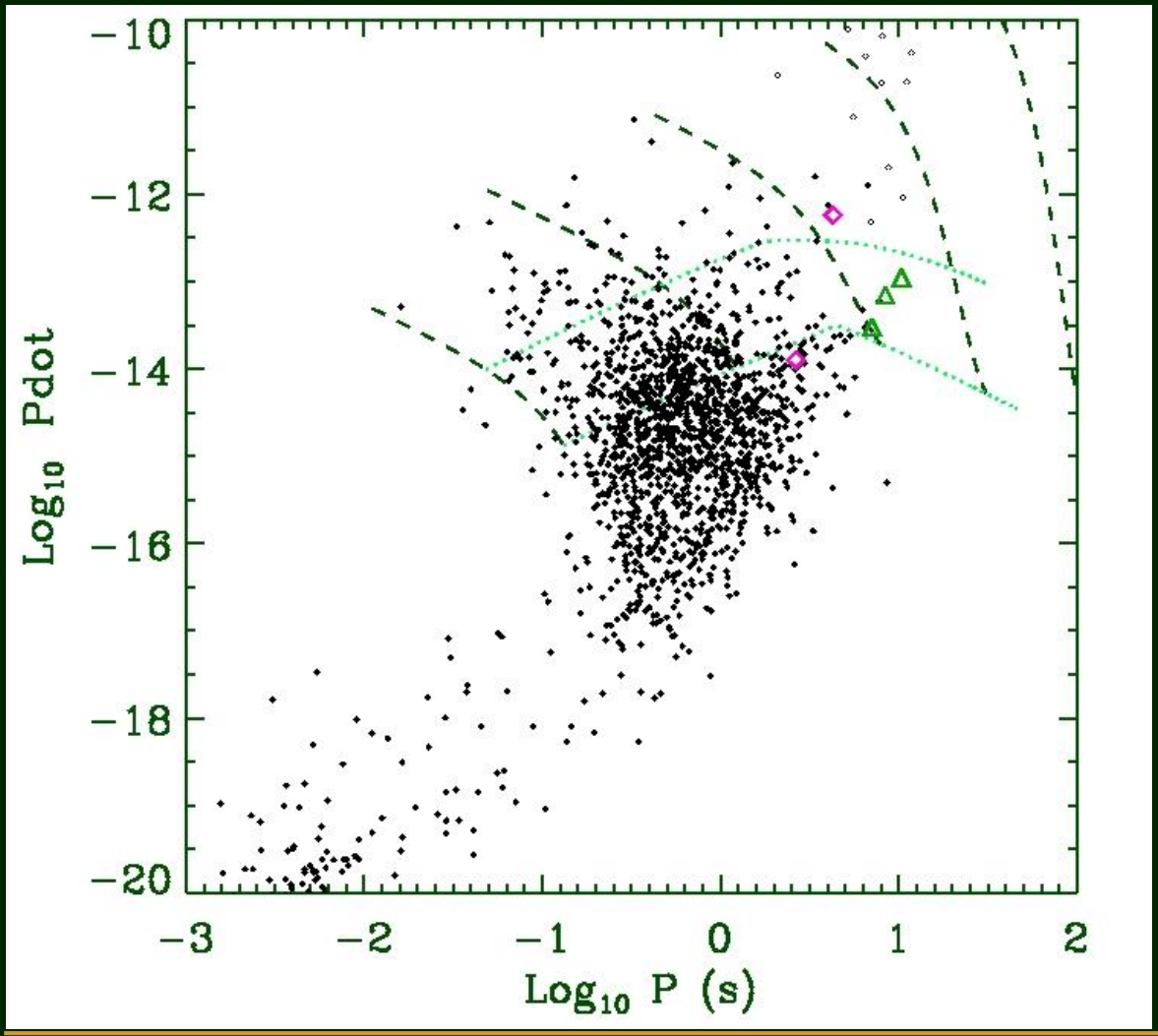

$$B = B_0 \frac{\exp(-t/\tau_{\rm Ohm})}{1 + \frac{\tau_{\rm Ohm}}{\tau_{\rm Hall}}(1 - \exp(-t/\tau_{\rm Ohm}))}$$

$\tau_{Ohm}=10^6$ yrs

$\tau_{Hall}=10^4/(B_0/10^{15}\ G)$ yrs

(Popov et al. MNRAS 2010. arXiv: 0910.2190)

Decay parameters and P-Pdot

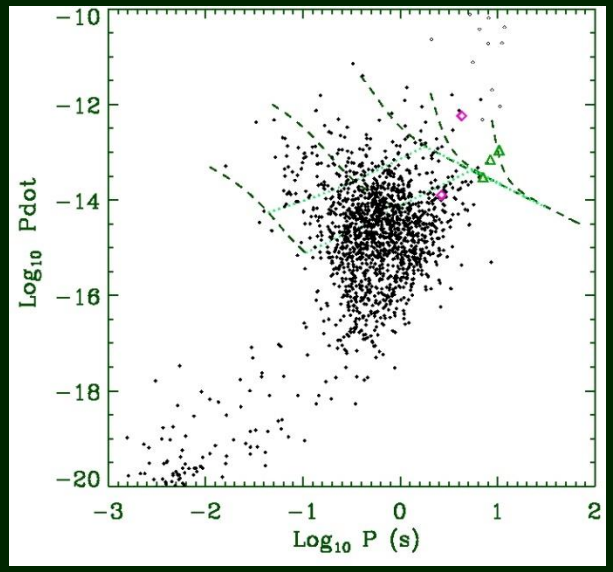

$T_{Ohm}=10^7$ yrs
$T_{Hall}=10^2/(B_0/10^{15}\,G)$

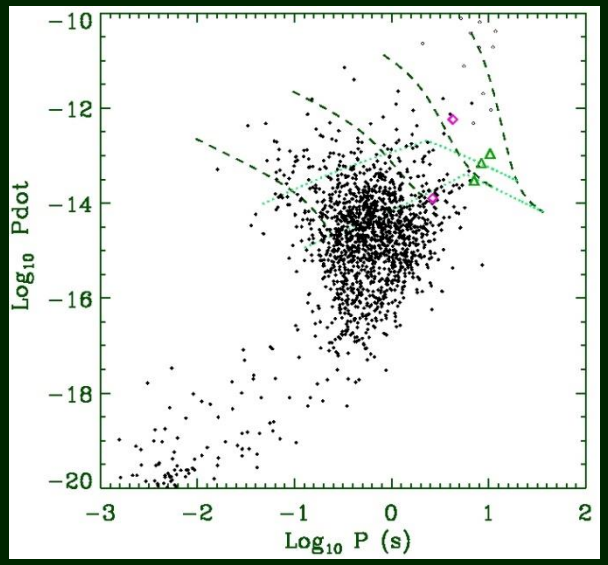

$T_{Ohm}=10^6$ yrs
$T_{Hall}=10^3/(B_0/10^{15}\,G)$

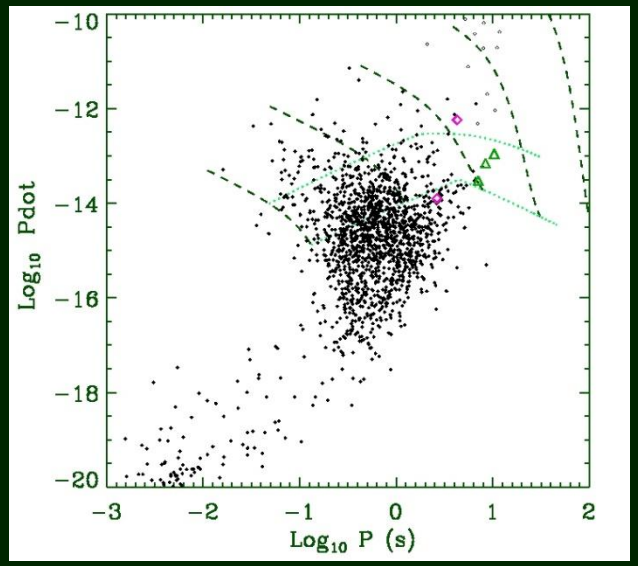

$T_{Ohm}=10^6$ yrs
$T_{Hall}=10^4/(B_0/10^{15}\,G)$

Longer time scale for the Hall field decay is favoured.

It is interesting to look at HMXBs to see if it is possible to derive the effect of field decay and convergence.

Realistic tracks

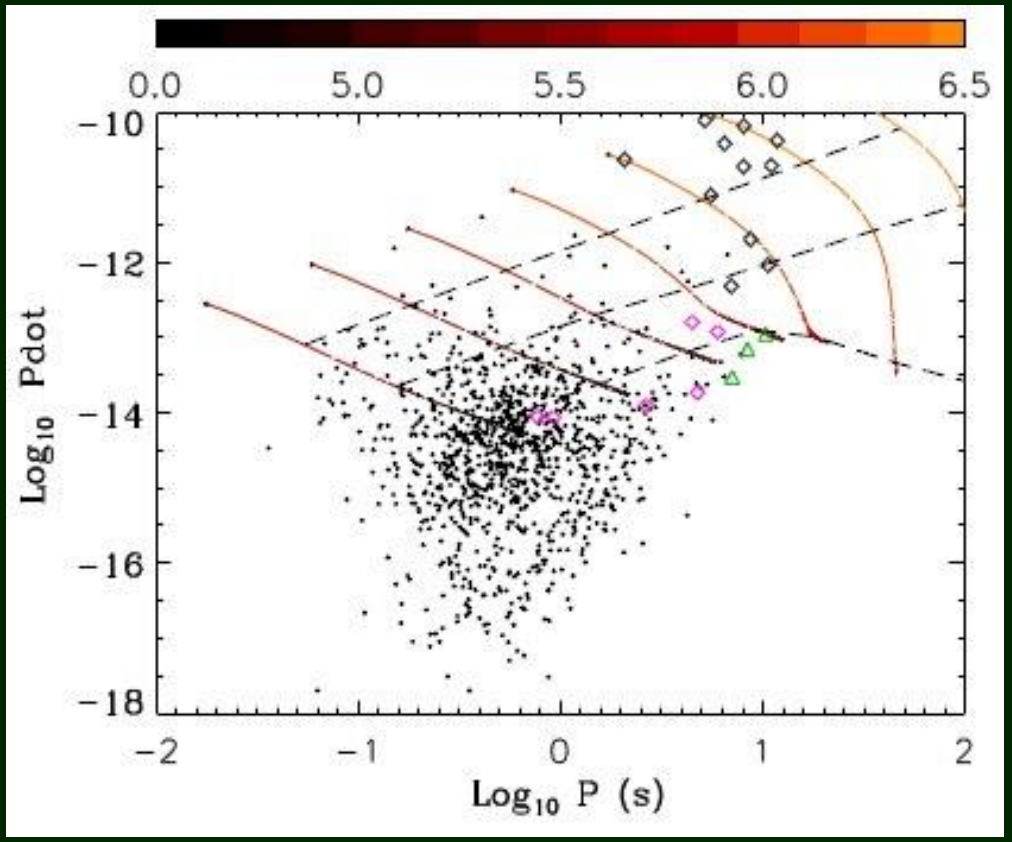

Using the model by Pons et al. (arXiv: 0812.3018) we plot realistic tracks for NS with masses 1.4 Msolar.

Initial fields are:
$3\ 10^{12}$, 10^{13}, $3\ 10^{13}$, 10^{14}, $3\ 10^{14}$, 10^{15}

Color on the track encodes surface temperature.

Tracks start at 10^3 years, and end at $2\ 10^6$ years.

(Popov et al. MNRAS 2010)

Joint description of NS evolution with decaying magnetic field

The idea to describe all types of NSs with a unique model using one initial distribution (fields, periods, velocities) and to compare with observational data, i.e. to confront vs. all available observed distributions:

- P-Pdot for PSRs and other isolated NSs
- Log N – Log S for cooling close-by NSs
- Luminosity distribution of magnetars (AXPs, SGRs)
- ……..

The first step is done in Popov et al. (2010)

The initial magnetic field distribution with $\langle \log B_0 \rangle \sim 13.25$ and $\sigma \sim 0.6$ gives a good fit. ~10% of magnetars.

Cooling curves with decay

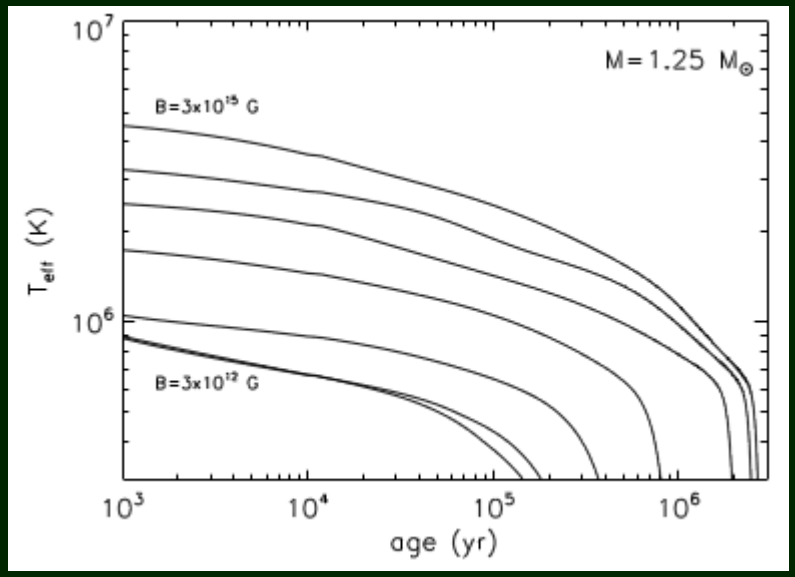

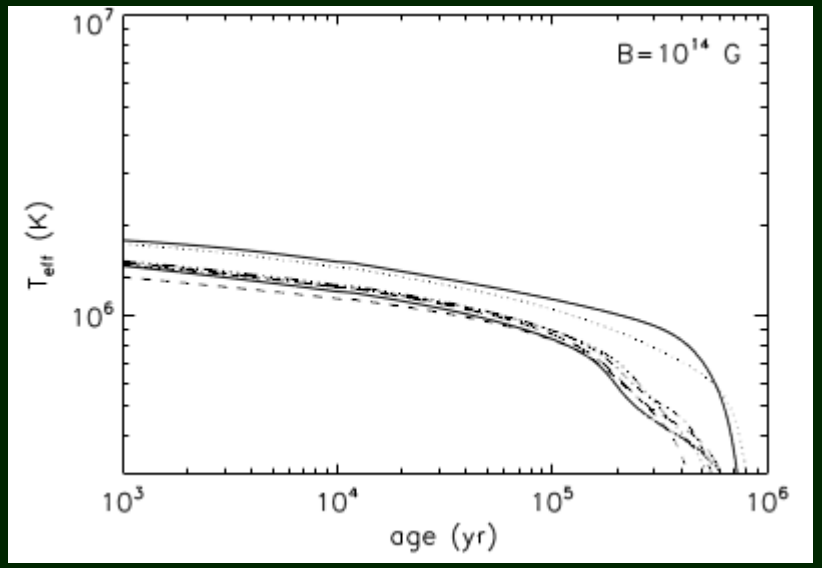

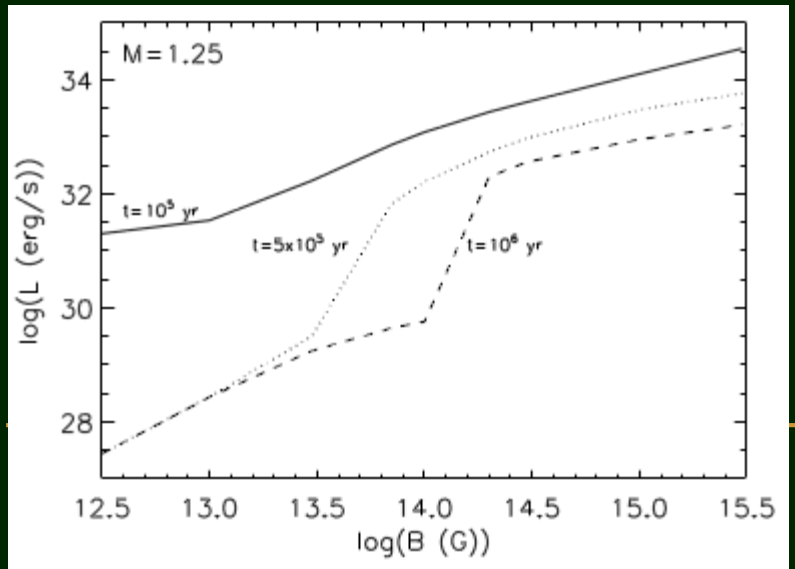

Magnetic field distribution is more important than the mass distribution.

Observational evidence?

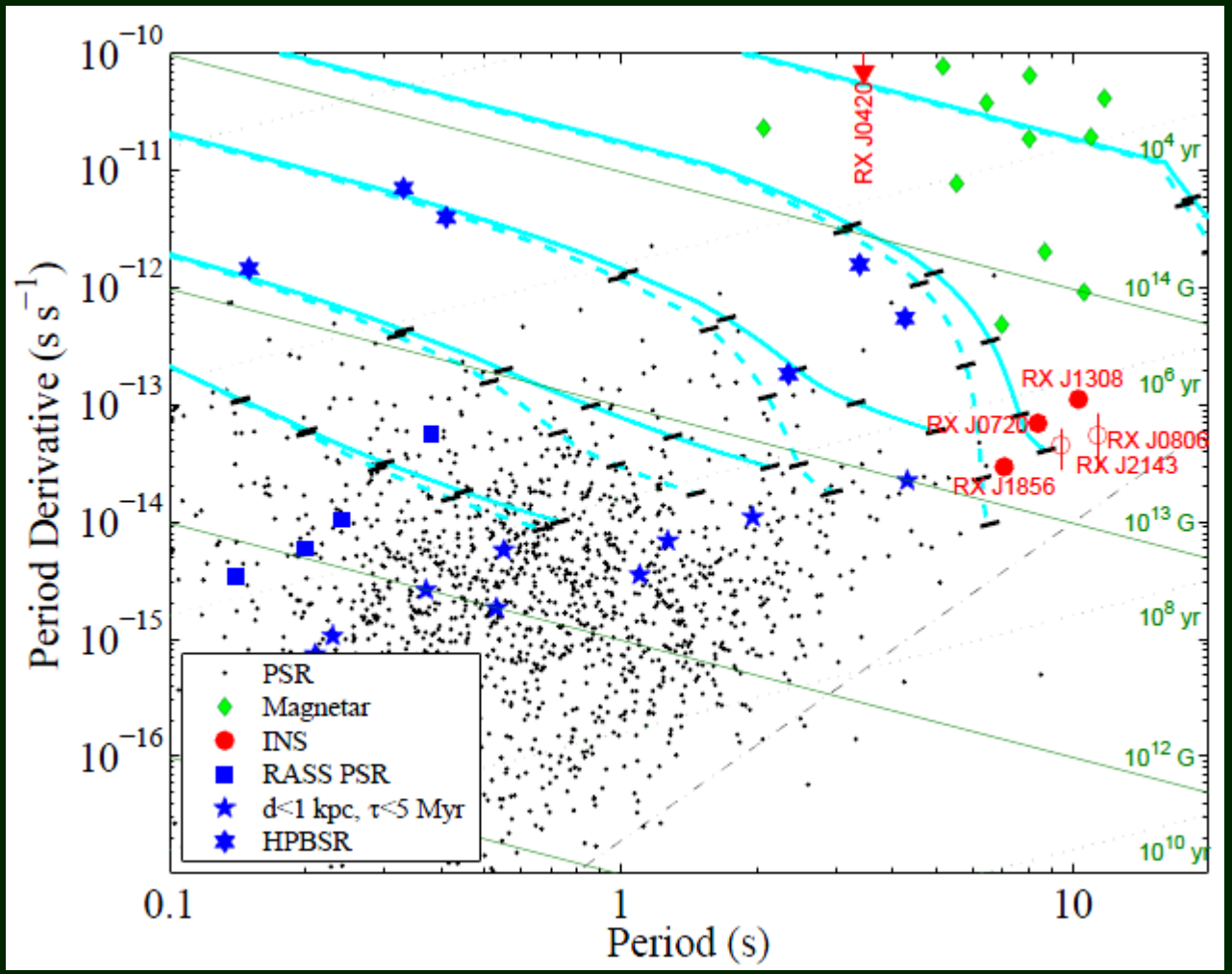

Kaplan & van Kerkwijk arXiv: 0909.5218

Extensive population synthesis: M7, magnetars, PSRs

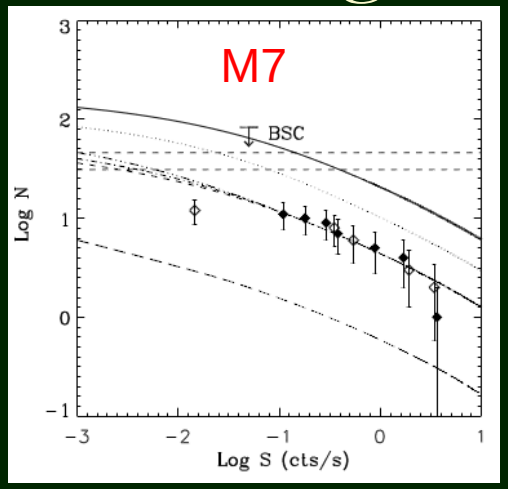

Using one population it is difficult or impossible to find unique initial distribution for the magnetic field

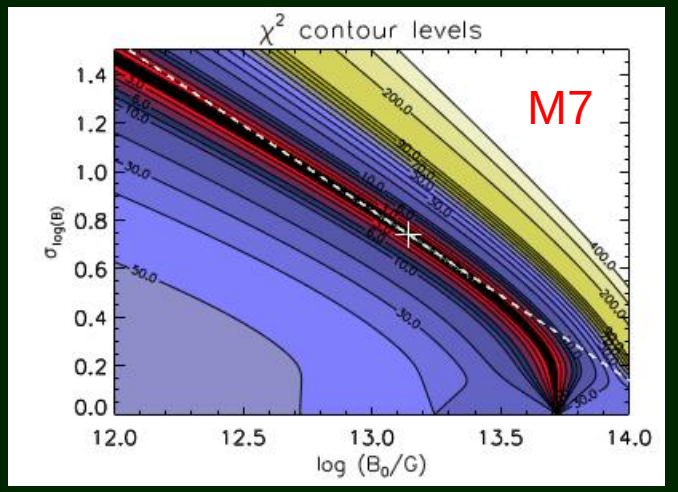

All three populations are compatible with a unique distribution.

Of course, the result is model dependent.

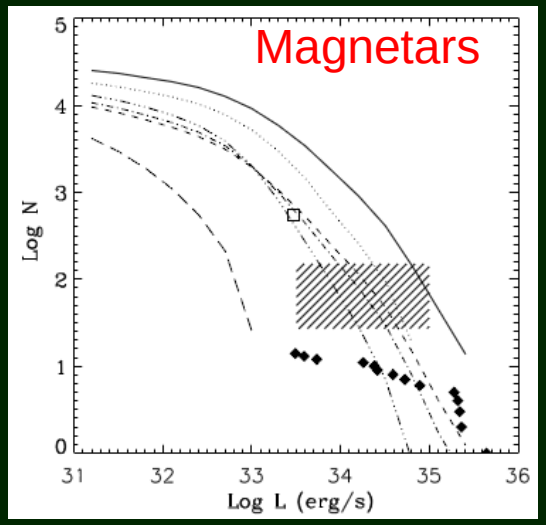

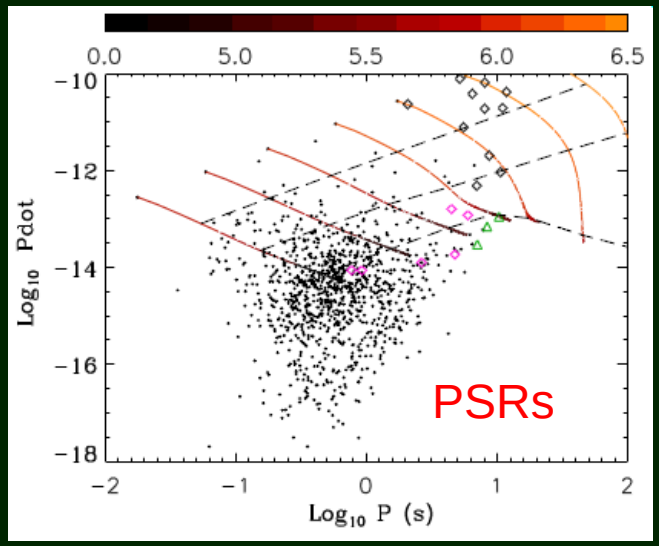

Magnetars bursting activity due to decay

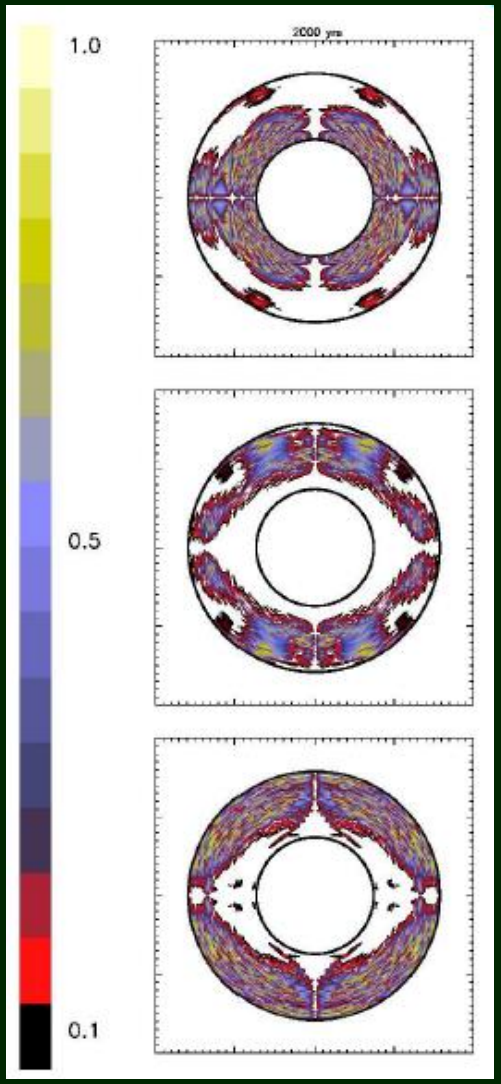

In the field decay model it is possible to study burst activity. Bursts occur due to crust cracking. The decaying field produce stresses in the crust that are not compensated by plastic deformations. When the stress level reaches a critical value the crust cracks, and energy can be released.

At the moment the model is very simple, but this just the first step.

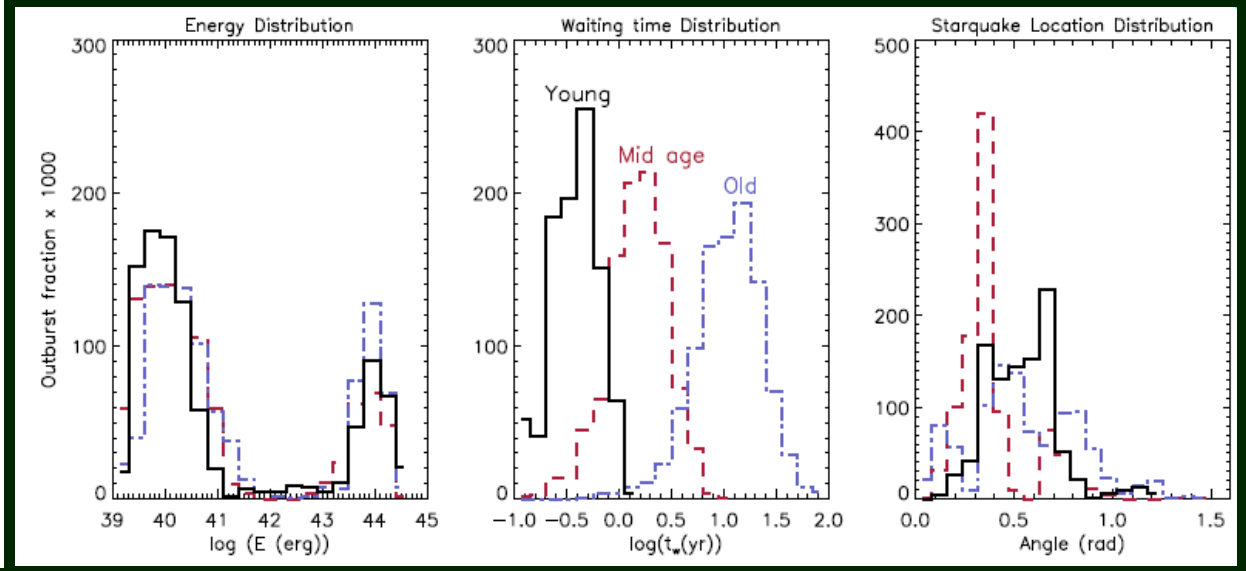

1101.1098

An illustrative model

Poloidal

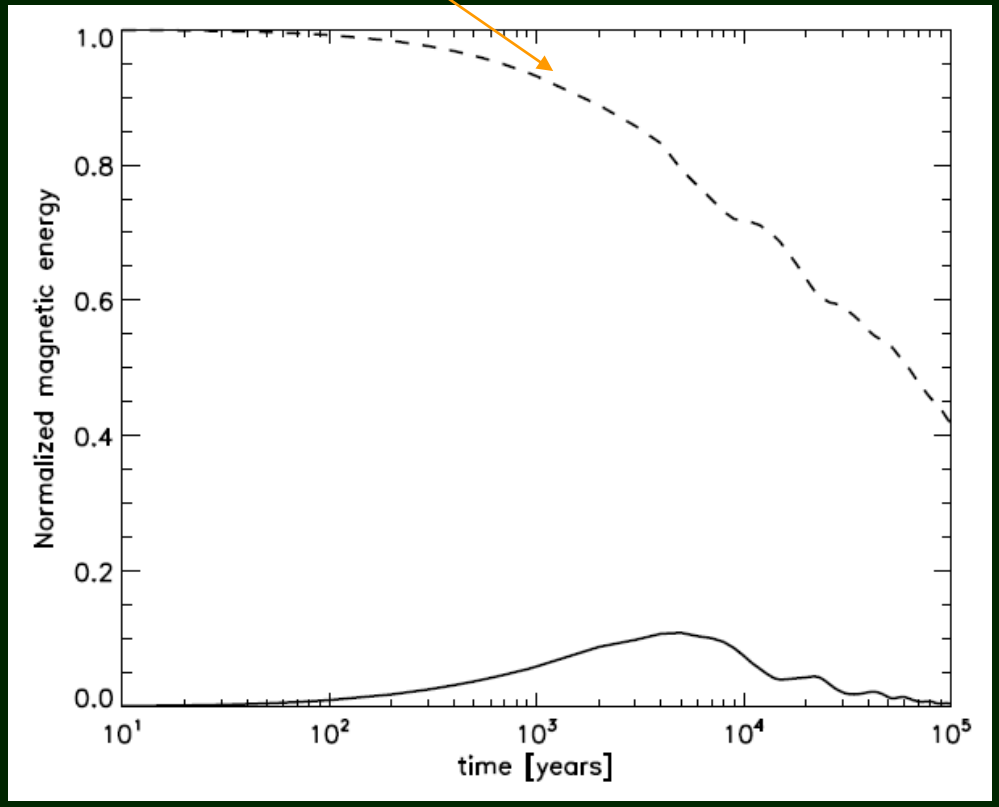

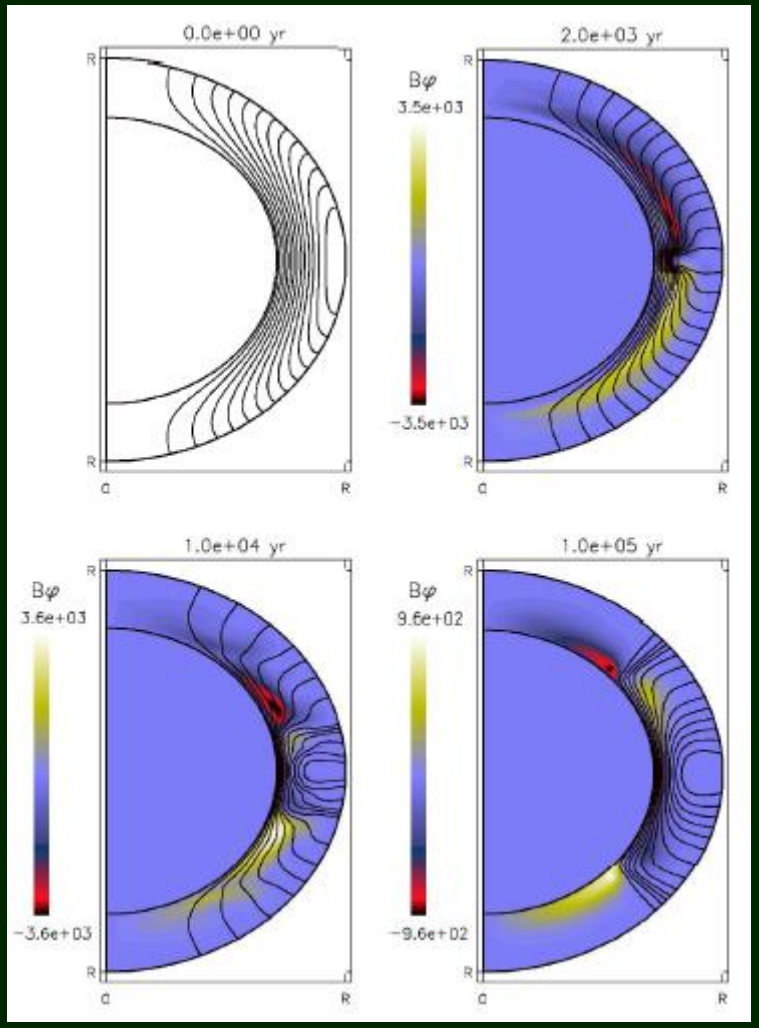

Test illustrates the evolution of initially purely poloidal field

1204.4707

Another model

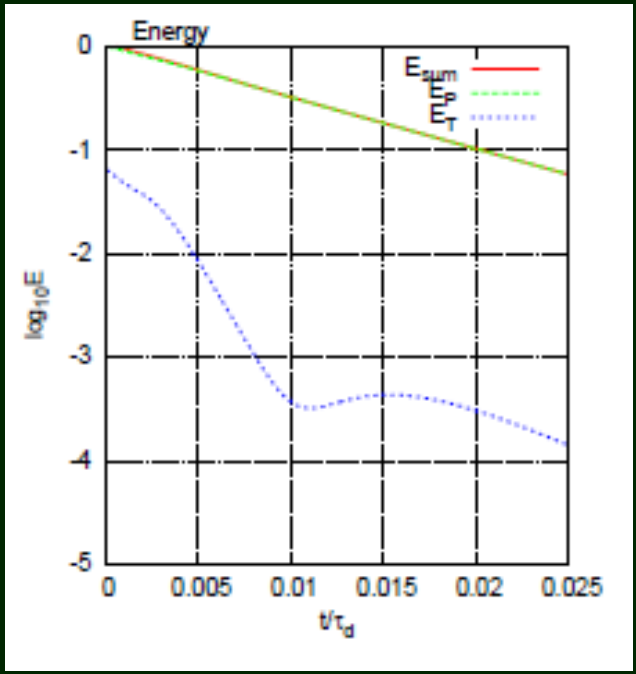

Initially the poloidal field is large.

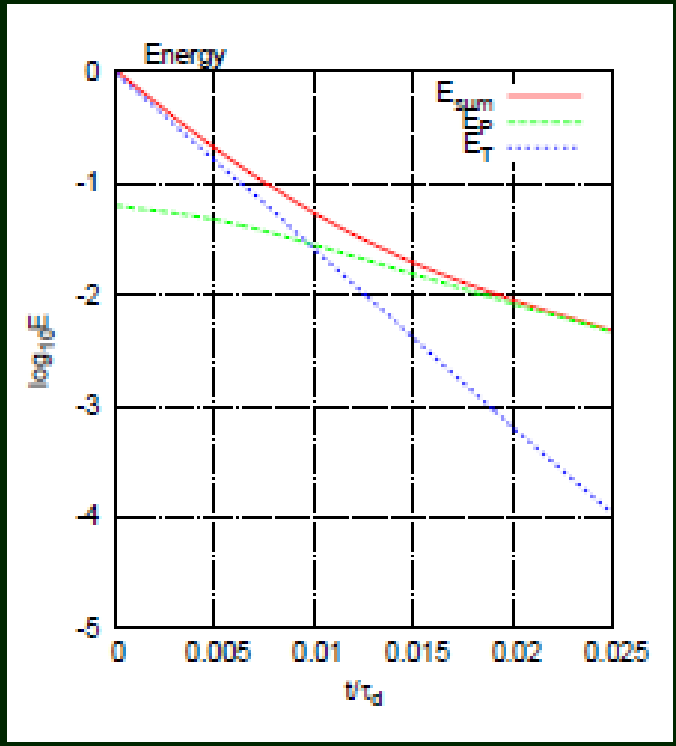

Initially the toroidal field is large.

If the toroidal field dominates initially then significant energy is transferred to the poloidal component during evolution.
In the opposite case, when the poloidal component initially dominates, energy is not transferred. The toroidal component decouples.

1201.1346

Hall cascade and attractor

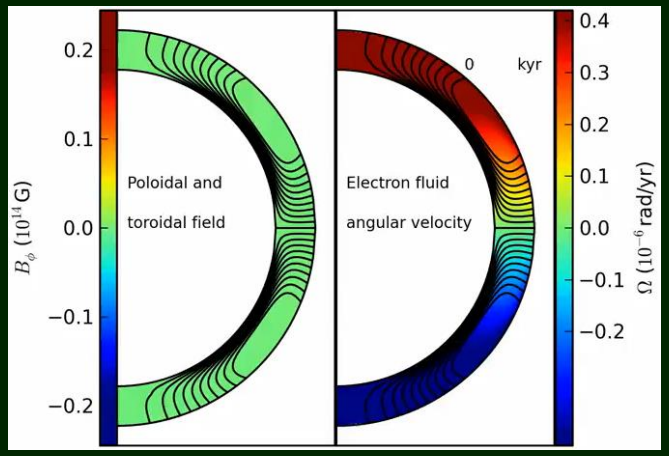

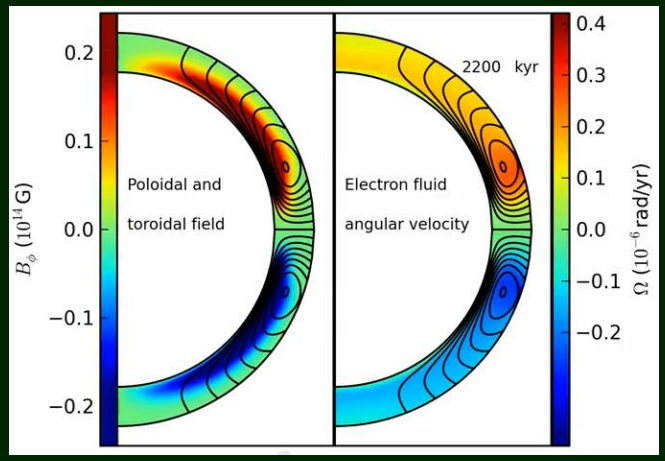

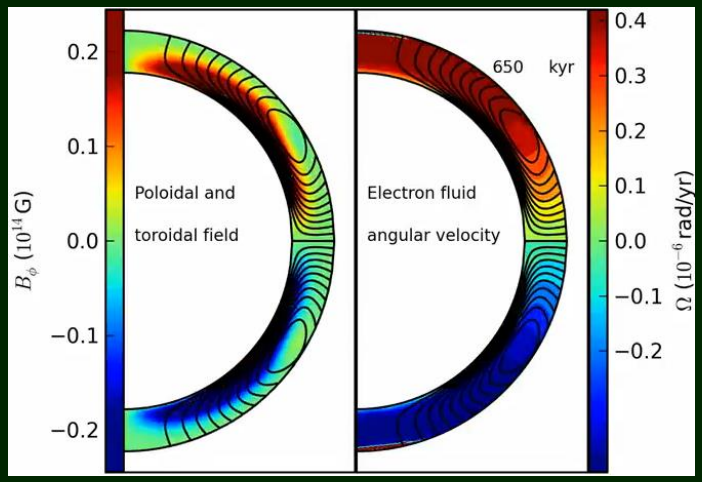

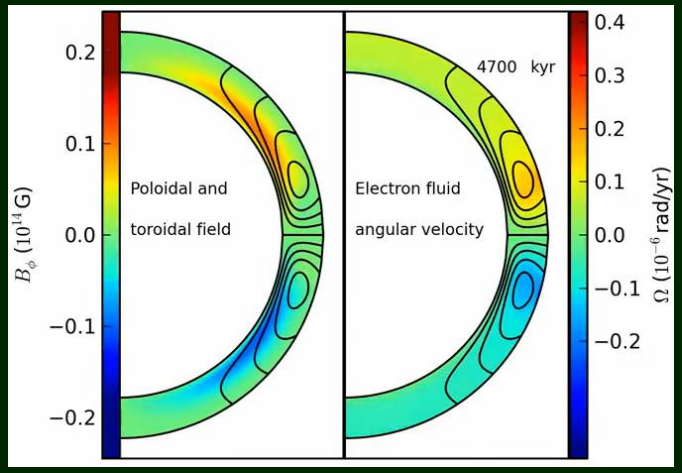

Gourgouliatos and Cumming 2013

Hall cascade can reach the stage of so-called Hall attractor, where the field decay stalls for some time (Gourgouliatos, Cumming).

http://www.physics.mcgill.ca/~kostasg/research.html

Evolution of different components

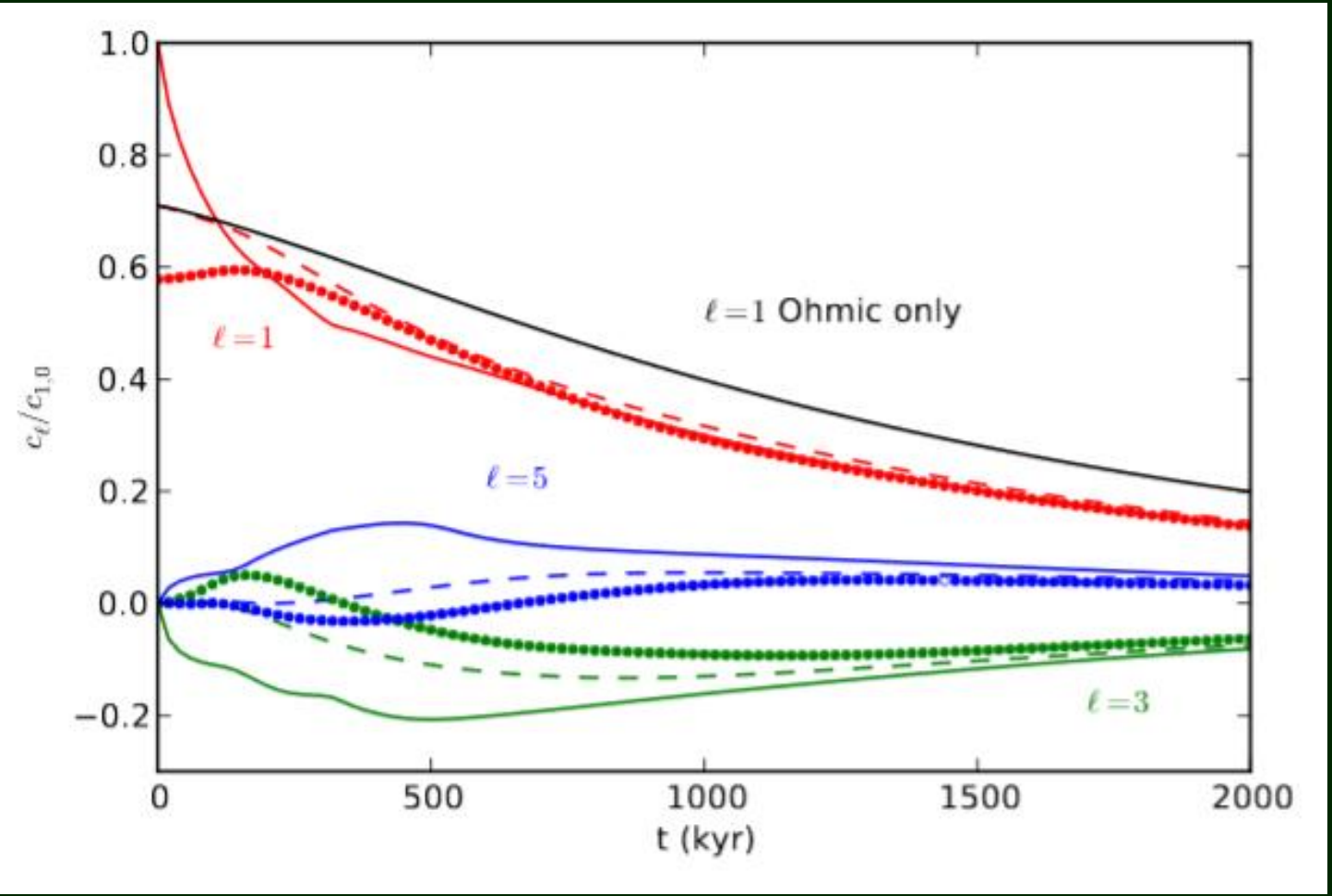

Hall attractor mainly consists of dipole and octupole (+l5)

1311.7004

New studies of the hall cascade

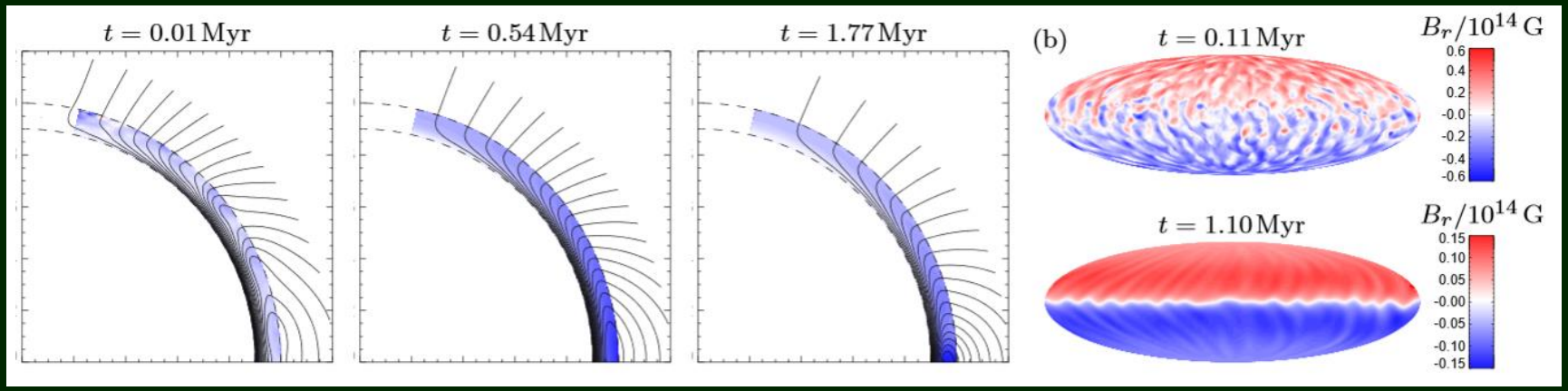

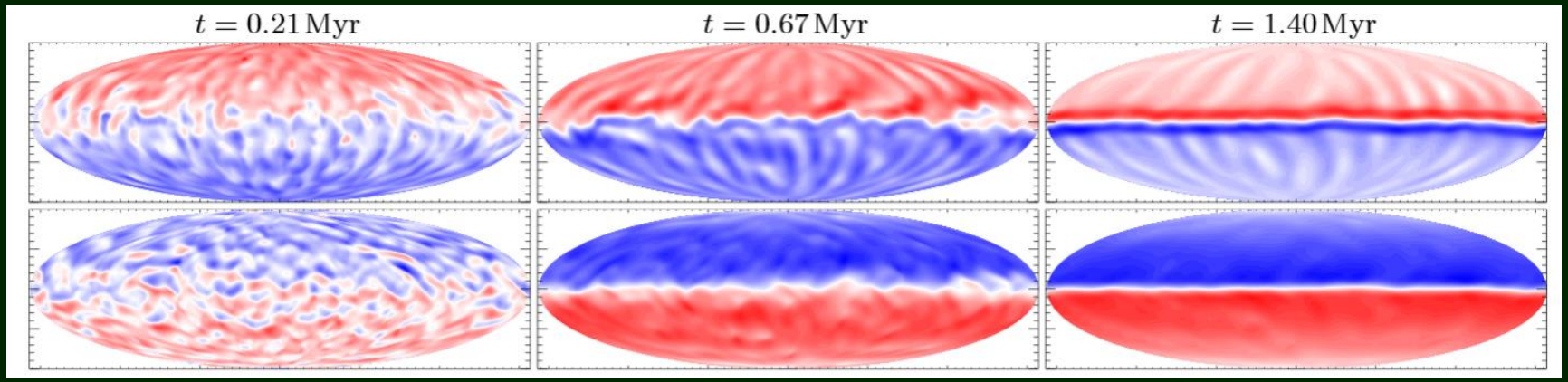

New calculations support the idea of a kind of stable configuration.

1501.05149

Core and crust field evolution

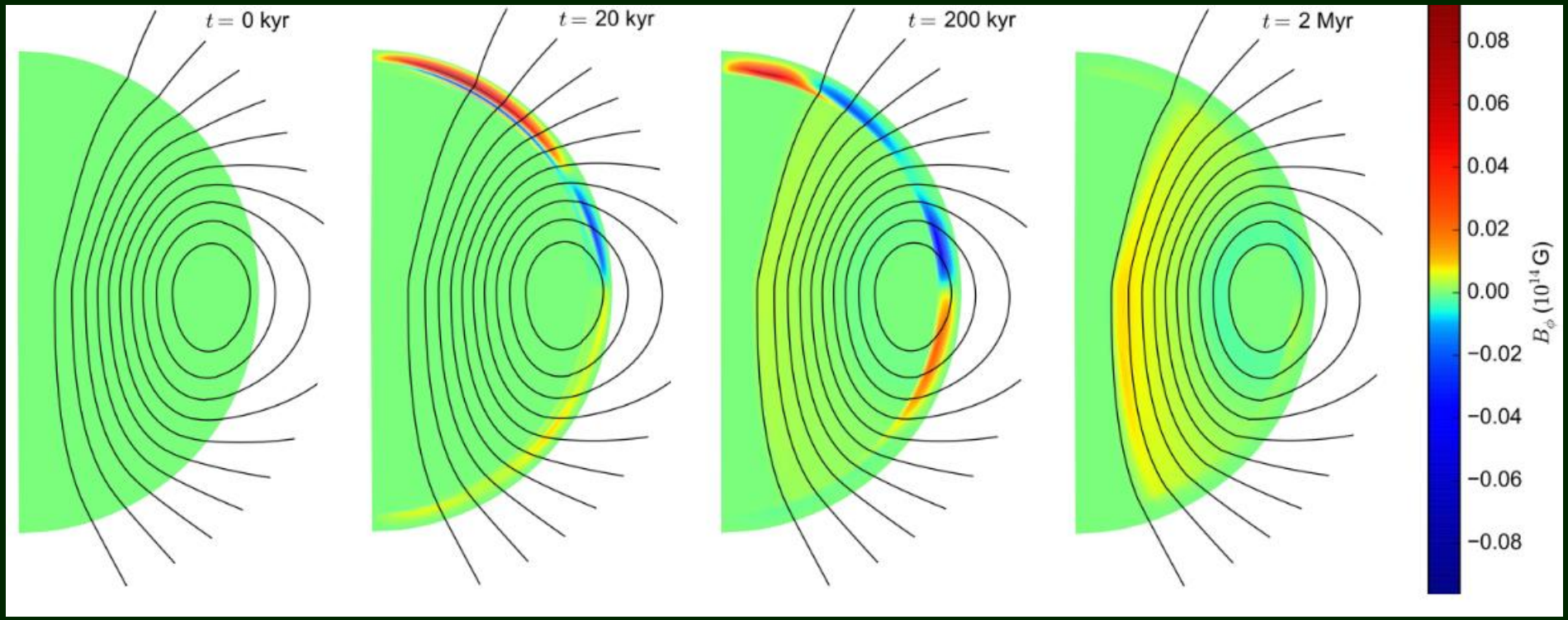

Hall attractor is confirmed.

1709.09167

Core field evolution

1805.03956

Wide initial spin period distribution

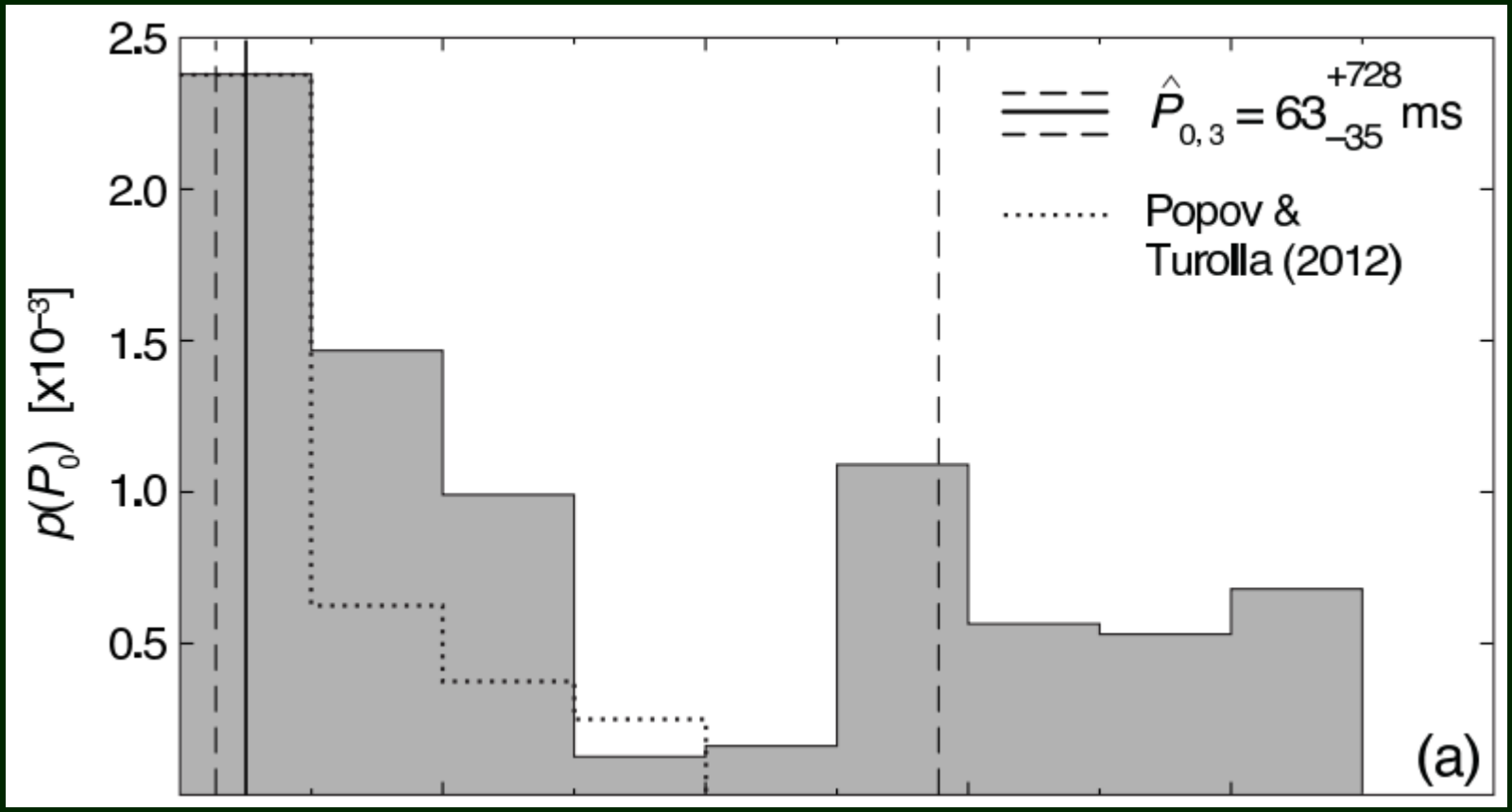

Based on kinematic ages. Mean age – few million years.
Note, that in Popov & Turolla (2012) only NSs in SNRs were used, i.e. the sample is much younger!
Can it explain the difference?

1301.1265

Magnetic field decay and P_0

One can suspect that magnetic field decay can influence the reconstruction of the initial spin period distribution.

Exponential field decay with τ=5 Myrs.
$\langle P_0 \rangle$=0.3 s, σ_P=0.15 s; $\langle \log B_0/[G] \rangle$=12.65, σ_B=0.55

$$P_0 = P\sqrt{1 - \frac{t}{\tau}}.$$

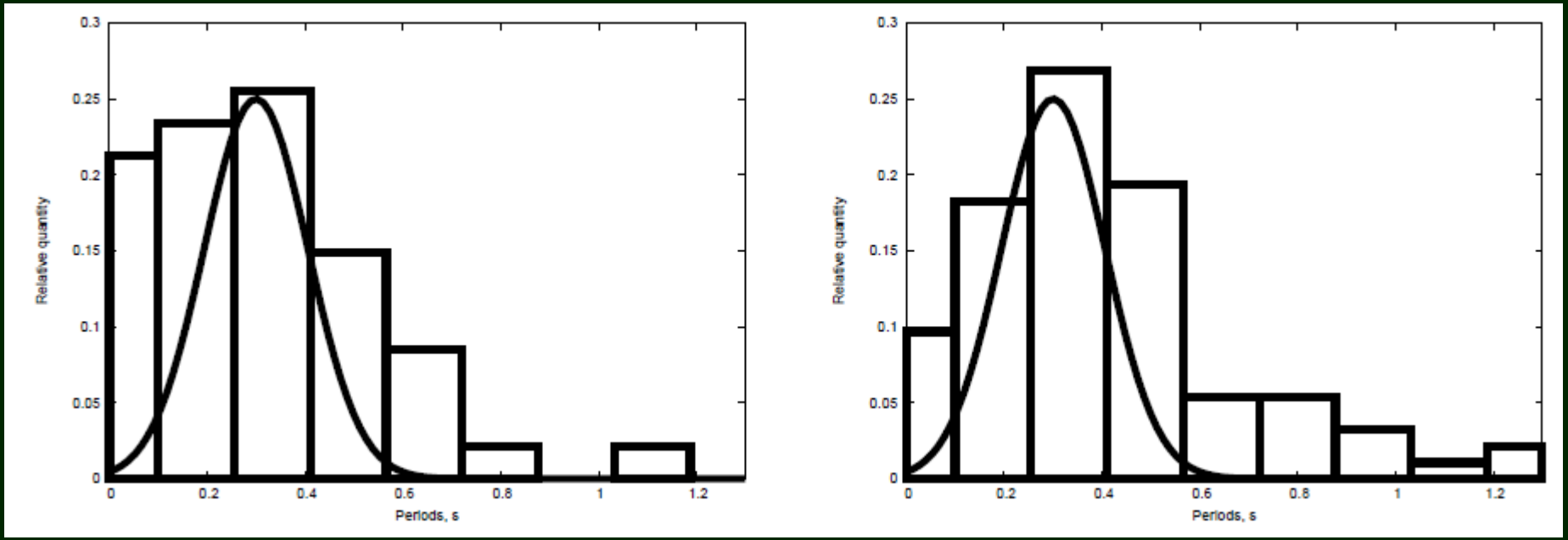

$\tau<10^7$ yrs, $10^5<t$

$10^5<t<10^7$ yrs

Igoshev, Popov 2013

Real vs. reconstructed P_0

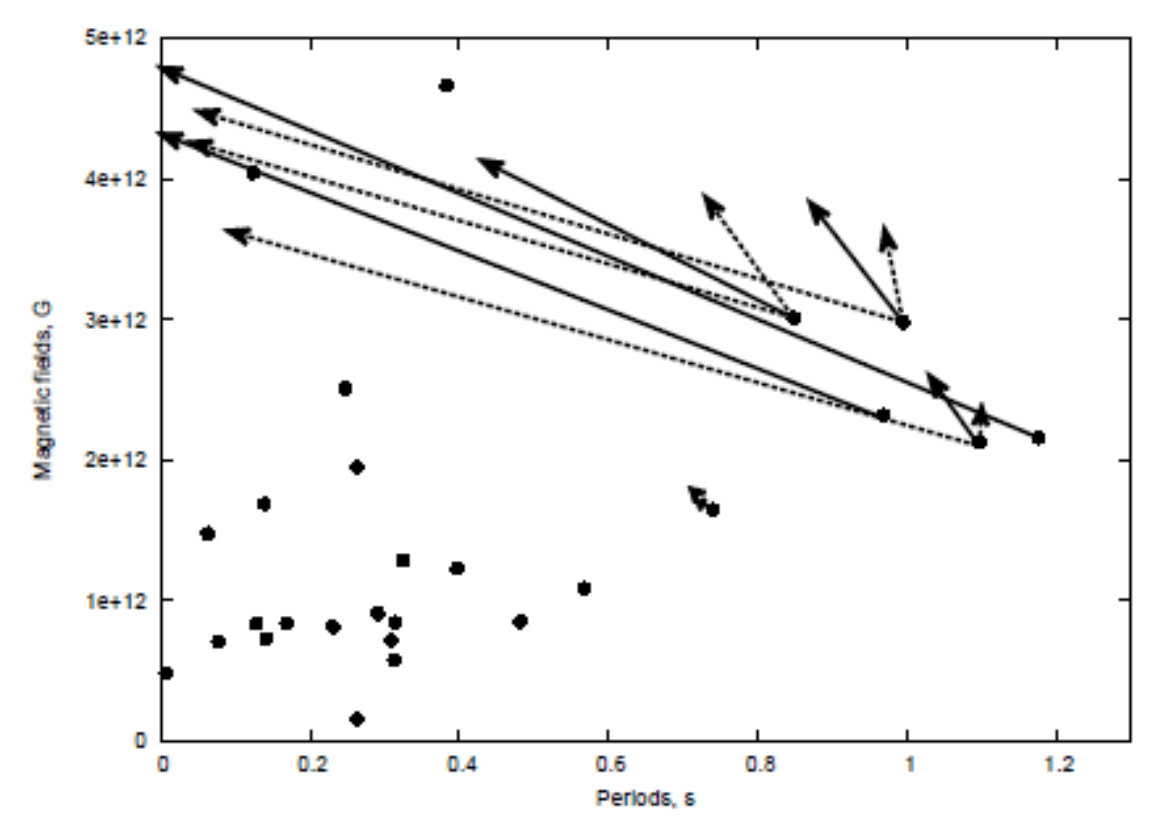

How significantly the reconstructed initial periods changed due to not taking into account the exponential field decay

Arrows point to initial parameters of pulsars if the exponential magnetic field decay was operating.

Igoshev, Popov 2013

Modified pulsar current

We perform a modified pulsar current analysis. In our approach we analyse the flow not along the spin period axis, as it was done in previous studies, but study the flow along the axis of growing characteristic age.

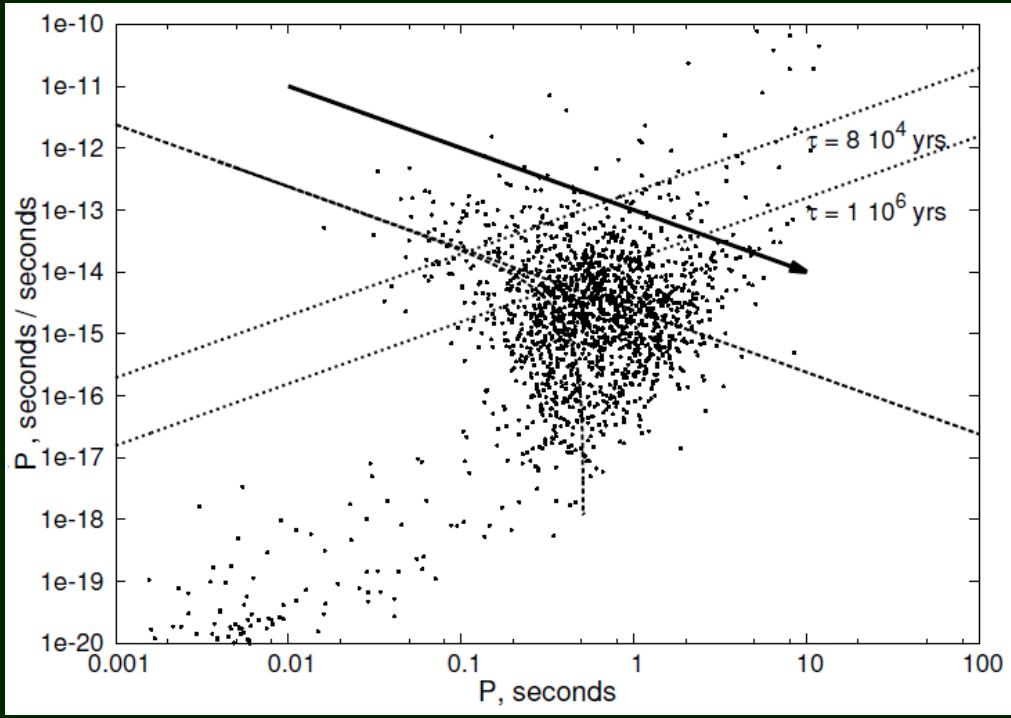

The idea is to probe magnetic field decay. Our method can be applied only in a limited range of ages.

We use distribution in characteristic ages to reconstruct the field evolution.

Igoshev, Popov (2014). MNRAS

Application to real data

We apply our methods to large observed samples of radio pulsars to study field decay in these objects. As we need to have as large statistics as possible, and also we need uniform samples, in the first place we study sources from the ATNF catalogue (Manchester et al. 2005). Then we apply our methods to the largest uniform subsample of the ATNF — to the PMSS (stands for the Parkes Multibeam and Swinburne surveys) (Manchester et al. 2001).

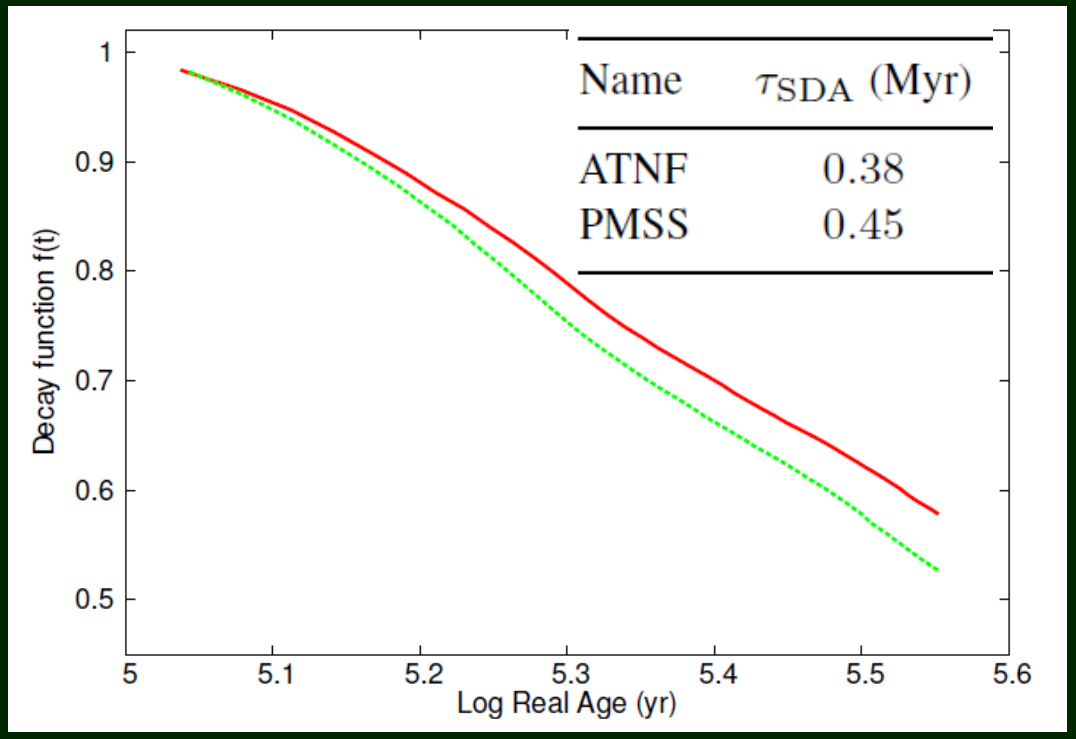

We reconstruct the magnetic field decay in the range of true (statistical) ages:
$8\ 10^4 < t < 3.5\ 10^5$ yrs
which corresponds to characteristic ages
$8\ 10^4 < \tau < 10^6$ yrs.
In this range, the field decays roughly by a factor of two.
With an exponential fit this corresponds to the decay time scale $\sim 4\ 10^5$ yrs.
Note, this decay is limited in time.

Igoshev, Popov (2014)

Comparison of different options

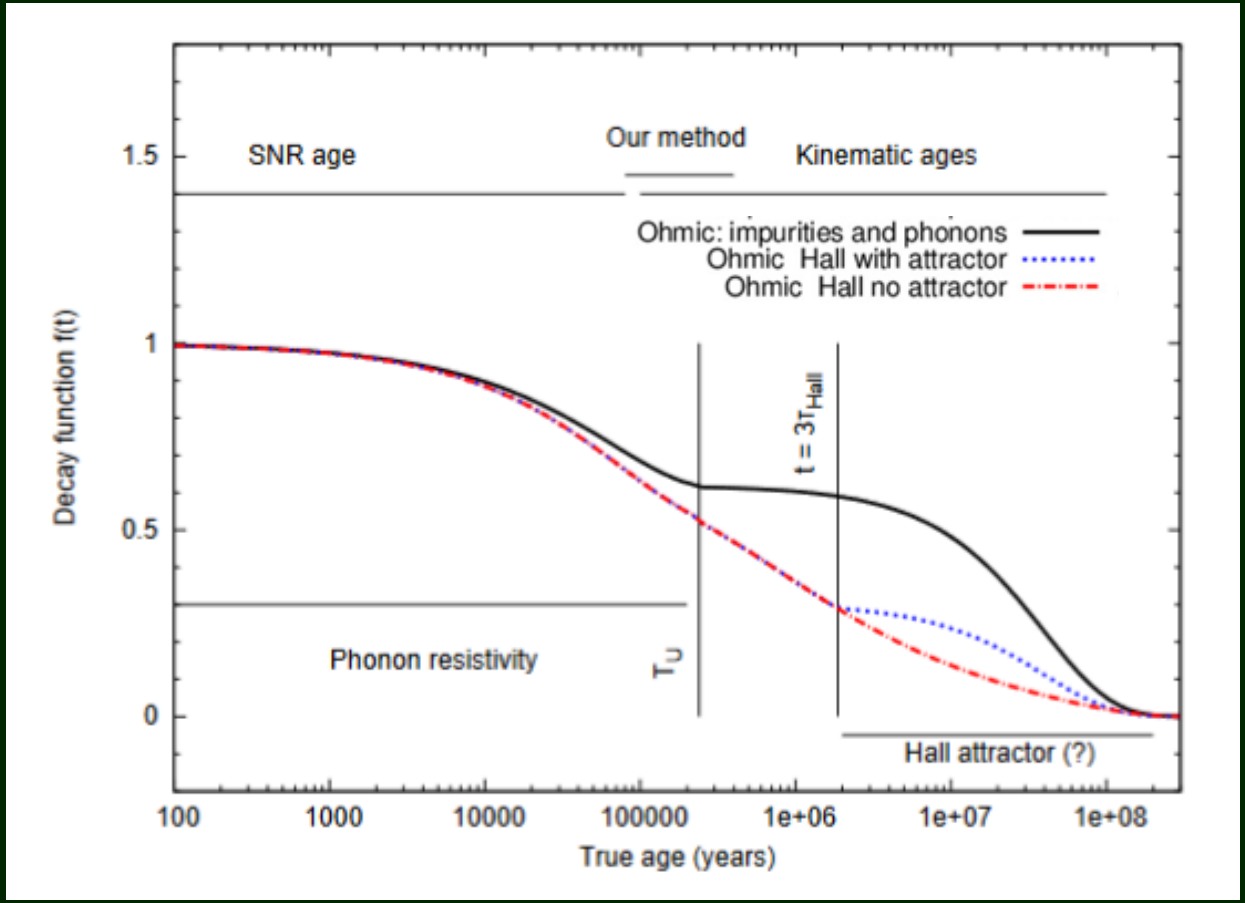

We think that at the ages ~10^5 yrs and below for normal pulsars we see mostly Ohmic decay, which then disappears as NSs cool down below the critical T.

Igoshev, Popov (2015)

Getting close to the attractor

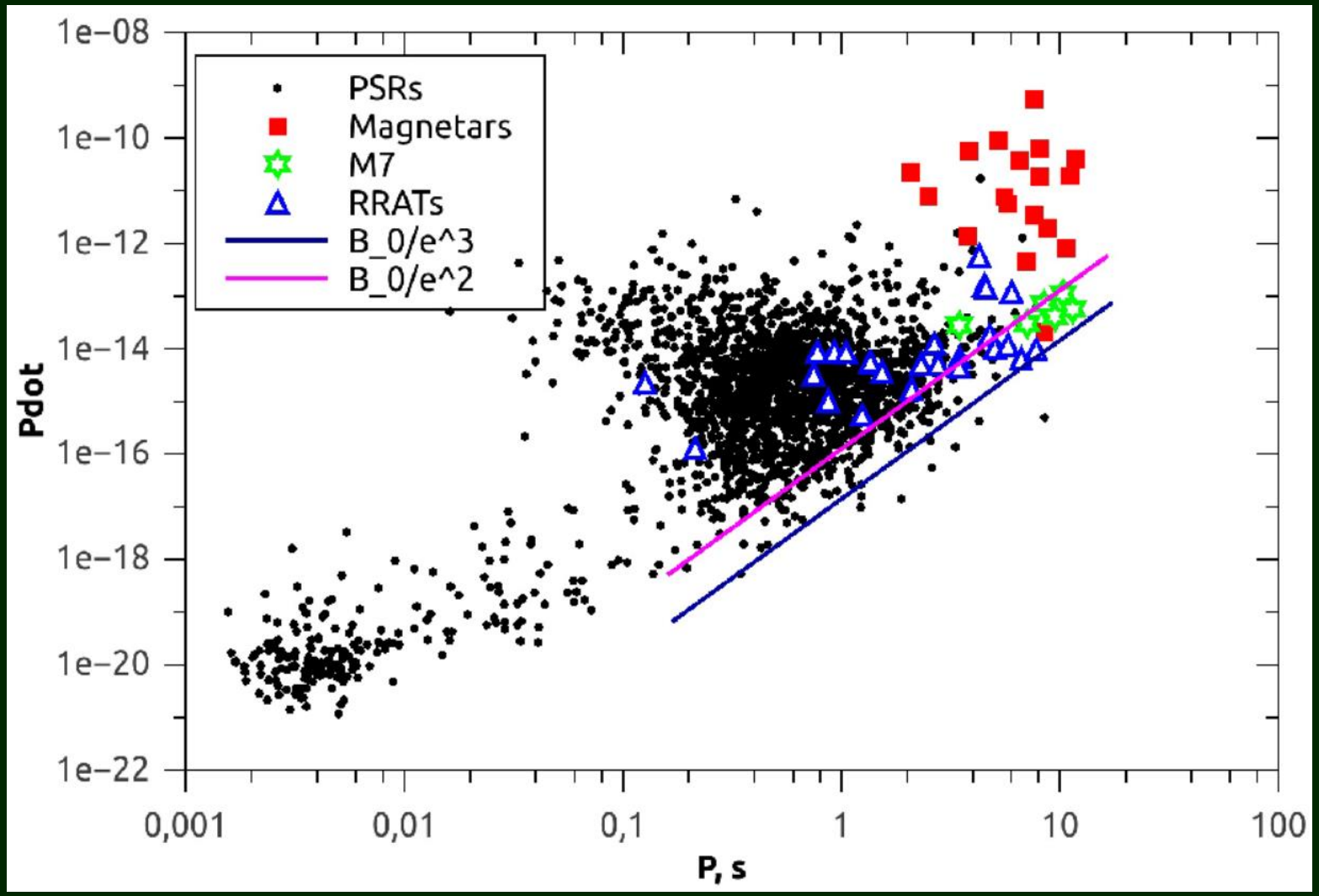

Tracks on the P-pdot diagram

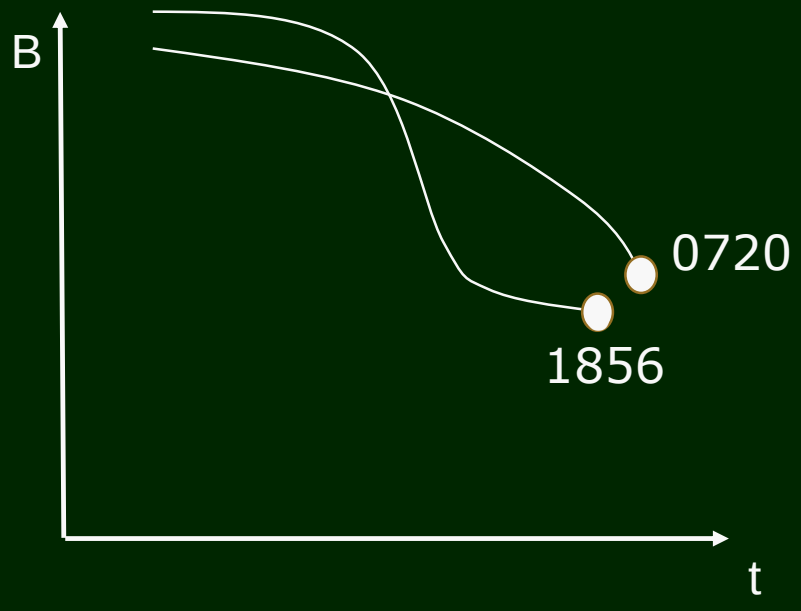

Kinematic age is larger for 0720, but characteristic age – for 1856.

It seems that 1856 is now on a more relaxed stage of the magneto-rotational evolution.

RX J0720 shows several types of activity, but RX J1856 is a very quiet source.

Non-monotonic evolution?

SXP 1062

A peculiar source was discovered in SMC.
Be/Xray binary, P=1062 sec.
A SNR is found. Age ~10^4 yrs.
(1110.6404; 1112.0491)

Typically, it can take ~1 Myr for a NS with B~10^{12} G to start accretion.

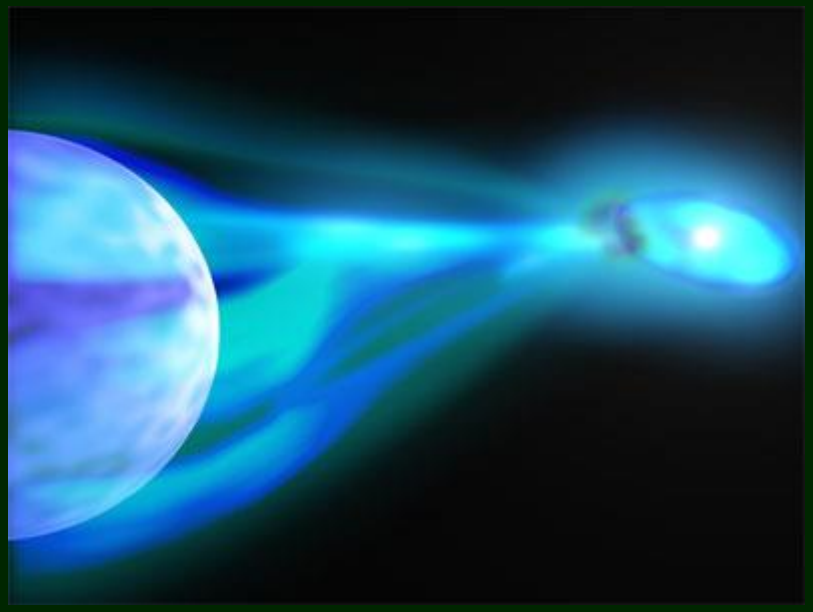

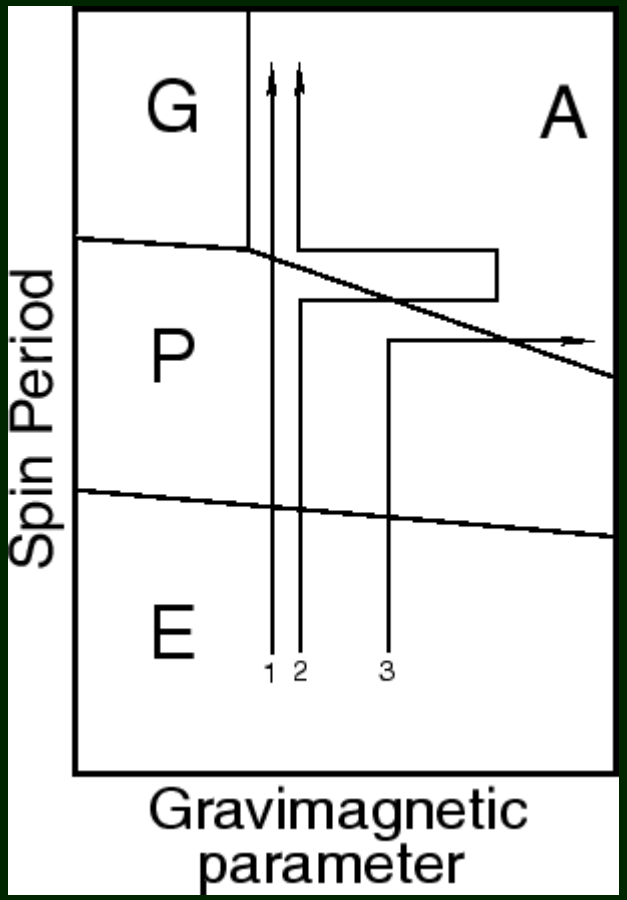

Evolution of SXP 1062

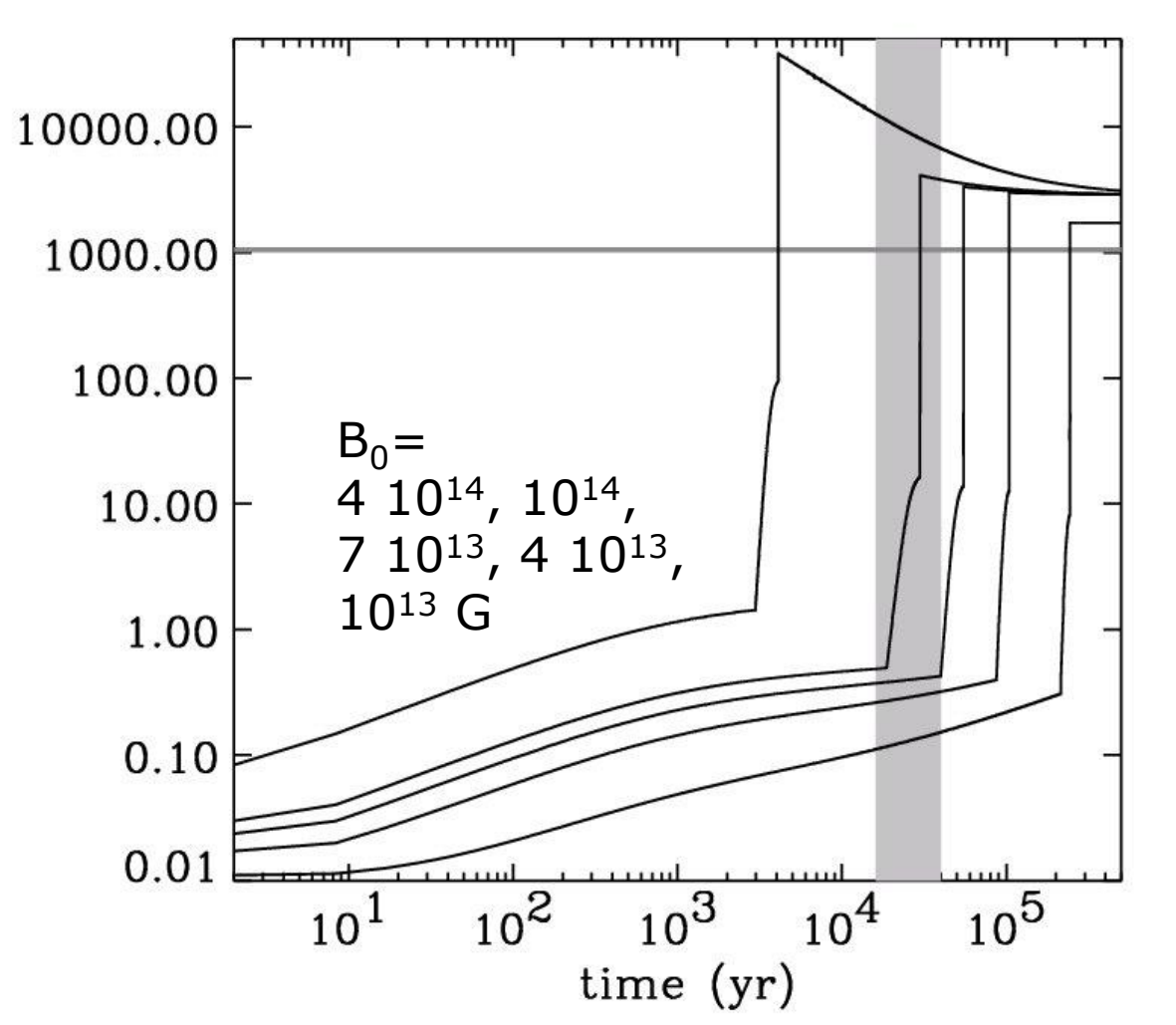

A model of a NS with initial field ~10^{14} G which decayed down to ~10^{13} G can explain the data on SXP 1062.

1112.2507

Some new data in 1304.6022

Many other scenarios have been proposed.
We need new observational data.

Accreting magnetars

Typically magnetic fields of neutron stars in accreting X-ray binaries are estimated with indirect methods.

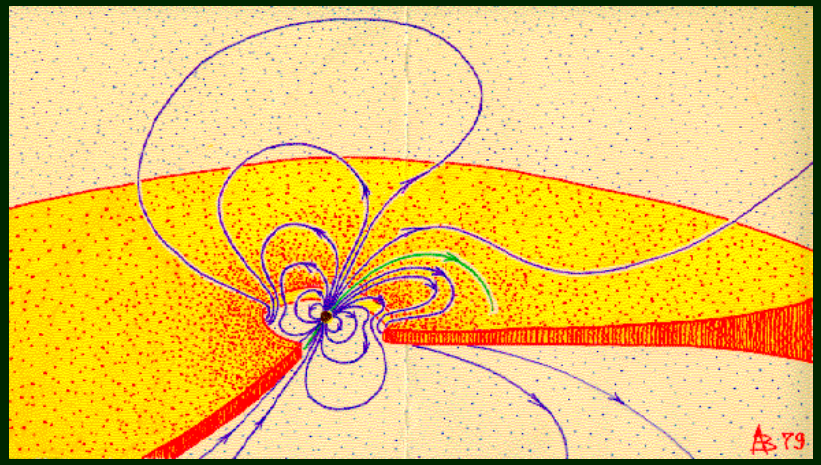

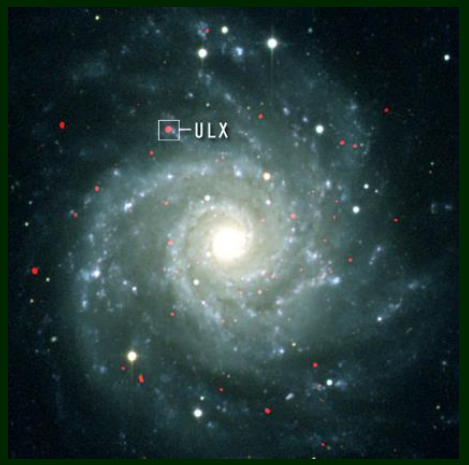

- Spin-up
- Spin-down
- Equilibrium period
- Accretion model
- …….

- ULX. NuSTAR J095551+6940.8 (M82 X-2). Ekşi et al. (2015).
- ULX. NGC 5907. Israel et al. (2017a)
- ULX. NGC 7793 P13. Israel et al. (2017b).
- 4U0114+65. Sanjurjo et al. (2017).
- 4U 2206+54. Ikhsanov & Beskrovnaya (2010).
- SXP1062. Fu & Li (2012)
- Swift J045106.8-694803. Klus et al. (2013).

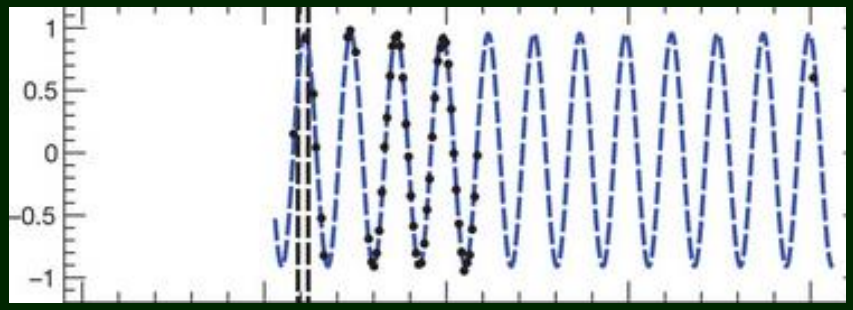

1709.10385

Field evolution in a magnetar

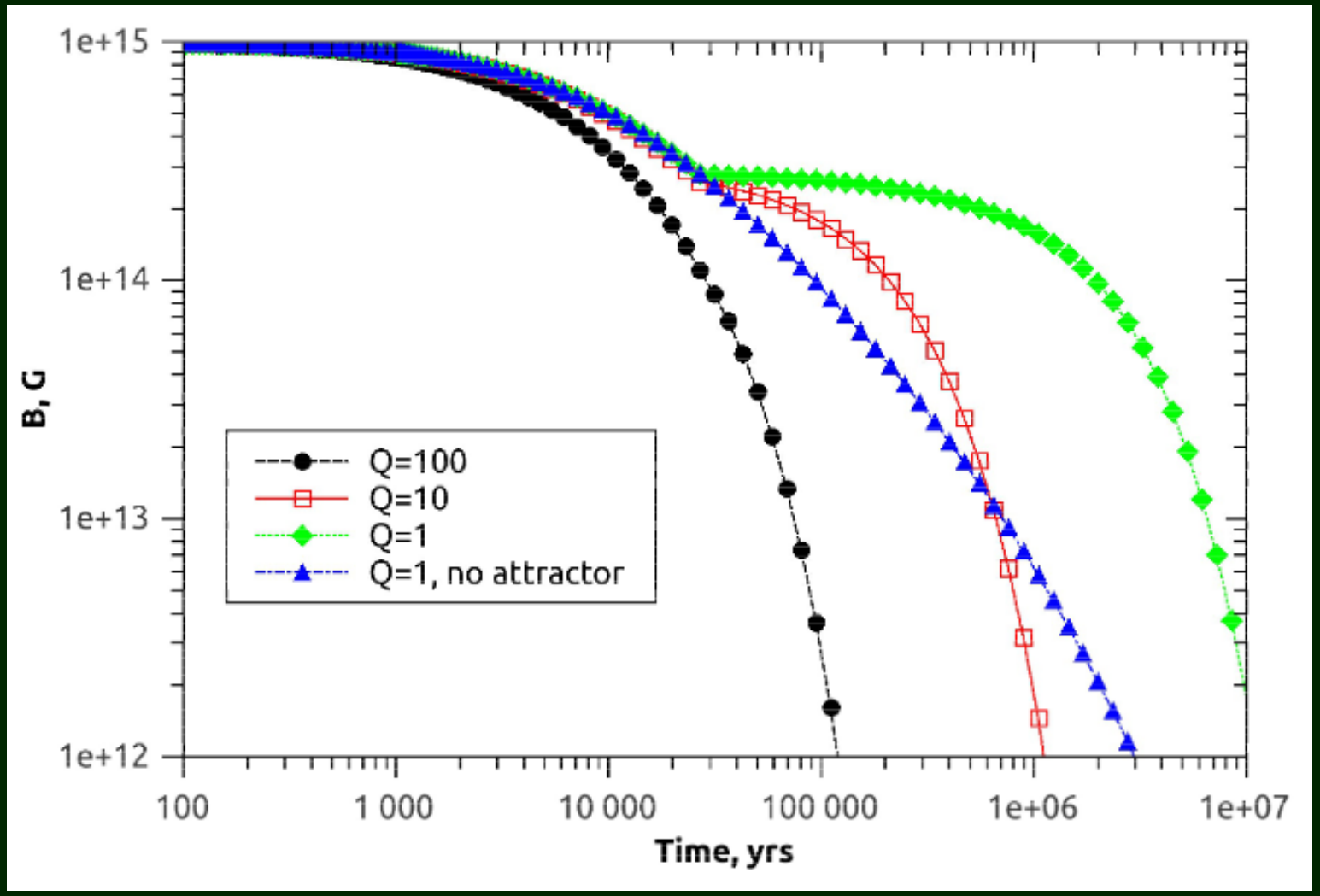

1709.10385

Parameters of ULX M82 X-2

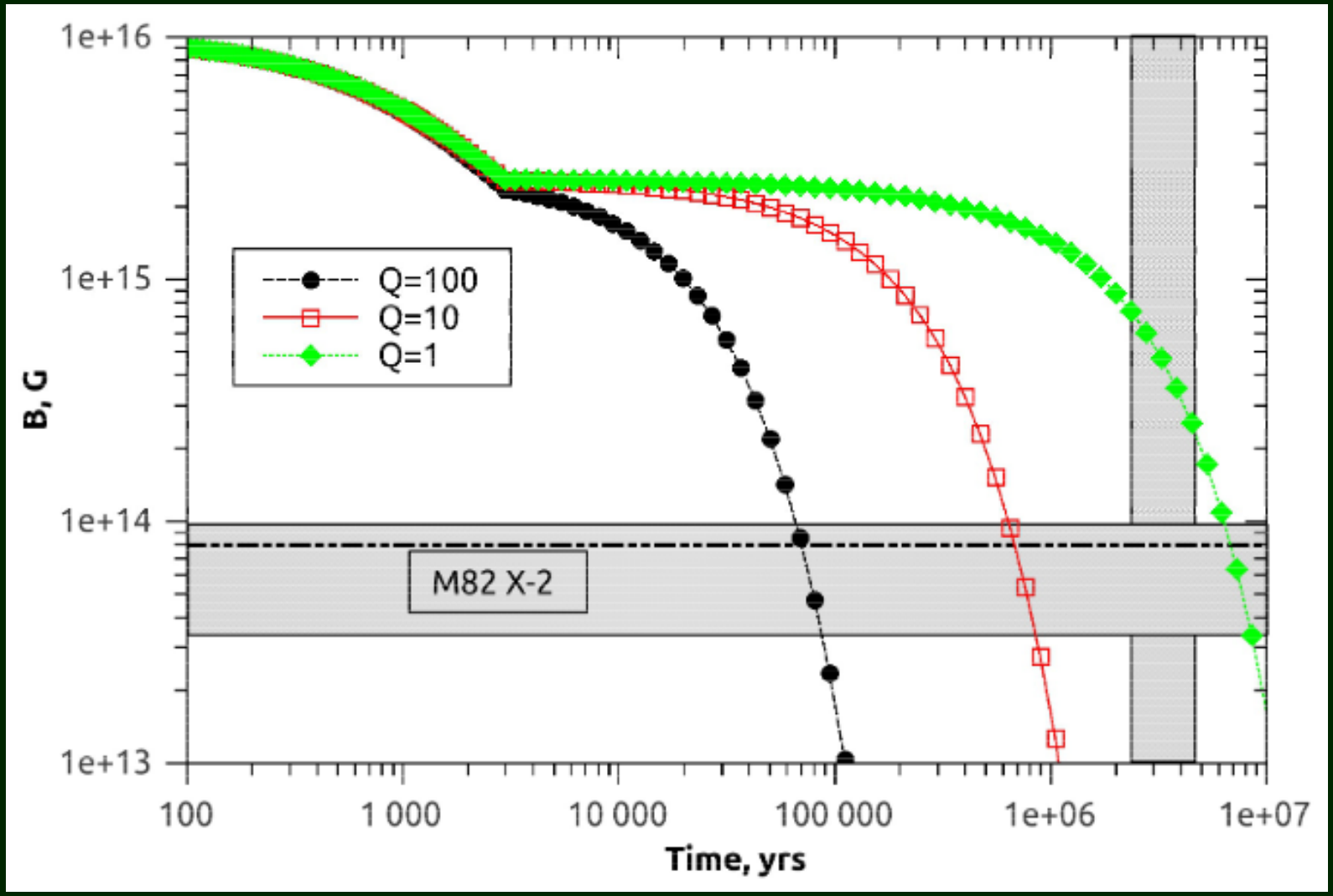

1709.10385

Anti-magnetars

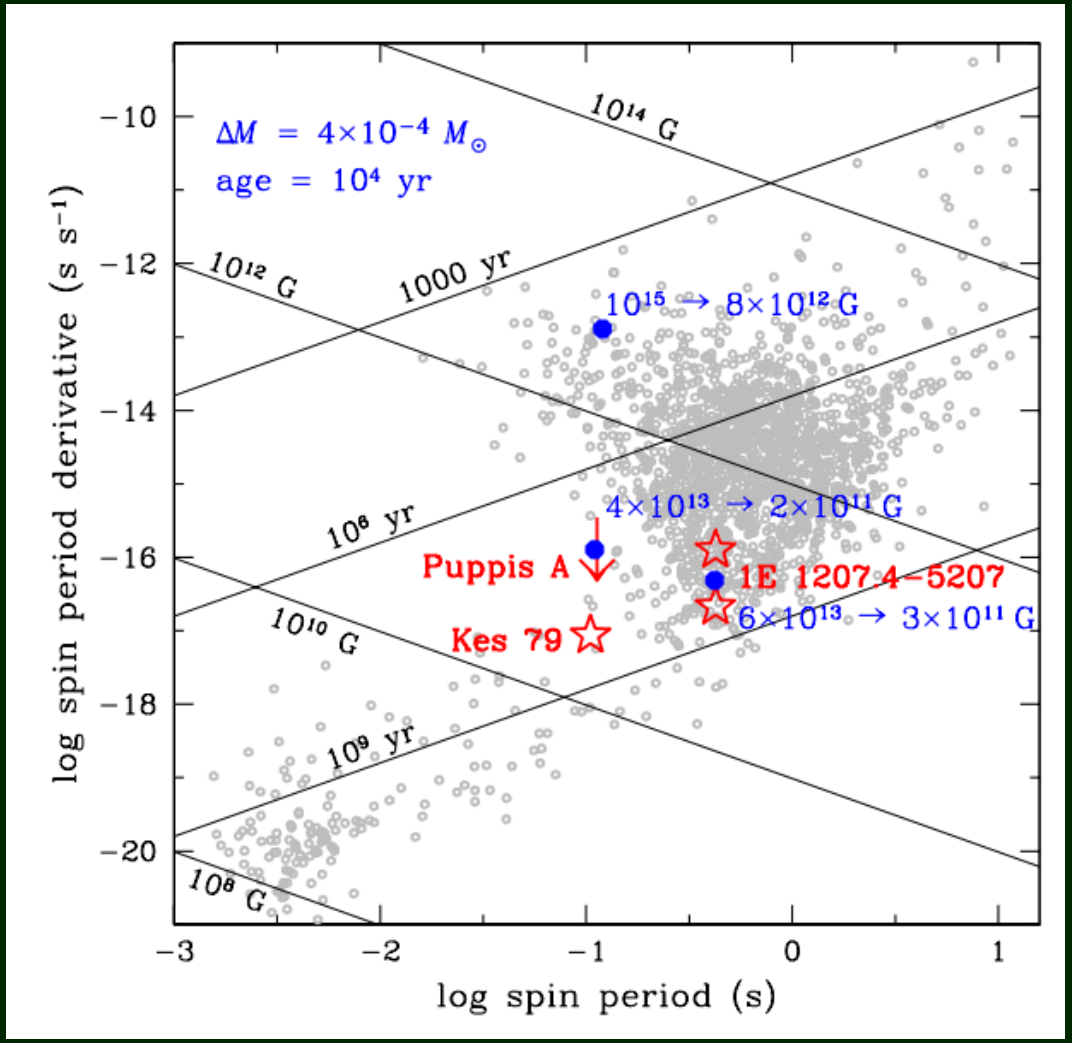

Note, that there is no room for antimagnetars from the point of view of birthrate in many studies of different NS populations.

New results 1301.2717
Spins and derivative are measured for
PSR J0821-4300 and
PSR J1210-5226

Ho 1210.7112

Evolution of CCOs

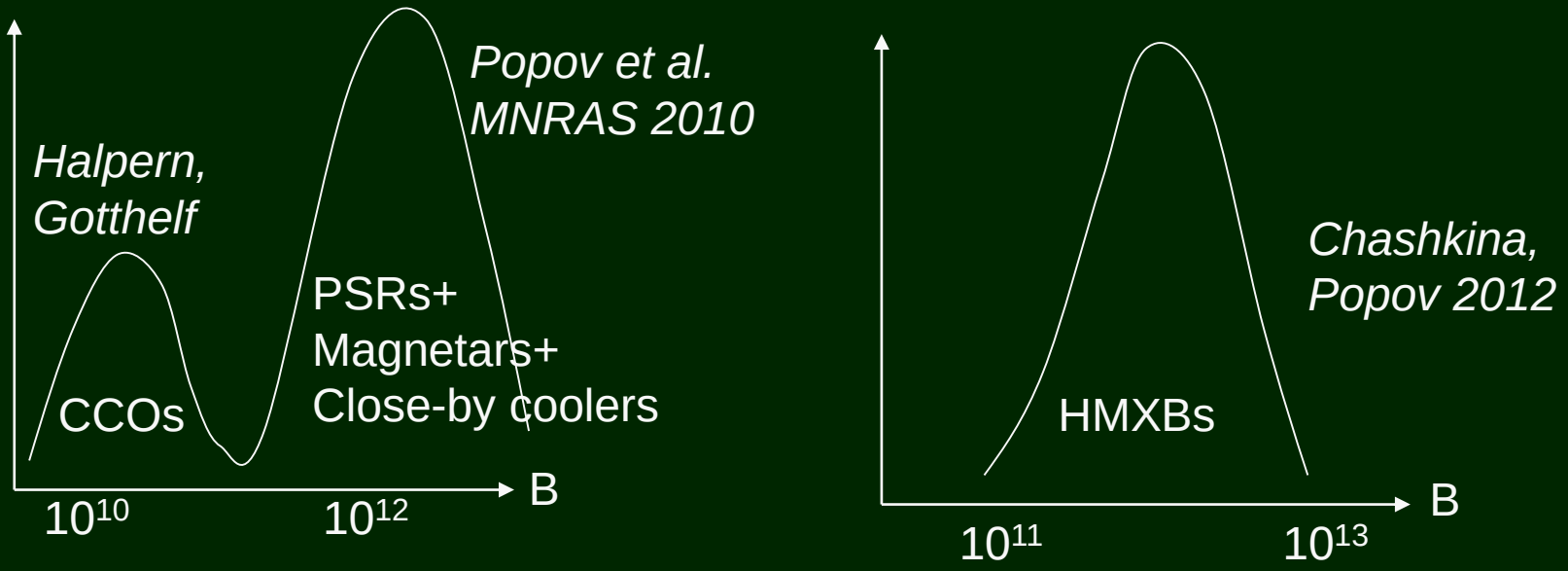

Among young isolated NSs about 1/3 can be related to CCOs.
If they are anti-magnetars, then we can expect that 1/3 of NSs in HMXBs are also low-magnetized objects.
They are expected to have short spin periods <1 sec.
However, there are no many sources with such properties.
The only good example - SAX J0635+0533. An old CCO?

Possible solution: emergence of magnetic field
(see physics in Ho 2011, Vigano, Pons 2012).

Observations vs. theory

We use observations of Be/X-ray binaries in SMC to derive magnetic field estimates, and compare them with prediction of the Pons et al. model.

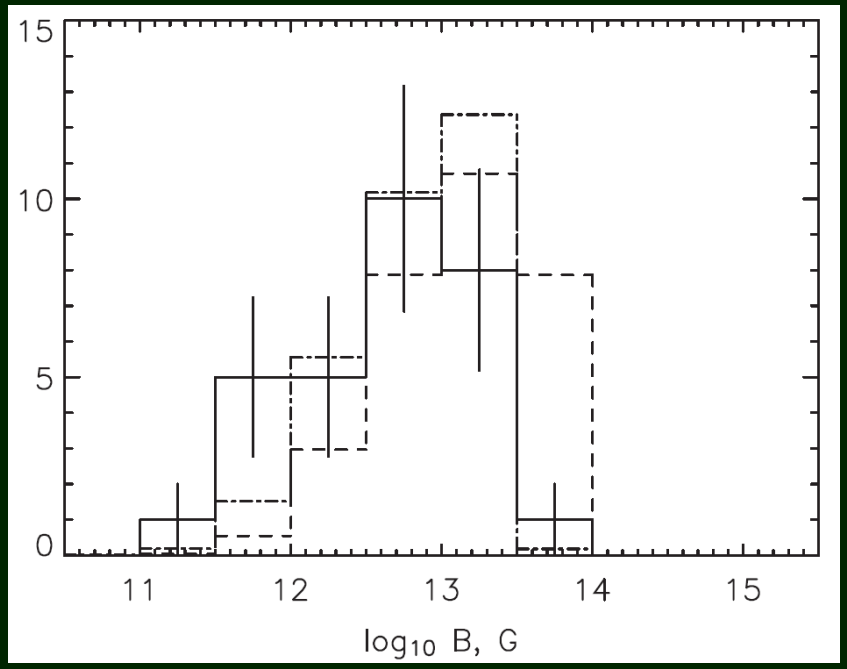

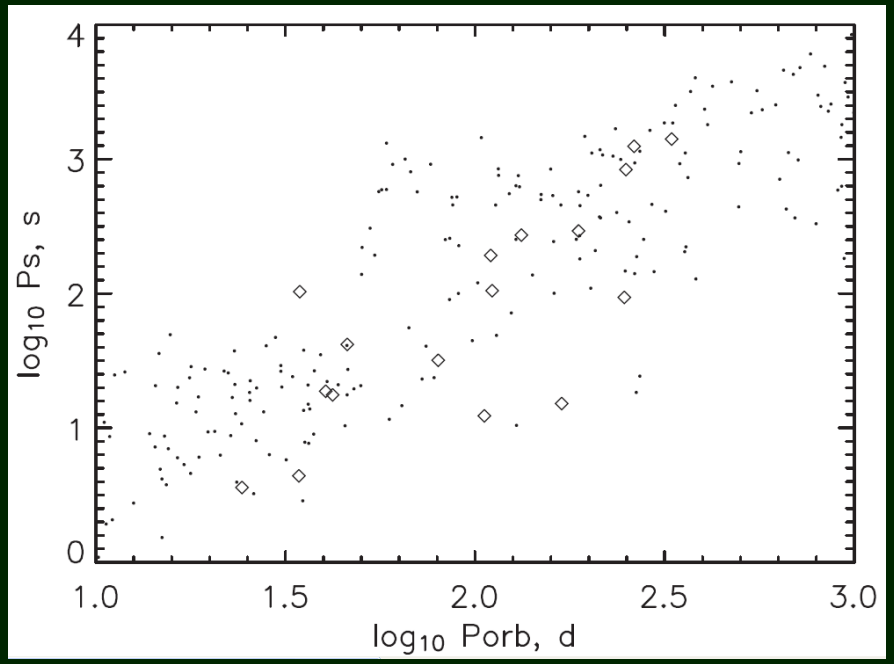

Chashkina, Popov (2012)

Where are old CCOs?

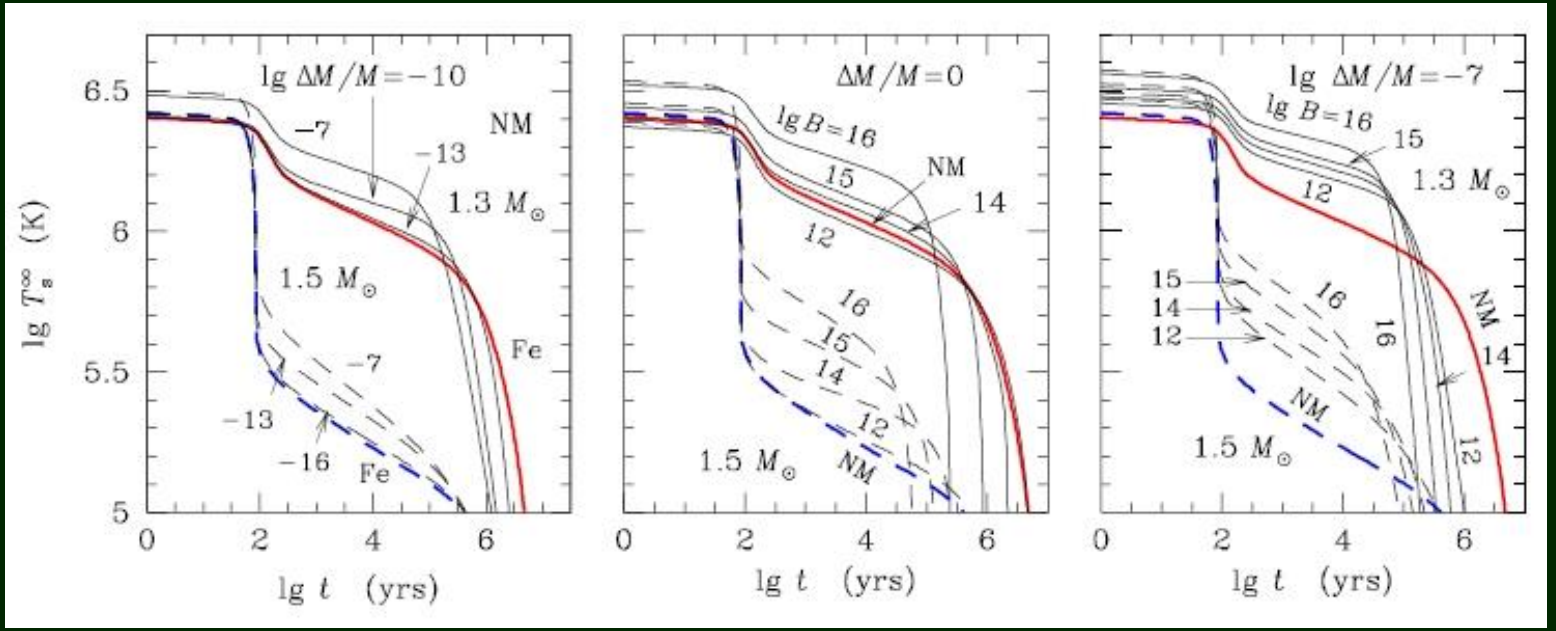

Yakovlev, Pethick 2004

According to cooling studies they have to be bright till at least 10^5 years. But only one candidate (2XMM J104608.7-594306 Pires et al.) to be a low-B cooling NS is known (Calvera is also a possible candidate).

We propose that a large set of data on HMXBs and cooling NSs is in favour of field emergence on the time scale $10^4 \le \tau \le 10^5$ years (arXiv:1206.2819).

Some PSRs with thermal emission for which additional heating was proposed can be descendants of CCOs with emerged field.

How the field is buried

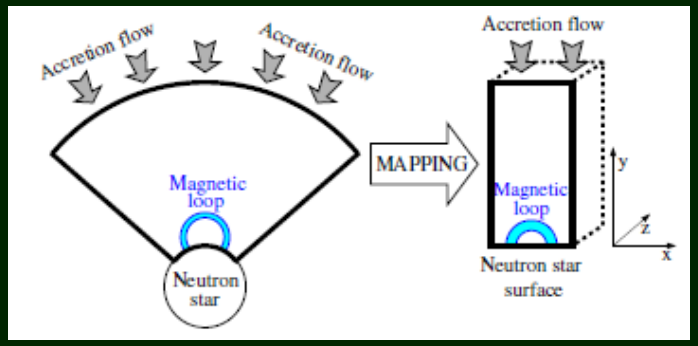

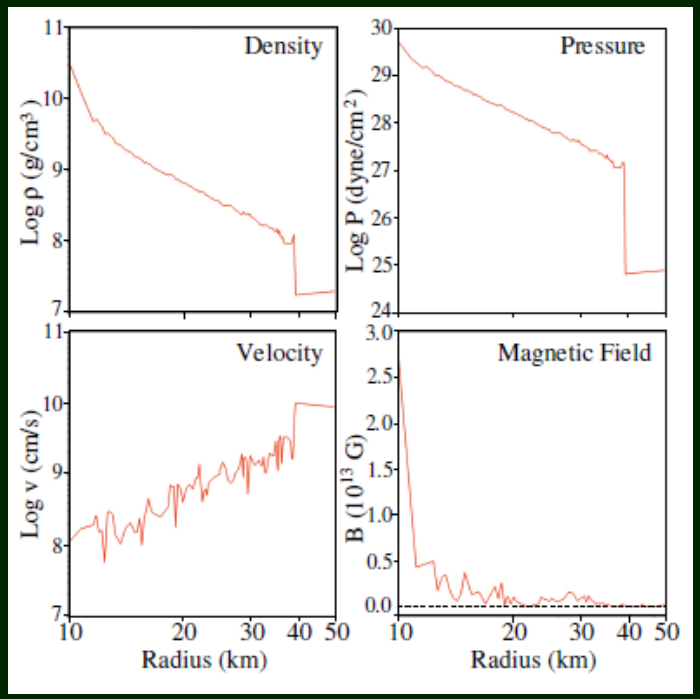

For t=60 msec

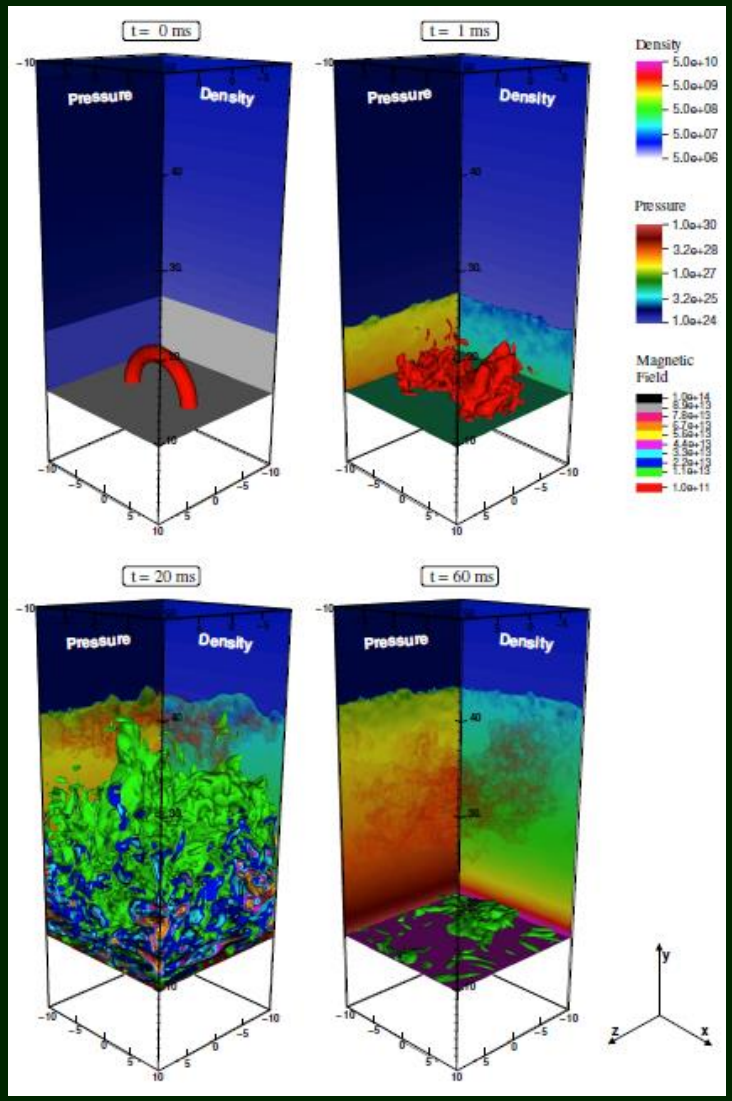

1212.0464

See 1210.7112 for a review of CCOs magnetic fields

Recent model

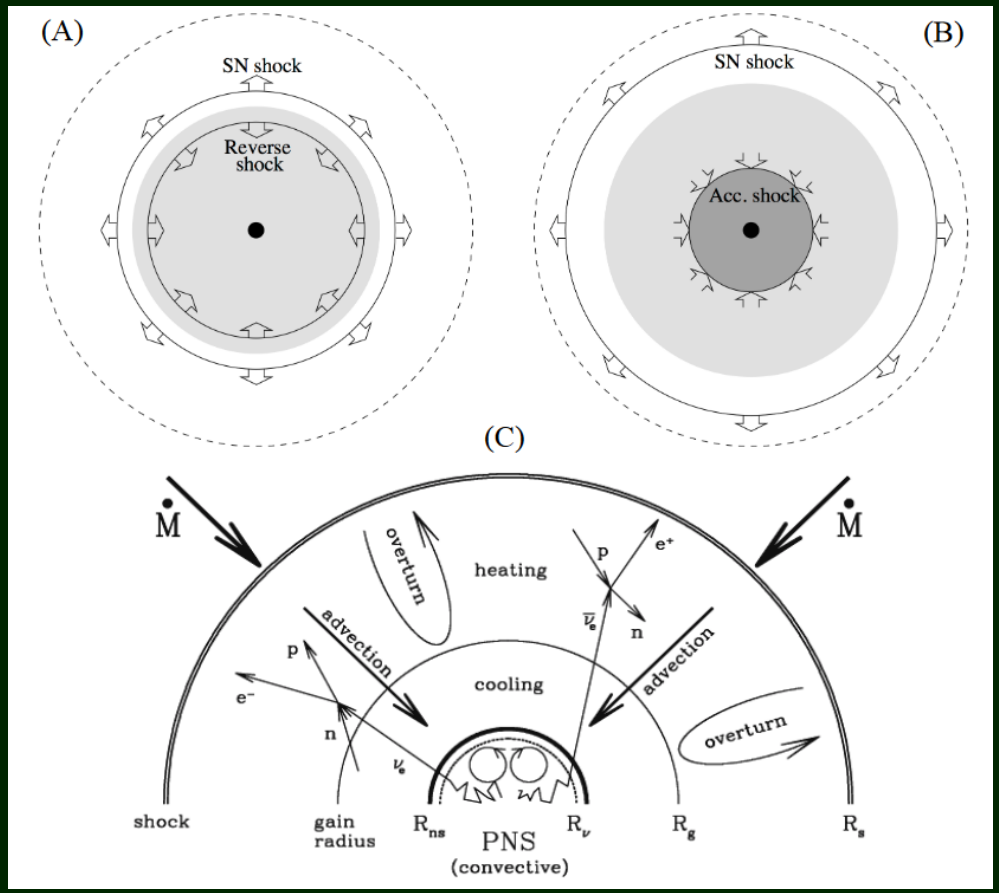

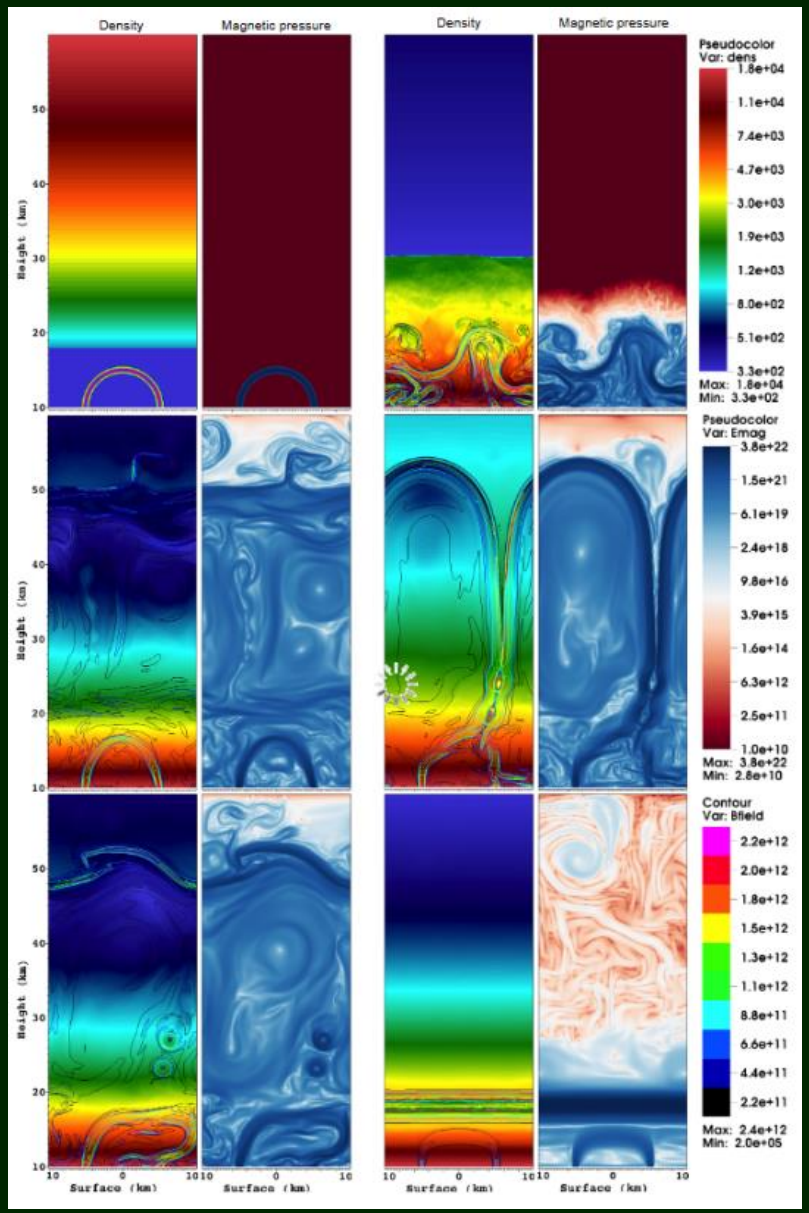

1809.07057

Emerging field: modeling

1D model of field emergence

Dashed – crustal, dotted – core field

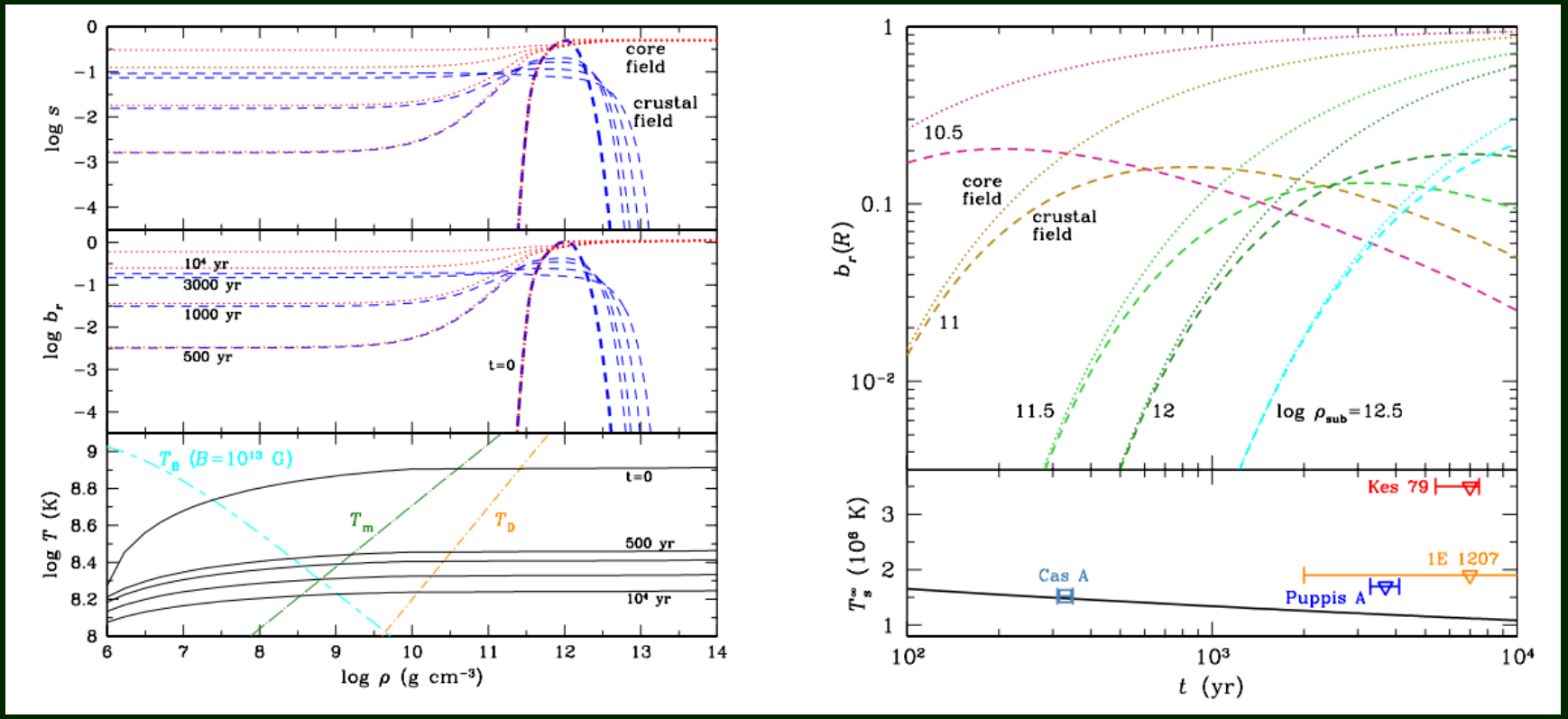

Ho 2011

Another model

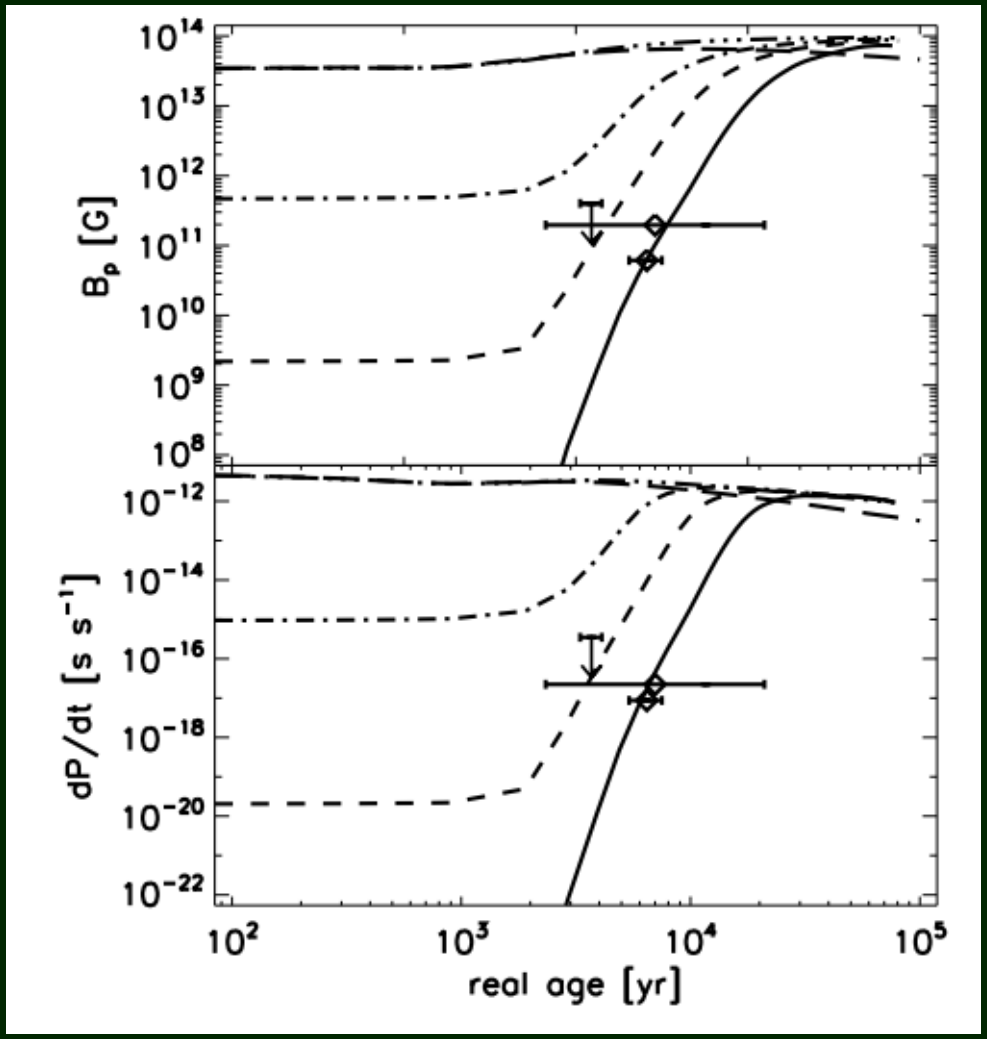

2D model with field decay

Ohmic diffusion dominates in field emergence, but Hall term also can be important.

Calculations confirm that emergence on the time scale 10^3-10^5 years is possible.

$B_{0p}=10^{14}$ G

Vigano, Pons 2012 1206.2014

Emerged pulsars in the P-Pdot diagram

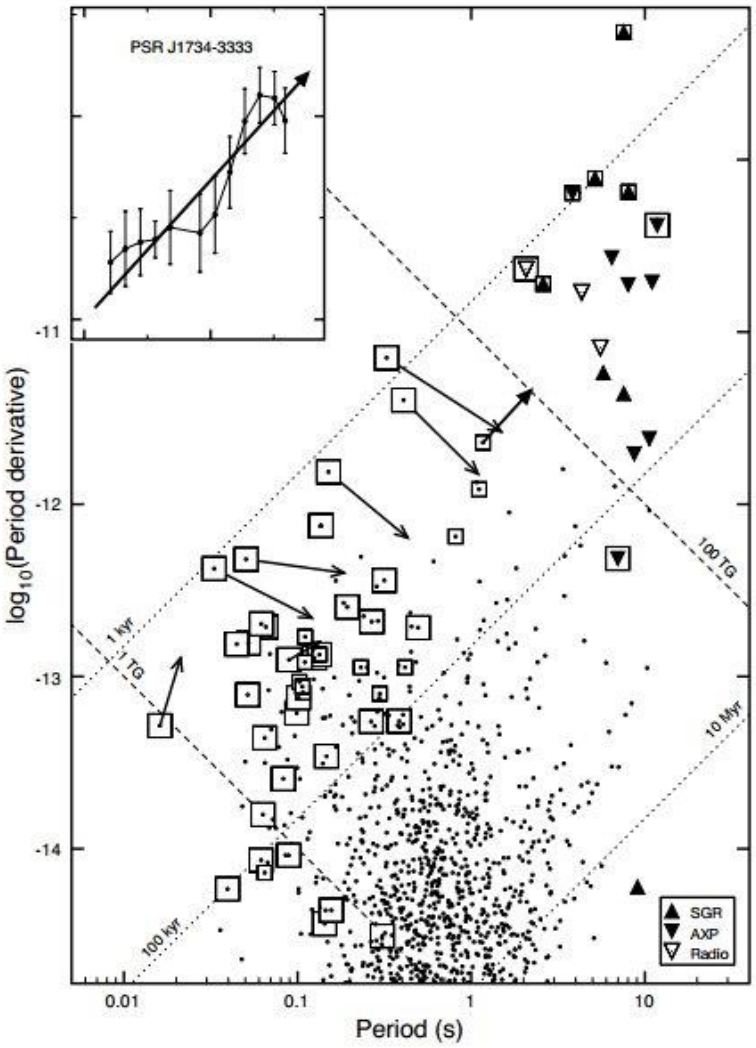

Emerged pulsars are expected to have
P~0.1-0.5 sec
B~10^{11}-10^{12} G
Negative braking indices or at least n<2.
About 20-40 of such objects are known.

Parameters of emerged PSRs:
similar to “injected” PSRs
(Vivekanand, Narayan, Ostriker).

The existence of significant fraction
of “injected” pulsars formally
do not contradict recent pulsar current studies
(Vranesevic, Melrose 2011).

Part of PSRs supposed to be born with
long (0.1-0.5 s) spin periods can be
matured CCOs.

Espinoza et al. arXiv: 1109.2740, 1211.5276

Field, rotation, fallback

$$\dot{M}_{\rm crit,repul} \sim 3\times10^{-5}\,M_\odot\,{\rm s}^{-1}\,\frac{\xi_{\rm s,crit}}{0.2}\,\frac{(4\pi D_{\rm fb}\sqrt{\xi_{\rm s}})_{\rm crit}}{5.3}\left(\frac{B_*}{10^{13}\,{\rm G}}\right)^2\left(\frac{P}{10\,{\rm ms}}\right)^{-2}\left(\frac{t_{\rm fb}}{20\,{\rm s}}\right)^{2/3}$$

$$\frac{B_*^{\,2}}{8\pi} \lesssim \rho v^2 \sim \frac{\dot{M}}{4\pi R_*^2}\sqrt{\frac{GM_{\rm c}}{R_*}}$$

$$\dot{M}_{\rm crit,bury} \sim 3\times10^{-6}\,M_\odot\,{\rm s}^{-1}\left(\frac{B_*}{10^{13}\,{\rm G}}\right)^2$$

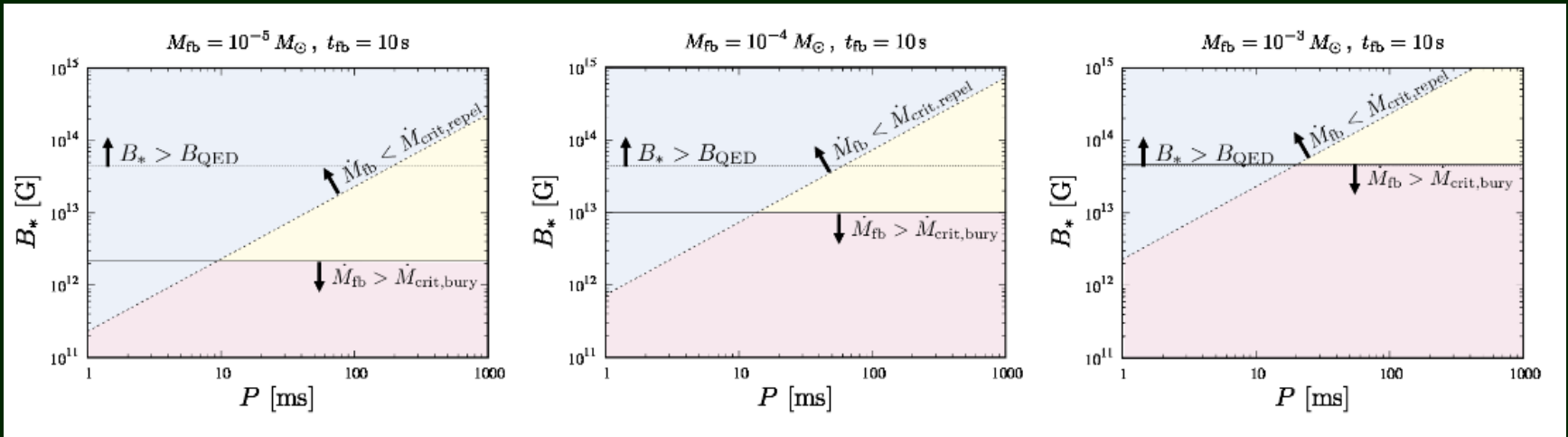

1809.00487

Growing field and kick velocities?

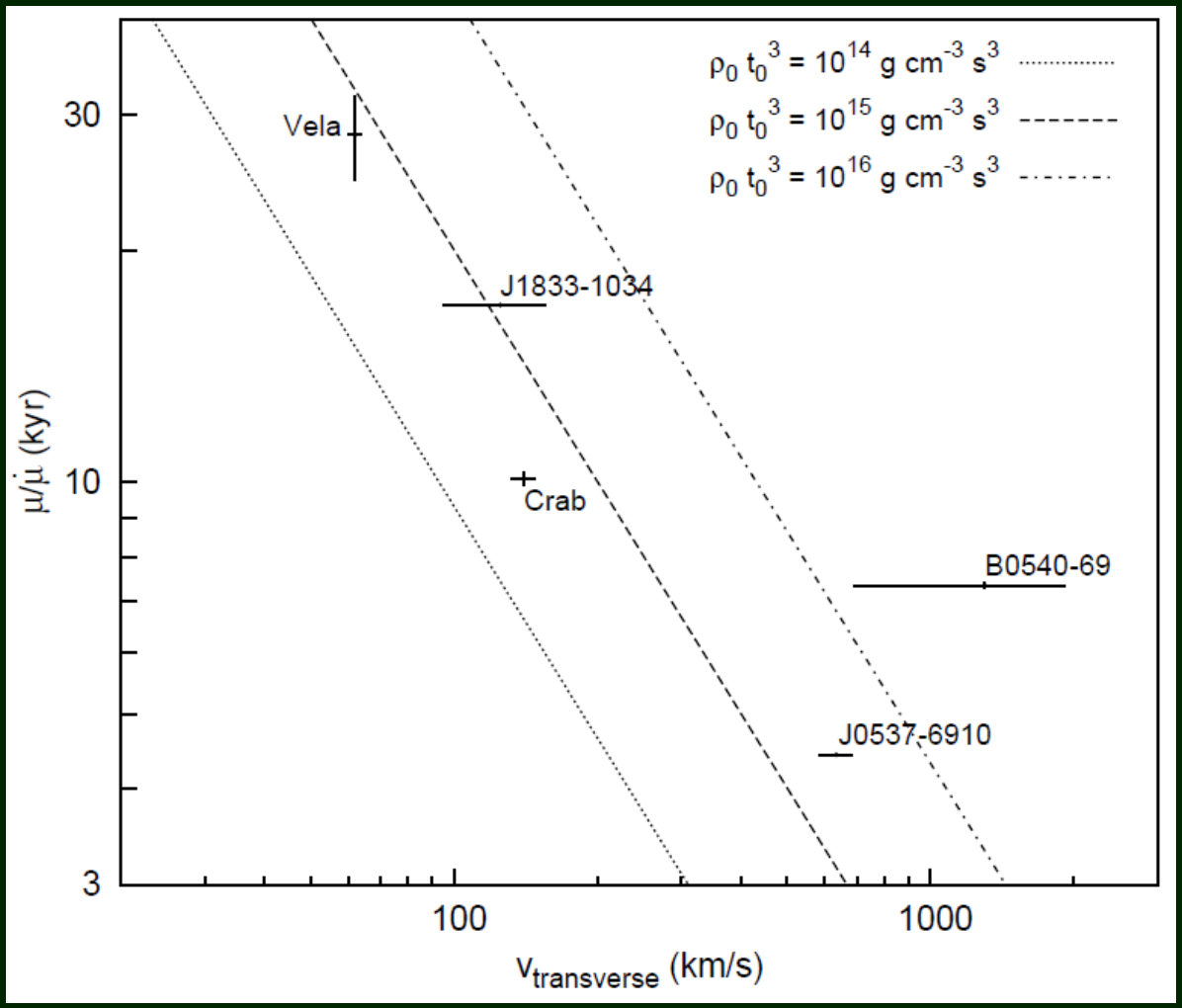

The idea is that
n<3 are explained
as due to growing field.
Then it is possible
to estimate the timescale
for growing and
plot it vs. velocity.

Larger kick –
- smaller fallback –
  - faster field growing

1207.1219

Evolution of PSRs with evolving field

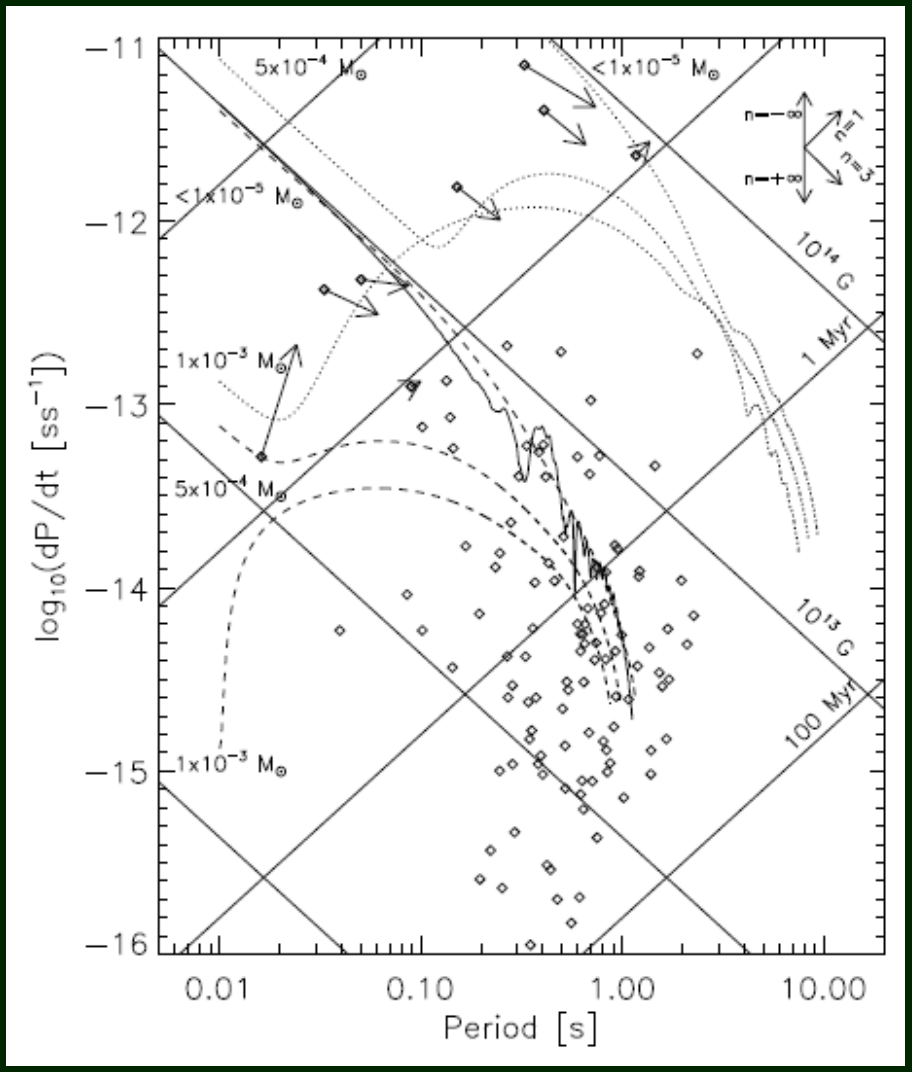

Three stages:

1. n<=3 Standard + emerging field
2. n>3 Orhmic field decay
3. oscillating and large n – Hall drift

$$n = 3 - 4\frac{\dot{B}_0}{B_0}\tau_c \equiv 3 - 4\frac{\tau_c}{\tau_B},$$

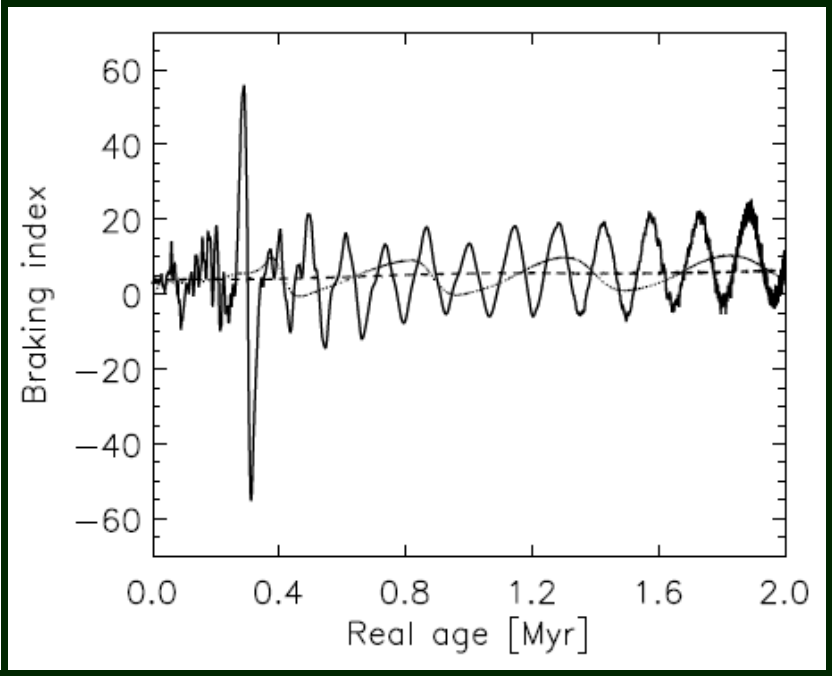

1209.2273

Buried field in Kes79?

The idea is to reconstruct surface temperature distribution, and then calculate which field configuration can produce it.

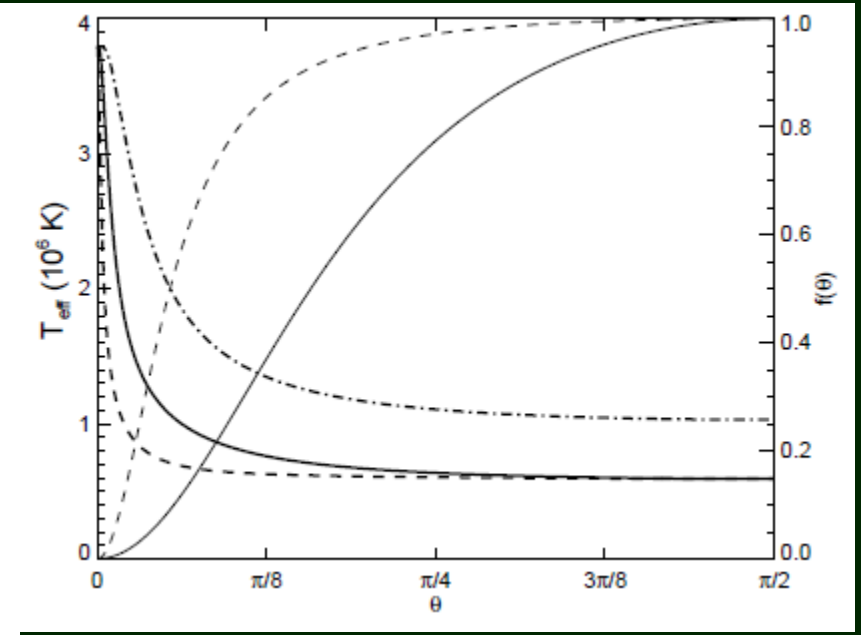

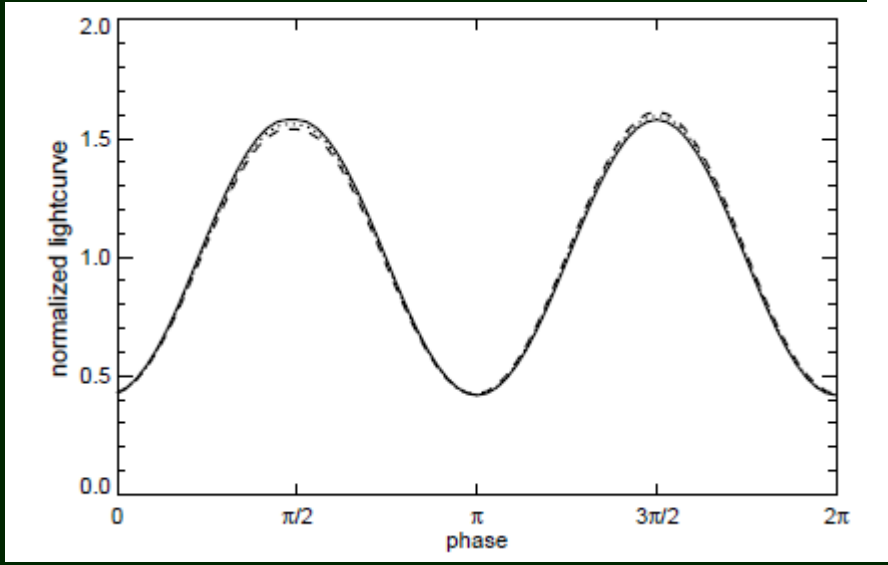

Very large pulse fraction (64%) in the anti-magnetar Kes 79.
Large sub-surface magnetic field can explain the existence of compact hot spots.
Then the field must have been buried in a fall-back episode.

1110.3129

Hidden magnetar in RCW103

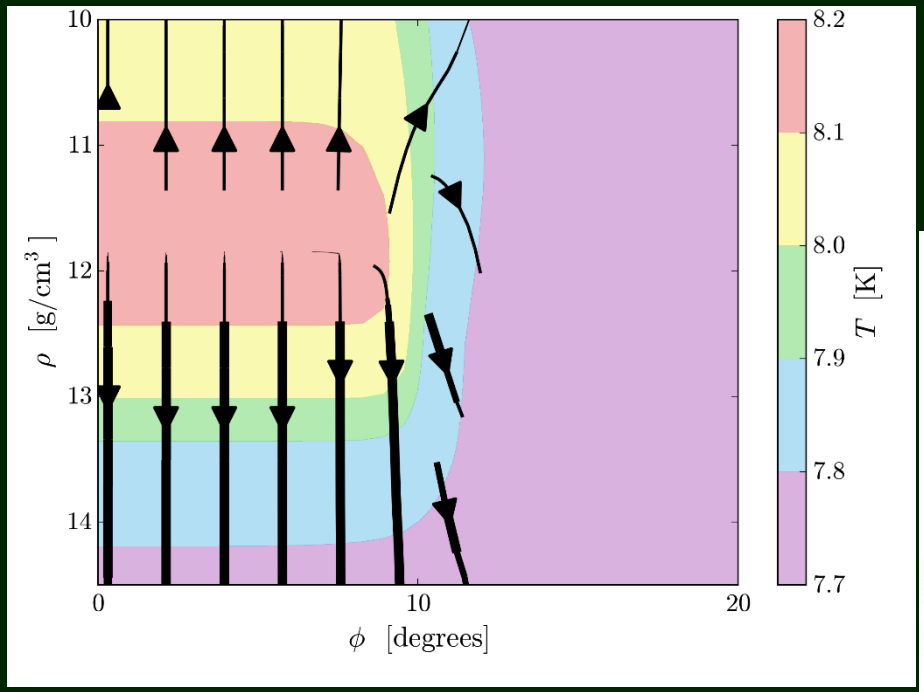

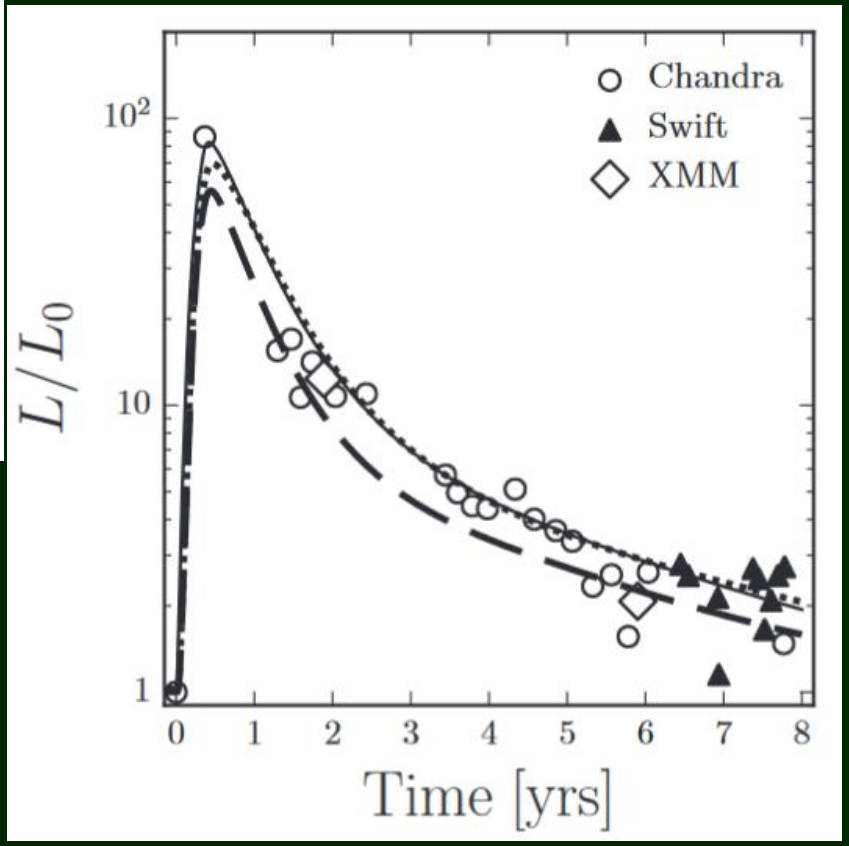

1504.03279

Not so hidden!

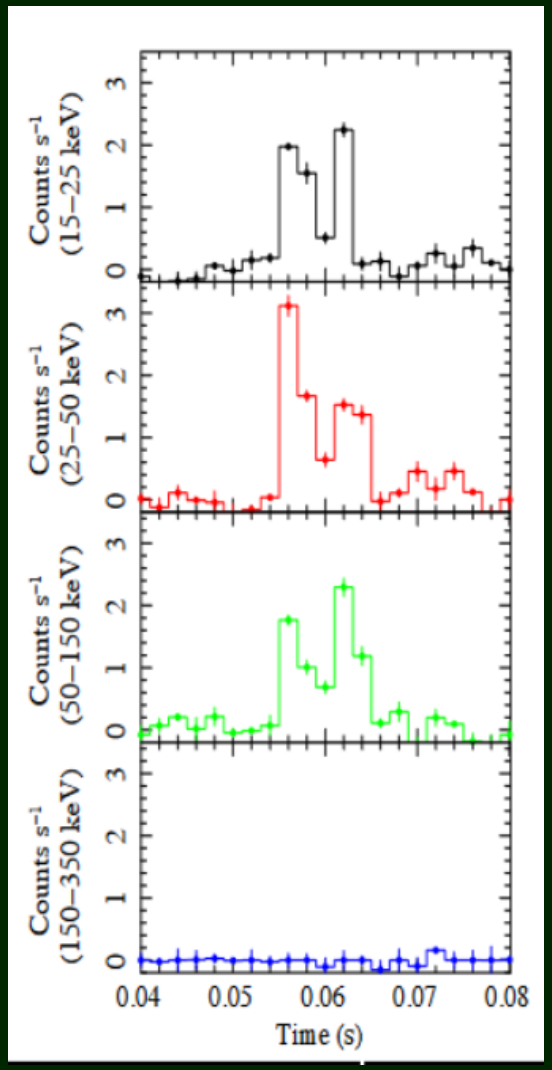

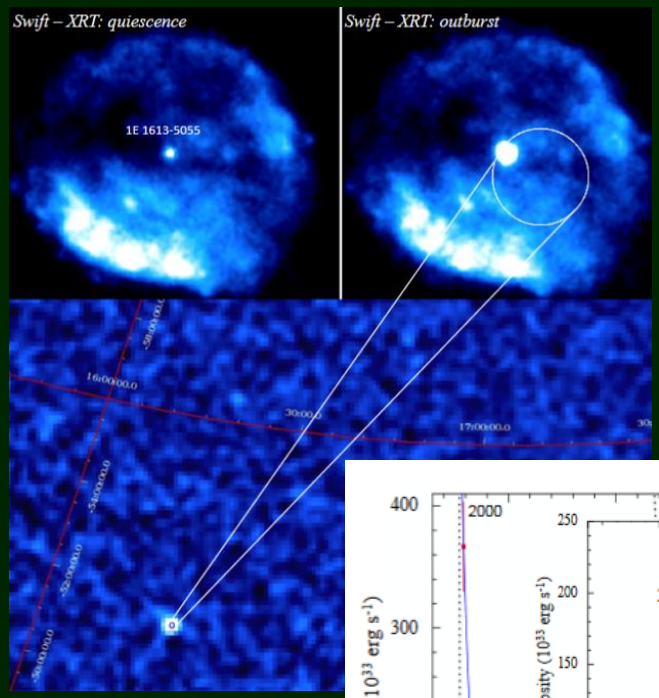

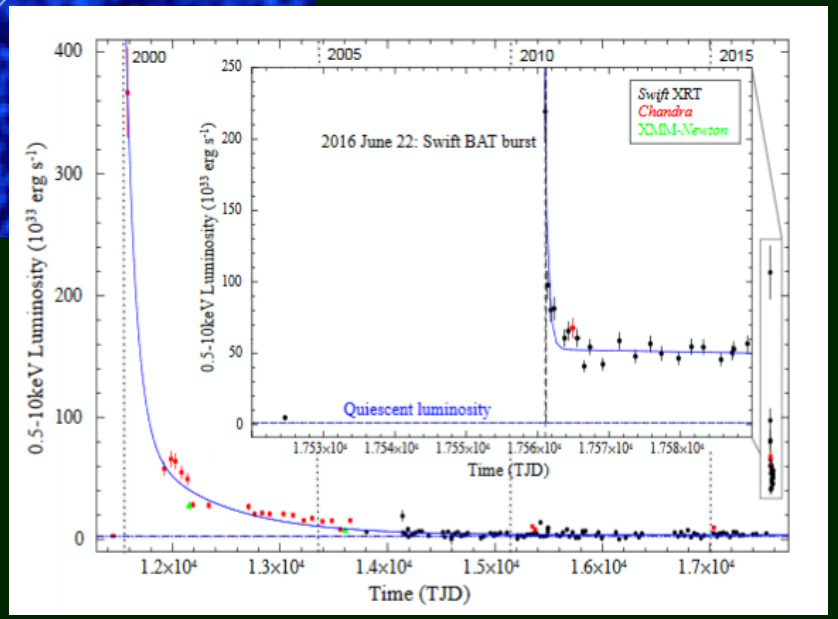

1607.04107

1607.04264

GRBs and fallback onto magnetars

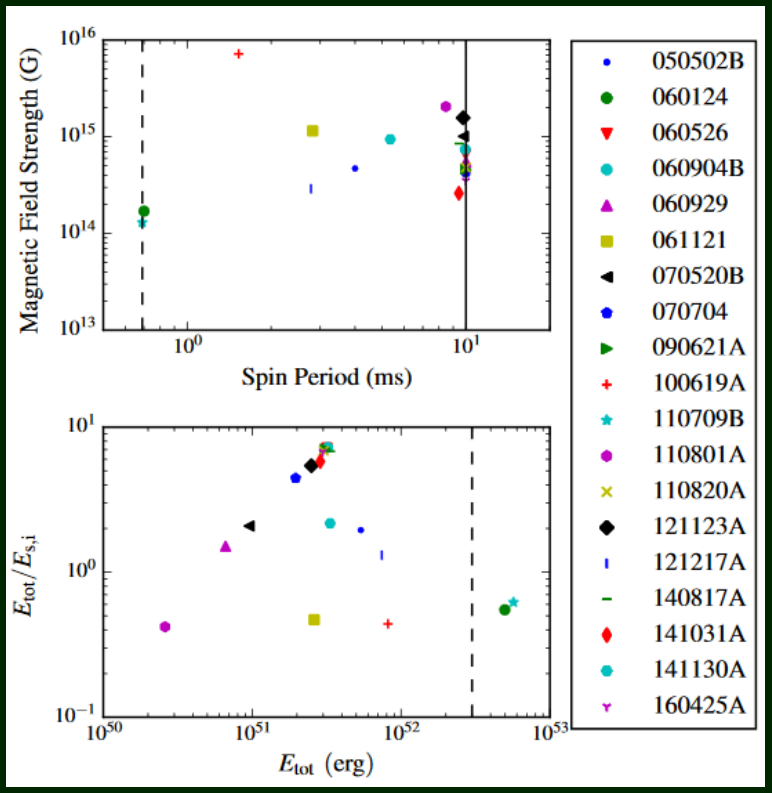

Giant X-ray flares in GRB happen after ~30-10^5 s.

Rotational energy ~2 10^{52} erg P_{ms}^{-2}

$$\dot{M}_{\rm D}(t) = \dot{M}_{\rm fb} - \dot{M}_{\rm acc} - \dot{M}_{\rm prop},$$

$$\dot{M}_{\rm fb}(t) = \frac{M_{\rm fb}}{t_{\rm fb}} \left(\frac{t + t_{\rm fb}}{t_{\rm fb}} \right)^{-\frac{5}{3}}$$

$$L_{\rm dip} = -\tau_{\rm dip}\omega$$

$$L_{\rm prop} = -\tau_{\rm acc}\omega$$

$\tau_{\rm acc}$ and $\tau_{\rm dip}$ are the accretion and dipole torques

$$L_{\rm tot} = \frac{1}{f_{\rm B}} \left(\eta_{\rm prop} L_{\rm prop} + \eta_{\rm dip} L_{\rm dip} \right)$$

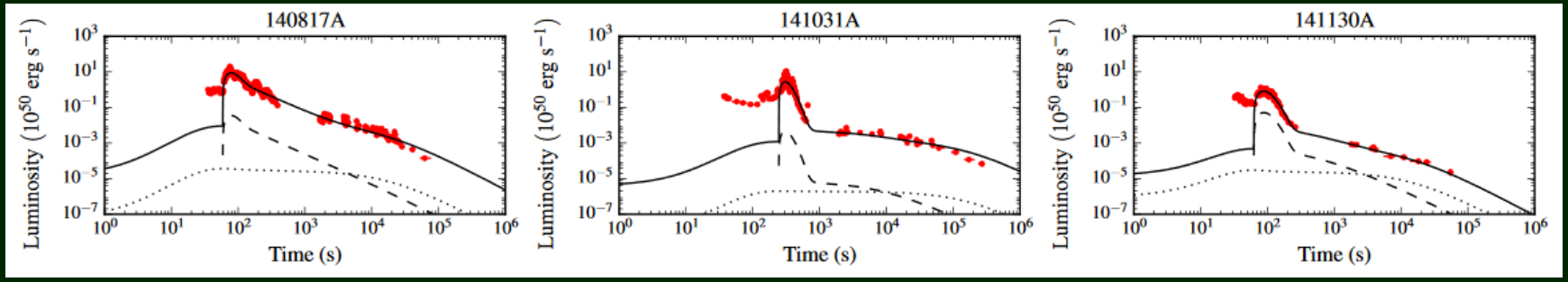

1805.09022

Fallback to power SN

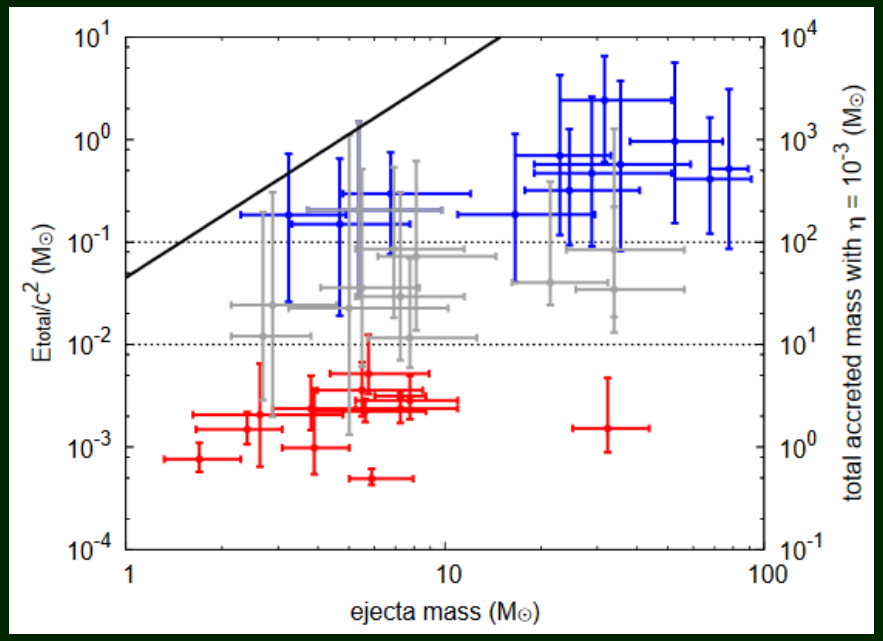

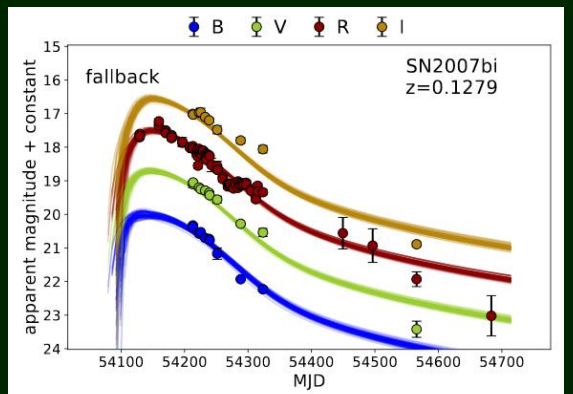

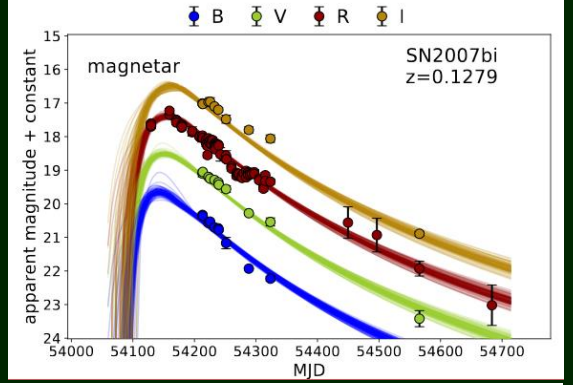

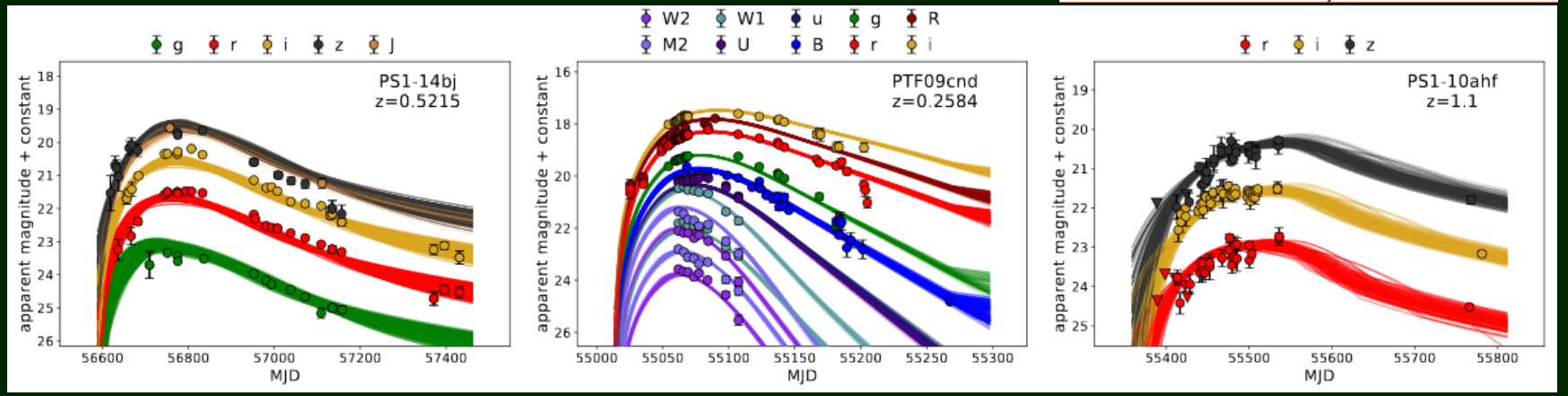

1806.00090

$$L_{\rm fallback}(t) = \begin{cases} L_1 \left(\frac{t_{\rm tr}}{1\ {\rm sec}}\right)^{-\frac{5}{3}} \equiv L_{\rm flat} & (t < t_{\rm tr}) \\ L_1 \left(\frac{t}{1\ {\rm sec}}\right)^{-\frac{5}{3}} & (t \geq t_{\rm tr}) \end{cases}$$

Conclusions

- Decaying magnetic field results in additional heating of a NS and decreasing its spin-down rate
- Field decay can be more important for large initial fields, for “standard” fields (~10^{12} G) it is not important
- It is possible to describe different types of young NSs (PSRs, magnetars, M7 etc.) in the model with decaying magnetic field
- Re-merging magnetic field can be an important ingredient
- With re-emerging field we can add to the general picture also CCOs.
- Recent studies indicate that in the life of normal radio pulsars there is a period when their magnetic field decay
- Hall cascade (and attractor) can be an important ingredient of the field evolution.
- At the moment we cannot state that we see the Hall attractor in the population of normal radio pulsars
- Also, we do not see that any of the M7 NSs are at the attractor stage, as its properties are predicted by GC2013
- Probably, the attractor stage is reached later, or its properties are different form the predicted ones.

Papers to read

- Pons, Geppert "Magnetic field dissipation in neutron star crusts: from magnetars to isolated neutron stars " astro-ph/0703267
- Popov et al. "Population synthesis studies of isolated neutron stars with magnetic field decay" MNRAS (2009) arXiv: 0910.2190
- Ho ``Evolution of a buried magnetic field in the central compact object neutron stars '' arXiv:1102.4870
- Pons et al. "Pulsar timing irregularities and the imprint of magnetic field Evolution" arXiv: 1209.2273
- Cumming et al. "MAGNETIC FIELD EVOLUTION IN NEUTRON STAR CRUSTS DUE TO THE HALL EFFECT AND OHMIC DECAY" astro-ph/0402392

Hall cascade and attractor

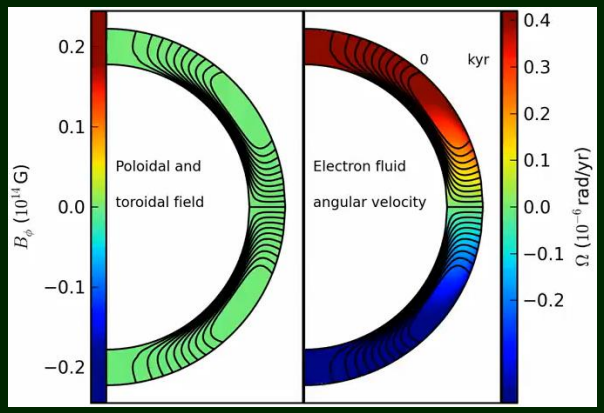

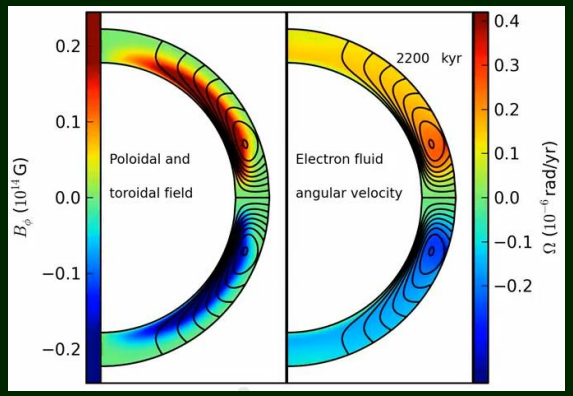

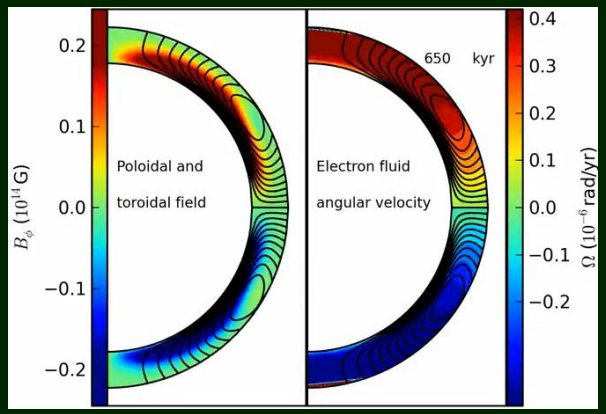

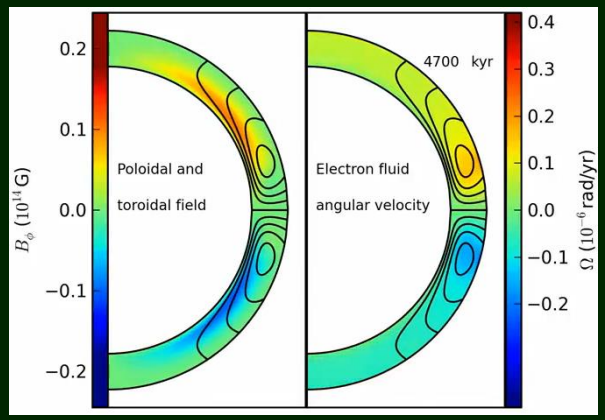

Hall cascade can reach the stage of so-called Hall attractor, where the field decay stalls for some time (Gourgouliatos, Cumming).

Gourgouliatos and Cumming 2013

http://www.physics.mcgill.ca/~kostasg/research.html

Hall attractor

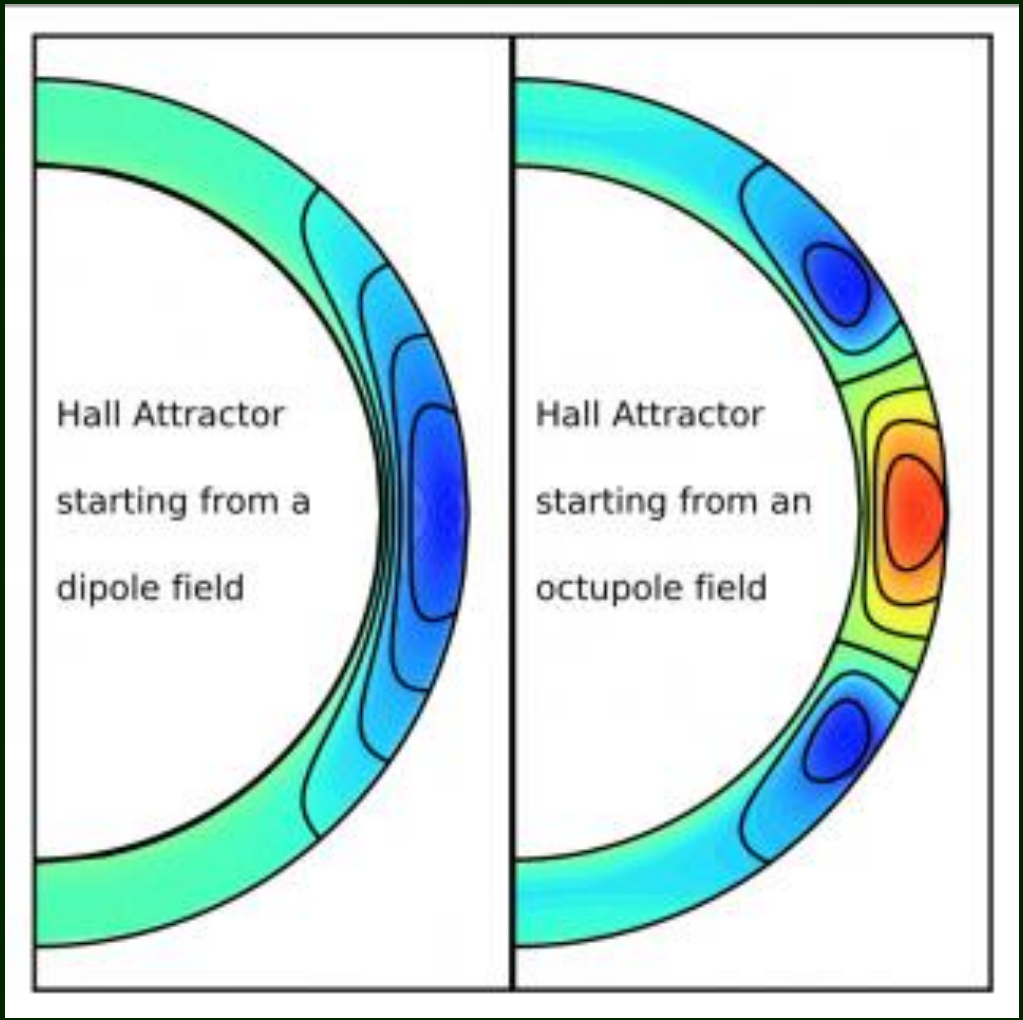

After some time the Hall cascade decays as the field finds a new| stable configuration.

1311.7345

Evolution of different components

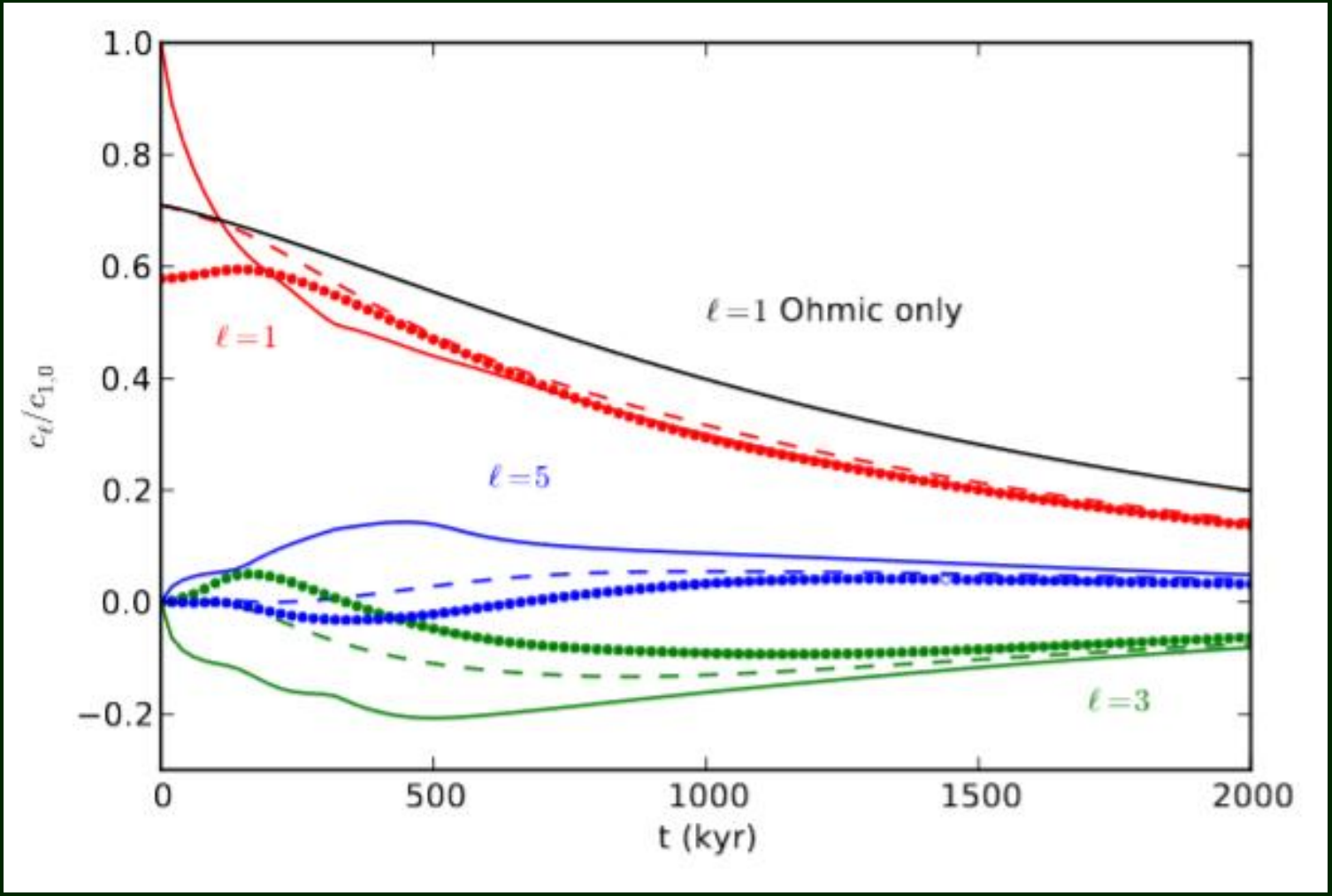

Hall attractor mainly consists of dipole and octupole

1311.7004

New studies of the hall cascade

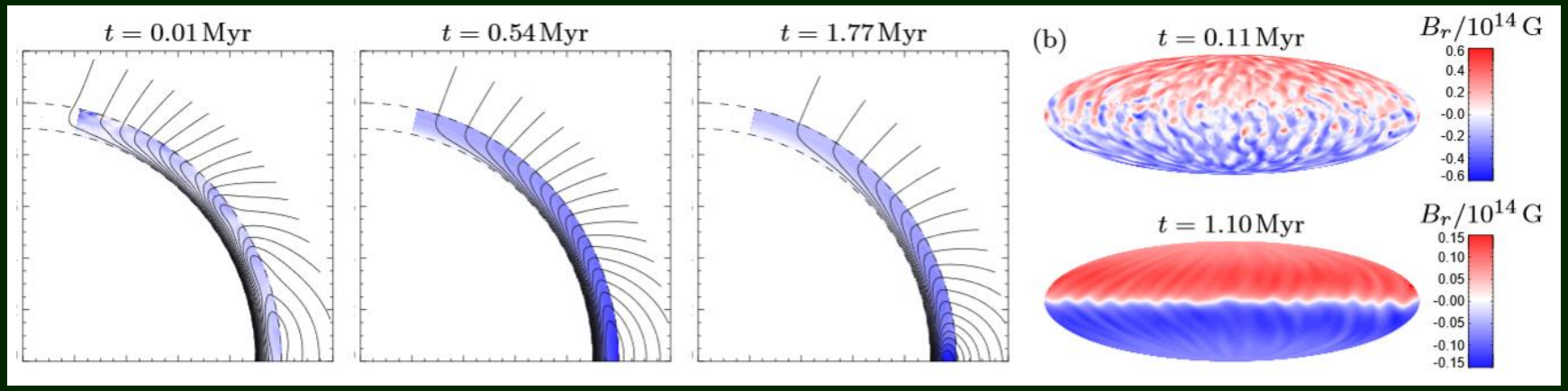

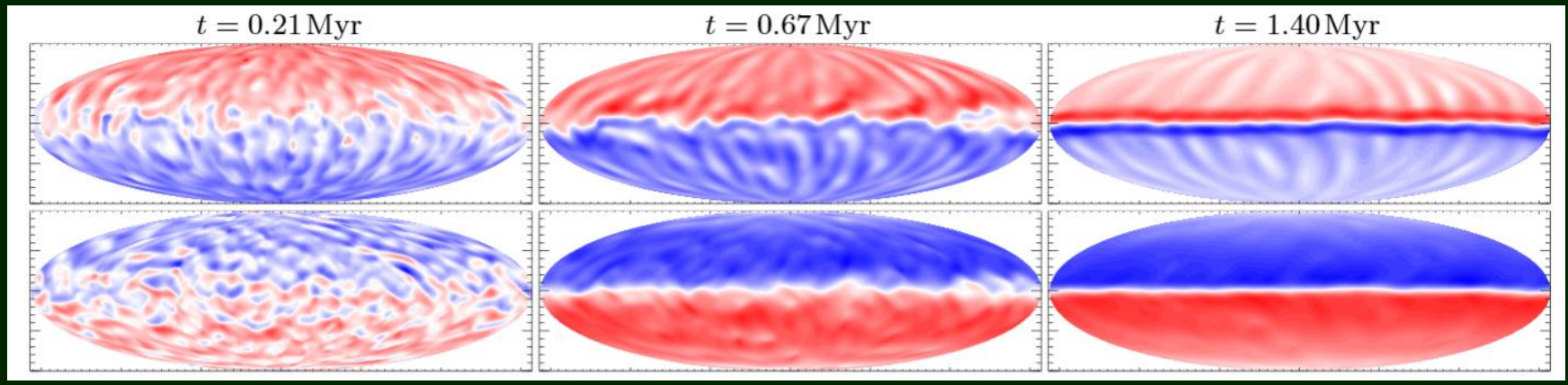

New calculations support the idea of a kind of stable configuration.

1501.05149

Where the currents are located?

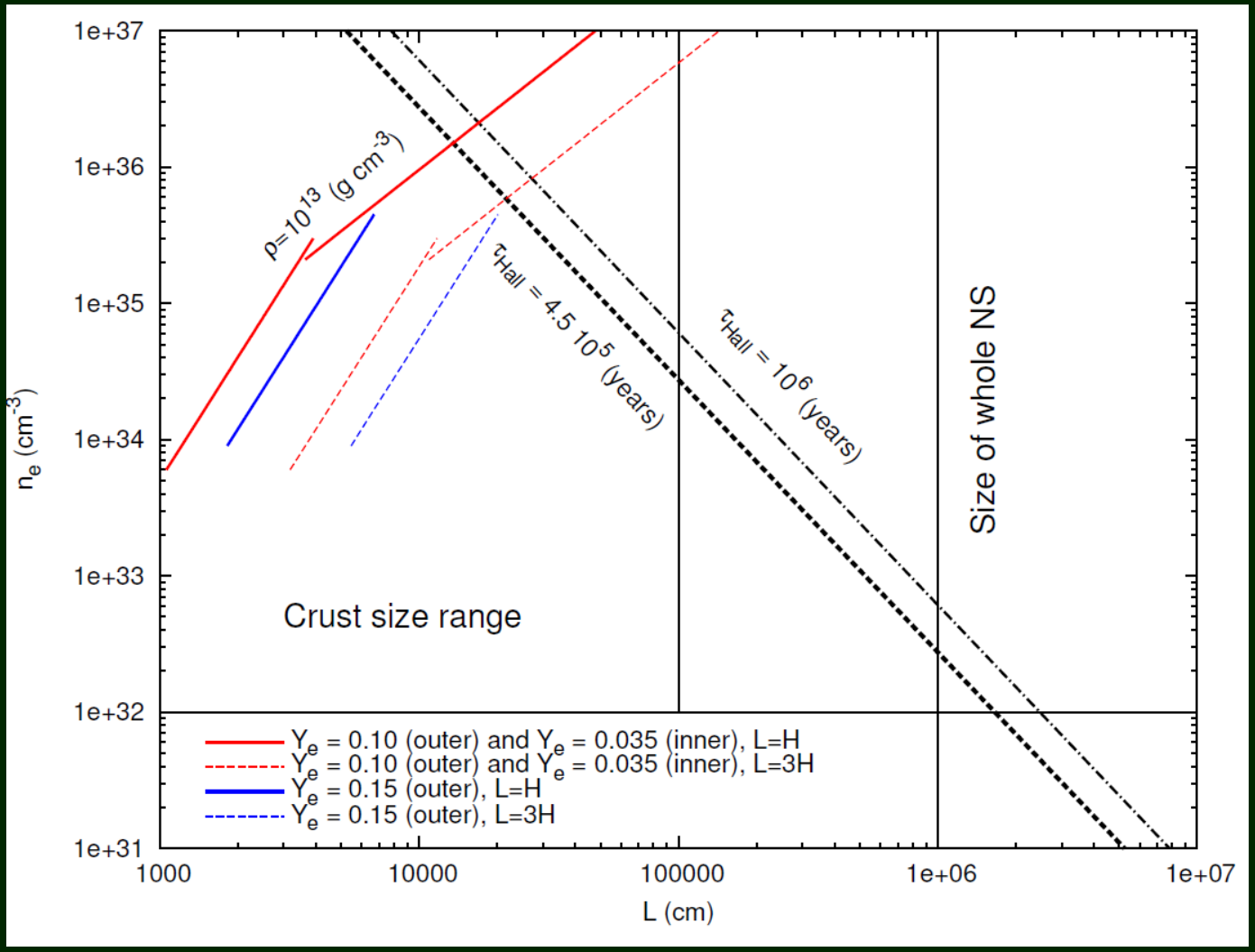

$$\tau_{\rm Hall} \approx \frac{4\pi e L^2 n_e}{cB}$$

$$L \approx H = P(\rho)/(\rho g)$$

Igoshev, Popov (2015)

Thermal evolution

Calculations are made by Shternin et al.

We fit the numerical results to perform a population synthesis of radio pulsars with decaying field.

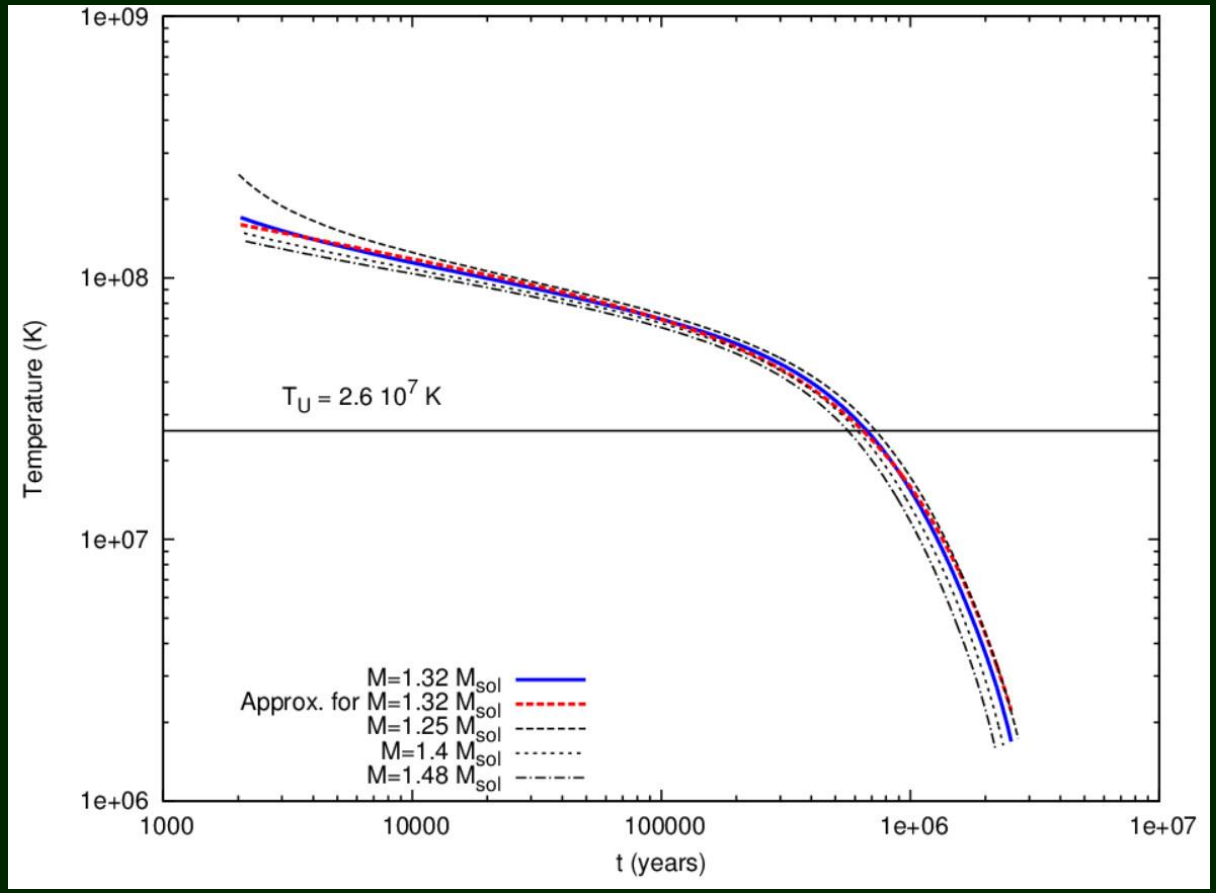

Different decay time scales

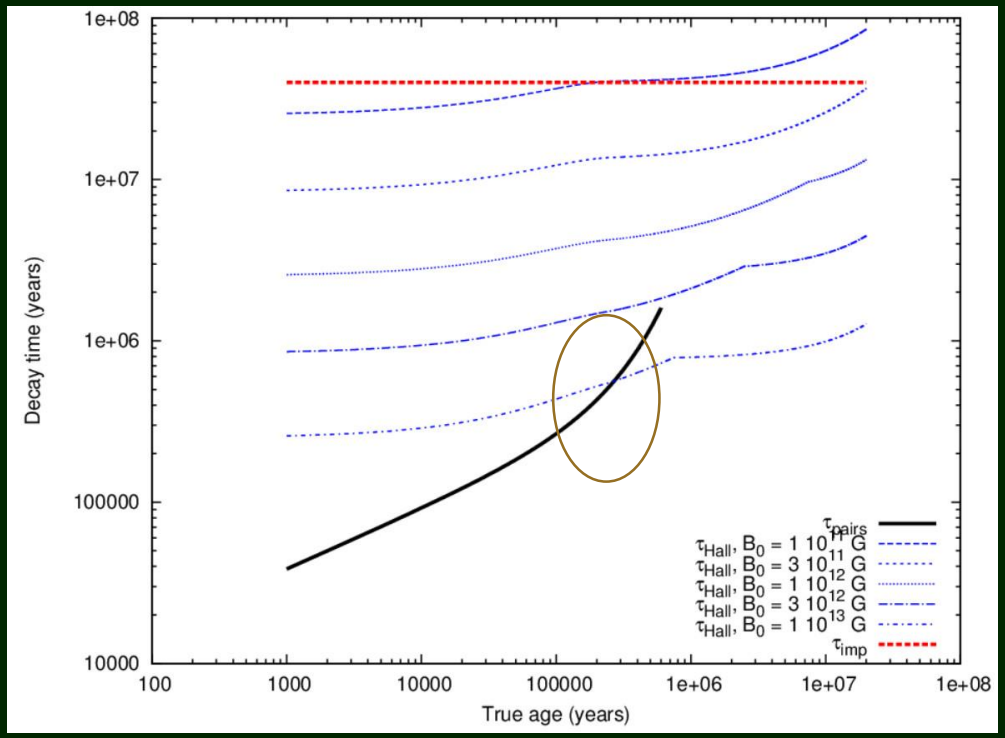

In the range of ages interesting for us the Hall rate is about the same value as the rate of Ohmic dissipation due to phonons.

$$B = B_0 \frac{\exp\left(-t/\tau_{\rm Ohm}\right)}{1+\frac{\tau_{\rm Ohm}}{\tau_{\rm Hall}}\left(1-\exp\left(-t/\tau_{\rm Ohm}\right)\right)}$$

$$\tau_{\rm imp} = 5.7\frac{\rho_{14}^{5/3}}{Q}\left(\frac{Z}{30}\right)\left(\frac{Y_e}{0.05}\right)^{1/3}\left(\frac{Y_n}{0.8}\right)^{10/3}\times$$
$$\times\left(\frac{f}{0.5}\right)^2\left(\frac{g_{14}}{2.45}\right)\ {\rm Myrs},$$

$$\tau_{\rm iphonon} = 2.2\frac{\rho_{14}^{15/6}}{T_8^2}\left(\frac{Y_e}{0.05}\right)^{5/3}\left(\frac{Y_n}{0.8}\right)^{10/3}\times$$
$$\times\left(\frac{f}{0.5}\right)^2\left(\frac{g_{14}}{2.45}\right)^{-2}\ {\rm Myrs},$$

Magnetic field evolution

$$B = B_0 \frac{\exp\left(-t/\tau_{\rm Ohm}\right)}{1 + \frac{\tau_{\rm Ohm}}{\tau_{\rm Hall}}\left(1 - \exp\left(-t/\tau_{\rm Ohm}\right)\right)}$$

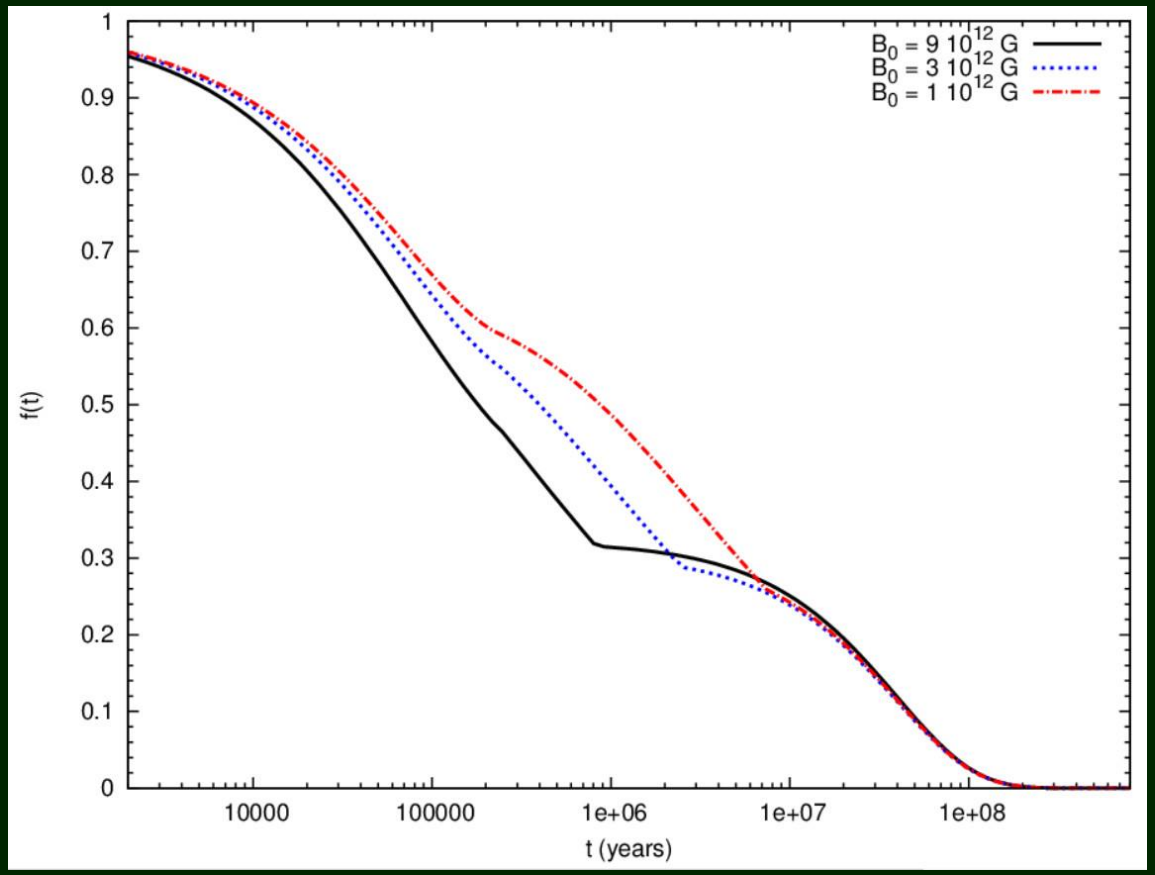

All inclusive:
- Hall
- Phonons
- Impurities

Igoshev, Popov (2015)

Only Ohmic decay

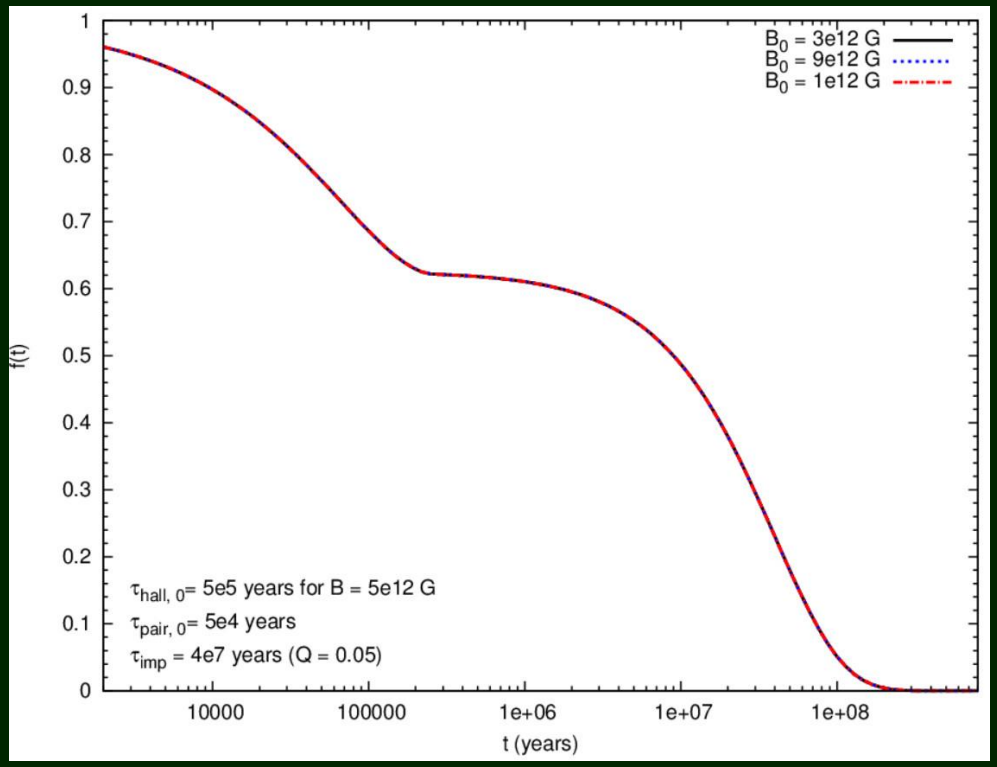

Here the Hall cascade is switched off

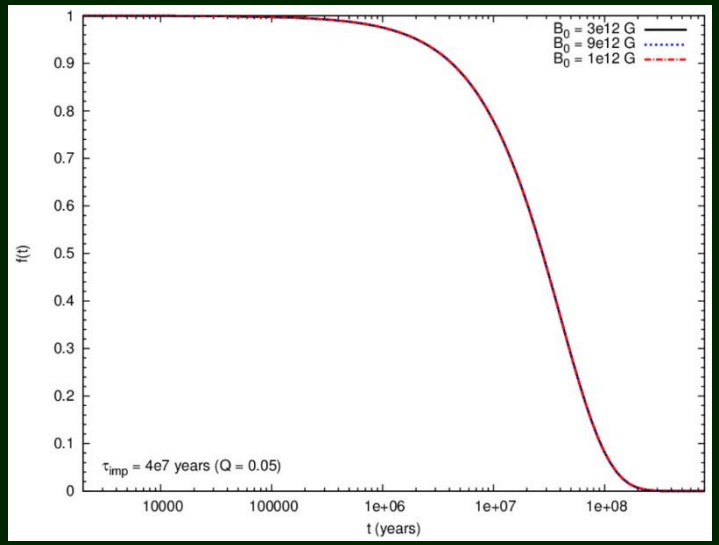

In one figure we have Ohmic decay only due to impurities, on another one – phonons are added.

Comparison of different options

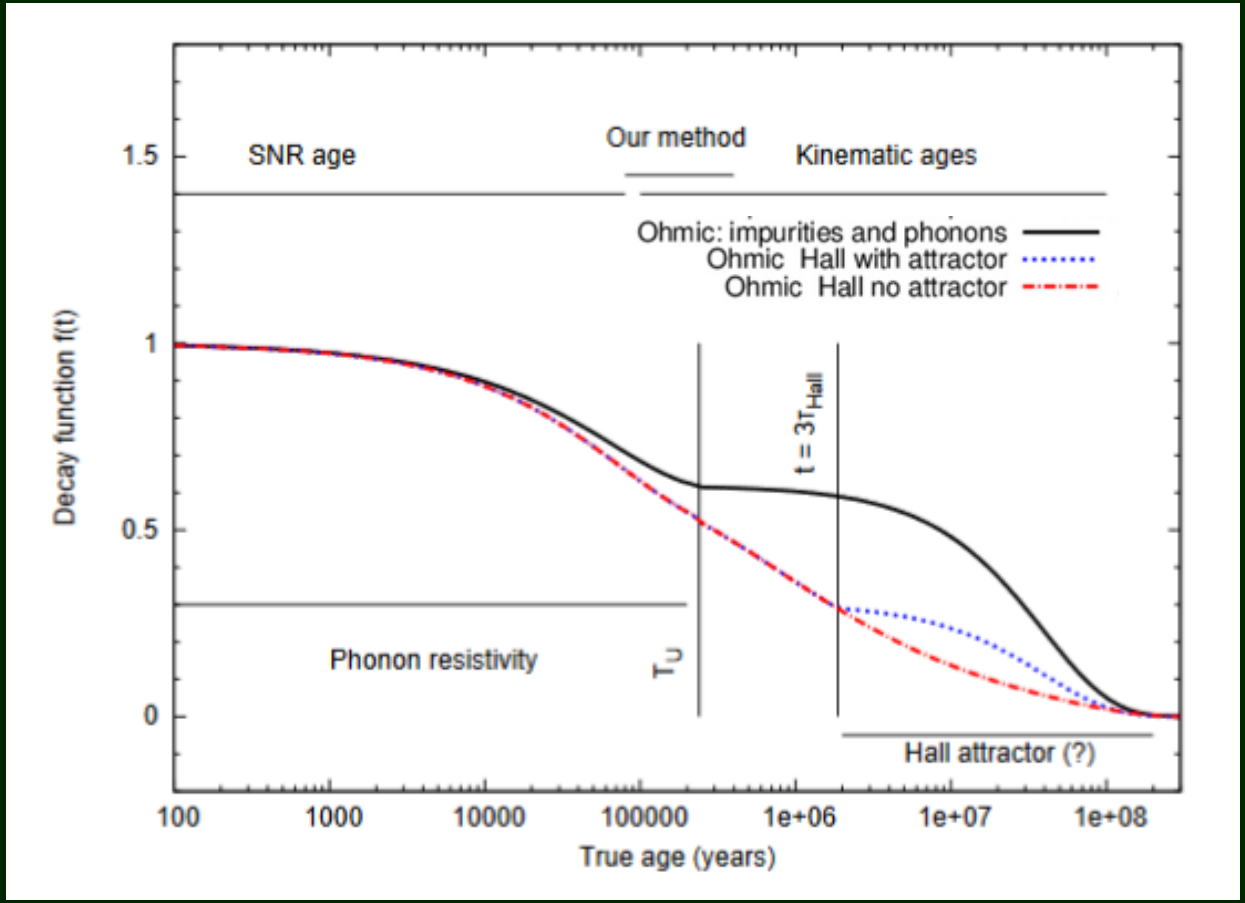

We think that at the ages ~10^5 yrs and below for normal pulsars we see mostly Ohmic decay, which then disappears as NSs cool down below the critical T.

Igoshev, Popov (2015)

Getting close to the attractor

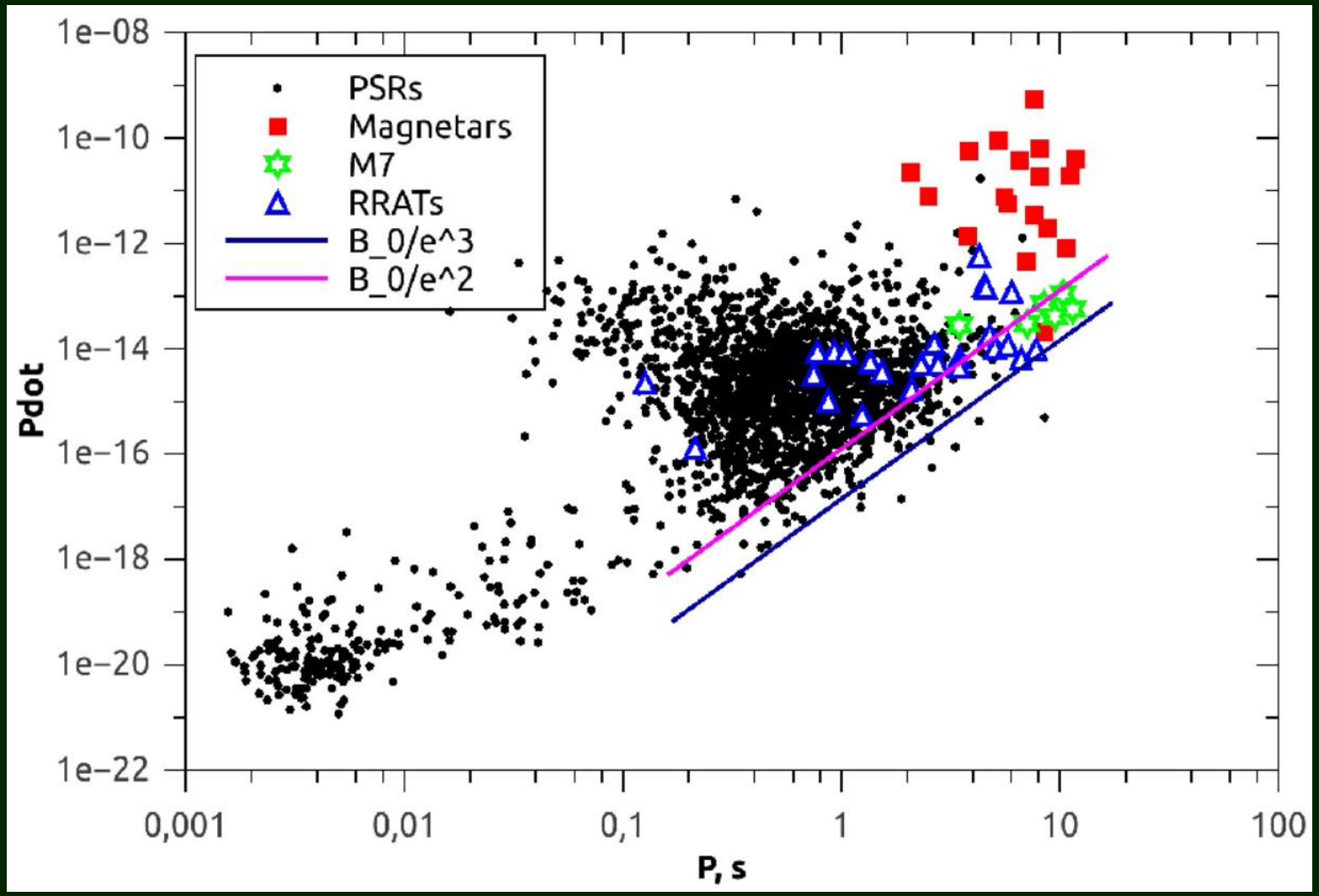

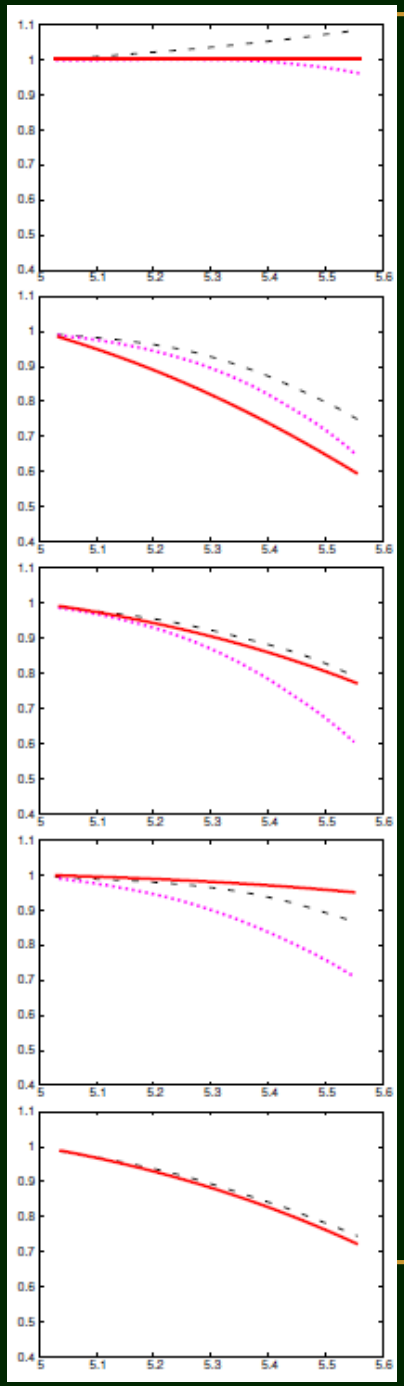

Tests

We make extensive tests of the method and obtain that in most of the cases it is able to uncover non-negligible magnetic field decay (more than a few tens of per cent during the studied range of ages) in normal radio pulsars for realistic initial properties of neutron stars.

Name	$\log \mu_{B_0}$ [G]	$\log \sigma_{B_0}$ [G]	μ_{P_0} [s]	σ_{P_0} [s]	α	$\tau_{\rm D}$ [Myr]	$\tau_{\rm SDA}$ [Myr]
A1	12.60	0.47	0.33	0.23	0.50	∞	∞
A2	12.95	0.55	0.30	0.15	0.50	∞	10
B1	12.60	0.47	0.33	0.23	0.50	0.5	1.00
B2	12.95	0.55	0.30	0.15	0.50	0.5	0.690
C1	12.60	0.47	0.33	0.23	0.50	1	1.15
C2	12.95	0.55	0.30	0.15	0.50	1	0.560
D1	12.60	0.47	0.33	0.23	0.50	5	2.00
D2	12.95	0.55	0.30	0.15	0.50	5	0.80
E	13.04	0.55	0.22	0.32	0.44	~ 0.8	0.880

(Synthetic samples are calculated by Gullon, Pons, Miralles)

Evolution with field decay

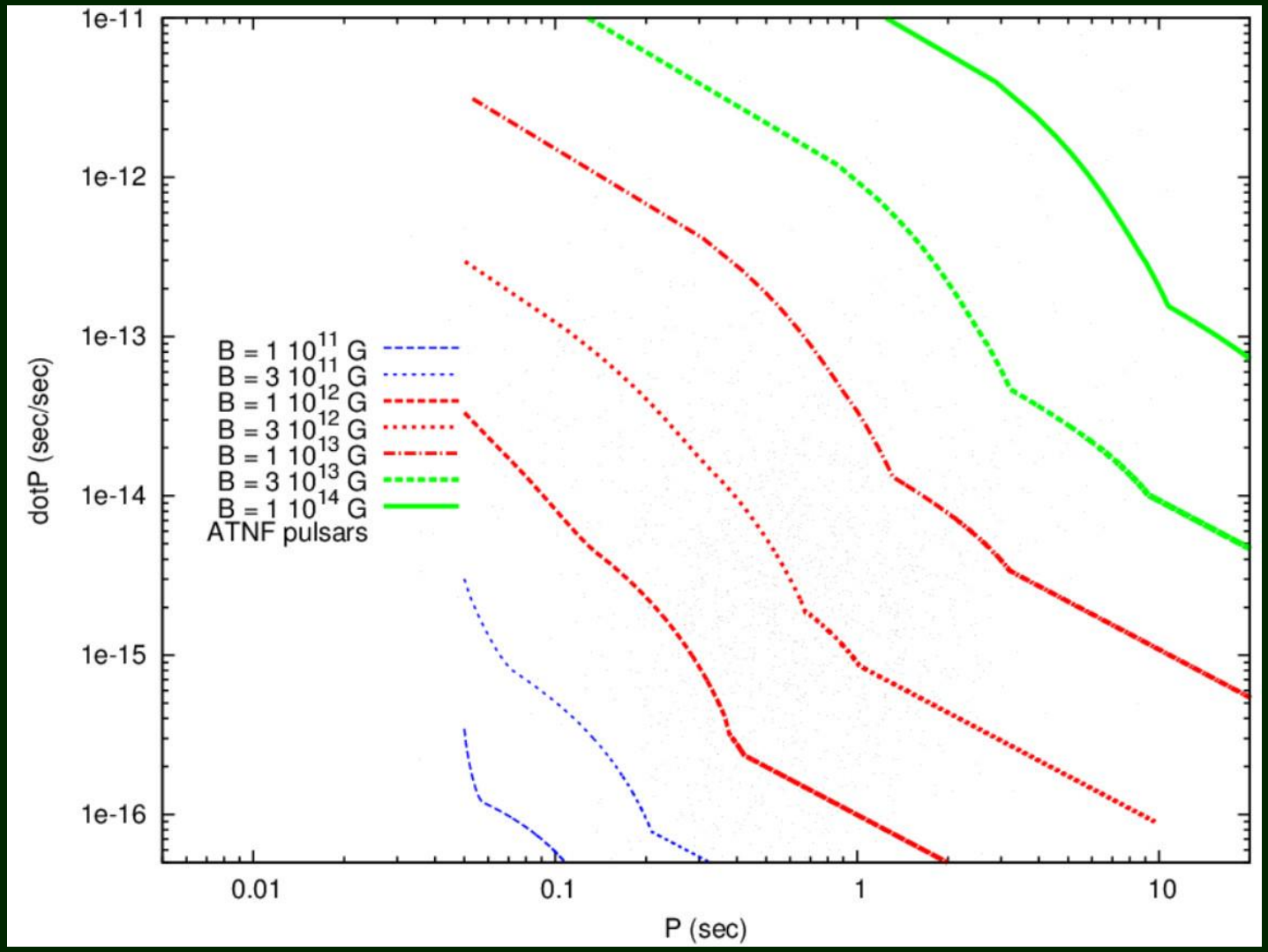

Who is closer to the attractor stage?

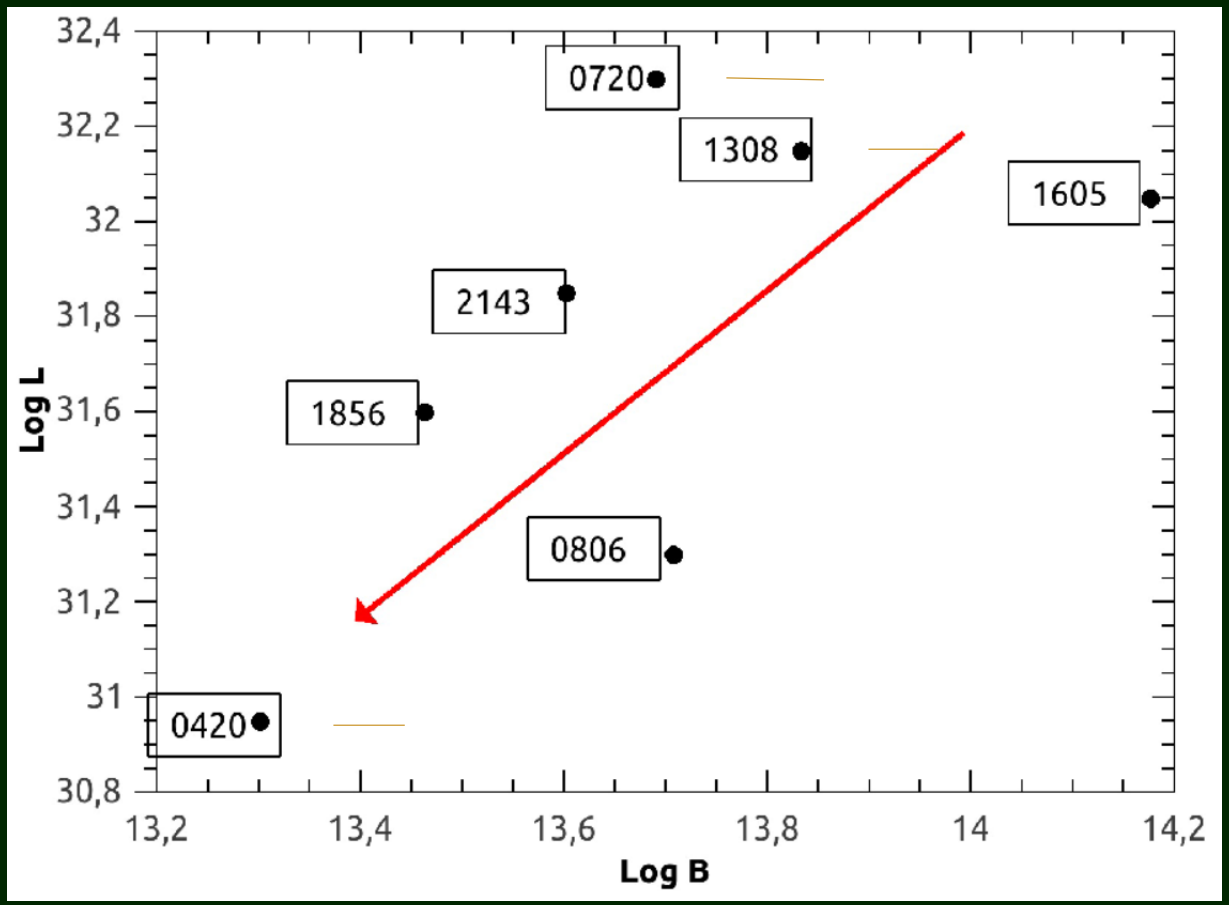

Evolution of different components

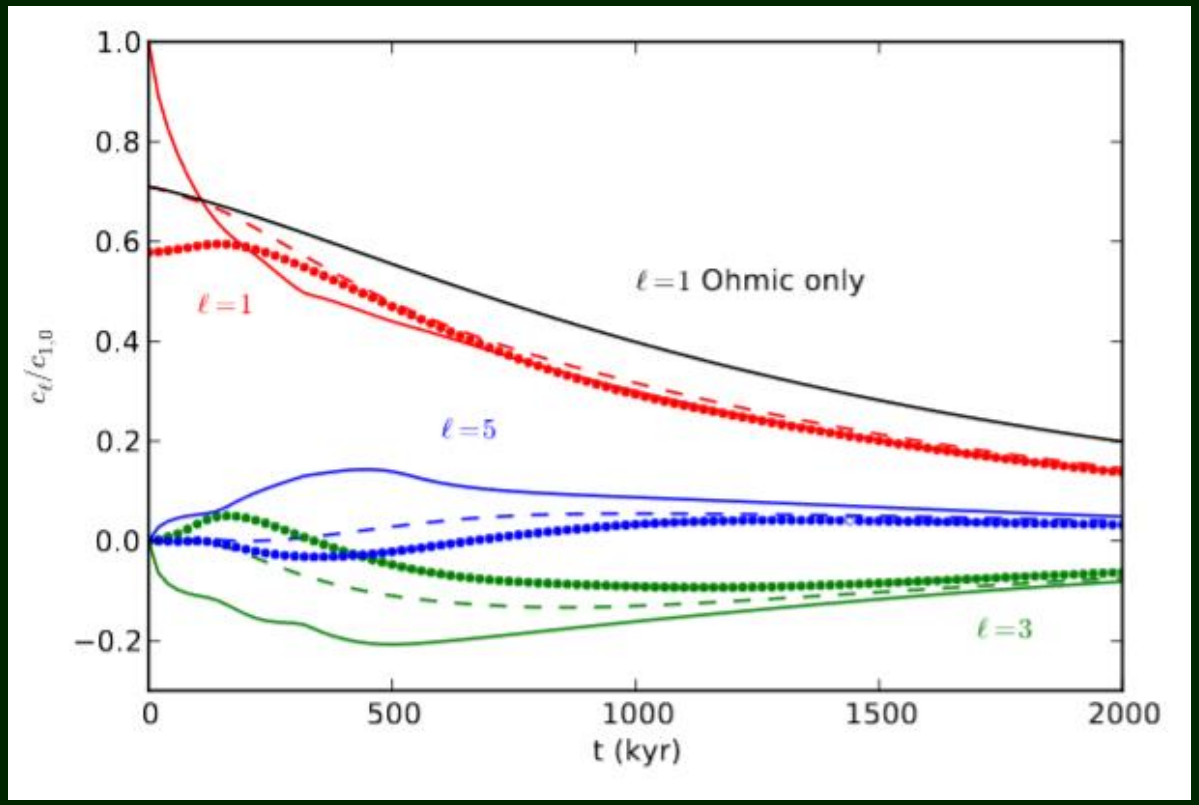

Hall attractor mainly consists of dipole and octupole

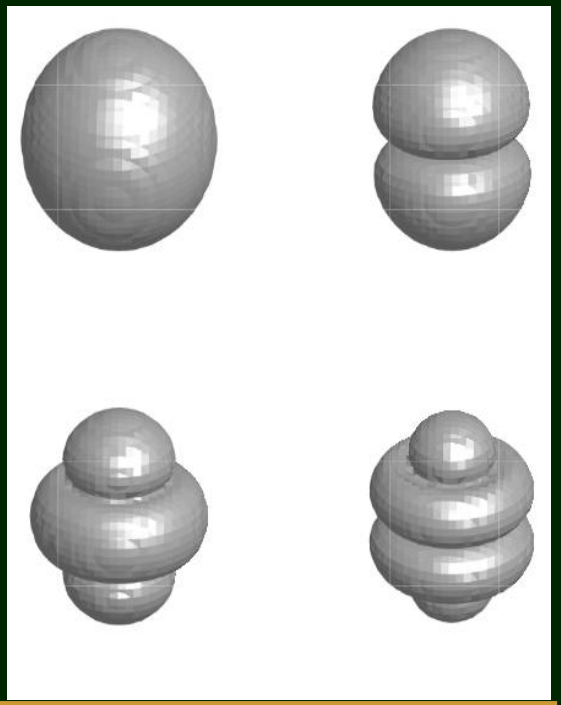

1311.7004

0902.0720

Temperature maps

Pure dipole

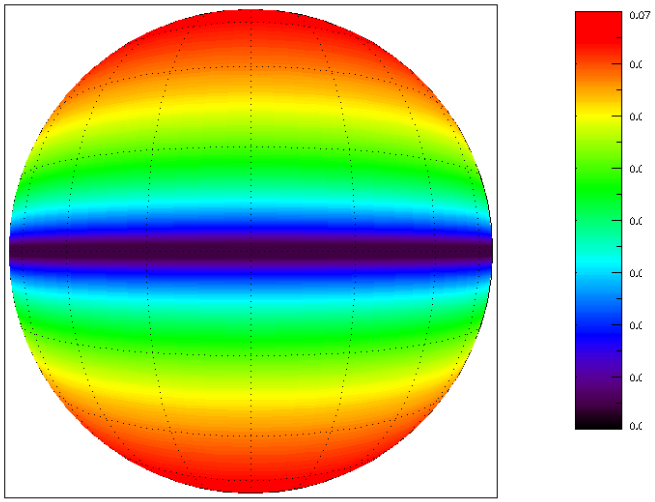

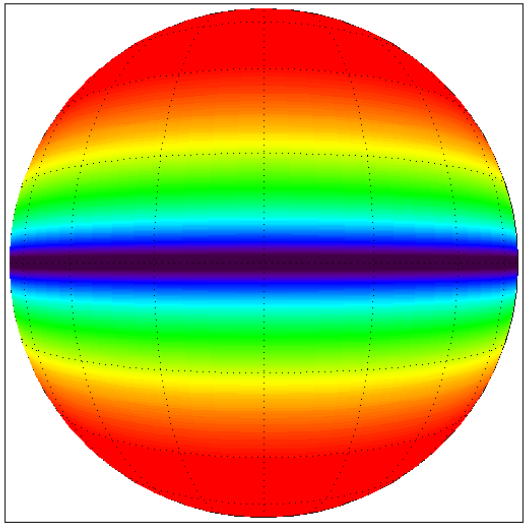

Dipole + octupole

Dipole+octupole+I5

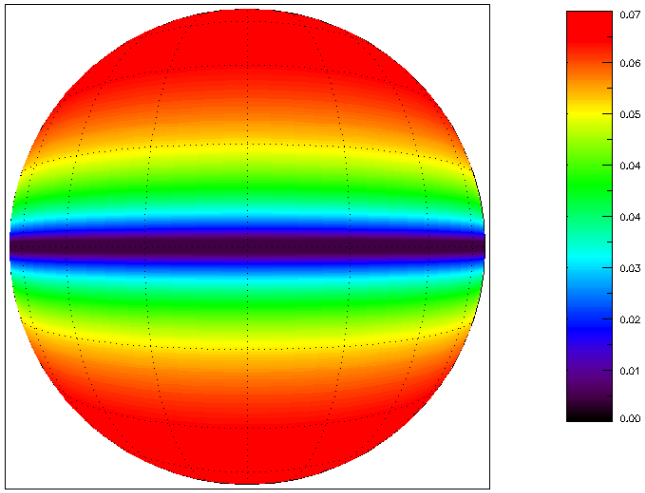

Spectral fits: single blackbody

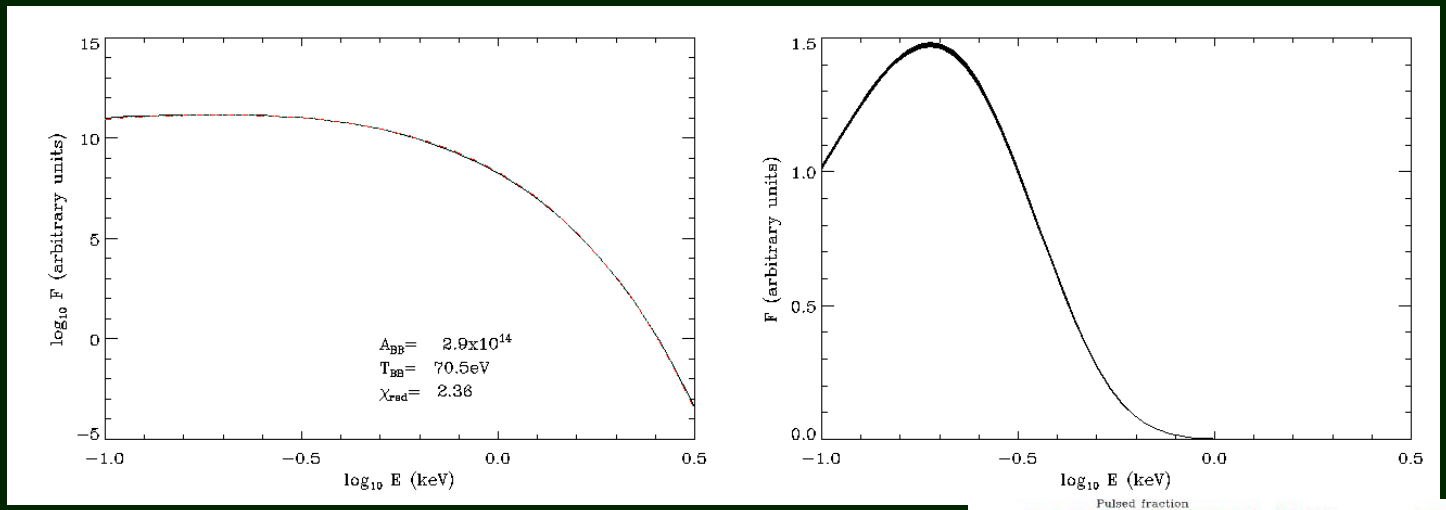

Single black body
does not provide
a good fit, even using,
in addition, a line,
or condensed surface.

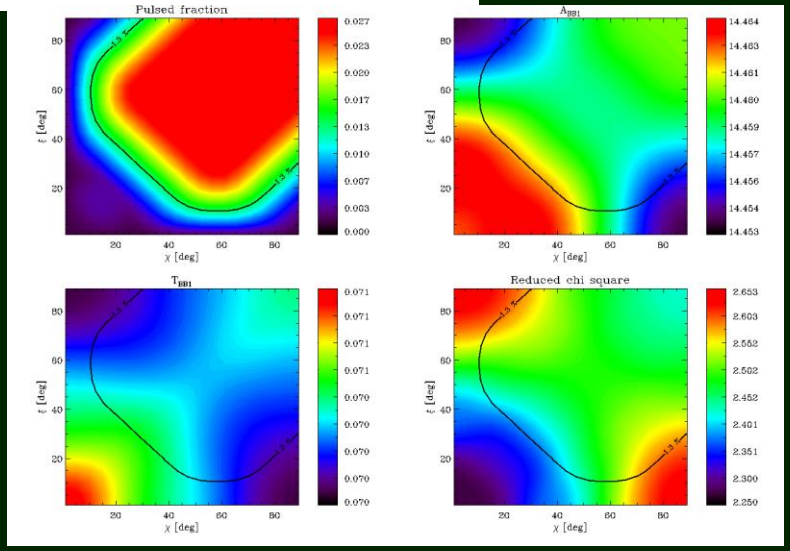

Spectral fits: two black bodies

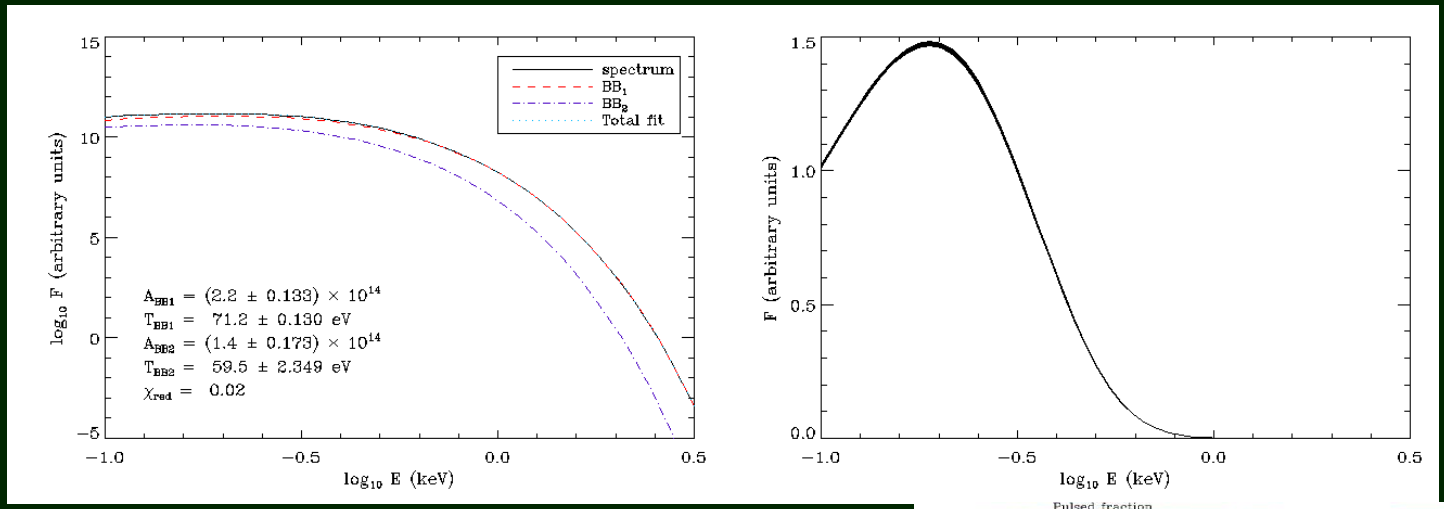

Formally, two black bodies
is the best fit for 1856.
And for dipole+octupole
we can obtain a very good fit.
But ….

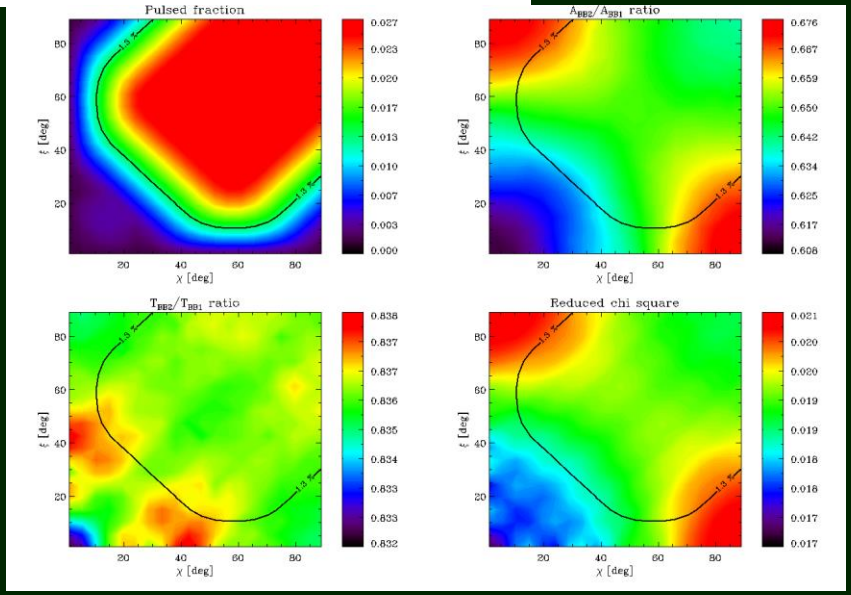

Observational data

Parameter	Single BB	Two BB
N_H $[10^{19}\ \mathrm{cm}^{-2}]$	$4.8^{+0.2}_{-0.2}$	$12.9^{+2.2}_{-2.3}$
kT_h^{∞} [eV]	$61.5^{+0.1}_{-0.1}$	$62.4^{+0.6}_{-0.4}$
R_h^{∞} [km]	$5.0^{+0.1}_{-0.1}$	$4.7^{+0.2}_{-0.3}$
kT_s^{∞} [eV]	-	$38.9^{+4.9}_{-2.9}$
R_s^{∞} [km]	-	$11.8^{+5.0}_{-0.4}$
σ_{sys}	1.5%	0.6%
χ^2_ν	1.12	1.11

Two black bodies is the best fit.
The colder component corresponds to larger surface area.
This is in contrast with our results for the Hall attractor proposed by GC2013 (dipole + octupole).

1202.2121

Synthetic populations

Constant field

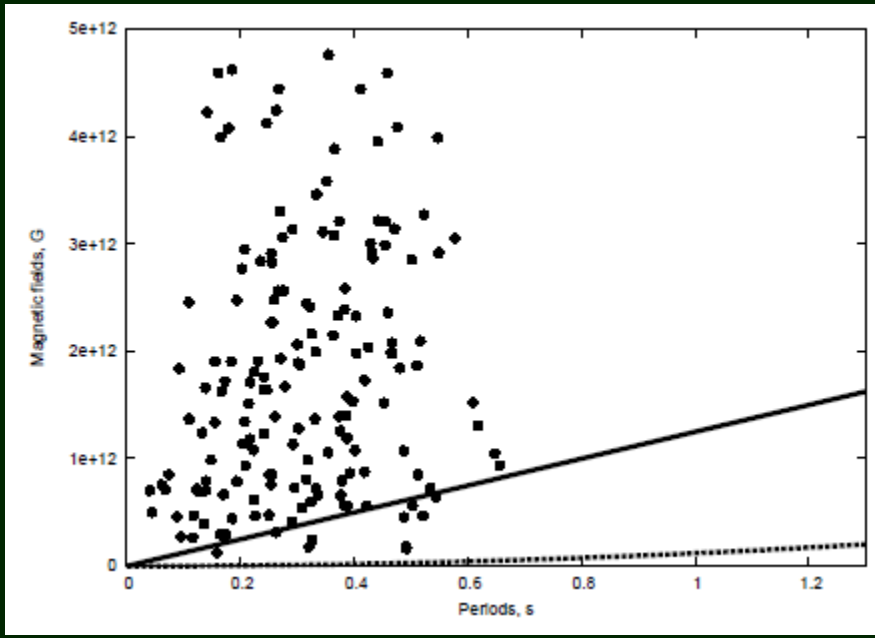

Exponential decay

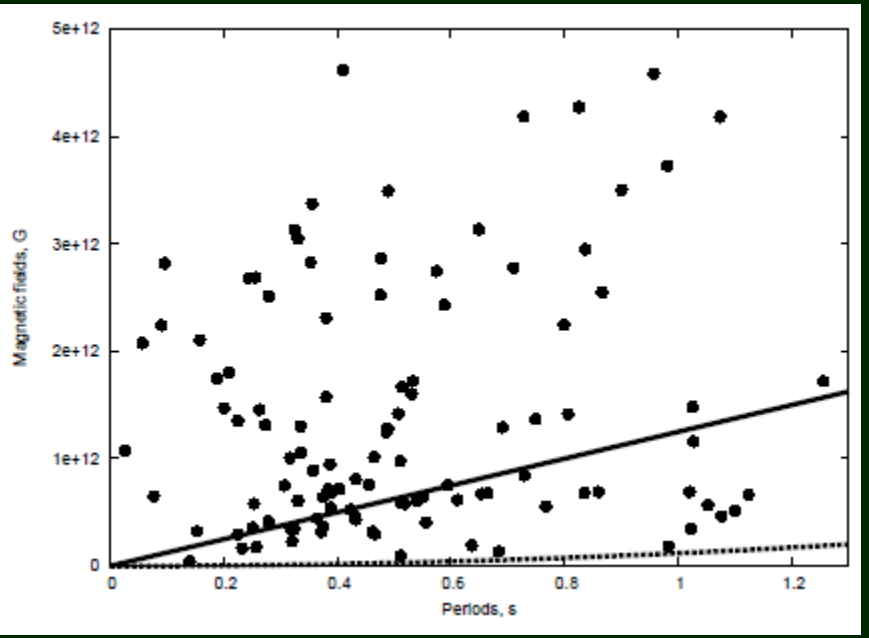

$$P_0 = P\sqrt{1 - \frac{t_{\rm true}}{\tau}}.$$

Igoshev, Popov 2013

Fitting the field decay

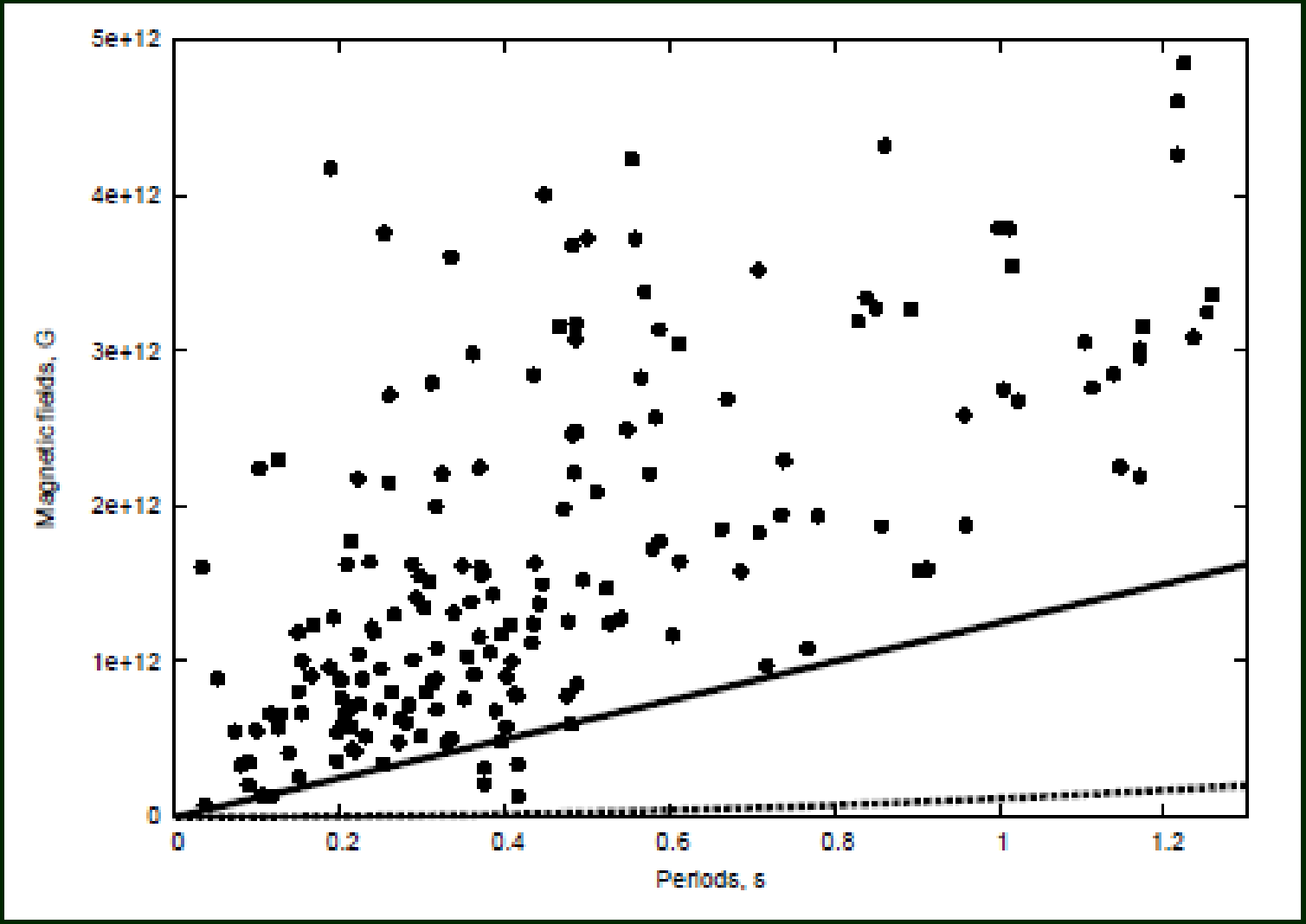

Igoshev, Popov 2013

Another option: emerging field

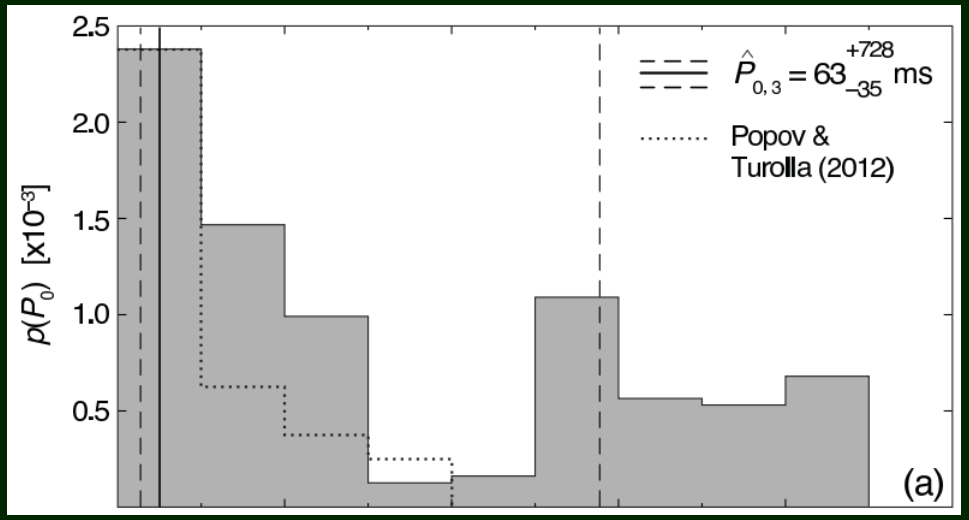

The problem is just with few (6) most long-period NSs.
Is it possible to hide them when they are young, and make them visible at the age ~few million years?

Yes! Emerging magnetic field!!!

Then we need correlations between different parameters.

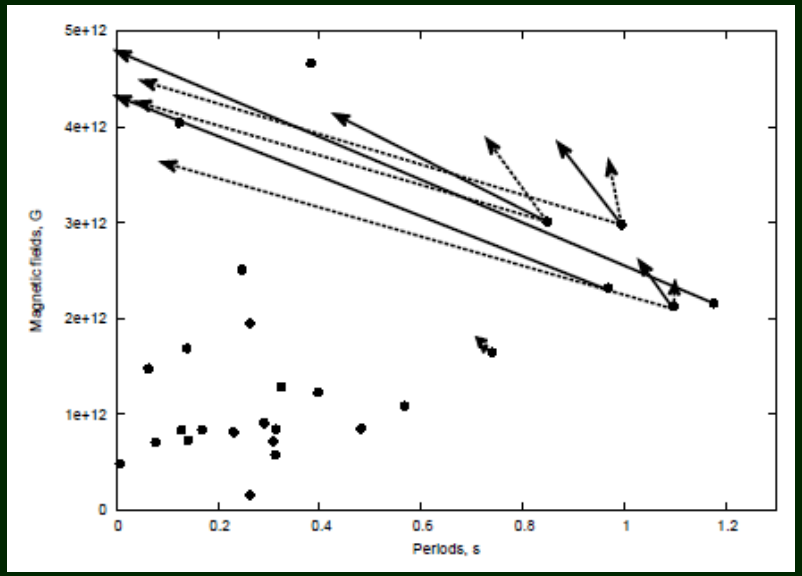

Igoshev, Popov 2013

Accreting isolated neutron stars

Magnetic rotator

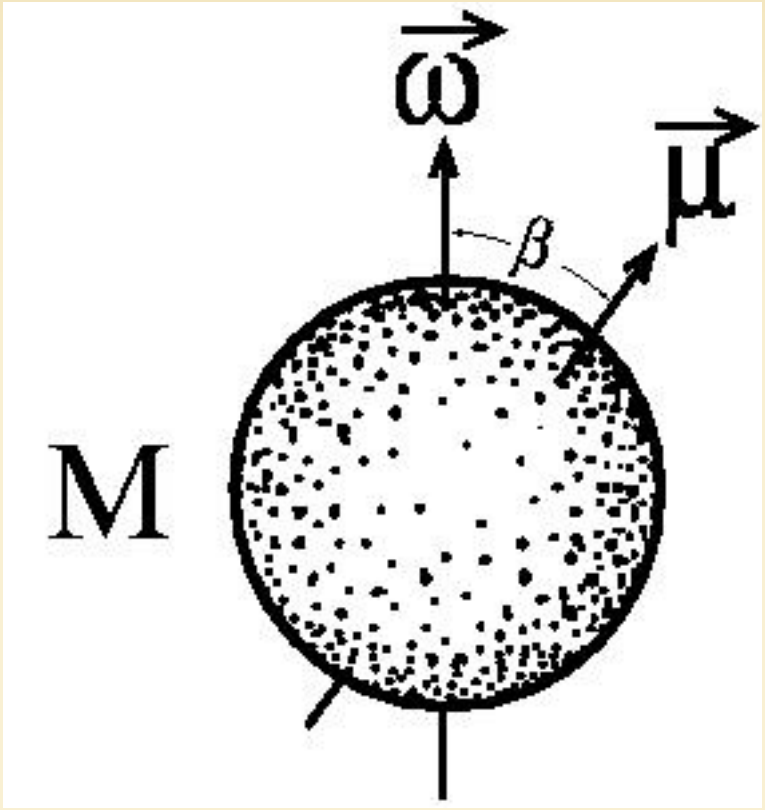

Observational appearances of NSs
(if we are not speaking about cooling)
are mainly determined by P, Pdot, V, B,
(also, probably by the inclination angle β),
and properties of the surrounding medium.
B is not evolving significantly in most cases,
so it is important to discuss spin evolution.

Together with changes in B (and β)
one can speak about

magneto-rotational evolution

We are going to discuss the main stages
of this evolution, namely:
Ejector, Propeller, Accretor, and *Georotator*
following the classification by Lipunov

Evolution of neutron stars: rotation + magnetic field

Ejector → Propeller → Accretor → Georotator

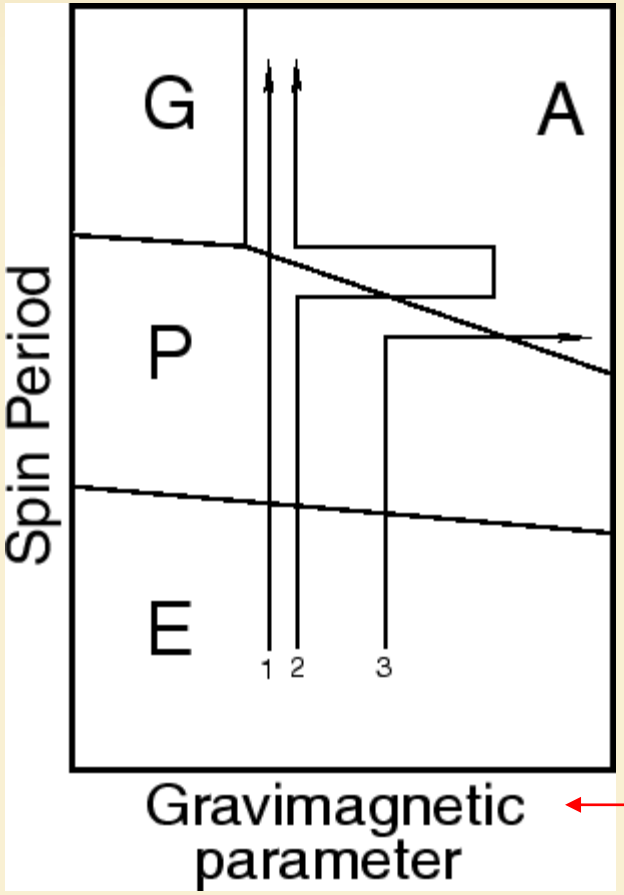

1 – spin down
2 – passage through a molecular cloud
3 – magnetic field decay

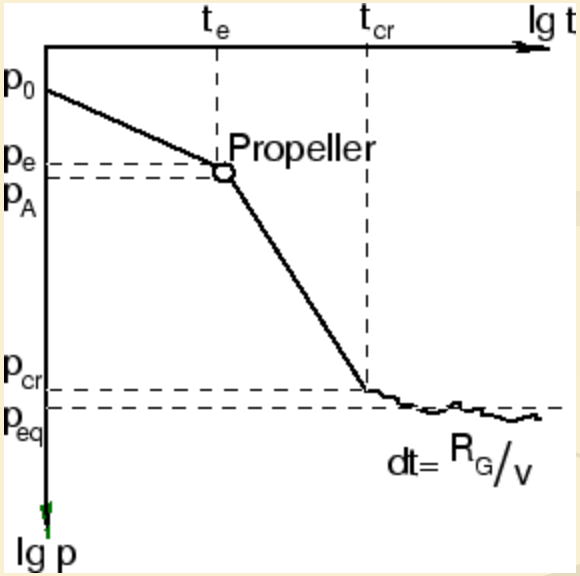

[astro-ph/0101031]

$\dot{M}/\mu^2$

See the book by Lipunov (1987, 1992)

Accreting isolated neutron stars

Why are they so important?

- Can show us how old NSs look like
  1. Magnetic field decay
  2. Spin evolution
- Physics of accretion at low rates
- NS velocity distribution
- New probe of NS surface and interiors
- ISM probe

Critical periods for isolated NSs

$$P_E(E \to P) \simeq 10\,\mu_{30}^{1/2}\,n^{-1/4}\,v_{10}^{1/2}\ \mathrm{s}$$

Transition from Ejector to Propeller (supersonic)

$$t_E \simeq 10^9\,\mu_{30}^{-1}\,n^{-1/2}\,v_{10}\ \mathrm{yr}$$

Duration of the ejector stage

$$P_A(P \to A) \simeq 420\,\mu_{30}^{6/7}\,n^{-3/7}\,v_{10}^{9/7}\ \mathrm{s}$$

Transition from supersonic Propeller to subsonic Propeller or Accretor

$$P_{eq} = 2.6 \times 10^3\,v_{(t)10}^{-2/3}\,\mu_{30}^{2/3}\,n^{-2/3}\,v_{10}^{13/3}\ \mathrm{s}$$

A kind of equilibrium period for the case of accretion from turbulent medium

$$v < 410\,n^{1/10}\,\mu_{30}^{-1/5}\ \mathrm{km\,s^{-1}}$$

Condition for the Georotator formation (instead of Propeller or Accretor)

(see, for example, astro-ph/9910114)

Accretion dynamics

Bondi-Hoyle-Littleton accretion (astro-ph/0406166)

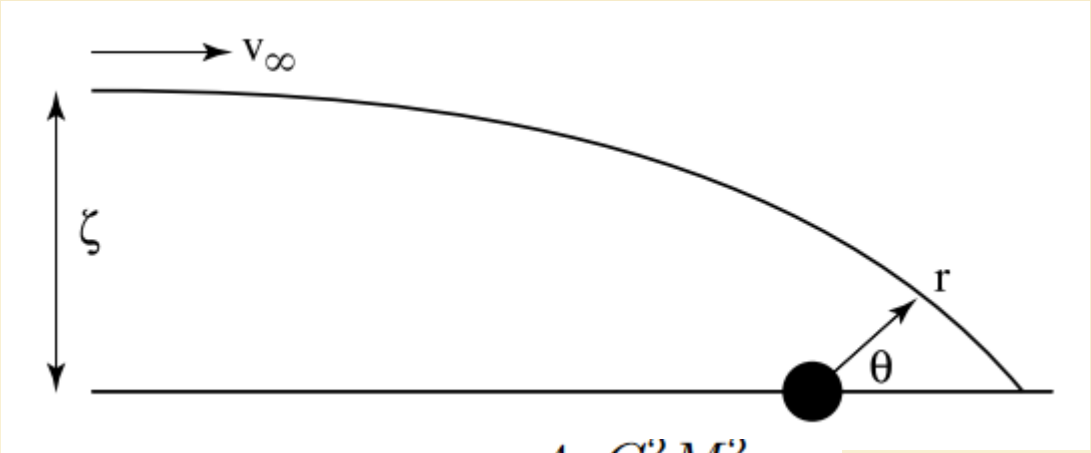

$$\dot{M}_{\rm HL} = \pi \zeta_{\rm HL}^2 v_\infty \rho_\infty = \frac{4\pi G^2 M^2 \rho_\infty}{v_\infty^3}$$

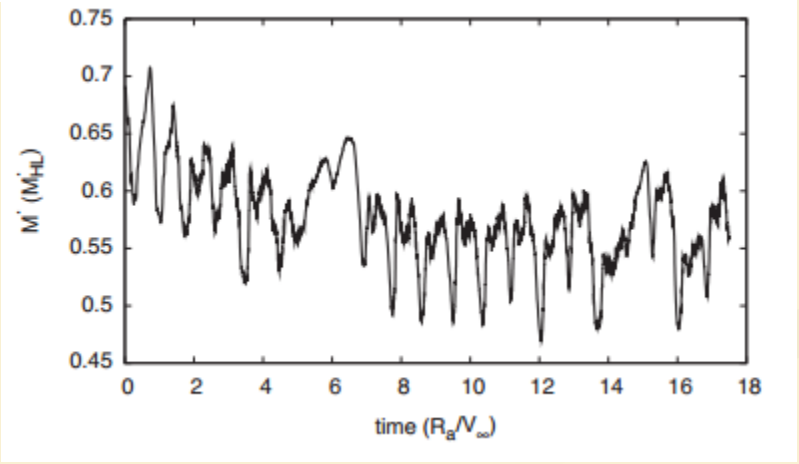

Recently BHL accretion for non-magnetized accretors have been studied in 1204.0717. Still, resolution in 3D is not high enough.

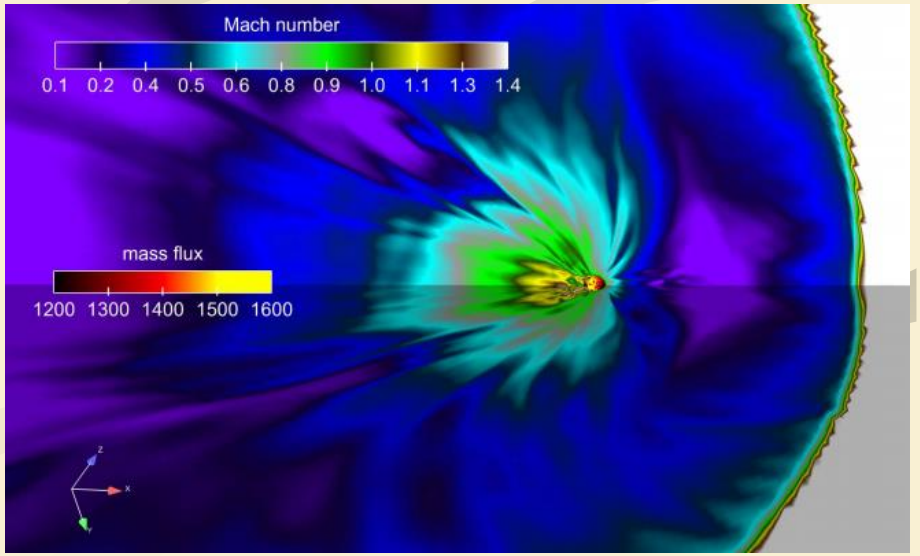

Expected properties

1. **Accretion rate**

An upper limit can be given by the Bondi formula:
$\dot{M} = \pi R_G^2 \rho v$, $R_G \sim v^{-2}$
$\dot{M} = 10^{11}$ g/s $(v/10$ km/s$)^{-3}$ n
$L = 0.1 \dot{M} c^2 \sim 10^{31}$ erg/s

However, accretion can be smaller due to the influence of a magnetosphere of a NS (see numerical studies by Toropina et al. 1111.2460).

2. **Periods**

Periods of old accreting NSs are uncertain, because we do not know evolution well enough.

$$p_A = 2^{5/14}\pi(GM)^{-5/7}(\mu^2/\dot{M})^{3/7} \simeq$$

$R_A = R_{co}$

$$300\,\mu_{30}^{6/7}(v/10\,\mathrm{km\,s^{-1}})^{9/7}n^{-3/7}\,\mathrm{s}.$$

Reduction of the accretion rate

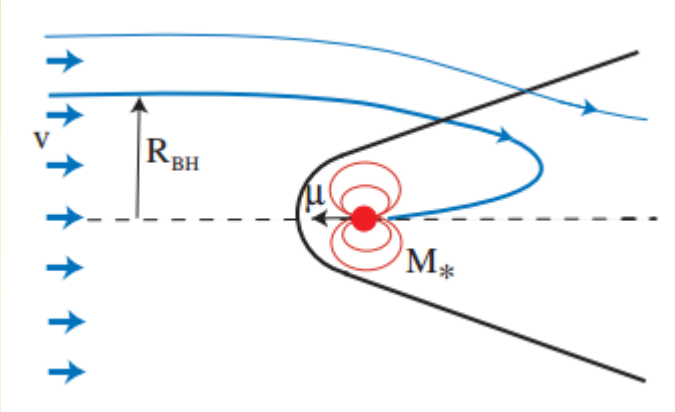

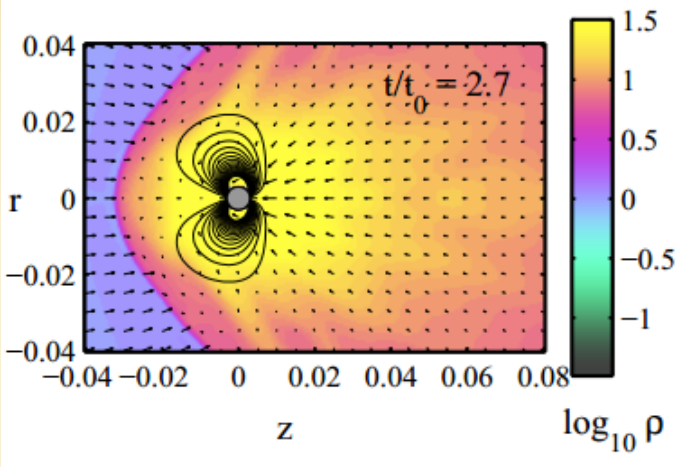

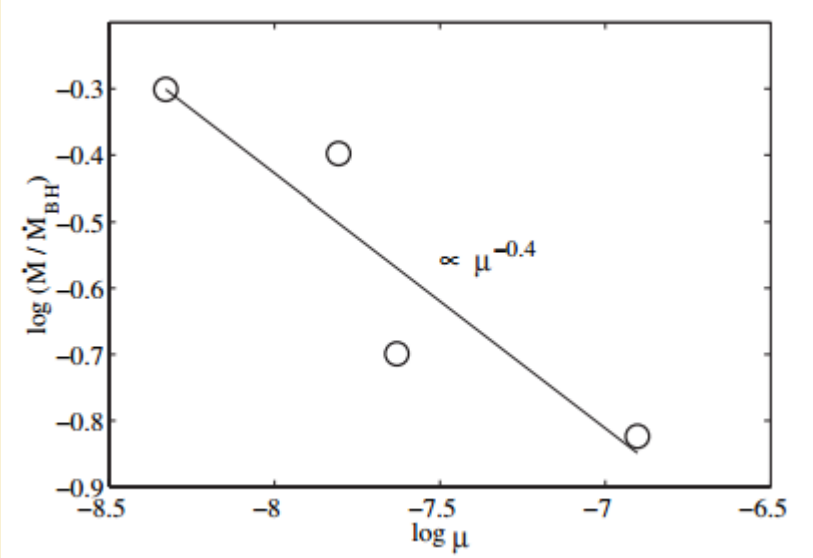

Surface accretion accretion rate can be much reduced due to the presence of large magnetosphere.

1111.2460

Subsonic propeller

Even after $R_{co}>R_A$ accretion can be inhibited.
This have been noted already in the pioneer papers by Davies et al.

Due to rapid (however, subsonic) rotation a hot envelope is formed around the magnetosphere. So, a new critical period appear.

$$P_{\rm br} \simeq 450\, \mu_{30}^{16/21}\, \dot{M}_{15}^{-5/7}\, m^{-4/21}\ {\rm s}.$$

(Ikhsanov astro-ph/0310076)

If this stage is realized (inefficient cooling) then
- accretion starts later
- accretors have longer periods

Equilibrium period

Interstellar medium is turbulized. If we put a non-rotating NS in the ISM, then because of accretions of turbulized matter it'll start to rotate.
This clearly illustrates, that a spinning-down accreting isolated NS in a realistic ISM should reach some equilibrium period.

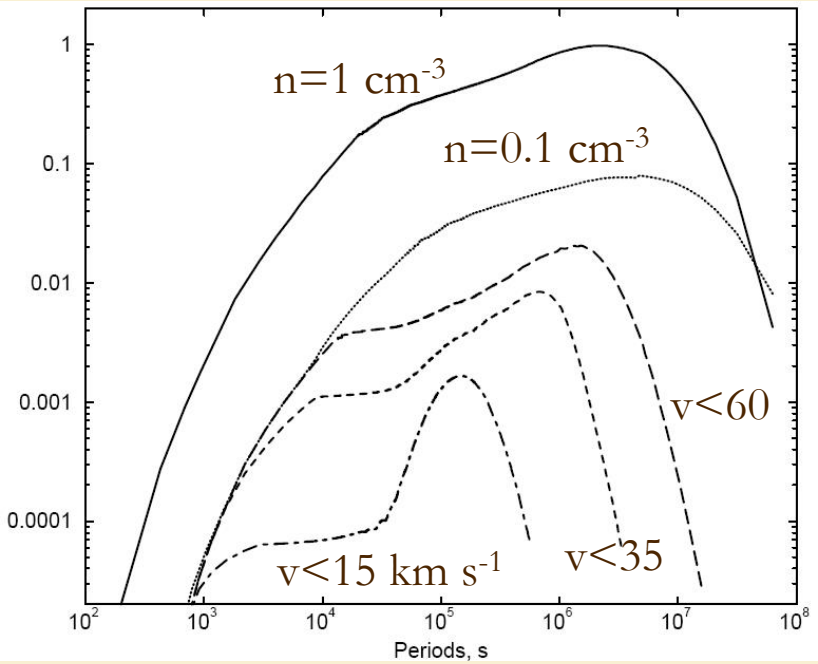

[A&A 381, 1000 (2002)]

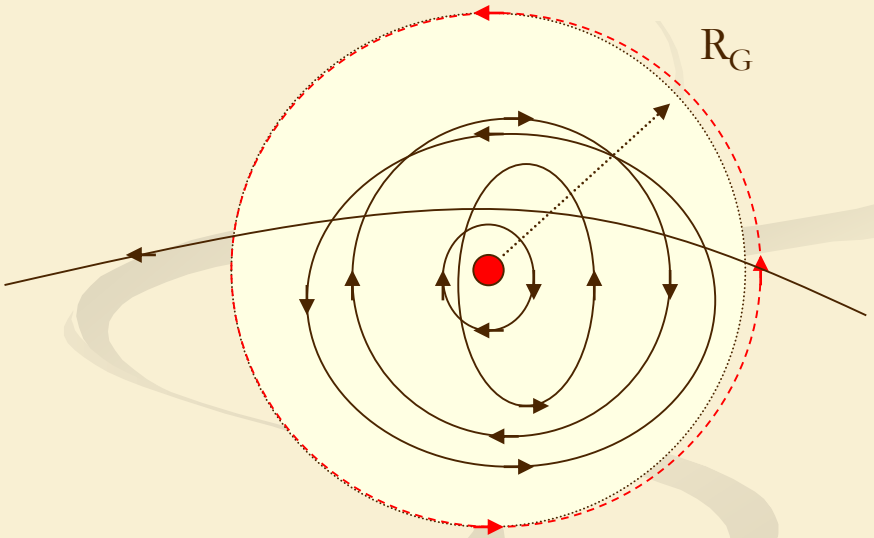

$$P_{eq} = 2.6 \times 10^3 \, v_{(t)10}^{-2/3} \, \mu_{30}^{2/3} \, n^{-2/3} \, v_{10}^{13/3} \ \mathrm{s}$$

A kind of equilibrium period for the case of accretion from turbulent medium

Disc formation

Accretion of turbulized matter can result in a transient accretion disc formation.

$$j_t = v_t(R_G) \cdot R_G = v_t(R_t) R_t^{-1/3} R_G^{4/3}$$

If j_t is larger than the keplerian momentum at the magnetospheric boundary (Alfven radius) then a disc can be formed.

$$j_K = v_K(R_A) \cdot R_A$$

Might happen for low magnetic fields
and low spatial velocities.
More prominent for accreting isolated BHs.

See, e.g., astro-ph/0108503

Expected properties-2

3. Temperatures

Depend on the magnetic field. The size of polar caps depends on the field and accretion rate: $\sim R\,(R/R_A)^{1/2}$

4. Magnetic fields

Very uncertain, as models of the field decay cannot give any solid predictions for very long time scales (billions of years).

5. Flux variability.

Due to fluctuations of matter density and turbulent velocity in the ISM it is expected that isolated accretors are variable on a time scale $\sim R_G/v \sim$ days - months

---

Still, isolated accretors are expected to be numerous at low fluxes (their total number in the Galaxy is large than the number of coolers of comparable luminosity). They should be hotter than coolers, and have much longer spin periods.

Properties of accretors

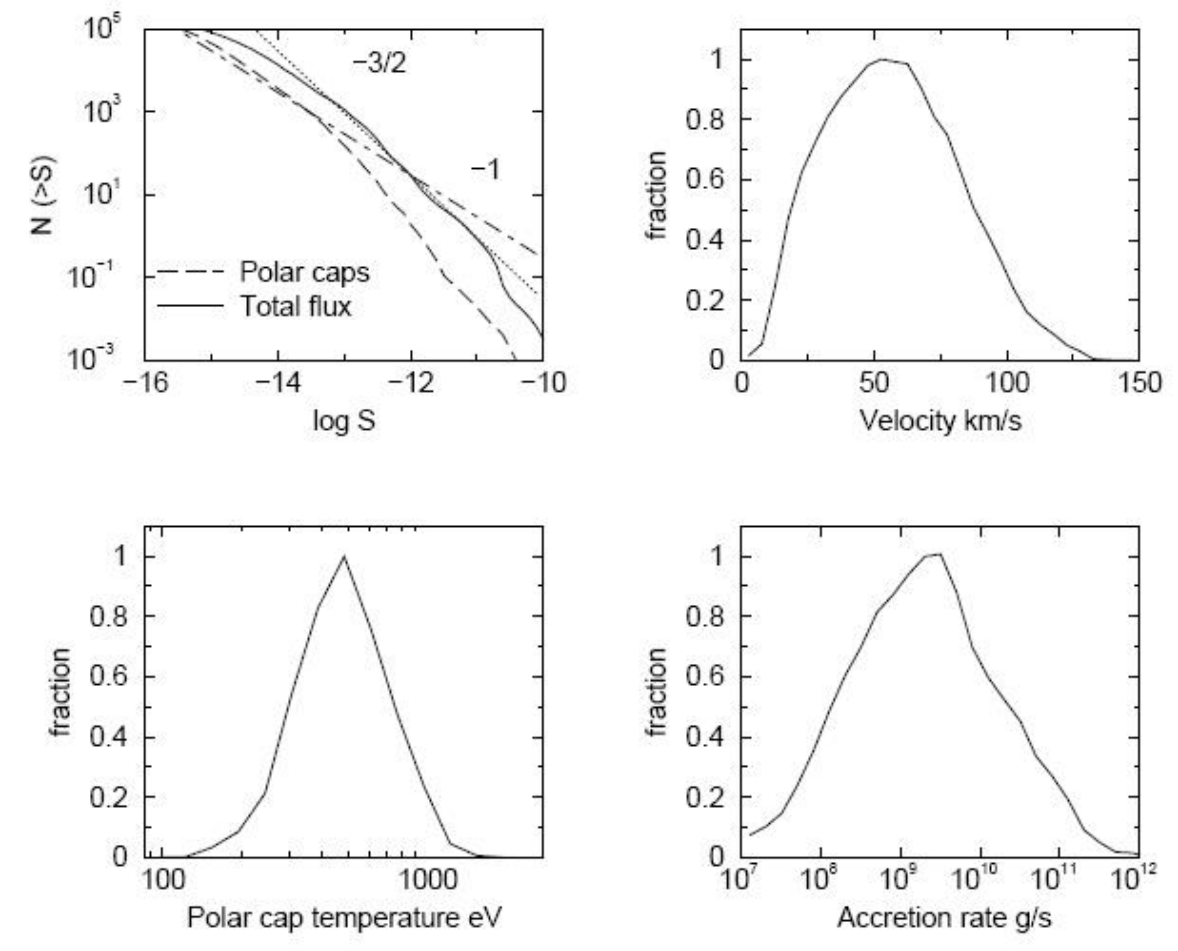

In the framework of a simplified model (no subsonic propeller, no field decay, no accretion inhibition, etc.) one can estimate properties of isolated accretors.

Slow, hot, dim, numerous at low fluxes ($<10^{-13}$ erg/cm^2/s)

Reality is more uncertain.

(astro-ph/0009225)

Accreting isolated NSs

At small fluxes $<10^{-13}$ erg/s/cm^2 accretors can become more abundant than coolers. Accretors are expected to be slightly harder: 300-500 eV vs. 50-100 eV. Good targets for eROSITA!

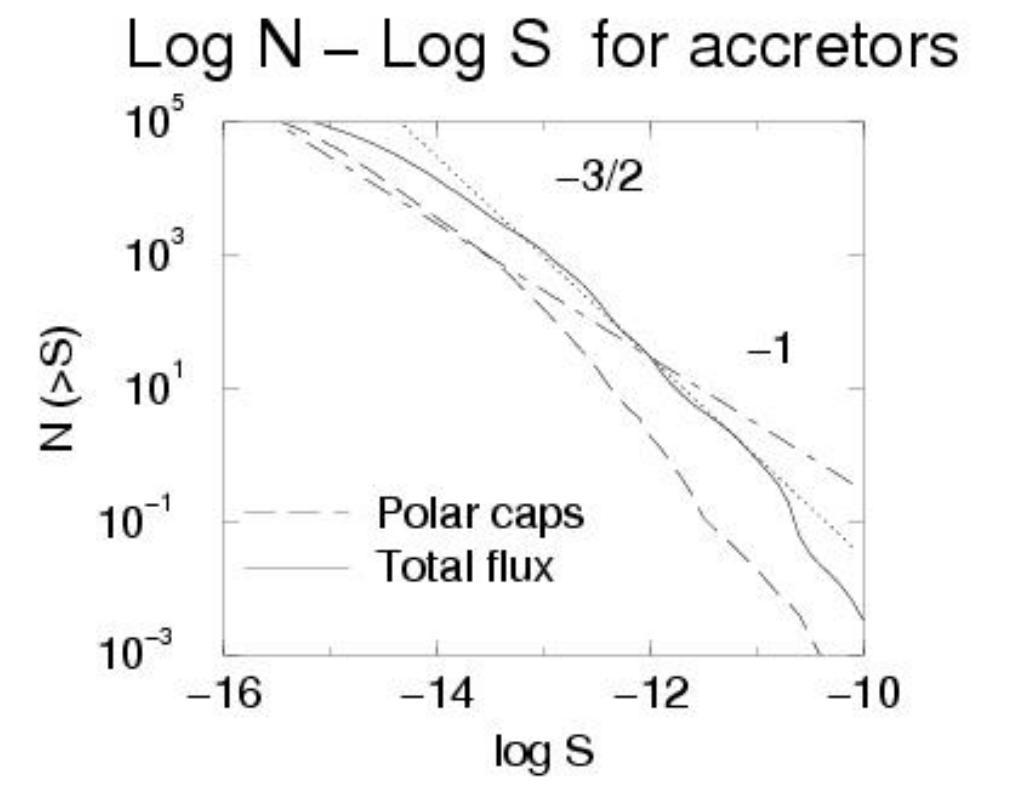

From several hundreds up to several thousands objects at fluxes about few $\cdot 10^{-14}$, but difficult to identify.

Monitoring is important.

Also isolated accretors can be found in the Galactic center (Zane et al. 1996, Deegan, Nayakshin 2006).

astro-ph/0009225

Where and how to look for

As sources are dim even in X-rays,
and probably are extremely dim in other bands
it is very difficult to find them.

In an optimistic scenario they outnumber cooling NSs at low fluxes.
Probably, for ROSAT they are to dim.
We hope that eROSITA will be able to identify accreting INSs.

Their spatial density at fluxes ~10^{-15} erg/cm^2/s is expected to be ~few per sq.degree in directions close to the galactic plane.

It is necessary to have an X-ray survey at ~100-500 eV with good resolution.

In a recent paper by Muno et al.the authors put interesting limits on the number of unidentified magnetars. The same results can be rescaled to give limits on the M7-like sources.

“Decayed” field distribution

We assume the field to be constant, but as an initial we use the “decayed” distribution, following Popov et al. 2010.

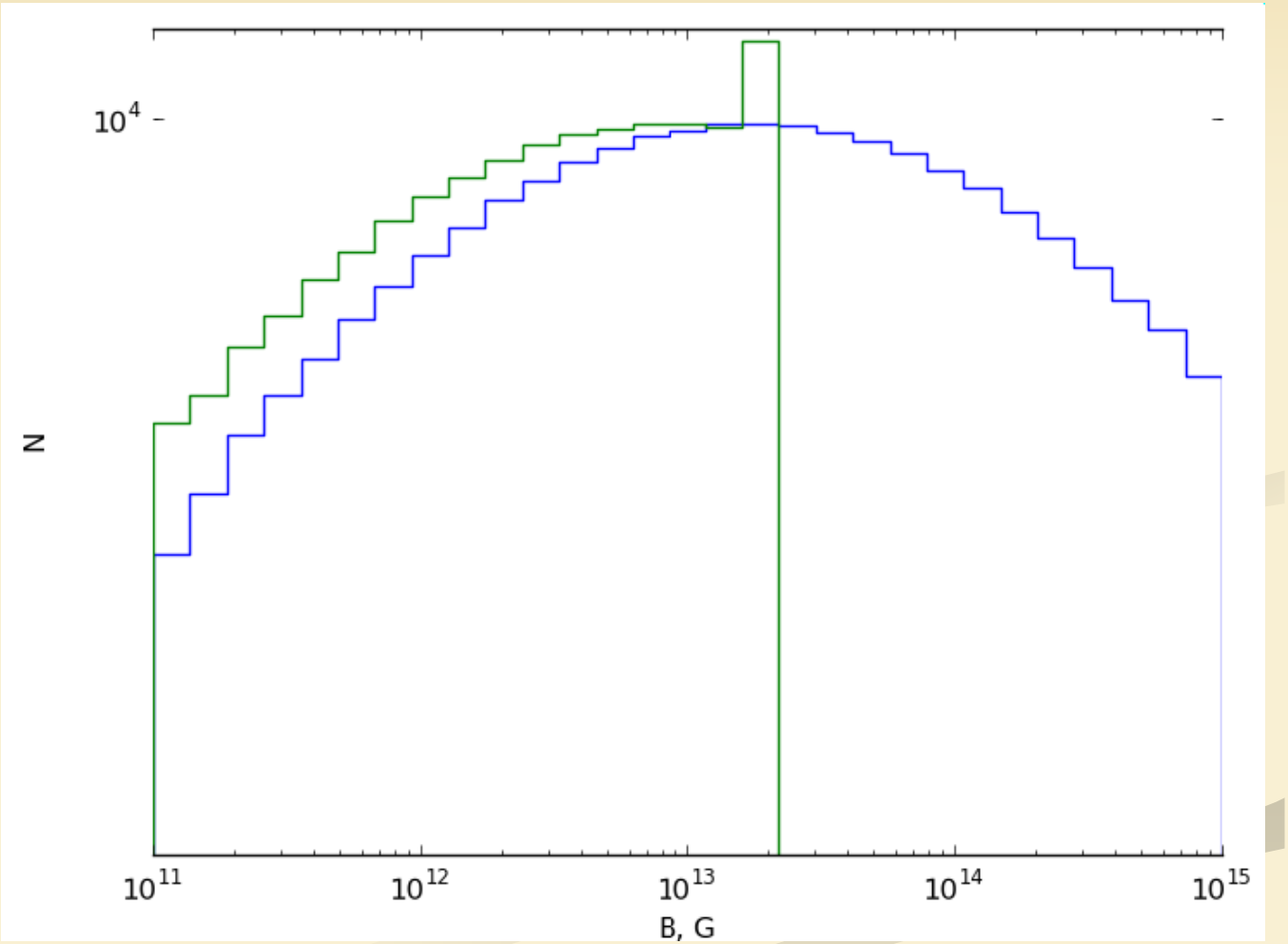

Boldin, Popov 2010

Simple semianalytical model

Fraction of accretors for different magnetic fields and ISM density.
Kick velocity distribution is taken following Arzoumanian et al. (2002).

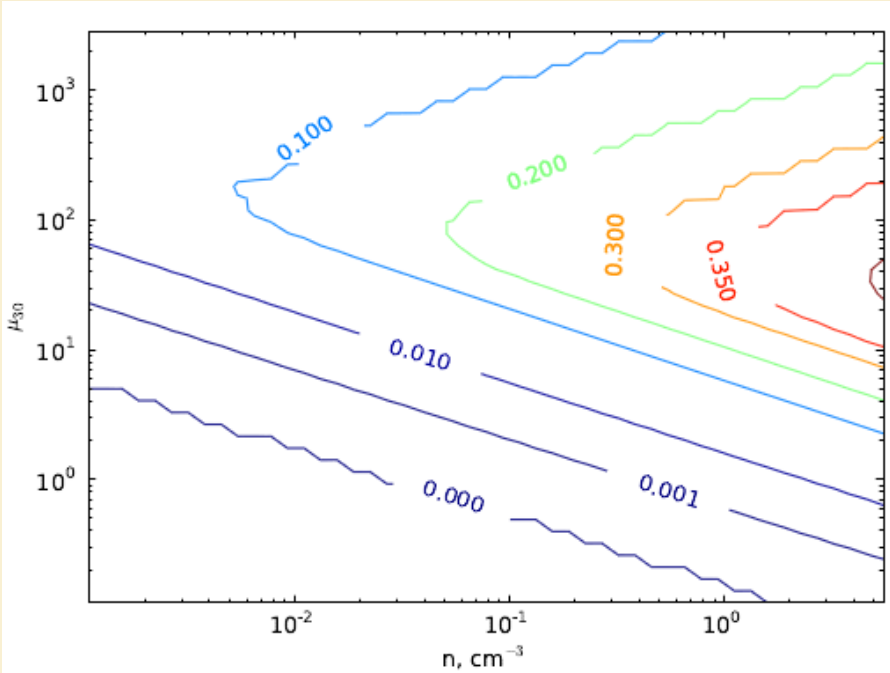

With subsonic

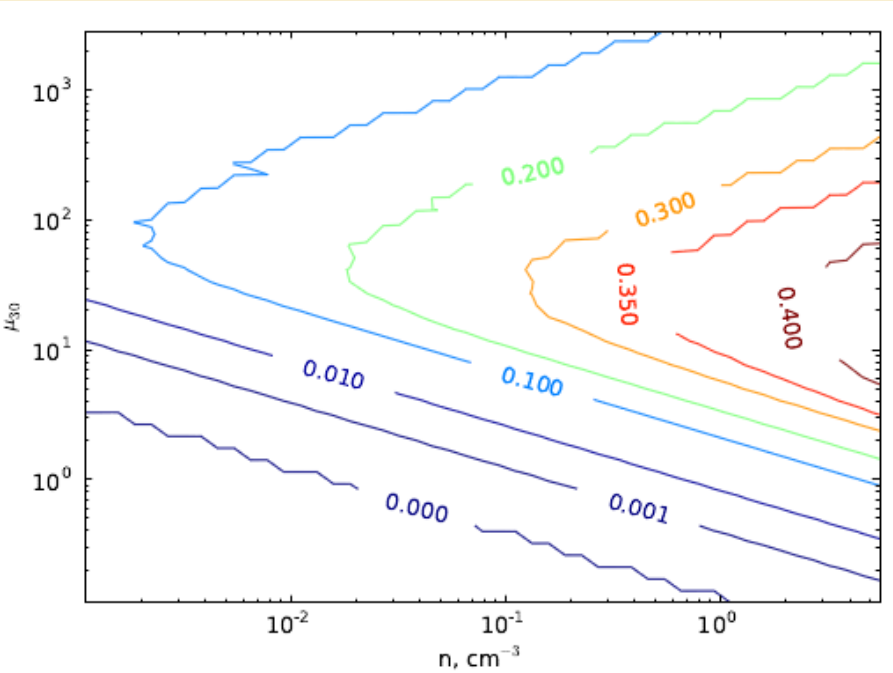

Without subsonic

Boldin, Popov 2010

Individual tracks

Individual tracks in the semianalytical model. Clearly, even with long subsonic propeller stage highly magnetized NSs (like the M7) can become accretors relatively soon.

Track	n, cm^{-3}	μ_{30}	v_{10}	$\tau_{\rm E}$	$P_{\rm E}$, s	$\tau_{\rm P}$	$P_{\rm P}$, s	$\tau_{\rm ssP}$	$P_{\rm break}$, s
Track I	0.5	1	5	0.419	16.051	0.423	3.163×10^3	0.850	2.278×10^6
Track II	0.5	1	20	–	–	–	–	–	–
Track III	0.5	1	40	–	–	–	–	–	–
Track IV	0.5	10	5	0.042	50.758	0.042	2.276×10^4	0.067	1.317×10^7
Track V	0.5	10	20	0.168	101.517	0.170	1.353×10^5	0.651	2.568×10^8
Track VI	0.5	10	40	0.163	100.091	0.169	1.523×10^5	Georotator	
Track VII	2.0	1	5	0.209	11.350	0.212	1.746×10^3	0.370	8.464×10^5
Track VIII	2.0	1	20	0.838	22.700	0.854	1.038×10^4	–	–
Track IX	2.0	1	40	–	–	–	–	–	–
Track X	2.0	10	5	0.021	35.892	0.021	1.257×10^4	0.030	4.892×10^6
Track XI	2.0	10	20	0.084	71.783	0.085	7.469×10^4	0.264	9.541×10^7
Track XII	2.0	10	40	0.103	79.442	0.106	1.077×10^5	Georotator	

Boldin, Popov 2010

Final distributions

Filled symbols – "decayed distribution".
Open squares – delta-function $\mu_{30}=1$.

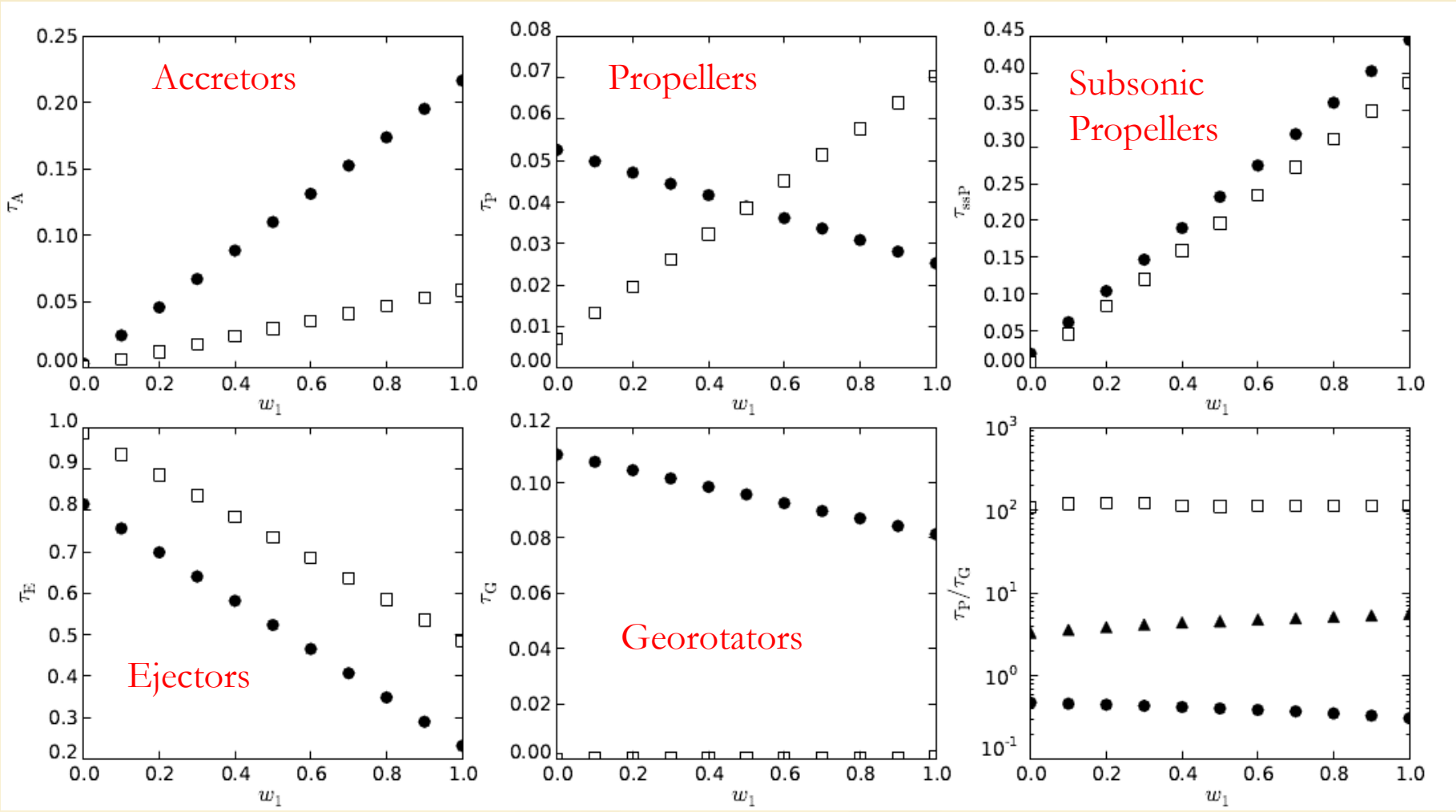

Boldin, Popov 2010

Spatial density of NSs

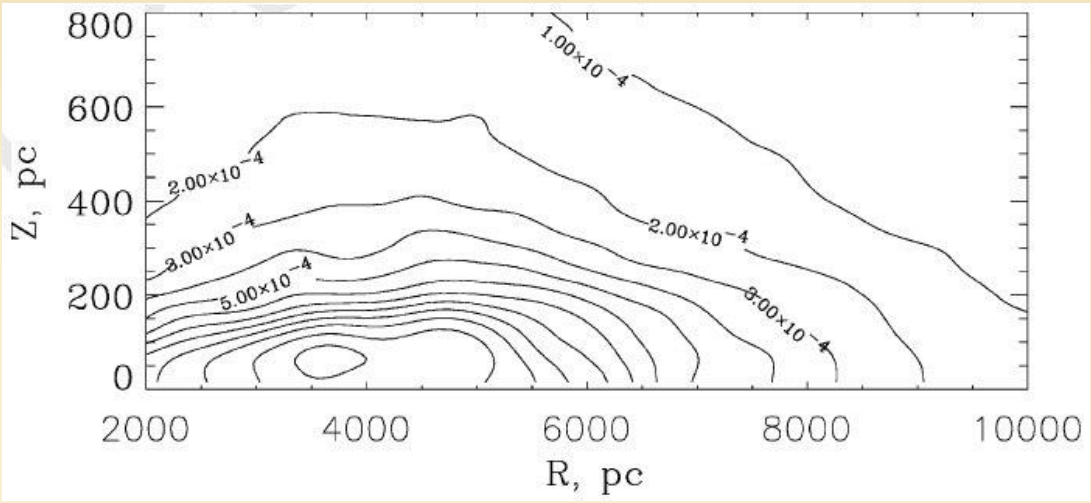

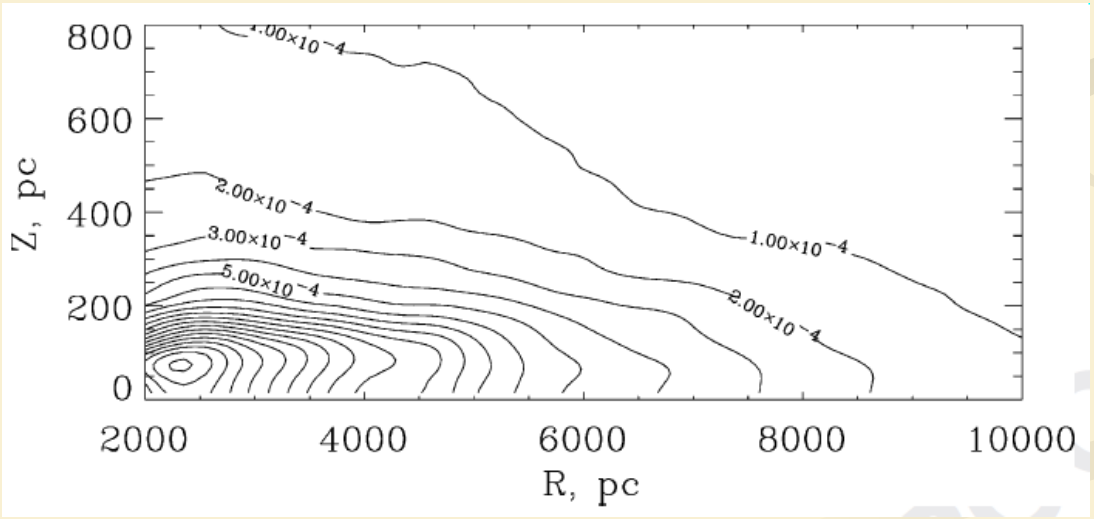

astro-ph/0305599

In both models N=5 10^8.
Kick: ACC02.
Potential: Paczynski 1990

NS formation rate is assumed to be proportional to the square of the ISM density at the birthplace.

Formation rate is proportional to $[\exp(-z/75\text{ pc})\exp(-R/4\text{ kpc})]$.

Who forms accretors?

NSs with stronger fields form more accretors, unless their field *and* velocities are so high, that they become Georotators.

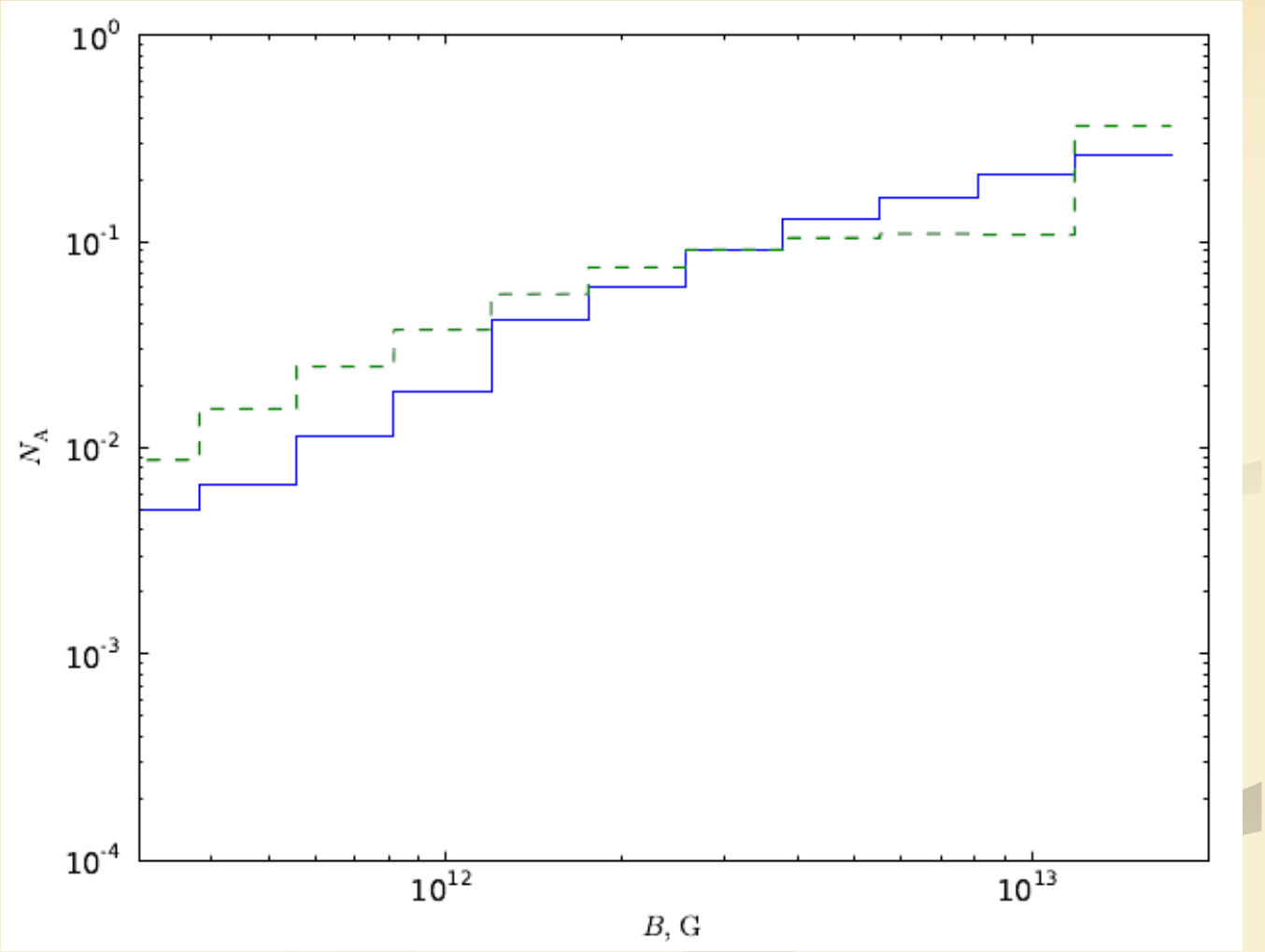

Boldin, Popov 2010

Running out of the Galaxy

2/3 of NSs leave the Galaxy.
Mostly, they stay as Ejectors, or become Georotators.

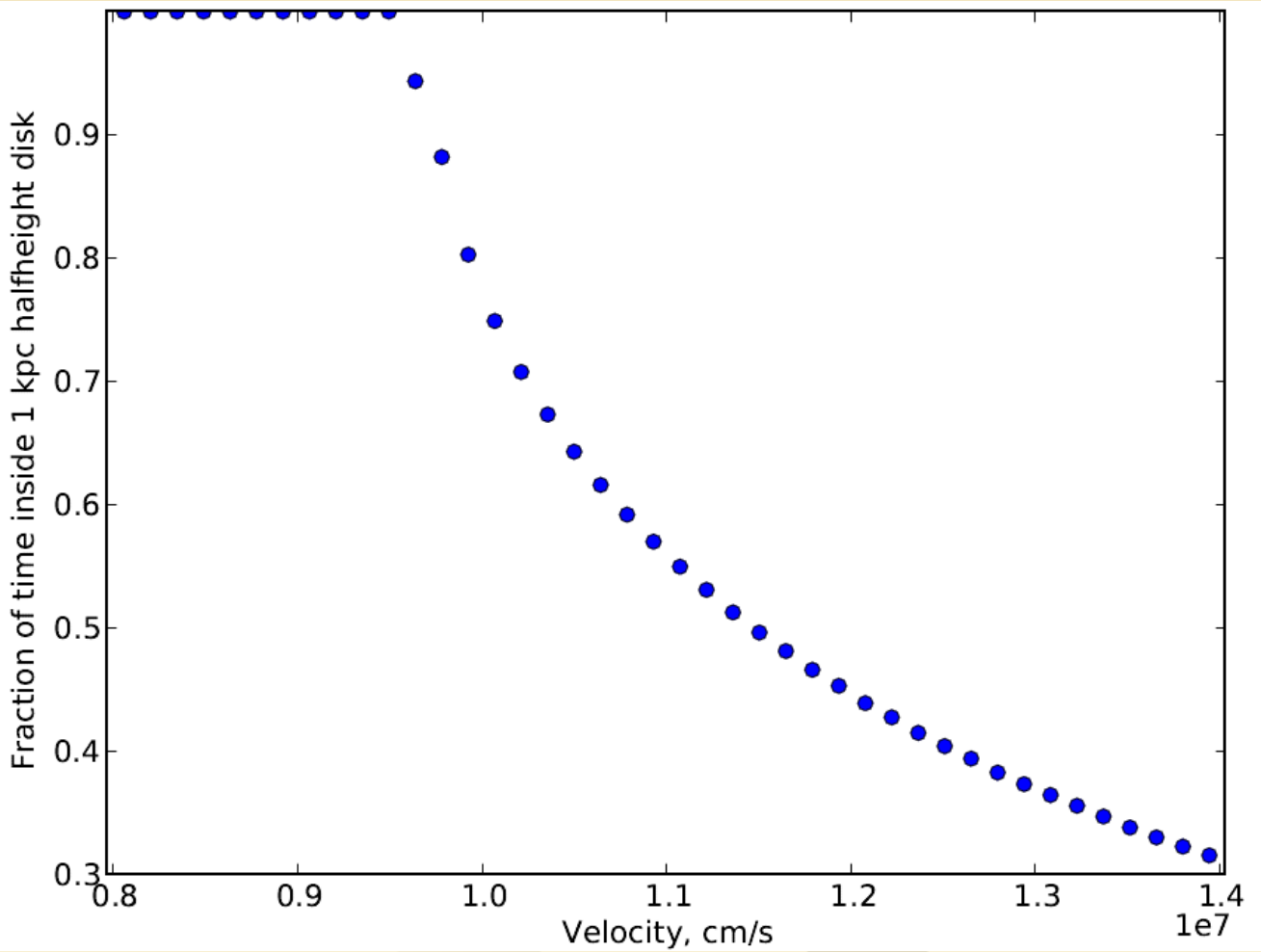

In the solar vicinity fractions of INSs at different evolutionary stages are:

- Ejectors: 18-20%
- Propellers: negligible
- subsonic P.: 40-45%
- Accretors: 35-40%
- Georotators: negligible

Boldin, Popov 2010

Some conclusions

•Highly magnetized INS (as the M7) can become Accretors even taking into account long subsonic Propeller stage.

• In the solar vicinity fractions of INSs at different evolutionary stages are:

- Ejectors: 18-20%
- Propellers: negligible
- subsonic P.: 40-45%
- Accretors: 35-40%
- Georotators: negligible

Boldin, Popov 2010

Settling accretion onto INSs

At low X-ray luminosities the captured matter, heated in the bow-shock, has no time to cool down and remains hot, which prevents it from entering the NS magnetosphere via Rayleigh-Taylor (RT) instability.

$$\dot{M}_{\rm x} \simeq (t_{\rm ff}/t_{\rm cool})^{1/3}\dot{M}_{\rm B}$$

$$\dot{M}_{\rm B} = \rho_\infty v(\pi R_{\rm G}^2) \sim 1.9\times10^9\, n\, v_7^{-3}\,{\rm g\,s^{-1}}$$

$$t_{\rm ff} = R^{3/2}/\sqrt{GM}.$$

$$t_{\rm cool} = 3\times10^8\left(\frac{R_{\rm A}}{10^{10}{\rm cm}}\right)\times \left(\frac{L_{\rm x}}{10^{30}{\rm erg\,s^{-1}}}\right)^{-1}\frac{f(u)}{0.01}(1+X)^{-1}\,{\rm s}.$$

$$f(u) = u_{\rm r}/u_{\rm ff} < 1$$

$$R_{\rm A} \approx 2.2\times10^{10} L_{30}^{-2/9}\mu_{30}^{16/27}\,{\rm cm}.$$

Thus, steady accretion luminosity is expected to be low, however, flares with duration hours-day are possible. Maximum luminosity can be ~10^{31} erg/s.

1412.4066

Papers to read

- Treves et al. PASP 112, 297 (2000)
- Popov et al. ApJ 530, 896 (2000)
- Popov, Prokhorov Physics Uspekhi 50, 1123 (2007) Ch. 5.4
- Boldin, Popov MNRAS vol. 407, pp. 1090-1097 (2010)
- Edgar astro-ph/0406166
- Popov et al. MNRAS 487, 2817 (2015)

Thermal evolution of neutron stars

Evolution of neutron stars. I.: rotation + magnetic field

Ejector → Propeller → Accretor → Georotator

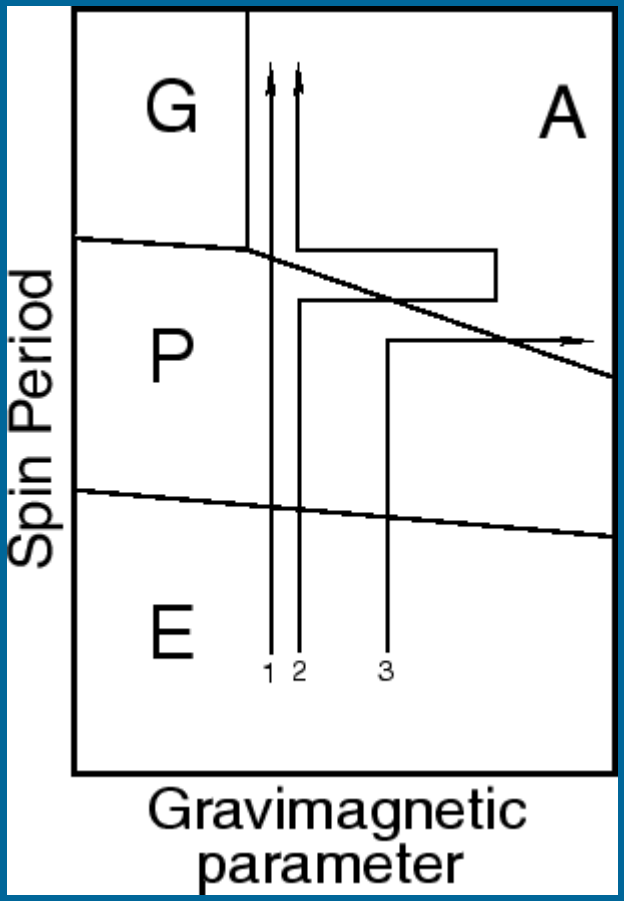

1 – spin down
2 – passage through a molecular cloud
3 – magnetic field decay

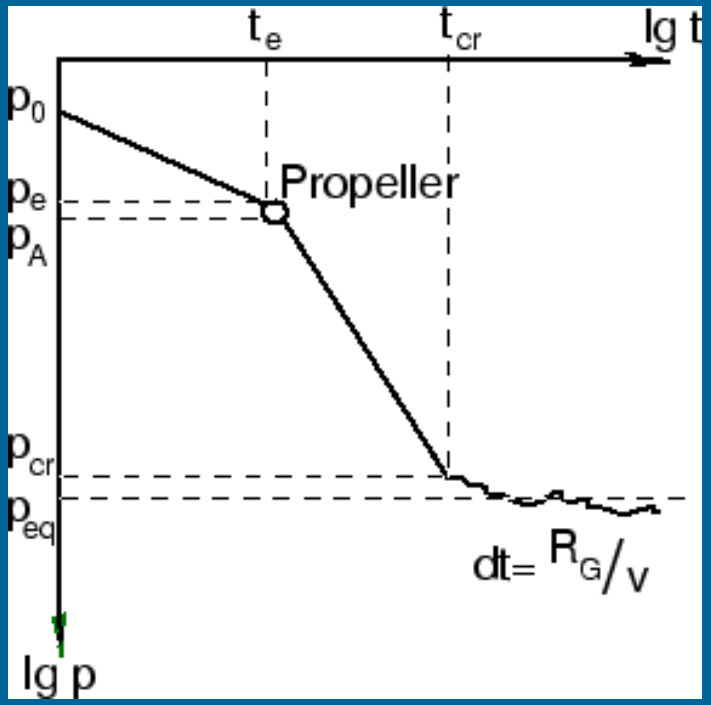

astro-ph/0101031

See the book by Lipunov (1987, 1992)

Magnetorotational evolution of radio pulsars

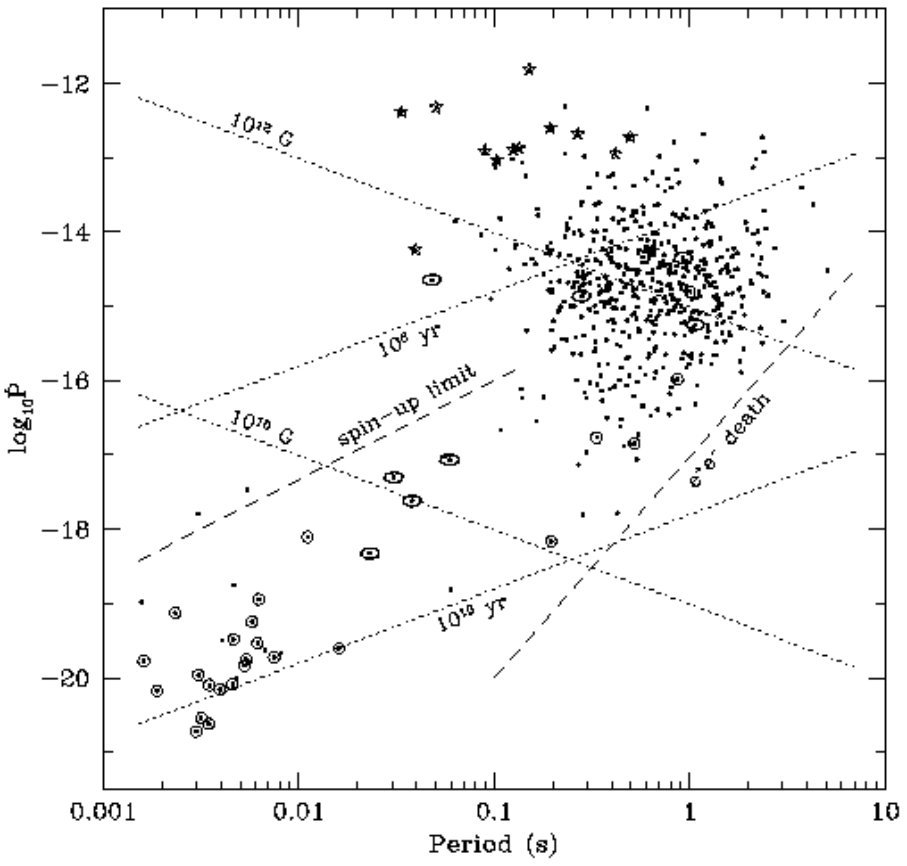

$$L_m = \frac{2}{3}\frac{\mu^2\omega^4}{c^3}\sin^2\beta = \kappa_t\frac{\mu^2}{R_l^3}\omega\,,$$

$$B \sim 3.2\times10^{19}\,(PdP/dt)^{1/2}\ \mathrm{G}.$$

Spin-down.
Rotational energy is released.
The exact mechanism is still unknown.

Evolution of NSs. II.: temperature

Neutrino cooling stage

Photon cooling stage

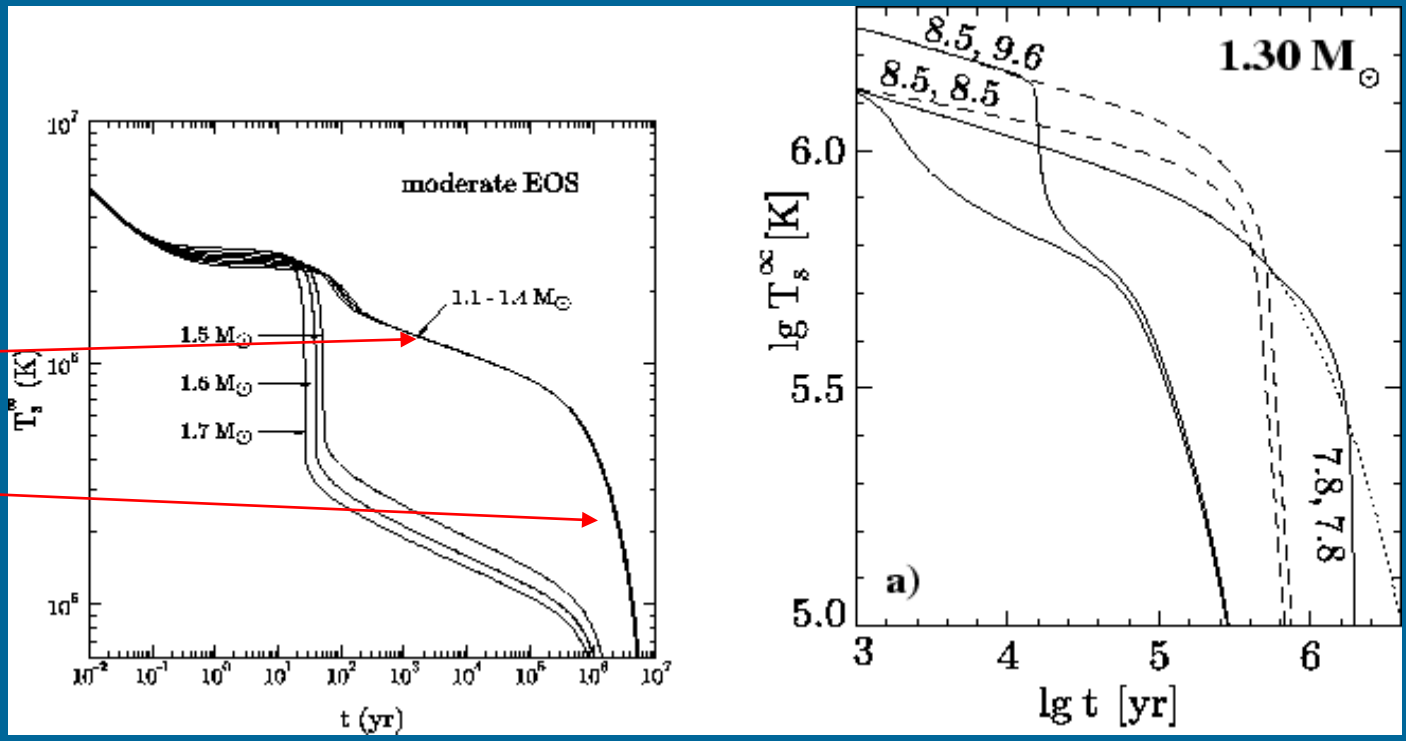

First papers on the thermal evolution appeared already in early 60s, i.e. before the discovery of radio pulsars.

[Yakovlev et al. (1999) Physics Uspekhi]

Early evolution of a NS

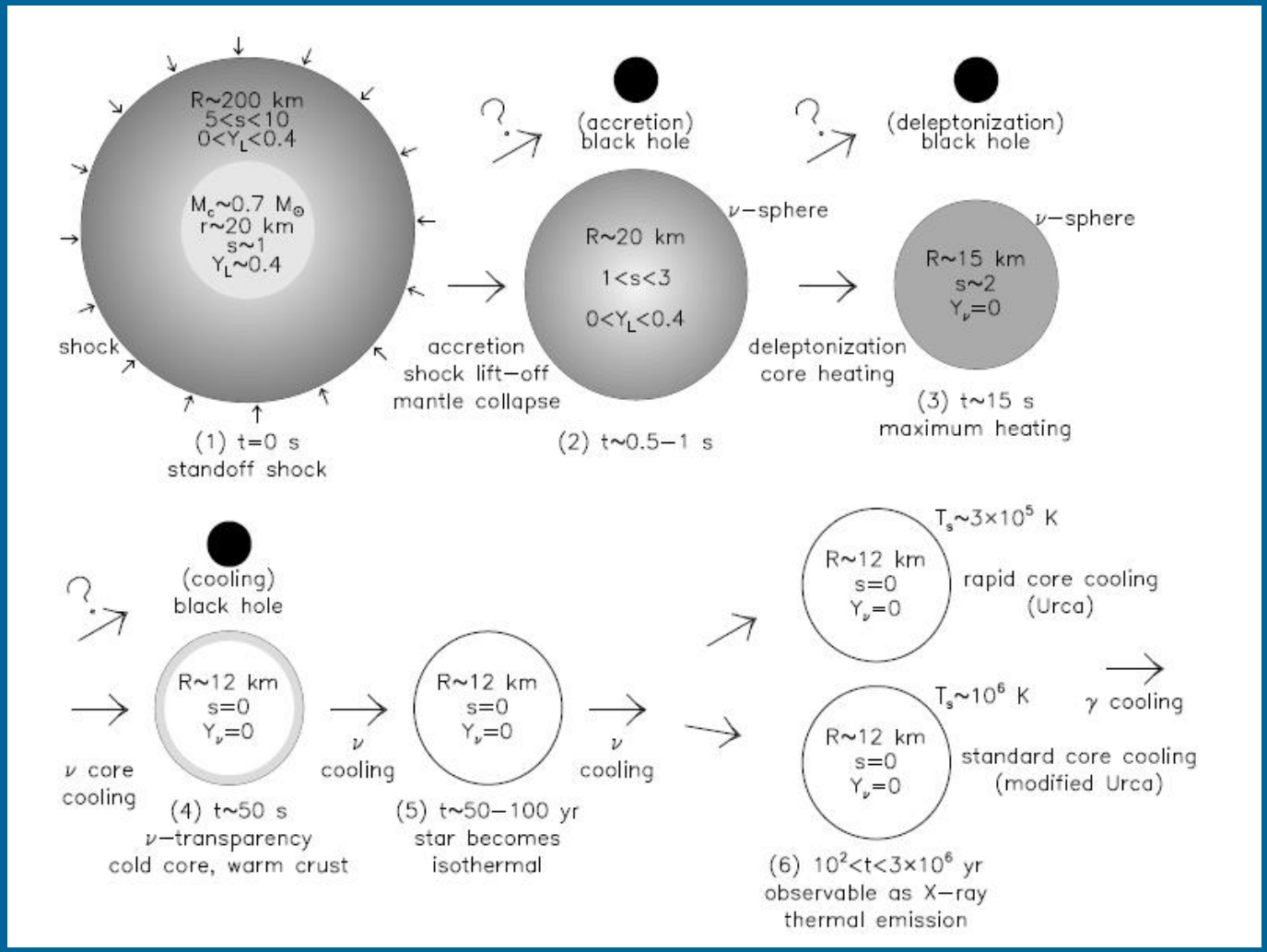

(Prakash et al. astro-ph/0112136)

Structure and layers

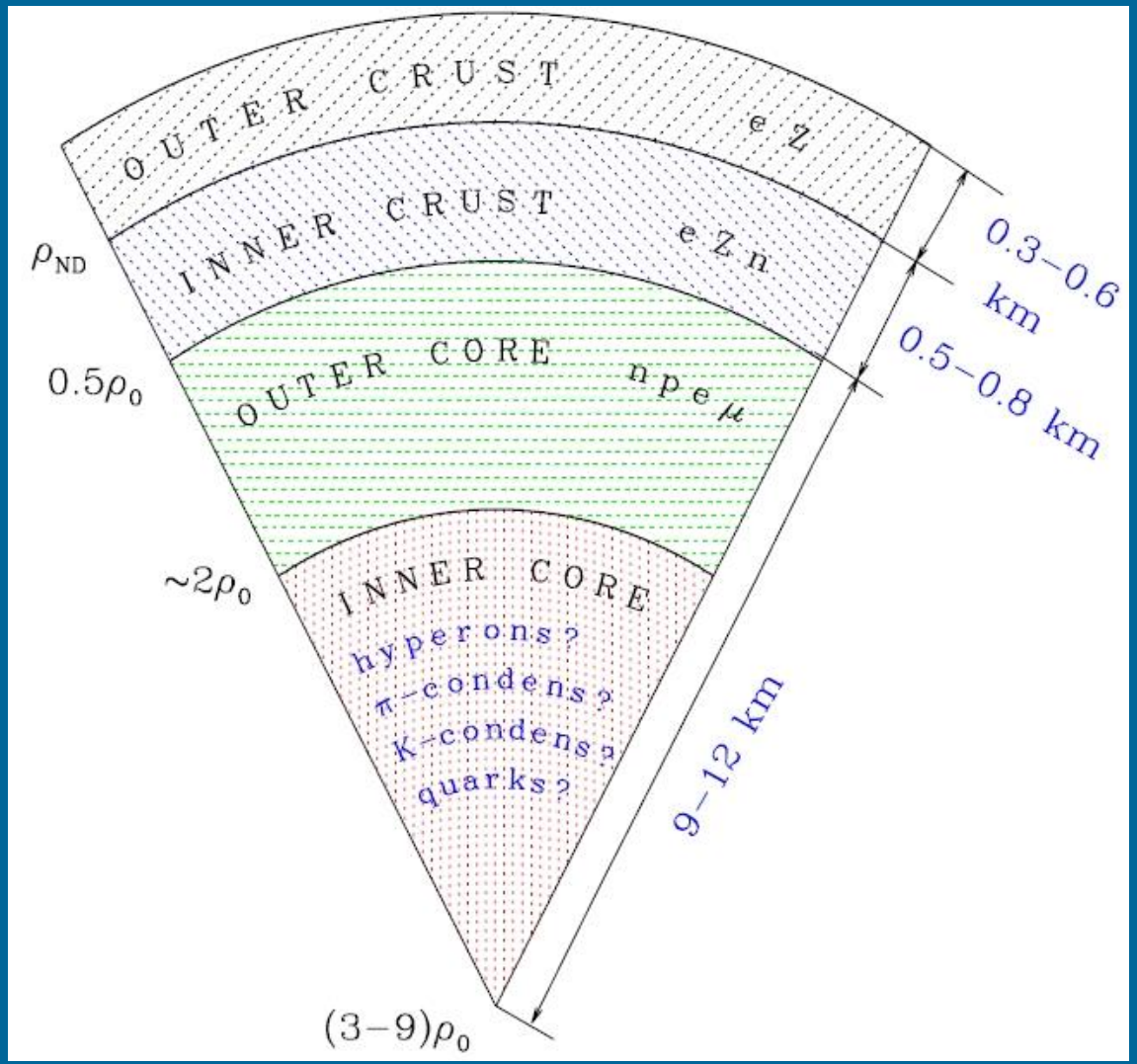

Plus an atmosphere...

See Ch.6 in the book by Haensel, Potekhin, Yakovlev

$\rho_0 \sim 2.8\ 10^{14}$ g cm^{-3}

The total thermal energy of a nonsuperfluid neutron star is estimated as $U_T \sim 10^{48}\ T^2_9$ erg.

The heat capacity of an *npe* neutron star core with strongly superfluid neutrons and protons is determined by the electrons, which are not superfluid, and it is ~20 times lower than for a neutron star with a nonsuperfluid core.

NS Cooling

- NSs are born very hot, T > 10^{10} K
- At early stages neutrino cooling dominates (exotic is possible – axions 1205.6940)
- The core is isothermal

$$\frac{dE_{th}}{dt} = C_V \frac{dT}{dt} = -L_\nu - L_\gamma$$

Photon luminosity

Neutrino luminosity

$$L_\gamma = 4\pi R^2 \sigma T_s^4, \quad T_s \propto T^{1/2+\alpha} \quad (|\alpha| << 1)$$

Core-crust temperature relation

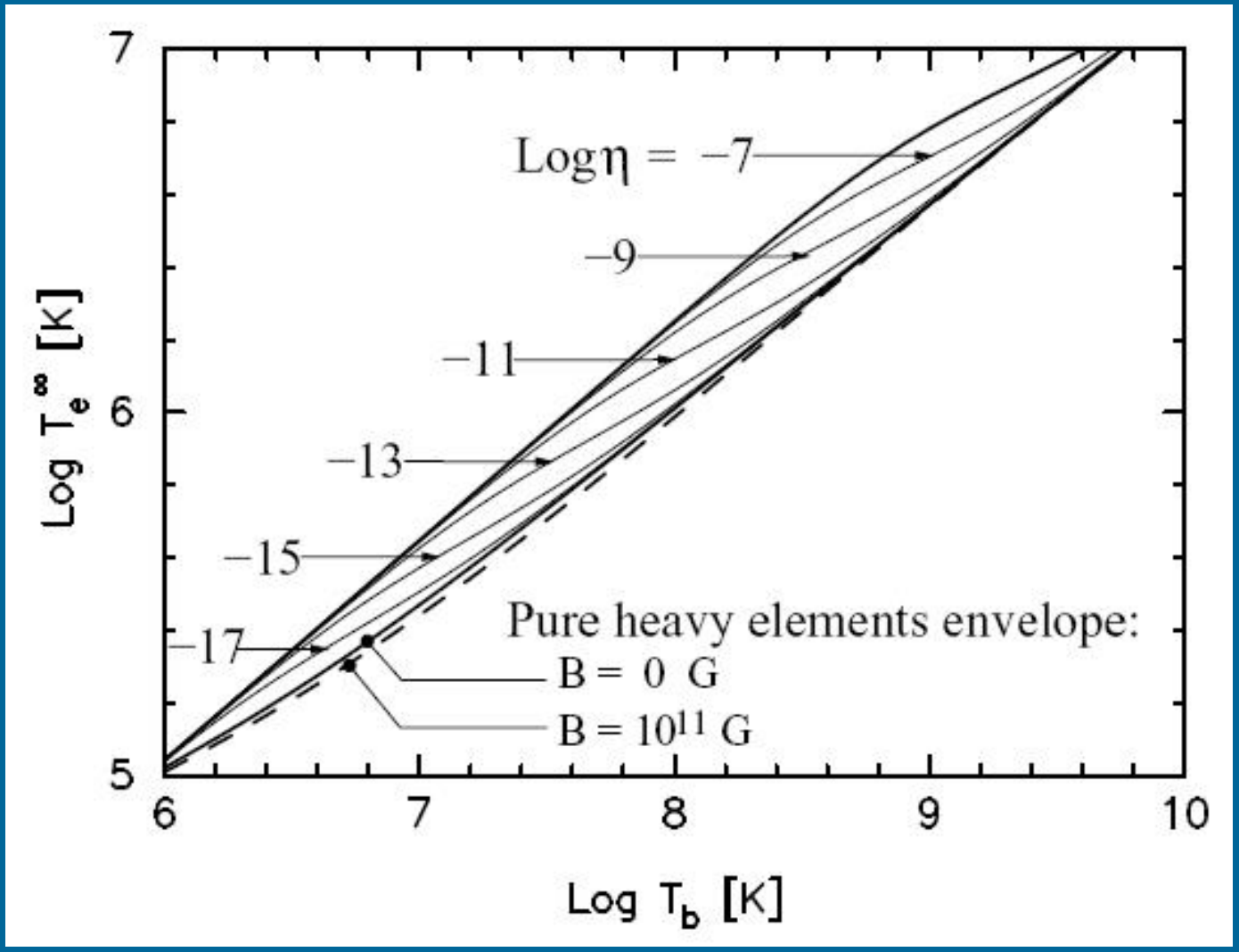

Heat blanketing envelope.
~100 meters
density ~10^{10} gcm^{-3}

See a review about crust properties related to thermal evolution in 1201.5602 and 1507.06186

Page et al. astro-ph/0508056

Cooling depends on:

1. Rate of neutrino emission from NS interiors
2. Heat capacity of internal parts of a star

} Depend on the EoS and composition

3. Superfluidity
4. Thermal conductivity in the outer layers
5. Possible heating

(see Yakovlev & Pethick 2004)

Main neutrino processes

Model	Process	$Q_{\rm f}$, erg cm^{-3} s^{-1}
Nucleon matter	$n \to pe\bar{\nu}$ $pe \to n\nu$	$10^{26} - 3 \times 10^{27}$
Pion condensate	$\tilde{N} \to \tilde{N}e\bar{\nu}$ $\tilde{N}e \to \tilde{N}\nu$	$10^{23} - 10^{26}$
Kaon condensate	$\tilde{B} \to \tilde{B}e\bar{\nu}$ $\tilde{B}e \to \tilde{B}\nu$	$10^{23} - 10^{24}$
Quark matter	$d \to ue\bar{\nu}$ $ue \to d\nu$	$10^{23} - 10^{24}$

Process		$Q_{\rm s}$, erg cm^{-3} s^{-1}
Modified Urca	$nN \to pNe\bar{\nu}$ $pNe \to nN\nu$	$10^{20} - 3 \times 10^{21}$
Bremsstrahlung	$NN \to NN\nu\bar{\nu}$	$10^{19} - 10^{20}$

$$Q_{\rm slow} = Q_{\rm s} T_9^8, \qquad Q_{\rm fast} = Q_{\rm f} T_9^6$$

(Yakovlev & Pethick astro-ph/0402143)

Fast Cooling (URCA cycle)

$$n \rightarrow p + e^- + \bar{\nu}_e$$

$$p + e^- \rightarrow n + \nu_e$$

Slow Cooling (modified URCA cycle)

$$n + n \rightarrow n + p + e^- + \bar{\nu}_e$$

$$n + p + e^- \rightarrow n + n + \nu_e$$

$$p + n \rightarrow p + p + e^- + \bar{\nu}_e$$

$$p + p + e^- \rightarrow p + n + \nu_e$$

- Fast cooling possible only if $n_p > n_n/8$
- Nucleon Cooper pairing is important
- Minimal cooling scenario (Page et al 2004):
  - no exotica
  - no fast processes
  - pairing included

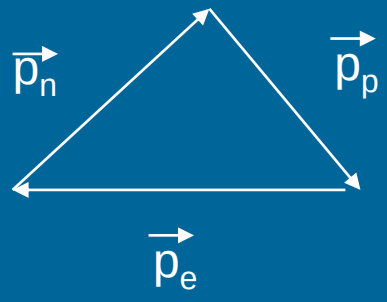

$p_n < p_p + p_e$

[See the book Haensel, Potekhin, Yakovlev p. 265 (p.286 in the file) and Shapiro, Teukolsky for details: Ch. 2.3, 2.5, 11.]

Equations

Neutrino emissivity

heating

$$\frac{\mathrm{e}^{-\lambda-2\Phi}}{4\pi r^2}\frac{\partial}{\partial r}\left(\mathrm{e}^{2\Phi}L_r\right) = -Q + Q_\mathrm{h} - \frac{c_T}{\mathrm{e}^{\Phi}}\frac{\partial T}{\partial t},$$

$$\frac{L_r}{4\pi\kappa r^2} = \mathrm{e}^{-\lambda-\Phi}\frac{\partial}{\partial r}\left(T\mathrm{e}^{\Phi}\right),$$

After thermal relaxation we have in the whole star: $T_i(t)=T(r,t)e^{\Phi(r)}$

$$\mathrm{e}^{-\lambda} = \sqrt{1-2Gm(r)/c^2r},$$

At the surface we have: $\Phi(R) = -\lambda(R)$

$$C(T_i)\frac{\mathrm{d}T_i}{\mathrm{d}t} = -L_\nu^\infty(T_i) + L_\mathrm{h}^\infty - L_\gamma^\infty(T_\mathrm{s}),$$

$$L_\nu^\infty(T_i) = \int \mathrm{d}V\, Q(T)\,\mathrm{e}^{2\Phi}, \text{ and } L_\mathrm{h}^\infty = \int \mathrm{d}V\, Q_\mathrm{h}\,\mathrm{e}^{2\Phi}, \quad C(T_i) = \int \mathrm{d}V\, c_T(T),$$

$\mathrm{d}V = 4\pi r^2 \mathrm{e}^{\lambda}\,\mathrm{d}r$ is the element of proper volume

L_ν^∞ is the total neutrino luminosity (for a distant observer)

L_h^∞ is the total reheating power.

(Yakovlev & Pethick 2004)

Total stellar heat capacity

Simplified model of a cooling NS

No superfluidity, no envelopes and magnetic fields, only hadrons.

The most critical moment is the onset of direct URCA cooling.

ρ_D= 7.851 10^{14} g/cm^3.

The critical mass depends on the EoS. For the examples below M_D=1.358 M_{solar}.

M ($M_\odot$)	R (km)	ρ_c (10^{14} g cm^{-3})	$M_{\rm crust}$ ($M_\odot$)	$\Delta R_{\rm crust}$ (km)	$\Delta M_{\rm D}$ ($M_\odot$)	$R_{\rm D}$ (km)
1.1	13.20	6.23	0.069	1.98	...	...
1.2	13.13	6.80	0.063	1.77	...	...
1.3	13.04	7.44	0.057	1.58	...	...
1.358[a]	12.98	7.85	0.054	1.48	0.000	0.00
1.4	12.93	8.17	0.052	1.40	0.023	2.40
1.5	12.81	9.00	0.049	1.26	0.137	4.27
1.6	12.64	10.05	0.042	1.10	0.306	5.51
1.7	12.43	11.39	0.035	0.96	0.510	6.41
1.8	12.16	13.22	0.030	0.84	0.742	7.10
1.9	11.73	16.33	0.023	0.69	1.024	7.65
1.977[b]	10.75	25.78	0.011	0.45	1.400	7.90

[a] Threshold configuration for the direct Urca process

[b] Maximum-mass stable neutron star

Simple cooling model for low-mass NSs.

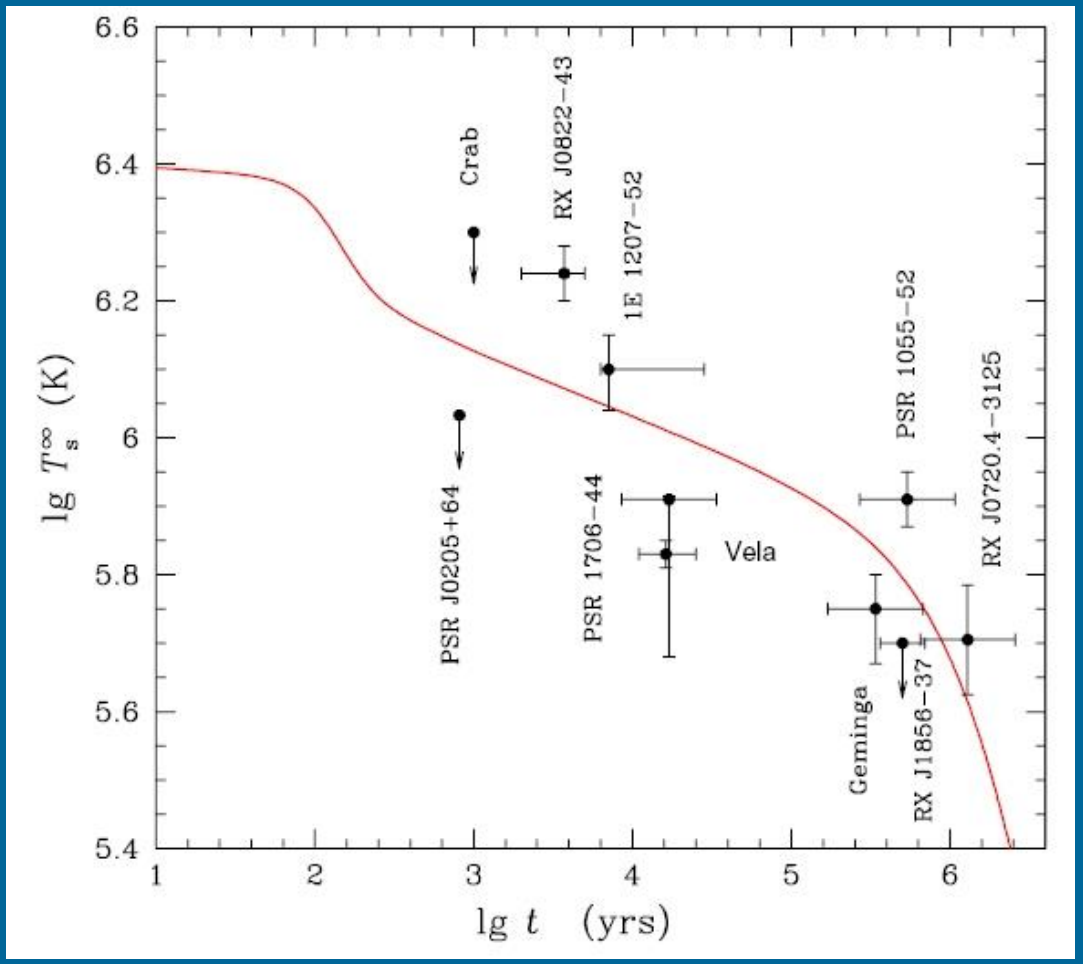

Too hot .....
Too cold ....

(Yakovlev & Pethick 2004)

Nonsuperfluid nucleon cores

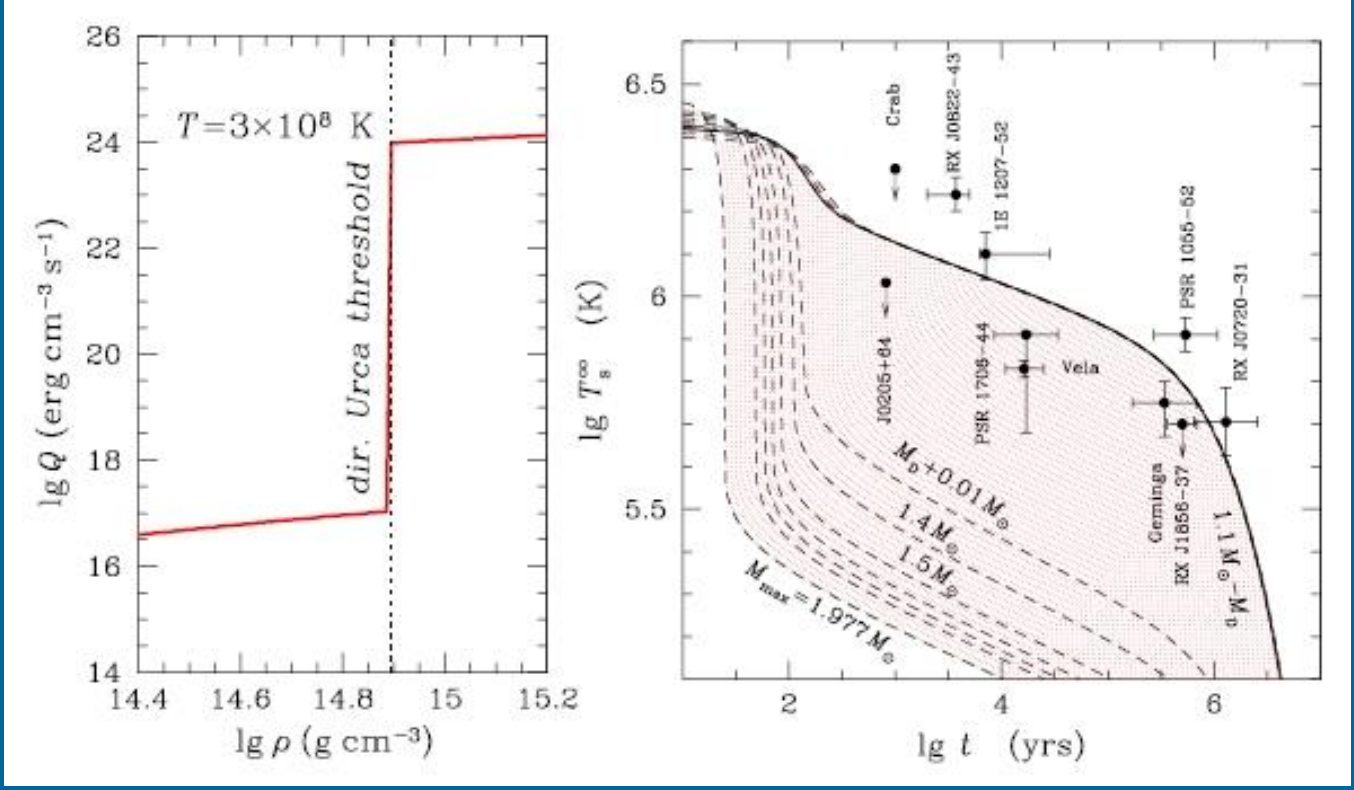

Note “population aspects” of the right plot: too many NSs have to be explained by a very narrow range of mass.

For slow cooling at the neutrino cooling stage t_{slow}~1 yr/T_{i9}^{6}
For fast cooling t_{fast}~ 1 min/T_{i9}^{4}

(Yakovlev & Pethick 2004)

Slow cooling for different EoS

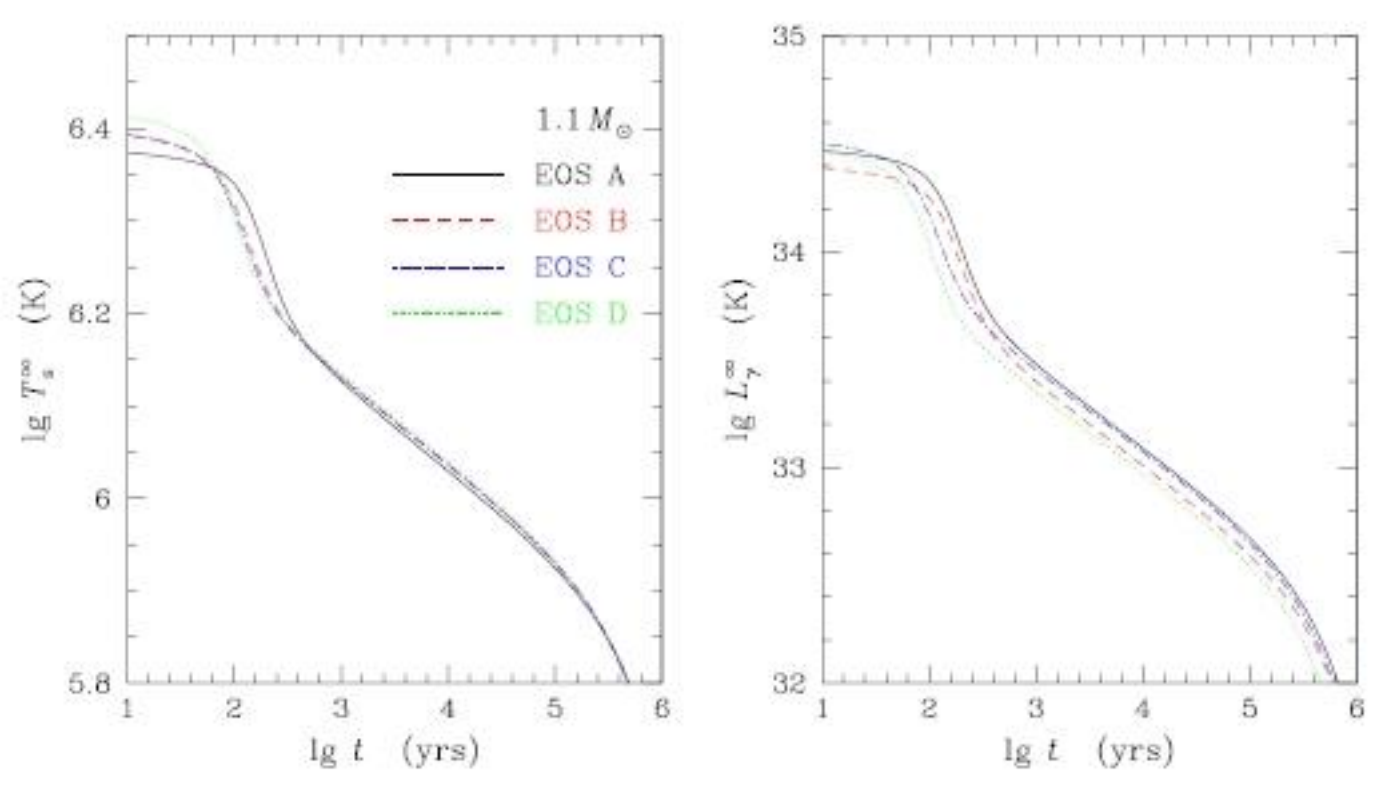

For slow cooling there is nearly no dependence on the EoS.
The same is true for cooling curves for maximum mass for each EoS.

(Yakovlev & Pethick 2004)

Envelopes and magnetic field

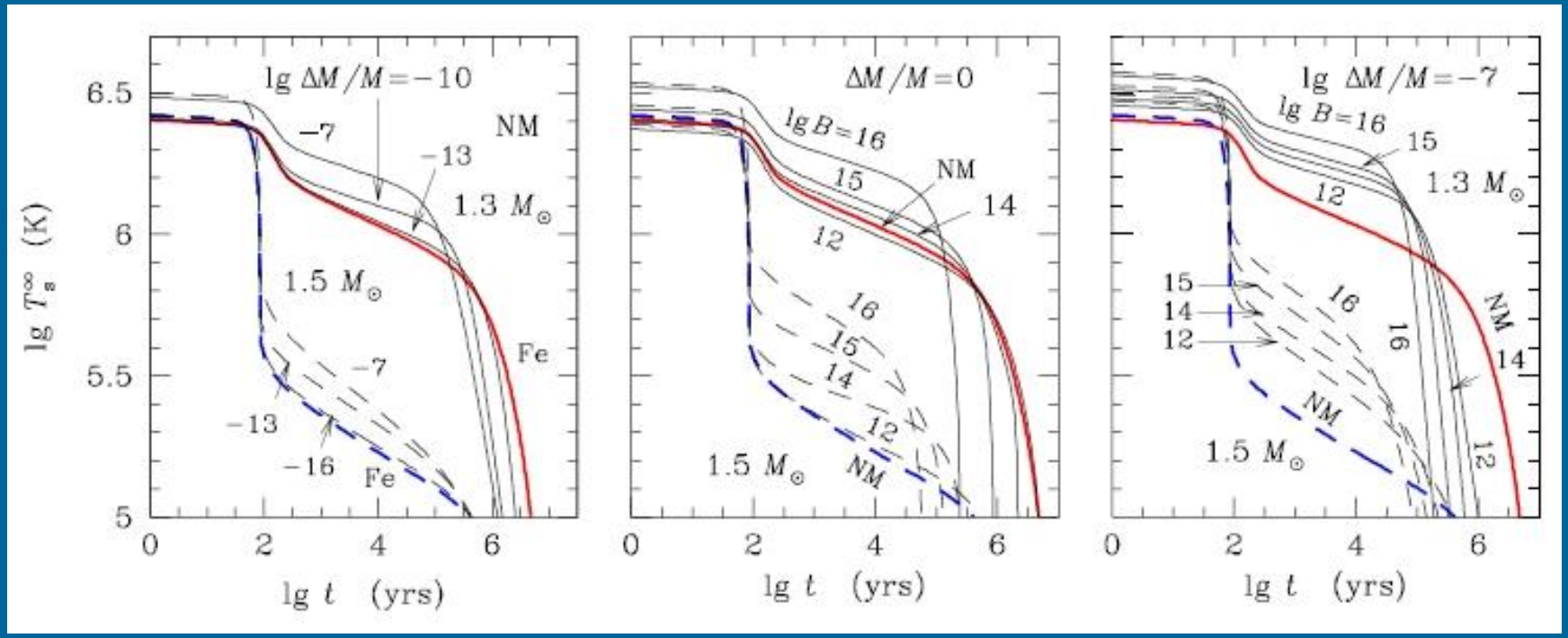

Non-magnetic stars
Thick lines – no envelope

No accreted envelopes, different magnetic fields.
Thick lines – non-magnetic

Envelopes + Fields

Envelopes can be related to the fact that we see a subpopulation of hot NS in CCOs with relatively long initial spin periods and low magnetic field, but do not observed representatives of this population around us, i.e. in the Solar vicinity.

Solid line M=1.3 M_{solar}, Dashed lines M=1.5 M_{solar}

(Yakovlev & Pethick 2004)

Simplified model: no neutron superfluidity

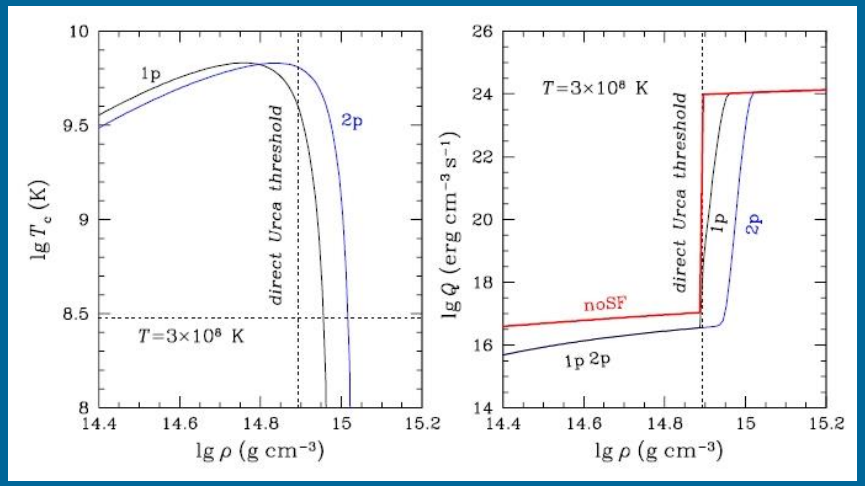

Superfluidity is an important ingredient of cooling models.
It is important to consider different types of proton and neutron superfluidity.

There is no complete microphysical theory which can describe superfluidity in neutron stars.

If proton superfluidity is strong,
but neutron superfluidity
in the core is weak
then it is possible
to explain observations.

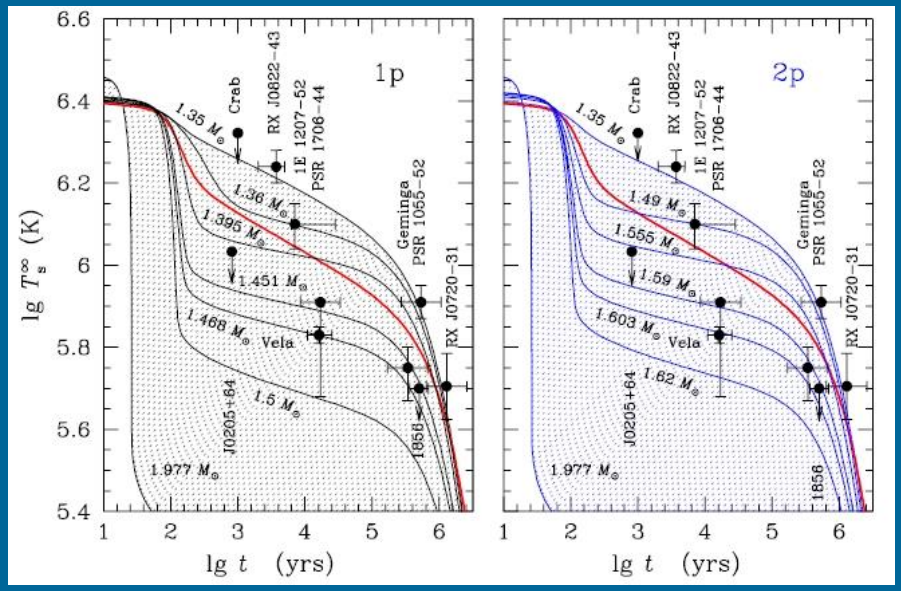

(Yakovlev & Pethick 2004)

Neutron superfluidity and observations

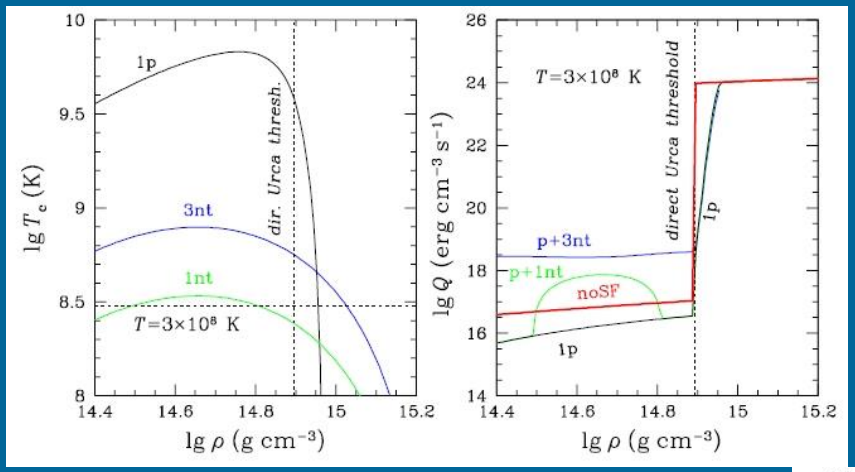

Mild neutron pairing in the core contradicts observations.

See a recent review about superfluidity and its relation to the thermal evolution of NSs in 1206.5011 and a very detailed review about superfluids in NSs in 1302.6626. A brief and more popular review in 1303.3282.

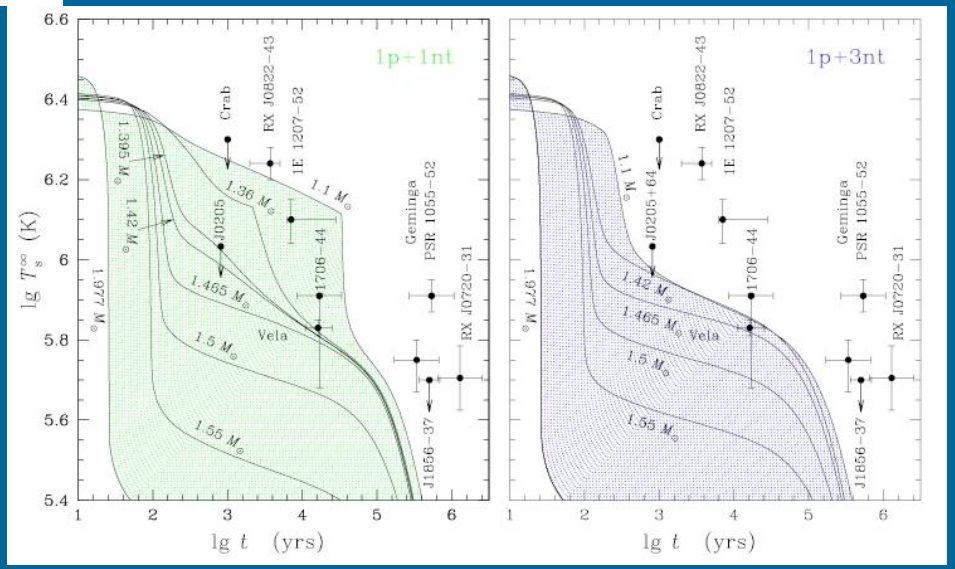

(Yakovlev & Pethick 2004)

Minimal cooling model

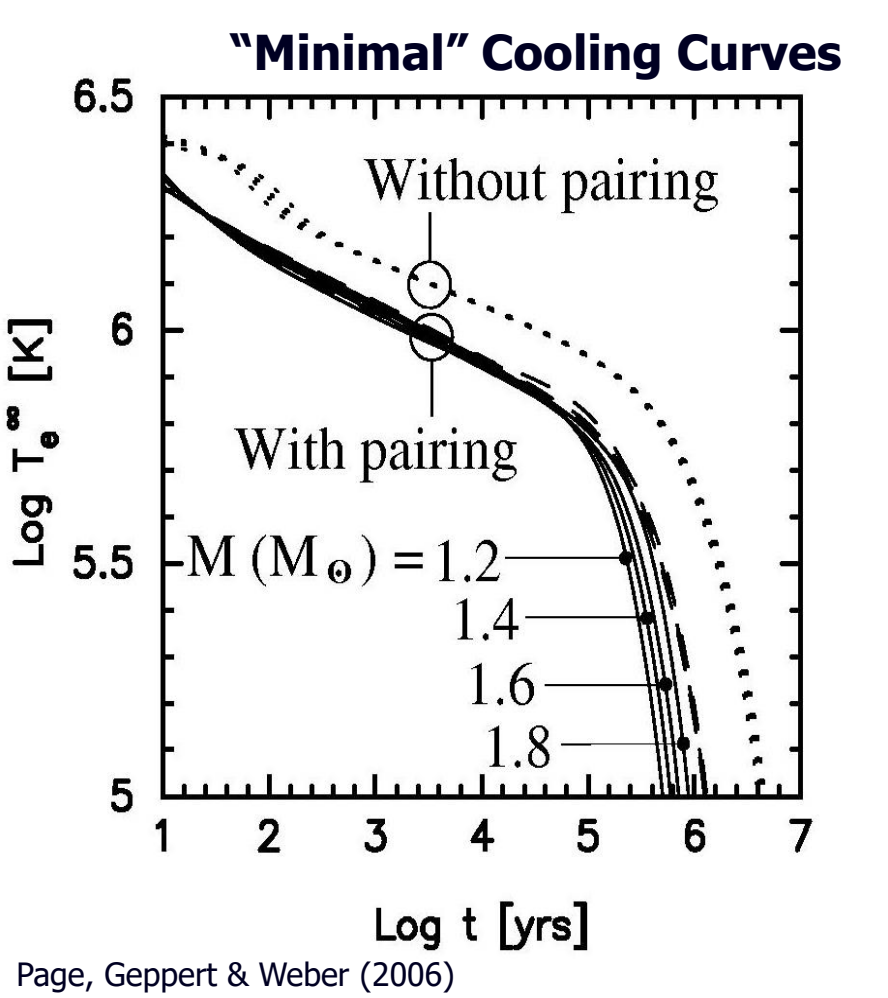

Page, Geppert & Weber (2006)

"minimal" means
without additional cooling
due to direct URCA
and without additional heating

Main ingredients of the minimal model

- EoS
- Superfluid properties
- Envelope composition
- NS mass

Analytical fits

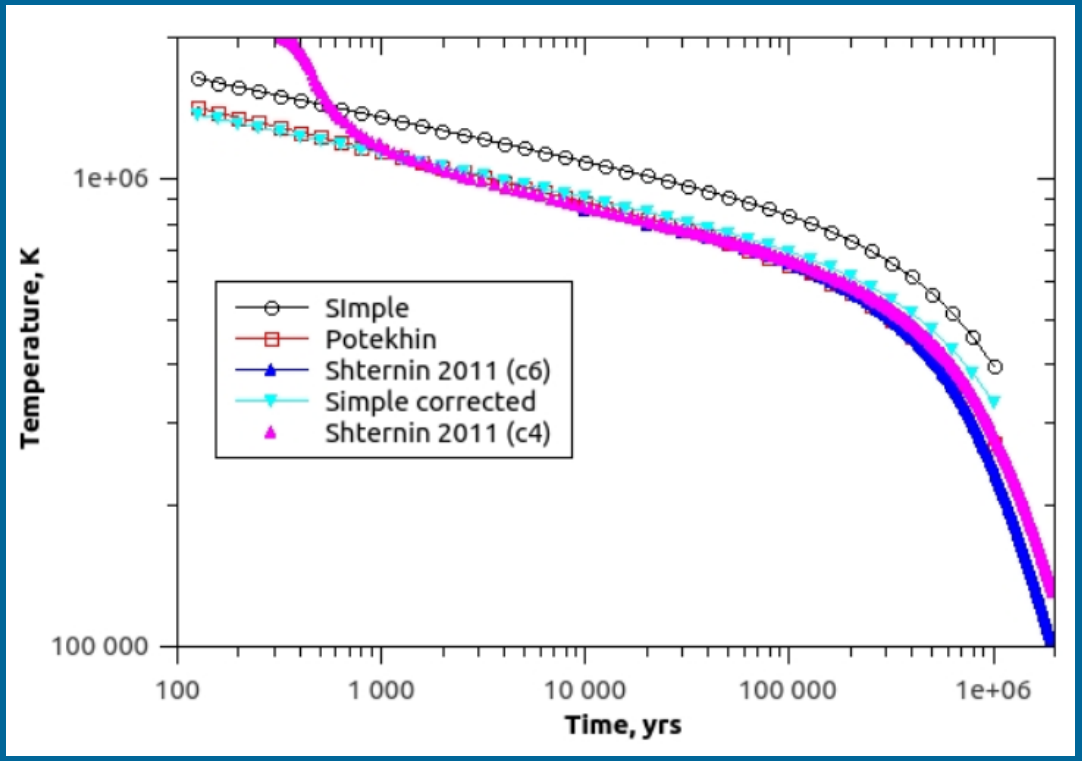

$T_{surface} \sim T_{core}^{1/2}$

$$T_{\rm eff6} = T_* \equiv (7\,T_{\rm b9}\sqrt{g_{14}})^{1/2}\,.$$

(iron envelope)

$$T^4_{\rm eff6,a} = g_{14}\,(18.1\,T_{\rm b9})^{2.42},$$

(accreted envelope)

astro-ph/9706148

astro-ph/0105261

$$T = b\left(\frac{t}{1\rm yr}\right)^a \exp(-t/\tau_{\rm c}).$$

1709.10385

$$T_{\rm s}^{(0)} \approx 10^6\, g_{14}^{1/4}\left[(7\zeta)^{2.25} + (\zeta/3)^{1.25}\right]^{1/4}\ \ {\rm K}, \qquad (27)$$

where $\zeta \equiv T_{\rm int,9} - 0.001\, g_{14}^{1/4}\sqrt{7\,T_{\rm int,9}}$, $T_{\rm int,9} \equiv T_{\rm int}/(10^9\ {\rm K})$ and $g_{14} \equiv g/10^{14}\ {\rm cm\ s^{-2}}$.

Luminosity and age uncertainties

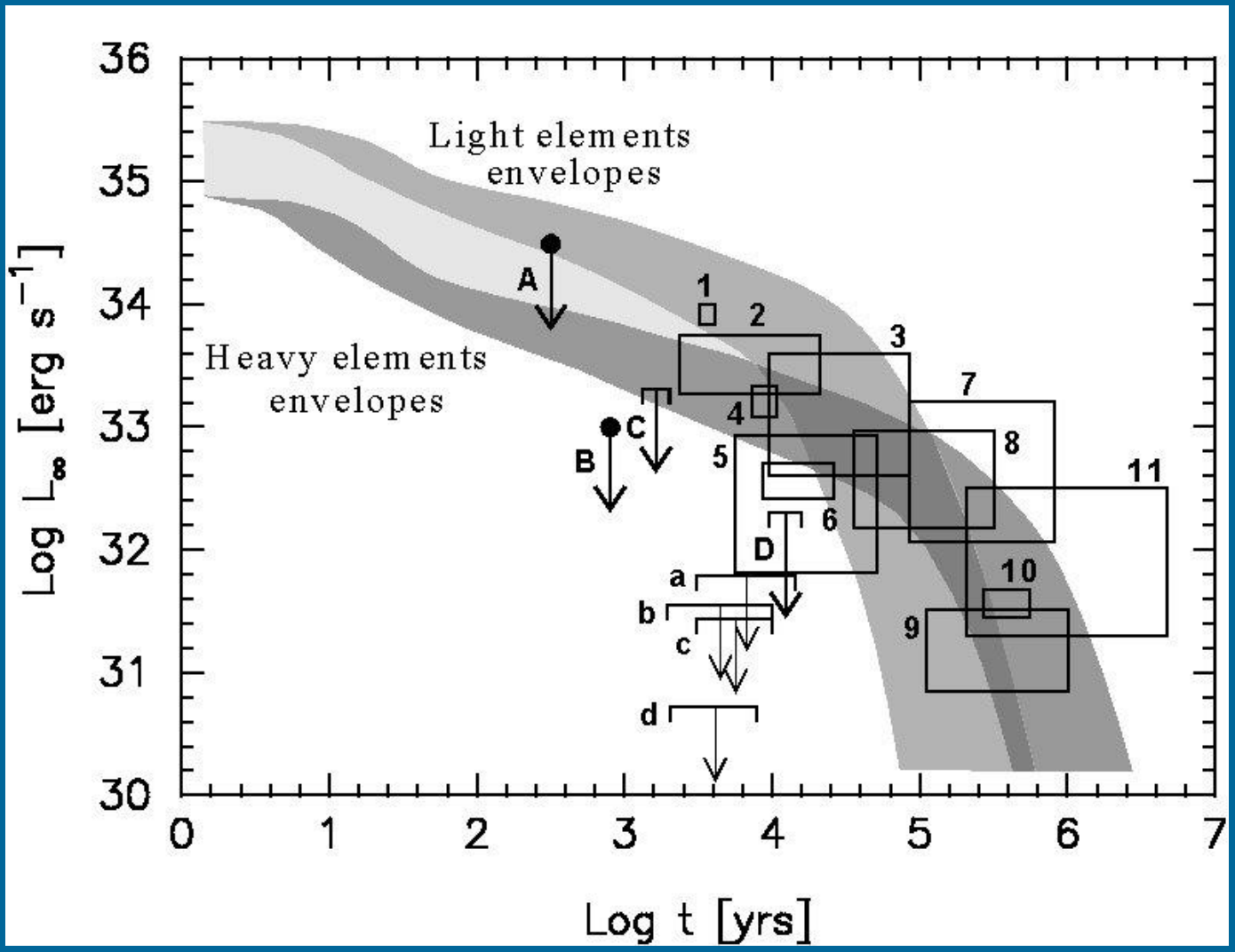

Page, Geppert, Weber
astro-ph/0508056

Standard test: temperature vs. age

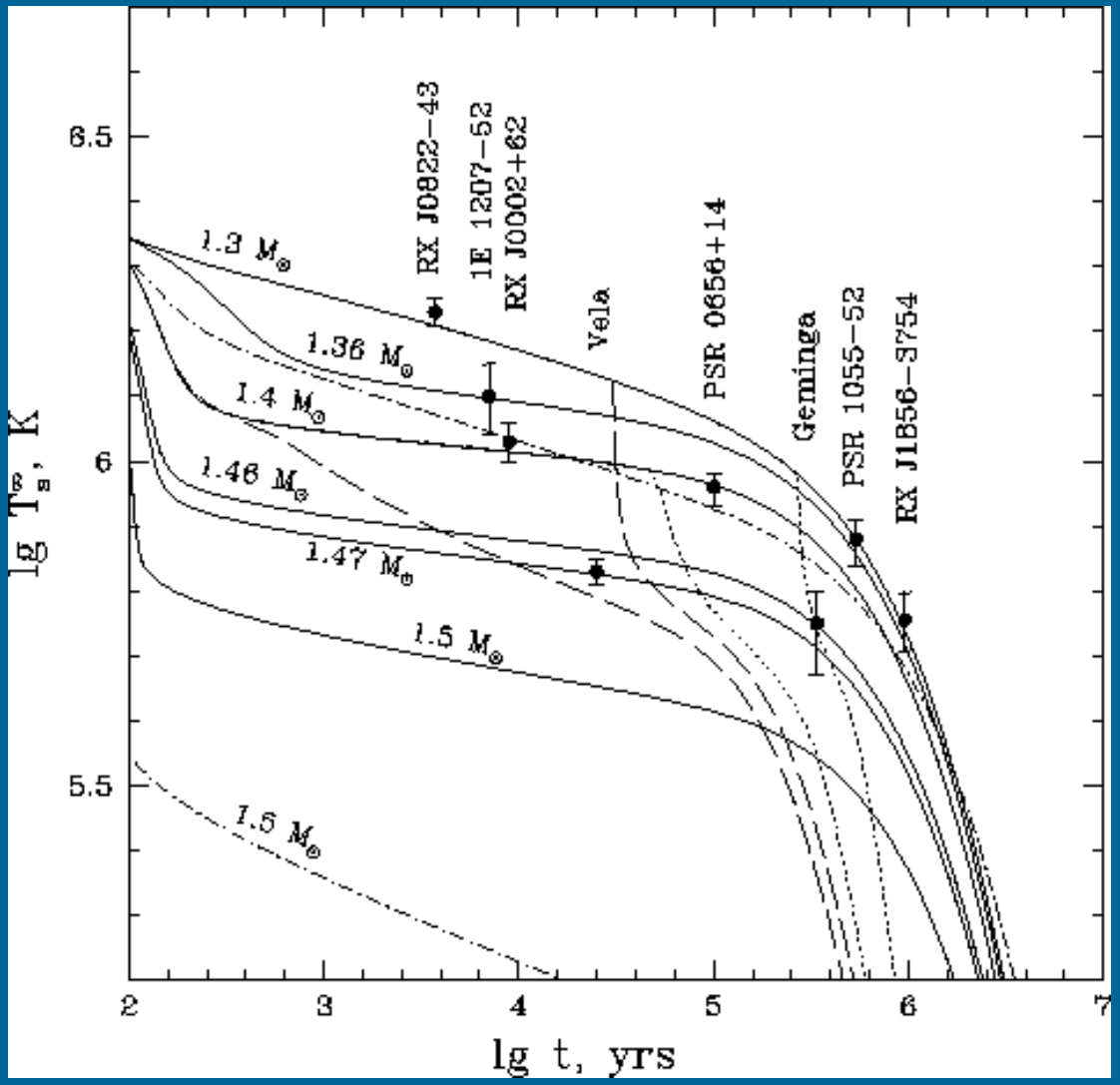

Kaminker et al. (2001)

Data

NEUTRON STAR PROPERTIES WITH HYDROGEN ATMOSPHERES

Star	$\log_{10} t_{sd}$ yr	$\log_{10} t_{kin}$ yr	$\log_{10} T_\infty$ K	d kpc	$\log_{10} L_\infty$ erg/s
RX J0822-4247	3.90	$3.57^{+0.04}_{-0.04}$	$6.24^{+0.04}_{-0.04}$	$1.9 - 2.5$	$33.85 - 34.00$
1E 1207.4-5209	$5.53^{+0.44}_{-0.19}$	$3.85^{+0.48}_{-0.48}$	$6.21^{+0.07}_{-0.07}$	$1.3 - 3.9$	$33.27 - 33.74$
RX J0002+6246	–	$3.96^{+0.08}_{-0.08}$	$6.03^{+0.03}_{-0.03}$	$2.5 - 3.5$	$33.08 - 33.33$
PSR 0833-45 (Vela)	4.05	$4.26^{+0.17}_{-0.31}$	$5.83^{+0.02}_{-0.02}$	$0.22 - 0.28$	$32.41 - 32.70$
PSR 1706-44	4.24	–	$5.8^{+0.13}_{-0.13}$	$1.4 - 2.3$	$31.81 - 32.93$
PSR 0538+2817	4.47	–	$6.05^{+0.10}_{-0.10}$	1.2	$32.6 - 33.6$

NEUTRON STAR PROPERTIES WITH BLACKBODY ATMOSPHERES

Star	$\log_{10} t_{sd}$ yr	$\log_{10} t_{kin}$ yr	$\log_{10} T_\infty$ K	R_∞ km	d kpc	$\log_{10} L_\infty$ erg/s
RX J0822-4247	3.90	$3.57^{+0.04}_{-0.04}$	$6.65^{+0.04}_{-0.04}$	$1 - 1.6$	$1.9 - 2.5$	$33.60 - 33.90$
1E 1207.4-5209	$5.53^{+0.44}_{-0.19}$	$3.85^{+0.48}_{-0.48}$	$6.48^{+0.01}_{-0.01}$	$1.0 - 3.7$	$1.3 - 3.9$	$32.70 - 33.88$
RX J0002+6246	–	$3.96^{+0.08}_{-0.08}$	$6.15^{+0.11}_{-0.11}$	$2.1 - 5.3$	$2.5 - 3.5$	$32.18 - 32.81$
PSR 0833-45 (Vela)	4.05	$4.26^{+0.17}_{-0.31}$	$6.18^{+0.02}_{-0.02}$	$1.7 - 2.5$	$0.22 - 0.28$	$32.04 - 32.32$
PSR 1706-44	4.24	–	$6.22^{+0.04}_{-0.04}$	$1.9 - 5.8$	$1.8 - 3.2$	$32.48 - 33.08$
PSR 0656+14	5.04	–	$5.71^{+0.03}_{-0.04}$	$7.0 - 8.5$	$0.26 - 0.32$	$32.18 - 32.97$
PSR 0633+1748 (Geminga)	5.53	–	$5.75^{+0.04}_{-0.05}$	$2.7 - 8.7$	$0.123 - 0.216$	$30.85 - 31.51$
PSR 1055-52	5.43	–	$5.92^{+0.02}_{-0.02}$	$6.5 - 19.5$	$0.5 - 1.5$	$32.07 - 33.19$
RX J1856.5-3754	–	$5.70^{+0.05}_{-0.25}$	$5.6 - 5.9$	> 16	$0.105 - 0.129$	$31.44 - 31.68$
RX J0720.4-3125	6.0 ± 0.2	–	$5.55 - 5.95$	$5.0 - 15.0$	$0.1 - 0.3$	$31.3 - 32.5$

(Page et al. astro-ph/0403657)

Not to mix with polar caps heating!

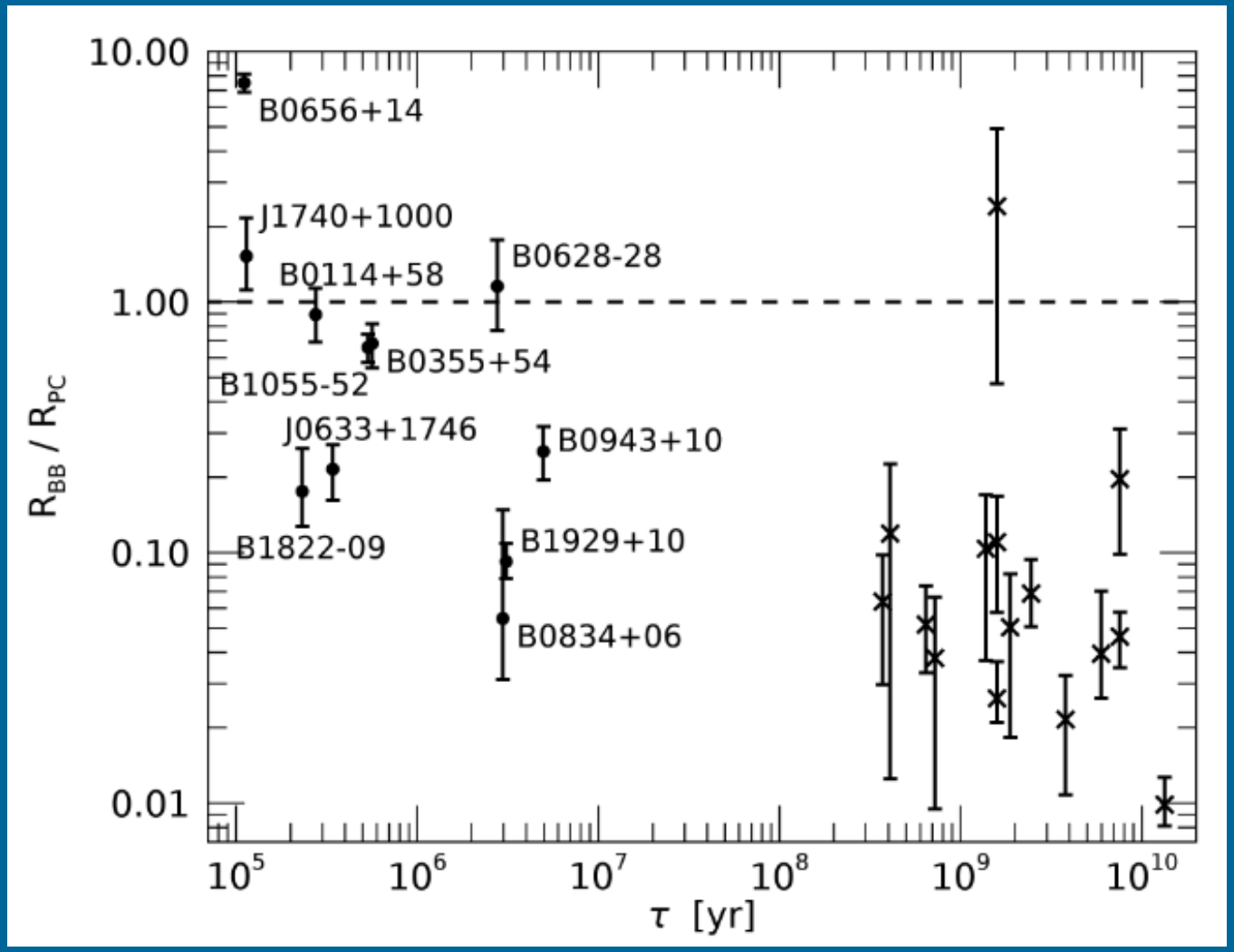

$R_{cap}=R_{NS}(R_{NS}/R_l)^{1/2}$

1802.09454

A puzzling source

Millisecond Pulsar J2124−3358

Characteristic age 3.4 Gyr

T~(0.5-2)x10^5K

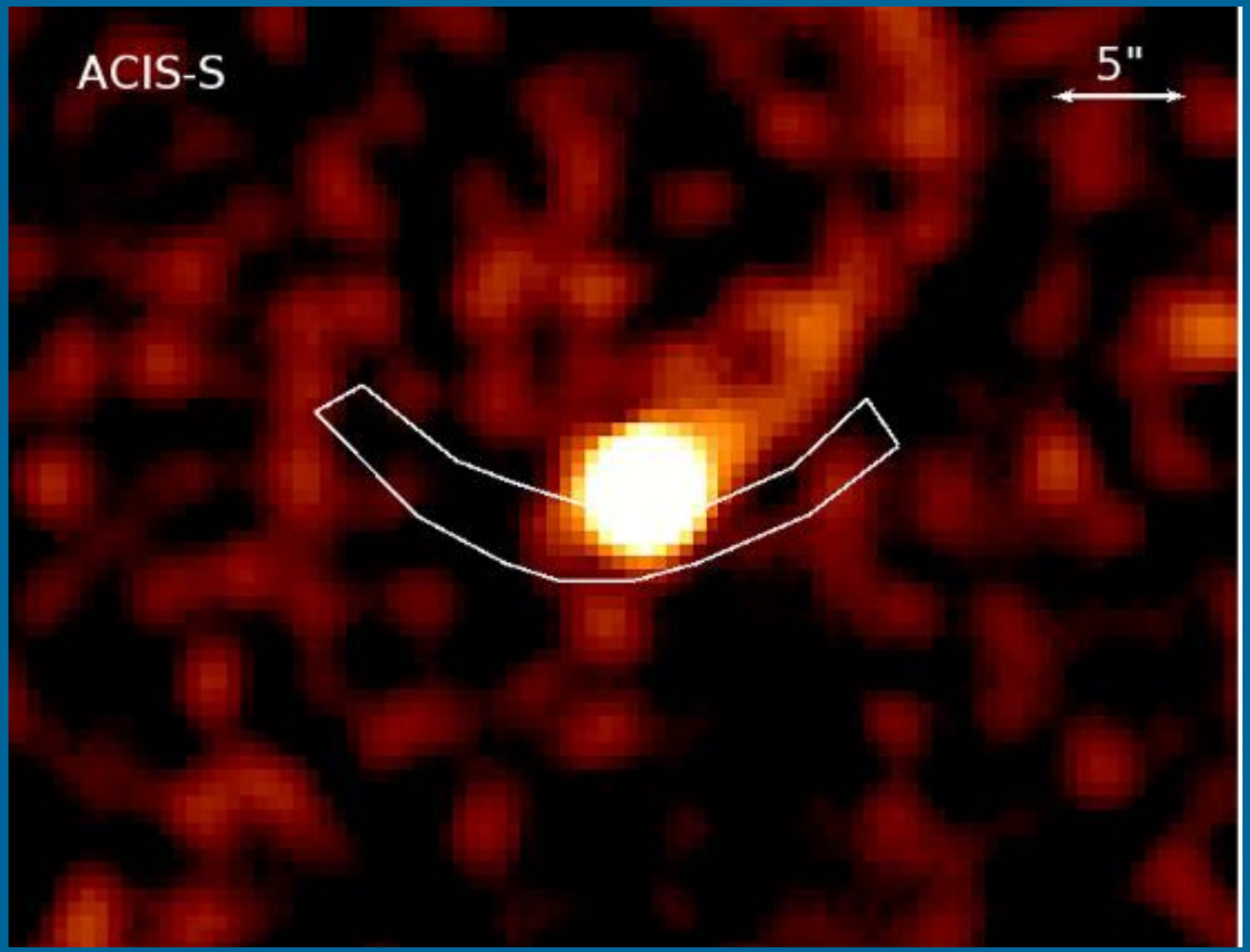

Rangelov et al. (2017)

Another old, but hot

PSR B0950+08

Characteristic age 17.5 Myr

T~(1-3)x10^5K

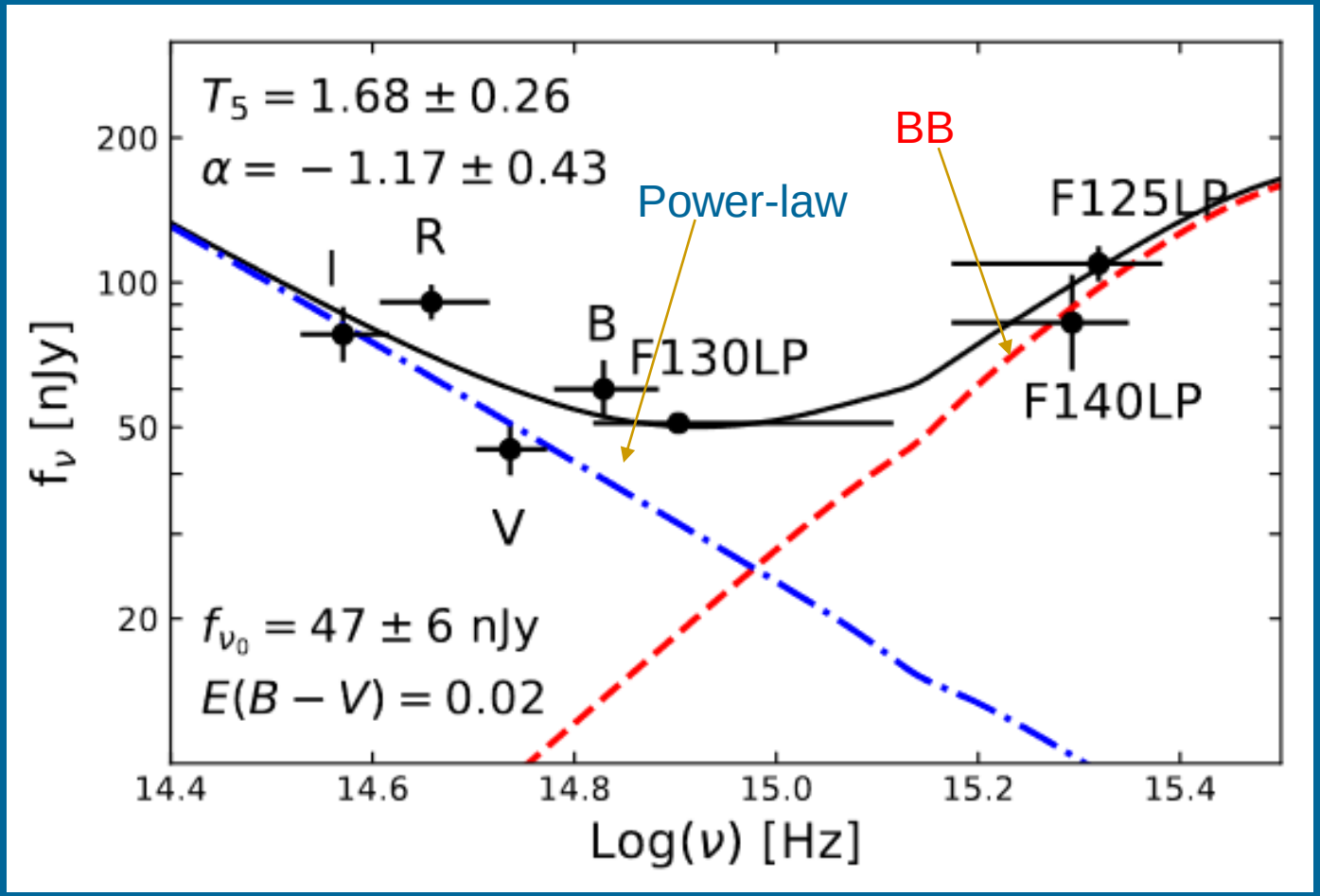

1710.06448

The coldest NS known

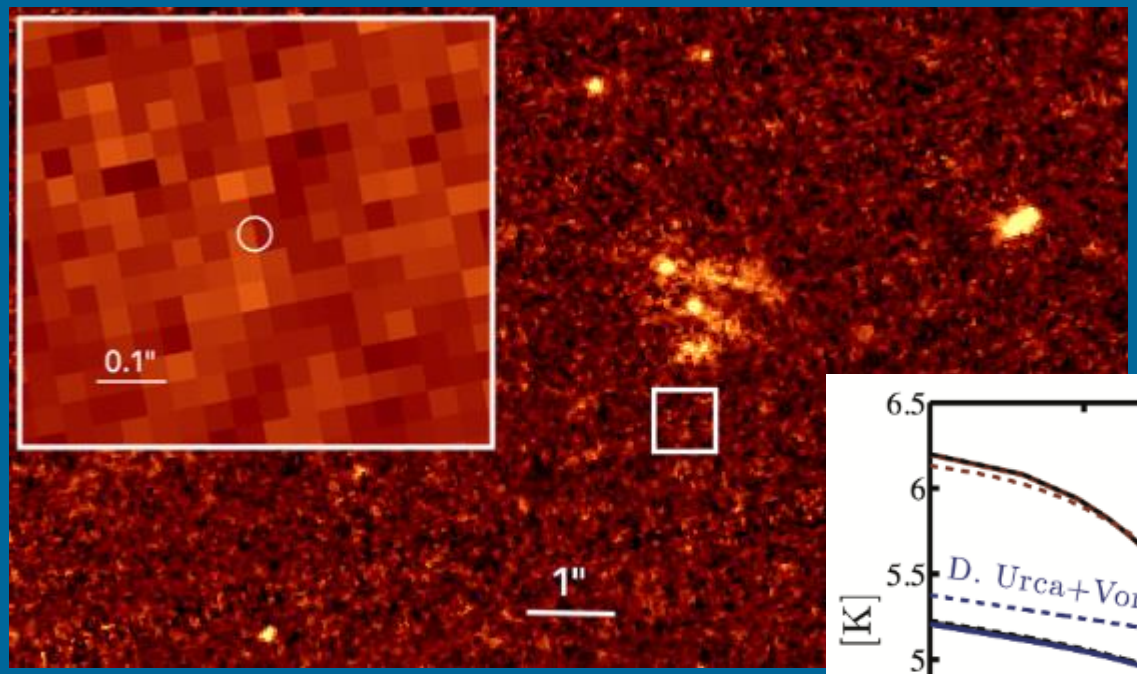

PSR J2144–3933
P=8.5 sec
B=2 10^{12} G
d=160-200 pc

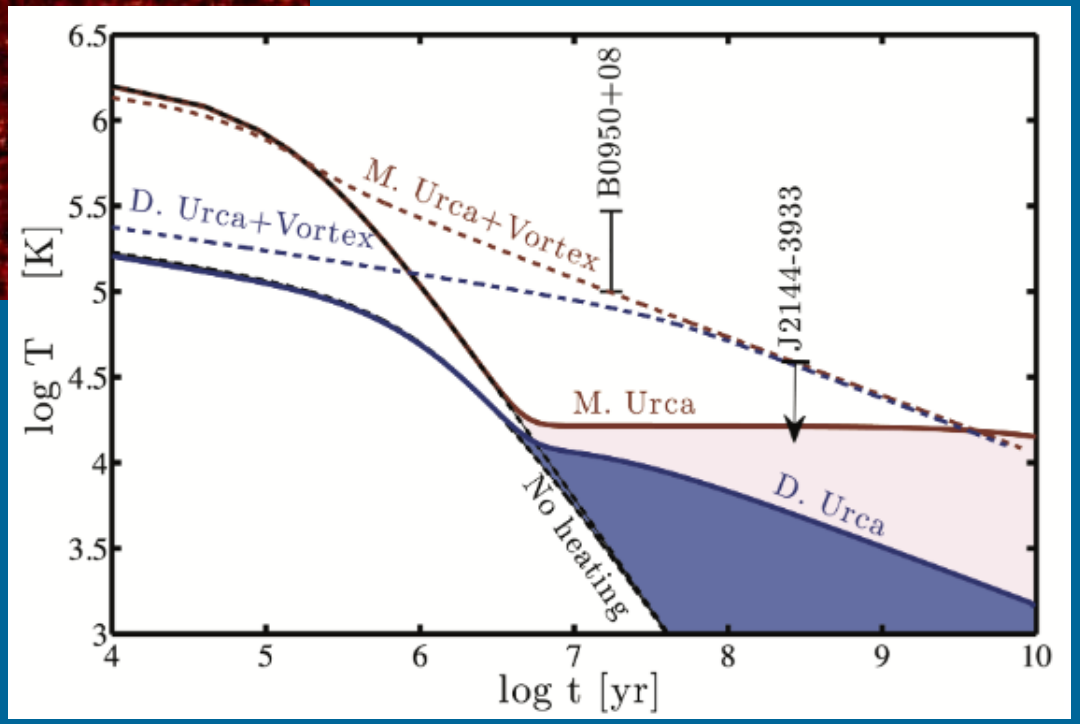

Limit: T<42000K

1901.0799

Brightness constraint

Different tests and constraints
are sensitive to different parameters,
so, typically it is better to use
several different tests

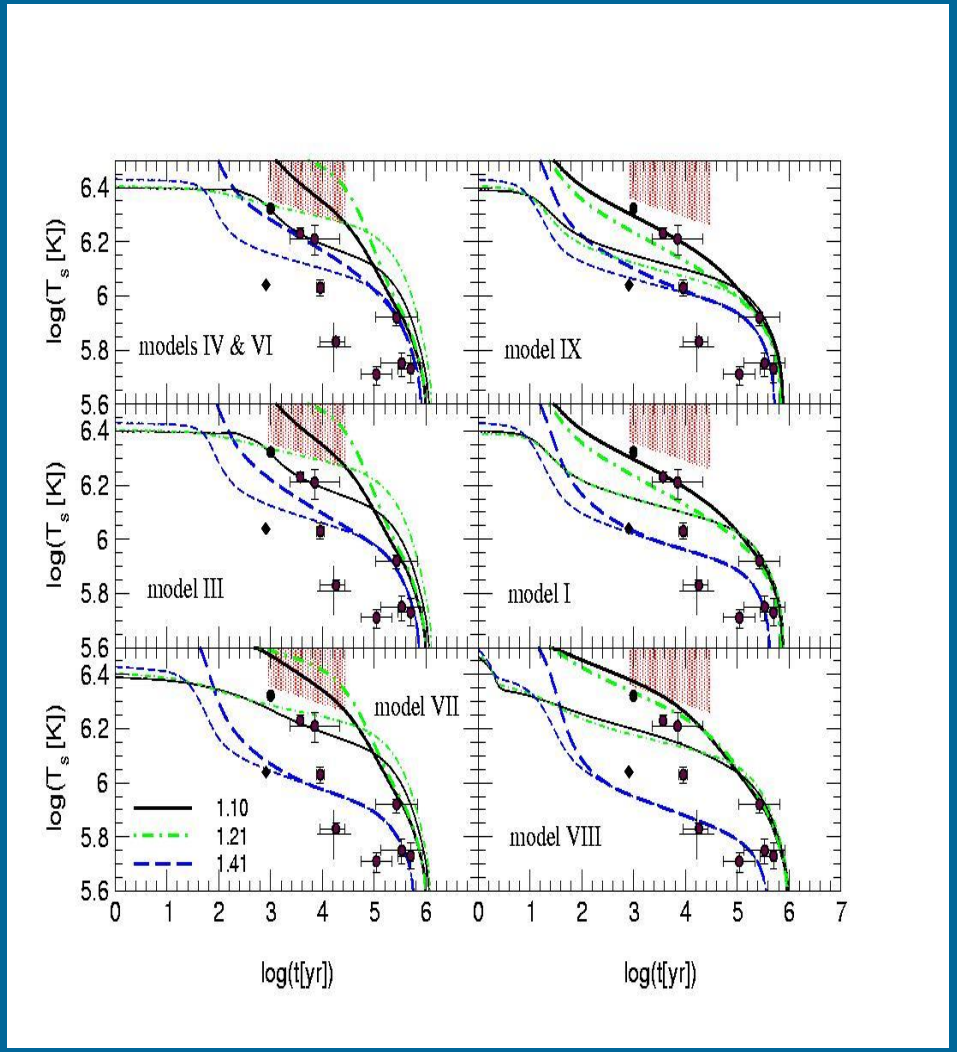

(H. Grigorian astro-ph/0507052)

CCOs

1. Found in SNRs
2. Have no radio or gamma-ray counterpats
3. No pulsar wind nebula (PWN)
4. Have soft thermal-like spectra

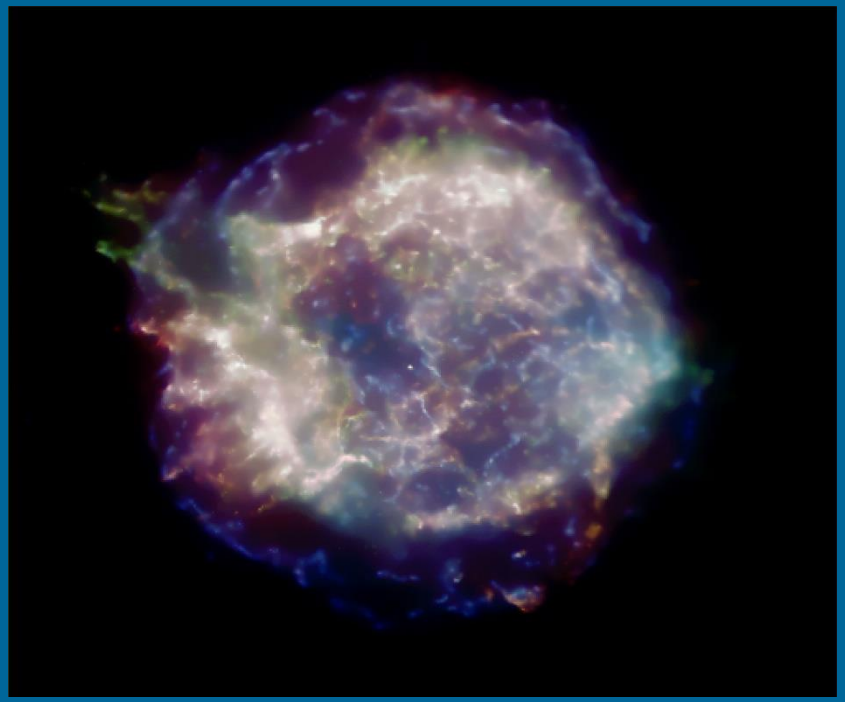

Known objects

Object	SNR	Age kyr	d kpc	P	$F_{\mathrm{x},-12}$
J232327.9+584843	Cas A	0.32	3.3–3.7	...	0.8
J085201.4−461753	G266.1−1.2	1–3	1–2	...	1.4
J161736.3−510225(x)	RCW 103	1–3	3–7	6.4hr	0.9–60
J082157.5−430017	Pup A	1–3	1.6–3.3	...	4.5
J121000.8−522628	G296.5+10.0	3–20	1.3–3.9	424ms	2.3
J185238.6+004020(n)	Kes 79	∼9	∼10	...	0.2
J171328.4−394955(n)	G347.3−0.5	∼10	∼6	...	2.8
J000256 +62465 (n,x)	G117.9+0.6[?]	?	∼ 3[?]	...	0.1

Object	kT keV	R km	$L_{\mathrm{bol},33}$	Γ	$L_{\mathrm{pl},33}$	$n_{\mathrm{H},22}$	$F^{\mathrm{bb}}/F^{\mathrm{pl}}$
J2323+5848	0.43	0.6	1.6	4.2	13	1.8	1.1
	0.43	0.7	1.9	2.5	0.2	[1.2]	4.5
J0852–4617	0.40	0.3	0.3	unconstr	...	0.4	...
J0821–4300	0.40	1.0	3.3	unconstr	...	0.3	...
J1210–5226	0.22	2.0	1.2	3.6	1.2	0.13	3.0
J1852+0040	0.50	1.0	8.0	unconstr	...	1.5	...
J1713–3949	0.38	2.4	15	3.9	72	0.8	0.9

New candidates appear continuously.

(Pavlov et al. astro-ph/0311526)

Correlations

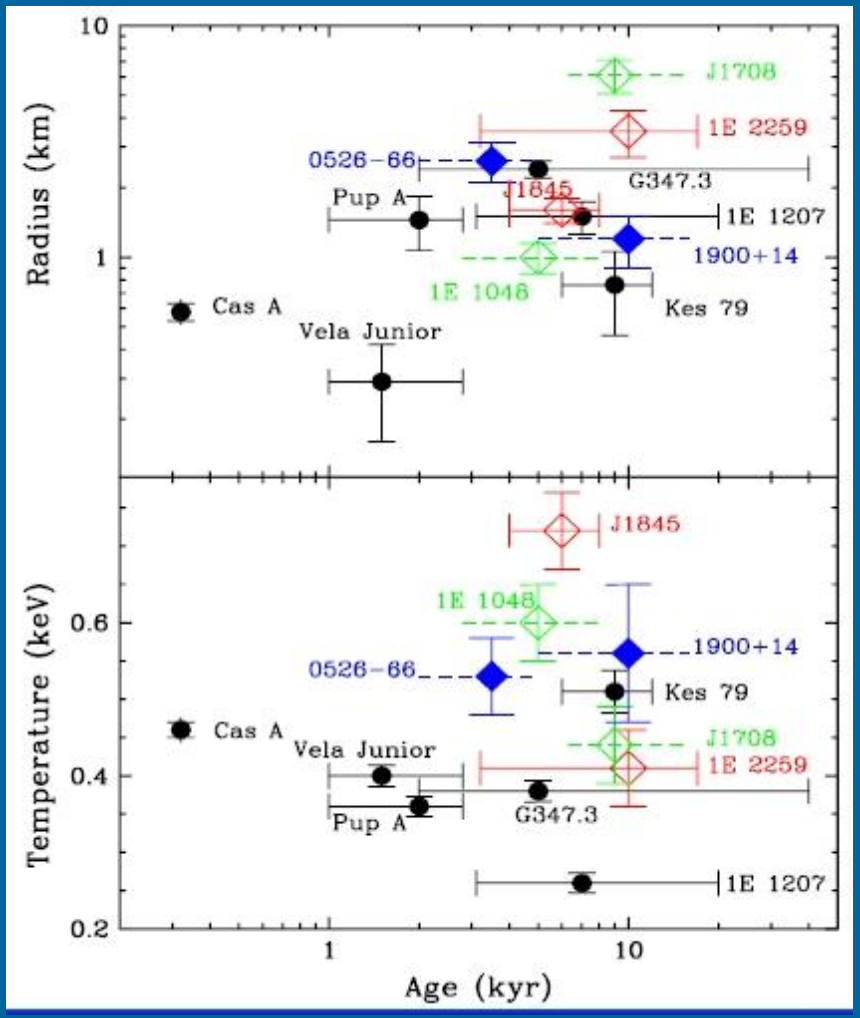

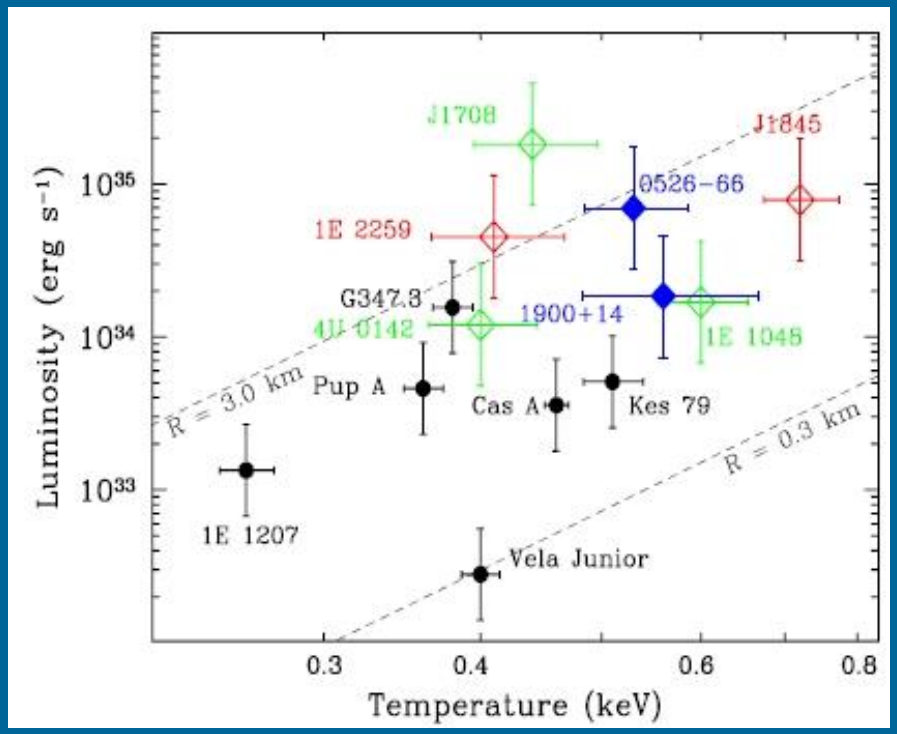

(Pavlov et al. astro-ph/0311526)

Cas A peculiar cooling

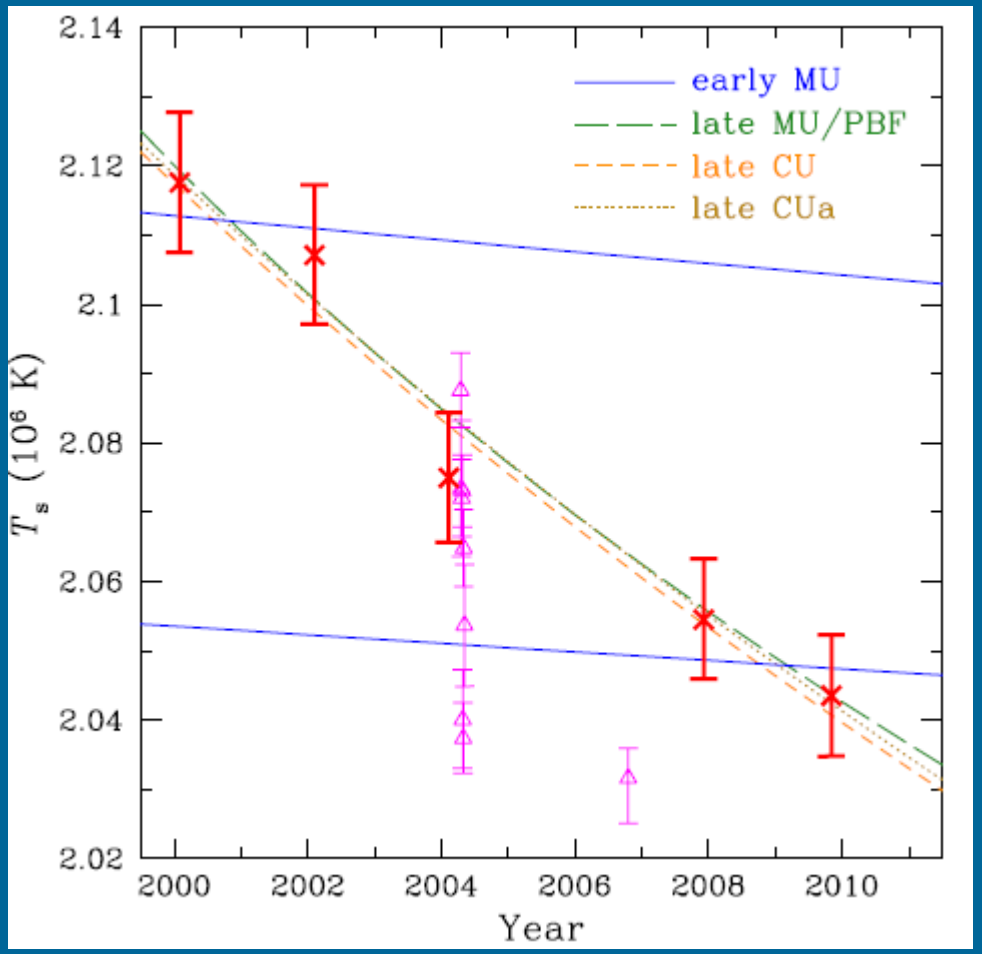

330 years
~3.5 kpc
Carbon atmosphere
The youngest cooler known

Temperature steadily goes down by ~4% in 10 years:
2.12 10^6K in 2000 – 2.04 10^6K in 2009

1007.4719

Onset of neutron $^3P_2$ superfluidity in the core

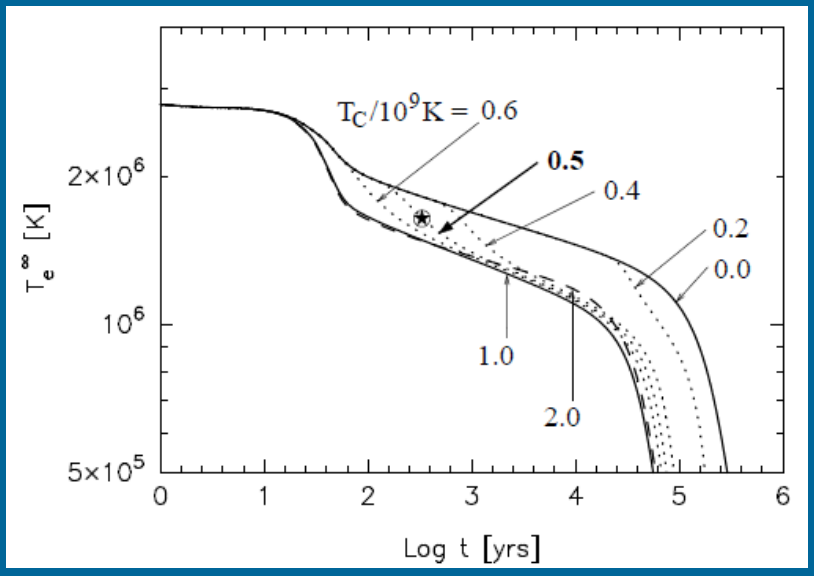

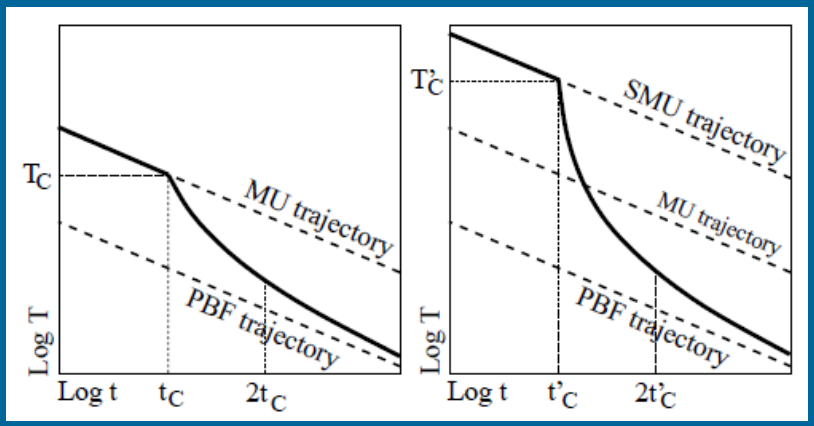

The idea is that we see the result of the onset of neutron $^3P_2$ superfluidity in the core.

The NS just cooled down enough to have this type of neutron superfluidity in the core.

This gives an opportunity to estimate the critical temperature: 0.5 10^9 K

1011.6142

The best fit model

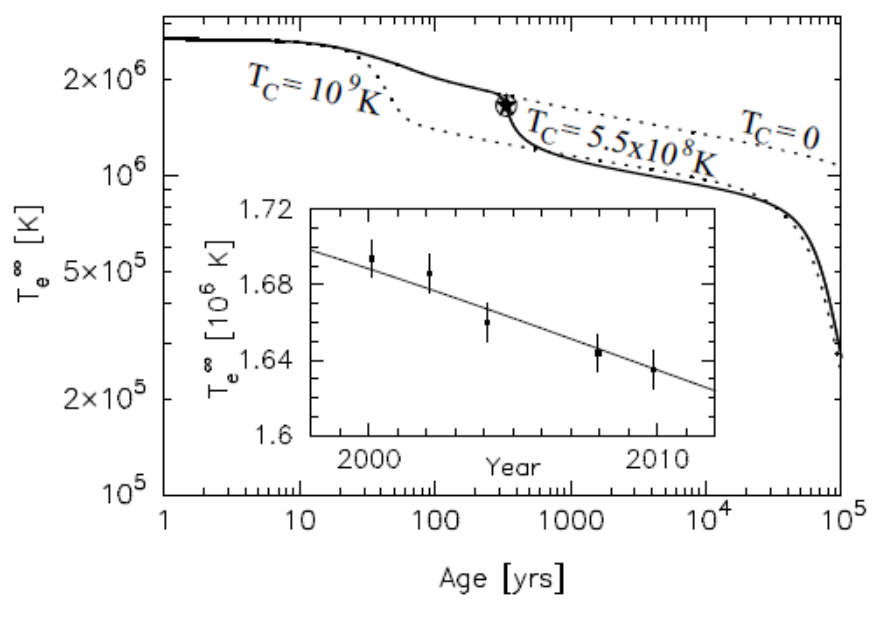

Cooling curves depend on masses, but the estimate of the critical temper. depends on M just slightly.

To explain a quick cooling it is necessary to assume suppression of cooling by proton $^1S_0$ superfluidity in the core.

Rapid cooling will proceed for several tens of years more.

The plot is made for $M=1.4M_O$

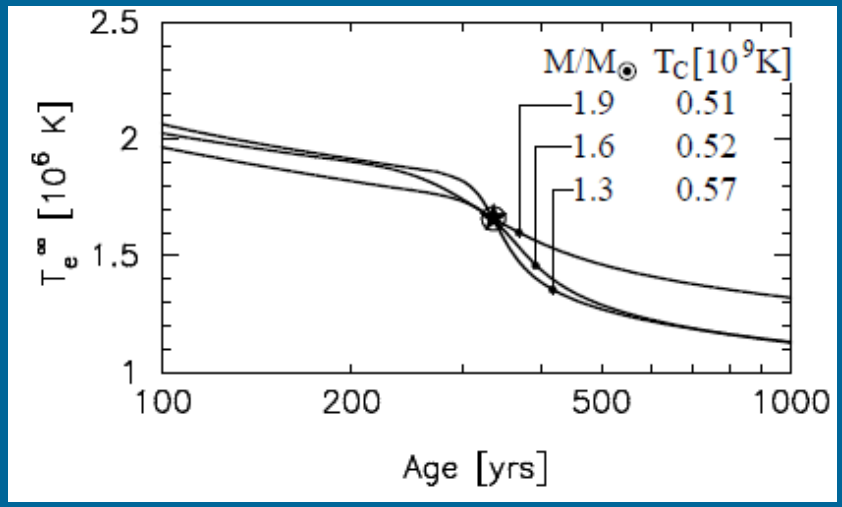

1011.6142, see many details in 1110.5116

Different superfluidity models

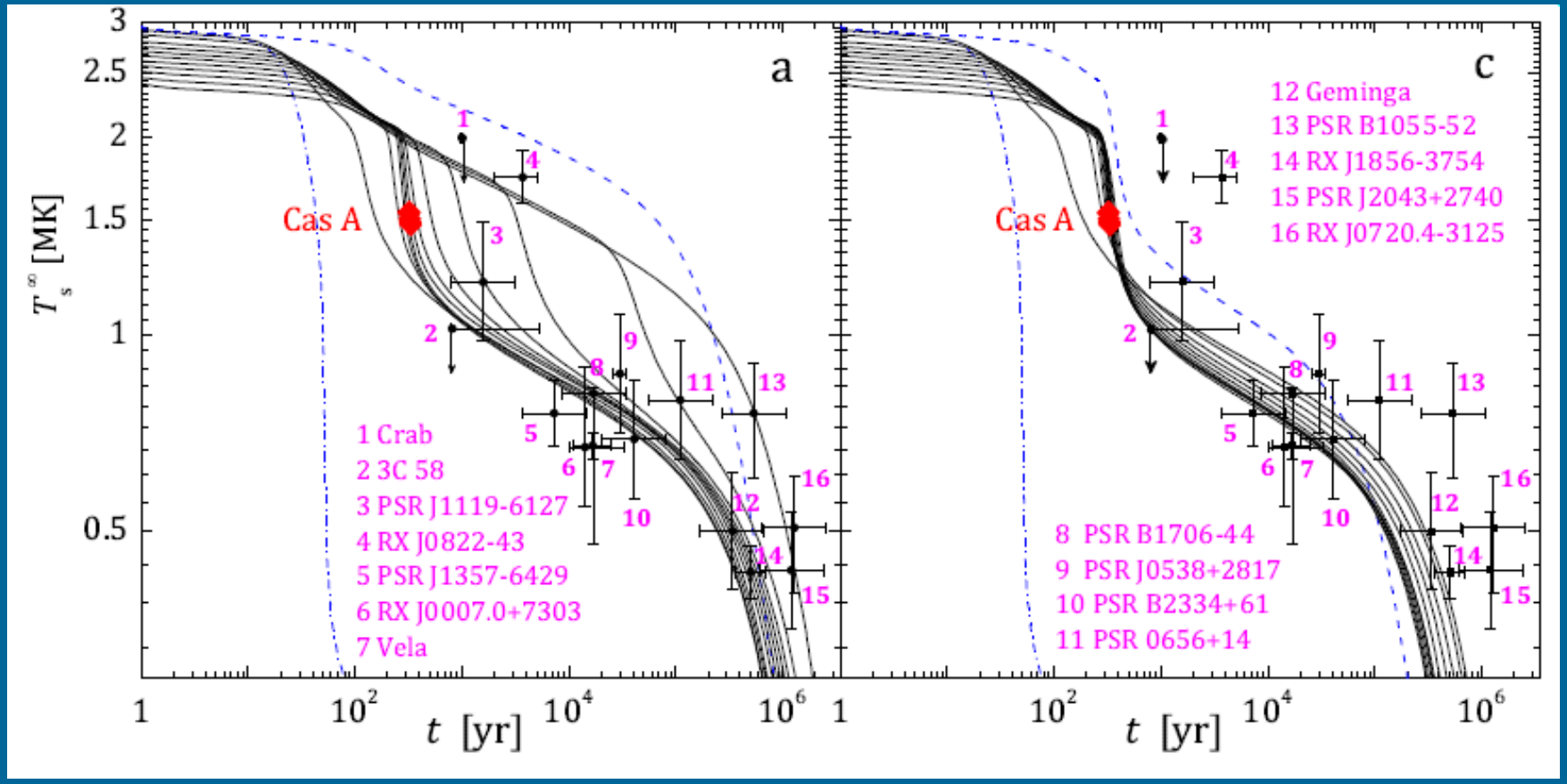

1012.0045

Nuclear medium cooling

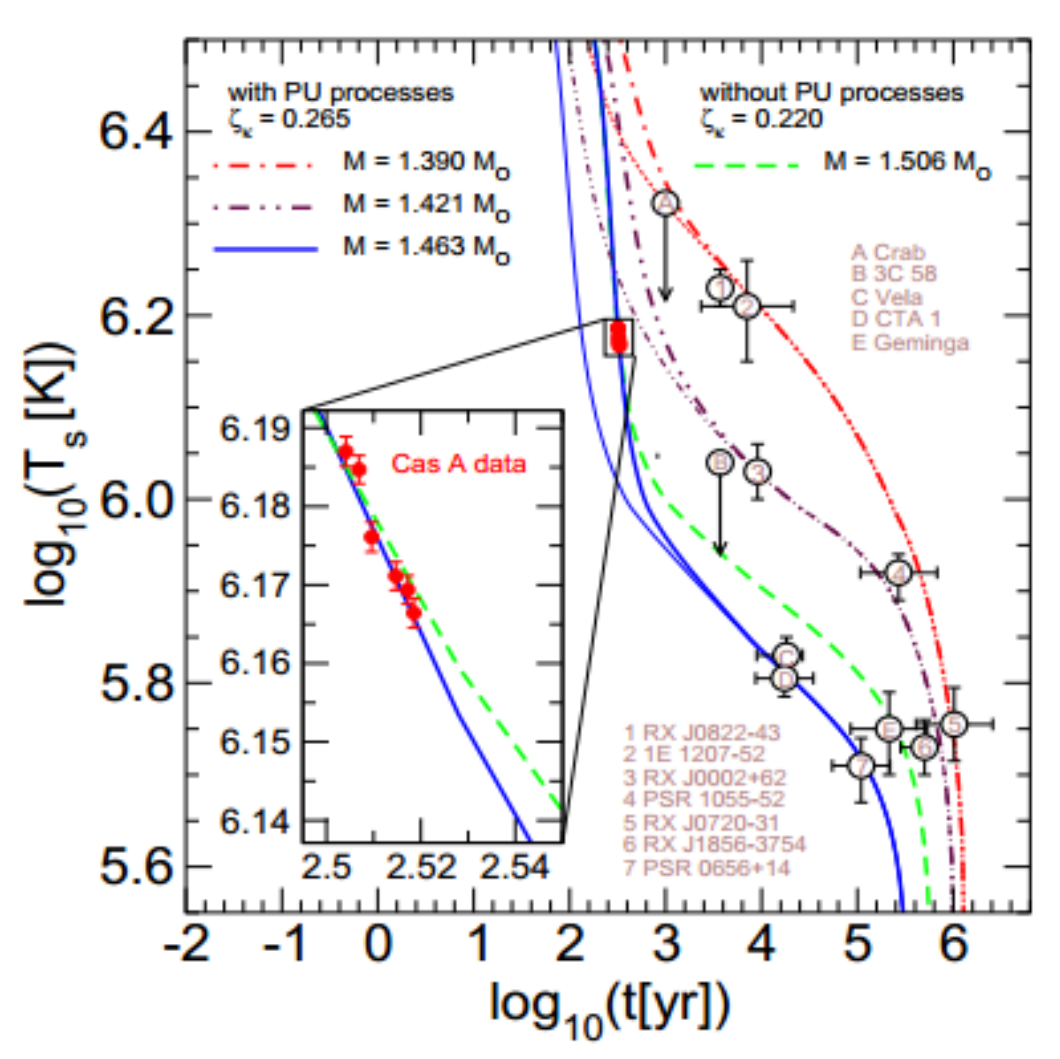

Crucial for the successful description of the observed data is a substantial reduction of the thermal conductivity, resulting from a suppression of both the electron and nucleon contributions to it by medium effects.

1108.4125

Diffusive nuclear burning

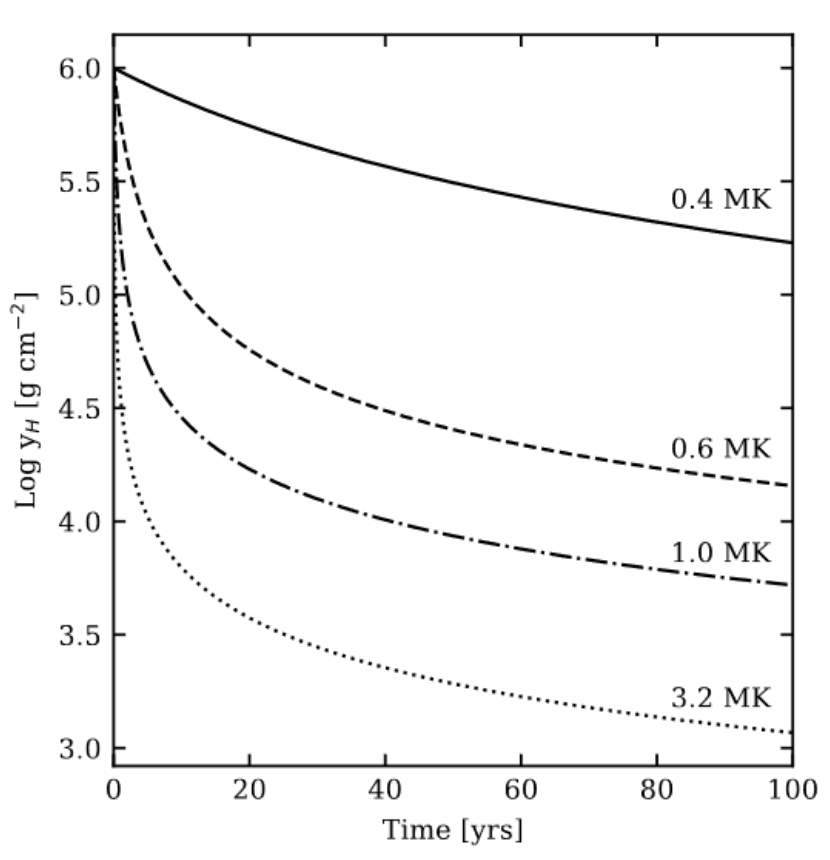

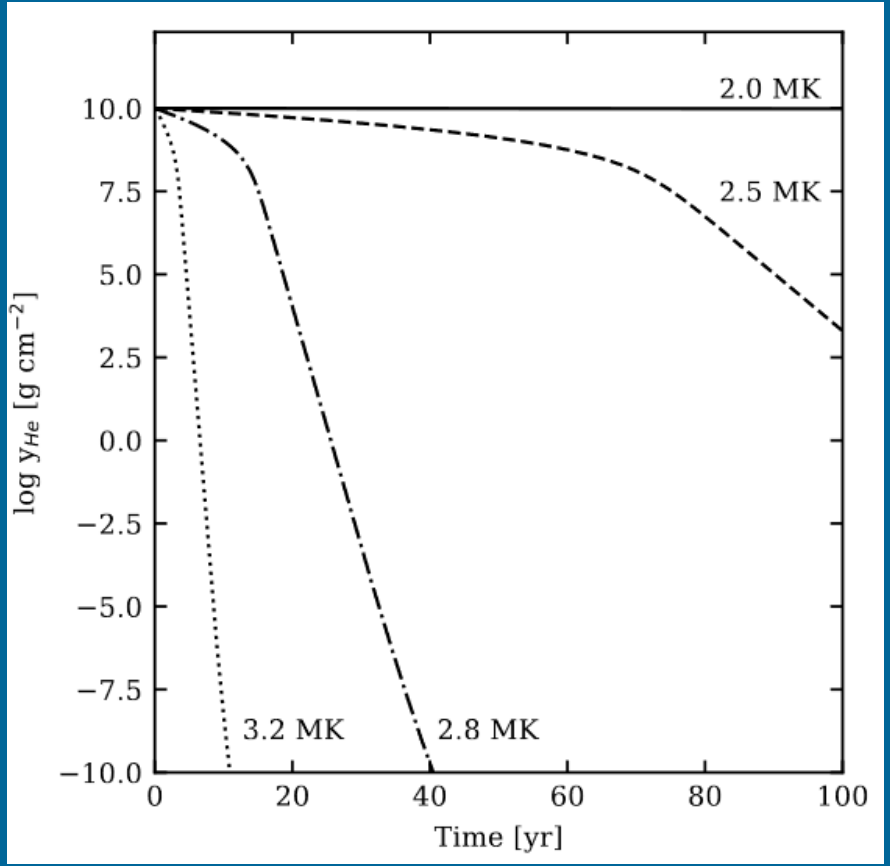

1901.01012

Cooling with DNB

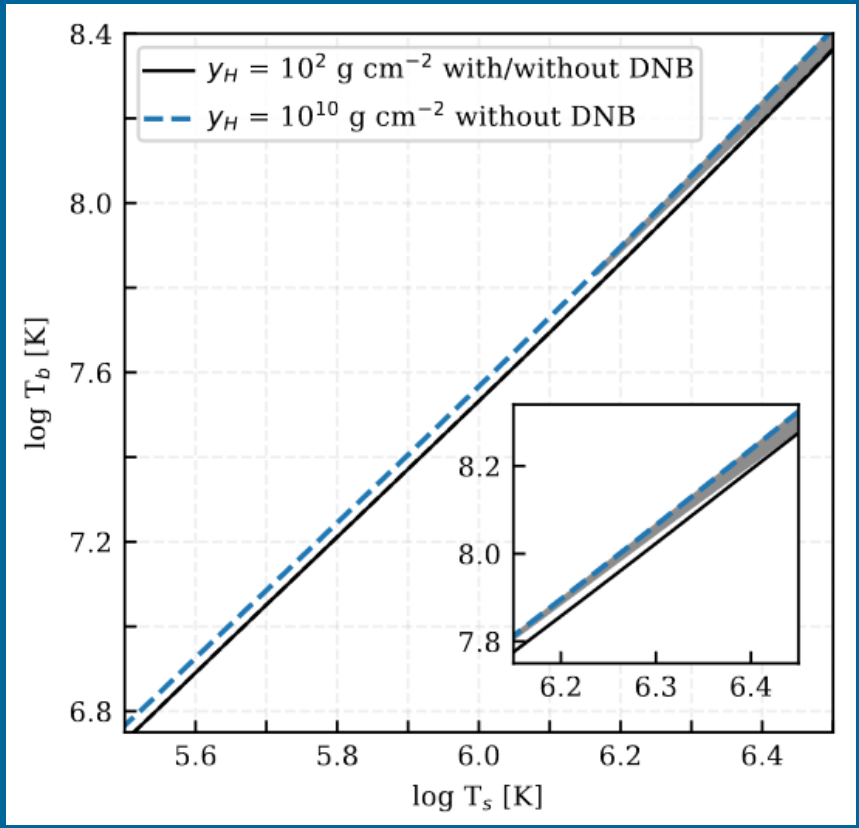

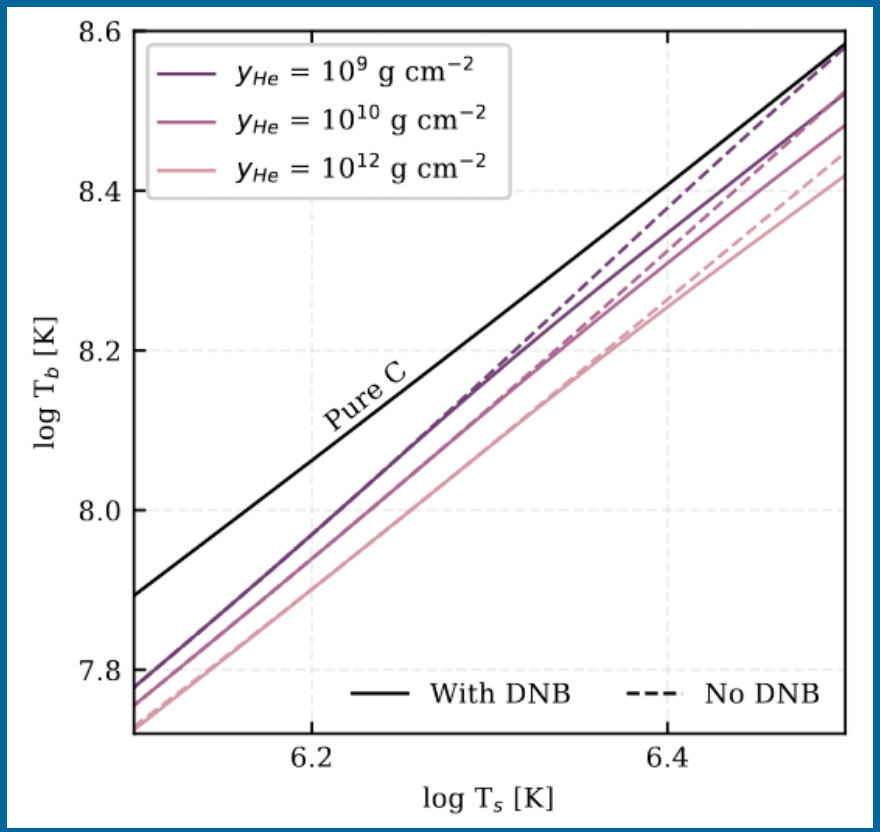

1901.01012

New twist: no cooling!

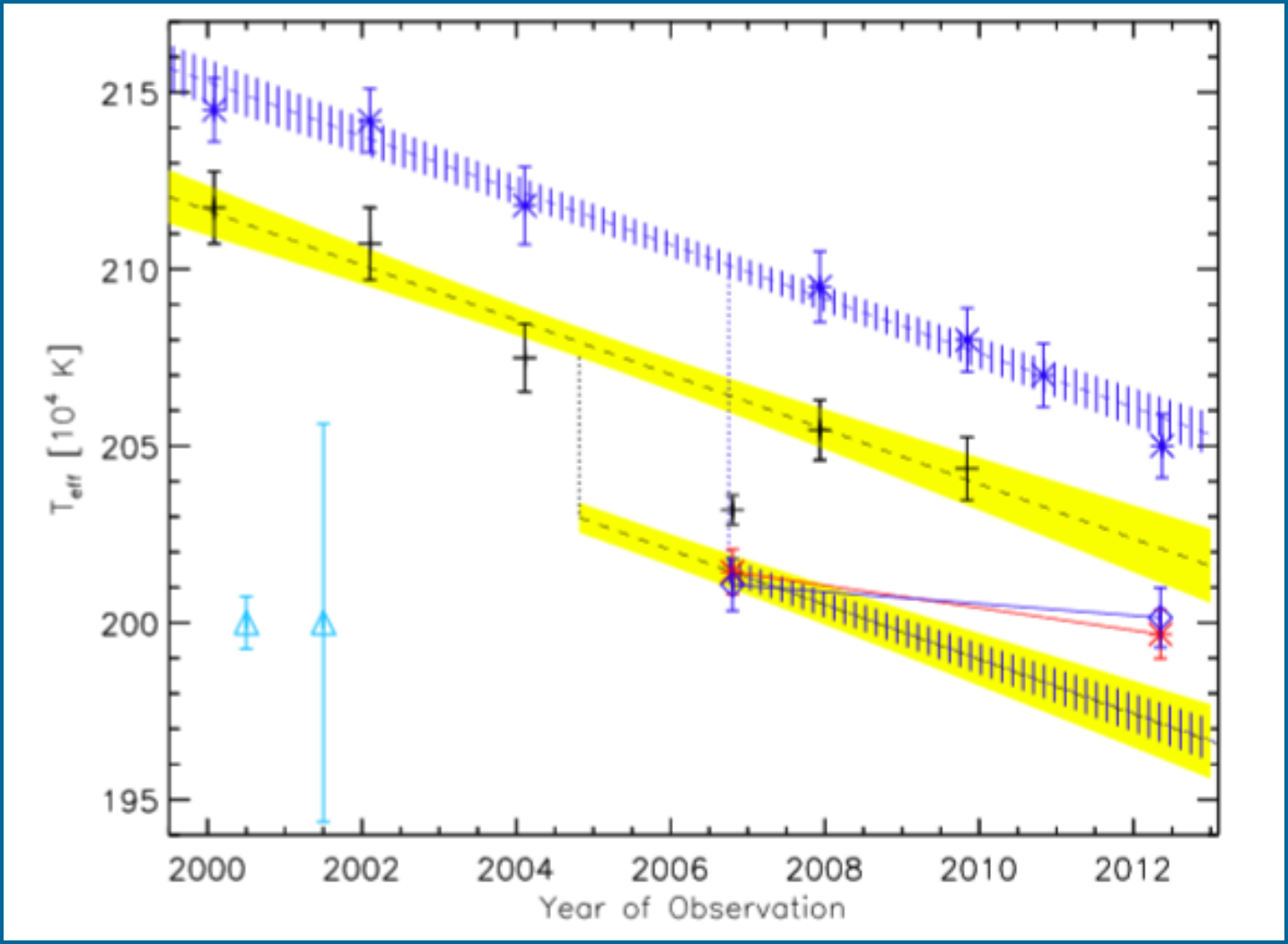

1311.0888

New data: still no cooling?

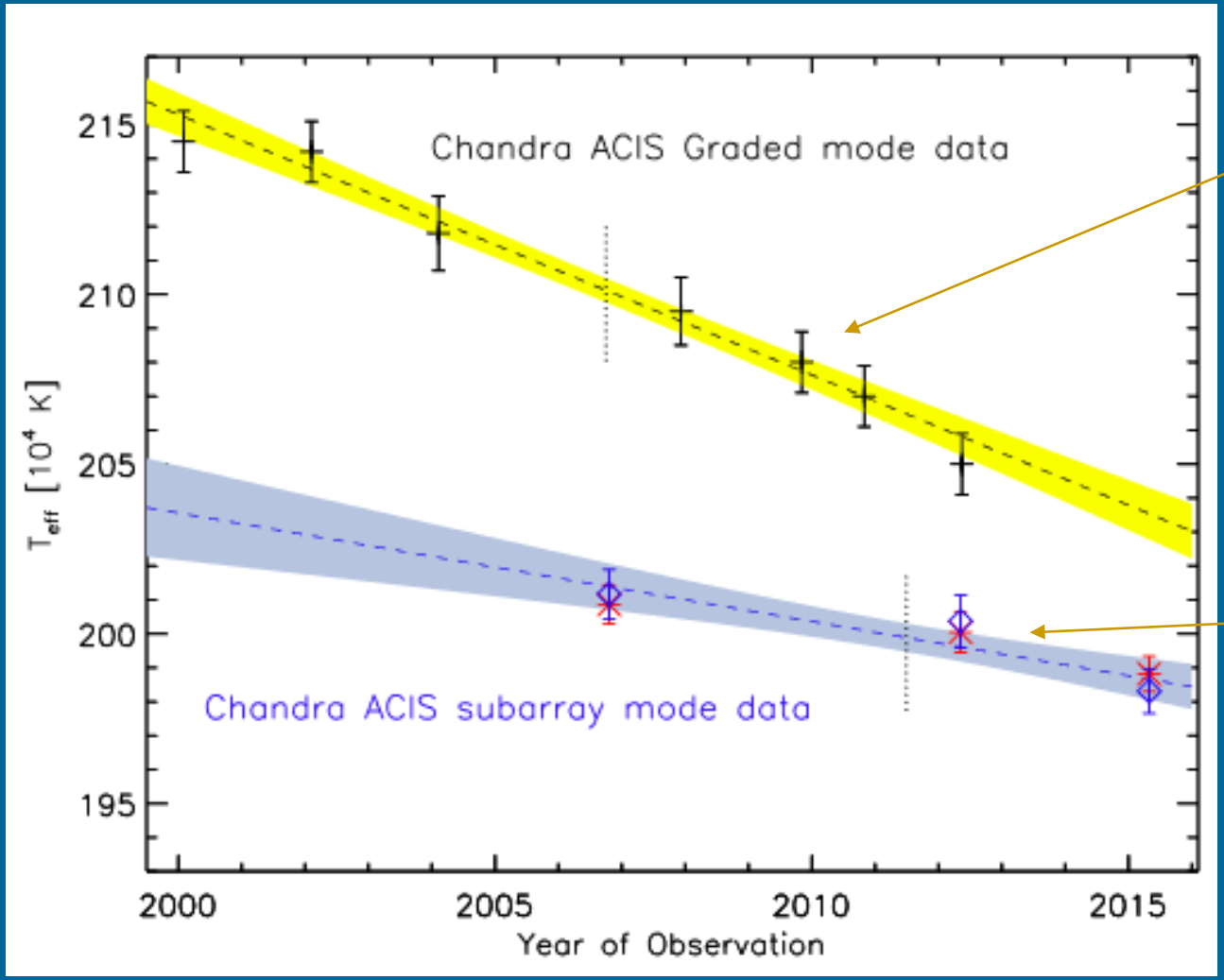

Elshamouty et al. 2013

Posselt et al.

1808.00531

Cooling and rotation

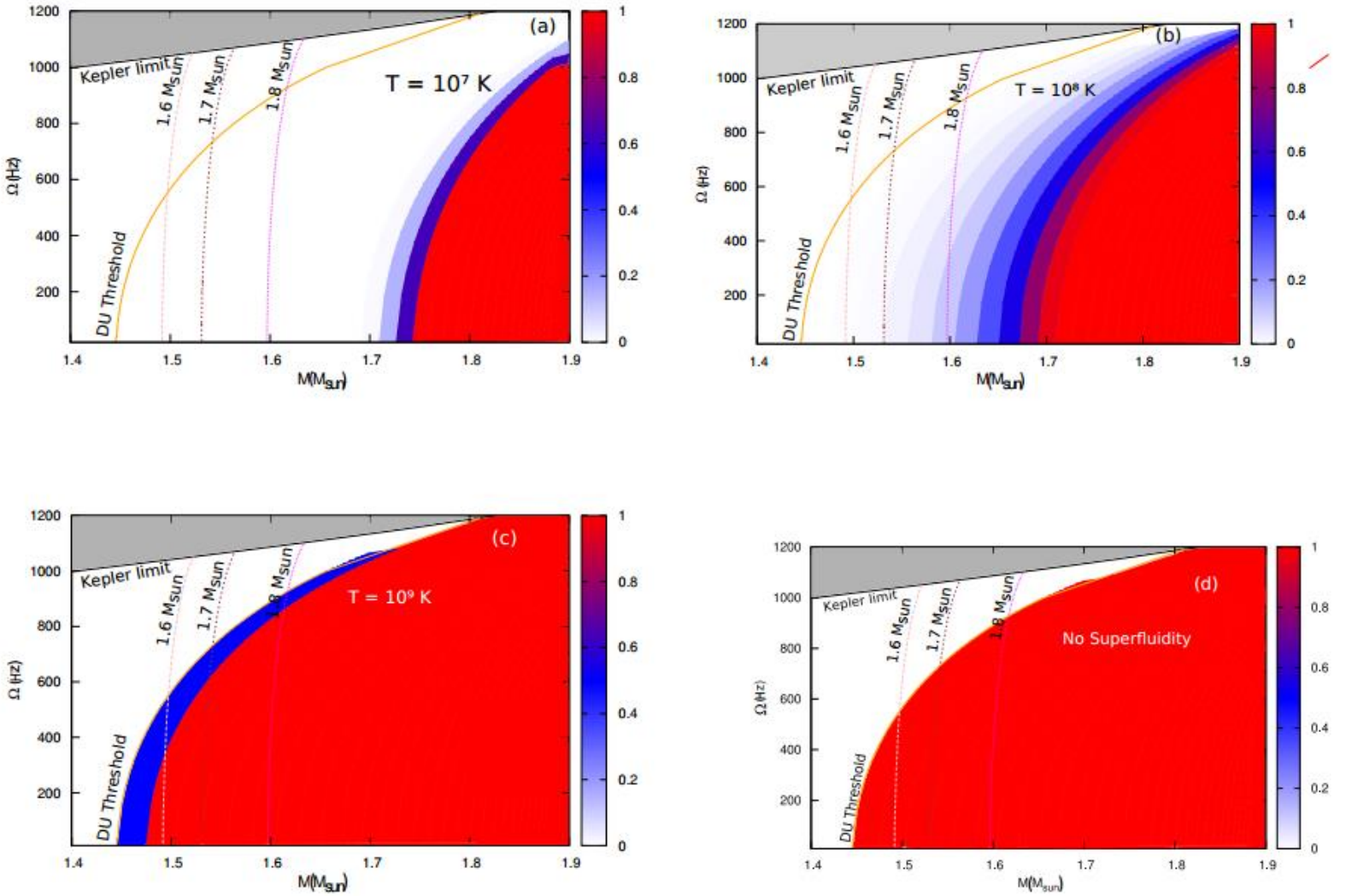

1103.3870

Cas A case

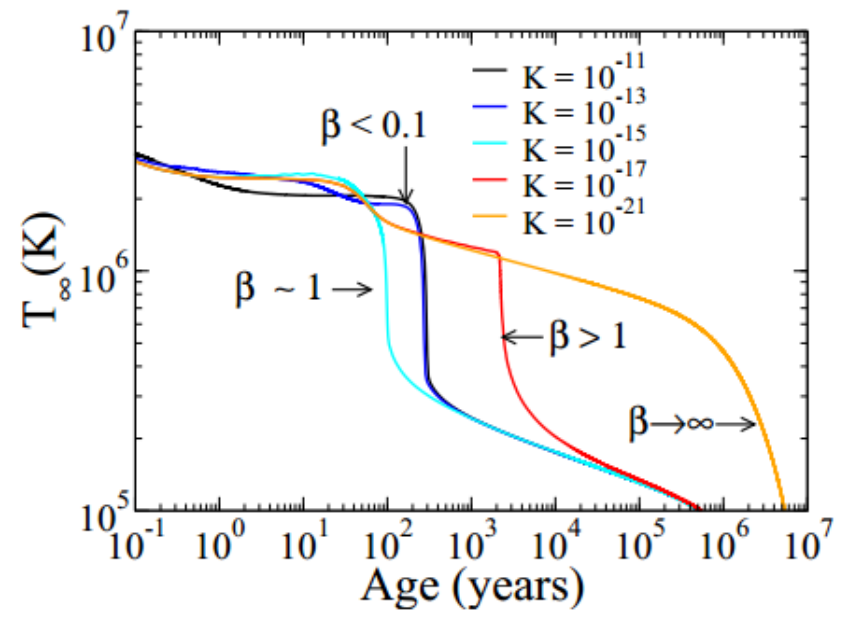

P_0=0.0025-0.00125 sec
B~10^{11} G

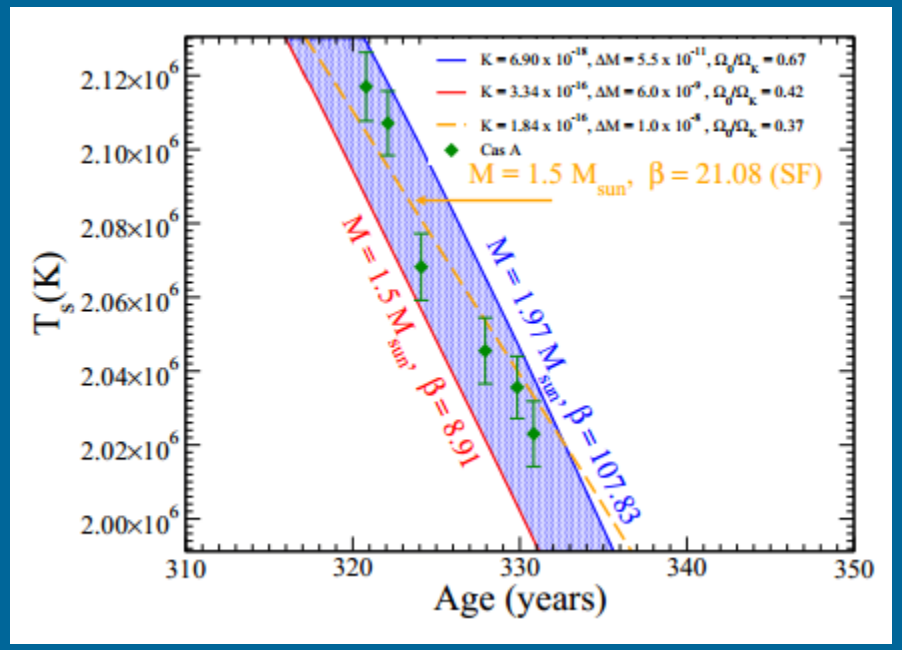

Other studies of the influence of effects of rotation see in 1201.2381

1103.3870

Exotic phase transition

Rapid cooling of Cas A can be understood
as a phase transition from the perfect 2SC phase
to a crystalline/gapless color-superconducting state

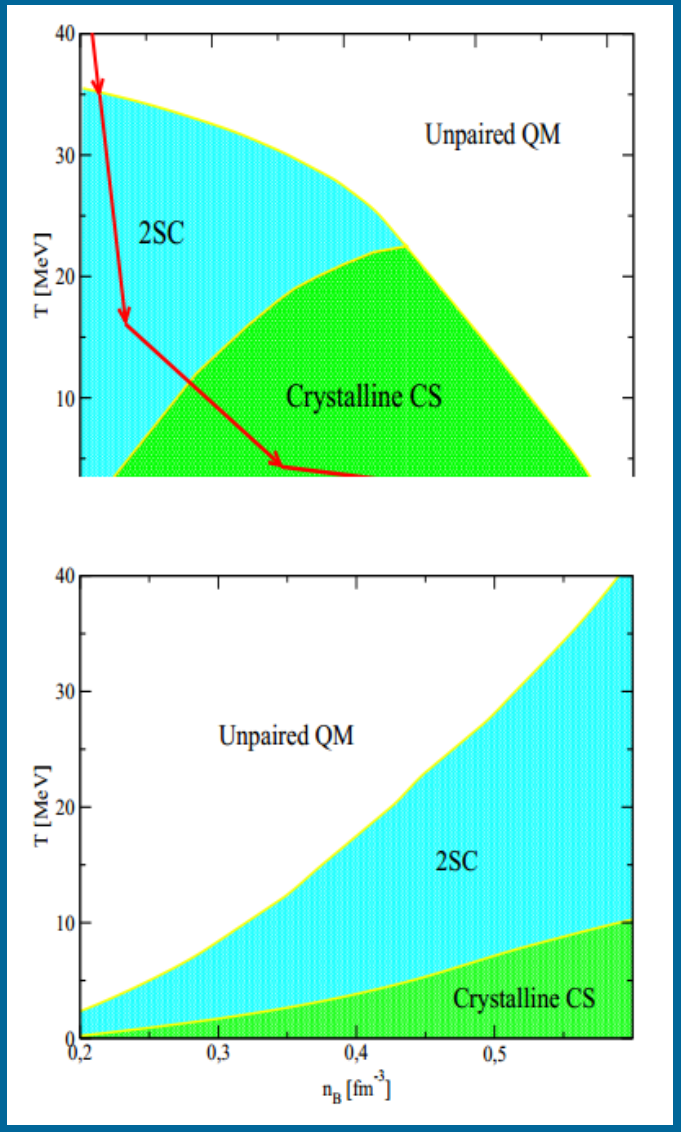

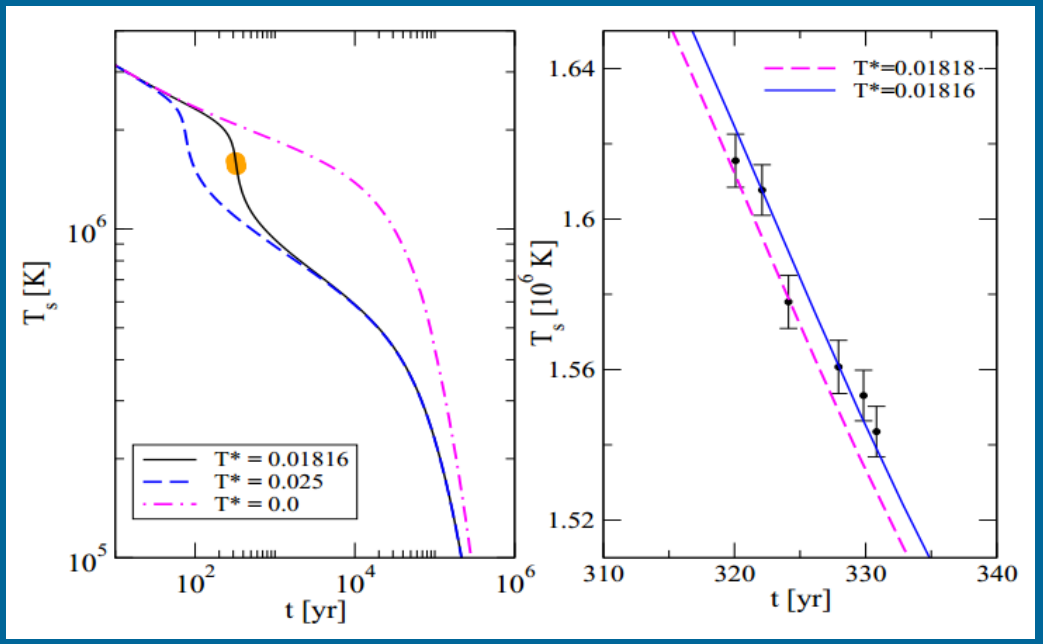

1301.2814

Cooling of X-ray transients

"Many neutron stars in close X-ray binaries are transient accretors (transients);
They exhibit X-ray bursts separated by long periods (months or even years) of quiescence.
It is believed that the quiescence corresponds to a lowlevel, or even halted, accretion onto the neutron star.
During high-state accretion episodes,
the heat is deposited by nonequilibrium processes in the deep layers (10^{12} -10^{13} g cm^{-3}) of the crust.
This deep crustal heating can maintain the temperature of the neutron star interior at a sufficiently high level to explain a persistent thermal X-ray radiation in quiescence (Brown *et al.*, 1998)."

(quotation from the book by Haensel, Potekhin, Yakovlev)

Cooling in soft X-ray transients

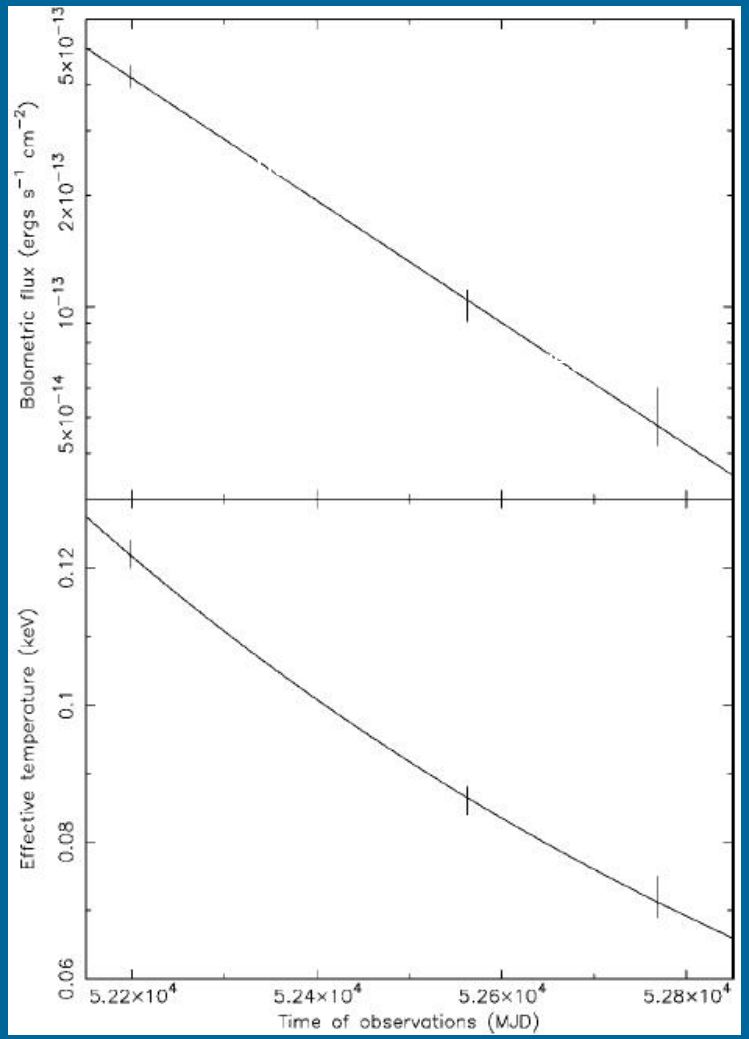

MXB 1659-29
~2.5 years outburst

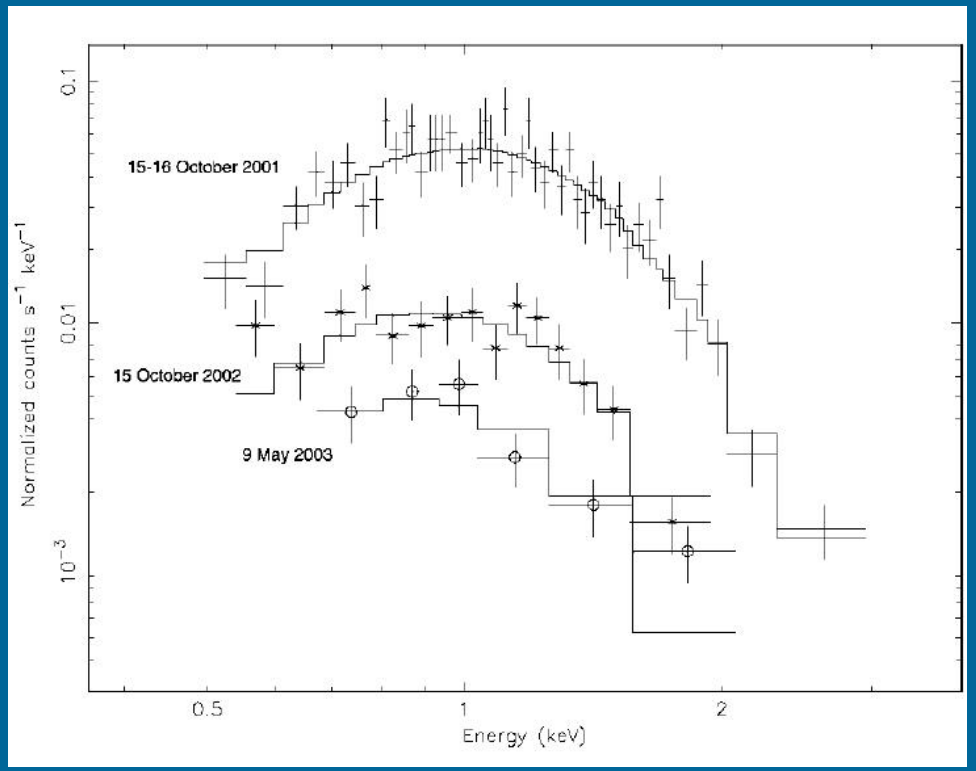

[Wijnands et al. 2004]

Deep crustal heating and cooling

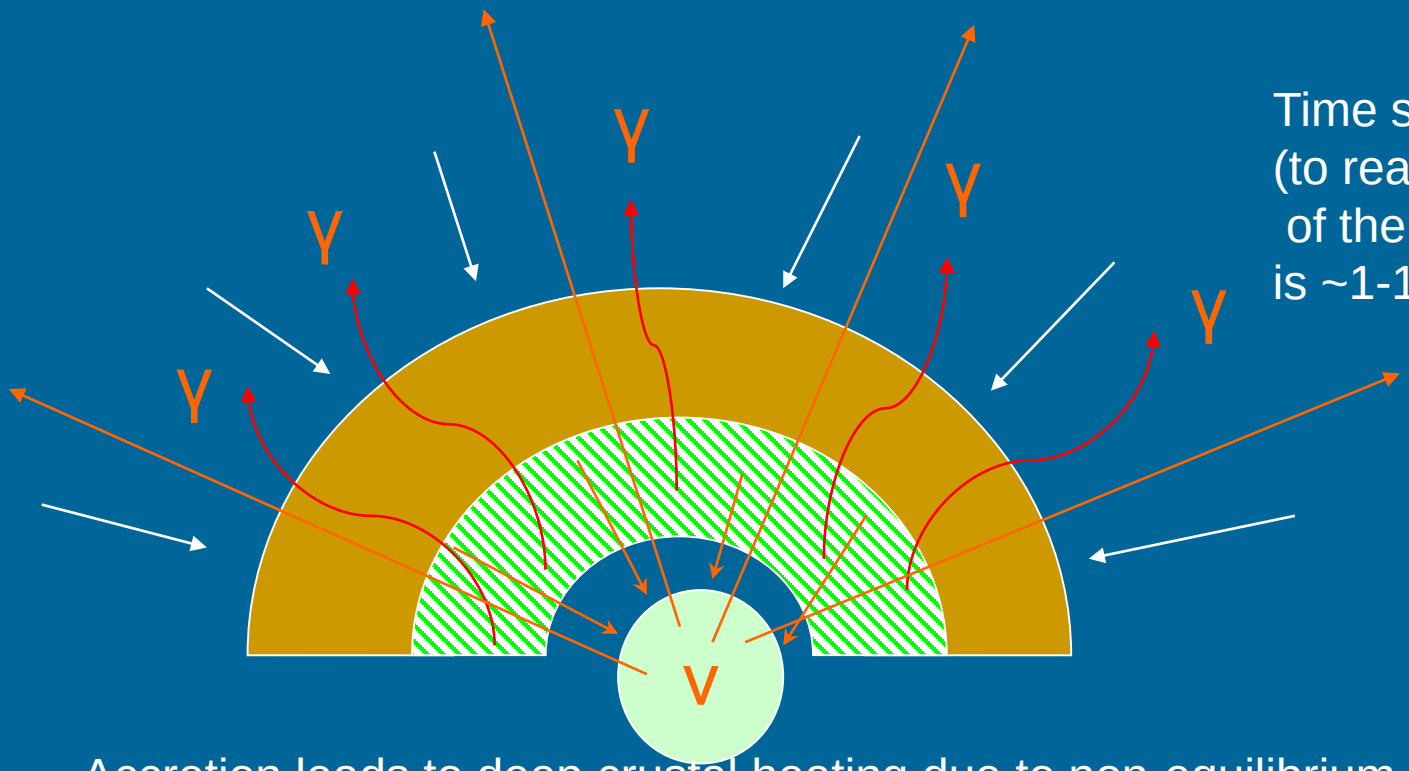

Time scale of cooling
(to reach thermal equilibrium
of the crust and the core)
is ~1-100 years.

To reach the
state “before”
takes ~10^3-10^4 yrs

Accretion leads to deep crustal heating due to non-equilibrium nuclear reactions.
After accretion is off:

- heat is transported inside and emitted by neutrinos
- heat is slowly transported out and emitted by photons

$\rho \sim 10^{12}$-10^{13} g/cm^3

See, for example, Haensel, Zdunik arxiv:0708.3996

New calculations appeared very recently 0811.1791 Gupta et al.

Pycnonuclear reactions

Let us give an example from Haensel, Zdunik (1990)

We start with ^{56}Fe
Density starts to increase

$^{56}Fe \rightarrow ^{56}Cr$
$^{56}Fe + e^- \rightarrow ^{56}Mn + \nu_e$
$^{56}Mn + e^- \rightarrow ^{56}Cr + \nu_e$

At ^{56}Ar: neutron drip
$^{56}Ar + e^- \rightarrow ^{56}Cl + \nu_e$
$^{56}Cl \rightarrow ^{55}Cl + n$
$^{55}Cl + e^- \rightarrow ^{55}S + \nu_e$
$^{55}S \rightarrow ^{54}S + n$
$^{54}S \rightarrow ^{52}S + 2n$

Then from ^{52}S we have a chain:
$^{52}S \rightarrow ^{46}Si + 6n - 2e^- + 2\nu_e$

As Z becomes smaller
the Coulomb barrier decreases.
Separation between
nuclei decreases, vibrations grow.
$^{40}Mg \rightarrow ^{34}Ne + 6n - 2e^- + 2\nu_e$

At Z=10 (Ne) pycnonuclear reactions start.

$^{34}Ne + ^{34}Ne \rightarrow ^{68}Ca$
$^{36}Ne + ^{36}Ne \rightarrow ^{72}Ca$

Then a heavy nuclei can react again:
$^{72}Ca \rightarrow ^{66}Ar + 6n - 2e^- + 2\nu_e$

$^{48}Mg + ^{48}Mg \rightarrow ^{96}Cr$
$^{96}Cr \rightarrow ^{88}Ti + 8n - 2e^- + 2\nu_e$

See a review in 1803.03818

Crust composition and reactions

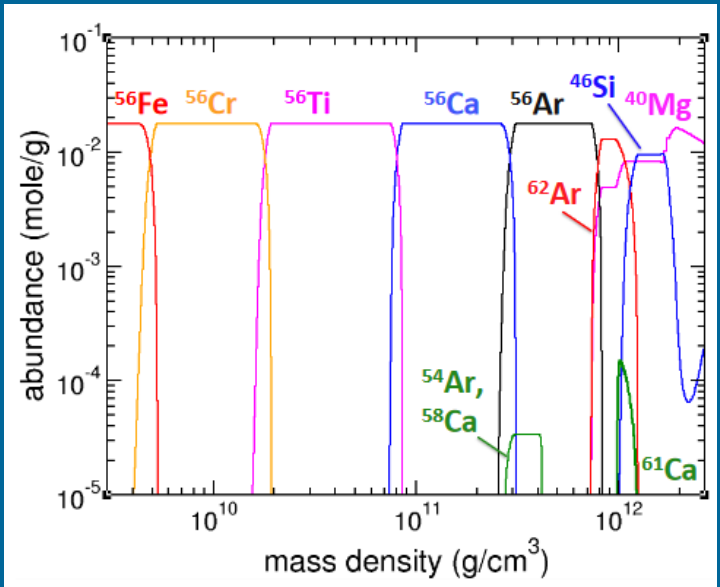

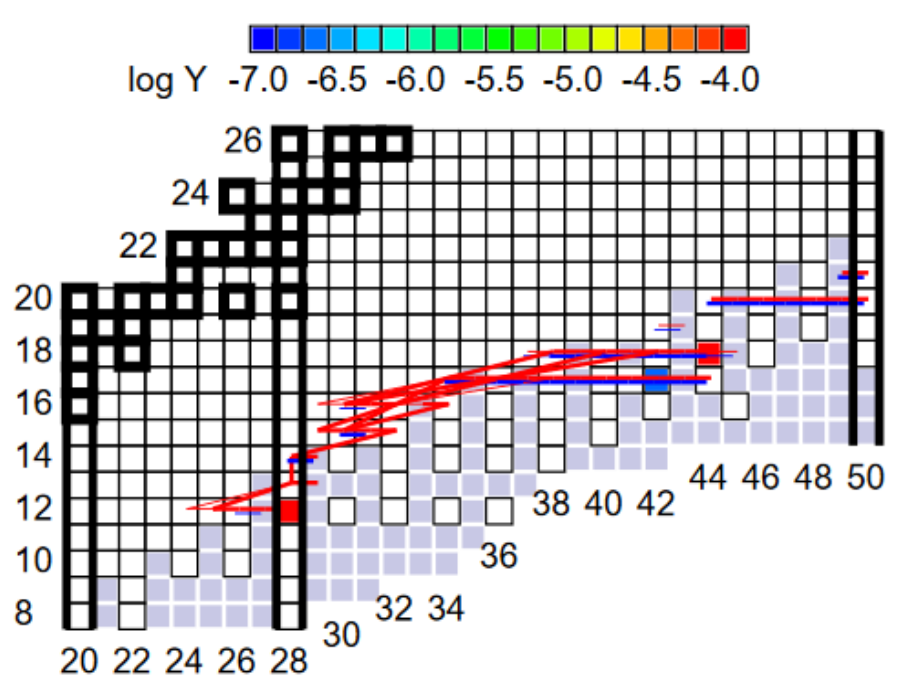

Transition	P^a	ρ^b	$\mu_e{}^c$	$X_n{}^d$
^{56}Fe→^{56}Cr	3.4×10^{27}	4.9×10^{9}	6.2	$<10^{-25}$
^{56}Cr→^{56}Ti	1.7×10^{28}	1.8×10^{10}	9.6	$<10^{-25}$
^{56}Ti→^{56}Ca	1.1×10^{29}	8.1×10^{10}	15.6	$<10^{-25}$
^{56}Ca→^{56}Ar,^{54}Ar,^{58}Ca	5.5×10^{29}	2.9×10^{11}	23.3	1.2×10^{-18}
^{56}Ar,^{54}Ar,^{58}Ca→^{56}Ar	8.3×10^{29}	4.2×10^{11}	25.9	7.2×10^{-20}
^{56}Ar→^{40}Mg,^{62}Ar	1.8×10^{30}	7.8×10^{11}	31.6	5.4×10^{-8}
^{40}Mg,^{62}Ar→^{40}Mg,^{48}Si	2.3×10^{30}	1.1×10^{12}	33.5	0.13
^{40}Mg,^{48}Si→^{40}Mg	4.2×10^{30}	2.8×10^{12}	37.1	0.54

1803.03818

Energy release vs. density and impurity

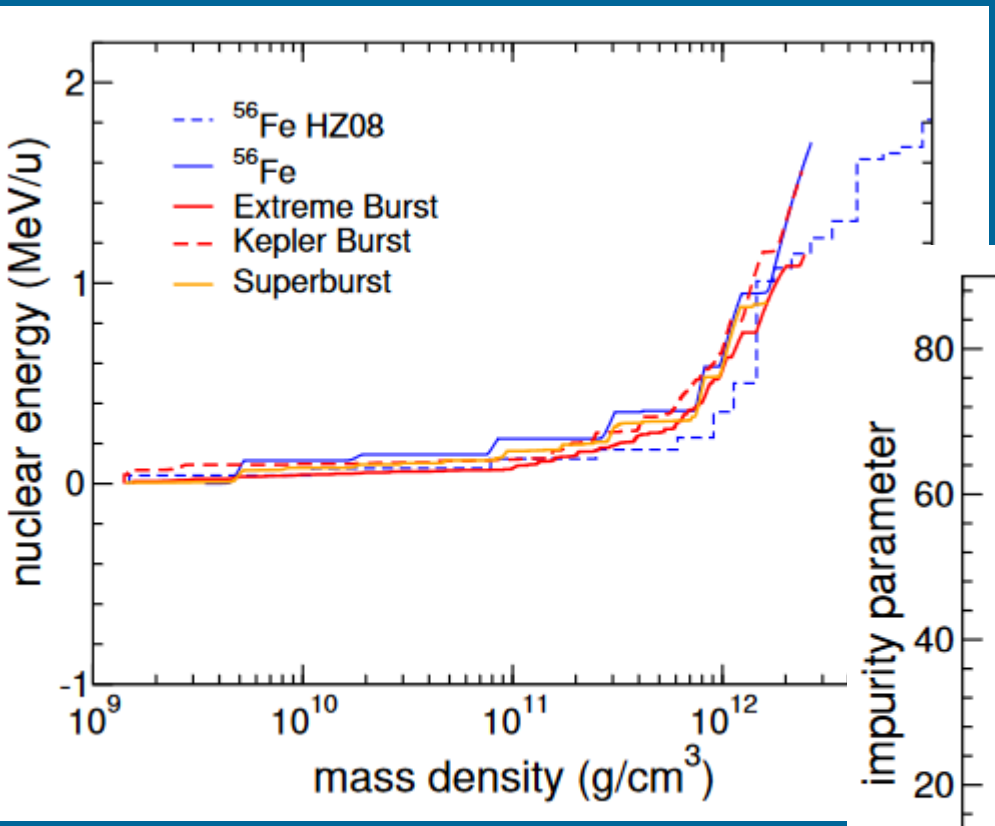

$$Q_{\rm imp} = \sum_i Y_i (Z_i - \langle Z \rangle)^2 / \sum_i Y_i$$

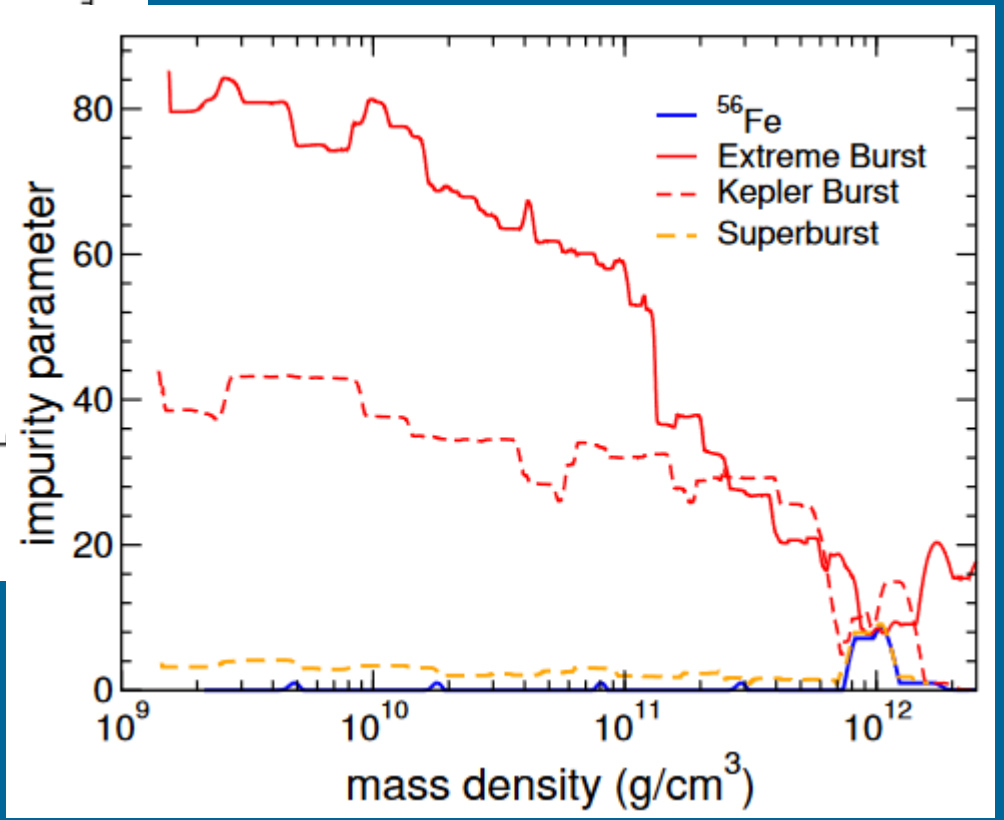

1803.03818

A simple model

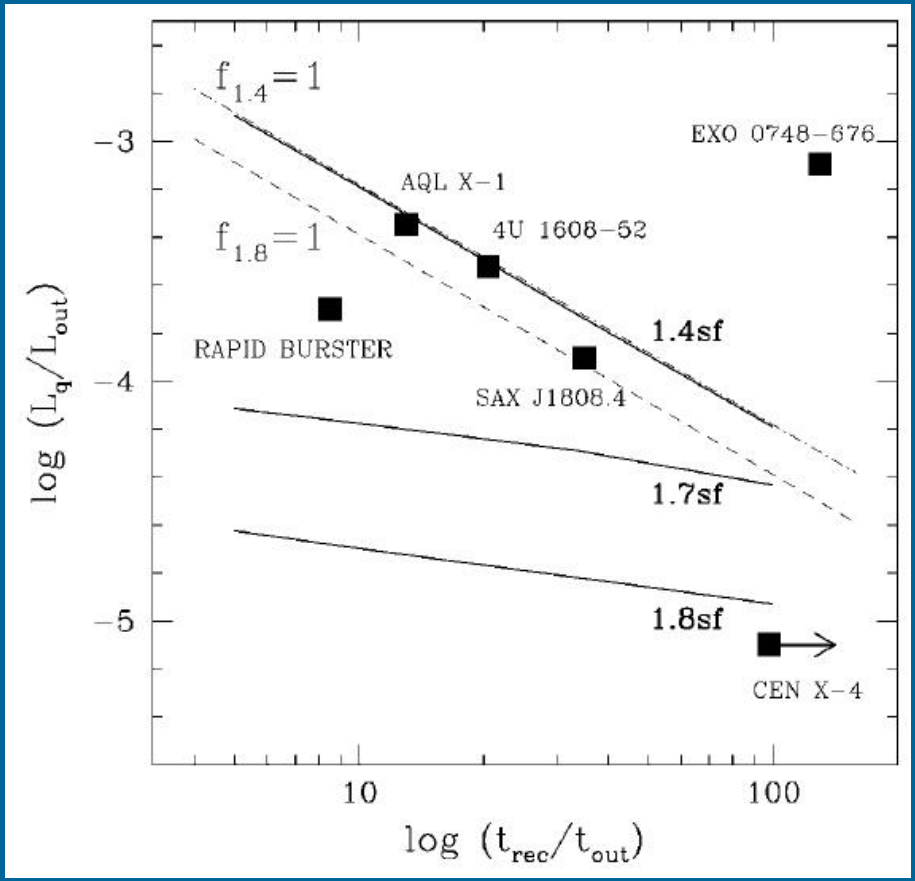

t_{rec} – time interval between outbursts
t_{out} – duration of an outburst
L_q – quiescent luminosity
L_{out} – luminosity during an outburst

Dashed lines corresponds to the case when all energy is emitted from a surface by photons.

$$L_q \sim \frac{Q_{\rm nuc}}{m_u}\langle \dot{M} \rangle \sim 6 \times 10^{32} \frac{\langle \dot{M} \rangle}{10^{-11}\ M_\odot\ {\rm yr}^{-1}}\ {\rm ergs\ s}^{-1}$$

[Colpi et al. 2001]

Deep crustal heating

~1.9 Mev per accreted nucleon
Crust is not in thermal equilibrium with the core.
After accretion is off the crust cools down and finally reach equilibrium with the core.

(see a recent model in 1202.3378)

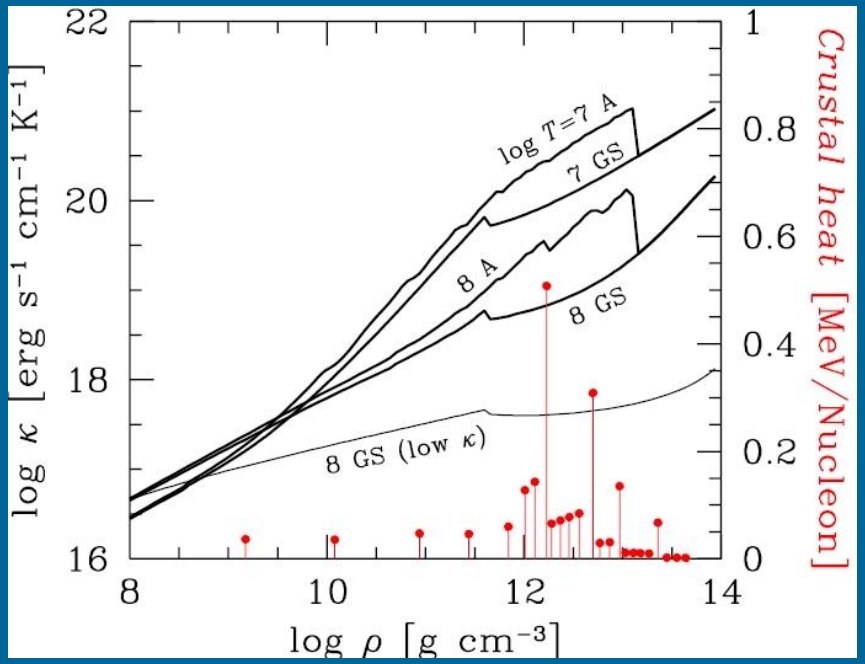

KS 1731-260

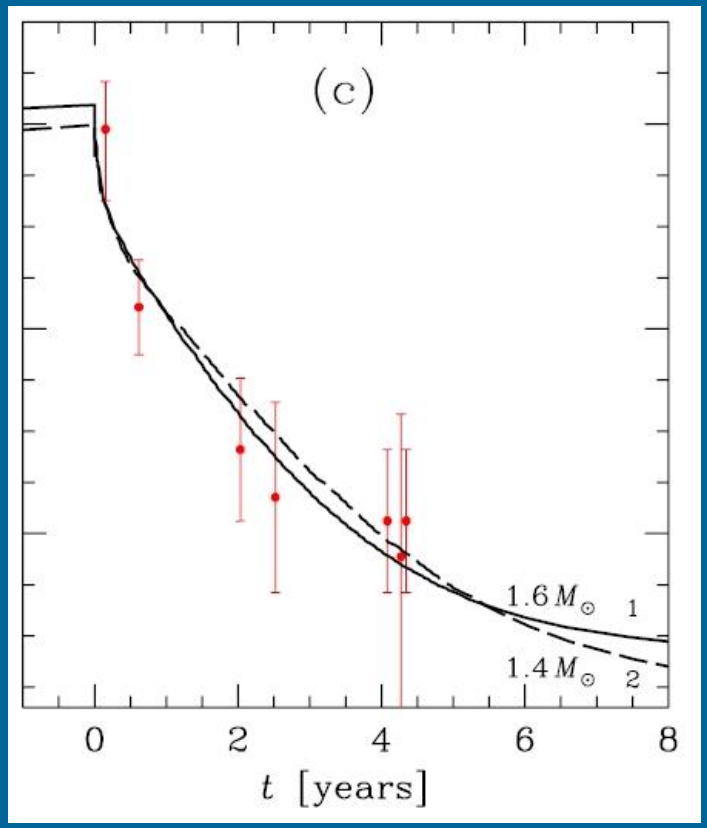

[Shternin et al. 2007]

See new results and discussion in 1702.08452

Visible cooling of a NS in a binary

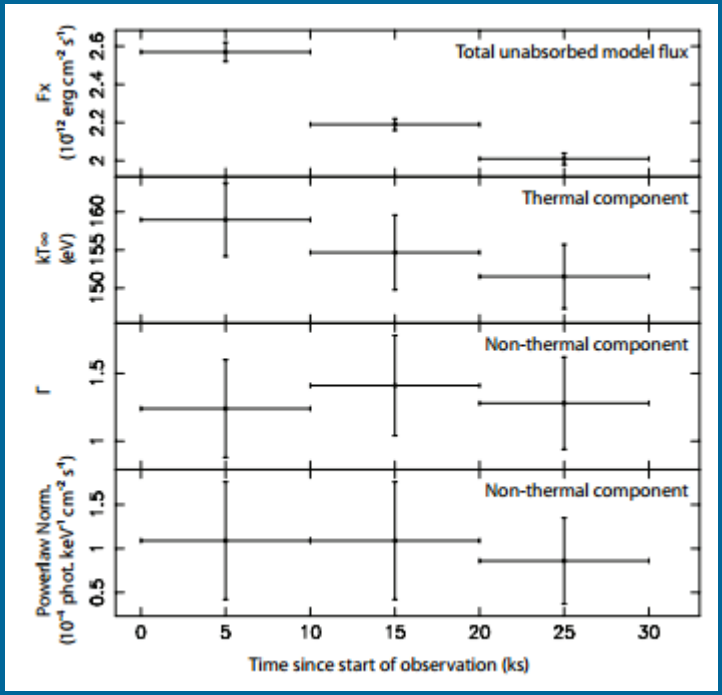

XTE J1709–267

The authors interpret this as cooling of a layer located at a column density of $y \simeq 5\times10^{12}$ g cm^{-2} ($\simeq$50 m inside the neutron star), which is just below the ignition depth of superbursts.

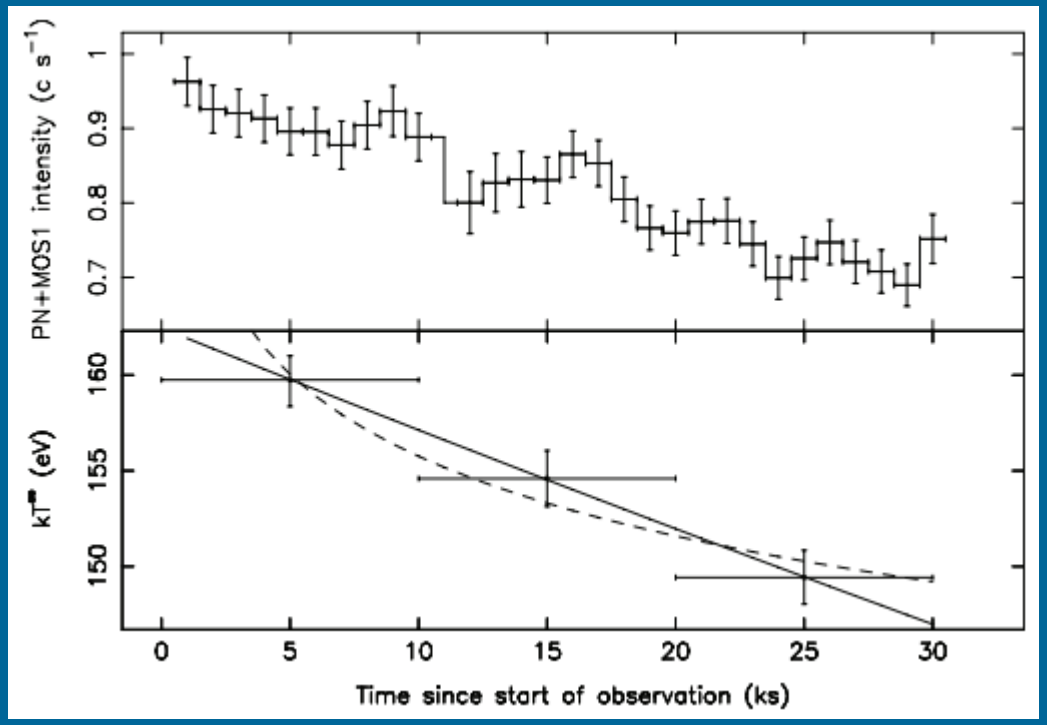

1212.1453

Fitting cooling of known sources

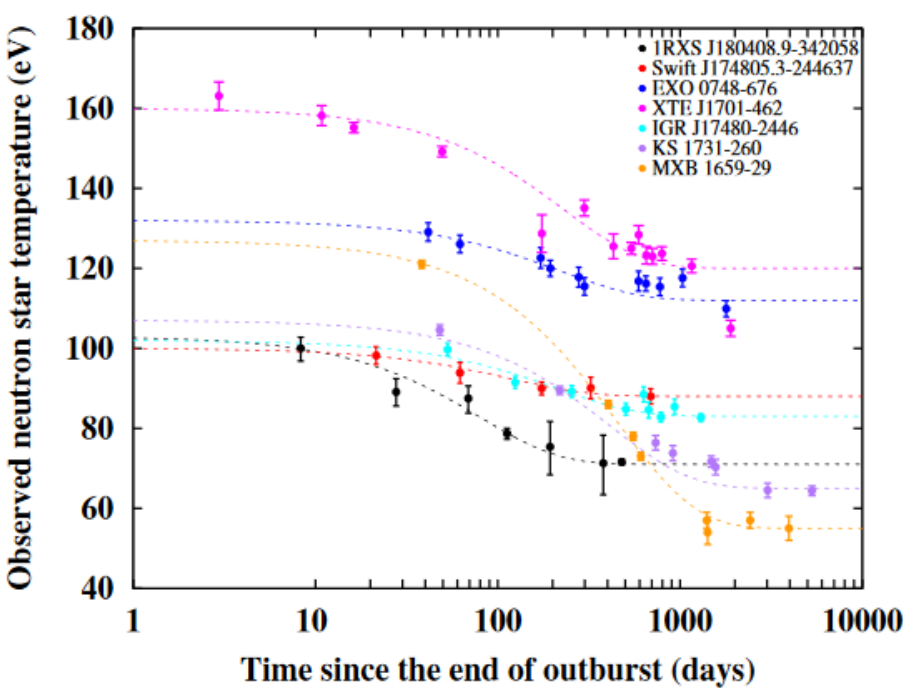

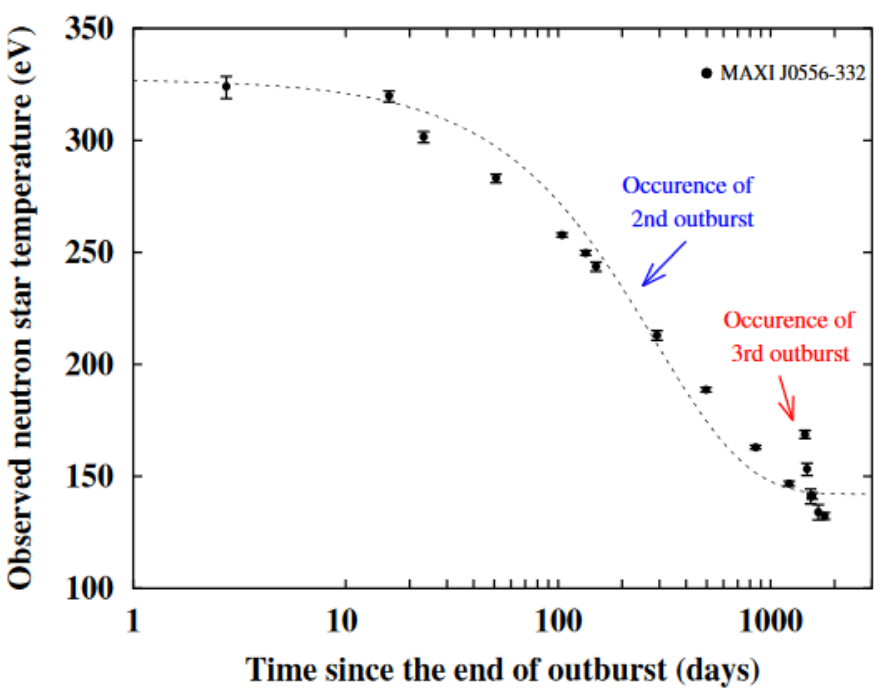

Different systems allow to probe different regimes of cooling and different layers of the crust.

1709.07034

Direct Urca in a cooling NS

MXB 1659-29

$$2.1 \times 10^{38}\ \mathrm{erg\ s^{-1}}\ \tilde{T}_8^6$$

$$C = 10^{37}\ \mathrm{erg\ K^{-1}}\ \tilde{T}_8.$$

About 1% of the core volume available for direct URCA.

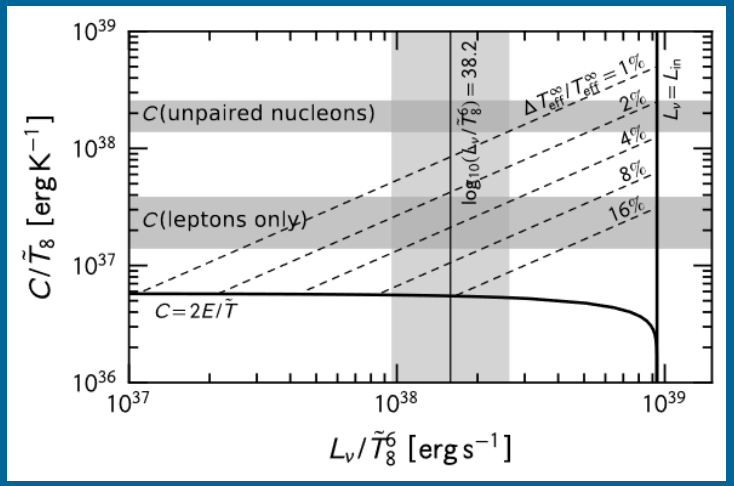

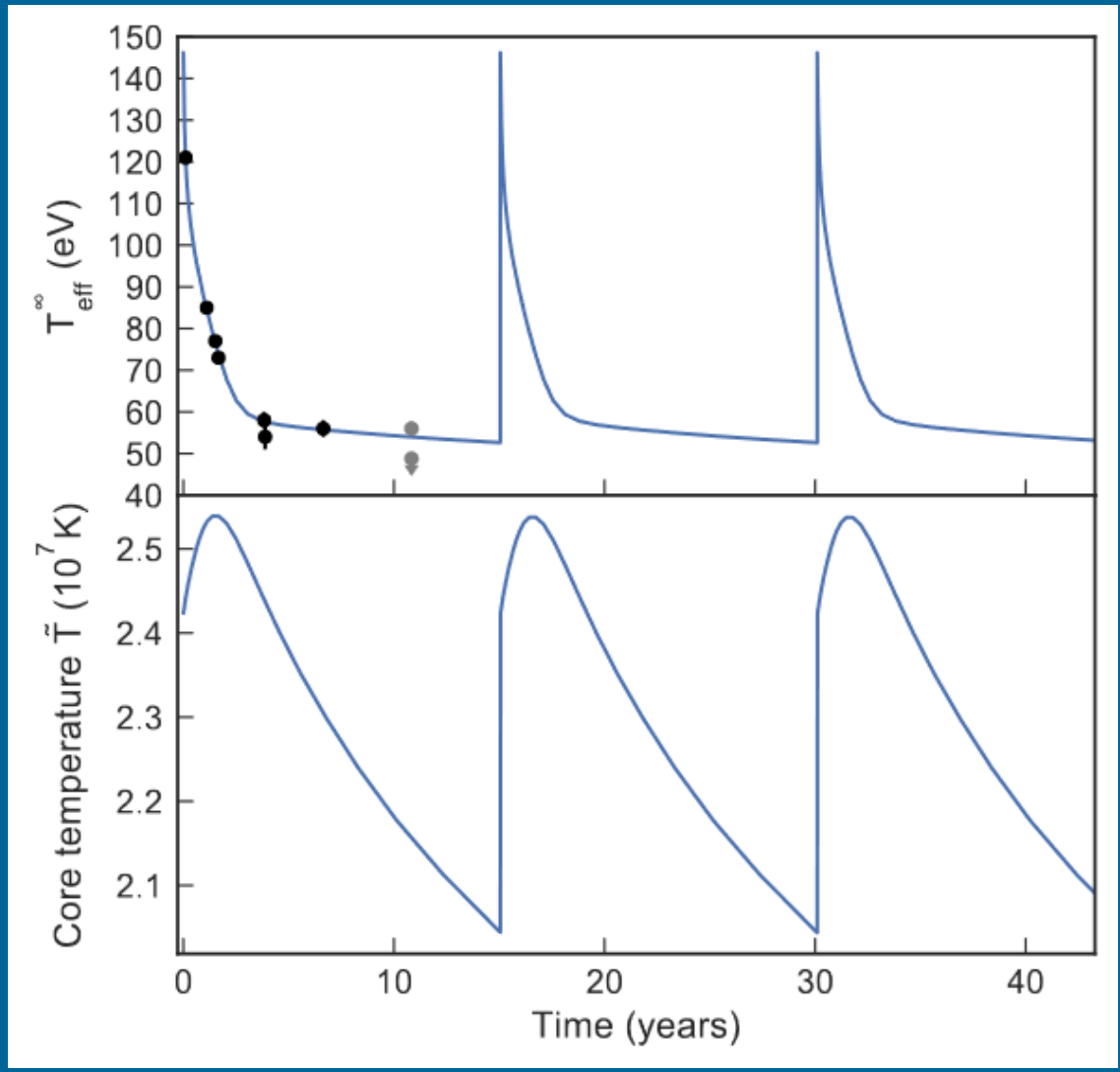

1801.00041

Cooling and crustal properties

RXS J180408.9−342058
LMXB

Rapid cooling
down to thermal
equilibrium between
the core and the crust.

Deep crustal heating +
shallow heat source.

The origin of the shallow
heating is unknown.

No DURCA.

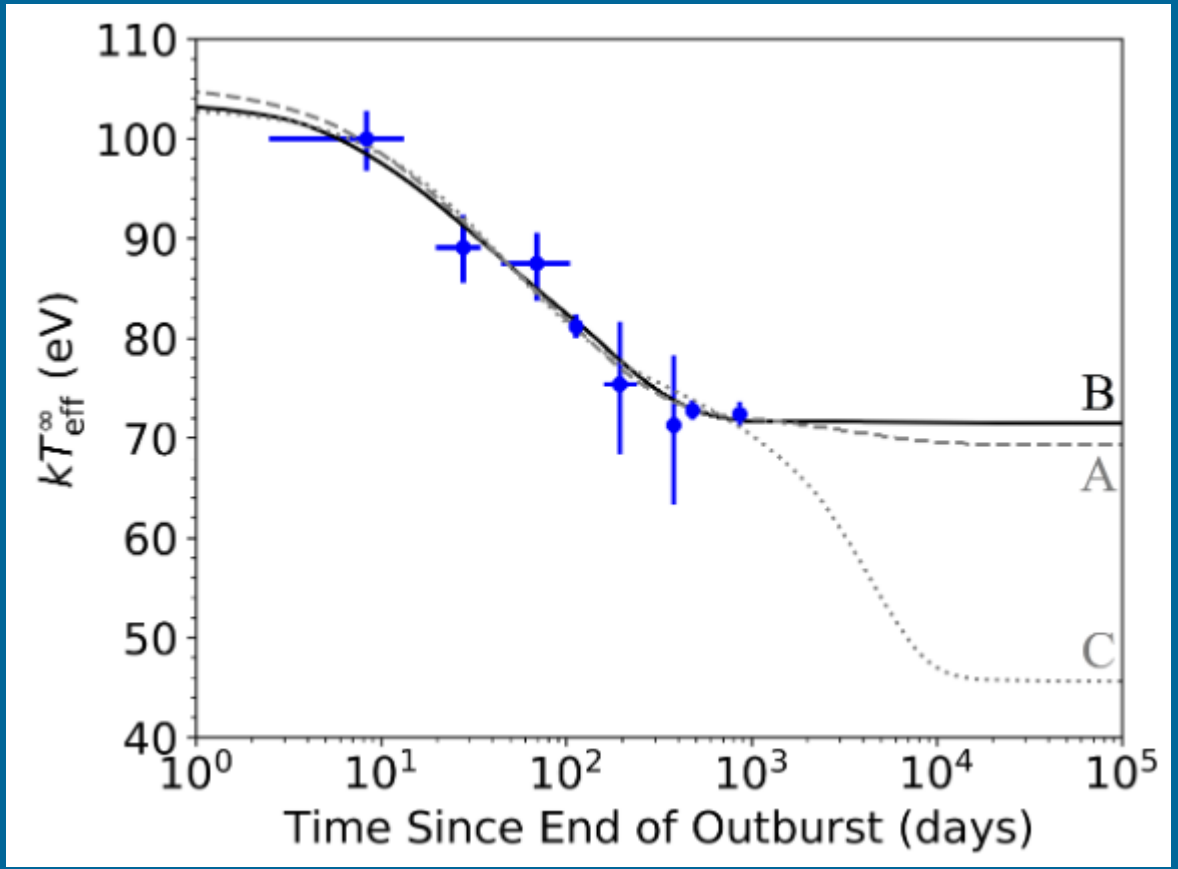

1802.05282

Aql X-1 transient

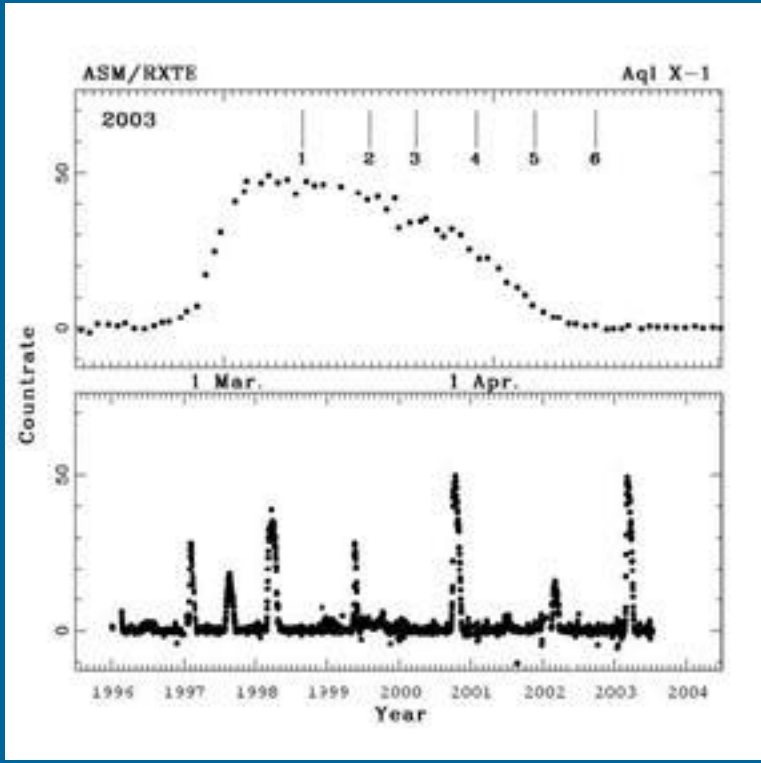

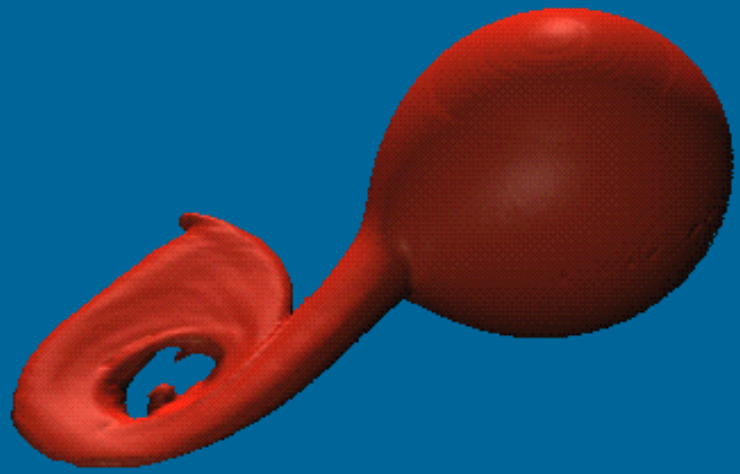

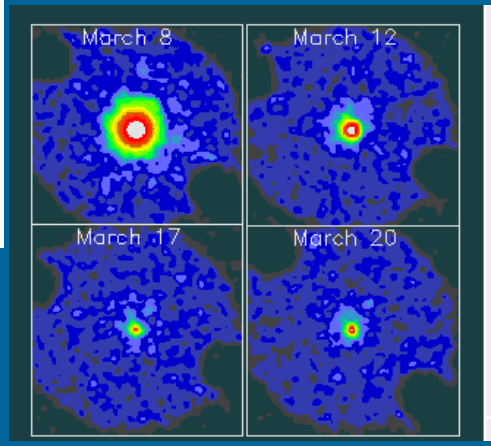

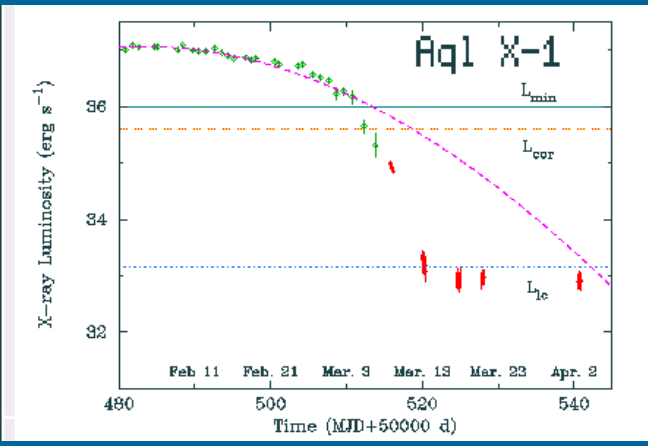

A NS with a K star.
The NS is the hottest among SXTs.

Aql X-1 modeling

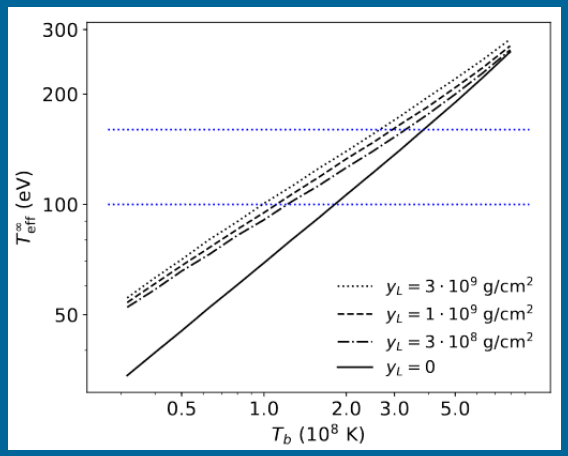

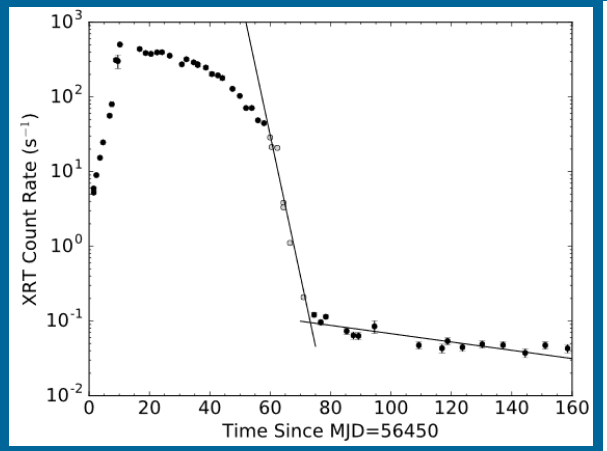

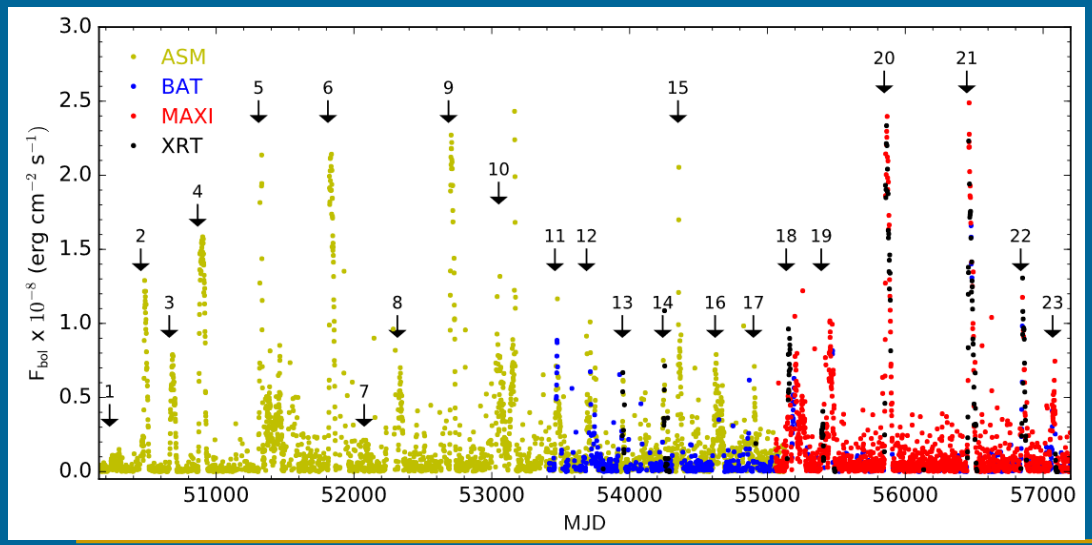

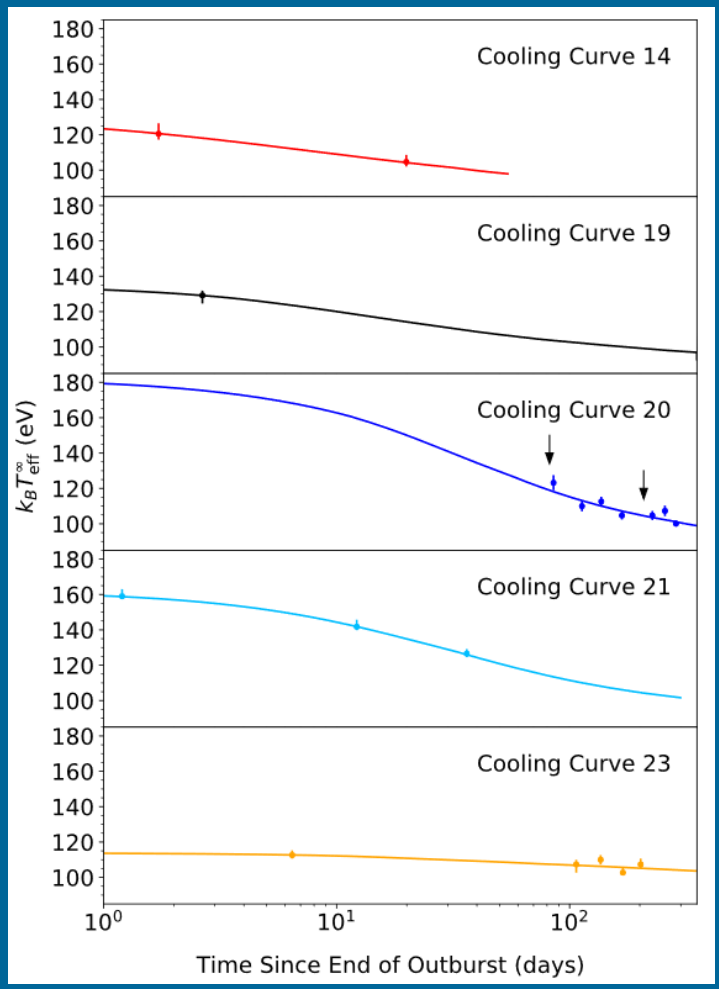

1802.06081

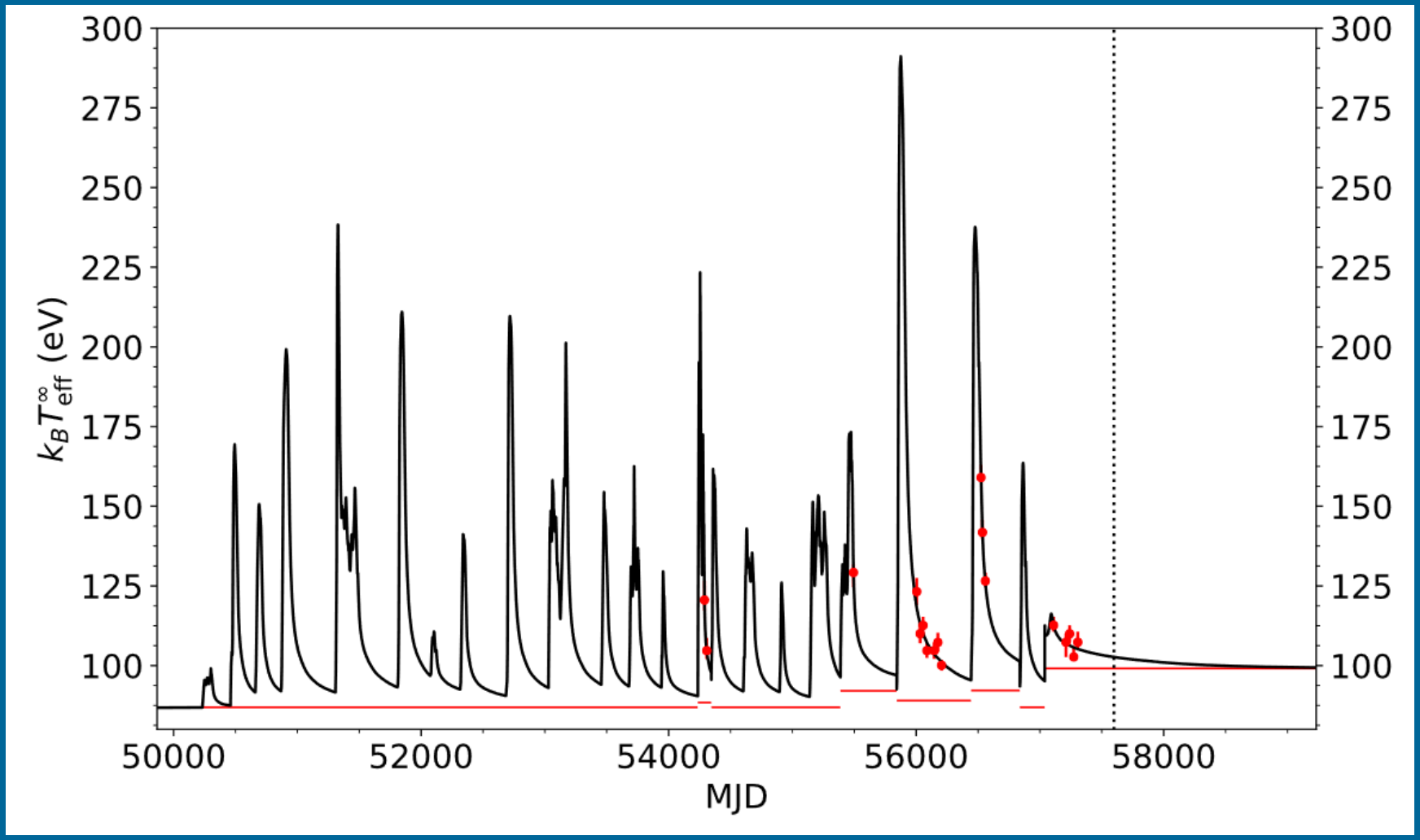
300
275
250
225
200
175
150
125
100
$k_B T^{\infty}_{\rm eff}$ (eV)
50000
52000
54000
56000
58000
MJD

1802.06081

Testing models with SXT

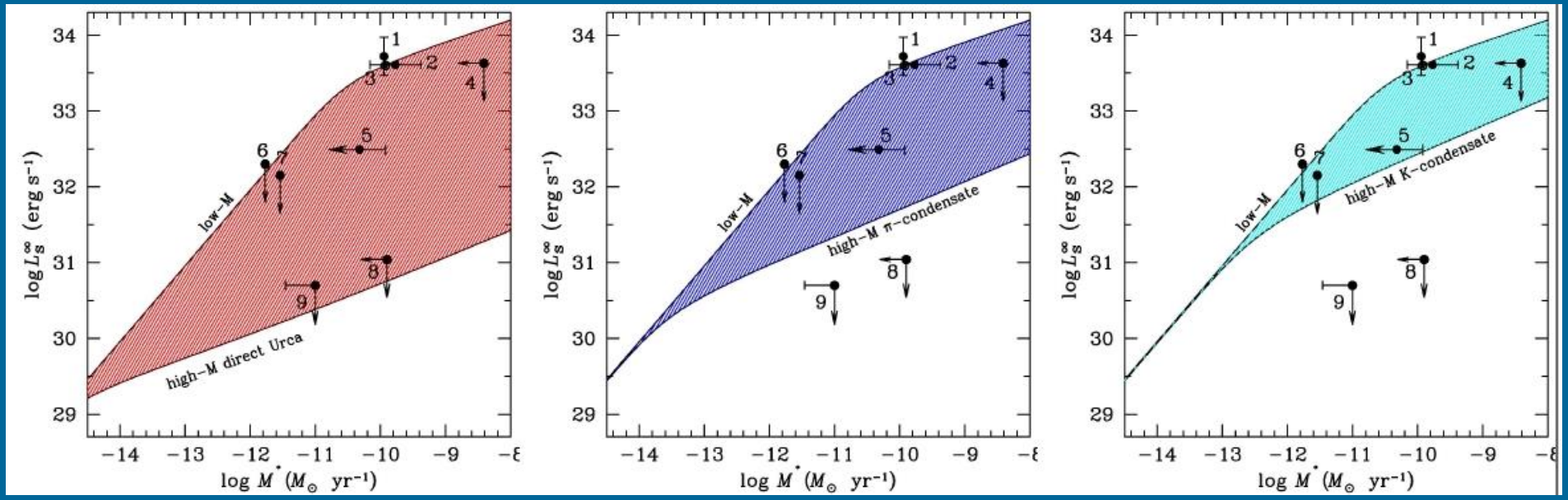

SXTs can be very important in confronting theoretical cooling models with data.

[from a presentation by Haensel, figures by Yakovlev and Levenfish]

Theory vs. Observations: SXT and isolated cooling NSs

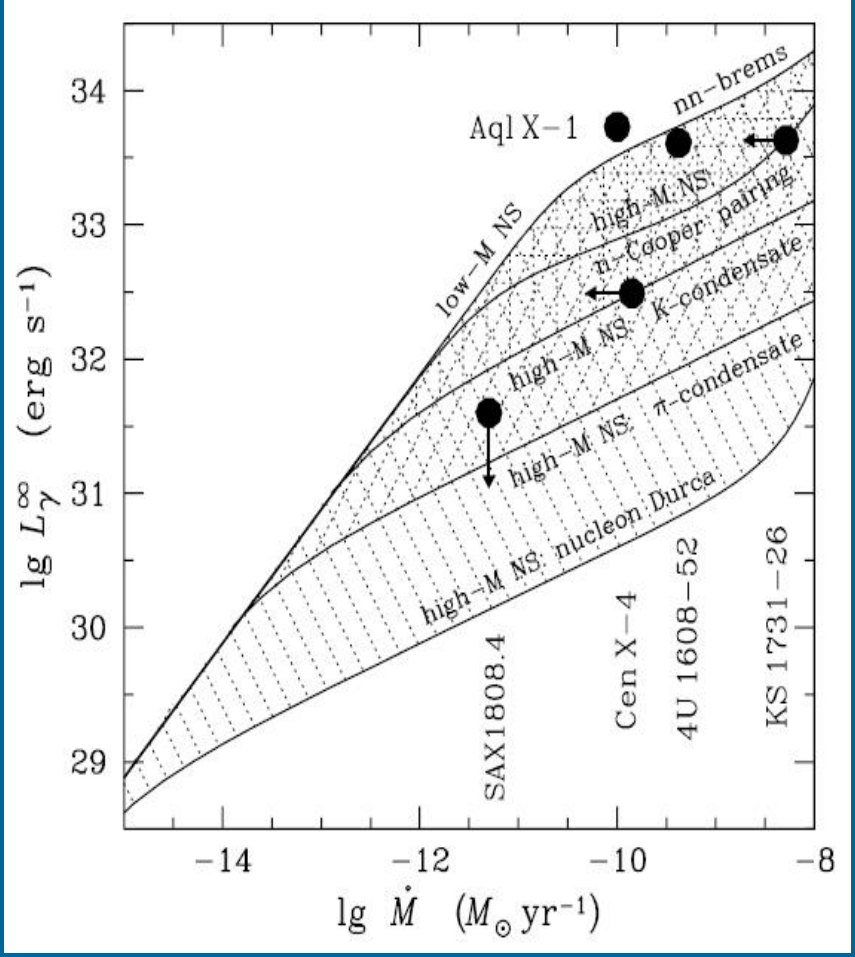

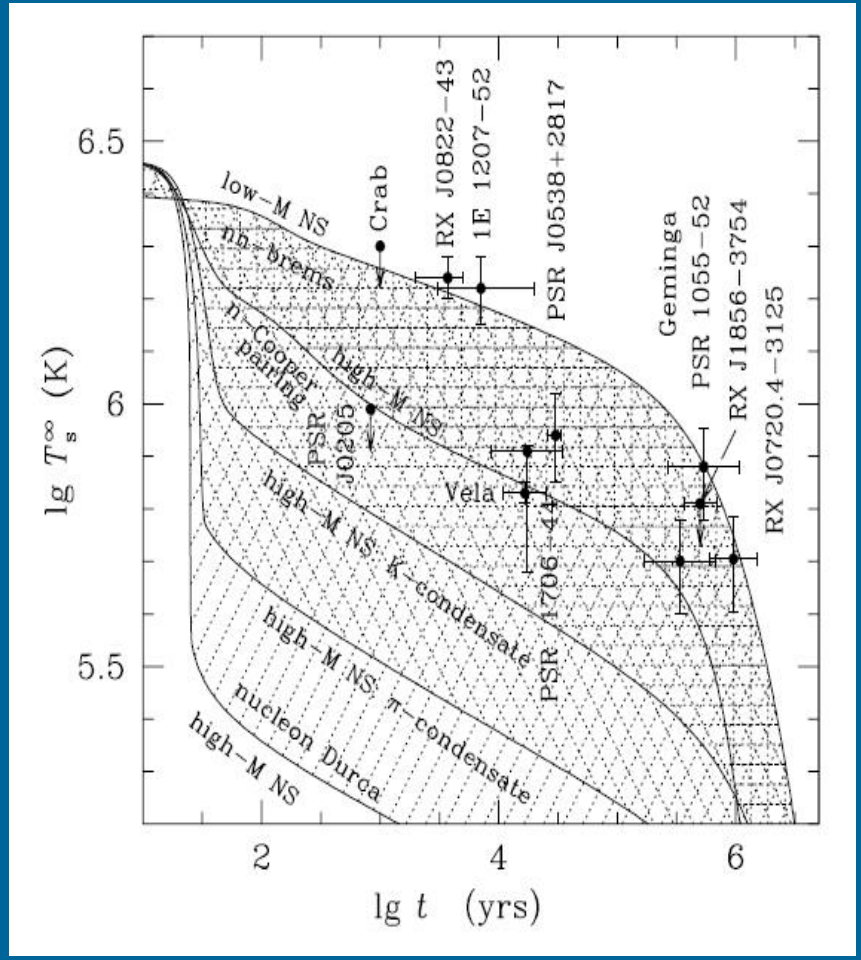

[Yakovlev et al. astro-ph/0501653]

Systems with deep crustal heating

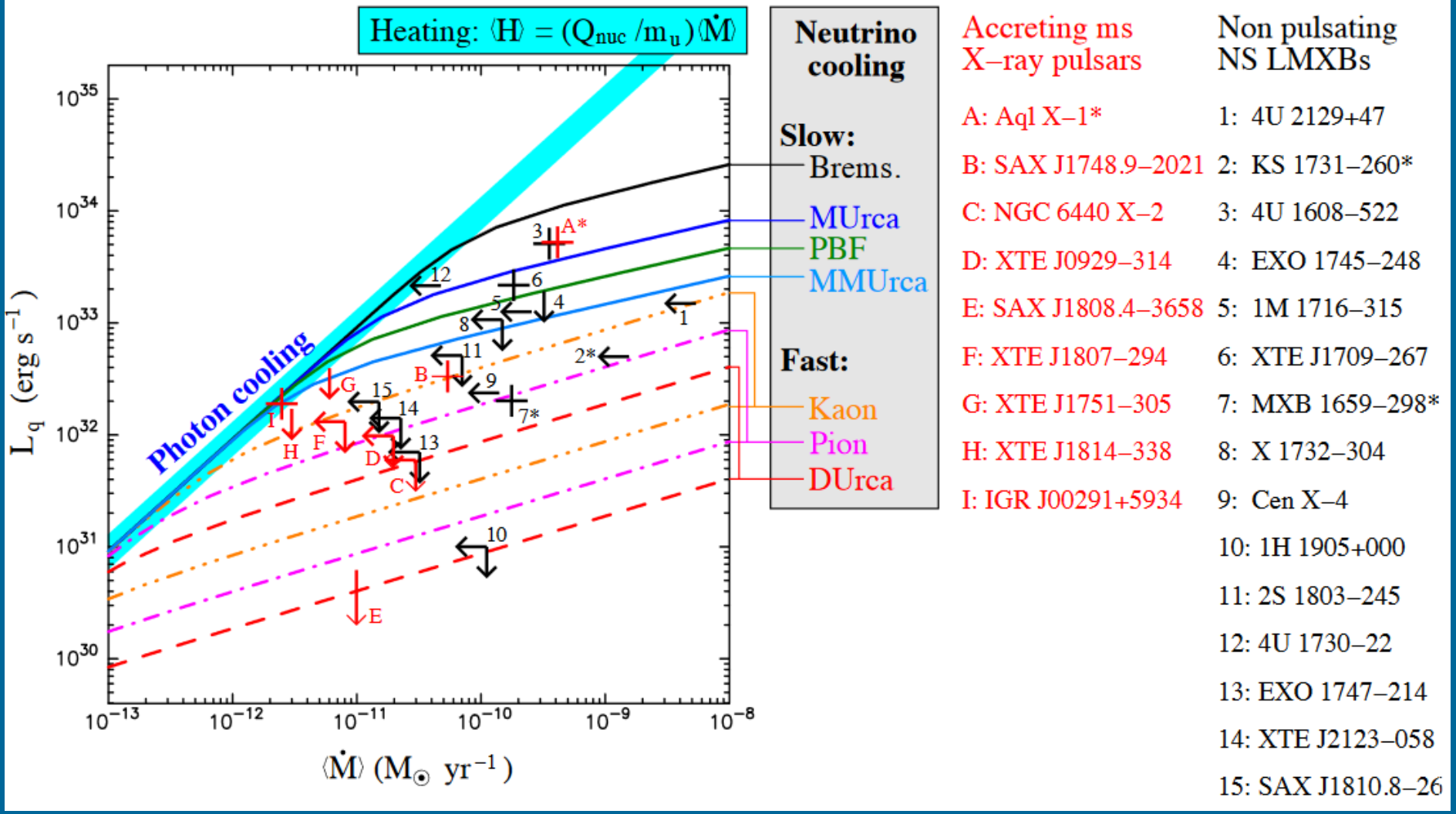

1709.07034

Conclusions

- NSs are born hot, and then cool down at first due to neutrino emission, and after – due to photon emission
- Observations of cooling provide important information about processes at high density at the NS interiors
- Two types of objects are studied:
  - isolated cooling NSs
  - NSs in soft X-ray transients

Papers to read

- Or astro-ph/0403657
  Or astro-ph/0508056
  Or astro-ph/0402143 ←
  Or 1507.06186
- arXiv:astro-ph/9906456 УФН 1999
- 1709.07034 – about cooling of NSs in binaries

M-R from spectral fit

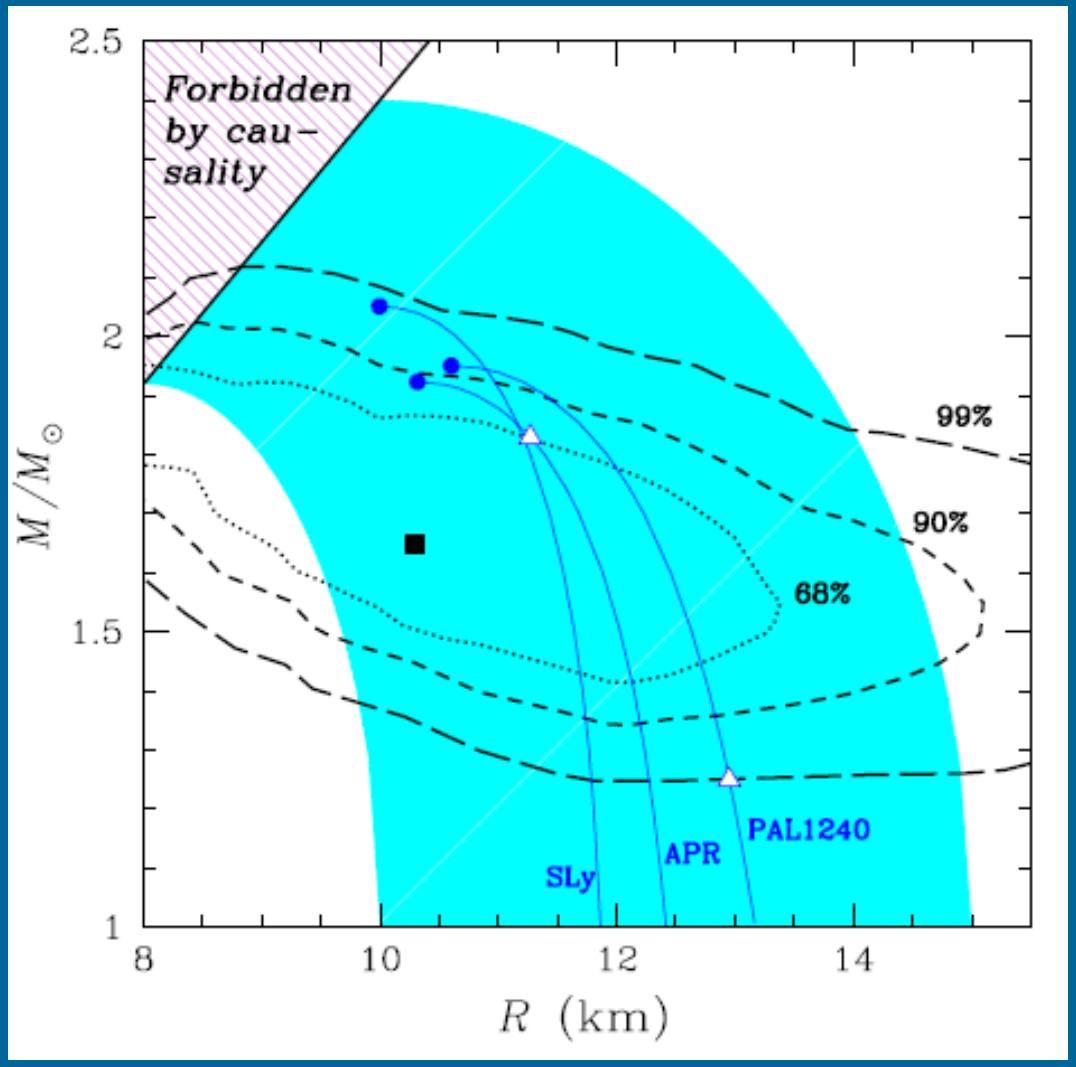

1010.1154

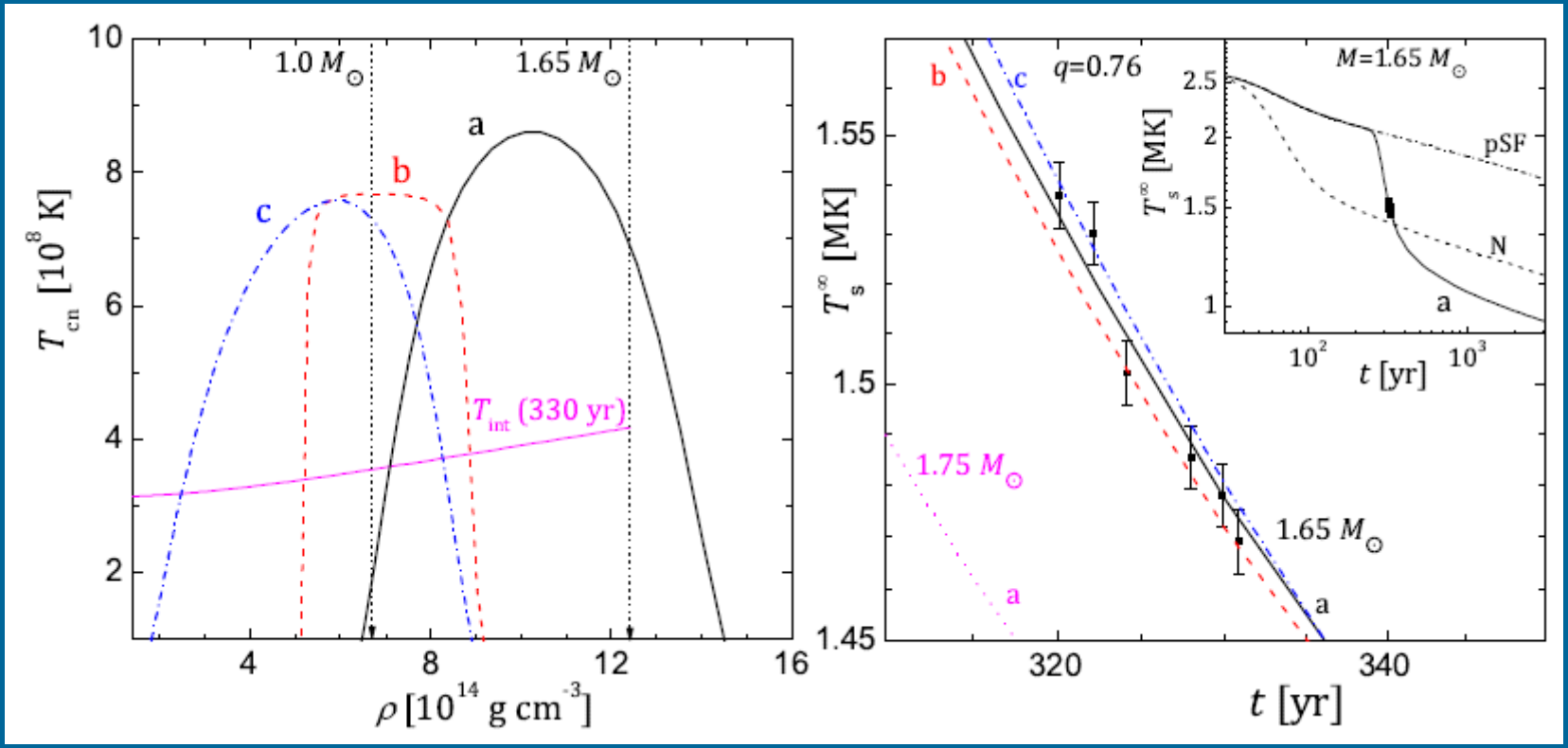
1.0 $M_\odot$
1.65 $M_\odot$
a
b
c
T_{int} (330 yr)
T_{cn} [10^8 K]
ρ [10^{14} g cm^{-3}]
q=0.76
1.75 $M_\odot$
1.65 $M_\odot$
T_s^∞ [MK]
t [yr]
M=1.65 $M_\odot$
pSF
N

1012.0045

Suppression in the axial-vector channel

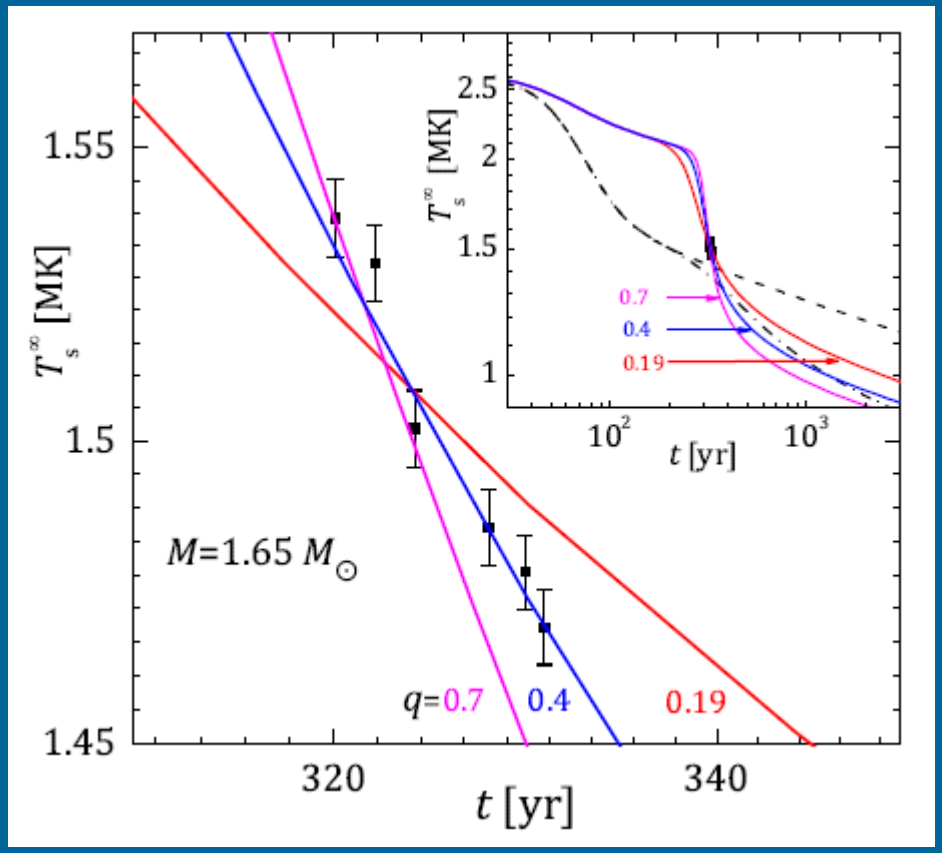

1012.0045

Cooling and grand unification for NSs

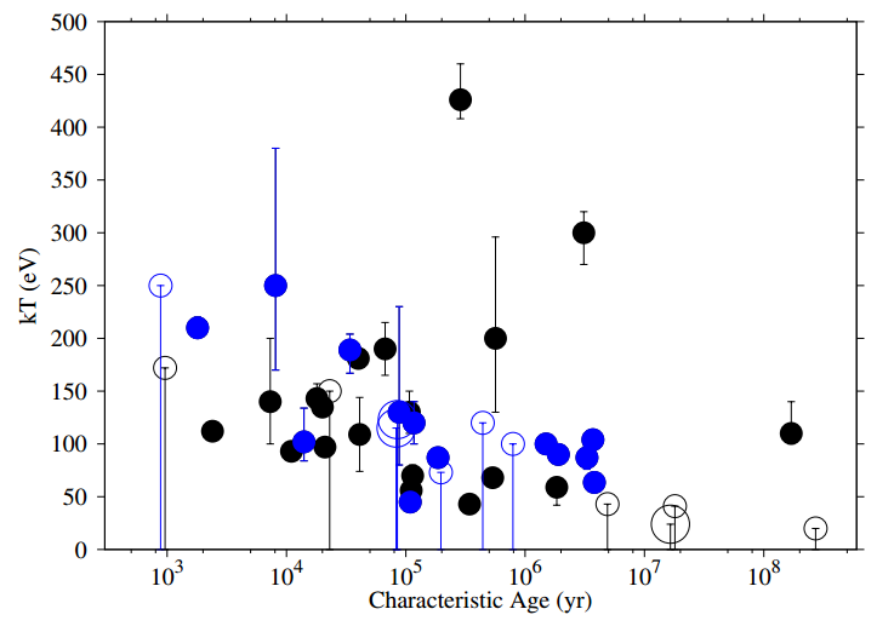

1301.2814

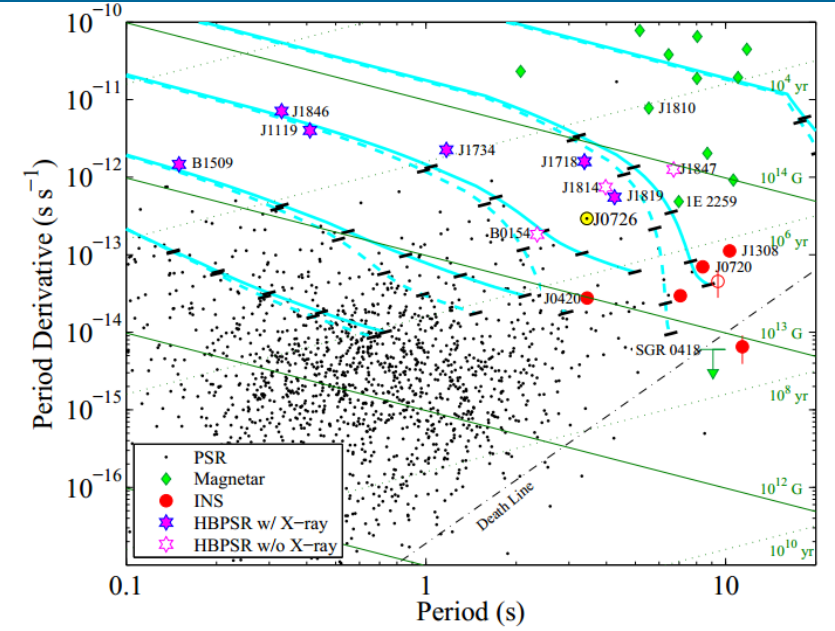

1111.2877

One study shows that highly magnetized NSs can be not hotter than NSs with standard magnetic fields.
Another study demonstrates that some young PSRs with relatively large field are hot, similar to the M7.

Влияние вращения

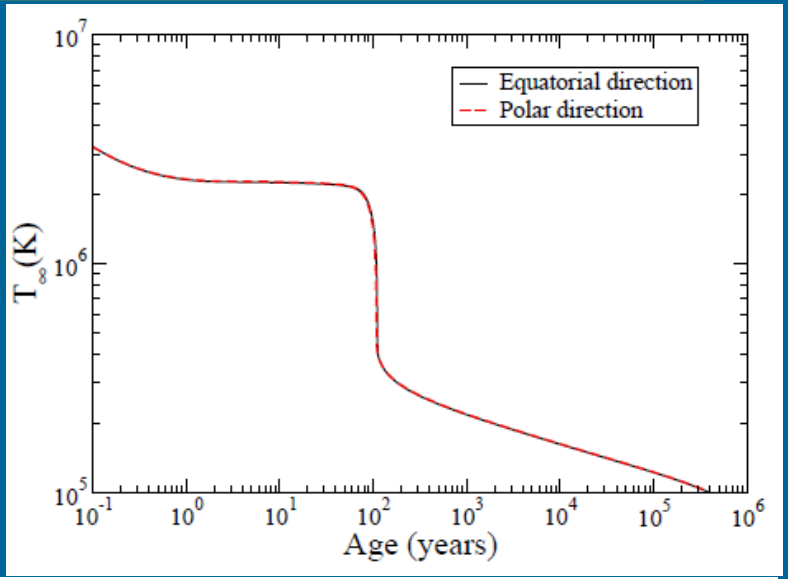

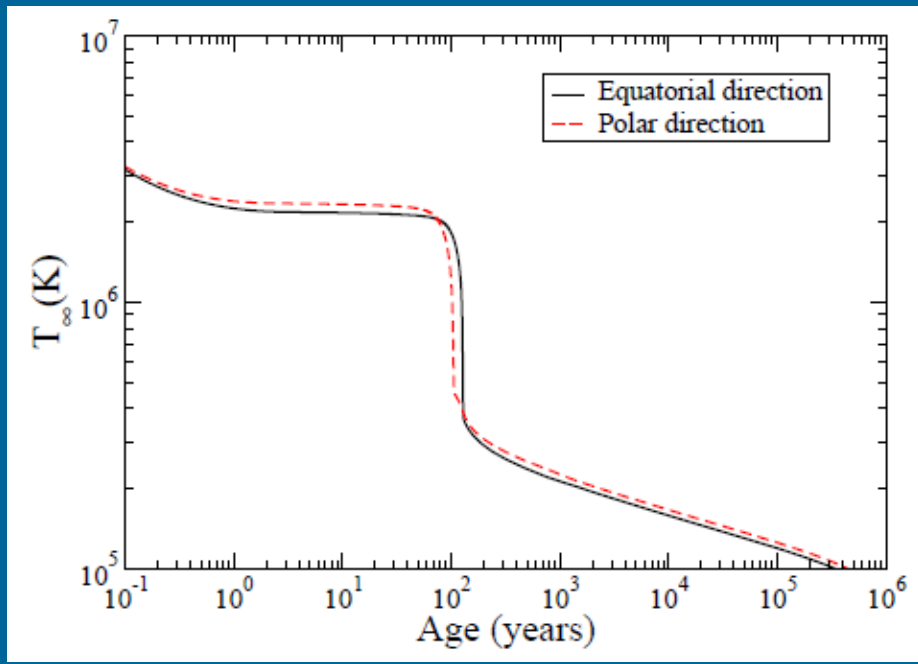

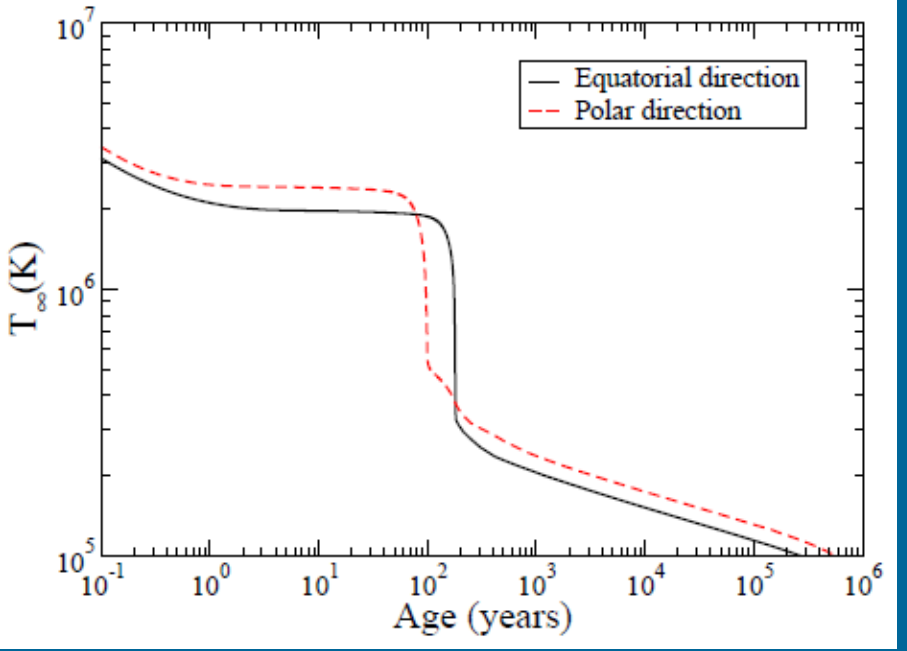

1307.7692

Records

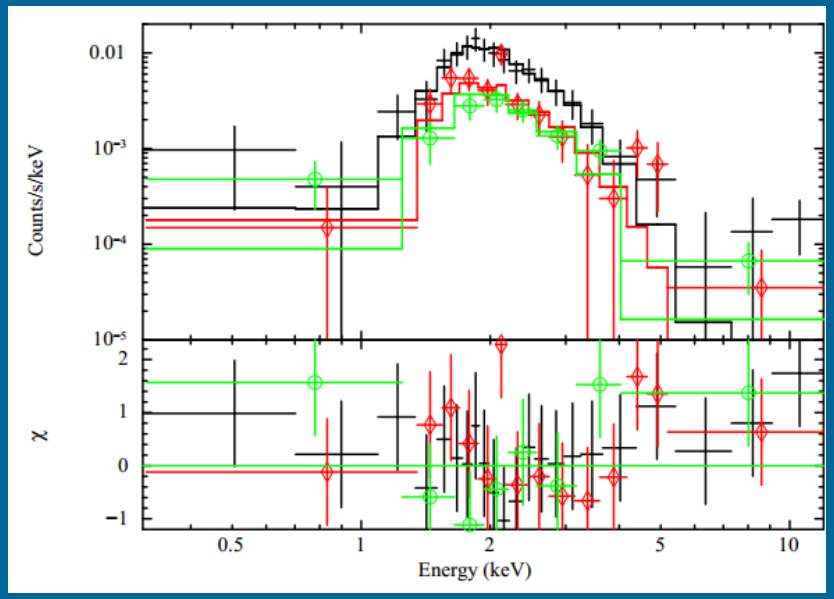

The hottest (in a binary, crustal heating) SAX J1750.8−2900. T~150 eV. 1202.1531

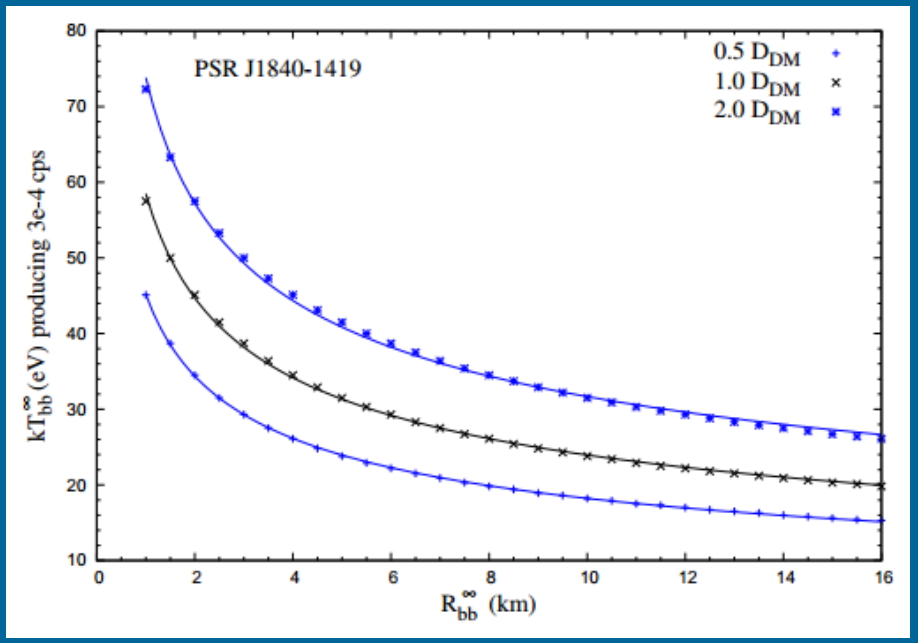

The coldest. Isolated pulsar. T<30 eV
PSR J18401419
1301.2814

Surface emission of neutron stars

NS Radii

- A NS with homogeneous surface temperature and local blackbody emission

$$L = 4\pi R^2 \sigma T^4$$

$$F = \frac{L}{4\pi D^2} = \left(R/D\right)^2 \sigma T^4$$

From dispersion measure

From X-ray spectroscopy

NS Radii - II

- Real life is a trifle more complicated…
  Atmospheres.

- Because of the strong B field
  - Photon propagation different
  - Surface temperature is not homogeneous
  - Local emission may be not exactly planckian

- Gravity effects are important

Uncertainties in temperature

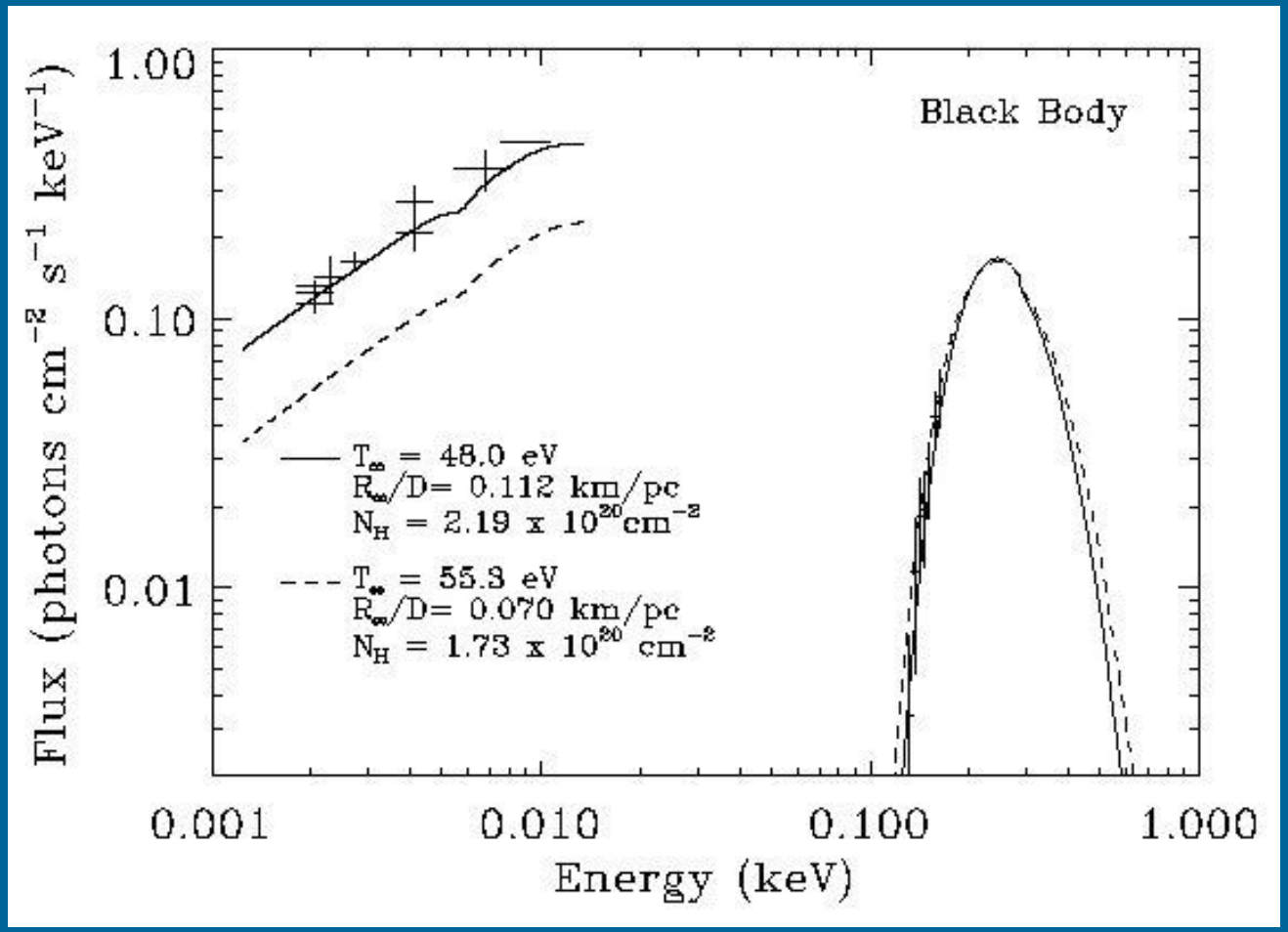

- **Atmospheres (composition)**
- **Magnetic field**
- **Non-thermal contributions to the spectrum**
- **Distance**
- **Interstellar absorption**
- **Temperature distribution**

(Pons et al. astro-ph/0107404)

Non-uniform temperature distribution

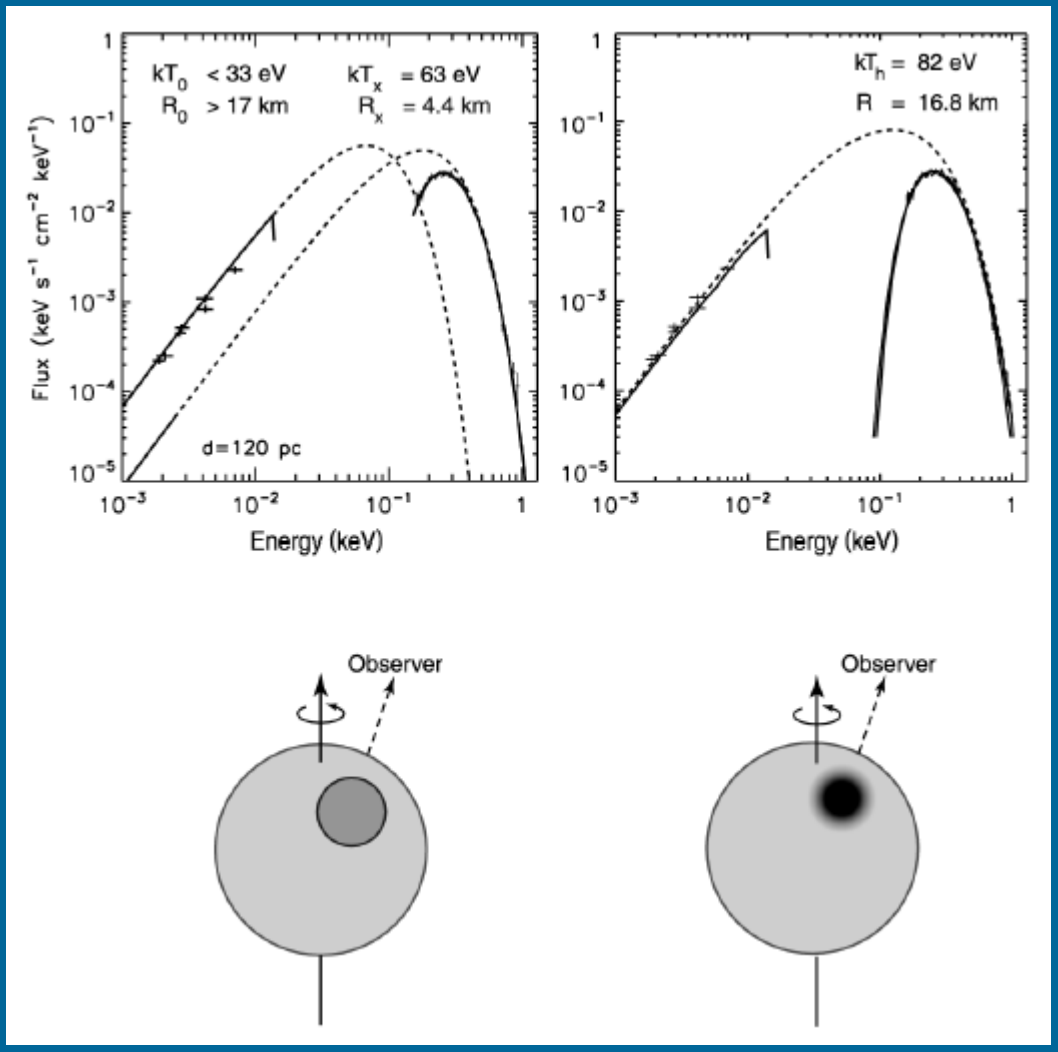

In the case of RX J1856 because of significant (~6) optical excess it was proposed that there is a spot, or there is a continuous temperature gradient.

Trumper astro-ph/0502457

NS Thermal Maps

- Electrons move much more easily along B than across B
- Therma… …opic inside a… …$h\nu_B$ or $\rho >> 10$…
- Envelop… …, B ~ cons… …1D

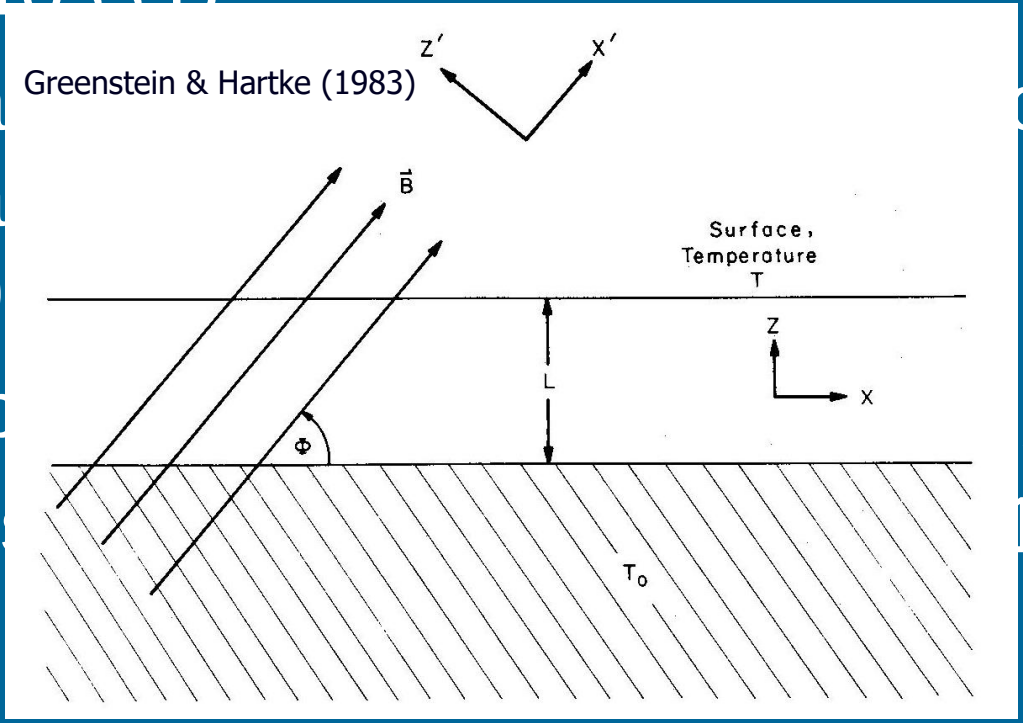

$$T_S = \left[\cos^2\Theta + \left(K_{perp} / K_{par}\right)\sin^2\Theta\right]^{1/4} T_{pole}$$

$$K_{perp} / K_{par} << 1$$

K - conductivity

$$T_S = \left|\cos\Theta\right|^{1/2} T_{pole}$$

Valid for strong fields: $K_{perp} << K_{par}$

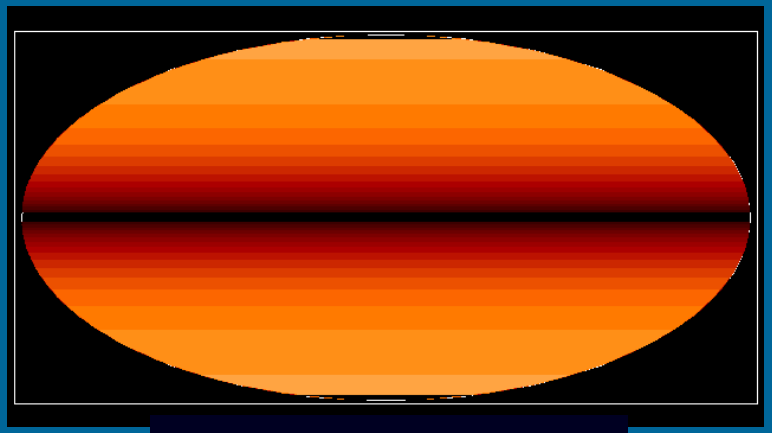

Core centered dipole

Core centered quadrupole

Zane, Turolla astro-ph/0510693

Local Surface Emission

- Much like normal stars NSs are covered by an atmosphere
- Because of enormous surface gravity, $g \approx 10^{14}$ cm/s^2, $h_{atm} \approx$ 1-10 cm ($h_{atm} \sim kT/mg$)
- Spectra depend on g, chemical composition and magnetic field
- Plane-parallel approximation (locally)

Atmospheric composition

A_1 The lightest

A_2 Light

A_3 Heavy

A_4 The heaviest

As $h<<R$ we can consider only flat layers.

Due to strong gravity an atmosphere is expected to be separated: lighter elements on top.

Because of that even a small amount of light elements (hydrogen) results in its dominance in the properties of the atmosphere.

10^{-20} solar mass of hydrogen is enough to form a hydrogen atmosphere.

See astro-ph/ 0702426

- Free-free absorption dominates

$$\kappa_\nu \propto \nu^{-3}, h\nu >> kT$$

- High energy photons decouple deeper in the atmosphere where T is higher

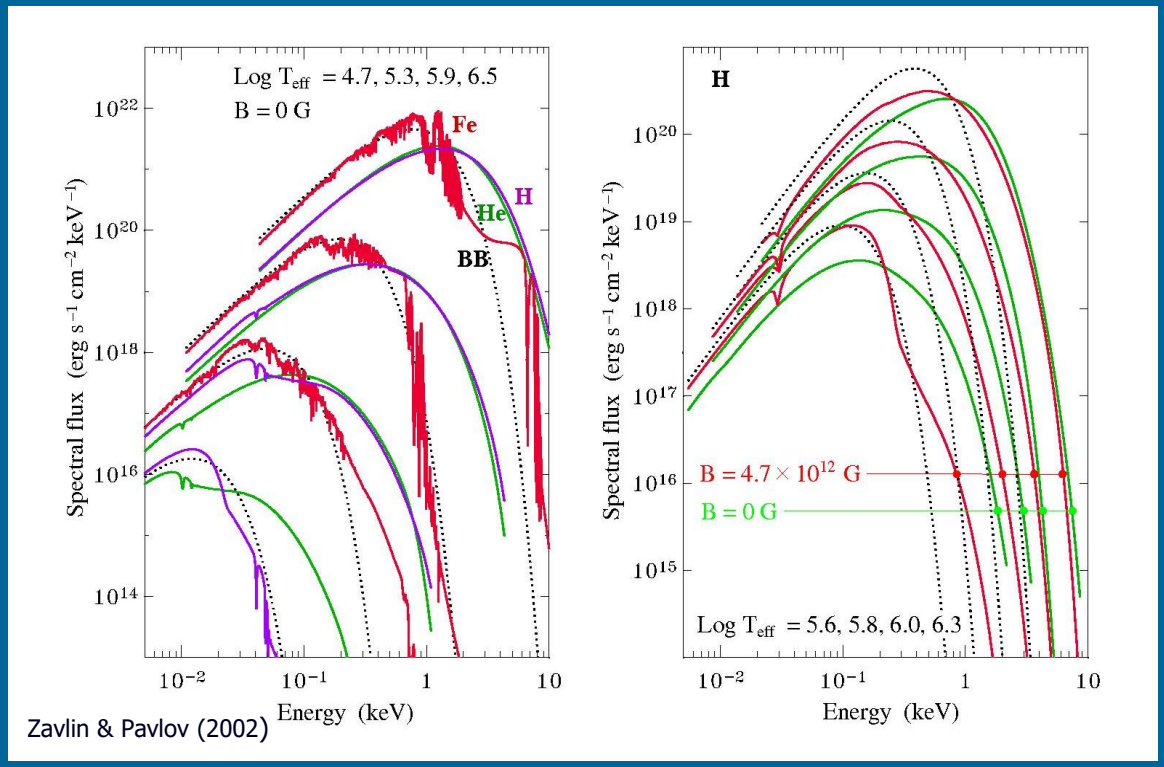

Zavlin & Pavlov (2002)

Rapid decrease of the light-element opacities with energy (~E^{-3})

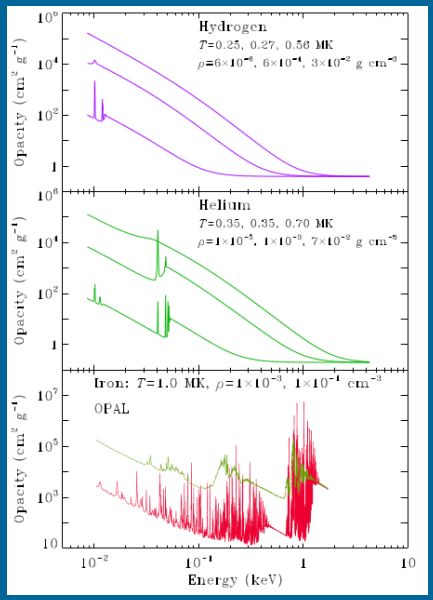

astro-ph/0206025

Emission from different atmospheres

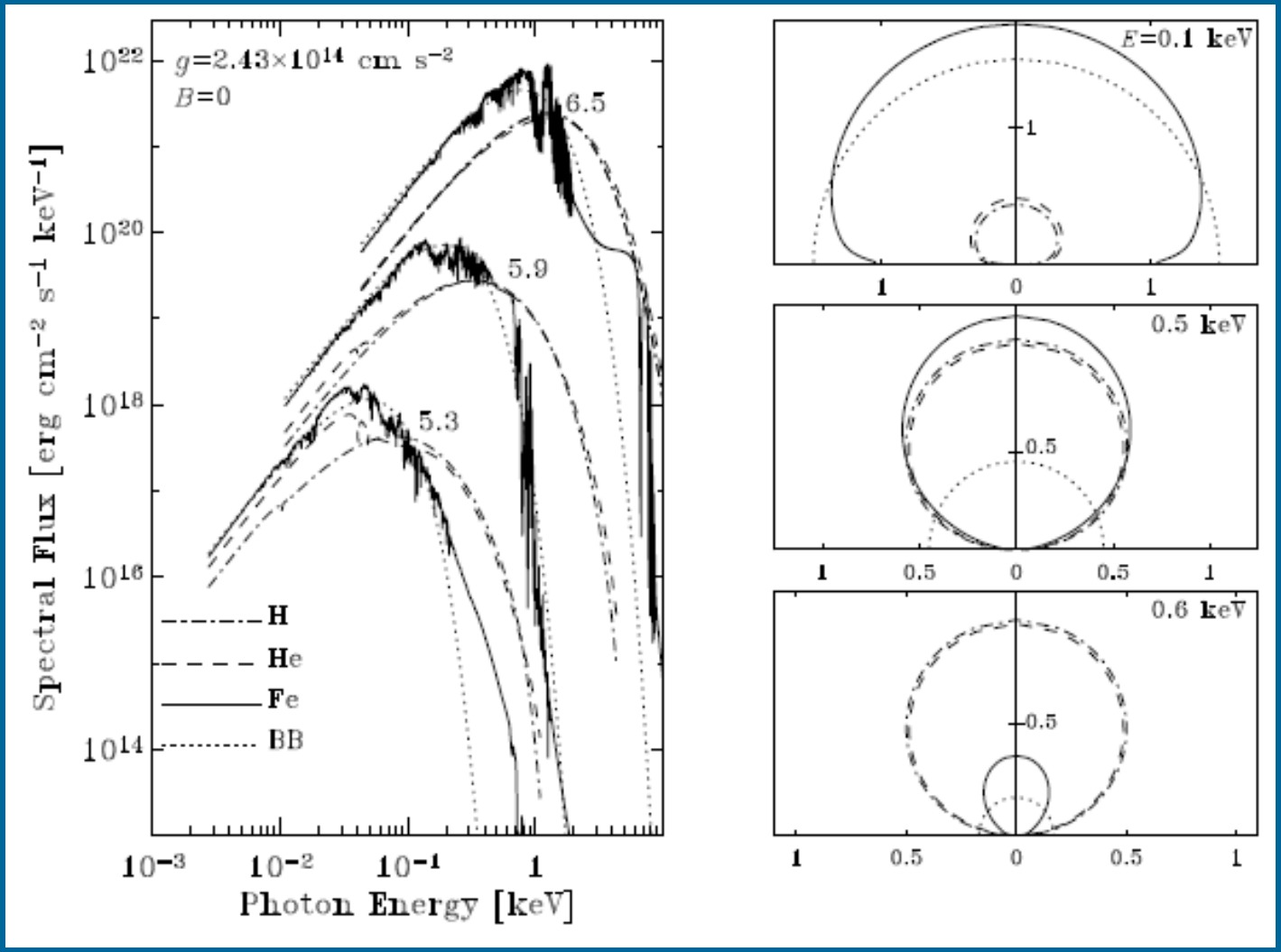

astro-ph/0702426

Fitting the spectrum of RX J1856

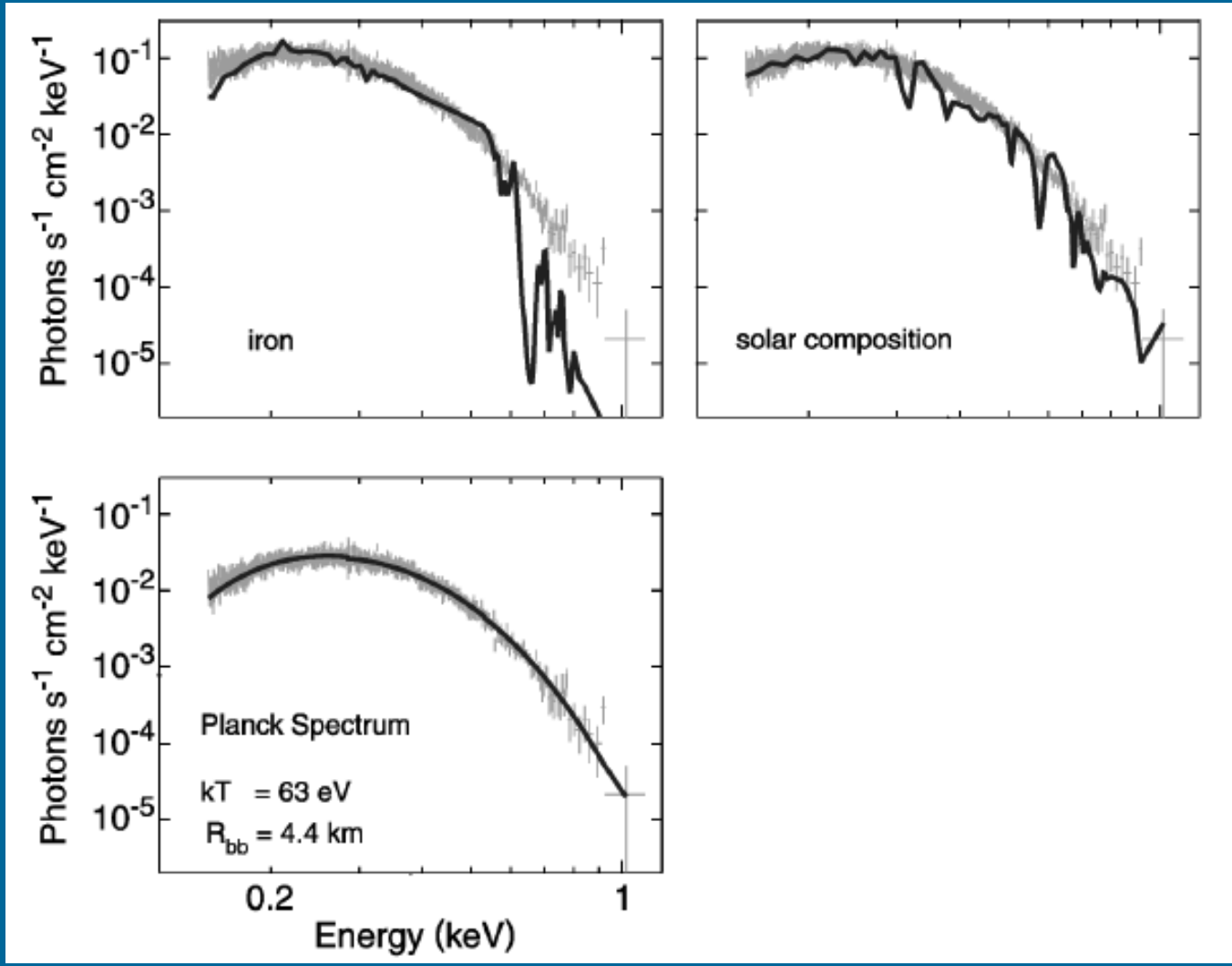

Trumper astro-ph/0502457

Different fits

PARAMETERS FROM MULTIWAVELENGTH FITS[a]

Model	n_H (10^{20} cm^{-2})	T_∞ (eV)	R_∞/D (km pc^{-1})	$T_\infty(R_\infty/D)^2$ [eV (km pc^{-1})^2]	Luminosity[b] (10^{31} ergs s^{-1})	P_{ox}^c
BB	$2.2^{+0.3}_{-0.4}$	48 ± 2	0.11 ± 0.01	$0.60^{+0.05}_{-0.4}$	$1.55^{+0.23}_{-0.17}$	3×10^{-4}
H	1.0 ± 0.1	26 ± 1	0.27 ± 0.01	1.94 ± 0.01	0.6 ± 0.01	$<10^{-14}$
Fe.....	1.8 ± 0.2	44 ± 1	0.13 ± 0.01	0.75 ± 0.05	$1.41^{+0.08}_{-0.06}$	7×10^{-7}
Si-ash.....	$1.9^{+0.3}_{-0.2}$	45^{+2}_{-1}	0.13 ± 0.01	$0.74^{+0.04}_{-0.05}$	$1.63^{+0.14}_{-0.21}$	0.53

[a] 3σ ranges, assuming $z = 0.305$. Weighting of the data is discussed in the text.
[b] Uncertainty does not include uncertainty in distance.
[c] The likelihood that the X-ray and optical parameters are the same.

Fits of realistic spectra of cooling NSs give higher temperature (and so smaller emitting surfaces) for blackbody and heavy element atmospheres (Fe, Si).
$T_{BB} \sim 2T_H$

Pons et al. 2002

Different fits

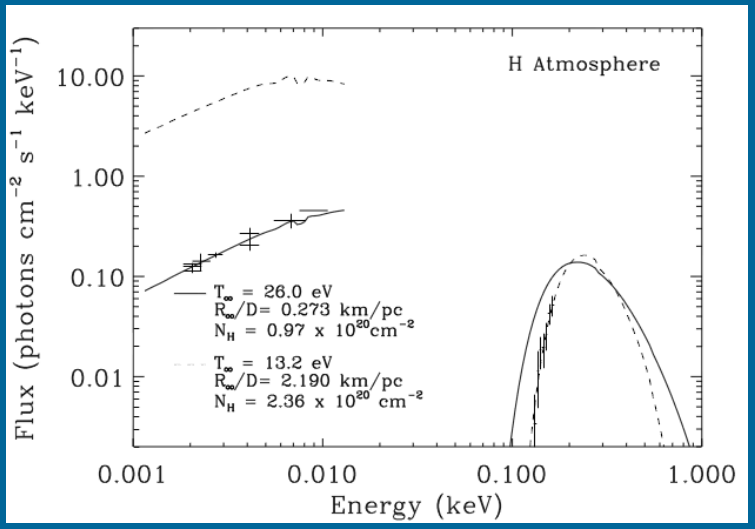

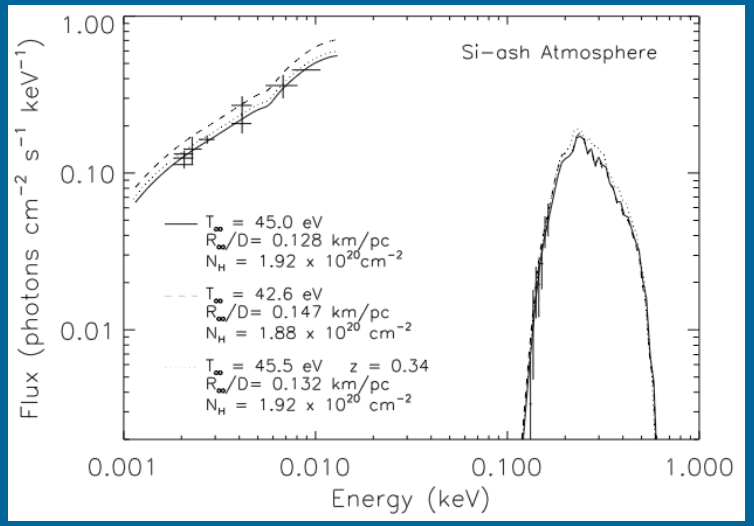

$T_{bb} \sim T_{Fe} > T_H$

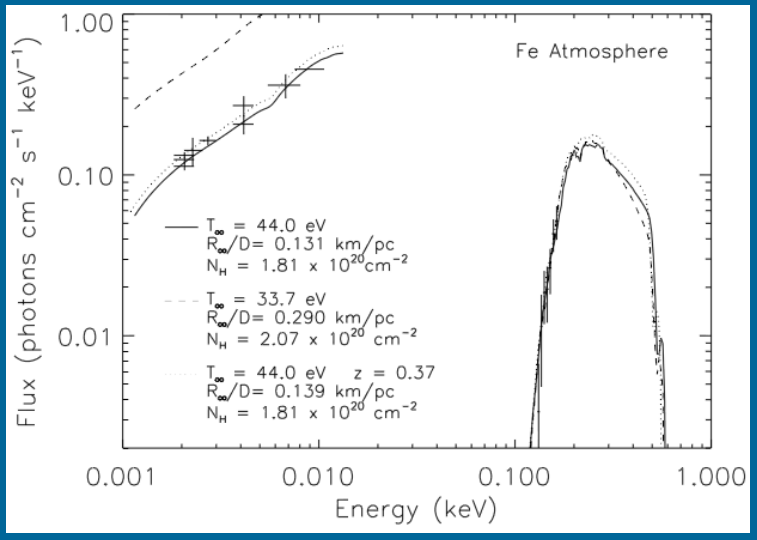

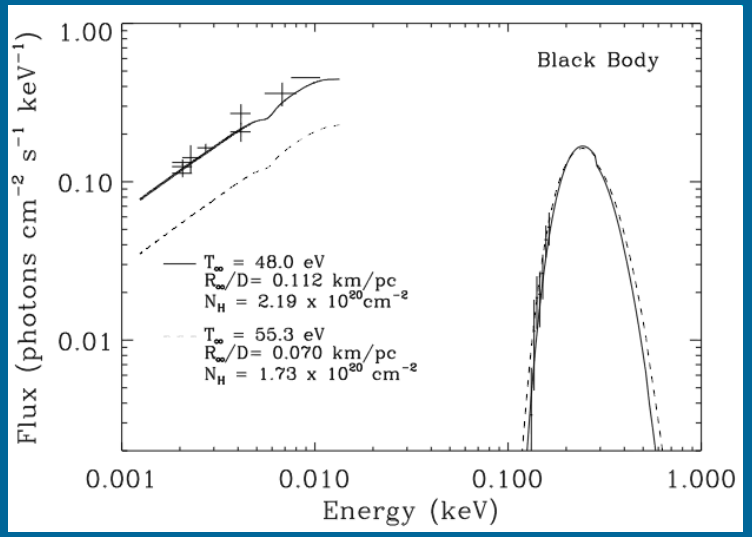

Pons et al. 2002

Cas A carbon atmosphere

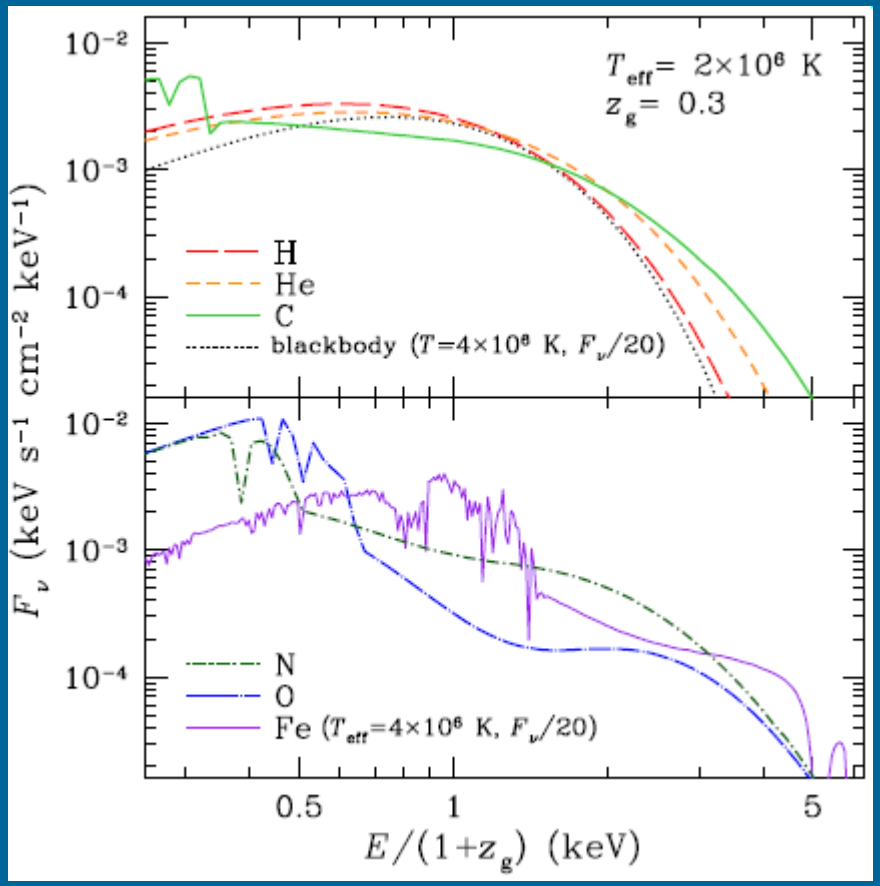

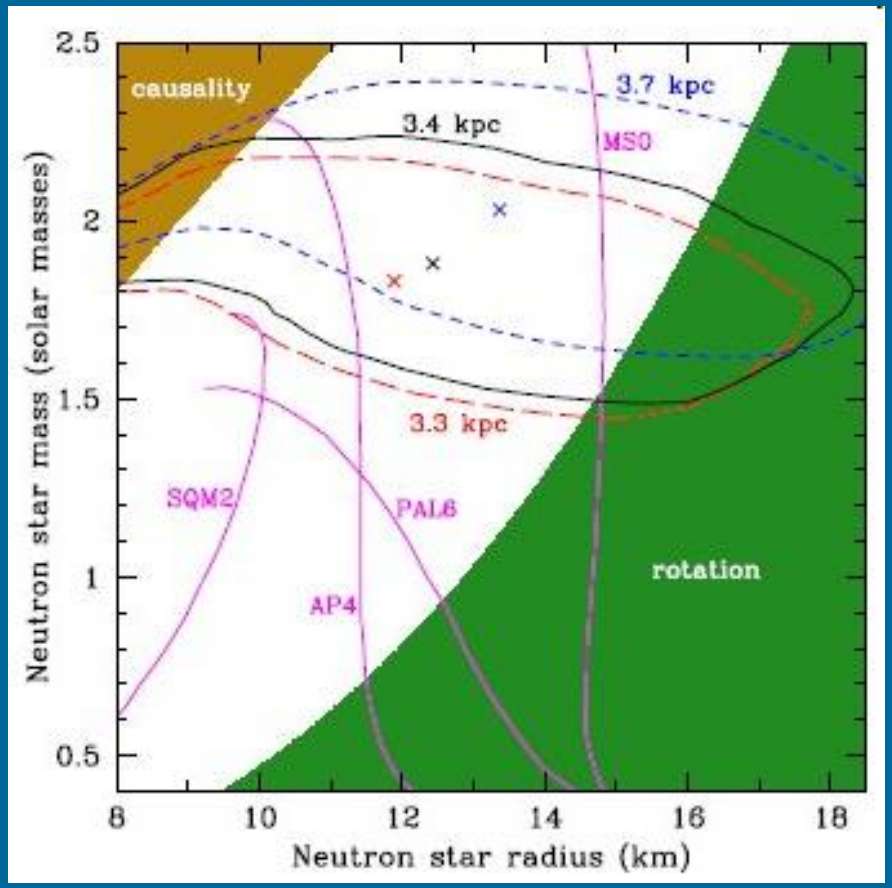

Low-field carbon atmosphere can fit the data.
Before all fits provided a very small emitting area.

0911.0672

Gravity Effects

- Redshift
- Ray bending

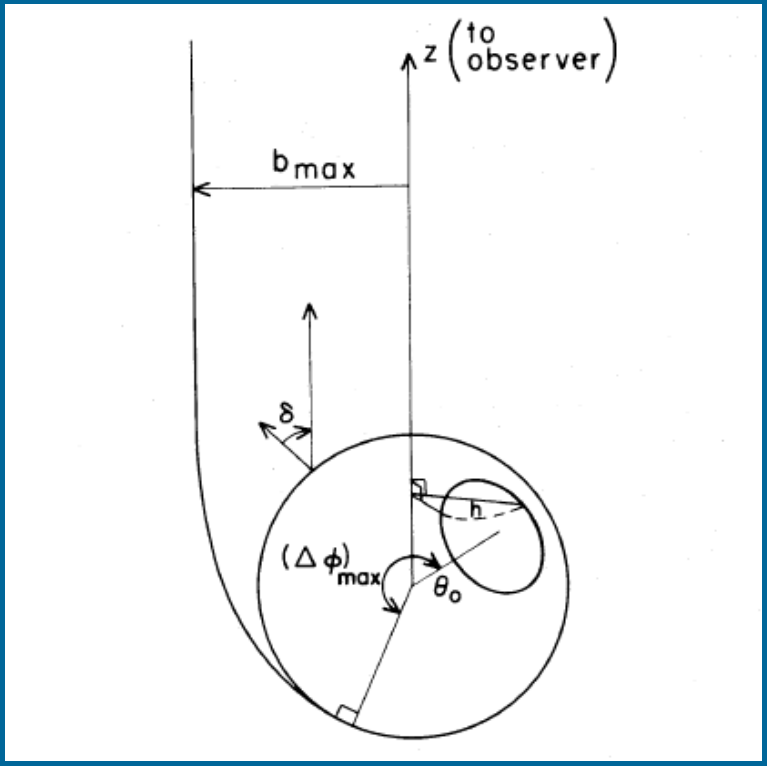

$$L_\infty = 4\pi R_\infty^2 \sigma T_\infty^4$$

$$4\pi\sigma T_\infty^4 \rightarrow \int_0^{2\pi} d\gamma \int_0^{2\pi} d\Phi \int_0^1 du^2 \int_{E_{\infty,1}}^{E_{\infty,2}} dE_\infty \; I(E, B, \cos\Theta, T_s, \gamma)$$

STEP 1
Specify viewing geometry and B-field topology; compute the surface temperature distribution

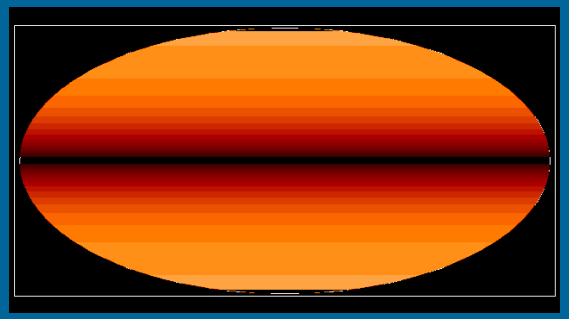

STEP 2
Compute emission from every surface patch

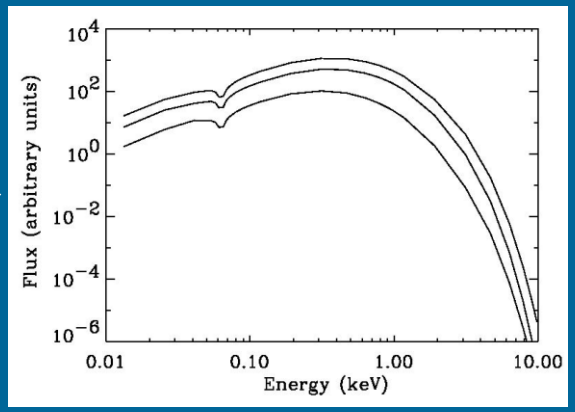

STEP 3
GR ray-tracing to obtain the spectrum at infinity

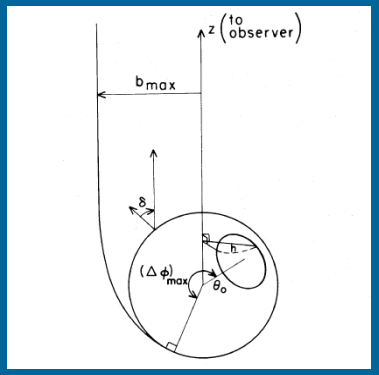

STEP 4
Predict lightcurve and phase-resolved spectrum
Compare with observations

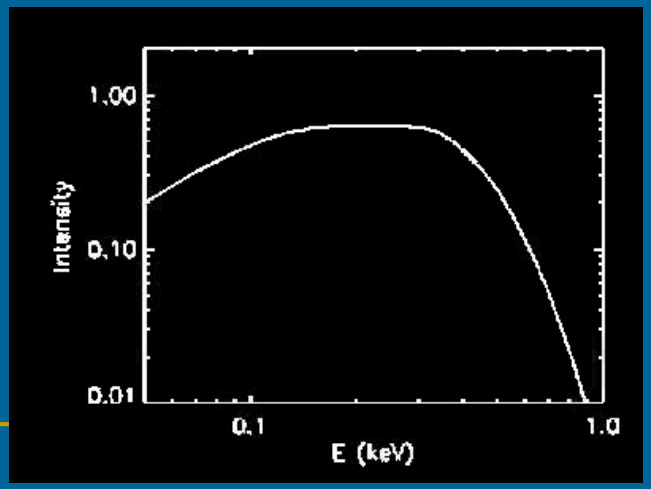

The Seven X-ray dim Isolated NSs

- Soft thermal spectrum (kT ≈ 50-100 eV)
- No hard, non-thermal tail
- Radio-quiet, no association with SNRs
- Low column density ($N_H \approx 10^{20}$ cm^{-2})
- X-ray pulsations in all (but one?) sources (P≈3-10 s)
- Very faint optical counterparts
- Broad spectral features

ICoNS: The Perfect Neutron Stars

ICoNS are key in neutron star astrophysics: these are the only sources for which we have a “clean view” of the star surface

- Information on the thermal and magnetic surface distributions
- Estimate of the star radius (and mass ?)
- Direct constraints on the EOS

ICoNS: What Are They ?

- ICoNS *are* neutron stars
- Idea number 1: Powered by ISM accretion?
  $\dot{M}_{Bondi} \sim n_{ISM}/v^3$ if $v < 40$ km/s and $D < 500$ pc
  (e.g. Treves et al 2000)
- Measured proper motions imply $v > 100$ km/s
- Just cooling NSs

Simple Thermal Emitters ?

Recent detailed observations of ICoNS allow direct testing of surface emission models

"STANDARD MODEL" thermal emission from the surface of a neutron star with a dipolar magnetic field and covered by an atmosphere

The optical excess

ICoNS lightcurves

The puzzle of RX J1856.5-3754

Spectral evolution of RX J0720.4-3125

Note a claim for an excess at harder (keV) X-rays: 1703.05995

The Magnificent Seven

Source	kT (eV)	P (s)	Amplitude/2	Optical
RX J1856.5-3754	60	7.06	1.5%	V = 25.6
RX J0720.4-3125 (*)	85	8.39	11%	B = 26.6
RX J0806.4-4123	96	11.37	6%	UV
RX J0420.0-5022	45	3.45	13%	B = 26.6
RX J1308.6+2127 (RBS 1223)	86	10.31	18%	m_{50CCD} = 28.6
RX J1605.3+3249 (RBS 1556)	96	3.39?	??	m_{50CCD} = 26.8
1RXS J214303.7+065419 (RBS 1774)	104	9.43	4%	B=27.4

(*) variable source

Featureless ? No Thanks !

- RX J … s (Chan…
- A bro… her ICoN… l 2004; Zane e…
- E_{line} … th E_1 ~ $2E_2$ i…
- Proto… high B ?

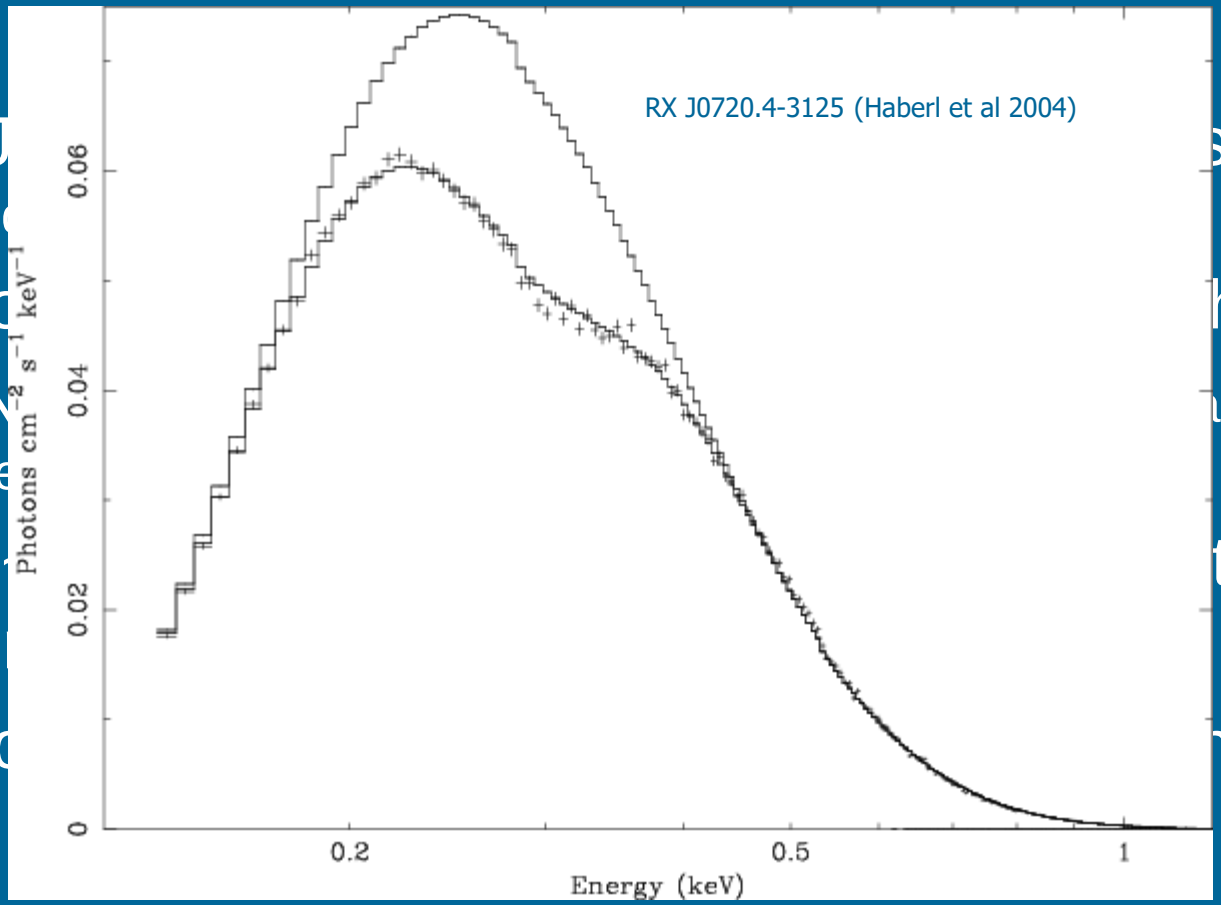

Source	Energy (eV)	EW (eV)	B_{line} (B_{sd}) (10^{13} G)	Notes
RX J1856.5-3754	no	no	?	-
RX J0720.4-3125	270	40	5 (2)	Variable line
RX J0806.4-4123	460	33	9	-
RX J0420.0-5022	330	43	7	-
RX J1308.6+2127	300	150	6 (3)	-
RX J1605.3+3249	450	36	9	-
1RXS J214303.7+065419	700	50	14	-

Phase variable spectral feature

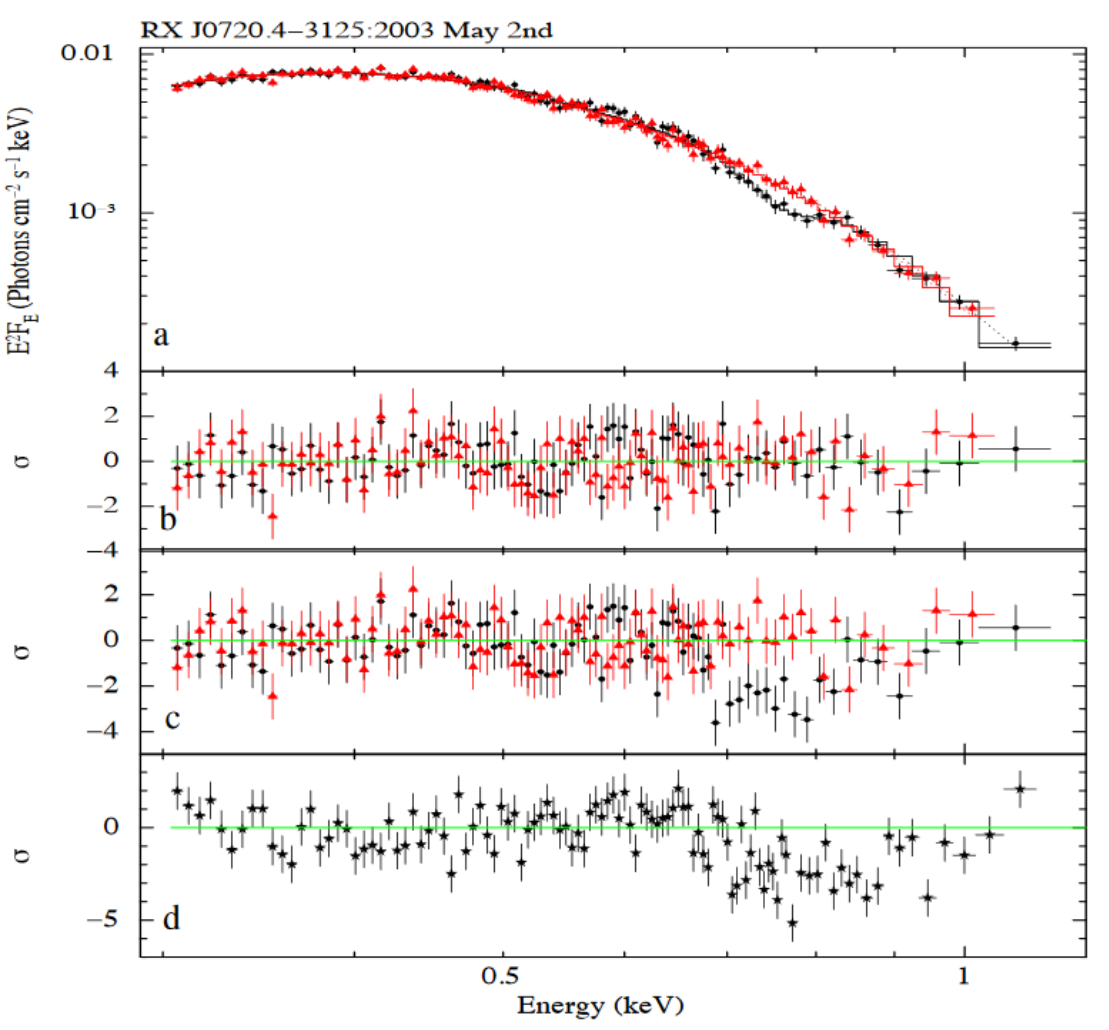

RX J0720.4−3125

Black: phase 0.1-0.3
red: phase 0.5-0.7

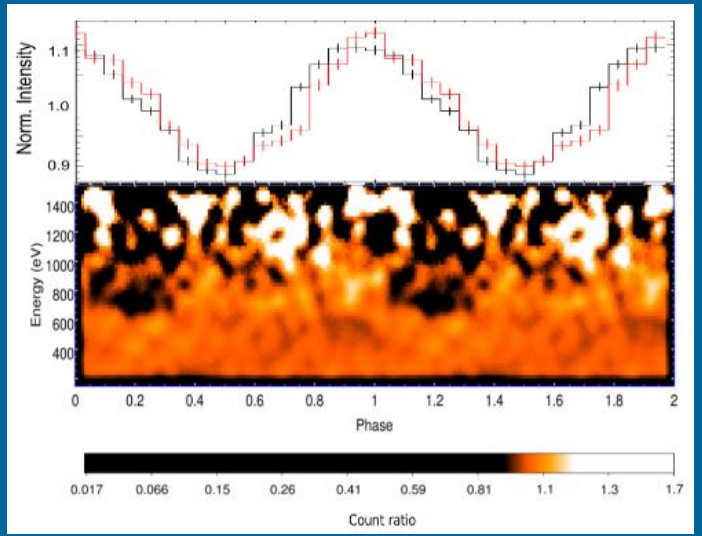

1506.04206

More phase-dependent features in M7

RX J1308.6+2127

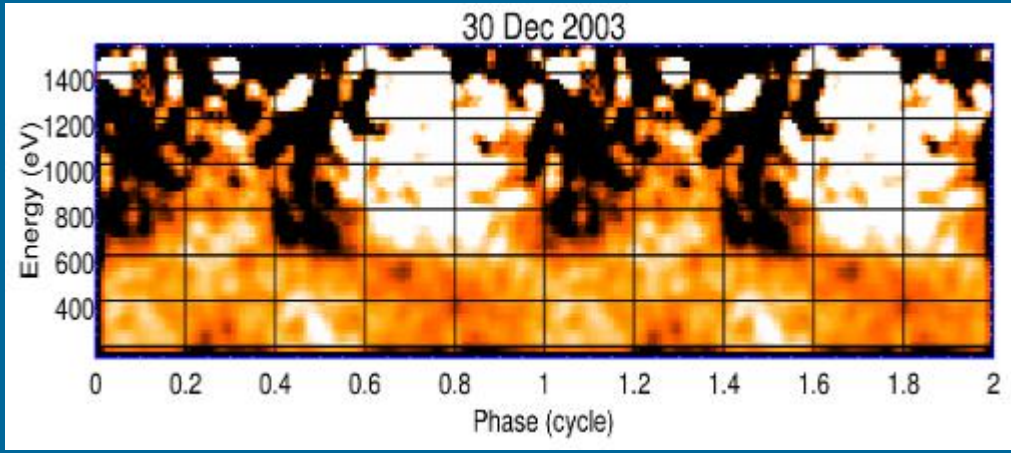

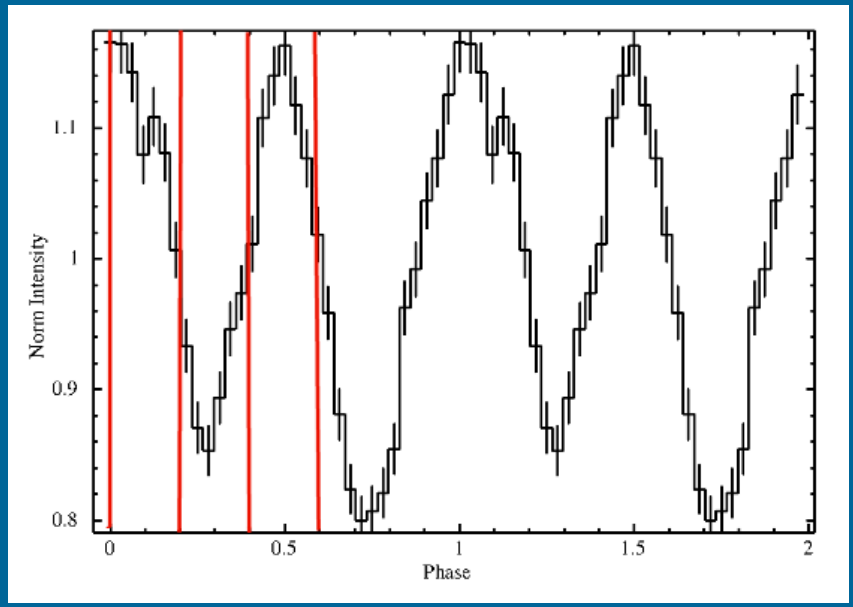

Parameter[a]	0–0.2	0.2–0.4	0.4–0.6	0.6–0.8	0.8–1
			BB+GAUSS		
kT_{BB} (eV)	$77.7^{+1.8}_{-2.0}$	$75.4^{+2.2}_{-2.5}$	$84.9^{+1.3}_{-1.4}$	$75.6^{+2.1}_{-2.7}$	$84.9^{+1.8}_{-2.0}$
R_{BB} (km)	4.3±0.5	5.6±1.0	2.6±0.1	5.8±1.1	3.4±0.3
Flux[b]	$3.34^{+0.04}_{-0.09}$	$3.67^{+0.15}_{-0.09}$	$3.10^{+0.05}_{-0.07}$	$3.68^{+0.07}_{-0.06}$	3.69±0.06
Unabs. Flux[b]	7.42±1.10	$7.69^{+1.70}_{-1.01}$	$6.63^{+0.63}_{-0.36}$	$8.26^{+1.35}_{-1.39}$	$7.77^{+0.55}_{-0.76}$
E_1 (eV)	173^{+32}_{-39}	107^{+44}_{-54}	256^{+22}_{-28}	109^{+41}_{-59}	198^{+30}_{-36}
σ_1 (eV)	143^{+13}_{-12}	169^{+15}_{-14}	105^{+13}_{-11}	168^{+16}_{-13}	146^{+14}_{-12}
Eq $Width_1$ (eV)	182^{+2}_{-8}	204^{+2}_{-35}	128^{+10}_{-14}	203^{+2}_{-5}	171^{+11}_{-29}
NHP[c]	1.6×10^{-1}	1.5×10^{-1}	5.4×10^{-2}	1.3×10^{-1}	2.8×10^{-3}
χ^2_ν	1.12	1.12	1.20	1.13	1.35
dof	141	149	139	147	150

1703.05336

Non-uniform temperature distribution

Source	Class	B_{dip} $[10^{12}\mathrm{G}]$	N_H $[10^{20}\mathrm{cm}^{-2}]$	kT_{bb} [eV]	E_0 [eV]	$\lvert E_w \rvert$ [eV]	PF %	Refs.
RX J0720.4-3125	XINS	49	1.0	84-94	311*	0-70	11	[1]
RX J0806.4-4123	XINS	51	0.9	95	486*	30	6	[2]
RX J1308.6+2127	XINS	68	3.7	93	390*	150	18	[3]
RX J1605.3+3249	XINS	148†	0	99	400*	70	5†	[4]
RX J2143.0+0654	XINS	40	2.3	104	750	50	4	[5]
2XMM J1046-5943‡	?	?	26	135	1350*	90	<4	[6]
1E 1207.4-5209	CCO	0.2	13	155,290	740,1390	60,100	4-14**	[7]
PSR J1740+1000	RPP	37	9.7	94	550-650	50-230	30	[8]
PSR J1819-1458	RPP	100	124	112	1120*	400	34	[9]
XTE J1810-197	MAG	410	73	300	1150	35	17-47**	[10]

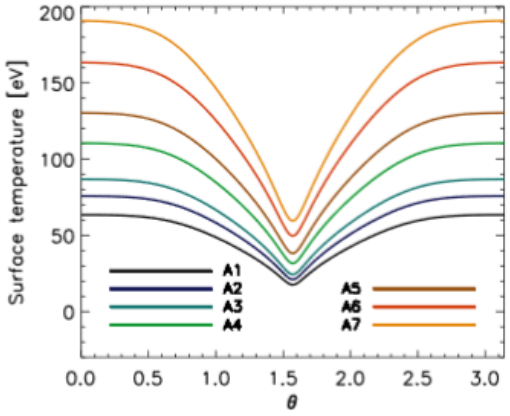

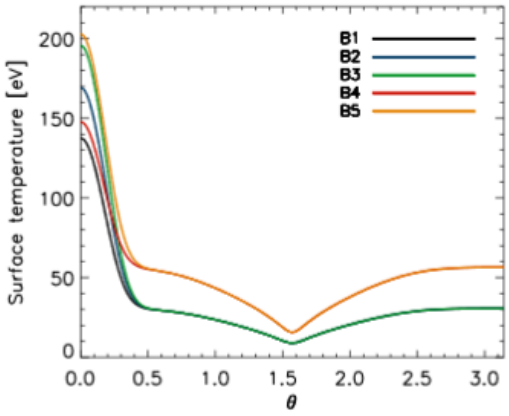

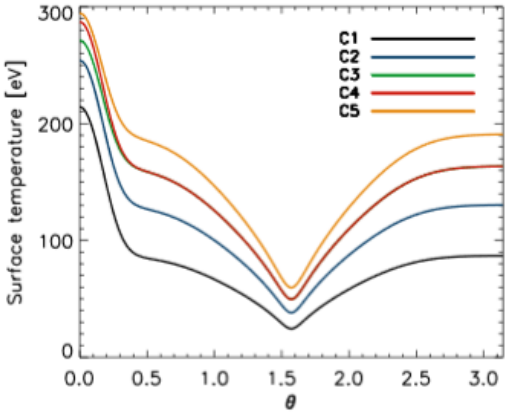

1406.0874

RX J0806.4-412

BB+line

Non-uniform distrubution

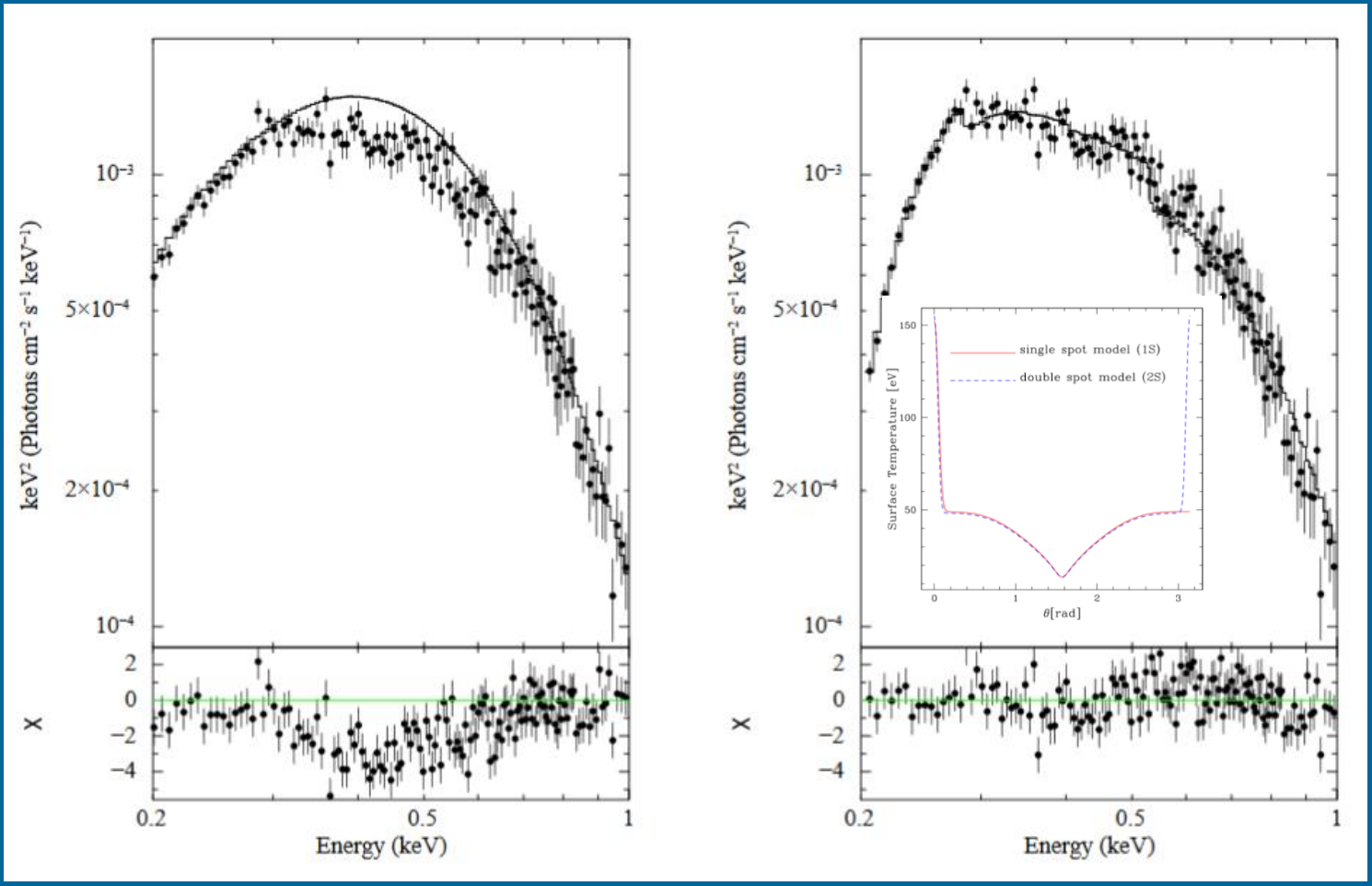

1406.0874

Pulsating ICoNS - I

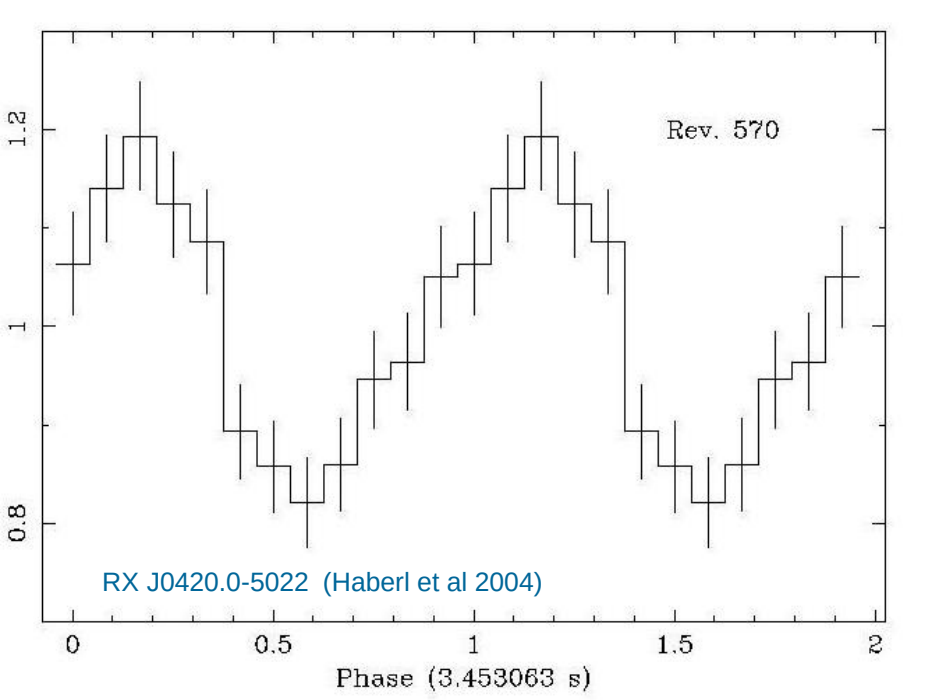

- Quite large pulsed fractions
- Skewed lightcurves
- Harder spectrum at pulse minimum
- Phase-dependent absorption features

Pulsating ICoNS - II

Core-centred dipole field + Atmosphere emission = Too small pulsed fractions Symmetrical pulse profiles (Zane & Turolla 2006)

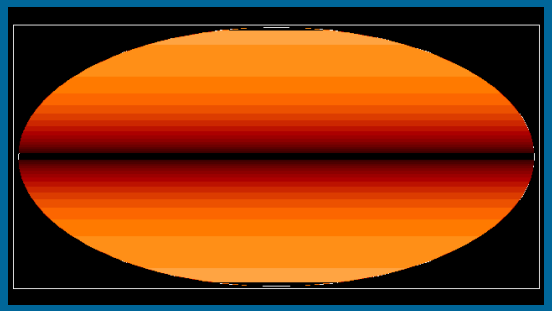

+

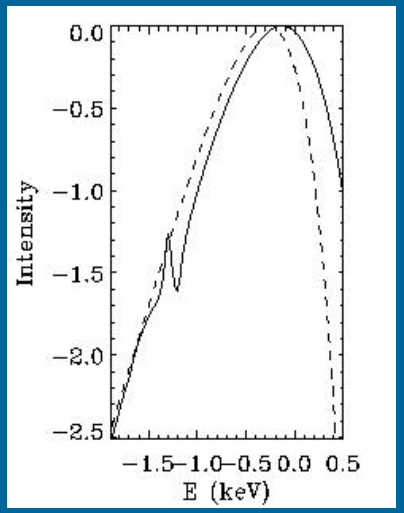

=

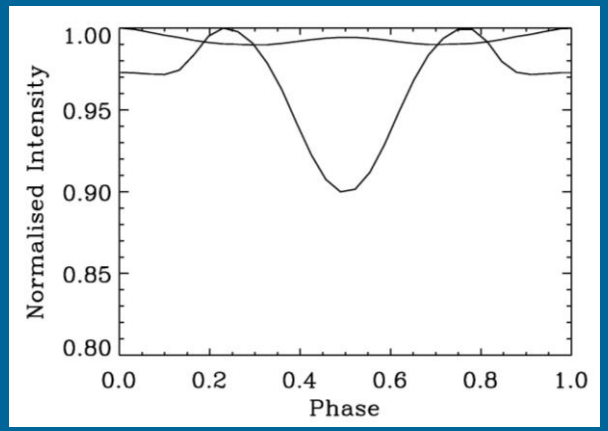

Crustal Magnetic Fields

- Star centred dipole + poloidal/toroidal field in the envelope (Geppert, Küker & Page 2005; 2006)
- Purely poloidal crustal fields produce a steeper meridional temperature gradient
- Addition of a toroidal component introduces a N-S asymmetry

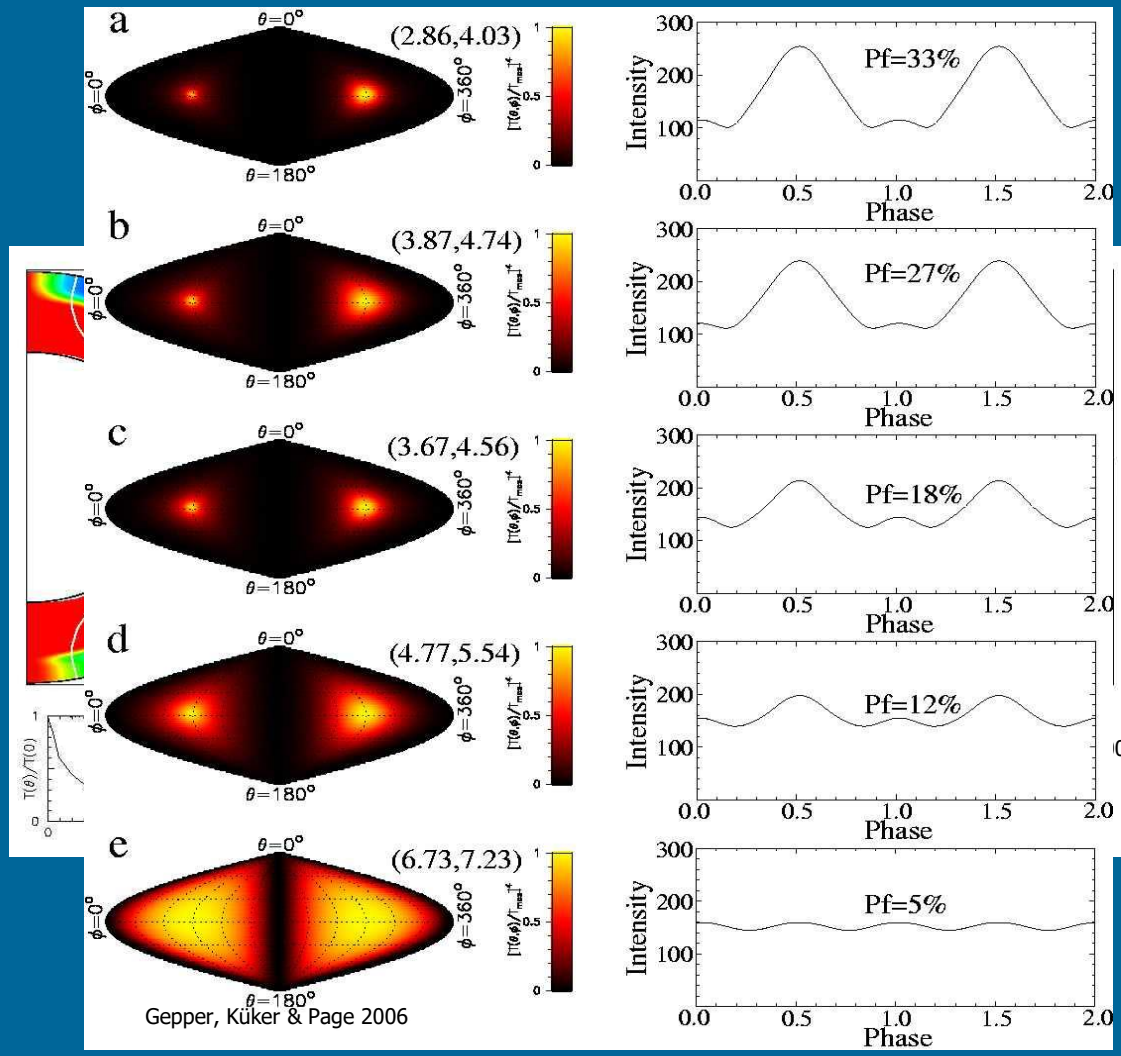

Gepper, Küker & Page 2006

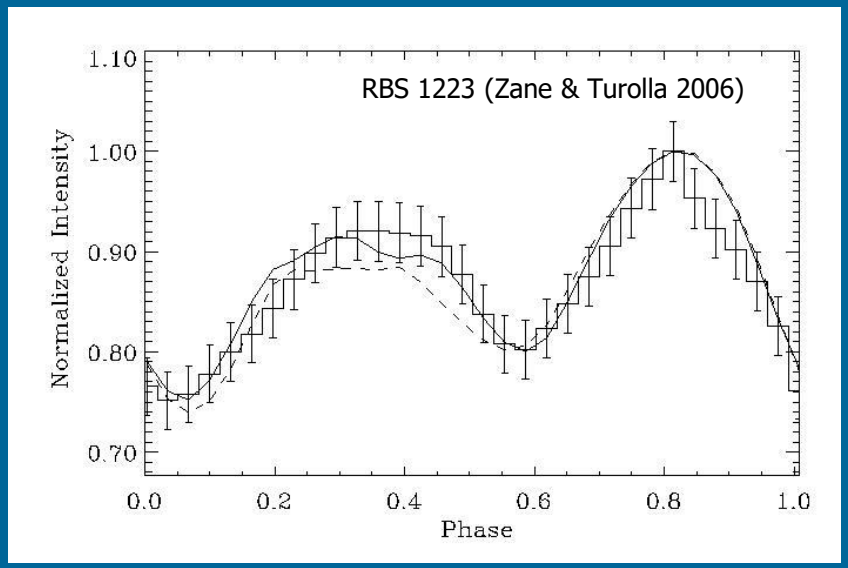

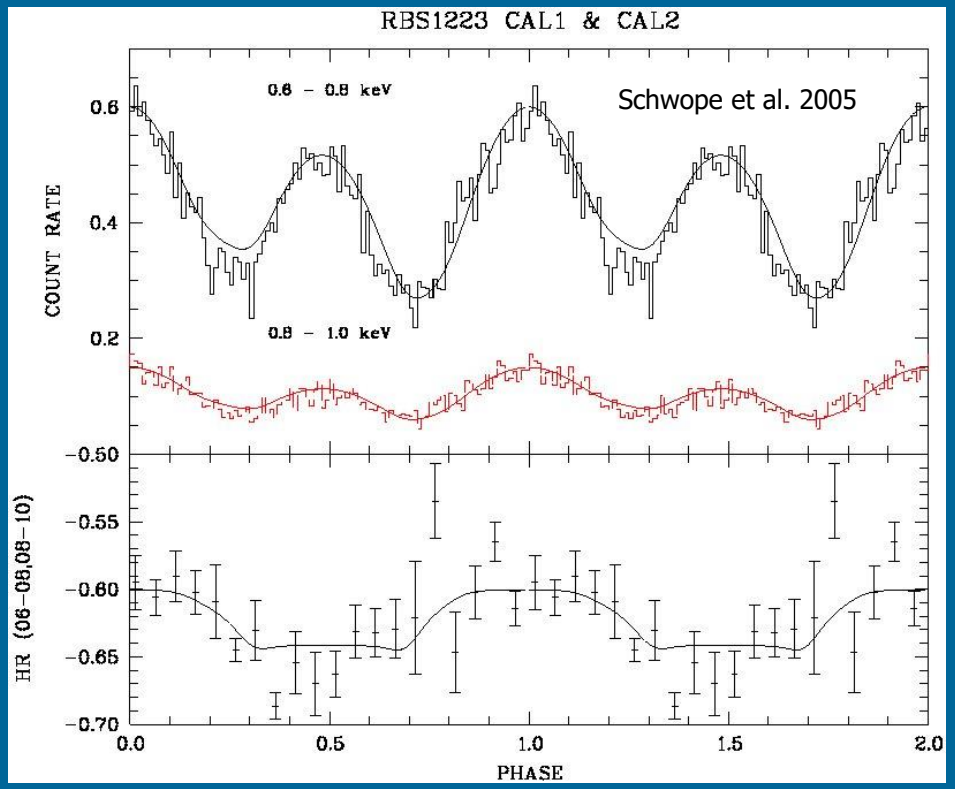

Indications for non-antipodal caps (Schwope et al 2005)

Need for a non-axisymmetric treatment of heat transport

RX J1856.5-3754 - I

Blackbody featureless spectrum in the 0.1-2 keV band (Chandra 500 ks DDT, Drake et al 2002); possible broadband deviations in the XMM 60 ks observation (Burwitz et al 2003)

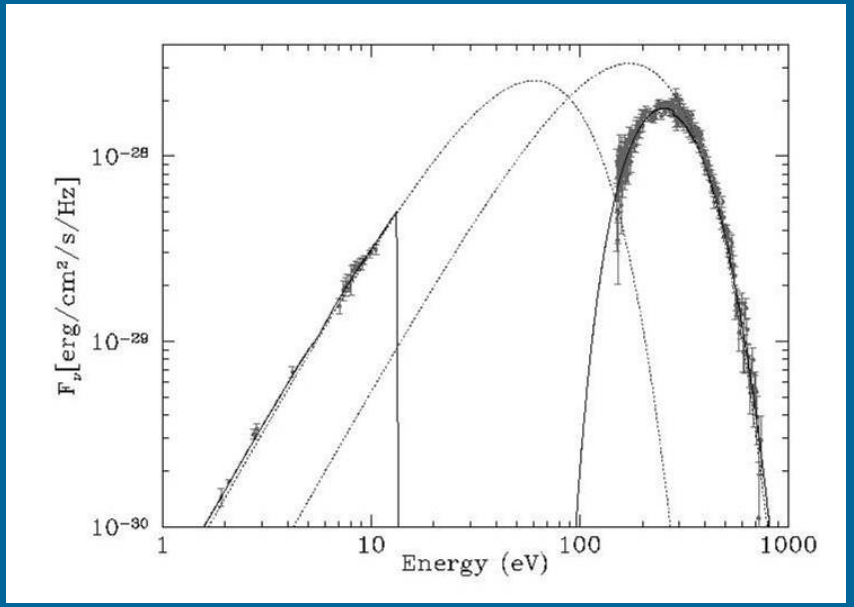

RX J1856 multiwavelength SED (Braje & Romani 2002)

Thermal emission from NSs is not expected to be a featureless BB ! H, He spectra are featureless but only blackbody-like (harder). Heavy elements spectra are closer to BB but with a variety of features

RX J1856.5-3754 - II

What spectrum ?
The optical excess ?

- A quark star (Drake et al 2002; Xu 2002; 2003)
- A NS with hotter caps and cooler equatorial region (Pons et al 2002; Braje & Romani 2002; Trűmper et al 2005)
- A bare NS (Burwitz et al 2003; Turolla, Zane & Drake 2004; Van Adelsberg et al 2005; Perez-Azorin, Miralles & Pons 2005)

A perfect BB ?

The Optical Excess

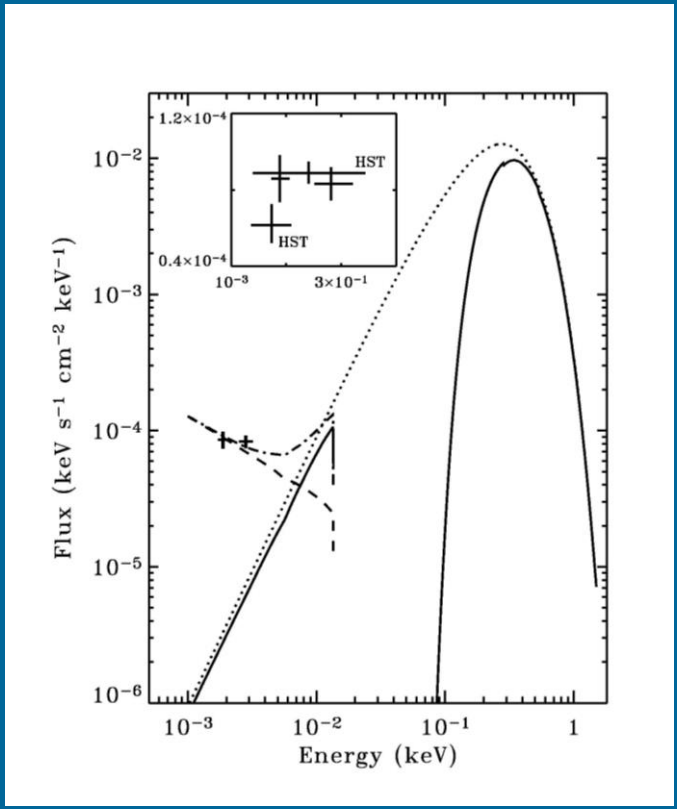

RX J1605 multiwavelength SED (Motch et al 2005)

- In the most of the sources with a confirmed optical counterpart $F_{opt} \approx 5\text{-}10 \times B_{\nu}(T_{BB,X})$
- $F_{opt} \approx \nu^2$?
- Deviations from a Rayleigh-Jeans continuum in RX J0720 (Kaplan et al 2003) and RX J1605 (Motch et al 2005). A non-thermal power law ?

Bare Neutron Stars

- At B >> B_0 ~ 2.35 x 10^9 G atoms

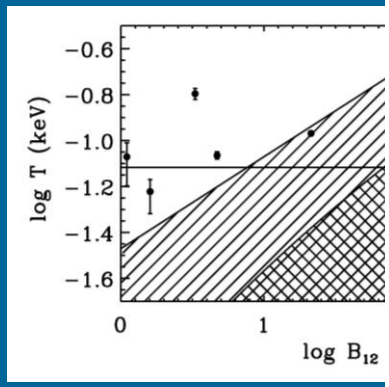

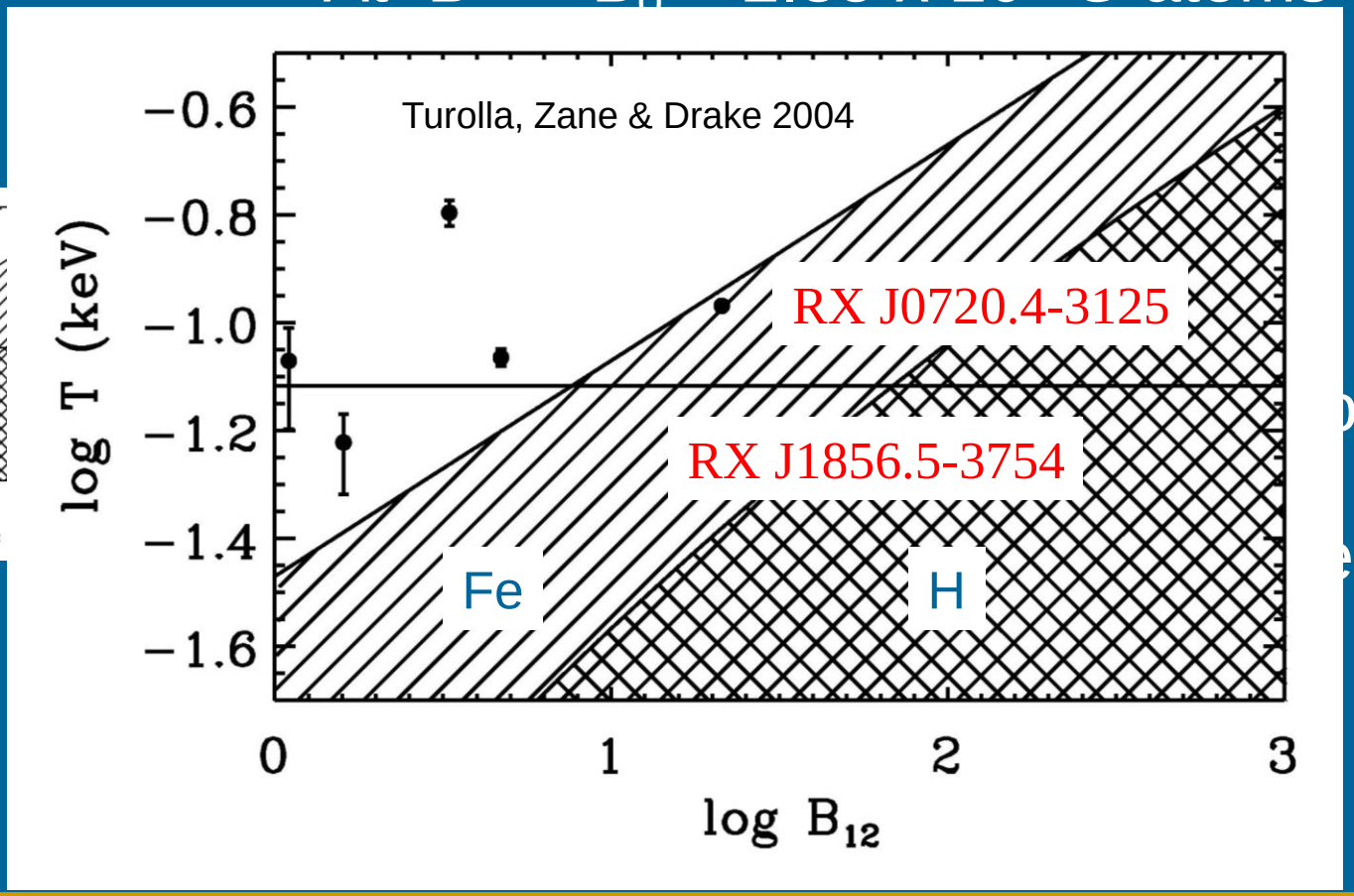

of a

e

Spectra from Bare NSs - I

The cold electron gas approximation. Reduced emissivity expected below ω_p (Lenzen & Trümper 1978; Brinkmann 1980)

Spectra are very close to BB in shape in the 0.1 - 2 keV range, but depressed wrt the BB at T_{eff}. Reduction factor ~ 2 - 3.

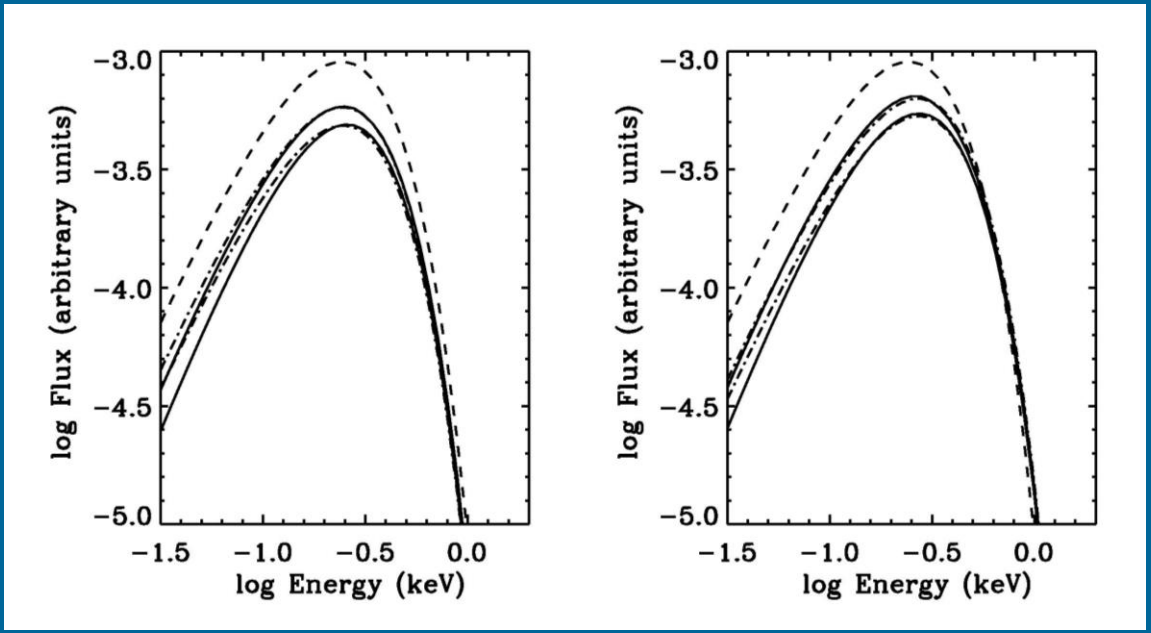

Turolla, Zane & Drake (2004)

Spectra from Bare NS - II

Proper account for damping of free electrons by lattice interactions (e-phonon scattering; Yakovlev & Urpin 1980; Potekhin 1999)

Spectra deviate more from BB. Fit in the 0.1 – 2 keV band still acceptable. Features may be present. Reduction factors higher.

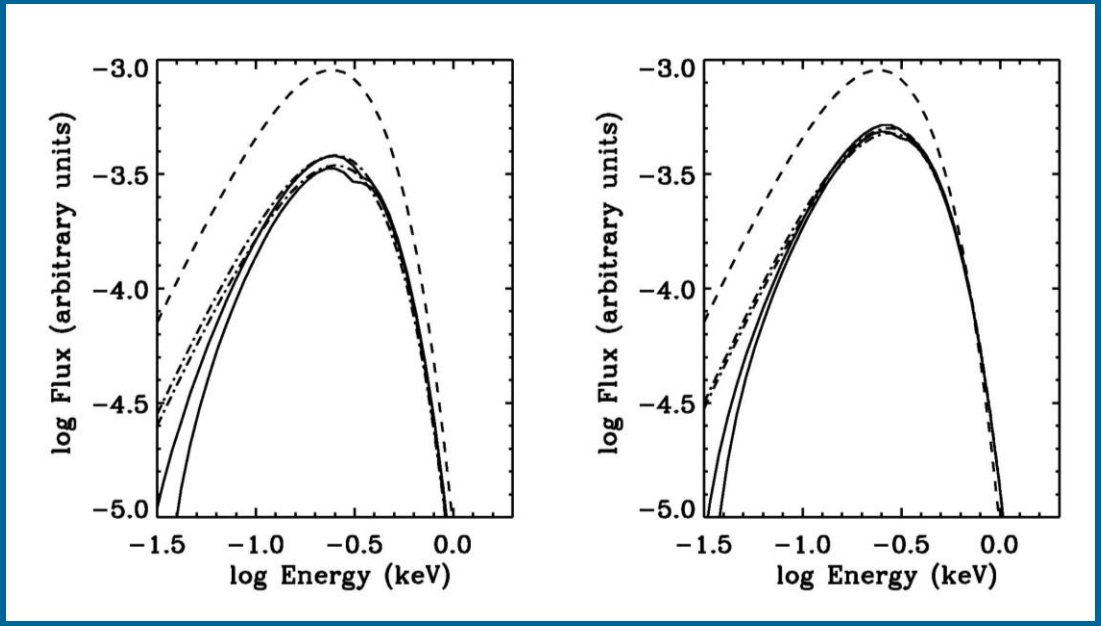

Turolla, Zane & Drake (2004)

Is RX J1856.5-3754 Bare ?

- Fit of X-ray data in the 0.15-2 keV band acceptable
- Radiation radius problem eased
- Optical excess may be produced by reprocessing of surface radiation in a very rarefied atmosphere (Motch, Zavlin & Haberl 2003; Zane, Turolla & Drake 2004; Ho et al. 2006)
- Details of spectral shape (features, low-energy behaviour) still uncertain

$$R_\infty = 4.25\, f_E^{-1/2} \left(\frac{D}{100\ \mathrm{pc}}\right)\left(\frac{T_{BB}}{60\ \mathrm{keV}}\right)^{-2} \mathrm{km}$$

Does the atmosphere keep the star surface temperature ?

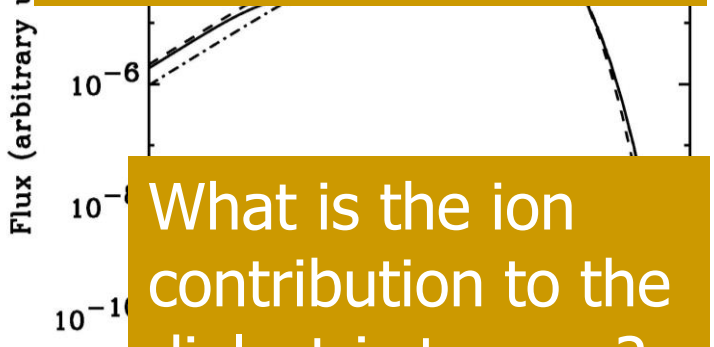

What is the ion contribution to the dielectric tensor ? (Van Adelsberg et al. 2005; Perez-Azorin, Miralles & Pons 2005)

Condensed iron surface emissivity

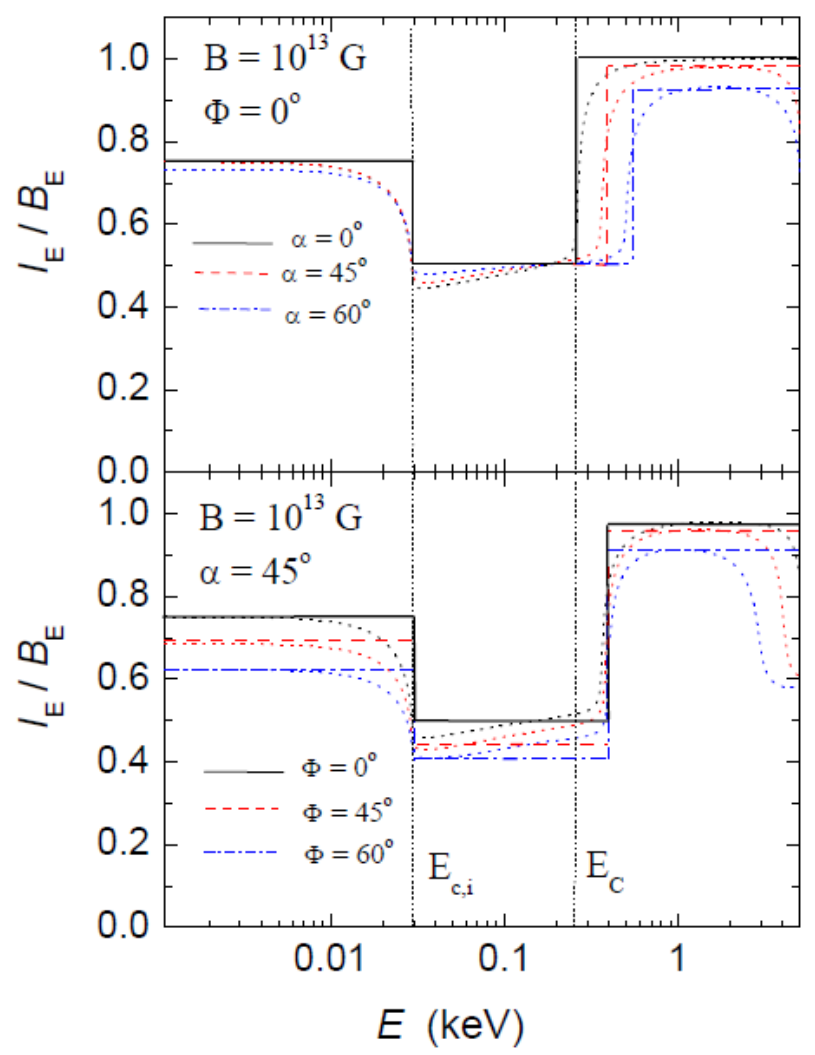

Free ions approximation.

1006.3292

Thin hydrogen magnetized atmosphere above blackbody and iron condensed surface

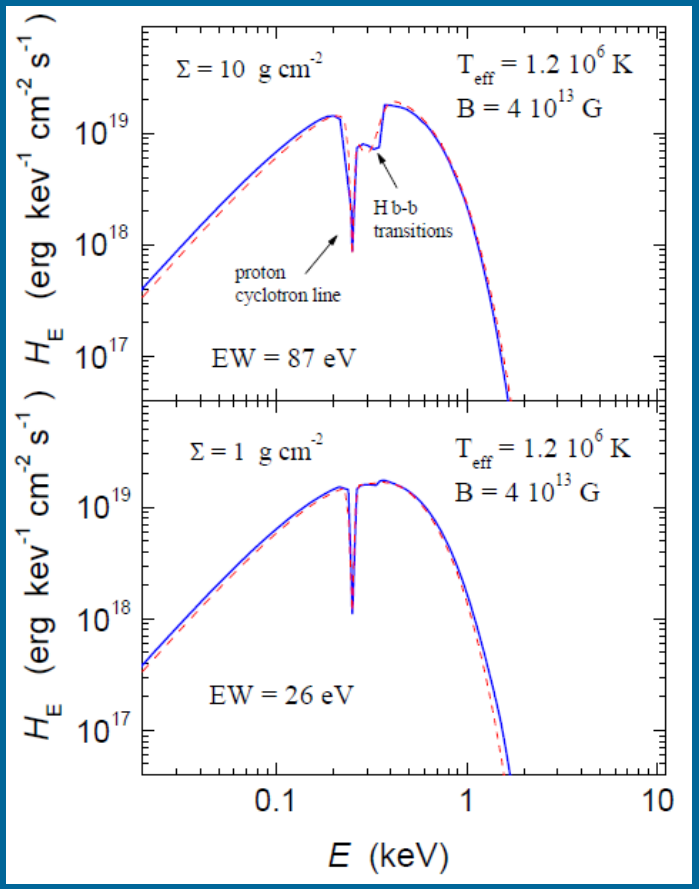

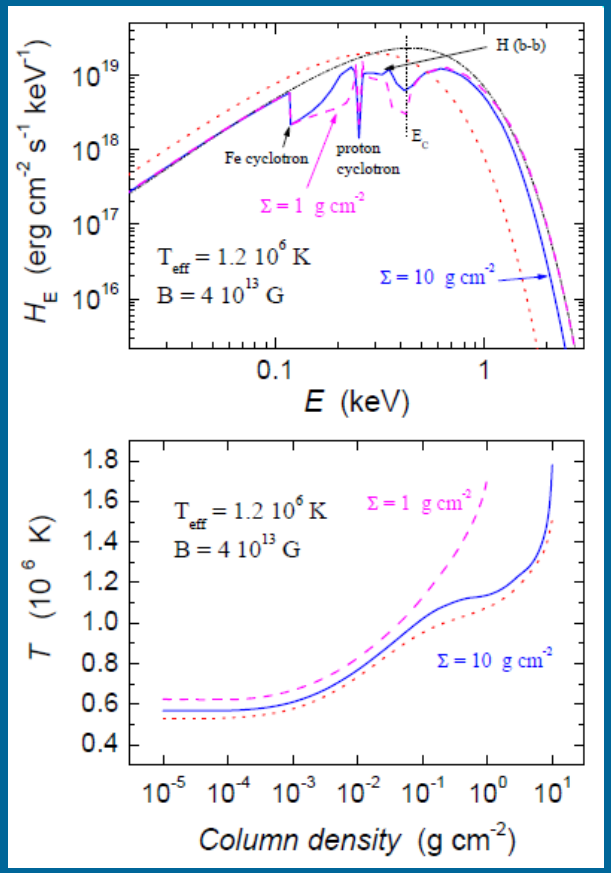

Below atmosphere was a blackbody spectrum

Below – iron condensed surface

1006.3292

Let us make it realistic

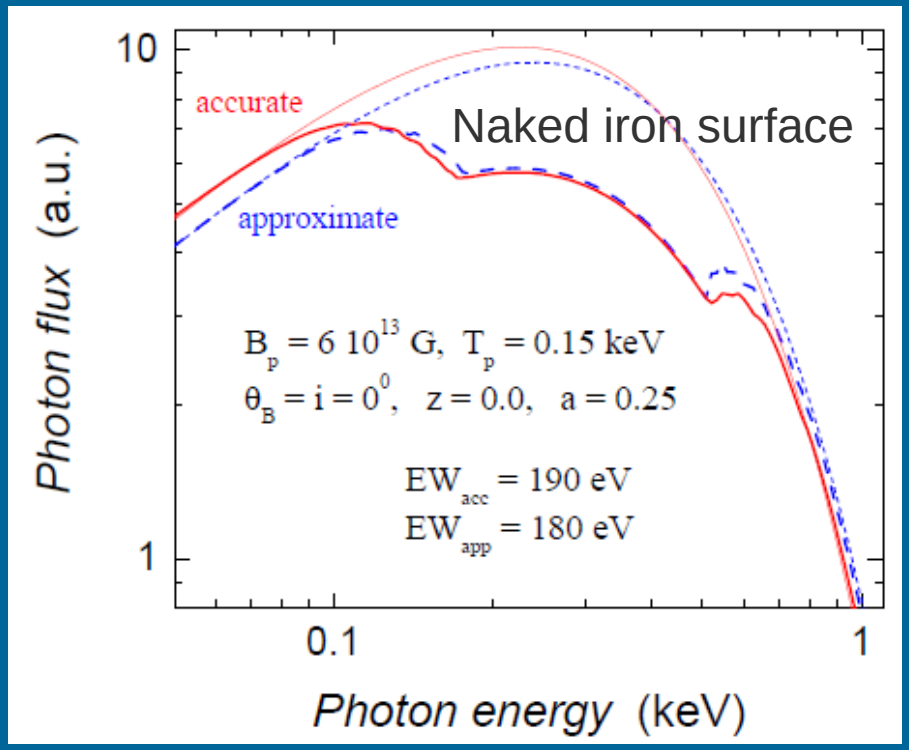

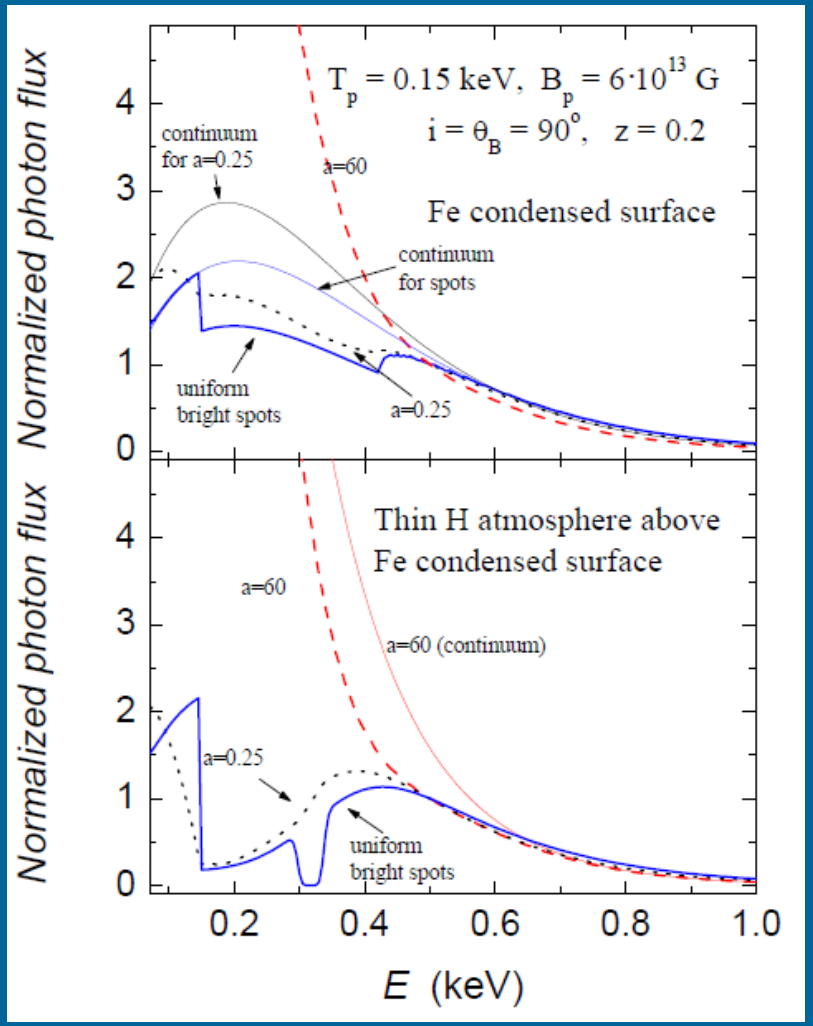

1006.3292

Excess at >1 keV?

Analysis of spectra of M7 demonstrated a strange excess at energies > 1 keV. This is somehow similar to what magnetars demonstrate.

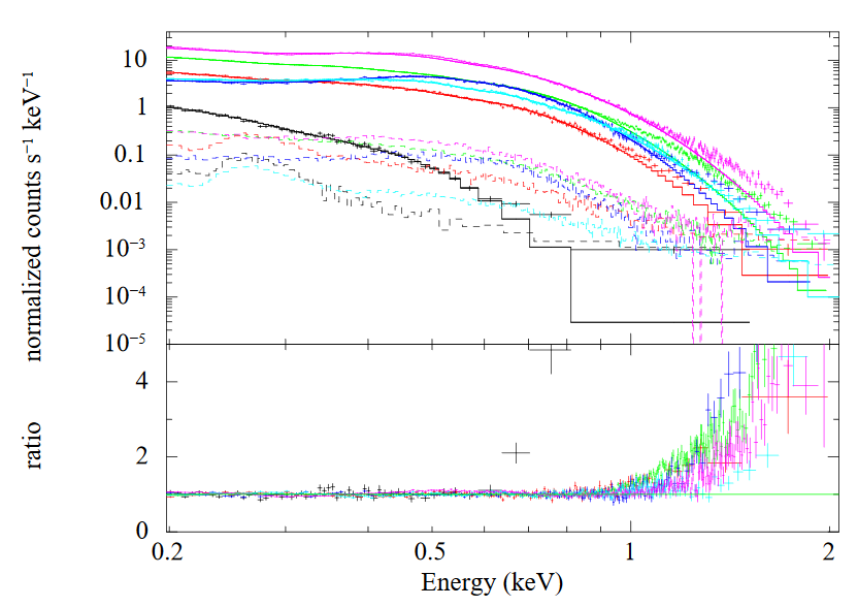

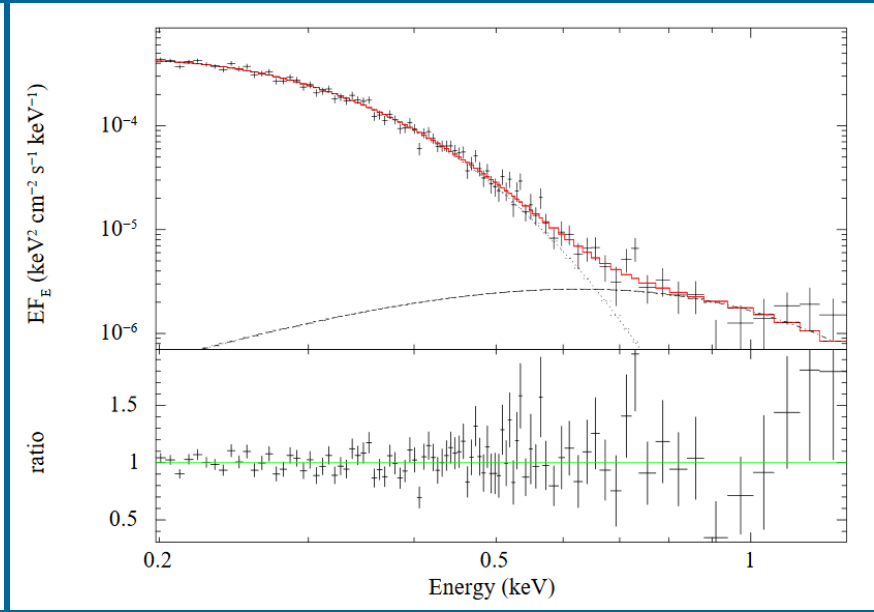

1811.11982

Calvera spectrum

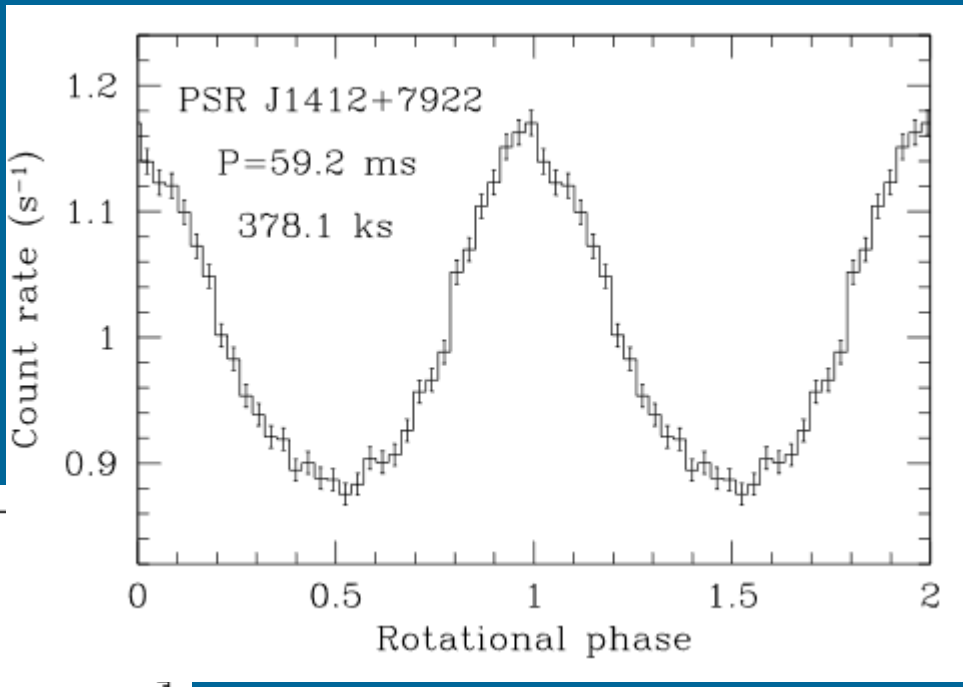

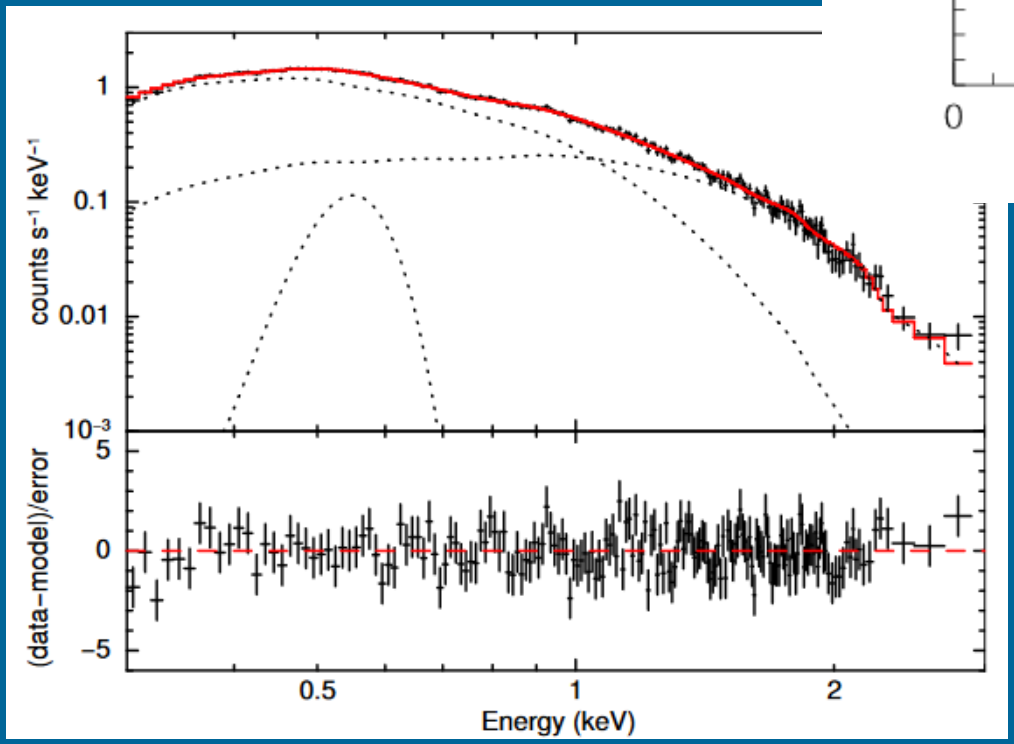

kT_1 (keV)	0.154 ± 0.004
R_1 (km) [b]	$2.21^{+0.08}_{-0.07}$
kT_2 (keV)	$0.319^{+0.013}_{-0.012}$
R_2 (km) [b]	0.37 ± 0.04

1902.00144

Light curves and pulsed fraction

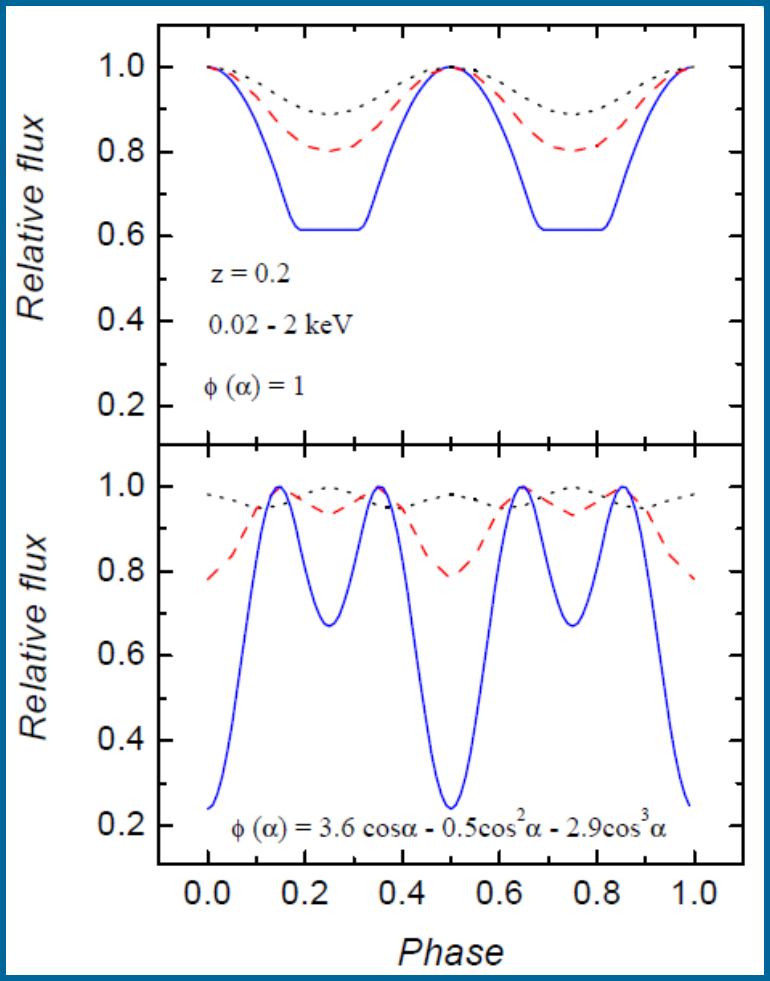

1006.3292

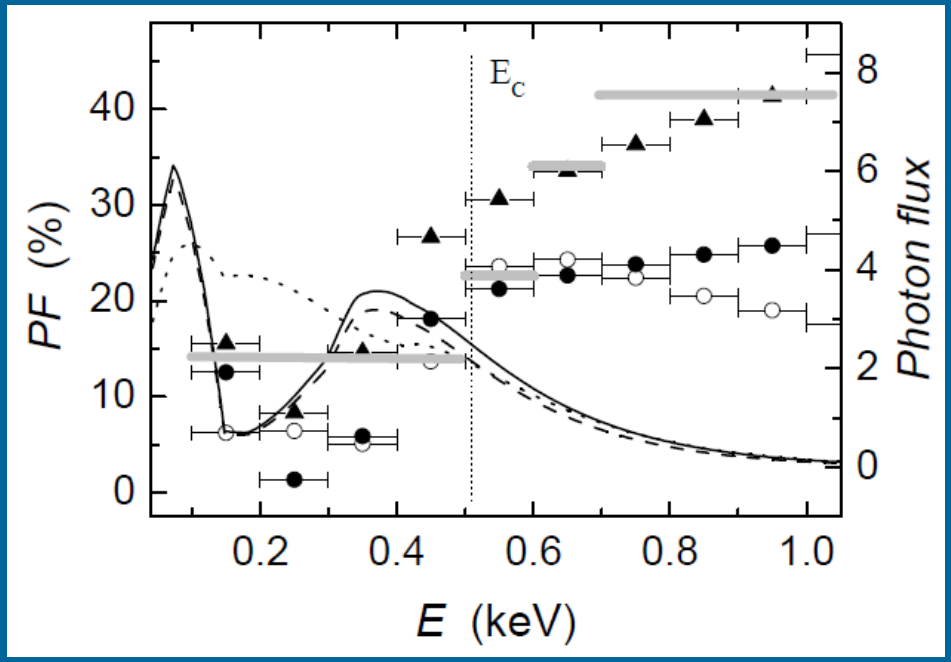

1010.0125

Low-field magnetar SGR 0418+5729

Fitting parameters of the magnetized atmosphere it is possible to show, that the low-field solution is not acceptable.
This can be due to non-dipolar field components.

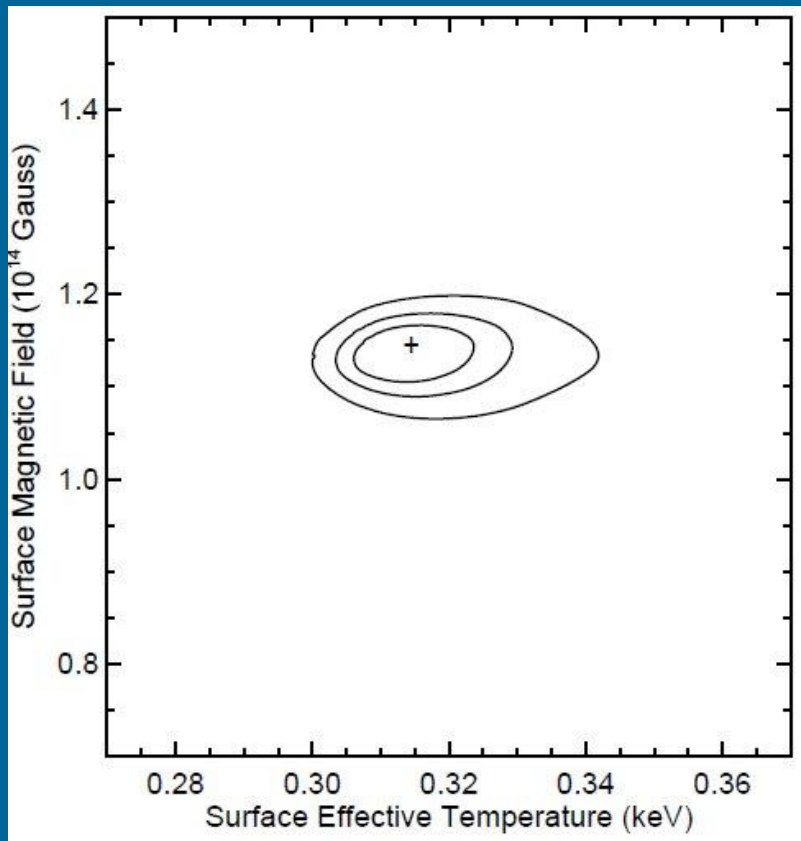

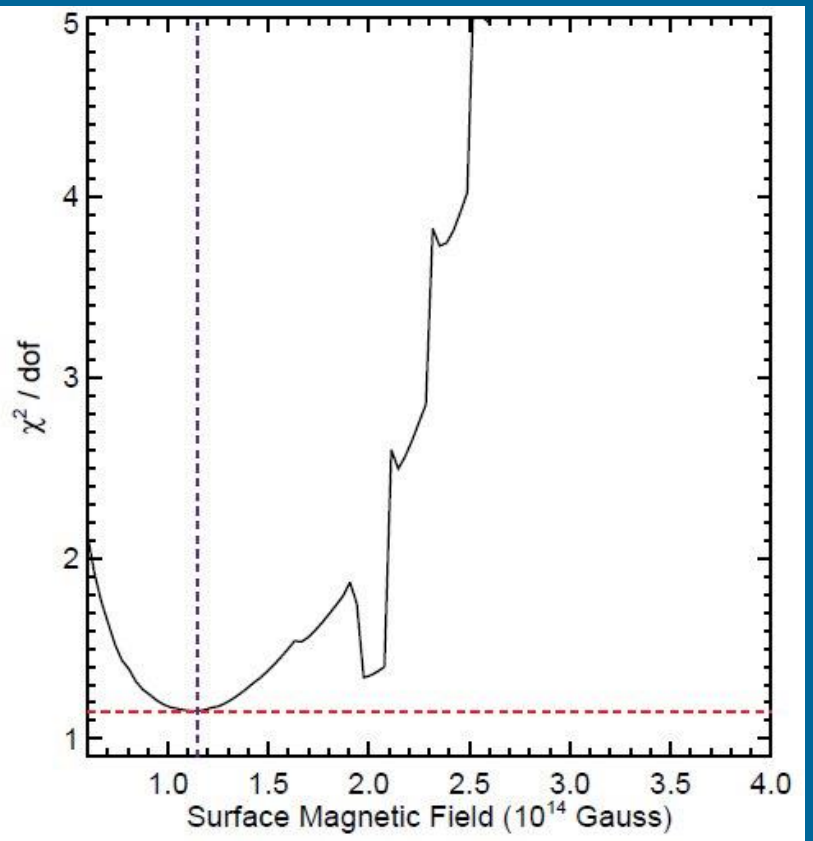

1103.3024

New results in 1507.02689

Conclusions

- Emission from cooling NSs is more complicated than a simple blackbody
- Light bending (gravity)
- Atmospheres
- Magnetic field distribution - effects on properties of atmospheres and emission
- Magnetic field (including toroidal) in the crust – non-uniform temp.distr.
- Condensate
- Rotation at ~msec periods can smear spectral lines

Papers to read

- astro-ph/0702426 ←
- arXiv: 0801.1143 or astro-ph/0609066 } Reviews on the M7
- astro-ph/0206025 ←
- arXiv: 0905.3276 } Recent calculations of spectra from magnetized atmos.
- arXiv: 1006.3292
- arXiv: 1210.0916 – review
- arXiv: 1409.7666 - review

Phase-resolved spectra and features

RX J1308.6+2127
A feature at the energy of ~ 740 eV
and an equivalent width of ~15 eV

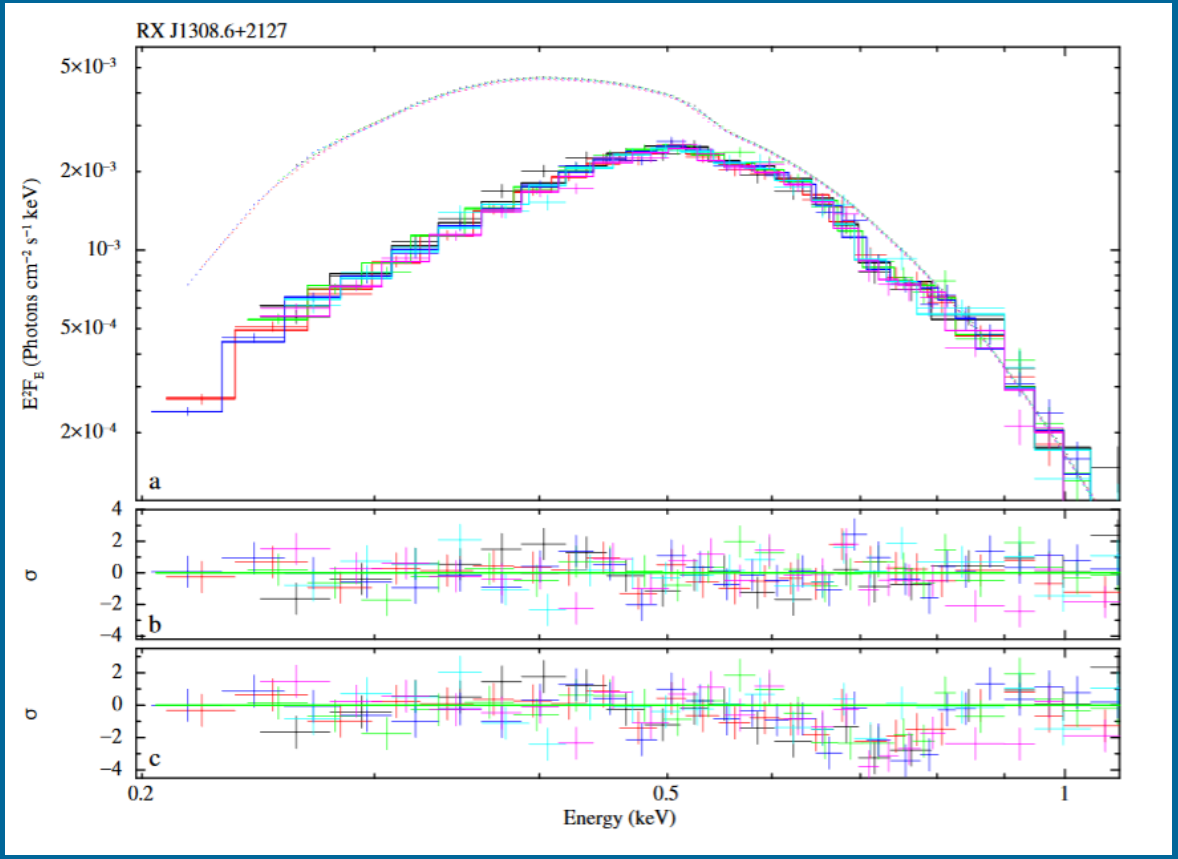

1703.05336

All in optics and UV

All seven objects have confirmed optical and ultraviolet counterparts.

The Rayleigh-Jeans tail would be flat. The best-fit power-laws with ±1σ uncertainties are shown by the cyan lines. The extrapolations of the X-ray blackbodies with ±1 σ uncertainties are shown by the magenta lines.

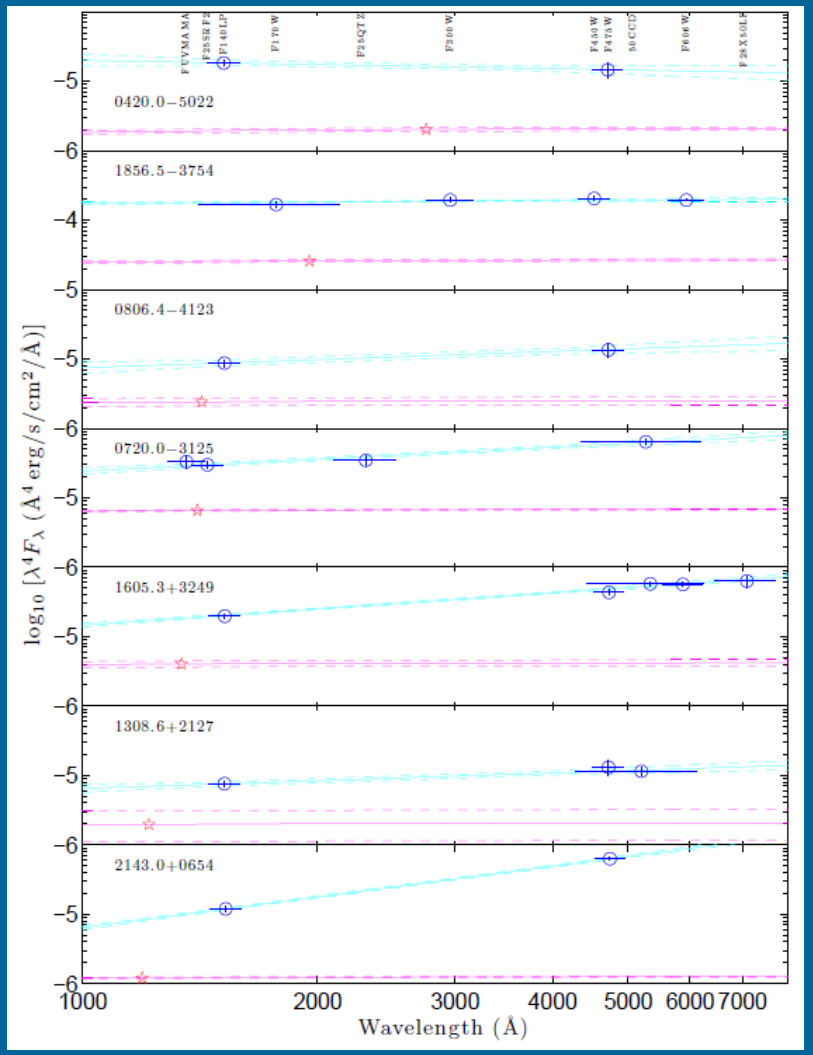

kT

New data: Kaplan et al. 1105.4178

Is RX J1856.5-3754 Bare ?

- Fit of X-ray data in the 0.15-2 keV band acceptable
- Radiation radius problem eased
- Optical excess may be produced by reprocessing of surface radiation in a very rarefied atmosphere (Motch, Zavlin & Haberl 2003; Zane, Turolla & Drake 2004; Ho et al. 2006)
- Details of spectral shape (features, low-energy behaviour) still uncertain

$$R_\infty = 4.25\, f_E^{-1/2} \left(\frac{D}{100\ \mathrm{pc}}\right)\left(\frac{T_{BB}}{60\ \mathrm{eV}}\right)^{-2} \mathrm{km}$$

Does the atmosphere keep the star surface temperature ?